Multi-storey Precast Concrete Framed Structures

2nd Edition

Kim S. Elliott and Colin K. Jolly

WILEY-BLACKWELL

Multi-storey Precast Concrete Framed Structures

Kim S. Elliott
BTech, PhD, CEng, MICE

Colin K. Jolly
MSc, PhD, CEng, MICE, FIStructE

WILEY Blackwell

This edition first published 2013

Registered office:
John Wiley & Sons, Ltd, The Atrium, Southern Gate, Chichester, West Sussex, PO19 8SQ, UK

Editorial offices:
9600 Garsington Road, Oxford, OX4 2DQ, UK
The Atrium, Southern Gate, Chichester, West Sussex, PO19 8SQ, UK
2121 State Avenue, Ames, Iowa 50014-8300, USA

For details of our global editorial offices, for customer services and for information about how to apply for permission to reuse the copyright material in this book, please see our website at www.wiley.com/wiley-blackwell.

Library of Congress Cataloging-in-Publication Data

Elliott, Kim S., author.
Multi-storey precast concrete framed structures / Kim S. Elliott, BTech, PhD, CEng, MICE, Colin K. Jolly, MSc, PhD, CEng, MICE, FIStructE. – [Second edition].
pages cm
Includes bibliographical references and index.
ISBN 978-1-4051-0614-6 (hardback : alk. paper) 1. Precast concrete construction. 2. Tall buildings–Design and construction. I. Title.
TH1498.E43 2013
693'.522–dc23
2012031585

A catalogue record for this book is available from the British Library.

Wiley also publishes its books in a variety of electronic formats. Some content that appears in print may not be available in electronic books.

Cover design by Andy Magee
Cover photo shows the North Galaxy Towers, Brussels (courtesy of Kim Elliott)

Set in 9.5/11.5 pt Minion by Toppan Best-set Premedia Limited

1 2013

Contents

Preface

Of all the major forms of multi-storey building construction, structural precast concrete is perhaps understood by the fewest practitioners. This is a significant 'blind spot' in that part of the building profession associated with the design and construction of large or small multi-storey precast and prestressed concrete frames. This is due mainly to two particular factors:

- The notion of using a modular form of construction, such as precast concrete, is not widely taught at undergraduate level because it is thought of as being too restrictive in the wider application of theory and design instruction.
- Precast concrete design is usually carried out in-house by the small number of specialist engineers employed by the precast manufacturing companies.

Consequently, the trainee structural designer is rarely exposed to the virtues of using precast concrete in this way. Opportunities to study the basic concepts adopted in the design, manufacturing and site erection stages are not often made available to the vast majority of trainees.

Even where precast concrete is accepted as a viable alternative form of construction to e.g. steelwork for medium to high-rise structures, or to insitu concrete for some of the more complex shaped buildings, or to masonry for low-rise work, it is often considered only at a late stage in the planning process. In these situations, precast concrete is then often restricted to the substitution of components carrying their own locally-induced stresses. The economic advantage of the precast components also carrying global stresses is lost in the urgency to commence construction. Indeed, precast component design has long been considered as having a secondary role to the main structural work. Only more recently have precast designers been challenged to validate the fundamental principles they are using, and to give clients confidence in precast concrete design solutions for entire structures.

To meet ever-increasing building specifications, precast manufacturing companies have considerably refined the design of their product. They have formed highly effective product associations dealing with not only the marketing and manufacturing of the product, but also with technical matters. These include common design solutions, research initiatives, education, unified design approaches, and, importantly, the encouragement of a wider appreciation of precast structures in the professional design office. Even so, the structural and architectural complexity of some of the more recent precast frames has widened the gap between precast designers and the rest of the profession. The latter have limited sources for guidance on how the former are working. Satisfying codes of practice and the building regulations plays only a minor role in the total package; there is so much more, as this book shows.

Nowadays, the use of precast reinforced and prestressed concrete for multi-storey framed buildings is widely regarded as an economic, structurally sound and architecturally versatile building method. Design concepts have evolved to satisfy a wide range of commercial and industrial building needs. 'Precast concrete frames' is a term which is now synonymous with high quality, strength, stability, durability and robustness. Design is carried out to the highest standard of exactness within the concrete industry and yet the knowhow, for the reasons given above, remains essentially within the precast industry itself.

Precast concrete buildings do not behave in the same way as cast-in situ ones. The components which make up the completed precast structure are subjected to different forces and movements from the concrete in the monolithic structure. It is necessary to understand where these physical effects come from, where they go to, and how they are transferred through the structure.

Consequently, this book aims to disseminate understanding of the disparate procedures involved in precast structural design, from drawing office practice to explaining the reasons for some of the more

intricate operations performed by precast contractors on site. The principal focus is upon on skeletal-frame type structures, the most extensively used form of precast structural concrete. They are defined as frameworks consisting essentially of beams, columns, slabs and a small number of shear walls.

From the structural and architectural viewpoints, skeletal frames are the most demanding of all precast structures. They contain the smallest quantity of structural concrete per unit volume. The precast components can be coordinated into the architectural façade, both internally and externally, to meet the social, economic and ecological demands that are now required. Ever greater accuracy, quality control, and on-site construction efficiency are being demanded and achieved. The construction industry is turning to high-specification prefabricated concrete for its advancement, using 'factory engineered' precasting techniques.

The chapters in this book have been arranged so that different parts of the design process can be either isolated (for example in the cases of precast flooring, or of connections), without the reader necessarily referring to the overall frame design, or read sequentially to realise the entire design. Chapters 1 to 3 present an overview of the subject in a non-technical way. Chapters 4 to 9 describe, in detail, the design procedures that would be carried out in a precast manufacturing company's design office. Chapter 10 describes the relevant site construction methods. Numerous examples have been used to demonstrate the application of design rules, many of which are not code-dependent.

There are many aspects to the design of precast skeletal frames that have evolved through the natural development of precast frame design since the 1950s. One aim of this book is to update and coordinate this information for the future. Historically, the precast concrete industry considered many of its design techniques commercially sensitive, particularly those for connector design, and was consequently criticised by developers and consultants. More information is now freely available since the expiry of many patents of ideas. One of the main purposes of the first edition was to bring together in a coherent manner, for the benefit of everyone, the widely varied design methods used in the industry. The second edition aims to extend that process in the context of continually developing technology and the introduction of Europe-wide design requirements embodied in the Eurocodes. It also demonstrates the trend towards greater, often fully serviced, spatial precast components.

Precast concrete designs are not entirely code-dependent, but the primary recommendations are in accordance with Eurocode 2 (BS EN 1992-1-1) and its predecessor BS 8110. Where the design procedures from the two codes differ, they are explained. Where major differences occur, or accumulate in design examples, the text is presented in two parallel columns with the Eurocode version in the left column and the BS 8110 text in the right column. When minor textual differences occur for the application of the two codes, Eurocode 2 forms the basic text, with the alternative BS text within braces or curly brackets thus: {to BS 8110}. It may help the reader to know that the authors have retained braces exclusively for this purpose, leaving the use of round brackets for the two contextually differentiable functions of parenthesis or mathematical grouping, and square brackets for references.

The combination of a broad overview, background research, and detailed analysis, the references to the familiar British Standards and the new Eurocodes, and an extensive range of illustrations together combine to offer a valuable resource for both undergraduate and practising engineers in the field of precast concrete.

The authors are indebted to the following individuals and companies for their personal assistance and corporate help in the preparation of this book: Beresford Flooring Ltd (Derby, UK), Bison Manufacturing (Swadlincote, UK), British Precast Concrete Federation and Precast Flooring Federation (Leicester, UK), CERIB (Epernon, France), Composites Ltd (formerly Composite Structures, Eastleigh, UK), Corsmit Consulting Engineers (Rijswijk, Netherlands), The Concrete Centre (formerly British Cement Association, Camberley, UK), Creagh Concrete (Antrim, UK), Ergon (formerly Partek, Lier, Belgium), Andrew T. Curd & Partners (USA), Federation International du Beton (*fib*), Gruppo Centro Nord (Cerano, Italy), Hume Industries Berhad (Malaysia), The New Civil Engineer (London), Peikko Finland Oy (Lahti, Finland), Precast Concrete Structures Ltd (Gloucester, UK), SCC Ltd (Stockport, UK), Spenncon AS (Sandvika, Norway), Spiroll Precast Services Ltd (Derby, UK), Strängbetong AB (Stockholm, Sweden), T&A Prefabricados (Igarrasu, Brazil), Tarmac Building Products Ltd (Ettingshall, UK), Trent Concrete Ltd (Nottingham, UK), University of California (San Diego, USA), Waycon (Plymouth, UK) and Mr Arnold van Acker (*fib* Commission member).

Notation

Latin upper-case letters

A	Accidental action
A	Cross-sectional area
A_b	Cross-sectional area of bolts
A_{bst}	Area of bursting reinforcement
A_c	Cross-sectional area of concrete
A_c'	Gross cross-sectional area of hollow-core slabs
$A_{c\,(net)}'$	Net cross-sectional area of hollow-core slabs
A_d	Area of diagonal reinforcement
A_f	Cross-sectional area of flange
A_{hd}	Area of diaphragm reinforcement
A_k	Contact area in castellated joint
A_p, A_{ps}	Area of a prestressing tendon or tendons
A_s	Cross-sectional area of tension reinforcement
A_s'	Area of compression reinforcement
A_s''	Area of longitudinal reinforcement in top of boot of beam
A_{sc}	Total area of reinforcement in column
A_{sh}	Area of horizontal reinforcement
A_{shv}	Area of horizontal punching shear reinforcement
$A_{s,min}$	Minimum cross-sectional area of reinforcement
A_{sv}	Area of shear reinforcement
A_{sw}	Cross-sectional area of shear reinforcement; area of reinforcing bars welded to plate
B	Breadth of void in slab; breadth of building; breadth of foundation
C	Compressive force
D	Diameter of mandrel; depth of pocket in foundation; depth of floor diaphragm; depth of hcu
D_{Ed}	Fatigue damage factor
E	Effect of action; Young's modulus of elasticity
E'	Equivalent Young's modulus in precast *in situ* joint
E_c	Tangent modulus of elasticity of normal weight concrete at a stress of $\sigma_c = 0$
E_c'	Young's modulus of *in situ* concrete
$E_{c(28)}$	Tangent modulus of elasticity of normal weight concrete at 28 days
$E_{c,eff}$	Effective modulus of elasticity of concrete
E_{cd}	Design value of modulus of elasticity of concrete
E_{ci}	Young's modulus of concrete at transfer
E_{cm}	Secant modulus of elasticity of concrete
$E_{c(0)}$	Tangent modulus of elasticity of normal weight concrete at a stress of $\sigma_c = 0$
$E_{c(t)}$	Tangent modulus of elasticity of normal weight concrete at time t

E_i	Young's modulus of infill concrete
E_p	Design value of modulus of elasticity of prestressing steel
E_s	Design value of modulus of elasticity of reinforcing steel
EI	Bending stiffness
EQU	Static equilibrium
F	Action; force
F_{bt}	Ultimate tensile force in bars at start of bends
F_c	Compressive force in concrete
F_{cR}	Ultimate compressive resistance force
F_d	Design value of an action; tensile force in diagonal reinforcing bars
F_h	Tensile force in horizontal reinforcing bars
F_k	Characteristic value of an action
F_s	Tensile force in reinforcing bars
F_t	Notional tensile force in stability ties
F_t'	Tensile force in stability ties
F_{tR}	Ultimate tensile resistance force
F_v	Shear force to one side of interface (composite construction)
G	Shear modulus
G_k	Characteristic permanent action
H	Total height of building; length of foundation; horizontal force
H_{bst}	Bursting force
H_v	Horizontal resistance of infill wall
I	Second moment of area of concrete section
I_c	Transformed second moment of area of composite section
I_{co}	Compound second moment of area
K	Stress factor $M/f_{ck}\, b\, d^2$ $\{M/f_{cu}\, b\, d^2\}$; shrinkage factor
K_b	Flexural stiffness of connections between members
K_s	Shear stiffness of connections between members
K_t	Bond length parameter
L	Length; span; length of void in slab; length of building base plate overhang distance
L'	Clear opening between columns; length of wall
L_e	Effective length
L_s	Clamping length
L_{sb}	Bond length
L_1	Distance from face of column to load
L_2, L_3	Length of stress block (insert design)
L_4	Length of embedment of insert
M	Bending moment
M'	Moment of resistance based on strength of concrete = $0.206\, f_{ck}\, b\, d^2$ $\{0.156\, f_{cu}\, b\, d^2\}$
M_{add}	Additional bending moment due to deflection = Na_u
M_b	Bending moment due to shrinkage
M_c	Balancing bending moment due to shrinkage
M_{Ed}	Design value of the applied internal bending moment
M_h	Bending moment in floor diaphragm
M_{max}, M_{min}	Maximum and minimum bending moment

M_{net}	M_{max}-M_{min}
M_o	Decompression bending moment
M_R	Moment of resistance
M_{sr}	Serviceability moment of resistance
M_{Rd} $\{M_{ur}\}$	Ultimate moment of resistance
M_1, M_2, M_3	Strength of connections in frames
N	Axial force; number of strands/wires/bolts
N_{Ed}	Design value of the applied axial force (tension or compression)
P	Prestressing force
P_0	Initial force at the active end of the tendon immediately after stressing
P_{po} $\{P_f\}$	Prestressing force after all losses
P_{pi} $\{P_i\}$	Initial prestressing force
P_{pmi}	Prestressing force at installation
P_{pm0} $\{P_t\}$	Prestressing force at transfer
P_r	Prestressing force after initial relaxation
P_t	Prestressing force at transfer
Q_k	Characteristic variable action
Q_{fat}	Characteristic fatigue load
R	Resistance; prop force
R_a	Roughness factor
R_y	Diagonal resistance of infill wall
S	Internal forces and moments; first moment of area; plastic section modulus
S_c	First moment of area to one side of interface
SLS	Serviceability limit state
T	Torsional moment; tension force
T_{Ed}	Design value of the applied torsional moment
ULS	Ultimate limit state
V	Shear force; reaction force
V_{co}	Shear resistance in flexurally uncracked prestressed section
V_{cr}	Shear resistance in flexurally cracked prestressed section
V_d	Shear force in dowel
V_{Ed}	Design value of the applied shear force
V_h	Horizontal shear force
V_r	Increased shear capacity due to additional reinforcement (insert design)
$V_{Rd,c}$ $\{V_{co}\}$	Shear resistance in flexurally uncracked prestressed section
$V_{Rd,cr}$ $\{V_{cr}\}$	Shear resistance in flexurally cracked prestressed section
$V_{Rd,CF}$	Ultimate shear capacity (compression field theory)
V_{uh}	Ultimate horizontal shear force
W	Self weight of column
W_k	Characteristic wind load
W_u	Ultimate wind load
X	Distance to neutral axis; stress block depth factor

Z	Elastic section modulus
Z_b, Z_t	Elastic section modulus at extreme bottom and top fibres
$Z_{b,co}$ $Z_{t,co}$	Compound elastic section modulus at extreme bottom and top fibres
Z_c	Elastic cracked concrete section modulus
Z_u	Elastic uncracked concrete section modulus

Latin lower-case letters

a	Distance; lever arm distance; distance to wall from shear centre; geometrical data
Δa	Deviation for geometrical data
a'	Distance from compression face to point where crack width is calculated
a_b	Clear distance between bars; cover to inside face of bars
a_{cr}	Distance from nearest bar to point where crack width is calculated
a_{eff}	Effective bearing length at corbel
a_f	Tangent of coefficient of friction, i.e. $\mu = \tan \alpha_f$
a_u	Sway deflection
a_v	Lever arm distance to shear force
b	Overall width of a cross-section, or actual flange width in a T- or L-beam
b_e, b_{eff}	Effective breadth
b_l	Length of bearing
b_p	Breadth of bearing
b_t	Breadth of section at centroid of steel in tension
b_v	Breadth of shear section or shear web
b_w	Width of the web on T-, I- or L-beams
c	Cover distance; distance to centre of bar
c_{min}	Minimum distance to bar in tension
c_w	Crack width
d	Diameter; depth; effective depth of a cross-section to tension steel; depth of web in steel sections
d'	Effective depth to compression steel
d''	Effective depth to tension steel in boot of beam
d_f	Effective depth to edge of foundation pocket
d_g	Largest nominal maximum aggregate size
d_h	Effective depth of half joint
d_n	Depth to centroid of compression zone
e	Eccentricity
e'	Effective eccentricity; lack of verticality
e_i $\{e_{add}\}$	Second order eccentricity
e_{net}	Net eccentricity
e_x	Minimum eccentricity (infill wall)
f_b	Ultimate bearing stress; limiting flexural compressive stress in concrete
f_{bc}	Bottom fibre stress due to prestress after losses
f_{bci}	Bottom fibre stress due to prestress at transfer
f_{bd}	Ultimate bond stress
f_{bpd}	Ultimate bond stress within the anchorage length
f_{bpt}	Bond stress within the transmission length
f_c	Compressive strength of bearing material

f_c'	Effective compressive strength of precast *in situ* concrete joint
f_{cc}	Prestress at centroid of tendons after losses
f_{cci}	Prestress at centroid of tendons at transfer
f_{cd}	Design value of concrete compressive strength
f_{ci}	Characteristic compressive cube strength of concrete at transfer
f_{ck}	Characteristic compressive cylinder strength of concrete at 28 days
f_{cm}	Mean value of concrete cylinder compressive strength
f_{cp}	Prestress at centroidal axis (taken as positive)
f_{cpx}	Prestress at centroidal axis at distance x from end of section
f_{ct}	Limiting flexural tensile stress in concrete
f_{ctk}	Characteristic axial tensile strength of concrete
f_{ctm}	Mean value of axial tensile strength of concrete
f_{cu}	Characteristic compressive cube strength of concrete
f_{cu}'	Characteristic compressive cube strength of infill concrete, ditto at lifting
f_{cyl}	Characteristic compressive cylinder strength of concrete
f_k	Characteristic compressive strength of brickwork
f_p	Tensile strength of prestressing steel
f_{pb}	Design tensile stress in tendons/wires
f_{pe}	Final prestress in tendons/wires after losses
f_{pi} $\{f_i\}$	Initial prestress in tendons
f_{pk}	Characteristic tensile strength of prestressing steel
f_{pm0} s_{pm0}	Prestress at transfer
f_{po} s_{po} $s_{pm\infty}$ $\{f_{pe}\}$	Final prestress in tendons/wires after losses
$f_{p0,1}$	0.1% proof-stress of prestressing steel
$f_{p0,1k}$	Characteristic 0.1% proof-stress of prestressing steel
$f_{0,2k}$	Characteristic 0.2% proof-stress of reinforcement
f_{pu}	Characteristic strength of prestressing tendons/wires
f_{Rd}	Ultimate bearing stress
f_s	Stress in reinforcing steel bars
f_t	Tensile strength of reinforcement; limiting direct (splitting) tensile stress in concrete
f_{tc}	Top fibre stress due to prestress after losses
f_{ti}	Top fibre stress due to prestress at transfer
f_{tk}	Characteristic tensile strength of reinforcement
f_v	Characteristic shear strength of brickwork
f_y	Yield strength of reinforcement
f_{yb}	Characteristic strength of bolts
f_{yd}	Design yield strength of reinforcement
f_{yk}	Characteristic yield strength of reinforcement
f_{ykw} $\{p_{weld}\}$	Strength of weld material
f_{yv}	Characteristic strength of reinforcing steel links/stirrups
f_{ywd}	Design yield of shear reinforcement
f_{ywk} $\{f_{yv}\}$	Characteristic strength of reinforcing steel links/stirrups
g_k	Characteristic uniformly distributed dead load
h	Height; floor-to-floor height; overall depth of section
h'	Clear floor-to-floor height; reduced depth at half joint
h_{agg}	Nominal size of aggregate
h_s	Depth of slab in composite construction
i	Radius of gyration

k	Coefficient; factor; core distance = $I/(0.5\,hA)$
k_s	Shear stiffness in joints
k_b	Flexural stiffness in joints
k_j	Rotational stiffness in joints
l	Length; span; distance between column-to-column centres
l_b	Bearing length
l_{bd}	Design anchorage length
l_e	Effective length
l_0	Clear height between restraints
l_{bpd} $\{l_p\}$	Prestress anchorage {development} length
l_{pt1}	Prestress transmission length, lower bound
l_{pt2} $\{l_t\}$	Prestress transmission length, upper bound
l_r	Distance between columns or walls (stability ties)
l_t	Prestress transmission length
l_w	Length of weldment
l_x	Penetration of starter bar into hole
l_z	Distance between positions of zero bending moment
m	Mass; distance from centre of starter bar to holding down bolt (base plate); modular ratio
m_{add}	Additional bending moment due to deflection = $N_{Ed}e_i$
m_s	Modular ratio (of elastic moduli) at service
m_u	Modular ratio (of strength) at ultimate
n	Number of columns in one plane frame, number of bars in tension zone of wall; number of storeys
p_b	Bearing strength of steel plate
p_{weld}	Strength of weld material
p_{yk} $\{p_y\}$	Strength of steel plate
q	Pressure (key elements)
q_k	Characteristic uniformly distributed live load
r	Radius; radius of gyration; bend radius of reinforcing bar
$1/r$	Curvature at a particular section
s	Spacing of reinforcing bars
t	Thickness; time being considered; temperature range
t_{eff}	Effective thickness
t_0	The age of concrete at the time of loading
u	Perimeter of concrete cross-section, having area A_c; perimeter distance
u, v, w	Components of the displacement of a point
v	Thickness of *in situ* infill; v_{Edi} $\{v\}$ ultimate shear stress
v_{ave}	Average interface shear stress
v_c	Design concrete shear stress
v_h	Design interface shear stress
v_{Rdi} $\{v_u\}$	Ultimate shear stress resistance
v_t	Design torsion stress

w	Length of steel plate; uniformly distributed load; breadth of compressive strut
w'	Diagonal length of infill shear wall
w_k	Characteristic uniformly distributed wind pressure
x	Neutral axis depth; dimension of stirrup in boot of beam; distance to centroid of stabilising system
x, y, z	Coordinates
x_{se}	Average crack spacing
y_{po}	Half bearing breadth ($b_p/2$)
y_0	Half section breadth ($b/2$)
z	Lever arm of internal forces

Greek upper-case letters

Δ	Second order deflection; deformation; construction tolerance distance
Φ	Reinforcing bar or dowel diameter; ductility factor

Greek lower-case letters

α	Angle; ratio; ratio Z_r/Z_b; coefficient of thermal expansion; characteristic contact length in infill wall
α_c	Ratio of sum of column stiffness to beam stiffness
α_{cmin}	Minimum value of α_{ca}
α_1	Ratio of distance to shear plane/transmission length l_x/l_{pt2}
β	Angle; ratio; coefficient
γ	Partial factor
γ_A	Partial factor for accidental actions, A
γ_C	Partial factor for concrete
γ_F	Partial factor for actions, F
$\gamma_{F,fat}$	Partial factor for fatigue actions
$\gamma_{C,fat}$	Partial factor for fatigue of concrete
γ_G	Partial factor for permanent actions, G
γ_M	Partial factor for a material property, taking account of uncertainties in the material property itself, in geometric deviation and in the design model used
γ_P	Partial factor for actions associated with prestressing, P
γ_Q	Partial factor for variable actions, Q
γ_S	Partial factor for reinforcing or prestressing steel
$\gamma_{S,fat}$	Partial factor for reinforcing or prestressing steel under fatigue loading
γ_f	Partial factor for actions without taking account of model uncertainties
γ_g	Partial factor for permanent actions without taking account of model uncertainties
γ_m	Partial factors for a material property, taking account only of uncertainties in the material property
δ	Increment/redistribution ratio; deflection; shear slip
ε	Strain
ε_b	Free shrinkage strain in precast beam or slab
ε_{bb}	Free shrinkage strain in bottom of precast beam or slab
ε_{bt}	Free shrinkage strain in top of precast beam or slab
ε_c	Compressive strain in the concrete

ε_{c1}	Compressive strain in the concrete at the peak stress f_c
ε_{cu}	Ultimate compressive strain in the concrete
ε_f	Strain of reinforcement or prestressing steel at maximum load
ε_m	Free shrinkage strain in *in situ* concrete flange or topping
ε_s	Average strain at level where crack width is calculated
ε_{sh}	Steel strain; relative shrinkage strain ε_f–ε_{bt}
ε_u	Shrinkage strain
ε_u	Strain at the level where crack width is calculated
ε_{uk}	Characteristic strain of reinforcement or prestressing steel at maximum load
ζ	Reduction factor/distribution coefficient
η	Total losses in prestressing force; force reduction factors
θ	Angle; slope of infill wall
λ	Slenderness ratio; relative stiffness parameter; joint deformability
μ	Coefficient of friction; degree of prestress force P_i/P
ν	Poisson's ratio; strength reduction factor for concrete cracked in shear
ξ	Ratio of bond strength of prestressing and reinforcing steel; bursting coefficient; prestress loss due to elastic shortening
ρ	Stress; reinforcement ratio = A/bd; oven-dry density of concrete in kg/m^3
ρ_{1000}	Value of relaxation loss (in %), at 1000 hours after tensioning and at a mean temperature of 20°C
ρ_l	Reinforcement ratio for longitudinal reinforcement
ρ_w	Reinforcement ratio for shear reinforcement
σ_c	Compressive stress in the concrete
σ_{cp}	Compressive stress in the concrete from axial load or prestressing
σ_{cp}	Spalling stress
σ_{cu}	Compressive stress in the concrete at the ultimate compressive strain, ε_{cu}
τ	Torsional shear stress; shear stress
ϕ	Diameter of a reinforcing bar or of a prestressing duct; rotation; diameter
ϕ_n	Equivalent diameter of a bundle of reinforcing bars
$\phi_{(t,t0)}$	Creep coefficient, defining creep between times t and t_0, related to elastic deformation at 28 days
$\phi_{(\infty,t0)}$	Final value of creep coefficient
ψ	Factor defining representative values of variable actions
ψ_0	Factor for combination values
ψ_1	Factor for frequent values
ψ_2	Factor for quasi-permanent values

CHAPTER 1

Precast Concepts, History and Design Philosophy

The background to the relevance of precast concrete as a modern construction method for multi-storey buildings is described. The design method is summarised.

1.1 A Historical Note on the Development of Precast Frames

Precast concrete is not a new idea. William H. Lascelles (1832–85) of Exeter, England devised a system of precasting concrete wall panels, 3 ft × 2 ft × 1 inch thick, strengthened by forged, ⅛ inch-square iron bars. The cost was 3d (£0.01) per ft^2. Afterwards, the notion of 'pre-casting' concrete for major structural purposes began in the late nineteenth century, when its most obvious application – to span over areas with difficult access – began with the use of flooring joists. François Hennebique (1842–1921) first introduced precast concrete into a cast-*in situ* flour mill in France, where the self-weight of the prefabricated units was limited to the lifting capacity of two strong men! White [1.1] and Morris [1.2] give good historical accounts of these early developments.

The first precast and reinforced concrete (rc) frame in Britain was Weaver's Mill in Swansea. In referring to the photograph of the building, shown in Figure 1.1, a historical note states: . . . *the large building was part of the flour mill complex of Weaver and Co. The firm established themselves at the North Dock basin in 1895–6, and caused the large ferro-concrete mill to be built in 1897–98. It was constructed on the system devised by a Frenchman, F. Hennebique, the local architect being H. C. Portsmouth* . . . At this time Louis Gustave Mouchel (1852–1908, founder of the Mouchel Group) was chosen to be Hennebique's UK agent. Mouchel used a mix of cast-*in situ* and prefabricated concrete for a range of concrete framed structures, building at the rate of 10 per year for the next 12 years.

The structure was a beam-and-column skeletal frame, generally of seven storeys in height, with floor and beams spans of about 20 feet. The building has since been demolished owing to changes in land utilisation, but as a major precast and reinforced concrete construction it pre-dates the majority of early precast frames by about 40 years.

Bachmann and Steinle [1.3] note that the first trials in structural precast components took place around 1900, for example at Coignet's casino building in Biarritz in 1891, and Hennebique and Züblin's signalman's lodge in 1896, a complete three-dimensional cellular structure weighing about 11 tons [1.3].

During the First World War storehouses for various military purposes were prefabricated using rc walls and shells. Later, the 1930s saw expansions by companies such as Bison, Trent Concrete and

Multi-storey Precast Concrete Framed Structures, Second Edition. Kim S. Elliott and Colin K. Jolly.

Figure 1.1 Weaver's Mill, Swansea – the first precast concrete skeletal frame in the United Kingdom, constructed in 1897–98 (courtesy of Swansea City Archives).

Girling, with establishments positioned close to aggregate reserves in the Thames and Trent Valley basins. The reason why precast concrete came into being in the first place varies from country to country. One of the main reasons was that availability of structural timber became more limited. Some countries, notably the Soviet Union, Scandinavia and others in northern Continental Europe, which together possess more than one-third of the world's timber resources but experience long and cold winters, regarded its development as a major part of their indigenous national economy. Structural steelwork was not a major competitor at the time outside the United States, since it was batch-processed and thus relatively more expensive.

During the next 25 years developments in precast frame systems, prestressed concrete (psc) long-span rafters (up to 70 feet), and precast cladding increased the precasters' market share to around 15 per cent in the industrial, commercial and domestic sectors. Influential articles in such journals as the *Engineering News Record* encouraged some companies to begin producing prestressed floor slabs, and in order to provide a comprehensive service by which to market the floors these companies diversified into frames. In 1960 the number of precast companies manufacturing major structural components in Britain was around thirty. Today it is about eight.

Early structural systems were rather cumbersome compared with the slim-line components used in modern construction. Structural zones of up to 36 inches, giving rise to span/depth ratios of less than 9, were used in favour of more optimised precasting techniques and designs. This could have been called the 'heavy' period, as shown in C. Glover's now classic handbook *Structural Precast Concrete* [1.4]. Some of the concepts shown by Glover are still practised today and one cannot resist the thought that the new generation of precast concrete designers should take heed of books such as this. It is also difficult to avoid making comparisons with the 'lighter' precast period that was to follow in the 1980s, when the saving on total building height could, in some instances, be as much as 100 to 150 mm per floor.

Attempts to standardise precast building systems in Britain led to the development of the National Building Frame (NBF) and, later, the Public Building Frame (PBF). The real initiative in developing these systems was entrenched more in central policy from the then Ministry of Public Building and Works than by the precasting engineers of the building industry. The NBF was designed to provide: . . . *a flexible and economical system of standardised concrete framing for buildings up to six*

storeys in height. It comprises a small number of different precast components produced from a few standard moulds [1.5].

The consumer for the PBF was the Department of Environment, for use within the public sector's expanding building programme of the 1960s. Unlike the NBF, which was controlled by licence, the PBF was available without patent restrictions to any designer. The structural models were simple and economical: simply supported, long-span, prestressed concrete slabs up to 20 inches deep were half recessed into beams of equal depth. By controlling the main variables, such as loading (3+1 kN/m^2 superimposed was used throughout), concrete strength and reinforcement quantities, limiting spans were computed against structural floor depths. Figures 1.2 and 1.3 show some of the details of these frames. Diamant [1.6] records the international development of industrialised buildings between the early 1950s and 1964. During this period the authoritative Eastern European work by Mokk [1.7] was translated into English, and with it the documentation of precast concrete had begun.

Unfortunately, the modular design philosophy was reflected in the façade architecture. The results were predictable, exemplified at Highbury Technical College in Portsmouth (now a part of the University of Portsmouth) shown in Figure 1.4. The precast industry has found it difficult to dispel the legacy of such architectural brutalism.

Following the demise of the NBF and PBF, precast frame design evolved towards more of a client-based concept. Standard frame systems gave way to the incorporation of standardised components into bespoke solutions. The result, shown in Figure 1.5 of Western House (1990), Surrey Docks (1990) and Merchant's House (1991), established the route to the versatile precast concrete concepts of the present day.

In the mid-1980s, the enormous demands on the British construction industry led developers to look elsewhere for building products, as the demands on the British precast industry far exceeded its capacity. Individual frame and cladding companies (with annual turnovers of between £1 m and £3 m) were being asked to tender for projects that were singularly equal to or greater in value than their annual turnovers. Programmes were unreasonably tight and it seemed that the lessons learned from mass-market-led production techniques of the 1960s had gone unheeded. One solution was to turn to Northern Europe, where the larger structural concrete prefabricators were able to cope with these demands. Concrete prefabricated in Belgium was duly transported to the London Docklands project, shown in Figure 1.6.

In making a comparison of developments in Europe and North America, Nilson [1.8] states: *Over the past 30 years, developments of prestressed concrete in Europe and in the United States have taken place along quite different lines. In Europe, where the ratio of labor cost to material cost has been relatively low, innovative one-of-a-kind projects were economically feasible. . . . In the U.S. the demand for skilled on-site building labor often exceeded the supply, so economic conditions favored the greatest possible standardisation of construction . . .*

North America's production capabilities are an order of magnitude greater than those of Europe. Figure 1.7 shows the construction of a 30-storey, 5000-room hotel and leisure complex in Las Vegas. The conditions to which Nilson refers are changing. The gap between labour and material costs in Europe is now closer to that of North America. At the same time, progressively lower oil and transportation costs into the early twenty-first century made it feasible to manufacture components virtually anywhere in the world and transport them to regions of high construction demand. Recent indications are that increasingly scarce energy resources and narrowing pay differentials will reverse this trend.

While the market share for complete precast concrete frames has remained constant in the UK, the development of high-strength concrete for columns and the use of innovative shallow prestressed concrete beams, together with speed of construction to rival that of steelwork, has led to successful tower buildings in Northern Europe, particularly in Belgium and Holland. The twin-tower building 'galaxy' in Brussels, Figure 1.8, is such an example. With column sizes of 600 mm diameter (cast in two-storey heights using 95 N/mm^2 concrete strength) and beam and floor spans up to 9.2 m × 405 mm depth, construction rates achieved 2 storeys in 8 working days [1.9].

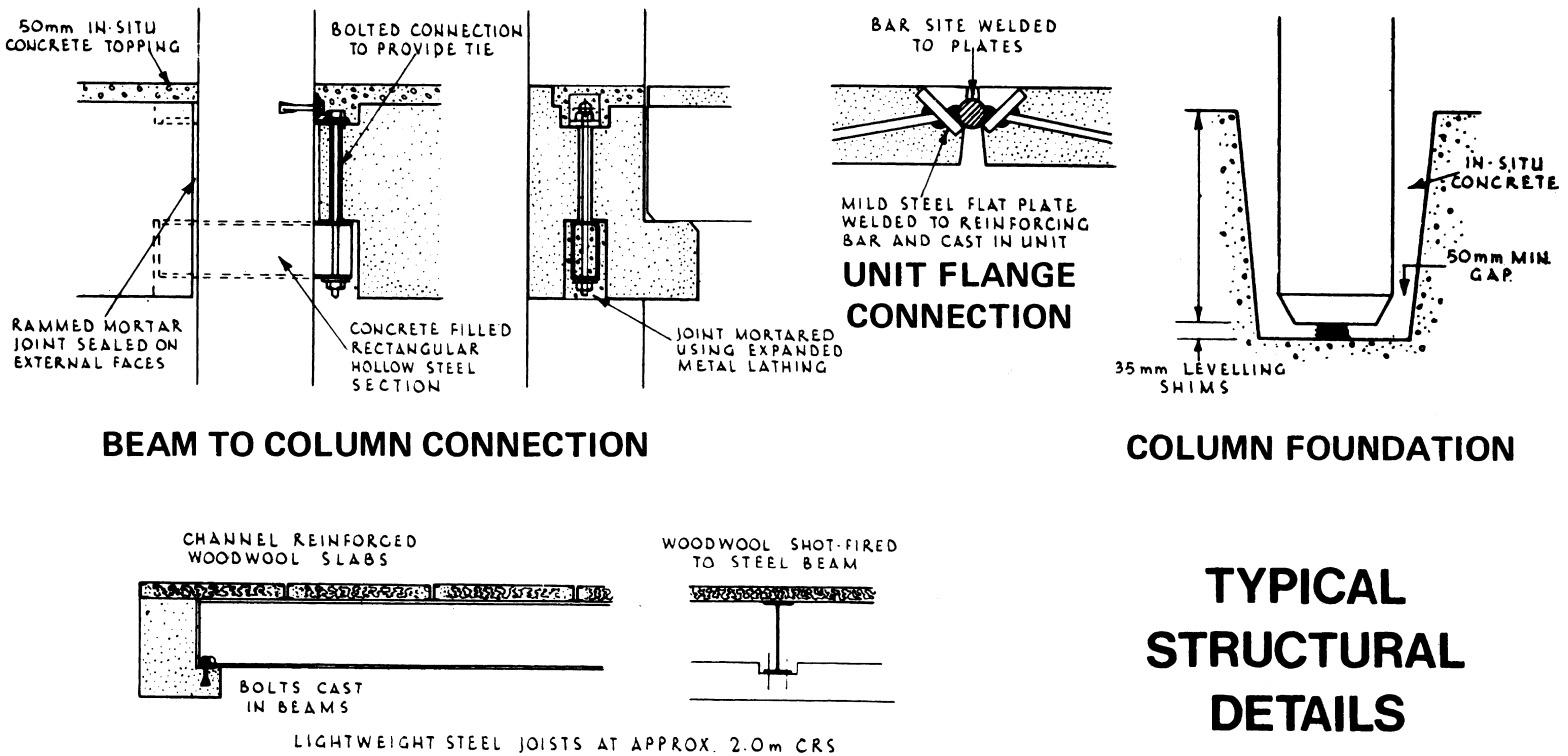

Figure 1.2 Typical structural details for the National Building Frame [1.4].

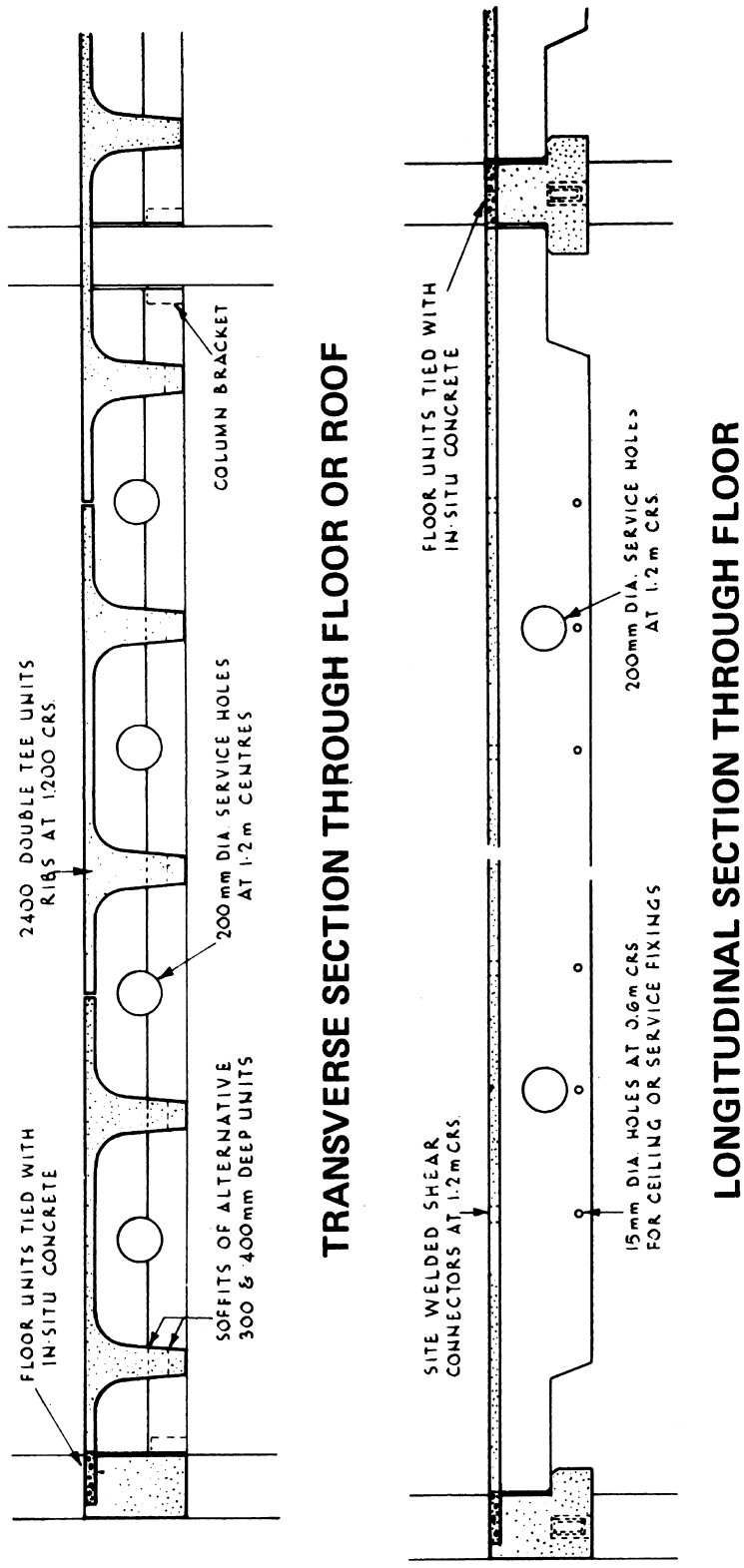

Figure 1.3 Floors used in the National Building Frame [1.4].

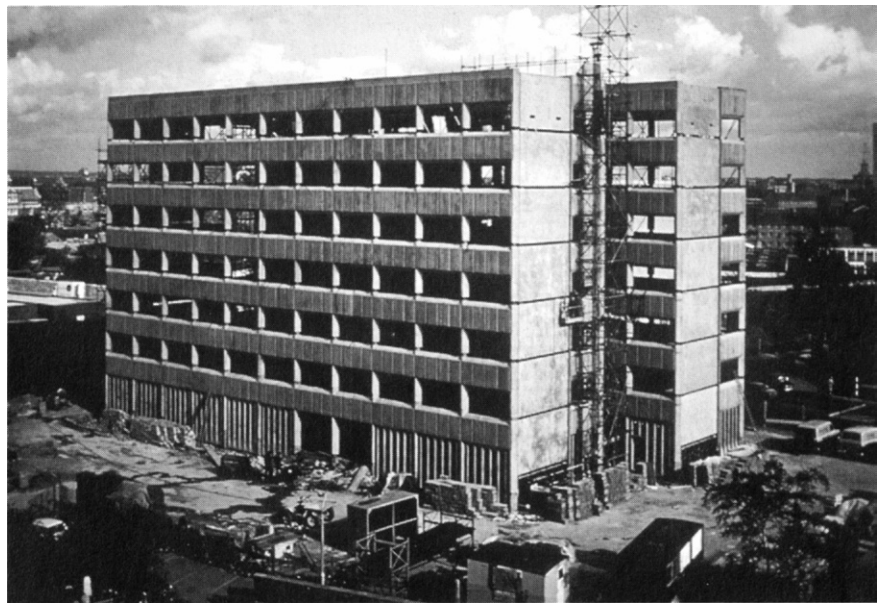

Figure 1.4 Precast construction of the 1960s using the National Building Frame, The building is Highbury College, now part of the University of Portsmouth (courtesy of Costain Building Products).

(a)

Figure 1.5 Examples of precast construction of the 1980s. (a) Western House, Swindon (courtesy Trent Concrete Ltd); (b) Surrey Docks, London (courtesy Crendon Structures); (c) Merchant House, London [1.10].

(b)

(c)

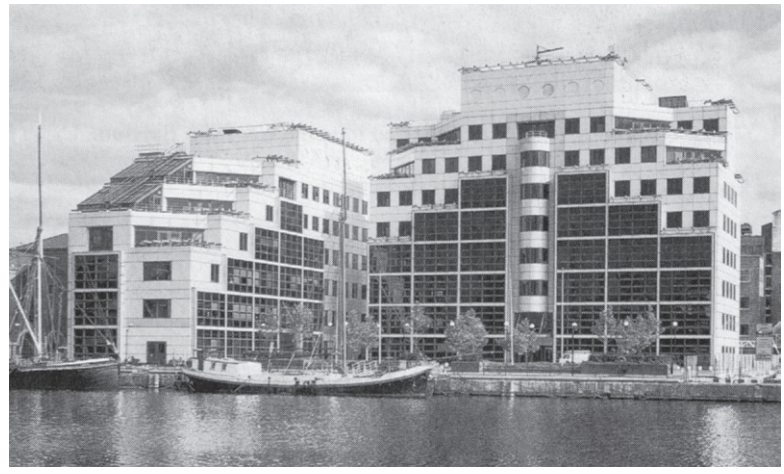

Figure 1.5 (*Continued*)

Changes to the way in which the construction industry should operate in a 'zero-waste and zero-defects' environment were given in the 1998 Egan Report [1.11]. The report called for sustained improvement targets: 10 per cent in capital construction costs; 10 per cent in construction time; 20 per cent of defects, and a 20 per cent increase in predictability. Further, the report goes on: . . . *The industry must design projects for ease of construction, making maximum use of standard components and processes.* Although the reports did not use the term 'prefabrication', to many people that is what 'predictability' and 'standard components' mean. The precast concrete industry is ideally placed to accommodate these higher demands by using experienced design teams and skilled labour in a quality-controlled environment to produce high-specification components. Figure 1.9 illustrates this in the repetitive use of granite cast spandrel beams and columns to form a building in the convoluted shape of a shell. Since 2000, high-quality architectural finishes have been more widely adopted for the exposed structural components, as illustrated in the integrated structure in Figure 1.10. The requirement for off-site fabrication will continue to increase as the rapid growth in management contracting, with its desire for reduced on-site processes and high-quality workmanship, will favour controlled prefabrication methods. The past five years have witnessed extensive developments in student accommodation – for example in Figure 1.11, where some 600 rooms were constructed using precast wall and floor systems in just over eight months, and were completed for occupancy within 18 months of site possession in 2009.

(a)

(b)

Figure 1.6 An early example of quality architecturally detailed precast concrete imported from Belgium. (a) Overall impression. (b) Architectural detail. (Courtesy of A. Van Acker, TU Ghent.)

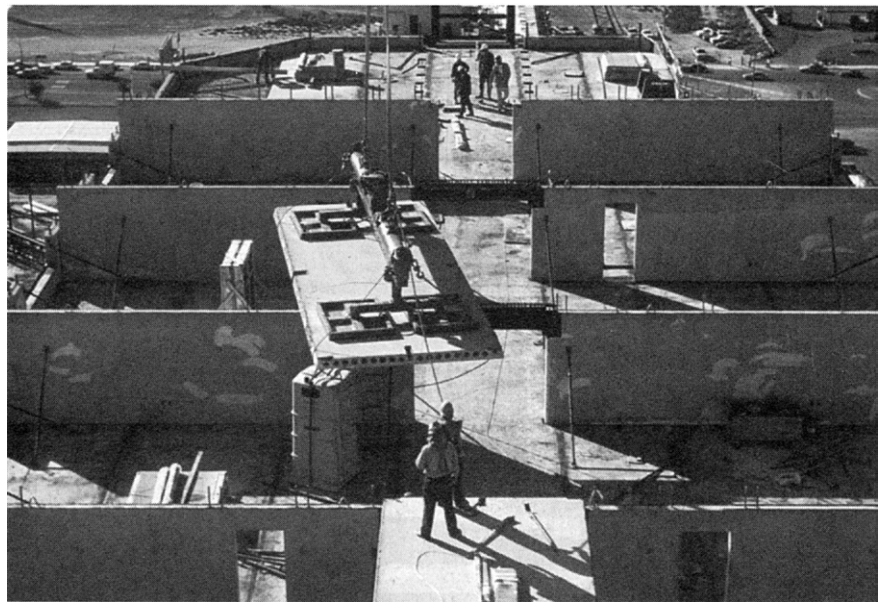

Figure 1.7 MGM Hotel and Casino at Las Vegas, US constructed in 1992 (courtesy of A. T. Curd).

Figure 1.8 36-storey precast skeletal tower buildings in Brussels (courtesy of Ergon, Belgium).

Figure 1.9 Granite aggregates in spandrel beams and columns, polished to reflect the Australian sunshine at No. 1 Spring Street, Melbourne, 1990.

(a)

(b)

Figure 1.10 Asticus Building, London, 2010. Precast cruciforms form (a) the exterior structure, and (b) architectural finish.

Figure 1.11 Student accommodation buildings at the University of West of England, Bristol. Precasted by Buchan, UK.

1.2 The Scope for Prefabricated Buildings

1.2.1 Modularisation and standardisation

The precast industry is still struggling to overcome the misconceptions of modular precast concrete buildings. This is not surprising, as many texts refer to: . . . *the design of a precast concrete structure on a modular grid. The grid should preferably have a basic module of 0.6 m* . . . [1.12]. The Continental Europeans introduced the phrase 'modular coordination', which meant the interdependent arrangement of dimensions, based on a primary value accepted as a module [1.13]. This dimension was 30 cm horizontally and 10 cm vertically. Moreover, the storey height in precast concrete apartment buildings was fixed at 280 cm, with the horizontal grid dimension on a 30 cm incremental scale between 270 cm and 540 cm. Strict observance of these rules facilitated the optimum assembly of prefabricated structures – in other words, all prefabricated buildings looked the same. And they were nearly all boxes – 'People are getting tired of this shoe-box architecture', said Harry Seidler, OBE, architect for the nautilus-shaped building in Figure 1.9.

There is a clear distinction between 'modular coordination' and 'standardisation'. The precast industry deplores the former and encourages the latter. What is the difference and how can this be?

Modularisation offers zero flexibility off the modular grid. The end product is evident in the comparison of the two buildings adjacent to Vauxhall Bridge in London, shown in Figure 1.12. Interior architectural freedom is possible only in the adoption of module quantities and configuration, and one cannot escape the geometrical dominance and lack of individuality of the older building on the left of the photograph. Exterior façades may of course be varied indefinitely, as in the 'twin façade'

Figure 1.12 Examples of past and present use of precast concrete, Vauxhall Bridge, London.

system shown in Figure 1.13, but that requires a full precast perimeter wall. In skeletal frames; one need go no further than the adoption of families of modular precast concrete components to obtain the optimum solution for any building, within reasonable limits.

Industrial modularised buildings were introduced in Europe in the 1950s, during the mass construction period following the Second World War. The problems in the architectural and social environment brought a re-emergence of traditional methods, and closer control on design and factory production. This has inevitably led to a new philosophy in what is called the 'modulated hierarchical building system' [1.14], which aims at the subdivision of a building into:

- functional systems, i.e. space utilisation both vertically and horizontally, personnel coordination, adaptability to changing needs
- technical systems, i.e. the structural design, the façade, mechanical and electrical services, waste disposal, and air-conditioning systems.

Precast modular frame manufacturers have been able to synthesise these requirements through continuous development of improved products and creative use of limited ranges of precast concrete products.

Standardisation is quite different from modularisation. It refers to the manner in which a set of predetermined components are used and connected. The buildings shown in Figures 1.14 to 1.16 were constructed using more or less the same family of standardised components. (The Reinforced Concrete Council has published case studies on precast frames, e.g. [1.10], where this may also be appreciated.) By adjusting beam depths, column lengths, wall positions, etc. the same components in any of these buildings could have been used to make a completely different structure. This is not possible with the modular system vision of the 1960s.

The four basic types of precast concrete structure are:

(1) The portal frame, Figure 1.17, consisting of columns and roof rafters or beams, provides large and adaptable ground-floor space. Portal frame structures are used for single-storey retail, warehousing, and industrial manufacturing facilities.

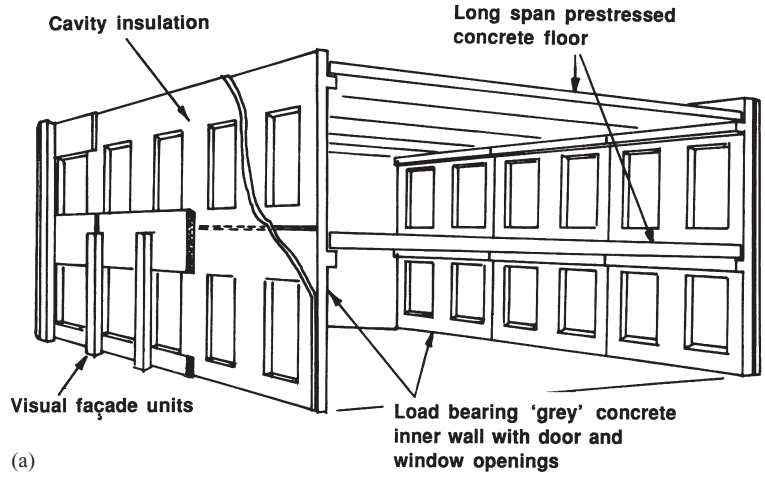

(a)

(b)

Figure 1.13 Principle of the twin facade system: (a) diagrammatic representation and (b) offices, Brussels.

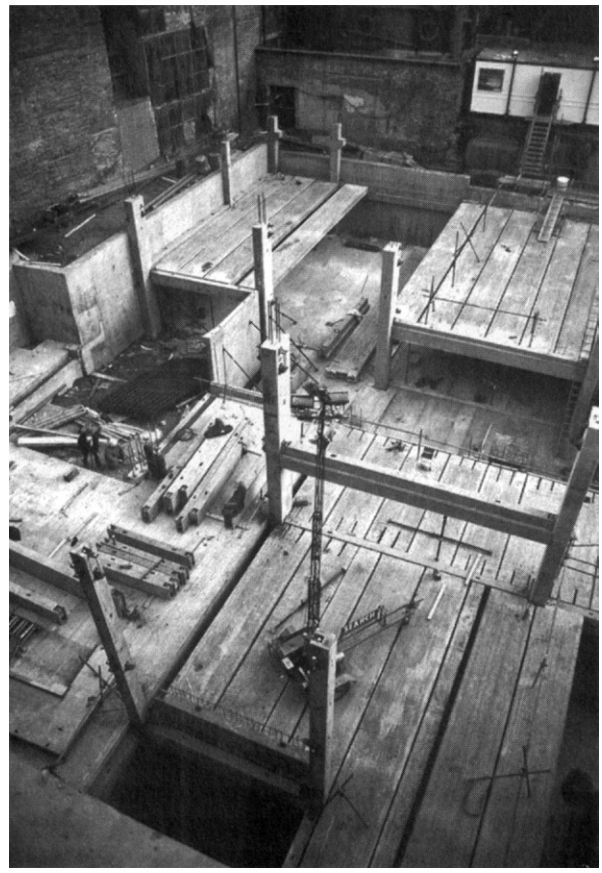

Figure 1.14 Structural 'grey' precast frame at Nottingham, UK (1995).

Figure 1.15 Commercial office development (courtesy of Crendon Structure, 1988).

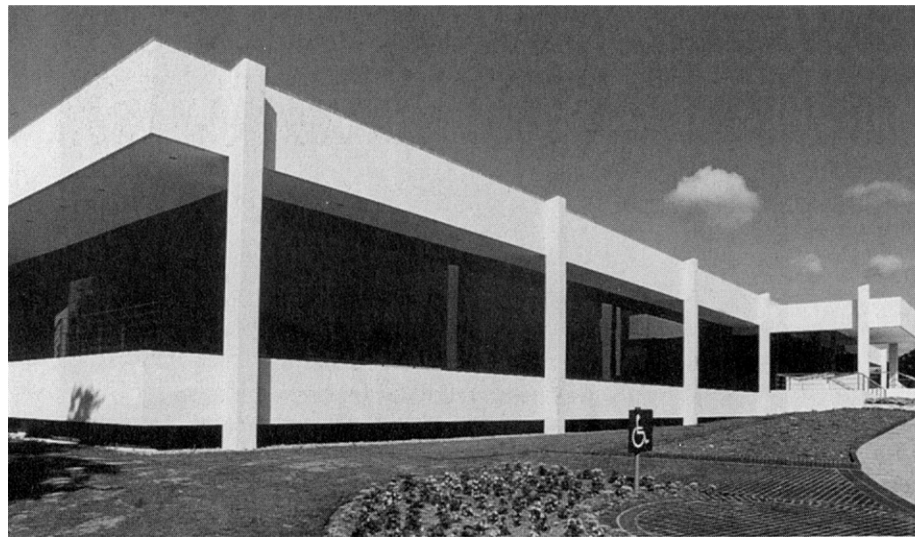

Figure 1.16 Visual structural units with a polished concrete finish (courtesy of Trent Concrete Ltd, 1992).

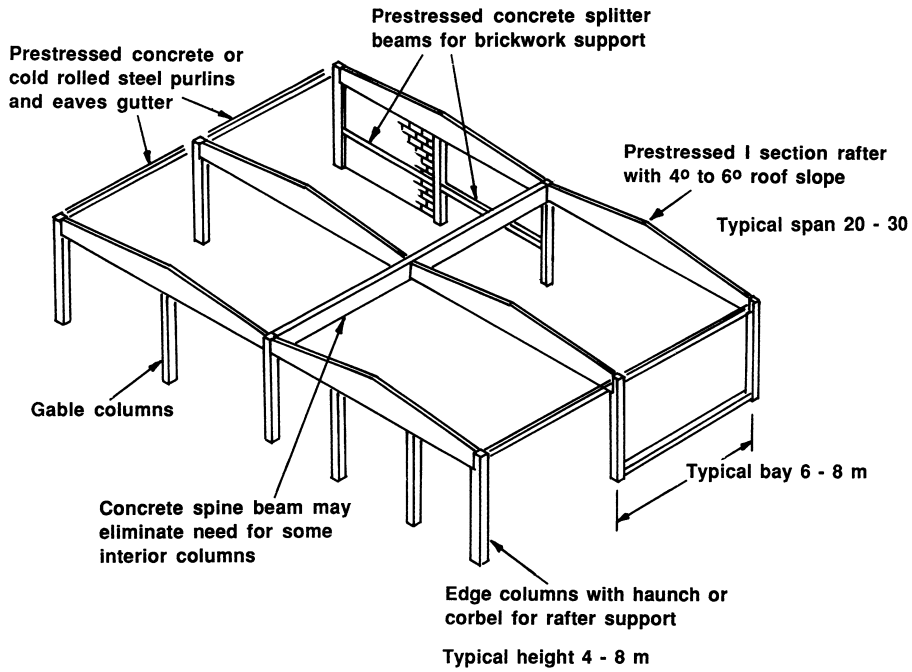

Figure 1.17 Typical arrangement of portal frames.

Figure 1.18 Wall frames used in apartment buildings and retail units near Sydney.

Figure 1.19 Crosswall construction.

(2) The crosswall frame, Figures 1.18 and 1.19, consisting of solid or voided vertical wall and horizontal slab units only. Here the structural walls serve as shear walls to resist lateral forces that increase with height, and also as acoustic and thermal partitioning. However, the walls interrupt the internal space and reduce functional flexibility. Wall frame structures are used extensively for multi-storey hotels, retail units, hospitals, housing, and partitioned offices.

(3) Volumetric, or cellular, structures such as that in Figure 1.20 are developments of wall frames in which a number of the walls and floors are constructed together as units. These units are suitable for high levels of factory installation of finishes and services, e.g. complete bathrooms, plumbing

Figure 1.20 Volumetric structure.

and wiring. Cellular units are then assembled to provide grouped, individual facilities such as student accommodation, hotel rooms or prisons.

(4) Skeletal structures, Figure 1.21, consisting of columns, beams and slabs for low- to medium-rise buildings, with a small number of walls for high-rise. Skeletal frames are used chiefly for commercial offices and car parks, where both clear spans and multiple storeys are required.

Skeletal frames are the most architecturally and structurally demanding, because in both disciplines designers feel that they have free rein to exploit the structural system by creating large, uninterrupted spans while reducing structural depths and the extent of the bracing elements. This results in a large proportion of the connections being highly stressed and difficult to analyse.

Non-structural or structural load-bearing panels or cells may also be incorporated in the frame, usually in the perimeter, and in the service cores. These units may be used as decorative cladding with a very wide range of finishes, textures, etc., thermal and sound insulation, fixings and other provisions. As decorative cladding, they are beyond the scope of this book and are documented elsewhere [1.15–1.17].

The skeletal structure is distinguished from other types because imposed gravity loads are carried to the foundations by beams and columns, and horizontal loads by columns and/or walls. The structural efficiency of a building is related, to a certain degree although not absolutely, to the mass of the structure. The volume of vertical structural concrete in a skeletal precast structure is in the order of 1 to 2 per cent of the volume of the building (for typical 3 to 3.5 m storey heights and 6 to 8 m beam spans). For a cross-wall frame the figure is closer to 4 per cent. Flooring is the most significant factor, with prestressed concrete voided slabs adding a further 4 per cent, compared with 7 to 8 per cent for solid concrete slabs.

1.3 Current Attitudes towards Precast Concrete Structures

The use of multi-storey precast concrete frames has evolved to improve the economy of high-specification buildings. Architectural precast concrete components are being used structurally on an

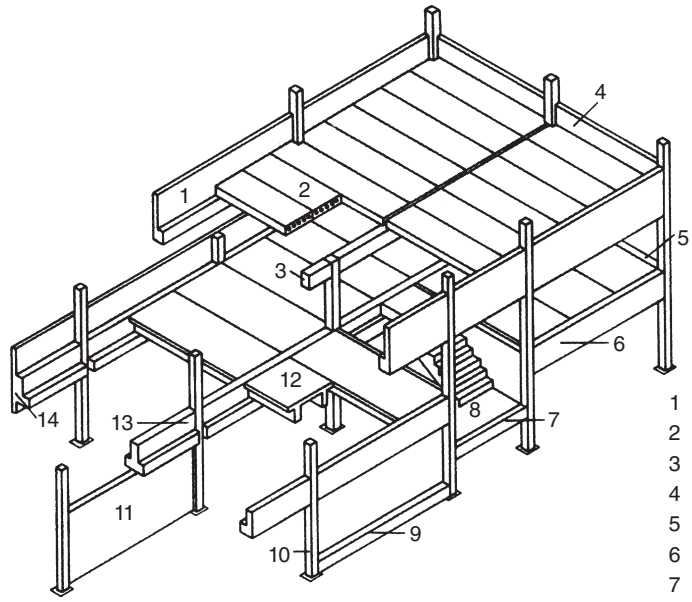

1 Main spandrel beam
2 Hollow-core unit
3 Internal rectangular beam
4 Gable spandrel beam
5 Gable beam
6 Main edge beam
7 Landing support beam
8 Staircase and landing
9 Ground beam
10 Column
11 Wall
12 Double-tee unit
13 Internal beam
14 Main edge spandrel beam

Figure 1.21 Skeletal structure and definition of components.

increasing number of prestigious commercial buildings, incorporating steelwork, timber and masonry for overall benefit. Designers are becoming more aware of the high-quality finishes possible in prefabricated units, affecting the way that the traditional precast structures are conceived and designed. The clients, and other parts of the construction industry, are calling for multi-functional design, where the use of all the components forming the building must be optimised.

The market share of commercial buildings, offices, schools, hotels, hospitals and car parks, etc. has fluctuated between as little as 5 per cent and nearly 15 per cent. Figure 1.22 shows the typical breakdown of market share in the multi-storey building market. Figure 1.23 shows the approximate breakdown of the UK's 2007 £2.6bn precast concrete market by product classification [1.18].

Compared with Continental Europe, Scandinavia and North America, the United Kingdom's precast concrete marketplace is small. Precast concrete frames, flooring and cladding represent approximately 22 per cent, 57 per cent, and 21 per cent of the total precast industry turnover, respectively.

To place this into context, Table 1.1 shows the approximate quantities of precast concrete flooring used in Europe in 1990 [1.19]. Total structural precast turnover in each country is nearly proportional. This variation in market penetration is not apparent in design and production matters, where concrete technology and production engineering are found to be broadly similar [1.20].

Use of precast concrete construction beyond five storeys has been rare in the UK until recently. Unlike the attitude in Continental Europe, North America and New Zealand, precast concrete is still considered as an alternative means of medium-rise (five to ten storeys) building construction to *in situ* concrete and structural steel. The possible reasons for this are three-fold:

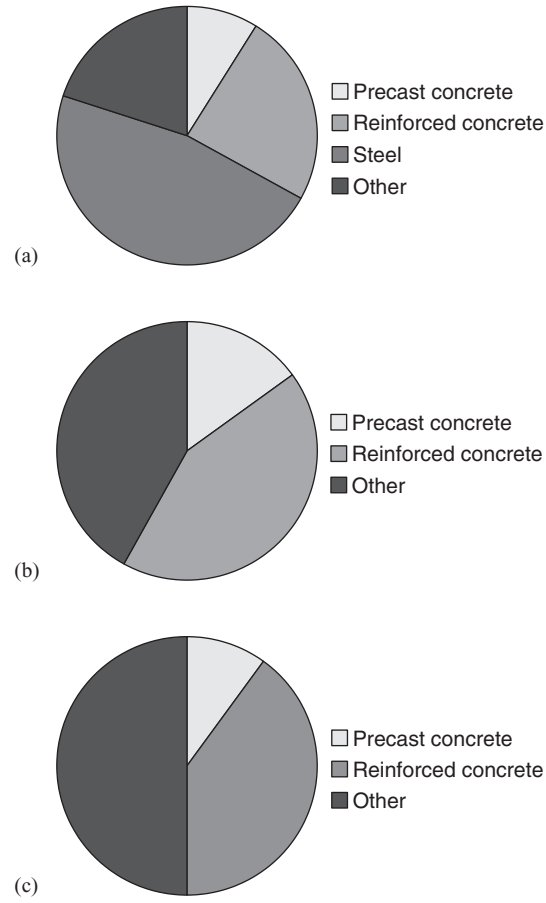

Figure 1.22 Market share for precast concrete in the multi-storey building market [1.18]. (a) Market share by value. (b) Non-housing market share. (c) Housing market share.

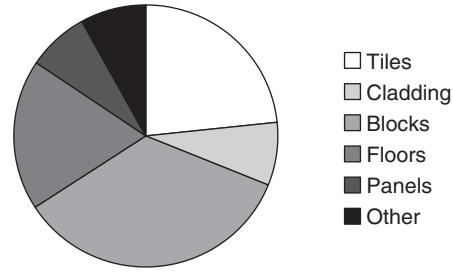

Figure 1.23 Market share for components of precast concrete.

Table 1.1 Quantities of precast concrete flooring used in Europe

	Production of hollow-cored flooring	
Country	**millions of m^2**	**m^2 per capita**
Germany	0.6	0.01
France	1.6	0.03
UK	2.8	0.05
Italy	3.4	0.06
Belgium	0.8	0.08
Denmark	0.7	0.15
Norway	0.9	0.22
Sweden	2.5	0.30
Netherlands	5.1	0.36
Finland	3.0	0.65

Note: On average 1 m^2 equates to about 0.12 m^3 of concrete, weighing 290 kg.

(1) There is a widespread lack of knowledge on the structural mechanics of precast construction, because the topic is rarely taught at a university and is not covered by post-graduate training in professional design practices. Precast has a low profile in academia, attracting little fundamental research funding from government. Few technical training courses have been organised, though the trade associations (The Concrete Centre, British Precast Concrete Federation, and Precast Flooring Federation) publish much general guidance and publicity material. As a result, precast concrete is perceived as difficult to specify for total building construction.

(2) Structural design and erection is nearly always (in 95 per cent of cases) carried out by the nominated precast manufacturer, thus depriving the consulting engineer of direct control over the frame design. Few clients, particularly government departments, will commit to a single-source manufacturer prior to design. There is a greater tradition of 'design and build' in the Continental construction industry.

(3) There is a lack of manufacturing capacity. Large-scale precast production demands capital investment. In a volatile economy, as has been seen in the UK since 1970, manufacturing companies have been forced to ride the crests and troughs with equal acumen if production capacities are to be maintained. Whereas structural steel can be stockpiled ready for cutting, and *in situ* concrete be poured at short notice, precast products must be manufactured to order.

In some countries precast concrete is viewed as a 'value-added product' and therefore carries a VAT surcharge over cast-*in situ* concrete.

On a worldwide scale the scope for high-specification precast concrete in buildings is still very large. The trend seems to be that in places where contracts are controlled by the contractor, rather than by the architect or client, precast is used mainly for the horizontal components, such as prestressed floors. This is reflected in the increase in use of precast concrete floors in residential building ground floors, up from 5 per cent in 1970 to 70 per cent in 2005. It is a well-known fact that precast manufacturers make less money from making vertical components than horizontal ones.

Furthermore, in certain regions, e.g. in the Middle East and Far East, the demand is growing at a rate greater than the increase in available technology. The major restraint for precast in the Far East is the very competitive cost for cast-*in situ* concrete, where site labour costs are typically single percentage points of the European costs. Building development is moving at such a swift pace that the frame geometry is fixed before the precast manufacturer has a chance to submit a more economical layout.

Table 1.2 Profit margins for US companies

Decade	Annual turnover	Annual profit (approx)
1970s	<$ 3.0 m	1.1%
	>$ 3.0 m	4.6%
1980s	<$ 7.5 m	1.8%
	>$ 7.5 m	8.2%
1990s	<$ 15.0 m	1.2%
	>$ 15.0 m	6.6%

Precast breaks down conveniently into three markets:

- residential (mainly 2–4 storeys) 5–15%
- commercial (offices, hotels, retail supermarkets, factories) 50–70%
- services (car parks, hospitals, colleges, sports stadiums) 20–40%

Product breakdown based on volume of concrete produced can be grouped into four markets:

- architectural façades, structural and non-structural 20–30%
- walls (non-decorative) 5–30%*
- floor slabs 50–60%
- beams and columns 10–15%

Note that volume of concrete produced is possibly not the best indicator with which to assess the industry. For example, the cost and the effort expended in manufacturing floor slabs is considerably less than for an architectural panel of similar weight, in some cases by a factor exceeding 10.

There is no doubt that the key to a successful precast concrete business is size. Output capacity has had a significant influence on the survival of precast companies in building. Using the American market as a role model (although a similar but scaled-down trend was seen in the UK and Europe), the profit margins for US companies were as shown in Table 1.2 [1.21].

Over this same period the approximate volume of precast reinforced and prestressed concrete produced per capita increased from 0.015 m^3 to 0.025 m^3 by the mid-1980s, but has fallen back to about 0.015 m^3 today.

1.4 Recent Trends in Design, and a New Definition for Precast Concrete

Responding to the reduced market of the 1990s, the industry saw a new movement in the design of precast structures, and a new definition to the word 'design'. It no longer meant '$\omega L^2/8$'. In a shrinking market the design of structural concrete frames for prestigious commercial buildings came under closer scrutiny as architects, design engineers and contractors strived to find optimum economy, speed of erection and the highest specification for their projects. The construction industry required a multiple choice in the selection of building components, and it was likely that the increasing demand on the performance of these components would overtake the existing technology used in their manufacture and utilisation.

Building design therefore became a multi-functional process, where the optimum use of all components forming the building was maximised. Attention was directed towards the structural frame,

*The production of walls for wall frames varies widely in different countries.

which could no longer be considered as serving only a structural function, but must be harmonised with the requirements of the building in total. Combined architectural/structural precast concrete components were therefore used on an increasing number of prestigious commercial buildings, as 'specifiers' became more aware of the high-quality finish possible in prefabricated units. However, changes had to be made to the way those traditional precast concrete structures were conceived and designed. Despite the cutbacks in staffing levels, the precast concrete industry was ideally placed to accommodate these higher demands by using experienced design teams and skilled labour in a quality-controlled environment to produce high-specification components, which served all the structural, architectural and services functions simultaneously.

An excellent example of the use of architectural/structural components is shown in Figure 1.16 above. White marble was originally chosen as separate cladding material to the external façade of a plain, precast concrete frame, including the expressed external columns. During the conceptual design stage it was realised that a white marble façade would have poor weathering characteristics, so it was replaced with a white, polished concrete, manufactured using 10 mm size Spanish Dolomite aggregate and white Portland cement, wet-ground and polished to produce a 'marble' appearance. The external façade was cast simultaneously with the structural components to reduce the overall cross section and eliminate unsightly joints to the front of the columns and beams [1.22].

Figure 1.24 shows prefabricated piers faced with load-bearing bricks used to support precast concrete floor units, spanning 14 m × 3.6 m wide, expressed as a rippling concrete band of vaulted units.

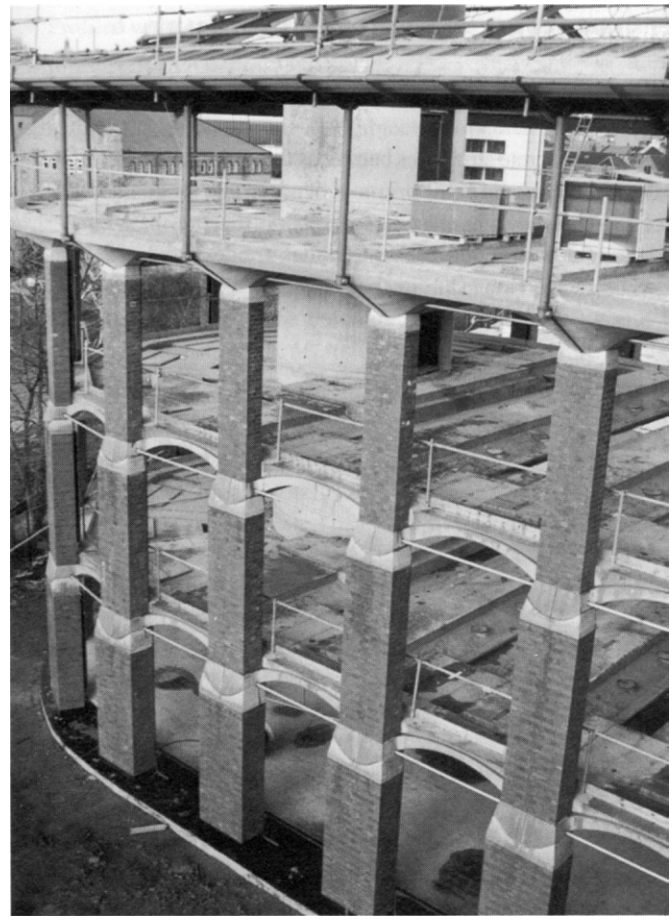

Figure 1.24 Prefabricated brick piers and concrete floor units.

Figure 1.25 Profiled white concrete columns supporting a steel roof (courtesy of Crendon Structures Ltd).

The components were manufactured as single long-span units, with dummy joints to give the appearance of numerous individual arched units in the short-span direction. The alternative design would have been to support vaulted panel units on longitudinal beams spanning between the piers. Structural and architectural variety was incorporated into this scheme at several levels. L-shaped blocks and quadrangles were joined with towers of glass blocks, which accommodated stairs and also acted as flue stacks to drive natural ventilation. Energy-saving features included structural components projected beyond the façade to shade windows, and the thermal mass of the floors limited peak summer temperatures.

The advantages of using single-piece visual concrete components are also evident from the photograph in Figure 1.25 of a building where cantilever columns support a lightweight steel roof. Concrete strengths of 50 MPa were achieved using white Portland cement and 10 mm down limestone aggregates. The structural capacity is no different from a column made from ordinary grey concrete.

1.5 Precast Superstructure Simply Explained

1.5.1 Differences in precast and cast-*in situ* concrete structures

Cast-*in situ* concrete structures behave as three-dimensional (3-D) frameworks. Continuity of displacements and equilibrium of bending and torsional moments, and shear and axial forces, are achieved by reinforcing the joints so that they have strengths equal to the members. However, for design purposes the frames are usually designed in 2-D plane stress, although the presence of the floor slab in the third dimension will affect the manner in which the plane frame behaves. This is particularly important in the end bay, where the beams and columns in the 2-D idealisation may be subject to torsional stresses and biaxial bending, respectively.

Figure 1.26(a) shows the approximate deflected shapes and bending moment distributions for a two-storey continuous frame subjected to gravity and horizontal loads. The foundations are assumed to be fully encastred in this example, which we may call frame F1. The relative magnitudes of the moments in the beams and columns depend on the relative stiffness (EI/L) of the columns and beams meeting at a joint. The joints depend on having equal strength M_1 to the members.

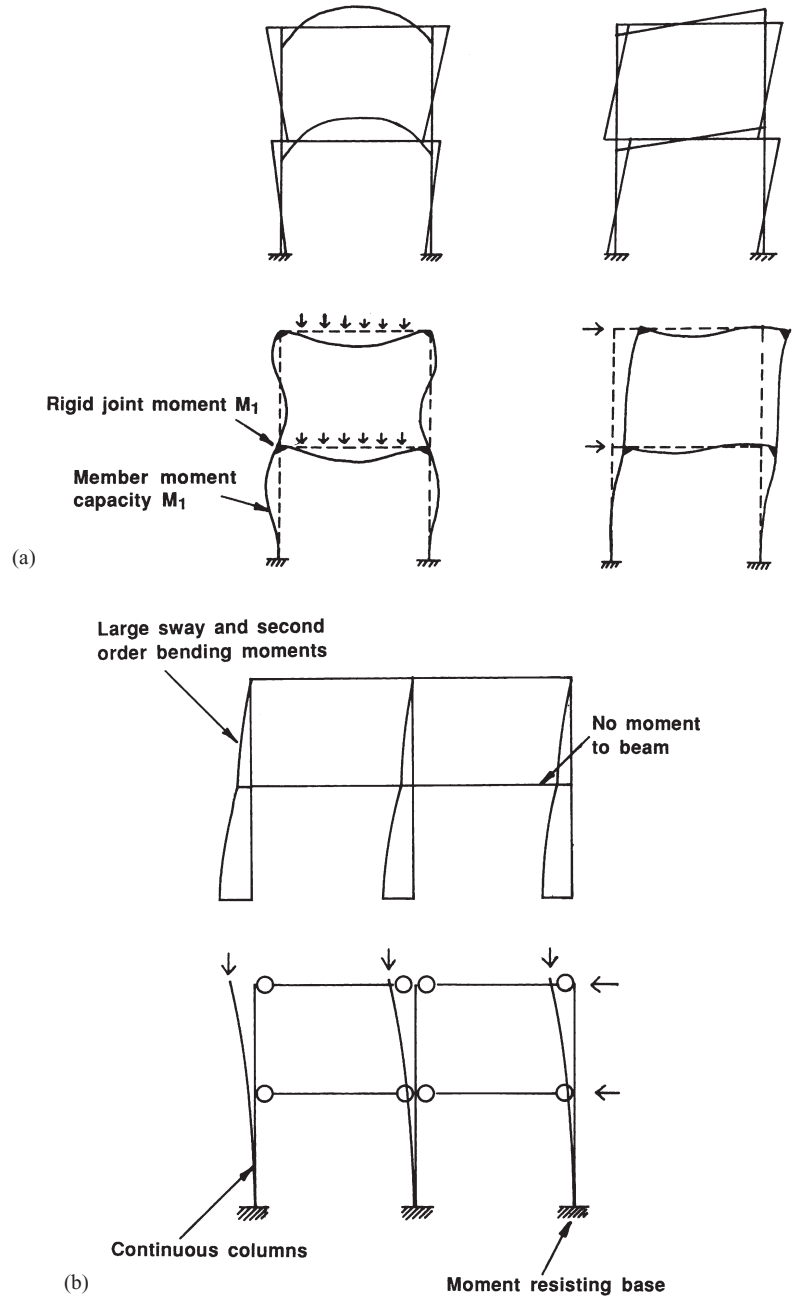

Figure 1.26 Moments and deflections: (a) in continuous frameworks and (b) in a unbraced structure.

If the strength of the joints in either of the beams in this frame were deliberately weakened to M_2 (e.g. by omitting reinforcement), the behaviour of the frame (called F2) would be equal to that of frame F1 up to the point where the moment in the joint reached M_2. Upon further loading the frame F2 would therefore develop plastic hinges at the joints. The difference between the bending moments in the column above and below the joint would be equal to the moment in the beam, M_2.

Taking this to the limit, if the joints were weakened to $M_3 = 0$, a pinned connection would result and the deflections and moments would be as shown in Figure 1.26(b). Note how the column moments have increased to allow for the fact that the moments can no longer be distributed into the beams. The difference between the bending moments in the upper and lower column at the joint is now zero. This is how a 'skeletal' precast structure behaves, because the beam–column connections are 'pinned' and the structure can be readily precast, with the individual components being bolted, dowelled or welded together on site. If there are no other stabilising elements in the structure, the ends of the columns at the foundations must be encastred.

The key elements in the design of skeletal structures are given by Elliott in journal papers and textbooks [1.23–1.25].

The term 'pin-jointed' refers essentially to the manner in which connections between columns, beams and floor slabs are made. The form of construction does not lend itself to seismic design and, conversely, in seismic zones fully rigid frame connections do not lend themselves to the safest and most economical use of precast concrete. Between these two extremes are semi-rigid connections, and design methods are now available for the post-elastic regime to be considered for the ultimate limit state design of columns in precast structures [1.26].

In buildings of more than about three storeys the horizontal sway deflections may become excessive, so that additional bracing must be used. Thus stability walls, cores or other forms of bracing are used. The usual practice is to place the stabilising units around lift shafts or stairwells so that the open-plan office space is not interrupted. The thickness of the walls varies from 125 mm to about 250 mm, depending on the size of the building. It is possible to cast door or window openings in walls, provided that viable force paths are maintained.

The structure is now classed as 'braced'. Figure 1.27 and the foundations may now be pinned. This simplifies foundation construction considerably and means that braced precast structures can be erected over *in situ* concrete retaining walls, beams, etc. and poor ground. The stabilising elements are so massive that the stiffness of the frame elements and connections is not important. Bending moments due to sway are small and columns can only deflect between floors as pin-ended struts.

In all cases, braced or not, horizontal wind loads are transmitted to the vertical frames through the precast floor, sometimes using unscreeded slabs, as though the floor were a deep beam on plan. One-way spanning, prestressed (or reinforced) precast floor slabs are seated on, or are recessed into, beams.

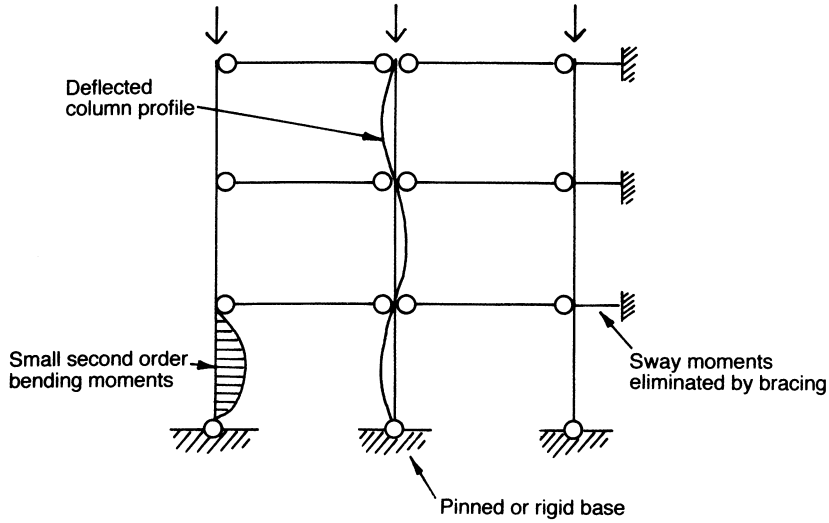

Figure 1.27 Moments and deflections in a braced structure.

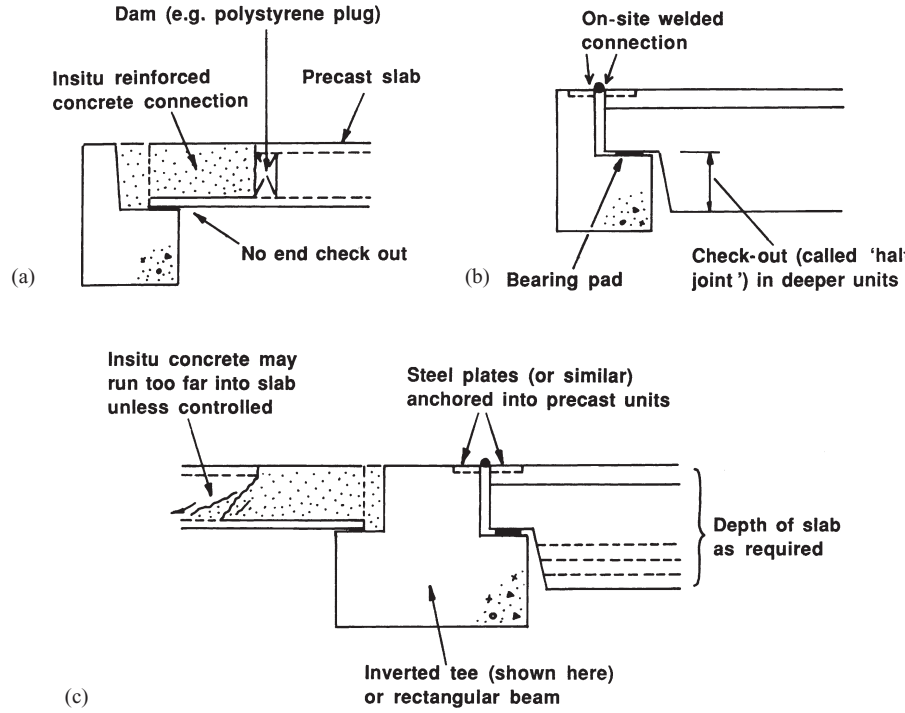

Figure 1.28 Detail of slab to beam bearing: (a) edge beam to hollow-core slab; (b) edge beam to double-tee slab; (c) internal beam to slab connections.

The structural zone is sometimes less than in an equivalent fire-protected steel frame, often showing a saving of 100 mm per floor [1.27, 1.28]. The slab bearing shown in Figures 1.28(a), 1.28(b) and 1.28(c) is designed as a simple pinned joint, despite the presence of the reinforced concrete *in situ* infill which penetrates into the floor slab and obviously provides some moment restraint. Beam design is to ordinary reinforced (rc) or prestressed concrete (psc) principles, and composite construction with the floor slab is occasionally appropriate. Precast staircases and landings are designed as inclined solid rc or psc units, and are omitted from the floor plate action.

Beams are connected to columns and walls using connectors that are, in the main, designed as pinned joints: Figure 1.29(a). Eccentric loading is applied to the column, which is continuous at the connection, and the bending moment is distributed in the column according to simplified 2-D frame analysis. Alternatively the beams may be connected on the tops of columns, Figure 1.29(b), or made continuous across the top of single-storey columns, Figure 1.29(c), and connected to the neighbouring beam away from the highly stressed column connection. Columns are considered continuous at floor joints, even though mechanical connections, called 'splices', are often made at this level, as shown in Figure 1.30.

In this book, architectural aspects will be dealt with in Chapter 3, the frame analysis and design methods in Chapter 4, component design in Chapters 5 and 6, the design of connections in Chapter 7, and the analysis and design for horizontal stability will be in Chapter 8.

1.5.2 Structural stability

Structural stability is the most crucial issue in precast concrete design, because it involves the design both of the precast concrete components and of the connections between them.

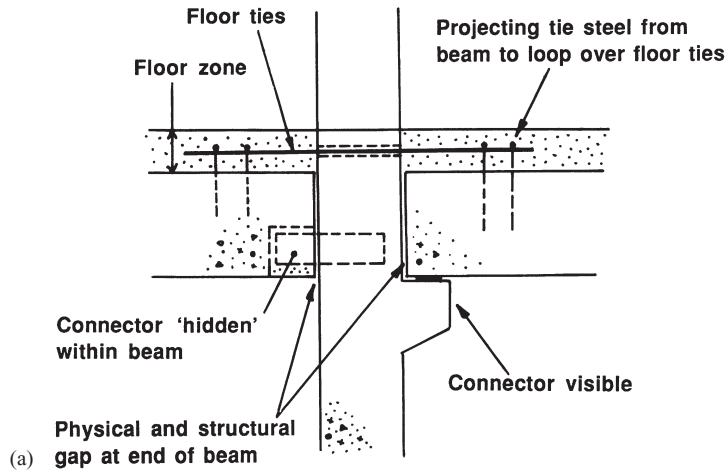

(a)

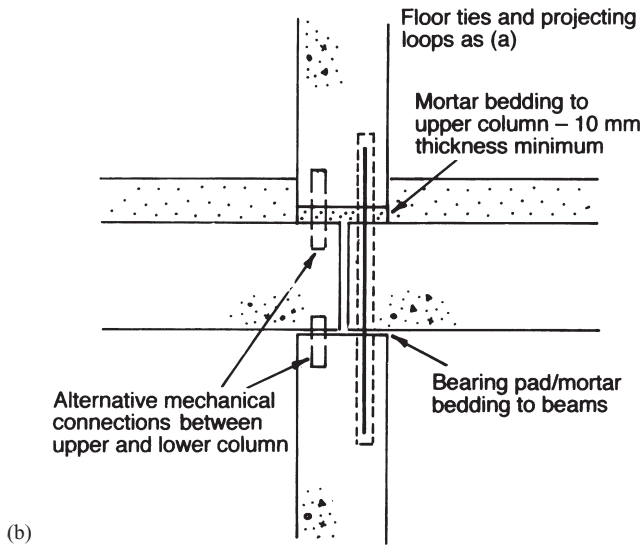

(b)

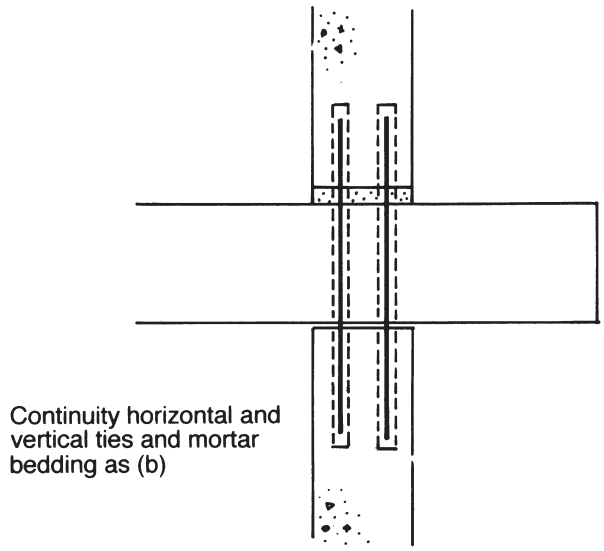

(c)

Figure 1.29 Beam to column connections: (a) beam to column connection – continuous column; (b) beam to column connection – discontinuous column and beam; (c) beam to column connection – continuous beam.

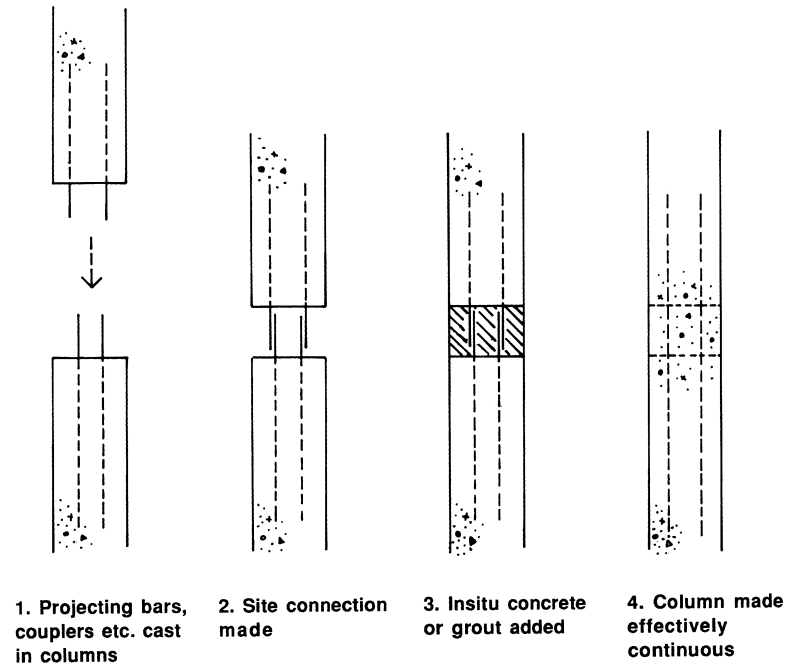

Figure 1.30 Principle of column splices. The substructure member could also be a wall or beam.

The first design features are stability and robustness. Precast systems are scrutinised by checking authorities more for structural stability, integrity, resistance against abnormal loading and robustness than for the design of individual precast components (slabs, beams, etc.), which usually have adequate factors of safety. In general 'stability' means adequate resistance against side-sway, and 'integrity and robustness' means correct joint design, attention to details and the prevention of progressive collapse. Chapter 9 describes in detail how to achieve structural integrity and resistance to accidental loading.

The problem is to ensure adequate ultimate strength and stiffness, but more importantly to ensure that the failure mode is ductile. Large factors of safety are less relevant to the overall performance criteria if brittle, or sudden, failures result. Brittle failures involve the rapid release of large amounts of energy.

Two design stages are considered:

- **Temporary stability during frame erection:** This has certain implications for design, e.g. the axial load capacity of temporary column splices must be greater than (at least) the self-weight of the upper column before the *in situ* infill grout has hardened and rendered the splice permanent. Chapter 10 will deal further with this topic.
- **Permanent stability:** This may be subdivided into four further stages:
  - horizontal diaphragm action in the precast floor slab;
  - transfer of horizontal loading from the floor slab and into the vertical bracing elements and thus into the foundations;
  - component design; and
  - connection and joint design.

The contribution to the lateral strength and stiffness of the structure from the *in situ* reinforced concrete infill strips is paramount. These strips provide the necessary tie forces that eliminate relative displacements between the various parts of the frame and ensure interaction between the components. The general idea is shown in Figure 1.31. These positions are not always easy to define, and no

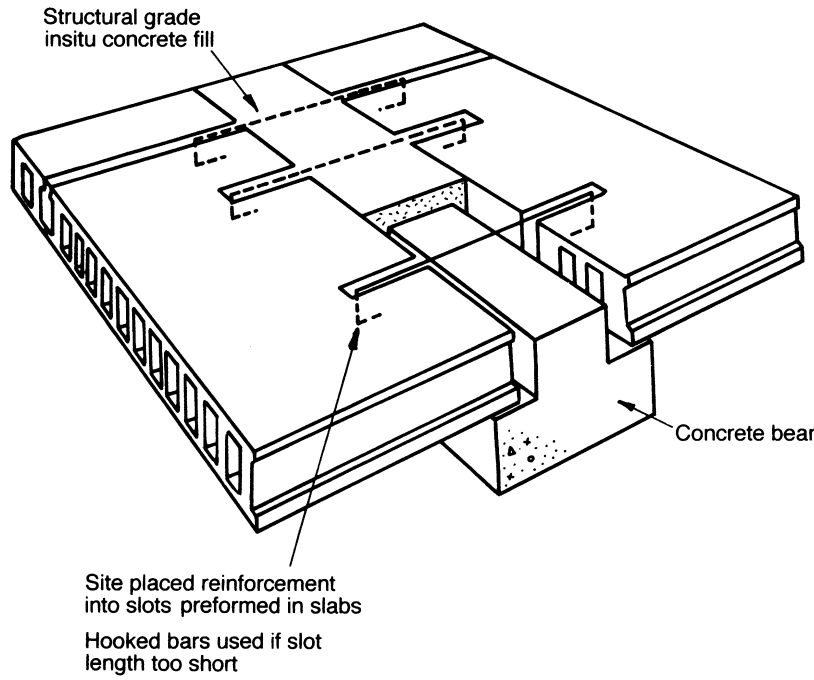

Figure 1.31 Continuity ties in the *in situ* concrete infill.

experimental work has addressed this problem directly. Engineers are cautious not to allow service openings or novel connections in these highly sensitive areas.

Stability may be achieved in several ways, but in the vast majority of cases it is based on either:

(1) an 'unbraced' (or 'sway') structure, Figure 1.26b, where stability is provided within the skeletal structure by cantilever action of the columns; or
(2) a 'braced' structure, Figure 1.27, where resistance against horizontal loading is not provided by the skeleton of the beams, columns and slabs. In other terminology, e.g. using *in situ* concrete, this would be called a 'no-sway' frame.

Combinations of the above are possible, giving what is then known as a 'partially braced' structure: Figure 1.32. It is perfectly reasonable for the frame to be braced in one plane and rely on column action in the other plane, particularly if the building is long and narrow. The design of these structural systems will be dealt with in Chapter 8, but it is important that sufficient bracing elements, e.g. walls, service shafts, columns, etc., are provided at the very outset of design, not at the end.

The positioning of shear walls is often a contentious issue. A conflict with architectural requirements as to the number of walls and their positions is usually the biggest problem. In general, it is necessary to 'balance' the flexural resistances (i.e. summation of stiffness) of the walls in the structure (in two mutually perpendicular directions) to avoid torsional effects as far as is reasonably practical. A design method for the different types of wall used in precast concrete frames is given in Chapter 8.

1.5.3 Floor plate action

Floor plate action means the transfer of horizontal loading across a building. It is sometimes called 'diaphragm action', because the floor is a relatively thin membrane. There has been a considerable

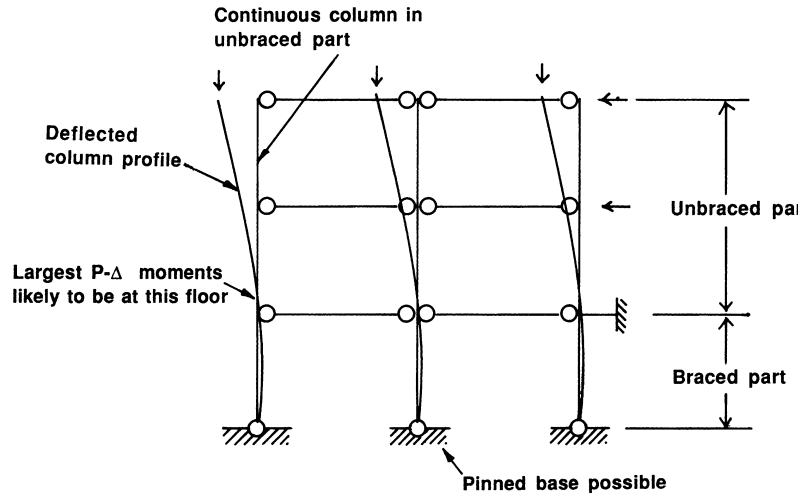

Figure 1.32 Partially braced structure.

debate about whether a precast concrete floor, consisting of a large number of discrete elements, tied together only around their edges as shown in Figure 1.33(a), can in fact be used as a floor diaphragm. The ability of discrete components to act compositely as a single diaphragm has now been demonstrated [1.29, 1.30]. Various structural models have been proposed for the shear transfer mechanism, which relies on the development of clamping forces generated in the tie bars placed in the *in situ* concrete strips at the ends of the slabs. Shear forces parallel with the span of the flooring units are transmitted to shear cores or other stabilising features by deep beam action. Shear forces perpendicular to the span of the floor slab are carried to successive bays of flooring by the shear friction reinforcements in the *in situ* concrete strips in the beam to slab connections.

If this cannot be achieved, for example in precast floor units with discontinuous or thin flanges, then a structural topping screed is used, as shown in Figure 1.33(b).

1.5.4 Connections and joints

The term 'connection' refers to major structural connections between precast components, whereas the term 'joint' is used to describe a more simplified jointing between components. For example, the entire junction between beams and column is called a connection, whereas the halving detail between landing and stair flight is classed as a joint.

Connections between components are the most important factors influencing the design, construction and in-service behaviour of precast structures. The many different types of connection used by designers make it difficult to generalise on rules and guidance notes, particularly because engineers practise different methods of making the same type of connection. The major connections are between:

- column or wall to the foundation
- column to column
- beam to column or wall
- beam to beam
- slab and/or staircase to beam or wall
- slab to slab
- structural steelwork, *in situ* concrete, timber and masonry to precast concrete components.

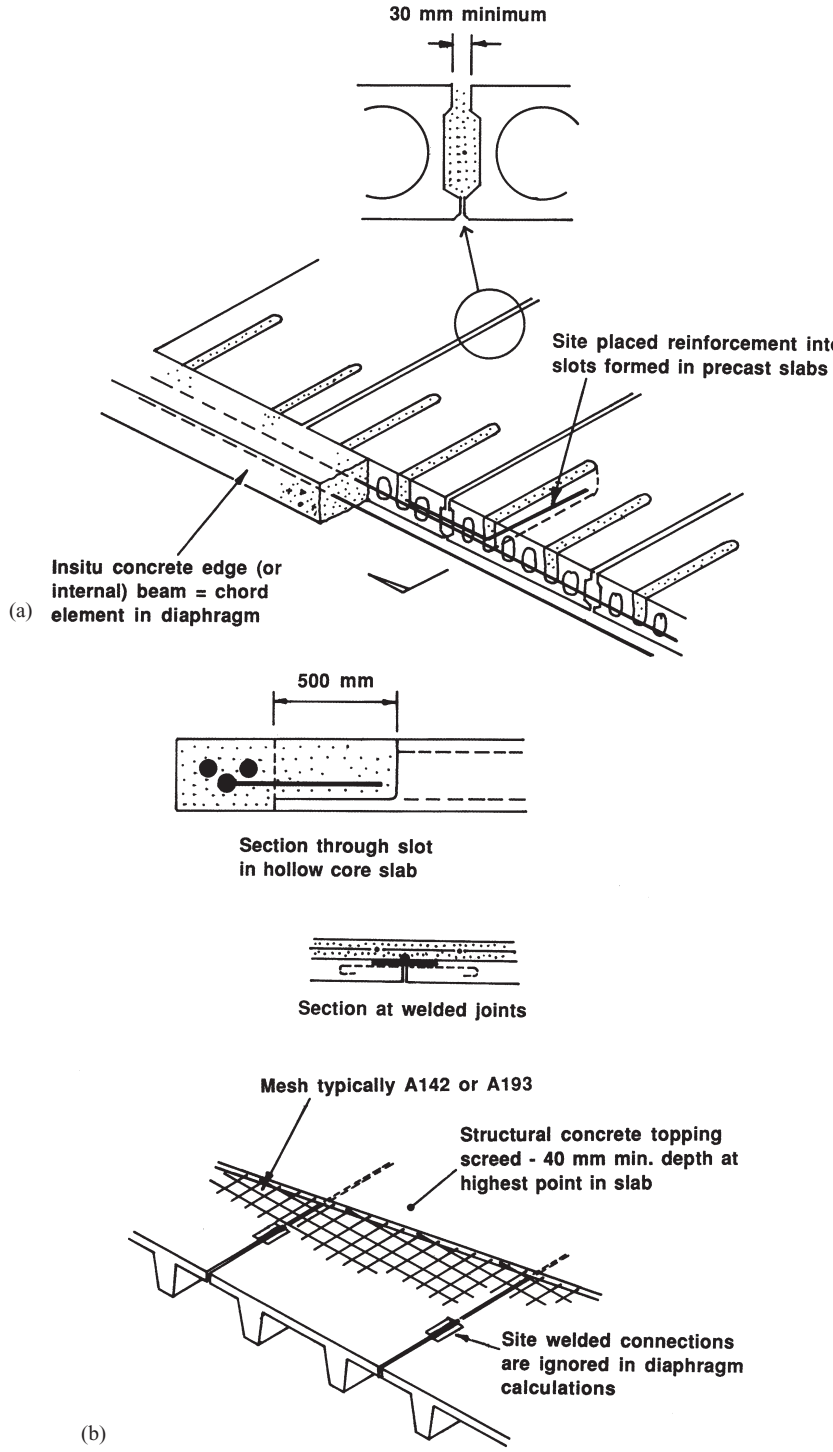

Figure 1.33 Basic principles of the precast floor diaphragm. (a) Precast concrete floors only and (b) precast floors with and *in situ* structural topping.

Joints are required mainly (but not exclusively) to transmit compression, tension and/or shear stresses. Bending and torsion moments can usually be resolved into these three components. Typical forms of joint construction involve wet grouting, dry-pack grout, adhesives, neoprene pads, welds, bolted cleats, dowels and screwed rods. Examples of joints are:

- bearings between slabs and beams or walls
- interfaces between precast and *in situ* concrete, e.g. structural topping
- scarf or halving joints between stair components
- trimmer angles forming holes in floor decks
- site erection aids (temporary or permanent).

1.5.5 Foundations

Loads and moments in columns are transferred to *in situ* concrete foundations through deep pockets, base plates or grouted sleeves. Wall loads and moments are usually spread over such a large area that the connections are made up of simple compression and tension joints.

The various options for foundations are shown in Figures 1.34(a), 1.34(b) and 1.34(c). The available depth of foundation may be the deciding factor in the type of stabilising system used in the structure, e.g. a shallow footing requires that a braced structure is used. The main criteria for foundations are simplicity in design and ease of erection of the precast superstructure.

Foundation design is much simplified in braced frames where only vertical axial loading is present, with small bending moments due to the carry-over couples resulting from eccentric loads at the first-floor beam connection. Simple pad footings are used in most instances, although the columns in a braced frame may be spliced onto the tops of *in situ* concrete retaining walls.

Moment-resisting foundations are required in unbraced frames. These may be very expensive in poor ground, and because of this it is often advisable to liaise with other bodies on the overall economics of unbraced structures. Structures exceeding three storeys or about 12 m in height should certainly be designed as braced. Precast box foundations have been tried, but the preparation of level ground for them outweighs most of the advantages.

1.6 Precast Design Concepts

1.6.1 Devising a precast solution

In their recent book, Bruggeling and Huyghe [1.31] state: *Prefabrication does not mean to 'cut' an already designed concrete structure into manageable pieces . . .*

The correct philosophy behind the design of precast concrete multi-storey structures is to consider the frame as a total entity, not an arbitrary set of elements each connected in a way that ensures interaction between no more than the two elements being joined. Thus it is clear that all the aspects of component design and structural stability are dealt with simultaneously in the designer's mind. The main aspects at the preliminary stage include:

- structural form
- frame stability and robustness
- component selection
- connection design.

These items cannot be dealt with in isolation. For example, the nature of the column–beam connection dictates the arrangement and function of the reinforcement in the ends of beams, and the manner in which floor slabs are connected to edge beams influences the torsional behaviour of the beam. Frame design is therefore an integrated process in which many of the iterative steps are not

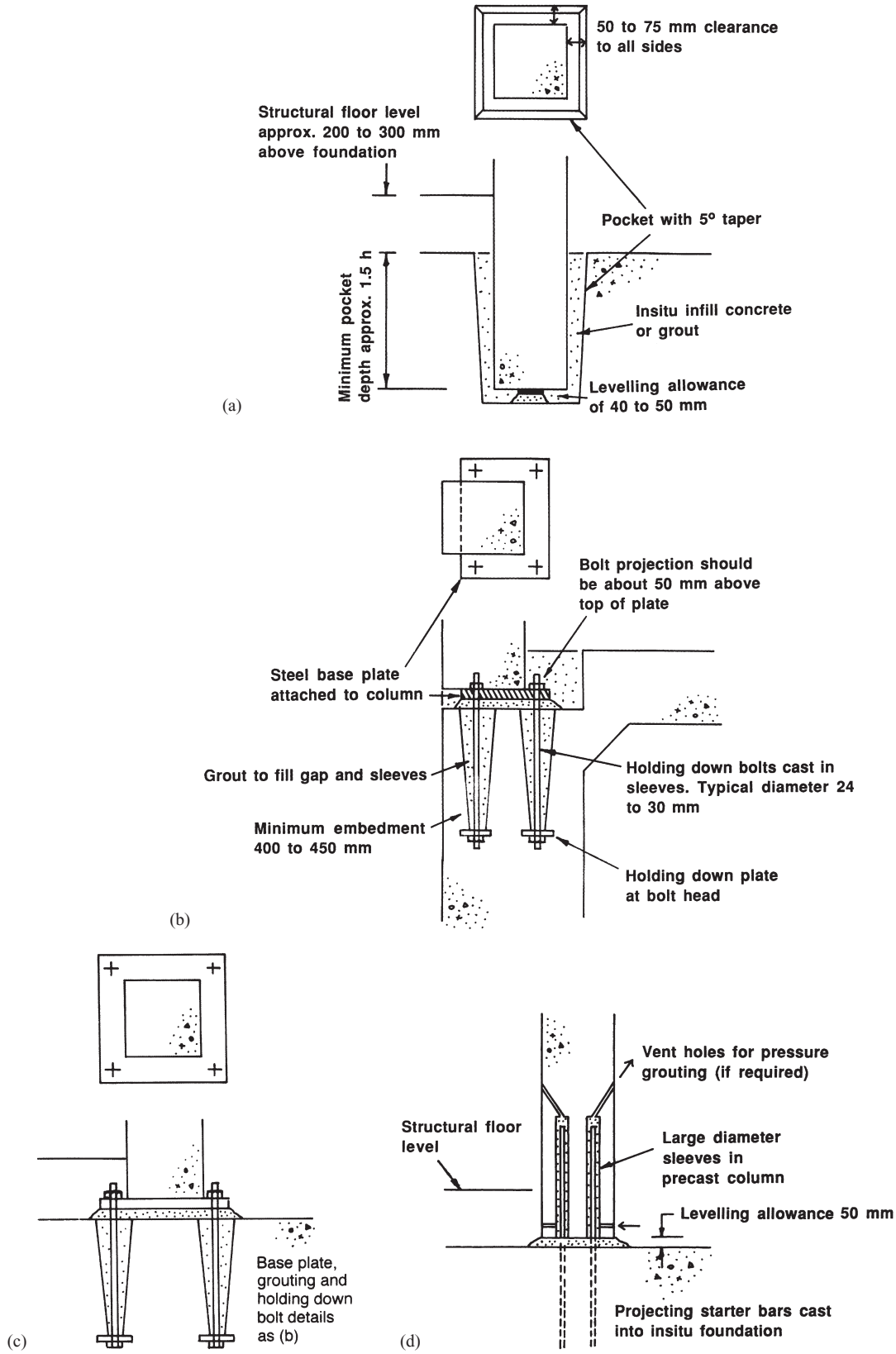

Figure 1.34 Alternative methods of making a column – foundation connection. (a) Pocket in pad footing; (b) base plate to *in situ* wall. Alternative methods of making a column-connection. (c) Base plate to pad footing. (d) Grouted projecting bars in pad footing or basement wall.

so obvious, because they are now hidden within the natural evolution of the design, detailing and site erection procedures. It must also be remembered that two additional procedures, namely manufacture and site erection, are also directly influential in making design decisions.

The correct order for dealing with the framing plan is:

- positions of construction joints
- positions of lift shafts and stairwells, which provide the locations for shear walls and/or cores
- positions of shear walls (if more than three storeys, or if on poor ground)
- positions of columns
- structural floor zones
- cantilevers
- direction of span and length of span of beams and slabs at all floors, and roof if different in plan
- use of non-preferred structural components
- use of structural precast concrete cladding
- positions of service areas and major holes in floor slabs
- staircases and precast lift-shaft boxes.

The main building function is assessed with respect to:

- architectural and aesthetic requirements
- loadings, i.e. dead, imposed dead, live, wind, seismic (occasionally), lateral load due to temperature, creep, shrinkage, and miscellaneous loads such as vibrating or mobile machinery
- fire and durability
- building regulations and codes of practice
- design guides and manuals.

The first task is therefore to establish an economical plan layout for the optimisation of the minimum number of the least-cost components versus overall building requirements. The optimum is usually found in a rectangular grid where the beams span in a direction parallel with the greater dimension of the frame. As a general rule, the minimum construction depth, for the same span and loading, is achieved when the ratio of the floor span/beam span = 1.5 to 2.0.

Figure 1.35 shows three options, for each of which there is a weighted function reflecting design, detailing, manufacture and construction effort and relative costs. There is a delicate balance between the architect's wishes and the precaster's pragmatism. Precast component selection will follow logically and simply once the optimum layout has been achieved. So too will service routes, as the most favourable option shown above will allow easy highways for pipes and cables.

The optimum solution in terms of building efficiency and cost is not always obvious. Consider the three different floor layouts shown in Figure 1.35. Scheme A (Figure 1.35(a)) may appear to give the best solution in terms of number of building components, and this is certainly the most favoured solution. However, as the data in Figure 1.36 show, scheme C (Figure 1.35(c)) offers the lowest ratio of floor zone to bay area, with a saving of about 100 to 150 mm per floor. If, in this case, the cost of the peripheral cladding is such that the saving in surface area exceeds the additional expense of the precast components, scheme C would be the cheapest. This simple example must be treated with caution, as there are many more variables affecting the final cost.

The rules for determining whether a structure is to be braced or unbraced are fairly clear-cut, and they affect both prefabricated steel and concrete frames alike. Table 1.3 gives guidance.

The robustness of the structure must also be considered at the conceptual stage, particularly if a structural floor topping is not being used. Making sure that all the necessary peripheral and internal ties can indeed be placed and be continuous and fully anchored at their ends is a design exercise in its own right. Dangerous congestion of ties can be avoided if the layout of beams is thought through at this early stage.

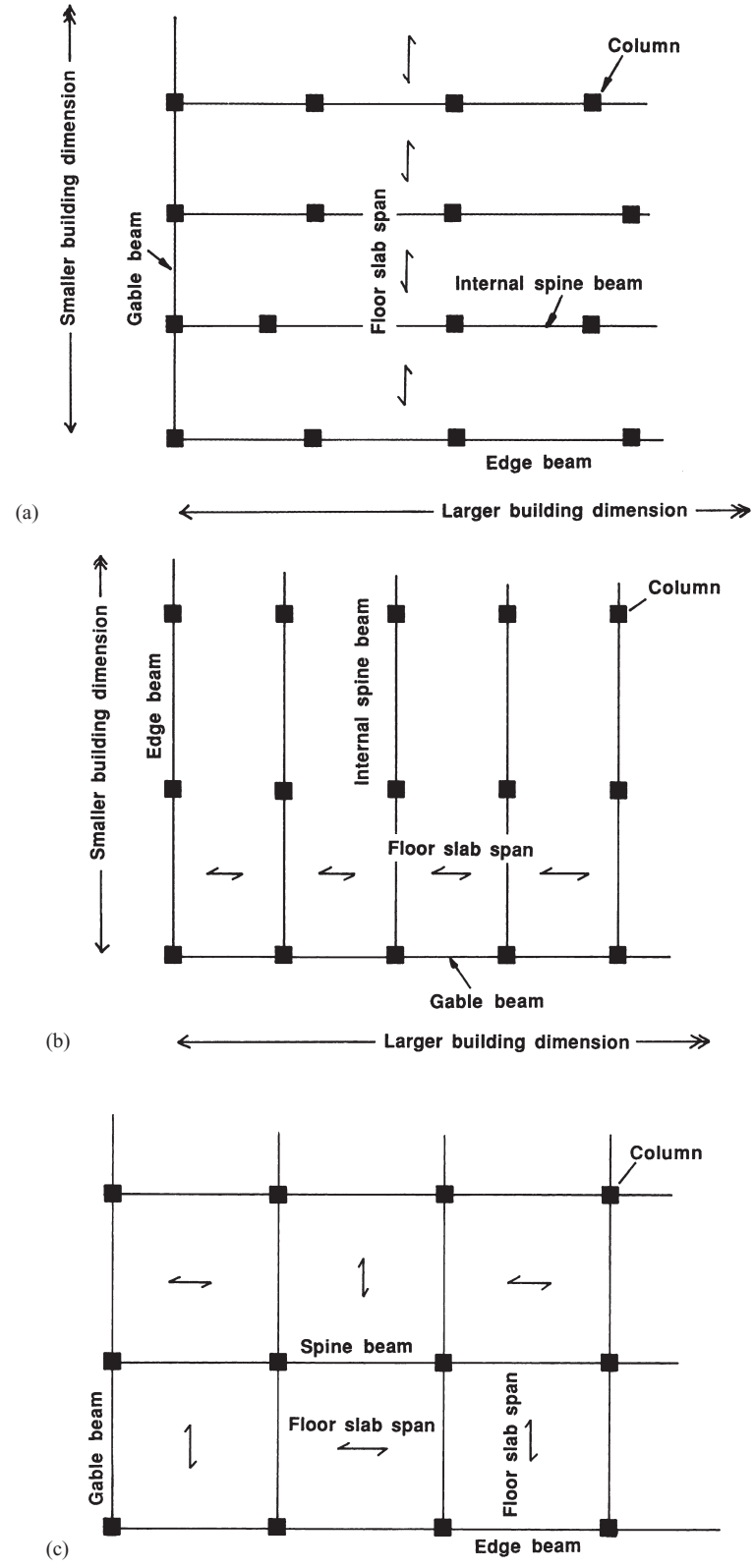

Figure 1.35 Options for layout of primary beams and floor slabs. (a) Scheme A: one-way spanning system with beams spanning in the larger building dimension. (b) Scheme B: one-way spanning system with beams spanning in the smaller building dimension. (c) Scheme C: two-way spanning system.

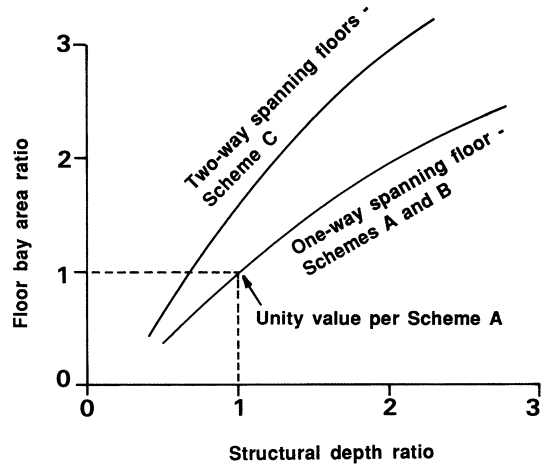

Figure 1.36 Structural zones versus bay area for the structural layouts shown in Figure 1.35.

Table 1.3 Storey heights of precast concrete frames and type of bracing [1.32]

Approximate economical range for number of storeys	Type of frame	Bracing element(s)
2	Unbraced	Cantilevered columns
Up to 3		Cantilevered columns (roof load small)
3 or 4 to 6		Precast wind posts (deep columns)
Up to 4	Braced	Steel cross bracing
Up to 5 or 6		Brick or block infill walls
3 to 5 or 6		Precast hollow-core infill walls
3 to 10		Precast solid infill walls
3 to 10		Precast solid cantilever walls
3 to 12		Precast hollow-core shear walls
10 to 15		Precast concrete shear box(es)
15 to 20		*In situ* conrete shear core(s)
Up to 5	Partially braced*	Brick or block infill walls
5 to 10		Precast infill walls
5 to 12		Precast hollow-core shear walls

* Uppermost one or two storeys unbraced.

1.6.2 Construction methods

Precast frames can greatly improve buildability, because many of the sensitive site operations are moved to the protective environment of the factory. Seasonal variations are less critical to site progress, and are totally nullified at the factory. Depending on the circumstances of the design, size and complexity of the building and the conditions at the construction site (i.e. access), prefabrication has the following approximate savings over cast-*in situ* construction at the site:

- scaffolding material and labour to erect scaffold 80–90%
- shuttering and formwork 90–95%
- delivery and pouring wet concrete* 75–95%

* Lower value where structural floor toppings are used.

- delivery and fixing of loose reinforcement 90–95%
- time of construction of superstructure (above foundations) 25–50%
- total construction time 10–30%
- site labour on superstructure 75–90%
- total site labour 50–75%

One of the key issues is programming the deliveries to site so that the construction team is not under pressure to construct hastily, nor to fix any of the components out of sequence. This could impair the temporary stability of the structure, as the height to the centre of the mass of the concrete above the level at which the frame is stable could be prohibitive to further progress. The rule is that components should not be fixed more than two storeys ahead of the last floor to be fully tied into the stabilising system. This allows time for the *in situ* concrete at the lower levels to mature. Theoretically it is possible to erect precast frames of up to about seven or eight storeys in height before the components are permanently structurally tied together; however, there is evidence that this is folly, and it leaves no room for error.

On-site construction methods have a significant influence on design. Most of these concern connection details, jointing materials, and temporary stability. In many instances the construction sequence will dictate the design of the frame. Often, the positions of shear walls, sizes of beams, spans, etc. can be finalised only when the construction programme is finalised, and the type and capacity of the crane is agreed. Significant economies can be achieved if the designer takes into account all the benefits available on site. In this respect construction sequences are self-defined, with columns, walls, beams, slabs and staircases being the obvious progression. However, the main decision to be made at the design stage is a logistical one.

The two main options are:

- completion of frame floor by floor, Figure 1.37
- completion of frame to roof block by block, Figure 1.38.

Figure 1.37 Construction sequence floor by floor (courtesy of Trent Concrete Ltd).

Figure 1.38 Construction sequence block by block (courtesy of Blatcon Ltd).

The following points should be considered:

- positions of shear walls and maturity of connections, which may dictate site progress
- possibility of temporary instability and the need to design some of the key components to eliminate it unless foundation fixity is available
- availability and/or positioning of equipment to transport and erect every component
- size and weight of components
- safety and speed of construction
- tolerances for economical construction.

The vast majority of precast structures are erected by fixing gangs with many years of experience in handling precast concrete. Many precasting companies employ their own fixing teams, and that is obviously beneficial as far as feedback to the design office and factory is concerned. Information about adequate tolerances is essential to the smooth running of a site. The UK Precast Concrete Industry Training Association [1.33], the UK Structural Products Association [1.34] and the UK Precast Flooring Federation [1.35] have published guides to the safe erection of precast concrete frames, cladding and flooring.

Programming can increase the overall speed of construction by allowing parts of the building to be released to following trades while work continues on erecting the rest of the precast structure. To construct bays to the full height while backing out of the building enables the structure to be released bay by bay. The alternative method, to construct floor by floor, releases lower floors while work continues on the erection of the floors above. Access can often be gained within two or three weeks of starting precast construction.

Table 1.4 Site fixing rates for generalised frame layouts

Frame layout	Example bay area* (m^2)	Site fixing rate per week (m^2)
Rectangular grid	100	1000–1500
Rectangular grid	40–50	600–800
Non-rectangular grid	100	900–1200
Non-rectangular grid with staggered columns	40–50	300–400

* A 'bay' is defined by the area enclosed between four columns.

The construction cost element, which includes transportation costs, varies with building size, number of storeys and the structural grid. In general it is about 8 to 12 per cent of the cost of the precast structure (not the finished building). The information may sometimes be deceptive, as the cheapest site cost may have hidden extras, e.g. the cheapest beams are the longer, which means greater depth and hence a greater structural zone.

Speed of construction is a major consideration in most building projects and it is there that the design of precast structures should be carefully considered. This advantage is maximised if the layout and details are not too complex. Designing for maximum repetition will make manufacture of the precast units easier and construction faster, but precast concrete can also be used in complex and irregular structures, although it may not then provide the same efficiency of construction as a rationalised design. The fixing rates shown in Table 1.4 vary depending on the shape and size of the structure, i.e. the number of linear components such as beams and columns per unit area of the building. The data refer to typical site progress using a fixing gang of no more than five persons, and one crane. A precast solution can stretch to a considerable number of non-standard details, say about 30 to 40 per cent of the total, before the fixing rates reduce dramatically.

The rates given in Table 1.4 are presented in terms of the floor area covered within the beam and column grid: for example, 100 m^2 could be a 12.0 m span floor carried on 8.5 m span beams, and so on. They do not include major volumes of cast-*in situ* concrete, such as structural toppings. The rates are affected by vertical transportation time, typically 3–5 minutes extra per item for buildings of more than about 6–10 storeys, respectively. The data also reflect the different environmental factors, e.g. winter versus summer weather and daylight hours, regionally available plant, particularly 5–10 tonne lifting capacity tower cranes, and ground conditions from green field to congested city sites. The data were collected from UK companies between 1990 and 1996.

The three-storey building shown in Figure 1.39 [1.36] achieved the following fixing rates on a 6 m × 6 m grid layout:

- columns (14.5 m long) — 30 per week
- beams (6 m long generally) — 45 per week
- floor slabs (6 to 17 m span) — 2335 m^2 per week
- façade panels — 750 m^2 per week

The structural form of a precast structure may be influenced by the manner in which it is built, the site access for long vehicles, and the capacity of the craneage. One of the most important decisions pertaining to temporary stability is the availability of a stiff shear core, or shear walls (or other forms of bracing) in two orthogonal directions at all times during construction. This may not seem to be a problem, but consider this structure shown in Figure 1.40, which would be constructed to its full height, bay by bay. If the shear core were available only up to point X, the previous bays would be unstable. In low-rise buildings of fewer than four storeys the columns can be stabilised by propping

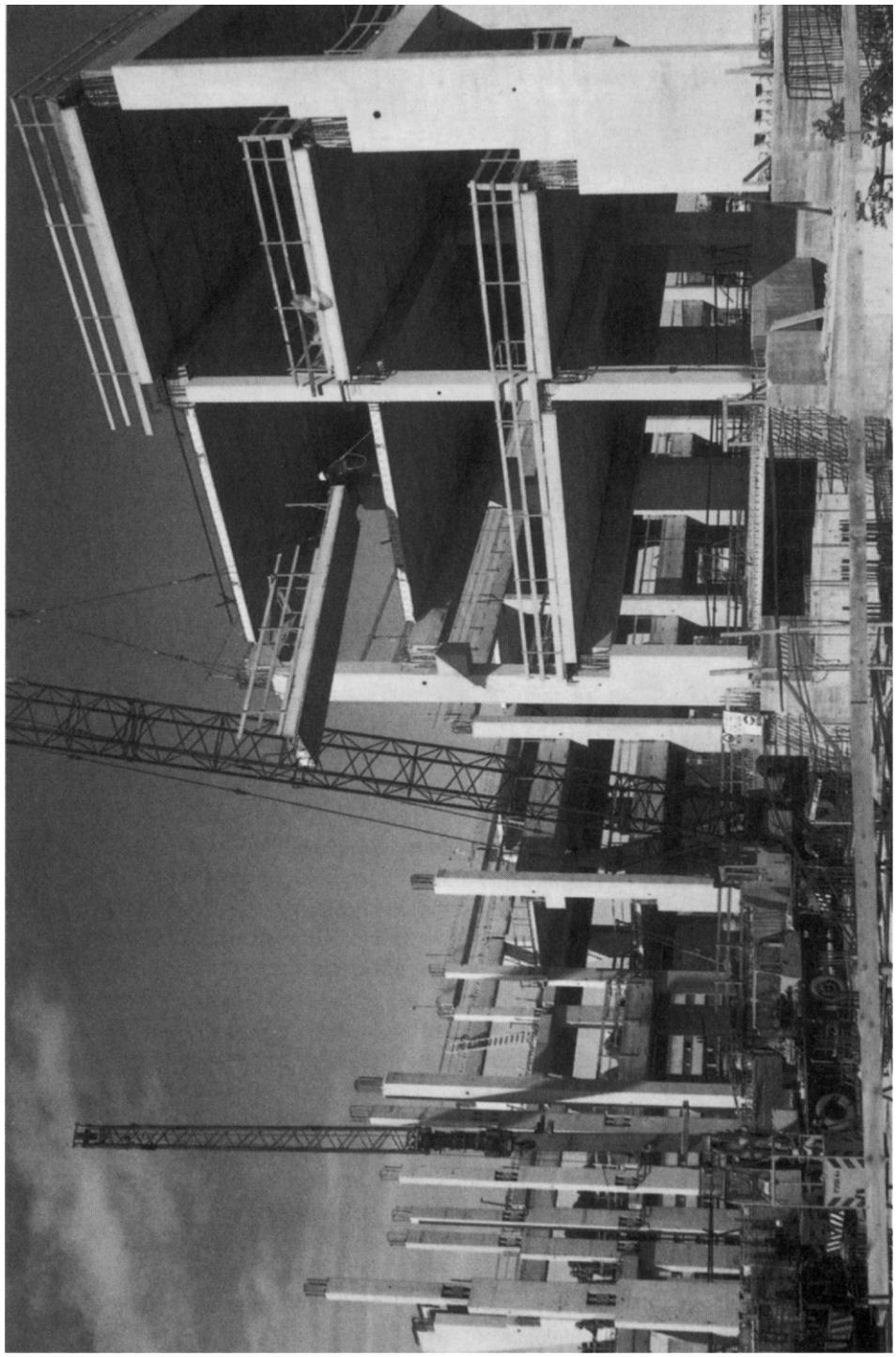

Figure 1.39 Skeletal frame (courtesy of B + FT Wisenbaden).

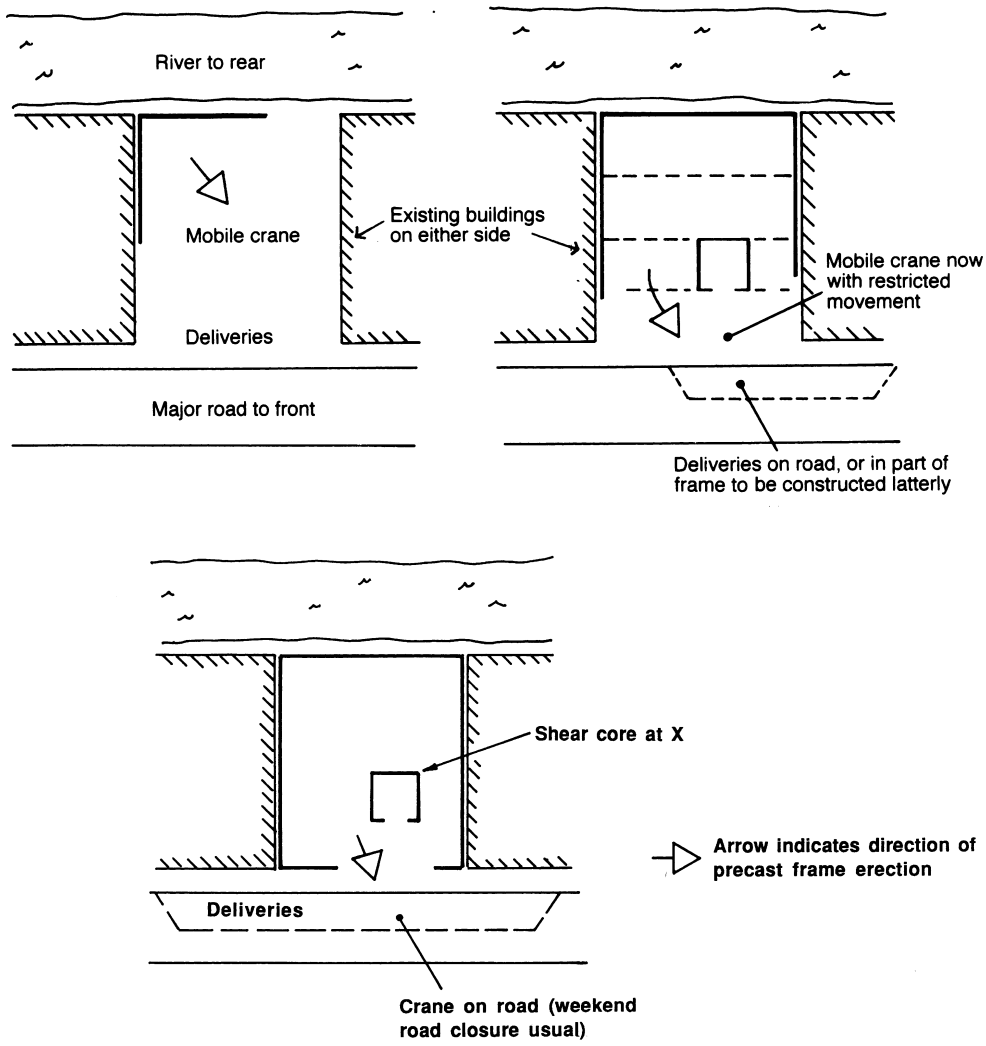

Figure 1.40 Preferred sequence of erection on confined sites.

at the ground level (assuming a sound footing is available, which is not always the case). However once a column splice is included, permanent stability is required.

In all cases the precast frame is correctly aligned and levelled as each floor is completed. Following trades may take up residence at each floor level immediately after the floor level above has been completed. Precast frames may lend themselves to partial completion and a phased hand-over. This depends very much on the form of the structure, and the divisions are dictated by the positions of fully stabilised subframes.

The construction programme may be dictated by the sequence in which components can be fixed. If the plan area is small, say less than 300 m^2, it is possible that the fixing rate can progress faster than the maturity rate of the connections. It may then be advantageous to design a connection that has no restriction on maturity, e.g. a bolted or welded plate, rather than specifying one with a cast-*in situ* 'stitch'.

CHAPTER 2

Procurement and Documentation

This chapter deals with the role of the precast frame designer as part of the project design team, and describes the design methodology. The literature is reviewed.

2.1 Initial Considerations for the Design Team

The International Federation for Structural Concrete, usually referred to as *fib* (Fédération Internationale du Béton) aims 'to develop at an international level the study of scientific and practical matters capable of advancing the technical, economic, aesthetic and environmental performance of concrete construction' [2.1]. *fib* was created in 1998 by the merger of the CEB (Comité Euro-International du Béton) and the FIP (Fédération Internationale de la Précontrainte). The success of *fib* may be attributed to the fact that while the CEB had excellent authorship of standards and codes, and good funding possibilities, the FIP had in-depth technical knowledge through its industrial and academic membership. Many members contributed to both organisations, making the transition almost seamless. *fib* publications are well respected throughout the world and many of the *Recommendations* and *Guides to Good Practice* are used in design offices, while several have been adopted into national codes – for example, there are substantial similarities between the Eurocode EC2 (which we shall refer to as BS EN 1992 in this textbook) and *fib*'s past and present Model Codes [2.2–2.4]. Many view the Model Codes as forerunners to normative standards. The FIP Commission on Prefabrication has produced a planning and design handbook [2.5] (currently being revised by *fib* Commission 6 for publication in 2013) in which the following advice for a design organisation is given:

> *Every construction system has its own characteristics, which to a greater or lesser extent influence the layout, storey height, stability, and statical system of the building. For best results the initial design should respect the specific and particular demands of the intended structure. The potential for profit seen at the signing of the contract documents by the client and the contractor often disappears during the construction period. . . . It is very important to realise that the best design for a precast concrete structure is arrived at if the structure is conceived as a precast structure from the very outset and is not merely adapted from the traditional cast-*in situ *or masonry methods.*

This is a particularly pertinent statement in the modern world and particularly important with regard to structural stability and the integrity of a precast concrete structure, where special details have evolved through the natural sequence of a 'design–manufacture–erection–design feedback' loop used in the precasting industry.

Multi-storey Precast Concrete Framed Structures, Second Edition. Kim S. Elliott and Colin K. Jolly.

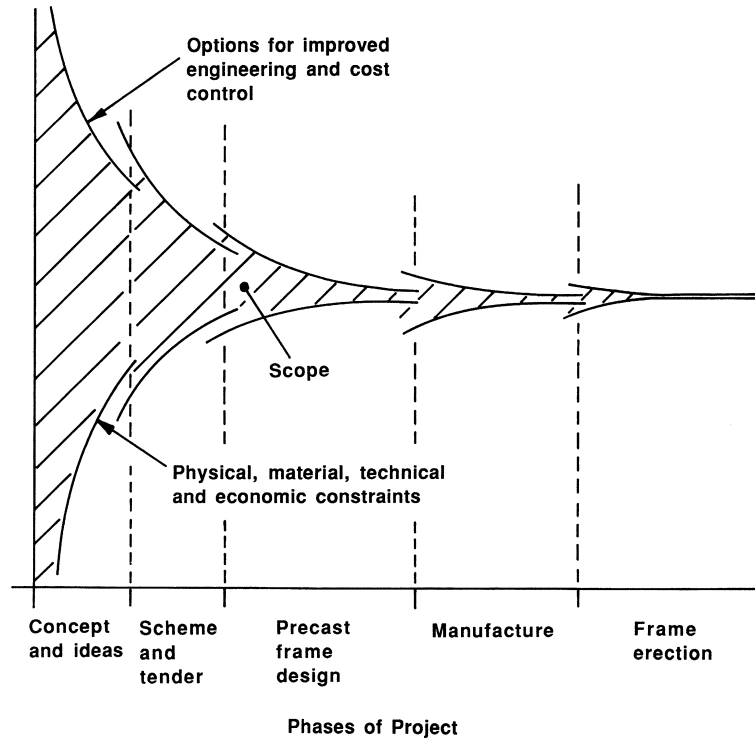

Figure 2.1 Scope for optimum project potential.

The major beneficial advantages of a precast concrete solution will accrue at the conceptual design stage. Figure 2.1 is a schematic representation of the 'scope for project potential', by whatever measure is chosen, as a function of the four major decisions taken prior to the construction of a precast building, when it is practically too late to implement substantial changes. Note that additional scope for potential savings is always present at the beginning of each of the five phases. Unfortunately the conceptual part of the design process is often carried out in the absence of the precast concrete engineer. It may be necessary to adjust the structural function of the building when the means of achieving maximum potential with the precast structure are realised. The initial design should be carried out at least with the assistance of the precast engineer, who will contribute to reducing the construction time and cost and ensure better quality by in-house expert knowledge.

The FIP handbook [2.5] concludes that

> *…designers should therefore consider the possibilities, restrictions, advantages and disadvantages of precast concrete, its detailing, manufacture, transport and erection and serviceability stages before completing a design in precast concrete. Precast concrete organisations will usually make available design and production information to the client, architect, consulting engineer, services engineers and all other disciplines to give unified guidance to the entire design team. This will ensure that all parties are aware of the particular methods adopted in all phases of the project, leading to maximum efficiency and benefit. This is particularly true with the manufacturing and erection stages, as many consulting engineers may not be familiar with some of the methods used.*

The Federation is conscious of the fact that precast concrete buildings are often adaptations of the more traditional and well-understood forms of construction, such as *in situ* concrete, structural steelwork or masonry.

2.2 Design Procurement

2.2.1 Definitions

The terminology used in this book to describe the functions of designers and contractors is as follows:

Precast company:	The organisation responsible for design, detailing, manufacture and erection.
In-house designer:	Designer employed by the company.
Specialist designer:	Private organisation or individuals offering a dedicated service to the manufacturer and occasionally the company.
Consultant designer:	Private consultancy or government-based design office offering a service to the manufacturer and occasionally the company, but not necessarily a dedicated specialist to precast.
Precast manufacturer:	Manufacturer of components made to details supplied by the designer, specialist or occasionally the company.
Precast contractor:	Frame erector specialising in this field.

2.2.2 Responsibilities

The chart shown in Figure 2.2 shows the responsibilities within the precasting organisation. It is shown that the involvement of the principal design engineer is wider than the structural design itself. It is important that this engineer is in close contact with the architect, foundation engineer and services providers, as well as the factory coordinator, estimator and the contracting staff. The need for excellent lines of communication between the design office, the factory and the site cannot be stressed too highly.

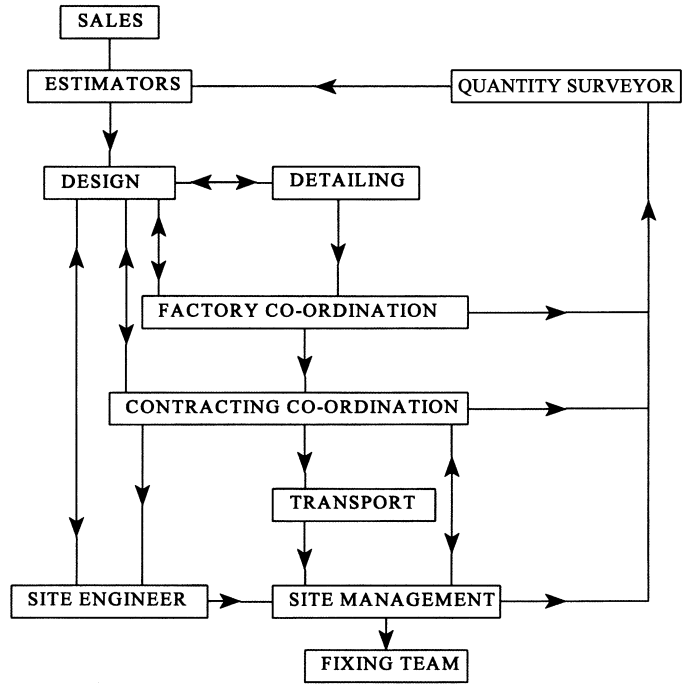

Figure 2.2 Responsibilities within a precasting organisation.

2.2.3 Routes to procurement

The design manual, *Precast Concrete Frame Buildings – A Design Guide* [2.6] includes a comprehensive chapter on precast project procurement (which was written by Andrew Dyson, Director of Advantage Precast, UK). The essential issues raised in this text were on the selection of the precasting company, and how the decisions leading to the appointment of the company were taken – the checks on quality control, qualifications of personnel, etc. The following section takes this a step further and describes the activities that take place after the precaster has been appointed and is invited to tender, i.e. the design procurement.

2.2.4 Design office practice

Design- and drawing-office practice is different from that experienced in a consulting engineer's practice, because the design procedures are highly dependent on the manufacturing and construction methods adopted by the particular precasting company. In some instances, design decisions are influenced more by ease of manufacture, repetition, handling and erection constraints than by economy of materials or form. Some prefabricators have excellent in-house mould-making facilities and are therefore able to offer structural units with intricate architectural features. The moulds and resulting units shown in Figures 2.3(a) and (b), respectively, are examples of this skill.

(a)

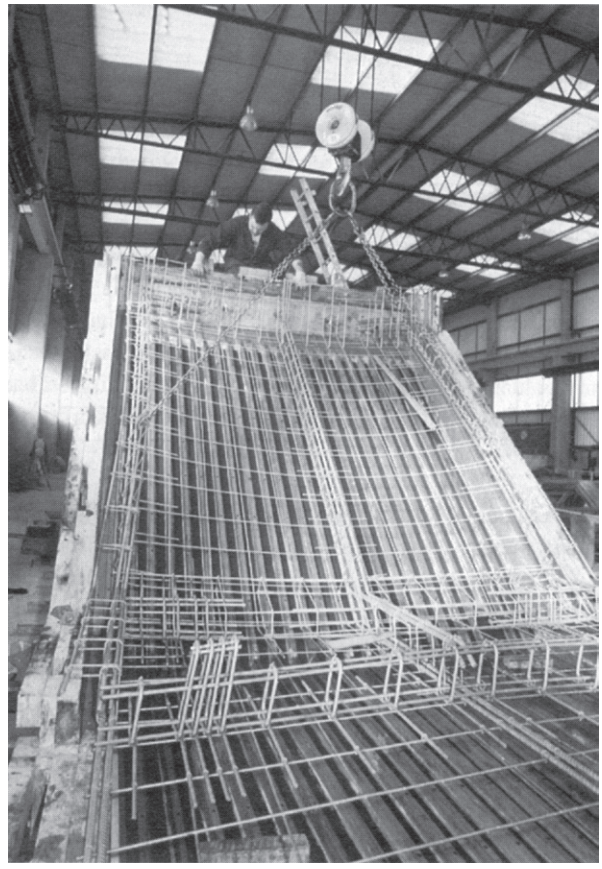

Figure 2.3 Manufacture of visual concrete units. (a) Timber moulds for prefabrication and (b) the final product. (Courtesy of Trent Concrete Ltd.)

(b)

Figure 2.3 (*Continued*)

Design-office practice is inextricably linked to the various shop-floor operations; bar bending, cage assembly, mould making, cage and connector positioning, casting, curing, lifting and handling are operations that must all be satisfied simultaneously in design to ensure that an economical and structurally sound product results. The thought process in the design of multi-storey buildings is essentially in two parts:

- the conceptual use of precast technology;
- detailed design work with a knowledge of load paths and prestressed and reinforced concrete stress analysis.

The designer attempts to utilise, as far as possible, a range of predetermined structural components in the skeletal structure while satisfying, again as far as possible, all the architectural and functional requirements of the building. Although the emphasis throughout is on the maximum use of factory-cast prefabricated concrete, there may be many economic, aesthetic or structural constraints that prevent the designer from using a totally precast solution. The reasons for these are numerous and the subject will be discussed in the appropriate chapter. However, the norm is to prefabricate a stable structure (columns, walls, beams and slabs), and then to consider the options of precasting other items such as staircases, lift shafts, balconies and arches, etc. to obtain the most economical solution for the completed building.

2.2.5 Project design stages

In the office, precast design is accomplished in four steps:

(1) preparation of the schematic building layout and quotation
(2) design calculations
(3) layout drawings
(4) component scheduling.

Step (1) is often termed the 'scheme' or 'quote' stage, whereas steps (2) to (4) are carried out upon receipt of an order and are termed the 'project' stage. Scheme and project engineers may be one and the same group, or may be affiliated to different parts of the company, or other companies with the relevant expertise. Whichever is the case, it is important that the scheme engineer is fully conversant with the project team's design practice.

The preparation of the schematic building layout drawings and the quotation forms the basis of the conceptual stage, in which the capability of the precast system is assessed and structural components are notionally designed for estimating purposes. The non-precast areas are identified at this stage and shown on the tender drawing as work by the general contractor. This list usually includes all foundations and other ground works (culverts, piling, ground beams, and retaining walls). The precaster may choose to carry out a small amount of *in situ* work himself in order to secure a contract, particularly if these items can include stitches connecting precast components, or if the finish must match the adjoining precast units. For example, it may be more economical and less disruptive to the construction programme if unusually shaped staircases are cast-*in situ* by the precast contractor employed by the precast company. In this case the area would be labelled '*in situ* staircase by the precaster'. Both responsibility and control then remain vested in a single company.

The tender drawing carries sufficient information for the client to judge the merits of the structure. The drawing(s) usually contain:

(1) a plan of every roof and floor level (or small variations to a single plan are noted if the floor layouts are similar)
(2) a cross section of the structure (in total, or in part if the floor-level details are repeated)
(3) a selection of structural components in cross section, e.g. hollow-cored flooring, spine and edge beams, spandrel beams and non-rectangular columns
(4) details to other *in situ* work, e.g. column pockets and/or base plate, or steelwork connections.

Items (3) and (4) are often considered optional, but are included at this early stage to assist other trades in assessing the viability of the precast structure. Points to look out for in this stage are:

- structural zones shown on the architect's drawing
- particularly large voids, service holes, etc. in the floor slab
- service routes above or beneath the floor, as these may affect the direction in which beams and floors will span
- heavy loading in one particular area, e.g. plant rooms, where beam spans selected for other lightly loaded areas are too great for the plant room area
- the possibility of using a structural steel or timber roof, e.g. truss or mansard-roof
- the possibility of using load-bearing or infill structural masonry, either prefabricated or built *in situ*
- obstructions to column positions, and the continuity of columns from roof to foundation
- possible positions of structural shear walls
- balconies, overhangs, etc. that must be structural in form, i.e. cannot be completed by the following trades
- splays in beams, chases in columns, holes in walls, etc., all of which may prove embarrassing at the project design stage.

At the completion of this exercise the designer should be confident that temporary stability is guaranteed no matter how the site erector may choose to build, and that the areas of *in situ* concrete may be allowed to cure and develop strength before further construction proceeds. To this end, the scheme drawing(s) are annotated for internal use during the billing stage with information to assist the estimator to assess craneage and site costs, in addition to the relatively simple task of pricing the precast concrete components.

A typical schedule for costing would include:

- beam cross section, either in dimensions or unit reference coding
- beam length
- reinforcement, usually in cage reference coding for both flexure and shear, or individually referred if no code exists
- beam end connector capacity
- any voids (size and position), chases, cut-outs, splays, etc.
- special requirements for surface finishes, exposed aggregates, etc.

For other components such as exposed aggregate spandrel beams, the texture, relief, colour, jointing, etc. are given on the drawing. Omission of this information could have very serious implications far in excess of omitting the exposed aggregate materials. An obvious example is the cost for a new mould in which to manufacture the unit.

Consideration must also be given to specifying a small number of very heavy units in situations where a larger number of smaller units would suffice. Although the golden rule to precast efficiency is an optimum number of components of approximately all the same weight, there are exceptions where the cost of hiring and using a large-capacity crane outweighs the benefit of a smaller number of components.

Preparing a final scheme and quotation is usually an iterative procedure; seldom are original layouts accepted after the first attempt. The points of contention are usually positions of shear walls, depths of beams and voids for service routes. Time spent on preparing schematic layouts may even exceed the time spent on final design, and unsuccessful tenders should not be considered as totally abortive; the experience assists the preparation of the next one.

2.2.6 Structural design calculations

Design calculations commence after discussions with the architect (or developer) that centre around the concurrence of details shown on the architect's current drawing with the precaster's latest scheme drawing. Loads are finalised and structural design commences in the manner described in Chapters

4 to 8. An example calculation for the design of hollow-core floors is shown in Figure 2.4. The terminology used here will be explained in Chapter 5. Structural drawings are often commenced early, and because of the increased use of computer-aided design or draughting (CAD) facilities this is not the problem it was as recently as the late 1980s. Computer-controlled detailing and scheduling of two-dimensional units, such as wall panels or floor slabs, have resulted in the kind of output shown in Figure 2.5, for example.

It is not always possible to delay tackling those areas that are commonly marked 'items in abeyance', returning to them at the end of the project. A case in point is the size of a void in the floor, where beyond a certain size (depending on spans and loading), additional measures may have to be taken to cater for the increased loads on adjacent units and the transfer of these loads to beams and columns.

Throughout the structural design process it is important not to lose sight of the overall behaviour. The sizes and positions of stability ties, often left until last, must be catered for in the design of the floor and/or beams. As with *in situ* concrete or structural steelwork, the design of a precast structure may be subdivided into a team effort, but there should be one engineer in charge to coordinate the input and output of information.

The design of most precast components can be committed to in-house or commercial software packages, resulting in predetermined design and detailing information. (In-house packages are merely an extension of the tabulated/graphical design data and standardised drawings for standard frames of yesteryear.) The main distinguishing feature of precast design software is that design output may be in coded form to be compatible with the chosen method for scheduling components.

2.2.7 Layout drawings

Until quite recently (c.1990) layout drawings were all prepared manually, but almost all drawings are now made using CAD methods. An argument against the use of CAD is rarely applicable to precast buildings in which there is an intention to replicate as many details as possible. The purpose of the layout drawings, e.g. Figure 2.6, is firstly to show the architect, engineer and other trades the details of the structure and its connections, and secondly to transmit to site information necessary to erect the structure.

To this end, precast concrete frame drawings tend to resemble structural steelwork layouts more than drawings for *in situ* concrete. Components are referred to individually and a reference number, which corresponds with its unit schedule number, is prominent on the drawing. Individual details, cross-referenced on the plan, are shown to an appropriate scale in Figure 2.7. Beams, walls, columns, staircases and cladding components are detailed on separate drawings.

The project drawings are not sufficient to describe fully the details of the precast components; they are to be read in conjunction with a set of 'project product drawings'. Because these drawings are generated within CAD software it is possible to store hundreds of details, recalling them when the specific requirements of a project are known. These drawings are used to show the exact details of the cast-in connections, reinforcements, joint details, connections, splices, ties, etc. assumed in the preparation of the project design and drawings. An example of a project product drawing is shown in Figure 2.8.

It is now common on larger sites for the entire building process to be managed by a Project Manager. This may be a separate management specialist, but is often a role adopted by either the architect or the precast company. The Project Manager will specify protocols (computer specification, software supplier, software revision, default settings, etc.) for a common database and CAD system that the architect, structural engineers and service engineers all agree in advance to use, both in their offices and on site. He will then retain the master documents, and only his latest approved revisions are accepted as details for inclusion in the building. This facilitates alterations and additions by different contributors during construction, and leads to a single set of 'as-built' drawings being available at the end of the project. While this arrangement helps to avoid the blame culture that can develop when contributors' details clash, it may cause delays while approval is sought, and force non-standard and thus less efficient practices on each organisation's office.

Design of prestressed concrete hollow-core floor units to Eurocode BS EN 1990 and BS EN 1992-1-1

Made by: K S Elliott
Date : 18.3.13
Checked by : C K Jolly

Re: Chart 5.1. Try 1200 x 250 unit
Floor use: Offices $\Psi_0 = 0.7$

Floor loading	kN/m^2	
Self weight *	3.73	
Finishes	1.50	
Services, ceiling	0.60	5.83
Partitions (as live)	1.00	
Imposed live	4.00	5.00

Service load $g_k + q_k = 10.83$ kN/m^2
w_s per unit = 1.2 x 10.83 = 13.00 kN/m

Ultimate load. BS EN 1990-1-1.
Eq. 6.10(a)
$w_{Ed} = 1.35 \times 5.83 + 1.5 \times 0.7 \times 5.00 = 13.12$ kN/m^2
Eq. 6.10(b) where 0.925 x 1.35 ≈ 1.25
$w_{Ed} = 1.25 \times 5.83 + 1.5 \times 5.00 = 14.78$ kN/m^2
w_{Ed} per unit = 1.2 x 14.78 = 17.74 kN/m

Unit 1.
$l_n = 4500 - 250 - 120 = 4130$ mm. Clause 5.3.3.2
$l_{eff} = 4130 + \min(250; 75/2 + 100/2) = 4218$ mm
Ignoring the restraint to imposed loads from the shear key between hollow-core units
$M_s = 13.00 \times 4.218^2/8 = 28.9$ kNm
$M_{Ed} = 17.74 \times 4.218^2/8 = 39.45$ kNm
Shear span = 4130 – 2 x 122* = 3886 mm
$V_{Ed} = 17.74 \times 3.886/2 = 34.45$ kN
Refer Chart 5.1. Use 25/68

Footprint spans = 2500 and 4500 – 150 = 4400 mm
Reactions to trimmer angles. Take all imposed loads as leading variable actions according to EC0, eq. 6.10(b).

$G_k = 1.2 \times 5.83 \times 2.5/2 = 8.75$ kN	and	15.39 kN
$Q_k = 1.2 \times 5.00 \times 2.5/2 =$ 7.50 kN	and	13.20 kN
Total 16.25 kN		28.59 kN

Ultimate 6.10(b) $P_1 = 22.18$ kN $P_2 = 39.04$ kN

Unit 2.
$l_{eff} = 7600 + \{\min 250; 75/2 + 75/2\} = 7675$ mm
Max BM at A
$M_s = 58.72 \times 4.288 - 13.00 \times 4.288^2/2 = 132.2$ kNm
$M_{Ed} = 80.13 \times 4.288 - 17.74 \times 4.288^2/2 = 180.5$ kNm
Shear is calculated at 75/2 + 122 = 160 mm from R
V_{Ed} max = 86.60 – 17.74 x 0.16 = 83.76 kN
Refer Chart 5.1. Use 25/88
$M_{sr} = 150.3$ kNm; $M_{Rd} = 214.2$ kNm; $V_{Rd,c} = 125.1$ kN. Further analysis not given in Chart 5.1 shows $V_{Rd,cr}$ = 89.0 kN and this is critical where $V_{Ed} = 20$ kN. The minimum capacity ratio = 150.3/132.2 = 1.14.

If trimmer live loads are taken as accompanying variable actions, then the ultimate loads reduce to:
$P_1 = 1.25 \times 8.75 + 1.05 \times 7.50 = 18.81$ kN
$P_2 = 1.25 \times 15.39 + 1.05 \times 13.20 = 33.10$ kN
$M_{Ed} = 78.31 \times 4.288 - 17.74 \times 4.288^2/2 = 172.7$ kNm
V_{Ed} max = 83.80 – 17.74 x 0.16 = 80.97 kN
Refer Chart 5.1. Use 25/88

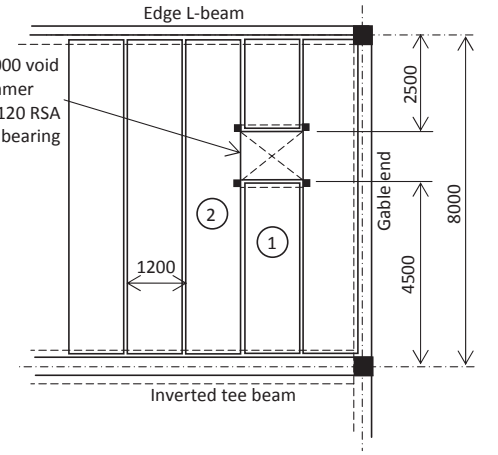

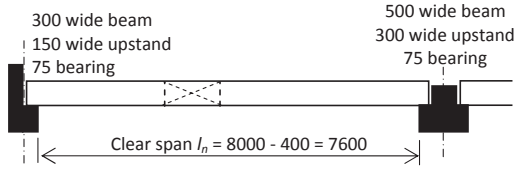

*Area concrete unit + longitudinal infill = 170480 + 8456 = 178936 mm^2 x 25 kN/m^3.
Self weight = 4.47 kN/m run or 3.73 kN/m^2.
Height to centroid = 122 mm.

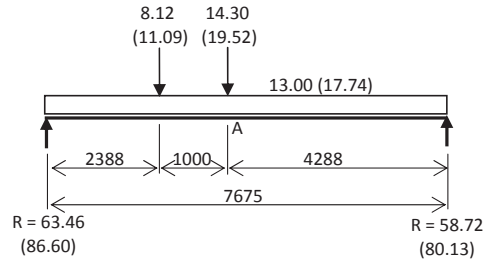

Trimmer loads are accompanying variable actions to the leading UDL

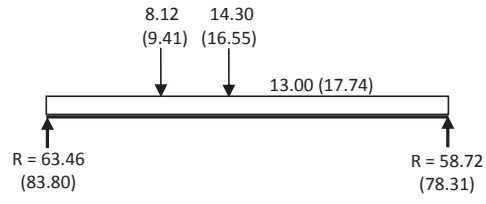

Further reductions in the trimmer live loads may be taken by allowing load spreading into the unit adjacent to Unit 2 only, see Section 5.2.7.

Figure 2.4 Calculation sheet for the design of a hollow-core floor bay containing a large void.

SLABS DISTRIBUTION: 1 TOOL: 6 SHIFT: 1

MANUFACTURING DATE: 12/04/93

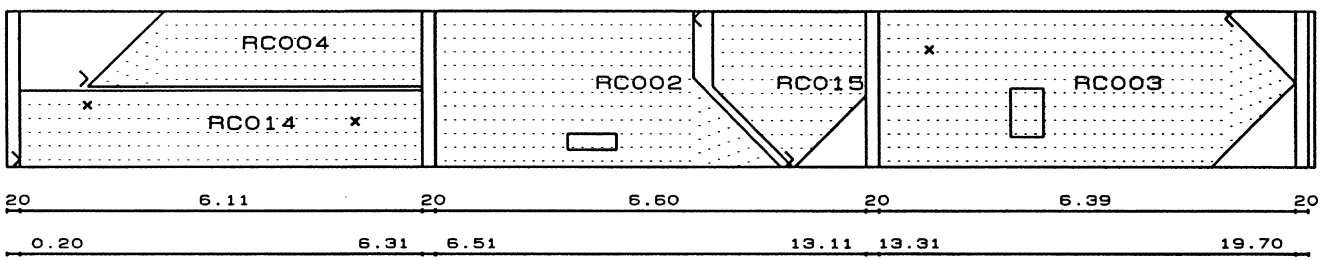

	Ref.	Leng. m	Widt. m	Concr. Thick.	Insu.	Insul. Thick.	d' cm	Area m2	Load.	Stack	Order	Weight Steel	Lay.	Case
1	RC014	6.11	1.17	5.00	0001	0.00	2.00	7.15	000001	001	002	0.00	01	8903
2	RC004	5.08	1.17	5.00	0001	10.00	2.00	5.94	000001	001	003	0.00	01	8903
3	RC002	5.30	2.41	5.00	0001	10.00	2.00	12.77	000001	002	001	0.00	01	8903
4	RC015	2.34	2.40	5.00	0001	0.00	2.00	5.62	000001	002	002	0.00	01	8903
5	RC003	6.39	2.41	5.00	0001	10.00	2.00	15.40	000001	001	001	0.00	01	8903

1/2

Figure 2.5 Computer-aided drawing and scheduling of precast components.

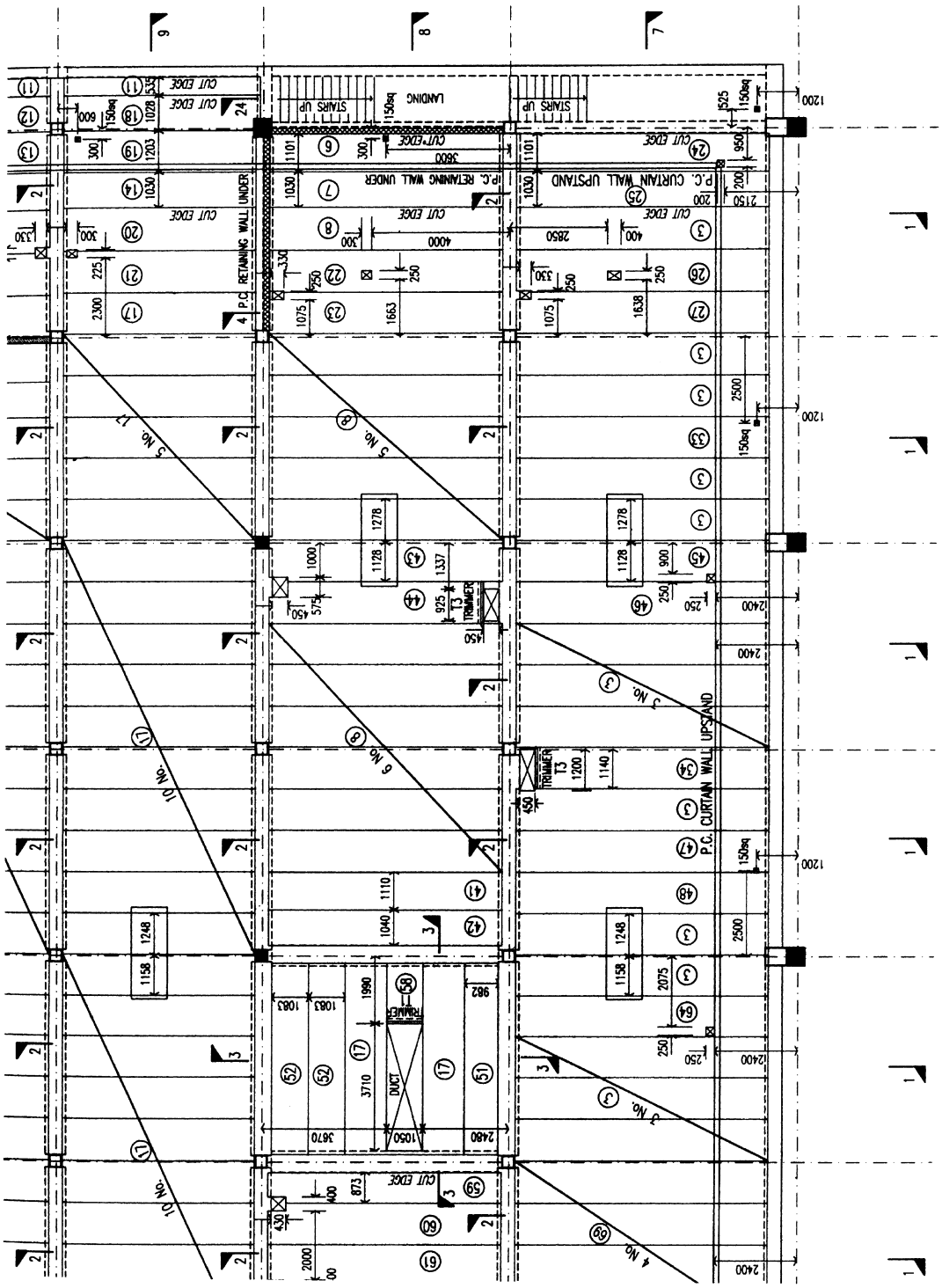

Figure 2.6 Example of a precast layout drawing (courtesy of Trent Concrete Ltd).

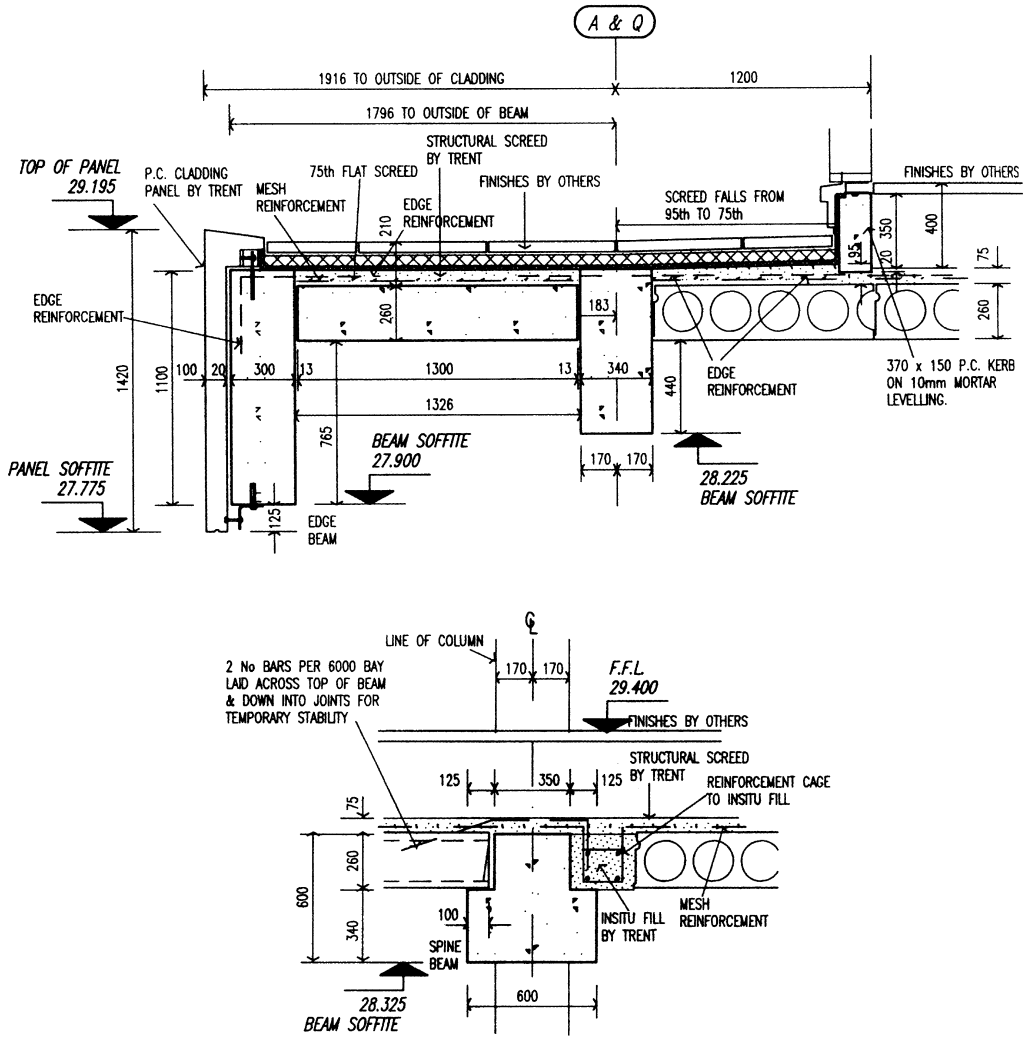

Figure 2.7 Examples of cross-sections (courtesy of Trent Concrete Ltd).

2.2.8 Component schedules and the engineer's instructions to factory and site

Unit schedules are prepared when the layout drawings are finalised or well advanced. CAD systems have usurped manual scheduling for the reasons given in Section 2.2.7. An example of a beam schedule (made using 'Autocad') is shown in Figure 2.9 and this must be read in conjunction with both the project product drawings (Figure 2.8) AND the project layout drawings (Figure 2.6) to be meaningful. Overall dimensions and tolerances are given in the schedules. The design procedure ends with the submission of component schedules to the casting factory. The casting works will make the necessary adjustments to cast-in inserts and moulds without violating the overall dimensions.

Sometimes instructions to the factory are not contained on product drawings and must be relayed by memoranda. These instructions include:

- special requests for additional quality control, e.g. cube testing, cover distances, curing, handling or storage
- special surface finishes, including exposed aggregate, retarded and scabbled faces and smooth finishes

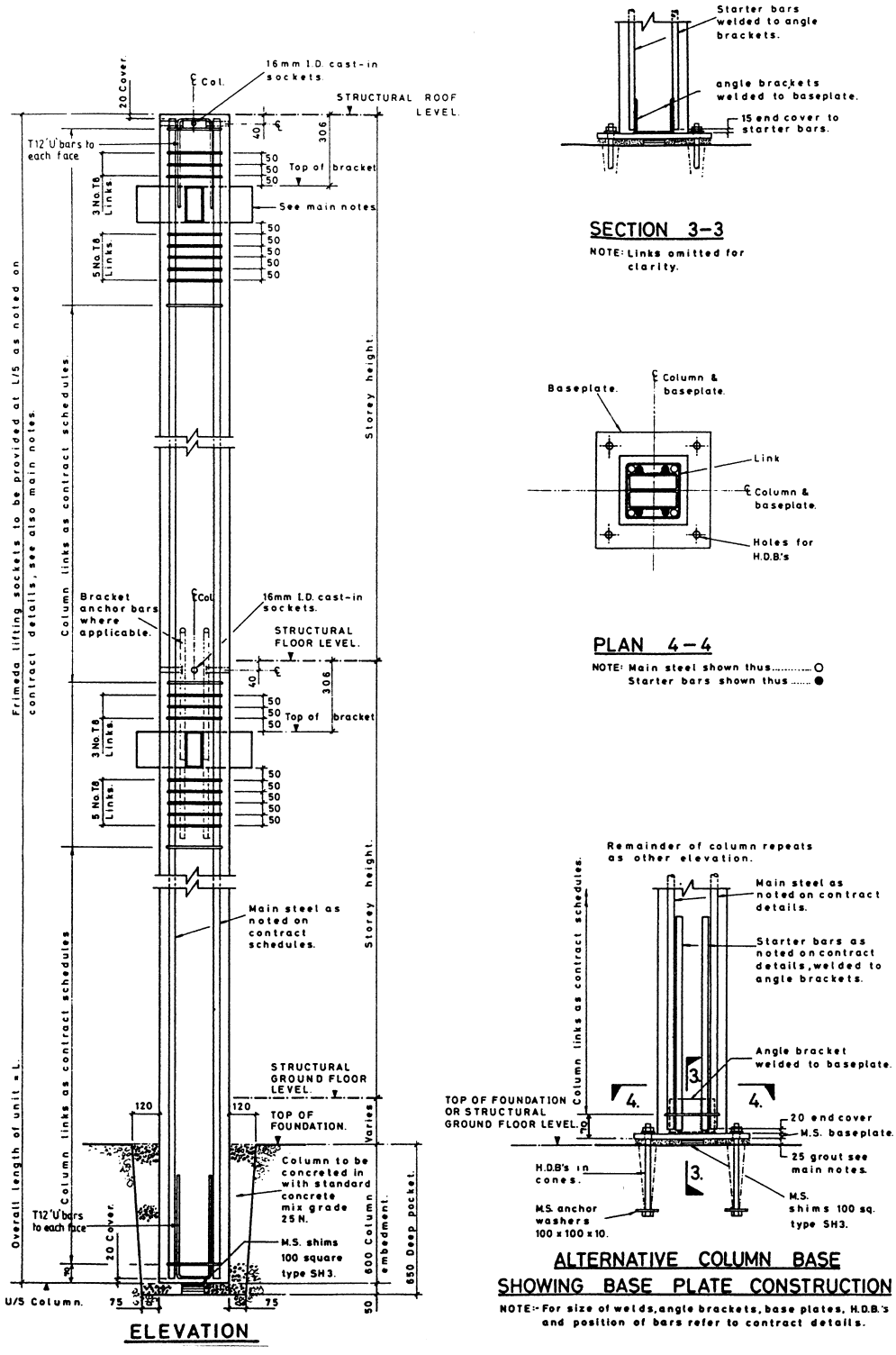

Figure 2.8 Standard detail for a column foot-to-steel base plate (courtesy of Crendon Structures Ltd).

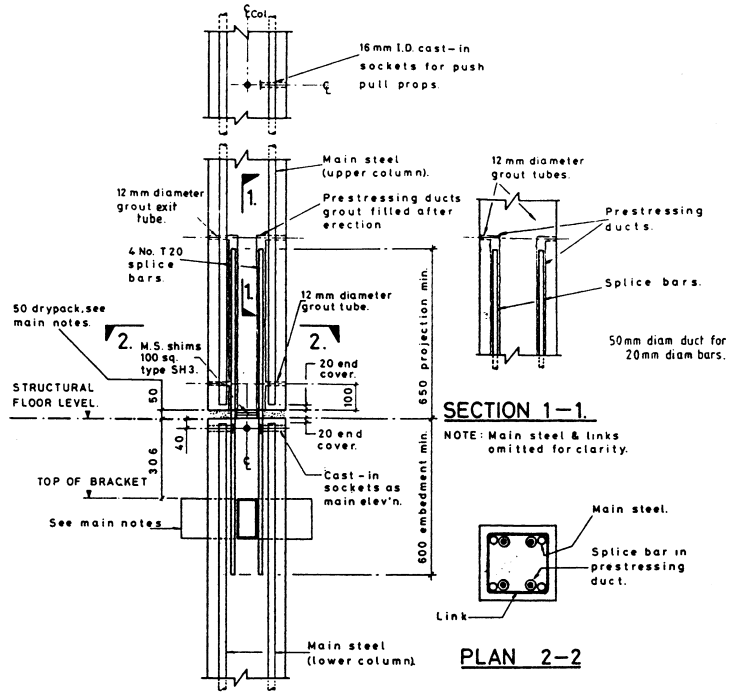

COLUMN SPLICE

NOTE: All links omitted for clarity.

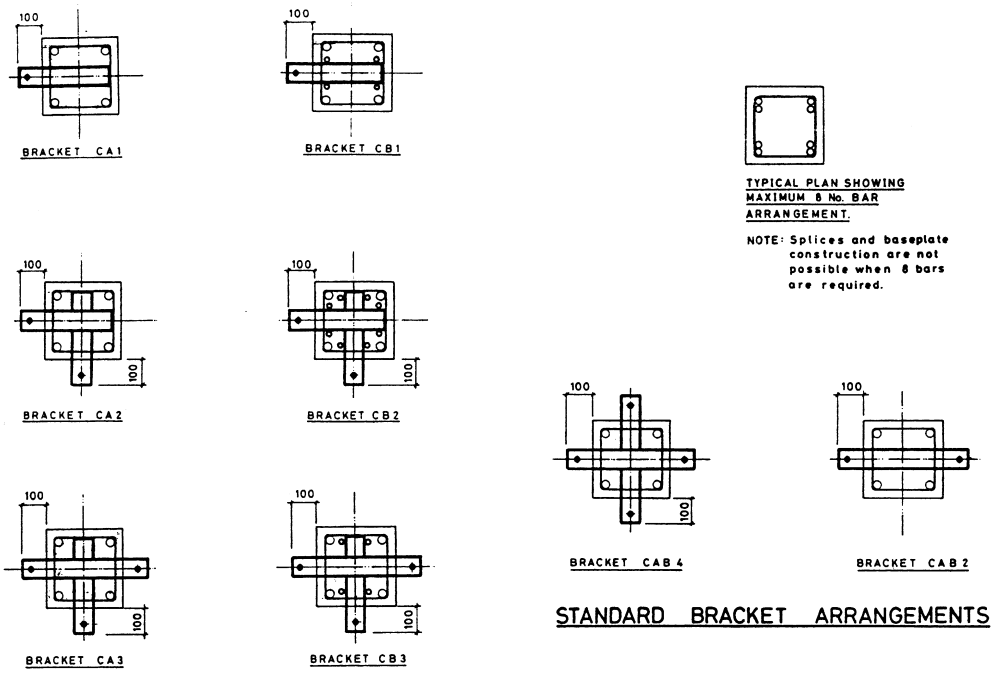

STANDARD BRACKET ARRANGEMENTS

Figure 2.8 (*Continued*)

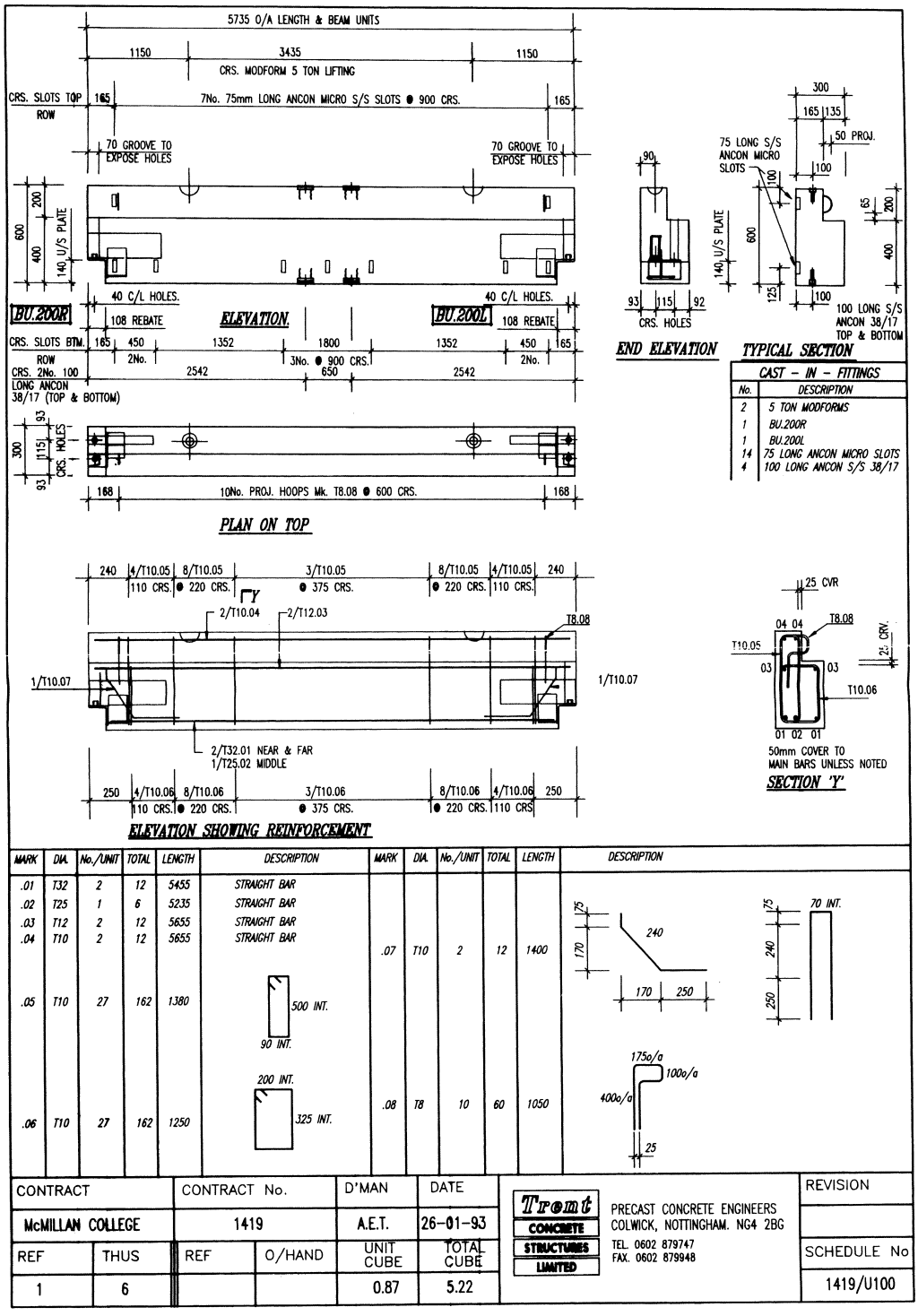

MARK	DIA.	No./UNIT	TOTAL	LENGTH	DESCRIPTION
.01	T32	2	12	5455	STRAIGHT BAR
.02	T25	1	6	5235	STRAIGHT BAR
.03	T12	2	12	5655	STRAIGHT BAR
.04	T10	2	12	5655	STRAIGHT BAR
.05	T10	27	162	1380	500 INT. / 90 INT.
.06	T10	27	162	1250	200 INT. / 325 INT.
.07	T10	2	12	1400	175 / 240 / 170 / 250
.08	T8	10	60	1050	175o/a / 100o/a / 400o/a / 25

CONTRACT	CONTRACT No.	D'MAN	DATE
McMILLAN COLLEGE	1419	A.E.T.	26-01-93

REF	THUS	REF	O/HAND	UNIT CUBE	TOTAL CUBE
1	6			0.87	5.22

Trent CONCRETE STRUCTURES LIMITED
PRECAST CONCRETE ENGINEERS
COLWICK, NOTTINGHAM. NG4 2BG
TEL. 0602 879747
FAX. 0602 879948

REVISION

SCHEDULE No 1419/U100

Figure 2.9 Examples of beam and column component schedules (courtesy of Trent Concrete Ltd).

- use of special mixes, e.g. using lightweight aggregates, selected aggregates and grading, white cement, sulphate-resisting cement, pigments, additives, etc.

Instructions to site are usually contained in what amounts to a 'code of practice', which is prepared by the precasting organisation at the tendering stage. Other instructions to site are self-evident from the drawings. The procedures adopted on site have grown out of many years' experience, and safe and structurally competent standard practices have evolved. Many site-fixing details are contained in the product drawings, e.g. the details for column-to-column splices are fully described, although the exact procedural methods are not. It is only where special or unusual components or joint details are being used that specific instructions are relayed to site. These might include:

- the sequence of erection, with particular reference to temporary stability (usually this is the decision of the contracting division, but special circumstances may prevail)
- temporary propping of components
- extra care, or specific instructions, in the handling and fixing of certain components
- changes to the specification or use of expanding agents, cementitious grouts, mortars, epoxy-based materials, adhesives, bolting and welding
- additional degree of quality control, e.g. cube sampling, curing protection, compaction
- extra details for the placement of important stability ties
- special requirements on construction tolerances.

2.3 Construction Matters

2.3.1 Design implications

The precast superstructure is designed and detailed to enable safe handling, transportation and fixing, without damage to the component and framework. The effects of small, hairline cracks that may occur in certain components when they are lifted are assessed on the basis of the nature of the component and its function within the structure. Due consideration should also be given to the location of the cracks, particularly in highly stressed regions close to connectors. In the event of structural cracks appearing in any component, reference is made to the designer prior to completion of the fixing.

The designer ensures that all lifting devices, whether bespoke or proprietary, are of sufficient load capacity to deal with all possible load magnitudes and directions. The lifting devices are located at the points given in the project product drawings. Detailed instructions and special provisions etc. are given on working drawings regarding the safe handling, lifting and storage of components, as well as any specific features regarding temporary and/or permanent stability. The sequence in which the structure is erected and the temporary measures taken to ensure the correct transfer of load to the ground are available in writing, as a 'method statement' for the fixing contractor to follow. Information is stated relating to the stage of construction at which an entire framework, or a part thereof (whether vertically or horizontally partitioned), is considered fully stable and may be allowed to stand free of any external restraint. Often there will be a time limit before which props cannot be removed, to permit *in situ* grout or concrete to develop a minimum strength.

Loading arrangements on delivery vehicles are such that the components are not subjected to forces and stress not catered for in the design. The components are loaded evenly so that the distribution of weight is uniform on each component, particularly when the vehicle is cornering, braking or inclined (Figure 2.10). Components are usually stacked on timber bearers for storage or transport. These bearers protect the concrete edges and assist easy access to lifting points. They must be located to ensure stability and to avoid temporary overstress, e.g. by creation of cantilevers that develop excessive hogging moments in members designed only to withstand sagging moments. The type of lifting equipment (crane, hoist, etc.) must be compatible with the geometry of the structure, weight and size of components, the nature of the ground and site access. Crawler cranes of 40 to 100 tonne capacity,

Figure 2.10 Correct transportation of precast components.

and smaller mobile cranes, are frequently used where all-round access is available. Otherwise 5 to 10 tonne capacity tower cranes are used. Lifting beams are used in situations where the inclination of the lifting chains will either cause cracking of the component, or will exceed the safe working load of the chains. Use of long chains is common, but can dictate use of a larger crane to achieve adequate jib height.

Components that are to be inclined by pitching are first placed on firm ground, and then pitched in a separate operation (Figure 2.11). A special (steel, concrete or timber) shoe may be required when pitching heavy and thin units that might otherwise be damaged locally.

Temporary imposed loads due to the combined storage of materials, storage of precast components, and construction traffic and plant are assessed, and maximum allowances are given to the various parts of the framework. Where a precast component has been designed to act compositely, consideration is given to the non-composite strength and stiffness of the component. Working drawings carry this information in the form of allowable loads per unit area, or per individual component, irrespective of the location of the imposed load. This is because site conditions may dictate that a load is landed temporarily and chains repositioned.

The total (fixed and stored) dead load present above the highest stabilised level in the structure is known to the contractor from his record of events during construction. The contractor will record dimensional inaccuracies, such as component dimensions (length, cross section, position of connectors, etc.), fixing tolerances (clear gaps, squareness and verticality) and report to the designer any major deviations from permitted tolerances.

There are a wide range of connections in a precast structure, many of which are used to perform a unique function. The contractor is made aware of the importance, or not, of each fixing type, and of the permitted deviations. The designer should ensure that the fixing(s) perform their intended function, either by strict compliance with manufacturer's details, or by full-scale testing. In the former case the influence of the position of the fixing in the component, and the measures taken to ensure the full, safe working capacity of the fixing, are observed. Construction tolerances are stated on the drawings.

The strengths of bolted or welded connections are assessed for both the temporary and permanent condition, such that no element is overstressed at any time. The effect of torsion and shear stresses

Figure 2.11 Pitching columns on site.

induced by non-symmetrical loading (e.g. slabs onto one side of a beam) that would not normally occur in service are catered for.

The contribution to strength and stiffness from *in situ* concreted connections is assessed with respect to the time taken for the concrete to mature. Although adequate strength may be achieved in compression, the bond resistance between rebar/dowel and the concrete may take longer to fully develop. The connections are protected from rapid drying or rain penetration.

2.4 Codes of Practice, Design Manuals, Textbooks and Technical Literature

2.4.1 Codes and Building Regulations

Past UK design practice has used a combination of statutory Building Regulation documents defining the general requirements, and non-statutory documents deemed to satisfy those requirements with respect to strength, safety, reliability and stability. British Standards (BS) defining acceptable methods of design and construction are based on an industry-wide consensus of best practice, and are listed as a means of satisfying the Regulations. Historically, the design has been carried out in accordance with BS 8110 [2.7], which allows the design of structures or structural components to be based on

testing, and permits the engineer to design in this manner which . . . *may be deemed satisfactory on the basis of results from an appropriate model test coupled with the use of model analysis to predict the behaviour of the actual structure…* (Part 1, clause 2.6.1), or . . . *if the analytical or empirical basis of the design has been justified by development testing of prototype units . . .* (Part 1, clause 2.6.1). For connections the code allows that: *Any other type of connection that can be shown to be capable of carrying the ultimate loads acting on it may be used*' (Part 1, clause 5.3.5.3). In other words, full-scale testing of structural components and connections is permitted.

The Eurocodes, together with their UK National Application Document (NAD) for locally determined parameters, are now published as BS EN (British Standard European Norm) codes to replace the British Standard (BS) codes. Although (at the time of publication of this book) there continues to be a period of transition, Eurocode 2 replaces all UK codes dealing with the design of structural concrete. Eurocodes will, in due course, be defined by the Building Regulations in 2013 as 'deemed to satisfy' its generic requirements. This will mean that a design to the Eurocodes must be acceptable to the client. However, it is anticipated that the British Standards will not be removed from the Regulations for some time (probably about five years), and hence designs to the existing standards may be accepted by the client during that period at least. There will be no further revisions of the British Standards, as they are no longer being supported by the British Standards Institute committee and will rapidly become outdated. It will become increasingly difficult to justify their use once they are no longer identified within the Regulations.

The Eurocodes are common in content across Europe, even in translation. The National Application Document then permits each country to vary certain parameters within each code. This permits each country to adjust parts of the Eurocode to reflect local conditions that have led to the development of parts of their historic design codes not recognised as essential across Europe. In other words, it is accepted that some parts of the codes will become identical to the former national code by insertion of relevant clauses or parameters into the NAD. Some changes are not permitted. For example, the partial load factors are lower than those used historically in Britain. Thus more economical solutions are possible using the Eurocodes, but with a reduced overall factor of safety and possibly of durability. In situations where the British climate leads to a lack of durability, the NAD introduces changes that should restore the serviceability requirements of the former codes.

Introduction of the Eurocodes means that all design and construction information is no longer contained in one volume. Thus generic design requirements, loading, and material-specific design information are contained in three separate volumes. The three that are relevant to precast concrete construction are:

- BS EN 1990: Basis of Structural Design [2.8]
- BS EN 1991: Actions on Structures (which is published with separate volumes for actions due to self-weight and imposed loads, fire loading, snow loading, wind loading, thermal changes, execution, accidental loads, loads on bridges, crane and machinery, and silos and tanks) [2.9–2.18]
- BS EN 1992: Design of Concrete Structures (rules for buildings and structural fire design [2.19, 2.20].

However, there is currently no Eurocode to cover site construction practices for each different construction material, which are addressed in the BS.

Traded items used in precast concrete construction, such as proprietary lifting-point inserts, already come under the European Construction Products Directive, which aims to remove national barriers to trade by an agreed system of attestation and conformity. Thus products deemed to satisfy European regulations in one country are given a CE mark and must then be accepted as a satisfactory product throughout Europe. This is the Europe-wide equivalent of the old BS kitemark.

The design of structural products is verified according to the following standards in relation to conformity, standardisation, durability, fire resistance, tolerances, inspection, quality control and testing. Product Standards linked to precast concrete elements include:

- Common rules for precast concrete products: EN 13369:2013 [2.21]
- Precast concrete products – Hollow-core slabs: EN 1168:2005+A3:2011 (+A3 means a third revision since 2005, but is due for a major revision c.2013) [2.22]
- Precast concrete products – Floor plates for floor systems: EN 13747:2005+A2:2010 [2.23]
- Precast concrete products – Beam-and-block flooring: EN 15037-1:2008, in 4 parts [2.24]
- Precast concrete products – Ribbed floor elements: EN 13224:2004 [2.25]
- Precast concrete products – Linear structural elements: EN 13225:2004 [2.26]
- Precast concrete products – Staircases: EN 14843:2007 [2.27]
- Precast concrete products – Wall elements: EN 14992:2007 [2.28]
- Execution of concrete structures: EN 13670:2007 [2.29]
- Background paper to the UK National Annexes to BS EN 1992-1 & 1992-3: PD 6687:2010 [2.30].

Generally PD 6687 deals with a number of topics that are not covered in BS EN 1992, but were found with specific reference to precast concrete in BS 8110, such as tie steel for precast stair flights, and stability tie forces in buildings. PD6687 gives (i) useful background information for the reasons for Nationally Determined Parameters; (ii) commentary on some specific subclauses from EN 1992-1-1 and EN 1992-1-2, and (iii) the requirements of the UK Building Regulations 2000 that are not covered in EN 1992-1-1 and the UK National Annexes.

The National Structural Concrete Specification Edition 4:2010, NSCS-4 [2.31] gives a comprehensive review of the Eurocodes against the background of BS EN 13670: 2009 *Execution of Concrete Structures* [2.29]. It provides a BS EN 13670-compliant specification for use in structural concrete, including precast and prestressed, together with an extensive list of references. A key point is: *The adoption in the UK for the first time of an execution or workmanship standard in place of the workmanship requirements forming part of a design standard . . . requires the use of an execution specification, consisting of documents and drawings to communicate additional and project-specific construction requirements between Client, Designer and Constructor*.

The Eurocodes retain the option of design justification based on a combination of testing and calculations, but with greater control of the statistical analysis of the resulting data than has been the case hitherto. Design by tests may be used when, for example:

- adequate calculation models are not available
- a large number of similar components are to be used
- control checks are needed to confirm assumptions made in the design.

Precast concrete designers have seized the opportunity to use the results of ultimate load tests and fire tests to demonstrate the adequacy of connections and components. Full-scale ultimate load testing has been carried out by independent authorities to determine factors of safety for a range of connector types and capacities (Figure 2.12). Beam-to-column shear connectors have been the subject of considerable load testing, but most of the data are confidential to the manufacturer. Certificates of validation for the connectors are issued to checking authorities as part of the design submission. In some instances it has been possible to supplement test results for connectors with a rudimentary structural design (see Section 7.10), but in general the behaviour is far too complex for simple analysis to be reliable and ultimate load testing is the sensible approach towards acceptance.

A similar approach has been adopted for fire resistance, particularly with hollow-cored flooring units where the hollow core renders fire-engineering calculations susceptible to oversimplification. There has not been a fully coordinated approach to fire testing in Europe in the past, and it is proving to be a difficult task to disseminate the available data. One stumbling block is that the results of fire tests are frequently confidential to the manufacturer, but in many cases resistances greater than those obtained by calculation with respect to BS 8110 have been measured.

Although precast concrete design has been carried out according to BS 8110, not all sections of the codes are used. Table 2.1 is a summary of the sections used, together with the comparable Eurocode reference.

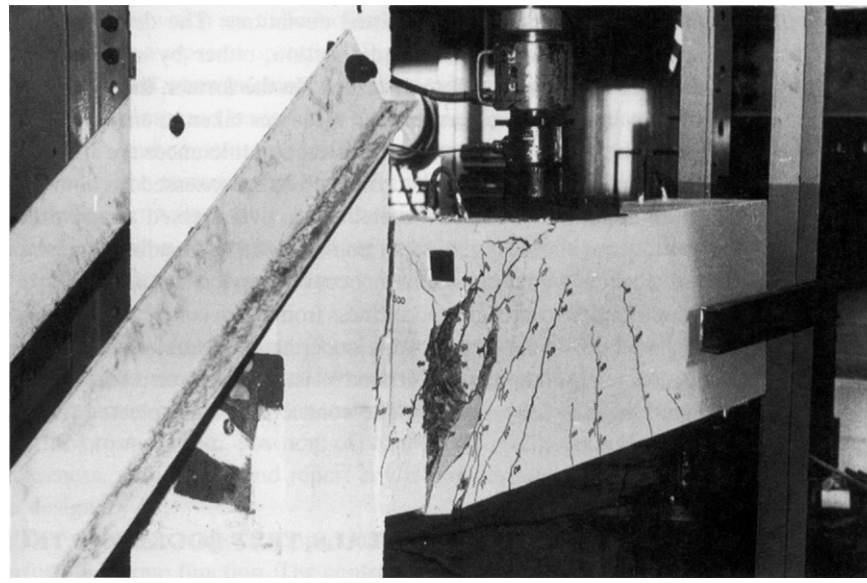

Figure 2.12 Beam end shear testing at Nottingham University (courtesy of Trent Concrete Ltd).

Table 2.1 BS 8110 requirements and their Eurocode equivalents

Design consideration	**Relevant section in BS 8110: Part 1**	**Relevant section in BS EN 1992**
Structural analysis and design, loading, materials and robustness	2	2, 3 and 5
Ultimate limit state for the design of reinforced precast concrete components in flexure, shear and compression	3.1 to 3.4, 3.8 to 3.10 and 3.12	6
Serviceability and ultimate limit state for the design of prestressed concrete components in flexure and shear	4.1, 4.3 to 4.10, and 4.12	3.3, 3.4, 5.10, and 8.10
Precast construction	5.1. to 5.3	10
Composite precast – *in situ* construction	5.4	6.2.5
Concrete and tolerances	6	8 and 9
Reinforced concrete components in torsion	2.4	6.3
Effective column height	2.5	5.8
Robustness	2.6	9.10
Serviceability limit state for reinforced concrete	3	4 and 7
Fire resistance	4	**EN 1991-1-2** and **EN 1991-1-5**: 1 to 5
Volumetric changes in concrete	7	3.1.4, 10.3 and 10.5
Movement joints	8	9.10

The Eurocodes use the now familiar limit-state design philosophy. There are numerous changes in detail, and in methods of implementation, in order to subsume the multiple differences in approach used historically by the former national code-setting countries within the EU. Some of the changes for those already familiar with BS 8110 and converting to using the Eurocodes can be summarised as:

- The weight of concrete is increased by 1 kN/m^3 (to 25 kN/m^3) when it contains normal ratios of reinforcing steel, and by 1 kN/m^3 for the additional water it contains when wet during construction.
- Load values and their consequences, referred to as actions, vary but are broadly similar, and are claimed to represent more uniform risks of being exceeded than the values in previous codes.
- The partial load factors of 1.4 and 1.6 for dead load and live load are replaced with 1.35 (called *persistent actions*) and 1.5 (called *transient actions*), respectively.
- Combined load cases assume more simultaneous loads, yet also attract reduced partial factors based on a statistical analysis of their likelihood of occurring simultaneously.
- Concrete material properties are based on cylinder test strengths, yet with equivalent cube strengths quoted.
- Once shear reinforcement is required, it must be provided to carry the total shear force using the truss analogy, with no reliance on dowel action, aggregate interlock, or shear in the compressive concrete.
- The design of slender columns requires the area of reinforcement as input in order to determine the second-order bending moments needed to design the area of reinforcement.

The net effect of the changes is to produce designs that are typically between 5 and 10 per cent more economical in use of materials, though that may not always translate into reduced cost.

2.4.2 Non-mandatory design documents

2.4.2.1 Structural Joints in Precast Concrete, The Institution of Structural Engineers [2.32]
This document has found wide acceptance in the UK and many design methods are used in conjunction with the ultimate design stresses given in BS 8110. The only criticism of the design methods is that many of the finer points are dealt with only in a qualitative manner, leaving the designer to propose numerical solutions to fit the specific problem. For example, column-to-column splices are described and well illustrated, but no design method to determine ultimate load or moment capacity is offered. Also, some of the connections shown are highly impractical and have rarely been used in the UK (e.g. Figures 4 and 18 in the manual). The danger here is that the inexperienced designer may be tempted to specify these types of connection without fully understanding precast construction.

2.4.2.2 Structural Connections for Precast Concrete Buildings, Fédération Internationale du Béton, Bulletin 43 [2.33]
This substantial, state-of-the-art publication strikes a good balance between the fundamental concepts of connection behaviour in the wider context of designing a precast concrete structure, and the minute detail of localised force equilibrium and strain compatibility in compression, shear, tension, bearing, bending and torsion. Although many of the design philosophies are linked to the Eurocodes' terminology and methodology, it is not always possible to adopt the methods directly into normative design. It provides excellent references for research. While the publication has its roots in Scandinavia and Northern Europe, there are contributions from *fib* members in over 15 countries worldwide.

2.4.2.3 Design and Typical Details of Connections for Precast and Prestressed Concrete, The Prestressed Concrete Institute [2.34]
The Prestressed Concrete Institute manual provides a library of connection details, with practical execution advice and detailed design information, although the latter is difficult to translate into

British or European standards owing to the dimensional requirements of US practice. Notwithstanding that problem, the manual is an excellent source of reference, such that it is possible to develop one's own solutions to connection details and apply the principles to BS 8110 or BS EN 1992 rules. Several of the solutions in this present book adopt this idea.

2.4.2.4 **PCI Design Handbook,** The Prestressed Concrete Institute [2.35]

Although many of the design methods presented are not appropriate to limit-state design, this manual is often used for detailing purposes. Some of these are used widely in Europe and successful designs have been converted from the American model. Many of the designs and details presented in this Handbook are the product of the experimental and analytical data generated in over five decades of research work. (Most of this work originates in the PCI Journal.) However, because many of the design principles are based on empiricism, they do not satisfy European legislation without national certification. Because of this, alternative methods have been sought by European designers and PCI rules are largely ignored. Many design equations are dimensional and care must be taken in using them with metric units.

2.4.2.5 **Design of Multi-Storey Precast Concrete Structures,** FIP Commission on Prefabrication [1.12]

This document from the Fédération Internationale de la Précontrainte focuses attention on the stability of high-rise structures and presents broad principles on structural analysis, with very little quantitative design data. The document is therefore useful only in the overall assessment of the integrity of precast structures, but is of little use in detailed design. The illustrations show only the principles involved in the design of joints and of structural stability and, as many appear to be outdated, the document has not found favour in some countries. A more comprehensive edition is published as follows.

2.4.2.6 **Planning and Design of Precast Concrete Structures,** FIP Commission on Prefabrication [2.5]

This book from the Fédération Internationale de la Précontrainte is primarily meant for beginners. It illustrates the wider issues of precast construction in many contexts – buildings, housing, stadiums and cladding – and takes the reader through the basic philosophy behind precast construction before focusing on specific details regarded as good practice within the Commission. The information is collected from more than 15 countries worldwide, showing the enormous scope in precast. There are no specific design rules.

2.4.2.7 **Precast Prestressed Hollow-cored Floors,** FIP Commission on Prefabrication [2.36]

This document from the Fédération Internationale de la Précontrainte has been used as a guide to both the design and detailing of hollow-cored floors and their connections to precast structural components, and to other hollow-cored units. The information may be used to design a structurally robust hollow-cored floor unit, capable of resisting flexural, shear, bond and bearing stresses in an economical manner. Connection details between adjacent slabs and at the ends of slabs, utilising the minimum volume of *in situ* concrete and expedient placement of site reinforcement, have been widely adopted in all European countries. At the present time (2013) *fib* is near to the publication of a more comprehensive second edition.

2.4.2.8 **Special Design Considerations for Precast Prestressed Hollow-Core Floors,** *fib* Commission on Prefabrication [2.37]

This Guide to Good Practice contains a number of specific cases linked to the analysis and design of prestressed hollow-core units, namely transfer of prestress, end splitting stresses, restrained supports, floor units on non-rigid (flexible) supports, floor diaphragm action, and floors under seismic action. While the articles are very informative and give a sound technical explanation of these complicated

subjects, it is often difficult to translate the information for the benefit of real design situations. Some chapters are reproductions of PhD thesis work. However, it is important that the information is made available as a tool for further interpretation.

2.4.2.9 Guidelines for the Use of Structural Precast Concrete in Buildings, Study Group of the New Zealand Concrete Society, and National Society of Earthquake Engineering [2.38]

This document is of primary importance to seismic-resistant structures, although some of the details and recommendations are relevant to non-seismic conditions. Special attention is given to support conditions and continuity in floors and frame connections, and to grouted and embedded connections. A positive aspect is the manner in which the document shows the relationship between the way in which connections are made and their influence on the behaviour of the structure as a whole. There is a very good section on tolerances.

2.4.2.10 Precast Concrete Framed Structures – *A Design Guide*, British Cement Association [2.6]

BCA's publication is very much a forerunner to this book. Their manual establishes the potential use of precast concrete in multi-storey building and although the basic design principles, both in the permanent and temporary stages, are comprehensively covered, no computational data is presented. The manual's place in the design process is therefore to harmonise design principles in a qualitative manner, and establish some basic rules for the design of precast buildings, e.g. stability methods, floor diaphragm action, connections, etc. There are only references to specific design rules, and no examples. There is a more recent publication, *Precast Concrete in Buildings: A Guide to Design and Construction*, covering much of the same content, from the BCA's successor, the Concrete Centre [2.39].

2.4.2.11 Hybrid Concrete Construction, Reinforced Concrete Council [2.40]

Working from a background of predominantly *in situ* concrete, this publication shows about 150 examples worldwide of how precast reinforced and prestressed concrete can be used both implicitly and explicitly with *in situ*. 'Hybrid' does not always mean composite construction, although both concretes may often benefit from the structural integrity of each other. There are numerous examples of where precast concrete is the dominant medium, and this philosophy is extended into the following review of mixed construction.

2.4.2.12 Precast Concrete in Mixed Construction, *fib* Commission on Prefabrication [2.41]

This is a well-illustrated, state-of-the-art review, prepared in response to the growing demand from architects and engineers asking for information on how to use precast concrete with other building materials. Although the document provides a holistic point of view for the benefit of the entire construction industry, it shows that precast concrete is central to most new buildings – over 75 per cent, in fact – worldwide. This includes (i) structural steelwork frames with prestressed concrete floors, and precast façades; (ii) cast-*in situ* frames with prestressed composite concrete floors, or precast floor soffits with composite *in situ* toppings; (iii) structural timber and glulam frames with precast floors; (iv) structural masonry with prestressed flooring, or a precast frame with masonry infill; and (v) precast concrete with structural glass. Note that the publication does not offer detailed design information.

2.4.2.13 Precast Eurocode 2: Design Manual, British Precast, UK [2.42] and Precast Eurocode 2: Worked Examples, British Precast, UK [2.43]

These documents aim to extend available design guidance by The Concrete Centre [2.44] and Institution of Structural Engineers [2.45] into the specialist area of precast concrete frame and component design. By distilling the volumes of the Eurocodes EC0, EC1 and EC2 into 92 pages, the Manual provides most of the important information required in precast design, except for slender columns and detailed deflection calculations. *Worked Examples* is more direct, and includes the design of an

entire precast structure, together with individual columns (not slender), beams, hollow-core floors, double-tee floors, and stability ties.

2.4.2.14 Economic Concrete Frame Elements to Eurocode 2, The Concrete Centre, UK [2.46]

This reference document provides preliminary design information for use in early project design when one is faced with the selection of building components. It provides charts and tables of load versus span data, reinforcement and prestressing quantities, ultimate loads and reactions, for a wide range of reinforced and precast/prestressed concrete floors, beams and columns. Chapter 4 deals exclusively with precast concrete, with technical data for the design of (i) floor slabs using either hollow-core, double-tee or half-slab (permanent concrete formwork such as Omnia); (ii) reinforced and prestressed beams; and (iii) reinforced columns. A brief specification and some worked examples are provided.

2.4.3 Other literature on precast structures

Precast design methods are not well documented, mainly because structural design is carried out largely in-house by the precasting companies and there has been no real requirement to publish. Nilson [1.8] covers precast building design, but most of the details and methods are based on PCI and ACI rules and therefore have limited applicability in Europe. A new edition of Sheppard & Phillips's extensive book [2.47] also focuses on American practice and covers such items as the thermal, acoustic and dynamic properties of precast products. Bruggeling & Huyghe [1.31] gives good coverage to most aspects of precast design, in particular in the design of joints, but as with Lewicki [1.13] and Haas [2.48] it leans towards the European ideal. Bachmann and Steinle's 2011 textbook [2.49] has its design work rooted in detailing and production matters, basing design information and calculations on German DIN standards and their European counterparts, making translations into BS EN design possible but tedious in places. Bljuger [2.50] deals with precast in a very analytical manner, and provides a firm basis for many design aspects, particularly connections and wall frames. Levitt's books [2.51, 2.52] are useful for production purposes, and as such have a place in the designer's library, but there is no structural design and the text is becoming rapidly outdated, particularly in Scandinavia and Northern Europe where nearly automated factories exist, e.g. [2.53]. Richardson has been a pioneer in the line of quality through manufacture and his books are particularly instructive [2.54, 2.55]. The National Precast Concrete Association of Australia has produced a very clear and comprehensive guide to antipodean practice in their Precast Concrete Handbook [2.56].

The PCI and FIP have large conventions every two or four years, in which approximately 10 per cent of time is devoted to prefabricated building. Recent events of note have been held in Washington D.C. (1993, 1994), Tokyo (1993), and Budapest (1992). The Secretariat for these organisations should be contacted for further details [2.57, 2.58].

In addition to the above there have also been a number of significant seminars and conferences dealing with precast frame design and construction – namely, the DoE & CIRIA Seminar on The Stability of Precast Concrete Structures [2.59]; Delft University Seminar on Prefabrication of Concrete Structures [2.60]; Noteworthy Developments in Prestressed and Precast Concrete in Singapore [2.61]; and The Engineering Institute of Malaysia Seminar on Trends, Innovations and Performance in Prestressed and Precast Concrete [2.62].

Structural Concrete, the official journal of the *fib*, contains the latest news from *fib* and a selection of technical papers. It provides conceptual and procedural guidance in the field of concrete construction, and features peer-reviewed papers, keynote research and industry news covering all aspects of the design, construction, performance in service and demolition of concrete structures [2.63].

Many papers may be found in academic and professional journals including (in approximate order of numbers of publications) the *PCI Journal* (US), *Nordic Concrete Research* (Scandinavia), *Concrete Precasting Plant and Technology*, otherwise known as *BF+T* (Germany), *ACI Structural Journal* (US), *ASCE Structural Division* (US), *The Structural Engineer* (UK), *Proceedings of the Institution of Civil*

Engineers (UK), *Journal of Structural Engineering* (US), *Magazine for Concrete Research* (UK), *Heron* (Netherlands), the *Canadian Journal of Civil Engineering* (Canada), and the *Malaysian Construction Research Journal* (Malaysia) for its focus on IBS (Industrialised Building Systems) [2.64].

2.5 Definitions

It is useful to define the main terms to be used in this book. The notation is given on pages xiii–xx.

2.5.1 General structural definitions

Frame:	a framework comprising columns, beams and slabs in which there is some degree of flexural (or torsional) continuity between the members, and part of the resistance to sway loads is carried by the horizontal members.
Skeletal structure:	a structure comprising columns, walls, beams, slabs and staircases, in which the connections are all designed as pin-jointed, and the resistance to sway loads is carried by the vertical members only.
Precast concrete structure:	the total structure, including any precast structural cladding, in situ floor screeds, etc.
Structural system:	the load-bearing components for both gravity and horizontal loads and the way in which these components are assumed to behave.
Structural cladding:	externally load-bearing exposed panels, serving both structural and architectural requirements simultaneously. Usually eliminates use of separate columns, beams and walls in external parts of the structure.
Unbraced structure:	in which resistance to horizontal loading is provided by columns in both orthogonal directions.
Braced structure:	in which resistance to horizontal loading is provided by the bracing in both orthogonal directions.
Partially braced structure:	in which part of the structure (usually the lower levels) is braced and the remainder is unbraced in both orthogonal directions.
Uniaxially braced structure:	in which the structure is braced in one direction and unbraced in the other.
Diaphragm, or floor plate, action:	mechanism in which horizontal loads are transferred in the floor slab to the vertical bracing.
Chord elements:	compression and tension beam members in the floor diaphragm.
Stability ties:	horizontal tie bars in situ, concreted into spaces between precast concrete components.
Component:	the discrete precast concrete units from which the structure is assembled.
Members:	two or more components working interactively with one another

2.5.2 Components

Column:	vertical load- and bending moment-resisting linear component.
Wind post:	deep columns in the direction of horizontal loading.
Shear wall:	general term given to vertical bracing walls.
Cantilever wall:	a structurally continuous shear wall designed as a deep cantilever.
Hollow-core wall:	a precast wall containing full height vertical holes into which reinforced *in situ* concrete is placed to form a continuous cantilever wall.
Infill wall:	a discontinuous solid precast shear wall positioned between adjacent columns and beams.
Hollow-core infill wall:	a factory-cast wall containing unfilled vertical or horizontal voids positioned between adjacent columns and beams.
Wall panel:	a solid precast shear wall positioned between columns only and connected vertically to one another.

Beams:	the primary load-carrying horizontal linear component.
Spandrel:	a beam with a deep upstand web, the face of which is flush with the front edge of the column.
Outstand spandrel:	one for which the upstand projects beyond the front edge of the column.
Slabs:	primary two-dimensional floor and roof components.
Composite slabs:	combined slab comprising precast concrete slab (also providing permanent shuttering) and *in situ* concrete topping (or structural screed).
Hollow-cored slab:	rectangular section slab with full-length longitudinal circular or oval (or similar) shaped voids.
Double-tee slab:	T-shaped solid units comprising two deep webs and a full-width top flange.
Flat plank:	rectangular solid section used either alone, or more usually as permanent shuttering in a composite floor.

2.5.3 Connections and jointing materials

Base plate:	steel plate anchored to the end of a column for foundation connection.
Splice:	connection between successive columns.
Connector:	mechanical device for the transfer of forces between precast components.
Shear box:	mechanical device for the sole purpose of transmitting end shear forces into beams.
Column insert:	mechanical device for the sole purpose of transmitting beam-end shear forces into columns.
Corbel:	bearing surface to a column or wall made by a reinforced concrete projection of defined width and finite depth.
Haunch:	bearing surface to a column (or beam) made by a varying increase of the cross section of the column (or beam) approaching the bearing face.
Scarf joint:	made between the recessed ends of two components, one bearing on top of the other on shallow sloping surfaces.
Halving joint:	a scarf joint with flat, horizontal bearing surfaces.
Simple bearing:	a direct dry bearing between precast components.
Extended bearing:	a reinforced *in situ* bearing made by *in situ* concreting of reinforcement left projecting from the adjoining components.
Dry bearing:	no additional material is used between the precast components.
Wet-bedding bearing:	mortar is used in the bearing surface before erection.
Dry-packed bearing:	mortar is packed in the gap between precast components after erection.
Elastomeric bearing:	neoprene (or similar) pads are used.
Simple connection:	where only shear and axial forces are transmitted.
Moment connection:	where bending and torsional moments, as well as shear and axial forces, are transmitted.
Trimmed hole:	a void made in a floor slab by supporting the curtailed members in line with the void on (usually) steel angles, which in turn are supported on adjacent components.
Cast-in-sockets, channels, etc.:	threaded sockets, channels, etc. fully anchored into the adjoining concrete.

CHAPTER 3

Architectural and Framing Considerations

This chapter describes the main features in the preliminary design stages that influence the interaction between the architectural concepts, the building's function and the precast concrete solution.

3.1 Frame and Component Selection

The criteria for the selection of internal and external layout are different in most buildings. The interior is governed by spatial requirements for function, and by the location, size and orientation of lift shafts, stairwells, mezzanine floors, major partitions, etc., while for the exterior the precast structure can be designed for a very wide range of architectural features. It is easy for the precast frame designer to respond to both of these requirements simultaneously by specifying an external structure that is, in the main, totally different from the internal arrangement. The first decision is therefore the selection of the structure. There are three main tasks in this selection process:

(1) selection of the structure
(2) recognition of the functional requirements of the building
(3) preparation of the framing plan by making optimum use of precast components.

These tasks are discussed separately below.

(1) Selection of the structure

The possibilities for the external structure are:

- an external structural envelope comprising either visual concrete spandrel beams, or structural precast concrete cladding: Figures 3.1 and 3.2.
- non-structural precast concrete cladding, *in situ* masonry, steel sheeting, or glass curtain walling supported on a plain concrete beam–column structure: Figure 3.3.

The external structure can be physically massive, by being overclad in some form, and may therefore be used as a primary horizontal stabilising structure. This means that the internal structure may be relatively lighter in construction and need not necessarily be established on the same dimensional grid as the exterior. The options here are then:

- a totally precast internal structure comprising a stable beam–column framework, floors, walls, staircases and lift-shaft walls: Figure 3.4.

Multi-storey Precast Concrete Framed Structures, Second Edition. Kim S. Elliott and Colin K. Jolly.

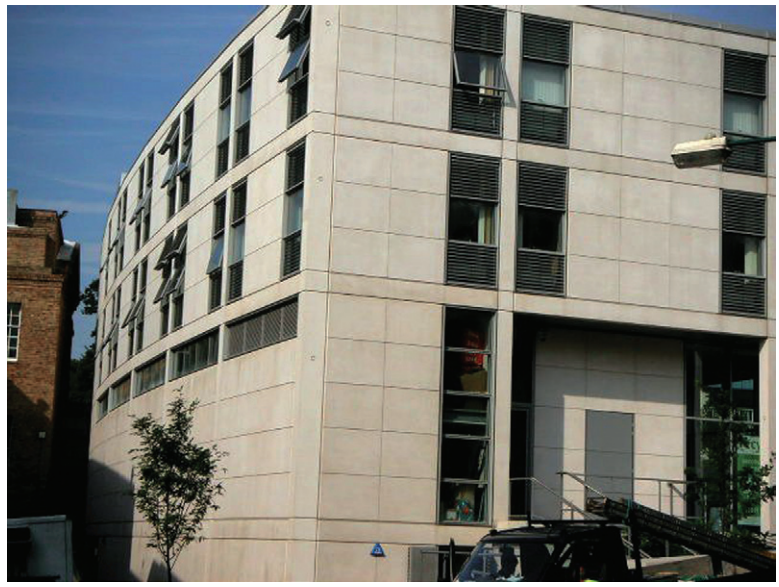

Figure 3.1 Architectural precast beams and columns, with an integrated structural façade, known as 'hard-wall': Portland Building, University of Nottingham, 2003.

(a)

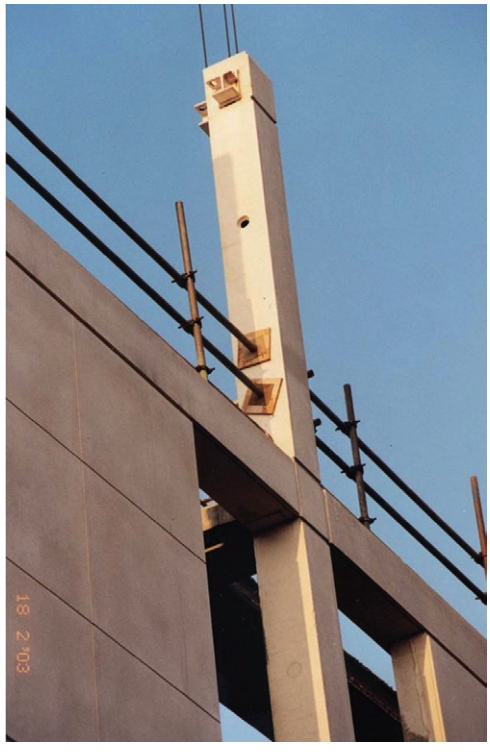

(b)

Figure 3.2 Portland Building, University of Nottingham, 2003. (a) Five-storey columns, in finished concrete, contain steel connectors to receive the cast-in box connector in the structural beams; (b) beams that are formed together with the insulated wall panel.

Figure 3.3 Grit-blasted reconstructed sandstone concrete cladding panels at Scottish Office, Leith (courtesy of Peter Stubbs, EdinPhoto, www.edinphoto.org.uk).

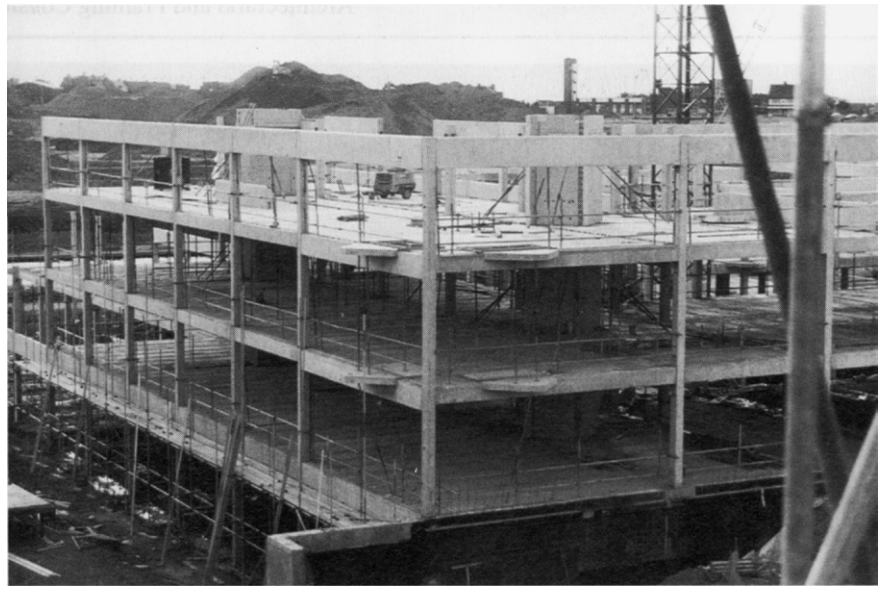

Figure 3.4 Precast skeletal structure under construction.

- a hybrid internal structure (see also Section 3.3.1) comprising a precast skeleton of beams, columns and slabs designed collectively with one or more of the following:
  - *in situ* concrete basement or ground-floor podium
  - structural steel or timber roof (mansard or Warren girder), atrium or gallery: Figure 3.5
  - structural steel portal frame (e.g. warehouse or factory attached to an office block).

Figure 3.5 Timber roof trusses seated on long span precast roof edge beams.

(2) Recognition of the functional requirements of the building

Different areas of the structure may require a higher building specification than other areas or floor levels – for example, with respect to fire resistance, thermal, acoustic or vibration characteristics. Other criteria may include the requirements for open spaces, natural light, the absence of fixed-position walls, unlimited freedom for vertical and horizontal service routes, future vertical and horizontal extensions, and changes in ownership. The design engineer must address all the aspects listed above, and often many more.

(3) Preparation of the framing plan by making optimum use of precast components

The example building plan shown in Figure 3.6 is subdivided into component rectangles and triangles. The flooring should span onto the beams or walls intersecting at an angle between 90° and 45°.

An orthogonal grid layout is specified as far as possible, with the columns and shear walls placed on beam lines. Primary columns are located at the strategic points (corners, changes in floor level, around stairwells and lift shafts) and secondary columns are introduced to satisfy architectural requirements, such as window bay widths, internal partitioning, or to obtain structural economy by using the minimum number of components giving acceptable structural zones. The distances between beams are equalised as far as possible in order to divide the building into equal bay widths. Beams should be placed beneath any major partitions, say 215 mm-thick brick or block walls, rather than supporting them on the floor slabs.

There are general rules regarding the provision and location of holes and cast-in fixings in precast components. Their availability varies with the different methods of manufacture. For example, some units are cast in steel moulds that become less adaptable for future use if drilled to locate fittings. It may be less expensive and time-consuming to drill and fix on site. Alternatively, if *ad hoc* timber or glass fibre moulds are used, then it is relatively easy to locate fittings to the inside of the mould. The best advice is to contact the precast manufacturer early in the project to ascertain which of these may be incorporated in the normal course of manufacture and which require additional attention. Some general guidelines are given in the following sections.

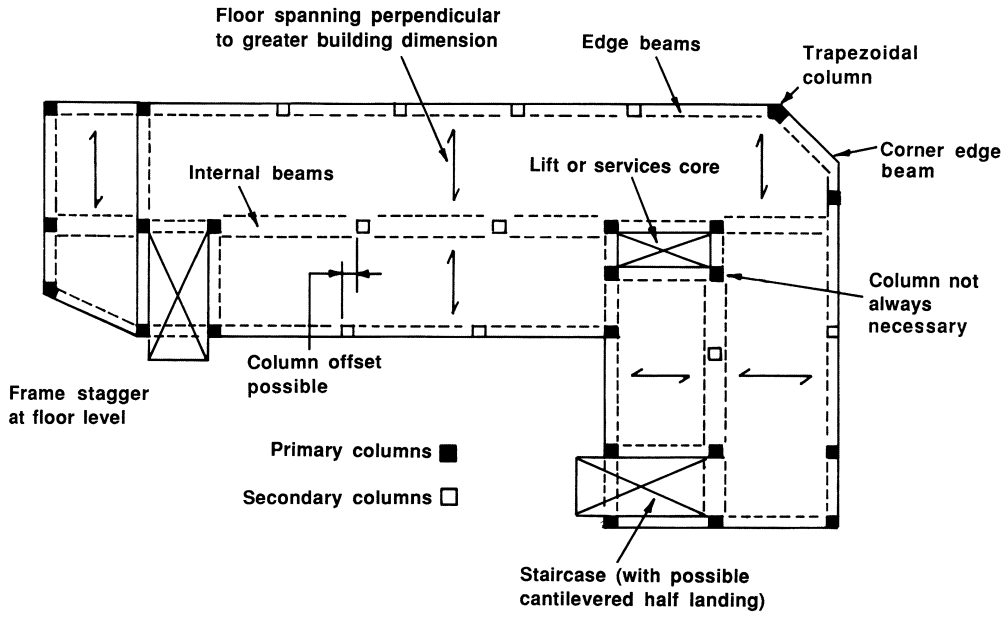

Figure 3.6 Subdivision of the floor layout into component rectangles and trapeziums.

Surface finishes will be specified according to BS EN 13670:2009 *Execution of concrete structures* [2.29]. However, the background document to the National Annex to BS EN 1992-1-1, PD6687 [2.30], states that the provisions of the National Structural Concrete Specification Edition 4:2010 (NSCS-4) [2.31] are considered equivalent to those in EN 13670 for all types. Until further information becomes available the surface finishes will be specified in NSCS-4 as Type A, B or C. The surface finish to all ex-mould faces is Type A. All non-contact surfaces have either a steel-trowelled finish, or are rough-tamped to develop a shear key with other concrete. The orientation for casting a component is often dictated by the need for a rough surface, and by which of the faces must be fair because they remain visible. Plain visual concrete for external use where the surface finish has not been specified, e.g. car parks, will be Type B. Plain concrete for other specified use will be Type B or C, according to the architect's specification.

3.2 Component Selection

3.2.1 General principles

Precast manufacturers have standardised their components by adopting a range of 'preferred' cross sections for each type of component. In fact it is the moulds that are standardised, and therefore non-preferred shapes will incur cost penalties because of the alterations to the mould. If a non-preferred cross section is to be used, there should be a sufficient number giving a piece-to-mark ratio (units per mould alteration) of 10, at least, to justify these alterations. Bespoke architectural details can often be achieved using inserts within a larger, more durable, standard mould. The framing plan may be adjusted according to this philosophy.

For the purpose of this study the components will be described in the design sequence:

- roof and floor slabs
- staircases
- beams

- columns
- bracing walls.

3.2.2 Roof and floor slabs

The wide range of precast concrete floors used in precast skeletal structures has, in recent years, been reduced to five main types (Figures 3.7 (a) to (e)):

- prestressed hollow-core floor
- reinforced and prestressed double-tee floor
- beam- (including wide beam-) and-block floors, which may or may not be used with a structural topping
- composite prestressed plank floor
- composite beam and plank, which must always be used with a structural topping.

Table 3.1 gives a performance guide to the self-weights and maximum spans for some of these units.

In most cases the floor construction is voided, thus producing a lighter floor having the same structural performance as a continuous *in situ* slab. The percentage void (volume of voids to total volume of a solid slab of equal depth) for hollow-core slabs is between 30 and 50 per cent (increasing with deeper units). For double-tee and beam/plank flooring the voids occupy about 75 per cent of an equivalent solid section.

Reinforced concrete versions of the above are equally valid, usually in short lengths for standard applications, e.g. housing. However, as explained in Chapter 1, unless there are special reasons for using a solid floor (e.g. vibration damping) or the prefabricator wishes to increase the turnover for the project and manufacture the units as reinforced, the advantages gained from maximum performance often outweigh the additional costs.

Beam-and-block flooring, shown in Figure 3.7(d), is restricted mainly to low-rise domestic or commercial work, while other forms of solid rc slabs or solid prestressed joists cannot compete structurally or economically with hollow-core or double-tee flooring systems. Comprehensive design and detailing information is given in Chapter 5. The following is a brief introduction to these units.

Table 3.2 compares the relative structural performance and costs of a selection of hollow-core and double-tee units. The data are for the cost of units supplied and fixed on site, but exclude the cost of pouring *in situ* infill and laying structural toppings. The higher costs for the larger double-tee units reflect the additional craneage and haulage costs associated with these units. The data were collected in the UK in 1993 and were based on the design of floor units for 5 kN/m^2 superimposed loading over a 6 m span. The haulage distance used in the exercise was 100 km.

3.2.2.1 Hollow-core units

Hollow-core units (hcu) are now the most widely used type of precast flooring; in Europe annual production is in the order of 30 million m^2, representing 40 to 60 per cent of the precast flooring market. This success is largely due to the highly efficient design and production methods, choice of unit depth and capacity, surface finish and (last but not least) structural efficiency. In this context only the machine-cast units will be discussed, although it is equally possible for hcus to be wet cast into moulds, recently using self-compacting concrete around rectangular or circular polystyrene void formers.

The load-bearing capacity of hollow-core slabs is such that they work most economically when the span/depth ratio is around 40, i.e. a 200 mm-deep unit spanning 8.0 m will carry a total uniformly distributed live load of 7.5 kN/m^2 plus 1.5 kN/m^2 finishes (already built into the graphs), suitable for many applications. Figure 3.8 is a guide to imposed load capacity (kN/m^2) versus clear span (m) for hollow-core units between 150 and 500 mm depth.

(a)

(b)

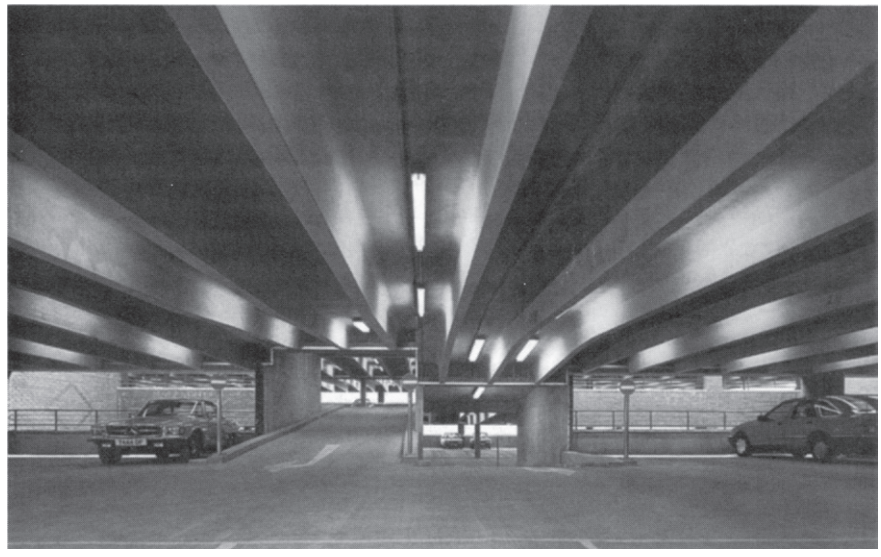

Figure 3.7 Most common types of precast floors used in skeletal structures. (a) Hollow-core units and double-tee slabs used in the same structure; (b) double-tee slabs used in parking structures (courtesy of Frank Graham Consulting Engineers). (c) The precast soffit part of a composite plank floor. The spaces between the girders may contain polystyrene blocks or similar for weight saving. (d) Beam-and-block flooring (courtesy of Bison Manufacturing Ltd, UK). (e) Wide beam and block floor.

The design of dry cast hcus originated in the USA in the early 1950s, following the development in 1951 of high-strength 3-wire and 7-wire helical strand that could be reliably pretensioned over distances of 100 to 150 m. This coincided with advancements in zero slump (hence the term 'dry') concrete production which, owing to quality-control constraints, inevitably led to factory-engineered units. Concrete extrusion techniques were first introduced in the USA following their development in Germany in the 1930s. Slip-forming followed later. The first units were 2 feet wide, and later ones

(c)

(d)

Figure 3.7 (*Continued*)

were 1.2 m wide, as is the case today. Attempts to produce units 3.6 m wide in the factory have not been successful, although very wide units (11 feet) have been produced in the open air for specific projects in the US. During the 1960s the industry experimented with different methods of forming the cores, using flexible pneumatic tubes (called 'flexicore') or tubes loosely filled with stones, but production rates could not compete with the extrusion or slip-forming production-line methods.

For many years the maximum depth of hcus was 400 mm; the restriction in depth was due mainly to instability in the narrow web. However, developments in Northern Europe have led to a 500

(e)

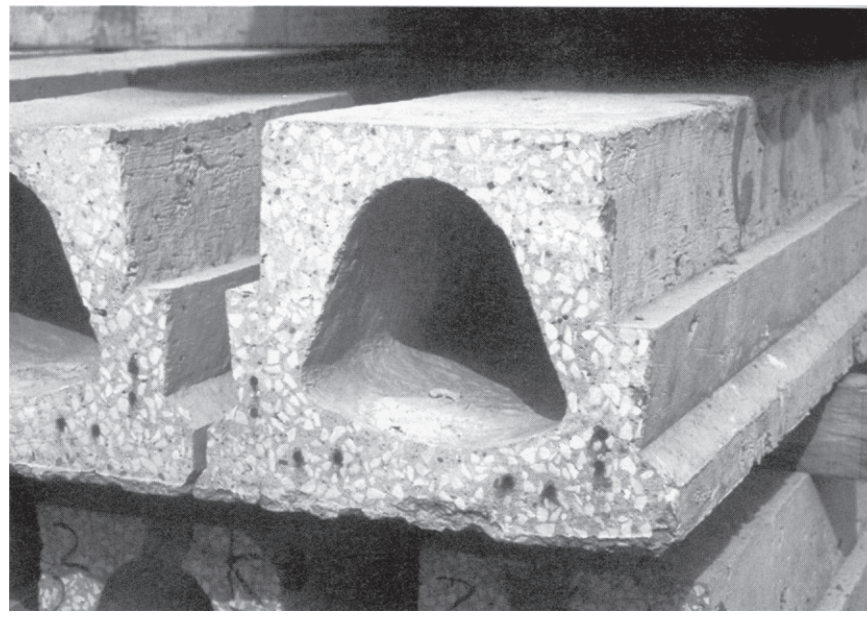

Figure 3.7 (*Continued*)

Table 3.1 Basic properties and performance characteristics of precast flooring

Type	Typical widths (mm)	Typical depths (mm)	Approximate self-weight (kN/m^2)[2]	Approximate maximum span[1] (m)
Hollow-core	**1200**, 600, 400, 333	110	1.90	7.0
		150	2.50	8.5
		200	3.35	10.5
		250	3.70	12.8
		300	4.20	14.5
		400	5.00	17.8
		500	6.30	20.3
Double-tee (composite[3])	**2400**, 3000	400	3.5–3.7[4]	14.5
		500	3.8–4.1	17.3
		600	4.2–4.5	20.0
		700	4.5–4.9	22.5
		800	4.9–5.4	25.2
Composite plank (rc)[7]	1200, **2400**	75/75[5]	3.75	5.40
		100/100	5.00	6.85
		150/150	7.50	9.80
Composite beam & plank	900–2400 beam centres	455/115[6]	4.2–6.6	17.8
		550/115	4.5–7.4	20.9

Data for exposure class XC1 using $f_{ck} = 45\,N/mm^2$ (55 cube) and limiting tension = f_{ctm}.
Quasi-permanent load factor $\psi_2 = 0.3$.
[1] Self-weight as site fixed, including infilled joints.
[2] Span for superimposed loading of $1.5\,kN/m^2$ plus $1.5\,kN/m^2$ of finishes.
[3] Composite slab with 75 mm topping, including finishes $1.5\,kN/m^2$.
[4] Self-weight varies with manufacturer.
[5] Depth of precast plank/depth of *in situ* topping, including finishes $1.5\,kN/m^2$.
[6] Depth of precast beam/depth of plank and topping, including finishes $1.5\,kN/m^2$.
[7] Propped at 2 points at 1/3 span.

Table 3.2 Economic and structural comparison of hollow-core and double-tee slabs

Flooring type	Depth (mm)	Structural performance index*	Mean cost index*
Hollow-core units	150	0.6 to 0.7	0.94
	200	1.00	1.00
	250	1.5 to 1.6	1.17
Double-tee units	400	2.0 to 2.8	1.7
	500	3.0 to 4.0	2.0
	700	5.5 to 6.5	2.6

* based on 200 mm-deep hollow-core unit.

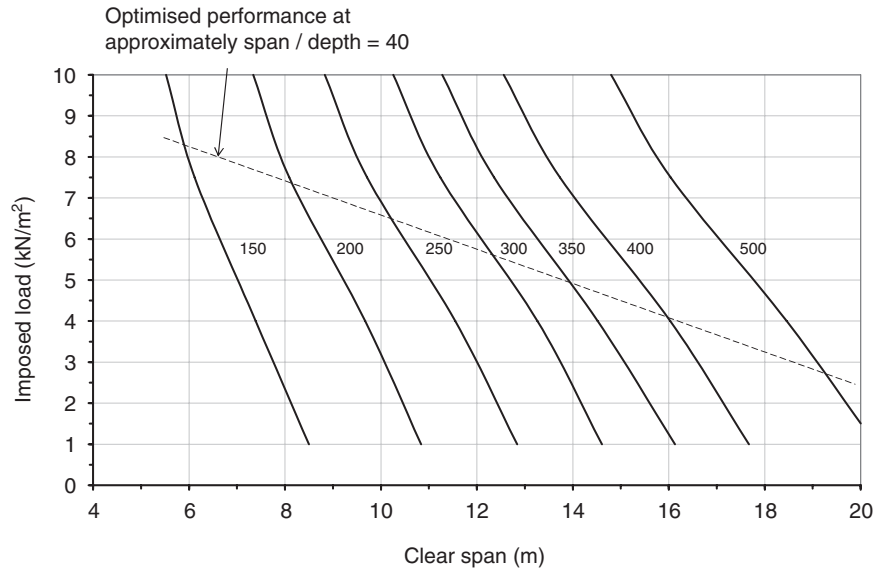

Figure 3.8 Imposed load versus clear span for prestressed hollow-core floor units; includes 1.5 kN/m^2 finishes. If finishes are less than this, deduct the difference when reading the *y*-axis.

mm-deep unit, shown in Figure 3.9. This slab has a 53 per cent void content and requires a special sturdy saw to cut it to length.

Hcus are manufactured using the long-line extrusion or slip-forming process, in which the degree of prestress and depth of unit are the two main design parameters. Steel beds, of very high accuracy, are used in lengths of up to 150 m. Many plants in warm and dry climates are uncovered, so there is less handling as the stockpile can be placed alongside the bed. Nearly all European plants are under cover, many in heated environments. Dimensional deviations are less than ±5 mm in depth and width, and ±10 mm in length. Cross section, concrete strength and surface finish are standard to each system of manufacture. Small variations include increased fire resistance by raising the level of the centroid of the tendons, provisions for vertical service holes, opening of cores for special fixings, cut-outs at columns, etc. Openings and cut-outs are easily formed while the concrete is 'green', i.e. less than 12 hours old, as shown in Figure 3.10, but afterwards the operation is more expensive.

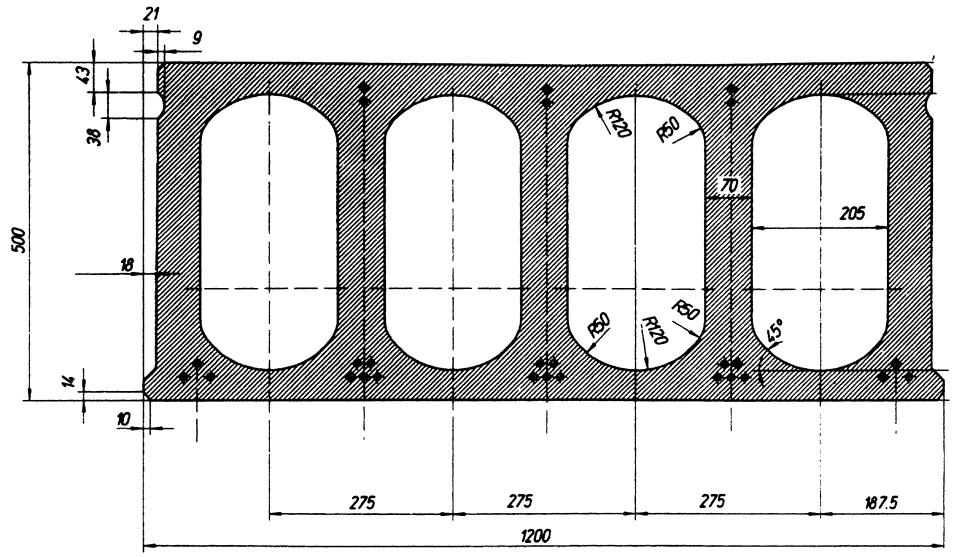

Figure 3.9 Cross-section of 500 mm deep hollow-core floor unit (courtesy of B + FT).

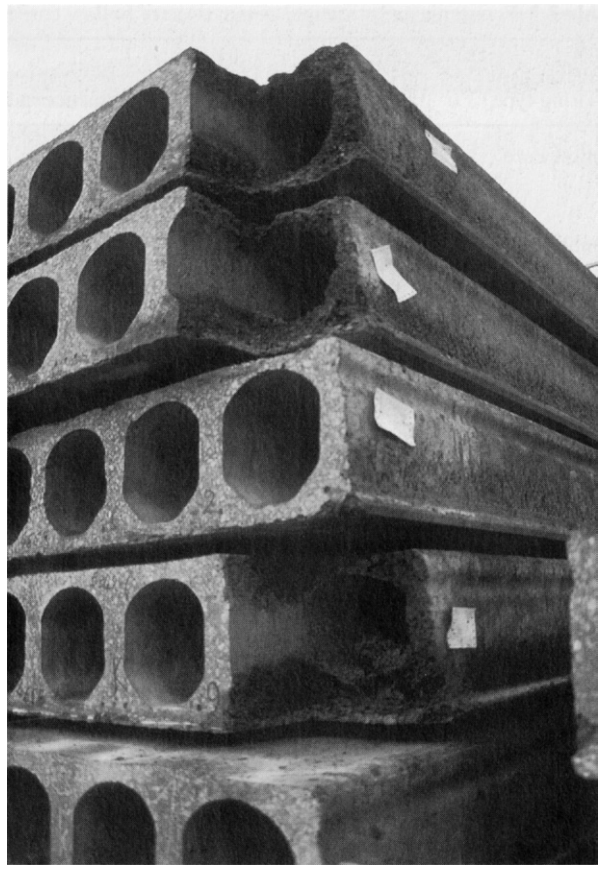

Figure 3.10 Cut-outs for services or check-outs around obstructions are made whilst the concrete is young.

Figure 3.11 2.4 metre-wide hollow-core units using Spirol equipment, manufactured by Preconco, Barbados.

The width of units is based on a nominal 1200 mm grid. More than 95 per cent of units produced are 1200 mm wide. The actual width of 1197 mm allows for constructional tolerances and prevents over-running of the floor layout due to cumulative errors. To maintain repetition in the flooring layout, and hence in the detailing of slabs and beams, the most economical framing plan is columns centred on a 1.20 m modular grid. Hollow-core units 2.40 m wide – see Figure 3.11 – are commonly produced in large quantities in the USA. Outdoor production of 11.0 m long × 3.35 m wide units was achieved for a specified project in the USA where a casting yard was established close to the site.

The slabs are cut to length using a circular saw. Although the cut gives a square end as standard, skew or cranked ends – which are necessary in a non-rectangular framing plan – may be specified. Longitudinal cutting is possible, as shown in Figure 3.12. This operation shows how *in situ* concrete, which was placed into the hollow core through a slot formed during the manufacturing process, penetrated the hollow core for a distance of about 600 mm along the slot. It also shows the degree of compaction possible when concrete is placed into hollow-core slabs, information which is particularly useful where a solid section is specified.

Hollow cores may be used as warm-air heating or cooling ducts, as shown in Figure 3.13. The UK's Building Research Establishment has been studying the cleanliness of conditioned air through the voids, and found it to be satisfactory [3.1]. Hollow-core slabs are also being used to cool the structure in summer and heat it in winter [3.2]. The webs of the slabs are punctured at various positions to create one continuous 'tube' snaking along the floor slab. The proprietary system 'TermoDeck®' was developed in Scandinavia for this purpose [3.3]. It is more a passive than an active system, where the hcus are cooled by the cooler air in the ducts. In the Middle East, where TermoDeck is very common on flooring projects up to 330,000 m^2, the reduction in installed cooling capacity has been measured at between 47 and 62 per cent of conventional air-con systems [3.4]. The cooling works at night, gradually gaining heat over a 12-hour cycle. There are obviously limitations to this method of air transport, particularly across beam lines where the cores are filled with *in situ* concrete, but alternative routes may be found at such locations.

A recent development, mainly in the Netherlands, is so-called 'pipe floor', shown in Figure 3.14. The top part of hollow-core slabs is thickened by 70–100 mm to allow grooves to be cut during manufacture, in which pipes, conduits, etc. are laid in the factory and connected on site. While the thermal mass is clearly advantageous, there is a small structural disadvantage due to the top

Figure 3.12 Longitudinal cutting of hollow-core slab is expensive, but often unavoidable.

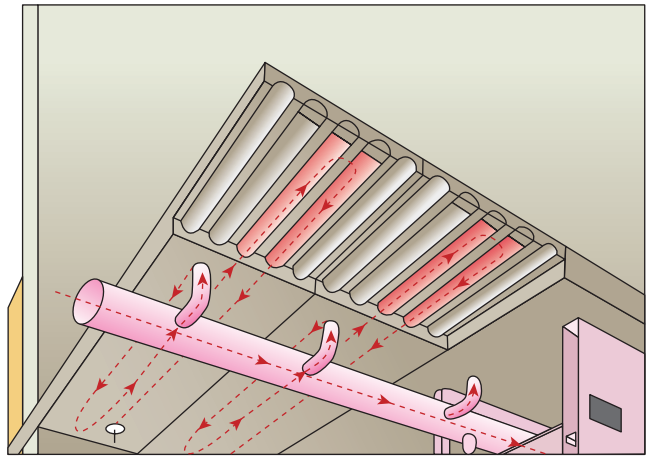

Figure 3.13 The principle of the air-conditioning system passing through the cores in hollow-core slabs (courtesy of Tarmac Building Products, 2010).

thickening, which cannot be used structurally because of the pipe grooves. In places without the pipe grooves, the imposed load capacity of, say, a 200 mm-deep hcu spanning 6.0 m would reduce from 12.7 kN/m^2 to 11.5 kN/m^2 when the thickness of the top flange of the hcu had been increased from 30 to 100 mm to cater for the ducts.

The fire resistance of hollow-core floor units is in accordance with EN 1168:2005+A3, 2011 [2.22], the European Product Standard for prestressed hollow-core units. See Table 3.3. Fire rating, e.g. R60 for 60 minutes' structural resistance, is a function of the mass of concrete, given by its effective thickness and the mean distance to the centroid of the tendons in the tension zone (called axis distance, *a*). For solid plank, refer to BS EN 1992, Part 1–2, clause 5.2(5) and Table 5.8 [2.20]. For hollow-core units, refer to EN 1168:2005, Annex G. The data in Table G.1 are for siliceous aggregates. Granite, sandstone, greywacke perform no worse. If calcareous aggregates (calcareous or dolomitic limestone)

Figure 3.14 The main features of pipe floor in hollow-core slabs. This demonstration floor is at VBI in Holland, 2008.

Table 3.3 The effective thickness and axis distance for solid plank and hollow-core slabs required for fire resistance

Fire resistance (mins)	Total effective thickness for solid, hollow-core units and composite slab (mm)		Axis distance *a* to BS EN 1992 or EN 1168 (mm)
	Solid unit to BS EN 1992	Hollow-core to EN 1168	
30	80	130	10
45	80	130	15
60	80	130	20
90	100	160	30
120	120	200	40
180	150	250	55

are used the required effective thickness t_e and average axis distance a are increased by 10 per cent, where: a = distance to centroid of tendons in tension zone = cover + tendon radius. The slab thickness is according to BS EN 1168+A3:2011, Table G.1 [2.22]. The thickness corresponds with the minimum solid floor thickness given in Table 5.8 of BS EN 1992, Part 1–2, summarised here in Table 3.3, and has been calculated using a conversion equation for hcu as $t_e = h\sqrt{\zeta}$ where h = actual depth and ζ = ratio of solid material (including infilled joints) to the whole. Unfortunately the data in Table G.1 are based on $\zeta = 0.4$, a rather low value for most proprietary hcu, where the ratio of solid material is typically $\zeta = 0.5$ for the deeper units (250 to 400 mm), where fire resistance is limited by axis distance rather than thickness, but about $\zeta = 0.65$ for shallower units (150 to 200 mm) that may be limited by thickness. For example, a certain 1200 mm wide × 150 mm hcu made of gravel aggregates has a fire resistance of 60 minutes. This hcu has gross concrete area plus infill in the joints of 120,000 mm^2. Then $\zeta = 120{,}000/180{,}000 = 0.667$, and $t_e = 150 \times 0.816 = 122.5$ mm. According to Table 3.3 a solid slab of this thickness will have a fire resistance of 120 minutes, not 60 minutes as the parent hcu. An hcu made of limestone aggregate with $h = 1.1 \times 150 = 165$ mm has 90 minutes.

For prestressed concrete reinforced using strand and/or wire, the axis distance a must be decreased by 15 mm in accordance with BS EN 1992-1-2, clause 5.2.(5) [2.20]. The axis distance for individual

tendons should not be less than 10 mm. Thus for a certain hollow-core unit pretensioned using 12.5 mm-diameter strands at 40 mm cover, axis distance $a = 40 + 12.5/2 - 15 = 31$ mm. According to Table 3.3 the slab will have a fire resistance of 90 minutes. If the aggregate is limestone, $a = 1.1 \times 46.25 - 15 = 36$ mm, and R90 still applies. It is clear that for depths of 150 mm or more, axis distance is the controlling factor.

Most of the fire tests and associated research work on hollow-core slabs was carried out between 1960 and 1980. The work covered a wide range of slab cross sections, together with variations in reinforcement quantities and position, cover to soffit and void, etc. Most tests were carried out in small furnaces on bare individual units – that is, without proper restraint or support details, no grouted joints between units, and an absence of the surrounding structure. Some European and UK tests at the BRE fire station indicated that there was a risk of premature shear failure during the heating cycle of a fire. Vertical splitting cracks were seen in the webs due to the incompatibility of the stress response to the stress gradient on heating. These results were disputed by some experts, as the test samples were not considered to be acting in a structural manner representative of that which occurs in a building, where different restraints due to a number of factors can be imposed on the floor slab.

In 2007 [3.5, 3.6]: 'It was decided by the UK Precast Flooring Federation (PFF), in conjunction with the International Prestressed Hollowcore Association (IPHA) and other member companies of the British Precast Concrete Federation, to undertake two full-scale fire tests as part of an ongoing product performance development programme, to see if premature shear failure was truly a potential problem, and by the use of significant instrumentation to better understand how precast hollow-core flooring behaves during the heating and cooling phases of a realistic fire. Both test structures were of single-storey construction using 200 mm-deep hollow-core floor units forming an area of 18 m × 7.5 m, supported 3.6 m above ground level on structural steelwork with infill blockwork panels (Figure 3.15). Average atmospheric temperatures in excess of 1050°C were recorded by thermocouples within the test structures, compared to 900°C required by the standard parametric fire test curve. Both tests were extremely successful, with the hollow-core floor areas maintaining their structural integrity for the full heating and cooling cycles of the tests. There was no shear failure of the type small standard furnace tests had indicated might occur, and these tests demonstrate that such unrepresentative small-scale testing should be treated with extreme caution.'

Until the results of this type of work are accepted in codes of practice, standard fire designs for hollow-core floors are currently based on a requirement for a 60-, 90- or 120-minute fire resistance, in accordance with BS EN 1168 [2.22] and BS EN 1992, Part 1–2 [2.20]. The latter offers three options: namely, calculation, fire testing or tabulated data, with the latter being commonly adopted by the industry. There is a slight penalty to pay in the flexural strength (about 10 per cent) of the units with increased fire resistance. For example, a certain 200 mm-deep unit pretensioned using 12.5 mm strands at 30 mm cover, $a = 36.25 - 15 = 21$ mm, will achieve R60 fire resistance and a moment of resistance of 87 kNm, compared with 79 kNm by raising the strands 20 mm extra to achieve R120. Greater fire ratings of up to R240 can be achieved by the application of soffit finishes.

Holes in the floor are dealt with in one of two ways, depending on size. Small holes of less than about 600 mm in size may be formed in the precast unit (except in 600 mm-wide hollow-core units, where the maximum size is 300 mm) during the manufacturing stage and before the concrete has hardened. The cost is small and the result is as shown in Figure 3.10. The rough edges are beneficial to the shear key with *in situ* concrete infill. The voids are usually formed manually, although there is scope to automate this within the machine's operations.

The maximum size of hole which may be formed in the units depends on the size of the voids in the slab and how much reinforcement may be removed without jeopardising the strength of the unit. For example, in a 200 mm-deep extruded unit (e.g. *Spiroll*) the diameter of the void is 150 mm and therefore a hole formed through the void may be of equal size. In a 200 mm-deep slip-formed unit (e.g. *Roth*) the diameter of a hole is limited to the width of the void, which is only 100 mm. General FIP information for restrictions on hole size and location is given in Figure 3.16(a) [2.36]. Figure 3.16(b) gives further information from product literature for a range of 1200 mm-wide units produced by the Partek Company [3.7]. Table 3.4 shows the limits on geometry applicable to Figure

(a)

(b)

Figure 3.15 Fire tests. (a) Three 6.0 m wide bays of 7.0 m span hollow-core slabs are on top of the blockwork walls during the 3-hour test, which reached 1050°C. (b) Afterwards the integrity of the floor was assured. (Courtesy of Precast Flooring Federation, Leicester 2007.)

Table 3.4 Limits imposed on cut-out geometry (see Figure 3.16 (b))

Depth of slab (mm)	Corner cut-out L × B (mm)	Edge cut-out L × B (mm)	End cut-out L × B (mm)	Middle cut-out L × B (mm)	Middle hole diameter, Φ (mm)
150	600 × 400	600 × 400	1000 × 400	1000 × 400	80
200	600 × 380	600 × 400	1000 × 380	1000 × 400	130
265	600 × 260	600 × 400	1000 × 260	1000 × 400	130
320	600 × 260	600 × 400	1000 × 260	1000 × 400	170
400	600 × 260	600 × 400	1000 × 260	1000 × 400	170

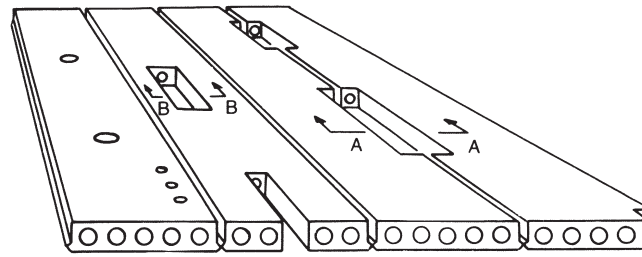

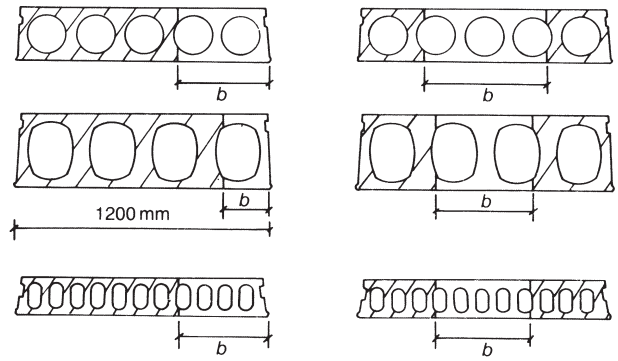

(a) Section AA, $b \leqslant 430$ mm Section BB, $b \leqslant 600$ mm

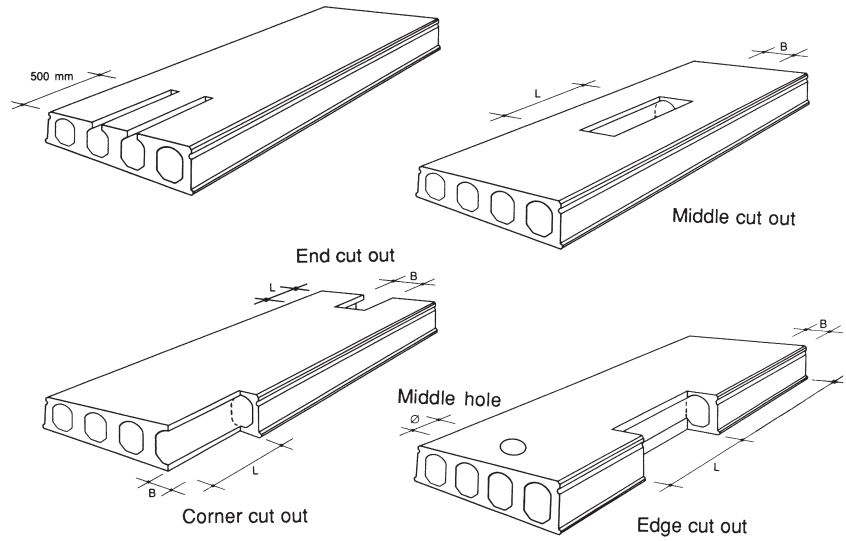

(b)

Figure 3.16 Trimmer details around floor voids: (a) restrictions on hole sizes in hollow-core units from FIP; (b) example hole limitation data for 1200 mm wide units (courtesy of Partek Company); (c) steel trimmer angles used to support floor units around a small void; (d) concrete trimmer beams used to support floor units around a large void (greater than about 2.4 m side).

(c)

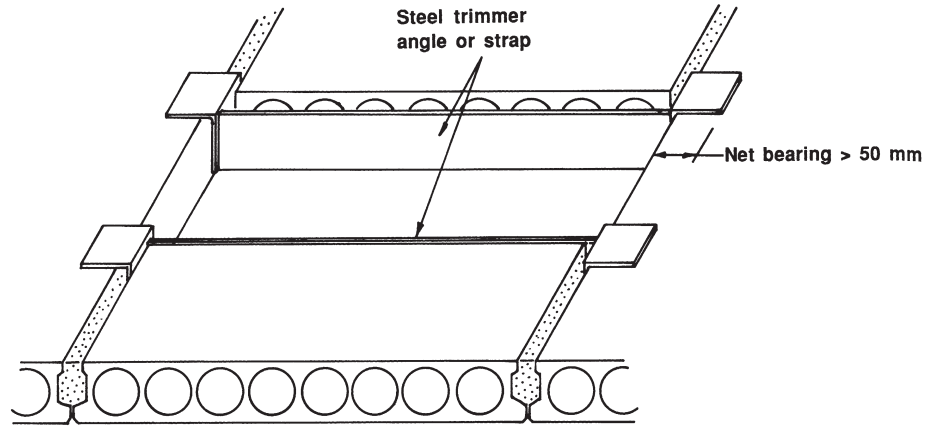

(d)

Figure 3.16 (*Continued*)

3.16(b). Small holes, up to about 150 mm diameter, can be core-drilled on site. The holes should pass through the hollow core, and the designers *must* be consulted if any of the reinforcing bars are accidentally removed. This can impose quite severe restrictions on the M & E services, but a way of increasing freedom is to provide additional reinforcement in the slab and to specify permitted 'zones' in which a limited number of holes at a predetermined spacing and size may be site-drilled.

Larger voids that are wider than the width of the precast units are 'trimmed' using transverse supports such as steel angles (i.e. perpendicular to the span of the floor), as shown in Figure 3.16(c), or concrete beams for larger openings as shown in Figure 3.16(d). A typical minimum section size for the steel trimmer is $100 \times 100 \times 8$ mm equal angle. The angles carry point loads to the edges of the adjacent units. The maximum practical size of hole is about 2.4 m × 2.4 m for normal office loading, but is less for superimposed floor loads greater than about 7.5 kN/m^2. There is some additional margin of safety in the design of trimmer angles, because the grouted longitudinal joints between the slabs will transfer some of the superimposed loading to adjacent slabs. The steel angles must be properly

fire-protected, either by precasting concrete to the soffit and sides of the angle or by spraying them with a fire-protective coating.

It is not possible to cast sockets or other fixings into the soffits or sides of prestressed floor slabs. These must be formed on site using proprietary anchor or toggle bolts. Shot-fired fixings are not recommended for prestressed units. Ceiling hangers are used extensively in commercial buildings, where ceilings and extensive electrical and mechanical services are suspended. Information sheets giving comprehensive details of these and other provisions are available from the flooring manufacturers.

One note of caution when using hollow-core slabs in wet and cold climates is that water may penetrate into the hollow cores through the open ends of the cores, or even through small drag cracks in the top flange. If this water is allowed to gather and expand by freezing there is a possibility that the bottom flange will explode off the unit. A simple remedy is to drill weep-holes in the bottom of the slabs, usually during manufacture.

3.2.2.2 Double-tee slabs

These units originate from the United States, where they have been used extensively since the 1940s for what are termed 'medium spans', i.e. up to 25 m simply supported span. Double-tees formed the principal slab units in the NBF (Figure 1.3), and they enjoyed the leading market share in precast flooring until the late 1960s, when hollow-core became the preferred slab. Their major structural advantage may be seen in Figure 3.17, where the deep web and shallow top flange maximise the moment of inertia compared to self-weight.

Single-tee units were found to be less economical in terms of quantity of concrete per unit area, in addition to lacking stability during erection. In the early days of development the units were reinforced; prestressing followed later.

Typical cross sections through prestressed precast double-tee units are shown in Figure 3.18. Various attempts were made to hide the longitudinal joint over the centres of the webs in an F configuration, shown in Figure 3.19. This failed, owing to non-symmetrical prestressing requirements and differential stiffness problems where the flange of one unit was bearing over the stiff web of its neighbour. After exhaustive research the double-tee section is still most widely used.

Figure 3.17 Prestressed (or sometimes reinforced) double-tee floor units.

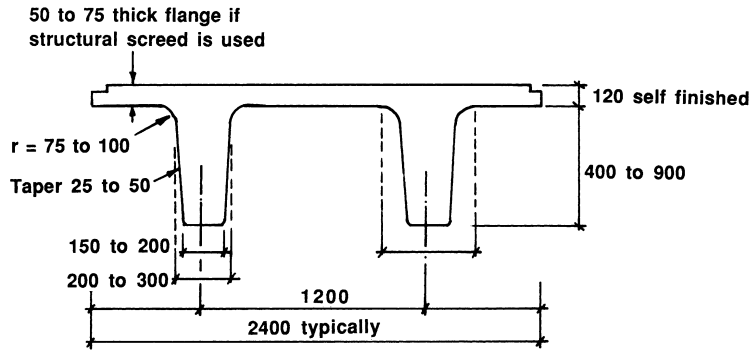

Figure 3.18 Shapes of double-tee floor units.

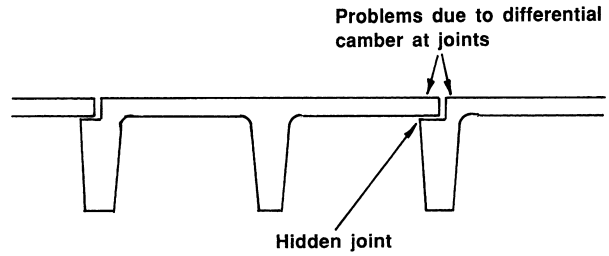

Figure 3.19 Historical development of shapes of double-tee slabs.

The main advantages in using these types of unit (over the hollow-core units) are:

- load-carrying capacity, although this advantage has been eroded by the introduction of 400 mm- and 500 mm-deep hollow-core slabs
- the ends of the units can be notched to one-third of overall depth to form a halving joint to reduce the overall structural depth
- the units are manufactured as standard up to 2400 mm wide (actually 2390 mm) or 2500 mm wide – thus reducing the number of units to be fixed on site. However, there is no reason why other widths, e.g. 3.0 m, should not be manufactured to meet the requirements of a particular project.

However, owing to the shallow flange depth an *in situ* reinforced concrete structural topping is required to ensure vertical shear transfer between adjacent units and develop horizontal diaphragm action in the floor plate.

The standard end profile is square, although contoured ends may be specified by shaping the flanges to suit the structure. The ends of ribs are always square. If vertical service voids are required adjacent to supporting beams, then forked ends may be formed by cutting back the flanges over the full width of the unit, as shown in Figure 3.20. The ribs must be maintained at full length to facilitate the welded connections at the supporting beam.

Double-tee units have a minimum fire rating of R120 providing the correct depth of screed is used. Other units with wider ribs and thicker flanges achieve a R240 rating. Greater fire rating can be achieved on all units by the application of soffit finishes. The slabs are manufactured in steel moulds with a high degree of dimensional stability and excellent surface finish. The soffit is type A to BS EN 13670 [2.29] (via the NSCS-4 [2.31]).

Holes may be formed in the positions shown in Figure 3.21. In no circumstances should vertical holes be formed through the webs of double-tee units. The circular holes through the webs are

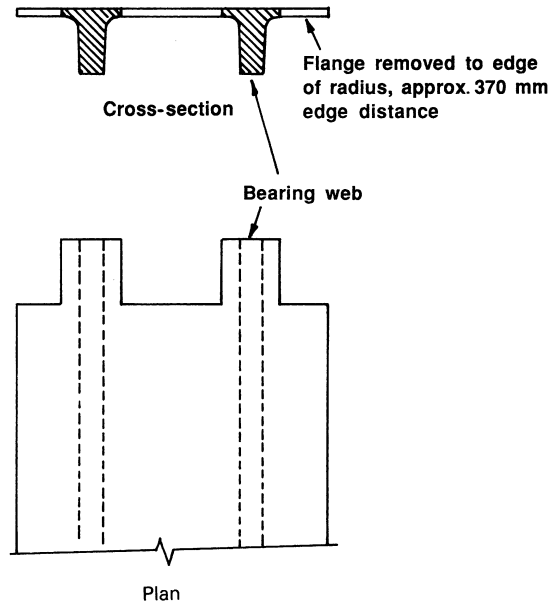

Figure 3.20 Forked ends in double-tee floor units.

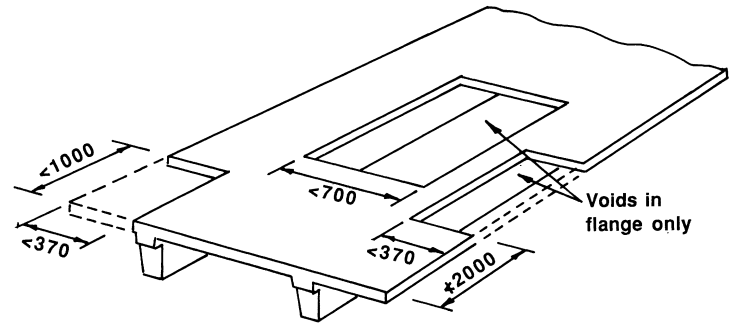

Figure 3.21 Guidelines for the permitted sizes and location of voids in double-tee floor units.

sometimes provided as standard at 1200 mm centres, so that they provide a passage for services where they cross the double-tee units at right angles.

The positions and sizes of additional horizontal holes need to be planned in advance because they may affect the shear capacity of the slab, or require alteration of the position of the prestressing reinforcement. Holes and notches in the flanges are best formed in the units immediately after manufacture and before the concrete has hardened, although site cutting is permitted with the manufacturer's consent and within their specified limitations.

3.2.2.3 Comparison of hollow-core and double-tee slabs

The designer is immediately faced with the choice of floor slab. The competition between hollow-core and double-tee units is still quite acute in some countries, particularly as double-tee units can be manufactured in house without the need for specialist equipment such as extrusion and slip-forming machines. The first restriction is often the total depth of floor slab and this must include an allowance for the upward camber of prestressed floor units, as the thickness of the finishes (or structural topping) is greater towards the support, typically 10–20 mm for a 6 m span, and 20–30 mm for spans

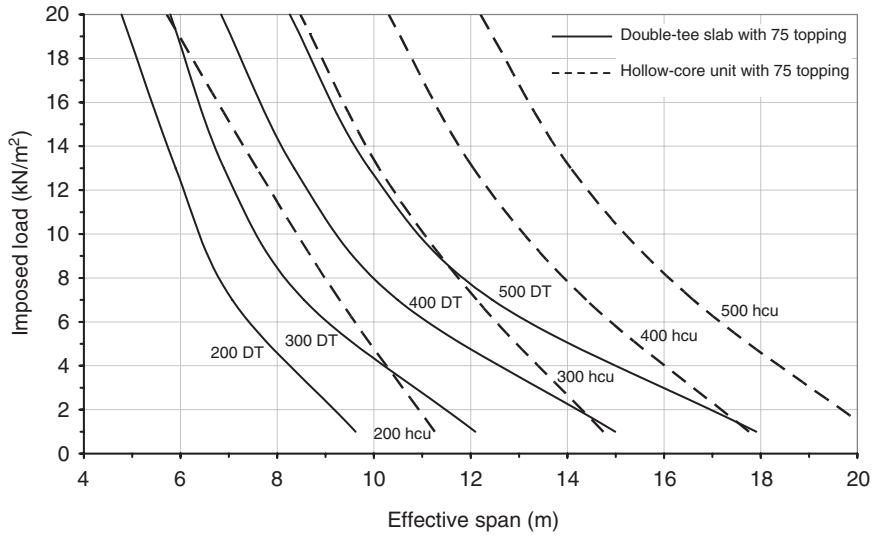

Figure 3.22 Load versus span graph comparing composite hollow-core and double-tee units.

around 10–12 m. Given the imposed floor loading (kN/m^2) and the effective span (= clear span plus ½ bearing length at both ends, typically 100 mm for hollow-core and 150 mm for double-tee), Figure 3.22 may be used to determine the structural depth of the floor slab, remembering to add the upward camber for the total depth. The precast depth varies from 200 to 500 mm, while the structural depth varies from 275 to 575 mm.

To allow a fair comparison between hollow-core and double-tee, this graph is for composite slabs, i.e. precast unit plus 75 mm structural topping. It already allows for 1.5 kN/m^2, leaving only the imposed loading to be read from the graph, which has been prepared using a live load subject to a quasi-permanent factor $\psi_2 = 0.3$ and an ultimate load factor $\psi_0 = 0.7$. As it happens, the units are mostly critical for the service moment, where neither of these two factors applies, so the imposed load may be a combination of dead and live without too much loss of accuracy. Exposure class is XC1. Concrete strength $f_{ck} = 45$ N/mm^2 and at transfer $f_{ck}(t) = 30$ N/mm^2. The precast units are all propped at two points, at ⅓ span.

More load versus span data are presented in Chapter 5 for non-composite units.

The key, e.g. 200 DT, means 200 mm-deep precast hollow-core plus 75 mm topping. Graph allows 1.5 kN/m^2 finishes. Load factors are $\psi_2 = 0.3$ for deflection and $\psi_0 = 0.7$ for ultimate. The units are propped at ⅓ span.

Figure 3.22 shows that the hollow-core slab outperforms the double-tee slab by on average 34 per cent on span, e.g. for an imposed load = 10 kN/m^2 and 375 mm structural depth, the limiting span is 7.5 m for double-tee and 11.0 m for hollow-core. Conversely, for a span of 10.0 m the load capacity of the double-tee is 4.2 kN/m^2, while the hollow-core is 13.4 kN/m^2. The double-tee is critical at the service moment of resistance, while the hollow-core is critical at the ultimate moment of resistance. Note that the double-tee unit has an area of tendons to concrete ratio $\rho = A_p/A_c = 0.45$ per cent, and a self-weight $w = 3.1$ kN/m^2, but the hollow-core is $\rho = 0.61$ per cent and $w = 4.0$ kN/m^2. Because the tendons in the double-tee unit may be debonded at the support, the level of prestress can be much greater than in the hollow-core unit, where tendons cannot be debonded. Thus, the bottom prestress at mid-span in the double-tee is possible up to about $f_{pB} = 24$ N/mm^2, but is limited to about $f_{pB} = 13$ N/mm^2 in the hollow-core.

The effect of not propping the precast unit while the topping is being cast (see Chapter 6, Section 6.5.3) has no effect on the hollow-core because it was previously critical at the ultimate moment, and propping has no influence there. However, because the 300 mm-deep double-tee has a much lower

section modulus at the bottom ($Z_B = 3{,}360\,\text{mm}^3$ per mm width) than the 300 mm hollow-core ($Z_B = 12{,}700\,\text{mm}^3$ per mm width), it was critical at the service moment. Without propping for a span of 10.0 m the load capacity of the double-tee is reduced to 2.8 kN/m^2, while the hollow-core remains at 13.4 kN/m^2.

It should be noted that as the factors ψ_2 and ψ_0 vary according to the usage of the floor, e.g. the data in Figure 3.22 are for offices and residential, the load versus span data will change. Factor ψ_2 affects only the longer spans and low loads where deflections are critical, but when ψ_2 increases to 0.6 and 0.8 for congregation, shopping and storage areas the higher loads will not render the slab critical in deflections. At these higher loads only $\psi_0 = 1.0$ for storage will cause a small change in the ultimate moment and hence a small reduction in span. For example, taking an imposed load of 10 kN/m^2, the limiting span for the 300 mm precast hollow-core was 11.0 m (Figure 3.22 with $\psi_0 = 0.7$). If $\psi_0 = 1.0$, the limiting span reduces to just 10.82 m.

3.2.2.4 Comparison of depth of structural topping on hollow-core floors

There is often a temptation to increase the thickness of the structural topping in the expectation that it will enhance the load-bearing capacity of the floor. This is certainly true in reinforced concrete slabs, where there is a squared proportional increase in ultimate moment capacity with depth, and a (nearly) linearly proportional increase in span with depth. However, in the particular case of composite prestressed floor slabs, the extra mass of the *in situ* topping, which has a considerably lower concrete strength and Young's modulus than the precast (say C50/60 precast and C25/30 *in situ*), does not always increase the load bearing or span of the basic prestressed unit by the ratio of the additional material. This is clearly shown in Figure 3.23, where 200 mm- and 400 mm-deep hollow-core units, with 0, 75 and 125 mm depth topping, have been selected to make this point.

In the case of the 200 mm-deep hollow-core: for 75 mm topping, the increase in effective span is +4% to +14% for an extra 64% in self weight, and for 125 mm topping the figures are +9% to +22% for an extra 101% in weight.

In the case of the 400 mm-deep hollow-core: for 75 mm topping, the increase in effective span is −1% to +3% for an extra 42% in self weight, and for 125 mm topping the figures are 0% to +7% for an extra 67% in weight. Specifying structural toppings on the deeper prestressed units must be carefully considered for reasons other than improvements in strength or stiffness.

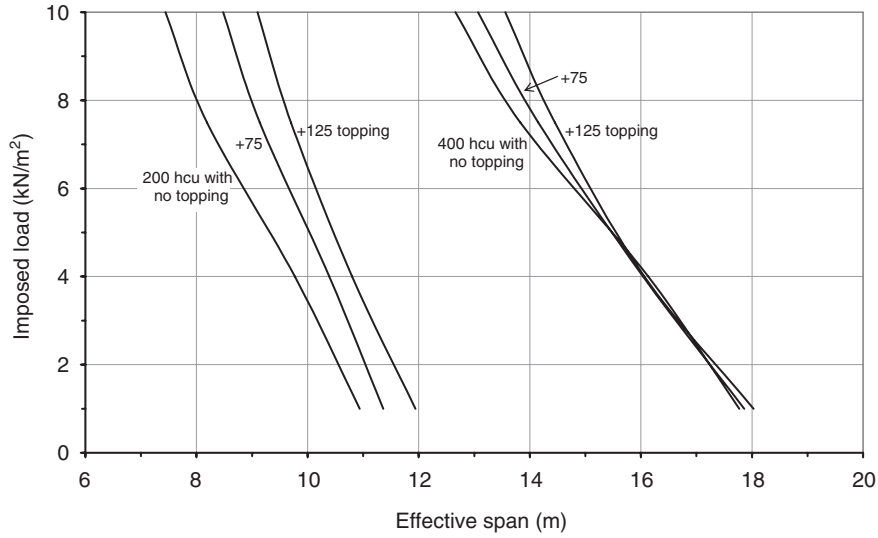

Figure 3.23 Load versus span graph comparing the depth of topping in non-composite and composite hollow slabs. The data are based on the same parameters as in Figure 3.22.

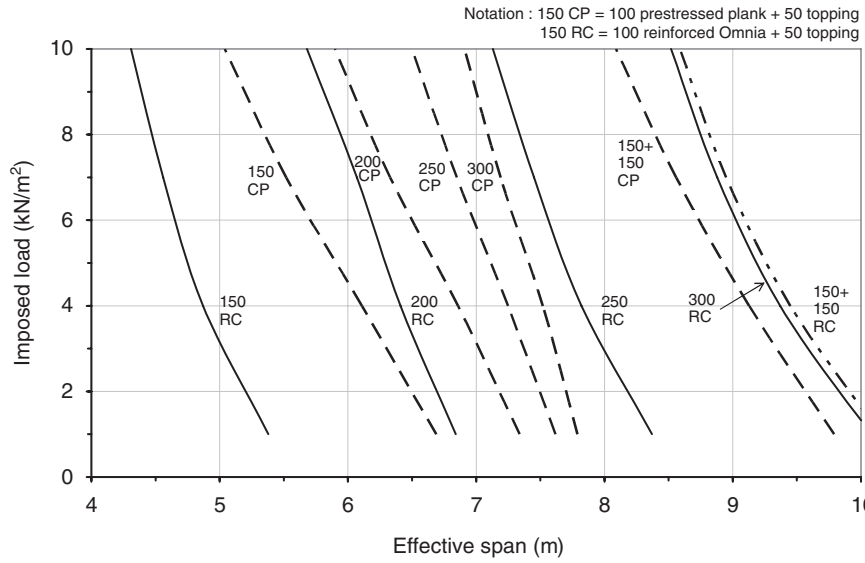

Figure 3.24 Load versus span graph comparing reinforced with prestressed composite plank (solid slabs). Each slab comprises 100 mm permanent formwork plus 50 to 200 mm-depth structural topping, except for 150+150 plots, which use 150 mm soffit plus 150 mm topping. The data are based on the same parameters as in Figure 3.22.

3.2.2.5 Composite plank floors

The principle of these precast units is quite simple: rectangular precast concrete beams or slabs are laid between supports and are used as permanent formwork for an *in situ* concrete topping. Steel bars, wires or tendons placed in the precast units act as the flexural sagging reinforcement, and a light steel mesh (e.g. A142) in the *in situ* concrete acts as hogging reinforcement. The floor slab may therefore be designed as continuous.

The two main versions are (i) rc permanent formwork, often referred to as Omnia, Figure 3.7(c), and (ii) prestressed plank, often called Half-slab, also used as permanent formwork. Figure 3.24 gives the load versus span information for both of these for simply supported slabs, propped during the construction of the topping at two points at ⅓ span. The technical data are the same as for the graph in Figure 3.22, except for one major difference – with the rc plank there is no limit to the amount of reinforcement used in the bottom of the precast part, and so the maximum area of rebars = 4% *bd* is used, where b = breadth (1200, 2400 mm) and d = structural depth minus 35 mm. By comparison the area of prestressing tendons in the prestressed plank is 0.67% (6 times less).

Figure 3.24 shows that for composite slabs up to 200 mm in depth, the prestressed plank has a load-bearing capacity 5–20 per cent greater than the rc Omnia type, in spite of the huge difference in area of steel used. The prestressed slab works very efficiently until the topping becomes excessive ≥ 150 mm and, as mentioned earlier, the extra topping is a hindrance to the prestressed unit. Conversely, the load-bearing capacity of the rc slab is almost linearly proportional to total depth. Increasing the depth of the reinforced soffit unit from 100 to 150 mm makes little difference, whereas when the prestressed soffit is increased from 100 to 150 mm the capacity increases by 17–26 per cent.

Figure 3.25 shows the construction of the composite floor using beams and slabs monolithically, and using slabs alone, respectively. Monolithic construction is structurally more efficient, and an example is shown in Figure 3.26. In terms of robustness this floor is considered equal to that of cast-*in situ* construction. This floor slab has advantages in using a prefabricated soffit unit (smooth finish, no formwork, up to 2.4 m wide units, rapid fixing), but carries performance penalties on span and self-weight; see Table 3.1. The slab may be made lighter by the use of lightweight block (or even

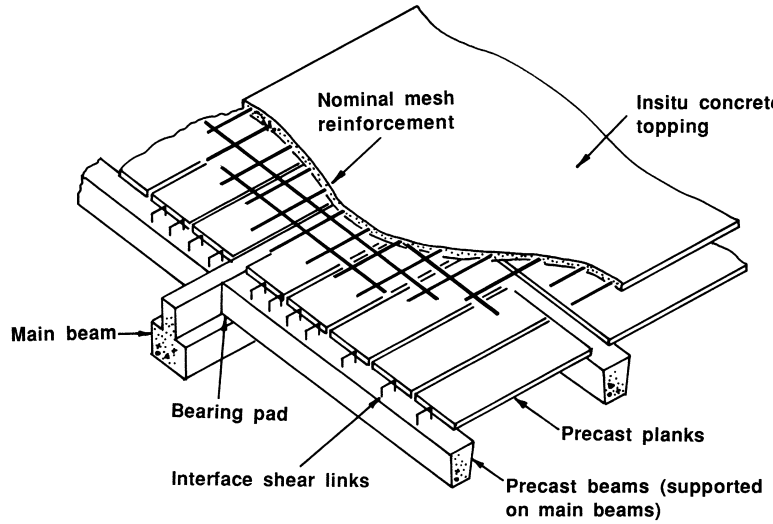

Figure 3.25 Composite beam and plank construction (the beam forms part of a tertiary system).

Figure 3.26 Composite plank construction.

polystyrene) void formers covering part of the planks, or by using a lightweight aggregate concrete topping. Splayed ends or other special shapes may be formed, usually at an extra charge due to the necessity to make alterations to the mould. Where the floor slabs bear onto beams (Figure 3.25), the maximum spans between the primary beams in the structure are in the order of 18 m.

Service openings up to 2.4 m wide may be formed by increasing the strength of the precast unit and placing addition steel around the hole in the *in situ* topping. Cantilevers up to 1.5 m span may be formed by placing additional top steel in the *in situ* topping. The usual fire resistance is R120.

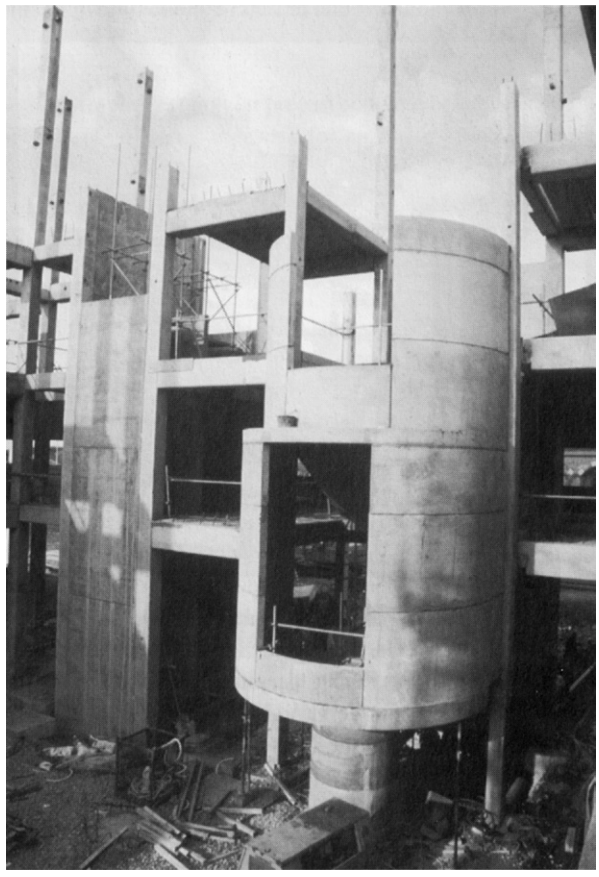

Figure 3.27 Circular staircase tower, later to be overclad in steel sheeting.

Thicker precast planks (up to 125 mm) are used for more onerous fire, durability and loading conditions.

3.2.3 Staircases

Precast concrete staircases are a viable alternative to cast-*in situ* staircases providing there are sufficient numbers and a reasonable amount of repetition. There were twelve identical stair towers on the six-storey Grand Island Project in Manchester, UK, enabling the precast circular staircase shown in Figure 3.27 to be designed economically. Precast staircases with high-quality finishes from steel moulds may be used in other types of structure, such as the *in situ* concrete frame shown in Figure 3.28.

Consistency in tread rise and go are the two main factors affecting repetition. The method of manufacture enables the depth of the waist, number of treads and the width of the flight to be varied readily. The most important factor in the use of the precast stairs is plan configuration and compatibility with the structure. This implies making optimum use of the structure to avoid introducing additional components to cater for the staircase. Various two-flight layouts are shown in Figure 3.29, and a typical three-flight staircase is shown in Figure 3.30 [2.39].

Figure 3.29(a) makes optimum use of the structure – only two short beams are required for the staircase support. It is the least satisfactory solution from the structural (greater span hence depth), and manufacturing points of view. Differential levels at floor and half-landings are difficult to avoid and either a finishing screed or an *in situ* levelling piece is necessary.

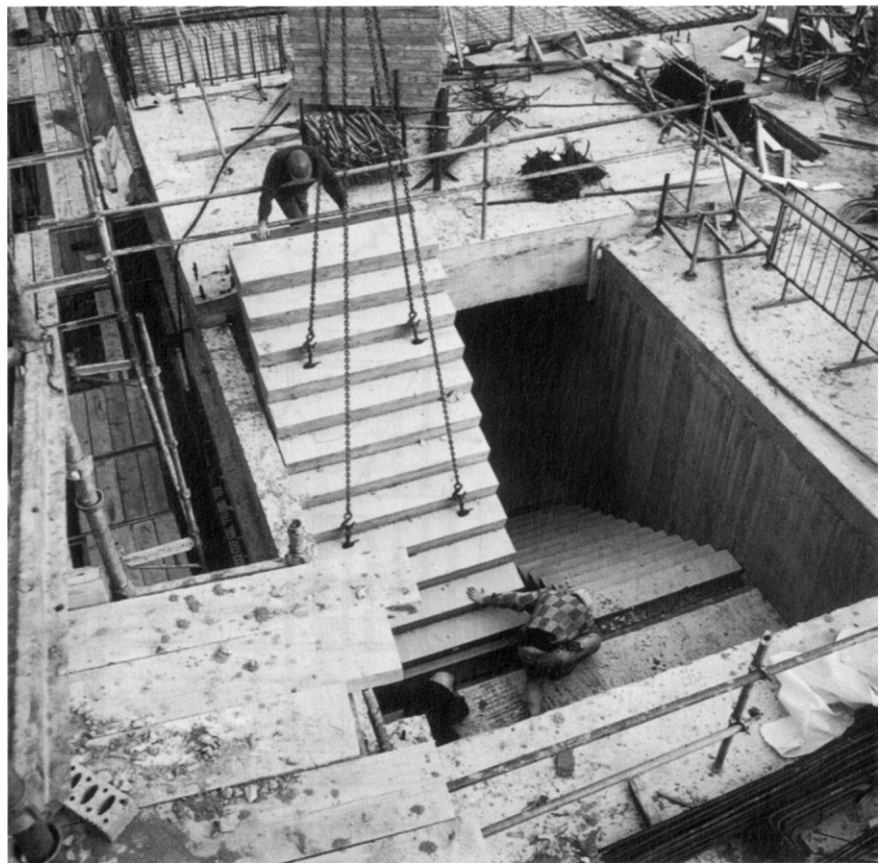

Figure 3.28 Precast concrete staircase positioned in an *in situ* concrete frame (courtesy of Breton Precast, UK).

This would not be the case in Figure 3.29(b), where optimum use of individual precast flights and landings is made possible by the use of halving joints, or support brackets, intended to eliminate construction errors. However, Figure 3.31 demonstrates the need for greater dimensional tolerances where close-fitting elements are to be positioned between two fixed points. The major disadvantage in the arrangement in Figure 3.29(b) is that long-span beams, or stub walls parallel with the flight (typically 4 m to 5 m long), are required both at floor and half-landing levels. *In situ* masonry may be used as half-landing support, but that enforces a strict programme both on the main contractor and the precast fixing team. Efforts should be made to make the floor and half-landings identical.

Figure 3.29(c) makes optimum use of the supporting beams and precast staircase units by casting the flight and half-landing in one piece. This solution enables cantilever half-landings to be expressed beyond the edge of the building, as shown in Figure 3.32. These may be rectangular, semi-circular or chamfered in plan, and the external stairway cladding may be carried by the precast members. A minimum waist of 150 mm is required in all cases for handling purposes and fire resistance.

In the three-flight staircase shown in Figure 3.30 various options are available to the designer, but the importance of minimising the number of precast components while maintaining simplicity of manufacture cannot be stressed too highly. Cantilevers may be specified providing consideration is given to an adequate tie back and to the design of the support beam, which must be profiled to suit the different landing levels.

Fixings for balustrades, lighting, security, etc. may be incorporated in precast staircase and landing units, but it is often more economical and accurate to drill and fix on site. The edge distance to holes

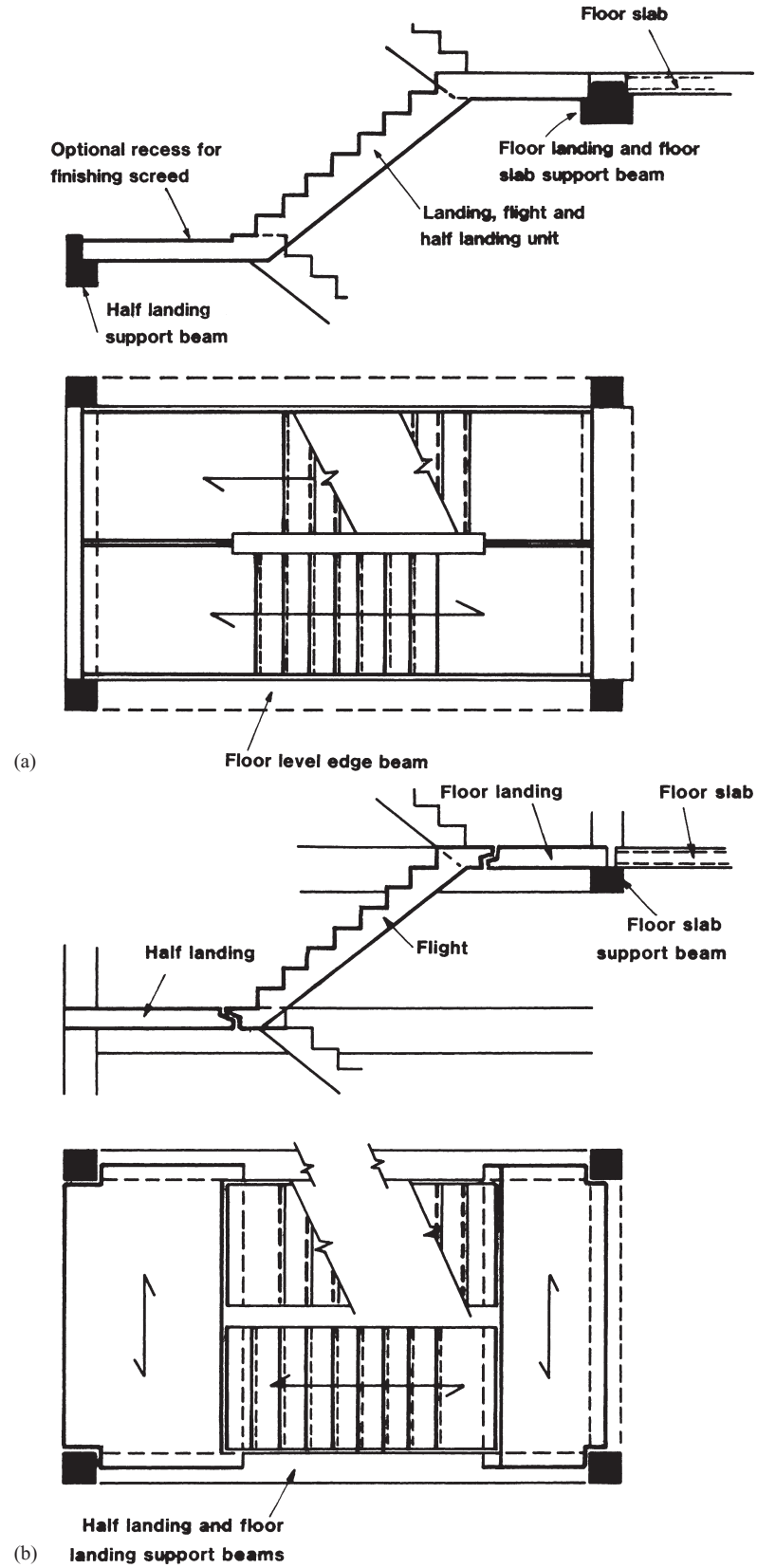

Figure 3.29 Possible options for the layout of a two flight staircase. (a) Option 1; (b) Option 2; (c) Option 3 [2.6].

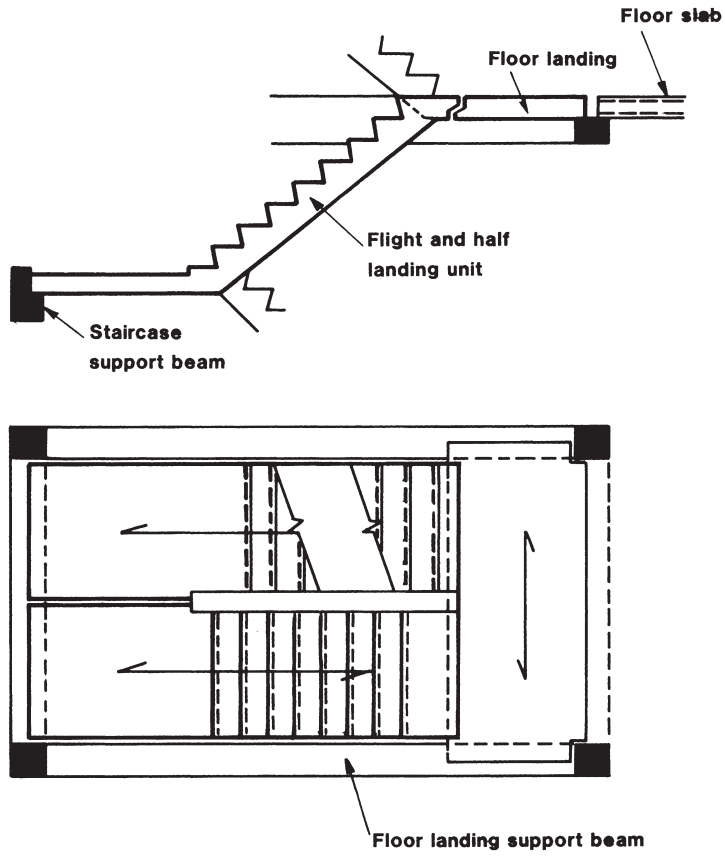

(c)

Figure 3.29 (*Continued*)

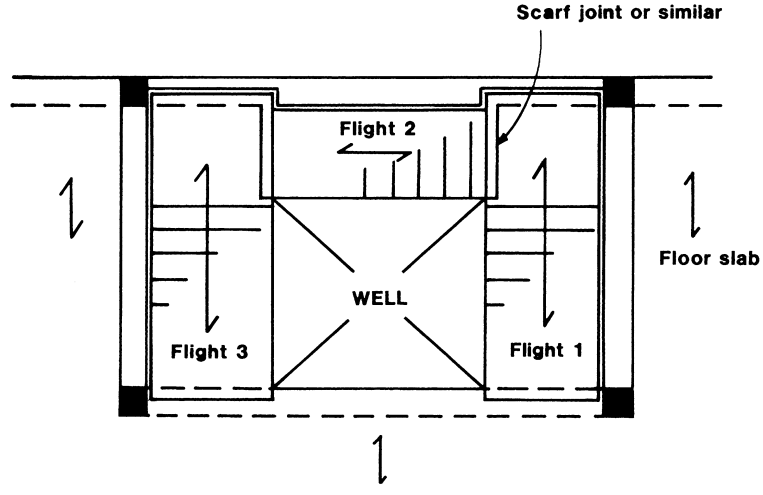

Figure 3.30 Possible layout of a three flight staircase [2.6].

Figure 3.31 Problems encountered with lack of tolerances in fitting a stairflight between two fixed point landings.

Figure 3.32 Cantilevered half landing with semi-circular balcony.

should be 50 mm minimum. Stair nosings, granolithic or non-slip surfaces are more easily added on site, although rebates or rounded arrises at the nose can be precast.

The finishes to be applied to stair units will dictate the method of manufacture. Units cast with the treads face down will have a surface finish (Type A to BS EN 13670 (via the NSCS-4)) from timber moulds, with a steel trowelled finish to the soffit and sides. Units cast in adjustable angle steel moulds with the treads face up will have all Type A finishes except for the treads, which will be trowelled. Information sheets supplied by the manufacturer of precast stairs provide further details on this.

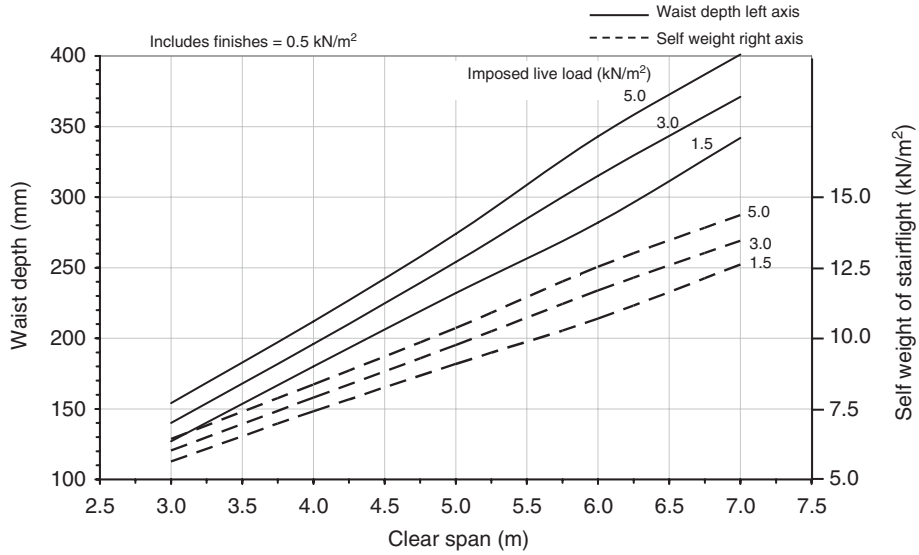

Figure 3.33 Waist depth and self-weight of precast reinforced concrete staircases based on clear span between landings. In all cases going = 250 mm, rise = 180 mm and recede (or rake) = 25 mm. Cover to main bars = 25 mm.

Inserts and holes are formed and located with exceptional accuracy, ±3 mm in position and less than 1° in alignment in most cases. Staircase and landing units can be designed with a fire rating equal to, or exceeding, that for the rest of the structure.

For estimating purposes only, the waist depth and self-weight of a simply supported stair flight may be obtained from Figure 3.33, calculated according to BS EN 1992-1-1. For example, for a span of 5.0 m with an imposed live load of 3.0 kN/m^2, the minimum waist depth (measured perpendicular to the sloping soffit) is 255 mm and the self-weight (measured on plan and not the sloping length) is 9.7 kN/m^2. This appears to be quite a heavy weight, but it includes the self-weight of the steps and is the horizontal projection of a slope of 35°.

3.2.4 Roof and floor beams

A wide range of beams are available in preferred cross sections, mainly composed of rectangles, and an unlimited range in non-preferred sections. What distinguishes a preferred section is simply a matter of available moulds in manufacturers' works. Beams may be classified either as:

- 'internal', where floor loading is approximately symmetrical, or
- 'external', where floor loading is predominantly non-symmetrical.

External beams may be manufactured using visual concrete incorporating external texture, colour, and weather protection, or in plain grey concrete. A nett structural section is used in the design of decorative components, allowing a thickness of about 40 to 50 mm for the finishes.

Internal beams may be prestressed or reinforced. The most common, shown in section in Figure 3.34(a), are called 'inverted-tee' or 'double boot', for which part of the structural section falls within the floor zone, thus reducing overall structural depth. Typical span-to-depth ratios for these beams are about 10 to 15, the former representing the worst possible situation using a reinforced beam rather than a prestressed beam.

The boot width is governed by two factors: (i) an adequate floor slab bearing distance of 100 mm minimum, i.e. 75 mm bearing length plus 25 mm tolerance, and (ii) the physical size of the connection

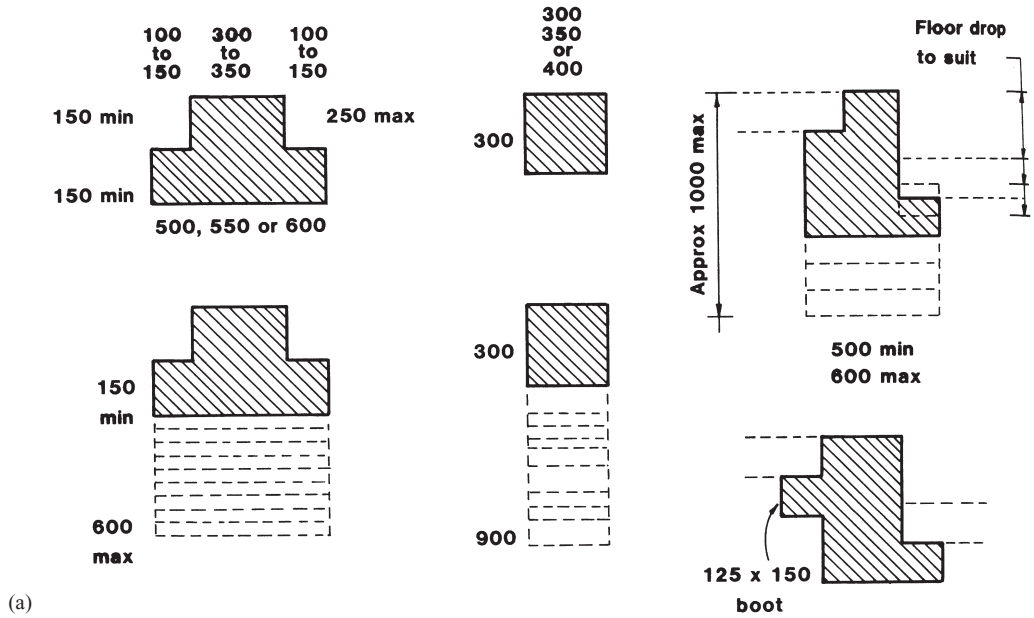

(a)

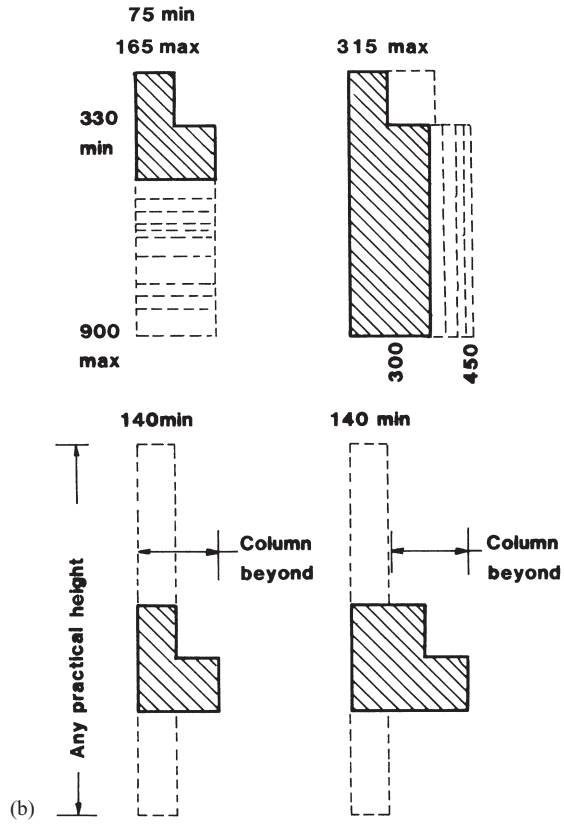

(b)

Figure 3.34 Shapes of standardised beams. (a) Internal beams and (b) edge and spandrel beams.

unit cast into the beam. Rectangular beams are less efficient structurally because a part of the floor slab is not concealed within the depth of the beam, but they may be more economical if the structural zone is not a limiting factor. The centre line of internal beams should preferably correspond with the centre of the column to avoid bi-axial bending effects in the column. Although the effects may be catered for in designing the connection, the maximum eccentricity from the centre of the column should not be greater than $b/3$. The exception to this rule may be in lift shafts or staircases where a flush edge at the beam-column interface is required architecturally. In this case the beam will be lightly loaded. The outstand boot of the beam is not continuous past the faces of the column.

Changes in floor level may be accommodated by using either an L-beam (or single boot beam), or building up one side of an inverted-tee beam, as shown in Figure 3.34(a), to form what is known as a 'dropped boot beam'. If the change of floor level exceeds about 750 mm an improved solution is to use two L-beams back to back, and separated by a small gap (say 100 mm) to facilitate site fixing.

External beams are usually reinforced because of their unsymmetrical L-shaped cross section, and as the depth of edge beams is not usually a restrictive dimension there is not much to be gained by attempting eccentric prestressing techniques. Preferred sections vary with different manufacturers, but a typical range is shown in Figure 3.34(b). Minimum dimensions are again dictated by the size of the beam connector making the connection with the column. The upstand serves two functions, by contributing to the strength of the beam and by providing permanent shuttering to the *in situ* infill concrete used with the floor slab. The depth of the upstand may be varied indefinitely. L-beams with large upstands are known as 'spandrel' beams (Figure 3.35). Structurally efficient, they form an

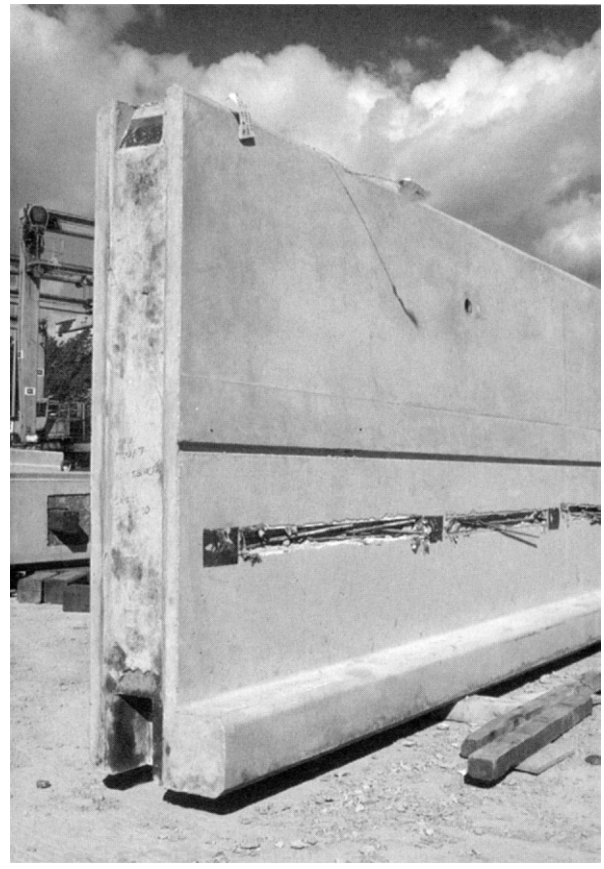

Figure 3.35 Example of long span roof spandrel beams (note the cast-in plate top connection).

immediate dry environment to the structure by providing the following construction trades with a simple means of weather protection. Parapet spandrel beams may contain specially shaped crenellations for weather proofing.

The width of L-shaped and spandrel beams may be confined within the width of the column, or may project forward of the column to form an outstand spandrel. Realistically, the gap between the face of the column and the inside edge of the upstand cannot be greater than about 250 mm. Architecturally they provide the structure with a continuous perimeter façade free from columns or other obstructions. Vertical joints between outstand spandrel beams may be pointed or sealed using a cold mastic. Alternatively the column may be revealed in front of the spandrel, as shown in Figure 3.36.

Because of their non-standard nature, these units may be fitted with window, brickwork and other service fixings at minimal additional cost. The range of decorative finishes is as wide as those available

Figure 3.36 Polished concrete columns and beams offset by up to 500 mm (courtesy of Trent Concrete Ltd, UK).

Table 3.5 Guide to the sizes and uses of beams

Location	Type	Range of typical sizes (mm)			
		Overall breadth	**Upstand breadth**	**Overall depth**	**Depth below slab**
Floor and roof main and gable edge beams	L-beam	250 to 450	75 to 315	330 to 900	150 to 750
	Spandrel	250 to 450	140 to 300	No limit *	–
	Outstand spandrel	400 min	140 min	No limit *	–
Internal main spine beams	Rectangular	300	–	300 to 900	300 to 900
	Inverted tee	500 to 750	300 to 450	300 to 800	150 to 600
Internal secondary beams	Rectangular	300	–	300 to 500	300 to 500
Staircase and lift-shaft beams	L-beam (mainly)	300	75 to 165	330 to 600	150 to 400

* within practical and architectural limits.

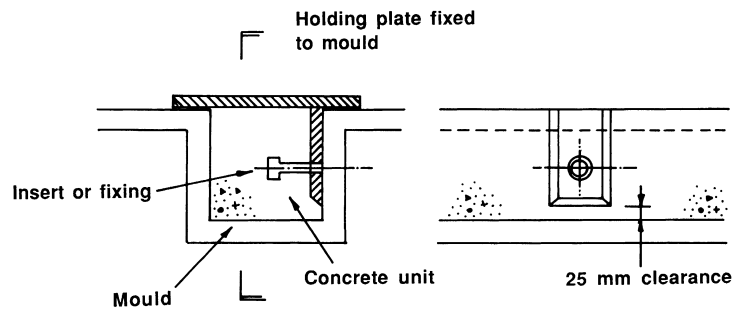

Figure 3.37 Fixing inserts inside a steel mould.

for cladding itself. Horizontal service holes may be provided transversely to the span of the beam. They should be located near to the neutral axis of the beam and/or near to the ends of the beam. Consultation with individual manufacturers with regard to maximum size and position of the holes should be made early in the design appraisal.

Table 3.5 is a guide to the different uses of the main types of preferred section for beams. Provisions for holes and fixings in beams and spandrels depend largely on the nature of the mould in which they are cast. In general, units having a preferred cross-sectional profile (as defined in Section 3.1) are manufactured in steel moulds, with the remainder cast in timber moulds. Fixings in concrete that are in contact with the sides and soffits of steel moulds are battened in the mould, as shown in Figure 3.37. In plain concrete units the rebate is not usually structurally or architecturally embarrassing. In some cases manufacturers prefer to drill holes in the mould and repair these later by plugging and grinding the inside face of the mould smooth.

The manufacturer can provide the following built-in fixings and fittings:

- cast-in-sockets (see also Table 3.3)
- galvanised steel dovetailed slots for masonry and other types of cladding

- dovetailed timber battens for window fixings, etc.
- crenellations for weatherproofing
- *in situ* brickwork support in either a bolted-on steel angle or a cast-on concrete nib with drip
- horizontal service holes.

3.2.5 Beam-to-column connections

One of the most important connections in multi-storey precast construction is the beam-to-column connection. The design, which will be dealt with in detail in Chapter 7, is based on a pinned joint, i.e. the beam is simply supported and no continuity moment transfer between the beam and column is considered. A bending moment is induced in the column, but this derives from the eccentric load reaction from the end of the beam, acting at about 50 mm from the face of the columns.

The main architectural decision to be taken is whether the connection is to be confined within the depth of the beam, or whether it may be permitted to project below the soffit of the beam, as in Figure 3.38. Concealed connections, shown in Figure 3.38(a), are frequently required at internal connections because of the restrictions on floor zones. Because of the reduced depth of beam and the highly localised forces in the column, steel inserts are cast into both beam and column components to ensure

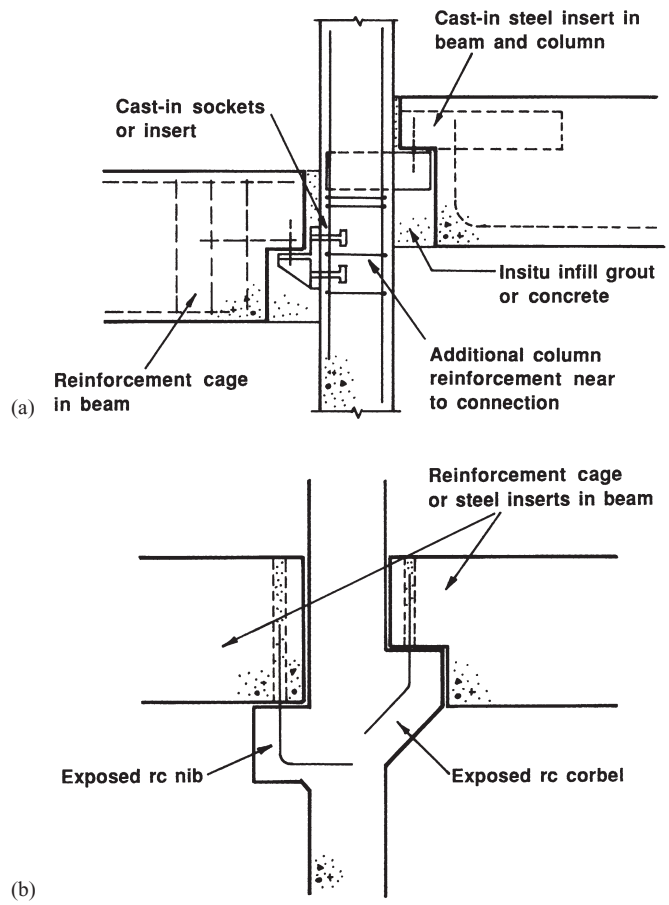

Figure 3.38 Beam-to-column connection: (a) enclosed; (b) expressed.

Figure 3.39 Beam to beam connections (courtesy of Trent Concrete Ltd).

that a positive connection is made. All steel inserts are protected against fire and exposure using an *in situ* grout or concrete. Corbelled connections, shown in Figure 3.38(b), may be used in the perimeter of the building where external cladding will hide the connection from view. However, it is unlikely that both types of connection will be used in the same building because of the different requirements on moulds.

In assessing the suitability of a precast concrete structure at certain intersections, due consideration must be made for the specialised nature of this connection. For example, it is not always possible to terminate beams on the column grid. In these circumstances a direct connection between the end of a secondary beam and a primary beam is made, as shown in Figure 3.39. This is usually a non-standard detail that requires special attention, particularly in the primary beam. As the shear force capacity of this type of connection is obviously restricted, the use of columns in the framing plan should be optimised accordingly.

The floor-to-beam connection is also based on a simple support, as shown in Figure 1.28, despite the presence of reinforced *in situ* concrete strips, or welded connections. Flooring is usually laid directly onto the shelf provided by the boot of the beam, but neoprene bearing pads or wet bedding onto grout is also used in certain circumstances.

The fire resistance of all beams is based on the recommendations of BS 8110, Part 2. Typical ratings for rc beams using a 'standardised' cage (i.e. a predetermined arrangement of bars most suited to the preferred range of beams), is R120, although R240 may be achieved without additional external protection. Fire ratings for most standardised prestressed beams is R90 to R120, although again with the use of a fine mesh and increased cover to the prestressing tendons R240 may be achieved. Lightweight aggregates are not used for beams of structural importance because of restrictions in strength, particularly at the connections. However, lightweight aggregates have been successfully incorporated into the upstand of deep spandrel beams (i.e. away from the structural connection) to reduce weight.

3.2.6 Columns

Column cross sections, shown in Figure 3.40(a) and (b), are based on a minimum of 300 mm × 300 mm plan dimension, because of the nature of the beam-to-column connection. Preferred increments

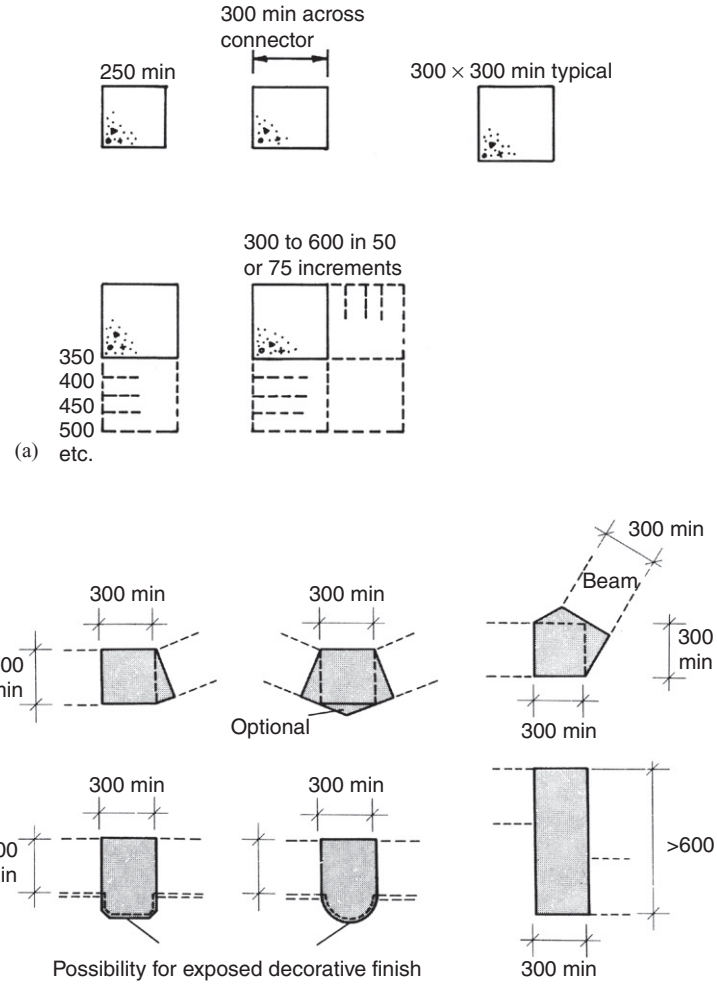

Figure 3.40 Preferred cross-section of columns. (a) Standard rectangular columns (in mm) and (b) non-standard columns (in mm) [2.6].

in size are 50 mm or 75 mm, in one or both faces. Non-preferred shapes (e.g. trapezoidal, hexagonal, round) are based around a column core size of 300 × 300 mm to accommodate structural connections: Figure 3.41. Columns may be erected in one piece, i.e. without mechanical splicing, up to 20 m in length, as in the five-storey building shown in Figure 3.42, where an unbroken finish in an exposed aggregate was required. However, the usual practical and more economical limit is 12 m to 13 m.

Column sizes in braced structures may be approximated by assuming that the cross-sectional area (mm^2) is equal to the maximum ultimate axial load (N) divided by 28. In using this simple approximation, check that the slenderness ratio (minimum cross-sectional dimension divided by length) is not greater than 15. In unbraced structures the quotient depends on the magnitudes of both axial force and overturning moment, which vary owing to many parameters, but in most practical cases column sizes are typically 350 mm square for three-storey buildings, and 300 mm square for two-storey buildings. These values take into account the effects of slenderness.

A more refined first estimate may be obtained from Figure 3.43. This diagram is taken from The Concrete Centre's publication *Economic Concrete Frame Elements to Eurocode 2* [2.46], which contains further information for the sizing of internal, external and corner columns in precast skeletal frames.

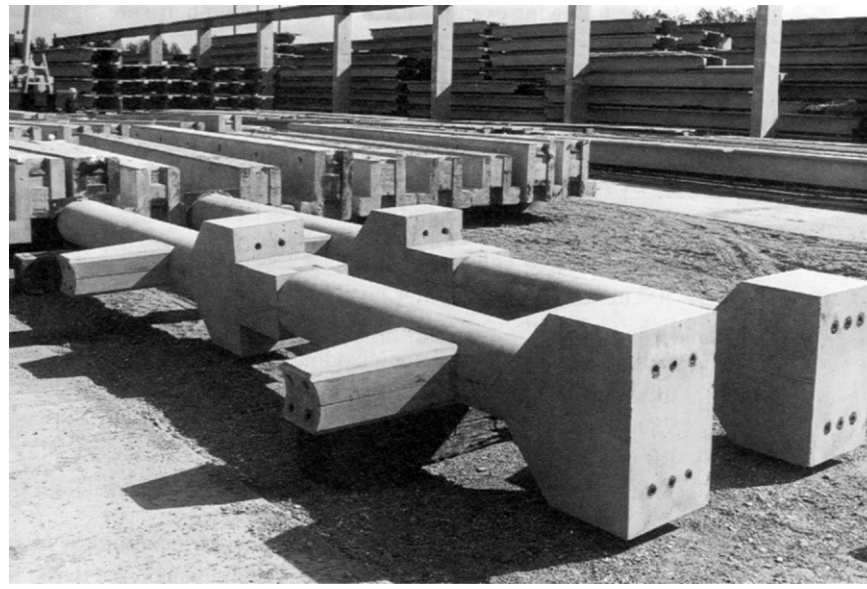

Figure 3.41 Non-preferred shapes of columns.

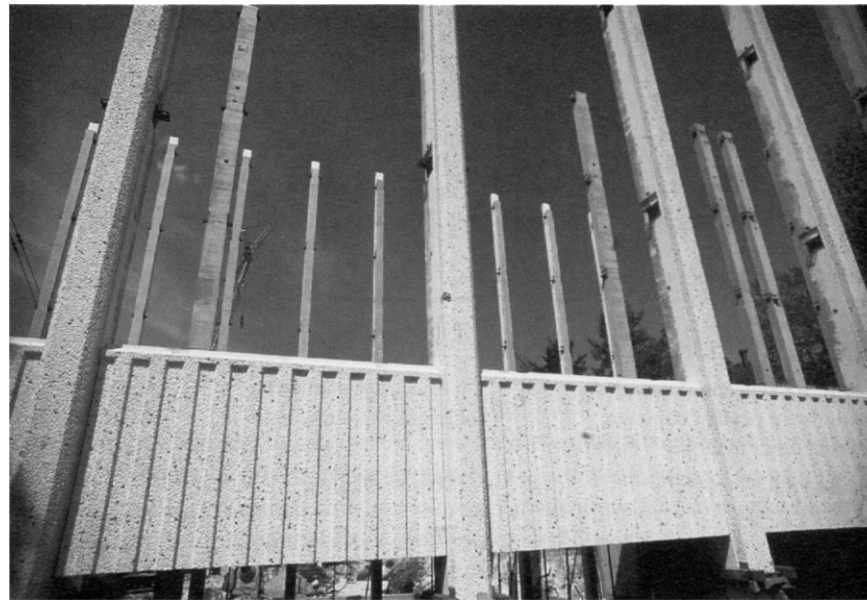

Figure 3.42 Five storey columns in exposed aggregate at Orpington, Kent (courtesy of Trent Concrete Ltd).

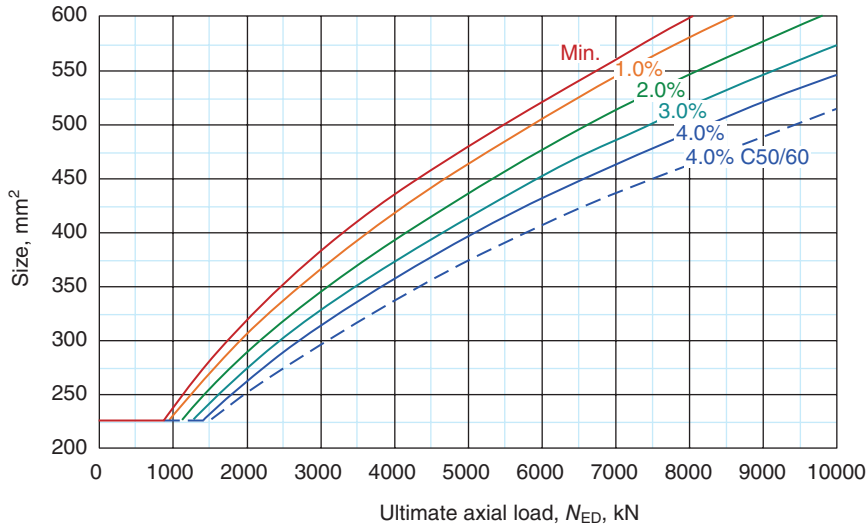

Figure 3.43 Initial precast concrete column sizes for axial load (courtesy of The Concrete Centre, UK).

Column finishes may either be plain grey or incorporate a decorative finish on any or all of the faces, as shown in Figure 1.16 where polished concrete, using white Portland cement and dolomitic limestone, was specified. In the latter case, conforming to standard shape or size does not carry cost penalties because of the special nature of the decorative finish. The design of the column makes due allowance for the finishes in computing a net cross section. Unless the concrete retains its gross section, e.g. when finished by polishing or acid etching, a thickness of 40 mm to 50 mm is typically subtracted for the finishes.

High-quality visual concrete in columns has only recently been fully exploited. Although the increase in cost in using visual concrete compared with plain concrete is between 50 and 250 per cent, depending on the complexity of the finish, a net saving is often made. Consider the following example for an external column in a prestigious four-storey office building:

Option		**Cost index**
1	Visual finish polished concrete column, grade C32/40 concrete, 13 m long × 350 mm × 350 mm section, reinforced with 4 no. H25 bars vertically and R10 links @ 300 c/c. **Total Option 1** =	**1.60**
2	Plain concrete column, grade C40/50, 13 m long × 300 mm × 300 mm, reinforced with four H32 bars vertically and R10 links @ 300 c/c.	1.00
	Polished concrete U-shaped cladding bolted on three sides of column, grade C25/30, four pieces totalling 13 m long × 75 mm thick, reinforced with five H10 bars vertically and R8 @ 200 c/c horizontally.	1.40
	Total plan dimensions in Option 2 = 470 mm × 385 mm. **Total Option 2** =	**2.40**

Table 3.6 lists the additional provisions that may be incorporated in columns, and the sizes and restrictions in using each facility. Columns may rise to the full height of the building, or may be terminated and stepped back into the structure to suit architectural features. As in any form of construction, it is desirable that the internal grid layout is not varied too extensively, except in terminating columns in places where the floor (or roof) construction can adequately span over the row of columns omitted beneath. Figure 3.44 shows examples of permissible practice.

Table 3.6 Additional provisions in columns

Provision	Typical sizes	Restrictions
Cast-in-sockets and dove-tailed channels for precast concrete, metal or other cladding	6 to 24 mm diameter	Centres > 2 × diameter
	Length > 30 mm	Edge distance > 50 mm
Internal rainwater pipes*	100 mm diameter	PVC (plastic) only, no steel
		May increase column size
		Blocked by certain splices
Protective cloaking for impact and damage resistance	50 × 50 mm bent plate	Galvanised or stainless steel only
	× 1 m long	
Chases for electrical fittings	50 mm wide	20 mm depth
	Full height if required	Edge distance > 30 mm
		Centres > 100 mm
Holes for horizontal services	Width < b − 200 mm	May increase column size.
	Length < 200 mm*	Not possible in beam zone
Ties for brickwork	100 mm long @ 150 c/c	Not in more than 3 faces

N.B. Consultation with precast concrete manufacturers is strongly advised before any of these provisions is considered, particularly those marked *.

3.2.7 Bracing walls

Precast skeletal structures of more than three storeys in height are usually braced. The need for permanent walls or cross-bracing is implicit in the design of a braced structure, and the design team must appreciate the need for these obstructions to clear open-plan floor areas, which may not always be necessary in a cast-*in situ* frame. The number and positions of walls in a precast structure is often a contentious issue, one that has to be accepted within the limitations of any prefabricated building system.

Precast concrete walls serve to provide stability and as surrounding walls or boxes for staircases and lift shafts. Walls may be classified as 'infill' or 'cantilever'. Users of infill walls attempt to design the wall as a single unit, but if the opening between beams and columns is particularly large, say 8 m × 4 m, it may be necessary to 'stitch' two separate units using a vertical reinforced *in situ* concrete joint. The effects of slenderness (= length/thickness < 30) are included in design. It is shown in Chapter 8 that the usual limiting strength for infill walls is given when the ultimate horizontal interface shear stress between the precast wall and the foundation is taken as 0.45 N/mm^2.

The thickness of the wall units varies between (the practical minimum thickness of) 150 mm and 300 mm, and is governed either by lifting in the factory or the ultimate shear capacity in service. Because the design considers the wall acting as a compressive diagonal strut it is not acceptable to provide large voids for windows, doors, etc. in these units. Service holes, up to about 500 mm in diameter, may be accommodated in the walls providing they do not interrupt the structural continuity by being less than approximately 250 mm from the edge of the wall. The wall openings shown in Figure 3.45 give an indication of the possible sizes in this respect.

Cantilever walls are designed as 'deep beams' with adequate tension anchorage to the foundation and between successive storey height units: Figure 3.46. In the case of isolated walls, the wall is braced laterally by other walls in the structure. No frame elements are used in this type of construction.

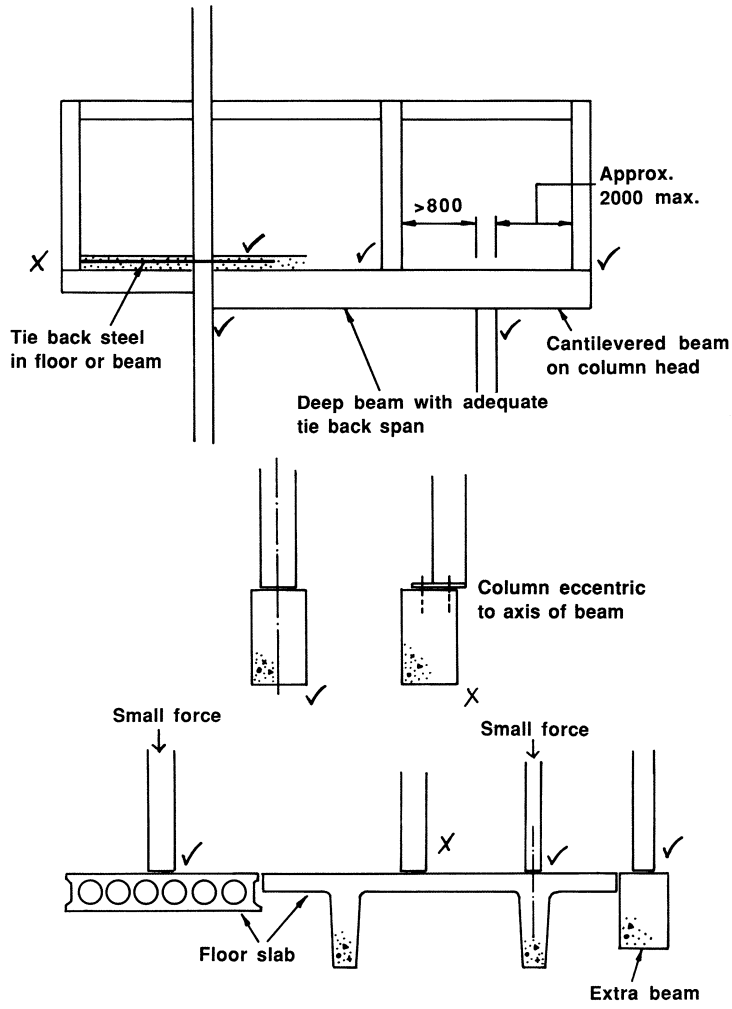

Figure 3.44 Guidance for the positioning of staggered columns founded on to walls and beams.

Therefore, corbel seatings are required for flooring or stair landings, and inserts are required for connecting beams or spandrels.

Precast shear cores or boxes, shown in Figure 3.47, are an extension of the single-cantilever wall. These units can contain large openings for doors and windows. They may be formed on site by 'stitching' two or more units, or manufactured as a complete storey (or part-storey) height box in the factory with door and window openings as required. The lift shaft shown in Figure 3.48 was erected to a height of 20 m before fixing of the skeletal frame commenced. Lift-motor rooms and basement pit boxes may be used to complete the prefabricated lift shaft. Lift-motor slabs may also be precast, but tend to be disproportionately expensive (per m^2) owing to their individual nature. Precast staircase boxes may be used similarly to provide access and/or architectural features to basements, roofs, plant rooms, etc.

The location and distribution of walls should be such that their centre of resistance coincides closely with the centre of mass and the geometric centroid of the completed building section plan. The most obvious location is around stairwells or lift shafts, although other internal or external walls may have to be used in order to 'balance' the structure. More precise design guidance will be given in Chapter 8.

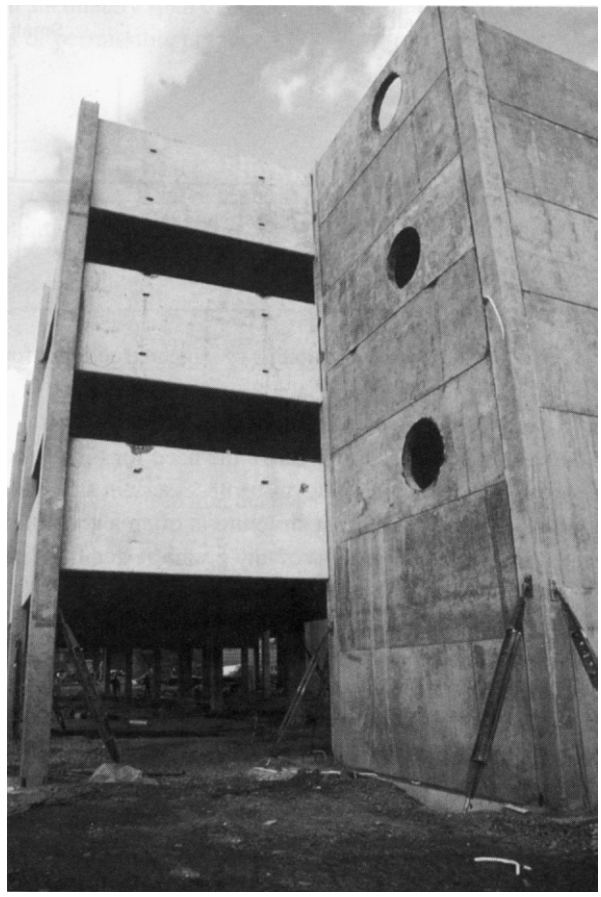

Figure 3.45 Holes in solid shear walls.

3.3 Special Features

3.3.1 Hybrid and mixed construction

The term 'hybrid' is used to describe mixed construction where precast concrete is used in combination with cast-*in situ* concrete. Reference should be made to the publication by the UK Reinforced Concrete Council [2.40], which deals extensively with this topic. Mixed construction is defined as that using two or more different structural materials in the same building. Precast concrete plays a central role because it can be readily integrated with structural steelwork, timber, cast-*in situ* concrete, brick and block masonry, fibre-reinforced materials, and glazing systems. The term must not be confused with 'composite' construction, which also uses both precast and another material, but where the structural performance relies on the interaction between the two.

Mixed construction gives architects the opportunity to utilise locally available materials. For example, precast concrete and glue-laminated timber were the dominant materials at Hydemoen airport, Norway, seen in Figure 3.51. There was a need to increase off-site prefabrication as much as possible, utilise local resources of concrete and timber, and allow the maximum clear head height in the critical service areas. Some 35 different schemes were considered for this structure, in which there are structural glazing (planar system), steel trusses and nodes, and cast-*in situ* concrete foundations and ground slabs.

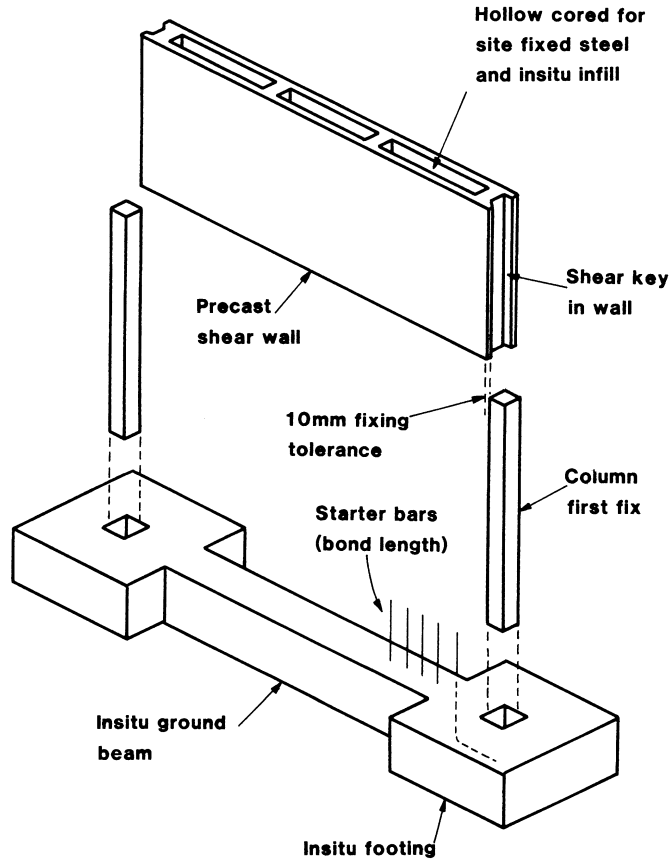

Figure 3.46 Hollow-core shear walls.

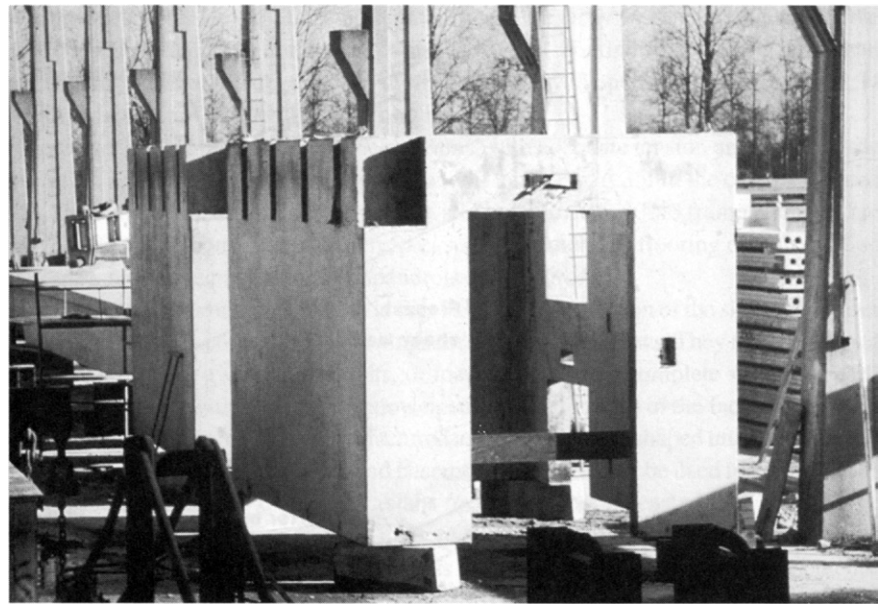

Figure 3.47 Shear core box complete with lift door opening and holes for electrical fittings (courtesy of Costain Building Products).

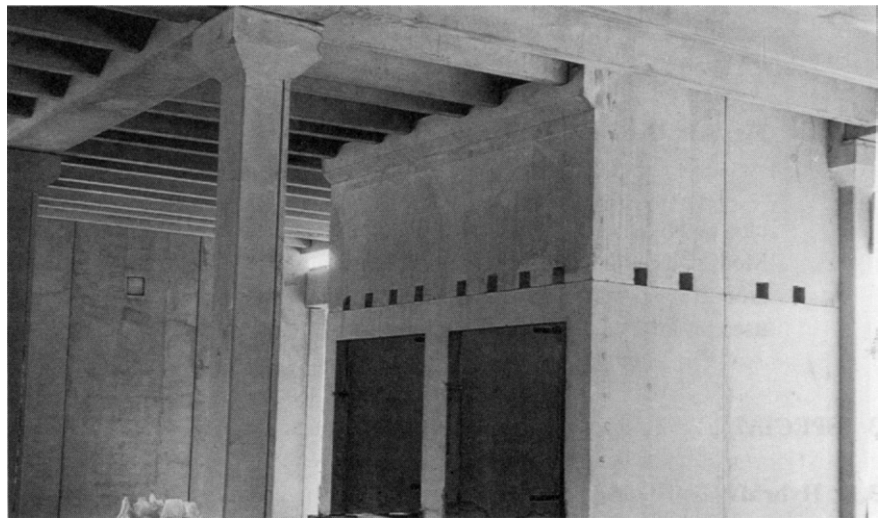

Figure 3.48 Twin lift shaft manufactured from two precast pieces (courtesy of Blatcon Ltd).

Figure 3.49 Precast concrete shear core box complete with openings and doors, which can facilitate internal fixings for services (courtesy of Waycon Precast Ltd).

Mixed precast construction is defined where precast concrete plays a central role. It was found, in a survey carried out between 2000 and 2002 on behalf of the *fib Commission on Prefabrication* [3.8], that up to 75 per cent of new buildings in some countries were designed in this way. The Commission points out that this is a 'high-tech' method that requires careful coordination between all parties, especially on site, where specialist fixers familiar with working in steel or precast have now to construct using other materials. The survey found that mixed precast construction has many advantages over a single material, not least in on-site construction time, where time savings of up to 20 per cent were reported.

Figure 3.50 Precast shear core for services of lift shaft.

Figure 3.51 Precast structure with glue-lam timber roof, beams, steel trusses, cast-*in situ* foundations and structural glazing at Hydemoen Airport, Oslo (courtesy of Spenncon AS).

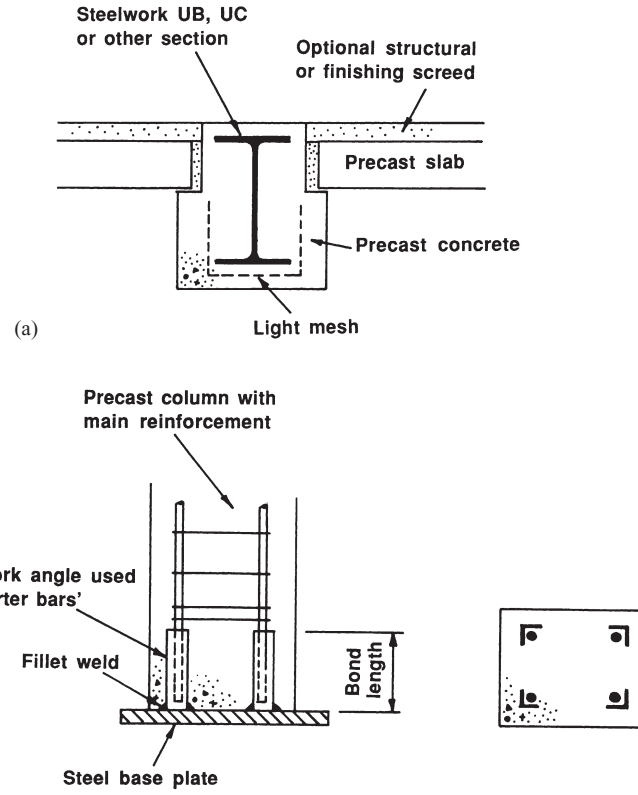

Figure 3.52 Structural steelwork encased in concrete at the factory. (a) UBs cased in concrete for fire protection and bearing purposes and (b) steel sections used for starter bars where the area of rebar would be too great in normal practical situations.

All hybrid structures take advantage of aspects of the excellent combination offered by concrete of durable strength, stiffness, thermal insulation combined with thermal mass, and sound insulation, with the added construction speed and convenience achieved by precasting.

Figures 3.52 and 3.53 show the combined use of steelwork and precast concrete in various situations. Figure 3.52 shows a steel Universal beam providing flexural strength with the concrete being used for the fire and corrosion protection only. Figure 3.53 shows separate structural precast concrete and steelwork members, where a conscious decision has been made to use precast in one part of the structure and another material in another.

Although mixed construction varies considerably with the type of construction and building function, buildings usually reflect local trends, environmental and physical conditions, relative material and labour costs, and local expertise. The permutations for mixed construction are numerous – Table 3.7 is a guide to their most common forms and combinations.

Other examples include:

- *in situ* concrete basement or lower-storey podium
- structural steel roof atrium, gallery, or portal frame
- timber roof or balcony
- load-bearing masonry walls or shear walls.

In a mixed structure, structural precast concrete members may be replaced with equivalent steel, timber, cast-*in situ*, or masonry members, because there is a cost or performance benefit or because the architect has called for this specific type of structure. A good example of the use of steel and

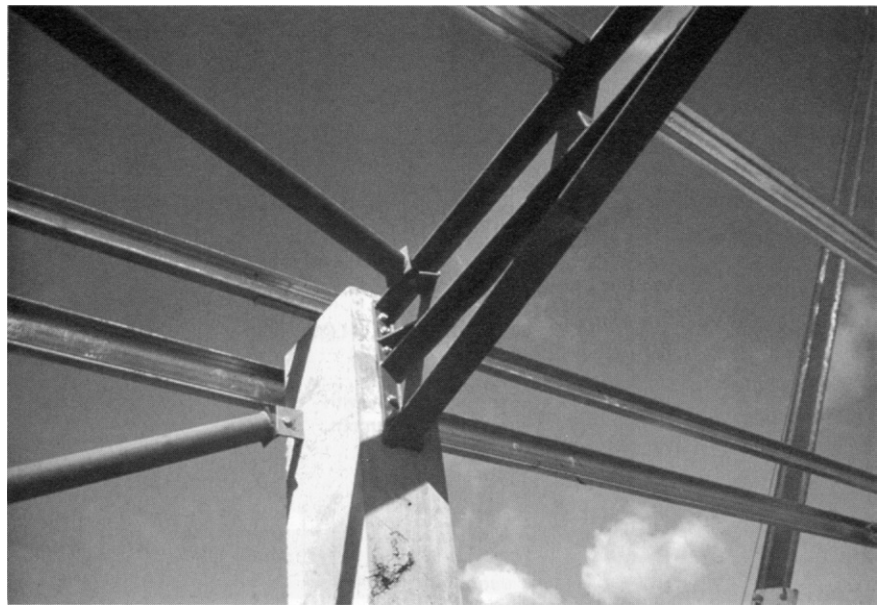

Figure 3.53 Precast concrete structural steelwork in mixed construction.

precast concrete is shown in Figure 3.54, where the more heavily loaded parts of the structure were manufactured using precast reinforced or prestressed concrete, and the lightly loaded roof members were steel. This was truly mixed construction, because the concrete foundations were cast *in situ*, and the diagonal bracing was also in steel.

3.3.2 Precast–*in situ* concrete structures

One of the most common mixed combinations is of precast concrete with cast-*in situ* concrete. The speed and quality of precast combine with the economy and robustness of small quantities of *in situ* to give high-quality, aesthetically pleasing structures quickly and economically. Structural compatibility is not a problem if the differential shrinkage rates are allowed for in the analysis. Providing the differences between continuous rigid *in situ* frame and pin-jointed precast structure behaviour can be accommodated in the stability analysis, the main problems are in the joints between the two structural media.

In internal locations, shallow precast (often prestressed or post-tensioned) beams provide temporary support for precast concrete floors and cast-*in situ* beams, as shown in Figure 3.55. Although there is some inevitable composite action between the precast soffit units and the *in situ* beam, the proportions are such that it is not significant, and certainly not an economic consideration. The *in situ* concrete must be confined in a transverse direction by site-placed bars positioned into the precast floor units. The same bars provide continuity of the hcus in a hogging mode across the beam. The resulting span-to-depth ratio for this construction is around 20:1, compared with about 15:1 if precast alone is used.

Matching the speed of casting *in situ* columns with that of fixing precast concrete spandrel beams and precast floor slabs was achieved in the 15-storey structure shown in Figure 3.56. The beams were positioned on column formwork and *in situ*-jointed to make a rigid connection. The floors were mixed construction, using rapidly erected prestressed precast concrete hollow-cored units with an *in situ* topping to form the horizontal wind diaphragms [3.9]. These rules for concurrent progression do not always hold. On the site shown in Figure 3.57 the cast-*in situ* work for an entire floor area, some 3000–4000 m^2, was completed before the precast terrace units were delivered.

Table 3.7 Options for mixed construction in precast concrete structures

Building type	Mixed precast construction methods	Comments
Commercial offices	*In situ* concrete frame with precast flooring and façades.	All combinations possible with *in situ* concrete underground or ground-floor podium.
	Steelwork frame with precast shear walls, flooring and façades.	
	Precast frame with steel raker or steel truss.	
	Precast frame with pitched timber truss.	
Retail and shopping	*In situ* concrete or steel frame with precast flooring and façades.	Ditto
	Precast load-bearing wall with cast-*in situ* floors.	
	Masonry load-bearing walls with precast floors.	
Parking garages	*In situ* concrete or steelwork frame with precast flooring and cast-*in situ* topping	Long-span double-tee floors up to 20 m
Industrial and warehouses	Steel frame with long-span precast wall units.	Hollow-cored or sandwich walls give thermal insulation.
	Precast columns with flat steel roof truss.	Long-span lightweight roof.
	Steel frame with precast floors (office areas).	
High-rise residential	Precast load-bearing walls with cast-*in situ* floors.	Composite floor plank often used because of complex floor-plan layout.
	Masonry load-bearing walls with precast floors.	
Domestic, low–medium density	Masonry load-bearing walls with precast floors.	Precast beam-and-block, and reinforced and prestressed hollow-core dominate.
	Precast walls with timber floors.	
Stadia	Steel frame including raker beams, with precast terraces.	All combinations possible with steel or pretensioned precast roof.
	Cast-*in situ* frames with precast terraces.	
	Precast columns with steel raker beams and precast terraces.	

Precast–*in situ* connections rely on accuracy in on-site work because the tolerances in precast work are small. Typical beam connections are shown in Figures 3.58(a) to (c). Precast–*in situ* connections may be less accurate, and rely on adequate bond developing between the two concretes. A check is necessary that the precast element can resist the new set of forces resulting from the changes in detail. Figure 3.58 illustrates this point. The effects of shrinkage must be considered, particularly if the connection is of major structural importance, as is the case in a moment-resisting joint.

Precast columns have been used in *in situ* concrete buildings for the dual purpose of speed and quality of finish. The main benefit is in multi-storey construction, where immediate load-carrying capacity is provided. The most common division of precast and *in situ* concrete is to construct the precast superstructure over the top of a basement or podium, which for reasons of structural form, strength or function cannot be part of the precast structure. Figure 3.59 shows *in situ* concrete being used to create column joints with U shaped precast beam formers.

Figure 3.54 Structural steelwork used in the roof of this precast structure (courtesy of Composite Ltd).

Figure 3.55 Wide *in situ* concrete beams supporting precast concrete hollow-core floors at an underground car park, Parma, Italy (courtesy of Gruppo Centro Nord, Italy, 2001).

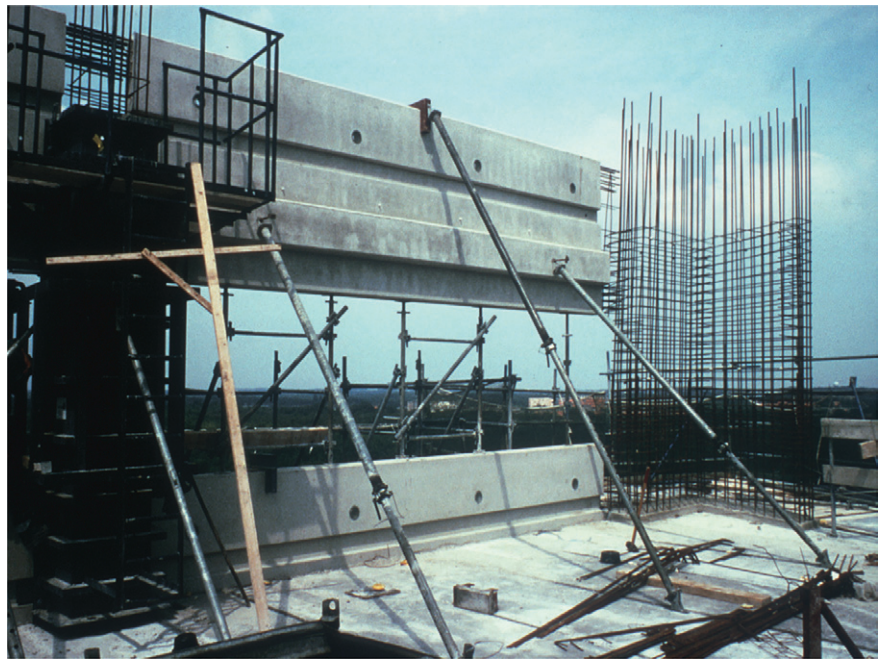

Figure 3.56 Precast spandrel beams are stitched on site at the Malietoren building in The Hague, the Netherlands (courtesy of Corsmit Consulting Engineers, Rijswijk, Netherlands).

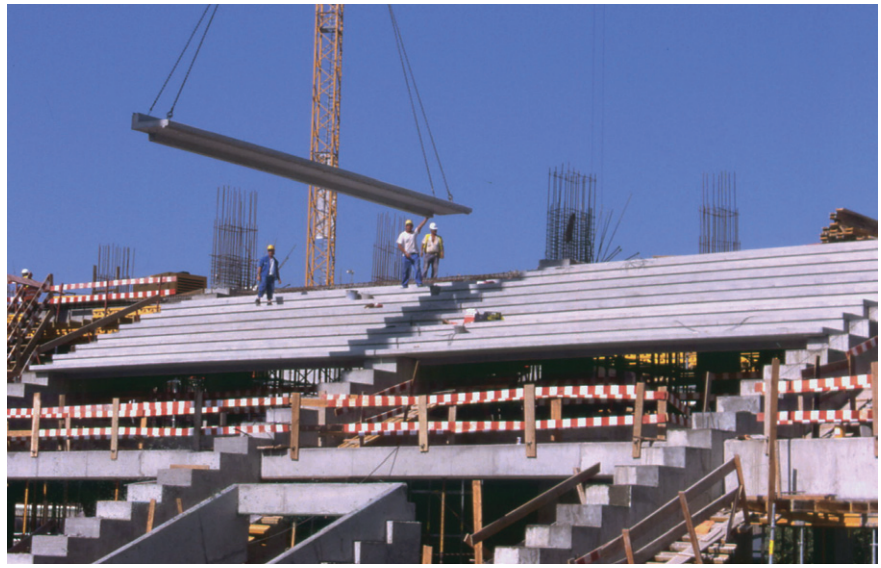

Figure 3.57 Cast-*in situ* concrete raker and tie beams support precast concrete terraces and (elsewhere) hollow-core floor slab (Sporting Lisbon stadium, 2003).

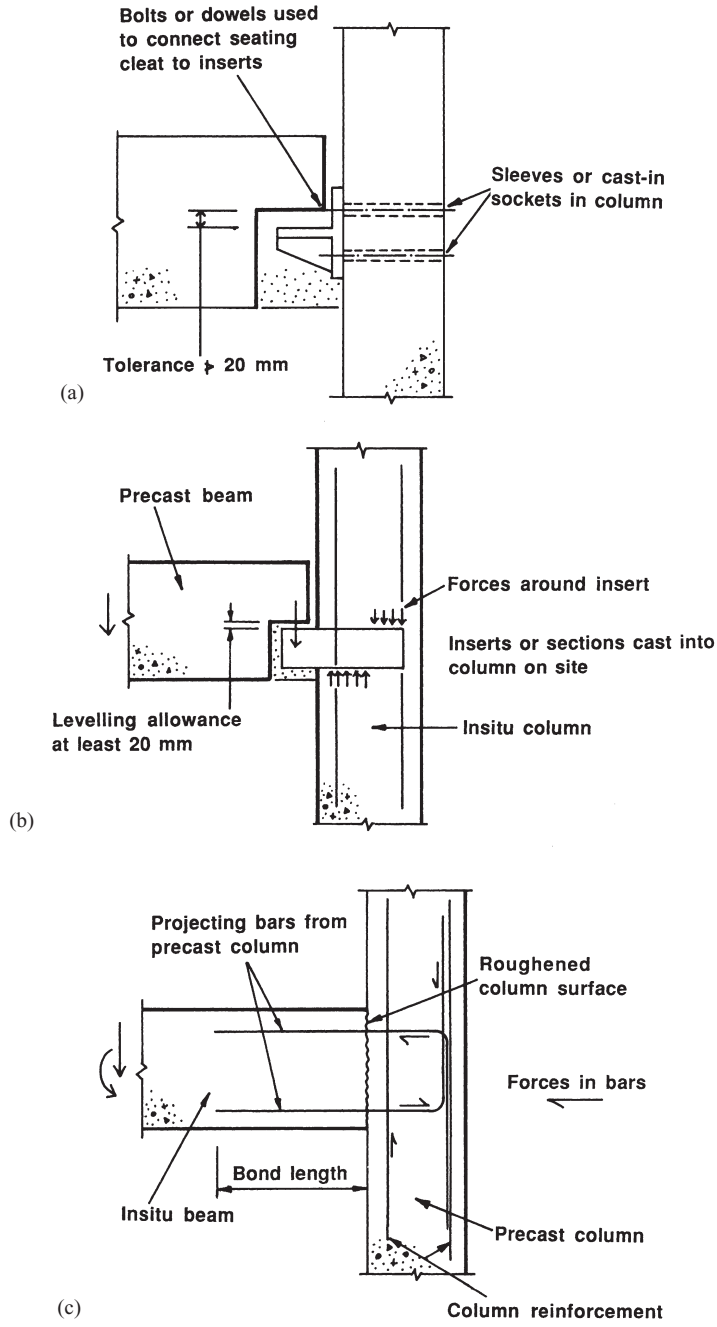

Figure 3.58 Beam–column connection details between precast and *in situ* concrete.

Figure 3.59 Precast superstructure founded onto *in situ* concrete basement (courtesy of New Zealand Concrete Society).

3.3.3 Structural steelwork and precast concrete in skeletal frames

When mixed with precast concrete, steel's structural properties are clearly beneficial (e.g. lightweight long-span roofs, stocky beams with shallow bearing ledges), but other properties are not. It is these properties, such as thermal, acoustic, maintenance, appearance and fire resistance, which are becoming increasingly dominant in modern times. Substituting a precast element with a steel one must be carefully considered.

Most engineers' vision of 'mixed' prefabricated construction is precast concrete floors supported on steel beams, often taking advantage of composite action that can be achieved using a small number of shear studs and small quantities of reinforced *in situ* infill at the ends of the slabs. The market for precast concrete floors in steel frames is huge – about 15 million m^2 in Europe alone in 2002. Hollow-core units of 6 to 16 m span and 200 to 400 mm depth are used mostly in steel frames. If the floors are structurally isolated from the steel beam, a horizontal diaphragm has to be provided either by steel cross-bracing (below the precast units) or in a reinforced structural topping, noting that the tie forces in either case must be continuous and connected to the stabilising elements.

The main advantage in this technique, shown in Figure 3.60, is to produce a (near) flat soffit, where the downstand is equal to the thickness of the bottom flange, say 15–25 mm. This form of construction is suited mostly to shallow floor units, i.e. prestressed hollow-core in particular. The span-to-depth ratio for the steel section is 20–25. The benefit from having a flat soffit must be considerable

Figure 3.60 A flat slab is achieved by placing precast floor units onto the bottom flanges of steel beams (courtesy of Strangbetong, Sweden, 2001).

Figure 3.61 Long-span prestressed hollow-core floors are recessed into rolled and prefabricated steel beams to produce a flat slab at The Big Apple, Helsinki, 2000.

in the total building, since the cost of some of the steel sections (e.g. Universal column) may be much greater than that of a standard steel I-beam or precast inverted-tee beam.

Precast, prestressed hollow-cored units of up to 15 m span and 400 mm depth are used mostly in steel frames. At the 'Big Apple' retail centre near Helsinki in Finland, Figure 3.61, 15 m long × 400 mm deep prestressed hollow-core units are supported on the bottom or top flanges of rolled steel or prefabricated box beams.

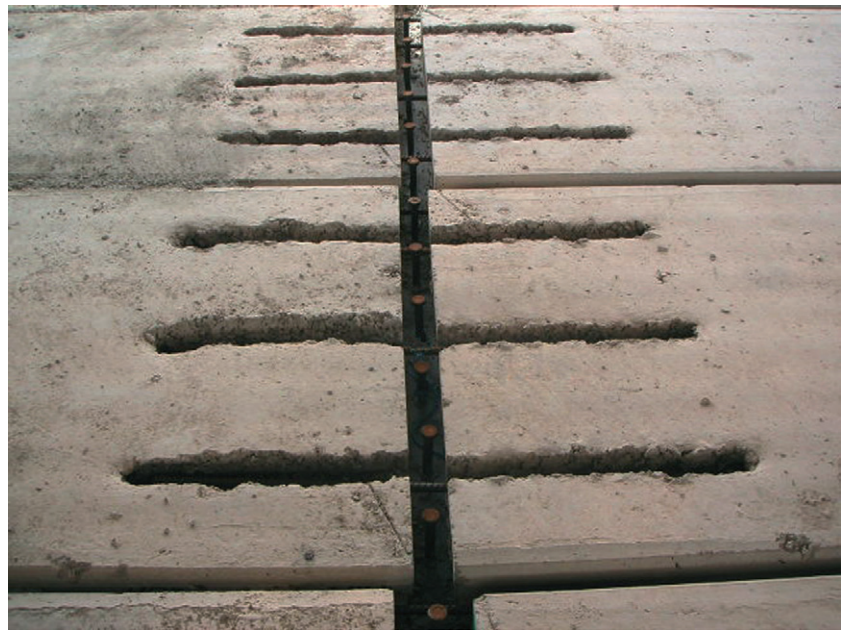

Figure 3.62 Hollow-core slabs bearing onto steel Universal beams made composite through small quantities of reinforced *in situ* concrete in the slots and gaps around the headed shear studs on the beams.

Composite action between precast hollow-core floor units may be achieved through a small quantity of reinforced *in situ* concrete placed into the gaps and milled slots at the ends of the hollow cores, as shown in Figure 3.62. Present design rules for the bending strength and flexural stiffness of the composite UB with hcu followed the research pioneered by Lam [3.10–3.13] using full-scale floor tests, supplemented with horizontal push-off tests to show that the moment of resistance of the composite beam varies between 1.42 and 2.02 times that of the bare steel beam – the range of values being attributed to the different amount of tie steel resisting lateral tension in the hollow-core units. The resulting clean soffit is evident in the long-span construction shown in Figure 3.63.

Grandstands for sports stadia are an alternative form of mixed construction to wholly precast structures. Massively damped spectator structures consist of a mix of cast-*in situ* and precast concrete, often post-tensioned for lateral stability, usually for the vertical and horizontal components respectively. A mixture of steel raker beams and precast concrete L-section bleachers is always used: Figure 3.64. To cater for dynamic loading the concrete frame is designed so that its flexural stiffness is disproportionately greater than its strength, compared with static frames. Conversely the roof structure is designed to be more flexible and this gives rise to lightweight steel trusses or lattices supported in a variety of ways – single bay cantilevers, arches, tensioned structures, transversely spanning trusses and so on, as shown in Figure 3.65. Here there is no composite action – the mixed construction is essentially two structures.

Structural steelwork and structural timber are used mainly for lightly loaded roofs, in the form of either portals or trusses. In most cases the precast concrete elements provide the sub-structure in the marriage. Simple connections are made to the precast components, as shown in Figure 3.66(a) to (c).

Fixings for structural steelwork can easily be accommodated in precast concrete column, beam and wall elements. This is because most precast components utilise steel inserts or cast-in sockets in their connections to other precast members anyway. Providing the stability of the structure is not impaired, the substitution of a steel girder, truss or portal frame for a precast component is taken care of entirely in the connection detail. Frame selection can therefore proceed to satisfy the economic and

Figure 3.63 Composite action between steel beam and precast hollow-core slabs increases the span of the beam by about 20 per cent for the same size of beam.

Figure 3.64 Precast concrete terraces in a steel-framed stadium.

architectural aspects. The main problems occur if connecting members are not coincident with the framing grid, and if connections are required in the floor slab. These are made as shown in Figure 3.66(a). An alternative method, but which is less satisfactory in terms of steelwork efficiency, shown in Figure 3.66(b), may achieve the same objective.

A less common combination of precast concrete with square hollow steel sections (SHS) columns and small steel joists is shown in Figure 3.67. In Figure 3.67(a) a steel frame comprising concrete-filled 120 × 120 SHS is braced using precast concrete shear walls. To complete this very lightweight structure, short-span RSJs support long-span, hollow-core floor units. Figure 3.67(b) shows similar slender SHS columns supporting precast spandrel beams. Both examples are from Scandinavian countries, where steel is relatively expensive compared with concrete.

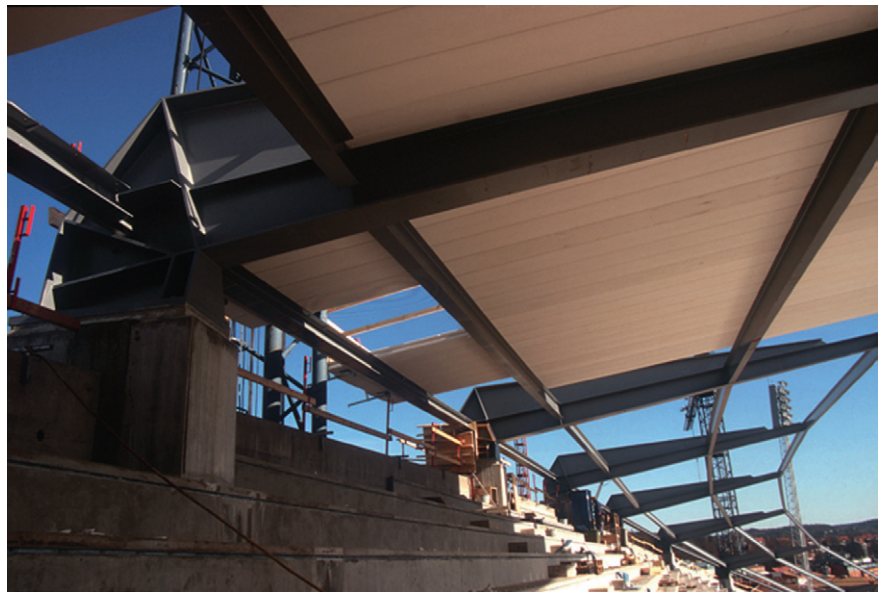

Figure 3.65 Steel roof beams cantilevered from the top of precast concrete columns.

3.3.4 Precast concrete with structural and glue-laminated timber

As with steelwork, timber can ostensibly be used to replace precast concrete for long-span roofs and lightweight floors, the two extremes being attributable to timber's excellent strength-to-weight ratio and good looks. Long-span timber trusses may easily be fixed to timber battens on precast concrete beams, as shown in Figure 3.68.

Although the market share for mixed precast–timber in multi-storey buildings is probably less than 1 or 2 per cent, it is growing rapidly, especially in parts of the world where timber and precast concrete are both 'local' materials. Recent developments came with economical and architectural advances in nail plate fin trusses and glue-laminated ('glulam') beams.

In the past 15 years timber has taken over some of the market for steel lattice roofs, especially in the 1990s when the relative price of timber dropped compared with steel and its availability increased. The erection time for a timber roof is comparable with that for steel, but haulage and hoisting costs are lower. One of the major drawbacks is the lack of R & D on the design and construction of the connection between timber and precast. Simple dowels or bolted cleats tend to be used, but the effects of flexural rotations and long-term temperature and creep movement, etc. are not fully understood.

Glue-laminated timber construction may be used for complete roof structures. In Figure 3.69 the glulam beams were dowelled to the column head in the same manner as precast beams are. Glulam rafters, supported on galvanised steel chairs, impose torsion in the beams and column head connection.

The glue-laminated timber frame shown in Figure 3.70 is included here to illustrate a possible solution for a small office or school. The glulam columns on a 3.6 m square grid, support precast rc slabs that span in two directions and bear directly onto the columns, so there are no beams. The connection at the column head has specially designed steel brackets in the corners of the slabs that are bolted to the columns. This is an option for the trend of demountable school buildings that can be moved around the country to follow the demographic population.

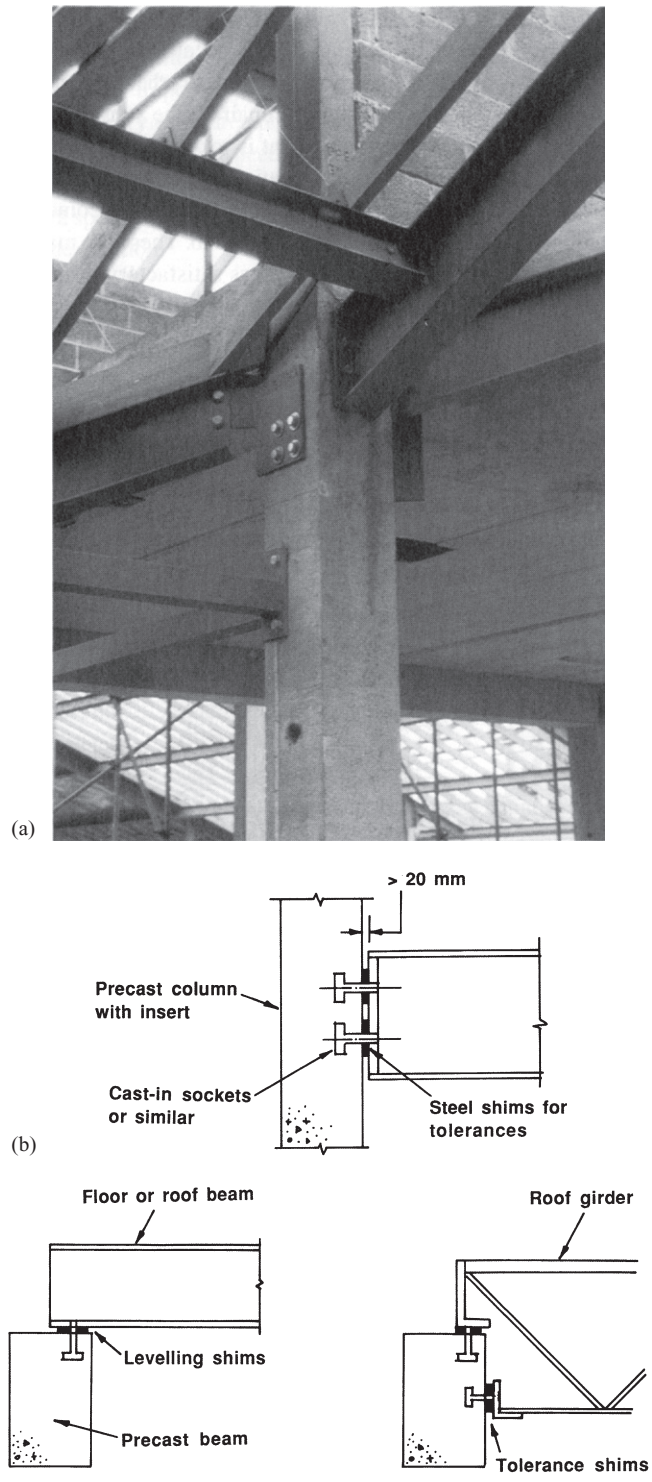

Figure 3.66 Connection details between precast and structural steelwork. (a) Connection details; (b) between precast column or wall; (c) to precast beam.

(a)

(b)

Figure 3.67 (a) Square hollow-section steel columns are braced using precast concrete walls and prestressed hollow-core floor units. (b) Precast concrete spandrel beams supported on square hollow-section steel columns.

Figure 3.68 Timber rafters fastened to battens on a precast concrete frame.

Figure 3.69 Glue-laminated beams and rafters provide the roof to a precast concrete supermarket structure (courtesy of Ergon, Belgium).

Figure 3.70 A glue-laminated timber frame supports two-way spanning precast concrete predales to form a flat slab effect (courtesy of Strangbetong, Sweden).

3.3.5 Precast concrete–masonry structures

Precast floor slabs such as reinforced and prestressed hollow-core units, beam-and-block, and composite plank are today common in UK house and apartment building. Load-bearing masonry walls tend not to be used to support precast concrete elements in parts of multi-storey frames because of on-site fixing sequences; the speed of erection of a precast structure is too rapid for the strength development of the load-bearing masonry. Occasionally masonry walls are built to support a special item, such as a lift motor-room floor that is not on the critical path of the frame erection.

Masonry is used extensively for infill walls or as structural shear walls in buildings of up to seven storeys (see Section 8.7.1), as shown in Figure 3.71. There is ambiguity over whether this is 'composite construction', because the precast structure relies on composite action with the wall, or whether it is 'hybrid construction'. The answer is unimportant because the methodology is proven in either case.

Some specialist projects, such as Hopkins's Inland Revenue building in Nottingham, have used prefabricated brickwork pillars as shown in Figures 3.72 to 3.74. They were of decreasing cross section to mirror reduced load by supporting 13.6 m long × 3.2 m wide precast concrete floors on precast concrete keystones, expressed as a rippling concrete band of vaulted units. The precast concrete components were manufactured in a single piece with dummy joints to give the appearance of a number of individual arched units. The six separate buildings comprising the 40,000 m^2 offices were erected in 18 weeks [3.14]. A raised floor and no suspended ceiling enabled the floor finishers to complete in 13 weeks. This example shows how only mixed construction could have been used to achieve the architectural demands and the speed of construction.

A similar reason for using prefabricated brickwork, this time as brick-halves cast into the columns and spandrel beams at a car park at Cheshire Oaks, was due to site restrictions and the speed of construction, coupled of course with the quality of the build, as shown in Figure 3.75. A shear key with the concrete is formed naturally when voided bricks are cut in half.

3.3.6 The future of mixed construction

In some countries mixed construction is today being used in up to 75 per cent of new multi-storey buildings – once the traditional domain of cast-*in situ* concrete and structural steelwork. Europe has

Figure 3.71 Precast concrete pinned-jointed skeletal structures may be stabilised by masonry infill walls.

led the way forward thanks to synergies developed between the respective precast concrete, steel and timber industries. Precast concrete is ideally suited to mixed construction as it may readily be combined with other materials, such as steelwork, timber, cast-*in situ* concrete, masonry and glass, for the benefit of the building process at large.

Using precast concrete as the dominant material in mixed construction, on-site operations are considerably reduced because there is less wet concrete to place, fewer loose rebars to fix and fewer structural components and formwork to erect. There is also less construction noise and disturbance to local communities. These factors result in a safer working environment, because prefabricated components provide working platforms, and workmen are less exposed to working at heights. Case studies claim that mixed construction saves up to 20 per cent on construction time.

Mixed construction is, by definition, cost-effective, because it maximises the beneficial structural and architectural advantages in using components made of different materials. The technique requires the cooperation of architects, consulting engineers, manufacturers, suppliers and contractors. It is possible that some client and architectural demands can be satisfied only by using mixed construction.

Figure 3.72 Prefabricated masonry pillars support radially curved precast floors and a steel roof.

Figure 3.73 Prefabricated masonry pillars and precast pad stones support vaulted precast concrete floor units at the Inland Revenue Buildings, Nottingham, UK.

Figure 3.74 Interior view of the masonry pillars and exposed precast concrete floor units (courtesy of Trent Concrete Ltd).

Figure 3.75 Prefabricated concrete columns and spandrel beams with brick halves cast into the concrete (courtesy of SCC, Stockport).

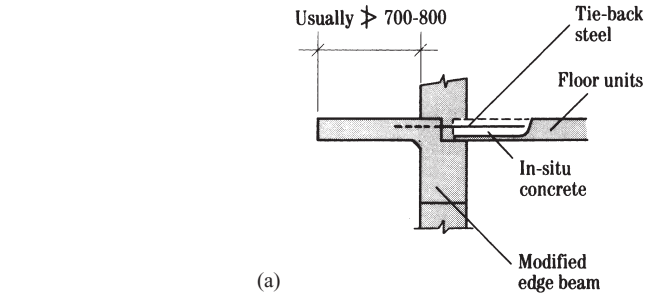

(a)

(b)

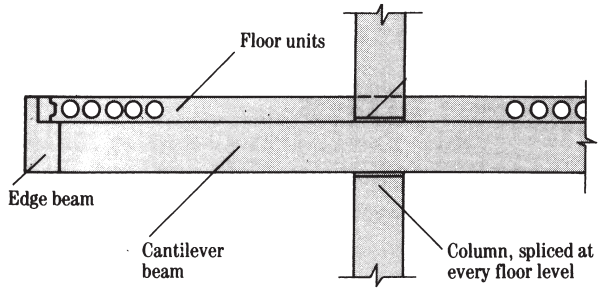

(c)

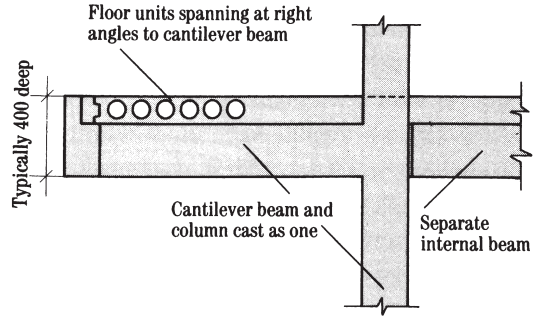

(d)

Figure 3.76 Options for forming cantilever balconies. (a) Cross-section of overhang beam [2.6]; (b) use of overhang beam; (c) cantilever beam [2.6]; (d) cantilever tee-columns [2.6].

3.4 Balconies

Cantilevered balconies may be formed in a number of ways, depending on the span of the balcony and its position relative to the main part of the structure:

- Edge beams can be adopted to provide a small projection up to about 700 to 800 mm overhang: Figures 3.76(a) and (b). The beam is a special casting, but if the quantity is large the cost implications of this are insignificant. *In situ* concrete tie backs may be necessary, as shown in the figure.
- Beams projecting over columns, as shown in Figure 3.76(c), provide cantilevers of up to about 2.5 m. This distance may be varied to produce a splayed effect. The disadvantages are:
  - column splicing at every floor level
  - a greater number of beams are required than in the usual solution
  - an additional edge beam is required at the end of the cantilever.
- Certain flooring, e.g. the double-tee, can be used to cantilever up to about 1.5 m directly over edge beams. The overall structural zone may be large, because it is not possible to use halving joints at the supporting beam. Hollow-core slabs are not recommended for direct cantilever action.
- Tee-columns or cruciform columns, where cantilever beams are cast integrally with the columns, have not been used extensively in the U.K. The shape of the unit (sometimes referred to as 'Christmas tree' columns) and the connection detail are shown in Figure 3.76(d). The limiting span of the cantilever, which is governed by the moment transfer capacity in the column, is about 2.0 to 2.5 m for typical floor loadings and external cladding arrangements. Manufacturing costs are likely to be high, particularly for a small number of units, owing to the individual nature of the units and consequent mould costs.

Exercise 3.1

Devise a precast concrete solution to the five-storey building shown in Figure 3.77, using a braced skeletal structure. The total depth of the floor zone may not exceed 600 mm and no structural topping is to be used. The floor finish is to be raised timber, and the ceiling suspended. The external façade may be taken as 50 per cent brickwork and 50 per cent glazing, except around the curved façade, which is to be aluminium curtain walling. The only internal blockwork (100 mm thick × 1500 kg/m^3 density) is around the service areas adjacent to the lift shaft. The side walls to the main staircases are to be full-height glazing.

Take the characteristic superimposed variable and permanent actions {live and dead loads} as 5.0 kN/m^2 and 1.5 kN/m^2 for the floors, and 1.5 kN/m^2 and 1.5 kN/m^2 for the roof, respectively, and the characteristic horizontal wind loading as 1.0 kN/m^2. Ignore local wind pressure coefficients for this exercise. For this exercise only take the maximum moment in the columns, due to precast beam eccentricity at the connections as 50 kNm.

Solution

The building is symmetrical about the *y-axis*. Therefore consider one half only. Assume that the top of the roof parapet beam is 1.0 m above the roof level. Thus the total height of the building, $H = 16.5$ m, and the column length $l = 17.0$ m.

Step 1: Positions of stabilising walls, possibly at any or all of lift shafts, main staircase and emergency staircase.

The total dead load G_k in the building may be estimated at 5.0 kN/m^2 for the floor loads, 4.5 kN/m^2 for the roof loads, plus allowances of 0.6 kN/m^2 for the beams and columns, 0.3 kN/m^2 for the shear walls, and 1.0 kN/m^2 for the external brickwork/glazing. Thus, total equivalent floor *udl* = 6.9 kN/m^2, and roof *udl* = 5.1 kN/m^2. Floor area = 1900 m^2. Hence the total $G_k = (6.9 \times 4 + 5.1) \times 1900 = 62130$ kN. The total live load $Q_k = (5.0 \times 4 + 1.5) \times 1900 = 40850$ kN.

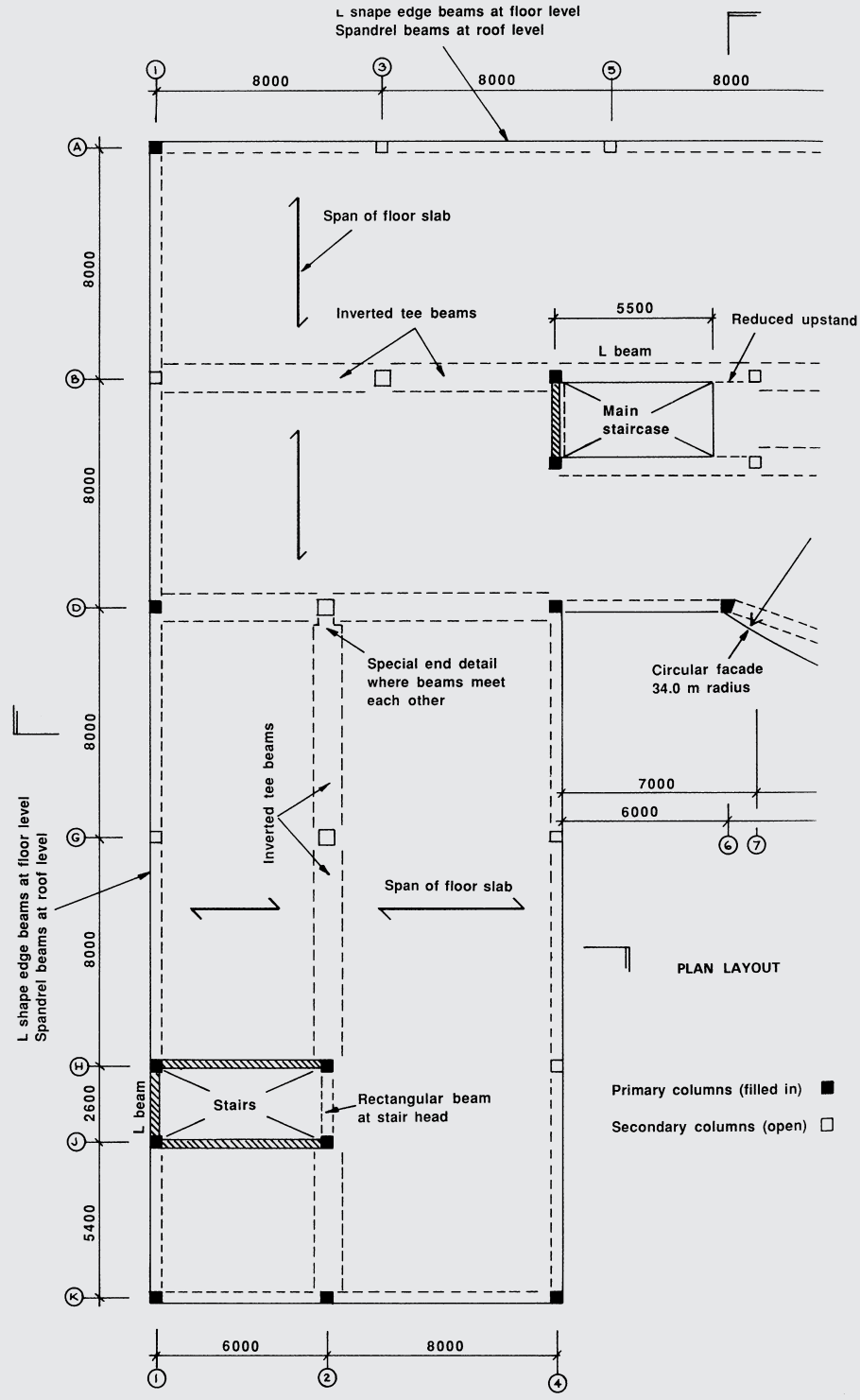

Figure 3.77 Schematic precast concrete structure used in Exercise 3.1.

(*Continued*)

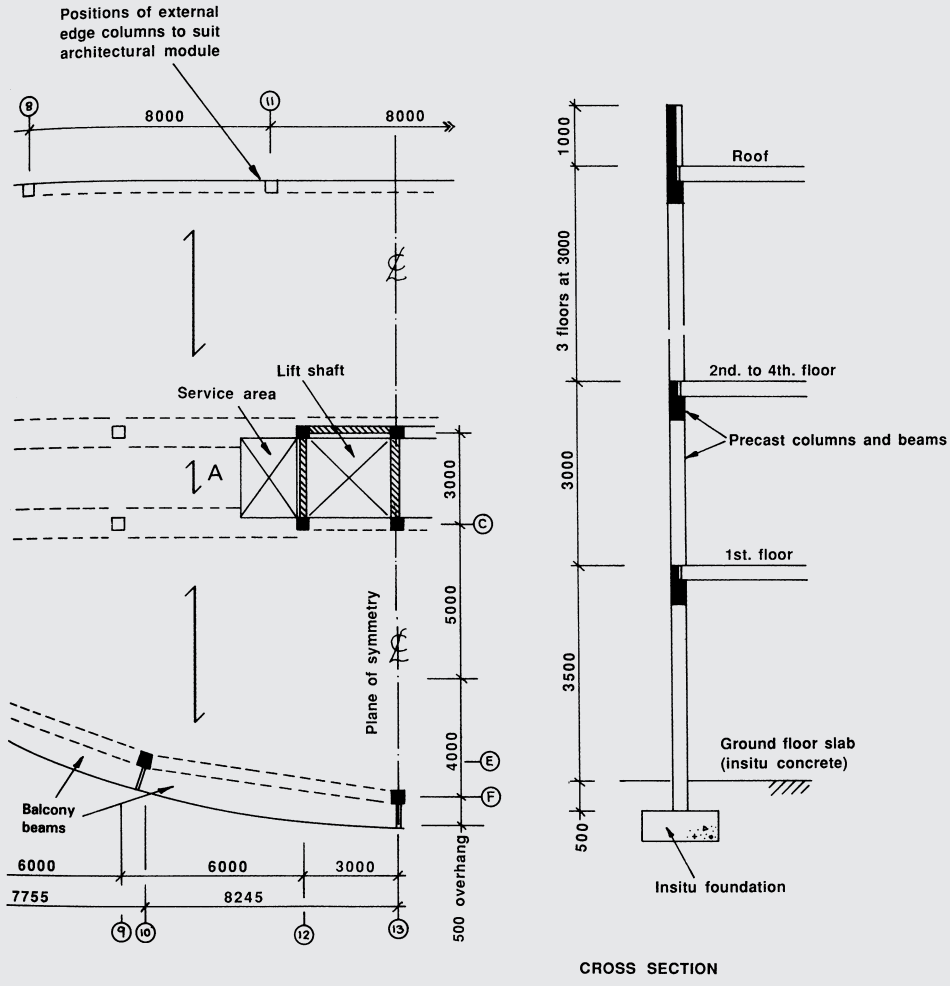

Figure 3.77 (*Continued*)

Total ultimate horizontal shear force in the ground floor shear walls is:

BS EN 1992-1-1:2004		**BS 8110:1997**	
Is the sum of the wind action $W_u = \gamma_f w_k L H$ plus the horizontal imperfection force (see Clause 5.2),		Is the greater of the wind force $W_u = \gamma_f w_k L H$ or the lateral force	
$F_H = \frac{1}{200} \times \frac{2}{\sqrt{l}} \times \sqrt{0.5\left(1+\frac{1}{m}\right)} \times V_1$		$F_H = 1.5\%\ G_k$.	
$\frac{2}{\sqrt{l}} = \frac{2}{\sqrt{17}} = 0.485 < 2/3$, so take 0.667			
m = 65 columns (see Step 2)			
$\sqrt{0.5\left(1+\frac{1}{m}\right)} = 0.7125$			

The ultimate gravity load at the first-floor level, $V_1 = 1.35 \times 62130 + 1.5 \times 40850$ Note that according to BS EN 1990, eq. 6.10a and 6.10b, ultimate = max {1.35 G_k + 1.5 y_0 Q_k; 1.25 G_k + 1.5 Q_k} (where e.g. $y_0 = 0.7$ for offices, see NA to BS EN 1990, Table NA.A1.1)	$V_1 = 145150\,\text{kN}$		

In the *y*-direction the wind action {force} is:

$W_{uy} = 1.5 \times 1.0 \times 72.4 \times 16.5$ $F_H = 0.005 \times 0.667 \times 0.7125 \times 145150$ Total =	$W_{uy} = 1792\,\text{kN}$ $F_H = 345\,\text{kN}$ $H_{uy} = 2137\,\text{kN}$	$W_{uy} = 1.4 \times 1.0 \times 72.4 \times 16.5$ $F_H = 1.5\% \times 62\,130$	$W_{uy} = 1673\,\text{kN}$ $F_H = 932\,\text{kN}$ $< W_{uy}$

and in the *x*-direction:

$W_{ux} = 1.5 \times 1.0 \times 40.4 \times 16.5$ $F_H = 0.005 \times 0.667 \times 0.7125 \times 145150$ Total =	$W_{ux} = 1000\,\text{kN}$ $F_H = 345\,\text{kN}$ $H_{ux} = 1345\,\text{kN}$	$W_{ux} = 1.4 \times 1.0 \times 40.4 \times 16.5$ $F_H = 1.5\% \times 62\,130$	$W_{ux} = 962\,\text{kN}$ $F_H = 932\,\text{kN}$ $< W_{ux}$

Choose to use precast concrete infill walls. These are plain walls reinforced lightly using mesh only for shrinkage, etc., and are therefore dealt with in BS EN 1992-1-1, Section 12, and in 6.2.5 {BS 8110, clause 3.9.4 and the interfaces in 3.2.7}. (Brickwork would be equally suitable, but adopt a totally precast solution here if possible.)

Assume column sizes are 400 mm square at the ground level and 300 mm square at higher levels, and of C40/50 concrete ($f_{ck} = 40\,\text{N/mm}^2$ and $f_{cd} = 0.85 \times 40/1.5 = 22.67\,\text{N/mm}^2$ {$f_{cu} = 50\,\text{N/mm}^2$}).

In the *y*-direction, the total length of shear wall available is $3 \times 2.6\,\text{m} = 7.8\,\text{m}$ at the lift shaft, plus $2 \times 2.6\,\text{m} = 5.2\,\text{m}$ at the main staircase, plus $2 \times 2.2\,\text{m} = 4.4\,\text{m}$ at the escape staircases. Hence $L = 17.4\,\text{m}$. The horizontal joint line between the ground-floor wall and the ground beam is subjected to in-plane shear v_{Edi} {v_h} and normal compression σ_n. σ_n is due to the vertical component of the diagonal force through the infill wall panel = $W_u \tan\theta/Lt$, where θ is the inclination of the diagonal from the horizontal, and t = thickness. This is a plain concrete wall with no reinforcement, and 'smooth' surface finish. Precast wall is grade C32/40. *In situ* infill is grade C25/30. Hence the maximum horizontal shear stress is:

(6.2.5(1) & (2), eq. 6.25) $v_{Rdi} = 0.2\,f_{ctd(i)} + 0.6\,\sigma_n$ $f_{ctd(i)} = 0.7 \times 0.3 \times 25^{0.67}/1.5$ $= 1.21\,\text{N/mm}^2$ Height of infill wall at ground level $l_w = 3500 - 600$ (beam) = 2900 mm. Considering $b = 2600$ mm walls (the final analysis would consider each wall in turn) $\theta = \tan^{-1}(2900/2600) = 48.1°$ Try $h_w = 200$ mm-thick wall $\sigma_n = 2137 \times 10^3 \tan 48.1°/17400 \times 200 = 0.685\,\text{N/mm}^2$ $v_{Rdi} = 0.2 \times 1.21 + 0.6 \times 0.685 = 0.59\,\text{N/mm}^2$ is not > $v_{Edi} = 2137 \times 10^3/17400 \times 200 = 0.61\,\text{N/mm}^2$	$t = 200\,\text{mm}$	For shear and compression a single figure is used: $v_{max} = 0.45\,\text{N/mm}^2$ (Clause 3.2.7), so the thickness of shear wall, $t = 1673/(17.4 \times 0.45)$ The minimum recommended thickness is 150 mm, so round up and take	$t \geq 214\,\text{mm}$ **$t = 225\,\text{mm}$**

(*Continued*)

In the *x*-direction, $L = (4 \times 5.6 + 2 \times 2.6) = 27.6$ m.

Considering $b = 5600$ mm $\theta = \tan^{-1}(2900/5600) = 27.4°$ Try h_w (min) = 150 mm $\sigma_n = 1345 \times 10^3 \tan 27.4°/27600 \times 150$ $= 0.17$ N/mm^2 $v_{Rdi} = 0.2 \times 1.21 + 0.6 \times 0.17 =$ 0.34 N/mm^2 > $v_{Edi} = 1345 \times 10^3/27600 \times 150 = 0.33$ N/mm^2		Hence $t = 933/(27.6 \times 0.45)$	$t \geq 75$ mm

It is likely that the thickness of the walls at the escape staircase will be governed by slenderness, i.e.:

(Clause 12.6.5) $b = 5600$ mm Diagonal length = 6306 mm (Table 12) Lateral restraint along all four edges. $b \geq l_w$ then $\beta = 1/(1 + (2900/5600)^2) = 0.79$ (eq. 12.9) $l_o = 0.79 \times 6306 = 4982$ mm (12.6.5.1(5), eq. 12.8) $\lambda = l_o/l_w \leq 25$ $l_w \geq 4982/25 = 199$ mm Try $h_w = 200$ mm $\lambda = 4982/150 = 24.9 < 25$ (5.2) $e_i = 2900/400 = 7.25$ mm (based on height not diagonal) (eq. 12.11) $\Phi = \min(1.14 \times (1 - 14.5/200) - 0.02 \times 24.9; 0.93) = 0.56$ Diagonal strut of $= 0.1 \times 6306 = 630$ mm (12.3.1(1)) $f_{cd} = 0.8 \times 0.85/1.5\, f_{ck}$ $= 14.5$ N/mm^2 $F_{Rd} = 630 \times 200 \times 14.5 \times 0.56 = 1023$ kN per 5.6 m wall. $H_{Rd} = 1023 \times \cos 27.4° =$ <u>908 kN</u> $\times$ 4 no. walls = 3632 kN > $H_{ux} = 1345$ kN	t = 200 mm	$t = 5600/30$	$t = 186$ mm < 225 mm

Therefore use the same thickness as per the walls in the *y*-direction.

For ease of further comparison, take $t = 225$ mm-thick precast walls for both solutions. The positioning of the walls is symmetrical and well balanced throughout the structure.

Step 2: Positions and shapes of primary columns

These are shown hatched solid in Figure 3.77. They are located at all the intersections identified so far, i.e. corners, lift shafts and staircases. Assume the columns are all rectangular or square in cross section. The special shaped columns in the curved part will be dealt with in Step 7(1).

Step 3: Positions and shapes of secondary columns

The positioning of these columns is not always straightforward. It is often dictated by architectural requirements, such as window bay sizes. Assume that the columns are all square in cross section. Split the task into two parts:

(1) Internal secondary columns. A suggested layout of columns is shown as open squares in Figure 3.77. The internal columns on grid line 2/A–K have been equispaced at 8 m centre-to-centre. The distance between the main stair (grid 7) and lift shaft (grid 12) is 12.0 m. This distance could be divided in many ways, depending on the architecture, but choose 6 + 6 m for this exercise. The distance between beams on grid lines B–C/9–12 has been made 3.0 m to enable the floor slab to be used to support the walls around the service void (see Step 7 (2)).

The maximum clear beam span (at the higher floor levels, where the column is 300 mm square) is therefore 7.7 m. Therefore internal beam depth = 600 mm. The span/allowable depth ratio = 7700/600 = 12.8.

This is within the permitted range according to Clause 7.4.2, provided $A_s < 3.3\%\ A_c$	**$A_s < 0.033\ A_c$**	This is within the permitted range according to Clause 3.2.4

(2) External secondary columns. There is no requirement, where flooring is spanning perpendicular to a building façade, that the centres of external and internal columns should be equal. Thus on grid line A column centres may be equidistant = 8.0 m. Similarly in the curved part columns are placed at 8.0 m centre-to-centre (*x*-axis), and on grid lines 1 and 4 also at 8.0 m centre-to-centre.

Where the flooring is spanning parallel with the edge of the building, the internal and external column centres should preferably be equal to avoid cranked beams and splayed floor slabs. Thus the maximum external beam span = 7.7 m, giving span/depth = 12.8, again within range. Therefore external beam depth also = 600 mm.

Step 4: Floor depths

The maximum floor span is 9.0 m centre-to-centre at grid 13/C–F, giving a clear span of 8.5 m (assuming the beams are 500 mm wide) and an effective span of 8.6 m (assuming 100 mm bearing lengths). For this type of building the choice of slab is realistically restricted to hollow-core or double-tee slabs, although with the majority of spans being 5.0 m to 8.0 m hollow-core flooring will be preferred. Given that the imposed live load on the floor and roof is 5.0 and 1.5 kN/m^2 from Figure 3.22, select depth of hollow-core slab = 200 mm for all. The self-weight of 200 mm-deep hcu, including infill concrete in the ≈ 50 mm-wide joints between them, is 3.35 kN/m^2. Thus the total dead *udl* for roof and floors = 3.35 + 1.50 = 4.85 kN/m^2.

Step 5: Column sizes

Some knowledge of column design is required to make a good estimate of column sizes, but referring to Section 3.2.6, use gross area = axial load/28.

(1) Internal columns. Maximum axial load occurs at grid D/2, where the floor area supported by that column is 8 × ((7+7)/2) = 56 m^2, and the length of beam = 3.5 + 3.5 + 4.0 = 11.0 m. Allowing 5 kN/m and 3 kN/m for the self-weight of the beams and column, respectively, the maximum axial force (kN) at the foundation is:

	Dead	Live			Dead	Live	
Roof slab = 56 m^2 =	272	84		Roof slab = 56 m^2	272	84	
Roof beam = 11 m	55	0		Roof beam = 11 m	55	0	
Floor slab = 4 × 56 = 224 m^2	1086	672**		Floor slab = 4 × 56 = 224 m^2	1086	784*	
Floor beams = 4 × 11 = 44 m	220	0		Floor beams = 4 × 11 = 44 m	220	0	
Column = 17 m	51	0		Column = 17 m	51	0	
Total in kN	1684	756		Total in kN	1684	868	
** live load reduction 30%, increased by area reduction to 40 %				* live load reduction 30% for design of the five-storey column supporting four floors.			
Ultimate force,				Ultimate force,			
$N_{Ed} = 1.35 \times 1684 + 1.5 \times 756$			$N_{Ed} = 3407$ kN	$N = 1.4 \times 1684 + 1.6 \times 868$			$N = 3746$ kN
Try 400 mm at the ground to third floor.			$b = h = 400$ mm	Hence $b = h = \sqrt{(3746 \times 10^3/28)}$			$b = h = 365$ mm
$l_0 = l = 4000$ mm				Use 400 mm at the ground to third floor. The slenderness ratio = 4000/400 = 10 < 15, hence the column is not slender.			
Radius of gyration $i = 400 / \sqrt{12}$			$b = h = 115$ mm				
$\lambda = 4000 / 115$							
$\lambda_{lim} = 20 \times A \times B \times C / \sqrt{n}$			$\lambda = 34.8$				
where A = 0.7, B = 1.1, C = 2.2 for braced columns where $r_m = -0.5$ (based on 50% carry over to foundation), and $n = N_{Ed}/A_c f_{cd} = 3407 \times 10^3 / 400 \times 400 \times 22.67 = 0.939$							
$\lambda_{lim} = 20 \times 0.7 \times 1.1 \times 2.2 / 0.969$ > 34.8 therefore column is short.			$\lambda_{lim} = 34.9$				

**The multi-storey live load reduction factor from EC1-1 National Annex NA.2.6: for 5 storeys, where all floors and the roof qualify, $\alpha_n = 1.1 - 5/10 = 0.6$.

(*Continued*)

This makes the length of the first and second lift columns 10 m and 7 m, respectively. A column splice can be made and concealed within the depth of the third-floor slab (where 200 mm depth is available in which to make the connection).

The axial force (kN) in the column above third floor is:

	Dead	Live			Dead	Live	
Roof slab = 56 m^2	272	84		Roof slab = 56 m^2	272	84	
Roof & floor beams = 22 m	110	0		Roof & floor beams = 22 m	110	0	
Floor slab = 56 m^2	272	252*		Floor slab = 56 m^2	272	280	
Column = 7 m	21	0		Column = 7 m	21	0	
Total in kN	675	336		Total in kN	675	364	
*live load area reduction to 10% remains.							
Ultimate force,				Ultimate force,			
$N_{Ed} = 1.35 \times 675 + 1.5 \times 336$			$N_{Ed} = 1416$ kN	$N = 1.4 \times 675 + 1.6 \times 364$			$N = 1527$ kN
Try 300 mm above the third floor.				Hence $b = h = \sqrt{(1527 \times 10^3/28)}$			$b = h = 233$ mm
$\lambda = 20 \times A \times B \times C/(N_{Ed}/A_c f_{cd})$				Use 300 mm at the roof to third floor.			
$l_0 = l = 3000$ mm				The slenderness ratio = 3000/300 = 10 < 15, hence the column is not slender.			
$b = h = \sqrt{(1416 \times 103/28)}$			$b = h = 225$ mm				
Radius gyration $i = 300/\sqrt{12}$			= 87 mm				
$\lambda = 3000/87$			$\lambda = 34.5$				
$\lambda_{lim} = 20 \times A \times B \times C/\sqrt{n}$							
where A = 0.7, B = 1.1, C = 0.7 for braced columns where $r_m = +1.0$ (based on single curvature), and $n = N_{Ed}/A_c f_{cd} = 1416 \times 10^3 / 300 \times 300 \times 22.67 = 0.694$							
$\lambda_{lim} = 20 \times 0.7 \times 1.1 \times 0.7/0.833$ < 34.5 therefore column is slender.			$\lambda_{lim} = 12.9$				
Clause 5.8.8.2. $M_{Ed} = M_{0Ed} + M_2$							
where $M_{0Ed} = 50$ kNm (is given)							
Second order $M_2 = N_{Ed}\, e_2$							
where $e_2 = 1/r\, l_o^2/10$							
Clause 5.8.8.3.							
(5.36) Take worst $K_r = 1.0$							
(5.37) $K_f = 1 + (0.35 + 0.2 - 34.5/150) \times 1.0 = 1.32$, letting $f_{ef} = 1$							
(5.34) $1/r = 1.0 \times 1.32 \times 0.002175/0.45 \times 350 = 18.2 \times 10^{-6}$ using $f_{yd} = 0.87 \times 500$ N/mm^2 and $E_s = 200000$ N/mm^2							
$e_2 = 18.2 \times 10^{-6} \times 3000^2/10 = 16.4$ mm							
$M_{Ed} = 50 + 1416 \times 0.0164 = 73.3$ kNm							
Using Figure 4.53, the column is satisfactory as 300 × 300 mm.							

Multi-storey live load reduction factor from EC1-1 National Annex NA.2.6: for 2 storeys, where the 4th floor and the roof qualify, $\alpha_n = 0.9$.

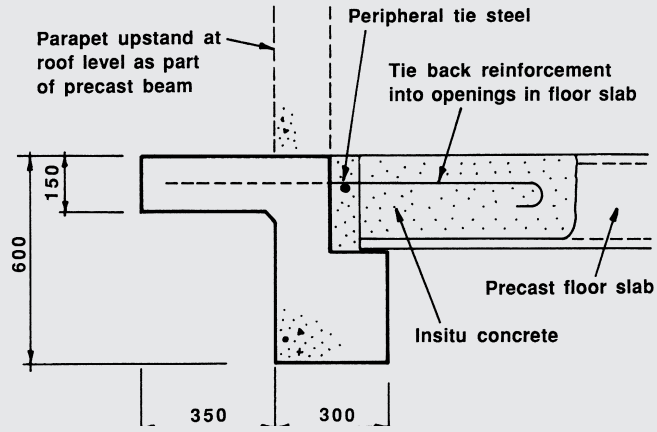

Figure 3.78 Edge details for the special beams used in the precast structure studied in Exercise 3.1.

(2) External columns External columns are usually smaller in cross section than internal columns. The maximum load in an external column occurs on grid line A (neglecting for the moment the columns in the curved façade, which are non-rectangular and will be dealt with in Step 7), where the area of floor slab supported by the column is $8 \times 8/2 = 32\,m^2$. The external façade *udl* is assessed to be 6.6 kN/m for 1.5 m high double-skin brickwork, plus 0.5 kN/m for glazing. Thus repeating the above procedures, at the foundation:

Try 300 mm square columns. 250 mm square columns could work here	$N = 2430$ kN $b = h = 96$ mm		$N = 2642$ kN $b = h = 307$ mm

Use 350 mm square or 400 × 300 mm ground to second floor, 300 mm square thereafter. The external column splice has been placed at the second floor in order to stagger the level of the splices. Note that changes in the external column section may cause severe problems in modular bay widths for window fixings, brickwork, etc. and should be discussed with the architect.

Step 6: Staircases

Figure 3.29(c) would be a good choice for all staircases. L-shaped edge beams would be used at the half-landing level. The stair side beams on grid lines B, C, H & J would be a rectangular shape with a cut-out to support the floor landing.

The depth of the flight unit would be approximately (5500/25) + 30 cover = 250 mm, i.e. equal to the floor depth. The landing could be either a 250 mm-deep hollow-core slab or a solid rc unit.

Step 7: Special Details

(1) Columns and edge beams to curved façade

The details in Figure 3.78 show the proposed shapes of these units. Because the angle offset at each of the 3 interior columns (grids 10, 13) is equal, these columns may be similar in cross section. The beam span = 8.31 m.

The column profile between floor levels would be circular, and in the region of the beam connection would be a rhombus. The maximum area of floor slab supported by these columns (grid F/13) is (4.5 + 0.5 overhang) × 8.245 = 41.23 m^2.

The maximum axial load on these columns is approximately 3500 kN. Thus a column diameter to BS EN 1992 of 250 mm could work {$b = 354$ mm to BS 8110}. Use 400 mm diameter over the full height, since a

(*Continued*)

special mould would be required to cast these columns. In order to reduce the cost of this mould, the column should be spliced at the third-floor level. (Here it is better for the upper column to be the shorter length.)

The four curved edge beams would all be equal length and identical in shape, requiring only one additional mould. The ends of the beams would be square to fit against the rhombus-shaped column.

Careful attention would be required when scheduling the lengths and splayed ends to the hollow-core floor slabs in this area.

(2) Framing around large floor voids

It is very important to appreciate the effect of a major floor void. It may involve additional components rather than merely strengthening existing components. In this case the major services void occurs adjacent to the lift shaft at grid B/12. Referring to the detailed plan in Figure 3.77, the walls around the 2 m × 2 m void may be supported on the floor slab marked A. The total ultimate load of the 100 mm blockwork (plus plaster) along the side of the void in that slab = 14 kN. This is easily catered for using 200 mm-deep units.

Step 8: Stability ties

Although the calculation for tie forces is carried out at the detailed design, it is necessary to ensure at this stage that the ties can be positioned and made structurally continuous throughout the building. In floors without structural toppings the ties will be collected over the tops of beams and pass either through sleeves in the columns or alongside the column. This poses no problems except at staircases and lift shafts, where the ties cannot be continued straight through. Threaded bars are screwed into cast-in threaded sockets at these positions.

The perimeter ties approaching the external corners (e.g. grid A/1, K/4, etc.) are allowed to pass in an arc around the corner. However the ties approaching the re-entrant corner (grid D/4) are not, because the resultant force pulls towards the outside of the structure. Here the ties should pass straight on and be fully anchored in the floor slab beyond. The detailed design solution is shown in Figure 9.27.

Step 9: Construction matters

At this point it is worth considering the craneage requirements, the construction sequence and the self-weights of the units obtained in the preliminary design. It may be assumed that the site is a 'green field', with no obstructions to crane or lorry access. For the purpose of this exercise it may be assumed that the nearest approach the crane may make is to a line drawn at 5 m from the edge of the structure, and that the crane may be positioned at the most convenient point on this locus. To identify a suitable crane, it is necessary to determine the maximum moment (weight of unit × reach) as shown in Table 3.8:

Table 3.8 Determining the maximum moment for the crane

Unit	Grid location	Weight (tonne)	Maximum reach (m)	Moment (t m)
200 mm-deep hollow-core floor	C–F/13	3.3	10.0	33
Edge beams	A/1–13	4.0	5.0	20
Edge beams in curved façade	D–F/6–13	4.8	6.0	29
Internal beam	B/2–4	4.0	13.0	52
Lift-shaft walls at ground level	B–C/13	5.6	14.5	81
Main stair wall at ground level	B–C/4	5.6	14.5	81
Escape stair wall at ground level	H & J/1–2	9.5*	8.5	81
Escape stair wall at upper level	H & J/1–2	6.6	8.5	56
Main stair flight	B–C/4–7	6.0	12.3	73
Escape stair flight	H–J/1–2	5.7	8.5	48
Internal column	D/2	3.9	13.0	51
External circular column	F/13	3.0	5.0	15

* This unit may be split into 2 units.

CHAPTER 4

Design of Skeletal Structures

Detailed design methods, with worked examples, are given for the design of beams, staircases, and columns subjected to gravity loads. Materials specifications are given.

4.1 Basis for the Design

The correct philosophy for the design of a precast concrete multi-storey structure is to consider it as a total entity, not an arbitrary set of components. The BCA's Frames Manual [4.1] states: *Precast concrete frames are often, but mistakenly, considered to consist of individual components which need to be designed and connected together in a manner that ensures adequate strength and interaction between them. . . . An assessment should be made of the requirements for each component and its contribution to the building as a whole.*

Precast structural frame design is an interactive procedure, and several iterations within the design routine are carried out. The result is that the subtleties of the process have been refined by the precasters to such a degree that it is difficult for the uninitiated to gain access to the thought process. Final solutions are born out of many years of trial and error in the design office, the testing laboratory and on site. Once the general (Chapter 1) and architectural (Chapter 3) aspects have been resolved, the order in which the design proceeds is as follows:

(1) precast concrete components: roof and floor slabs, staircases, beams, columns and walls
(2) connections between components
(3) stability: floor diaphragm action, walls, columns, and temporary safety
(4) structural integrity: robustness, ties, and progressive collapse.

The components of the structure are classified by considering their functions as either:

(a) slabs, simply supported between beams and providing the horizontal floor diaphragm;
(b) beams, supported between columns and providing the chords to the horizontal diaphragm; or
(c) columns and walls, carrying gravity forces to the foundations and providing the stabilising system.

In this context, staircases do not contribute to the structural system. The design considers individual precast components, the connections between them and their behaviour in the global structure at

Multi-storey Precast Concrete Framed Structures, Second Edition. Kim S. Elliott and Colin K. Jolly.

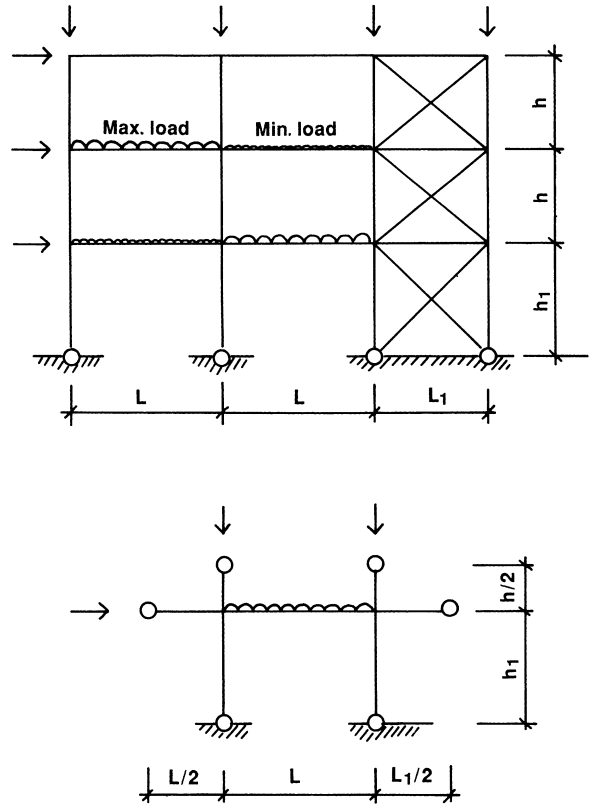

Figure 4.1 Substructuring methods for precast frame design.

both the serviceability and ultimate limiting states. In the former the components are proportioned so that crack and deflection criteria are satisfied and the effects of thermal, creep and shrinkage movements are not adverse. At ultimate limit state, the components and their connections are checked for sufficient strength, stability and ductility.

Simplified 2-D sub-structuring of frames is used to determine the internal forces and moments in the members and connections; Figure 4.1. An elastic analysis of the structure is carried out and plastic methods are used for the design of the components. No redistribution of bending moments is considered. The effects of imperfections, e.g. lack of verticality, positions and stiffness of shear walls, creep, thermal movement and shrinkage, are catered for in the global structural frame analysis. The latter items are not generally considered in buildings where the plan dimension is less than 30 m. Equilibrium is checked on the basis of an undeformed structure, using first-order deflections to compute force eccentricities. Second-order deflections are used in the design of individual components, e.g. columns and walls. Occasionally numerical finite element methods or full-scale experimental strain analysis of localised areas, e.g. supports, concentrated load points, anchorage zones and abrupt changes in geometric section, are used to validate design assumptions.

In the main, precast concrete buildings are analysed as pin-jointed, braced structures; Figure 4.2(a). The beams are simply supported between columns or walls, and the columns are required to resist axial loads and small moments produced by eccentric forces at the ends of beams. The foundations are pinned, and subjected only to axial compression. Although the design of the stabilising system is separate from the design of the components, the two are carried out simultaneously.

In certain cases, for example in buildings of up to three storeys, the structure is considered unbraced, relying for stability on cantilever action in the columns and moment-fixity at the

foundation. As an alternative to every column resisting moments, a small number of large columns acting as deep beams may be used as wind posts at intervals along the structure; Figure 4.2(b). In both of these cases the stability design is an integral part of the component design.

Partially braced structures, Figure 4.2(c), offer a compromise between fully braced and fully unbraced structures. Here the component design is directly influenced by the stabilising system, and vice versa.

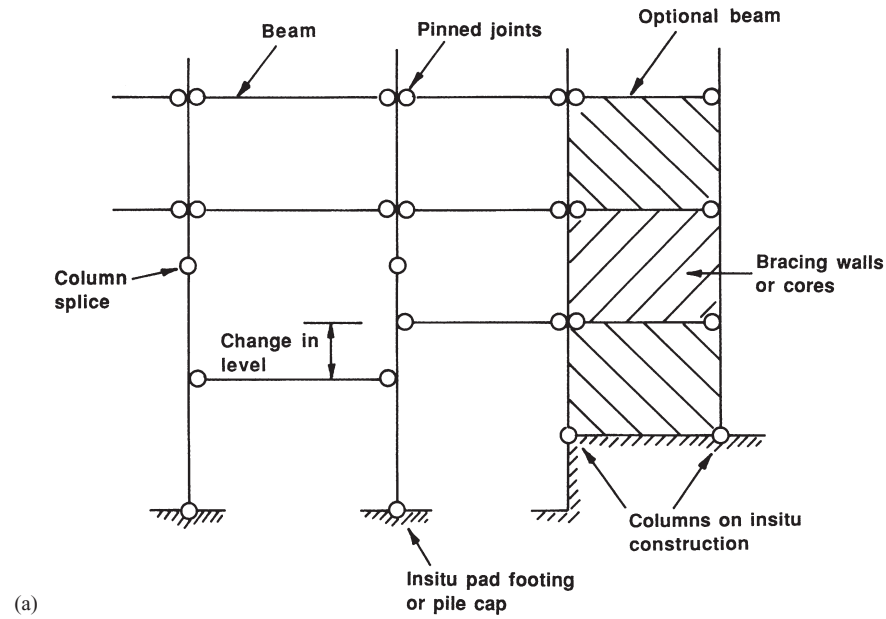

(a)

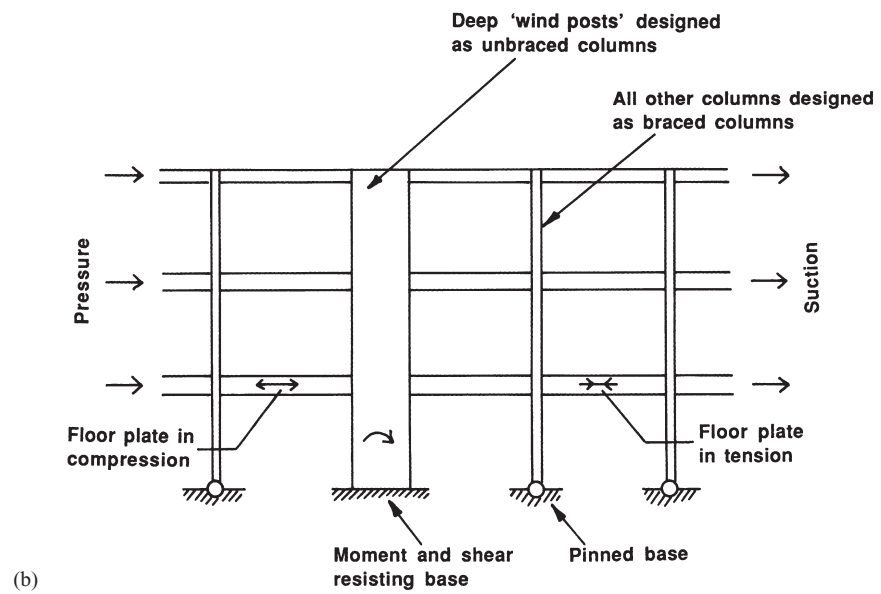

(b)

Figure 4.2 Principles of braced structures. (a) Principle of a pin-jointed braced structure; (b) principle of a bracing using deep columns; (c) principle of a partially braced structure.

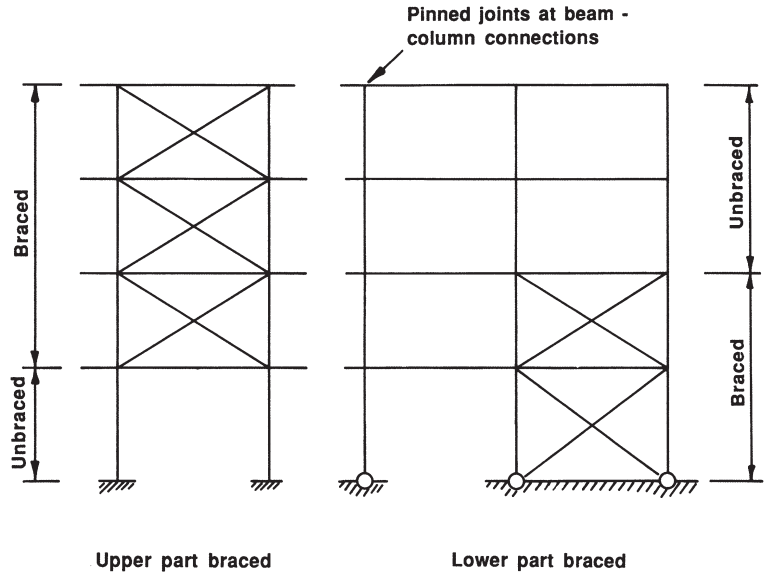

Figure 4.2 (*Continued*)

However, it is generally accepted that the most economical solution, in terms of manufacture and erection, is to use the pin-jointed braced version. The main advantages are:

- Minimisation of precast components, e.g. columns may be multi-storey and beams need only be provided primarily in one direction (Figure 3.6).
- Pin-jointed connections are made on site without the necessity of a seven-day (or longer) curing period required for *in situ* concrete joints.
- The structure is structurally stable floor by floor.
- Foundations are optimised because the column base is pin-jointed.

The main disadvantage is that shear walls etc. are often sought in places other than staircases and lift shafts in order to avoid torsional effects; see Section 8.2. Conflicting architectural and structural requirements occasionally lead to additional framing to satisfy both aspects.

4.2 Materials

Prefabrication of reinforced and prestressed concrete components has much greater potential for economy, structural performance and durability than cast-*in situ* concrete. Most precasting works use computer-controlled batching and mixing equipment, leading to a reduction in the standard deviation in the appropriate performance index, i.e. workability, strength gain, ultimate strength and uniformity. Typical values for the standard deviation of compressive cylinder {cube} strengths are 2 to 3 N/mm^2 {3 to 4 N/mm^2} for mean design strengths of 40 to 50 N/mm^2 {50 to 60 N/mm^2}.

The working platform for casting concrete is adjacent to the mould and is therefore conducive to geometrical accuracy and good concrete compaction. The result is that the grade of concrete used can be exactly suited to the requirements of each type of component in order to expedite the use of the more expensive and exhaustible materials. Enhanced concrete stresses, i.e. up to the characteristic cylinder strength {0.8 of the cube strength}, may be used in certain situations. Tests on bespoke precast

components and connections have been used to substantiate this assumption, which would not be possible with cast-*in situ* work.

4.2.1 Concrete

The 28-day characteristic and design strengths and short-term elastic moduli (N/mm^2 units) for the range of standard mixes used are given in Table 4.1. The 28-day cylinder {cube} crushing strengths f_{ck} $\{f_{cu}\}$ refer to cylinders or cubes stored in water at 20°C (not air-cured), and refer to the grade indicator C, followed by cube/cylinder strength.

Cement is classified according to BS 8500-2:2006 +A1:2012, Table 1. Cement type shall conform to BS EN 197-1:2000 *Cement – Composition, specifications and conformity criteria for common cements*. The grade of cement (e.g. 52.5R, 42.5N) shall be appropriate to the required 28-day cylinder {cube} strength and the strength at the time of demoulding or transfer of prestress.

Normal-weight coarse aggregates from natural land sources conform to BS EN 12620:2002, *Aggregates for concrete*. Sea dredged aggregates are not used. The precast manufacturer can confirm the sources of all aggregates and suppliers' name(s) for each category stored. Aggregates should be free from impurities such as pyrites, which may cause surface defects.

Mixing water conforms to EN 1008:2002 *Mixing water for concrete,* clause 3.1, and is potable from land sources. Water reclaimed from cement slurry is filtered such that the cement content is less than 10 per cent by weight, or the specific gravity of the filtered slurry is less than 1.1. Sea water is not used.

The design of concrete mixes is in accordance with national design data, e.g. in the UK that is *Design of Normal Concrete Mixes* [4.6]. Producers may modify the mix proportions according to BS EN 206-1:2000 [4.7] to obtain the greatest benefit from local materials, superior in quality to those in the national standard. One of the main mix-design parameters is the strength of concrete at an age

Table 4.1 Design strengths and moduli used in precast components [4.2, 4.3]

Component	Type	Grade	Characteristic strength (N/mm^2)	Design strength (N/mm^2)	Tensile strength (N/mm^2)	Modulus (N/mm^2)
To BS EN 1992-1			f_{ck}	$0.567f_{ck}$	f_{ctm}	E_{cm}
Beams, staircases, floors, shear walls	rc	C32/40	32.0	18.13	3.0	33 350
Columns, load-bearing walls	rc	C40/50	40.0	22.67	3.5	37 000
Beams, floors, staircases	psc	C50/60	50.0	28.33	4.1	32 000
To BS 8110			f_{cu}	$0.45f_{cu}$	f_{ct}	E_c
Beams, staircases, floors, shear walls	rc	C32/40	40.0	18.0	–	28 000
Columns, load-bearing walls	rc	C40/50	50.0	22.5	–	30 000
Beams, floors, staircases	psc	C50/60	60.0	27.0	3.50	32 000

Note: E_{cm} $\{E_c\}$ is the 28-day mean value. Long-term values are derived from the creep coefficients in BS EN 1992, Part 1, clause 3.1.4 [4.4], or BS 8110, Part 2, clause 7.3 [4.5].

Table 4.2 Indicative strength gain and mix proportions in standard mixes

Mix proportions (kg/m³)									
		28-day strength					Aggregates		
Grade	Lifting strength (N/mm²)	f_{ck} (N/mm²)	f_{cu} (N/mm²)	RHPC	Water	Sand	<14 mm	<10 mm	Admixture[1] (kg/m³)
C32/40	21	32	40	375	170	575	850	430	0
C40/50	25	40	50	400	150	525	890	445	0
C50/60	30	50	60	410	150	500	895	445	0
C50/60[2]	35–38	50	60	410	100	685	775	480	0–60[3]

Notes: Actual values used depend on quality of local materials and the lifting requirements of the precast producer.
[1] See Section 3.3.3.
[2] Refers to machine-produced hollow-core, which accounts for the marked difference in the mix proportions of the C60 and C60[2] grades.
[3] Includes Pozzolana used in certain hollow-core slab mixes, but a problem with blowholes in the soffits has limited wider use of these additives.

of 24 hours for beam, column, wall and staircase units, and between 12 and 24 hours for prestressed hollow-core slabs. This is the optimum age when the units are removed from the mould, and the strength at this time is termed the lifting strength. For prestressed units it coincides with the stress transfer strength. It is important that the cylinders {cubes} used for de-tensioning purposes are cured in the identical manner to the actual concrete. This may present a problem where an electrical heating method, such as induction in the tendons, is used. Accelerated-cure cylinders {cubes}, possibly no more than 24 hours old, are frequently used to predict the 28-day strengths. These strengths may be as high as 85 to 90 per cent of the 28-day value, and excellent correlation (within 5 per cent) is found.

Indicative values for concrete lifting strengths and design strengths, and mix proportions, are given in Table 4.2. The sand is medium zone, and the aggregates are normal-weight gravels, crushed limestone or crushed granite.

Cast-*in situ* concrete is used to complete many types of connection. The strength of the *in situ* concrete is required to be the same as the precast concrete only where the load-carrying capacity must be equal to that in the parent precast member, e.g. column splices, but should not be less than grade C20/25. A special mix may be specified for pumped concrete to structural toppings. Notional values for infill *in situ* concrete strengths and mix proportions for the site-placed concrete are given in Table 4.3.

Expanding agents are occasionally used as an admixture. The data given here should not be used in favour of manufacturer's instructions, which must be followed to give the correct dosage with respect to the type of cement used and the intended purpose of the mix.

Creep and shrinkage strains are determined according to BS EN 1992-1-1, clause 3.1.4 Figure 3.1, or BS 8110, Part 2, Figures 7.1 and 7.2, and by detailed calculation using Annex B. The age at loading is usually taken as 28 days. Relative humidity is taken as 50 per cent {45%} in internal situations, and 80 per cent {85%} externally.

4.2.2 Concrete admixtures

Admixtures will comply with BS EN 934-1:2008, BS EN 934-2:2009 +A1:2012 and BS EN 934-3:2009 +A1:2012 [4.8], *Admixtures for concrete, mortar and grout*. Self-compacting admixtures will comply with BS EN 206-9:2010 [4.9], *Concrete – Additional rules for self-compacting concrete*. Precast manufacturers will make known the dosages of all admixtures and provide certificates of conformity. The main types of admixture sometimes used in factory-cast concrete are as follows:

- Pozzolana, such as pulverised fuel ash, used as a partial cement replacement in certain prestressed units;
- retarding agents, used to retard the hardening of concrete surfaces that are to be removed to expose the aggregate matrix. The retarding agent is applied only to the surface of the mould, and is not added to the mix;
- air entrainment agents, such as liquid lignosulfanate plasticising air entrainment, used to increase the plasticity of concrete for use in slip-formed products;
- self-compacting concrete and rheology modifier, used in wet-cast work and for visual concrete;
- colouring pigments, for visual concrete.

Table 4.3 Indicative infill *in situ* concrete strengths and mix proportions

Mix proportions (kg/m^3)										
		28-day strength						Aggregates		
Location	Grade	f_{ck} (N/mm^2)	f_{cu} (N/mm^2)	OPC	RHPC	Water	Sand	<20 mm[1]	<6 mm	Admixture (kg/m^3)
Floor infill Structural toppings Beam end connections[2]	C20/25	20	25	325	–	180	660	1235	–	0
Beam end connections	C32/40	32	40	–	425	250	1700	–	0	0–4
Wall infill					425	250	850		850	0–4
Column splices	C40/50	40	50	–	500	300	1575	–	0	0–5
Columns to foundations					500	300	785		785	0–5

Notes: Actual values used depend on quality of local materials and the specific requirements of the contractor.
[1] Graded through 20–5 mm.
[2] Some end connections are large enough for concrete, rather than grout, to be used. See Section 7.9.

4.2.3 Reinforcement

High-tensile steel bars conform to BS EN 10080:2005 [4.10], *Steel for the reinforcement of concrete* as H500A, H500B and H500C, depending on the requirements for ductility. H500B is the most common. At present (year 2013), however, the technical specification is actually according to the UK National Annex, and is given by values of R_e = yield strength = 500 N/mm^2; R_m/R_e = ratio of tensile strength/yield strength = 1.05, 1.08 and 1.15 to 1.35 for classes A, B and C; A_{gt} = percentage total elongation at maximum force = 2.5%, 5.0% and 7.5%, respectively; fatigue strength, bend performance, weldability, bond strength, shear and weld strength for use in welded fabric, tolerances and dimensions. Note that H500 in 6 mm-diameter reinforcing steel does not comply with BS EN 1992-1-1 in respect of ductility. Shape codes are to ISO 3766:2003 [4.11].

High-tensile ribbed steel bar is used in the majority of cases, including shear links, where the increased tensile strength and lower cost outweigh the reduced ductility. This is particularly relevant in the highly stressed areas around connections and supports, where smaller volumes of reinforcement give greater access for concrete and vibrating pokers. Welded fabric (or mesh), produced from reduced plain high-tensile bar or indented wire, is used in 2-D units such as slabs and walls. It is a false economy to specify too many different bar types and sizes in precast production.

Stainless-steel ribbed reinforcement is used in very exceptional circumstances where the thickness of a section is small with respect to the conditions of exposure, e.g. 75 mm thickness if the exposure category is severe or worse. Stainless-steel rebars conform to BS 6744:2001 [4.12], *Stainless Steel Bars for the Reinforcement of and Use in Concrete.* The yield strength is given as $R_e = 500\,\text{N/mm}^2$, and $R_m/R_e = 1.10$. For non-chloride exposure the grade shall be at least 1.4301 (was BS 6744 grade 304); otherwise grades 1.4401 or 1.4436 shall be used (was BS 6744 grade 316). Stainless-steel mesh fabric is to BS 4483:2005 [4.13].

Epoxy fusion-bonded reinforcement, galvanised steel reinforcement, and fibre-reinforced polymer reinforcement are not usually used.

The bar diameters commonly used are 8 and 10 mm for column stirrups; 8, 10 and 12 mm for beam links and distribution (crack control) bars; and 16, 25, 32 and 40 mm for the main flexural bars. Popular mesh sizes are A142 (6 mm bars at 200 mm centres) and A193 (7 mm bars at 200 mm centres) for flat precast units such as plank floor slabs and walls, and for structural toppings. C283 mesh (6 mm bars at 100 mm centres in one direction and 5 mm bars at 400 mm centres in the other) is used in the flanges of double-tee slabs. The 5 percentile characteristic strength (N/mm^2) for hot-rolled, high-yield steel is taken as $500\,\text{N/mm}^2$ {and for mild steel is $250\,\text{N/mm}^2$ (note that grade 250 rebar is not recognised in BS EN 1992-1-1, clause 3.2.2)}. The modulus of elasticity is taken as $200\,\text{kN/mm}^2$.

4.2.4 Prestressing steel

Two main types of prestressing steel tendon are commonly used:

- 5 or 7 mm-diameter (occasionally 9 mm) indented (or crimped) wire or plain wire.
- 9.3, 10.9, 12.5 or 15.2-mm diameter 7-wire standard helical strand.
- 9.6 and 15.7 mm-diameter 7-wire super-stress strand.

Prestressing tendons conform to BS EN 10138-1, *Prestressing steel – Part 1: General requirements* (in draft) [4.14]. Helical strand comprising of 3 or 7 hot-rolled wires, and individual hot-rolled plain or Belgian indented wire, are all, in accordance with BS EN 1992-1-1 clause 3.3.2 (4), having 'low' relaxation class 2, i.e. 2.5 per cent after 1000 hours stressed. In some cases the manufacturer may use the supplier's data, where relaxation as low as 1.6 per cent is possible. Plain and indented wire of 5 and 7 mm diameter, and ribbed wire of 9 mm diameter, may be used. Maximum diameters for use in hollow-core units are given in BS EN 1168:2005, clause 4.1.1.1 [4.15].

Smaller diameters are possible, such as 6.5 mm-diameter strand made from three wires, but less frequently used. A popular type of helical strand, called 'Dyform', is drawn through a die to partly flatten the six outer wires. Both wire and strand are classified as 'class 2: 2.5 per cent low relaxation', meaning the final stress in the wire after elastic relaxation over 1000 hours will be 97.5 per cent of the original prestress. The 5 per cent characteristic strength is taken as f_{pk} $\{f_{pu}\} = 1750\,\text{N/mm}^2$, except for 7 mm wire f_{pk} $\{f_{pu}\} = 1670\,\text{N/mm}^2$. Super-stress strand is also available, where f_{pk} $\{f_{pu}\} = 1860\,\text{N/mm}^2$ and the relaxation is 2.5 per cent.

The modulus of elasticity E_p is taken as $195\,\text{kN/mm}^2$ for helical strand, and $205\,\text{kN/mm}^2$ for indented wire.

4.2.5 Structural steel and bolts

Structural steelwork conforms to BS EN 10025-1:2004, *Hot rolled products of structural steels: General technical delivery conditions*, and is designed according to EC3. Rolled steel sections and bent or flat steel plate are welded to form steel connectors in many highly stressed support situations where direct contact between concrete surfaces is to be avoided. Steelwork is usually coated with zinc phosphate high-performance metal primer, to give a mean dry coating thickness of at least 0.08 mm, or polyamide cured epoxy primer at least 0.08 mm thick.

The steel most used is grade S275 {43} or grade S355 {50}. Welding electrodes are of minimum grade E43. The most common types of rolled section used in beam shear boxes and/or column inserts are rectangular hollow sections (typically 200 × 100 mm or 150 × 100 mm cross section), square hollow sections (typically 150 mm or 100 mm size), channels and angles. Solid steel billets are also used in column inserts. Steelwork entirely cast in concrete is cleaned by blasting to ISO 8501-1 to standard SA1, where poorly adhering mill-scale, rust and old paint and foreign matter are removed, but well-adhered contaminants remain. No primer is used.

Hot-dipped galvanised steel is used for exposed connections, usually those of secondary structural significance, such as dovetail channels for brick ties. The basic plate is grade 43 steel, and grade 50 is used in the more highly stressed plates. It conforms to ISO 1461:1999, *Hot-dip galvanised coatings on fabricated iron and steel articles.*

Metric bolts, set screws and nuts still conform to BS 3692:2001, *ISO metric precision hexagon bolts, screws and nuts. Specification*, and washers to BS 4320:1968, *Specification for metal washers for general engineering purposes. Metric series*. (There are no current documents as EN.) The minimum diameter for a structural bolt or threaded rod is 12 mm. Strength grades for 'black bolts' of carbon steel are to Grade 4.6, 5.6, 6.8, 8.8 (both ≤16 mm and >16 mm) and 10.9. Grade strength of nuts is 4, 5, 6, 8 and 10, respectively. Grade 8.8 galvanised, preferably sherardised, bolts are now more commonly specified. Strength classes of stainless-steel bolts and screws are 50, 70, 80 and 100.

High-strength friction-grip bolts (HSFG) are used in special circumstances where the integrity and safety (both temporary and permanent) of connections made with ordinary bolts in clearance holes cannot be guaranteed. HSFG bolts conform to the National Annex A to BS EN 1993-1-8:2005, UK National Annex to Eurocode 3, *Design of steel structures. Design of joints*. Grades are 8.8, 10.9 and 12.9. Preloading of HSFG bolts is to BS EN 14399-1:2005, *High-strength structural bolting assemblies for preloading. General requirements*.

Welding of steel plates to plates or rebars is carried out to BS EN 1011-1:2009, *Welding. Recommendations for welding of metallic material. General guidance for arc welding*. The importance of the welding to the structural behaviour of many connections cannot be overstated. Welding electrodes conform to BS EN 1011-2:2001, *Arc welding of ferritic steels*, and BS EN 1011-3:2000, *Arc welding of stainless steels*. Welding of reinforcement bars is mostly by metal–inert gas, known as 'MIG-welding'. Electrodes are quite small and are usually between 2.5 and 6 mm in diameter. Preheating is not required, and post-weld heat treatment is not normally carried out on such small items.

4.2.6 Non-cementitious materials

Polymers and additives are used extensively in site work. Epoxy-based mortars are used to make, either partially or completely, connections where a rapid gain in strength is required, e.g. up to 40 N/mm^2 in 2 to 3 hours. Care is taken to ensure that these materials have not exceeded their shelf life, are being used correctly and for the right application. Neoprene, rubbers and mastics are used for soft bearings, backing strips, etc. The specification and design are according to BS EN 1337-3:2005, *Structural bearings – Part 3*: Elastomeric bearings (currently under revision as prEN 1337-3:2011, *Structural bearings – Part 3*). The *PCI Manual on Architectural Precast Cladding* [4.2] gives extensive guidance on the use of these materials. Although they are not used extensively in precast structures, a typical range of applications and representative material properties is given in Table 4.4. See also the *Institution of Structural Engineers' Manual*, Section 3 [4.16].

4.3 Structural Design

4.3.1 Terminology

The term 'component' is used to describe the single prefabricated artefact, e.g. a beam. Occasionally the term 'unit' is used to describe single floor components, such as hollow-core units.

Table 4.4 Use of non-cementitious materials in precast construction

Material	Application	Data (at 20°C)
Elastomeric bearings, e.g. neoprene, rubber	Bearing pads	Compressive strength = 7 N/mm^2 Shear strength = 1 N/mm^2 Compressive strain = 15%
Bitumen-impregnated sealing strip	Backing strip to concrete joints	Compressibility = 85%
Polysulfide sealants	Expansion joints	Elongation strain < 50%
Epoxy resin mortars	Compression, shear or tension joints	Compressive strength = 55–110 N/mm^2 Tensile strength = 9–20 N/mm^2 Elongation strain < 15%
Polyester resin mortars	Compression, shear or tension joints	Compressive strength = 55–110 N/mm^2 Tensile strength = 6–15 N/mm^2 Elongation strain < 2%
Polystyrene	Filler, back-up blocks	

Precast components are divided into the following groups:

- linear components: beams and columns
- 2-D components: floors, walls, stairs and landings
- 3-D components: towers, cores
- others: foundations, cladding panels, plant room roofs, etc.

The term 'members' is used to describe a situation where the construction is completed by the use or two or more components, e.g. composite members consist of precast floor components and *in situ* concrete. 'Non-isolated members' are those that interact with other members and would sustain loads in the event of failure to their supporting member. For example, hollow-core floor units with fully grouted joints would sustain load if the supporting beam failed.

4.3.2(a) Design methods

Horizontal components are designed as simply supported. The effective span is calculated either in accordance with BS EN 1992-1-1, clause 5.3.2 [4.4] {BS 8110, Part 1, clause 3.4.1 [4.5]} (see Figure 4.3), or by determining the point of effective rotation between the members. Maximum flexural and torsional moments and shear forces are computed for the fundamental serviceability and ultimate limit states, the accidental load condition, and for lifting at the factory and on site.

Particular care must be taken when flexible members (e.g. long-span permanent formwork for structural toppings) bear onto boot lintels. Small changes of the support location can create large percentage changes of the torsional moments. Figure 4.4 shows how slab deflections can increase the effective lever arm of the reaction. Precambering of slab members can be used advantageously to pre-empt this effect, or stepped bearing surfaces can be created at the support. Similarly, large torsional moments can be induced in supporting beams by fixing slab members (e.g. by welding lugs) prior to application of screeds or toppings. Curvature of the slab members can result from wet screed loads, or from overnight cooling of slab top surfaces fixed on sunny days. The bridge loading code BS 5400 [4.17] provides means of estimating temperature gradients through the slabs and thus quantifying the curvature in accordance with BS EN 1991-1-5 [4.18] which accounts for thermal gradients in building components as well as in bridges.

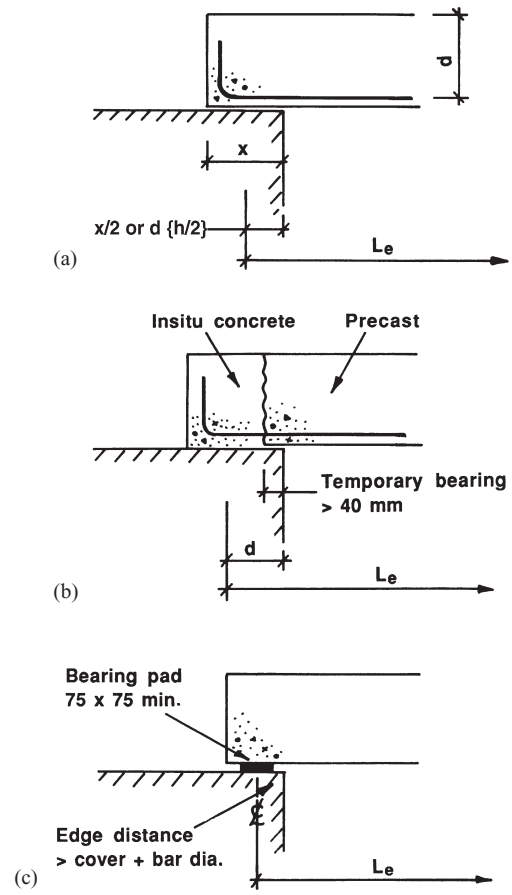

Figure 4.3 Point of effective rotation of simply supported members. (a) Precast unit bearing directly on support. (b) *In situ* bearing cast onto support. (c) Use of bearing pad.

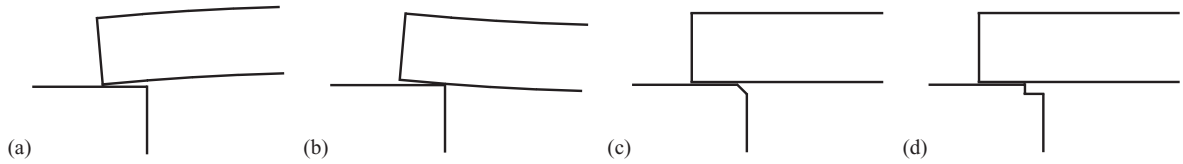

Figure 4.4 Effect of geometry changes at bearings: (a) precamber in beam; (b) deflection within span under load; (c) chamfer to exposed corner; and (d) stepped bearing surface.

Prestressed components are designed to BS 8110 mainly as 'Class 2', but in some situations to 'Class 3(0.1)' or even 'Class 3(0.2)' with regard to serviceability stress limitations. The Eurocode BS EN 1992-1-1 does NOT specify the appropriate tensile strength (nor do the product standards EN 13369 or EN 1168), and this can be the subject of some discussion. The *mean* axial tensile strength f_{ctm} (Table 3.1) is more appropriately used if the stress distribution in the bottom of the section is nearly linear, as in the case of hollow-core units that have wide but shallow bottom flanges. But in solid sections where the stress distribution is triangular, the mean flexural tensile strength $f_{ctm,fl} = \max(f_{ctm}\,;\,(1.6 - h/1000)f_{ctm})$, where h = depth in plane of bending in mm (clause 3.1.8.(1)) might be used. These differences are explained in Figure 4.5. Note that f_{ctm} is roughly comparable to Class 2, as $f_{ctm,fl}$ is to Class 3.

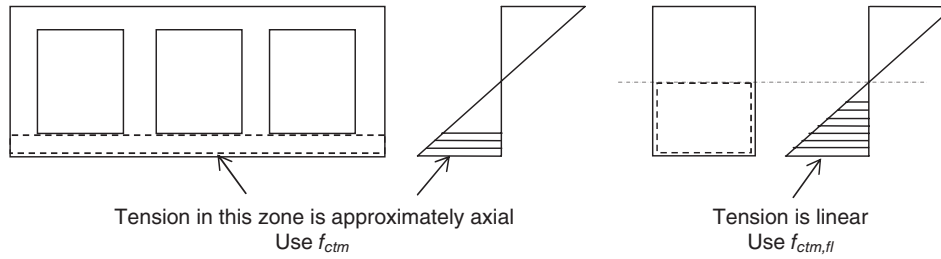

Figure 4.5 Defining mean axial tensile strength and mean flexural tensile strengths.

The permissible tensile stress in BS EN 1992-1-1 is controlled by crack width requirements in Table 7.1N (also National Application document Table NA4) and is related to durability as follows:

Exposure Class	Crack width (mm)	Permissible tension	Service live load
X0, XC1	0.2	f_{ctm} or $f_{ctm,fl}$	Characteristic
XC2, XC3, XC4	0.2	Zero	Quasi-permanent
XD1, XD2, XS1, XS2, XS3	0.2	Zero	Frequent

In BS EN 1992-1-1, it is more convenient to take f_{ctm} as the permissible tension because according to clause 7.3.2.(4): . . . *no minimum reinforcement is required . . . where under the characteristic combination of loads . . . the absolute value of the tensile stress in the concrete is below* $\sigma_{ct,p}$ (where $\sigma_{ct,p} = f_{ct,eff}$ in clause 7.3.2.(2) = f_{ctm}).

Therefore in order to use $f_{ctm,fl}$ minimum reinforcement A_p is required according to BS EN 1992-1-1, Eq. 7.1 and clause 7.3.2.(3) as $\sqrt{\xi} A_p \, \Delta\sigma_p \geq k_c \, k \, f_{cteff} \, A_{c,eff}$, where $\Delta\sigma_p$ is the stress variation in the tendons from the state of zero strain in the concrete at the level of the tendons *after* the concrete there has been decompressed by the characteristic loads, i.e. $\Delta\sigma_p = m(M_s/Z_z - f_z)$, where m = modular ratio, taken here as 15; f_z is the pre-compression after losses; and Z_z is the section modulus at the level of the tendons. Unfortunately if tendons are considered alone (no static reinforcement), this equation is often unworkable, as shown in the following example. Consider a typical 200 mm-deep hollow-core unit with a small area of strands of, say, 370 mm^2 in which $f_z = +4.2$ N/mm^2 and the service moment of resistance $M_{sr} = 80.0$ kNm. Then $\Delta\sigma_p$ is only = $15 \times (80.0/11.1 - 4.2) = 45$ N/mm^2. Using $f_{ctm} = 4.07$ N/mm^2 (for $f_{ck} = 50$ N/mm^2), $f_{ctm,fl} = 4.07 \times (1.6 - 0.200) = 5.7$ N/mm^2, $\xi = 0.6$ for strands (BS EN 1992-1-1, Table 6.2), $k_c = 0.4$, k is taken as 1.0, $A_{c,eff}$ is the portion of the unit in tension and is found to be 33 000 mm^2. Thus $A'_p = 0.4 \times 1 \times 4.07 \times 33\,000 / 45\sqrt{0.6} = 1540$ mm^2. This is not a practicable procedure in design, and is an unreasonable answer that is clearly due to using the post-decompression stress $\Delta\sigma_p$, compared with the full value of f_{yk} used in rc calculations for $A_{s,min}$. For this reason, f_{ctm} is the preferred choice for permissible tension.

Most walls are designed as 'plain' because of the small quantities of reinforcement required, and are in accordance with BS EN 1992-1-1, Section 12, clause 12.6.

Although minimum section sizes are nearly always governed by influences other than design strength, the minimum practical dimensions for components are 50 mm for the flanges of solid slabs, 75 mm for solid slabs, and 140 to 150 mm for horizontally cast beams, columns and shear walls.

Dimensional deviations from the nominal cross section are in accordance with BS EN 1991, clause 4 [4.4] {BS 8110, Part 1, clause 6.11.3 [4.5]}. (Section 3 of the BCA Manual [4.1] gives further guidance on tolerances.) The design assumes that the effects of deviations are included as part of the relevant partial safety factors and the designer should not design using the reduced sections. Table 4.5 gives the results of a sensitivity analysis on 300 mm wide × 300 mm and 600 mm deep rectangular

Table 4.5 Effects of dimensional deviation on flexural serviceability strength of prestressed beams

Nominal cross section height h × breadth b (mm)	Dimension deviation (mm)	Relative flexural strength for deviation of positions of tendons*		
		−5 mm	0	+5 mm
300 × 300	−5	0.92	0.96	1.00
	0	0.95	1.00	1.04
	+5	1.00	1.04	1.07
600 × 300	−5	0.96	0.98	1.00
	0	0.98	1.00	1.02
	+5	1.01	1.02	1.04

Notes:
Negative value means nearer to the neutral axis of the section.
All prestressing parameters are constant for each size of beam.
Concrete grade C50/60.

psc beams (refer to Figure 4.6) and shows the effects that deviations of both the position of the centroid of the tendons and the dimension of the beam have on strength.

The results for the ultimate condition were broadly similar, but with slightly smaller differences for the larger deviations. The table shows that the effects of negative beam and positive tendon deviations, and vice versa, cancel each other out irrespective of the depth of the beam, e.g. the relative strength of a beam 305 mm deep with the tendons raised by +5 mm = 1.00. Where the 5 mm deviations are cumulative, the reductions or increases are in the order of 8 percentage points for the 300 mm deep beam and 3 percentage points for the 600 mm deep beam.

Minimum and maximum volumes of reinforcement can be optimised to give the most benefit in prefabricated concrete. Maximum volume ratios in the order of 10 per cent are possible in flexural components, particularly where the higher-strength concretes (grade > C50/60) are used, in order to minimise depth. Because factory-cast units are cured in a controlled environment, it is possible for minimum quantities of reinforcement to be less than for *in situ* concrete. All major structural components are reinforced in accordance with BS EN 1992-1-1, clause 7.3 {BS 8110, Part 1, clause 3.12.5.} for cracking, and in BS EN 1992-1-1, clause 9.5.3 [4.4] {BS 8110, Part 1, Table 3.27 [4.5]} generally. The requirements are summarised in Table 4.6.

The spacing of reinforcement will be described in the individual component design in Sections 4.3.3 to 4.3.5. The cover to all reinforcement (including links) is as indicated in Figure 4.7. Cover to BS EN 1992-1-1 will normally be the bar diameter plus dimensional deviation for inside buildings, but see clause 4.4.1 for durability requirements [4.4]. {The exposure class, according to BS 8110, Part 1, Table 3.2 [4.5] is mild for internal use.} The dimensional deviation Δc_{dev} to the reinforcement cover is taken as 5 mm, from equation 4.3N.

4.3.2(b) Reduced partial safety factors for precast design

The safety of design carried out to BS EN 1992-1-1 is based on the probabilistic approach in the Eurocode BS EN 1990:2002: *EC0 Basis of Structural Design*. The code outlines possible reasons for reducing partial safety factors (PSF) for dead load (self-weight), and for concrete and steel reinforcement used in precast manufacture, due to the beneficial influence of the prefabrication process. For example, according to a report *Precast Concrete Safety Factors* [4.19], the self-weight of precast elements was found to vary by less than half of the current hypothesis adopted for dead weight. The PSF for materials given in BS EN 1992-1-1, clause 2.4.2.4, i.e. $\gamma_{mc} = 1.5$ for concrete and $\gamma_{ms} = 1.15$ for rebars (previously 1.05 in BS 8110:1985), correspond to geometrical deviations of Class 1 in BS EN

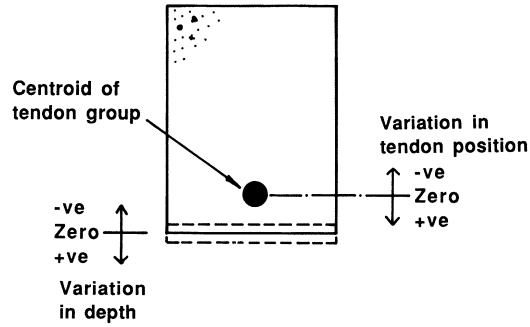

Figure 4.6 Definitions of dimensions used in Table 4.5.

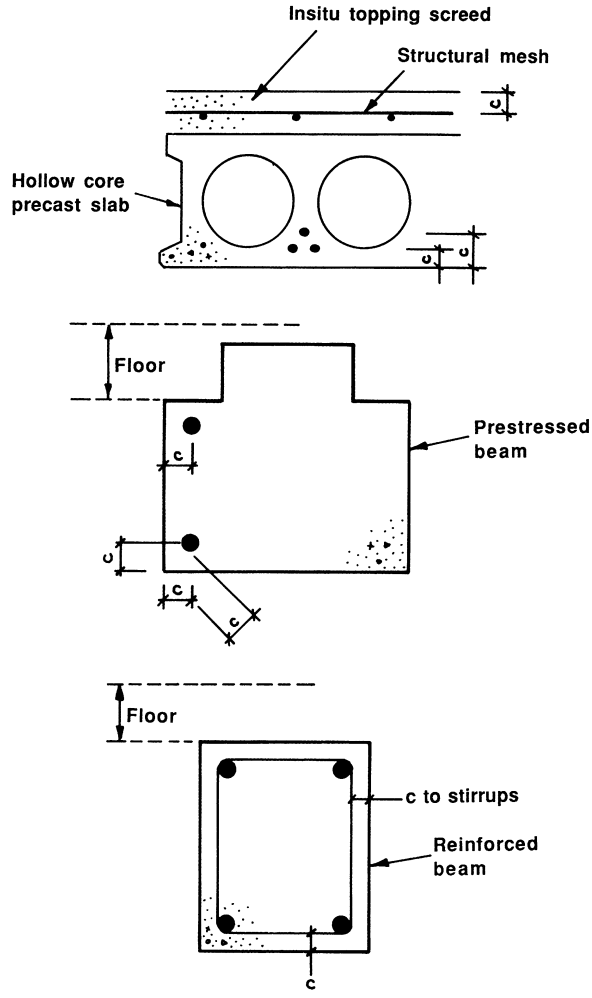

Figure 4.7 Cover to reinforcement in prestressed and reinforced components (centroidal cover distance is often used in psc).

Table 4.6 Maximum and minimum reinforcement quantities as percentage of effective areas

		Primary		Transverse[+]	
Component	**Steel**	**Min %**	**Max %**	**Min %**	**Max %**
To BS EN 1992-1-1					
Rectangular, tee or inverted L-beam	HT/ MS	$0.26\frac{f_{ctm}}{f_{yk}} \geq 0.13$	4.0	As for primary reinforcement, but if cracking is likely see Clause 7.3.	
Columns	HT/ MS	0.40	4 (8 at laps)	Clause 9.5.3	**
Walls	HT/ MS	0.20	4.0	1.0 & Clause 9.6.3/4	4.0
To BS 8110					
Rectangular, tee or inverted L-beam, $b_w \geq 400$ mm	HT	0.13	4.0	0.15*	4.0
	MS	0.24	4.0	0.15*	4.0
Tee or inverted L-beam, $b_w < 400$ mm	HT	0.18	4.0	0.15	4.0
	MS	0.32	4.0	0.15	4.0
Inverted-tee beam	HT	0.26	4.0	0.15	4.0
	MS	0.48	4.0	0.15	4.0
L- beam	HT	0.20	4.0	0.15	4.0
	MS	0.36	4.0	0.15	4.0
Columns	HT/ MS	0.40	8 (10 at laps)	Clause 3.12.7.1	**
Walls	HT	0.40	4.0	0.25 & Clause 3.12.7.4	4.0 or Clause 3.12.7.5
	MS	0.4	4.0	0.3 & Clause 3.12.7.4	4.0 or Clause 3.12.7.5

Notes:
HT = high-tensile rebar, f_{yk} {f_y} = 500 N/mm^2; MS = mild steel plain bar, f_{yk} {f_y} = 250 N/mm^2.
[+] Transverse bars at 90° to primary bars, or minimum links for beams.
* In slabs and staircases, provision for torsion may be required to BS EN 1992-1-1, Clause 9.3 [4.4] {BS 8110, Clause 3.5.3.5 [4.5]}.
** No requirement, but in practice limited to between 1.5 and 2.0 per cent.

13670-1:2009, *Execution of concrete structures* and to the normal levels of workmanship and inspection in the same EN.

Recommendations for reduced PSF for precast concrete are given in BS EN 1992-1-1, Annex A.3. This refers to Annex A.2, clause A.2.1(1) and states that if deviations in the cross-section dimension Δ_b *and* the position of reinforcement $\Delta_c \leq 5$ mm within a depth $h \leq 150$ mm, or Δ_b and $\Delta_c \leq 10$ mm within a depth $h \leq 400$ mm, then a reduced PSF for rebar of $\gamma_{ms} = 1.1$ may be used. If this is satisfied, *and* the coefficient of variation of concrete strength is less than 10 per cent, then a reduced PSF for concrete $\gamma_{mc} = 1.4$.

To test these criteria, a Working Party from nine European countries, including BRE (UK), CERIB (France) and RTT (Finland), published a report *Precast Concrete Safety Factors* [4.19], in which the following are proposed: see Table 4.7.

Table 4.7 Proposed reduced partial safety factors for steel rebars, concrete and dead load

	Reinforcement generally γ_{ms}	Reinforcement in special elements* γ_{ms}	Concrete γ_{mc}	Dead load γ_G
Cast-*in situ*	1.15	1.15	1.50	1.35
Precast concrete	1.15	1.09	1.42	1.28
Precast with tightened tolerance quality**	1.15	1.07	1.42	1.21

* Elements with a high sensitivity to geometrical uncertainty, e.g. less than 250 mm-thick, hollow-core units.
** Tightened tolerances and strict quality control conditions apply when variation in geometry < 2.5% mean.

Figure 4.8 Hundreds of measurements were taken of the self-weight of precast elements in the report *Precast Concrete Safety Factors,* in CERIB Publication [4.19]. (Courtesy Photothèque CERIB.)

A measurement campaign was carried out on precast reinforced and prestressed concrete beams, columns, and ribbed, solid and hollow-core floors at 20 factories in 10 countries (see Figure 4.8). Measurements included concrete strength, density, element volume and self-weight, placement of bars and cover, widths of webs and flanges, and camber.

Figure 4.9 shows that probability density function (p.d.f., i.e. the likelihood for the position to occur at a given point in the precast element) for deviations in the position of rebars of ±10 mm was less than 3 per cent. Figure 4.10 shows the mean deviation from nominal (mean) and standard deviations (s.d.) for the depth and width of precast elements; in 65 product groups of measurements, only four were outside the mean variation of ±5 mm, and there were only three results where the s.d. > 6 mm. For 991 measurements of depth, ranging from 200 to 2000 mm, the range was generally ±10 mm, the mean = 0.85 mm and the s.d. = 5.0 mm. For 730 measurements of width, up to 3000 mm, the range was generally −5 to +10 mm, the mean = 0.23 mm and the s.d. = 4.9 mm. The linear trend lines are confusing, as the s.d. for width decreases to about 2 mm for wider elements, but the opposite is found

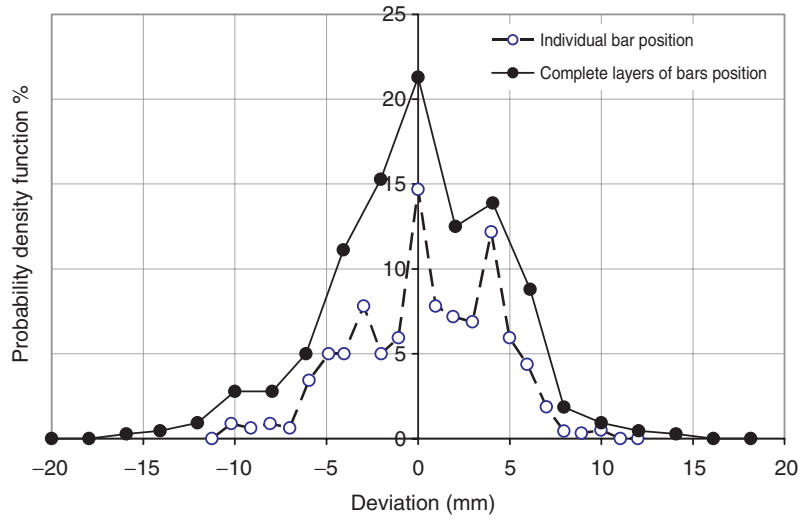

Figure 4.9 Probability density function for the position of reinforcement in beams, adapted from pages 34–35 of ref. [4.19].

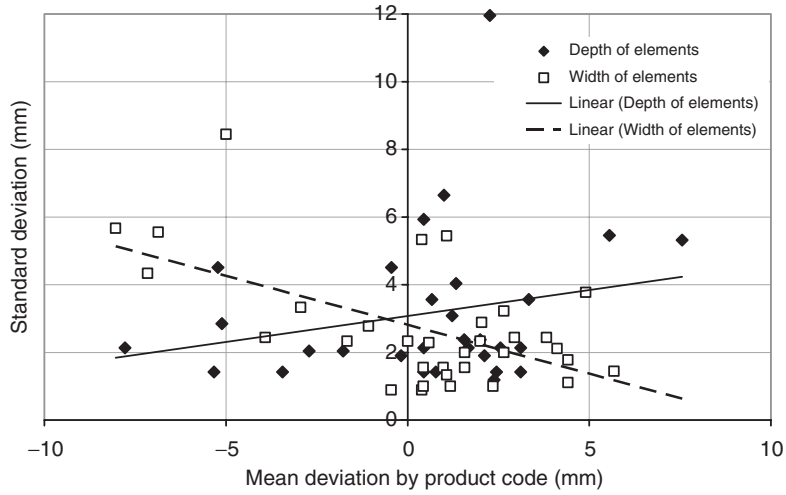

Figure 4.10 Standard and mean deviations in the depth and width of precast elements, adapted from pages 38–39 of ref. [4.19].

for deeper elements, although the scatter may be distorting the picture here. The results from this study suggest that a reduced PSF for concrete of $\gamma_{mc} = 1.4$ is appropriate, providing a manufacturer supplies the appropriate corroborated data. However, $\gamma_{mc} = 1.4$ will *not* be used in this textbook. The proposed reduced PSF for dead load of $\gamma_f = 1.28$ has already been recognised in EC0, equation 6.10(b), where $\gamma_f = 0.925 \times 1.35 = 1.25$.

BS EN 13369, Annex C, clause C.2 [4.20] reiterates the tightened tolerances given in BS EN 1992-1-1, Annex A.2. Hollow-core floor units may have difficulty in meeting the requirements for dimension deviation on depth, i.e. ±5 mm for $h \leq 150$ mm, or ±10 mm for $h \leq 400$ mm. The author has measured the depth of more than 1400 hcus over the period 2005–2008 at three different UK producers. The deviation in depth, ranging from −10 mm to +15 mm, is shown in Figure 4.11. For units $h \leq 150$ mm (including a solid plank made in the same process as an hcu) the

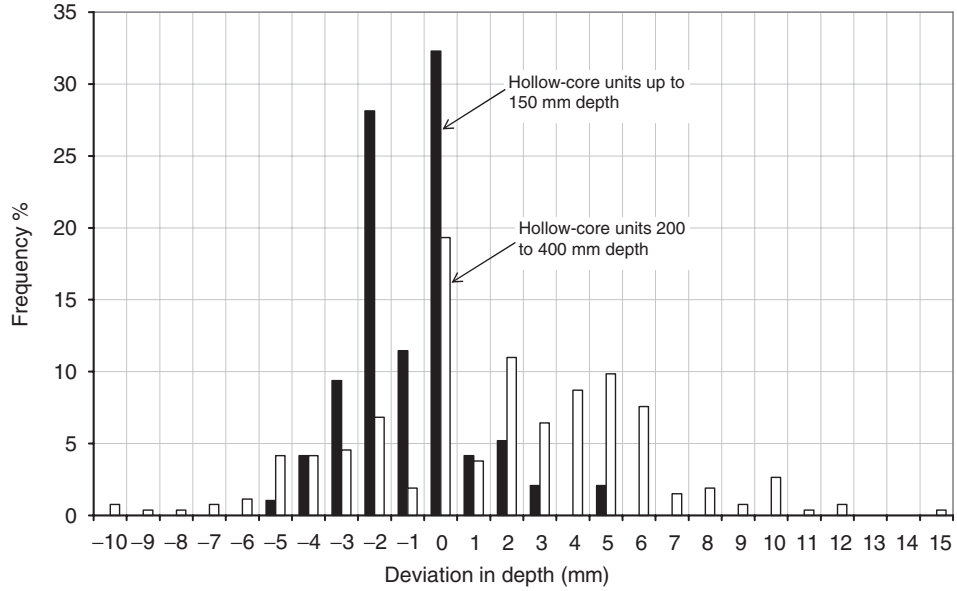

Figure 4.11 Dimensional deviations for measured depths of precast concrete hollow-core floor slabs.

results just fall within range, but not for $200 \leq h \leq 400$ mm, where deviations up to −10 to +15 mm are found. The positive deviation is often a local effect where part of the cross section is deeper, over a breadth of about 150–200 mm out of 1200 mm. Negative deviations of more than −10 mm are localised, but negative deviations less than that may be due to a top plate in slip-forming machines pushing and tamping down the top flange. Extruded units are generally more accurate. The accuracy in length, typically ±10 mm, but in the newer factories within ±3 or better, is not an issue, as the limit is 30 mm.

4.3.3 Design of beams

The design of beams is based on ordinary reinforced or prestressed concrete principles for specified loads and support conditions. Complications in design are associated with beam-to-beam connections, large asymmetrical loadings, and the provision of service holes near to the ends of beams where special shear cages or shear boxes are provided to transmit shear forces to the support. A predetermined set of standardised beam section geometries is selected according to the requirements of most building structures, and both flexural and shear reinforcements are computed for the optimum reinforcement quantities appropriate to each size of beam. PC-compatible software is generally used, and checks for deflections, crack widths, etc. are made simultaneously with strength calculations.

Extensive testing has been carried out over many years to prove the satisfactory performance of precast reinforced and prestressed beams, e.g. [4.3, 4.21, 4.22].

Standardised designs are prepared for beams which vary only in depth, breadth and quantity of reinforcement. Ultimate moments and shear resistances are thus equated with particular project requirements. Families of curves or tabulated data are usually prepared in advance. Standard calculations often allow for service holes up to 50 mm in diameter, with their axes located near the neutral axis of the beam.

Precast concrete beams are mostly simply supported and singly reinforced, thanks to the higher strength of concrete used in precast versus *in situ* construction, although doubly reinforced sections are possible. In BS EN 1992-1-1 the limiting depth to the neutral axis is not obvious, as Figure 6.1 explicitly defines the limiting value of X only for the linear-parabolic ($X = 0.4286h$) and bilinear

($X = 0.5h$) stress block conditions. Clause 5.5(4), equation 5.10 gives the expression $\delta \geq k_1 + k_2\, x_u/d$, where δ is the ratio of moment to redistributed moment, and the National Annex Document to BS EN 1992-1-1 permits $k_1 = 0.4$ and $k_2 = 0.6 + 0.0014/\varepsilon_{cu}$. If $\varepsilon_{cu} = 0.0035$ and rearranging, $x_u/d \leq \delta - 0.4$. If $\delta = 1$, then $x_u/d \leq 0.6$. Thus $X/d \leq 0.6$ will be used in this text for checking single reinforcement in simply supported beams. It should be noted that in some textbooks (in particular the *ISE Manual* [4.23] to which the textbooks refer) on reinforced concrete, $x_u/d = 0.45$ is used. This is because in BS EN 1992-1-1, clause 5.6.3(1) & (2) where plastic rotations occur, for example over supports in the region of yield hinges in slabs, where there is a frequent assumption of 15 per cent redistribution, the expression for δ implies a restriction to $x_u/d \leq 0.45$ for concrete ≤ grade C50/60. The limiting depth X to the neutral axis in singly reinforced sections in BS 8110 is clearly stated as $X \leq 0.5d$.

Given that the depth of the idealised compressive stress block in BS EN 1992-1-1 is $0.8X = 0.48d$ {and $0.9X = 0.45d$ in BS 8110}, the limiting value for single reinforcement is $K' = M_{Ed}/f_{ck}bd^2 = 0.2067$ {$M_u/f_{cu}bd^2 = 0.156$}. Values for elsewhere in Europe are $k_1 = 0.44$, $k_2 = 1.25(0.6 + 0.0014/\varepsilon_{cu})$, $X/d \leq 0.56$, and $M_{Ed}/f_{ck}bd^2 = 0.158$.

Design methods are either 'non-composite' – in which the *in situ* concrete infill between the ends of the slab and beam is ignored – or 'composite'. Composite beam design is dealt with in Chapter 6.

4.3.4 Non-composite reinforced concrete beams

Non-composite construction utilises the properties of the basic beam. Ultimate moments and shear resistances are equated with particular project requirements. Load versus span data may be presented, as shown in Figure 4.12, for a range of reinforced concrete edge beams and prestressed concrete internal beams, as seen in Figures 3.34(a) and 3.34(b).

L-shaped edge beams, otherwise known as 'ledger beams', support non-symmetrical floor loads, usually at the edge of the structure. In this book the part of the beam supporting the floor is called the 'boot' and the main web is the 'upstand'. Edge beams are designed as under-reinforced and either singly reinforced or doubly reinforced, because the lacer bars in the top of the upstand will increase the moment of resistance. The only complication to design is if the breadth of the upstand varies, but a simple computer program can be written to deal with this. There are two types of edge beam, shown in Figures 4.13 and 4.14:

- Type I, where a wide upstand is part of the structural section, or
- Type II, where a narrow upstand (less than 100 mm) provides a permanent formwork to the floor slab, and is considered monolithic with the *in situ* concrete infill at the ends of the floor slab. The *in situ* concrete is adequately confined by the floor slabs.

Type I edge beams

In type I beams, the minimum width of the upstand should be approximately $b_w = 160$ mm. This allows for two 16 mm-diameter bars to be placed within a 12 mm-diameter shear stirrup, with adequate cover and bar spacing, as shown in Figure 4.15. The ledge width is worked out by adding together the nominal slab bearing length (75 mm), a fixing tolerance (10 mm) and the clear space required for *in situ* infill (50 mm), giving a typical total dimension of 135 mm. Thus the minimum breadth of a type I beam is 295 mm, say 300 mm. The precast concrete upstand width in type I beams is about 75 to 100 mm, but that is because the *in situ* concrete is considered as part of the beam. Then $b_w = (b - 75\,\text{mm})$ and the minimum breadth is about $b = 250$ mm.

Minimum depth is often determined by the size of the connector in the end of the beam, but there is no reason why the beam should not be shallower away from the connection. In this case the minimum depth would be equal to the depth of the floor slab (h_s) plus the minimum boot depth of 150 mm. In most buildings floor depth is at least 150 mm.

The general approach is to limit the increments to 50 mm for both depth (from 300 to 900 mm) and breadth (from 250 to 450 mm) and compute ultimate moments and shear resistances as follows.

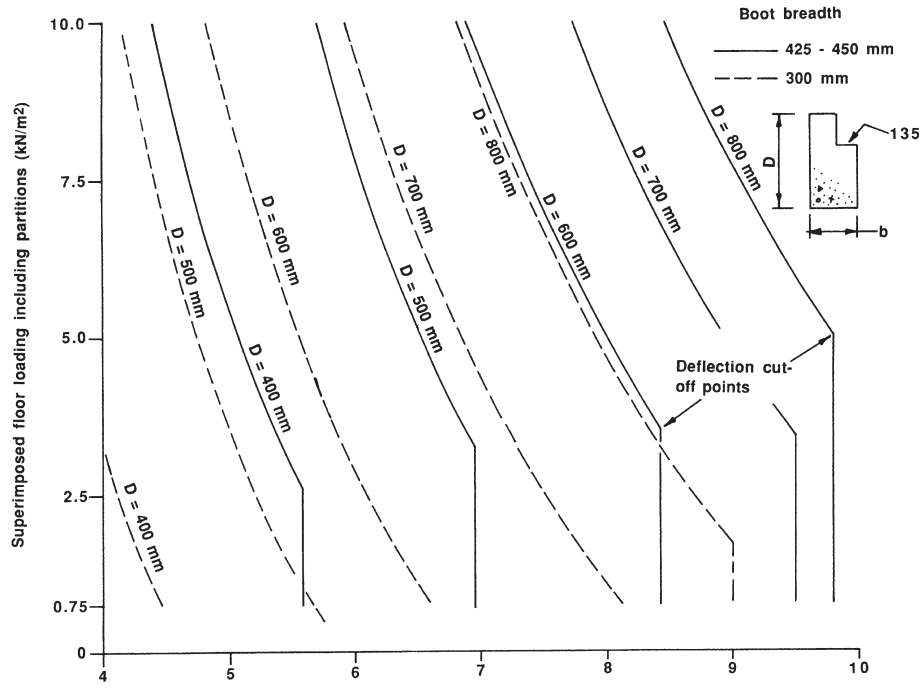

(a)

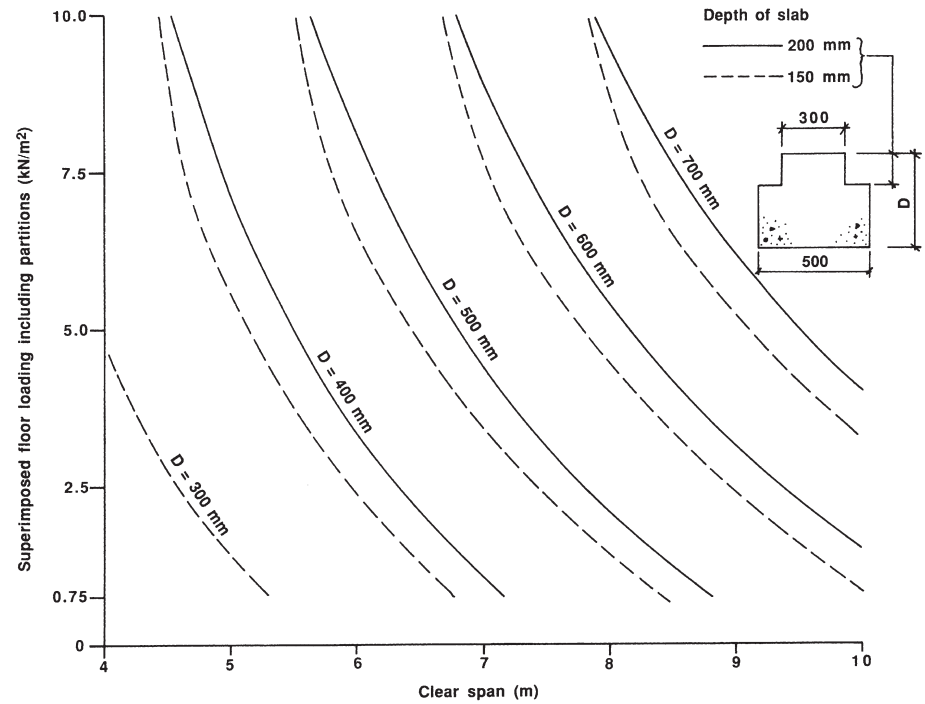

(b)

Figure 4.12 Typical superimposed load versus span data for prestressed and reinforced beams. (a) Reinforced external L beams. (b) Prestressed inverted-tee beams.

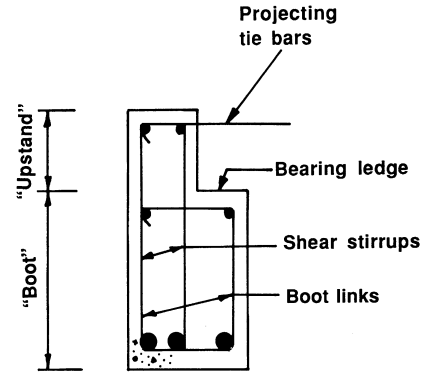

Figure 4.13 Type I edge beams.

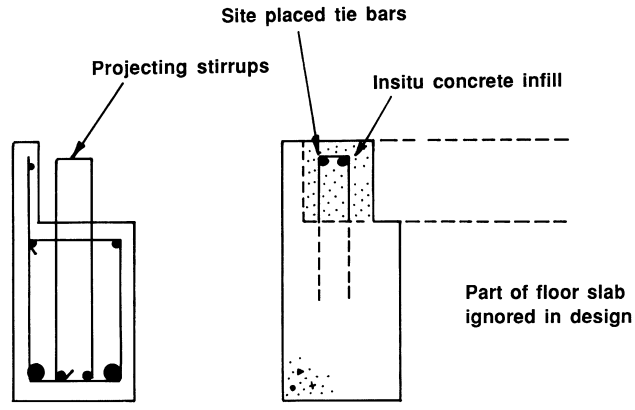

Figure 4.14 Type II edge beams.

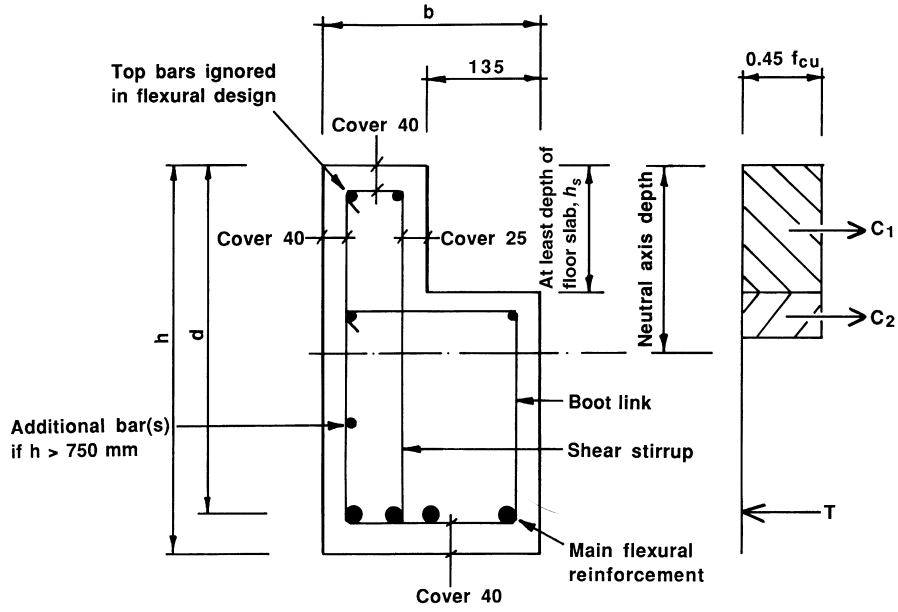

Figure 4.15 Definitions of geometry for Type I beams.

Referring to Figure 4.15, let $\rho = A_s/bh$ and assume that in type I beams the depth to the neutral axis $X > h_s$. Then, for the rectangular concrete stress block assumption:

$T = 0.87\, f_{yk} \rho b\, h$	(4.1)	$T = 0.87\, f_y \rho b\, h$	(4.1)
$C_1 \leq 0.567 f_{ck}\, (b - 135)\, h_s$	(4.2)	$C_1 \leq 0.45\, f_{cu}\, (b - 135)\, h_s$	(4.2)
$C_2 = 0.567 f_{ck}\, b\, (0.8\, X - h_s)$	(4.3)	$C_2 = 0.45\, f_{cu}\, b\, (0.9\, X - h_s)$	(4.3)
$T - C_1 = C_2$		$T - C_1 = C_2$	
hence X, and check:		hence X, and check:	
$X < 0.6\, d$		$X < 0.5d$	
$z_1 = d - h_s/2$ and	(4.4a)	$z_1 = d - h_s/2$ and	(4.4a)
$z_2 = (d - 0.4X) - h_s/2$	(4.4b)	$z_2 = (d - 0.45X) - h_s/2$	(4.4b)
$M_{Rd} = C_1\, z_1 + C_2\, z_2$	(4.5)	$M_r = C_1\, z_1 + C_2\, z_2$	(4.5)
If		If	
$C_1 > T$, then $X < h_s$ and		$C_1 > T$, then $X < h_s$ and	
$M_{Rd} = T\, (d - 0.4\, X)$	(4.6)	$M_r = T\, (d - 0.45\, X)$	(4.6)

Type II edge beams

The design for type II beams (Figure 4.14) is similar, except that the upstand width is $b - 75$ mm.

Table 4.8 gives examples of the flexural capacities of some typical singly reinforced 300 mm-wide L-shaped edge beams, using $b_w = 165$ mm, $h_s = 200$ mm, $f_{ck}/f_{cu} = 32/40$ N/mm^2, f_{yk} $\{f_y\} = 500$ N/mm^2, cover to reinforcement = 35 mm, and assumed diameter of links = 12 mm. The table shows that the beam is more frequently under-reinforced to BS EN 1992-1-1, with $0.534 \leq X/d \leq 0.6$, whereas the section is over-reinforced to BS 8110.

The designed shear links are placed in the upstand of the beam, as shown in Figure 4.16, and not in the boot, to ensure that the reinforcement crosses the plane of potential shear cracking where the shear stress is a maximum. Links to locate bars in the boot do not normally contribute towards shear capacity.

The design of shear reinforcement in BS EN 1992-1-1 is based on the inclined-strut method given in clause 6.2.3, equations 6.8 and 6.9. In their presented form they do not yield a solution to the area of links, but this may be determined as follows:

(See Eq. 6.9)

$$V_{Rd,max} = \frac{\alpha_{cw} b z \nu_1 f_{cd}}{\cot\theta + \tan\theta} = \alpha_{cw} \nu_1 b z f_{cd} 0.5 \sin 2\theta \tag{4.7}$$

where $\alpha_{cw} = 1$, $\nu_1 = 0.6\ (1 - f_{ck}/250)$, $z = 0.9d$ and $f_{cd} = f_{ck}/1.5$.

Table 4.8 Flexural strength of Type I L-shaped edge beams

Overall depth of beam, h (mm)	Bars in bottom of beam	A_s (mm^2)	d (mm)	To EC2		To BS 8110	
				X/d	M_{Rd} (kNm)	X/d	M_r (kNm)
400	2 H25 + 1 H12	1095	340	0.600	112	0.500	101
500	3 H25	1473	440	0.571	217	0.500	199
600	2 H32 + 1 H20	1922	537	0.547	341	0.500	330
700	3 H32	2413	637	0.534	506	0.496	498
800	2 H40 + 1 H25	3004	733	0.540	720	0.500	704
900	3 H40	3770	833	0.562	1013	0.500	950

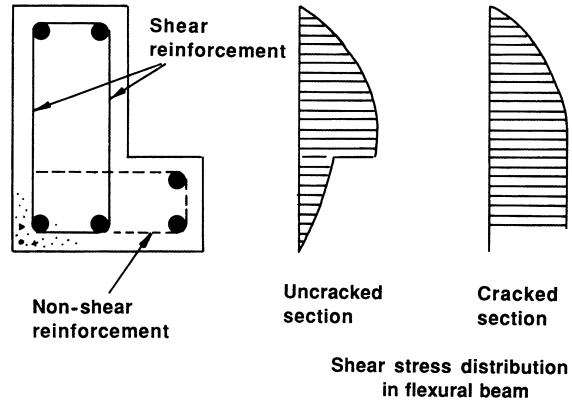

Figure 4.16 Positions of shear links and shear stresses in L beams.

Rearranging and replacing $V_{Rd,max}$ with V_{Ed}

$$\theta = 0.5\sin^{-1}\left(\frac{V_{Ed}}{0.5\nu_1 bzf_{cd}}\right) \tag{4.8}$$

$\therefore \cot\theta$ is determined and $1.0 \leq \cot\theta \leq 2.5$
(See Eq. 6.8)

$$\frac{A_{sw}}{s} \geq \frac{V_{Ed}}{zf_{ywd}\cot\theta} \tag{4.9-a}$$

(see Eq. 9.5N)

$$\frac{A_{sw}}{s}\min \geq \frac{0.08\sqrt{f_{ck}}b}{f_{ywk}} \text{ with } s \leq 0.75d \tag{4.9-b}$$

4.3.5 Beam boot design

The boot of the beam must be reinforced using links around the full perimeter of the boot. If the depth of the boot is less than 300 mm, it should be designed as a short cantilever in bending – otherwise the behaviour is nearer to the strut-and-tie action. The bending method gives a slightly greater area of tie-back steel (about 5–10 per cent).

As with all projecting nibs, it is first necessary to preclude a shear failure at the root of the nib. The enhanced shear stress given in BS EN 1992-1-1, clause 6.2.2 (6) [4.4] {BS 8110, Part 1, clause 3.4.5.9 [4.5]} usually takes care of any vertical shear problems. If not, then the depth of the boot should be increased in preference to providing shear reinforcement. Punching shear beneath point loads is dealt with later.

A 'shallow' boot is one where the lever arm, a, in Figure 4.17 is greater than $0.6d''$, where d'' is the effective depth to the steel in the top of the boot from the bottom of the beam. Otherwise the nib is classed as 'deep'. The design of the boot is very different for the two cases of wide- and narrow-slab flooring. In the former, e.g. hollow-core slab or composite plank, the reactions are uniformly distributed along the boot, whereas in the latter, e.g. double-tee or beam-and-plank, the reactions are point loads applied by the slab beams' webs. The case of uniformly loaded beams will be discussed first.

4.3.5.1 Uniformly loaded boot beams

If the floor slab is placed in direct contact with a shallow bearing nib, a horizontal force resulting from possible contractions or other movement (e.g. thermal effects) of the floor slab relative to the

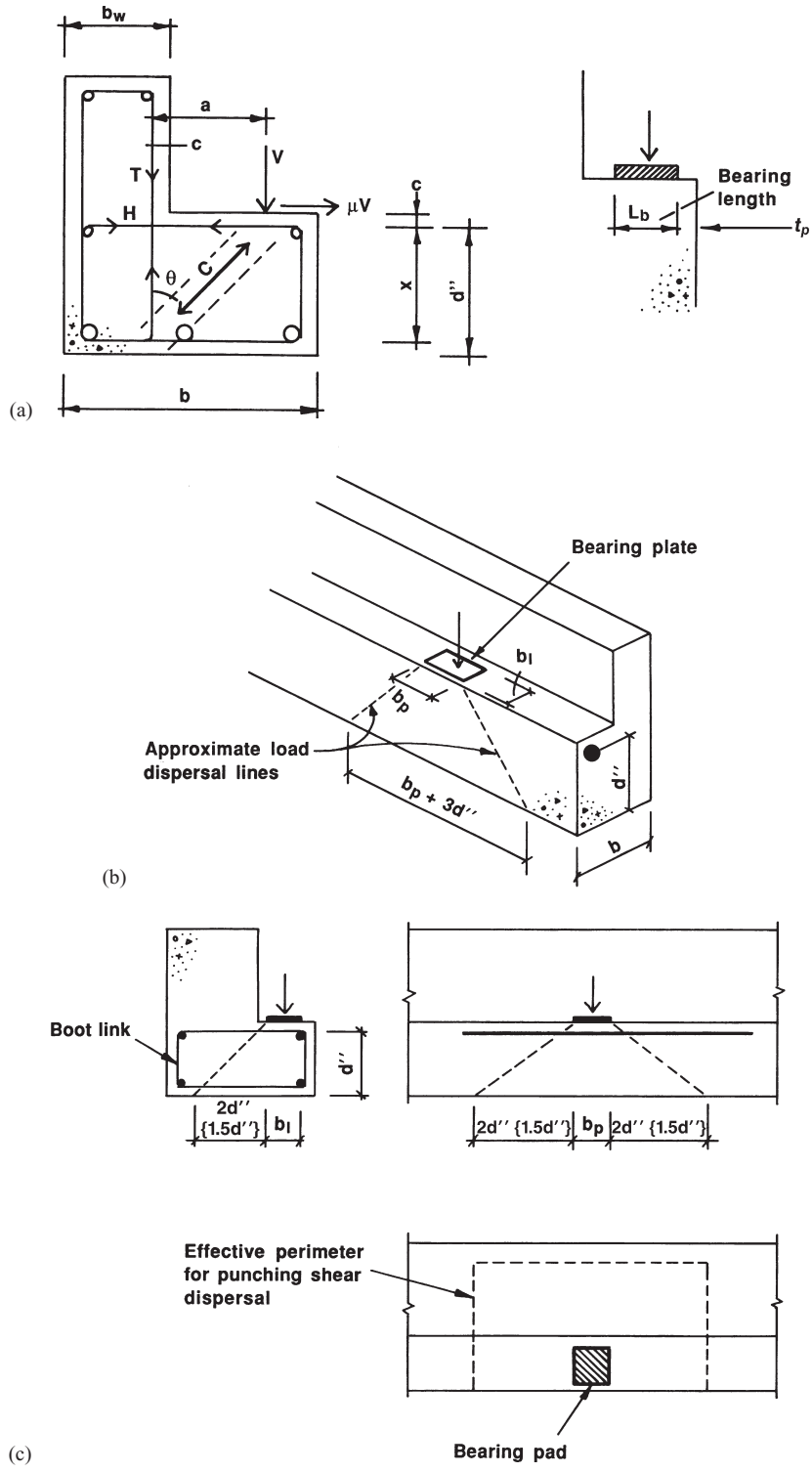

Figure 4.17 Design of boot reinforcement in L beams. (a) Strut and tie model; (b) beam geometry for designing for point loads; (c) design parameters for punching shear design in L beams.

beam will develop at the interface. Referring to Figure 4.17(a), if the floor reaction is V per unit length of beam, the maximum horizontal force is μV, where μ is the coefficient of friction between two concrete surfaces, often taken as 0.7 (see also Section 4.3.10.). Thus the tie force is:

$$H = V\tan\theta + (x + c/x)\mu V \tag{4.10}$$

where $x = (d'' - c)$ is the centre-to-centre distance of the boot link, and c the edge distance to the centroid of the steel bar in the top of the boot. The horizontal bars placed in the top of the boot must satisfy:

$$A_{sh} = \frac{H}{0.87 f_y}. \tag{4.11}$$

The bars are formed into links, but do not contribute to vertical shear strength of the beam unless the boot is sufficiently deep that the vertical leg of the boot link extends at least one-third of the depth of the beam above the neutral axis of the section. Because the upstand width is fairly small, typically 150 mm, the bars in the top of the boot must extend a full anchorage length in the rear face of the beam. This means that the bars are stressed beyond a point that is more than four diameters from the corner of the bar, and the bend radius must be checked so that the bursting stresses caused by small bend radii are not a problem. The usual practice is to provide H8 or H10 links at a spacing no greater than 280 mm for mild steel bars and 155 mm for high-tensile bars ($2(d'' + c) < 0.75d < 250$ mm to BS EN 1992-1-1, clauses 9.3.1.1(3) and 9.3.2(4) {BS 8110, Part 1, Table 3.28}).

The strut force is given by:

$$C = V/\cos\theta \tag{4.12}$$

which must be resisted by a compressive strut in the uncracked part of the nib. The uncracked zone may extend to a point, based on the maximum depth to the neutral axis, at $0.6d''$ {$0.5d''$} from the bottom of the beam. The limiting compressive strength of the concrete, which is subjected to transverse tension in the bottom of the beam, is $0.6(1 - f_{ck}/250)f_{cd}$ from clause 6.5.2(2), equation 6.56 {$0.4f_{cu}$}.Thus the strut capacity per unit length of beam is:

$C = 0.24(1 - f_{ck}/250)f_{ck}\, d''\sin\theta$ (4.13-b) | $C = 0.2\, f_{cu}\, d''\sin\theta$ (4.13-a)

The vertical force T in the stirrup in the main body of the beam is given by:

$$T = V\left(1 + \mu\left(\frac{x + c}{a}\right)\right) \tag{4.14}$$

where a is the centre distance from the stirrup to the line of action of the slab reaction. Then:

$$A_{sv} = \frac{T}{0.87 f_y}. \tag{4.15}$$

This steel must be in addition to any shear requirement.

If the floor slab is fully tied to the beam using reinforced *in situ* strips capable of generating the frictional force μV, then this force may be ignored in the above design, in which case $T = V$.

In a deep boot, the floor slab reactions would be carried directly into the web of the beam by diagonal strut action, assuming $\theta = 45^{\circ}$. If the level of the bearing surface is above the neutral axis, the only steel required would be the horizontal steel A_{sh}.

In fact the design of all the above reinforcement should be carried out in two stages, before and after *in situ* concrete has been added to the ends of the slab. This is because the *in situ* concrete potentially increases the bearing length to the full ledge width, and hence reduces the lever arm a. Before the *in situ* concrete is added, the lever arm is $a = c + (b - b_w) - (t_p + L_b/2)$, and the slab reaction

is due to the self-weight of the slab plus the *in situ* concrete infill. Afterwards $a = c + (b - b_w - t_p)/2$, and the slab reaction is due to superimposed permanent and variable loading.

4.3.5.2 Point-loaded boot beams

Consider the case of isolated point loads due to the reactions from double-tee slabs, for example. Additional punching shear and bursting checks should be made.

Punching shear is dealt with by considering the first zone shear perimeter u (according to BS EN 1992-1-1, clause 6.4.4 & 6.4.5 {BS 8110, Part 1, clause 3.7.7}) spreading into the upstand of the beam in an approximately 45° trajectory on one side, and spreading to the edge of the boot on the other. The first task is to decide the boundary of the effective shear perimeter over which the shear is punching. Using the notation in Figures 4.17(b) and (c), if the beam if sufficiently wide such that the spread of load from the bearing is encompassed on three sides of the beam, the shear perimeter u may be taken as:

(BS EN 1992-1-1, clause 6.4.2(2) restricts u to

$$u = 2\,(b - b_w + c) + (b_p + 2\,(2d'')) \qquad (4.16\text{-b})$$

$$u = 2\,(b_l + 1.5d'') + (b_p + 2\,(1.5d'')) \qquad (4.16\text{-a})$$

If the bearing pad is square (the usual case), then:
$b_p = b_l$ and
$u = 3b_p + 6d''$.
However if the breadth of the beam
$b < b_l + 1.5d''$
the situation is similar to a concentrated load near to a free edge, and

$$u = 2b + (b_p + 2 \times 1.5d'') \qquad (4.17)$$

Note that a shear perimeter is allowed only if reinforcement crosses each plane.
If the design shear stress, v

$$v_{Ed} = \frac{2V_{Ed}}{u(d_y + d_z)}\frac{0.5}{2} \quad \text{for } a \le 0.5d$$

$$v_{Ed} = \frac{2V_{Ed}}{u(d_y + d_z)}\frac{a}{2d''} \quad \text{for } a \le 2d$$

and to ensure no links,
$v_{Ed} < v_{Rd,c}$ given by clauses 6.4.2 to 4 with
$v_{min} = 0.0035\ k^{3/2}\ (f_{ck})^{1/2}$

$$k = 1 + \sqrt{\frac{200}{d}} \le 2.0$$

$C_{Rd,c} = 0.12$
$k_1 = 0.10$

$$\rho_l = \sqrt{\rho_{ly}\rho_{lz}} \le 0.02$$

Using $A_{sly} = A_{sh}$ from Eq. 4.15
and $A_{slz} = A_s''$ from Eq. 4.21
(See clause 6.4.4(1), eq. 6.47)
$v_{Rd,c} = C_{Rd,c}k(100\rho_l f_{ck})^{1/3} + k_1\sigma_{cp}$
$v_{Rd,c} \ge v_{\min} + k_1\sigma_{cp}$

$v = V/ud''$
is less than the enhanced concrete shear stress $1.5d''v_c/a_v$ (where a_v is taken as the distance from the edge of the bearing to the shear plane considered), shear reinforcement A_{shv} is not required. Otherwise it is provided according to

$$A_{shv} = \frac{(v - v_c)ud''}{0.87f_y} \text{ for } v_c < v < 1.6v_c \qquad (4.18\text{-a})$$

or

$$A_{shv} = \frac{5(0.7v - v_c)ud''}{0.87f_y} \text{ for } 1.6\,v_c < v < 2.0v_c \qquad (4.18\text{-b})$$

but not less than $\dfrac{0.4ud''}{0.87f_y}$

Note that the link area, A_{shv} in Eq. (4.18) must be in addition to any bending or tie steel A_{sh} provided in Eq. (4.11), because the link is being stressed by two separate forces.

The concrete shear strength v_c is a function of the area of steel A_s crossing the shear plane. In beams this is different in the longitudinal and transverse directions. BS EN 1992-1-1 [4.4] takes this into account in the formulae whereas BS 8110 [4.5] does not consider such a situation and so a reasonable approach is to use the length-averaged value. Therefore, it is necessary in both methods to have designed the longitudinal steel in the top of the boot and the boot links before a punching shear check is made.

The reaction force V is carried to the beam through a neoprene (or similar) spreader pad (of breadth b_p) and is distributed into the upstand of the beam on a 45° trajectory from a point near the edge of the bearing pad. Thus the steel A_{sh} in Eq. (4.11) must be concentrated into a zone of effective width b_e where:

$$b_e = b_p + 4d'' \qquad (4.19\text{-b})$$

$$b_e = b_p + 2a + 400\,\text{mm} \qquad (4.19\text{-a})$$

(assuming a stiff compression zone will extend from a point about 200 mm either side of the edge of the bearing).

In most cases this distance is about 800 mm. The *PCI Manual* states that an effective width of six times the boot depth to either side of the bearing may be used, but this seems to be stretching the limits of load spreading.

The vertical upstand (hanger) stirrups, called A_{sv} above and designed in the same way, must be positioned in the same localised zone according to the forces generated in the compressive strut-and-tie steel A_{sh}, i.e. over the same effective breadth as above. The upstand stirrups are most easily located by tying them to the boot links.

If the boot depth is less than 300 mm, bending steel is required to resist the moment $M = Va$, according to the usual bending theory. Here the effective breadth used in the stress factor equation $k = M / f_{ck} b_e d''^2 \{k = M / f_{cu} b_e d''^2\}$ is defined by Eq. (4.19).

In all cases (irrespective of the design theory used), at least one boot link should be placed within 50 mm from the edge of the bearing to prevent a shear crack forming under the pad. In between these areas of localised concentrations the boot links should be distributed along the beam as nominal steel at a rate of 0.13 per cent A_c {>0.15% A_c}, typically H10 bars at 250 mm centres. However, most precasters would continue the links at the closer spacing to simplify cage manufacture. This also has the added advantage that the position of the nib links is independent of the location of the double-tee bearing point. Typical reinforcement cages for this type of beam are shown in Figure 4.18.

In long-span floors where the end slab reaction is greater than about 200 kN, a minimum depth of boot of about 250 mm is required to enable a 45° compressive strut to develop according to Eq. (4.12) and (4.13), and to satisfy local punching shear either side of the bearing point. If the ultimate slab reaction is less than about 150 kN, a minimum boot depth of about 200 mm may be used. The BS EN 1992-1-1 formulation allows for this, but for BS 8110 the value of Eq. (4.13) should be modified as follows:

$$C = 0.2 f_{cu} (b_p + 2a) d'' \sin\theta. \qquad (4.20)$$

No composite action may be used in this case, as the *in situ* concrete infill does not penetrate to the level of the slab bearing. Although some of the end shear due to superimposed loads will be transferred to the beam through the reinforced interface at the level of any structural topping, this is ignored in design and the boot is reinforced for the full end reaction.

Where the floor slab is connected to the supporting beam by mechanical fasteners the frictional force μV may be ignored, providing of course that the mechanical fastener is capable of mobilising this force. This may occur in double-tee slabs where, as explained in Section 5.3.2, fully anchored end plates in the flanges of the slab are fillet-welded to plates cast into the beam.

The concentrated point loads cause longitudinal bursting tensile forces in the top and outer surfaces of the boot and must be resisted by a longitudinal bar in the corner of the boot. This bar, of area A_s'', is also necessary in forming the cage, but its size and type is determined as follows:

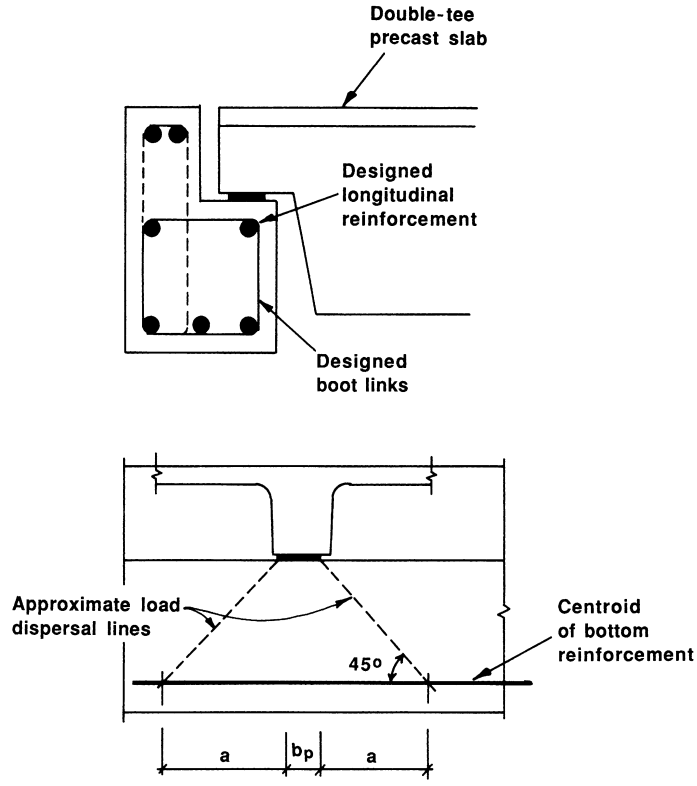

Figure 4.18 Reinforcement in the boot of a beam supporting point loads (e.g. double-tee slabs).

$$A_s'' = \frac{0.25V_{Ed}}{0.87f_{yk}} \quad \left\{ A_s'' = \frac{0.23V}{0.87f_y} \right\} \tag{4.21}$$

where the quotient figure of 0.25 {0.23} is the maximum value derived from bursting theory, as explained in Section 4.3.10. A single longitudinal bar will suffice at not more than 50 mm centroidal distance below the top of the boot. This bar, which is typically H8 or H10, does not contribute to the flexural strength of the beam. If the depth of the boot is greater than 500 mm, a second longitudinal bar is positioned at 250 mm below the first. (Note that these bars are also provided even if wide slab flooring is used.)

In reinforcing beams to support narrow-slab flooring, some knowledge of the positions of the bearing points must be known in advance. It is therefore extremely important that the floor layout is finalised before the beam detailing proceeds.

4.3.6 Upstand design

Edge beams with narrow breadth upstands – which are in compression, of course – are checked for lateral stability or slenderness in the temporary condition before the *in situ* concrete connection with the floor is made. It is possible that this is a limiting criterion with respect to span. The maximum effective span is the lesser of (to BS EN 1992-1-1, clause 5.9) 70 $b_w/(h/b)^{1/3}$ or $300t_f$

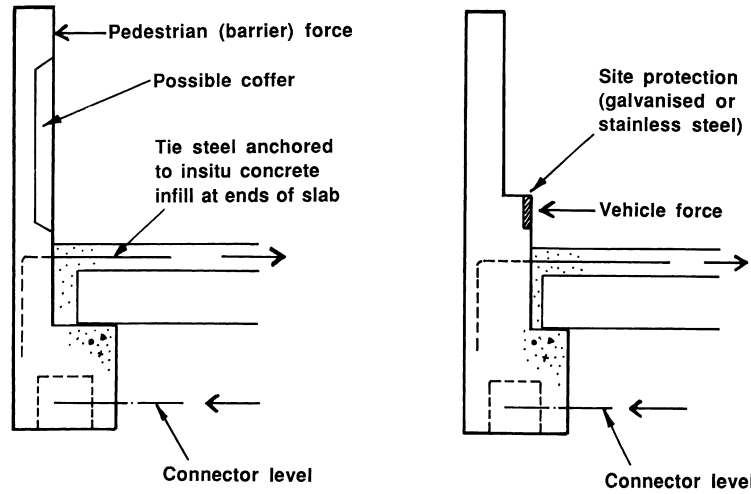

Figure 4.19 Reactions in spandrel beams due to horizontal parapet loading.

where t_f is the floor unit location tolerance [4.4] {or to BS 8110, 60 b_w or $250b_w^2/d$ [4.5]} for type I beams only.

The upstands may be designed to resist vehicle impacts in accordance with BS EN 1991-1-5 [4.18] {BS 6399, Part 1 [4.24]}. A horizontal line force is applied at a height of between 375 mm and 610 mm above the top of the floor slab, and the upstand is designed as a vertical cantilever. The bending moment is transmitted to the slab through the top reinforcement in the structural topping, in the case of double-tee and composite plank units, or through top steel in the broken-out cores of hollow-core slabs. The structural model is shown in Figure 4.19. As a precautionary measure, a fixing cleat is provided at each end of the beam at the top connection with the column. This is designed to carry one-half of the impact force, although it will actually be less than this. Horizontal equilibrium is maintained through the beam-to-column connection at the bottom of the beam (Figure 3.35).

Edge beams subjected to asymmetrical loading are not always reinforced against torsion, on the assumption that the floor plate provides a horizontal prop force and the lateral stiffness of the beam is sufficiently large to prevent excessive horizontal deflections under the action of the propping force. This may be the case once the floor-to-beam joint is completed. It is more difficult to justify the elimination of torsion using the sole propping action of the structural topping, because of the problems in establishing a practical shear transfer mechanism in this type of construction. However, torsion cannot be neglected prior to completion of the joint, particularly if the floor loading and/or floor span is large, as is often the case where double-tee slabs are specified. Diurnal temperature variation and the exposed surface heating temperature gradient will cause a horizontal frictional force at the floor slab bearing onto the boot that can add to the gravity-induced torsion.

An example of this concerns the design of edge beams subjected to asymmetrical loading. It would appear that the beam shown in Figure 4.20(a) should be designed against the torque $T = \dfrac{wL}{2}e$. The value of T can be in the order of 30 to 40 kNm, resulting in a torsional stress (for a typical 300 × 600 mm-deep beam) of around 1.5 to 2.0 N/mm^2. The Eurocode expects a design check to demonstrate adequate resistance to this load case, clause 6.3.2(5), equation 6.31, using a torsion stress = f_{ctd}. The torsional stress is in excess of v_{tmin} and, according to BS 8110, Part 2, clause 2.4.6, torsional links are required. However, edge beams such as the one shown in Figure 4.20(b) have not always been

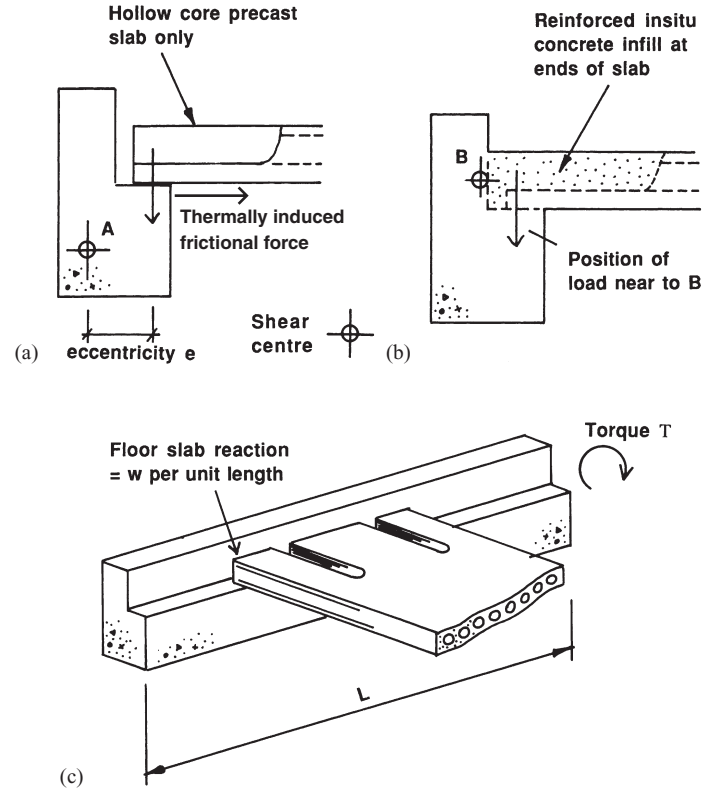

Figure 4.20 Response of asymmetrically loaded L beams. (a) Without *in situ* concrete infill; (b) with *in situ* concrete infill between the beam and slab; (c) general arrangement.

reinforced against torsion, on the assumption that the precast concrete floor plate, which is not monolithic with the beam but is tied into the beam as shown, will provide a horizontal propping force to prevent beam rotations occurring.

Adlparvar [4.25] and Elliott *et al.* [4.26] tested some typical precast edge beams in combined bending, shear and torsion. The beams were 600 mm deep × 300 mm wide, and were of both types I and II defined above. Because the emphasis was on torsion, the torque was exaggerated to produce torsional failures in the beam. In the first tests the beams were loaded without hollow-core floor slabs, i.e. in their temporary condition before the *in situ* infill concrete had hardened. The torsional stress at cracking, according to the 'sand heap' analogy, was 1.8 N/mm^2, as expected, and the beams failed in torsion when the applied torque at either end of the beam was about 60 kNm. However, in the second set of tests, when the same beams were tested under asymmetrical loading through 200 mm-deep hollow-core floor slabs, equivalent floor loads of up to 80 kN/m caused shear failure in the slab. The only cracking in the beam was due to bending at mid-span and shear near to the connector. Figures 4.21(a) and 4.21(b) show failure crack patterns for the beam alone and for the beam when it was tied into the floor slab, respectively.

In the temporary construction stage the beam is not tied to the slab, and therefore only the friction between the floor slab and bearing ledge of the beam will prevent beam rotations. However, the torque induced from the self-weight of the floor slab is only about 0.3 of the total torque in service. This was found not to be great enough to cause torsional cracking in the absence of thermal stress. The conclusions from this work were that, once the joint was complete:

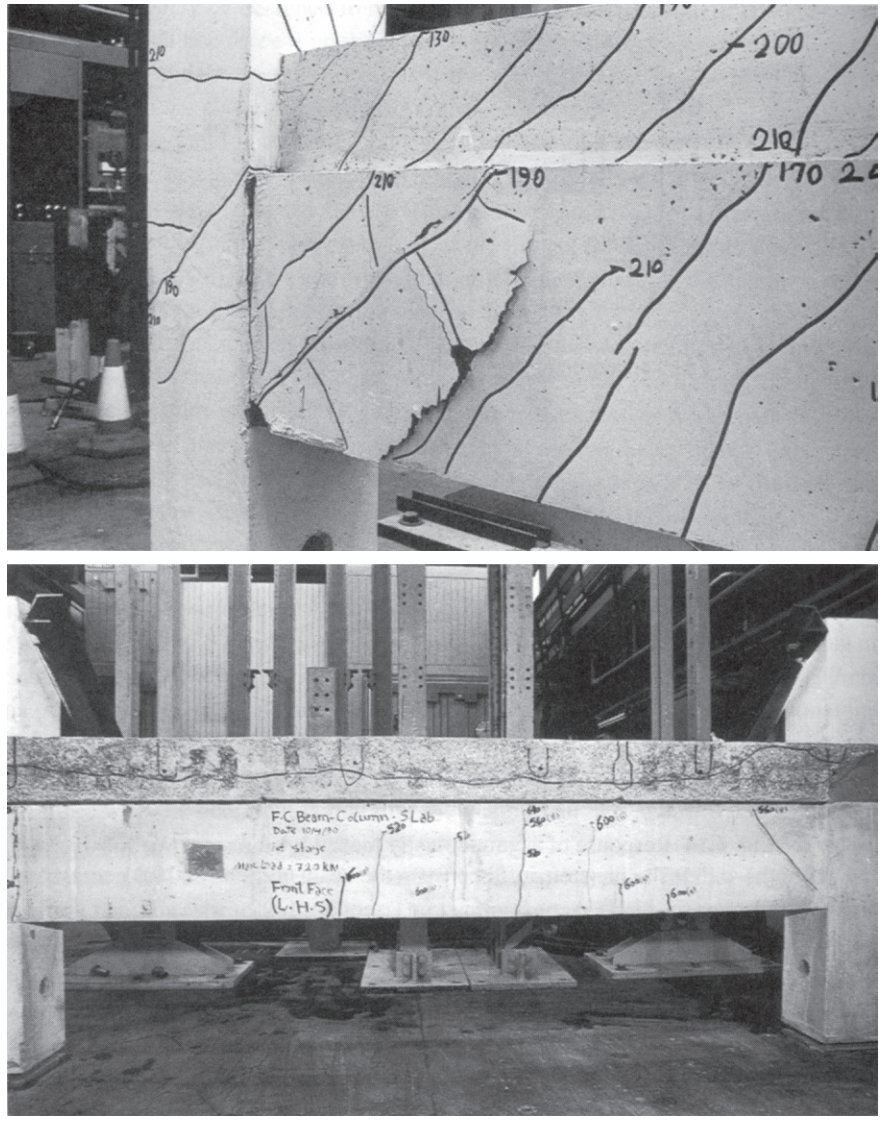

Figure 4.21 Cracking in L beam subjected to asymmetrical load. (a) Without *in situ* concrete infill and (b) with *in situ* concrete infill between the beam and slab.

- the *in situ* concrete infill produces an extended bearing, thus reducing the eccentricity of the load, as shown in Figure 4.20(b);
- composite action between the beam and slab alters the position of the shear centre for the beam from point A to B in Figure 4.19, thus reducing the eccentricity even more; and
- the beam cannot possibly rotate because of the flexural stiffness of the precast floor slab, causing the equilibrating stresses as shown in Figure 4.22.

The minimum required compressive strength of *in situ* concrete is grade C20/25, and the minimum amount of tie steel to the slabs, H10 bars at 600 mm centres, was used to produce these results.

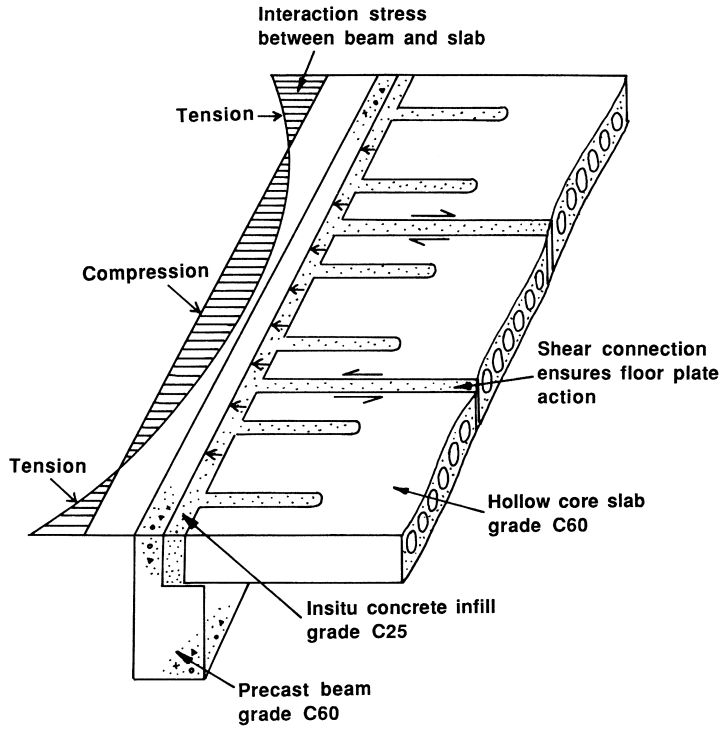

Figure 4.22 Horizontal stresses in the interface between floor slabs and L beams subjected to asymmetrical floor load.

Exercise 4.1 Precast L-beam design

Design the flexural and shear reinforcement for a precast concrete L-shaped edge beam over a simply supported effective span of 7.0 m, to carry a 200 mm-deep hollow-core floor slab and an external cavity wall, as shown in Figure 4.23. Check the serviceability limit state for deflection. The characteristic superimposed permanent and variable beam loading are given in Table 4.9. The beam is to support office flooring, such that the EC0 ultimate load combination factors are $\zeta = 0.925$ and $\psi_0 = 0.7$. Thus $w = \max(1.35\ G_k + 1.05\ Q_k\ ;\ 1.25\ G_k + 1.5\ Q_k)$.

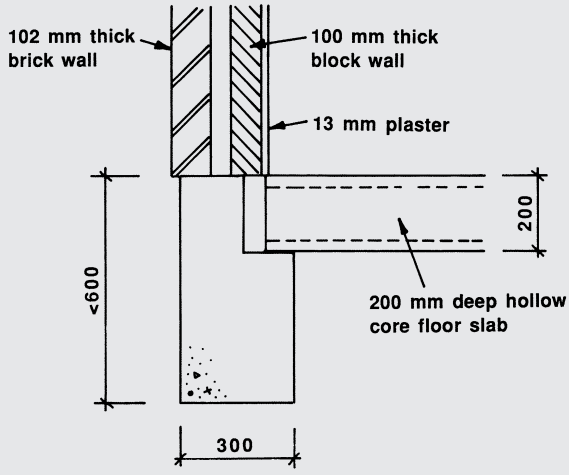

Figure 4.23 Details for Exercise 4.1.

Table 4.9 Characteristic superimposed permanent and variable beam action for Exercise 4.1

	Loading (kN/m)
Floor slab permanent action, including services and ceiling	14.5 to allow for steel {14.0}
Floor slab variable action, including partitions	20.0
Brickwork (2.2 kN/m^2 × 3.0 m high)	6.6
Blockwork and finishes (1.3 kN/m^2 × 2.4 m high)	3.1

The floor slab bearing is 75 mm, with a 40 mm toe projection. Use grade C32/40 concrete, high-tensile reinforcement, XC3 exposure and a 60 minutes {1 hour} fire resistance. Assume density of concrete = 25 kg/m^3 {24 kg/m^3}.

Solution

Step 1: Section sizes and cover

Exposure. Cover to reinforcement (BS 8500, Part 1, Table A3) for C32/40 concrete = 30 mm.
Fire. Minimum beam width (EN 1992-1-2 table 5.2a {BS 8110, Part 1, Fig. 3.2} for 60 mins = 200 mm.
Use b = 300 mm-wide beam.

Fire. (EN 1992-1-2 table 5.2a) assuming minimum size main bars 16 mm and links 8 mm, for 60 mins		Fire. Cover to reinforcement (BS 8110, Part 1, Table 3.4) for 1 hour	= 20 mm < 30 mm
= 31 − 8 − 8	= 15 mm < 30 mm		

Minimum upstand width (assume H8 stirrups) = 30 + 4(8 × 8) + 30 = 124 mm.
Slenderness check

(Clause 5.9)		(Clause 3.4.1.6.)	
b_w > L/70 $(h/b)^{1/3}$		b_w > L/60 = 7000/60 or	$b_w \geq 117$ mm
= 7000/70 × $(600/300)^{1/3}$	$b_w \geq 126$ mm	$\sqrt{Ld/250} = \sqrt{(7000 \times 550/250)}$ (see later d = 550 mm)	$b_w \geq 124$ mm

Use maximum possible upstand width b_w = 170 mm with 200 mm-deep floor recess.
Effective depth of beam d is controlled by deflection and the design of the flexurally balanced section.

Step 2: Flexural design

Try initial depth of beam h = 600 mm, and d = 550 mm

Self-weight		Self-weight	
= 25((0.4 × 0.3) + (0.2 × 0.17))	= 3.85 kN/m	= 24 ((0.4 × 0.3) + (0.2 × 0.17))	= 3.47 kN/m
Total permanent load		Total permanent load	
= 14.5 + 6.6 + 3.1 + 3.85	= 28.05 kN/m	= 14 + 6.6 + 3.1 + 3.47	= 27.20 kN/m
so maximum ultimate load on beam,		so maximum ultimate load on beam,	
Eq. 6.10(a)			
ω = 1.35 × 28.05 + 1.5 × 0.7 × 20.00	= 58.86 kN/m	ω = 1.4 × 27.20 + 1.6 × 20.00	= 70.07 kN/m
Eq. 6.10(b)			
ω = 1.25 × 28.05 + 1.5 × 20.00	= 65.06 kN/m		
M_{Ed} = 65.06 × 7.00^2/8	= 398.5 kNm	M_u = 70.07 × 7.00^2/8	= 429.2 kNm
V_{Ed} = 65.06 × 7.00/2	= 227.7 kN	V_u = 70.07 × 7.00/2	= 245.3 kN
$k = M_{Ed}/bd^2f_{ck}$ = 0.242 > 0.2067		$k = M_u/bd^2f_{cu}$ = 0.209 > 0.156	
compression reinforcement required to carry M'_{Ed}		compression reinforcement required to carry M'	

(*Continued*)

$M'_{Ed} = M_{Ed} - 0.2067 \times 170 \times 550^2 \times 32$	= 58.4 kNm
$d - d' = 550 - 50$	= 500 mm
Top steel,	
$A'_s = 58.4 \times 10^6 / (0.87 \times 500 \times 500)$	= 268 mm^2
Minimum compression steel	
(Not given, use) = 0.15% $b\ h$	
= 0.15% × 170 × 600	= 153 mm^2
	<268 mm^2
$A_s = \dfrac{340.2 \times 10^6}{0.87 \times 500 \times 0.76 \times 550} + 268$	= 2138 mm^2
Minimum tension steel	
See Clause 9.2.1.1, $A_{s,min}$ = max(0.13% $b_t\ d$	
or 0.26 $f_{ctm}\ b_t\ d/f_{yk}$)	
= 0.13% × 170 × 550, or	= 122 mm^2
= 0.26 × 3.02 × 170 × 550/500	= 147 mm^2

Use three H12 bars (399 mm^2) in top of upstand.
Use two H32 plus two H20 bars (2236 mm^2) in bottom
Use two H10 additional bars at top of boot.

$M' = M_u - 0.156 \times 170 \times 550^2 \times 40$	= 108.3 kNm
$d - d' = 550 - 50$	= 500 mm
Top steel,	
$A'_s = 108.3 \times 10^6 / (0.87 \times 500 \times 500)$	= 497 mm^2
Minimum compression steel (Clause 3.12.5.) = 0.2% $b_w\ h$	
= 0.2% × 170 × 600	= 204 mm^2
	< 497 mm^2
$A_s = \dfrac{320.9 \times 10^6}{0.87 \times 500 \times 0.775 \times 550} + 497$	= 2229 mm^2
Minimum tension steel	
$A_{s,min}$ = 0.13% $b\ d$	
= 0.13% × 170 × 550	= 122 mm^2

Use four H16 bars paired vertically (804 mm^2)
Use two H32 plus two H20 bars (2236 mm^2) in bottom.
Use two H10 additional bars at top of boot.

Step 3: Deflection check

(See Clause 7.4.2(2) equation 7.16b)	
$\rho_0 = 0.005657$	
$\rho = 2236/(170 \times 550) = 0.02047$	
$\rho' = 268/(170 \times 550) = 0.00263$	
$K = 1$	
$\dfrac{l}{d} = K\left(11 + 1.5\dfrac{\rho_0}{\rho - \rho'}\sqrt{f_{ck}} + \dfrac{\sqrt{f_{ck}}}{12}\sqrt{\dfrac{\rho'}{\rho_0}}\right.$	= 13.78
$d \geq 7000/13.78$	≥ 508 mm

(BS 8110, Part 1, Table 3.9) Basic factor for rectangular section = 20.	
If beam were to be balanced, then $M/bd^2 = K' f_{cu} = 0.156 \times 40 = 6.24$	
(BS 8110, Part 1, Table 3.10) Modification factor when	
f_s = 333 N/mm^2 is 0.72	
$d > 7000/(20 \times 0.72)$	> 486 mm

Step 4: Curtailment of flexural steel
Reduce top bars to nominal when:

M_{Ed} = 340.1 kNm, i.e. at 2 m from support. Here V_{Ed} = 87.2 kN, causing a shift in the bending moment diagram $\Delta M = 0.5 V_{Ed}\ 0.9d$ = 21.6 kNm. (Clause 6.2.3(7))
Then top rebar curtailment is when M_{Ed} = 340.1 − 21.6 = 318.4 kNm, at 1.93 m from support.
Minimum steel = 153 mm^2.
Curtail top steel to two H12 (226 mm^2) at 1.93 m from centre of support.

Reduce bottom bars to 2H32 (1608 mm^2), where M_{Rd} = 305.2 kNm at 1.81 m from centre of support. Here V_{Ed} = 110.1 kN, ΔM = 27.2 kNm. Then curtailment is when M_{Ed} = 305.2 − 27.2 = 278.0 kNm, at 1.58 m from support.
Curtail bottom steel to two H32 (1608 mm^2) at 1.58 m from centre line of support.

M = 304.2 kNm, i.e. at 1.74 m from support, minus an anchorage length. (Clause 3.12.9.1 and Table 3.27)
Anchorage length = d or 35 Φ
= 560 mm.

Minimum steel = 204 mm^2.
Curtail top steel to two H16 (402 mm^2) at 1.18 m from centre of support.
(Clause 3.12.10.2.)
Reduce bottom bars by up to 50 per cent A_s at 0.08L = 560 mm.
Or curtail bottom steel to two H32 (1608 mm^2) where M_u = 304.2 kNm, which is at 1.61 m from the centre of support, minus 0.56 m. i.e. at 1.05 m from centre of support.

Step 5: Shear design

It is necessary to check the shear at the following positions:

(1) end of the beam
(2) curtailment point for the bottom steel
(3) where nominal links are required.

(1) *End of the beam*

The shear capacity without links,
$v = 0.12 \times 1.603 \times (100 \times 0.02 \times 32)^{(1/3)}$ $= 0.769$
or $v_{min} = 0.0035 \times 1.603^{1.5} \times 32^{0.5}$ $= 0.04$
$V_{Rd,c} = 0.769 \times 170 \times 550$ $= 71.94\,\text{kN}$
$< 227.7\,\text{kN}$

Clause 6.2.3, Eq. 6.9 rearranged
$v_1 = 0.6\,(1 - f_{ck}/250) = 0.523$
$\theta = 0.5 \sin^{-1}\,(227.7 \times 10^3/(0.5 \times 0.523 \times 170 \times 0.9 \times 550 \times 32/1.5)) = 14.5°$
$\therefore \cot\theta = 3.87 > 2.5$ so use 2.5
Clause 6.2.3, Eq. 6.8 rearranged
Try H8 links. $A_{sw} = 100\,\text{mm}^2$ for 2 legs
$s = 100 \times 0.9 \times 550 \times 0.87 \times 500 \times 2.5/227.7 \times 10^3 = 236\,\text{mm}$
Use H8 at 230 mm centres from end of beam to point of minimum links.

$V = 245.3\,\text{kN}$
$v = 245.3 \times 10^3/(170 \times 550)$ $= 2.62\,\text{N/mm}^2$
$\dfrac{100A_s}{b_w d} = \dfrac{100 \times 2236}{170 \times 550} = 2.77$ Hence
$v_c = 0.82 \times ((40/25)^{0.33})$ $= 0.92\,\text{N/mm}^2$
$\dfrac{A_{sv}}{s_v} = \dfrac{(2.62 - 0.92) \times 170}{(0.87 \times 500)}$ $= 0.668\,\text{mm}^2/\text{mm}$
Use 2-leg stirrup
$A_{sv}/s_v = 0.668 \times 1000/2$ $= 334\,\text{mm}^2/\text{m/leg}$

Use H8 at 125 mm centres ($402\,\text{mm}^2/\text{m}$) from end of beam to 560 mm from centre of support.

(2) *Curtailment point for the bottom steel*

$V = 304.2 - (70.07 \times 0.56)$ $= 265.0\,\text{kN}$
$v = 2.21\,\text{N/mm}^2$ $= 2.21\,\text{N/mm}^2$
$\dfrac{100A_s}{b_w d} = \dfrac{100 \times 1608}{170 \times 550} = 1.72$
Hence $v_c = 0.70 \times ((40/25)^{0.33})$ $= 0.82\,\text{N/mm}^2$
$\dfrac{A_{sv}}{s_v} = \dfrac{(2.21 - 0.82) \times 170}{(0.87 \times 500)}$ $= 0.216\,\text{mm}^2/\text{mm}$
Use 2-leg stirrup
$A_{sv}/s_v = 0.185 \times 1000/2$ $= 93\,\text{mm}^2/\text{m/leg}$
Use H8 at 200 mm centres ($251\,\text{mm}^2/\text{m}$) beyond 560 mm from centre of support to point 3.

(3) *Where nominal links are required*

Minimum links (Eq. 9.5N)

$$A_{sw}/s = 0.08\frac{\sqrt{f_{ck}}}{f_{yk}} b_w = 0.08\frac{5.66}{500}170$$

$= 0.154\,\text{mm}^2/\text{mm}$
Use 2-leg stirrup
$A_{sw}/s = 0.154 \times 1000/2$ $= 77\,\text{mm}^2/\text{m/leg}$
But the maximum spacing, $0.75d = 412\,\text{mm}$
Use H8 at 300 mm centres ($168\,\text{mm}^2/\text{m/leg}$).

Where $v = v_c + 0.4\,\text{N/mm}^2$
$v = 0.4 + 0.92 = 1.32\,\text{N/mm}^2$
$V = 1.32 \times 170 \times 550 \times 10^{-3}$ $= 123.4\,\text{kN}$
This point occurs at 1.761 m from centre of support
$\dfrac{A_{sv}}{s_v} = \dfrac{(0.4) \times 170}{(0.87 \times 500)} = 0.156\,\text{mm}^2/\text{mm}$
Use 2-leg stirrup
$A_{sv}/s_v = 0.156 \times 1000/2$ $= 78\,\text{mm}^2/\text{m/leg}$
But the maximum spacing, $0.75d = 412\,\text{mm}$

(*Continued*)

This resists a shear of (Eq. 6.8)
$V_{Rd,min} = 100 \times 0.9 \times 550 \times 0.87 \times 500 \times 2.5/300 = 179.4\,\text{kN}$ which is at 0.75 m from centre of support

Use H8 at 300 mm centres (168 mm²/m) beyond 1.59 m from centre of support

Step 6: Boot reinforcement (Ignore horizontal frictional force μV in this exercise)
Floor slab loading

$\omega = 1.35 \times 14.5 + 1.05 \times 20.00 = 40.6\,\text{kN/m}$
$\omega = 1.25 \times 14.5 + 1.5 \times 20.00 = \underline{48.1\,\text{kN/m}}$

$\omega = 1.4 \times 14.00 + 1.6 \times 20.00 = 51.6\,\text{kN/m}$

Boot depth = 400 mm, therefore use strut-and-tie method.

The triangle of forces (see Fig. 4.16) gives $\theta = \tan^{-1}\left(\dfrac{300-170-40-75/2+30+4}{600-200-2\times30-2\times4}\right) = 14.6°$

Thus, $H = V \tan\theta$

$H = 48.1 \times 0.261 = 12.53\,\text{kN/m}$
$A_{sh} = 12.53 \times 10^3/0.87 \times 500 = 29\,\text{mm}^2\text{/m/leg}$
Maximum spacing $= 0.75 \times 366 = 275\,\text{mm}$

$H = 51.6 \times 0.261 = 13.44\,\text{kN/m}$
$A_{sh} = 13.44 \times 10^3/0.87 \times 500 = 31\,\text{mm}^2\text{/m/leg}$
Maximum spacing $= 155\,\text{mm}$

Although 6 mm bars are suitable, the availability is poor and the ductility of such bars does not satisfy BS EN 1992-1-1.

Use H8 at 200 mm centres (251 mm²/m) links in boot for full length.

Use H8 at 150 mm centres (335 mm²/m) links in boot for full length.

Exercise 4.2 Boot reinforcement under uniform load

Design the boot reinforcement in a 900 mm-deep × 400 mm-wide L-beam which supports 250 mm-deep hollow-core flooring over a clear span of 10 m. Tie bars H12 at 600 mm centres are cast into the beam and are to be concreted into the broken-out cores of the slabs. The floor slab is to be completed using grade C20/25 *in situ* concrete. The slab bearing length is 80 mm. The dimensions of the boot are 250 mm × 300 mm deep. The superimposed permanent and variable loads are 2.0 kN/m² and 5.0 kN/m², respectively.

Use C32/40 concrete and $f_y = f_{yv} = 500\,\text{N/mm}^2$. Cover to links in protected faces = 25 mm, and to exposed outer and bottom faces = 40 mm.

Solution
The boot depth is exactly 300 mm, hence use strut-and-tie design method.

Step 1: With slabs laid dry before *in situ* concrete is cast.
Length of slab = 10.0 + 0.1 + 0.1 = 10.2 m
Self-weight of slab (see Table 3.1) = 3.35 kN/m²
Assume H12 links.
Ultimate slab reaction

$V_{Ed1} = 1.35 \times 0.925 \times 3.35 \times 10.2/2 = 21.33\,\text{kN/m}$

$V_1 = 1.4 \times 3.35 \times 10.2/2 = 23.92\,\text{kN/m}$

Beam bearing length, $b_l = 100$ mm, thus $a = 25 + 6 + 250 - 100/2 = 231$ mm
Boot $x = 300 - 25 - 40 - 12 = 223$ mm
Diagonal strut inclination $\theta = \tan^{-1} 231/223 = 46.01°$

$H = 21.33\left(\tan\theta + \frac{223+6+25}{223}0.7\right)$ = 39.11 kN/m

$A_{sh1} = \frac{39.11\times10^3}{0.87\times500} = 90\ \text{mm}^2/\text{m}$

The diagonal force, C

$C = 21.33/\cos 46.01°$ = 30.72 kN/m

$C_r = 0.24 \times 269 \times (1 - 32/250) \times 32 \times \sin 46.01°$ = 1296 kN/m

> 30.72 kN/m

$T = 21.33\left(1 + \frac{0.7\times248}{231}\right)$ = 37.37 kN/m

Hence

$A_{sv1} = \frac{37.37}{0.87\times500} = 86\ \text{mm}^2/\text{m}$

$H = 23.92\left(\tan\theta + \frac{223+6+25}{223}0.7\right)$ = 43.85 kN/m

$A_{sh1} = \frac{43.85\times10^3}{0.87\times500} = 101\ \text{mm}^2/\text{m}$

The diagonal force, C

$C = 23.92/\cos 46.01°$ = 34.44 kN/m

$d' = 300 - 25 - 6$ = 269 mm

$C_r = 0.2 \times 40 \times 269 \times \sin 46.01°$ = 1548 kN/m

> 34.44 kN/m

$T = 23.92\left(1 + \frac{0.7\times248}{231}\right)$ = 41.89 kN/m

Hence

$A_{sv1} = \frac{41.89}{0.87\times500} = 96\ \text{mm}^2/\text{m}$

Step 2: After *in situ* concreting

Effective length of slab = 10.0 + 0.25 + 0.25 = 10.5 m due to extended bearings.

Ultimate slab reaction

V_{Ed2} = (1.25 × 2 + 1.5 × 5.0) 10.5/2 = 52.5 kN/m

V_2 = ((1.4 × 2.0) + (1.6 × 5.0)) × 10.5/2 = 56.7 kN/m

Beam bearing length b_l = 250 mm, thus a = 25 + 6 + 250/2 = 156 mm

Boot x = 300 − 25 − 40 − 12 = 223 mm

Total frictional force

$= \mu\ (V_1 + V_2) = 0.7\ (21.33 + 52.5)$ = 51.68 kN/m

Tie steel capacity

$= 0.87 \times 500 \times 113/0.6 \times 10^{-3}$ = 81.93 kN/m

> 51.68 kN/m

Hence frictional force is not mobilised in the composite situation.

H_2 = 36.72 kN/m and

A_{sh2} = 85 mm²/m

Total A_{sh} = 175 mm²/m

Use H10 at 300 centres (262 mm²/m)

C increases to 75.6 kN, still $< C_r$

Also T = 52.5 kN/m and

A_{sw2} = 121 mm²/m

Total A_{sw} = 207 mm²/m

$= \mu\ (V_1 + V_2) = 0.7\ (23.92 + 56.70)$ = 56.43 kN/m

Tie steel capacity

$= 0.87 \times 500 \times 113/0.6 \times 10^{-3}$ = 81.93 kN/m

> 56.43 kN/m

Hence frictional force is not mobilised in the composite situation.

H_2 = 39.7 kN/m and

A_{sh2} = 91 mm²/m

Total A_{sh} = 192 mm²/m

Use H10 at 300 centres (262 mm²/m)

Compressive strut not critical by inspection.

Also T = 56.7 kN/m and

A_{sv2} = 130 mm²/m

Total A_{sv} = 226 mm²/m

Use H10 at 300 centres (262 mm²/m) links in boot for full length.

Exercise 4.3 Boot reinforcement under concentrated load

Determine the minimum depth of the boot and design the boot reinforcement for a 400 mm-wide L-beam to support double-tee floor slabs spanning 11.0 m and with webs at 1.2 m centres. The characteristic floor loading is 8.5 kN/m^2 permanent plus 5.0 kN/m^2 variable. The floor slabs are seated on 150 × 150 × 10 mm neoprene pads at 1200 mm centres. The fixing tolerance for the slab is 15 mm at each end of the slab. Immediately after fixing, the end plates in the slabs are welded to side plates in the beam.

Use grade C32/40 concrete and $f_{yv}\{f_y\}$ = 500 N/mm^2. Cover to links in all faces = 40 mm.

Solution

Bearing dimensions $b_l = b_p$ = 150 mm
Ledge width = bearing pad 150 mm plus 2 × tolerance 15 mm = 180 mm
Upstand width = 400 − 180 = 220 mm
Assume H12 links.
Thus, maximum eccentricity a = 40 cover + 6 bar + 30 gap + 75 half ledge = 151 mm
Boot height >a for <45° truss, so try boot depth of 200 mm
d'' = 200 − 40 − 6 = 154 mm
Load spread width (eq. 4.16)

= 150 + 4 × 154 = 766 mm	= 150 + (2 × 151) + 400 = 852 mm
Ultimate end reaction in floor webs,	Ultimate end reaction in floor webs,
V_{Ed} = ((1.25 × 8.5) + (1.5 × 5.0)) × 1.20 × 11.0/2 = 119.55 kN	V = ((1.4 × 8.5) + (1.6 × 5.0)) × 1.20 × 11.0/2 = 131.34 kN
Bursting force beneath bearing pad:	Bursting force beneath bearing pad:
Referring to Eq.4.21 (Clause 6.5.3(3), Eq. 6.58):	Referring to Eq.4.21:
$A_s'' = 0.25 \times 119.55 \times 10^3 / 0.87 \times 500$ = 69 mm^2	$A_s'' = 0.23 \times 131.34 \times 10^3 / 0.87 \times 500$ = 70 mm^2

Use one longitudinal H10 bar (78 mm^2) in top corner of boot.
Also provide one H10 bar in top corner of link in outside face of beam.

Bending steel

Bending moment

M_{Ed} = 119.55 × 0.151	M = 131.34 × 0.151
$k = \dfrac{18.06 \times 10^6}{32 \times 766 \times 154^2} = 0.031$ = 18.06 kNm	$k = \dfrac{19.83 \times 10^6}{40 \times 852 \times 154^2} = 0.024$ = 19.83 kNm
z = 151 mm	z = 0.95 d
$A_{sh} = \dfrac{18.06 \times 10^6}{0.87 \times 500 \times 151}$ = 276 mm^2	$A_{sh} = \dfrac{19.83 \times 10^6}{0.87 \times 500 \times 0.95 \times 154}$ = 312 mm^2
Minimum = 0.15% = 300 mm^2/m	Minimum = 0.13% = 260 mm^2/m

Use five H10 at 150 mm centres (393 mm^2), ensuring that at least one link is within 50 mm of each edge of the bearing pad.

It is interesting to note that if the 45° strut-and-tie method is used, the reinforcement in the localised zone is e.g.

A_{sh} = 119.55 × 10^3/0.87 × 500 = 275 mm^2	A_{sh} = 131.34 × 10^3/0.87 × 500 = 302 mm^2

The answer is about the same.

Reinforcement between localised zones:
Distance between the localised zones

= 1200 − 766 = 434 mm | = 1200 − 852 = 348 mm

In this region use nominal steel at 0.15% = 300 mm²/m
Use H10 at 250 mm between centres.

Punching shear check

Use Eq. 4.16.
$u = 2(150 + 139.5) + (150 + 2 \times 2 \times 154)$
= 1345 mm
$d_{eff} = (154 + (154 - 12/2 - 10/2))/2$
= 148.5 mm
$a > 0.5\ d_{eff}$
$v_{Ed} = 119.55 \times 10^3 \times 151/(1345 \times (143 + 154) \times 154)$ = 0.30 N/mm²
$k = 1 + \sqrt{(200/154)} = 2.139$, but ≤ 2.0
$v_{min} = 0.0035 \times 2^{(3/2)} \times 32^{(1/2)}$ = 0.056 N/mm²

$\rho_l = \sqrt{(0.262 \times 0.196)} = 0.227\%$
$v_{Rd,c} = 0.12 \times 2.0 \times (0.227 \times 32)^{(1/3)}$ = 0.464 N/mm²
$v_{Ed} < v_{Rd,c}$, so no punching shear reinforcement required > 0.056 N/mm²

Consider 3-sided perimeter because
$b_l + 1.5d'' = 150 + 1.5 \times 154$
= 381 mm < 400 mm beam breadth.
Use Eq. 4.16.
$u = (2 \times (150 + 1.5 \times 154)) + (150 + 3 \times 148.5) = 1341$ mm
$v = 131.34 \times 10^3/(1341 \times 154)$ = 0.64 N/mm²
To determine critical value for v_c, consider the steel crossing the shear perimeter and use the mean value.
Longitudinal steel in top of boot is two H10 bars, then
$100A_s/bd'' = 100 \times 2 \times 78.5/381 \times 154$
= 0.27%
Boot links H10 at 150 c/c, then
$100A_{sh}/bd'' = 100 \times 78.5/150 \times 154$
= 0.34%
Then v_c(average) = 0.63 N/mm²
But 1.5 d″/a_v = 1 at this point
Then $v < v_c$, so no punching shear reinforcement required.

4.3.7 Non-composite prestressed beams

4.3.7.1 Flexural design

The design of prestressed beams is less versatile than in reinforced beams, because the tendons' positions are restricted to a predetermined pattern by an array of holes in the jacking heads, which is usually a permanent fixture in a precasting works. The opportunity for architectural freedom is limited to symmetrical sections of modular depth – usually 50 mm increments. A range of rectangular or inverted-tee beams (L-beams are not symmetrical) from 200 to 600 mm deep will usually satisfy the flexural and shear requirements in most structures.

Figure 4.24 shows a full array of possible tendon positions in an inverted-tee beam, and an example of a typical tendon layout. Note the symmetry. The tendons are placed at all the corners, a 40 to 50 mm centroidal cover distance being used in most cases. The positions of the tendons are such that they do not interfere with any of the beam end connections, such as shear boxes or shear hanger plates. They can also be arranged to allow service holes to pass through the beam by leaving a clear zone of about 75 mm near the centroid of the uncracked concrete section.

As shown in Figure 4.24(a), a referencing system of letters (A, B, C, etc.) and numbers (1, 2, 3, 4, etc.) is used to convey information to the manufacturer as to which strands are to be used in a particular beam. Where debonding of strands is required a coded message relating to the requirements is also given, e.g. B 2 – 800, means the strand at position B 2 is to be sheathed for a distance of 800 mm

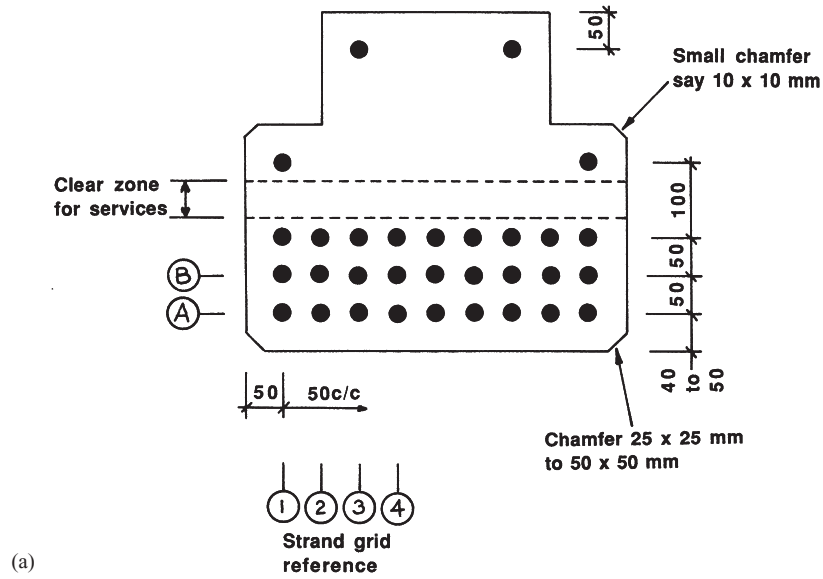

(a)

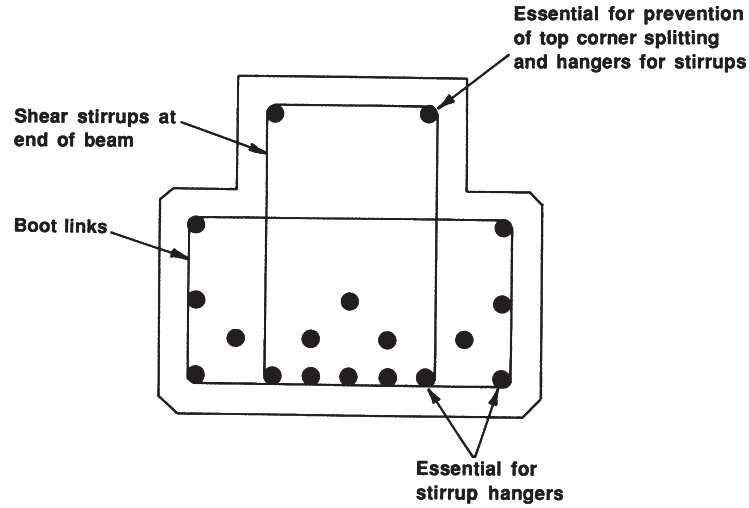

(b)

Figure 4.24 Location of tendons in inverted-tee beams. (a) Full array and (b) typical arrangements. (c) Detail of inverted-tee beam used in beam design example and (d) strand pattern to beam design example.

from the end of the beam. Figure 4.24(b) shows a typical arrangement of strands – note the strand positions which are essential for use.

The minimum breadth of the beam is a function of the type of floor slab to be used. The breadth is equal to twice the recess width, plus the upstand width. The same reasoning as for the L-beam is used if floor ties are intended to be placed within the recess and concealed in the depth of hollow-core floor slabs. The minimum recess width for this condition is 100–125 mm. If the ties are to be located elsewhere, the recess width may be 90–100 mm. The width of the upstand depends largely on accommodating end connections, particularly in shallow beams where the connector may be positioned near to the top of the beam (e.g. see Figures in Section 4.3.12). The minimum upstand breadth is therefore 250–300 mm, depending on the type of connector used. Thus the breadth of internal tee-beams usually varies between 450 mm and 600 mm.

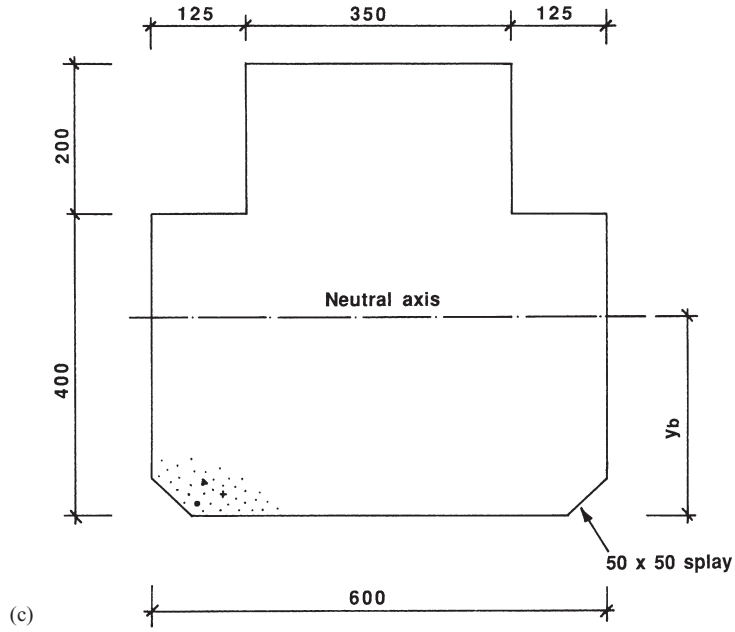

(c)

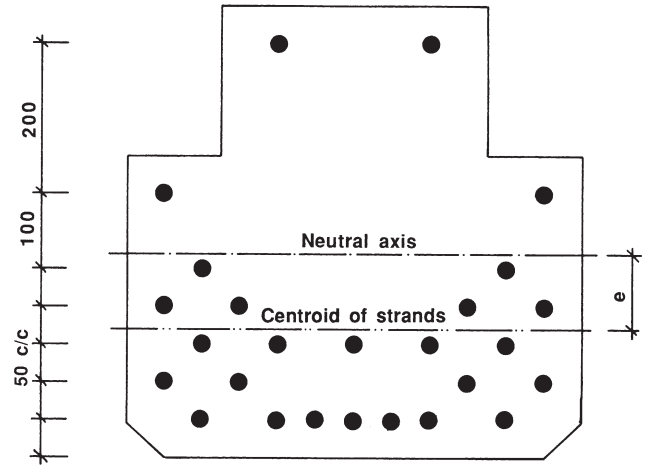

(d)

Figure 4.24 (*Continued*)

Beam depths depend on three factors:

(a) the flexural and shear capacities
(b) the size of the end connector
(c) the depth of the boot required to carry the floor loads.

Factor (a) is self-evident from standard designs as mentioned above. Factor (b) will be dealt with in Section 4.3.10.

The process of selecting the prestressing requirements can be optimised by choosing a reinforcement pattern that will simultaneously satisfy transfer at the ends of the beam and working loads at the point of maximum imposed bending moment, without having to debond or deflect the tendons.

This method is further refined if the permissible stress at transfer, $f_{cd(t)} = 0.6\,f_{ck(t)}$ {$0.5\,f_{ci}$} after the initial losses (due to elastic shortening), is made equal (or as close as possible) to the working stress 0.45 $f_{ck(t)}$ {$0.33f_{cu}$} after all losses. In most beam designs the initial losses are about 7–8 per cent and the final losses 20–25 per cent, meaning that the ratio f_{ci}/f_{ck} {f_{ci}/f_{cu}} should be at least 0.55. In fact the transfer strength for grade C50/60 concrete is usually at least 32 N/mm^2 {40 N/mm^2}. This is because precasting factories regularly test for early age strength at the maturity they need for stress transfer. Consequently, the default values from BS EN 1992-1-1 can be replaced with more accurate, usually higher, early age concrete strengths. Transfer stresses will, therefore, (nearly) always govern for parallel, unbonded tendons. To overcome this problem it is desirable to debond a small number of strands, say four in a typical situation.

There are two scenarios for assessing strength at transfer:

- In on-site casting, or with a new curing regime, or with new concrete in use, a curing regime is known but there is no statistically reliable strength measurement. In this case the maturity can be estimated from the equations in BS EN 1992-1-1, Appendix B. For example, a curing regime for C50/60 concrete of 16 hours at 40°C will give a maturity of 16/24 × 4.776 (from equation H10) = 3.184 days. BS EN 1992-1-1 equations 3.1 & 3.2 then give $f_{cm(t)} = 0.675 \times f_{cm} = 0.675 \times 58 = 39.15$ N/mm^2 cylinder strength. The concrete equivalent grade for design at transfer $f_{ck(t)}$ would then be C31.1/35.8 (39.1 − 8 = 31.1 & 31.1/0.83 = 35.8), and all other design stresses can be derived from this value.
- A precaster with statistically significant test data may test concrete samples stored with the precast units and tested to ensure attainment of a mean target strength immediately prior to stress transfer. For example, if there is a test-proven cube strength at time of transfer of 40.0 N/mm^2 for a C50/60 mix, then the exothermic reaction of the curing concrete will have maintained the cast units at a higher temperature than that controlled by the curing regime. Now the concrete equivalent grade is C33.2/40.0 (0.83 × 40.0 = 33.2, with test strengths specified to an accuracy of 0.1). Maturity from BS EN 1992-1-1 equations 3.1 & 3.2 is back-calculated as 9.22 days, and all other transfer design values follow from $f_{ck(t)} = 33.2$ N/mm^2. The results obtained by comprehensive monitoring of concrete strength at transfer against a statistical database will usually provide higher design values at transfer (i.e. there will be some economic benefit).

It is wise to actually restrict the top fibre stress to something less than $f_{ctm(t)}$ {$0.45\sqrt{f_{ci}}$}, say 2/3 or even 1/2 this value (i.e. $0.5f_{ctm(t)}$ {$0.225\sqrt{f_{ci}}$}), while accepting that there will be a small loss in moment capacity. This factor of safety is based on the experience gained from transporting and handling highly stressed prestressed beams, and the need to avoid flexural cracking for the sake of durability. It also allows some freedom in choosing a final tendon arrangement if the eccentricity of the tendons needs to be greater than the calculated design value.

A further factor is that the actual initial pretensioning force achieved in practice may be higher than the design value. In order to avoid understressing, the manufacturer will deliberately overstress by 2 or 3 per cent to compensate for slippage in the chucks, losses in the hydraulic stressing system, etc.

Simple algebra will give a set of relationships to solve for the prestressing force P and the eccentricity e, as follows. The geometric centroid of the section is computed for the gross concrete section ignoring the area of reinforcement (which is barely significant). The total initial force (in all the tendons) is therefore governed by the state of stress at transfer and is given by:

$$P_{pi} = \frac{A}{2(1-\xi)}\left((0.6f_{ck(t)} - 0.5f_{ctm(t)}) + (0.6f_{ck(t)} + 0.5f_{ctm(t)})\left(\frac{1-\alpha}{1+\alpha}\right)\right)$$
$$\left\{ P_i = \frac{A}{2(1-\xi)}\left((0.5f_{ci} - 0.225\sqrt{f_{ci}}) + (0.5f_{ci} + 0.225\sqrt{f_{ci}})\left(\frac{1-\alpha}{1+\alpha}\right)\right)\right\} \quad (4.22)$$

where the limiting tensile stress at transfer is either measured and directly known, or is given in BS EN 1992-1-1 Eq. 3.1 & 3.4, as $f_{ctm(t)} = f_{ctm}\,f_{cm(t)}/f_{cm}$. Also ξ = initial prestress loss due to elastic shortening

(expressed as a decimal fraction), and $\alpha = Z_t/Z_b$. The number of tendons required $N = P_{pi}/\mu\ A_p\ f_{pk}$ $\{P_i/\mu\ A_{ps}\ f_{pu}\}$ (where μ = degree of prestress, the minimum of 0.8/1.15 and 0.9 $f_{p,0.1k}/1.15\ f_{pk}$ {usually taken as 0.65 to 0.7 for larger strands, and 0.7 to 0.75 for smaller strands} depending on the type of tendon used) should be rounded down to the next integer to prevent overstress, particularly in the tensile fibres at the top of the beam. The eccentricity z_{cp} $\{e\}$ is given by:

$$z_{cp} = \frac{0.6f_{ck(t)} + 0.5f_{ctm(t)}}{(1-\xi)P_{pi}\beta} \quad \left\{ e = \frac{0.5f_{ci} + 0.225\sqrt{f_{ci}}}{(1-\xi)P_i\beta} \right\} \tag{4.23}$$

where $\beta = \dfrac{1}{Z_t} + \dfrac{1}{Z_b}$, and P_i is based on the value obtained from Eq. (4.22).

The design then follows the procedures given in Section 5.2.8.

The bending stress due to the service moment, $\sigma = M_s/Z$, may be calculated using the compound section modulii $Z_{b,co}$ and $Z_{t,co}$, determined from the compound second moment of area, using a modular ratio $m - 1 = ((1+\Psi_{28})E_p/E_{cm}) - 1$ for the transformed areas of strands $A_{ps}(m-1)$. Use of the compound section is not common practice, but Calevera ([4.27], page 175) shows that, using $\alpha = E_p/E_c$, where E_c is the short-term modulus, the compound values for Z_b, Z_t and I divided by the basic values, may be taken as:

$$\text{For the second moment of area: } I_{co}\ /\ I = (1+\alpha\rho) \tag{4.24}$$

$$\text{For the bottom section: } Z_{b,co}\ /\ Z_b = (1+1.5\alpha\rho) \tag{4.25}$$

$$\text{For the top section: } Z_{t,co}\ /\ Z_t = (1+0.5\alpha\rho) \tag{4.26}$$

where ρ is the reinforcement to concrete section ratio. Clearly the effects of (i) different rates of creep on the concrete at the bottom and top, and (ii) the position of the centroidal axis, where the compound section at the bottom increases more than it does at the top, are evident.

Thus M_{sr} is the lesser of

$$M_{sr} = (f_{bc} + f_{ctm(t)})Z_{b,co} = (f_{bc} + 0.3(f_{ck})^{(2/3)})Z_{b,co} \quad \{M_{sr} = (f_{bc} + 0.45\sqrt{f_{cu}})Z_{b,co}\} \tag{4.27}$$

$$M_{sr} = (f_{tc} + f_{cd})Z_{t,co} = (f_{tc} + 0.567f_{ck})Z_{t,co} \quad \{M_{sr} = (f_{tc} + 0.45f_{cu})Z_{t,co}\} \tag{4.28}$$

Note that f_{bc} and f_{tc} are calculated for the concrete section alone. Here Ψ_{28} is the creep coefficient at the date of installation, generally taken as 28 days. This is the minimum time when the service moment will be fully imposed. The $m - 1$ term is used so that the concrete area occupied by the strands is not counted twice.

The above analysis will give the maximum possible serviceability moment capacity M_{sr} for a single arrangement of tendons for the beam, but if M_{sr} is limited by tension in the top fibre, then a smaller number of strands will give the same moment of resistance. The designer has to be careful in checking that the above analysis does not lead to an uneconomical solution by using too many strands. This is particularly important in inverted-tee beams, where non-symmetry leads to the serviceability moment of resistance M_{sr} governed by bottom fibre stresses being about 15 per cent greater than M_{sr} governed by the top fibre stress. It is also advantageous to use more than one arrangement of tendons in situations where smaller bending moments are required in beams of the same cross section. This is achieved by reducing the number of tendons by, say, 2 or 3 at a time, and finding new values for the eccentricity z_{cp} $\{e\}$ that will satisfy maximum fibre stresses as before. The following example shows the basic idea.

Consider a prestressed inverted-tee beam 600 mm deep × 600 mm wide, having a 200 mm deep × 350 mm wide upstand, as shown in Figure 4.24(c). In this example use C50/60 concrete, $E_{cm(t)} = 37.28\,\text{kN/mm}^2$ $\{E_c = 32\,\text{kN/mm}^2\}$, achieving grade C32/40 at transfer, $E_{cm(t)} = 33.35\,\text{kN/mm}^2$, $\{E_{ci} = 28\,\text{kN/mm}^2\}$, $A_{ps} = 94.2\,\text{mm}^2$, P_i per strand for 0.7 prestress = $0.7 \times 1750 \times 94.2 = 115.4\,\text{kN}$, $E_s = 195\,\text{kN/mm}^2$, and 2.5% strand relaxation. The beam is used for internal exposure taking 50%

relative humidity in service. Installation takes place at 28 days when the creep factor $\psi_{28} = 0.4 \times 1.8 = 0.72$ {0.72}. The cement is grade 52.5R and the aggregates are gravel.

Geometric data:

$A = 307.5 \times 10^3\,\text{mm}^2$ | $y_b = 269.8\,\text{mm}$
$Z_b = 30\,215 \times 10^3\,\text{mm}^3$ | $Z_t = 24\,685 \times 10^3\,\text{mm}^3$
$\alpha = 0.817$ | $\beta = 7.36 \times 10^{-8}\,\text{mm}^{-1}$

The limiting bottom and top fibre stresses at transfer are:

$\sigma_c < 0.567\, f_{ck(t)} = 0.567 \times 32 = 18.13\,\text{N/mm}^2$
$\sigma_t > 0.467 \times 3.02 = -1.41\,\text{N/mm}^2$
where $f_{ctm} = 0.3 \times 32^{2/3} = 3.02\,\text{N/mm}^2$
Note. Based on the 28-day strengths, the measured strengths are approximately equivalent to a maturity of 8.7 days.

$f_b < +20.00\,\text{N/mm}^2$
$f_{ct} > -0.225\sqrt{40} = -1.42\ \text{N/mm}^2$

Assuming that the elastic shortening loss is 0.08 of the initial, from equations (4.22) and (4.23):

$$P_i = \frac{307.5\times10^3}{2\times(1-0.08)}\left(16.72+\left(19.54\times\frac{0.183}{1.817}\right)\right) = 3123.6\,\text{kN}$$

$$e = \frac{19.54}{0.92\times3123.6\times10^3\times7.36\times10^{-8}} = 92.41\,\text{mm}$$

The maximum number of tendons
$N = 3123.6/115.4 = 27.1$
This is taken as 27,
so the actual initial prestressing force
$P_{pi} = 27 \times 115.4 = 3115.7\,\text{kN}$
and after initial losses, $P_{pmo} = 2866.4\,\text{kN}$

$$P_i = \frac{307.5\times10^3}{2\times(1-0.08)}\left(18.58+\left(21.42\times\frac{0.183}{1.817}\right)\right) = 3465.2\,\text{kN}$$

$$e = \frac{21.42}{0.92\times3465.2\times10^3\times7.36\times10^{-8}} = 91.30\,\text{mm}$$

The maximum number of tendons
$N = 3465.2/115.4 = 30.03$
This is taken as 29,
so the actual initial prestressing force
$P_i = 29 \times 115.4 = 3346.5\,\text{kN}$
and after initial losses, $P_t = 3078.7\,\text{kN}$

The maximum fibre stresses at transfer (suffix i) are:

$$f_{bi} = \frac{2866.4}{307.5}+\frac{2866.4\times92.41}{30215} = 18.09\,\text{N/mm}^2 < +18.13\,\text{N/mm}^2$$

$$f_{ti} = \frac{2866.4}{307.5}-\frac{2866.4\times92.41}{24685} = -1.41\,\text{N/mm}^2 > -1.41\,\text{N/mm}^2$$

The initial stress at the level of the centroid of the strands
$f_{cci} = 12.36\,\text{N/mm}^2$.
Instantaneous deformation loss (see Eq. 5.44)

$$= \frac{195\times12.36}{33.35\times(0.7\times1750)} = 5.28\%$$

Relaxation loss at transfer = 0.49%
Total loss at transfer = 5.77%
Original assumption of 8% OK.
The other final losses, conservatively ignoring the measured strengths and assuming maturity based on mould stripped at 2 days, and with 28 days at 70% RH to installation, and 50% RH in service, give strain losses as follows:

$$f_{bi} = \frac{3078.7}{307.5}+\frac{3078.7\times91.30}{30215} = 10.01+9.30 = 19.32\,\text{N/mm}^2 < +20\,\text{N/mm}^2$$

$$f_{ti} = \frac{3078.7}{307.5}-\frac{3078.7\times91.30}{24685} = 10.01-11.39 = -1.38\,\text{N/mm}^2 > -1.42\,\text{N/mm}^2$$

The initial stress at the level of the centroid of the strands
$f_{cci} = 13.63\,\text{N/mm}^2$.
The elastic shortening loss

$$= \frac{195\times13.63}{29\times(0.7\times1750)} = 7.75\%$$

Original assumption of 8% close.
The other final losses are as follows (see Section 5.2.8):
creep = 1.8 × 7.75% = 13.94%
shrinkage = $300 \times 10^{-3} \times 195/0.7 \times 1750$ = 4.78%
relaxation = 1.2 × 2.5 = 3.00%
Final losses = 29.47%

creep (see Eq. B.2 & 5.46)	= 10.25%		
480 με shrinkage (see Eq. 3.8 & 5.46)	= 8.36%		
long term relaxation (see Eq. 3.29)	= 2.25%		
plus transfer losses above	= 5.77%		
Final losses	= 20.86%		
Thus the final prestress force		Thus the final prestress force	
$= (1 - 0.2086) \times 3231.1$	= 2465.8 kN	$= (1 - 0.2947) \times 3346.5$	= 2360.3 kN
The final working fibre stresses are		The final working fibre stresses are	
$f_{bc} = +15.56\,\text{N/mm}^2$ and		$f_{bc} = +14.81\,\text{N/mm}^2$ and	
$f_{ct} = -1.21\,\text{N/mm}^2$.		$f_{ct} = -1.05\,\text{N/mm}^2$.	
The long-term value of f_{ctm} = $4.07\,\text{N/mm}^2$		The long-term value of f_{ct} $f_{ct} > -0.45\sqrt{60} = -3.49\,\text{N/mm}^2$	
$f_{ct} > -4.07\,\text{N/mm}^2$			
Service moment of resistance	= 645.68 kNm	Service moment of resistance	= 612.7 kNm
$m = (1 + 0.72) \times 195/37.28 = 9.$		$m = (1 + 0.72) \times 195/32 = 10.5.$	
For A_p and Z_{cp} determined above, compound section		For A_{ps} and e determined above, compound section	
$Z_{b,co} = 32\,890 \times 10^3\,\text{mm}^3$ (9% greater)		$Z_{b,co} = 33\,490 \times 10^3\,\text{mm}^3$ (11% greater)	
$Z_{t,co} = 25\,830 \times 10^3\,\text{mm}^3$ (5% greater)		$Z_{t,co} = 26\,070 \times 10^3\,\text{mm}^3$ (6% greater)	
Then M_{sr} is the lesser of		Then M_{sr} is the lesser of	
$M_{sr} = (15.56 + 4.07) \times 32\,890 \times 10^{-3}$ = 645.68 kNm		$M_{sr} = (14.81 + 3.49) \times 33\,490 \times 10^3 \times 10^{-6}$ = 612.7 kNm	
based on the bottom fibre stress, or		based on the bottom fibre stress limit, or	
$M_{sr} = (1.21 + 28.35) \times 25\,830 \times 10^{-3}$ = 745.04 kNm		$M_{sr} = (1.05 + 27.0) \times 26\,070 \times 10^3 \times 10^{-6}$ = 709.2 kNm	
based on the top fibre stress limit.		based on the top fibre stress limit.	

Note: had Calevera's Eq. (4.25) been used for $Z_{co,}$ it would have given $Z_{b,co} = 32\,100 \times 10^3\,\text{mm}^3$ (2.4% less than here) and $Z_{t,co} = 25\,200 \times 10^3\,\text{mm}^3$ (2.5% less).

Figure 4.24(d) shows a possible pattern for the strands for the BS solution. Note that the actual eccentricity derived from the strand pattern should not (but may) exceed the theoretical value; in this case the difference is −0.67 mm. The strand pattern for the BS EN 1992-1-1 solution has an extra strand at 150 and 200 mm from the bottom, resulting in a difference in actual and theoretical eccentricity of −1.3 mm.

The restricted 'no strand' zones along the vertical centre line of the beam are to enable the end shear connector to be positioned uninhibited. The other restricted zone across the centre of the beam (near to the neutral axis position of 269 mm above the soffit) is to facilitate a 50 mm service pipe.

The arrangement of the strands is very important in order to avoid splitting stresses (although this would be rare in a beam of this shape). The layout must be symmetrical about the vertical centre line, and there should be no large concentration of strands (called bunching) vertically.

The prestressing arrangement may now proceed using a smaller number of strands, say 23, 21 and 19 in this example, until the level of prestress renders the section uneconomic. This will occur when the moment of resistance of a beam with a smaller depth is greater than the beam in question. As mentioned above, the depth increment for prestressed beams is usually 50 mm. Thus, considering 550 mm as the next smallest size, it is found that the balanced moment of resistance for a 550 mm-deep inverted-tee beam is 431 kNm when using 24 strands. The number of strands required in the 600 mm-deep beam to give a slightly higher moment capacity than this is found to be 19. This therefore represents the lower-bound prestressing arrangement for the 600 mm-deep beam, and the overall economics of choosing either the deeper or shallower section must be considered.

Ultimate limit-state design is based on a rectangular section of effective breadth b_w, and effective depth, d, calculated to the centroid of those strands below the neutral axis, i.e. discounting the two strands in the top of the upstand and the two in the top of the boot. Refer to Section 5.2.8.2 for details.

Table 4.10(a) (to BS EN 1992-1) and Table 4.10(b) {to BS 8110} show an example of calculations carried out for a series of 500 mm wide by 300 mm boot depth (450 mm total depth) inverted-tee beams with varying numbers of 10.9 mm-diameter low-relaxation strands.

In Chart 4.1 (to BS EN 1992-1) and Chart 4.2 {to BS 8110} the moments and shear force capacities are given for a range of beams of varying depth and using 12.5 mm-diameter Class 2 {low-relaxation} strands.

In Table 4.10(a) and Chart 4.2, the values for M_{sr} according to BS EN 1992-1-1 are based on the compound section moduli using $m - 1 = ((1+\psi_{28})E_p/E_{cm}) - 1$. Here $\psi_{28} = 0.72$ at the date of installation, taken as 28 days. The height to the centroid of the strands can be deduced from the eccentricity, i.e. $y_s = y_b - z_{cp}$, from which the compound values are calculated using the parallel axis theorem. The ratio $Z_{b,co}/Z_b$ is between 1.05 and 1.10, depending on the area of strands to area of concrete.

Table 4.10(a) Specimen inverted tee-beam flexural design to BS EN 1992-1-1

(a) Beam Geometry

$b = 500$ mm; $b_{upstand} = 300$ mm; $h_{boot} = 300$ mm; $h_{upstand} = 150$ mm

Bottom corner triangular chamfer = 50 × 50 mm

$A = 192.5 \times 10^3$ mm^2; $y_b = 204.3$ mm; $I_c = 2874.5 \times 10^6$ mm^2

$Z_b = 14.069 \times 10^6$ mm^3; $Z_t = 11.699 \times 10^6$ mm^3; $\alpha = \dfrac{Z_t}{Z_b} = 0.8316$

(b) Material Data

$f_{ck} = 40$ N/mm^2; $E_{cm} = 35.2$ kN/mm^2; $f_{ck(t)} = 28$ N/mm^2; $E_{cm(t)} = 32.3$ kN/mm^2

Cement = 42.5R; Aggregates = gravel; Transfer at 2 days; Installation at 28 days

$f_{pk} = 1750$ N/mm^2; $A_p = 71.0$ mm^2 per strand; $E_p = 195$ kN/mm^2

Degree of initial prestress $\mu = 0.7$. Hence $P_{pi} = 87$ kN per strand.

		At transfer								
N	***P_{pi}***	**Loss %**	***P_{pmo}***	***z***	***P_{pmo}/A***	***$P_{pmo}\,z/Z_b$***	***$P_{pmo}\,z/Z_t$***	***f_{bi}***	***f_{ti}***	***f_{cci}***
16	1392	5.3	1318	73.1	+6.85	+6.85	−8.23	+13.69	−1.39	+9.77
14	1218	4.8	1159	75.8	+6.02	+6.24	−7.51	+12.27	−1.48	+8.71
12	1044	4.2	1000	75.2	+5.20	+5.34	−6.43	+10.54	−1.23	+7.44

	Losses %								
N	**Shortening**	**Creep**	**Shrinkage + Relaxation**	**Total**	***P_{po}***	***f_{bc}***	***f_{tc}***	***M_{sr} (bottom)***	***M_{sr} (top)***
16	4.81	10.27	9.78	24.86	1046	+10.86	−1.10	215.9	231.3
14	4.29	9.32	9.96	23.57	931	+9.85	−1.19	200.1	232.4
12	3.66	8.13	10.18	21.97	814	+8.58	−1.00	180.3	229.9

N_T	***A_p***	***d***	***x/d***	***d_n***	***f_p***	***M_{Rd}***	***M_{Rd}/M_{sr}***
12	852	368.0	0.55	84.4	1354	327.3	1.619
10	710	380.3	0.50	77.9	1493	320.5	1.706
8	568	393.8	0.37	60.0	1406	266.6	1.567

Notes:

N = total number of strands, all of which are equally stressed and fully bonded.

N_T = number of strands in tension zone. In this example it is assumed that 2 strands are located in the top of the upstand and 2 in the top of the boot. Hence $N_T = N - 4$.

Table 4.10(b) Specimen inverted tee-beam flexural design to BS 8110

(a) Beam Geometry

$b = 500\,\text{mm}$ $b_{upstand} = 300\,\text{mm}$ $h_{boot} = 300\,\text{mm}$ $h_{upstand} = 150\,\text{mm}$

Bottom corner triangular chamfer = $50 \times 50\,\text{mm}$

$A = 192.5 \times 10^3\,\text{mm}^2$ $y_b = 204.3\,\text{mm}$ $I = 2874.5 \times 10^6\,\text{mm}^2$

$Z_b = 14.069 \times 10^6\,\text{mm}^3$ $Z_t = 11.699 \times 10^6\,\text{mm}^3$ $\alpha = \dfrac{Z_t}{Z_b} = 0.8316$

(b) Material Data

$f_{cu} = 50\,\text{N/mm}^2$ $E_c = 30\,\text{kN/mm}^2$ $f_{ci} = 35\,\text{N/mm}^2$ $E_{ci} = 27\,\text{kN/mm}^2$

$f_{pu} = 1750\,\text{N/mm}^2$ $A_{ps} = 71.0\,\text{mm}^2$ per strand $E_s = 195\,\text{kN/mm}^2$

Degree of initial prestress $\mu = 0.7$. Hence $P_i = 87\,\text{kN}$ per strand.

		At transfer								
N	P_i	**Loss %***	P_t	e	P_t/A	$P_t\,e/Z_b$	$P_t\,e/Z_t$	f_{bi}	f_{ti}	f_{cci}
16	1392	5.0	1322.4	72.5	+6.87	+6.81	−8.20	+13.68	−1.33	+9.28
14	1218	4.0	1169.3	74.0	+6.07	+6.15	−7.40	+12.22	−1.33	+8.29
12	1044	3.5	1007.5	76.2	+5.23	+5.46	−6.56	+10.69	−1.33	+7.27

* Estimate prior to transfer stress analysis.

	Losses %								
N	**Shortening**	**Creep**	**Shrinkage + Relaxation**	**Total**	P_t	f_{bc}	f_{tc}	M_{sr} ***(bottom)***	M_{sr} ***(top)***
16	5.47	9.85	7.77	23.09	1070.5	+11.07	−1.08	200.7	205.6
14	4.88	8.78	7.77	21.43	957.0	+10.00	−1.09	185.7	205.7
12	4.28	7.71	7.77	19.76	837.7	+8.89	−1.11	170.1	206.0

N_T	A_{ps}	d	$\dfrac{f_{pu}A_{ps}}{f_{pu}bd}$	$\dfrac{f_{pb}}{0.87f_{pu}}$	x/d	d_n	M_{ur}	M_{ur}/M_{sr}
12	852	380.8	0.261	0.87	0.475	81.4	337.7	1.683
10	710	385.0	0.215	0.90	0.420	72.8	303.7	1.635
8	568	391.3	0.169	0.95	0.350	61.6	270.8	1.592

Notes:
N = total number of strands, all of which are equally stressed and fully bonded.
N_T = number of strands in tension zone. In this example it is assumed that 2 strands are located in the top of the upstand and 2 in the top of the boot. Hence $N_T = N - 4$.

4.3.7.2 Boot reinforcement

The boot of inverted-tee beams is designed and reinforced in exactly the same way as in the L-shaped beam, except that a single link A_{sh} is used to satisfy tension in both sides of the beam. The vertical steel A_{sv} carries the maximum reaction, in accordance with equations (4.14) and (4.15).

In most cases the depth of the recess is smaller than or equal to the depth of the floor slab, or the depth of the half-joint in double-tee slabs. This means that the depth of the boot on which the floor rests is sufficient for there to be no requirement for horizontal tie steel. Here the concrete is in longitudinal compression and is usually uncracked flexurally. Only in cases where the boot depth is less than about 250 mm, or the beam is heavily loaded using double-tee slabs, are links required in the boot. As shown earlier in Figure 4.18, links (typically H8 or H10) are placed with at least one either side of the slab reaction points.

Chart 4.1 Example Moments and Shear Force Capacities for Inverted-Tee Beams to BS EN 1992-1-1

Geometric data	Overall width = 500 mm Bearing ledge width = 100 mm Boot depth = variable 300 to 600 mm		Upstand width = 300 mm Upstand depth = 200 mm No corner chamfers
Material data	Concrete Strand Initial prestress Transmission length	f_{ck} = 50 N/mm^2 A_{ps} = 94.2 mm^2 η = 0.70 = 790 mm	$f_{ck(t)}$ = 32 N/mm^2 f_{pk} = 1750 N/mm^2 P_{pi} = 115.4 kN per strand Cement 52.5R, Aggregates gravel
Transfer at 2 days.	Installation at 28 days		RH = 70% stockyard, 50% in service
Curing 40°C	Shrinkage loss = 6.6% to 6.9%		Relaxation loss = 2.5% to 2.7% Ecc. = eccentricity

Beam ref	Boot depth (mm)	No. of strands	Ecc. (mm)	Final f_{bc} (N/mm^2)	Final f_{tc} (N/mm^2)	M_{sr} (kNm)	M_{Rd} (kNm)	$V_{Rd,c}$ (kN)	$V_{Rd,cr}$ (kN)
TB300	300	13	79.1	+10.66	−0.87	289	487	341	167
y_b =	221.4 mm	15	81.4	+12.21	−1.19	321	546	355	182
		17	83.2	+13.68	−1.50	353	577	368	195
TB400	400	15	99.2	+10.38	−1.12	408	698	482	188
y_b =	269.2 mm	18	97.0	+12.04	−1.15	457	727	509	214
		21	95.4	+13.62	−1.18	504	792	534	233
TB500	500	17	126.6	+10.43	−1.60	560	889	660	219
y_b =	317.7 mm	21	124.9	+12.45	−1.82	643	1025	705	244
		25	123.7	+14.35	−2.03	724	1134	746	270
TB600	600	20	146.7	+10.68	−1.66	748	1192	786	247
y_b =	366.7 mm	25	144.7	+12.86	−1.91	868	1380	839	279
		30	143.3	+14.92	−2.13	980	1530	888	309

Chart 4.2 Example Moments and Shear Force Capacities for Inverted-Tee Beams to BS 8110

Geometric data	Overall width = 500 mm Bearing ledge width = 100 mm Boot depth = variable 300 to 600 mm		Upstand width = 300 mm Upstand depth = 200 mm
Material data	Concrete Strand Initial prestress Transmission length	f_{cu} = 60 N/mm^2 A_{ps} = 94.2 mm^2 η = 0.70 = 475 mm	f_{ci} = 40 N/mm^2 f_{pu} = 1750 N/mm^2 P_i = 115.4 kN per strand
Fixed losses	Shrinkage = 58.5 N/mm^2 = 4.77%		Strand relaxation = 1.2 × 2.5% = 3.0%

Beam reference	Boot depth (mm)	Number of strands	Final f_{bc} (N/mm^2)	Final f_{tc} (N/mm^2)	M_{sr} (kNm)	M_{ur} (kNm)	V_{co} (kN)	Min. V_{cr} (kN)
TB300	300	13	+11.1	−1.0	263	459	309	92
		15	+12.3	−1.1	286	485	321	99
		17	+13.5	−1.1	303	509	333	106
TB400	400	15	+10.4	−1.0	363	638	380	106
		18	+12.2	−1.1	409	692	399	119
		21	+13.7	−1.1	448	743	417	129
TB500	500	17	+10.2	−1.0	488	851	449	123
		21	+12.0	−1.1	555	913	477	138
		25	+13.8	−1.1	617	1001	502	152
TB600	600	20	+10.4	−1.0	655	1122	526	144
		25	+12.4	−1.1	747	1211	562	162
		30	+14.2	−1.1	832	1300	593	181

4.3.7.3 Shear design

Shear reinforcement is rarely necessary, because the ultimate shear resistance of prestressed members is a function of the ultimate flexural requirements. The shear span (M_{Rd}/V_{Rd}) $\{M_u/V_u\}$ for most beams in precast structures is $L/4$. Thus the shear force at the position of flexural decompression rarely exceeds 0.5 V_{cr}. The uncracked shear capacity $V_{Rd,c}$ is in accordance with BS EN 1992-1-1, Eq. 6.4. It extends to the position where the service moment exceeds the cracking moment of resistance $M_{cr} = (f_{bc} + f_{ctk,0.05}/\gamma_c)\, Z_b$ where f_{bc} = prestress at bottom after losses. The flexurally cracked shear capacity, called $V_{Rd,cr}$ in this textbook to distinguish it from $V_{Rd,c}$, is in accordance with BS EN 1992-1-1, the greater of Eq. 6.2(a) or (b). Note that there is no gradual reduction in $V_{Rd,cr}$, as there is with V_{cr} in BS 8110.

Deflected tendons may be specified to increase shear capacity in very special cases, but complications to the long-line prestressing outweigh the enhancements in structural performance.

Prestressed beams are highly efficient, both structurally and economically. Attempts to reduce the depth of the downstand below the soffit of the slab have inevitably led to composite construction, as discussed in Chapter 6.

Exercise 4.4 Inverted tee-beam design

Calculate the flexural serviceability and ultimate moments of resistance, and the uncracked and cracked shear resistances of the prestressed concrete inverted-tee beam shown in Figure 4.25. Bearing length = 150 mm. Show the detailed calculation for losses.

Use grade C50/60 concrete, $E_{cm} = 37.28\,\text{kN/mm}^2$, $\{E_c = 32\,\text{kN/mm}^2\}$, achieving grade C32/40 at transfer after 48 hours, during which the mean curing temperature was $T = 40°\text{C}$. $E_{cm(t)} = 33.35\,\text{kN/mm}^2$, $\{E_{ci} = 28\,\text{kN/mm}^2\}$, and 12.5 mm-diameter low-relaxation helical strand stressed to 70% ultimate with f_{pk} $\{f_{pu}\} = 1751\,\text{N/mm}^2$ (quoted values) and $f_{p,0.1k} = 1520\,\text{N/mm}^2$. The beam is stored externally for 28 days where relative humidity is 70%, and is then used for internal exposure Class XC1 {Class 2}, where RH = 50% in service. The creep factor at installation $\psi_{28} = 0.72$ {0.72}. The cement is grade 52.5R and the aggregates are gravel.

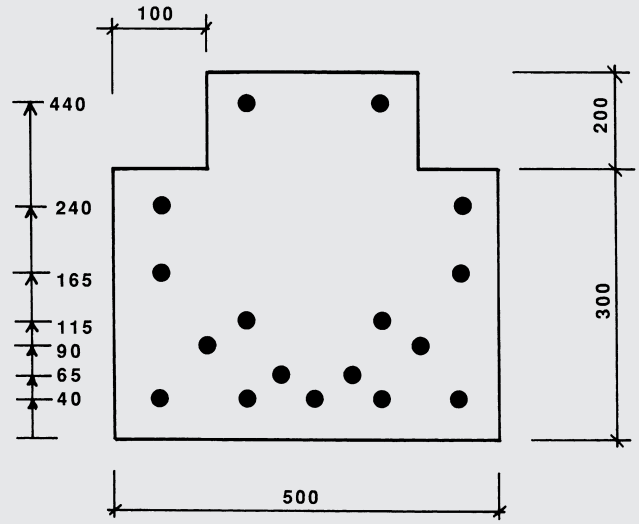

Figure 4.25 Details for Exercise 4.4.

(*Continued*)

Solution

Step 1: Component cross-sectional properties

Component dimensions: Overall width = 500 mm; Overall depth = 500 mm; Upstand width = 300 mm; Upstand depth = 200 mm

Exposure. Cover to reinforcement = 40 − 12.5/2 = 33.75 mm > 20 mm {BS 8500-1, table A.4, exposure XC1}

Area = 210 000 mm^2 $I = 4003.57 \times 10^6\ mm^4$

Height to centroid of concrete from bottom y_b = 221.4 mm, and y_t = 278.6 mm
$Z_b = 18.080 \times 10^6\ mm^3$ $Z_t = 14.37 \times 10^6\ mm^3$
No. of tendons = 17 at 12.5 mm diameter Area per strand = 94.2 mm^2
Relaxation type 2 = 2.5% loss Centroid of strands from bottom = 143 mm

Eccentricity e from $A_{ps} = 1601.4\ mm^2$ $f_{pu} A_{ps} = 2805.0$ kN $E_s = 195\ kN/mm^2$
Neutral axis depth = 78.4 mm

Characteristic strength at 28 days	= 50 N/mm^2	Characteristic strength at 28 days	= 60 N/mm^2
E_{cm} (28 days) using gravel	= 37.28 kN/mm^2	E_c (28 days)	= 32 kN/mm^2
Transfer strength	= 32 N/mm^2	Transfer strength	= 40 N/mm^2
$E_{cm(t)}$	= 33.35 kN/mm^2	E_{ci}	= 28 kN/mm^2
Self-weight of concrete = 25 kN/m^3		Self-weight of concrete = 24 kN/m^3	
Self-weight	= 5.25 kN/m	Self-weight	= 5.04 kN/m

Step 2: Serviceability limit state of bending

Initial prestressing stress = 0.7 × 1751	= 1225.7 N/mm^2	Initial prestressing stress = 0.7 × 1751	= 1225.7 N/mm^2
Initial prestressing force		Initial prestressing force	
P_{pi} = 0.7 × 2805	= 1962.8 kN	P_i = 0.7 × 2805 = 1962.8 kN	
Estimate initial losses at transfer = 6%		Estimate initial losses at transfer = 6 %	
Prestress at transfer:		Prestress at transfer:	
f_{bc} = 16.80 N/mm^2 (bottom)		f_{bc} = 16.80 N/mm^2 (bottom)	
f_{tc} = −1.29 N/mm^2 (top)		f_{tc} = −1.29 N/mm^2 (top)	
		f_{cc} = 11.63 N/mm^2 (centroid of strand)	
Losses:		Losses:	
Instantaneous relaxation loss		Elastic shortening = 11.63 × 195/28	
Eq. 3.29. μ = 0.7 and t = 48 hours		= 81.0 N/mm^2	= 6.61%
Loss $\Delta\sigma_{p,r} = 1225.7 \times 0.66 \times 2.5 \times e^{(9.1 \times 0.7)} \times 0.048^{0.75(1-0.7)}$ = 5.97 N/mm^2	= 0.49%	Creep loss = 1.8 × elastic shortening loss	= 11.90%
		Steel relaxation quoted as 2.50% at 100 hr	= 3.00%
Elastic shortening		Concrete shrinkage at 300 $\mu\varepsilon$ =	
$\Delta\sigma_{p,el}$ = 11.63 × 195/33.35 = 68.0 N/mm^2	= 5.55% = 6.04%	58.5 N/mm^2	= 4.77%
Total loss at transfer		Total losses	= 26.27%
Creep from transfer to installation			
(See Cl. 3.1.4(5)) (all faces exposed)			
h_0 = 2 × 210 000/2000 = 210 mm			
RH = 70%			
$\alpha_1 = 0.7$, $\alpha_2 = 0.9$, $\alpha_3 = 0.78$			
(See Eq. B.3b/B.8c) $\varphi_{RH} = 1.224$			
(See Eq. B.4)			
$\beta_{(fcm)} = 16.8/\sqrt{58} = 2.206$			

(See Eq. B.10) $t_{o,T} = e^{-(4000/313 - 13.65)} \times 2$
= 4.77 days' equivalent maturity (conservatively ignoring the measured strength, which implies 55.3°C curing temperature or greater maturity).
(See Eq. B.9) $t_o = 4.77 \times ((9/(2 + 4.77^{1.2}) + 1)^1 = 9.8$ days
(See Eq. B.5) $\beta_{(to)} = 1/(0.1 + 9.8^{0.2}) = 0.596$
(See Eq. B.8b) $\beta_H = 523$ days
(See Eq. B.7) $\beta_{c(t,to)} = ((28–2)/(523+28–2))^{0.3} = 0.400$
$\varphi_{(ti,to)} = 1.224 \times 2.206 \times 0.596 \times 0.4 = \underline{0.644}$
$f_{cc} = 11.62\,\text{N/mm}^2$ (centroid of strand)
(See Eq. 5.46) Loss
$\Delta\sigma_{p,c,i} = 195 \times 11.62 \times 0.644/(37.28 \times 1.089) = \underline{35.9\,\text{N/mm}^2}$ = 2.93%
$\sigma_{pmi} = 1115.8\,\text{N/mm}^2$
P_{pmi} after losses to install = 1786.9 kN
Creep from install to life, $t_o = 28$ days to $t = 500\,000$ hours (20833 days)
$h_0 = 2 \times 210\,000/1100 = 382$ mm (sides and bottom exposed)
RH = 50%
$\beta_{(to)} = 1/(0.1 + 28^{0.2}) = 0.488$
$\beta_H = 767$ days
$\beta_{c(t,t0)} = ((20\,833 - 28)/(767 + 20\,833 - 28))^{0.3} = 0.989$
$\varphi_{(ti,to)} = 1.341 \times 2.206 \times 0.488 \times 0.989 = \underline{1.43}$ = 6.17%
$f_{cc} = 11.613\,\text{N/mm}^2$
Loss $\Delta\sigma_{p,c,i} = 195 \times 11.26 \times 1.43/(37.28 \times 1.113) = \underline{75.6\,\text{N/mm}^2}$
Total creep loss = 9.10%
Shrinkage from transfer to life

$h_0 = 382$ mm
(See Table 3.3) $k_h = 0.73$
Cement Class R ($\alpha_{ds1} = 6$, $\alpha_{ds2} = 0.11$)
(See Eq. B.12)} RH = 50%
$\beta_{RH} = 1.356$
(See Eq. B.11) $\varepsilon_{cd,o} = 0.85 \times (220 + 110 \times 6)\, e^{-(0.11 \times 58/10)} \times 1.356 = 0.000536$
(See Eq. 3.10) $\beta_{ds(t,ts)} = 0.986$
(See Eq. 3.9) Drying $\varepsilon_{cd} = 0.73 \times 1.356 \times 0.986 \times 0.000536 = 0.000523$
(See Eq. 3.12) $\varepsilon_{ca(\infty)} = 2.5 \times (50 - 10) \times 10^{-6} = 0.000100$

(*Continued*)

(See Eq. 3.13) $\beta_{as} = 1$ for long term
(See Eq. 3.11) Autogenous
$\varepsilon_{ca(t)} = 0.000100$
(See Eq. 3.8})Total shrinkage
$\varepsilon_{cs} = 0.000623$
(See Eq. 5.46) Loss $\Delta\sigma_{p,s} = 195 \times 0.000623/1.113 = 109.1\,\underline{\text{N/mm}^2}$ $= 8.90\%$
Final tendon relaxation
(See Eq. 3.29) $\mu = (1 - 0.06) \times 0.7 = 0.66$
(See Eq. 3.29) $\sigma_{pr} = 39.64\,\text{N/mm}^2$
(See Eq. 5.46) Loss $\Delta\sigma_{p,r} = 0.8 \times 37.25/1.113 = \underline{28.49\,\text{N/mm}^2}$ $= 2.32\%$
Total losses $= \underline{26.39\%}$
Effective prestressing force after losses at transfer $P_{pmo} = 1844.4\,\text{kN}$
Check, prestress at transfer:
$f_{bi} = +16.79\,\text{N/mm}^2 < 0.6\,f_{ck(t)} = +19.2\,\text{N/mm}^2$
$f_{ti} = -1.29\,\text{N/mm}^2 > f_{ctd(t)} = -1.41\,\text{N/mm}^2$
Effective prestressing force after final losses $= 1444.8\,\text{kN}$

Prestress after losses:
$f_{bc} = +13.15\,\text{N/mm}^2$
$f_{tc} = -1.01\,\text{N/mm}^2$
$f_{cc} = +9.10\,\text{N/mm}^2$ (strand centroid)
$f_{cp} = +6.88\,\text{N/mm}^2$ (section centroid)
Service moment of resistance using compound section where
$m = (1 + 0.72) \times 195/37.28 = 9.0$
$Z_{b,co} = 19\,730 \times 10^3\,\text{mm}^3$
$Z_{t,co} = 15\,120 \times 10^3\,\text{mm}^3$
For XC1 exposure, allowable tension (for $f_{ck} = 50\,\text{N/mm}^2$) $f_{ctm} = -4.07\,\text{N/mm}^2$
$M_{sr} = (13.15 + 4.07) \times 19.730 = \underline{339.8\,\text{kNm}}$
Allowable compression $= 22.5\,\text{N/mm}^2$
or $M_{sr} = (1.01 + 22.5) \times 15.12 = 355.5\,\text{kNm}$ $= \underline{339.8\,\text{kNm}}$

Effective prestressing force after losses at transfer = 1833.2 kN
Check, prestress at transfer:
$f_{bi} = +16.69\,\text{N/mm}^2 < 0.33\,f_{cu} = +20\,\text{N/mm}^2$
$f_{ti} = -1.28\,\text{N/mm}^2 > 0.45\sqrt{f_{civ}} = -2.85\,\text{N/mm}^2$

Effective prestressing force after final losses $= 1447.3\,\text{kN}$

Prestress after losses:
$f_{bc} = +13.17\,\text{N/mm}^2$
$f_{tc} = -1.01\,\text{N/mm}^2$
$f_{cc} = +9.12\,\text{N/mm}^2$ (strand centroid)
$f_{cp} = +6.89\,\text{N/mm}^2$ (section centroid)
Service moment of resistance using compound section, where
$m = (1 + 0.72) \times 195/32 = 10.5$
$Z_{b,co} = 20\,040 \times 10^3\,\text{mm}^3$
$Z_{t,co} = 15\,250 \times 10^3\,\text{mm}^3$
For class 2 elements, allowable tension (for $f_{cu} = 60\,\text{N/mm}^2$) $= -3.49\,\text{N/mm}^2$
$M_{sr} = (13.17 + 3.49) \times 20.04 = 333.9\,\text{kNm}$
Allowable compression $= 20.0\,\text{N/mm}^2$
Service Resistance Moment,
$M_{sr} = (1.01 + 20.0) \times 15.25$ $= 320.4\,\text{kNm}$ $= \underline{320.4\,\text{kNm}}$

Step 3: Ultimate limit state of bending

No. of strands below neutral axis in tension zone = 13
$d = 417.7\,\text{mm}$
$b = 300\,\text{mm}$

Centroid of these bars is 82.3 mm from bottom face
$A_{ps} = 1224.6\,\text{mm}^2$

Final stress in tendons
$\sigma_{cp} = 1444.8 \times 10^3/1601.4$
$= 902.2\,\text{N/mm}^2$
(See clause 5.10.9) Pre-strain
$\varepsilon_{po} = 902.2/195\,000 = 0.00463$
$\varepsilon_{LOP} = 0.9 \times 0.87 \times 1751/195\,000$
$= 0.00703$
By solving quadratic or iterative solutions,
$X = 247.0\,\text{mm}$, and
$0.8X = 197.6 < 200\,\text{mm}$ upstand depth
$d_n = 98.8\,\text{mm}$
Ultimate strain $\varepsilon_p = 0.00714$
$> \varepsilon_{LOP} < \varepsilon_{ud}$
(See Fig. 3.10) $f_p = 1371.5\,\text{N/mm}^2$
$F_s = f_p\,A_p = 1371.5 \times 1224.6 = 1679.5\,\text{kN}$
Ultimate moment of resistance
$M_{Rd} = 1679.5 \times (417.7 - 98.8)$ $= \underline{535.6\,\text{kNm}}$
Check equilibrium
$F_c = 0.567 f_{ck}\,b\,0.8\,X = F_s$
Hence $X = 246.98\,\text{mm}$ (agrees 247 mm)
The ratio $M_{Rd}/M_{sr} = 1.55 > 1.5$
So the serviceability limit state will be critical.

Limiting value of $f_{pb}/f_{pu} = 0.737$
$F_s = f_{pb}\,A_{ps} = 1291 \times 1224.6 = 1581.0\,\text{kN}$
$f_{cu} = 60\,\text{N/mm}^2$
$F_c = 0.45\,f_{cu} b\,0.9\,X$
Hence $X = 216.9\,\text{mm}$, and $0.9X =$
$195.2 < 200\,\text{mm}$ upstand depth
$d_n = 0.45 \times 216.9 = 97.60\,\text{mm}$

Ultimate moment of resistance
$M_{ur} = 1581.0 \times (417.7 - 97.6) = 506.1\,\text{kNm}$
However, $X > 0.5(500 - 82.3) = 208.8\,\text{mm}$,
so section is over-reinforced and the ultimate moment is limited to
$M_{ur} = 0.156 \times 300 \times (500 - 82.3)^2 \times 60$ $= \underline{489.9\,\text{kNm}}$
Thus the ratio $M_{ur}/M_{sr} = 1.47$ approx < 1.6
So the serviceability or limit state may be critical.

Step 4: Ultimate limit state of shear

(a) *Uncracked*, at the level of the intersect between the upstand and the boot:

$b_v = 300\,\text{mm}$
$y_t = 500 - 221.4 = 278.6\,\text{mm}$
$I\,b_v/A\,y = 112\,100\,\text{mm}^2$

$A_v = 300 \times 200 = 60\,000\,\text{mm}^2$
$y = 278.6 - 100 = 178.6\,\text{mm}$

$\alpha_{ct} = 1$
(See clause 8.10.2.2)
$f_{ctd(t)} = 0.7 \times 3.02/1.5 = 1.41\,\text{N/mm}^2$
(See Eq. 8.15)
$f_{pbt} = 3.2 \times 1.0 \times 1.41 = 4.52\,\text{N/mm}^2$
Transfer $\sigma_{pmo} = 1844.4 \times 10^3/1601$
$= 1152\,\text{N/mm}^2$
(See Eq. 8.16) $l_{pt} = (1.0 \times 0.19 \times 1152/4.52) \times 12.5 = 606\,\text{mm}$
(See Eq. 8.18) $1.2\,l_{pt} = 727\,\text{mm}$
$l_x = 40 + 417.6 = 457.6\,\text{mm}$
$\alpha_l = 457.6/783 = 0.619$
σ_{cp} at level of the intersect $= 4.23\,\text{N/mm}^2$
(See clause 2.4.2.2.(1)) $\gamma_{p,fav} = 0.9$
$f_{ctd} = 0.7 \times 4.07/1.5 = 1.9\,\text{N/mm}^2$
Ultimate Shear Resistance
(See Eq. 6.4)
$V_{Rd,c} = 112.1 \times \sqrt{(1.9^2 + 0.574 \times 0.9 \times 4.23 \times 1.9)}$
$= 320.3\,\text{kN}$
The reader should verify that at centroidal axis $V_{Rd,c} = 499\,\text{kN}$, and is clearly not critical (steps $\sigma_{cp} = 7.12$; $l_x = 371$; $\alpha_l = 0.475$; $S = 12.26 \times 10^6$; $b_w = 500$)

f_{cp} (at intersect plane) $= +4.66\,\text{N/mm}^2$
$f_t = -1.86\,\text{N/mm}^2$

Ultimate Shear Resistance
$V_{co} = 0.67 \times 300 \times 600 \sqrt{(1.86^2 + 0.8 \times 4.66 \times 1.86)}$
$= 324.0\,\text{kN}$

(*Continued*)

(b) *Cracked* (see also Section 5.2.8)

(See Eq. 6.3) $v_{min} = 0.545\,\text{N/mm}^2$
(See clause 6.2.2.(1)) $k = 1.692$
$k_1 = 0.15$
$\rho_1 = 0.00977$
$V_{Rd,cr} = ((0.12 \times 1.692 \times (100 \times 0.00977 \times 50)^{(1/3)}) + 0.15 \times 0.2 \times 28.33) \times 300 \times 417.7 = 199.5\,\text{kN}$
$V_{Rd,cr,min} = (0.545 + 0.15 \times 5.67) \times 300 \times 417.7 = 174.8\,\text{kN}$
Critical $V_{Rd,cr} = \underline{199.5\,\text{kN}}$
(See clause 6.2.2.(2)) Use $V_{Rd,cr}$
where $M_s > (\sigma_b + f_{ctd}/\gamma_c)\, Z_b$
$= (13.15 + 1.9) \times 19.73$
$= 297.0\,\text{kNm}$

$\sqrt{60} = 7.74$
Decompression moment
$M_o = (0.37 \times 7.74 + 0.8 \times 13.17) \times 18.08 = 242.3\,\text{kNm}$
$f_{cpx} = 3.916\,\text{N/mm}^2$
$V/M = V_{co}/\gamma_{f,mean}\, M_{sr} = 324.0/(1.5 \times 333.9) = 0.647$
$V_{cr} = (0.037 \times 7.74 \times 500 \times 417.7 \times 10^{-3} + 242.3 \times 0.647) = 216.6\,\text{kN}$

But not less than $0.1 \times 300 \times 417.7 \times 7.74 = 97.06\,\text{kN}$
Critical $V_{cr} = \underline{216.6\,\text{kN}}$

4.3.8 Beam end shear design

Special attention is given to shear reinforcement near the end connections. Stirrups and bent-up reinforcing bars are provided to ensure the transfer of shear in the critical region. Bent-up bars may be used to resist approximately one-half of the shear force. In some instances a prefabricated shear box, comprising welded angles, channels, composite plates, or RHS sections, partially or wholly replaces the stirrup cage. These are used to:

- transfer the shear forces to a point in the beam where the stirrups are considered to be fully effective
- prevent bursting of the concrete at ends of the beam
- provide a steel bearing plate with which to make a steel-to-steel connection to the supporting member.

Extensive testing has been carried out to prove the shear capacity of beams with steel inserts (e.g. [4.28] and [4.29]).

Recessed or pocketed beam ends, shown in Figures 4.26 and 4.27, are used where the beam is to be supported on a member projecting from the face of the column. The structural connection is made entirely within the depth of the beam. The generalised structural model, presented here in Figure 4.28, is similar in principle to the design of reinforced concrete corbels. The dotted lines represent principal stress trajectories as determined using a finite element solution [4.30]. The stresses fan out in a 45° manner and principal compressive and tensile forces are in equilibrium. The concrete provides the compressive force, providing it is restrained against later bursting by the binding steel, and tie bars provide the tensile force resistance.

One of the most comprehensive dissertations on this subject is by Martin and Korkosz [4.31], which cites 147 references (up to 1982) and studies the analytical and experimental aspects of many of the connections given in the various PCI design manuals on precast structures [4.2] and connections [4.32].

Beam-to-beam connections may also be made, as shown in Figure 3.39, where it is not possible to position a column at the end of a beam. The design of the end shear reinforcement is no different from the above. Additional reinforcement is required in the primary supporting beam to cope with the combined effects of bending, shear, torsion and bearing stresses. The design method involves the resolution of actions into shear or axial forces, and the superposition of resulting stresses in the

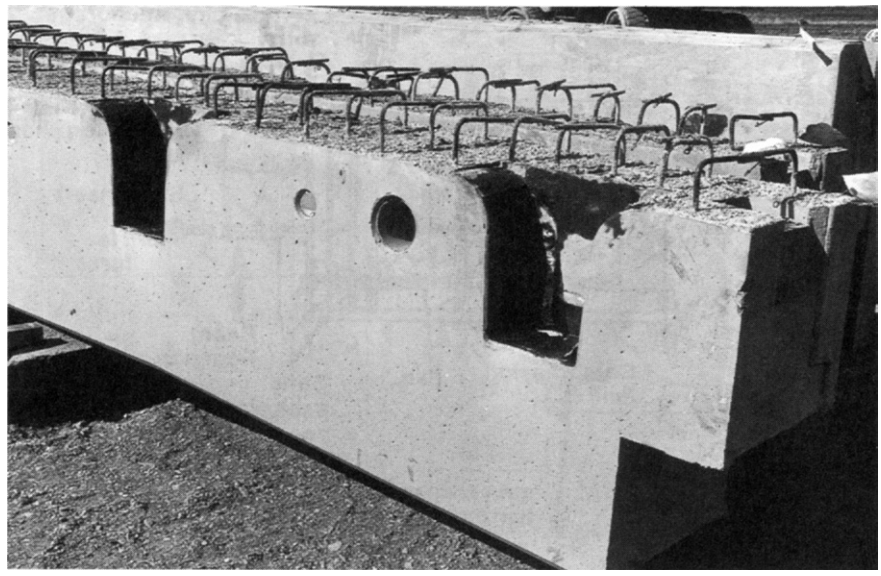

Figure 4.26 Recessed beam end.

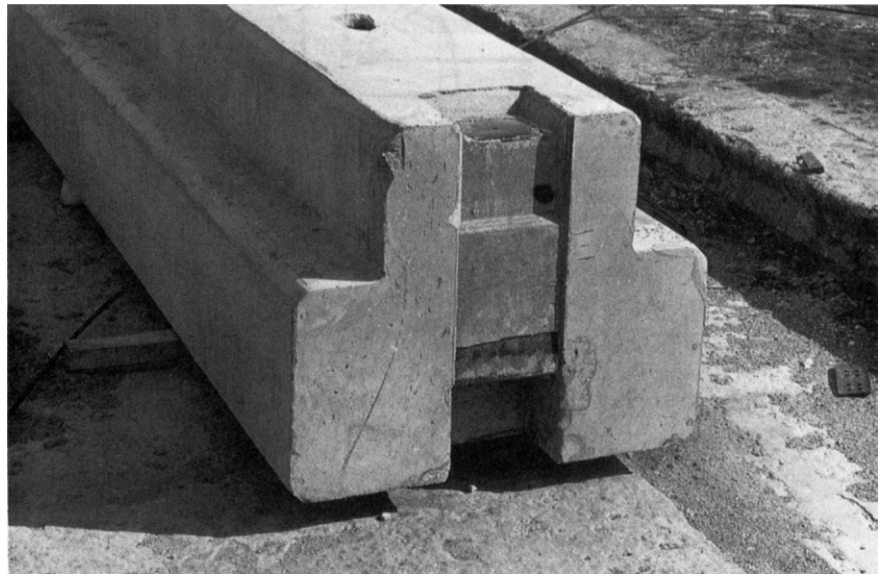

Figure 4.27 Pocketed beam end.

connection. Steel inserts are most widely used, particularly if the ultimate beam reaction is greater than about 200 kN. The design of this connection is discussed further in Section 7.12.

4.3.9 Recessed beam ends

Recessed beam ends are used where the beam is to be supported on a member projecting from the face of the column, and the structural connection is made entirely within the depth of the beam. The design methods presented here are similar in principle to the halving joint or corbels given in BS

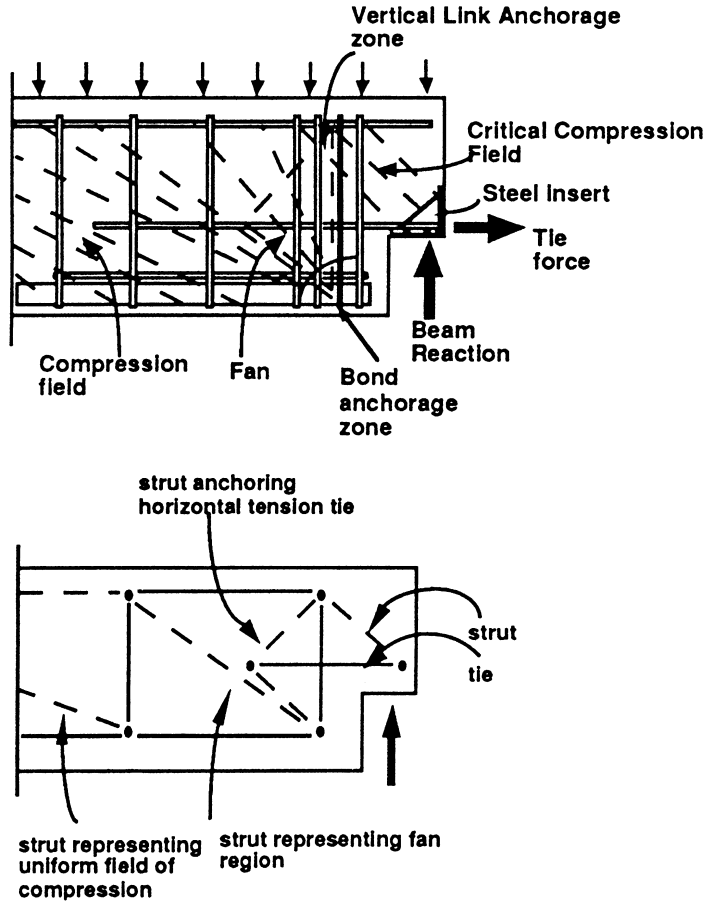

Figure 4.28 Generalised structural model of halving joint in beams [4.30].

8110, Part 1, clause 5.2.7. The general dimensions for a recessed beam are given in Figures 4.29 and 4.30.

A special type of beam end, shown in Figures 4.27 and 4.30, is the pocketed end type. Two concrete wings, Y in the diagram, are reinforced to allow the main flexural steel in the bottom of the beam to develop full anchorage without the use of anchor plates or bent-up bars.

In all cases the ends of the beams are reinforced at the ultimate limit state using an arrangement of vertical links and diagonal or horizontal bars to cater for tie forces and bursting pressures in the compression zones, respectively. The horizontal bars in direct contact with the bearing surface are often used in all cases to avoid the risk of local spalling and crushing and to ensure uniformity of bearing pressures in this highly stressed zone.

The serviceability limit state is equally important in this region, and the design should check that service strains, based on a short-term modulus of rupture of $0.556\sqrt{f_{cu}}$ [4.33], are not exceeded. A method of calculating the service-load stresses, strains and crack widths is proposed by Clark and Thorogood [4.34] (see Figure 4.31). By limiting either the strain in the concrete ε_c (to say 0.0018) or steel ε_s (to say 0.0020) considered along the cracked section OA, it is possible to determine the forces F_c and F_s, and hence the serviceability force V_s. The most significant factor in controlling service-load stresses is the inclined reinforcement across the inside corner of the recess. Mattock and Chan also measured crack widths in 'dapped-end' beams subjected to vertical end shear forces, and vertical plus horizontal end forces [4.35].

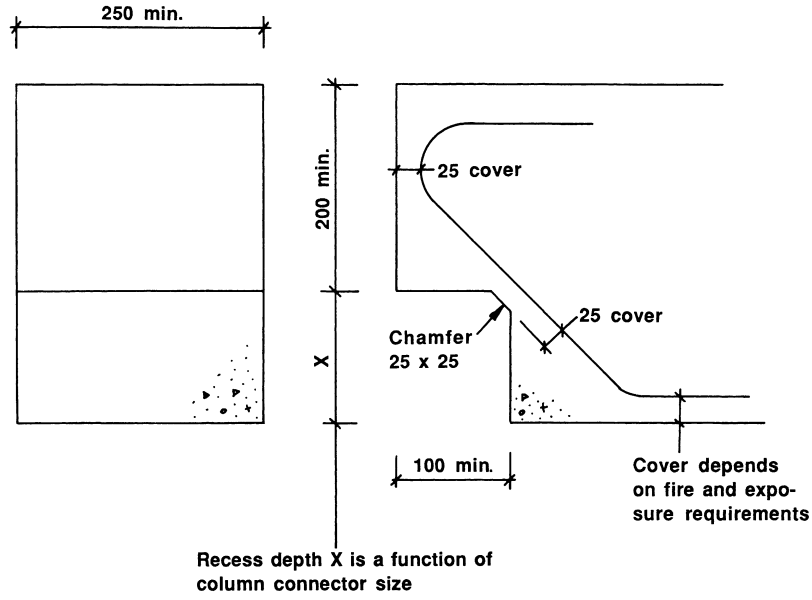

Figure 4.29 Geometry of recessed beam end.

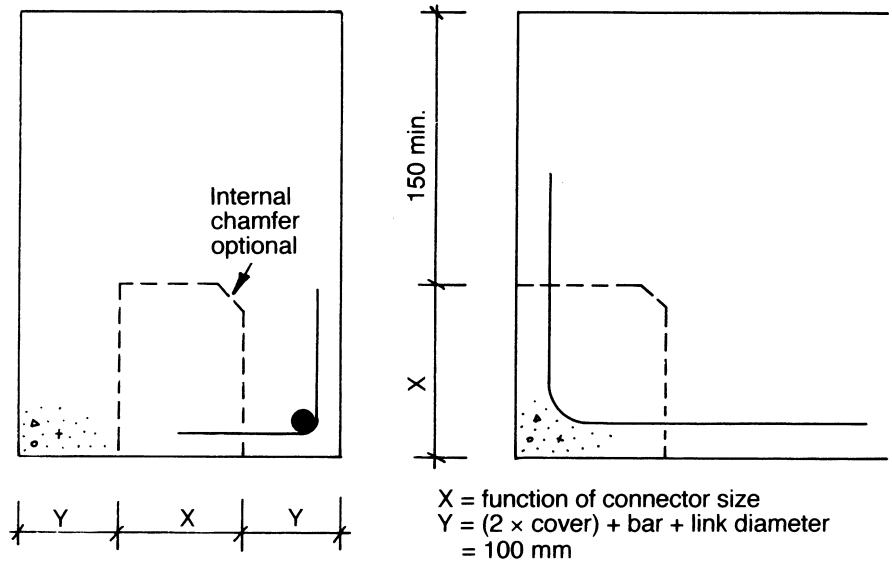

Figure 4.30 Geometry of pocketed beam end.

The inclination of the shear crack (α to the horizontal) propagating from the root depends on the relative magnitude of the shear and normal stress at that point. Remote from local stress concentrations, this ratio is a function of the reduced depth h' to the full depth h of the beam. Windisch [4.36] states that extensive linear elastic finite element analysis has shown that:

$$\alpha = 90h'/h \tag{4.29}$$

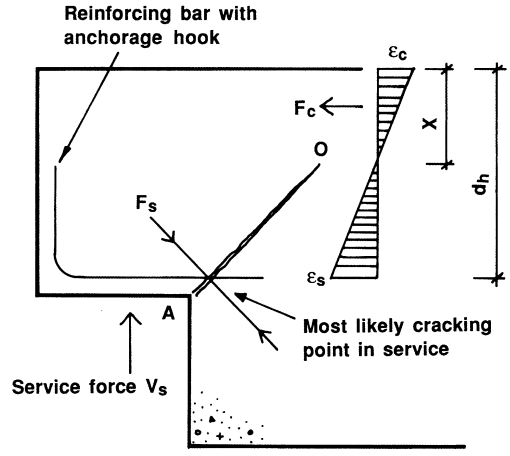

Figure 4.31 Strains in half joint.

in degrees, and that the strength of the diagonal bar placed at the root should be down-rated if the crack is not normal to the bar. In most cases the angular discrepancy will not be more than about 20°, such that the down-rating is only 10 per cent [4.36].

These types of joint are also subject to large stress concentrations in the vicinity of the bearing surface. In the beam end test shown in Figure 4.32, four H12 diagonal bars were provided to resist a vertical end shear force of 80 kN (service) and 125 kN (ultimate), together with one H12 U-bar to resist lateral bursting. The reinforcement cage is shown in Figure 4.32(a) and the grade of concrete was C32/40. The first sign of cracking was found at 90 kN, but it did not occur at the half-joint, as shown in Figure 4.32(b). Instead the cracks propagated from a point directly over the edge of the steel bearing plate, and occurred when the bearing stress was approximately 12 N/mm^2, or 0.33 f_{cu}. Figure 4.32(c) shows the ultimate test condition.

Noor and Elliott [4.37, 4.38] tested a range of precast concrete half-joints, reinforced using horizontal loops and vertical links, rather than using diagonal bars. In some tests short steel fibres (*Dramix* 50 mm long × 0.5 mm diameter at 0.5–1.5 per cent by volume) were used to replace some of the rebars and ease congestion. The steel fibres were able to control post-cracking behaviour and help the remaining rebars to develop full yield strength. Although cracking at the ultimate failure was extensive, as shown in Figure 4.33, the joint demonstrated adequate strength and ductility, such traditional equations for the ultimate strength based on the combined effects of reinforcement and steel fibres were able to predict failure loads with accuracy to ±10 per cent of the tests. Figure 4.34 shows a rebar cage at a precaster's works that has the same arrangement of loops and links as in Noor's work. However, the absence of diagonal bars in a half-joint is not common.

Plates cast into the beam are sized to ensure that the average bearing stress in the plate does not exceed 0.85 f_{cd} (See clause 10.9.5.2(2)) {0.6 f_{cu}}. In the more highly stressed situations reinforcement is sometimes welded to the plates to ensure that concrete in contact with the plate is confined. It is clear that the failure mode of these beams is affected by the width of the bearing plate, as the shear crack in the half-joint began above the edge of the bearing plate. Narrow plates will produce the type of failure shown in Figure 4.35. Cracks above the end plate will propagate rapidly into shear cracks in the sides of the beam.

In the test the ultimate limit state was reached following yielding of the links directly above the recess. The average failure shear stress in the beam was 1.20 N/mm^2 in the main body of the beam and 1.75 N/mm^2 in the half-joint.

The width of the bearing plate b_p in the beam should not be greater than 0.4b [4.16], to avoid punching through the concrete above the plate, and should also be less than (b − 100) mm to give adequate cover, with tolerances, to the sides of the beam. In most cases $b_p = b/3$. The thickness of the

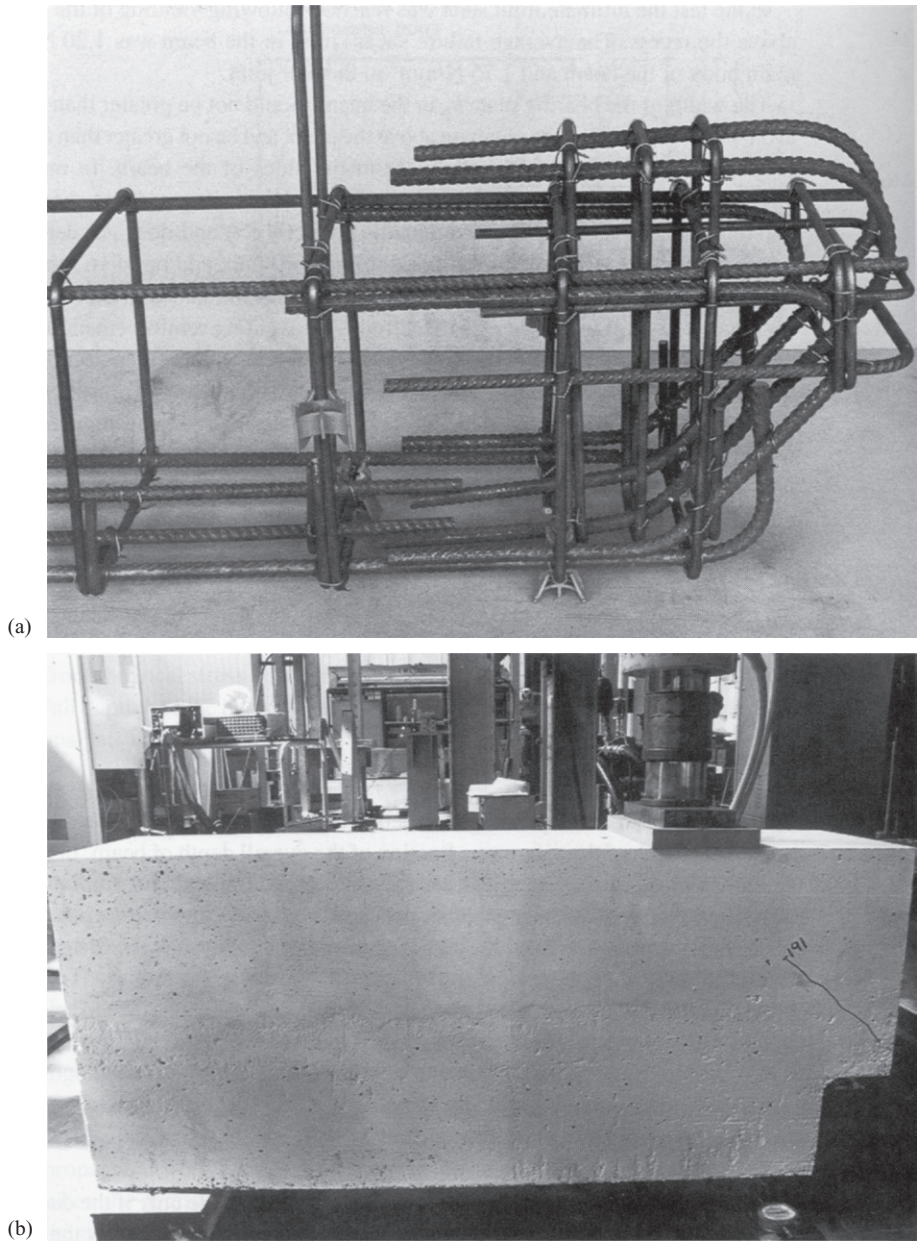

(a)

(b)

Figure 4.32 Beam end shear test. (a) Reinforcement cage; (b) first crack at 90 kN end reaction; (c) ultimate failure at 180 kN end reaction (design value = 125 kN).

plate is determined from its punching shear and lateral bursting capacity, so that the plate remains perfectly flat and does not deform over the bearing point. Plate thickness is at least 8 mm to 10 mm, and up to 16 mm in the more heavily loaded connections (>250 kN). In most cases mild steel grade S275 {43} or S355 {50} is used for the plate and grade E43 or E51 electrodes for welding reinforcement to it.

The end cover to the edge of the plate should not be greater than 25 mm, with some designers preferring to take the plates to the end of the beam to prevent spalling. The stress distribution over

(c)

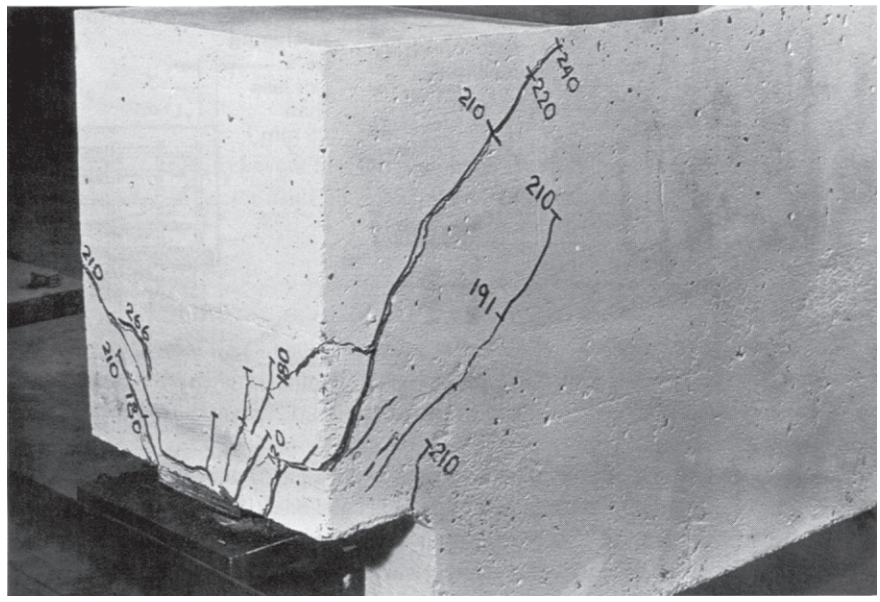

Figure 4.32 (*Continued*)

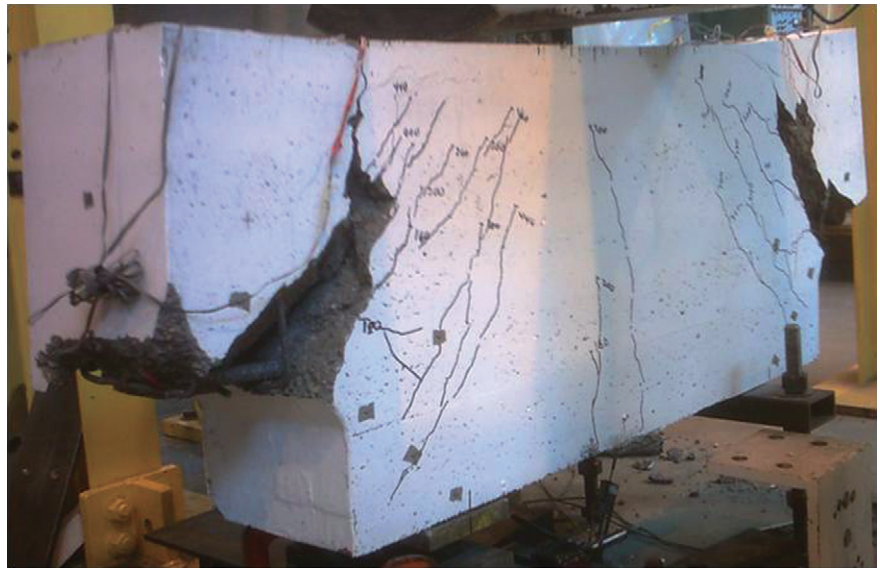

Figure 4.33 Ultimate failure of precast beam half-joint reinforced with horizontal loops, and in some cases adding steel fibres.

the surface of the plate is assumed to be triangular (trapezoidal would be nearer the reality) and therefore the resultant of the force V acts at a distance $b_1/3 + 25$ mm (end cover distance) from the end of the beam. Cumulative deviations in manufacture and erection will give the most onerous eccentricity, and therefore the gap between beam and column should be increased by the possible site-fixing tolerances at each end. Thus the total eccentricity from the face of the column may be calculated. In practice, dimensional accuracy for precast beams (particularly those cast in steel moulds) is much better than the values quoted in BS 8110, Part 1, clause 5.2.4 [4.5] of 3 mm per metre distance between supports.

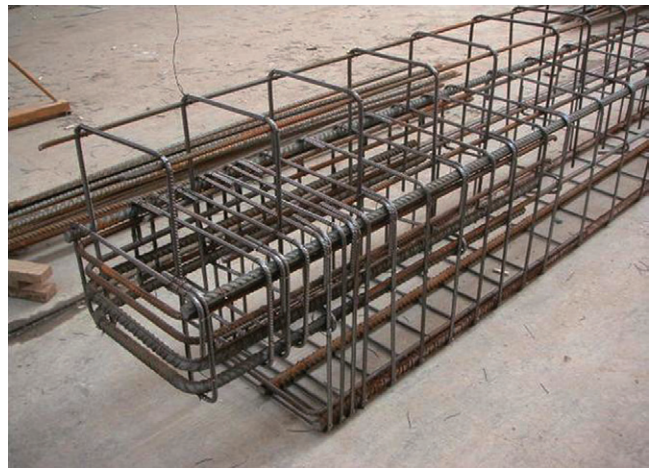

Figure 4.34 Alternative reinforcement for beam half-joint using horizontal loops instead of diagonal bars.

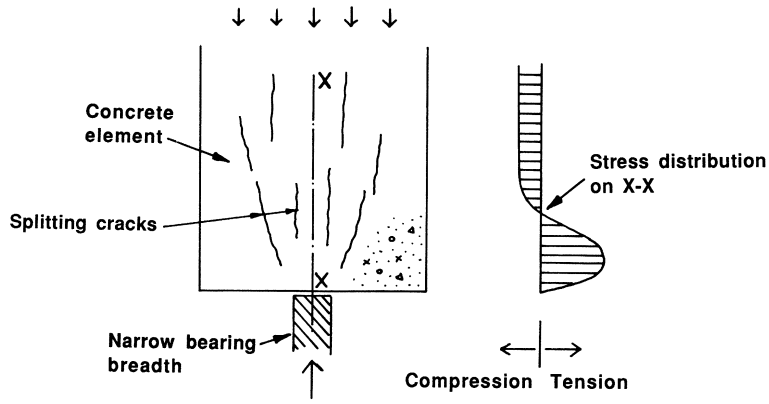

Figure 4.35 Narrow plate beam failure.

4.3.10 Design methods for end shear

Two methods are used, depending on whether the end of the beam is recessed or pocketed, and on the depth of the recess as a fraction of the overall depth of beam. In both cases truss action develops in the beam and adequate shear friction and shear bond anchorage are provided either mechanically or physically. Reinforcement normal to the potential cracking plane provides the normal force required to maintain the ultimate shear resistance by shear friction.

Although two different shear transfer mechanisms exist and may be analysed separately, it is common practice to add the shear resistances in the following:

- vertical links and compressive struts
- diagonal bars,

to obtain the total ultimate shear capacity. This is permissible only if the ductility factors for high-tensile bars are not exceeded, i.e. the shear capacity obtained by the two different methods does not differ by more than about 40 per cent in favour of the diagonal bars. This is the most economical solution, because it is necessary to include the vertical links over the bearing surface in order to mobilise the forces in the anti-bursting bars in this region.

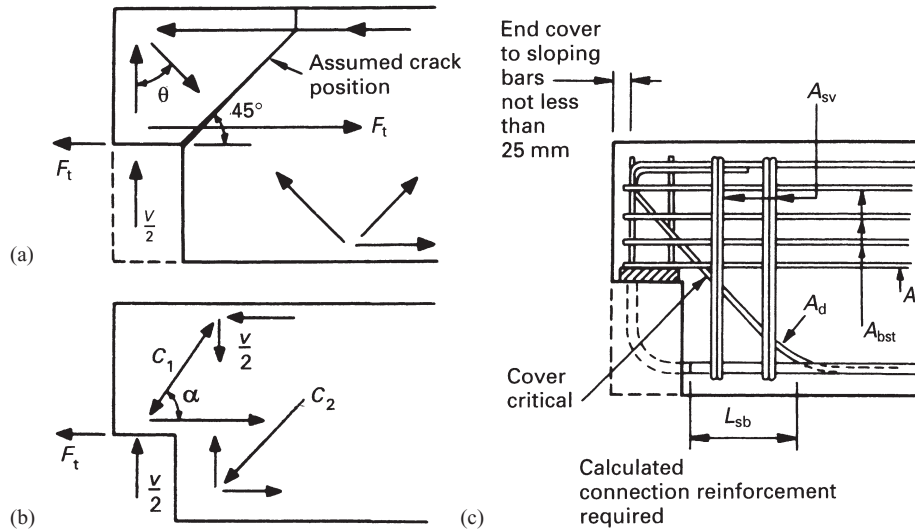

Figure 4.36 Structural action and typical reinforcement arrangements. (a) Truss action in half joint with deep pocket [4.16]; (b) truss action in half joint with shallow pocket [4.16]; (c) reinforcement positions.

The best way of dealing with this problem is first to calculate the steel requirements for lateral bursting, which has to be provided in all cases, and then to calculate the vertical shear resistance of the vertical links placed above the bearing surface. The remaining reaction force, which should not be greater than $0.5V$ (because bent-up bars should not be used to carry more than 50 per cent of shear forces) may then be carried by the diagonal bars.

Figure 4.36(a) [4.16] shows the first of the two structural models and typical details for this connection, where the recess is about one-half of the total depth. The breadth of the beam is b, the effective depth of the beam is d, and the reduced effective depth is d_h.

The first task is to check that the bearing stress between the beam and the bearing surface does not exceed $0.6\ (1 - f_{ck}/250)\ f_{ck}/1.5$ $\{0.85\ f_{cu}\}$. Bearing stresses $f_{Ed} = V_{Ed}/b_p\ b_l$ $\{f_b = V/b_p\ b_l\}$ are calculated in accordance with the recommendations given later in Section 7.6 and BS EN 1992-1-1, clause 10.9.5.2 [4.4] {BS 8110, Part 1, clause 5.2.3.4 [4.5]}. The assumption is that the distribution of bearing stresses is trapezoidal, such that the maximum ultimate stress is approximately equal to $0.8\ f_{ck}$ $\{f_{cu}\}$. If $f_b > 0.85\ f_{cd}$ $\{0.6\ f_{cu}\}$, a steel bearing plate is provided and the concrete in contact with the plate is confined, where an ultimate stress of $\sigma_c \leq 0.85\ f_{ck}\ S_q$, where S_q is a confinement factor – see Eq. (7.15) $\{0.8\ f_{cu}\ S_q\}$ may be used in contact with the plate. The plate is fully bonded to the beam by virtue of tie bars welded to the inside surface of the plate. The thickness of the plate is determined from two factors:

- tensile force T in the tie bars
- punching shear capacity of the plate, but only if the width of the plate is greater than the width of the bearing, otherwise the force is transferred directly through the plate.

If $f_b < 0.85\ f_{cd}\ (1 - f_{ck}/250)\ f_{ck}/1.5$ $\{0.6\ f_{cu}\}$, the concrete beam may be bedded directly onto a felt, neoprene (or similar) pad, of 10 mm minimum thickness, and covering the whole of the bearing surface. This is to allow small rotations, in the order of 0.001 radians, to take place without causing damage to the edges of the bearings.

The second task is to check that the shear stress in the recessed section of the beam does not exceed $0.5\ v\ f_{cd}$ (clause 6.2.2(6)) $\{0.8\sqrt{f_{cu}}\}$, e.g. for C32/40 concrete $t = 5.58$ and $\{5.05\}$ N/mm^2, respectively. This is to ensure that the section will not fail by shear, even though reinforcement is providing the entire shear resistance.

When a precast concrete beam is positioned firmly onto a bearing surface, axial deformations in the beam will induce axial tension or compression at the point of contact. This is due to the fact that the beam cannot slide on the bearing until the frictional force is overcome. The axial strain required to induce the frictional force is quite small, in the order of 50 με for most types of precast components. Thus a horizontal frictional force $T = \mu V$ is generated over the bearing at the interface, where μ = shear friction coefficient, as follows:

- 0.7 for plain concrete-to-concrete surfaces
- 0.4 for steel-to-concrete surfaces
- 0.4 for steel-to-steel surfaces.

The reinforcement A_h required to provide this force is given by:

$$A_h = \frac{mV}{0.87 f_y} \tag{4.30}$$

In the (rather unlikely) event that the peripheral stability tie force F_t(see Chapter 9) is carried by the connector itself, then A_h should be increased to:

$$A_h = \frac{mV + F_t}{0.87 f_y} \tag{4.31}$$

At least two mild steel bars should be used to provide A_h and they should preferably be welded to the bearing plate, as it is unlikely that full anchorage would be achieved by other means. If no plate is required, a single bar should be formed into a U-shape and placed directly over the bearing with 15 mm to 20 mm cover. The size of this bar should not be greater than 25 mm diameter in order to achieve the correct position. It is important that the internal radius of the bend should be checked for bursting forces. If more than one bar is required, the vertical separation distance should not exceed 50 mm.

Although codes of practice do not require the steel A_h to carry flexural forces, they will undoubtedly exist if the nib is long, say, greater than one effective depth. It is therefore worth checking that the bars provided will resist any bending moment at the root of the nib.

According to BS EN 1992-1-1, clause 8.3(3), Eq. 8.1 [4.4] {BS 8110 (Part 1, Eq. 50) [4.5]} the internal radius r of a bar of diameter Φ that extends for more than 4 {5} diameters beyond the point at which it is required to resist the full force F_{bt} at the start of the bend is given by:

$$r = \frac{F_{bt}\left(\frac{1}{a_b} + \frac{1}{2\Phi}\right)}{2 f_{cd}} \quad \left\{ r = \frac{F_{bt}(1 + 2(\Phi / a_b))}{2 f_{cu} \Phi} \right\} \tag{4.32}$$

where a_b = the distance from the edge bar centre to the nearest free surface, i.e. cover plus $\Phi/2$, or half of the centre–centre distance between bars {BS 8110 is cover plus Φ, or the centre–centre distance between bars}.

Cover to the end of the beam and to the internal root of the recess should be not less than 25 mm. The area of diagonal bars A_d is given by:

$$A_d = \frac{0.5V \sec\theta}{0.87 f_y} \tag{4.33}$$

where θ is usually 40° to 45°.

If truss action is to develop, these bars must be fully anchored in both the top and bottom of the beam. The bend at the top is usually 135° and so the bending radius must not be contravened, because

the concrete is already in a 'high-risk' zone and localised effects must not be allowed to exacerbate the situation. For this reason, H25 bars are considered to be the largest practical bar size for A_d. The diagonal bar must continue a full anchorage length from the root of the recess. The cover to this bar is critical, 25 to 30 mm being the correct cover to use. A small triangular chamfer, say 25 × 25 mm, is often used to reduce the possibility of cracks developing at the internal corner.

The remaining $0.5V$ is carried by the first diagonal compressive strut, assumed to be inclined at α to the horizontal. The compression in the strut is:

$$C_1 = 0.5V\text{cosec}\,\alpha \tag{4.34}$$

The limiting compressive force in this strut is given by:

$$C_1 = 0.85 f_{ck} b 0.45 d_h \cos\alpha \quad \{C_1 = 0.8 f_{cu} b 0.5 d_h \cos\alpha\} \tag{4.35}$$

as shown in Figure 4.36(b). This ensures that not too much of the effective depth is in compression. If the compression is exceeded, two courses of action are possible:

- either the depth of the recess is reduced, or d_h is increased, or
- the 40 per cent ductility allowance is called upon and the proportion of the force carried by the compressive strut is reduced to $0.42V$ (with a corresponding increase in the force carried by the diagonal bars to $0.58V$).

The bursting force T is given in BS EN 1992-1-1, clause 6.5.3(3) [4.4], Eq. 6.58 as

$$\varsigma = T/H = 0.25(b-a)/a$$

The values are reproduced here in Table 4.11(a). Linear interpolation is used. These values are about 25 per cent lower than in BS 8110.

The vertical force V gives rise to a lateral horizontal bursting force H_{bst} across the end of the beam, which may be obtained from BS 8110, Part 1, Table 4.7 'end block' theory – the most appropriate method [4.5]. Thus $H_{bst} = \varsigma V$, where ς is the bursting force coefficient, typically 0.20 to 0.23 for $b_p/b = 0.2$ to 0.4. The BS table is reproduced here in Table 4.11(b). Linear interpolation is used.

The derivation of the above data may be seen from Figure 4.37, where the dispersal of forces away from a bearing plate may be given by the resolution of the triangulation of forces. If the angle subtended to the direction of load is given by:

$$\theta = \frac{\sqrt{2}}{4}\frac{b-b_p}{0.4b}, \tag{4.36}$$

the tensile bursting force coefficient ς between two such struts is given by:

$$\varsigma = \frac{\theta}{2\sqrt{2}} = 0.312\left(1-\frac{b_p}{b}\right) \tag{4.37}$$

Table 4.11(a) Bursting force coefficients to BS EN 1992-1-1 (code uses a/b instead of b_p/b).

b_p/b	0.3	0.4	0.5	0.6	0.7
ς	0.175	0.15	0.125	0.10	0.075

Table 4.11(b) Bursting force coefficients to BS 8110 (code uses y_{po}/y_o instead of b_p/b)

b_p/b	0.3	0.4	0.5	0.6	0.7
ς	0.23	0.20	0.17	0.14	0.11

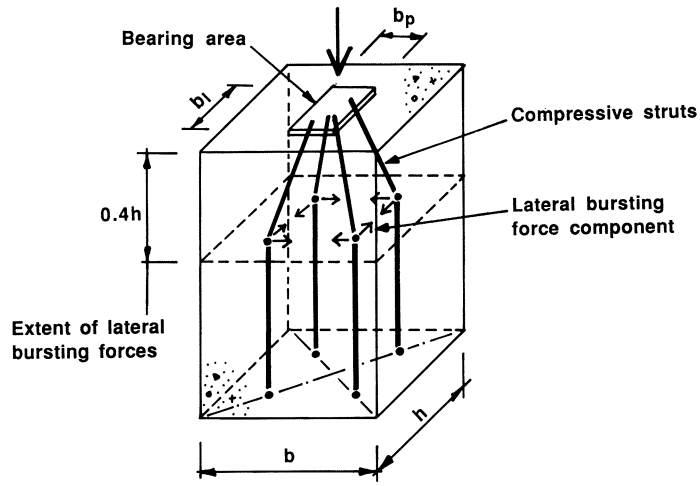

Figure 4.37 Dispersal of forces above bearing plates.

The results, which are given in Table 4.12, are in better agreement with BS 8110 than in BS EN 1992-1-1.

In the beam end, horizontal hairpins are provided such that:

$$A_{bst} = \frac{H_{bst}}{0.87 f_y} \tag{4.38}$$

across the end face of the beam.

PCI recommendations [4.2] give $A_{bst} = A_h/2$, and here the result is about the same as carrying out the above analysis. Part of this steel may form part of the U-bars provided for A_h above. However, whereas A_h need only be provided directly above the bearing, bursting steel must be positioned over the full height of the end of the beam. Thus at least two, and preferably three, hairpin bars should be provided. H8 or H10 rebars at 50 mm centres are the norm. The bars should extend across the full face of the beam and enclose any vertical bars. The anchorage length, which is standard, should start at 25 mm beyond the face of the recess. Two or three vertical stirrups should be used to support the hairpins over the top of the bearing plate. The area of vertical bar in each face should be not less than A_{bst}.

The horizontal component of the force taken by bars A_d is given by $H = 0.5\ V \tan\theta$. This is a compressive force in the top of the beam. The horizontal component of the force, C_1 is $H = C_1 \cos\alpha$. The steel required for the total H is given by:

$$A'_s = \frac{H}{0.87 f_y} \tag{4.39}$$

The bars providing A'_s must not be less than the minimum percentage steel for concrete in compression, and they must be surrounded by links up to the end of the beam in order to be fully effective. The bars should extend to within a cover distance from the end of the beam and be lapped to the diagonal bars a distance equal to 1.4 times the basic lap length. Occasionally the top bars are welded to the first vertical link to provide the necessary anchorage at the end of the cage.

To complete the shear cage, the first full-depth vertical links A_{sv1} designed using the truss action, shown in Figure 4.36(a), should be placed at one cover distance from the inside face of the recess. The area of the links is:

$$A_{sv1} = \frac{0.5V}{0.87 f_y} \tag{4.40}$$

Note that the concrete shear stress v_c is ignored.

Table 4.12 Bursting force coefficients using strut-and-tie methods

b_p/b	0.3	0.4	0.5	0.6	0.7
ς	0.22	0.19	0.16	0.13	0.09

It is likely that pairs of links are required. The links should *enclose* the diagonal bars A_d, the hairpin bars A_{bst} and the tie bars A_h. Although in theory the full vertical shear resistance of the section does not depend entirely on these first links, they are nevertheless provided to ensure the gradual transfer of shear from the truss to stirrup actions.

The vertical force in these links is equilibrated by a second compressive strut C_2, inclined at 45° to the horizontal, where:

$$C_2 = 0.5V\text{cosec}\,45° \tag{4.41}$$

The limiting compressive strut stress is $0.6(1 - f_{ck}/250)(f_{ck}/1.5)$, using clause 6.5.2, Eq. 6.56 $\{0.4\,f_{cu}\}$ acting over a depth of $0.6d$ $\{0.5d\}$.

The limiting value of C_2 is given by:

$$C_2 = 0.45 f_{ck} b 0.6d \cos 45° \quad \{C_2 = 0.4 f_{cu} b 0.5d \cos 45°\} \tag{4.42}$$

As before, the horizontal component of the force at the bottom end of A_d produces a tension $H = 0.5V \tan\theta$. In addition to this the horizontal component of the force C_2 is $H = C_2 \cos 45°$. The steel required for the total H is given by:

$$A_s = \frac{H}{0.87 f_y} \tag{4.43}$$

The bars providing A_s are, of course, the same bars as used in the curtailment of flexural steel.

Finally, where the diagonal bar meets the bottom steel a second set of links A_{sv2} should be provided to carry the full shear force V within the nodal distance L_{sb}, so that:

$$A_{sv2} = \frac{V}{0.87 f_y} \tag{4.44}$$

Note that the nodal distance L_{sb} is much less than that which would be calculated by applying anchorage bond stresses. This is because it is assumed that the force is transferred not only by bond, but also by friction between the links, which are tied tightly to the inclined bar. Beyond L_{sb}, the development of shear resistance is subsequently catered for by the links and concrete according to BS EN 1992-1-1, clause 6.2.3(3) [4.4] {BS 8110, Part 1, clause 3.4.5 [4.5]}.

Where the recess is smaller, about one-third of the depth, a diagonal compressive strut develops alone instead of the tension tie above. Figure 4.36(b) shows the structural model for this second case. Note the differences compared to Figure 4.36(a). The similarities are that horizontal hairpin bars are placed directly over the top of the pocket as a restraint against lateral bursting forces F_{bst}. The bars are held in position by an equal amount of fully anchored vertical steel. They form the basis of the shear reinforcement cage, in which the spacing of the links is gradually increased as in normal reinforced concrete design.

The main differences with the previous case are that the net depth of concrete above the bearing surface is sufficiently large to enable a compressive diagonal strut $C_3 = V\,\text{cosec}\,\alpha$ to form. Here α depends on the geometry of the recess, and is usually about 60–70°. The simple resolution of forces enables the reinforcement of areas A'_s, A_h, A_{bst}, A_{sv} and A_s to be determined as before. Here the longitudinal bars A_h carry an additional force to the previous case, the horizontal component of the diagonal force $V \sec\alpha$. Thus, if the peripheral tie force F_t is included, then:

$$A_h = \frac{\mu V + F_t + V\cot\alpha}{0.87 f_y} \tag{4.45}$$

Proper anchorage is required to carry the forces in the diagonal truss member by ensuring that the forces in the horizontal steel A_h are fully active. This means that the end of the horizontal bar A_h may have to be welded to the inside of the bearing plate or fully anchored, as discussed above. The remote end of the bar enters into an area of compression, as shown in Figure 4.36(a).

Cook [4.30, 4.39] developed a non-linear finite element program called 'FIELDS', which uses compression field theory to study the strut-and-tie action in these and similar types of joint, i.e. corbels (see Figure 4.28). The dashed lines represent principal stress trajectories. Full-scale testing on precast beams with deep recessed ends, i.e. 350 mm in a total beam depth of 600 mm, has verified the computational work and shows that reinforcing beams using the strut-and-tie analogy gives conservative estimates of the ultimate shear resistance. Factors of safety against ACI code equations are about 1.2, but the failures occur in a very ductile manner.

A detailing problem occurs at the end of the beam for the bars marked A_h in Figure 4.36(c), where proper anchorage is required. The first link (from the end of the beam) will be displaced beyond its effective position because of the radius of the hook required to anchor the reinforcement A_h at the end of the recess. There are two possible solutions to this:

- to weld an anchor plate or angle to the end of the main steel, as shown in Figure 4.36(c). This would require fire protection as is drawn here; or
- to provide an additional straight bar in the corner of the cage for the sole purpose of providing a link hanger. This bar would be additional to the curtailment requirements for the main longitudinal reinforcement, and is a less popular option in congested cages.

4.3.11 Hanging shear cages for wide beams

The analysis considered in Section 4.3.10 is used in narrow beam design, where it is not possible to carry the end shear forces in the plane of the connection. In wider beams, as shown in Figure 4.38, where the net cross section of concrete at point B is sufficient to carry the shear force, hanger steel may be used to transfer the end reaction from A to B. In this case the diagonal bars A_d in Figure 4.36(c) are replaced with hanger bars A_{dd}. The most important section occurs in inverted-tee beams, where the breadth of concrete at section z–z in the figure is small, i.e. less than 150 mm. Referring to Figure 4.38, the area of hanger steel is given by:

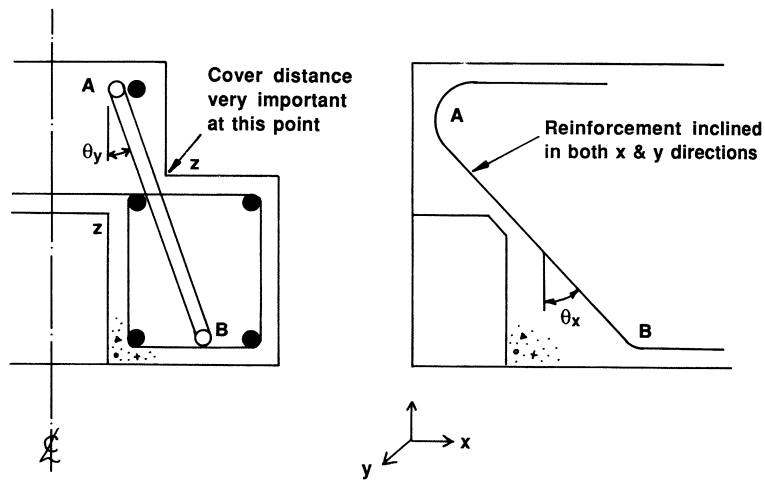

Figure 4.38 Hanger reinforcement in wide pocketed end beam.

$$A_{dd} = \frac{V}{0.87 f_y \cos\theta_x \cos\theta_y} \tag{4.46}$$

where θ_x and θ_y are the inclination of the bar to the vertical in the x and y planes. Bars inclined to both axes are *extremely* difficult to bend, particularly where accuracy is very important, as is the case here. Ideally the hanger bar(s) should be vertical in the y plane for ease of cage manufacture.

In practice this reinforcing method may be used only in pocketed beams where the breadth of the beam either side of the pocket is at least 200 to 300 mm, depending on the shear force. Thus the overall breadth of the beam is likely to be at least 600 mm.

Exercise 4.5 Beam end shear design

Beam end shear reinforcement is required in a 10.0 m long × 600 mm deep by 300 mm wide beam to carry an ultimate shear force of 200 kN. The shape of the end of the beam is to be recessed across the full width of the beam to a depth of 200 mm and length 130 mm. A steel bearing plate is to be used in the horizontal bearing surface. The width of the supporting steel billet is 80 mm.

Given the following data, design the end shear reinforcement and bearing plate. The peripheral tie force is taken care of elsewhere. Use concrete grade C32/40, f_{yk} {f_y} = 500 N/mm^2, f_{yk} {f_y} = 250 N/mm^2 for welded bars, p_{yk} {p_y} for plate = 275 N/mm^2 for Grade 43 steel, f_{ydw} = 275/1.25 = 220 N/mm^2, see Table 7.12 {f_{weld} = 215 N/mm^2} for 6 mm CFW. Cover to links = 25 mm. Allow an end tolerance for factory positioning the plate = 10 mm.

Solution

Step 1: Bearing plate width

$b/3 \le b_p \le b - 100$ mm or $0.4\,b$

Try $b_p = 100$ mm

To determine S_q try $b_l = 80$ mm.
Resistance width = 100 + 2 × 100 either side = 300 mm.
Resistance length = 80 + 0 at end of beam + 80 = 160 mm.

$$S_q = \sqrt{\frac{300 \times 160}{100 \times 80}} = 2.45 < 3$$

A steel plate design ultimate average bearing stress = $0.567 f_{ck} S_q$ = 44.4 N/mm^2

$$b_l > \frac{200 \times 10^3}{100 \times 44.4} = 45.0 \text{ mm}$$

Allow 10 mm end tolerance as given, plus (See clause 10.9.5.2) Δa_3 = 10 000/2500 = 4 mm
(See Table 10.5) Δa_2 = 10 mm
$b_l \ge 45 + 10 + 4 + 10 = 69$ mm
Try 80 mm as a minimum < 130 available
Effective plate bearing length, = 80 − 24 = 56 mm

A steel plate design ultimate average bearing stress = 0.8 f_{cu} = 32 N/mm^2

$$b_l > \frac{200 \times 10^3}{100 \times 32} = 62.5 \text{ mm}$$

Allow 10 mm end tolerance as given, plus a further 10 mm fixing tolerance.

$b_l \ge 62.5 + 10 + 10 = 82.5$ mm
Try 90 mm < 130 available
Effective plate bearing length = 90 − 20 = 70 mm

Step 2: Plate thickness

The plate is subjected to an axial tension force = $\mu V = 0.4 \times 200 = 80$ kN

Cross-sectional area of plate $= \frac{80 \times 10^3}{275} = 291 \text{ mm}^2$, so $t > \frac{291}{100} = 2.9$ mm

The plate is also subjected to double shear of design stress 0.6 p_{yk} {0.6 p_y} from the steel billet.

$t > \dfrac{200\times10^3}{2\times0.6\times275\times56}$	$= 10.8\,\text{mm}$
Total $t > 2.9 + 10.8$	$= 13.7\,\text{mm}$
>12 mm preferred, therefore increase b_l to 90 mm, and effective $b_l = 66$, such that $t = 2.9 + 9.2$	$= 12.1\,\text{mm}$
Use $100 \times 90 \times 12$ plate	

$t > \dfrac{200\times10^3}{2\times0.6\times275\times70}$	$= 8.7\,\text{mm}$
Total $t > 2.9 + 8.7$	$= 11.6\,\text{mm}$
Use $100 \times 90 \times 12$ plate	

Step 3: Reinforcement

Using the compressive strut-and-tensile-tie analogy, shown in Figures 4.36(b) and 4.39(a), it is first necessary to determine the angle θ of the primary strut C_1 . From Figure 4.39(a), assuming 8 mm links, 12 mm top bars and 20 mm bars welded to the plate, $d = 400 - 25 - 8 - 12/2 - 12 - 20/2 = 339$ mm, and the reaction point at ½ plate length $a_v = 130 + 25 + 8/2 - 90/2 = 114$ mm. $\theta = \tan^{-1}(114/339) = 18.6°$.

Compressive strut force $C_1 = V/\cos\theta = 200/0.948 = 211.0$ kN.

The width of the compressive strut w_1 must be checked to ensure that it does not extend beyond the end of the beam. The depth of the compressive block is also limited to $0.6d_h$ {$0.5d_h$}, where d_h is the effective depth to the horizontal tie bars attached to the plate. Referring to Figure 4.39(a), $d_h = 400 - 12 - 20/2 = 378$ mm.

Hence the maximum value of w_1 $= 0.6 \times 378 \times \sin\theta$	$= 72.3\,\text{mm}$
The actual value of w_1 is given by limiting the concrete stress to $0.6(1 - f_{ck}/250)\, f_{ck}/1.5 = 11.16\,\text{N/mm}^2$	
$w_1 > \dfrac{211.0\times10^3}{300\times11.16} =$	$= 63\,\text{mm} < 72.3$

Hence the maximum value of w_1 $= 0.5 \times 378 \times \sin\theta$	$= 60.3\,\text{mm}$
The actual value of w_1 is given by limiting the concrete stress to $0.4f_{cu} = 16.0\,\text{N/mm}^2$	
$w_1 > \dfrac{211.0\times10^3}{300\times16.0}$	$= 44.0\,\text{mm} < 60.3$

The effect of the reaction creates two types of tensile force. The first is a lateral bursting force across the end of the beam and is a function of the width of the plate divided by the width of the beam, i.e. end block theory mentioned in the text.

Using $b_p/b = 0.33$ (see Table 4.11b), the bursting force is given by	
$F_{bst} = 0.167 \times 200$	$= 33.3\,\text{kN}$
and the area of the horizontal bars to resist this force is:	
$A_{bst} = \dfrac{33.3\times10^3}{0.87\times500}$	$= 77\,\text{mm}^2$

Using $b_p/b = 0.33$ (see Table 4.11a), the bursting force is given by	
$F_{bst} = 0.22 \times 200$	$= 44\,\text{kN}$
and the area of the horizontal bars to resist this force is:	
$A_{bst} = \dfrac{44\times10^3}{0.87\times500}$	$= 101\,\text{mm}^2$

Use two H8 bars at 100 mm centres, i.e. within the lower half of the end face of the beam. Also provide 77 mm^2 {101 mm^2} of vertical links above the plate; use two H12 links (diameter to be same as main links later).

The second force is a longitudinal tie force as given by $F_h = \mu V + V\tan\theta = (\mu + \tan\theta)\, V$.

Thus: $F_h = (0.4 + 0.336) \times 200 = 147.3$ kN

The horizontal bar is welded to the steel plate using a strength f_y {f_{yk}} = 250 N/mm^2, even though a high-tensile bar is used.

$$A_h = \frac{147.3\times10^3}{0.87\times250} = 667\ \text{mm}^2$$

Use two R25 bars welded to the plate using electrodes Grade E43.

The bars must have a bond length of 40 {35} diameters = 1000 mm {875 mm} beyond the intersection node with compressive strut C_2. Because of the remoteness of the mid-span tension reinforcement, 1.5 times this is often provided.

(*Continued*)

The length of a 6 mm double-sided fillet weld required to resist the rebar force distributed equally between two bars is:

$$l_w = \frac{147.3\times10^3}{4\times6\times220} = 27.9\,\text{mm} \quad \Big| \quad l_w = \frac{147.3\times10^3}{4\times6\times215} = 28.5\,\text{mm}$$

plus 12 mm run-outs.

Use 50 mm weld length.

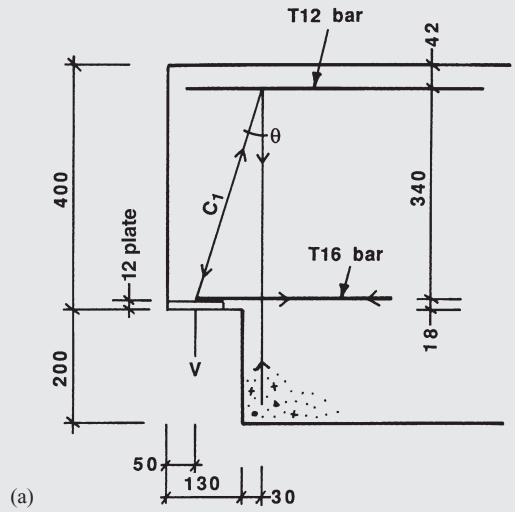

(a)

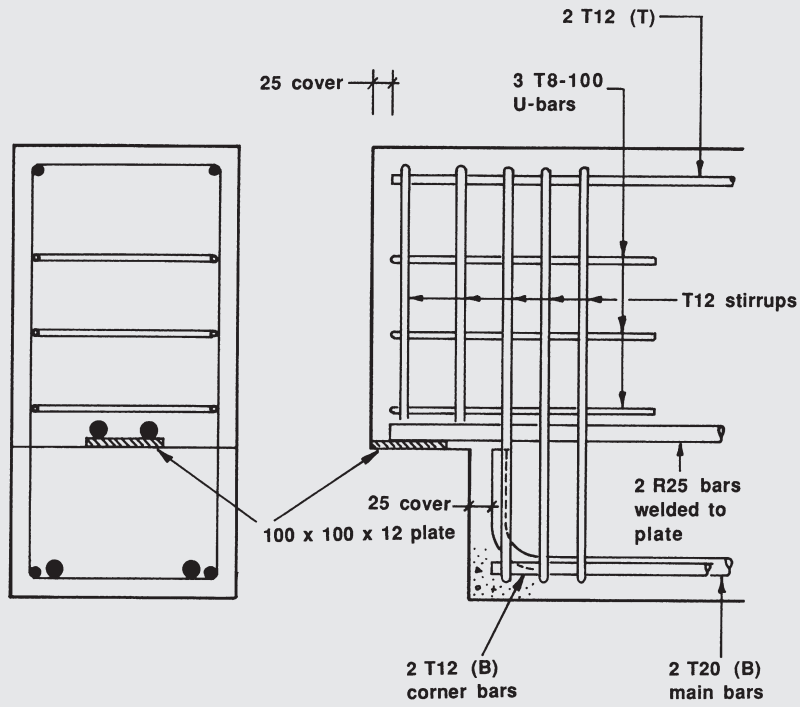

(b)

Figure 4.39 Details for Exercise 4.5. (a) Strut and tie forces used and (b) reinforcement cage.

The vertical force V in the stirrups gives $A_{sv} = \dfrac{200 \times 10^3}{0.87 \times 500} = 460\ \text{mm}^2$.

Use three H12 links at 50 mm centres, the first of which should be placed as close to the end of the beam as possible, i.e. one cover distance. This means that two additional longitudinal bars (say two H12 bars) must be placed in the bottom corners of the beam to carry the first stirrup.

The horizontal compressive force H in the top of the beam is:
$H = V \tan\theta = 200 \times 0.336 = 67.3\ \text{kN}$

$$A_s' = \frac{67.3 \times 10^3}{0.87 \times 500} = 155\ \text{mm}^2$$

Use two H12 bars.

Anchorage length of bar required from nodal point = 40 {35} × 12 = 480 mm {420 mm}, or length of bar from end of beam = 420 + 155 = 635 mm {575 mm}.

The maximum diagonal compressive force C_2 is given by $V/\sin 45° = 282.8\ \text{kN}$.

Using the same method as before to check confinement of the compressive strut, where $d = 550\ \text{mm}$

$w_{1,max} = 0.6 \times 550 \times \sin 45^\circ$	$= 233\ \text{mm}$	$w_{1,max} = 0.5 \times 550 \times \sin 45^\circ$	$= 194\ \text{mm}$
Actual width required $w_1 > \dfrac{282.8 \times 10^3}{300 \times 11.16}$	$= 84.5\ \text{mm}$	Actual width required $w_1 > \dfrac{282.8 \times 10^3}{300 \times 16.0}$	$= 58.9\ \text{mm}$

Figure 4.39(b) shows the reinforcement cage.

Finally the tension in the bottom of the beam is $T = V$ (because the compressive strut C_2 is assumed to act at 45°). Hence

$A_s = 460\ \text{mm}^2$

Use two H20 bars, with an internal radius of 60 {70} mm.

Anchorage length of bar from nodal point = 40 {35} × 20 = 800 mm {700 mm}. These bars should be properly anchored, either to a corner angle using a fillet weld designed as before (for direct tension), or the bars should be fully anchored using a standard end hook for simply supported beams. Note that the area of this steel may be increased owing to the curtailment requirements of the main flexural reinforcement.

Exercise 4.6

Repeat Exercise 4.5, but where the depth of the halving joint recess is increased from 200 mm to 350 mm.

Solution

The size of the bearing plate will be as before. The reduction in the half-joint depth will create diagonal tension across the face of the joint, as shown in Figure 4.36. The shear stress at this point is $v = 3.07\ \text{N/mm}^2$ and, when combined with the horizontal tensile stresses and the stress concentration at the sharp 90° corner, is surely going to cause a diagonal failure. One way of reducing the stress concentration is to chamfer the corner with a 45° 20 mm × 20 mm fillet.

Reinforcement

Referring to Figure 4.40, it is possible to place the diagonal bar at 45° to the direction of the force V to resist the diagonal force F_d resulting from $0.5V$. Hence:

$F_d = \dfrac{100}{\sin 45°} = 141.4\ \text{kN}$. From which $A_d = 325\ \text{mm}^2$.

(*Continued*)

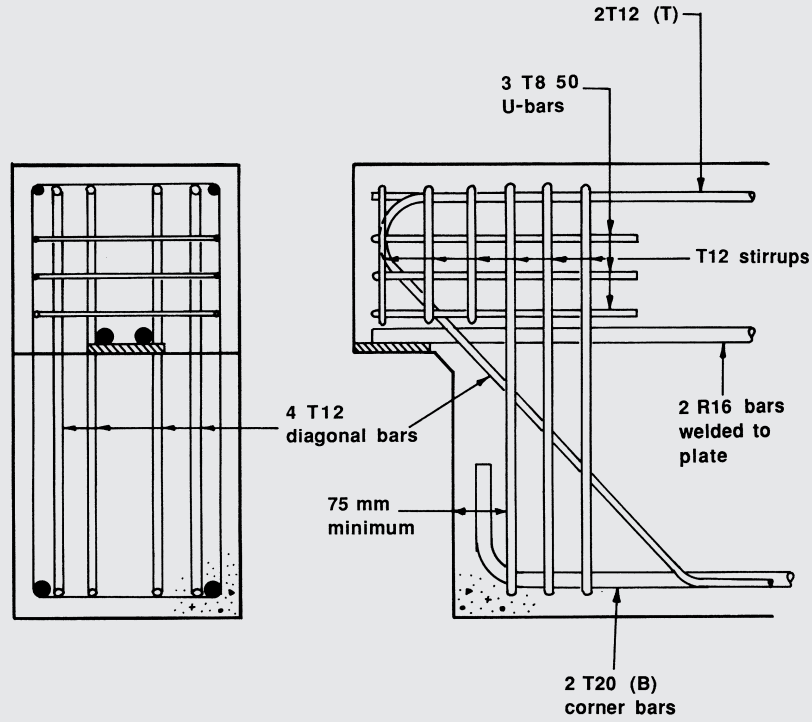

Figure 4.40 Diagonal reinforcement in half joint shear cage in Exercise 4.6.

The preference is to use bars that may be bent easily and will not violate the bearing stresses inside bends BS EN 1992-1-1, clause 8.3(3) [4.4] {BS 8110, Part 1, clause 3.12.8.25 [4.5]}). Therefore use four H12 bars, in preference to two H16 bars. To satisfy bearing stresses, where $F_{bt} = 141.4/4 = 35.4\,\text{kN}$ per bar, the internal bar radius should be greater than r obtained from:

$a_b = 58/2 = 29\,\text{mm}$, but less than
cover + $\phi/2 = 25 + 12 + 20 + 12/2 = 63\,\text{mm}$

$$r = \frac{35.4\times10^3(1/29+1/(2\times12))}{2\times32/1.5} = 63\,\text{mm}$$

Let r = 65 mm

$a_b = (300 - 2(25 + 12 + 20) - 12)/3 = 58\,\text{mm}$
less than cover + ϕ
$= 25 + 12 + 20 + 12 = 69\,\text{mm}$

$$r = \frac{35.4\times10^3(1+2(12/58))}{2\times40\times12} = 52\,\text{mm}$$

Let r = 55 mm.

The bars should be fully anchored a full bond length of 40 {35} × diameter = 480 mm {420 mm} from the corner of the halving joint or the nodal point, as shown in Figure 4.40.

The design for lateral bursting and vertical shear is as before. The design for longitudinal tie steel anchored to the plate is given by $F_h = \mu V$. Thus $A_h = \dfrac{0.4\times200\times10^3}{0.87\times250} = 368\,\text{mm}^2$.

Use two R20 bars welded to the plate in the same manner as before.

The weld leg length may be kept at 50 mm. Anchorage length = 800 mm {700 mm}. The bars are to be positioned on the inside of the outer diagonal bars.

4.3.12 Prefabricated shear boxes

An alternative to the reinforced shear cage is the so-called 'shear-box' approach, in which a solid plate, rectangular hollow section (RHS), or other structural steel section projects from the end of the beam (see Figures 4.41 to 4.43). Shear boxes are necessary in situations where the depth of the beam becomes prohibitively large because of the large amount of reinforcement required in the end cage. Depending upon the circumstances, a steel box section or two channel sections back to back can reduce the depth of the beam by 100 mm. This may be greater in L-shaped beams, where non-symmetrical boxes form part of the upstand. A typical RHS section size of $150 \times 100 \times 6$ (grade S275 {43} steel) will carry shear forces in the region of 250 kN. About 75 mm cover distance is required to the top of the insert, and links must pass over the top of the insert in order to carry tensile forces to the bottom of the beam. A minimum bearing length of 60 mm is recommended.

Design recommendations are based on adequate bearing stresses both in the plate and concrete beam, the prevention of spalling, bursting and splitting, and an adequate tie-back in the concrete beam. The ultimate shear capacity of the section is based on the shear capacity of the shear box itself, and is gradually transferred into the reinforced concrete beam. Tie back forces are distributed into the concrete beam by an appropriate concentration of vertical stirrups, by bent bars, or by welding a wide plate (or similar) to the bottom of the shear box.

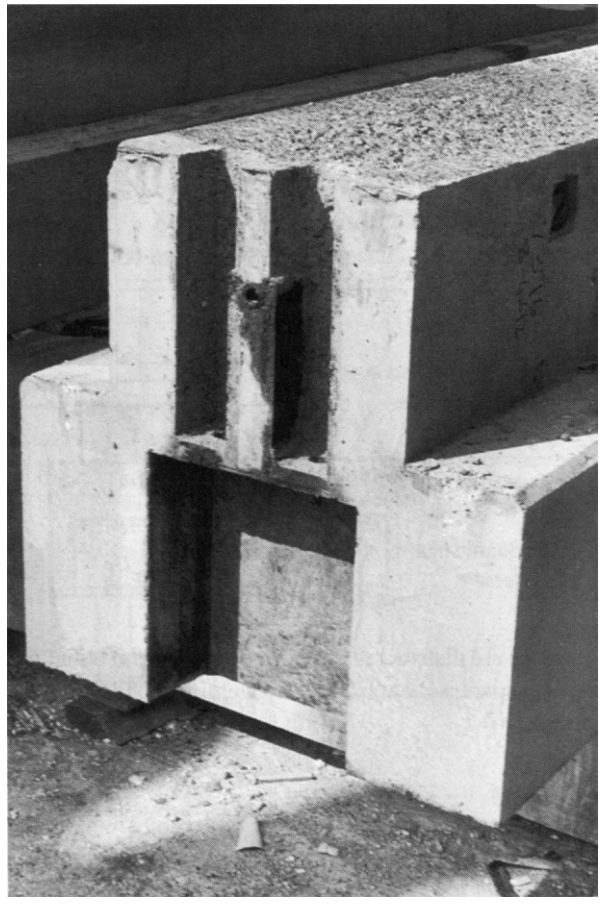

Figure 4.41 Photograph of a beam shear box.

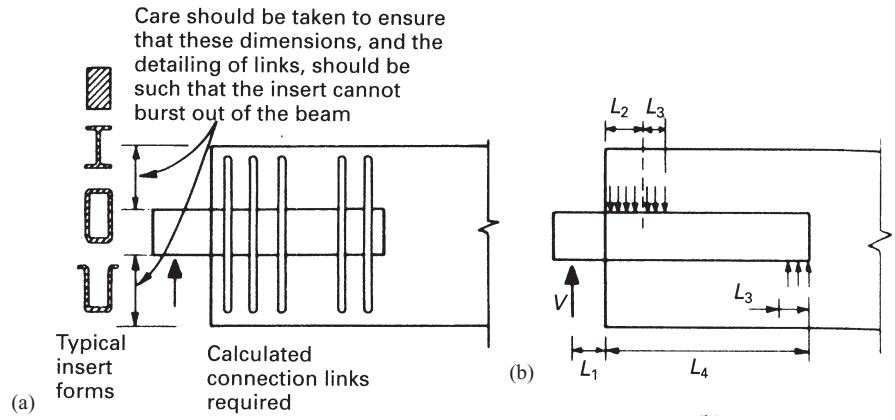

Figure 4.42 Prefabricated beam shear box design (taken from [4.16]).

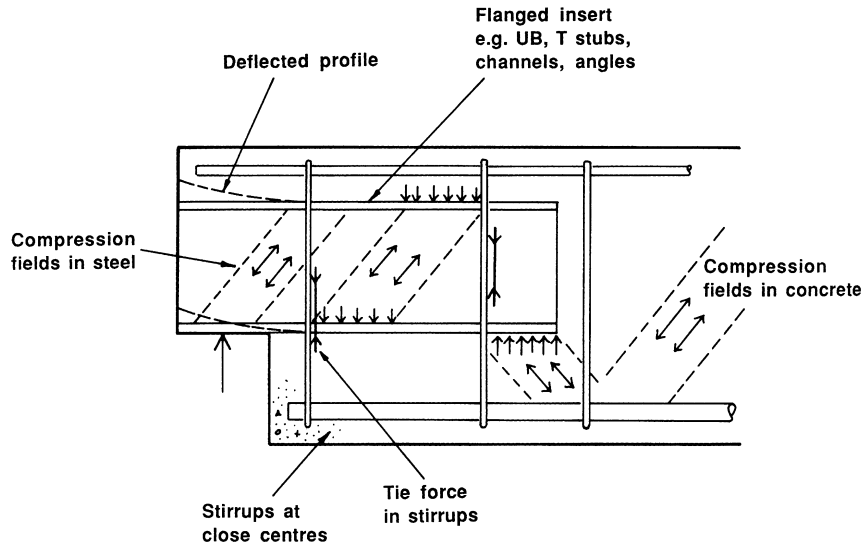

Figure 4.43 Beam shear box design principles.

4.3.12.1 Wide box design

The wide box design is based on three-point bending, and is therefore statically determinate. The section is completely filled with concrete and surrounded by reinforced concrete to prevent local wall buckling etc. The concrete is otherwise ignored up to a point near the end of the box where truss action takes over, as in a normal beam.

End reactions V are transferred to the box either directly, providing the local bearing stresses allow and the connection is stable in the temporary fixing condition, or through a flat plate welded to the bottom of the box. If the position of the box is near the top of the beam, i.e. less than 200 mm, the box is restrained vertically and prevented from bursting out of the top of the beam by a tension hanger in the form of plate strap reinforcement, as shown in Figure 4.44. The strap, which generates a force T, may consist of a bent plate, 6 mm thick × 50 mm to 100 mm wide depending on the required capacity, welded to a bottom bearing plate. A compressive strut force must be allowed to develop above the bottom plate acting at 45° to the horizontal. Thus the 'clearance' between the underside of

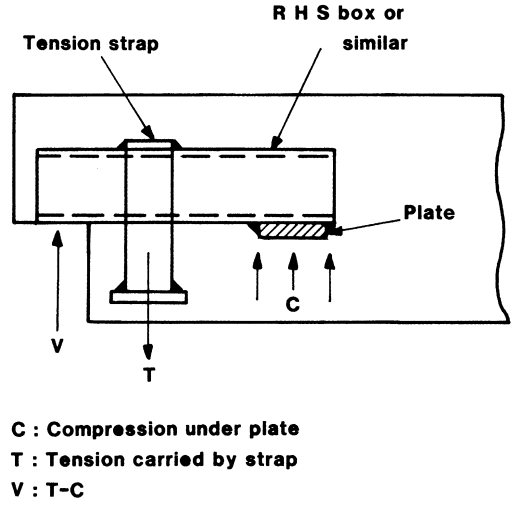

Figure 4.44 Beam shear box with additional steel plate strap hangers.

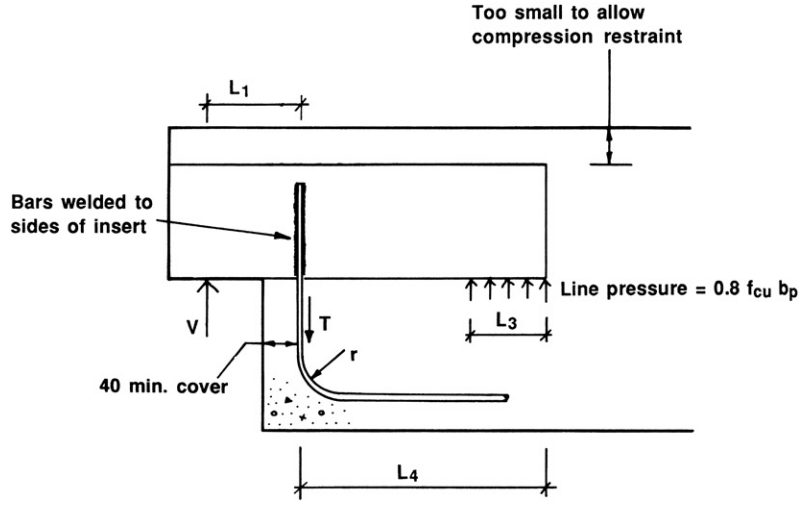

Figure 4.45 Beam shear box with additional rebar hangers.

the wide shear box and the bottom plate must be at least equal to the length of the strap, plus a little extra, say 25 mm.

Alternatively, rebars may be welded to the sides (or bottom) of the box and provided with a full anchorage length and correct bend radius Eq. (4.32). In no circumstances should roughened surfaces of the steel box be used to generate shear friction – a ductile, mechanical connection is required.

The equilibrium compression force $C = T - V$ is provided at the remote end of the box, either by direct bearing or through an additional bearing plate. The line pressure may be taken as $0.85\, f_{ck}$ $\{0.8\, f_{cu}\, b_p\}$, providing that the concrete beneath the bearing is confined laterally. Links are provided in the beam at a spacing of not more than 150 mm in readiness to carry the shear force as explained above, and these are usually more than adequate for this purpose. Taking moments about the centre of the tension strap, then referring to Figure 4.45:

$$V = 0.85 f_{ck} b_p L_3 (L_4 - 0.5L_3)/L_1 \quad \{V = 0.8 f_{cu} b_p L_3 (L_4 - 0.5L_3)/L_1\} \tag{4.47}$$

The length of the box ($L_4 + L_1$) is in the order of 500 mm for connector capacities of about 250 kN, reaching 700 mm for 400 kN capacity connectors. Resolving vertically:

$$V = T - 0.85 f_{ck} b_p L_3 \quad \{V = T - 0.8 f_{cu} b_p L_3\} \tag{4.48}$$

Hence T may be computed. The area of reinforcement is:

$$\begin{aligned} &A_s = T / 0.87 f_y \text{ for rebar} \\ &\text{or} \quad A_s = T / p_y \text{ for steel plate} \end{aligned} \tag{4.49}$$

The thickness of the plate at the bottom of the strap is based on the shear capacity of the plate, and a sufficient thickness to be welded to the strap, typically 6 mm. Figures 4.44 and 4.45 show examples of the completed shear box using steel straps and rebars, respectively.

Exercise 4.7 Beam end shear box design

Design a RHS (or SHS) shear box to carry an ultimate end reaction of 250 kN in a 300 mm-wide reinforced concrete beam. Determine the minimum depth of beam required to support the shear box, and design the shear reinforcement. Assume that the beam bearing is onto a mild steel plate. Use two methods for the tie force: (a) rebars, (b) straps.

Use concrete grade C32/40, f_{yk} $\{f_{yv}\} = 500\,\text{N/mm}^2$, f_{yk} $\{f_y\} = 250\,\text{N/mm}^2$ for welded bars, $p_y = 275\,\text{N/mm}^2$, $p_b = 190\,\text{N/mm}^2$, $f_{ydw} = 275/1.25 = 220\,\text{N/mm}^2$ $\{f_{weld} = 215\,\text{N/mm}^2\}$. Cover to reinforcement = 40 mm.

Solution

Breadth of box = $b/3$ = 100 mm.
Length of bearing = $250 \times 10^3/190 \times 100$ = 13.2 mm, plus 10 mm fixing tolerance = 25 mm.
Use minimum recommended steel bearing length = 60 mm.
Beam rebate length = 60 + 20 mm grouting gap = 80 mm.

(a) Using reinforcement hanger (see Figure 4.45)

L_1 = 80 − 60/2 + 40 cover + say 16 = 106 mm, assuming 32 mm bar diameter
Try L_4 = 300 mm

Line pressure under box = $0.85 \times 32 \times 100 = 2720\,\text{N/mm}$
Moments about tie gives
$250 \times 10^3 = 2720\, L_3\, (300 - 0.5\, L_3)/106$
Hence L_3 = 34.5 mm, say 35 mm.
$C = 2720 \times 35 \times 10^{-3} = 95.2\,\text{kN}$
$T = 250 + 95.2 = 345.2\,\text{kN}$

$$A_s = \frac{345.2 \times 10^3}{0.87 \times 250} = 1587\,\text{mm}^2$$

Line pressure under box = $0.8 \times 40 \times 100 = 3200\,\text{N/mm}$
Moments about tie gives
$250 \times 10^3 = 3200\, L_3\, (300 - 0.5\, L_3)/106$
Hence L_3 = 29.0 mm, say 30 mm.
$C = 3200 \times 30 \times 10^{-3} = 96.0\,\text{kN}$
$T = 250 + 96.0 = 346.0\,\text{kN}$

$$A_s = \frac{346.0 \times 10^3}{0.87 \times 250} = 1591\,\text{mm}^2$$

Use two H32 bars (1608 mm^2) welded to side of box.

(1) Bend radius to R32

Cover distance + radius = 84 mm.

$$r = \frac{172.6 \times 10^3 (1/84 + 1/(2 \times 32))}{2 \times 32/1.5} = 112\,\text{mm},$$

say 115 mm
Minimum required depth beneath box
= 115 + 32 + 10 link + 40 cover = 197 mm, use 200 mm

Cover distance + diameter = 100 mm.

$$r = \frac{173.0 \times 10^3 (1 + 2(32/100))}{2 \times 40 \times 32} = 110.8\,\text{mm},$$

say 115 mm
Minimum required depth beneath box
= 115 + 32 + 10 link + 40 cover = 197 mm, use 200 mm

(2) Confinement of concrete beneath box

$F_{bst} = 0.167 \times 95.2 = 15.9\,\text{N/mm}^2$
$A_{bst} = 37\,\text{mm}^2$

$F_{bst} = 0.22 \times 96.0 = 21.1\,\text{kN}$
$A_{bst} = 49\,\text{mm}^2$

Use a pair of H10 bars ($157\,\text{mm}^2$) at end of box.

(3) RHS design

$M_{max} = 250 \times 106 = 26\,500\,\text{kN mm}$

Plastic modulus $S_{xx} > \dfrac{26500}{0.6 \times 275} = 96.4\,\text{cm}^3$

$V_{max} = 250\,\text{kN}$

Web area, $dt > \dfrac{250 \times 10^3}{0.6 \times 275} \Big/ 2 = 758\,\text{mm}^2$

Use 100 × 100 × 8 RHS grade S275 {43} steel ($S_{xx} = 99.9\,\text{cm}^3$, $dt = 800\,\text{mm}^2$).

(4) Weld design to side of box
Maximum length available = 100 mm.
Assume 8 mm leg length, then:

Weld length $l_w = \dfrac{172.6 \times 10^3}{2 \times 5.6 \times 220} = 70\,\text{mm}$

Weld length $l_w = \dfrac{173.0 \times 10^3}{2 \times 5.6 \times 215} = 71.1\,\text{mm}$

Use 8 mm × 100 mm-long CFW to tie bars.

(5) Shear links in concrete between tie and end of box, and for an effective depth beyond end of box.
Assume flexure requires a minimum of two H25 bars.

Total depth of beam, h
= 50 top cover + 100 box + 200 below = 350 mm
$b = 300\,\text{mm}$
d = 350 − 40 cover − 10 link
− 12 bar radius = 287.5 mm
$z = 0.9 \times 287.5 = 258.7\,\text{mm}$
(See Eq. 6.8 with $\cot\theta = 2.5$)

$A_{sw} = \dfrac{250 \times 10^3}{258.7 \times 0.87 \times 500 \times 2.5} \Big/ 2 = 0.444\,\text{mm}^2/\text{mm}$
$= 444\,\text{mm}^2/\text{m/leg}$

Use H10 links at 175 mm centres.

Total depth of beam, h
= 50 top cover + 100 box + 200 below = 350 mm
$b = 300\,\text{mm}$
d = 350 − 40 cover − 10 link
− 12 bar radius = 287.5 mm
$100\,A_s/bd = 100 \times 982/(300 \times 288)$ = 1.14%
$v_c = 0.66\,\text{N/mm}^2$

$v = \dfrac{250 \times 10^3}{300 \times 287.5} = 2.89\,\text{N/mm}^2$

$A_{sv} = \dfrac{(2.89 - 0.66) \times 300}{0.87 \times 500} \Big/ 2 = 0.771\,\text{mm}^2/\text{mm}$
$= 771\,\text{mm}^2/\text{m/leg}$

Use H10 links at 100 mm centres.

(b) Using plate strap hanger (refer to Figure 4.44)
Because the plate strap occupies a greater length than a single rebar above, the lever arm L_1 is increased to half the length of the plate minus the radius of the bar. Using the tie force above as a guide, adding about 10% extra for the additional lever arm, try 6 mm thick × 120 mm long strap.

$L_1 = 80 - 60/2 + 40\,\text{cover} + 120/2 = 150\,\text{mm}$

Try $L_4 = 300\,\text{mm}$ as before and increase if necessary.

(*Continued*)

Moments about tie

$250 \times 10^3 = 2720\ L_3\ (300 - 0.5\ L_3)/150$
Hence $L_3 = 50.1$ mm, say 51 mm
$C = 2720 \times 51 \times 10^{-3} = 138.7$ kN
$T = 250 + 138.7 = 388.7$ kN.
$A_{plate} = 388.7 \times 10^3/275 = 1414\ mm^2$
Length of strap = $1414/(2 \times 6) = 117.8$ mm

$250 \times 10^3 = 3200\ L_3\ (300 - 0.5\ L_3)/150$
Hence $L_3 = 42.0$ mm, say 42 mm
$C = 3200 \times 42 \times 10^{-3} = 134.4$ kN
$T = 250 + 134.4 = 384.4$ kN
$A_{plate} = 384.4 \times 10^3/275 = 1398\ mm^2$
Length of strap = $1398/(2 \times 6) = 116.5$ mm

Use two 6 mm-thick x 120 mm-long straps.

(1) RHS design
$M_{max} = 250 \times 150 = 37\ 500$ kNm.
Plastic modulus $S_{xx} > 37\ 500/275 = 136.4\ cm^3$.
$V_{max} = 250$ kN
Web area $dt > 250 \times 10^3/(0.6 \times 275 \times 2) = 758\ mm^2$.
Use $150 \times 100 \times 6.3$ RHS grade S275 {43} steel ($S_{xx} = 148\ cm^2$, $dt = 945\ mm^2$).

(2) Weld design to side of box
Maximum length available = 150 mm. Assume 8 mm leg length, then:

Weld length
$= 388.7 \times 10^3/(2 \times 2 \times 5.6 \times 220) = 79$ mm

Weld length
$= (384.4 \times 10^3)/(2 \times 2 \times 5.6 \times 215) = 79$ mm

Use 8 mm × 100 mm-long CFW to side strap.

(3) Width of bottom plate for an 8 mm weld leg = $100 + (2 \times 6) + 2 \times 8 = 128$ mm.

Use 150 mm plate width.
Bearing capacity above bottom plate
$= 0.85 \times 32 \times 120 \times 150 \times 10^{-3} = 489.6$ kN
> 388.7 kN
Shear thickness, t
$= 388.7 \times 10^3/(2 \times 150 \times 0.6 \times 275) = 9.8$ mm

Use 130 mm plate width.
Bearing capacity above bottom plate
$= 0.8 \times 40 \times 120 \times 130 \times 10^{-3} = 499.2$ kN
> 384.4 kN
Shear thickness, t
$= (384.4 \times 10^3)/(2 \times 120 \times 0.6 \times 275) = 9.7$ mm

Use 130 mm x 120 x 10 mm thick bottom plate.

Weld leg length to bottom plate (assuming 8 mm run-outs):

$l = 388.7 \times 10^3/(2 \times 2 \times 5.6 \times 220) = 79$ mm

$l = (384.4 \times 10^3)/(2 \times 2 \times 5.6 \times 215) = 79$ mm

Use 4 no. 8 mm welds across the full 120 mm bottom plate.

(4) Depth of concrete clearance between RHS box and bottom plate

$= 150 + 25 = 175$ mm

$= 130 + 25 = 155$ mm

(5) Shear links in concrete between tie and end of box, and for an effective depth beyond end of box.

Minimum total depth of beam = 2 × cover + 2 × links + box + clearance + plate

$= 2 \times 40 + 2 \times 12 + 150 + 175 + 10 = 439$ mm

$= 2 \times 40 + 2 \times 10 + 150 + 155 + 10 = 415$ mm

So total depth of beam rounded up is 450 mm.
Assume two H25 bars in end of flexural cage.

$d = 450 - 40 - 12 - 25/2 = 385.5$ mm
$z = 0.9 \times 385.5 = 347.0$ mm

$$A_{sw} = \frac{250 \times 10^3}{347 \times 0.87 \times 500 \times 2.5} \Big/ 2$$

$= 0.331\ mm^2/mm = 331\ mm^2/m/leg$
Use H12 links at 230 mm centres ($491\ mm^2/m$).

$d = 450 - 40 - 10 - 25/2 = 387.5$ mm
$100\ A_s/bd = 100 \times 982/(300 \times 338) = 0.84\%$
$v_c = 0.60\ N/mm^2$
$v = 250 \times 10^3/(300 \times 387.5) = 2.15\ N/mm^2$

$$A_{sv} = \frac{(2.15 - 0.6) \times 300}{2 \times 0.87 \times 500} = 0.536\ mm^2/mm$$

$= 536\ mm^2/m/leg$
Use H10 links at 145 mm centres ($541\ mm^2/m$).

4.3.12.2 Narrow plate design

A narrow shear plate is defined as one where the width (or thickness) of the plate, t, is in the range $0.1b < t < 75$ mm. Figure 4.46 shows three details of design methods using a narrow plate insert instead of the wider shear box. The narrow plate is used mostly with the welded plate column connector (see Figure 7.68(c)), where the plate is fillet-welded to a steel billet cast in the column. If a wide bearing plate is added to the end of the plate, the beam may be connected to many of the other types of column connector, e.g. the cleat type. In order to safely transfer the end reaction to the beam, the narrow plate is supplemented with any of the following:

(a) additional bearing plates welded to the underside of the vertical plate at a distance of 75 mm from the end of the beam, and if necessary a plate welded to the top of the remote end of the plate (Figure 4.46(a))

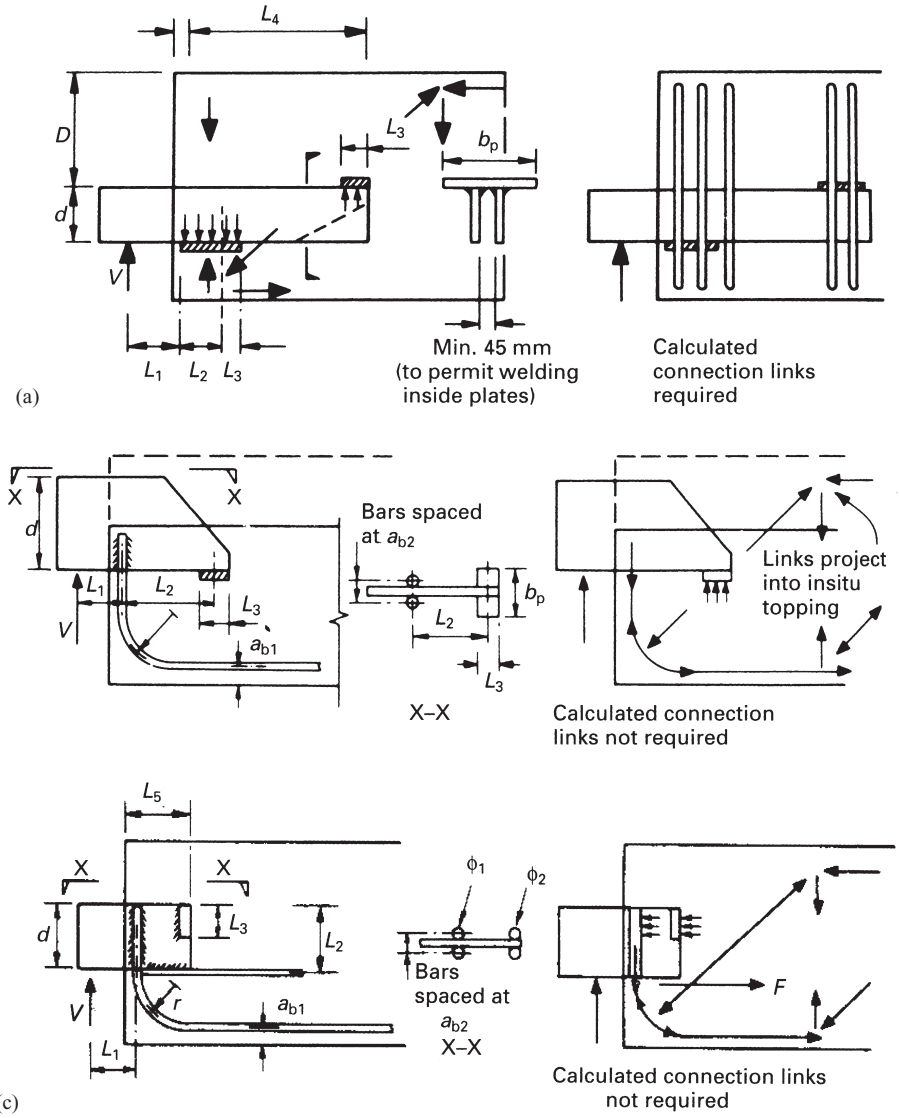

Figure 4.46 Narrow plate beam end design. (a) With additional bearing plate [4.16]; (b) with additional rebar and remote end plate [4.16]; (c) with additional remote end plate and rebar [4.16].

(b) additional (two minimum) rebars welded to the sides of the plate at a centre distance of 75 mm from the end of the beam, and a bottom plate welded to the underside of the vertical plate (Figure 4.46(b))

(c) rebars as (b), but with a vertical end plate and horizontal tie-back steel bars welded to the bottom of the plate (Figure 4.46(c)). This option is used where the length of the plate is restricted, for example by a service hole or check-out in the beam.

As with the wide shear box, the narrow shear plate is designed in three-point bending, and is therefore statically determinate. The plate is completely surrounded by concrete to prevent twisting and buckling, etc. The concrete is otherwise ignored up to a point just beyond the tie bars, where truss action takes over as in a normal beam. Unlike the wide box connector, which may be embedded in a deep concrete beam without additional ties, the plate *must* be restrained vertically and prevented from splitting through the concrete, no matter how deeply embedded it is, either by the additional bearing plates or by closely spaced links near to the reaction points.

Option (a) is used if the distance from the bottom of the beam to the underside of the plate is small, say less than about 75 mm, and where insufficient compression can develop over the top of the steel insert. The concrete at the top of the beam should be at least capable of resisting punching shear and of generating a diagonal compressive strut to the steel in the top of the beam. The top cover distance depends on the magnitude of V, but if the distance L_4 is large the end reaction is obviously small and a cover distance of about 150 mm is adequate.

Referring to Figure 4.46(a), the depth of the plate d is calculated from the greater of:

$$d = \frac{V}{0.6 p_y t} \tag{4.50}$$

or

$$d = \sqrt{\frac{4V(L_1 + 0.5L_2)}{p_y t}} \tag{4.51}$$

The equilibrium compression force $C = T - V$ is provided at the remote end of the plate. The bearing pressure may be taken as 0.85 f_{ck} {0.8 f_{cu}} providing that the concrete around the plate is confined laterally, although some designers prefer to restrict the stress (not code values) to 0.6 f_{ck} {about 0.6 f_{cu}} to guard against cracking at the corner of the plate or on narrow bearings. Small-diameter links are provided in the beam at a spacing of not more than 150 mm, as explained above. The overall difference in the design compared with the wide box connector is directly related to the position of the plate in the beam, or more specifically the amount of concrete cover beneath the plate.

The first step is to choose a length L_4 for the narrow shear plate. As an initial guess try $L_4 = 300$ mm for $V < 150$ kN, increasing to $L_4 = 500$ mm for $V < 300$ kN (assume $b > 300$ mm, and $f_{ck} > 32$ N/mm^2 {$f_{cu} > 40$ N/mm^2}). The width of the bearing plate b_p should be approximately $b/3$. Then:

$$V = 0.85 f_{ck} b p L_2 \quad \{V = 0.8 f_{cu} b p L_2\} \tag{4.52}$$

Assuming that both plates have the same width, L_3 is calculated from equilibrium of moments:

$$L_3(L_4 - L_2 - L_3) = L_2(L_1 + 0.5L_2) \tag{4.53}$$

Check that the bearing stresses do not overlap such that $L_2 + 2\,L_3 < 0.9\,L_4$.

The force in the end plate must be upheld by steel stirrups A_{sv} as follows:

$$A_{sv} = \frac{0.85 f_{ck} b_p (L_2 + L_3)}{0.87 f_y} \quad \left\{ A_{sv} = \frac{0.8 f_{cu} b_p (L_2 + L_3)}{0.87 f_{yv}} \right\} \tag{4.54}$$

equally spaced over a distance $L_2 + L_3 + 125\,\text{mm}$ from the end of the concrete. Note that if $0.85\,f_{ck}\,b_p\,(L_2 + L_3) > V$ $\{0.8\,f_{cu}\,b_p\,(L_2 + L_3) > V\}$, the stirrups are required to carry a force greater than the end reaction.

The force at the end of the shear plate $0.85\,f_{ck}\,b_p\,L_3$ $\{0.8\,f_{cu}\,b_p\,L_3\}$ is resisted by a diagonal compressive strut C acting at an assumed angle of 45°.

$$C = 0.85 f_{ck} b_p L_3 / \sin 45° \quad \{0.8 f_{cu} b_p L_3 / \sin 45°\} \tag{4.55}$$

and the horizontal component of that force, $C \cos 45°$, is carried into the bottom reinforcement, while the vertical component $C \sin 45°$ is absorbed into the shear stirrups at the end of the plate, which carry the full reaction V.

Where no remote end bearing plate is used, taking moments about the centre of the tension tie steel, and referring to Figure 4.46(b):

$$V = \frac{0.6 f_{ck} t L_3 (L_4 - 0.5 L_3)}{L_1} \quad \left\{\frac{0.6 f_{cu} t L_3 (L_4 - 0.5 L_3)}{L_1}\right\} \tag{4.56}$$

Typical sizes for the plate are in the order of 20 mm thick × 500 mm long for connector capacities of about 250 kN, reaching 25 mm × 700 mm for 400 kN capacity connectors.

Resolving vertically:

$$V = T - 0.6 f_{ck}\, t L_3 \quad \{T - 0.6 f_{cu} t L_3\} \tag{4.57}$$

Hence T may be computed. The area of reinforcement is:

$$A_s = T / 0.87 f_y \tag{4.58}$$

Option (b) is also used where the narrow plate is projecting above the top of the beam, or is very close to the top, i.e. less than 50 mm cover. This design follows the methods used for the wide shear box, and the design principle is based on the so-called 'Cazaly hanger', developed by Lawrence Cazaly of Ontario, Canada, in which the top plate supports the bars that carry the shear to the beam. Tests on this device were carried out by Ife *et al.* [4.40]. In all cases the anchor rebars must be formed over large-radii mandrels (typically 150 to 200 mm diameter for 25 mm diameter bars) to avoid excessive local bearing stresses causing diagonal tensile splitting directly beneath the steel section, where the shear stress is large. Variations of the Cazalay hanger have been designed in which the anchor steel is connected to the underside of a channel or back-to-back steel angles. The bars are either fillet- or butt-welded to the steel sections (depending upon the force required) or are threaded and pass through holes in the section. The same design equations (4.52) through to (4.55) are used here.

In using option (c) there must be sufficient top and bottom cover to the plate to enable the reaction forces to generate compressive struts and bond strengths, respectively. If a bearing plate of length X and width b_p is used, Eq. (4.56) is altered to:

$$V = \frac{0.6 f_{ck} b_p X (L_4 - 0.5 X)}{L_1} \quad \left\{\frac{0.6 f_{cu} b_p X (L_4 - 0.5 X)}{L_1}\right\} \tag{4.59}$$

Hence X is found. Then:

$$V = T - 0.6 f_{ck} b_p b_l \quad \{T - 0.6 f_{cu}\, b_p b_l\} \tag{4.60}$$

and the analysis proceeds as before.

Finally, factors of safety for the shear capacities of precast beams using shear cages and bearing plates, wide shear boxes or narrow plates are usually obtained by individual manufacturers by full-scale laboratory testing. Most of this work remains unpublished, but it is known that the results show that ultimate failure is a function of the shear reinforcement as in ordinary reinforced concrete, despite excessive local cracking near the bearing plate. Shear cages and boxes are usually rated in increments

of 50 kN up to 300 kN, and at 100 kN or 150 kN increments thereafter. Shear cages and boxes are capable of transmitting end shear forces up to about 700 kN. At greater load magnitudes the practical construction of such a connection is difficult to achieve.

4.4 Columns Subjected to Gravity Loads

The design of columns for overturning is given in Chapter 8.

4.4.1 General design

A column is specified where the ratio of the greater to the lesser cross-sectional dimension is less than 4; otherwise the component is designed as a wall. Precast column design is no different from the design of ordinary reinforced concrete columns and walls once all the aspects of manufacture, different types of structural connection, and temporary stability have been resolved. In fact, with a few isolated cases where columns have been prestressed axially to enable very long units to be pitched without (flexural) cracking, designs are based on the recommendations given in BS EN 1992-1-1, clause 5.8 [4.4] {BS 8110 [4.5]} for reinforced columns subjected to combined axial compression and bending (uniaxial or biaxial).

Precast columns and walls are manufactured horizontally, often in very accurate steel moulds. The standards of control are therefore greater than in vertically cast-*in situ* work and congested arrangements or reinforcement, particularly at column splices and foundations, can be specified with confidence in the knowledge that full compaction of concrete and correct spacing of bars will always be achieved. It is also possible to precast a concrete column having up to 10 per cent reinforcement (the recommended maximum value) at the level of the splices, although this quantity of reinforcement is rarely used in preference for a larger gross section. Figure 2.8 shows some reinforcement details in column sections. The design characteristic strength of the concrete is usually (cylinder/cube) 40/50 N/mm^2, but, because of the early strength required for lifting in the factory, actual characteristic strengths are in the range 50 to 65 {60 to 80} N/mm^2. The columns in the 30- to 40-storey precast frames in Belgium – see Figures 1.8 and 4.47 – were manufactured using grade C95/120 concrete for the lower

Figure 4.47 High-strength columns in 40-storey precast concrete frames (courtesy of Ergon, Belgium).

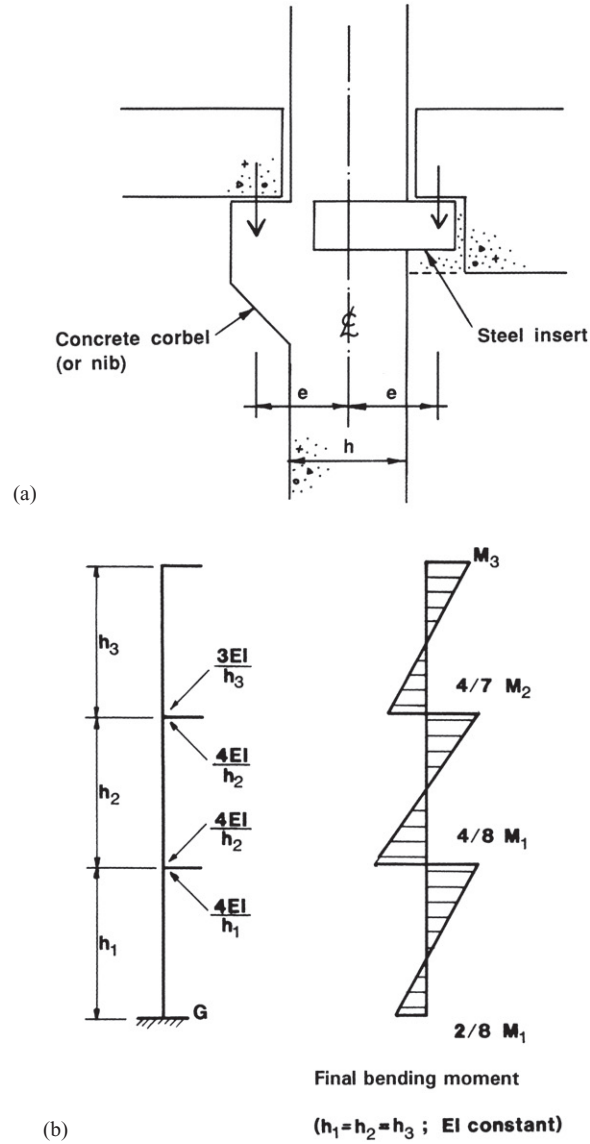

Figure 4.48 Bending moments in columns due to connector eccentricity. (a) Definition of eccentricity and (b) distribution of bending moments in columns.

storeys, and grade C50/60 for the upper storeys. Manufactured in two-storey sections, with rectangular bearing corbels for beams, the diameter of the columns was limited for architectural reasons to 600 mm. Even at 36 storeys, the axial compression in the ground-floor columns would only be about $N_{Ed}/f_{ck}\ A_c = 0.7$, such that the area of reinforcement would be about 5 per cent of the area of concrete.

The design commences with an assessment of structural stability, and of the axial loadings and bending moments at each floor level. As shown in Figures 1.29 and 4.48(a) and (b), column bending moments are the result of eccentric loading in the connection. The eccentricity varies with the type of connection, corbel or haunch. Typical values are $e = (h/2 + 50)$ mm to $(h/2 + 150)$ mm.

In edge columns supporting a single beam, the ultimate reaction V produces a bending moment at the connector node $M = Ve$. At internal columns supporting a (near) symmetrical arrangement of

beams, the moment is obtained by the summation of moments at each side of the column. Patch loading is used where the maximum and minimum beam reactions on either side of the column are:

$$V_{max} = 1.35\{1.4\} \times \text{permanent load} + 1.5\{1.6\} \times \text{variable load}$$

$$V_{min} = 1.0 \times \text{permanent load.}$$

The net overturning moment is obtained from the worst possible scenario when the construction tolerance Δ is added to the eccentricity of the greater load and deducted from the eccentricity of the smaller. Thus if the distance from the centroid of the column to the centre of the beam reaction is e, the net column moment is:

$$M_{net} = M_{max} - M_{min} = V_{max}(e + \Delta) - V_{min}(e - \Delta) \tag{4.61}$$

The net eccentricity is given by:

$$e_{net} = M_{net} / (V_{max} + V_{min}) \tag{4.62}$$

The analysis may now proceed in the same manner as for the single-sided beam.

A similar approach is adopted for 3-way and 4-way beam connections where biaxial bending moments are present in the column.

The resulting bending moments are distributed in the column in proportion to the stiffness EI/H of the column between adjacent floor levels, Figure 4.48(b) (where the stiffness factors $4EI/H$ and $3EI/H$ assume equal storey heights), and the column is designed accordingly to BS 8110 [4.5] using the clauses reproduced below for column effective length factors and second-order moments.

Design rules for columns in precast structures

Effective column height according to equations from clause 5.8.3.2(3) in BS EN 1992-1-1. {BS 8110 Part 2, clause 2.5 gives similar results.}

(a) Braced columns: the effective height for columns in framed structures may be taken as the lesser of:

$$l_e = l_0(0.7 + 0.05(\alpha_{c1} + \alpha_{c2})) < l_0$$

$$l_e = 0.5l\sqrt{\left(1 + \frac{\alpha_{c1}}{0.45 + \alpha_{c1}}\right)\left(1 + \frac{\alpha_{c2}}{0.45 + \alpha_{c2}}\right)} \tag{4.63}$$

$$l_e = l_0(0.7 + 0.05(\alpha_{cmin})) < l_0 \tag{4.64}$$

(b) Unbraced columns: the effective height for columns in framed structures may be taken as the lesser of:

$$l_e = l_0(1.0 + 0.15(\alpha_{c1} + \alpha_{c2}))$$

$$l_e = l\left(\max\left(\sqrt{\left(1 + \frac{10\alpha_{c1}\alpha_{c2}}{\alpha_{c1} + \alpha_{c2}}\right)}, \left(1 + \frac{\alpha_{c1}}{1 + \alpha_{c1}}\right) \times \left(1 + \frac{\alpha_{c2}}{1 + \alpha_{c2}}\right)\right)\right) \tag{4.65}$$

$$l_e = l_0(2.0 + 0.3(\alpha_{cmin})) \tag{4.66}$$

where:

α_{c1} = ratio of the sum of the column stiffnesses to the sum of the beam stiffnesses at the lower end of a column and $\alpha_{c1} \geq 0.1$)

α_{c2} = ratio of the sum of the column stiffnesses to the sum of the beam stiffnesses at the upper end of a column

α_{cmin} = lesser of α_{c1} and α_{c2}
l_e = effective height of a column in the plane of bending considered
l_0 = clear height between end restraints.

In the calculation of α_{cmin}, α_{c1} and α_{c2}, only members properly framed into the end of the column in the appropriate plane of bending should be considered. The stiffness of each member equals I/l_0, where I is the uncracked second moment of area for the section considered.

In specific cases of relative stiffness the following simplifying assumptions may be used:

(i) simply-supported beams framing in to a column: α_c to be taken as 10;
(ii) connection between column and base designed to resist only nominal moment: α_c to be taken as 10;
(iii) connection between column and base designed to resist column moment: α_c to be taken as 1.0.

For columns in precast concrete structures, effective length factors are based on $\alpha_c = 10$ for pinned connections, and actual frame geometry. The value of $\alpha_c = 10$ leads to $\beta = 1.35$ in a braced structure, and so $\beta = 1.0$ is used, and $\beta = 2.3$ in an unbraced structure. Although the designated value of $\alpha_c = 10$ for the relative stiffness of pin-jointed connections is somewhat arbitrary, it is adopted to justify the design of unbraced columns.

(c) Deflection induced moments in solid slender columns, BS EN 1992-1-1, clause 5.2 {BS 8110 Part 1, clause 3.8.3}.

Account has to be taken of the additional moment induced in the column by its deflection. The deflection of a rectangular or circular column under ultimate conditions may be taken to be:

$$e_i = \theta_i l_0 / 2 \le l_0 / 400 \quad \{a_u = \beta_a K h\} \tag{4.67}$$

$$\text{where } \beta_a = ((l_e / b)^2) / 2 \tag{4.68}$$

K = a reduction factor that corrects the deflection to allow for the influence of axial load
h = overall depth of a column in the plane considered
b = smaller dimension of a column
e_i = the load eccentricity
θ_i = 0.005
l_0 = the effective length.

In some precast structures there are only beams (except at gable ends or around lifts or stairwells) in one of the two orthogonal directions. In this case the clear height is taken to the centre depth of the first-floor slab based on the ground- to first-floor height. Subsequent upper-storey columns are designed using the same effective length factor as before, because the column is structurally continuous in these types of structure. Bending moments due to eccentric loading, horizontal forces and second-order deflection (a_u) effects are combined to give the most onerous design condition. Deflection-induced moments, M_{add}, are distributed throughout the structure in proportion to the stiffness of all the columns.

This assumes that the floor plate – a rigid diaphragm in any multi-storey structure – is capable of transmitting small prop forces that are the result of reactions from differential additional moments in various parts of the structure. An example of the application of this analysis is where large additional moments are created in only a few columns surrounding a roof-level lift motor or plant room. The natural structural response of the columns below this level ensures the full distribution of additional moments throughout the structure by generating a prop force in the floor, and thereby slightly altering the notional magnitude of a_u (i.e. initial value) at each floor level.

The resulting bending moments are usually large and this precludes the use of column splices and pinned bases. The magnitudes of the forces and moments also restrict the capacities of most columns to three storeys – particularly if the ground- to first-floor height exceeds about 3.5 m. Here the design

value of the deflection-induced eccentricity is in the order of 80 mm to 110 mm for 300 mm to 400 mm minimum column dimensions, respectively. It is difficult to visualise the reality of this without the column experiencing cracking far in excess of that which is normally associated with ultimate failure. Coupled with the bending moments generated by horizontal forces, the dimensions of the columns easily exceed architectural expectations for the sizes of columns in three-storey buildings, i.e. 300 × 300 mm. This leads to the use of braced or partially braced structures.

4.4.2 Columns in braced structures

Braced columns in so-called 'no-sway frames' ('small-sway frames' would be more precise) are checked for slenderness, an effective length factor of 1.0 being used in all upper floors and 0.9 between a fixed base and first floor. There is still inadequate analytical or experimental evidence to show the beneficial effects of moment rotation stiffnesses in the beam-to-column connection in reducing column effective lengths. Base plates and pocket foundations may be considered as fully moment-resisting, but the stiffness coefficient $\alpha_c = 1.0$ means that they are not fully rigid in the interpretation of the code. Sometimes the base is considered as a pinned connection (despite the moment fixity) in order to simplify column manufacture and foundation design.

Braced slender columns are analysed in the usual manner, taking into consideration the second-order deflection (or additional) bending moments as appropriate. The design axial load N is considered in combination with eccentric connector moments, Ve.

4.4.3 Columns in unbraced structures

In unbraced structures stability is shared between the columns in proportion to the flexural stiffness of each column and degree of moment fixity provided at the foundation.

Most unbraced columns are slender, although deep columns acting as 'wind posts' are deliberately proportioned so as to be designed as short. The effective length factor for cantilever columns in pin-jointed structures founded on moment-resisting bases is 2.3. Bending moments due to eccentric loading, horizontal forces and second-order deflections are combined to give the most onerous design condition.

4.4.4 Columns in partially braced structures

According to BS 8110 [4.5], columns in the unbraced part of the structure are designed as cantilevers with an effective length ratio of 2.3. This is a conservative value, because some of the columns immediately adjacent to the stabilising walls may have an effective length factor of 2.0. This is because their connection to the braced structure can be considered as infinitely rigid (although BS 8110 does not recognise such an end condition). A special case, shown in Figure 4.49, is where columns are supporting raking steelwork, which is connected at its other end to a rigid (no-sway) part of the structure. These columns are designed as propped cantilevers with an effective length factor of 1.6.

An issue of particular concern arises in partially braced structures because the lower end conditions for the columns, which are not in direct contact with shear walls, are not defined in BS 8110. The structure can be idealised, as shown in Figure 4.50. In Figure 4.50(b) the deflected profile of a column held in position, but not in direction, at level N, and a free cantilever up to level (N+1) are shown. The effective length of the column at level (N+1) is 2.85. Thus the true manner of slenderness-induced deflections would be as shown in Figure 4.50(c), where the effective length of *all* columns is 2.35. This has been computed from critical buckling loads obtained using stability functions given by Elliott, Davies and Mahdi [4.41, 4.42] and following the work carried out by Cranston [4.43]. The shear forces at the base of the unbraced columns are carried in the floor plate to the stiffening elements in accordance with their stiffnesses and position. However, bending moments resulting from sway in the unbraced part are carried over into the braced part of the structure, diminishing to zero with distance

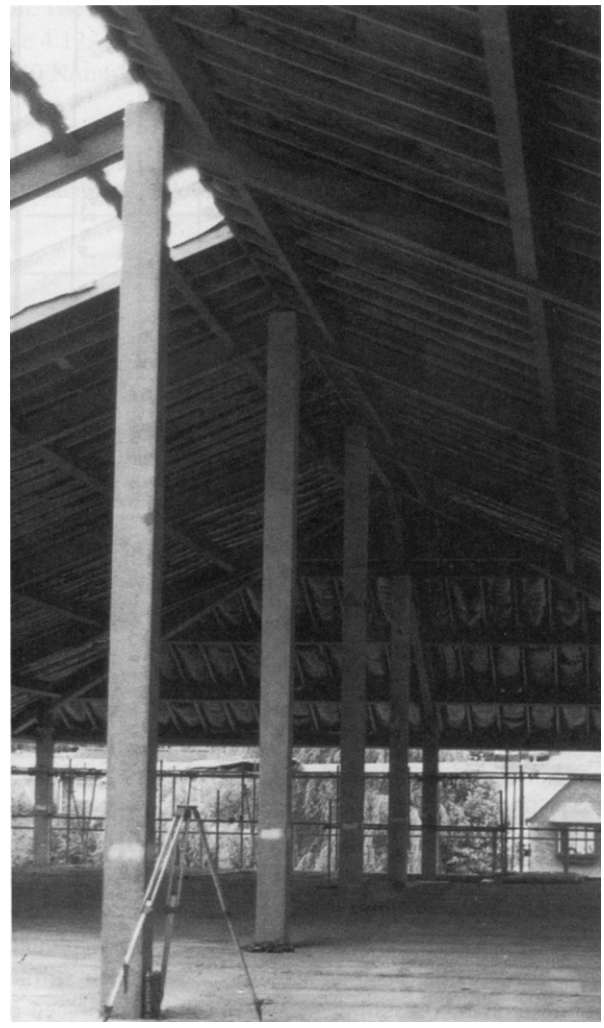

Figure 4.49 An example of propped cantilever columns.

to the level of the floor plate below. The effective length factor for the columns in this lower region is 1.0.

The situation where the ground-floor area is free of walls for architectural reasons is not a common option, for the following reasons:

(a) The columns will be founded in moment-resisting bases. Where the ground- to first-floor column is unbraced, the column effective length factor is 1.15 (because according to BS 8110, Part 2, clause 2.5 this gives $\alpha_{c1} = 1$ and $\alpha_{c2} = 0$). In the two-storey unbraced version it is 2.3 in the ground- to first-floor column and 1.15 in the first- to second-floor column. The major problem is that the columns surrounding the upper-floor walls are heavily loaded axially, because the overturning moments are concentrated there.

(b) This gives rise to very large second-order bending moments in the columns, with the inherent problems that these bring to foundation design.

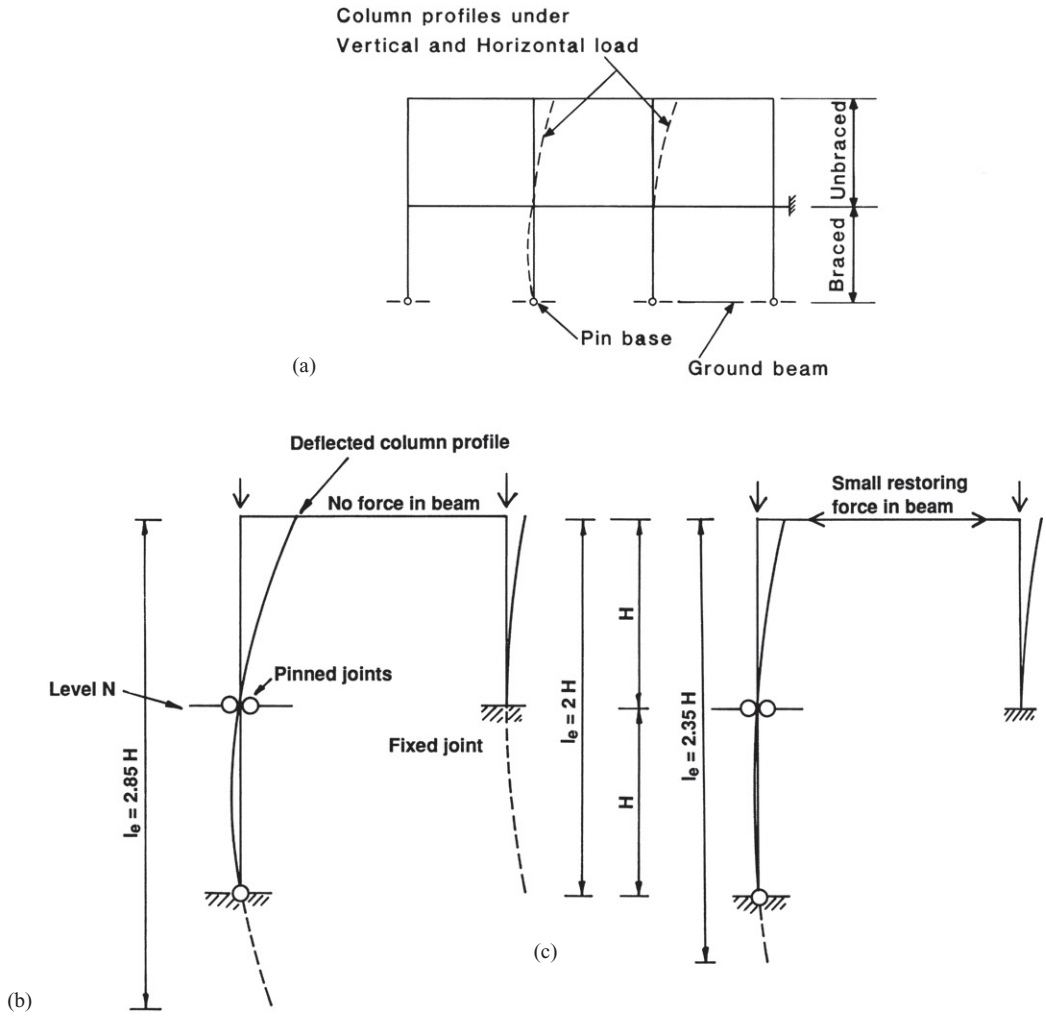

Figure 4.50 Partially braced structures. (a) Idealised structure. (b) Column buckling considering each column separately and (c) column buckling in framed structure.

Exercise 4.8 Column design

The four-storey braced column shown in Figure 4.51 carries beams on either side in a symmetrical arrangement. The distance from the face of the column to the point load V is nominally 60 mm. The construction allowance is 10 mm. The beam end reactions are given in Table 4.13. For the purpose of this exercise use the ultimate load combination factor $\psi_o = 1.0$. Let the effective creep factor $\varphi_{ef} = 1.0$.

Given concrete grade C40/50, steel f_{yk} $\{f_y\} = 500\,\text{N/mm}^2$, and cover = 35 mm to 10 mm diameter links:

i) calculate maximum and minimum axial loads and moments
ii) draw bending moment and axial force diagrams
iii) design column reinforcement and column size
iv) check reinforcement for factory lifting if $f_{ck} = 12.75\,\text{N/mm}^2$ $\{f_{cu} = 15\,\text{N/mm}^2\}$
v) check site pitching if $f_{ck} = 25.5\,\text{N/mm}^2$ $\{f_{cu} = 30\,\text{N/mm}^2\}$

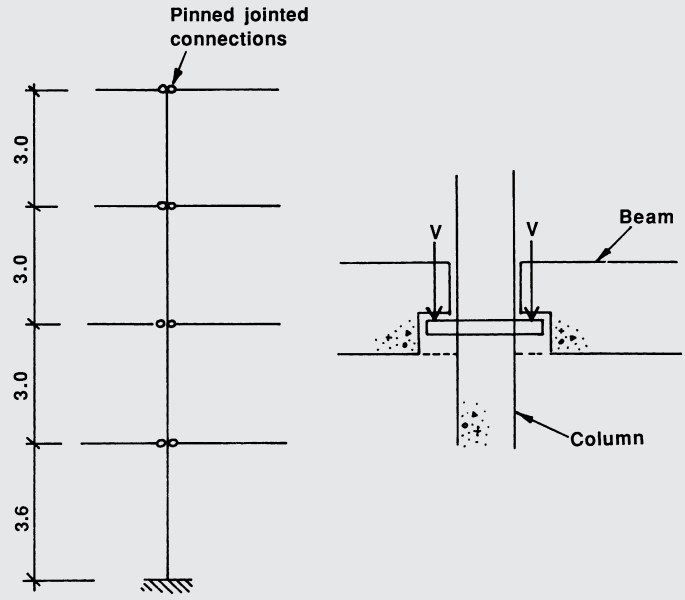

Figure 4.51 Details for Exercise 4.8.

Table 4.13 Beam end reactions *V* (kN)

	Permanent action	Variable action
Roof	80	27
Floors	108	90

Solution

Try 300 × 300 mm column, this being the smallest recommended size for a four-storey building.
$b = h = 300$ mm. Assume 20 mm diameter bars. $d = 300 - 35 - 10 - 20/2 = 245$ mm.

Self-weight = 0.3 × 0.3 × 25 × 12.6
= 28.4 kN
Maximum axial load per floor
= 1.35 × permanent + 1.5 × variable load.

$N_{Ed,max}$ = 1.35 (28.4 + 160 + (3 × 216)) = 1129.1
+1.5 (54 + (3 × 180)) = 891.0
2020.1 kN

Total $N_{Ed,min}$ = 1.0 × permanent action = 836.4 kN
N_{Ed} at 1st floor = 1447.6 kN
Column effective length factor l_o/L for ground to 1st floor
(See clause 5.8.3.2) k_1 at foundation = 0.1
k_2 at first-floor slab that is nominally restrained, use = 100
(See Eq. 5.15)

$$l_o/L = 0.5\sqrt{((1+0.1/0.55)\times(1+100/100.45))} = 0.768$$

(See Eq. 5.14) $$\lambda = \frac{l_o}{i} = \frac{0.768\times 3600}{86.6} = 31.9$$

(See Eq. 5.13N) $\lambda_{lim} = 20ABC/(\sqrt{n})$

Self-weight = 0.3 × 0.3 × 24 × 12.6
= 27.2 kN
Maximum axial load per floor
= 1.4 × permanent + 1.6 × variable load.

N_{max} = 1.4 (27.2 + 160 + (3 × 216)) = 1169.3
+1.6 (54 + (3 × 180)) = 950.4
2119.7 kN

Total N_{min} = 1.0 × permanent action = 835.2 kN
N at 1st floor = 1519.6 kN
Column effective length factor β for ground to 1st floor = 0.9

$$\frac{l_e}{h} = \frac{0.9\times 3600}{300} = 10.8 < 15$$ hence short column

M_{min} due to min eccentricity of 0.05 h
M_{min} = 0.05 × 0.300 × 2119.7 = 31.80 kNm
β factor 1st to 2nd floor = 1.0

$$\frac{l_e}{h} = \frac{1.0\times 3000}{300} = 10 < 15$$ hence short column

(*Continued*)

$A = 0.833$ ($\varphi_{ef} = 1.0$)

$\omega = A_s f_{yd}/A_c f_{cd}$ = say $4 \times 314 \times 0.87 \times 500/(300^2 \times 40/1.5) = 0.227$

$B = \sqrt{(1+2\times0.227)} = 1.20$

In the case of alternate patch loading on subsequent floors, $r_m = +1$

$C = 1.7 - (+1) = 0.7$

$n = 2020 \times 10^3/300^2 \times 40/1.5 = 0.842$

$\lambda_{lim} = 20 \times 0.833 \times 1.20 \times 0.7/0.917 = 15.2$

< 31.9 column is slender

Ultimate design moment

(See Eq. 5.31, 5.33) $M_{Ed} = M_{0Ed} + N_{Ed}\, e_2$

$l_o = 0.768 \times 3600 = 2765$ mm

(See Eq. 5.34) Try $K_r = 0.35$

(See Eq. 5.37) K_φ

$= 1 + (0.35 + 40/200 + 31.9/150) \times 1.0$

$= 1.76$

$1/r_o = (0.87 \times 500/200\,000)/0.45 \times 245$

$= 19.7 \times 10^{-6}\,\text{mm}^{-1}$

$1/r = 0.35 \times 1.76 \times 19.7 \times 10^{-6}$

$= 12.1 \times 10^{-6}$

$e_2 = 12.1 \times 10^{-6} \times 2765^2/10 = 9$ mm

$M_2 = 0.009 \times 2020.1 =$ <u>18.18 kNm</u>

(See clause 5.2(9)) Min eccentricity

$e = 2765/400 = 7$ mm, or

(See clause 6.14)

$e_o = \max(300/30 = 10; 20)$ mm

$M_{Ed,min} = 0.02 \times 2020.1 =$ <u>40.40 kNm</u>

Slenderness 1st to 2nd floor $l_o/L = 1$

$$\lambda = \frac{l_0}{r_y} = \frac{1.0\times3000}{86.6} = 34.6$$

Following the same procedures

$\lambda_{lim} = 15.2 < 34.6$ column is slender

$K_r = 0.35$; $K_\varphi = 1.78$

$1/r = 0.35 \times 1.78 \times 19.7 \times 10^{-6}$

$= 12.3 \times 10^{-6}$

$e_2 = 12.3 \times 10^{-6} \times 3000^2/10 = 11$ mm

Case (i) for $N_{Ed,max} = 1447.6$ kN

$M_2 = 0.011 \times 1447.6 =$ <u>15.92 kNm</u>

$M_{Ed,min} = 0.02 \times 1447.6 =$ <u>28.95 kNm</u>

Case (ii) for $N_{Ed,patch} = 1137.1$ kN

$M_2 = 0.011 \times 1137.1 =$ <u>12.51 kNm</u>

$M_{Ed,min} = 0.02 \times 1137.1 =$ <u>22.74 kNm</u>

Case (i) for $N_{max} = 1519.6$ kN

$M_{min} = 0.05 \times 0.300 \times 1519.6 =$ <u>22.79 kNm</u>

Case (ii) for $N_{patch} = 1188.4$ kN

$M_{min} = 0.05 \times 0.300 \times 1188.4 =$ <u>17.83 kNm</u>

Maximum bending moment occurs owing to patch loading alternating on successive floors, where the beam action V = minimum on one beam and V = maximum on the other beam. The eccentricity of V at each side of the column about the centre line of column $e = 0.5\ h + 60 \pm$ construction allowance of 10 mm = 200 mm minimum and 220 mm maximum.

Maximum moment

= 0.22 (1.35 permanent + 1.5 variable) − 0.200 × 1.0 permanent

At roof $M = 32.67 - 16.00$ = 16.67 kNm

At floors $M = 61.78 - 21.60$ = 40.18 kNm

Maximum moment

= 0.22 (1.4 permanent + 1.6 variable) − 0.200 × 1.0 permanent

At roof $M = 34.14 - 16.00$ = 18.14 kNm

At floors $M = 64.94 - 21.60$ = 43.34 kNm

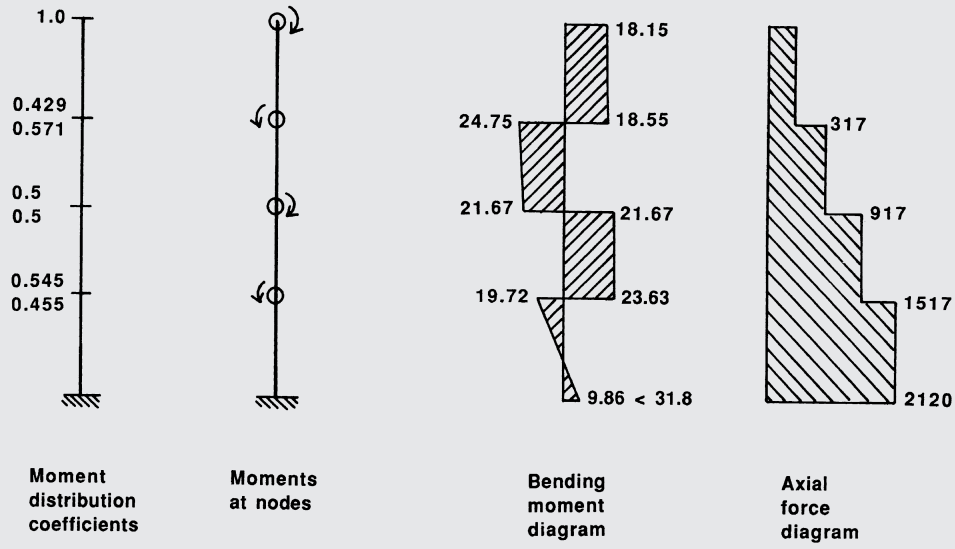

Figure 4.52 Moments and axial forces in Exercise 4.8.

Moment distribution factors:

at roof = 1.0 and complement = 0

at 3rd floor $= \dfrac{3}{3+4}$ = 0.429 and complement = 0.571

at 2nd floor $= \dfrac{4}{4+4}$ = 0.5 and complement = 0.5

at 1st floor $= \dfrac{3.6}{3.0+3.6}$ = 0.545 and complement = 0.455, with 50% carry over to foundation.

The bending moment and axial force diagrams are given in Figure 4.52.

Maximum moment due to patch loads at the 1st floor M_{Ed}	= 21.90 kNm
where the axial force N_{Ed}	= 1137.1 kN
Maximum moment due to patch loads at the 1st floor M	= 23.62 kNm
where the axial force N	= 1188.4 kN

Reinforcement design

$d/h = 245/300 = 0.81$

From design chart given in Figure 4.53 for $d_2/h = 0.2$ (or $d/h = 0.8$).

(a) Case 1, at foundation

$N_{Ed} = 2020.1$ kN, $M_{Ed} = 40.40 + 18.18 = 58.58$ kNm

$$\frac{N_{Ed}}{f_{ck}bh} = \frac{2020.1\times10^3}{40\times300\times300} = 0.561$$

$$\frac{M_{Ed}}{f_{ck}bh^2} = \frac{58.58\times10^6}{40\times300\times300^2} = 0.054$$

$A_s = 0.17 \times 300^2 \times 40/500 = 1224\,\text{mm}^2$

A_s not critical for N_{min}

Also $K_r \approx 0.32 <$ initial estimate of 0.35

Use $d/h = 0.8$ given in BS 8110, Part 3, Chart 47 [4.5].

(a) Case 1, at foundation

$N = 2119.7$ kN, $M = 31.80$ kNm

$$\frac{N}{bh} = \frac{2119.7\times10^3}{300\times300} = 23.55$$

$$\frac{M}{bh^2} = \frac{31.8\times10^6}{300\times300^2} = 1.18$$

$A_{sc} = 1.15\% = 1035\,\text{mm}^2$

Use four H20 main bars (1256 mm^2) and R6 links at 240 centres

(*Continued*)

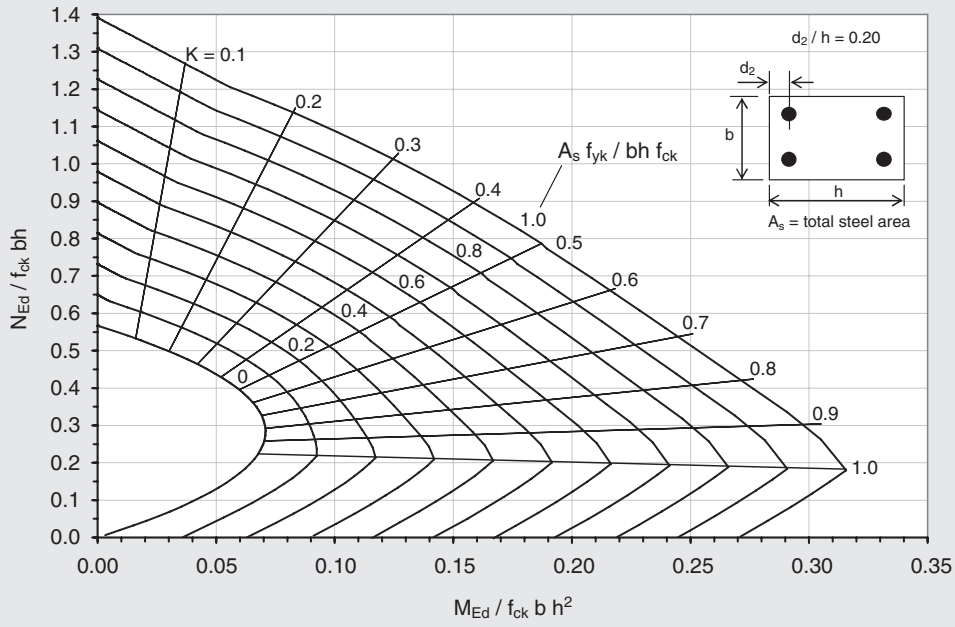

Figure 4.53 Column design chart to BS EN 1992-1-1 used in Exercise 4.8.

(b) Case 2 at 1st floor

(i) $N_{Ed} = 1447.6\,\text{kN}$, $M_{Ed} = 28.95 + 15.92 = 44.87\,\text{kNm}$

$$\frac{N}{f_{ck}bh} = \frac{1447.6\times10^3}{40\times300\times300} = 0.402$$

$$\frac{M_{Ed}}{f_{ck}bh^2} = \frac{44.87\times10^6}{40\times300\times300^2} = 0.042$$

$A_s = 0$

(ii) $N_{Ed} = 1137.1\,\text{kN}$

$M_{Ed} = \max(21.90; 22.74) + 12.51 = 35.25\,\text{kNm}$

Not critical compared to (b)(i)

(i) $N_{max} = 1519.6\,\text{kN}$, $M = 22.79\,\text{kNm}$

$$\frac{N}{bh} = \frac{1519.6\times10^3}{300\times300} = 16.88$$

$$\frac{M}{bh^2} = \frac{22.79\times10^6}{300\times300^2} = 0.844$$

$A_{sc} = 0.4\% <$ above

(ii) $N_{patch} = 1188.4\,\text{kN}$, $M = \max(23.62; 17.83)\,\text{kNm}$

$$\frac{N}{bh} = \frac{1188.4\times10^3}{300\times300} = 13.2$$

$$\frac{M}{bh^2} = \frac{23.62\times10^6}{300\times300^2} = 0.87$$

$A_{sc} = 0.4\% <$ above

Factory lifting (see Section 10.2.2 before proceeding)

Self-weight of column plus 50% suction and impact allowance

$= 2.25 \times 1.5 = 3.38\,\text{kN/m}$

Lifting points at $0.2L$ from ends $= 0.2 \times 12.6 = 2.52\,\text{m}$

$M_{Ed} = 1.35 \times 3.38 \times 2.52^2/2 = 14.47\,\text{kNm}$

or $= 1.35\times\left(3.38\times\frac{12.6}{2}\times\left(\frac{12.6}{2}-2.52\right)-3.38\times\frac{\left(\frac{12.6}{2}\right)^2}{2}\right) = 18.1\,\text{kNm}$

$k = 18.1 \times 10^6/(12.75 \times 300 \times 245^2) = 0.0788$

giving $z = 231.0\,\text{mm}$ which is < 0.2067

$A_s = 18.1 \times 10^6/(0.87 \times 500 \times 231.0) = 180\,\text{mm}^2$

for two bars $<$ above

$= 2.16 \times 1.5 = 3.24\,\text{kN/m}$

Lifting points at $0.2L$ from ends $= 0.2 \times 12.6 = 2.52\,\text{m}$

$M_u = 1.4 \times 3.24 \times 2.52^2/2 = 14.4\,\text{kNm}$

or $= 1.4\times\left(3.24\times\frac{12.6}{2}\times\left(\frac{12.6}{2}-2.52\right)-3.24\times\frac{\left(\frac{12.6}{2}\right)^2}{2}\right) = 18.0\,\text{kNm}$

$k = 18.0 \times 10^6/(15 \times 300 \times 245^2) = 0.0667$ giving $z = 225.3\,\text{mm}$ which is < 0.156

$A_s = 18.0 \times 10^6/(0.87 \times 500 \times 225.3) = 184\,\text{mm}^2$

for two bars $<$ above

On-site pitching
Add 25% to self-weight for impact

$= 2.25 \times 1.25 = 2.813\,\text{kN/m}$		$= 2.16 \times 1.25 = 2.70\,\text{kN/m}$	
Pitching point $= 0.3L$ from end	$= 3.78\,\text{m}$	Pitching point $= 0.3L$ from end	$= 3.78\,\text{m}$
$M_{Ed,max} = 1.35 \times 2.813 \times 3.78^2/2$	$= 27.1\,\text{kNm}$	$M_{u,max} = 1.4 \times 2.70 \times 3.78^2/2$	$= 27.0\,\text{kNm}$
$k = 27.1 \times 10^6/(30 \times 300 \times 245^2) = 0.0591$		$k = 27.0 \times 10^6/(30 \times 300 \times 245^2) = 0.0500$	
giving $z = 231.6\,\text{mm}$ which is	< 0.2067	giving $z = 230.5\,\text{mm}$ which is	< 0.156
$As = 27.0 \times 10^6/(0.87 \times 500 \times 226.0)$	$= 270\,\text{mm}^2$	$As = 27.0 \times 10^6/(0.87 \times 500 \times 230.5)$	$= 269\,\text{mm}^2$
for two bars	< above	for two bars	< above

4.5 Staircases

4.5.1 Reinforced concrete staircases

Staircase design is by reinforced or prestressed concrete solid slab or tee-beam analysis. The main features that distinguish it from traditional *in situ* design are the manufacture (i.e. early age tilting and lifting), layout (i.e. allocation of flights, landings and half-landings per single item, as described in Section 3.2.3.) and the design of the joints.

Precast staircases are manufactured in one of three positions, with the tread facing up, down or to one side. In the former, so called 'ski-slope' moulds made of high-quality steel are used so that the unit is manufactured in its final orientation, i.e. treads horizontal. Three of the four faces and the risers are ex-mould – only the treads are trowelled. Tread-down casting is more ideally suited to the manufacture of flight units only. The unit is likely to be doubly reinforced, because the soffit is cast face up. Individual moulds are used only for flights of similar inclination and therefore tend to be made of timber. In the latter a variable tread mould is used so that the inclination of the stair is fully adjustable – see Figures 4.54 and 4.55. Flexural reinforcement is provided for lifting and ultimate service conditions.

Figure 4.54 Staircases cast using an adjustable tread and riser mould.

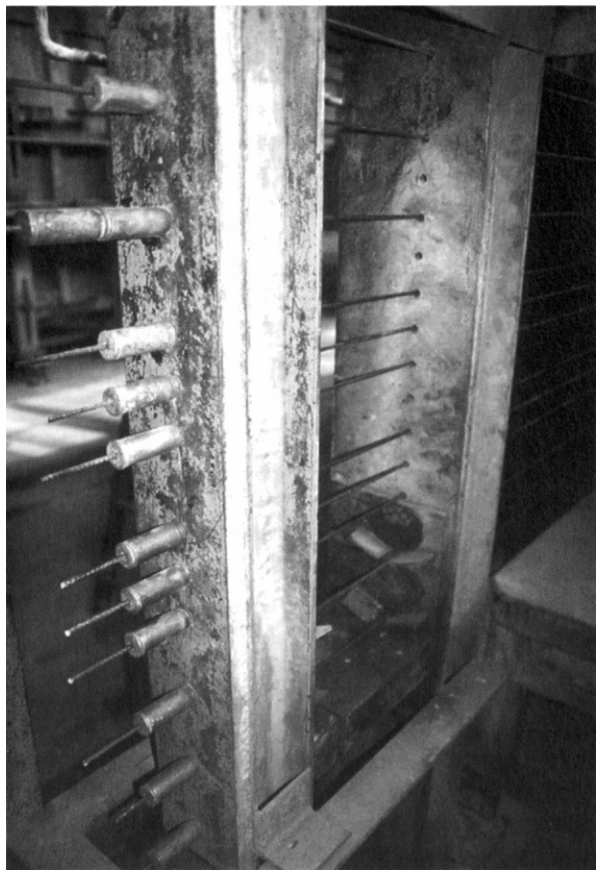

Figure 4.55 Pretensioning head block for prestressed concrete staircase production.

The flights are designed as one-way spanning solid slabs. Typical reinforcement consists of a square cage using H12 to H16 bars in the longitudinal direction of the span, and H8 or H10 bars transversely. An alternative economical design for long-span units (exceeding 6 m) uses so-called 'stringer' beams designed as rc tee-beams (Figure 4.56). The steps cantilever transverse to the flight span and are reinforced with transverse steel in the top of the flight. The stringer beam is checked for torsion for the case of non-symmetrical superimposed loading.

Landings, whether simply supported or cantilevered, are designed as rc solid slabs. Spans rarely exceed 4 m and it is therefore possible to design units not exceeding 250 mm in depth. It is usual for the landing to be shallower than the stair flight, and this also allows for a levelling screed to be used over the landing. Composite action with a structural topping is used where appropriate (but rarely). Precast, prestressed flat planks or hollow-core slabs are used if correct details at the connections can be found.

Other specialist precast rc components, such as lift-motor slabs, partition walls, roof gangways with a bund wall, steps, ramps or *ad-hoc* bases for machinery, etc., are usually classified as 'non-structural' and dowelled or bolted to the appropriate part of the structure.

4.5.2 Prestressed concrete staircases

The main benefit in prestressing stair-flight units compared with rc is the ease of production and the reduced depth of unit (waist) and amount of reinforcement required. Depths of 150 mm are

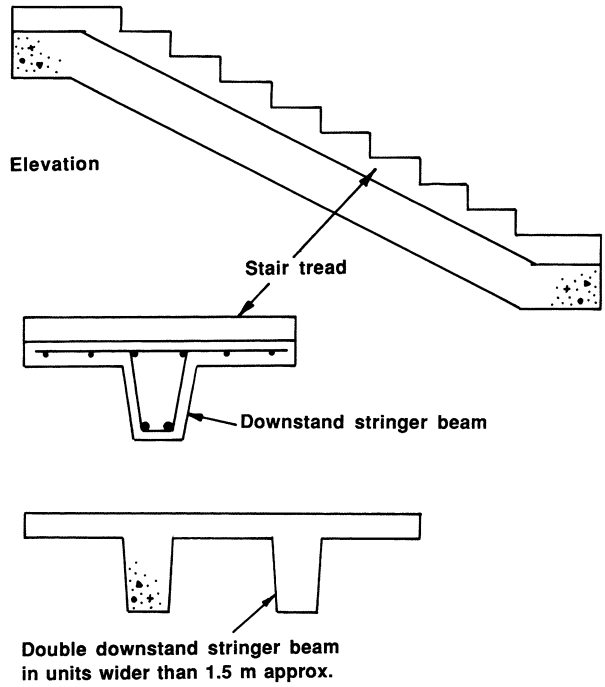

Figure 4.56 Stringer beam design for staircases.

commonplace for spans of up to 3.5 m. The reinforcement is simply in the form of several 5 mm- or 7 mm-diameter wires (the pretensioning force is usually too small for the use of strands), typically six per 1 m wide unit as shown in Figure 4.55. The grade of concrete is usually C40/50 or C50/60. Because the maximum stair-flight length is governed by the maximum number of steps in a single flight, the flexural moments are small in comparison with other types of prestressed work.

4.5.3 Staircase and landing end reinforcement

The ends of staircase units may be shaped into scarf joints, or halving joints. These may be visualised as two identical continuous bearing nibs in which the forces acting on each are equal and opposite in direction and magnitude. The design is based on a short cantilever nib principle, rather like the beam bearing nib design, but where accuracy in the positioning of the flexural reinforcement is of the utmost importance. In order to increase the depth at the root of the nib, the bearing ledge is sloping at a gradient α, about 1 in 7 to 1 in 10. This naturally affects the resultant force, as the frictional force $\mu V \cos\alpha$ in Figure 4.57 is acting down the slope, where V is the uniformly distributed ultimate stair-flight end shear force. In concrete-to-concrete joints $\mu = 0.7$, and so the resultant force is inclined at $\theta \approx \tan^{-1}(\mu \cos\alpha) + \alpha$ relative to the surface of the bearing ledge. Typically, $\theta = 40°$ to 45°.

Figure 4.57 shows the notation and triangle of forces at the reaction point, which gives the following forces and areas of reinforcement:

$$H = \frac{V}{(\sin\alpha + (\cos\alpha \tan\beta))} + \mu V \cos\alpha \frac{x+c}{x} \tag{4.69}$$

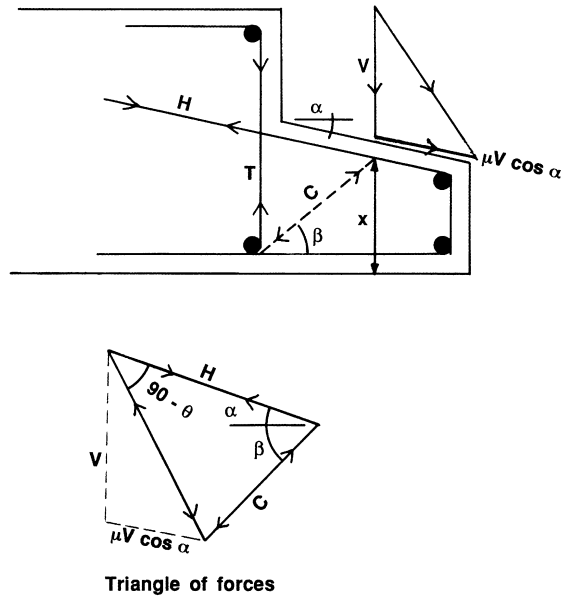

Figure 4.57 Scarf joint geometry in staircase.

and by the resolution of forces at the load point:

$$C = \frac{V}{((\cos\beta\tan\alpha)+\sin\beta)} \tag{4.70}$$

with

$$T = V + \mu V\cos\alpha\sin\alpha \tag{4.71}$$

The corresponding areas of reinforcement are given by:

$$A_{sh} = \frac{H}{0.87 f_y} \tag{4.72}$$

$$A_{sv} = \frac{T}{0.87 f_y} \tag{4.73}$$

Note that T should not be less than V.

Small-diameter bars at frequent intervals, say H8 at 100 mm centres, are preferred to larger bars where bending restrictions may violate cover requirements. Figure 4.58(a) shows typical dimensions and ideal reinforcement details. Neoprene pads, or steel packing shims with a soft mortar bed, are used to ensure the correct bearing. Although ultimate design pressures rarely exceed about 1.0 N/mm^2 (for typical spans of 3 m and 5 kN/m^2 superimposed loading), the line of action of loading is very important. This should pass through a point which is well behind the line of the longitudinal bar in the front of the rib, and not less than about 30 mm from the ends of either the upper or lower half of the joint.

Continuous end details of this type do not provide continuity between precast units. This may be achieved using intermittent scarf joints, as shown in Figure 4.58(b) in which pockets of reinforced *in situ* concrete tie the precast units together. These units are obviously more expensive to manufacture. Welded connections made between fully anchored plates (similar to double-tee floor slabs) may also

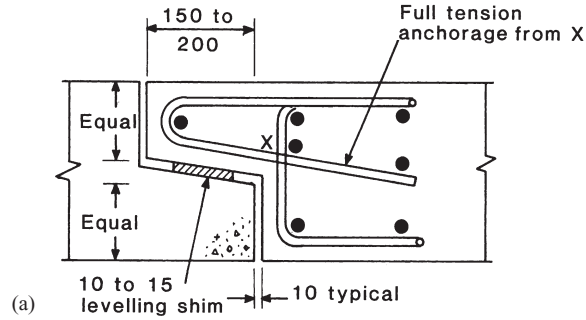

(a)

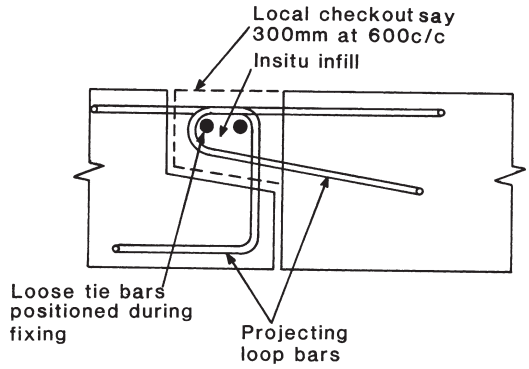

(b)

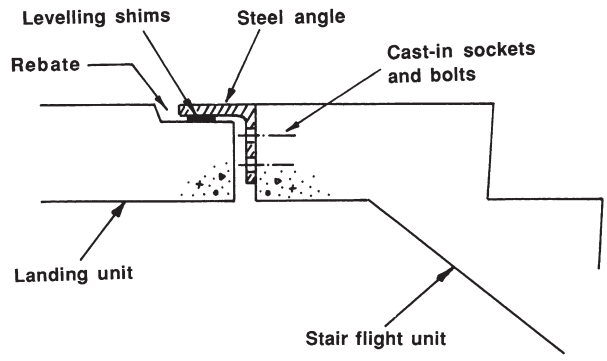

(c)

(d)

Figure 4.58 Staircase to landing joint details. (a) Reinforcement in stair scarf joint; (b) intermittent scarf joint; (c) steel shelf angle method; (d) precast concrete stair flight with steel angle supports detail.

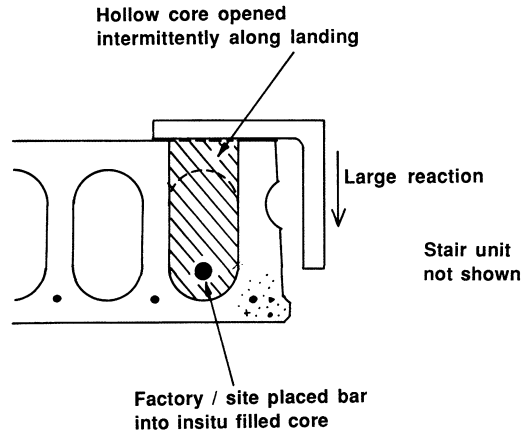

Figure 4.59 Hollow-core floor slabs used as landings, with filled edge core.

be specified if structurally required. Concrete cover to the welding is required for fire protection and cosmetic purposes.

Shelf angles are a popular alternative to concrete scarf joints in that production is simplified by the simple provision of cast-in sockets for the bolted connection. The detail is 'inverted' (relative to the normal use of a shelf angle), as shown in Figure 4.58(c) and (d). A small check-out in the supporting (landing) member is prepared to receive the flange of the angle attached to the flight unit. At least two angles are used in the connection. The assembly is designed on the basis of an eccentric vertical load acting at the most onerous position. Flexural and shear stresses are considered at the root of the angle, and pull-out forces and shear stresses are used in designing the bolt and socket. Friction-grip bolts in slotted holes are required for fixing tolerances. Concrete cover is required to give fire protection to the angle. Typical details of angle and bolt are given in Figure 4.58(c).

Hollow-core floor slabs may be used to replace solid rc landing units. The depth of the hollow-core slab is about 50 mm less than that of the precast stair flight, to enable a finished structural topping to cover the steel angle (hollow-core units cannot be recessed). If the hollow-core slab unit is cut to the required landing width, the stair flight should not bear solely on the top flange of the slab. Figure 4.59 shows the correct practice, where the first hollow-core is opened and filled with grade > C25/30 concrete, and a rebar (12 mm diameter minimum) is placed near to the bottom of the core. The use of hollow-core units as landings must be carefully designed and executed. Some authorities will not allow this detail following a fatal accident after the bearing end of a hollow-core unit failed and led to progressive collapse of a multi-storey staircase.

Exercise 4.9 Staircase half-joint design

Design the reinforcement for the scarf joint shown in Figure 4.60 for an ultimate landing reaction of 30 kN/m run. Allow a 10 mm vertical gap between the units.

Use C40/50 concrete, f_{yk} $\{f_y\}$ = 500 N/mm^2, and cover to reinforcement = 25 mm.

Solution

Using Figure 4.57 notation:

$\mu = 0.7$, $\alpha = \tan^{-1}(20/150) = 7.6°$

Bearing length = 150 − 10 gap = 140 mm.

Centre of bearing = 10 + 140/2 = 80 mm from face of nib.

Assume 10 mm bar diameter. Lever arm to vertical tie steel = 80 + 25 + 10/2 = 110 mm.

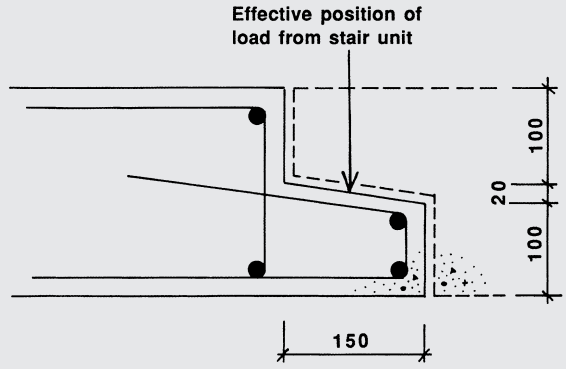

Figure 4.60 Details for Exercise 4.9.

$$\text{Depth } x = 120 - \frac{80}{150} \times 20 - \left(25 + \frac{10}{2}\right) \times \sec\theta = 79.1 \text{ mm}$$

Then $\beta = \tan^{-1}(79.1/110) = 35.7°$
Consider 1.0 m wide unit, then $V = 30$ kN/m

$$H = \frac{30}{(\sin 7.6° + (\cos 7.6° \times \tan 35.7°))} + 0.7 \times 30 \times \cos 7.6° \times \left(\frac{79.1 + 25}{79.1}\right) = 62.9 \text{ kN/m run}$$

$$C = \frac{30}{(\cos 35.7° \times \tan 7.6°) + \sin 35.7°} = 43.36 \text{ kN/m}$$

and $T = 30 + (0.7 \times 30 \times \cos 7.6° \times \sin 7.6°) = 32.75$ kN/m

Thus: $A_{sh} = \dfrac{62.9 \times 10^3}{0.87 \times 500} = 145 \text{ mm}^2/\text{m}$

Use H8 at 200 mm centres (251 mm^2) U-shaped bars in nib.

$$A_{sv} = \frac{32.75 \times 10^3}{0.87 \times 500} = 76 \text{ mm}^2/\text{m}$$

Use H8 at 300 mm centres (168 mm^2) U-shaped bars in end of landing. Provide H8 transverse steel as shown in Figure 4.58(a).

CHAPTER 5

Design of Precast Floors Used in Precast Frames

The options for using precast floors in frames are given, together with the fundamental design methods and some in-depth analysis for individual units and complete floors.

5.1 Flooring Options

Precast concrete flooring offers an economic and versatile solution to ground and suspended floors in any type of building construction. It has been widely used in commercial, industrial and domestic building, offering both design and cost advantages over traditional methods such as *in situ* concrete, composite and timber floors. There is a wide range of flooring types available to give the most economical solution for all loadings and spans. The floors give maximum structural performance with minimum weight and may be used with or without structural topping screeds, non-structural finishes (such as granolithic screed), or with raised timber floors. The main types of flooring are shown in Figure 5.1 (a) to (e):

- hollow-core slab
- double-tee slab
- beam-and-block
- solid composite plank
- beam and composite plank.

There is a market for each type of slab, which is dictated by load capacities, spans, preferred construction methods, integrity of the floor plate, and cost. The main building functions of these slabs were discussed in Chapter 3, in which Table 3.1 summarises the performance criteria.

The two main criteria in the design of floors are strength and stiffness, both in the vertical direction under gravity loading and in the horizontal direction under wind (or earthquake) loading. In each case, in the event of overload or accidental damage, the floor system must be ductile. Other design criteria include fire resistance, thermal and acoustic properties, vibrations, durability, handling, and construction methods.

Multi-storey Precast Concrete Framed Structures, Second Edition. Kim S. Elliott and Colin K. Jolly.

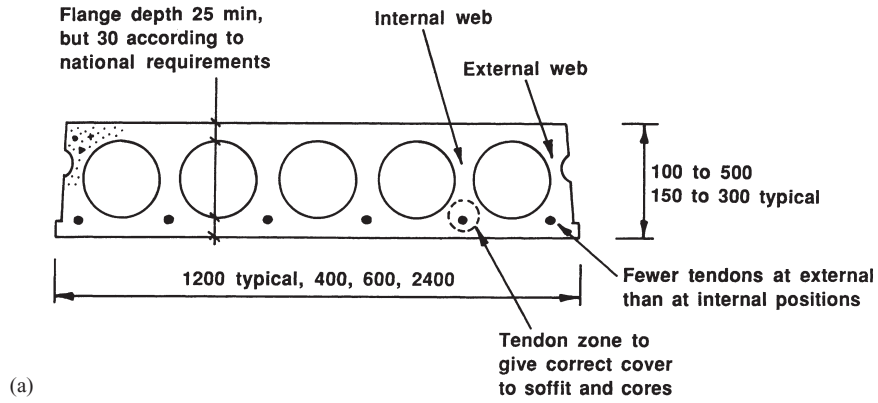

(a)

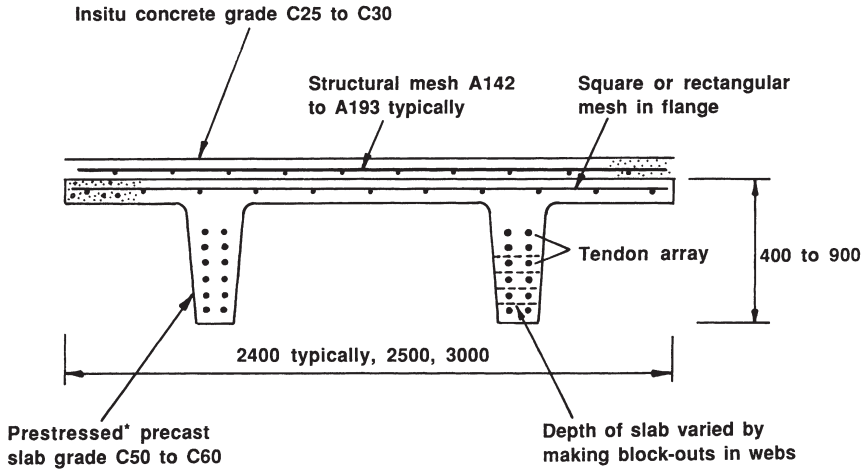

(b) * may be rc grade C40

Figure 5.1 Types of precast concrete flooring: (a) hollow-core slab; (b) double-tee slab; (c) beam and block; (d) solid composite plank; (e) beam and composite plank.

Hollow-core floors may be used without a topping screed, because the individual floor units are keyed together over the full surface area of their edges. Thus vertical and horizontal load transfer is effective over the entire floor area and the units are classified, in accordance with Section 4.3.1 of this document, as non-isolated. This is not the case with all the other types of precast floor, where a structural (i.e. containing adequate reinforcement) topping must be used either for horizontal load transfer, flexural and shear strength, or simply to complete the construction.

More than 90 per cent of all precast concrete used in flooring is prestressed. The slabs are designed in accordance with BS EN 1992-1-1 [5.1] or BS 8110 [5.2] and other selected literature produced by I.Struct.E [5.3], BCA [5.4], FIP [5.5, 5.6], CEN product standards [5.7–5.11], British Precast [5.12], PCI [5.13] and individual research (e.g. [5.14–5.17]).

All slabs are designed as single spanning. Lateral load distribution perpendicular to the span is only permitted if the longitudinal joint is capable of transmitting a shear stress of 1 N/mm^2. This is not

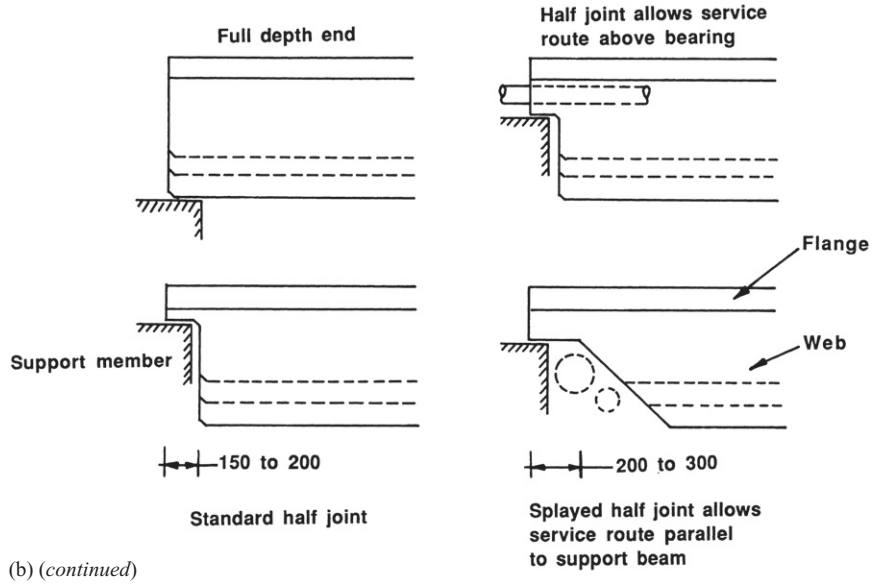

(b) (*continued*)

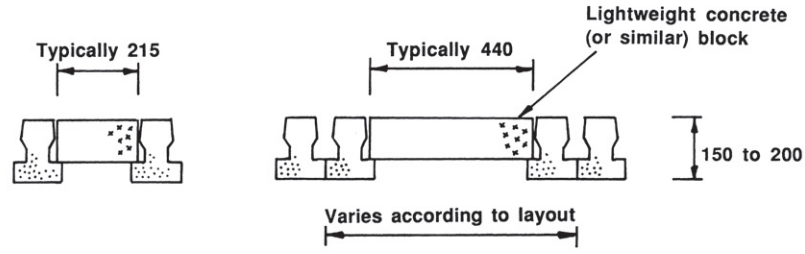

(c)

Figure 5.1 (*Continued*)

possible with unscreeded beam-and-block floors, but in the case of hollow-core slabs loads may be distributed across several slabs. Heavy point loads or line loads are distributed over at least three individual slabs. See Section 5.2.7 for further details.

Figure 5.2 shows, diagrammatically, the five different limiting design criteria for the capacity of flooring units. These are, from short to long spans, respectively:

- bearing capacity
- shear capacity
- flexural capacity
- deflection limits
- handling restriction.

Shear is usually critical only in very short (e.g. < 3 m) or heavily loaded spans, particularly where large line loads (e.g. > 100 kN/m) are present.

Thus for each type of floor slab a family of standardised cross sections and reinforcement patterns to cover the widest possible combination of floor loading and spans is produced. A computerised output is submitted, as the standard calculations are easy to commit to software. Section sizes are selected at incremental depths, usually 50 mm, and a set of reinforcement patterns is chosen. From

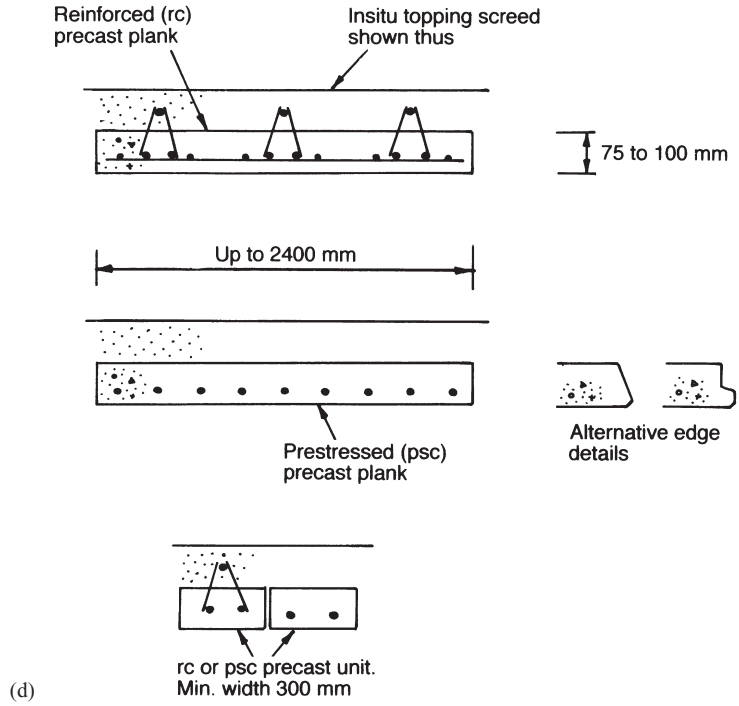

(d)

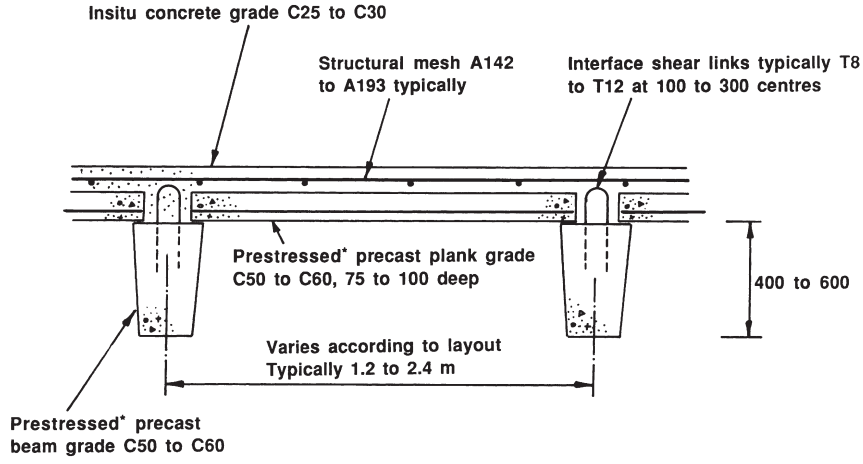

(e) * may be rc grade C40

Figure 5.1 (*Continued*)

these data a predetermined set of bending moment and shear force capacities is compared with project design requirements. Usually the engineer has at least two, and sometimes three, different depths of unit to choose from. The most economical choice is usually the shallowest and most heavily reinforced unit, although unacceptable deflections may rule this one out. The additional advantage is that the structural floor zone is then kept to a minimum.

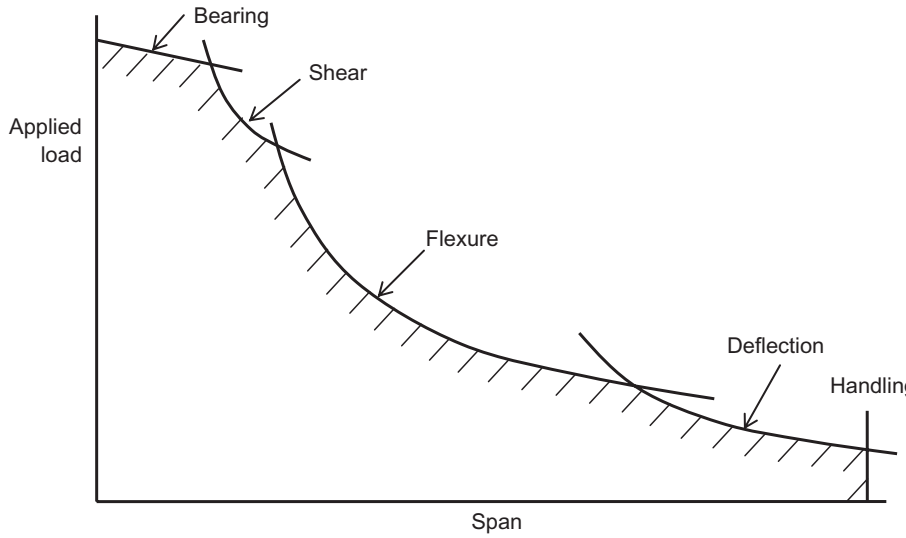

Figure 5.2 Load versus span criteria for prestressed concrete flooring.

Although cambers and deflections are easy to calculate, actual measurements are smaller than calculated values by up to 25 per cent. This is because of unreliable data for Young's modulus and variations in material properties due to temperature and humidity fluctuations throughout the casting, curing and manufacturing cycle. The precamber should not exceed span/250. Deflections are usually critical where the span-to-depth ratio is more than 40:1.

5.2 Hollow-core Slabs

5.2.1 General

A general introduction to hollow-core slab units (hcus) is given in Section 3.2.2.1. They are available as either reinforced or prestressed concrete units. The span-to-weight ratio is better in a prestressed slab, but the unit is less versatile when it comes to forming cantilevers, dealing with point loads, or reinforcing around large holes, etc. Although the cross sections and versatility of these units vary widely, the differences are largely due to the manufacturing process.

There are two main proprietary types:

- Type A hcus, with oval or non-circular voids, shown in Figure 5.3, are produced by the slip-forming technique. Compaction is by vibration, often in two or three layers, and the machine is pulled by an external cable and winch.
- Type B hcus, with mainly circular voids, shown in Figure 5.4, are produced by the extrusion technique. Compaction is by pressing and vibrating the concrete behind the point of delivery, and the machine pushes itself forward from the rear thrust.

The manufacturing process is shown in Figures 5.5 and 5.6. The concrete is a dry mix with zero or very low slump [5.18]. The water/cement ratio (w/c) for extrusion is about 0.36, but some extra water is used to flood the casting bed in front of the machine so that the local $w/c = 0.6$, as shown in Figure 5.7. The w/c for slip forming is about 0.42. Coarse gravel or crushed limestone aggregate graded 10 mm

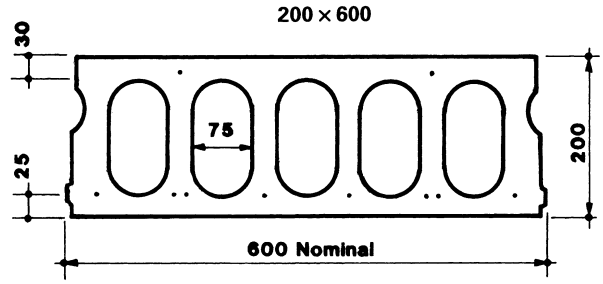

Figure 5.3 Types of hollow-core units – Type A: slip-formed with non-circular voids.

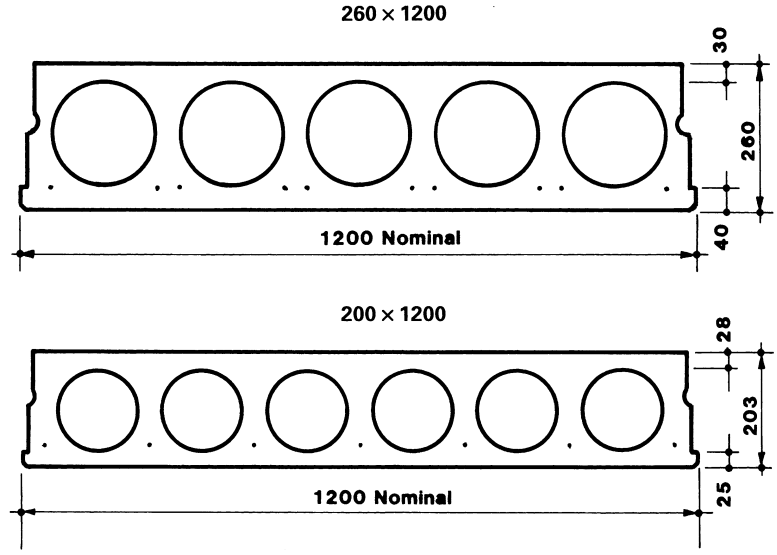

Figure 5.4 Types of hollow-core units – Type B: extruded with circular voids.

to 4 mm or 14 mm to 4 mm is used, together with medium-grade sand of crushed gravel or limestone. Lightweight aggregates are not used because of the excess wear on the machinery, and because the density of aggregate required to achieve the necessary strength is quite high. Recycled concrete, crushed down from waste production to 10 mm aggregate, is used at not more than 9 per cent of the total aggregate content. Addition of short steel fibres to the mix may be considered, to improve concrete toughness and bonding performance.

The positions of the tendons, for both vertical cover and side cover to cores, is controlled by a set of guides, sometimes called 'soldiers', as shown in Figure 5.7. Tolerances for the vertical positions of strands are given in BS EN 1168 [5.8] as 10 mm for units of depth to 200 mm (15 mm for greater). Unfortunately, horizontal tolerances are not given. BS 8110, Part 1, clause 8.6 recommends ±5 mm horizontally.

Type A units are slip-formed by feeding concrete around steel formers. A profiled form is moved during placement and the concrete is vibrated around these forms without too much pressure. Figure 5.5 shows the operation by using the 'Roth' technique. The machine lays the concrete in three layers – the bottom flange, the webs and the top flange. The shape of the former is designed to give the optimum flexural and shear performance, as well as providing adequate cover to the reinforcing tendons.

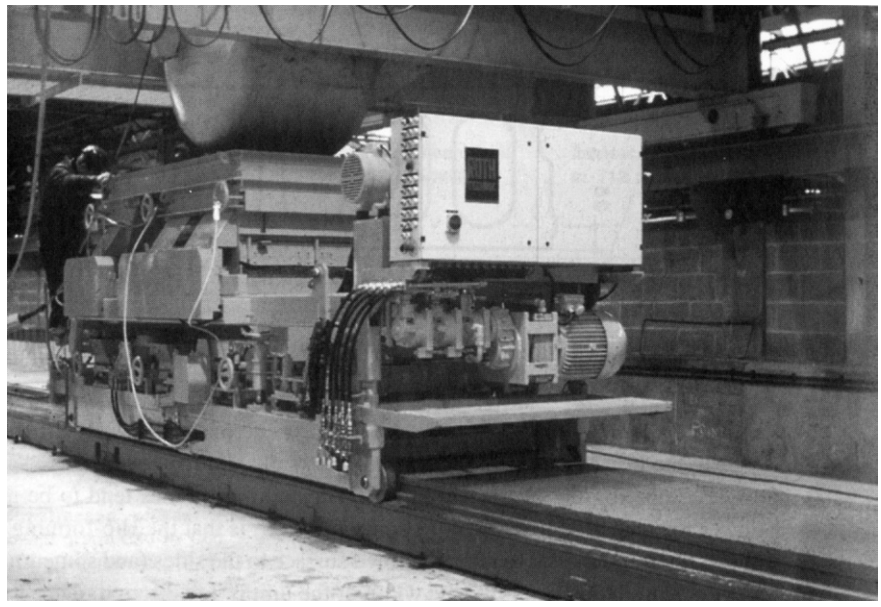

Figure 5.5 Production of hollow-core slab – the slip-forming machine.

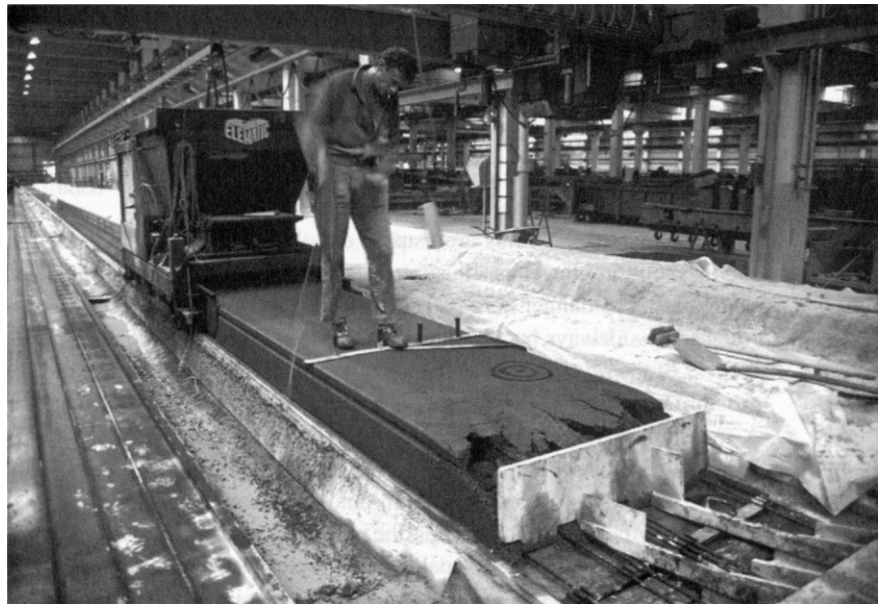

Figure 5.6 Production of hollow-core slab in Belgium.

In the extrusion process the concrete is pressed out by screws during compaction into the required cross section. Figure 5.8 shows the result of the extrusion technique; handling takes place within 12 hours of casting. The voids are circular in profile, with the result that in order to optimise the cross-sectional properties of the slab, the thickness of the web at the mid-height of the voids is usually only about 30 mm.

In comparing the two techniques, slip-forming machines tend to be noisy but have lower maintenance costs. One problem, however, is that the slip-forming machine may move forward in jerks,

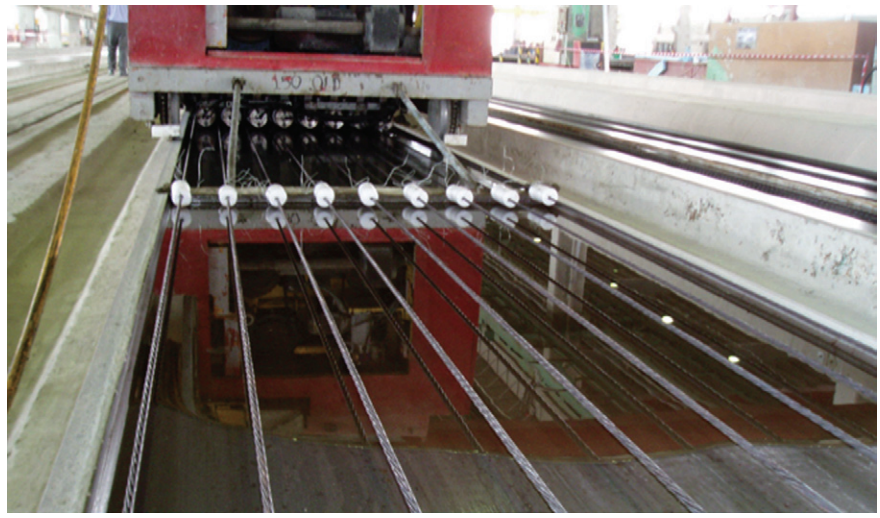

Figure 5.7 Production of hollow-core floor unit showing pooling of water in front of the machine, and guides to control the cover to the strands.

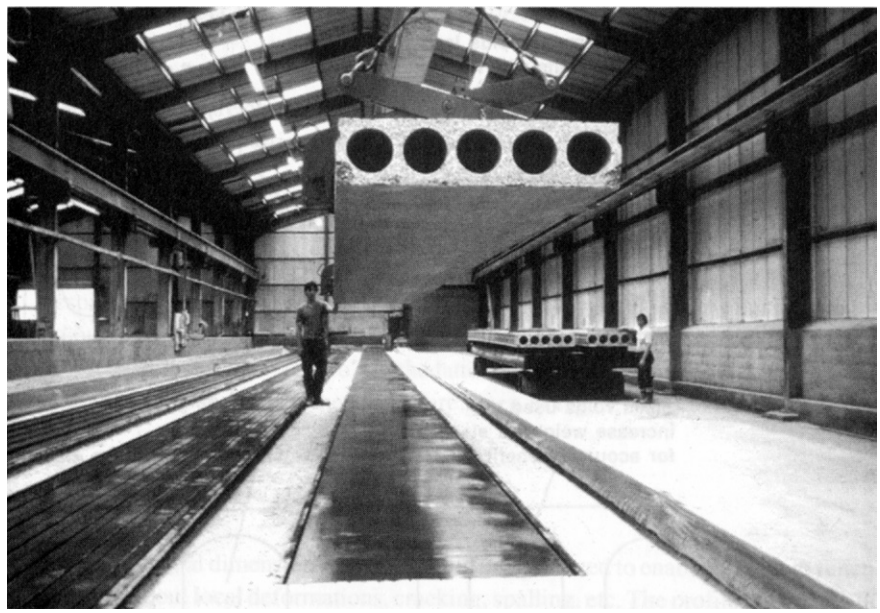

Figure 5.8 Production of hollow-core slab – extrusion through helical screws.

leaving a rippled surface to the sides (and sometimes the tops) of the units, with the result that the width of the unit is 2 mm to 3 mm too large. Ironically, this profile may actually improve the horizontal diaphragm capacity of the floor slab. New investors in hollow-core machinery seem to prefer the slip-forming process, although the extrusion process gives a better finish and is more dimensionally accurate.

Wet-cast units are manufactured both as prestressed and reinforced, in depths from 150 to 250 mm, and are dealt with in Section 5.2.16. One solution is the reinforced hcu shown in Figure 5.9, which provides an excellent solution for spans of around 4–6 m for depths of 150 and 225 mm in domestic

Figure 5.9 Reinforced hollow-core units suitable for medium spans in domestic use.

use. Perhaps less versatile for cut-outs and holes, it is a serious competitor to beam-and-block flooring thanks mainly to its speed and simplicity of erection.

Cross section, concrete strength, fire resistance and surface finish are standard to each system of manufacture. Small variations, which may be included at an extra cost, should be discussed early in the design appraisal. These include increased fire resistance, provisions for vertical service holes, opening of cores for special fixings, cut-outs at columns, etc.

The edges of the slab are profiled to ensure that an adequate shear key of *in situ* concrete (10 mm size aggregate), rather than grout, is formed between adjacent units. The manufacturing process is not sympathetic to providing projecting reinforcement across the joint. The capacity of the shear key between the units is sufficient to prevent the adjacent slabs from differential movement. Despite a slight roughening of the surfaces during the manufacturing process, where indentations of up to 2 mm are present, the surface is classified in BS EN 1992-1-1, clause 6.2.5 [5.1] and BS 8110, Part 1, clause 5.3.7 [5.2] as 'smooth', as opposed to being 'rough'.

5.2.2 Design

Hollow-core slabs are designed as a series of I-sections with semi-circular or parallel-sided webs. The concrete is usually grade C40/50 (for slip-forming with a higher *w/c* than for extrusion) or C50/60. The section is structurally very efficient and the design is well documented [5.5]. The maximum practical span-to-depth ratio is about 55, and the holes guarantee the maximum possible radius of gyration in addition to reducing the self-weight of the slab by 40 to 50 per cent.

The shapes of the voids are usually circular, oval, or parallel-sided with triangular and/or semi-circular ends, illustrated in Figure 5.10 from various manufacturers' product catalogues. The danger here is that the webs become slender and have been known to collapse by sideways buckling in 300 mm-deep units, although the problem is rare owing to the dryness of the mix. There is a tendency for manufacturers to make the voids as large as possible for obvious reasons: less concrete and improved performance-to-weight ratio. A measure of this latter parameter is expressed in terms of the radius of gyration ($r = \sqrt{I/A}$) for the section. Table 5.1 gives approximate data for a range of extruded (e.g. former 'Spiroll') and slip-formed (e.g. 'Roth' and 'Elematic') units. The 'Roth'-type units

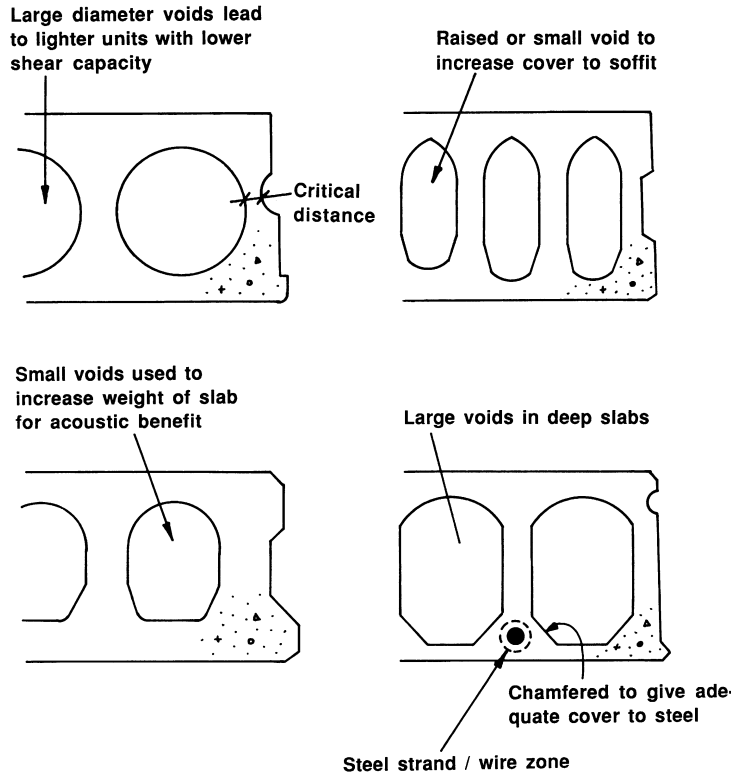

Figure 5.10 Shapes of voids and edge profiles in hollow-core units.

Table 5.1 Some section properties of hollow-core slabs per 1.2 m width

Type of Unit	Depth (mm)	Second Moment of area $I \times 10^6$ (mm^4)	Cross-sectional area $A \times 10^3$ (mm^2)	Radius of gyration r (mm)
Extruded	400	4950	247	142
	320	2500	190	115
	250	1290	170	87
	200	635	127	71
	150	295	117	50
Slip-formed 'Roth'	300	2130	215	100
	250	1270	183	83
	200	670	151	66
	150	300	123	49
Slip-formed 'Elematic'	400	4405	224	140
	350	3115	207	123
	300	2080	190	105
	250	1270	168	87
	200	700	152	68
	150	305	123	50

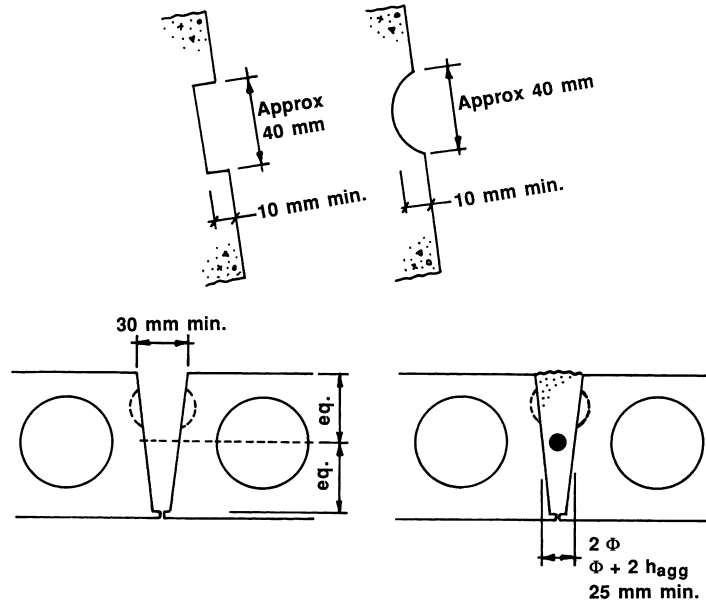

Figure 5.11 Rules for determining the size of the longitudinal joint between units.

(other proprietary names exist) usually contain 11 cores and tend to have a greater cross section (except for 150 depth), and hence lower radius of gyration than those units with fewer larger cores.

Owing to the absence of stirrups, the minimum web thickness is governed by limitation of the tensile stresses due to either spalling upon release of prestress from the tendons to the concrete, or by shear. The maximum spalling stress is the criterion, with a resulting web thickness of 30 mm, giving a total web-to-unit-breadth ratio of between 0.25 and 0.35.

The rules for the size of the longitudinal gap are shown in Figure 5.11. They are based on the premise that tie steel might be placed in the joint. FIP Recommendations [5.5] for edge profiles are also included in Figure 5.11.

Although in 95 per cent of cases a mid-span flexural failure is more likely at ultimate limit state, much attention is devoted to the shear capacity of hollow-core slabs. The reasons for this include:

- shear failures are catastrophic due to an absence of stirrups, and
- shear behaviour, particularly in the transmission zone, is not fully understood.

Design is carried out to the normal prestressed concrete methods in BS EN 1992-1-1 or BS 8110, but the level of prestress in the transmission zone is often obtained from the FIP Recommendations [5.5].

In spite of the large number of proprietary dry-cast units available, the two major types are distinguishable only in the shape of the voids – circular or oval. In the former group are 'Spiroll', 'Flexicore' and 'Tembo', while in the latter are 'Roth', 'Dynaspan' and 'Spancrete'. Although depths vary from 100 to 750 mm, the common range is 150 to 400 mm.

Typical load-versus-span data for these units are given in Figure 5.12 for two cases of exposure, limiting tension and load factors. Internal exposure class XC1 may use limiting tension f_{ctm} in the soffit with the full service load. External exposure class XD1 is limited to zero tension in the soffit, but may use the frequent imposed load $\psi_1 Q_k$, where $\psi_1 = 0.5$ in this figure. Because of the three sets of load combination factors in BS EN 1992-1-1, namely ψ_0, ψ_1 and ψ_2, together with the requirements of EC1, Eq.s 6.10(a) and 6.10(b), the critical loading and limiting capacity is changing for the range of imposed loads.

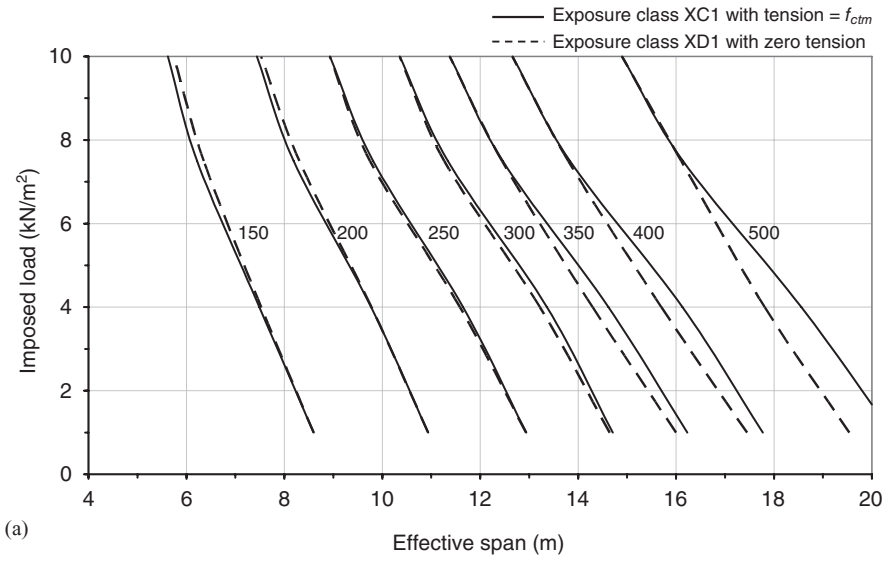

(a)

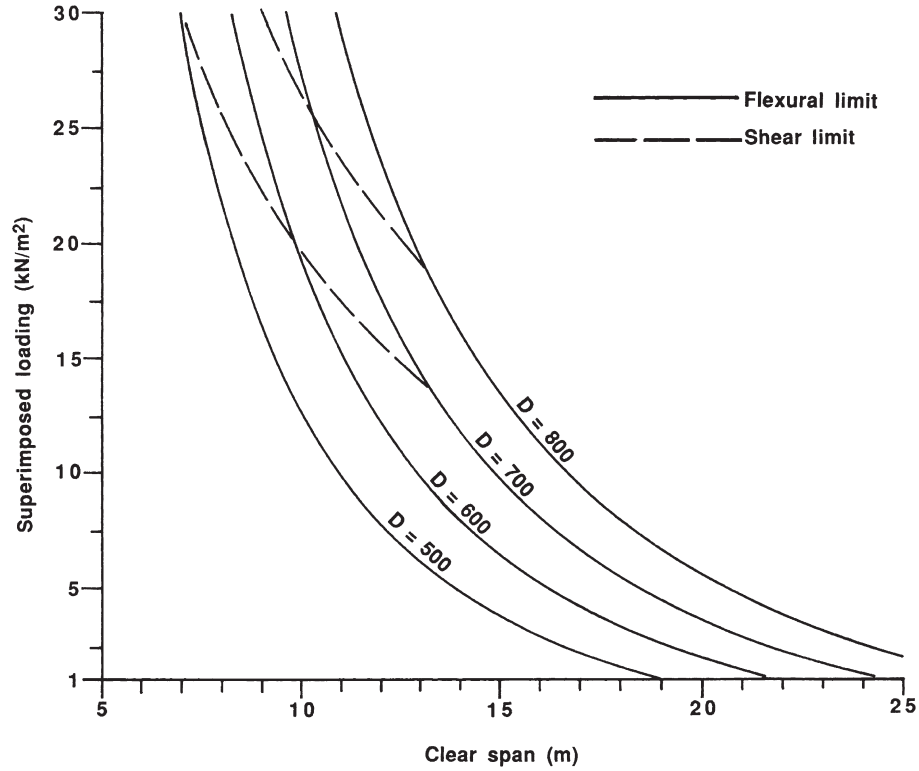

(b)

Figure 5.12 (a) Imposed load versus effective span for prestressed hollow-core units for two different conditions of exposure and limiting tension. (b) Superimposed load versus clear span for double-tee units.

For imposed loads of less than about 4.0 kN/m^2 and unit depth less than 300 mm, the limiting span criterion is deflection and is therefore sensitive only to changes in ψ_2. This explains why the limiting span is unaffected by the exposure conditions. However, at greater depths the criterion changes from deflection to service moment of resistance, such that there is a reduction in load-bearing capacity of about 10–15 per cent, or a reduction in span of about 0.5 m. For imposed loads greater than about 7.5 kN/m^2 the limiting span criterion is ultimate moment or shear capacity, which also explains why the limiting span is unaffected by the exposure conditions. In between, the limiting span criterion is service moment of resistance, but the balance between dead and live load is such that the net effect of losing the permissible tension f_{ctm} and the reduced live load $\psi_1 Q_k$ cancels out.

5.2.3 Design of cross section

The cross-sectional dimensions of hcus should be optimised to enable each unit to function in service without local deformations, cracking, spalling, etc. The profile must also allow for the concrete to be correctly placed, compacted and cured uniformly. The geometry of the unit includes size, shape and spacing of voids, web thickness, depth of flanges, concrete cover to tendons, and edge profile.

Although the size and shape of the voids depend on the manufacturing process, some general rules as regards size and spacing of voids may be given. The height of voids should not exceed $h - 50$ mm, where h is the overall depth of the unit. The minimum flange thickness h_f is given in BS EN 1168, clause 4.3.1.2 [5.8] as not less than the largest value of 17 mm, d_g (coarse aggregate size) + 5, or $\sqrt{2h}$, where h is the overall depth of the unit h. This gives 23 mm for a 250 mm-deep unit, etc. However, the upper flange is controlled by the shape of the top of the core, and should be at least 0.25 b_c, where b_c is defined in Figure 5.13. This rule is intended to prevent wide and shallow flanges, and is rarely critical, e.g. a semi-circular-shaped core of say $r = 60$ mm radius, $h_f = 6$ mm, and for $r = 200$, $h_f \geq 20$ mm, and therefore the practicalities of specifying a top flange thickness that will not collapse is about 30 mm. However, it is usually necessary for the bottom flange to be at least 30 mm thick because of cover requirements. The width of the void (i.e. clear distance between webs) is governed by the maximum stresses that may develop in the transverse direction. To prevent localised collapse of the flange, the ratio of the width of the (non-circular) void to flange depth is about 3:1 or 4:1.

5.2.4 Web thickness

The critical region is near the ends of the units, where web thickness is governed by the limitations in the tensile stress capacity of the concrete at the onset of the transfer of prestress to the concrete. These stresses manifest themselves in spalling, splitting and bursting of the concrete in what is known as the 'transmission zone'. This is shown in Figure 5.14 as distance l_{pt} {l_t}. Although the most important

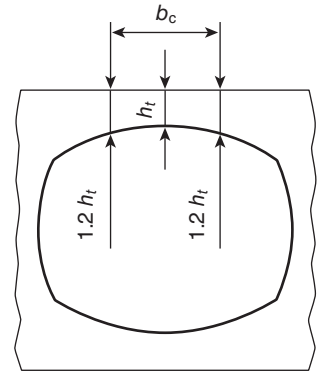

Figure 5.13 Minimum thickness of top flange of hollow-core units according to BS EN 1168 [5.8].

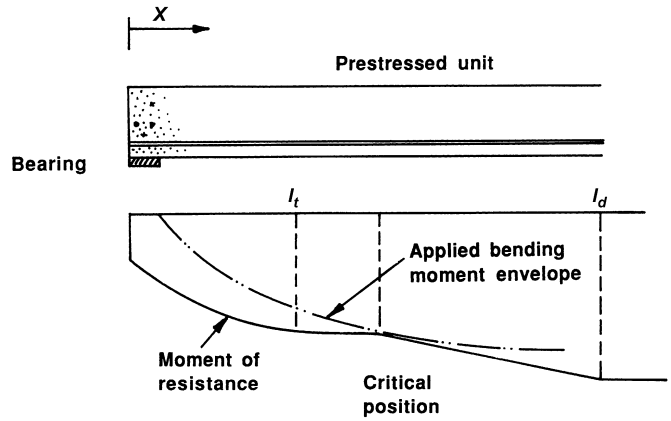

Figure 5.14 Development and anchorage lengths of helical strand in hollow-core units.

of these is the splitting due to bond failure around the prestressing tendon, spalling in the webs must be avoided by following some fairly comprehensive design rules by Den Uijl [5.19], as adopted in BS EN 1168, clause 4.3.3.2.1 [5.8]. Den Uijl's research was applicable to hcu < 400 mm deep, but this is not mentioned in BS EN 1168. (Note that 'spalling' is the term used in BS EN 1168 for what is really splitting due to lateral tension around the ends of the tendons. Spalling is when concrete breaks up, flakes, or becomes pitted; however, the code uses this term to distinguish between other splitting cracks and so it will be used in this context.)

Figure 5.15(a) defines the terminology used to determine the spalling (or vertical splitting) stress σ_{sp} according to BS EN 1168 [5.8] shown in Figure 5.15(b) in terms of the prestressing force P_0, transmission length $l_{pt1} = 0.8\, l_{pt}$ and cross-sectional geometry eccentricity e_o, depth h, web breadth b_w, and k (the so called 'core distance') = $I/0.5\,hA$, defined in Fig 5.15(a). Designers of hollow-core sections show that the resulting value of σ_{sp} is less than the tensile strength of concrete at transfer $f_{ct(t)}$ on the basis of tests. However, spalling is not easily predicted by simply calculating σ_{sp}. It is significantly affected by mix design (cement type, fine aggregates), detensioning rate, prestress level (when f_{bc} is greater than about 14 N/mm^2), bond slip and transmission length, and the environmental conditions during curing. However, for an initial estimate, a typical value for $f_{ct(t)}$ is about 2 N/mm^2 for f_{ck} = 30–35 N/mm^2 after 16 to 20 hours curing.

The usual result for the breadth of the web for a grade C50/60 concrete in fully stressed units of up to 300 mm in depth is a minimum b_w = 30 mm. The minimum web thickness is given in BS EN 1168, clause 4.3.1.2 [5.8] as not less than the largest value of 20 mm, d_g (coarse aggregate size) + 5, or h/10 where h is the overall depth of the unit. This gives 25 mm for a 250 mm-deep unit, etc.

Excessive prestressing (the result of trying to increase the strength capacity along the length of the unit) in these relatively thin regions has resulted in horizontal cracking along the length of the unit due to shear-compression. The cracks propagate from the ends of the units with the appearance of a crocodile's mouth; hence the term 'crocodiling' was coined. Thicker webs, greater than 30 mm, mostly prevent this from happening, although excessive prestressing and poor control of fine-aggregate grading can still cause problems in some deeper units.

5.2.5 Edge profiles

Standard edge profiles have evolved to ensure an adequate transfer of horizontal and vertical shear between adjacent units. The main function of the joint is to prevent relative displacements between units. In hcus these objectives are achieved using structural-grade *in situ* concrete (C20/25 minimum), compacted by a small-diameter poker in dampened joints. Typical profile geometries are specified in BS EN 1168, Annex B [5.8] and shown in Figure 5.11. Some shallow units, e.g. 110 mm deep,

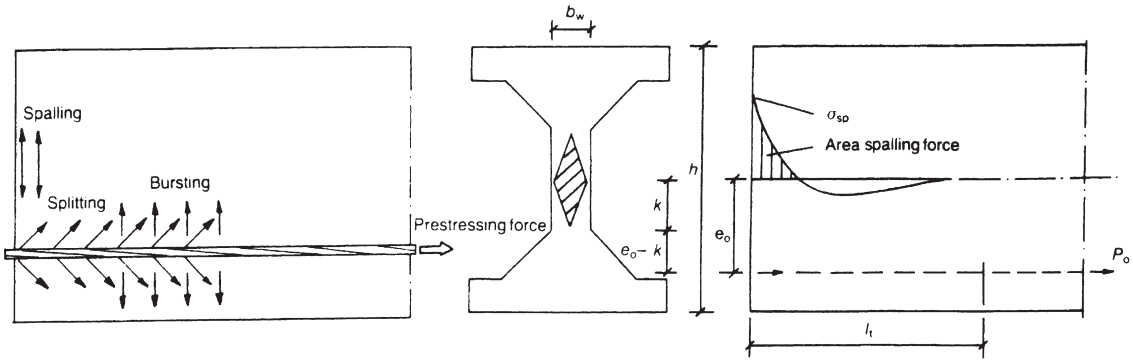

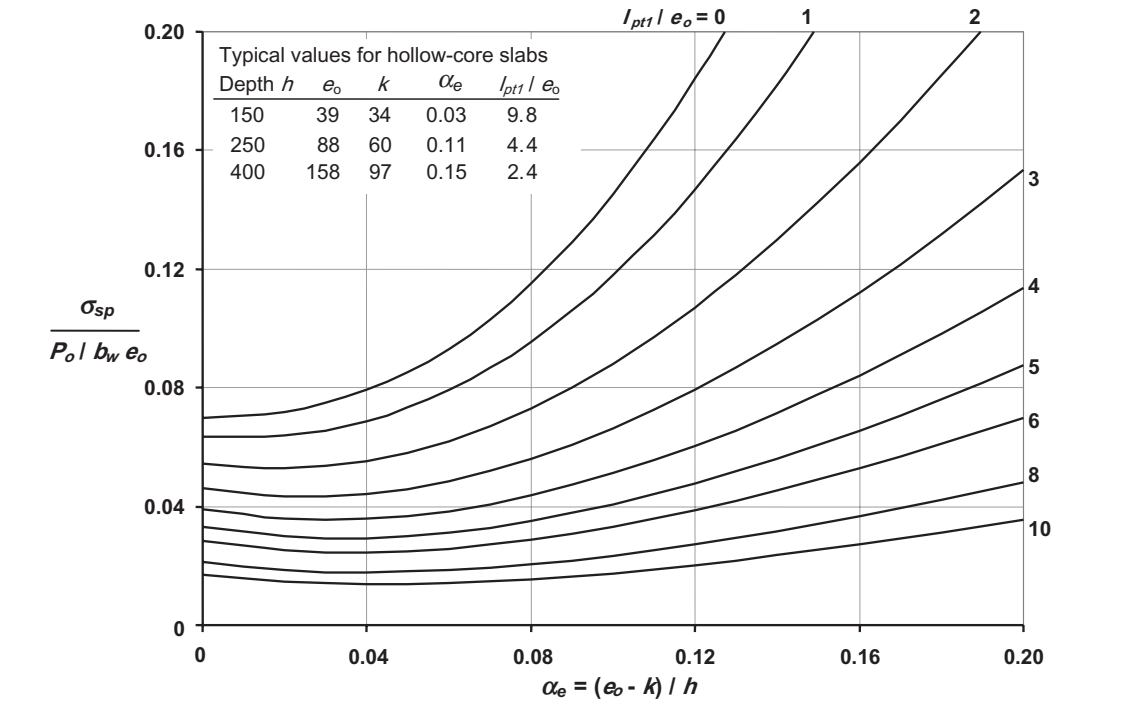

Figure 5.15 Spalling (or vertical splitting) stresses according to BS EN 1168 [5.8].

struggle to have a 35 mm shear key and may be made only 20–25 mm deep, yet still perform adequately in tests.

The sides of the units have natural random roughness, with indentations up to 2 mm in depth. The design ultimate horizontal shear stress, given in BS EN 1992-1-1 for the type of joint conforming to Figure 5.11, is 0.25 N/mm^2, {BS 8110 value is 0.23 N/mm^2}. For a typical 6 m long, 200 mm deep unit, V_{uh} > 275 kN; a value which is rarely critical. Vertical shear capacity is based on single castellated joint design with minimum root indentation 40 mm × 10 mm deep. An ultimate shear stress of 0.5 N/mm^2 for this indented surface yields an ultimate shear resistance equivalent to 45 kN/m^2 floor loading for 1.2 m wide units.

If reinforcing bars are placed in the joint, the joint should be wide enough at the level of the bar to enable *in situ* concrete to be compacted around the bar. This should not be less than 25 mm if

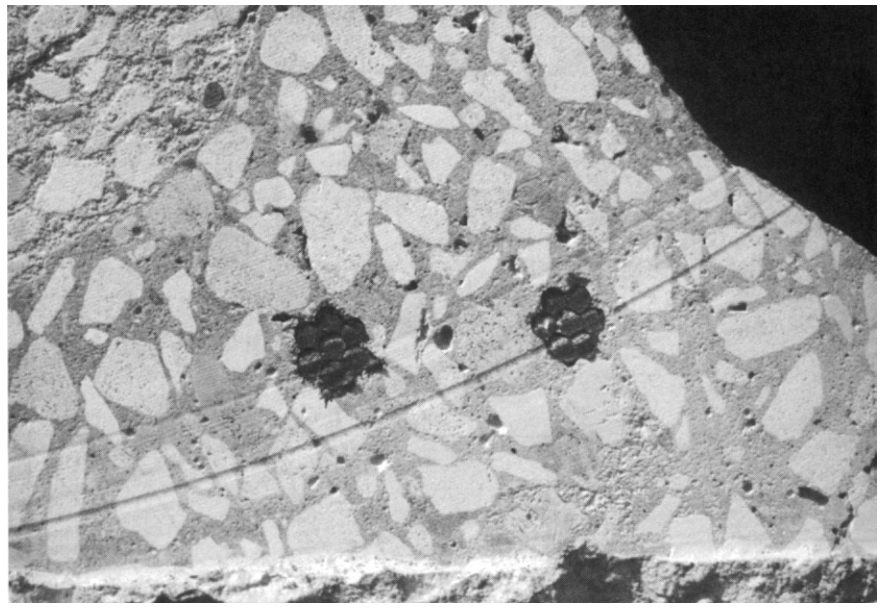

Figure 5.16 Close-up of helical strand in hollow-core units.

10 mm maximum size of aggregate is used. The diameter of the bar should not be greater than half the gap width.

5.2.6 Reinforcement

Hollow-core units have, in general, no reinforcement other than longitudinal prestressing tendons (helical strand or wire) anchored by bond. It is therefore desirable to take advantage of the tensile strength of concrete in the determination of M_{sr} and $V_{Rd,c}$ $\{V_{co}\}$.

The low-relaxation (class 2) strand is of the 7-wire helical form, and the wire is crimped or plain according to the specification given in Section 4.2.4. Test certificates for the ultimate tensile strength are available from all manufacturers. Stressing is restricted to between 65 and 75 per cent of the characteristic strength. Tendons are exposed at the ends of the member, as shown in Figure 5.16. The slippage (or pull-in) of the tendon should be between 1 and 2 mm. If it is greater than this, see Section 5.2.12 for further analysis. The slippage of the tendon is measured using a depth gauge.

The percentage area of steel is relatively small, particularly in comparison with a reinforced section of comparable flexural capacity. The steel ratio $\rho = A_{ps}/bd$ varies from 0.10 to 0.25 per cent in most of the units manufactured in the UK. The failure mode for these slabs is excessive deflections, flexural cracking in the soffits and, finally, rupture in the tendons.

5.2.7 Lateral load distribution

The question often arises of whether hcus can safely distribute line and point loads to adjacent units, and to what extent a slab 'field' exists, due to compressive membrane action and shear interlock.

Patch loads and line loads parallel with the direction of span give rise to bending moments in a direction at right angles to the direction of span, and to vertical shear forces in the longitudinal joints between adjacent units. Similar situations occur where steel trimmer angles are used to frame out large floor voids. The problem is that hollow-core floors are not provided with transverse reinforcement in the precast units or in the joints between the units. Load transfer depends on adhesion, bond

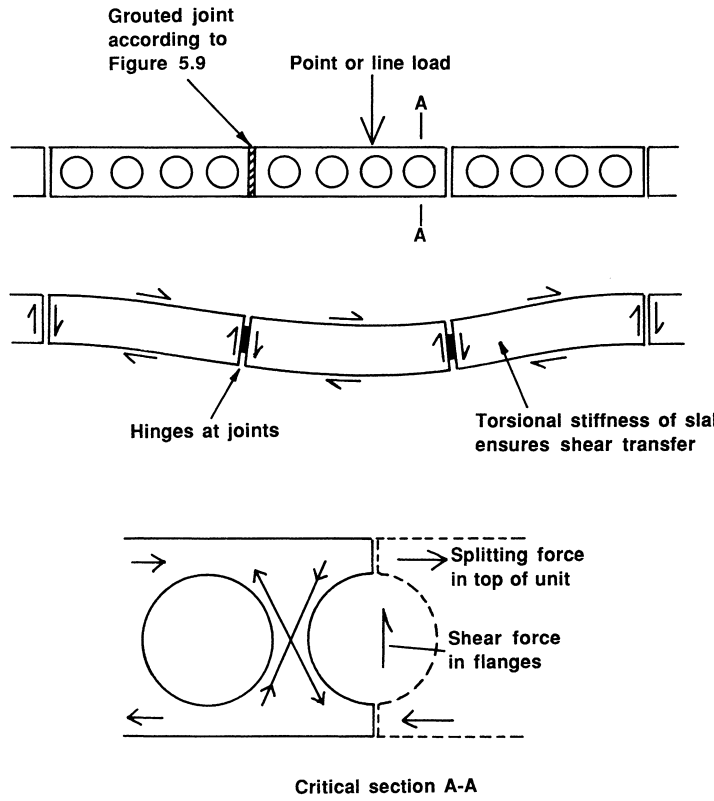

Figure 5.17 The torsional hinge concept to lateral load distribution in one-way spanning elements.

and friction in the shear key between the units, and the possible shear-torsion failure of the hcu is likely to be sudden and without warning.

Although the behaviour of thin-plate floors is well understood, the behaviour of hollow-core slabs is complicated by the partial moment interaction between adjacent units. The joints between adjacent units behave as hinges, capable of finite moment and full shear transfer. However, the former is not well understood and relies extensively on the quality of the infill grout. In the interest of safety the moments are ignored. The point or line load in Figure 5.17 produces a shear reaction in the longitudinal edge of the adjacent units, and this induces torsion in the slab. The capacity of the hollow-core slab to carry the torsion is limited by the tensile capacity of the concrete. The magnitude of the shear reaction depends on the torsional stiffness and the longitudinal and transverse stiffnesses of all the adjacent slabs. Low stiffnesses result in low load sharing. The precast units themselves may be assumed to be cracked longitudinally in their bottom flanges, but shear friction generated by transverse restraints in the floor grillage ensures integrity at the ultimate state. The deflected profile of the total floor slab is computed using finite strips and differential analysis. The cross section of each floor element is considered as a solid rectangular element and the circular (or oval) voids are ignored. The result is unconservative and therefore reduction factors are applied to the shear reactions.

The transverse moments and shear forces may be distributed (in accordance with BS EN 1992-1-1, clause 10.9.3(5) [5.1] and BS 8110, Part 1, clause 5.2.2.2 [5.2]) over an effective width equal to the total width of three precast units, or one-quarter of the span either side of the loaded area, plus the width of the loaded area. If a composite topping is used, the spreading width is 4 units. If a free edge interrupts these distances, the spreading width is the lesser of the edge distance or 1½ (or 2) unit widths. The equivalent uniformly distributed loading on each slab unit may thus be computed. This

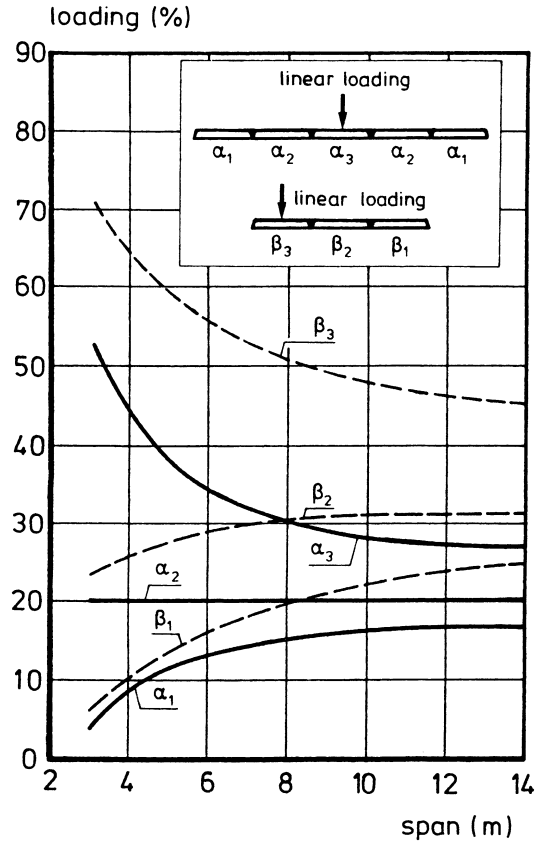

Figure 5.18 Lateral load distribution coefficients for a central load [5.5].

is a conservative approach, as data given in BS EN 1168, Annex C, Figure C.1 [5.8] (previously given in FIP Recommendations [5.5] and reproduced here in Figure 5.18 following the work of Van Acker [5.20]) show that up to five units are effective for spans exceeding 4 m. The data are based on the theory of elasticity for service loads, noting that at ultimate limit state, the load on the directly loaded unit is multiplied by 1.25, and the total share on to the other units is decreased by the same amount, depending on the coefficient, such that the total ultimate load does not change.

Data in Figure C.2 (reproduced in Figure 5.19) show that for edge elements, e.g. adjacent to a large void, only three units, α_1 to α_3, contribute significantly in carrying the load. If the load is acting at an edge distance between 0 and 2½ units (≤3.0 m) from a free edge, linear interpolation may be used (see later example). If the distance from the load to a free edge is less than 2½ unit widths, BS EN 1168 Annex C (Figure C.5) provides reaction coefficients to an edge support such that the net effect of a line load less than 3.0 m from the edge of a three-side supported slab may be determined. The reaction force is then distributed into the units according to Figure C.1 as a negative edge load (see example later). When using Figure C.5, the contractor must ensure that a full and effective edge bearing is provided, particularly in the long term when the negative deflection effects of creep may lift the hcu from the bearing in places and render the reactions null. Note that the coefficients in these charts are based on moment distributions, and are not applicable to spreading of shear forces due to point loads, as shown in Figure 5.20 of data by Lundgren *et al.* [5.21], who tested a slab field comprising five 1.2 m wide hcus subjected to a point load at mid-span. The analysis was carried out using idealised 'beams', which represented the bending and torsional stiffness of each hcu, and finite element 'shell' elements. Lateral load distribution factors were confirmed for bending moments (shown in

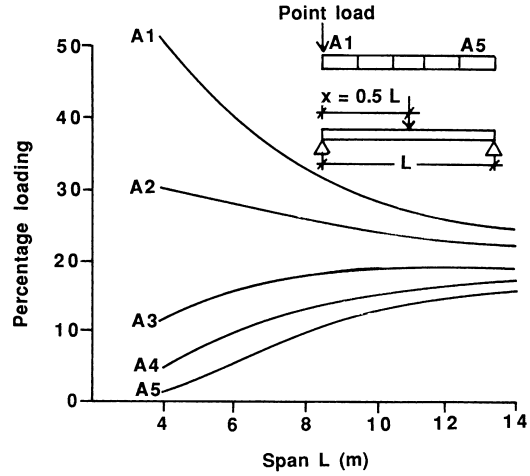

Figure 5.19 Lateral load distribution coefficients for an edge load [5.5].

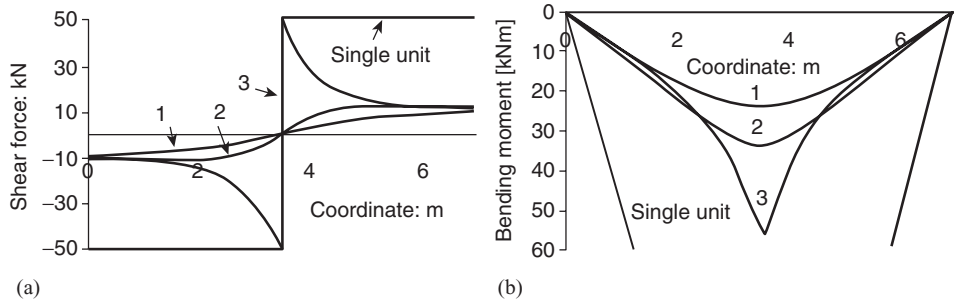

Figure 5.20 (a) Shear force diagrams and (b) bending moment diagrams, for a point load at mid-span for hollow-core units in a slab field by Lundgren *et al*. [5.21]. Line 1 is for the loaded hcu, line 2 for the adjacent hcu, and line 3 beyond. (Courtesy of fédération internationale du béton (*fib*), www.fib-international.org, and ICE Publishing.)

Figure 5.21(a)), but not for shear forces at supports (shown in Figure 5.21(b)). However, for the important units α_3 and α_2, the coefficients for shear force are lower than those for bending, and so the latter may be used conservatively for bending and shear. The coefficients for α_1 are small and would not be critical in a slab field unless α_1 and α_3 were combined, and then the loss of accuracy would be very small.

As an example from BS EN 1168, a wall load of 20 kN/m acts along an hcu of span 6.0 m, and is 3.0 m (2.5 b) from an edge support. The net load on the loaded unit is obtained as follows: from Figure C.1, using the load portion (curve 5), $\alpha_3 = 0.26$. From Figure C.5, the reaction under unit α_1 is $R = -0.34$. From Figure C.1 the distribution factor of R (curve 4) $\alpha_1 = 0.40$. The net coefficient $\alpha_1 = 0.26 - 0.34 \times 0.40 = 0.124$, or $w = 0.124 \times 20 = 2.48$ kN/m. If the load is more than 4.5 b from the edge support, $w = 0.26 \times 20 = 5.2$ kN/m. Repeating the example for the edge unit, the net coefficient will be $\alpha_1 = 0.15 - 0.55 \times 0.40 = -0.07$, or $w = -0.07 \times 20 = -1.4$ kN/m (negative load).

The author has observed that the effect of three supporting edges, together with negative end restraint from tie bars, considerably reduces deflections in hollow-core slab fields. Tested individually to 1.25 times ultimate design load, the mid-span deflections were 15 to 17 mm, but when tested under the same load magnitude in a slab field 8 units wide the maximum mid-span deflections were only 4 to 6 mm. The hollow-core slab field was clearly acting as a two-way slab.

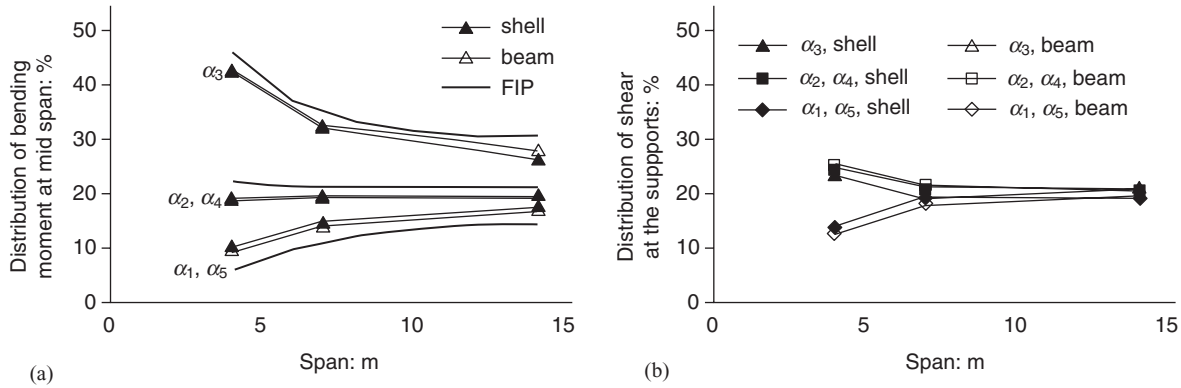

Figure 5.21 Lateral load distribution percentages by Lundgren *et al*. [5.21]: (a) bending moments at mid-span; (b) shear force at supports. The α references are the same as in BS EN 1168 notation. (Courtesy of fédération internationale du béton (*fib*), www.fib-international.org, and ICE Publishing.)

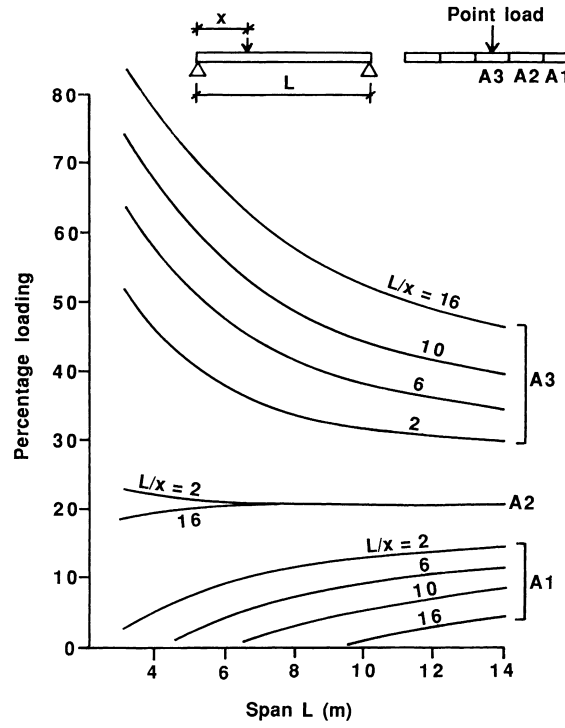

Figure 5.22 Lateral load distribution coefficients for point loads [5.5].

BS EN 1168 does not explain what course of action should be taken for hcu widths of less than 1200 mm, e.g. a 'ripped' unit or a 600 mm manufactured unit; it merely states '. . . the graphs may be elaborated', which is not helpful. The common opinion is to ignore the narrow unit and consider it as a full-width unit if there is only one narrow-width unit in the field; it would be very unusual if all units in a slab field were narrow units.

BS EN 1992 accepts test results to justify exceeding the quarter span criterion quoted above, and this is explicitly called for by BS 8110. This information is not readily available, and therefore bending moment distribution factors, given in Figure 5.22, may be used to show that the effective width is

equal to the width of at least three slabs, irrespective of the position of the load. BS EN 1992-1-1, clause 10.9.3(12) limits the average longitudinal shear stress to 0.15 N/mm^2 when distributing actions between adjoining units.

Some designers of hollow-core find the load distribution charts in BS EN 1168 difficult and cumbersome to use, particularly if there are a number of walls of partial span, or at right angles, crossing several units, etc., and they prefer to use the BS 8110 approach of considering a panel width of 3 (or 4 if composite) units. To BS EN 1168, the total load on the panel width is simply scaled, pro rata to the width of one unit. For example, for a span of 6.0 m, panel width = 2 × 0.25 × 6000 + load width, say, 150 = 3150 mm. If the sum of the line and cross-wall loads and point loads in that panel equates to a bending moment of (say) 40 kNm, the moment per unit = 40 × 1.2/3.15 = 15.2 kNm.

Design rules for determining the lateral distribution of concentrated vertical loads in decks made from hcus were derived using the finite strip method [5.22]. The analysis considered the torsional, shear and flexural stiffness of units up to 1.2 m wide containing circular voids. The longitudinal joint between the units was considered as a rotational hinge with a shear capacity equal to the minimum shear capacity of the precast unit. The results showed that the lateral bending moment, vertical shear and vertical deflection responses were all different; the shear response is the most concentrated around the loaded unit. Because the curves shown in Figure 5.23 for bending moment factors α are closed-form solutions (i.e. require iterations to obtain the final result) and seemingly difficult to handle in design situations, adopting a value of $\mu = 1$ (where μ = ratio of torsional to flexural stiffness of an

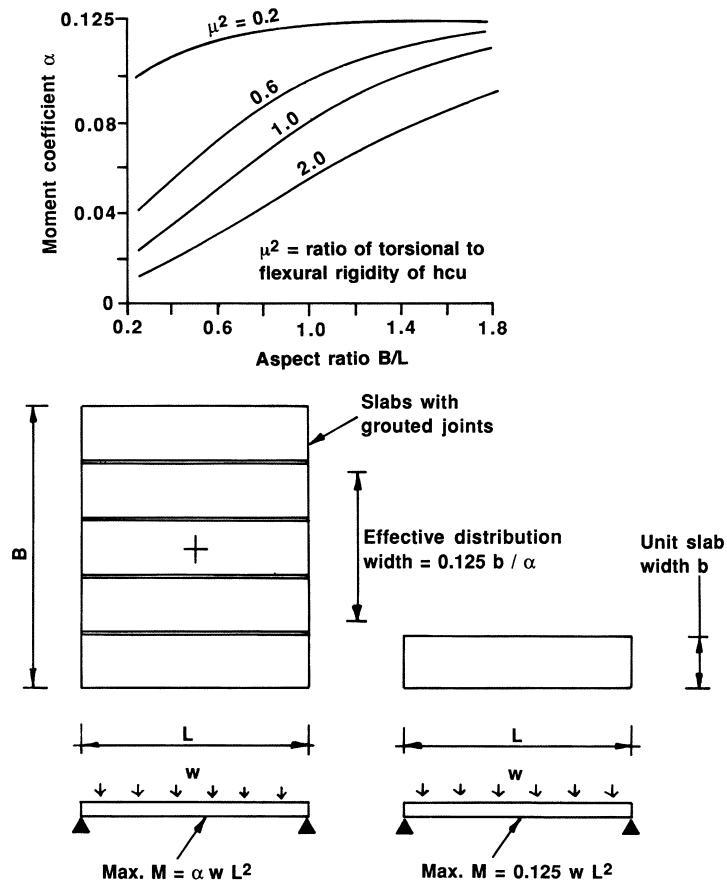

Figure 5.23 Bending coefficients for lateral load distribution [5.22].

hcu) gives a good approximation and enables a realistic value to be assigned to the effective breadth of the slab field = 0.125 b/α.

Stanton [5.23] found distribution widths for bending, shear and deflection resulting from point loads not only near the centre of the floor area, but also close to a free longitudinal edge. This is the effective width over which a point load may be distributed. In summary, Stanton's equations suggest that if a point load is acting at mid-span over a length L, then the distribution width is 0.35L either side of the centre of the loaded unit. If the point load is at 1/4 span, the distribution is 0.28L either side. Applying these results to spans of 6 to 8 m, the loads are being distributed over 5 units of 1.2 m width. These results are in good agreement with the FIP values presented in the figures.

Shear is the most complex response, because the effects of torsion must be separated from vertical shears. The distribution of shear is largely dependent on the separation distance between the load and response positions. Shear distribution widths increase rapidly with this increasing distance, but are seldom greater than 0.125L, and the distribution curve is triangular.

Aswad and Jacques [5.24] tested some 203 mm-deep 'Dycore' units to determine allowable magnitudes for a single point edge load. Two modes of failure, in which the slabs failed without warning, were found:

- by edge punching shear under the load at mid-span
- shear-torsion failure at the corners of the units when the load point was nearer to the support (see Figure 5.24).

With the load point at mid-span the lowest failure load was 51.2 kN, while the lowest failure load for a load point at quarter-span was 44.5 kN. The former failed by punching shear, while the latter was by shear-torsion. Factors of safety of 2.80 ($\approx$1.60/0.85 $\times$ 1.5) were applied to these results, which gave good agreement (within 5 per cent) with the equation in *FIP Technical Report* [5.25].

Lateral spreading of section properties, where holes in units are formed, is not covered in codes of practice or product standards, but may be considered using the same approach for lateral distribution of loads within a panel width = 2 $\times$ 0.25 $\times$ span. First, the section properties $Z_{b,1}$ and prestress $f_{bc,1}$ in the

Figure 5.24 Edge failures in tests by Aswad and Jacques [5.24] (courtesy of PCI Journal).

hcu containing the hole are determined, and the net bending stress calculated for the self-weight (and topping if present) moment M_1 at installation, $\sigma_{b1} = f_{bc1} - M_1/Z_{b1}$. The section properties $Z_{b,2}$ prestress $f_{bc,2}$ of the hcu without holes are calculated, and the mean values obtained across the panel width, e.g. if the panel width is 3.0 m (2.5 b), $Z_{b,mean} = (1.5Z_{b,2} + Z_{b1})/2.5$ and $f_{bc,mean} = (1.5f_{bc,2} + f_{bc1})/2.5$. The net bending stress calculated for imposed loads after the units have been grouted or connected using a structural topping is $\sigma_{b2} = f_{bc,mean} - M_2/Z_{b,mean}$. Finally $\sigma_{b1} + \sigma_{b2} \geq -f_{ctm}\{-0.45\sqrt{f_{cu}}\}$. The method is repeated for the net top stress.

Lateral load spreading is not possible where large holes are formed by using trimmer angles, as the load from an adjacent unit is simply carried back into that unit via the trimmer angle. The analysis of complete slab fields consisting of up to 7 × 1.2 m wide hcus, with large holes up to 2.4 m wide, was carried out by Bernardi *et al.* at the University of Parma [5.26, 5.27]. A finite element (FE) model was first calibrated against full-scale tests carried out at VTT in Finland by Pajari [5.28] and Suikka [5.29], where 7.1 m × 4.8 m wide hcu slab fields with a large opening were subjected to point and line loads. The FE results by Bernardi *et al.* [5.27] show that load spreading around large voids gives end reactions in the supporting units that are almost exactly statically determinate, e.g. for a 300 mm deep × 10.5 m span unit supporting a 1.2 m wide × 9.3 m long unit on a trimmer angle at the end of a 1.2 m hole, the calculated reaction in the supporting unit is 27.2 per cent of the total floor load, compared to the FE results of 27.0 per cent at service and 28.5 per cent at ultimate in a composite slab with 40 mm topping. This suggests that although the shear forces due to the self-weight of the unit (and where present the topping) are carried by the trimmer angle, and the imposed loads are distributed via the longitudinal joints (and where present the topping), end reactions may be calculated using simply supported statics via the trimmer angle.

5.2.8 Flexural capacity

The flexural capacity of a prestressed hcu is checked at both the serviceability and ultimate limit states. It is usual for the ratio of the ultimate moment of resistance M_{ur} to the serviceability moment of resistance M_{sr} to be in the order of 1.7 to 1.8 for critical longer spans. Thus with the use of the present load factors (<1.5 for all actions in BS EN 1992-1-1 {<1.6 for all actions in BS 8110}, the serviceability condition will usually be critical.

The problem of cracking in the unreinforced zones of hcus is particularly important with regard to the uncracked shear capacity. It is therefore necessary to ensure that tensile stresses are not exceeded.

Prestressed concrete is well documented and the reader should refer to standard texts such as Mosley, Bungay and Hulse [5.30] and O'Brien, Dixon and Sheils [5.31] for BS EN 1992-1-1 {Kong and Evans for BS 8110 [5.32]}. Figure 5.25 shows the basic ideas. Units are classified mostly as Class XC1 members to BS EN 1992-1-1 {Class 2 to BS 8110} with respect to the serviceability limit state of cracking. This means that a certain amount of tension is allowed. For spans exceeding about 3 to 4 m it is usual for the governing design criteria to be the flexural tensile stresses at the serviceability limit state.

5.2.8.1 Serviceability limit state of flexure

The serviceability flexural resistance M_{sr} is limited by the following:

(a) flexural tensile and compressive stresses in the concrete
(b) precamber
(c) deflections.

Items (b) and (c) are particularly relevant to the more highly stressed units, exceeding about 7 to 10 m in length. Item (a) is applicable to all units of all ages and under all possible loading conditions (including handling and temporary conditions).

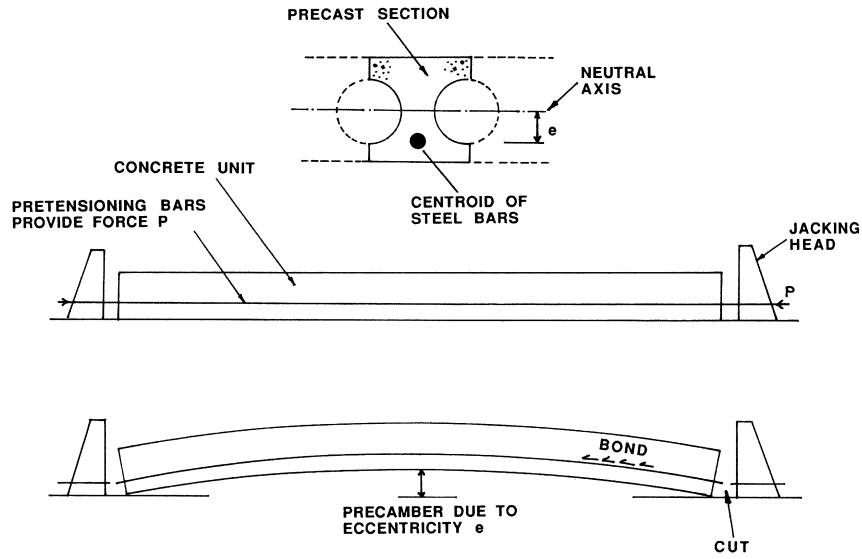

Figure 5.25 Basic prestressing principles.

For units designed to Class XC1, BS EN 1992-1-1 limits the tensile stress in prestressed members with no reinforcement in the tensile zone to $f_{ctm} = 0.3 f_{ck}^{2/3}$, which for the classes of concrete normally used (C40/50 to C50/60) is a minimum of 3.5 N/mm^2.

The amount of flexural tensile stress f_{ct} allowed classifies the units designed to BS 8110 as follows:

- Class 1: No flexural tensile stress.
- Class 2: Flexural tensile stresses are allowed, but not exceeding the smaller of $0.45\sqrt{f_{cu}}$ or 3.5 N/mm^2, and with no visible cracking.
- Class 3: Flexural tensile stresses allowed, but for crack widths less than 0.1 mm in units in a severe environment the stress is ($1.34\sqrt{f_{cu}} - 2.2$ N/mm^2) or 6.3 N/mm^2, whichever is the smaller. With crack widths less than 0.2 mm in units in all other environmental conditions the stress is ($1.34\sqrt{f_{cu}} - 3.2$ N/mm^2) or 7.3 N/mm^2, whichever is the smaller. Class 3 tensile stresses are considered 'hypothetical' in that, because the concrete is cracked and the actual stresses close to the cracks are virtually zero, an equivalent average stress is used. This would be the tensile stress immediately prior to cracking. Depth factors and certain enhancements to the basic tensile stress, given in codes of practice, may be used.

Most designers specify Class 2, but occasionally Class 1 if deflection is excessive. This means a higher prestressing level is required to compensate for the zero tension in the soffit – which is nearly always the limiting case. The flexural compressive stress in the top surface of simply supported units (the only condition used in precast work) is limited to $0.45 f_{ck}$ {$0.33 f_{cu}$}. It is rarely critical in slabs other than the temporary condition in the prestressed solid plank units.

It is necessary to calculate stresses due to the loading arrangement for the following cases:

(a) immediately after the transfer of prestress
(b) after all the losses in the prestressing tendons have occurred
(c) as (b), but in service using $\gamma_f = 1.0$.

The calculated transfer stress, expressed in the usual manner as the characteristic strength f_{ci}, is a function of the cylinder strength at transfer $f_{ck(t)}$ {or of the final concrete cube strength f_{cu}}. In practice,

the concrete strengths achieved are monitored by the manufacturer for a particular process. For concrete grade C50/60 (the typical strength), f_{ci} should be 31 to 33 N/mm^2 {38 to 40 N/mm^2}. For concrete grade C40/50, $f_{ck(t)} = 28$ N/mm^2 { $f_{ci} = 35$ N/mm^2}.

Use of rapid-hardening cements, semi-dry mixes and humid indoor curing conditions are all conducive to early strength gain. The transfer strength is achieved in less than 24 hours – 16 hours if the conditions are favourable. The design compressive and tensile strengths for Class XC1 {Class 2} members are, respectively, 0.6 $f_{ck(t)}$, clause 5.10.2.2.(5), where $f_{ck(t)}$ is defined by clause 3.1.2(5) {0.5 f_{ci}}, and 0.9 × splitting test strength, or $f_{ctm(t)}$, where $f_{ctm(t)}$ is defined by clause 3.1.2(6) and (9) {$0.45\sqrt{f_{ci}}$}. Assuming that the initial pretensioning force is 70 per cent of ultimate (in other countries between 60 and 75 per cent is used), the magnitude of the prestressing force per wire or tendon is taken as $0.7(1 - \eta)A_{ps}f_{pk}/\gamma_m$ {$0.7(1 - \eta)A_{ps}f_{pu}/\gamma_m$}, where $\gamma_m = 1.0$ in this situation, and η is the losses in the prestressing tendons. In the majority of cases f_{pk} {f_{pu}} = 1670 and 1750 to 1770 N/mm^2, although super-strand, with f_{pk} {f_{pu}} = 1860 N/mm^2 and 3.5 per cent relaxation loss at 75 per cent prestress level, may be obtained in certain situations.

If low-relaxation wires are used, $\eta = 0.04$ at transfer, i.e. typically half the final value of the 8 per cent relaxation loss given in the specification. If low-relaxation helical wire strands are used, $\eta = 0.0125$ at transfer, i.e. half of the 2.5 per cent final relaxation loss. In BS EN 1992-1-1 the initial relaxation at the time of transfer is given by clause 3.3.2(7), which either is from the manufacturer's specification or is in accordance with code equations 3.28 to 3.30, depending on the class.

The state of stress after case (a) includes immediate losses due to initial relaxation and 'instantaneous deformation', which is generally known as the 'elastic shortening' loss. This is based on the initial short-term modulus of elasticity for the concrete at transfer taken from the usual database, and is summarised in Table 6.1. (See BS EN 1992-1-1, clause 3.1.3(3). Note that the type of aggregate must be specified.) Elastic shortening is calculated using the prestress in the concrete f_{cc} at the level of the tendon. Hence the elastic loss in the steel is $f_{cc}\ E_s/E_{ci}$. The loss due to the instantaneous deformation according to clause 5.10.5.1 of BS EN 1992-1-1 is $f_{cc}\ E_p/E_{cm(t)}$ and the effective prestress after transfer is given by $f_{pm0} \leq 0.75\ f_{pk}$ in clause 5.10.3.(2). If the losses are required at mid-span, or at some other position along the span of the floor slab, the compressive stress f_{cc} may be reduced owing to the tension caused by the self-weight of the floor unit. This can be quite significant in the longer, heavier units, and can reduce the instantaneous deformation loss by about 2 percentage points. Of course the losses at the ends of the unit, where the prestress at transfer is often critical, cannot be reduced in this way.

The state of stress after *all* losses have occurred in case (b) is similar to the above, except that η now refers to the total losses. These can be estimated from the codes of practice, and are typically:

(i) Prestressing steel relaxation losses, as given above:
The long-term loss for wire and strand for Class XC1 is given in BS 5896 [5.33] or BS EN 1992-1-1, clause 5.10.6(1b) & (2) for the final loss, or Annex D for the loss at intervals in time [5.1] and BS EN 10138 [5.34] {Class 2 is 1.25 times the 1000-hour relaxation test value provided by manufacturers}.

(ii) Concrete shrinkage losses:
These are the product of the shrinkage per unit length (obtained from BS EN 1992-1-1, clause 3.1.4(6) [5.1] {typically as 300×10^{-6} for indoor manufacture and exposure}) and modulus of elasticity of the tendons (taken as 205 kN/mm^2 {200 kN/mm^2}, although 195 kN/mm^2 is more applicable to helical strand, which has a slight tendency to unwind when stretched). The loss due to the concrete shrinkage in BS EN 1992-1-1 is according to clause 5.10.6(1a) and code equation 5.46, which contains stiffening and ageing terms in its denominator. The shrinkage loss to BS 8110 is 60 N/mm^2, or 4.89 per cent at 70 per cent prestress, using $f_{pu} = 1750$ N/mm^2, i.e. $100 \times 60/(0.7 \times 1750)$.

(iii) Creep of concrete losses:
This is proportional to the stress in the concrete at the level of the tendon (see BS EN 1992-1-1, clause 3.1.4 (2 to 4)). The loss due to the creep in BS EN 1992-1-1 is according to clause 5.10.6(1a) and code equation 5.46. Annex B contains detailed equations, and allows the maturity

of the concrete to be calculated at the time when the concrete is deemed to be loaded. The work is based on the Arrhenius equation (nineteenth-century Swedish chemist Svante Arrhenius) for the temperature dependence of the reaction rate of cement, and is cement type-dependent, although BS EN 1992-1-1 uses OPC only. For example, if concrete is cured at 40°C for 24 hours, the maturity is calculated as 57 hours, or 2.38 days. Thus, creep losses begin not at 1 day, but at 2.38 days of age. As before, the compressive stress f_{cc} may be reduced owing to the tension caused by the self-weight and dead loads (not live loads) acting on the floor slab. This can reduce the creep loss by about 3–5 percentage points. A specific creep strain (i.e. creep per unit length per unit of stress) of 1.8, for indoor curing and loading at 90 days, has been used hitherto in the UK. Hence, the creep loss is 1.8 times $f_{cc}\ E_s/E_{ci}$.

Exact solutions for each of these are easy to compute (and will be given in a design exercise). However, typical values for strands or wires stressed to 70 per cent of their ultimate are:

- 2% to 8% for relaxation
- 5% shrinkage
- 5% to 7% for elastic shortening
- 9% to 12% for creep loss.

Total losses range from 20 to 30 per cent for minimum to maximum levels of prestress. The design effective prestress in the tendons after all losses is given by f_{po} $\{f_{pe}\}$.

For the service condition in case (c), the section is considered uncracked and the net cross-sectional area A and moment of inertia I are used to compute maximum fibre stresses f_{bc} and f_{tc} in the bottom and top of the section. The section is subjected to a final prestressing force $P_{po} = 0.7 f_{po} A_p$ $\{P_f = 0.7 f_{pe} A_{ps}\}$ acting at an eccentricity z_{cp} $\{e\}$ from the geometrical neutral axis. The design method is standard prestressed concrete procedure. When calculating the service stress due to imposed bending moment, the section moduli Z_b and Z_t may be taken as the compound value using the transformed area of tendons, $(m-1)A_p$, where m = modular ratio = $(1+\psi)E_p/E_{cm}$, where ψ is the creep factor at installation, which at 1 month is typically = 40% × 1.8 = 0.72.

Using the usual notation, the service moment of resistance M_{sr} is given by the lesser of:

$$M_{sr} = (f_{bc} + 0.3 f_{ck}^{(2/3)}) Z_b \quad \{M_{sr} = (f_{bc} + 0.45\sqrt{f_{cu}}) Z_b\} \tag{5.1(a)}$$

or

$$M_{sr} = (f_{tc} + 0.45 f_{ck}) Z_t \quad \{M_{sr} = (f_{tc} + 0.33 f_{cu}) Z_t\} \tag{5.1(b)}$$

where $f_{bc} = P_f(1/A + e/Z_b)$ and $f_{tc} = P_f(1/A + e/Z_t)$.

Adopting the above concepts, Figure 5.26 shows the moments of resistance and ultimate shear capacities to BS EN 1992-1-1 for a standard range of hollow-core composite units from 150 to 500 mm depth. The material properties are $f_{ck} = 45\,\text{N/mm}^2$ and $f_{ck(t)} = 30\,\text{N/mm}^2$ at transfer with gravel aggregates. Final prestress in the bottom fibre is set at about $f_{bc} = 12\,\text{N/mm}^2$. The permissible tension is f_{ctm} for exposure class XC1 and zero for > XC1.

5.2.8.2 Ultimate limit state of flexure

The ultimate flexural resistance M_{ur} when using bonded tendons is limited by the following:

- ultimate compressive strength of concrete, $0.85/1.5 = 0.567 f_{ck}$ $\{0.45 f_{cu}\}$
- the design tensile stress in the tendons, f_p $\{f_{pb}\}$.

The depth of the (strain-responsive) neutral axis X is obtained by considering the equilibrium of the section. The tensile strength of the steel depends on the net prestress f_{pe} in the tendons after all

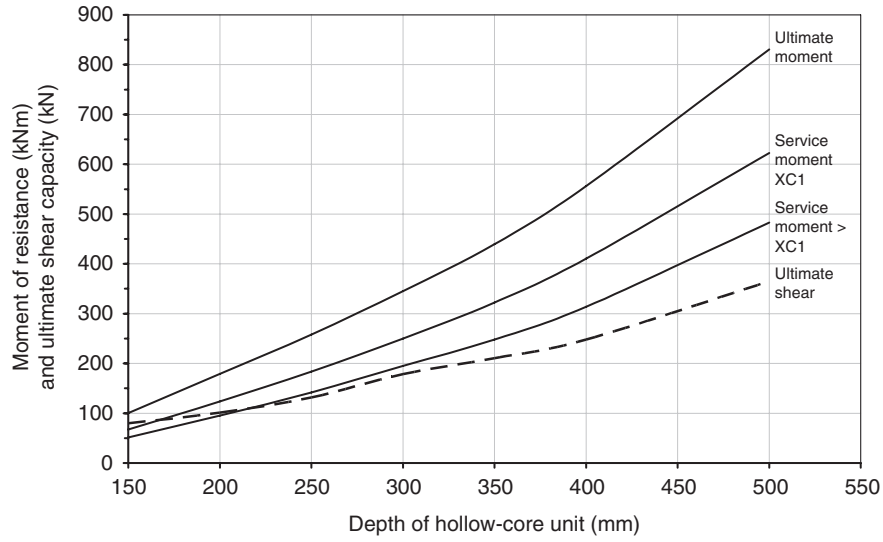

Figure 5.26 Moments of resistance and ultimate shear capacity of hollow-core floor units.

losses and initial prestress levels have been considered. In most hollow-core production the ratio f_{po}/f_{pk} $\{f_{pe}/f_{pu}\} = 0.50$ to 0.55. If the neutral axis remains in the top flange above the top of the cores, the value from BS EN 1992-1-1, clause 3.3.6 is according to the inclined branch B in Figure 3.10 at a limiting strain of $\varepsilon_{ud} = 0.02$, commencing at $f_{pd} = 0.9f_{pk}/1.15 = 0.783f_{pk}$. {The values for X/d and f_{pb} may be obtained from BS 8110, Part 1, Table 4.4 [5.2]; otherwise a solution for X is found by compatibility of final strains and equilibrium of forces in the concrete and tendons.} The ultimate moment of resistance of a (rectangular) section containing bonded tendons, all of which are located in the tension zone at an effective depth d, is given by:

$$M_{Rd} = f_p A_{ps}(d - 0.4X) \quad \{M_{ur} = f_{pb} A_{ps}(d - 0.45X)\} \tag{5.2}$$

If the compressive stress block is not rectangular, as in the case of hollow-core slabs where $0.8X$ $\{0.9X\}$ > top flange depth to cores, the depth to the neutral axis must be found by geometrical or arithmetic means (see Section 5.6). An allowance for other non-prestressed reinforcing bars in the tension zone is made by replacing the area of reinforcement A_s by an equivalent area of prestressing tendons $A_s f_{yd}/f_p$ $\{A_s f_y/f_{pu}\}$, about 0.31 A_s $\{0.28\ A_s\}$ for high-tensile bar. This additional area should be used in the calculation of X, f_p and hence M_{Rd} $\{M_{ur}\}$.

5.2.8.3 Strength sensitivity exercise

A sensitivity analysis was carried out on 200 mm-deep 'Roth'-type hollow-core floor units to determine the effects that 5 mm deviations in both the position of the centroid of the tendons and the overall depth of the slab have on strength. The results are given in Table 5.2 for flexural serviceability and ultimate strengths.

The results show some interesting statistics at the serviceability limit state in that lowering the tendons by 5 mm increased the moment by only 1 percentage point, and yet raising the tendons by the same amount reduced the moment by 3 percentage points. The results for the ultimate condition showed that the effects of negative slab depth and positive tendon deviations, and vice versa, cancelled each other. Where the 5 mm deviations were cumulative, the reductions or increases were in the order of 8 percentage points for both limiting states.

Table 5.2 Effects of dimensional deviation on flexural serviceability and ultimate strength of hollow-core floor slabs

Limiting state	Dimension depth deviation (mm)	Relative flexural strength for deviation of positions of tendons*		
		−5 mm	0	+5 mm
Serviceability	−5	0.92	0.95	0.96
	0	0.97	1.00	1.01
	+5	1.02	1.04	1.05
Ultimate	−5	0.93	0.96	1.00
	0	0.97	1.00	1.03
	+5	1.00	1.03	1.06

Note: * −ve value means nearer to the neutral axis of the section. A mean value of 40 mm was taken for the zero deviation. All prestressing parameters are constant for each size of beam. Concrete grade = C50/60.

5.2.9 Precamber and deflections

5.2.9.1 Basis for calculation and limits

The calculated values for precamber and deflections are based on a stiffness $E_{cm}I$ {E_cI} using an average value for the long-term modulus obtained from the design concrete strength (N/mm^2). Young's modulus (kN/mm^2) is taken as $E_{cm(t)} = 22\ (f_{ck} + 8/10)^{0.3}$ for gravel from BS EN 1992-1-1, Table 3.1, and reduced by 10 per cent for limestone {$E_c = 20 + 0.2\ f_{cu}$}. The same equations may be used with the transfer strength. When considering the gain in Young's modulus over time between the age at transfer (typically 16 hours) and at installation, say 28 days, a factor may be used representing the approximate integration of E_c over that period, i.e. $E_{cm(t)}/0.5(E_{cm(t)} + E_{cm})\{E_{ci}/0.5(E_{ci} + E_c)\}$. This factor may be used to adjust the short-term creep coefficients when calculating deflections at installation.

The I value may be based on the compound section I_{co}, as mentioned in Section 5.2.8.1. Inevitable creep variations in E_c lead to variations in the deflection stiffness. However, the final upward camber δ is calculated using the following approximation:

$$\delta = \frac{P_{po} z_{cp} L^2}{8 E_{cm} I_{co}} \quad \left\{ \delta = \frac{P_f e L^2}{8 E_c I_{co}} \right\} \tag{5.3}$$

where P_{po} {P_f} includes *all* losses. In BS EN 1992-1-1, clause 7.4.1(4), the net upward deflection due to precamber and self-weight in hcus is limited to span/250 and is usually about L/300.

In-service deflections are calculated in the usual manner, taking into consideration the support conditions and loading arrangement for characteristic dead and factored (quasi-permanent) live loads (clause 7.4.1(4)); see Section 5.2.9.2. For normal office loading, deflections are in the order of 10 mm to 20 mm for 6 m to 9 m simply supported spans.

Deflections after construction, defined in clause 7.4.1(5), are limited to span/500. They are due either to (i) imposed loads alone, both short-term immediately after finishes are applied, or (ii) long-term due to imposed loads, visco-elastic dead loads and visco-elastic upward camber. The net deflection, i.e. imposed deflection minus precamber, is typically less than span/1000. The historical requirement of limiting the span to effective depth ratio to control deflection of rc beams is not applicable to prestressed concrete because of the major influence of the prestressing.

The creep coefficients used for deflections ψ are obtained from the Italian Concrete Association *ASSAP Manual* [5.35], also used in the new EC2 publications by British Precast [5.12]. Because the stress conditions in the top and bottom of the unit are different, the values for ψ determined for the effect of dead and imposed loads are *not* the same as the internal creep coefficients φ used for

calculating losses in prestress. The value of ψ at time t is found by multiplying the basic creep coefficient $\psi_\infty = 2.5$ by a coefficient of development, as follows:

Coefficient of development at:		
	transfer	= 0.1
	15 days	= 0.3
	28 days	= 0.4
	2 months	= 0.5
	3 months	= 0.6
	6 months	= 0.7
	12 months	= 0.8
	∞	= 1.0

The long-term concrete ageing coefficient to allow for stress increments after initial loads $\chi = 0.8$. For example, from transfer to 28 days $\psi_1 = 2.5 \times (0.4 - 0.1) = 0.75$. From 28 days to life $\psi_{28} = 2.5 \times 0.8 \times (1 - 0.4) = 1.2$. For long-term live loads, $\psi_\infty = 2.5 \times 0.8 = 2.0$. In effect, the visco-elastic creep deflections may be calculated at any point in time, since interpolation of the coefficients is permitted.

5.2.9.2 Deflection calculations

Deflections are required at installation and in the long term. The installation value is required for two reasons:

- to inform the contractor how much camber (which most often is negative) to expect when laying floor finishes or structural topping to level, or if a 'step', or differential camber, is to be expected in the floor level;
- to enable the deflection after the installation of brittle finishes, ceilings, services, etc. to be calculated due to imposed live loads and the visco-elastic portion of dead loads, self-weight and camber due to prestress.

Let L = effective span (assume same as actual length of unit); P_{pm0} = prestress force at transfer, P_{pmi} = prestress force at installation, P_{po} = final prestress force, z_{cp} = eccentricity, E_{cm} and $E_{cm(t)}$ = Young's modulus at transfer and 28 days, I_c = 2nd moment of area of compound section, ψ_1 = creep coefficient from transfer to installation, ψ_{28} = creep coefficient from installation (assume 28 days) to long term, and ψ_∞ = creep coefficient at long term, w_o, w_1, w_2 and w_3 = uniformly distributed loads due to self-weight of unit, self-weight of slab after grouting, dead loads and imposed live loads, respectively, ψ_2 = quasi-permanent live load factor.

(a) At Transfer

Immediate camber

$$\delta_1 = -P_{pm0} z_{cp} L^2 / 8 E_{cm(t)} I_c \tag{5.4}$$

Deflection due to self-weight

$$\delta_2 = 5 w_o L^4 / 384 E_{cm(t)} I_c \tag{5.5}$$

Resultant deflection at transfer = $\delta_1 + \delta_2$

(b) At Installation, taken here as 28 days

Referring to the creep development coefficients in Section 5.2.9, the effective creep coefficient ψ_1 takes into account the mean change in E_{cm} as:

$$\psi_1 = (E_{cm(t)} / 0.5(E_{cm} + E_{cm(t)})) \times 2.5 \times (0.4 - 0.1) \tag{5.6}$$

Camber at installation is due to the camber at transfer, plus further visco-elastic movement $\psi_1\ \delta_1$ minus a small reduction (optional) due to the reduction in pretensioning force from transfer P_{pm0} to installation P_{pmi}. The second term is often ignored as it makes about a 2–3 per cent difference in δ_3.

$$\delta_3 = -(1+\psi_1)P_{pm0}z_{cp}L^2 / 8E_{cm(t)}I_c + (P_{pm0} - P_{pmi})z_{cp}L^2 / 8E_{cm}I_c \tag{5.7}$$

Deflection at installation due to self-weight is due to further visco-elastic movement of the hcu at transfer, plus the static deflection

$$\delta_4 = +\delta_2(1+\psi_1) \tag{5.8}$$

Resultant deflection at installation = $\delta_3 + \delta_4$.

(c) Long term

The effective creep coefficient after installation takes into account the increase in strength given by $X = 0.8$, and Young's modulus after 28 days.

$$\psi_{28} = 0.8 \times 2.5 \times (1.0 - 0.4) \tag{5.9}$$

Long-term camber is due to camber at installation plus further visco-elastic movement due to the pretensioning force at installation P_{pmi}, minus a reduction (optional) due to the reduction in pretensioning force from installation P_{pmi} to long-term P_{po}

$$\delta_5 = \delta_3 - (\psi_{28}P_{pmi} - (P_{pmi} - P_{po}))z_{cp}L^2 / 8E_{cm}I_c \tag{5.10}$$

Long-term deflection due to self-weight and infill w_1 is due to further visco-elastic movement of w_1 at installation, plus the static deflection:

$$\delta_6 = +\delta_4\psi_{28} + 5w_1L^4 / 384E_{cm}I_c \tag{5.11}$$

Deflection due to UDL dead w_2 added after installation:

$$\delta_7 = +(1+\psi_{28})5w_2L^4 / 384E_{cm}I_c \tag{5.12}$$

Deflection due to UDL live load $\psi_2\ w_3$ using long-term creep coefficient = 0.8 ψ_∞

$$\delta_8 = +(1+0.8\psi_\infty)5\varphi_2 w_3L^4 / 384E_{cm}I_c \tag{5.13}$$

plus similar expressions for imposed point loads and line loads, where φ_2 is the quasi-permanent live load factor.

(d) Deflection after installation

Long-term movement due to live load, visco-elastic response to self-weight and dead loads after installation using post-installation creep factor ψ_{28}, and changes in camber after installation:

$$\delta_9 = 5((1+\psi_{28})\varphi_2 w_3 + \psi_{28}(w_1 + w_2))L^4 / 384E_{cm}I_c + (\delta_5 - \delta_3) \tag{5.14}$$

See Section 5.6 for a worked example.

(e) Maximum spans for limiting deflection

It is often required to back-calculate maximum effective span(s) for the limiting deflections of $L/250$ or $L/500$ (or 20 mm), as follows:

Case 1: Final deflection ≤ *L*/250

$$\text{Final camber} = \frac{z_{cp}L^2}{8E_{cm}I_c}(-P_{pmo}(1+\psi_1)\alpha - P_{pmi}\psi_{28} + 0.5(P_{pm0} - P_{po})) = -AL^2$$

$$\text{Final downward} = \frac{5L^4}{384E_{cm}I_c}(w_o(1+\psi_1)\psi_{28}\alpha + w_1 + w_2(1+\psi_{28}) + \varphi_2 w_3(1+0.8\psi_\infty)) = BL^4$$

where $\alpha = E_{cm}/E_{cm(t)}$

$$\text{Then: } -AL + BL^3 - \frac{1}{250} = 0, \text{ and solve by iteration } \therefore L \to \sqrt[3]{\frac{\frac{1}{250} + AL}{B}} \tag{5.15}$$

Case 2: Movement after installation ≤ *L*/500

$$\text{Movement camber} = \frac{z_{cp}L^2}{8E_{cm}I_c}(-P_{pmi}\psi_{28} + 0.5(P_{pmi} - P_{po})) = -CL^2$$

$$\text{Movement downward} = \frac{5L^4}{384E_{cm}I_c}((w_1 + w_2)\psi_{28} + \varphi_2 w_3(1+\psi_{28})) = DL^4$$

$$\text{Then: } -CL + DL^3 - \frac{1}{500} = 0, \text{ and solve by iteration } \therefore L \to \sqrt[3]{\frac{\frac{1}{500} + CL}{D}} \tag{5.16}$$

5.2.10 Shear capacity

Shear is not usually a problem in hcus under uniformly distributed loading. The only time shear is critical is in simply supported units of less than about 3 to 6 m in span for depths of 150 to 400 mm, respectively. Large point or line loads, particularly at a free edge (i.e. hcu not grouted to a neighbour), must be considered on an individual basis according to BS EN 1168 [5.8], see Section 5.2.10.4. An extensive discussion on this is given by Girhammer [5.36].

As in any prestressed concrete elements the design shear capacity is calculated for two conditions: the flexurally uncracked section and the cracked section in flexure. The uncracked ultimate shear capacity $V_{Rd,c}$ $\{V_{co}\}$ is greater than the ultimate cracked value $V_{Rd,cr}$ $\{V_{cr}\}$ because the full section properties are considered and a small amount of diagonal tension in the concrete is permitted. The ratio of $V_{Rd,c}/V_{Rd,cr}$ to BS EN 1992-1-1 is typically 1.3 to 2.0 (the latter being for maximum prestress). However, V_{co}/V_{cr} to BS 8110 is typically 2.0 to 2.4. This is advantageous because the maximum design shear, which usually occurs where the flexural moments are small, may be equated with $V_{Rd,c}$ $\{V_{co}\}$, the greater shear capacity. The position of the cracked section depends very much on the loading conditions, but for uniformly distributed loads it is usually far enough into the span of the slab so as to render a check against $V_{Rd,cr}$ $\{V_{cr}\}$ as unwarranted. Strictly speaking, $V_{Rd,cr}$ $\{V_{cr}\}$ should always be checked.

It is not possible to provide shear reinforcement in hcus, and therefore the prestressed concrete must do the work. (There are some production systems that enable a light mesh to be cast in the webs of very deep units, e.g. 500 to 750 mm, but this is not common.) A note of caution must be added here; it is not economical to increase the number of prestressing wires merely to satisfy shear. For example, increasing the area of prestressing reinforcement by a factor of 4 increases the flexural capacity by about 2.5 and the shear capacity by only 1.2. The most economical method of increasing the shear capacity is to make solid the ends of the units by opening the tops of the cores and filling them

with structural-grade concrete, often using self-compacting concrete [5.37]. A less popular alternative is to increase the depth of the slab.

The additional shear capacity with a number n (at least 2) of filled cores is, according to BS EN 1168, Annex F, clause F.3 as

$$V_{Rd,t} = 2/3nb_c df_{ctd(i)} \tag{5.17}$$

where

b_c = breadth of core (mean if different)
d = depth of core (although BS EN 1168, Figure F.1 shows this as the effective depth to the tendons)
$f_{ctd(i)}$ = design tensile strength for the infill.

Some hcus have a greater shear capacity, with all things being equal, than others. The slip-formed-type floor with the large number of webs has a shear capacity about 30 per cent greater than its extruded counterpart.

Two modes of shear failure are possible: flexural shear and shear tension. The occurrence of each is not merely a function of the shear span ratio, although the latter does usually occur when $a_v/d < 2$ to 3.

Flexural shear occurs if a flexural crack develops into a shear crack. Because of the relatively large amount of prestress in hcus, it is usually the first (or second) flexural crack that causes the shear failure. Failure occurs where the shear force exceeds the shear compression capacity, and a single flexural crack initiates shear failure.

Shear tension failures are also possible, and embrittled diagonal cracks are found close to the ends of the units propagating through the unprestressed and unreinforced regions of the slab (see Figure 5.27). Figure 5.28 (from [5.14]) shows the development of prestress in a simple rectangular section. Stresses in hcus are further complicated by the cross-sectional shape of the unit. It is further assumed that the extremity of the support bearing pressure spreads at an angle of about 45° from the inner

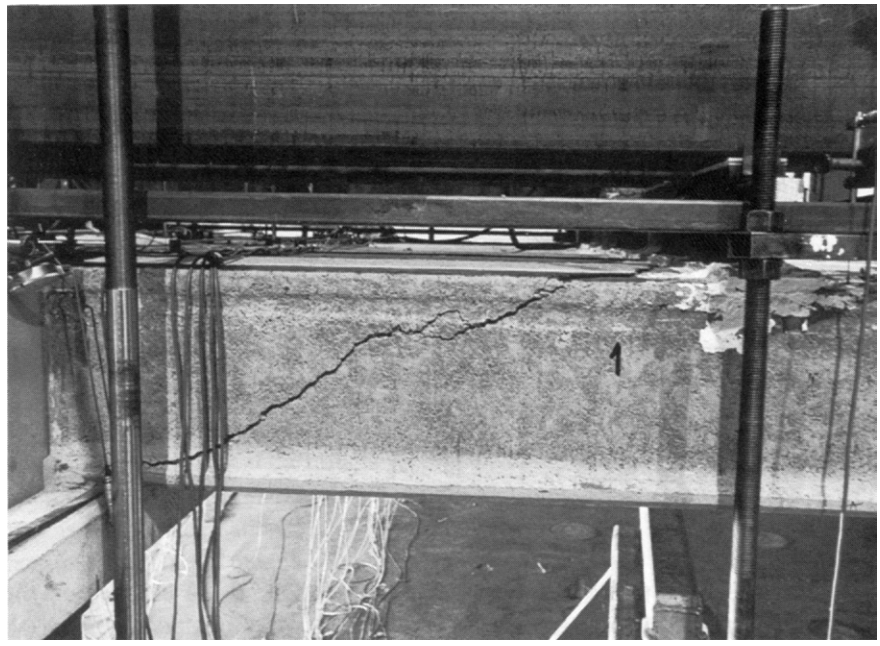

Figure 5.27 Shear cracking in hollow-core slabs.

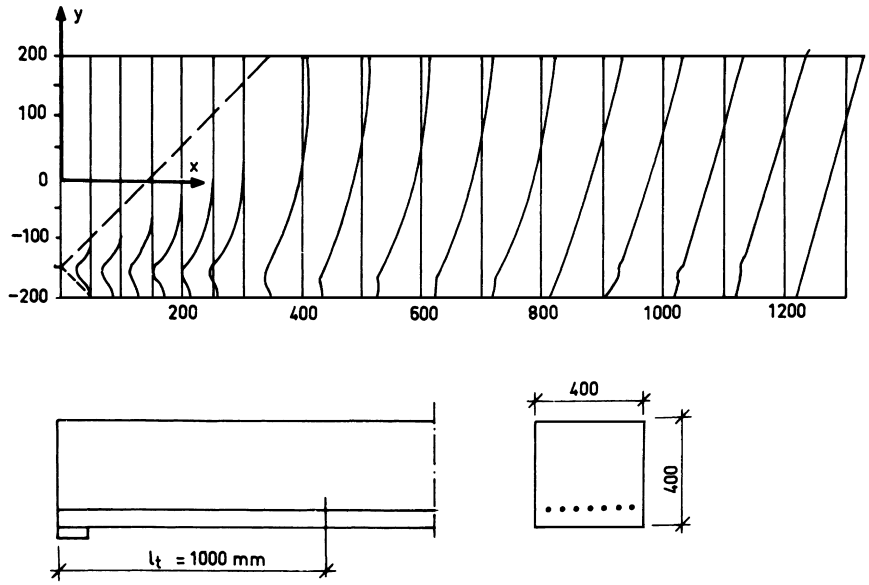

Figure 5.28 Contours of prestress development in ends of hollow-core units [5.14].

bearing point. Walraven [5.14] suggests that an increment equal to half the depth of the slab is required for a shear-tension crack to develop. The direct transmission of forces, by strut-and-tie action, does not occur in prestressed members, which rely on the development of bond to satisfy the truss analogy. The codes do not recognise this fact; the equation for the uncracked shear capacity given in Section 5.2.10.2 is considered adequate in all respects.

5.2.10.1 Compression field theory for shear capacity

Shear failures are difficult to characterise in prestressed hollow-core units, because of the large number of variables close to the support and the rapidly changing stress distributions, both longitudinally in the transmission zone and vertically through the webs. Because the most common mode of failure lies somewhere between flexure-shear and shear-tension, and may be of either mode for nominally identical situations, the principal stress equations (5.22) may not always be the most accurate, particularly if high shear forces and bending moments occur in the transmission zone. Adopting Vecchio and Collins's various shear hypotheses [5.38], Araujo *et al.* [5.39] presented a modified compression field theory to rival principal stress models and, further, compared the results of their analysis against 129 shear tests compiled by Bertagnoli and Mancini [5.40]. Using a variable strut inclination method with cot $\theta = 2$, the ultimate shear capacity $V_{Rd,CF}$ (CF = compression field) is given as:

$$V_{Rd,CF} = 2\beta b_w 0.9d\sqrt{f_{ck}/\gamma_c} \tag{5.18}$$

(note in this book the original term $\sqrt{f_{ck}}$ has been used rather than the approximation $2f_{ctm}$ in Araujo's paper) where, after Collins *et al.* [5.41]

$$\beta = \frac{0.4}{(1+1500\varepsilon_x)}\frac{1300}{(1000+s_{xe})} \tag{5.19}$$

where the average strain in the cracked section is:

$$\varepsilon_x = \frac{M_{Ed}/0.9d + V_{Ed} - A_{ps}f_{p0(x)}}{2E_pA_{ps} + 0.5E_cb_w0.9d} \tag{5.20}$$

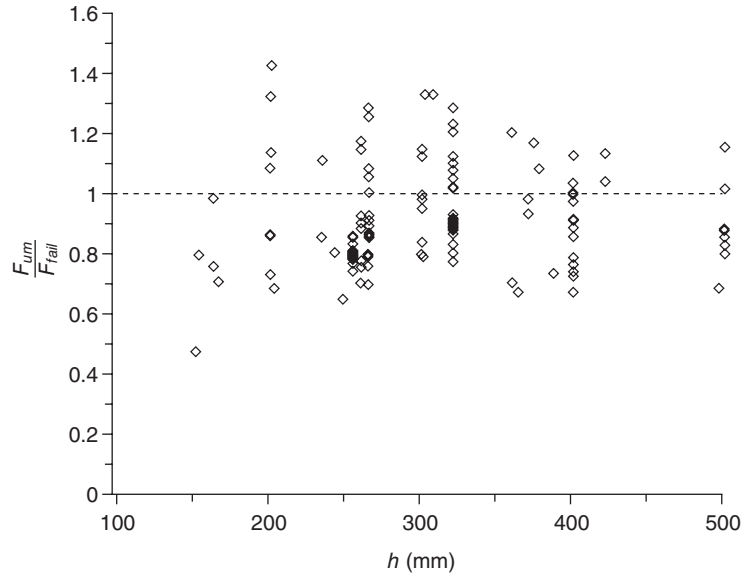

Figure 5.29 Ratio of theoretical ultimate shear capacity using mean material properties of Araujo [5.39] to experimental results of Bertagnoli and Mancini [5.40]. (Courtesy of Araujo/Bertagnoli/Mancini and Ernst & Sohn.)

and average spacing of cracks is:

$$s_{xe} = s_{xe} = \frac{35 \times 0.9d}{15 + a_g} \geq 0.85 \times 0.9d \tag{5.21}$$

where a_g = maximum size of coarse aggregate.

In this analysis, $V_{Rd,CF}$ is position-dependent, and may therefore be calculated at various positions from the support, e.g. along a 45° shear plane at $0.9d$ from the edge of the support (of bearing length L_b). To find the critical value for $V_{Rd,CF}$, let the design shear force $V_{Ed} = V_{Rd,CF}$, and $M_{Ed} = V_{Ed}$ $(0.5L_b + 0.9d)$. The effective prestress $f_{po(x)}$ at the edge of the support = $(L_b/l_{pt2})\ \sigma_{pmo}$, where σ_{pmo} = prestress after transfer losses.

Araujo's theoretical versus experimental ratios are shown in Figure 5.29. 95 per cent of the results fall within +15% to −25% of the experimental data, with the most conservative values belonging to depths of 250 to 300 mm, where shear-tension and flexural-shear failures are more in balance than at other depths.

Comparing $V_{Rd,c}$ and $V_{Rd,CF}$ for the 250 mm-depth hollow-core unit reference 25/108 (with ten 12.5 mm-diameter helical strands) in Chart 5.1, in which an expected experimental shear capacity would be in the order of 220 to 240 kN:

Data: $I = 1289 \times 10^6\ \text{mm}^4$; $S = 6.866 \times 10^6\ \text{mm}^3$; $b_w = 285$ mm; $d = 209$ mm; $0.9d = 188$ mm; $A_{ps} = 930\ \text{mm}^2$; $f_{pk} = 1770\ \text{N/mm}^2$; $\sigma_{pmo} = 0.95 \times 0.7 \times 1177\ \text{N/mm}^2$ (5% losses); $E_p = 195\ 000\ \text{N/mm}^2$; $f_{ck} = 50\ \text{N/mm}^2$; gravel aggregates; $a_g = 14$ mm; $E_c = 37\ 300\ \text{N/mm}^2$; $f_{ctd} = 1.90\ \text{N/mm}^2$; $l_{pt2} = 830$ mm; $L_b = 100$ mm; $y_b = 122$ mm; $l_x = 100 + 122 = 222$ mm; $\alpha = 222/830 = 0.268$; $f_{cp} = 4.45\ \text{N/mm}^2$. Therefore, $V_{Rd,c} = (1289 \times 10^6 \times 285 / 6.866 \times 10^6)\sqrt{(1.90^2 + 0.268 \times 4.45 \times 1.90)10^{-3}} = \underline{129.7\ \text{kN}}$. Removing γ_c from f_{ctd} and the 0.9 factor in f_{cp} gives $V_{Rd,c} = \underline{198.6\ \text{kN}}$.

To calculate $V_{Rd,CF}$ at $0.9d$ from the support: using iteration, try $V_{Rd,CF} = 181.7$ kN. Then $M_{Ed} = 181.7 \times (50 + 188) = 43.2$ kNm; $f_{po}(x) = (100/830) \times 1177 = 142\ \text{N/mm}^2$; $\varepsilon_x = 0.000206$; $s_{xe} = 227$ mm; then $\beta = 0.324$.

$V_{Rd,c} = 2 \times 0.324 \times 285 \times 188 \times \sqrt{50/1.5} = \underline{181.7\ \text{kN}}$. Removing γ_c gives, by iteration, $V_{Rd,c} = \underline{243.7\ \text{kN}} > 198.6$ kN. The failure mode would be closer to shear tension.

5.2.10.2 Shear capacity in the uncracked region, $V_{Rd,c}$ {V_{co}}

The term 'uncracked' refers to flexural cracking (i.e. tensile stress < f_{ctd} {f_t}), and where cracking exists $V_{Rd,c}$ {V_{co}} must not be used. The ultimate shear capacity is given by:

BS EN 1992-1-1 Eq. 6.4

$$V_{Rd,c} = \frac{Ib_w}{S}\sqrt{f_{ctd}^2 + \alpha_1 \gamma_{\text{p,fav}} \sigma_{cp} f_{ctd}} \qquad (5.22)$$

where $f_{ctd} = 0.7 \times 0.3\, f_{ck}^{2/3}/1.5$

$\alpha_1 = l_x/l_{pt2} \leq 1.0$

l_x = distance from end of unit to point where a 45° plane drawn from edge of support meets the centroidal axis

$l_x = 0.5l_b + y_b$

$l_{pt2} = 1.2\ l_{pt}$

l_{pt} = transmission length

(see clause 2.4.2.2(1)) $\gamma_{p,fav} = 0.9$ for prestress at ultimate

$\sigma_{cp} = P_{po}/A_c$ (final prestress)

I, S = 2nd and 1st moments of area about the centroidal axis

b_w = breadth of webs at centroidal axis.

For sections where the width varies over the height, the maximum principal stress may occur other than at the centroidal axis and the shear resistance should be checked at various heights in the cross section. Equations for $V_{Rd,c}$ in BS EN 1168, clause 4.3.3.2.2.1 require uncracked shear resistance to be checked on a 35° plane from the edge of bearing (not 45°) using the equations:

$$V_{Rd,c} = \frac{Ib_{w(y)}}{S_{(y)}}\sqrt{f_{ctd}^2 + \sigma_{cp(y)} f_{ctd}} - \tau_{cp(y)} \qquad (5.24)$$

where, +ve if compressive

$$\sigma_{cp(y)} = \sum_{t=1}^{n}\left(\left(\frac{1}{A_i} + \frac{(Y_c - y)(Y_c - Yp_t)}{I}\right)P_{t(lx)}\right) - \frac{M_{Ed}}{I}(Y_c - y)$$

$$\tau_{cp(y)} = \frac{1}{b_{w(y)}}\sum_{t=1}^{n}\left(\left(\frac{A_{c(y)}}{A_i} - \frac{S_{c(y)}(Y_c - Yp_t)}{I} + Cp_{t(y)}\right)\frac{dP_{t(lx)}}{dx}\right)$$

BS 8110, Eq. 55

$$V_{co} = 0.67 b_v h \sqrt{f_t^2 + 0.8 f_{cp} f_t} \qquad (5.22)$$

where $f_t = 0.24\sqrt{f_{cu}}$

Design rules recognise the fact that the critical shear plane may occur in the prestress development zone, where f_{cp} is not fully developed. It is shown [5.14] that prestressing forces develop parabolically and therefore a reduced value f_{cpx} is used. It may be shown that f_{cpx} is given by:

$$f_{cpx} = \frac{x}{l_p}\left(2 - \frac{x}{l_p}\right) f_{cp} \qquad (5.23)$$

where l_p is the prestress development length, taken as the greater of the transmission length l_t (see Section 5.2.12) of depth h. x is from the end of the unit measured at 45° to the inner bearing edge. All these factors have been taken into account in the design data given at the end of this chapter.

Pisanty [5.17] has found that a reduction of less than 2 per cent in calculated EC2 values {10 per cent in the calculated value of V_{co}} brings the design value into good agreement with full-scale experimental test results. The larger BS 8110 reduction is necessary because the BS 8110 term $0.67b_vh$ is less than the EC2 term $I\ b_v/S$ for the shape of the hollow-core web. See also Table 5.3, where the mean value of the ratio of the test failure load divided by $0.9V_{co}$ is 1.05.

Although this expression is derived using a rectangular section and not the actual flanged section appropriate to hollow-core units, the difference is accepted as being small. Safety factors are built into the equations for $V_{Rd,c}$ {V_{co}}, because as a favourable effect $\gamma_{p,fav} = 0.9$ {0.8} of the compressive stress σ_{cp} at the centroidal axis is used. The value for f_{ctd} {f_t} is also conservative.

Lin Yang [5.42] has proposed a design method to calculate the shear web capacity. The equation allows for changes in cross section, material properties and prestress levels. Web shear is critical at a

point at the narrowest part of the web between the voids on a diagonal line inclined at 35° to the horizontal from the edge of the support. This is typically 0.72 h from the support, where h is the depth of the slab. Comparisons with 118 tests at VTT in Finland found that a 95 per cent confidence limit could be used in this equation if the value so obtained is decreased by (approximately) 50 kN.

Test results, starting with Yang, have shown that where hollow-core units have narrow webs just above the top of the strands, the maximum shear stress occurs there, and there is a reduction in $V_{Rd,c}$ of between 0.7 and 1.0, depending on the shape of the web. The ratio of the minimum value of $V_{Rd,c}$ to $V_{Rd,c}$ at the centroid is about 0.95 in circular cores, where the web is narrow on the centroidal axis.

The vast majority of shear tests have been carried out on hollow-core units up to 250 mm deep, where the correlation of the ultimate shear capacity $V_{Rd,c}$ {V_{co}} has generally been within about 10 per cent. The calculation for $V_{Rd,c}$ {V_{co}} has always been carried out on a 45° shear plane at the centroidal axis, where it is understood shear cracks will first propagate. This is certainly the case in any type of prestressed section where the web is narrowest at the centroidal axis, e.g. hollow-core units having circular webs, but may not be the case in more parallel-sided webs, e.g. oval or pear-shaped cores, where the combined effects of the transfer of prestress and the principal shear stress may cause the shear failure to initiate at a point below the centroidal axis.

The Eurocode recognises this in BS EN 1992-1-1, clause 6.2.2.(2): *For cross-sections where the (web) width varies over the height, the maximum principal stress may occur on an axis other than the centroidal axis. In such a case the minimum value of the shear resistance should be found by calculating* $V_{Rd,c}$ *at various axes in the cross section*. The amended version of the European Product Standard for hollow-core units BS EN 1168:2005+A3(2011), clause 4.3.3.2.2.1 presents Eq. (5.25) to calculate $V_{Rd,c}$ at various points along the shear plane, as shown in Figure 5.30. Following the recommendation of Yang [5.42], the inclination of the shear plane is 35° from the end of the bearing.

The ultimate shear capacity at distance l_x from the end of the unit and height y from the bottom of the section, where $l_x \geq l_b + 0.5\,h$, is given as:

$$V_{Rd,c(y)} = \frac{Ib_{w(y)}}{S_{(y)}}\sqrt{f_{ctd}^2 + \sigma_{cp(y)}f_{ctd}} - \tau_{cp(y)} \tag{5.25}$$

where the compression due to prestress at l_x and y is:

$$\sigma_{cp} = \left(\frac{1}{A_c} + \frac{(Y_c - y)z_{cp}}{I}\right)P_{t(l_x)} \tag{5.26}$$

and the concrete shear stress due to transmission of prestress at l_x and y is:

$$\tau_{cp} = \frac{1}{b_{w(y)}}\left(\frac{A_{c(y)}}{A_c} + \frac{S_y(Y_c - y_{Pt})}{I} + C_{Pt(y)}\right)\frac{\partial P_{t(l_x)}}{\partial x} \tag{5.27}$$

where

I = 2nd moment of area about centroidal axis
$S_{(y)}$ = 1st moment of area above y and about centroidal axis
A_c = net concrete section area (note that BS EN 1168 calls this a *fictive* area)
$A_{c(y)}$ = net concrete section area above height y
$P_{t(lx)}$ = prestressing force at distance l_x
$\partial P_{t(lx)}/\partial x$ = gradient of the prestressing force in the transmission zone = P_t/l_{pt2}
$C_{pt(y)}$ = a factor according to position of tendons. $C_{pt(y)} = -1$ if $y \leq Y_{Pt}$ otherwise = 0

Other definitions are shown in Figure 5.30.

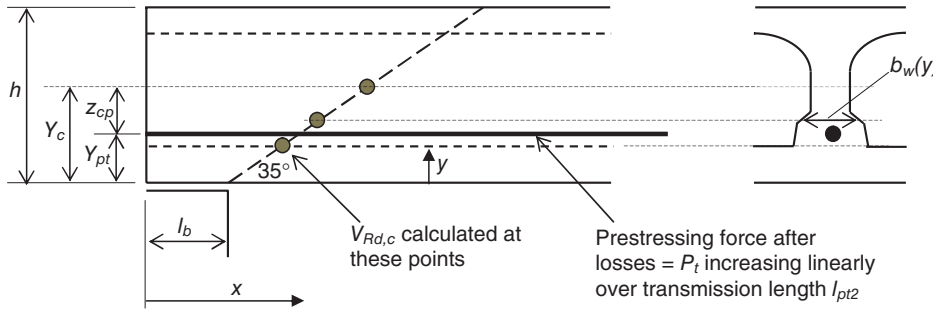

Figure 5.30 Principles and definitions used in the calculation of $V_{Rd,c(y)}$ in hollow-core units.

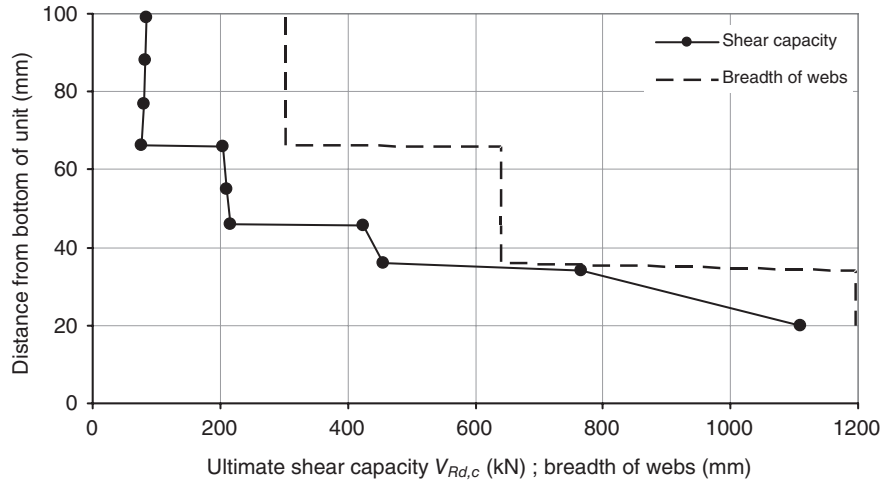

Figure 5.31 Variation in $V_{Rd,c}$ according to Eq. (5.25) in 200 mm-deep × 6 core, hollow-core unit of same cross section, section properties and ultimate stresses used in Section 5.6.

As an alternative to Eq. (5.25) the shear capacity at the centroidal axis may be according to Eq. (5.22), but factored as follows:

$$V_{Rd,c} = \frac{0.8Ib_w}{S}\sqrt{f_{ctd}^2 + \alpha_l 0.9\sigma_{cp} f_{ctd}} \tag{5.28}$$

For hollow-core units deeper than 450 mm, $V_{Rd,c}$ ($V_{Rd,cr}$) in Section 5.2.10.3 shall be multiplied by 0.9. BS EN 1168 states that $V_{Rd,c}$ need not be checked at points less than $0.5h$ from the edge of the support, $l_x < l_b + 0.5h$. This clause effectively rules out checking $V_{Rd,c}$ at the bottom of the webs, where the greatest principal stresses actually occur. For example, in a 200 mm-deep unit with a 40 mm bottom flange, 100 mm bearing length, $l_b + 0.5h = 200$ mm, whereas $l_x = 100 + 40/\tan 35^\circ = 157$ mm. In other words, $V_{Rd,c}$ is not checked until the height $y = (200 - 100)\tan 35° = 70$ mm, which is only about 29 mm below the centroidal axis.

Referring to the 200 mm-deep hollow-core unit designed in Section 5.1, $V_{Rd,c(y)}$ has been recalculated according to Eqs. (5.25 to 5.27). The results are shown in Figure 5.31, in which $V_{Rd,c(\text{c.g.})} = 84.8$ kN, and minimum $V_{Rd,c(y)} = 78.4$ kN, a reduction of 8 per cent. The steps in the results occur at changes in (a) breadth of webs, i.e. b_w at the centroidal axis and in the lower core are 303 and 640 mm, respectively, as shown in the dashed line in Figure 5.31, and (b) at the level of the tendons (where $C_{Pt(y)}$ changes from 0 to −1 and causes τ_{cp} to become negative) at $y = 45$ mm.

Applying the same analysis to units of greater depth, and keeping $b_w = 303$ mm and the axial prestress $\sigma_{cp} \approx 5.4\,\text{N/mm}^2$, gave the results in the following table. The minimum value of $V_{Rd,c(y)}$ always occurred at the bottom of the parallel-sided part of the webs (except for $h = 150$ mm), or where $l_x < l_b + 0.5\,h$ ($l_b = 100$ mm).

Depth h mm	$V_{Rd,c(c.g.)}$ kN	Minimum $V_{Rd,c(y)}$ kN	y mm	Ratio $V_{Rd,c(y)}/V_{Rd,c(c.g.)}$
150	54.7	53.3	52	0.98
200	84.8	78.4	70	0.92
300	163.9	146.4	105	0.89
400	231.6	196.1	140	0.85
500	365.6	308.7	175	0.84

The reduction in shear capacity becomes marked when $h \geq 300$ mm. In perfectly parallel-sided webs, the reductions have been shown by IPHA to be as low as 0.61, although this may have been at the very bottom of the webs and violated the $l_x < l_b + 0.5\,h$ rule. However, there is a clear message that in deeper units $V_{Rd,c(y)}$ will surely be less than $V_{Rd,c(c.g.)}$. In 2008, ACI-318 stated that hollow-core units greater than 320 mm deep should have shear reinforcement when the ultimate shear force $V_u > 0.5\ V_{cw}$; i.e. without using shear reinforcement, which is impractical in production, V_{cw} is halved!

Palmer and Schultz [5.43] carried out 24 full-scale shear tests on 12-, 16- and 20-inch (305, 407, 508 mm) deep units. The units were supplied by two manufacturers A and B with quite differing material properties and strand slippage, factors that appear to be as much responsible for the scatter in results as for the behaviour of the units at failure. Concrete strengths were 53.9 and 68.2 N/mm^2, core densities were 2140 and 2400 kg/m^3 and the range of strand slippage 0.7–2.9 and 0.5–1.1 mm, for units from manufacturer A and B, respectively. These measurements of slippage appear to be quite low, particularly for B in such deep units, where slippage values closer to 3 mm would be expected. This was questioned by Logan in Discussion [5.44]; however, the authors defended the values as typical of those units in general. Figure 5.32 shows the influence of strand slippage on

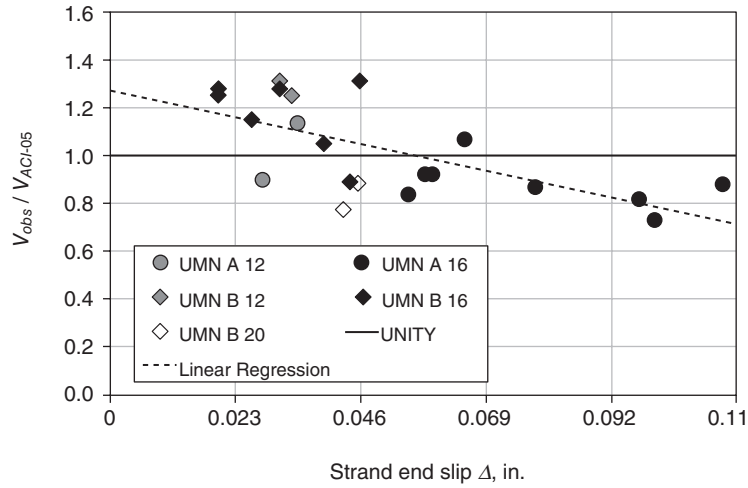

Figure 5.32 Normalised ultimate shear/ACI-2005 capacity versus strand slippage [5.43]. The notation is *A, B* = manufacturer; *12, 16, 20* = depth in inches. (Courtesy of Arturo E. Schultz.)

the ratio of the observed test load V_{obs} to calculated shear capacity $V_{ACI\text{-}05}$ according to ACI-2005. Several 16 inch-deep results have $V_{obs}/V_{ACI\text{-}05}$ ratios ≈ 1.1 to 1.3, which casts doubt over the move to halve V_{cw} in ACI-2008, although 20 inch-deep results have $V_{obs}/V_{ACI\text{-}05} \approx 0.8$, which supports the claim in BS EN 1168 to multiply $V_{Rd,c}$ for $h > 450$ mm by 0.9. The mean ratio is almost 1.0, where the regression line crosses the unity line at a strand slippage $\delta = 1.46$ mm, which is in agreement with the limiting slippage given in BS EN 13369, clause 4.2.3.2.4. of $\Delta L_o = 0.4\ l_{pt2}\ \sigma_{pmo}/E_p$. Using an example of $l_{pt2} = 50\ \phi$, 5% losses, 70% prestress, $\Delta L_o = 0.4 \times 50 \times 12.5 \times 0.95 \times 0.7 \times 1860/195\ 000 = 1.58$ mm. These results suggest that all tests referenced UMN A 16 *may* have had extended transmission lengths (according to $L_t = 2\delta\ E_p/\sigma_{pmo}$) that could have impaired the shear capacity.

Test results were compared to design equations based on BS EN 1992-1-1 and after Yang, and are summarised in Figure 5.33. Comparisons with BS EN 1992-1-1 are mostly unconservative, with only six out of twenty-four tests having $V_{obs}/V_{EC2} > 1$. Tests with the largest slippage (UMN A 16) have a mean $V_{obs}/V_{EC2} \approx 0.75$, and $V_{Rd,c} = 100$ kip = 445 kN. These units had nominal $b_w \approx 390$ mm, resulting

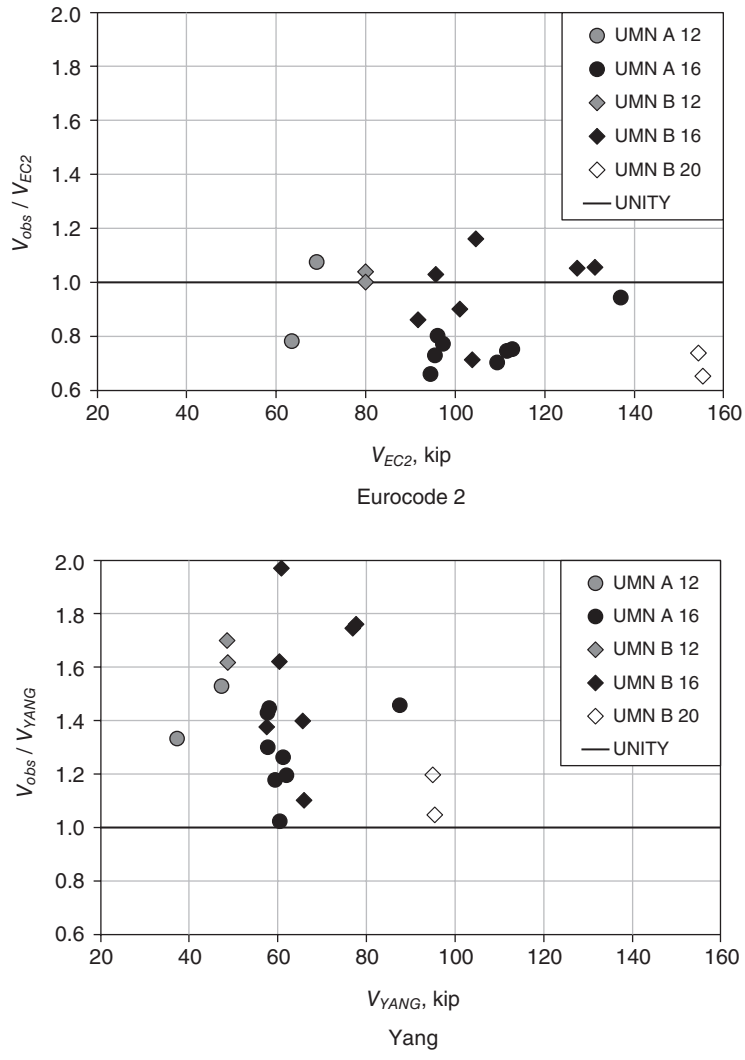

Figure 5.33 Normalised ultimate shear/EC2 and Yang's equation capacity versus calculated capacity (100 kip = 445 kN) [5.43]. (Courtesy of Arturo E. Schultz.)

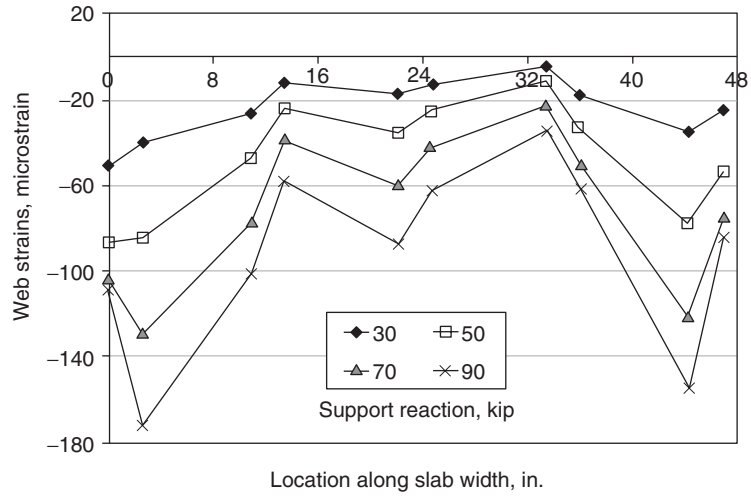

Figure 5.34 Distributions of web strains across 16 inch-deep hollow-core units at various test loads [5.43]. (Courtesy of Arturo E. Schultz.)

in $V_{Rd,c}/b_w h \approx 2.25\,\text{N/mm}^2$, which is within the typical range for a fully stressed 400 mm-deep unit. Therefore a greater shear load would have been expected. However, comparisons with Yang, on which Eq. (5.25) is based, are all conservative, with $V_{obs}/V_{EC2} = 1.0$ to 2.0. Tests identified as UMN A 16 have a mean shear stress of $V_{YANG}/b_w h \approx 1.4\,\text{N/mm}^2$, which by itself is less than the design tensile stress f_{ctd} for C50/60 concrete. The results indicate that while BS EN 1992-1-1 is largely unconservative for deep units, Yang's approach has tipped the balance too far.

Palmer and Schultz judicially measured surface strains in the webs and found large variations on both sides of the same web, and between outer and inner webs, as shown in Figure 5.34, measured on 407 mm-deep units × 60 mm-wide webs. Strains in the outer webs are in the region of −160 με, compared to internal values of −40 to −80 με. The authors report 60 per cent differences in surface strain on both sides of the same web, suggesting bulging of the outer webs, where shear cracking may have been initiated. There was also redistribution of stress in the webs indicated by reversals of strain at higher loads, and some post-cracking strengthening that is unusual in prestressed hollow-core units in shear.

These important test results of shear strength and web-strain distributions show that shear behaviour in deep webs is non-symmetric, leading to reductions in the shear load at the onset of cracking in individual webs. This behaviour is not seen in shallower units. The cross-section profile of deep units may therefore be optimised beneficially by increasing the width of outer webs, in order to bring the symmetric nature found in shallow units into line with design equations.

5.2.10.3 Shear capacity in the region cracked in flexure, $V_{Rd,cr}$ {V_{cr}}

Note that in this book $V_{Rd,cr}$ is used, to distinguish it from $V_{Rd,c}$.

The value of $V_{Rd,cr}$ {V_{cr}} is calculated using the following (semi-empirical) equation:

BS EN 1992-1-1, equation 6.2 gives the usual formulation for $V_{Rd,cr}$ for shear:

$$V_{Rd,cr} = \left(0.12k(100\rho_1 f_{ck})^{1/3} + 0.15\gamma_{p,fav}\sigma_{cp}\right)b_w d \quad (5.29)$$

But not less than

$$V_{Rd,cr} = (v_{min} + 0.15\sigma_{cp})b_w d \quad (5.30)$$

$$v_{min} = 0.035k^{3/2} f_{ck}^{1/2} \quad (5.31)$$

$$V_{cr} = \left(1 - 0.55\frac{f_{pe}}{f_{pu}}\right)v_c b_v d + M_o \frac{V}{M} \quad (5.29)$$

One of the problems in using the above equation is that the decompression moment, M_o, and the shear force and bending moment values, V and M, must be known before V_{cr} may be computed.

where

$$k = \min\left(\left(1+\sqrt{\frac{200}{d}}\right); 2.0\right) \tag{5.32}$$

$$\rho_1 = \min\left(\left(\frac{A_{sl}}{b_w d}\right); 0.002\right) \tag{5.33}$$

$$\sigma_{cp} = \min\left(\left(\frac{0.9 f_p A_p}{A_c}\right); 0.2 f_{cd}\right) \tag{5.34}$$

A_{sl} is the area of tendons, which extends $\geq (l_{bd} + d)$ beyond the shear plane. This is not satisfied by calculation in hcus, but the condition is satisfied by tests.

This is an obvious drawback in the preparation of predetermined shear capacity data tables, much favoured in the precast industry. A short cut is possible here by using the expression given in the Handbook to BS 8110 as follows:

$$V_{cr} = 0.037\sqrt{f_{cu}} b_v d + (0.37\sqrt{f_{cu}} + 0.8 f_{bc}) Z_b \frac{V}{M} \tag{5.35}$$

All values except V and M are known for specified section geometry and prestressing levels. It is assumed that at the critical section the design shear V cannot exceed V_{cr}, and so therefore $V = V_{cr}$. Similarly the ultimate design moment M cannot exceed $\gamma_f M_s$. In most cases floor dead and live loads are roughly equal, and so therefore $M = 1.5\, M_s$ approximately. Thus a unique value for V_{cr} exists.

It appears from tests carried out on 1.93 m long × 300 mm deep extruded slabs in 3-point bending [5.17] that Eq. (5.35) is conservative. Table 5.3 summarises the test data and comparisons with BS 8110 [5.2].

5.2.10.4 Punching shear and concentrated loads

Trying to initiate a classical punching shear failure in hollow-core floor units is very difficult, and the author has not been successful in several tests carried out on 150- and 200 mm-deep units of around 4 m in length. The failure mode is always by longitudinal cracking along the line of the cores, even though the footprint of the load ($w = 300$ mm square) was wider than the breadth of the core. A footprint as little as $w = 50$ to 100 mm square (e.g. as specified for computer-room cabinet bearings, for which unscreeded slabs would be inappropriate) is required to punch through the top flange directly over the core.

Table 5.3 Summary of Shear Tests by Pisanty [5.17]

Test failure load	Predicted V_{cr} (kN)	Predicted V_{co} (kN)	Test load/ 0.9 V_{co}
178.50	133.63	188.60	1.050
172.50	133.84	189.75	1.008
174.00	133.73	189.17	1.021
173.50	133.54	187.45	1.027
47.50	41.92	69.44	0.760
67.00	41.98	69.71	1.068
78.00	41.92	69.44	1.248
53.75	41.77	68.88	0.867
47.00	36.57	47.36	1.103
57.25	36.54	47.04	1.352

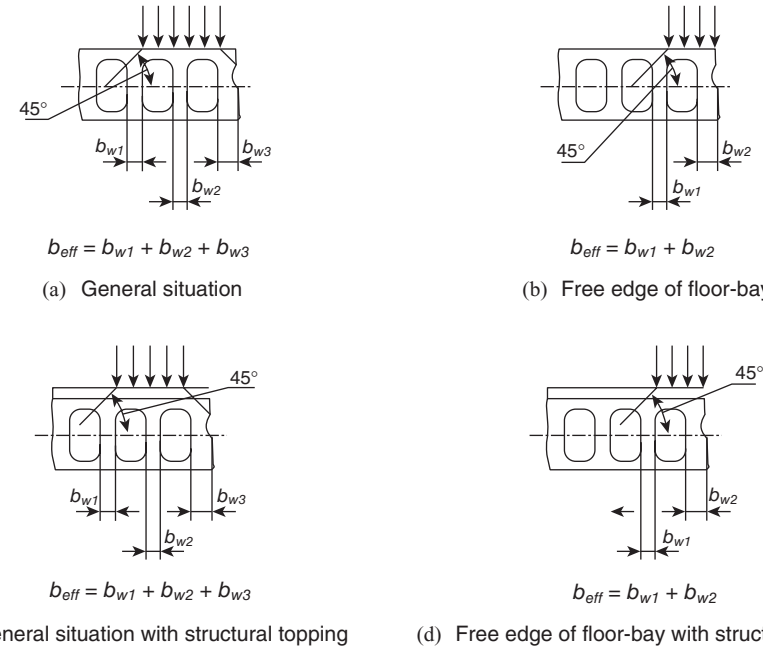

Figure 5.35 Effective breadth of webs under action of punching shear (reproduced from BS EN 1168 Figure 5(a) and (b)).

In spite of this evidence, BS EN 1168 [5.8], clause 4.3.3.2.4 (there is no equivalent in BS 8110) gives an expression for punching shear capacity V_{Rd} in untopped hcu as:

$$V_{Rd} = b_{eff} h f_{ctd}(1 + 0.3\alpha\sigma_{cp} / f_{ctd}) \geq V_{Ed,p} \text{ reaction from the point load(s)} F_{Ed} \tag{5.36}$$

where

b_{eff} = effective widths of webs according to Figure 5.35
h = depth of unit
α = $l_x/l_{bpd} \leq 1$ if the point load is within a distance less than the flexural development length.

By rearranging Eq. (5.32), V_{Rd} is equal to the shear-tension capacity of the webs ($b_{eff}\ h\ f_{ctd}$) plus 0.3 times the effective prestress in the webs ($0.3\alpha\ \sigma_{cp}\ b_{eff}\ h$), similar to historic values. V_{Rd} is heavily influenced by the width of the footprint relative to the breadth of the cores, particularly if $w <$ ½ core breadth, e.g. in some deeper slip-formed units core breadth = 150 to 250 mm. Clause 4.3.3.2.4 states that if $w <$ ½ core breadth, h in Eq. (5.32) is replaced by h_f (top flange depth) and $b_{eff} = w$. There are several complications at free edges in the outermost web, for which the best solution is to open and *in situ* infill the first core. Clause 4.3.3.2.4 states that if more than 50 per cent of the load is acting on the outermost web (i.e. only two webs active), Eq. (5.36) is applicable if one tendon is in that web and transverse reinforcement is present, i.e. in reality a structural topping with $A_s = F_{Ed}/0.87f_{yk}$ locally. The topping could be localised over the edge unit if it is possible for this to be (say) 50 mm shallower than the rest of the units. If one or both of these is not satisfied, then use 0.5 V_{Rd}.

BS EN 1168 does give guidance in the case of two point loads in close proximity, or what that proximity might be in both longitudinal and transverse directions of the unit. If the transverse gap between the point loads is greater than $2b_{eff}$, they may be considered separately. However, as

many point loads in hollow-core floors are due to trimmer angles at voids, they will be acting together. This is dealt with by drawing a shear force diagram $V_{Ed,p}$ for multiple point loads F_{Ed}'s such that $V_{Ed,p} \leq V_{Rd}$.

Consider a point dead load of 50 kN acting over a footprint 300 mm square at 1.0 m from the centre of support of a 6.0 m, simply supported, 200 mm-deep hcu. The unit is grouted in and the load is not at a free edge. The hcu contains 140 mm-wide cores and 40 mm webs. Concrete $f_{ck} = 45\,\text{N/mm}^2$, $f_{ctd} = 1.77\,\text{N/mm}^2$, axial prestress $\gamma_{p,fav}\ \sigma_{cp} = 0.9 \times 4.95 = 4.46\,\text{N/mm}^2$, the unit contains 12.5 mm strands such that $l_{bpd} = 1410$ mm. If the bearing length is 100 mm, $\alpha = (10\,000 + 100/2)/1410 = 0.744$. Referring to Figure 5.35(a), a 300 mm-wide footprint will be resisted by two webs; then $b_{eff} = 80$ mm. Thus Eq. (5.36)

$$V_{Rd} = 80 \times 200 \times 1.77(1 + 0.3 \times 0.744 \times 4.46/1.77) \times 10^{-3} = \underline{44.2\ \text{kN}}$$

Maximum reaction from the load $V_{Ed} = 1.35 \times 50 \times (6.0 - 1.0)/6.0 = \underline{56.3\,\text{kN}} > 44.2$. Fails.

Concentrated point and line loads, anywhere on the floor slab, are in accordance with BS EN 1168, clause 4.3.3.2.5. The first decision is whether the hcus are grouted to form a complete floor. If this is not the case (isolated units), the limiting tension is $f_{ctk,0.05}$ $(= 0.7f_{ctm})$ and the capacities are at the serviceability limit state q_k and F_k. If the units are grouted to permit transverse load distribution, the limiting tension $f_t = f_{ctd}$ $(= 0.7f_{ctm}/1.5)$ and the capacities are now at the ultimate limit state q_d and F_d.

BS EN 1168 does not explain how to deal with multiple loads in close proximity, nor diagonally crossing loads, but these should be resolved into loads parallel with the longitudinal span as long as the load is covering at least a width of one core plus one web. For multiple loads in close proximity, the shear force diagram may be drawn such that the design shear force should not exceed the capacities in Eqs. (5.37 to 5.39).

For a linear (line) load <u>not</u> at an edge

$$q_k = 20W_{lb}f_{ctk,0.05} / (l + 2b) \tag{5.37}$$

For a linear (line) load at an edge

$$q_k = 10W_{lt}f_{ctk,0.05} / (l + 2b) \tag{5.38}$$

For a point load anywhere

$$F_k = 3W_l f_{ctk,0.05} \tag{5.39}$$

where W_{lb} and W_{lt} = section modulus in transverse direction per unit length in the bottom and top fibres, respectively.

W_l is smaller of W_{lb} or W_{lt}
l = length of the line load
b = breadth of unit.

The section modulus W is calculated from the second moment of area, taking a longitudinal cut through the unit, and considering the top and bottom flanges as rectangles 1 mm wide. For example, if $h = 200$ mm and both flanges have thickness $h_f = 40$ mm, $I_l = 522\ 667\,\text{mm}^4/\text{mm}$, $W_l = 5227\,\text{mm}^3/\text{mm}$. If $f_{ctk,0.05} = 0.7 \times 3.80 = 2.66\,\text{N/mm}^2$, length of line load = 1000 mm and $b = 1200$ mm, then for an innermost line load Eq. (5.37)

$$q_k = 20 \times 5227 \times 2.66 / 3400 \leq 81.7\ \text{N/mm} = 81.7\ \text{kN/m service load for an isolated unit.}$$

If the start of the line load is less than b from the end of the unit, the load spread term $(l + 2b)$ is reduced, e.g. if the same line load starts at 600 mm from the end of the span, $(l + 2b) = 600 + 1000 + 1200 = 2800$ mm, and $q_k = 99.3$ kN/m. If the floor slab is grouted, part of the load will be distributed across the longitudinal joints and the ultimate capacity is now $q_d = 20 \times 5227 \times 1.77/3400 \leq 54.4$ kN/m. If this is a dead load, then $q_k = 54.4/1.35 = 40.3$ kN/m. Line loads at edges Eq. (5.38) are half of the above.

Global resistance to point loads is given in Eq. (5.39). The size of the footprint is not given, but at least 300 mm is prudent. This is not the same as a punching shear capacity, but is derived in the manner in which full-scale test behaviour shows longitudinal splitting running through the entire span. However, for the same example, $F_k = 3\ W_l f_{ctk,0.05} = 3 \times 5227 \times 2.66 = 41.7$ kN on an isolated unit, and $F_d = 27.8$ kN on a grouted floor.

This section has considered the local load capacities of hcus in a one-way spanning floor slab. If the edge unit is supported along one edge by a gable wall or beam, the unit is classed as supported on three edges and is subjected to shear, bending and torsion. BS EN 1168, clause 4.3.3.2.6 provides semi-empirical data for the imposed service load capacity (excludes self-weight) of such units as

$$q_k = W_t f_{ctk,0.05} / 0.06 l^2 \tag{5.40}$$

where

W_t = elastic torsional section modulus = $2t\ (h - h_f)(b - b_w)$
t = $\min(h_f;\ b_w)$.

Continuing the same example, with $b_w = 50$ mm outermost web, $W_t = 2 \times 40 \times 160 \times 1150 = 14.72 \times 10^6$ mm^3. $q_k = 14.72 \times 10^6 \times 2.66/(0.06 \times 6000^2) = 18.12$ kN/m^2. This imposed load (assumed to be all live load) would exceed the service moment of resistance of the hcu considered, and is therefore shown to be not critical should it happen to be supported on three edges.

5.2.11 Anchorage and bond development lengths

The notion of anchorage and bond transfer lengths in prestressed concrete is well established. However, in cases where helically wound strand is used as the prestressing medium, the unique properties give rise to increased stress transfer lengths, known as total anchorage lengths in BS EN 1992-1-1 {or 'development lengths' in BS 8110}. These distances are indicated in Figure 5.14. Development lengths may be of the order of 1.5 to 2.0 m for 12.5- or 12.9 mm-diameter strand and therefore must form part of this study so that the designer can assess the implications of flexural cracking in this region. The situation is exacerbated by the fact that shear, which is most critical at about $0.5h$ from the support at the narrowest point in the web, relies entirely on the development of prestress.

When the tendon is released at transfer, frictional bond stresses develop around the tendon. Equilibrium is reached when the total bond force equals the prestressing force in the tendon, and the tendon stops slipping. The length of tendon necessary to reach the state of equilibrium is called the 'transmission length' l_{pt} in BS EN 1992-1 {or 'transfer length', l_t in BS 8110}. Typical values for l_t are 40 to 80 diameters, and so 70 {50} diameters is frequently used in design for strand, and 100 {100} for plain or indented wire. A major difference in BS EN 1992-1-1 compared with BS 8110 is that l_{pt} is a function of the prestress in the tendons at transfer/release σ_{pm0}. It is also subject to an upper-bound factor of 1.2 for ultimate design, e.g. for $V_{Rd,c}$. When checking service stress limits, such as for slippage or bursting stresses, a lower bound is used $l_{pt1} = 0.8\ l_{pt}$.

A comparison of transmission length/diameter ratio, between EC2 and previous research data, is shown in Figure 5.36. Most of the research uses 12.7- and 15.2 mm-diameter strand, except in Kong's work for 5- and 7 mm-diameter wires. It is clear that the research data are nearly all below the

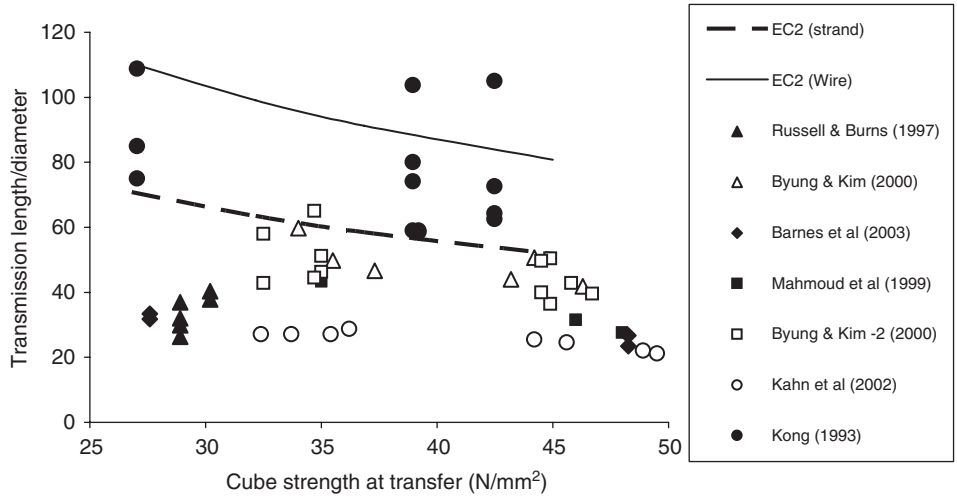

Figure 5.36 Normalised transmission length between EC2 and past research data. Note: EC2 data do not contain the 1.2 l_{pt} factor.

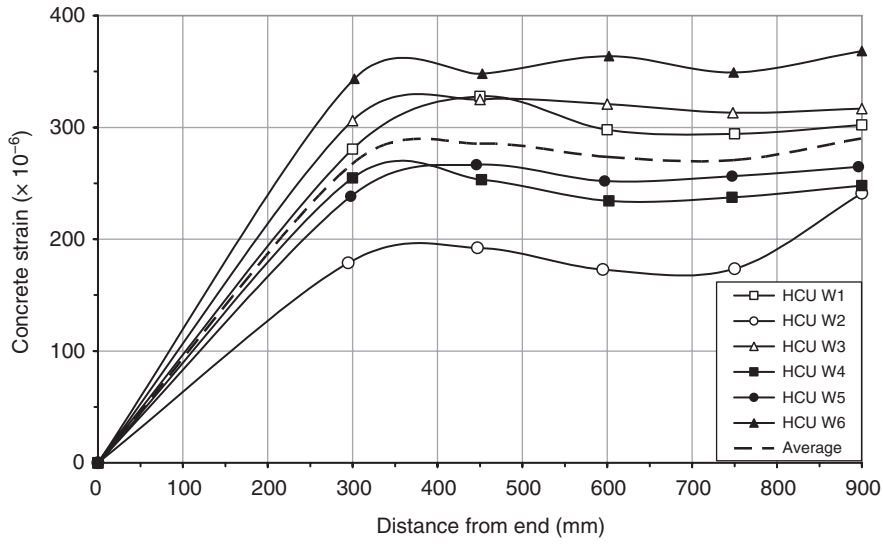

Figure 5.37 Distributions of soffit surface strain near the ends of hollow-core units.

requirements in EC2. The discrepancies are even greater when the 1.2 l_{pt} factor is added. There is clearly scope for 'improvement' in the EC2 values, i.e. experimental evidence that l_{pt} is reduced in hcus cut from long line production, where the fully developed anchorage bond is interrupted during the sawing operation, rather than developing from a cast end.

Figure 5.37 shows some experimental results produced by Elliott for the UK Precast Flooring Federation. Soffit strains were measured from the ends of hcus pretensioned using 5 mm wires to about $f_{bc(t)} = 11\,\text{N/mm}^2$. Using $\sigma_{pm0} = 1158\,\text{N/mm}^2$, and $f_{bpt} = 2.8\,\text{N/mm}^2$, l_{pt} was calculated as 515 mm, hence $1.2l_{pt} = 618\,\text{mm}$. Figure 5.38 shows the measured transmission length is between 260 and 340 mm,

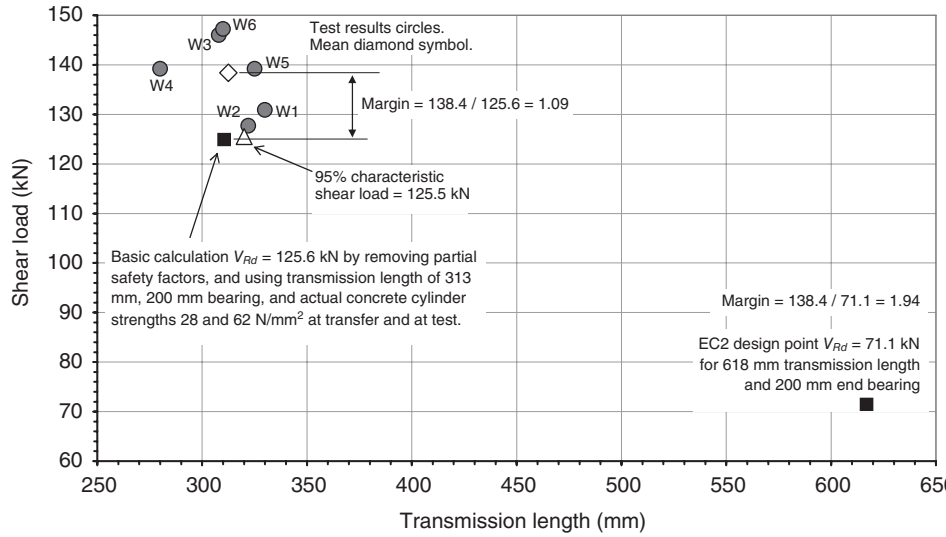

Figure 5.38 Transmission length versus ultimate shear resistance of 150 mm-deep prestressed hollow-core slabs pretensioned using 5 mm wire.

with a mean value of 313 mm, i.e. 61 per cent of l_{pt}. Furthermore, using $1.2l_{pt} = 618$ mm the design value for these units was $V_{Rd,c} = 71.1$ kN, compared with the average ultimate shear capacity in the six tests of 138.4 kN and a 95 per cent characteristic strength of 125.5 kN. A more meaningful comparison is to (i) replace $1.2l_{pt}$ with 315 mm; (ii) remove all partial safety factors from the design equation, i.e. $\gamma_{m,fav} = 0.9$ and $\gamma_m = 1.5$; (iii) substitute actual material properties for design strengths, and (iv) recalculate $V_{R,mean} = 125.6$ kN. This is equal to the 95 per cent characteristic strength of 125.5 kN and shows that, with further research, there may be scope to reduce transmission lengths in hcus.

Previous research has shown that transmission lengths are longer at the end where the prestress is released at a cast end, compared to the remote dead end. In the case of hcus the prestress never develops at a 'cast' end, but always at a 'dead' end during cutting. Russell *et al.* [5.45] showed an increase in L_t of 34%; Kaar *et al.* 20%, and Oh and Kim (2000) [5.46] 16% and 13% for 12.7 and 15.2 mm strands, respectively. It is possible that EC2 equations are based on transfer at a cast end, and have not taken into consideration the unique manufacturing practice for hcus.

If a flexural crack occurs within the transfer length it is not possible to develop the full prestressing force, because the equilibrium has been destroyed. Thus in flexurally cracked concrete an additional length is necessary to ensure that the ultimate stress in the tendon is developed. This additional distance is called the 'flexural-bond length', and the total length is the 'development length' l_{bpd} $\{l_d\}$.

The stress at the end of the transfer length is equal to the prestress after losses. The stress at the end of the development length is equal to the rupture stress in the tendon. Thus if a flexural crack occurs at a distance x from the end of the slab (Figure 5.14), then if:

- $x > l_{bpd}$ $\{l_d\}$, full flexural capacity is achieved;
- l_{pt} $\{l_t\} < x < l_{bpd}$ $\{l_d\}$, the capacity is larger than the flexural cracking moment, but smaller than the ultimate moment;
- $x < l_{pt}$ $\{l_t\}$ the anchorage capacity is smaller than the cracking moment, so that failure occurs subsequent to flexural cracking. Also the cracking moment is reduced owing to incomplete development of prestress in that zone.

BS EN 1992-1-1, clause 8.10.2.2 [5.1].
For helical strand with gradual release of prestress. 'Good' bond conditions are known.
(Eq. 8.16) $l_{pt} = 0.19\ \sigma_{pm0}\ \phi / f_{bpt}$ (5.41)
(Eq. 8.15) $f_{bpt} = 3.2\ f_{ctd(t)}$
σ_{pm0} = tendon stress at release.
For plain and indented wire:
$l_{pt} = 0.25\ \sigma_{pm0}\ \phi / f_{bpt}$
$f_{bpt} = 2.7\ f_{ctd(t)}$
(Eq. 8.18) Design $l_{pt2} = 1.2\ l_{pt}$
Eq. 8.19 calls for the greater of $1.2\ l_{pt}$ or a dispersion length l_{disp}. It is found that $1.2\ l_{pt}$ is critical for hollow-core.
(from Eq. 8.21)

$$l_{bpd} = l_{pt2} + 1.131 \frac{(\sigma_{pd} - \sigma_{pm\infty})}{f_{ck}^{2/3}} \phi \qquad (5.42)$$

where
$f_{bpd} = 0.168 f_{ck}^{2/3}$ (from Eq. 8.20)
for strands and
$f_{bpd} = 0.196 f_{ck}^{2/3}$ for wire
σ_{pd} is the tendon stress for a cracked section where the concrete stress > $f_{ctk,0.05}$
$\sigma_{pm\infty}$ is the prestress after all losses.

Walraven and Mercx [5.14] have reported that the ACI Code [5.37] formulae for:

$$l_t = f_{pe} \frac{\phi}{21} \qquad (5.41)$$

$$l_d = l_t + (f_{pu} - f_{pe}) \frac{\phi}{7} \qquad (5.42)$$

are adequate, where
ϕ = bar diameter.
BS 8110, Part 1, clauses 4.3.8.4. and 4.10.3 give l_d as the greater of h, or $K_t \phi / \sqrt{f_{ci}}$, where $K_t = 240$ for strand, 400 for crimped wire and 600 for plain wire.
Finite element work by Akesson [5.47] has simulated the bond around 7-wire 12.9 mm-diameter helical strands in 215, 265 and 380 mm-deep hollow-core slab sections shown in Figure 5.39. The concrete strength was 47.5 N/mm^2. The main objectives of the study were to determine the extent of cracking in the interface, measure transmission lengths, and compare strand slippage with actual values measured by Tassi [5.48] and Gylltoft [5.49]. The strands were stressed to $f_{pe} = 0.54\ f_{pu}$ to $0.60\ f_{pu}$ and the results show transfer lengths were in the order of 340 mm, i.e. 26ϕ. In other words the denominator in Eq. (5.41) would read 38, not 21. The strand slippage was about 0.8 mm. A failure analysis was also carried out using $f_{pe} = f_{pu}$, whereupon l_t increases to 719 mm and the slippage increases to 2.19 mm in the worst case.
Figure 5.40 shows contours of the splitting stresses through the centre of the web. The maximum stress is 2.18 N/mm^2, i.e. $0.32\sqrt{f_{cu}}$, which under normal circumstances would probably not lead to cracking. However in this case cracking was found in the concrete closest to the interface over a distance of between 172 and 191 mm.

High concrete strengths do not guarantee good anchorage capacity; that depends mainly on good compaction around the tendon. There is more laitance around the strands in units produced by the extrusion process (compared with slip-forming), which may have a slight effect on the bond characteristics.

5.2.12 Slippage of tendons

Slippage (sometimes called 'pull-in') ΔL_o is the shortening of tendons after transfer of prestress. It is the cumulative effect of movement of tendons relative to the concrete due to bond slip within the

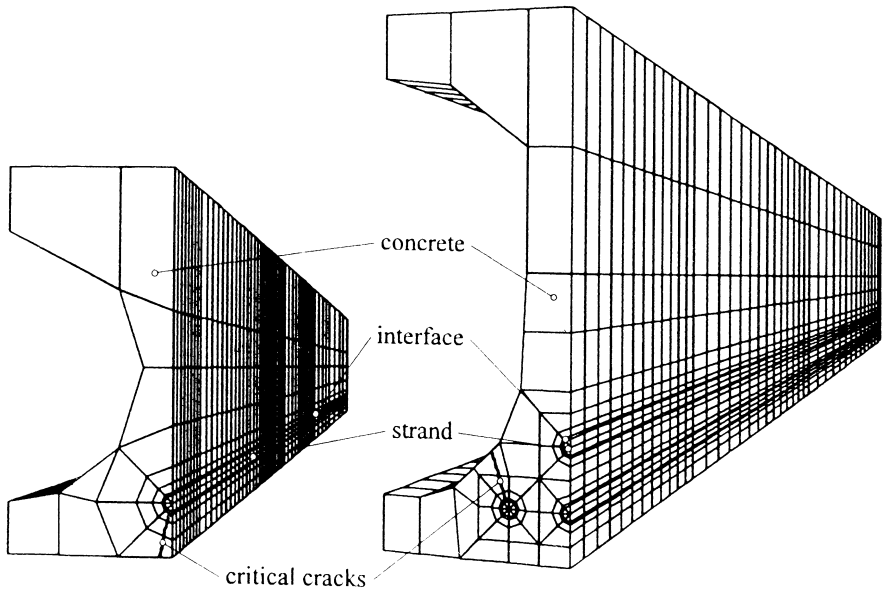

Figure 5.39 Finite element mesh used by Akesson [5.47].

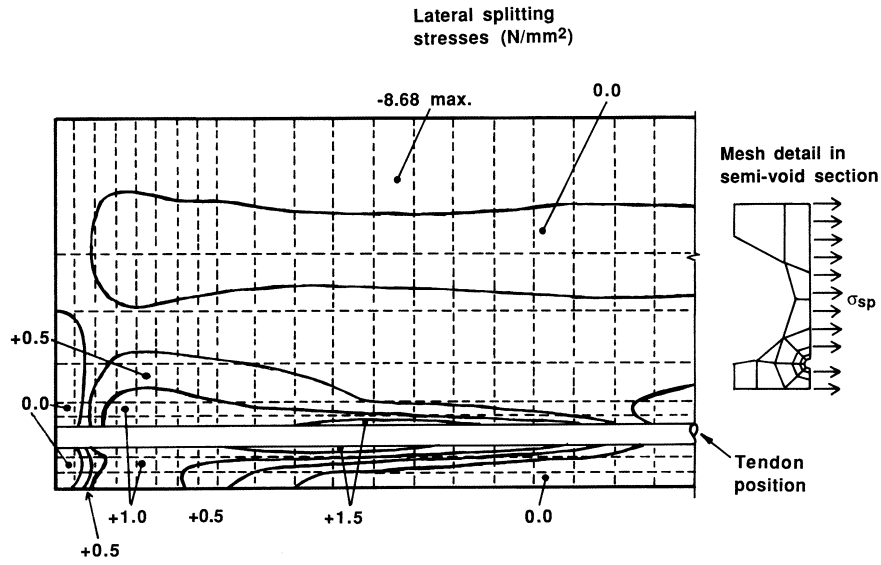

Figure 5.40 Principal tensile stress contours around tendons by Akesson [5.47].

transmission length, l_{pt} $\{l_t\}$. It appears at the ends of prestressed elements, as shown in Figure 5.41 and 5.42, and gives an indication that prestress has developed correctly, particularly in the transmission zone, but it is not a definitive measurement of prestress.

The subject is comprehensively reviewed and the relationship between ΔL_o and l_t analysed in a thesis by Paul Kong [5.50]. Referring to Figure 5.41:

$\varepsilon_{si} - \varepsilon_{sx}$ = steel strain change at distance x after transfer
ε_{cx} = concrete strain at distance x after transfer
$(\varepsilon_{si} - \varepsilon_{sx}) - \varepsilon_{cx}$ = steel strain change at distance x after transfer net of concrete strain

Figure 5.41 Pull-in and slippage of 5 mm-diameter wires.

Figure 5.42 Slippage of 9.3 mm-diameter helical strand between 2 and 10 mm.

$$\Delta L_o = \int_0^{L_t} (\varepsilon_{si} - \varepsilon_{sx} - \varepsilon_{cx})\delta x \quad \text{(the area OAB)}$$
$$= \varepsilon_{si} l_{pt} / 2 = \sigma_{pm0} l_{pt} / 2E_p \quad \{= f_{si} l_t / 2E_p\} \tag{5.43}$$

where σ_{pm0} is the prestress at transfer $\{f_{si}\}$.

BS EN 1992-1-1, clause 8.10.2.1 specifies a linear increase in prestress, and so $\Delta L_o = f_{si}\ l_t/2\ E_p$. However, BS 8110 specifies a parabolic increase and so $\Delta L_o = f_{si}\ l_t/3\ E_p$. If it is linear-parabolic (as shown in the strain distributions in Figure 5.37), it takes the familiar form

$$\Delta L_o = f_{si} l_t / 2.5E_p = 0.4 f_{si} l_t / E_p \tag{5.44}$$

Slippage is routinely observed (and often measured and recorded) by manufacturers of hollow-core, as shown in Figures 5.42 and 5.43, according to methods given in BS EN 13369:2013, clause 4.2.3.2.4, *Common Rules for Precast Concrete Products*. A single measurement is required for single wires, but in the case of helical strand, where the slippage across a single strand will vary as the saw progressively cuts through the wires, the mean of three circumferentially positioned measurements is required on the outer wires. In typical production, with good-quality and well-graded aggregates

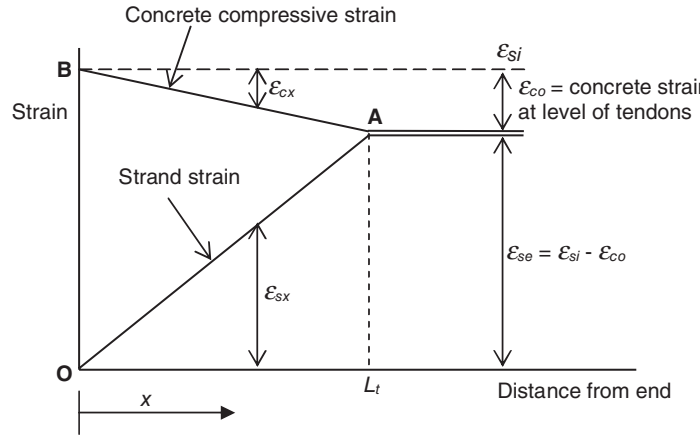

Figure 5.43 Strand and concrete strain profiles without slippage, both assumed linear according to BS EN 1992-1-1.

(particularly fine aggregate grading around the 1 mm sieve size), adequate maturity and careful detensioning and sawing operations, slippage is about 1 to 2 mm. Theoretically it cannot be zero, but often appears to be so. Slippage of wire tends to be more consistent than with strand, particularly if there is a concentration of large-diameter strands in a small area, and is quite common if a group of three strands are positioned in a line rather than in a triangular formation.

The limit for slippage is a manufacturing issue, rather than a design issue, and as such is not given in BS EN 1992-1-1 or BS 8110. However, BS EN 13369, clause 4.2.3.2.4 states that mean slippage in an element (both ends) should not exceed:

$$\Delta L_o = 0.4 l_{pt2} \sigma_{pm0} / E_p \tag{5.45}$$

and for an individual tendon not more than $1.3\Delta_o$.

For an example of strand, if $\sigma_{pm0} = 0.7 \times 1770 \times 0.95$ (5% loss), and l_{pt2} = (say) 600 mm, $\Delta L_o = 0.4 \times 1177 \times 600/195\,000 = 1.45$ mm, and $1.3\Delta L_o = 1.88$ mm. These are reasonable limits to work to, but this clause does not explain how, or whether, the capacity of a prestressed element may be reassessed if ΔL_o is exceeded. Clearly if the measured slippage $\delta_s > \Delta L_o$ by 2 or 3 mm in a couple of tendons, the effect on transmission length and mechanical strength will be small, but if $\delta_s = 5$ or 6 mm in all tendons, re-analysis for residual prestress, or rejection of the unit, are possible courses of action. The FIP Manual: *Quality assurance of hollow-core slab floors*, clause 3.5.3 [5.51], gives a production limit based on an upper-bound value for transmission length $l_t = 13\phi\sqrt{\sigma_{pm0} / f_{cu}}$ and slippage $\Delta L_o = ½ \varepsilon_{pm0} l_t$. For example, consider an hcu with $f_{ci} = 35$ N/mm^2, with 12.5 mm strands stressed to 70% × 1770 N/mm^2 and 5% losses at transfer, $l_t = 13 \times 12.5 \times \sqrt{1177/35} = 942$ mm, and $\Delta L_{o,limit} = 0.5 \times 0.00604 \times 942 = 2.85$ mm. This is multiplied by 1.5 for an individual tendon $\Delta L_{o,limit} = 4.3$ mm, and this would be an acceptable limit. The PCI Manual for the design of hollow-core slabs (Section 2.6.1) [5.13] suggests a 'free end slip' $\Delta_{ct} = f_{si}\, d_b/950$ (Imperial units) that approximates the shortening over the transfer length, i.e. $\Delta L_{o,limit} = l_{pt2}\, \sigma_{pm0}/E_p = 3.6$ mm for the same example. The evidence now suggests that if $\delta_s \le \Delta L_o$ as per Eq. (5.45) no action is required, but if $\Delta L_o < \delta_s \le \Delta L_{o,limit}$ some reassessment is advisable.

The PCI Manual also offers a method to back-calculate transmission length from slippage, i.e. if $\delta_s > \Delta L_o$, then $l_t = 2\, E_p/f_{si}\, \delta_s$, and goes on to determine the total anchorage length {flexural development length}, as explained later.

For the relationship between slippage and residual prestress, some designers of hcus take the FIP limit for a tendon to be non-contributory, and recalculate the capacity on a reduced number of

tendons. Others use a linear scale to determine residual prestress, taking the ratio of prestress with/without slippage from 1.0 where $\delta_s = \Delta L_o$, to zero, where δ_{free} = free elastic shortening over half the length of the unit for the tendons having $\delta_s > \Delta L_o$. Then $\delta_{free} = 0.5\ L\ \sigma_{pm0}/E_p$.

Continuing the example above, let slippage $\delta_{s,mean} = 4.0$ mm occur in half the number of tendons in an hcu of 6.0 m length. Now $\delta_{free} = 1177 \times 3000/195\ 000 = 18.1$ mm. The prestress in tendons with slippage is given pro rata as $(\delta_{free} - \delta_s)/\delta_{free})\ \sigma_{pm0} = ((18.1 - 4.0)/18.1) \times 1177 = 917\ \text{N/mm}^2$. The mean effective prestress $\sigma_{pm0,\text{eff}} = (0.5 \times 917 + 0.5 \times 1177) = 1047\ \text{N/mm}^2$, and this is used to calculate losses due to instantaneous deformation, creep and relaxation, leading to reduced values of σ_{po}, f_{bc} and hence M_{sr}. Comparison can be made with the research by Evans [5.52], who measured the loss of strain at the end of the transmission zone as 0.14 $\delta_{mean}/L_t = 0.14 \times 2.7/600 = 0.00063$, where $\delta_{mean} = (0.5 \times 4.0 + 0.5 \times 1.45) = 2.7$ mm. Then the residual strain is 0.00604 − 0.00063 = 0.00541, and residual stress = 0.00541 × 195 000 = 1055 N/mm^2 (giving reasonable agreement with 1047 N/mm^2).

The increase in l_{pt2} for strands with slippage is given as $l'_{pt2} = \delta_s E_p\ /\ 0.4\sigma_{pm0} = 4.0 \times 195\,000\ /\ 0.4 \times 1177 = 1656$ mm. The mean length by superposition $l'_{pt2,mean} = (0.5 \times 1656 + 0.5 \times 600)\ /\ 10 = 1128$ mm. This is used to recalculate the reduced shear capacity $V_{Rd,c}$.

If $\delta_s > \Delta L_o$, l_{pt2} and the total anchorage length l_{pbd} are both increased. The PCI Manual [5.13] shows that the increase in l_{pbd} is directly proportional to the increase in l_{pt2}, i.e. $l_{pbd,mean} = l_{pbd} l'_{pt2,mean}\ /\ l_{pt2}$. Thus for the example, it is found from the above that the final prestress (with no slippage) is 970 N/mm^2 and σ_{pd} = maximum allowed (according to BS EN 1992-1-1, Fig. 3.19) = 1517 N/mm^2. Then (Eq. 8.20 & 8.21) $l_{pbd} = 600 + 0.19 \times 12.5 \times (1517 - 970)/(1.2 \times 1.0 \times 1.77) = 1212$ mm, so $l_{pbd,mean} = 1212 \times 1128\ /\ 600 = 2278$ mm. If this distance is greater than half the span of the floor unit, full flexural capacity cannot be achieved.

Figure 5.44 shows stress profiles for this example for strands with and without slippage. Based on this stress profile, the service and ultimate moments of resistance M_{sr} and M_{Rd} may be computed at positions in the span, and compared with design service and ultimate moments, as shown in Figure 5.45.

Slippage will cause a reduction in camber according to the effective prestress. Changes in l_{pt2} have no influence on flexural stiffness when calculating floor deflections due to live loads, but would nevertheless result in greater long-term positive deflections due to reduced visco-elastic negative camber.

5.2.13 Calculation of crack width

Prestressed concrete elements designed as Class 1 or Class 2 (limiting tensile stress of zero or f_{ctm} $\{0.45\sqrt{f_{cu}}\}$) should not, by definition, require a check for crack width, and such has been the practice

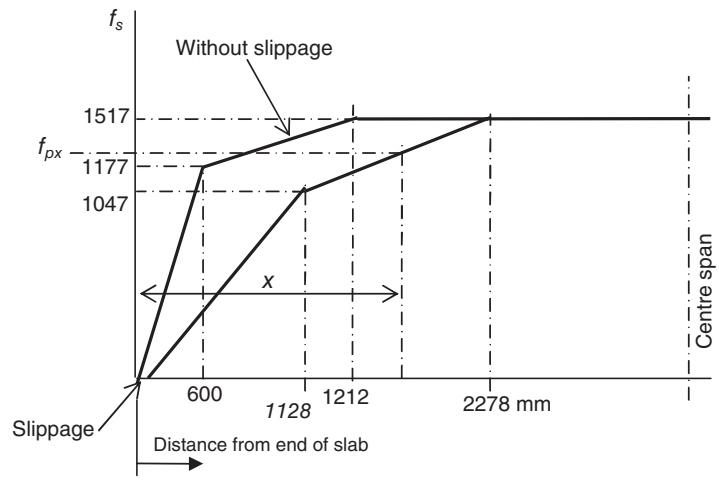

Figure 5.44 Stress profile for the worked example of the transmission and anchorage lengths, with and without slippage.

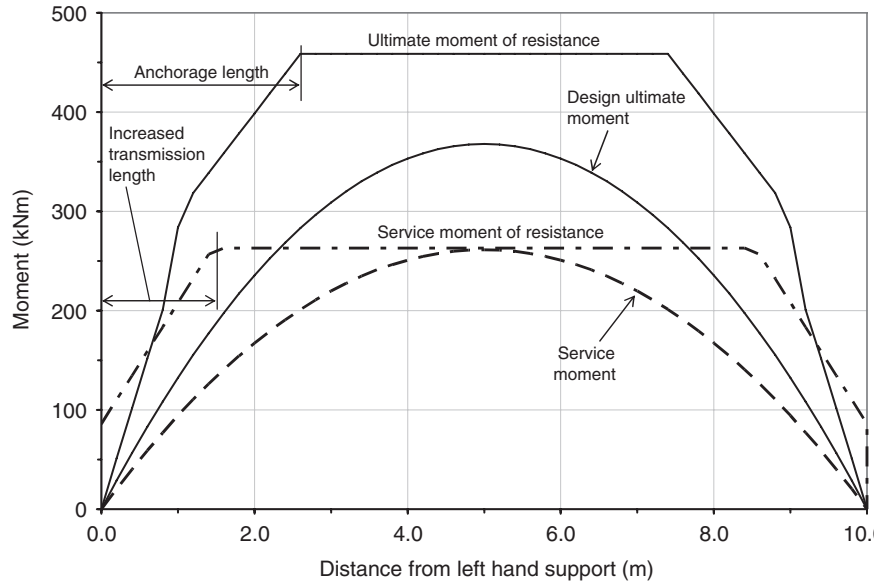

Figure 5.45 Moment of resistance distributions for the effects of slippage of tendons, showing increased transmission and anchorage lengths.

for many years. BS 8110 Class 3 elements which have a hypothetical crack width of 0.1 or 0.2 mm, have likewise not been the subject of crack-width checks. Unacceptable cracking may be avoided if the level of prestress does not exceed 0.75 f_{pk} in service, typically 1330 N/mm^2, which is uncommon and means that the initial prestress needs to as high as 0.85 f_{pk}.

BS EN 1992-1-1, clause 7.1(2) states that for the purpose of calculating crack widths, service stresses should be for the flexurally uncracked section and the flexural tensile stress $\leq f_{ctm}$. Further, clause 7.3.2(4) states that where crack control is necessary no minimum reinforcement is required providing that, under characteristic loading, the tensile stress is less than f_{ctm}. This is always the case; as the only time characteristic loading is not used, the limiting tensile stress is zero for exposure classes greater than XC1, according to Table 7.1N (from the UK NAD Table NA4). Table 5.4 shows the part of Table 7.1N applicable to prestressed concrete with bonded tendons. Note that Table 7.1N has not been accepted in all European countries, particularly for zero tension for exposure classes XC2 to XC4, where a limiting tensile stress of $f_{ctm}/1.2$ is used, for example. Although Table 7.1N suggests that crack widths are required by calculation, and should be ≤ 0.2 mm under the frequent load combination, it is not common practice to calculate crack widths. Two alternatives are therefore possible:

1. Under the frequent combination of load the tensile stress is maintained as $\leq 1.65\ f_{ctm}$. This is proposed in Technical Report 43 [5.53], albeit on post-tensioned concrete slabs. This figure is generally in line with Class 3 stresses in BS 8110, i.e. 5.8 to 6.7 N/mm^2.
2. Crack-spacing and crack-width calculations are undertaken according to clause 7.3.4.

The design crack width w_k is the product of crack spacing $s_{r,max}$ and effective tensile strain between the steel bars ε_{sm} and the concrete ε_{cm}, allowing for tension stiffening, as:

$$w_k = s_{r,max}(\varepsilon_{sm} - \varepsilon_{cm}) \quad \text{(from Eq. 7.8)} \tag{5.46}$$

Note that in calculating ε_{sm} only the *additional* strain (not the total strain) beyond the state of zero strain in the concrete should be considered, i.e. for prestressed concrete this means after decompression.

Table 5.4 Maximum crack width (mm) for prestressed concrete with bonded tendons

Class designation	**Frequent load combination** $= 1.0\ G_k + \psi_1\ Q_k$	**Quasi-permanent load** $= 1.0\ G_k + \psi_2\ Q_k$
XC1	0.2	–
XC2 XC3 XC4	0.2	Decompression i.e. zero tension in soffit*
XD1/XS1 XD2/XS2 XS3	Decompression i.e. zero tension in soffit*	–
XD3	Depends on nature of aggressive agent	

* All wires lie at least 25 mm within concrete in compression, i.e. cover from soffit ≥ 25 mm.

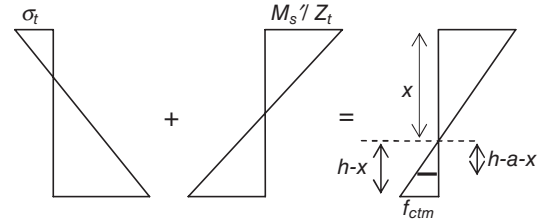

Figure 5.46 State of stress used in the calculation of $\Delta\sigma_p$ and crack width in prestressed concrete.

The net strain is given as:

$$\varepsilon_{sm} - \varepsilon_{cm} = \frac{\sigma_s - k_t \dfrac{f_{ct,eff}}{\rho_{eff}}(1 + \alpha_e \rho_{eff})}{E_s} \geq 0.6\frac{\sigma_s}{E_s} \quad \text{(from Eq. 7.9)} \tag{5.47}$$

For prestressed concrete, the steel stress σ_s may be replaced by $\Delta\sigma_p$. The stress variation in the tendons from the state of zero strain in the concrete at the level of tendons nearest to soffit $= \dfrac{h-a-x}{h-x} f_{ctm}$. See Figure 5.46. (Note that for reinforced concrete σ_s is the stress based on the flexurally cracked section.)

where a = axis distance = minimum cover + tendon diameter

x = depth to zero stress after decompression

$$x = \left(\frac{M_s' / Z_t - \sigma_t}{M_s' / Z_t - \sigma_t + f_{ctm}}\right) h \tag{5.48}$$

k_t = 0.4 for long-term loading
$f_{ct,eff} = f_{ctm}$
$\alpha_e = E_s / E_{cm}$
$\rho_{eff} = A_p / A_{c,eff}$
$A_{c,eff}$ = area in tension zone to a height of $\min((h - x)/3;\ 2.5(h - d);\ 0.5h)$
M_s' = service moment due to frequent load combination = $1.0\ G_k + \psi_1\ Q_k$.

Note that for the majority of prestressed sections that are critical at M_{sr} based on f_{ctm}, x is very close to the bottom of the section, and because the bending stress M'_s / Z_t is from the frequent load < characteristic load, decompression will not be attained and hence $\Delta\sigma_p = 0$.

The design crack spacing (mm)

$$s_{r,max} = k_3 c + k_1 k_2 k_4 \phi / \rho_{eff} \quad \text{(from Eq. 7.11)} \tag{5.49}$$

where

$k_1 = 1.6$, $k_2 = 0.5$, $k_3 = 3.4$, $k_4 = 0.425$
ϕ = mean tendon diameter based on area (if mixed sizes at minimum cover)
c = minimum cover

Finally, check that tendon spacing $< 5(c + \phi/2)$ (from 7.3.4.(3)) (5.50)

See worked example in Section 5.6.

5.2.14 Cantilever design using hollow-core slabs

Cantilever spans of up to about 1.5 m long for units 200 to 250 mm deep may be designed using one of two methods. If no structural topping screed is used, one solution is to provide top steel in the cantilevered part and in the main span for a considerable distance, to provide a tie-back with an adequate factor of safety of 2. Figure 5.47 shows an example of 750 mm-long cantilever units with additional top steel. The disruption to production is considerable, as seen in Figure 5.48. The most onerous partial load factors are used. Figure 5.49 shows a 2.65 m cantilever in a negative bending and shear test. The 300 mm-deep hcu contained seven 9.3 mm-diameter strands in the top, with a design tensile force resistance of 561 kN. The negative bending moment due to self-weight and the applied load of 9.5 kN induced a top stress of $-3.1\ \text{N/mm}^2$ (tension) which, when added to the compressive prestress in the top, gave a net top stress of $+0.5\ \text{N/mm}^2$ (compression). There was no evidence of cracking and the deflections were fully recoverable.

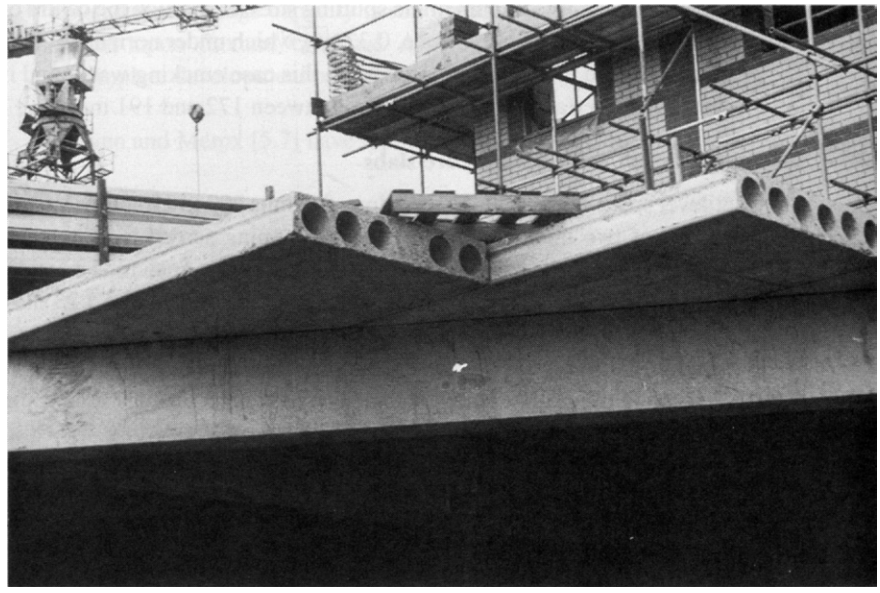

Figure 5.47 Cantilevered hollow-core slabs.

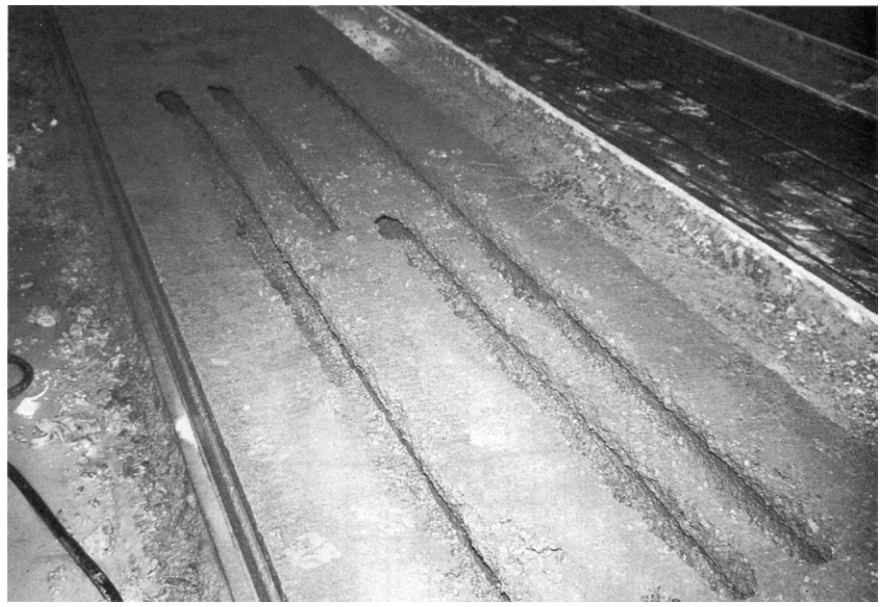

Figure 5.48 Making cut-outs in to the tops of hollow-core units to form reinforced concrete slots to resist hogging bending moments.

Figure 5.49 Cantilever hollow-core unit under negative moment and shear.
(Courtesy of Creagh Concrete Ltd., N. Ireland).

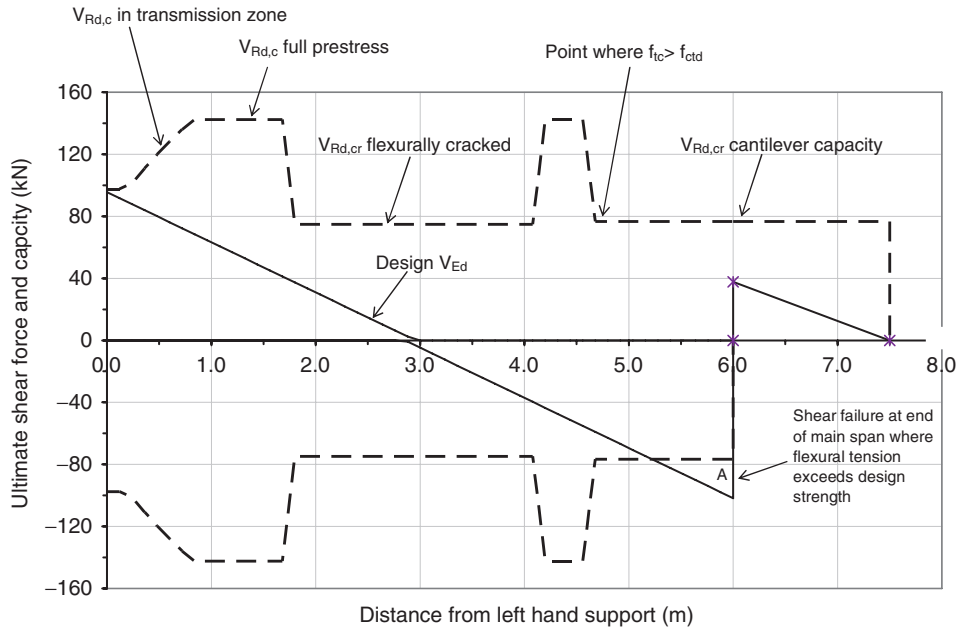

Figure 5.50 Shear force and shear capacity diagram for cantilever hollow-core unit, showing regions of reduced shear in the main span (A) where flexural tension exceeds design tensile strength.

The second solution is to use debonded strands so that no upward prestressing force is applied in the cantilevered portion, but this may be wasteful if the cantilever is short compared with the main span. Where debonded tendons are used, the transmission lengths for top steel should be increased by 50 per cent, owing to the varying nature of concrete close to the tops of units.

In either case there is considerable disruption to the manufacturing procedures and a cost increase in the order of 10 to 15 per cent.

The combined tensile stresses due to negative moment and prestress may exceed the design tensile strength of the concrete f_{ctd} $\{f_{ct}\}$ in the region of the support. In this case the design ultimate shear strength should be reduced to the flexurally cracked capacity $V_{Rd,cr}$ $\{V_{cr}\}$ (see Section 5.2.10.3). This may have a serious consequence in the shear capacity of the main span. As an example, Figure 5.50 shows the shear force diagram for a particular 200 mm-deep hcu containing a 1.5 m cantilever. The loading in the main span has been set to the most common criterion of being critical at the mid-span bending moment. This illustration shows that the ultimate shear is now exceeded only at the support.

5.2.15 Bearing capacity

The terminology used in BS EN 1992-1-1 and BS 8110 for bearing 'lengths' and 'widths' are different: BS 8110 uses 'width' measured with the span, whereas BS EN 1992-1-1 uses 'length' for this and 'breadth' perpendicular to the span. In this book the BS EN 1992-1-1 terminology will be used, so bearing 'length' is parallel to the span and 'breadth' is perpendicular, e.g. in a hollow-core slab, length say $a = 75$ mm and breadth $b = 1200$ mm.

Nominal bearing lengths a $\{L_b\}$ are specified on construction drawings, typically 75 to 100 mm on concrete, 75 mm on steelwork and 100 to 150 mm on masonry, depending on the quality and thickness of the wall. The net bearing length a_1 is less than a to account for manufacturing and construction tolerances, according to clause 10.9.5.2(1), Eq. 10.6 {clauses 5.2.3.7 and 5.2.4} as:

$$L_b = \text{net} + 2 \text{ ineffective lengths} + \text{allowance } a = a_1 + a_2 + a_3 + \sqrt{\Delta a_2^2 + \Delta a_3^2} \tag{5.51}$$

Tabulated values for the ineffective distances and allowances (BS EN 1992-1-1, Tables 10.2 to 10.4 {BS 8110, Tables 5.1 and 5.2}) are given in Section 7.6.

The ultimate bearing capacity is:

$$F_{Rd} = a_1 b_1 f_{Rd} < F_{Ed} \quad \{F_R = L_b L_w f_b < F_u\} \tag{5.52}$$

The effective breadth b_1, clause 10.9.5.2.(3) {width L_w (called 'length' in clause 5.2.3.3)} is taken as the actual breadth if a bedding material is used, such as mortar, neoprene strips, etc., but not greater than 600 mm for slabs such as hcus on dry bearings.

The design procedure for bearing length L_b in BS 8110 is a simple addition of nominal and ineffective lengths. If the unit is isolated, i.e. its bearing capacity does not rely on other elements, add 20 mm to L_b (5.2.3.5).

The design procedure in BS EN 1992-1-1 for a is iterative because the bearing stress $\sigma_{Ed} = F_{Ed}/a_1\ b_1$ is required before a_1 is calculated. However, for back-calculation to F_{Rd} the length a_1 is already known. There is also a danger of entering a loop in the calculation of a_1 when σ_{Ed}/f_{cd} is close to the limits of 0.15 and 0.4 in Tables 10.2 and 10.3; in this situation the greater value for a_1 is used. Minimum values of a_1 are given in Table 10.2, where 'line supports' include wide slabs such as hcu, plank, Omnia slab, etc. 'Ribbed' floors include double-tee units, beams in beam-and-block. 'Concentrated' supports include isolated beams in a beam-and-composite slab floor system. The ineffective lengths for line supports are: a_2 {Table 10.3}, $a_3 = 5$ (Table 10.4 for tendons exposed at ends of members), $\Delta a_2 = 10 \le$ span/1200 < 30 mm onto steel or precast, or $\Delta a_2 = 15 \le$ span/1200 < 40 mm onto brickwork or *in situ* concrete (Table 10.5), and $\Delta a_3 = l_n/2500$ (length l_n).

The ultimate bearing stress to BS 8110 is (a) $f_b = 0.4\ f_{cu}$ for a dry bearing, where f_{cu} is the weaker strength of the slab or support; (b) $0.6\ f_{cu}$ on a bedded material, and (c) $0.8\ f_{cu}$ for contact with steel plates that in size do not exceed 40 per cent of the dimension of the concrete units.

To BS EN 1992-1-1, clause 10.9.4.3(2) for a dry bearing $f_{Rd} = 0.4\ f_{cd}$, where $f_{cd} = f_{ck}/1.5$ is the weaker strength. Otherwise $f_{Rd} = 0.85\ f_{cd}$, where f_{cd} is the weaker strength of the slab, support or bedding material, such as elastomeric strip, or wet mortar bedding on plastic (not steel) levelling shims according to the contractor's preference. Normally spans up to about 10 m do not require bedding materials on steel or precast concrete supports. (Note that these values are not applicable to concentrated forces at 'nodes'; see BS EN 1992-1-1, Section 6.5.4. and Section 7.6.1.)

For example, the required nominal bearing length for a 1200 mm-wide hcu spanning 6.0 m and subject to an ultimate reaction of 200 kN, with a dry bearing onto a precast concrete beam grade C32/40:

$f_{Rd} = 0.4 \times 32/1.5 = 8.53\ \text{N/mm}^2$
$b_1 = \min(600;1200)\ \text{mm}$
$a_1 = 200 \times 10^3/(600 \times 8.53) = 39\ \text{mm}$
$\sigma_{Ed}/f_{cd} = (200 \times 10^3/600 \times 39)/(32/1.5)$
$= 8.55/21.33 = 0.4$

$a_1 \ge 30\ \text{mm} < 39$ OK, $a_2 = 10\ \text{mm}$, $a_3 = 5\ \text{mm}$,
$\Delta a_2 = 10\ \text{mm}$, $\Delta a_3 = 2.4\ \text{mm}$
Then $a = 39 + 10 + 5 + 10.3 = 64.3\ \text{mm}$,
use <u>65 mm</u>.

$f_b = 0.4 \times 40 = 16.0\ \text{N/mm}^2$
$L_w = \min(600;1200)\ \text{mm}$
$L_b = 40 + 20 + 10 =$ <u>70 mm</u>
$F = 200 \times 10^3/600 \times 40 = 8.33\ \text{N/mm}^2 < 16$

Note that in this example σ_{Ed}/f_{cd} is on the borderline between sets of values in Tables 10.2 and 10.3. If it happened that σ_{Ed}/f_{cd} is just greater than 0.4, then $a_1 = 40$ mm, $a_2 = 15$ mm, $a_3 = 5$ mm, $\Delta a_2 = 10$ mm, $\Delta a_3 = 2.4$ mm, such that $a = 70.3$ mm. But now $\sigma_{Ed}/f_{cd} = (200 \times 10^3/600 \times 40)/21.33 = 0.39$ and $a_1 \ge 30$ mm once more, entering the loop. In this case use $a = 70$ mm.

5.2.16 Wet cast hollow-core flooring

Not all hollow-core flooring units are manufactured using the long line extrusion or slip-forming methods described above. These types of unit are described as 'dry-cast' because of the very low water

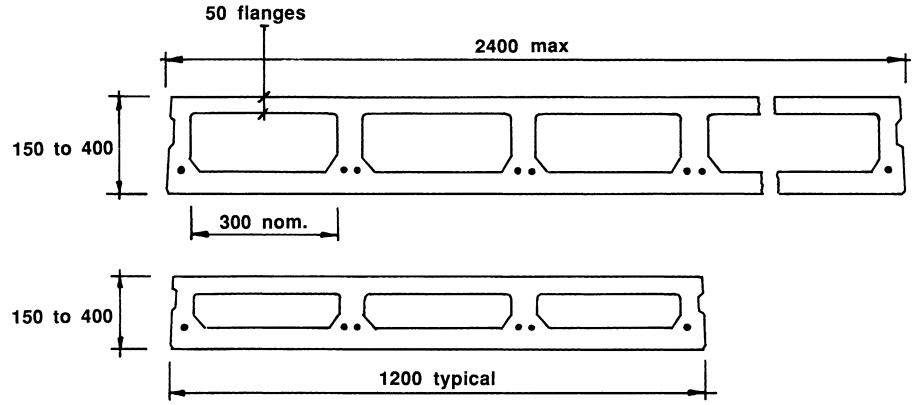

Figure 5.51 Wet cast hollow-core floor slab profiles.

content in the mixes. However, wet-cast units are manufactured to the typical profiles shown in Figure 5.51. There are two main types:

(i) concrete manually placed into moulds around void formers, either prestressed or reinforced
(ii) concrete placed by machine into vibrating moulds around mandrel void formers that are extracted after casting, only reinforced.

For type (i), the cores may be formed using prismatic blocks of high-density polystyrene (approx. 3 kg/m^3) in lengths of about 2 m, with short solid sections of 300 mm between the ends. The ends of the hcu are solid for a distance of about 500 mm. The process involves three stages – (a) casting the bottom flange, typically 50 mm minimum thickness, to enable adequate cover to the soffit and infill block; (b) placing the infill blocks; and (c) second casting of the webs and top flange. The time delay between (a) and (c) should not be more than about 45 minutes (depending on consistency of the mix), as it is important to achieve coarse aggregate penetration between the two layers. The development of prestress through the flange–web interface must be assured. The introduction of self-compacting concrete (SCC) has made the operational task of using such delicate core-former materials easier. However, the cast joint after stage (a) can be smooth owing to the thixotropic nature of SCC, its absence of bleeding, and the tendency of coarse aggregate to settle beneath its surface. Consequent horizontal cracks may be seen along the casting line at the ends of the unit, where bond stress in the transmission zone and vertical splitting stresses (known as 'spalling stresses' in BS EN 1168) are greatest. Hollow-core units manufactured using SCC should therefore be tested for shear flow across the casting line at transfer, and tested in shear. There remains a tendency for the buoyancy of the polystyrene to cause problems in maintaining the thickness of the top flange. Straps across the top of the moulds are used to support the blocks. Tying the blocks to the bottom tendons should be avoided.

Type (ii) (Figure 5.9) are cast upside down into trapezoidal moulds, 600 mm wide at the bottom (at the top when cast) by 150 or 225 mm deep (for the purpose of 75 mm brick courses). The mix is semi-dry with $w/c = 0.4$, allowing a machine to make two passes over the mould, which has (typically) five circular mandrels forming the cores, as shown in Figures 5.52 and 5.53. The reinforcement cage, comprising (typically six) rebars of H8 to H20 size, and transverse bars H8 at 200 centres, is spot-welded and lifted into position automatically, giving 25–30 mm cover. Immediately after the second pass of the casting machine, and following mould vibration for several seconds, the mandrels are withdrawn, a steel plate is lowered onto the top of the cast surface, and the entire slab is lifted and inverted into its rightful position ready for 24 hours' steam curing. The casting operation takes around three minutes.

To be competitive in terms of load capacity versus span, these units must be designed to BS EN 1992-1-1 using the partially cracked section for deflections (clause 7.4.3(3), Eq. 7.18 and 7.19), and quasi-permanent live loads with $\psi_o = 0.3$. BS 8110 does not permit the use of the partially cracked section.

In tests, the section responds linearly before cracking, and measured deflections are 5 to 10 per cent lower than predicted values using calculated values for $E_{cm(t)}$ (see Table 3.1). The cracking moment of

Figure 5.52 Second pass of the semi-dry concrete mix to manufacture reinforced hollow-core slabs. The top of the mould is the bottom of the slab. Manufactured by Creagh Concrete, N. Ireland.

Figure 5.53 After turning over, steam curing of reinforced hollow-core slabs. Manufactured by Creagh Concrete, N. Ireland.

resistance can be reasonably well predicted using a flexural tensile stress $f_{ctm,fl}$ (see clause 3.1.8(1)). However, the post-cracking stiffness reduces quickly, and the tension stiffening term in BS EN 1992-1-1, Eq. 7.19, of 2 can reach 3, 4 or 5, particularly in the lightly reinforced section. However, using the tensile stress at cracking as f_{ctm} (rather than $f_{ctm,fl}$) in deflection calculation renders BS EN 1992-1-1, Eq. 7.19 reasonable. The ultimate mode of failure is by excessive yielding of rebars and is predictable.

The UK market for wet-cast hcu is small (around 5 per cent of the precast flooring market) but up to 40 per cent of the North European market for domestic hollow-core is prestressed (or rc) wet-cast into moulds of fixed dimensions (length and width) and stockpiled for building contractors to purchase as the need arises. This is not the case with long-line manufacture, which is mostly made to order.

Section properties and moment and shear capacities are comparable with the dry-cast units and self-weights are lower in the deeper units, e.g. 300 mm. The big advantage with the wet-cast method is that additional reinforcement may be added to standard cages for any special requirement, e.g. point loads, large voids, high shear, cantilevers, etc. The cost penalty is small.

The American trade name for this type of unit is 'Span-Deck', and they have been used for floors, walls and self-finished cladding panels, as illustrated in Figure 5.54. Manufactured in a two-part process; a 50 mm-thick (and sometimes lightweight concrete of low strength) soffit is first cast,

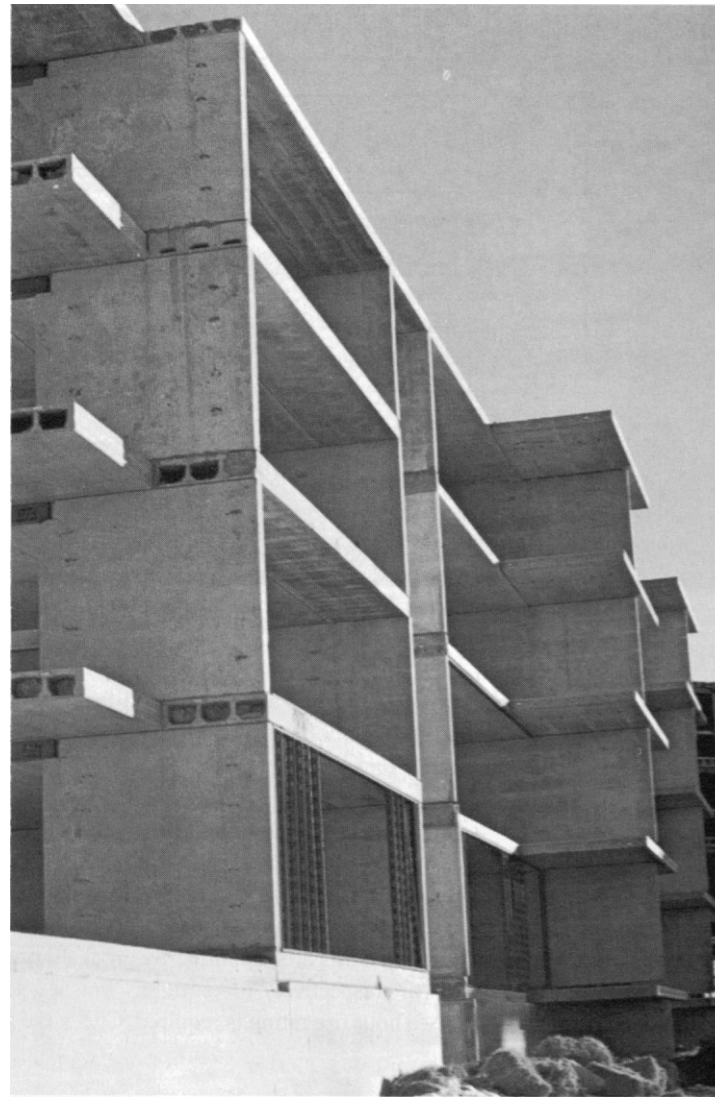

Figure 5.54 Wet cast hollow-core units used for floors as well as walls (courtesy of Span-Deck, US).

followed by the webs (which contain the prestressing tendons) and the top flange. Voids are formed using fibreglass or timber formers, which are drawn out 24 hours after casting.

5.2.17 Summary examples of product design data

Data in Chart 5.1 is for hcus with a small number of large cores, typically six in a 200 mm-deep unit, and Chart 5.2 with a larger number of large cores, typically eleven. They are derived for a particular cross section of slab, and should not be used for commercial design of floor slabs. Current product data should be referenced for this purpose, since they may have different sectional and material properties.

Although Chart 5.2 gives the most widely used design data, further information is often required to enable a designer to check the behaviour of the floor slab if more than just the service and ultimate moments are required. For example, in composite design conditions the designer needs to be able to check the stresses at the different loading stages, and to calculate the depth to the centroid of the tendons. Therefore, to complete the design data file, prestressing magnitudes and tendon locations are given in Chart 5.3.

Chart 5.1 Example non-composite section properties and load capacities for 150 to 250 mm-deep prestressed concrete hollow-core slabs with large cores and narrower webs

Sample section properties

b = 1197 tapering to 1160 mm
A_c (net) = 127 200 mm^2
$I_{xx} = 633 \times 10^6$ mm^4
b_w = 236 mm
Concrete grade C50/60
Transfer grade C30/40
Gravel aggregates

h = 200 mm
y_t = 101.0 mm
$Z_t = 6.267 \times 10^6$ mm^3
L_b = 75 mm
f_{pu} = 1770 (1670 for 7 dia.) N/mm^2

y_b = 99.0 mm
$Z_b = 6.394 \times 10^6$ mm^3
$S_{xx} = 4.17 \times 10^6$ mm^3

			To BS EN 1992-1-1			To BS 8110		
Unit type	**100 A_{ps} / A_c'**	**Cores no. × dia.**	**M_{sr} (kNm)**	**M_{Rd} (kNm)**	**$V_{Rd,c}$ (kN)**	**M_s (kNm)**	**M_u (kNm)**	**V_{co} (kN)**
15/7322	0.171	8 × 96	37.7	48.8	87.8	36.5	49.5	96.2
15/7622	0.224		44.7	61.3	92.5	44.0	62.5	99.8
15/96	0.260		48.8	69.0	94.1	48.4	71.2	101.3
15/97	0.351		58.8	87.6	96.2	59.0	88.0	105.7
20/3643	0.129	6 × 150	60.8	72.0	78.4	59.0	73.2	80.6
20/76	0.152		67.4	83.7	81.1	66.1	84.9	82.2
20/77	0.206		80.0	111.6	82.7	80.3	112.8	85.7
20/78	0.271		95.4	136.6	84.2	95.8	134.8	88.7
25/68	0.186	5 × 175	125.5	165.5	120.1	123.3	167.6	123.7
25/88	0.248		150.3	214.2	125.1	149.3	218.1	131.9
25/108	0.310		173.9	252.6	129.7	173.8	249.5	138.9

Notes: A_c' = gross nominal cross-sectional area including voids, e.g. 1200 × 200 mm^2.
Serviceability moments are for Class 2, XC1 elements.
Shear forces are calculated for a 75 mm bearing at each end of the unit.

Key: First digits: 15, 20, 25 = nominal depth in cm
Each following pair of digits gives the number and type of bar:
- type 2 = 5 mm dia. wire (area = 19.6 mm^2)
- type 3 = 7 mm dia. wire (area = 38.5 mm^2)
- type 6 = 9.3 mm dia. strand (area = 52 mm^2)
- type 7 = 10.9 mm dia. strand (area = 71 mm^2)
- type 8 = 12.5 mm dia. strand (area = 93 mm^2)

Chart 5.2 Example non-composite section properties and load capacities for 1200 × 200 mm-deep prestressed concrete hollow-core slabs with eleven narrow cores and wider webs

Basic section properties

b = 1200 tapering to 1165 mm	h = 200 mm	No. of 58 mm wide voids = 11
A_c (net) = 142 311 mm^2	y_t = 102.7 mm	y_b = 97.3 mm
I_{xx} = 628.1 × 10^6 mm^4	Z_t = 6.1154 × 10^6 mm^3	Z_b = 6.4558 × 10^6 mm^3
b_w = 544 mm	L_b = 75 mm	S_{xx} = 4.21 × 10^6 mm^3
Concrete grade C40/50	f_{pu} = 1570 N/mm^2	A_{ps} = 19.6 mm^2/wire

		To BS EN 1992-1-1 Fire rating = 1 hour			To BS 8110 Fire rating = 2 hours		
Unit type	**100 A_{ps} / A_c'**	**M_{sr} (kNm)**	**M_{Rd} (kNm)**	**$V_{Rd,c}$ (kN)**	**M_s (kNm)**	**M_u (kNm)**	**V_{co} (kN)**
R (0 + 8)	0.065	40.6	36.7	115.5	36.54	35.94	129.8
R (0 + 10)	0.082	44.7	45.4	120.4	40.35	44.58	133.0
R (0 + 12)	0.098	48.8	54.1	125.1	44.09	53.10	136.1
R (0 + 14)	0.114	52.7	62.3	129.4	47.64	61.33	139.0
R (0 + 16)	0.131	56.5	70.4	133.5	51.13	69.43	141.8
R (0 + 19)	0.155	62.2	82.9	139.2	56.55	81.88	145.8
R (0 + 21)	0.172	65.7	90.6	142.8	59.84	89.60	148.4
R (0 + 23)	0.188	69.1	98.1	146.1	63.14	97.24	150.9
R (0 + 25)	0.204	72.4	105.5	149.3	66.30	104.60	153.2
R (0 + 27)	0.221	75.6	112.7	152.3	69.46	111.80	155.6
R (0 + 29)	0.237	78.7	119.8	155.2	72.56	117.60	157.8
R (0 + 31)	0.235	81.6	126.7	157.9	75.53	122.60	160.0
R (0 + 33)	0.270	84.1	132.4	160.7	78.05	125.60	162.1

Notes: A_c' = gross nominal cross-sectional area including voids, e.g. 1200 × 200 mm^2.
Serviceability moments for Class 2, XC1 elements.
Shear forces are calculated for a 75 mm bearing at each end of the unit.
Key: Letters: R = manufacturer's code.
Following pairs of digits give number of 5 mm wires in top and bottom of slab, respectively.

Exercise 5.1

Design a 200 mm-deep non-composite dry-cast hollow-core slab to carry a superimposed loading of 5.0 kN/m^2 over a simply supported clear span of 6.6 m. End bearing lengths are 75 mm nominally, and the units are supported by grade C30/37 precast concrete beams. Allow 1.0, 1.0 and 0.6 kN/m^2 for partitions, finishes, services and suspended ceiling, respectively. Ultimate load combination factors to EC1 are taken as $\zeta = 0.925$ and $\psi_o = 0.7$. Check the unit for flexure, shear and bearing.

Solution Use unit type 20 from Table 5.1
Effective span = 6600 + 75/2 + 75/2 = 6675 mm

Loading		**Service**	**EC2 Ultimate Eq. 6.10(b)**	**BS 8110 Ultimate**
Permanent actions:	Self-weight of slab, incl. infill in joints*	2.73	3.41	3.82
	Partitions, finishes, services and ceilings	2.60	3.25	3.64
		5.33	6.66	7.46
Superimposed actions:		5.00	7.50	8.00
Total		10.33	14.16	15.46

* Self-weight of unit given by manufacturer = 2.67 kN/m^2.

Step 1: Design in flexure

$M_{Es} = 10.33 \times 6.675^2/8$	$= 57.5\,\text{kNm/m}$	$M_s = 10.33 \times 6.675^2/8$	$= 57.5\,\text{kNm/m}$
M_{Es} per hollow-core unit		M_s per hollow-core unit	
$= 57.5 \times 1.2$ (for unit width)	$= 69.0\,\text{kNm}$	$= 57.5 \times 1.2$ (for unit width)	$= 69.0\,\text{kNm}$
$M_{Ed} = 14.16 \times 6.675^2/8$	$= 78.9\,\text{kNm/m}$	$M_u = 15.46 \times 6.675^2/8$	$= 86.1\,\text{kNm/m}$
M_{Ed} per hollow-core unit		M_u per hollow-core unit	
$= 78.9 \times 1.2$ (for unit width)	$= 94.6\,\text{kNm}$	$= 86.1 \times 1.2$ (for unit width)	$= 103.3\,\text{kNm}$

Step 2: Design in shear

V_{Ed} at y_b from edge of support		V at y_b from edge of support	
$V_{Ed} = 14.16 \times 6.396/2$	$= 45.3\,\text{kN/m}$	$V_u = 15.46 \times (6.600 - 2 \times 0.102)/2$	$= 49.4\,\text{kN/m}$
V_{Ed} per hollow-core unit		V_u per hollow-core unit	
$= 45.3 \times 1.2$ (for unit width)	$= 54.3\,\text{kN}$	$= 49.4 \times 1.2$ (for unit width)	$= 59.3\,\text{kN}$

Referring to design data Chart 5.1, use unit ref. 20/77, requiring seven 10.9 mm-diameter strands of total $A_{ps} = 497\,\text{mm}^2$ (0.206% A_c').

Step 3: Design in bearing (see also Section 6.7)

(10.9.5.2(3)) Net bearing width	$= 600\,\text{mm}$	Net bearing length (clause 5.2.3.3)	$= 600\,\text{mm}$
Assume $\sigma_{Ed}/f_{cd} < 0.15$		Net bearing width (clause 5.2.3.7 &	
(Eq. 10.6) Nominal bearing length	$=$ say 41 mm	5.2.4) $= 75 - 20 - 15$	$= 40\,\text{mm}$
$a = 25 + 5 + 5 + \sqrt{(5.56^2 + 2.67^2)}$	$<75\,\text{mm}$ actual		
End reaction F_{Ed}			
$= 1.2 \times 14.16 \times 6.675/2$	$= 61.9\,\text{kN}$		
Bearing stress		Bearing stress	
$= 61.9 \times 10^3/600 \times 41$	$= 2.51\,\text{N/mm}^2$	$= 61.59 \times 10^3/600 \times 40$	$= 2.57\,\text{N/mm}^2$
$< 0.4\,f_{cd}$ (beam) $= 0.4 \times 30/1.5$	$= 8.00\,\text{N/mm}^2$	$< 0.4\,f_{cu}$ (beam)	$< 14.8\,\text{N/mm}^2$
Check $\sigma_{Ed}/f_{cd} = 2.51/(30/1.5)$			
$= 0.125 < 0.15$ assumed.			

Exercise 5.2

Repeat Exercise 5.1 using 'Roth'-type 200 mm deep × 1200 mm wide slabs.

Solution

Loading		**Service**	**BS 8110 Ultimate**	**EC2 Ultimate Eq. 6.10(b)**
Permanent actions:	Self-weight of slab, incl. infill in joints*	3.00	4.20	3.75
	Partitions, finishes, services and ceilings	2.60	3.64	3.25
		5.60	7.84	7.00
Superimposed actions:		5.00	8.00	7.50
Total		10.60	15.84	14.50

* Self-weight of unit given by manufacturer = $2.94\,\text{kN/m}^2$.

(*Continued*)

Step 1: Design in flexure

M_s per unit = $10.60 \times 6.675^2/8 \times 1.2$ wide = 70.84 kNm per unit

M_{Ed} per unit		M_u per unit	
$= 1.2 \times 14.50 \times 6.675^2/8$	= 96.9 kNm	$= 1.2 \times 15.84 \times 6.675^2/8$	= 105.8 kNm

Step 2: Design in shear

V_{Ed} at y_b from edge of support		V_u at y_b from edge of support	
$= 1.2 \times 14.50 \times 6.406/2$	= 55.7 kN	$= 1.2 \times 15.84 \times (6.600 - 2 \times 0.097)/2$	= 60.88 kN

Referring to design data Chart 5.2, use unit ref. R (0 + 25) {R (0 + 29)}, requiring 25 {29} 5 mm dia. wires of total $A_{ps} = 490\ \text{mm}^2 (0.204\%\ A_c')$ {$A_{ps} = 568\ \text{mm}^2 (0.237\%\ A_c')$}. Chart 5.3 gives the tendon locations and prestressing values for these slabs. Note that this unit requires 2 per cent less {but 14 per cent more} area of tendons than the hcu in Example 5.1. Also note that in spite of the lower ultimate prestressing force for BS EN 1992-1-1, giving for example M_{Ed} = 96.9 versus 105.8 kNm, the unit is still critical at the service stress limit where the characteristic load is the same.

Chart 5.3 Example prestressing data for 200 mm-deep 'Roth' prestressed concrete hollow-core slabs

	Position above soffit (mm)				To BS EN 1992-1-1			To BS 8110		
	Row 1 27.5	Row 2 42.5	Row 3 62.5	Prestress eccentricity (mm)	Prestress force (kN)	f_{bc} (N/mm^2)	f_{bt} (N/mm^2)	Prestress force (kN)	f_{bc} (N/mm^2)	f_{bt} (N/mm^2)
Unit type	Number of tendons									
R (0 + 8)		8		54.8	178.6	2.77	–0.34	158.7	2.46	–0.31
R (0 + 10)		10		54.8	220.5	3.42	–0.42	196.6	3.05	–0.38
R (0 + 12)		12		54.8	261.3	4.05	–0.50	233.7	3.63	–0.45
R (0 + 14)	1	12	1	54.4	301.1	4.65	–0.56	270.2	4.18	–0.51
R (0 + 16)	2	12	2	54.2	339.8	5.24	–0.62	306.1	4.72	–0.56
R (0 + 19)	4	12	3	54.8	395.2	6.13	–0.76	358.2	5.56	–0.69
R (0 + 21)	5	12	4	54.6	431.2	6.67	–0.81	392.3	6.07	–0.74
R (0 + 23)	6	12	5	54.4	466.1	7.20	–0.86	425.8	6.58	–0.79
R (0 + 25)	7	12	6	54.2	499.9	7.71	–0.91	458.7	7.07	–0.84
R (0 + 27)	8	12	7	54.1	532.7	8.20	–0.96	490.9	7.56	–0.89
R (0 + 29)	9	12	8	53.9	564.3	8.68	–1.01	522.5	8.04	–0.94
R (0 + 31)	10	12	9	53.8	595.0	9.14	–1.05	553.4	8.50	–0.98
R (0 + 33)	10	12	11	52.7	626.8	9.52	–1.00	585.1	8.89	–0.93

Notes: The sign convention is compression positive.
Prestress force is after all losses.
An axis distance of 42.5 mm has 15 mm deducted according to BS EN 1992-1-2 clause 5.2.(5), giving a = 27.5 mm. This gives only 1 hour of fire resistance according to BS EN 1168, Annex. G, Table G.1, because $a < 30$ mm. If limestone aggregates are used 10 per cent is added to the axis distance, hence $a = 1.1 \times 42.5 - 15 = 32$ mm, giving 1.5 hours. {The value chosen for the axis distance to the majority number of tendons, i.e. 42.5 mm, ensures that the average cover to the tendons is equal to or exceeds 40 mm. This is the cover distance necessary to achieve a two-hour fire resistance to BS 8110.}

Key: Letters: R = manufacturer's code.
Following pairs of digits give number of 5 mm wires in top and bottom of slab, respectively.
Thus slab unit reference R (0 + 19) contains nineteen 5.0 mm-diameter tendons, of which four are located at a centroidal distance of 27.5 mm from the soffit of the slab, twelve at 42.5 mm, and three at 62.5 mm from the soffit.

5.3 Double-Tee Slabs

5.3.1 General

A general introduction to double-tee slabs is given in Section 3.2.2.2. Double-tees are cast in long steel moulds and, in more than 90 per cent of cases, are prestressed for strength. Reinforced double-tees are used, but long-term deflections have precluded their economical use for spans in excess of about 8 m. Concreting 'trains' driven by two operatives are used in some high-production factories: Figure 5.55(a) and (b). The concrete is of medium workability (75 mm to 100 mm slump) and is

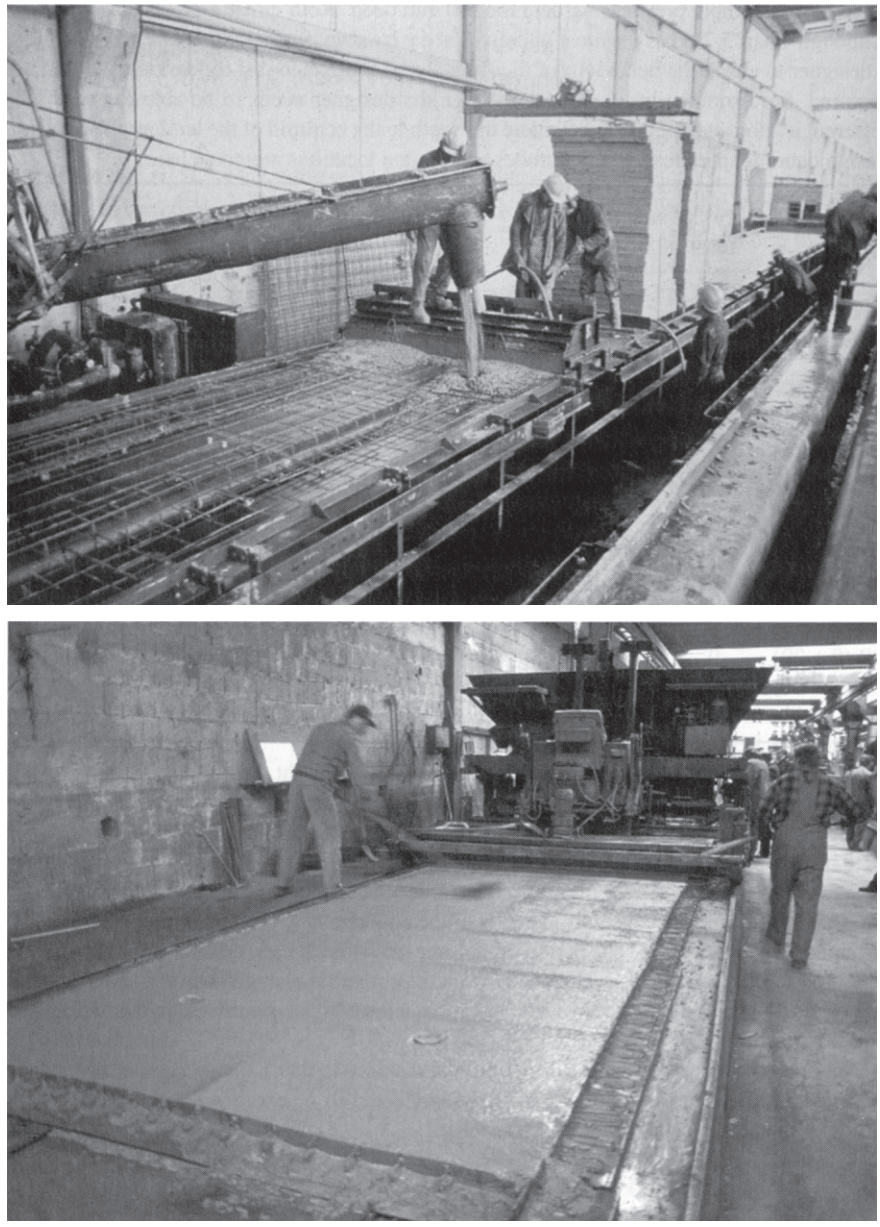

(a)

(b)

Figure 5.55 Manufacture of double-tees. (a) Using concrete pouring arms and (b) using concreting train.

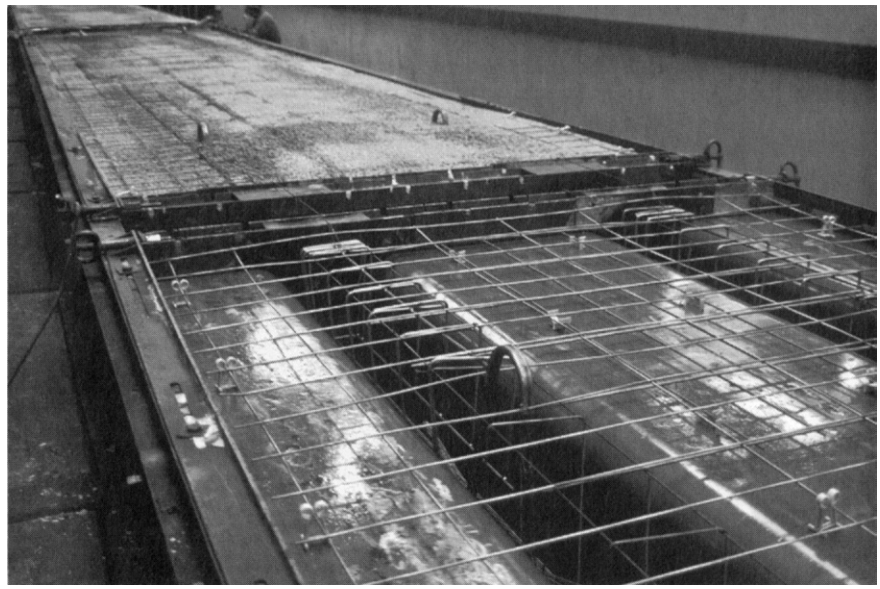

Figure 5.56 Two part casting process for double-tee slabs – the web is poured and vibrated first, followed by the flanges.

Figure 5.57 Surface finishes to the tops of double-tee slabs are tamped rough.

pumped or skipped to the mould. The top surface is hand-tamped to give up to 6 mm furrows in the surface (Figures 5.56 and 5.57). This provides an excellent shear key to the *in situ* concrete topping, and no interface shear reinforcement is necessary. The design strength is at least 50 N/mm^2. Detensioning takes place between 12 and 24 hours after casting and at a strength as required by the design prestress, which is usually 35 to 40 N/mm^2 after steam curing. Self-compacting concrete (SCC) is often used, as shown in Figure 5.58, thanks to the recent development of admixtures that enable the required

Figure 5.58 Self-compacting concrete grade C50/60 is often used for wet-casting double-tee slabs (courtesy of EFNARC).

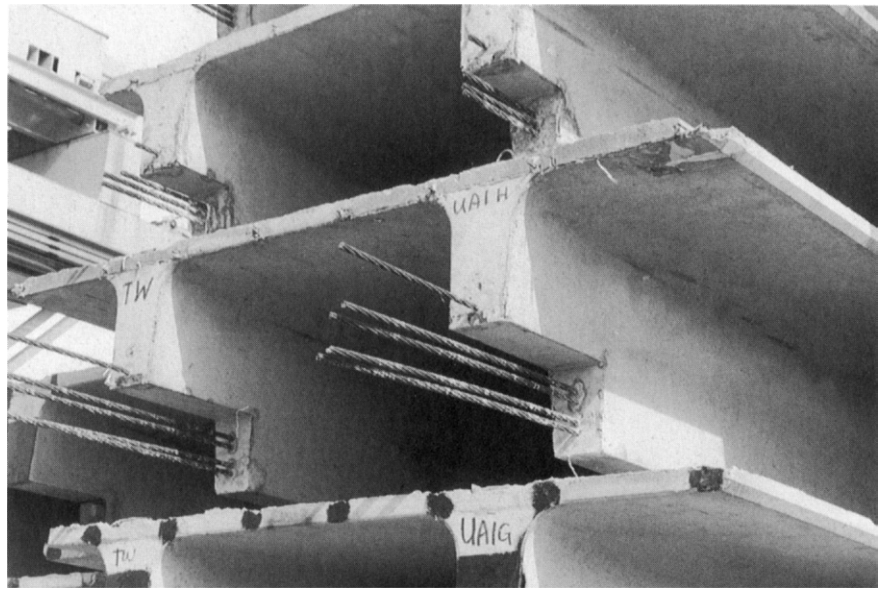

Figure 5.59 Half joint in the ends of double-tee units.

early strength for detensioning and demoulding. The ratio of the cost of the workforce to the value of the product has been halved since the introduction of SCC, more than compensating for the additional expense of the admixture.

The ends of the prestressing tendons require protection because they will be exposed in the building, particularly in car parks. A cold bitumen paint is used, as shown in Figure 5.59. Flame-cut tendons do not require additional protection.

Figure 5.60 Mesh reinforcement in the top flange, and the anchor bars for the connection plate at the edge of the top flange.

5.3.2 Design

The slabs are designed as T-sections. The flexural and shear strength derives from the deep webs, with the thin flanges providing lateral stability to the units. Deflected or debonded tendons are used in some cases to overcome transfer stress problems in long-span units. Figure 5.12(b) shows typical load versus span data for proprietary units up to 800 mm deep.

The depth of the section is reduced at the ends of the units to facilitate a recessed bearing onto the supporting beam or wall (see Figure 5.1(b)). The concrete is heavily reinforced at this point because it is subjected to shear, bending and bearing. Stress concentrations also occur at the internal corner, which is why triangular chamfers are used there. A truss analogy, or strut-and-tie method of analysis (similar to Section 4.3.9), is used to calculate the forces. Figure 5.61 shows a typical end shear cage in which the vertical bars are provided for the ultimate shear capacity, and the horizontal U-bars are for the lateral bursting resistance.

Welded connections between adjacent double-tee units, or between the units and a supporting member, shown in Figure 5.62, provide an ultimate shear capacity of about 25 kN/m, but that is ignored in the final design. The anchorage is provided by inclined loops, typically H12 or H16 and 600 mm long, fillet-welded to the plate, as shown in Figure 5.60. Electrodes grade E43 are used to form short, continuous fillet welds between fully anchored mild steel plates (stainless-steel plates and electrodes may be specified in special circumstances). A small saw cut is made at the ends of the cast-in plate to act as a stress reliever to the heated plate during welding.

Double-tee units are either designed compositely with a structural topping, in which case the flange thickness is 50 to 75 mm, or are self-topped with thicker flanges of around 120 mm. In the former, vertical and horizontal shear are transferred entirely by the *in situ* structural topping, using a design value for shear stress of (from clause 6.2.5(1) and (2)), $v_{Rdi} = 0.35\, f_{ctd(i)}$ for 'smooth' interface $\{0.45\,\text{N/mm}^2\}$. In the latter, projecting reinforcement loops, typically H8 at 200 mm c/c and lapped to the mesh inside the flange, are provided in recesses. These are grouted on site, and as such are a source of major concern with regard to thermal and shrinkage effects, and waterproofing in parking structures.

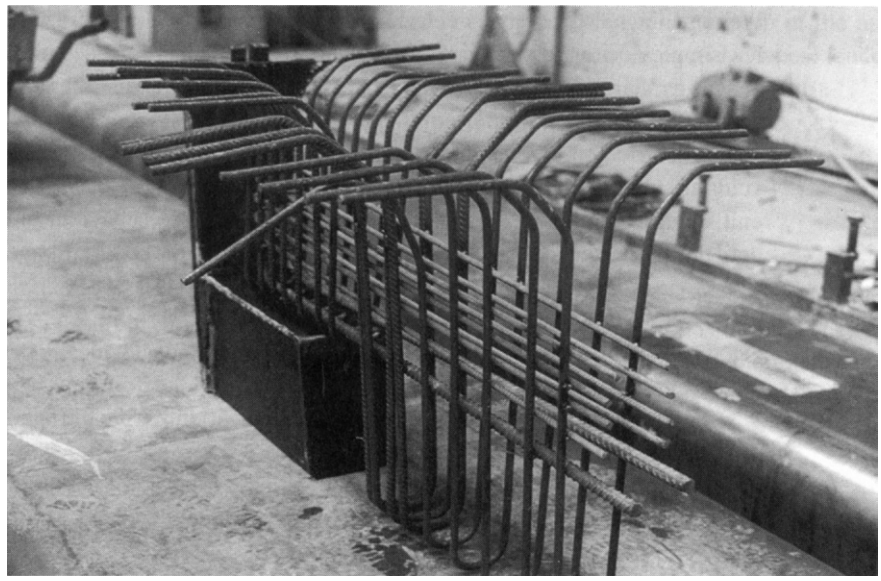

Figure 5.61 Shear cage in the ends of double-tee units.

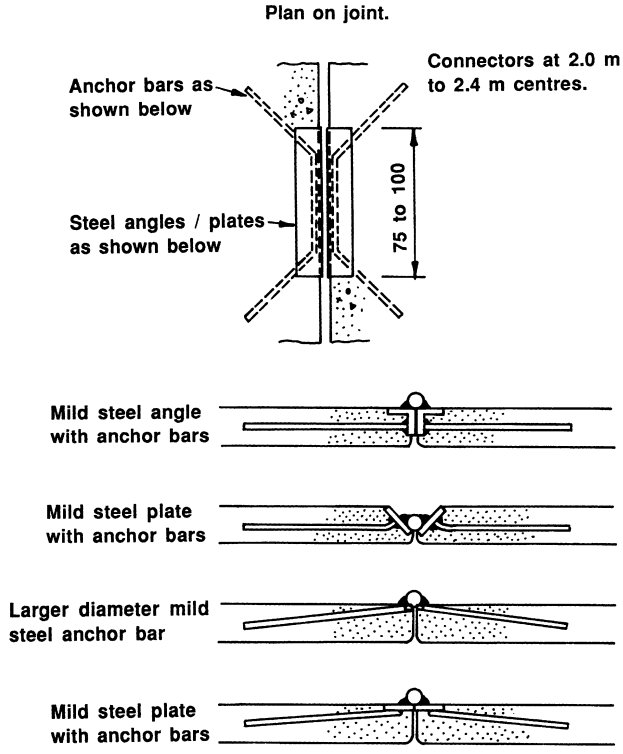

Figure 5.62 Welded connections between adjacent double-tee units.

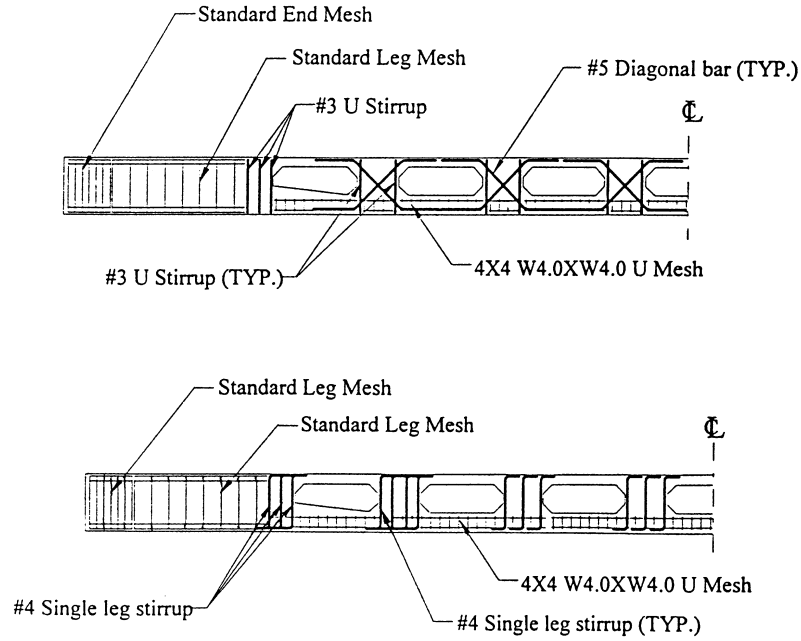

Figure 5.63 Reinforcement around large openings in the webs of double-tee slabs [5.56].

Double-tee units often contain web openings at positions that will not coincide with the longitudinal strands and are preferably near to the geometric centroid of the unit. Web openings do not have a deleterious effect on strength or stiffness providing that a few simple rules are observed [5.54, 5.55]. It is found that prestressed units with openings behave as Vierendeel trusses, and the shear at the opening is distributed between the top and bottom chords in proportion to the chords' stiffness.

Tests carried out by Savage *et al.* [5.56] on 24-inch-deep units have shown that where voids are placed directly beneath the flange and are not greater than half the depth of the unit, as shown in Figure 5.63, the openings do not affect the behaviour of the voided slab until the applied bending moment was equal to 1.4 times the service moment. The general rules are as follows:

- Web openings should not be placed in high-shear regions, typically in the first quarter span.
- Web openings should not be placed nearer than 50 mm from the nearest prestressing strand.
- The centre of the void should coincide with the centroid of the unit.
- Reinforcement, either in the form of stirrups or inclined links, should be placed on either side of the opening to aid crack control.
- The corners of the openings should be chamfered or rounded.

5.3.3 Flexural and shear capacity, precamber and deflections

The analysis given in Sections 5.2.8 to 5.2.13 is also adopted for double-tee units, with due consideration for the cross-sectional geometry and the concentration of the main flexural reinforcement in the webs. Additional shear capacity is provided where tendons are deflected.

Typical load-versus-span data for these units are given in Figure 5.64 for the internal exposure class XC1 with limiting tension f_{ctm}. Limiting spans for external exposure XD1, with zero tension and a service bending moment using the frequent live load factor $\psi_1 = 0.5$, are equal or (surprisingly) greater than these, by as little as 3 per cent. The main reason for this is in the ratio between the ultimate and service moments of resistance, which for double-tees is 1.4 to 1.5 such that the ultimate moment is

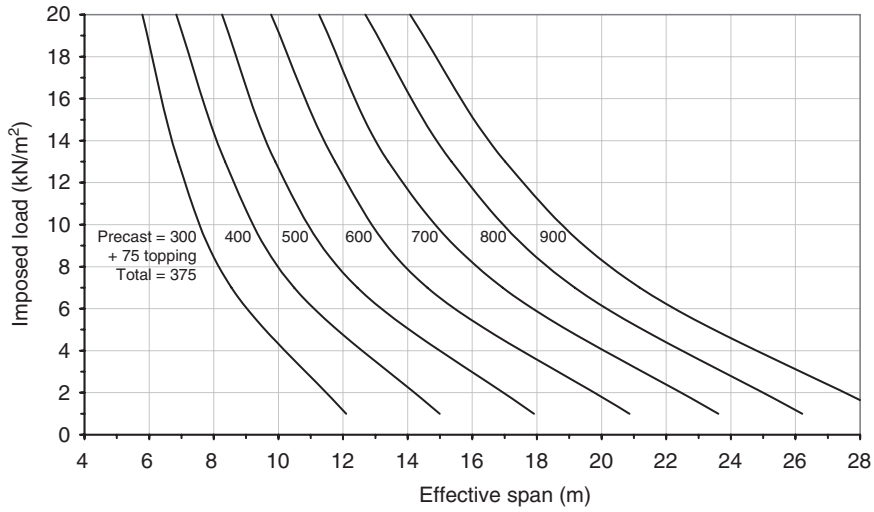

Figure 5.64 Imposed load versus effective span for composite prestressed double-tee slabs for internal exposure condition XC1. Finishes and self-weight of topping are included as 1.5 kN/m^2 and 2.05 kN/m^2, respectively. The composite slab is propped at 1/3 points.

often critical. This contrasts with hcus which have a reduction for external exposure because the service stress is critical.

The data in Figure 5.64 are for propped slabs at two points at 1/3 span. With no props, the load capacity is unaffected if the critical design constraint in span is due to the ultimate moment or the deflection after installation, since these are post-topping criteria. Thus the limiting span without props is unaffected when the ratio of the characteristic live load to dead load is greater than 2.5 (where M_{Rd} is critical) and where the span/depth ratio is greater than 30 (where deflection is critical). In between these limits, the ratio of limiting span without props/with props is 0.96 to 0.99, for the 300- to 900 mm-deep units, respectively, i.e. a 4 per cent reduction at worst. Propping has little effect for XD1 exposure, as M_{Rd} or deflection criteria are usually critical.

5.3.4 Special design situations

Double-tees may be used as cantilever balconies by adding additional reinforcement in the top flange. It is not possible to use halving joints over cantilever support beams and therefore the structural zone is often a prohibitive factor in this design. The main problems are in the detailing and the avoidance of cold bridging if the units remain physically exposed. Precast rib-end closure pieces may be used to complete the precast assembly.

5.4 Composite Plank Floor

5.4.1 General

A general introduction to composite plank flooring is given in Section 3.2.2.3. The precast concrete is typically grade C28/35 if reinforced or C40/50 if prestressed. The *in situ* topping need only be grade C20/25 to C25/30, and a lightweight aggregate concrete grade C20/25 is often used. The precast planks are manufactured from normal and lightweight aggregate concrete. Self-compacting concrete is used by most manufacturers, although the ease of casting and vibrating a simple flat rectangular element is offset by the additional cost and quality control aspects of SCC, e.g. casting before the effect of the admixture diminishes.

Figure 5.65 Prefabrication of the lower half of prestressed concrete plank floor.

There are several proprietary types of plank floor, including 'Omnia' and 'Katzenburger'. The precast part varies in depth from 65 to 100 mm, although some European producers manufacture 40 mm-deep planks. Land [5.57, 5.58] gives a good account of many aspects of the use of these units, aspects beyond the scope of this book. The plank floor system lends itself to automated manufacture where robots are used to measure out, select and assemble the reinforcement, and the concreting and lifting operations are carried out using minimal labour (see Figure 5.65).

Figure 3.26 showed the construction of the composite plank floor, and in terms of robustness this floor is considered equal to a cast-*in situ* floor. This floor system has the advantage of using a prefabricated soffit unit (with benefits of smooth finish, no formwork, rapid fixing of up to 100 m^2 per hour), but carries performance penalties on span and self-weight; see Table 3.1.

Solid plank floor is prestressed or reinforced as shown in Figure 5.66. The triangulated lattice girders are manufactured using drawn wire spot-welded in a semi-automatic production. The lattices provide four important functions:

- the links ensure mechanical bond between the precast and *in situ* concrete
- the links provide the precast plank with vertical stiffness in the temporary condition
- the lower bars provide the flexural reinforcement
- the lattice makes a convenient lifting point.

In prestressed units the lattices are positioned next to the prestressing wires. Although the longitudinal bars in the lattices are ignored at the serviceability condition, they *may* be included in the flexural design at ultimate.

5.4.2 Design

The lattice girder is manufactured from 5- or 7 mm-diameter hard-drawn wire, or 8- to 20 mm-diameter ribbed high-tensile bar with a characteristic 0.2 per cent proof stress of 500 N/mm^2. The lattice girder consists of:

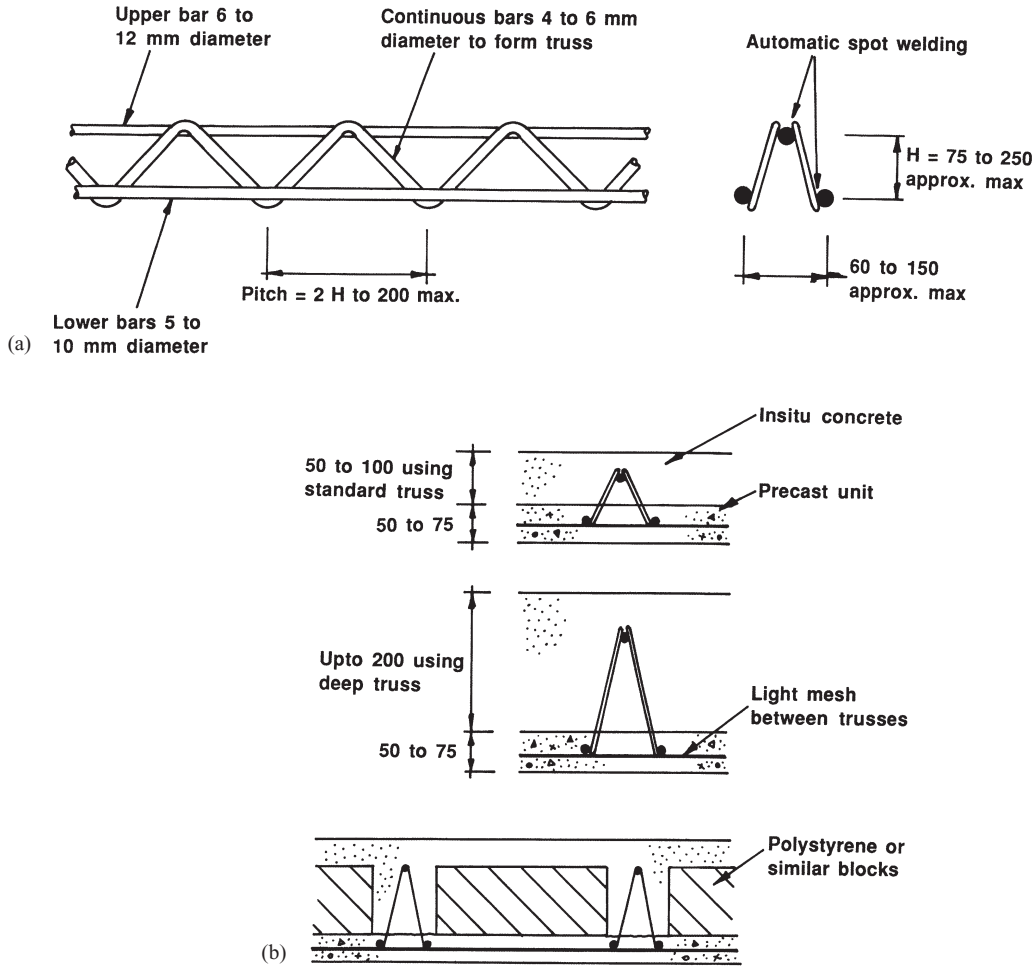

Figure 5.66 Details of composite plank floor. (a) Lattices made using automatic production; (b) construction details.

- small-diameter bars in pairs, typically 5-, 6- or 7 mm-diameter bars, bent into a zigzag girder where the inclination of the links is between 45° and 65° to the longitudinal direction, and about 70° to the transverse direction. The links provide the shear strength in the temporary condition, and, if required, the shear capacity at ultimate;
- a single top bar, typically H8 to H20, depending on the span of the floor and the propping methods used; and
- at least two bottom bars of similar size, depending on the tensile strength in the reinforcement at ultimate.

The lattices are cut so that a complete stirrup is left intact at both ends of the girder. The buckling strength of the diagonal link and the top bar is checked according to BS EN 1993-1-1, clause 6.3.1.3, the steelwork Eurocode [5.59] {BS 5950, Part 1:2000, Table 24, curve (b)}. The effective length ratio of the compression leg is taken as 0.7 {0.7} because of rigid end restraints between the diagonals and top bars, and so the slenderness ratio $\lambda = 0.7\, l_o/i$ $\{\lambda = 0.7\, l_o/r_y\}$ ($r_y = i = \phi/4$, the radius of gyration for round bar).

In EC3 λ is checked against $\lambda_{crit} = 93.9 \times \sqrt{235/f_{yk}}$, which gives the non-dimensional slenderness $\bar{\lambda} = \lambda / \lambda_{crit}$. The α factor for the curve = 0.49 (Tables 6.1 and 6.2, buckling curve (c)). The buckling strength $f_{ykb} = \chi\, f_{yk}$ where the stress reduction factor $\chi = 1/(\phi + \sqrt{(\phi^2 - \bar{\lambda}^2)}) \leq 1.0$, where $\phi = 0.5(1 + \alpha(\bar{\lambda} - 0.2) + \bar{\lambda}^2)$. For example, if the lattices are spaced at 200 mm, and the top bar is 10 mm in diameter, $\lambda = 140/2.5 = 56$, $\lambda_{crit} = 64.4$ (for $f_{yk} = 500$), $\bar{\lambda} = 0.87$, and $\chi = 0.618$. Buckling strength $f_{ykb} = 0.618 \times 500 = 309\,\text{N/mm}^2$.

In BS 5950 λ is checked against $\lambda_{limit} = 15$, and if greater is used to find the buckling strength p_c in BS 5950, Table 24. For example if the lattices are spaced at 200 mm, and the top bar is 10 mm in diameter, $\lambda = 140/2.5 = 56 > 15$. Grade 500 steel is not given in Table 24, but using S460 pro rata, $p_c = (500/460) \times 347 = 377\,\text{N/mm}^2 < 0.87 f_y$. (This is considerably higher than EC3.)

Any additional high-yield reinforcement is attached to the lattice prior to placement in the mould. The cover to the bottom reinforcement is typically 20 mm for internal exposure and R60 minutes fire resistance {1-hour} for a simply supported slab. If the slab is designed continuously, this may be increased to R90 minutes {1.5 hours}. The clear distance between the top of the precast surface and the bar in the top of the girder should be 20 mm.

The floor slab is designed as one-way spanning, despite the introduction of transverse reinforcement in the topping. The two-way spanning capabilities have not been fully exploited to date.

In the temporary stage, the precast plank is simply supported. The unit may be designed so that unpropped spans of up to 4 m are possible, usually by increasing the number of lattices to increase shear stiffness, but not necessarily increasing the number of bottom bars. The top bar is in compression, but is firmly restrained both vertically and horizontally by the inclined bars making the lattice. By adjusting the size of the top bar and the spacing between the lattices, it is possible to vary the strength of the plank alone. The unit is most critical when the self-weight of the wet *in situ* concrete is added to the self-weight of the precast plank. An allowance for construction traffic of up to 1.5 kN/m^2 is added to the temporary loading when calculating the sizes of bars required.

In the permanent situation the hardened *in situ* concrete provides the compressive resistance. The flexural sagging resistance at mid-span is governed by the strength of the bottom reinforcing bars, as in an ordinary under-reinforced situation. The flexural hogging moment over the supports is provided by a combination of precast and *in situ* concrete, as shown in Figure 5.67, together with some additional site-placed reinforcement in the top of the slab.

If the maximum bending moment in the temporary condition is M_1 (inclusive of the construction traffic), then the area of top steel in the lattice is given by:

$$A'_s = \frac{M_1}{z_1 0.87 f_{yk}} \quad \left\{ A'_s = \frac{M_1}{z_1 0.87 f_y} \right\} \tag{5.53}$$

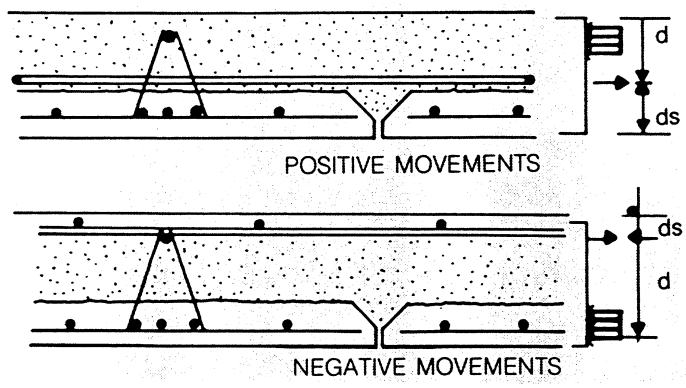

Figure 5.67 Flexural resistances due to positive (sagging) and negative bending moments.

where z_1 is the centre-to-centre vertical distance between the bars in the lattice. f_{yk} {f_y} is checked for its buckling capacity f_{ykb} as above. The area of the bottom steel is specified after the full service load is considered, but without the effects of the construction load as this load will have been removed when in service. Hence, if the net temporary moment is M_1' and the ultimate moment due to superimposed loading is M_2, the area of bottom steel in the lattice is given by:

$$A_{s1} = \frac{M_1'}{z_1 0.87 f_{yk}} + \frac{M_2}{z_2 0.87 f_{yk}} \quad \left\{ A_{s1} = \frac{M_1'}{z_1 0.87 f_y} + \frac{M_2}{z_2 0.87 f_y} \right\} \tag{5.54}$$

where z_2 is the lever arm obtained from the flexural design.

The shear reinforcement in the lattices is designed by taking the vertical component of the axial force in the inclined bars as the only shear resistance against the temporary shear force V_1. The area of the lattice's 'shear links' is given by:

$$A_{sv} = \frac{\sqrt{2} V_1}{0.87 f_{yv}} \tag{5.55}$$

Two lattice bars are used to provide the shear reinforcement. They are stiffened by the plank concrete, and must not be long enough to buckle. The buckling capacity f_{ykb} {p_c} is checked as above, and can often be considerably lower than $f_{ywk.}$ For example, if 6 mm diagonals are used in a 150 mm-deep lattice, their diagonal length will be about 185 mm and i {r_y} = 1.5 mm, λ = 129/1.5 = 86. To BS EN 1992-1-1, λ_{crit} = 91 (f_{yk} = 250 N/mm^2), $\bar{\lambda} = 0.94$, and ξ = 0.575. Buckling strength f_{ykb} = 0.575 × 250 = 144 N/mm^2 (and is in close agreement). Note, that if f_{yk} = 500 N/mm^2 slenderness is exceeded, λ_{crit} = 64, and $\bar{\lambda} = 1.33 > 1$. {To BS 5950, table 24b, p_c = 149 N/mm^2.}

The diagonal bars are also used to transfer shear forces due to superimposed loads V_2 in the precast-*in situ* interface.

Then the applied shear force must be less than $V_{Rd,c}$, given again by:

$$V_{Rd,c} = (0.12k(100\rho_1 f_{ck})^{1/3} + 0.15\sigma_{cp}) b_v d \tag{5.56}$$

where $k = \min\left(\left(1 + \sqrt{\frac{200}{d}}\right); 2.0\right)$

$$\rho_1 = \min\left(\left(\frac{A_s}{b_v d}\right); 0.002\right)$$

$$\sigma_{cp} = \min\left(\left(\frac{f_p A_p}{A_c}\right); 0.2 f_{cd}\right)$$

Thus, if the applied shear stress, v given by:

$$v = \frac{V_2}{bd} \tag{5.56}$$

is greater than the limiting value in BS 8110, Table 5.5 [5.2], then the area of shear steel should be increased to carry the whole interface shear force, $F = vb$ per unit length of the interface.

The precast unit may be propped at one or two positions. The design of propped slabs is dealt with in Section 6.5.3. In this case spans of up to 6.5 m are possible.

The design for the temporary stage should consider the forces from back-propping of the floor(s) above, if they indeed exist. Successive storeys of props should align vertically and be firmly founded.

Vertical shear is rarely critical because of the large cover width at the support. It may become critical in the presence of large voids where the effective width of the slab at the support is less than about one-quarter of the full width. Additional shear reinforcement is used to take care of the ultimate shear and the problem of stress concentrations near the corners of voids. The effects of point loads or line loads (e.g. walls around voids) are dealt with in the same manner as for any *in situ* concrete floor.

Table 5.5 Typical clear span data for composite slab construction

(a) Units unpropped

Construction		Clear span (m) for imposed loading (kN/m²)									
Unit Depth (mm)	Total Depth (mm)	0.75	1.5	2.0	2.5	3.0	4.0	5.0	7.5	10.0	15.0
75	115	3.75	3.75	3.75	3.75	3.75	3.75	3.75	3.75	3.50	3.09
	150	3.75	3.75	3.75	3.75	3.75	3.75	3.75	3.75	3.75	3.49
	175	3.75	3.75	3.75	3.75	3.75	3.75	3.75	3.75	3.75	3.61
	200	3.75	3.75	3.75	3.75	3.75	3.75	3.75	3.75	3.75	3.65
100	150	5.00	5.00	5.00	5.00	5.00	5.00	5.00	5.00	4.78	4.42
	200	5.00	5.00	5.00	5.00	5.00	5.00	5.00	5.00	4.78	4.42
	250	5.00	5.00	5.00	5.00	5.00	5.00	5.00	4.88	4.75	4.51
	300	4.90	4.87	4.85	4.83	4.82	4.78	4.74	4.66	4.58	4.43

(b) Units propped at mid-span

Construction		Clear span (m) for imposed loading (kN/m²)									
Unit Depth (mm)	Total Depth (mm)	0.75	1.5	2.0	2.5	3.0	4.0	5.0	7.5	10.0	15.0
75	115	6.58	6.14	5.89	5.67	5.47	5.13	4.84	4.28	3.87	3.32
	150	7.50	7.36	7.08	6.83	6.60	6.21	5.88	5.24	4.77	4.12
	175	7.50	7.50	7.50	7.43	7.20	6.79	6.45	5.78	5.28	4.58
	200	7.50	7.50	7.50	7.50	7.50	7.24	6.90	6.21	5.69	4.96
100	150	8.08	7.56	7.27	7.01	6.78	6.37	6.03	5.37	4.89	4.22
	200	9.07	8.57	8.29	8.03	7.79	7.38	7.02	6.32	5.79	5.04
	250	9.40	9.23	8.96	8.72	8.49	8.08	7.72	7.01	6.46	5.67
	300	9.40	9.40	9.39	9.16	8.94	8.55	8.20	7.50	6.95	6.13

The only point to note is that the additional bottom steel has to be cast into the precast plank at the factory.

Interface shear is checked according to the details given in Section 6.3. Unless the unit width is greatly reduced for the same reasons as given above, the reinforcement provided by the lattices is sufficient for all purposes. Indeed, it is designed to be that way. The top surface of the plank is tamped to give an undulating surface with furrows up to 2 to 3 mm deep.

The resulting load-versus-span performance of these units is given in Table 5.5.

5.4.3 Voided composite slab

Lightweight void formers – typically, but not always, made of expanded polystyrene – are pressed into the top surface of the precast plank during manufacture; see Figure 5.68. The adhesion and friction between the polystyrene and wet precast concrete is sufficient to hold the block in position throughout the erection and *in situ* concreting operations. (This is quite important, because the blocks are buoyant in the wet *in situ* concrete.) The reduction in self-weight of a voided floor compared to a solid floor is 30 to 60 per cent for depths of slab from 200 to 350 mm, respectively.

Figure 5.68 Voided composite plank floor (courtesy of MWE Precast Concrete Bhd.).

Exercise 5.3

Design a composite plank floor to carry a characteristic superimposed live load of 5 kN/m^2 over a simply supported effective span of 3.5 m. No propping is allowed. The temporary construction traffic load is 1.03 kN/m^2 {1.0 kN/m^2}.

Use concrete grade C32/40 for the precast, and grade C20/25 for the *in situ*. Use drawn wire for the bars in the precast plank, and a square wire mesh in the *in situ* topping, using $f_{yk} = 500$ N/mm^2 and $f_{ywk} = 250$ N/mm^2 for diagonals inclined at 45°. Cover to all reinforcement = 25 mm. Ultimate load combination factors to EC1 are taken as $\zeta = 0.925$ and $\psi_o = 0.7$.

Check the design at both the temporary and permanent stages for flexural and vertical shear only. (Interface shear will be dealt with in Chapter 6.)

Solution

Step 1: Design in shear

Deflection control:

Assume 16 mm-diameter bottom bars.

BS EN 1992-1-1, NAD Table NA.5.

Assume $\rho = 0.34$

$$\frac{\rho_0}{\rho} = \frac{\sqrt{32} \times 10^{-3}}{0.0034} = 1.664$$

$$\left(\frac{\rho_0}{\rho} - 1\right)^{3/2} = (1.664 - 1)^{3/2} = 0.146$$

$$3.2\sqrt{32} \times 0.146 = 2.647$$

$$l/d = 1.0\left(11 + 1.5\sqrt{32} \times 1.664 + 2.647\right) \quad = 27.8$$

d = 3500/27.8 $\quad d$ = 127 mm

BS 8110, Part 1, Tables 3.10 & 3.11.

Basic span/d = 20.

Modification factor is 1.38

(for an initial estimate $M/bd^2 = 1.0$)

Thus d = 3500/(20 × 1.38) = 127 mm

h = 127 + 25 + 8 = 160 mm

Consider 1 m width of floor, using 50 mm-deep precast with 110 mm-deep *in situ* topping.

(*Continued*)

Step 2: Loading on lattice in temporary condition
Assume lattice top and bottom bar size = 16 mm

Loading		BS 8110 Service (kN/m²)	EC2 Service (kN/m²)
Permanent actions:	Self-weight of 50 mm-deep precast unit	1.20	1.25
	Self-weight of 110 mm-deep wet concrete	2.64	2.75
		3.84	4.00
	Construction traffic allowance	1.00	1.03
Total		4.84	5.03

Ultimate load Eq. 6.10(a) or (b)
= 1.35 × 4.0 + 1.05 × 5.0 or = 10.65 kN/m²
1.25 × 4.0 + 1.5 × 5.0 = 12.50 kN/m²
Use $\gamma_f = 1.25$ and 1.50

$$M_{Ed1} = (1.5 \times 3.78 + 1.25 \times 1.25)\frac{3.5^2}{8} = 11.07\ \text{kNm/m}$$

$$V_{Ed1} = (1.5 \times 3.78 + 1.25 \times 3.75)\frac{3.5}{2} = 12.65\ \text{kN/m}$$

Lever arm = 160 − 33 − 33 = 94 mm
Force in top and bottom bars
= 11.07 × 10³/94 = 117.8 kN/m run

Slenderness of top bars
Pitch = 2 × 94 = 188 mm
$\lambda = 0.7 \times 188/4 = 32.9$
$\lambda_{lim} = 93.3 \times \sqrt{235/500} = 64$
$\lambda = 0.514$
$\phi = (1 + 0.49\ (0.514 - 0.2) + 0.514^2)$
= 0.709
$\chi = 1/(0.709 + \sqrt{(0.709^2 - 0.514^2)})$
= 0.835
f_{ykb} = 0.835 × 500 = 417 N/mm²
< 0.87 × 500

$$A_s = \frac{117.8 \times 10^3}{417} = 282\ \text{mm}^2\text{/m}$$

A_s per lattice at 0.6 m centres
= 282 × 0.6 = 169 mm²

$$M_{u1} = (1.4 \times 3.84 + 1.6 \times 1.00)\frac{3.5^2}{8} = 10.68\ \text{kNm/m}$$

$$V_{u1} = (1.4 \times 3.84 + 1.6 \times 1.00)\frac{3.5}{2} = 12.21\ \text{kN/m}$$

Lever arm
= 160 − 2 × 25 − 2 × 8 = 94 mm
Force in top and bottom bars
= 10.68 × 10³/94 = 113.6 kN/m run

Slenderness of top bars
Pitch = 2 × 94 = 188 mm
$\lambda = 0.7 \times 188/4 = 32.9 > 15$
$p_c \approx (500/460) \times 422$
= 459 N/mm² > 0.87 × 500

$$A_s = \frac{113.6 \times 10^3}{0.87 \times 500} = 262\ \text{mm}^2\text{/m}$$

A_s per lattice at 0.6 m centres
= 262 × 0.6 = 157 mm²

Use one H16 top bar (201 mm²) in lattices at 600 mm centres.

Lattice bars at 45° inclination, with a diagonal length = 94/sin 45° = 133 mm

Bottom bars will be specified after full service load is considered. Subtract the effects of the construction load when calculating the force in bottom steel (as this load will have been removed when in service). Hence:

A_s = (5.00/6.54) × 286 = 196 mm²/m
Shear per lattice = 0.6 × 12.6 = 7.59 kN
Slenderness of lattice (try 6 mm dia.)
$\lambda = 0.7 \times 133/1.5 = 62$
$\lambda_{lim} = 93.3 \times \sqrt{235/250} = 91$
$\lambda = 0.682$
$\chi = 0.736$
f_{ykb} = 0.736 × 250 = 184 N/mm²
< 0.87 × 250

A_s = (5.38/6.98) × 262 = 202 mm²/m
Shear per lattice = 0.6 × 12.21 = 7.33 kN
Slenderness of lattice (try 6 mm dia.)
$\lambda = 0.7 \times 133/1.5 = 62 > 15$
p_c = 200 N/mm² < 0.87 × 250

Thus force in diagonal bar

= 7.59/sin 45° = 10.74 kN		= 7.33/sin 45° = 10.4 kN	
$A_s = \frac{10.74 \times 10^3}{184}$	= 56 mm^2	$A_s = \frac{10.4 \times 10^3}{200}$	= 52 mm^2
A triangular truss with 2 diagonal lattice bars requires each to be	= 28 mm^2	A triangular truss with 2 diagonal lattice bars requires each to be	= 26 mm^2

Use double R6 diagonal lattice bars (28 mm^2) inclined at 45°.

Step 3: Service loading

When the *in situ* concrete has hardened it is effectively stress-free, because the deflections have all occurred while the concrete was wet. Therefore the only stresses in the *in situ* topping derive from superimposed load of 5.00 kN/m^2.

$M_{Ed2} = 1.5 \times 5.00 \times 3.5^2/8$	= 11.48 kNm/m	$M_{u2} = 1.6 \times 5.00 \times 3.5^2/8$	= 12.25 kNm/m
$V_{Ed2} = 1.5 \times 5.00 \times 3.5/2$	= 13.13 kN/m	$V_{u1} = 1.6 \times 5.00 \times 3.5/2$	= 14.0 kN/m

Step 4: Flexural design

$k = \frac{11.48 \times 10^6}{1000 \times 127^2 \times 20}$	= 0.035<0.2067	$k = \frac{12.25 \times 10^6}{1000 \times 127^2 \times 25}$	= 0.03 < 0.156
$z = d(0.5 + \sqrt{0.25 - k/1.133})$		$z = d(0.5 + \sqrt{0.25 - k/0.9}) \leq 0.95\,\mathrm{d}$	
$z/d = 0.95 \times 127$	= 120.7 mm	$z = 0.95 \times 127$	= 120.7 mm
$A_s = \frac{11.48 \times 10^6}{120.7 \times 0.87 \times 500}$	= 219 mm^2/m	$A_s = \frac{12.25 \times 10^6}{120.7 \times 0.87 \times 500}$	= 234 mm^2/m
plus 196 mm^2/m from the construction stage = 415 mm^2/m		plus 202 mm^2/m from the construction stage = 436 mm^2/m	
Bottom bar area per lattice at 0.6 m centres requires		Bottom bar area per lattice at 0.6 m centres requires	
$A_s = 415 \times 0.6$	= 249 mm^2	$A_s = 436 \times 0.6$	= 262 mm^2

Use two H16 bottom bars (402 mm^2) in lattices at 600 mm centres.

Step 5: Shear design

$k = 1 + \sqrt{(200/127)} = 2.139$ but ≤ 2.0	$k = 2$	$v = \frac{14.00 \times 10^3}{1000 \times 127}$	= 0.11 N/mm^2
$v_{min} = 0.0035 \times 2^{(3/2)} \times 32^{(1/2)}$	= 0.056	< minimum value in BS 8110, Part 1, Tables 3.9 and 5.5.	
$\rho_l = 249/(600 \times 127)$	= 0.328%		
$v_{Rd,c} = 0.12 \times 2.0 \times (0.328 \times 32)^{(1/3)}$	= 0.5255		
$V_{Rd,c} = 0.5255 \times 600 \times 127 \times 10^{-3}$	= 40.04 kN		
	> 13.13 kN/m		

Therefore no additional reinforcement to the lattice is required.

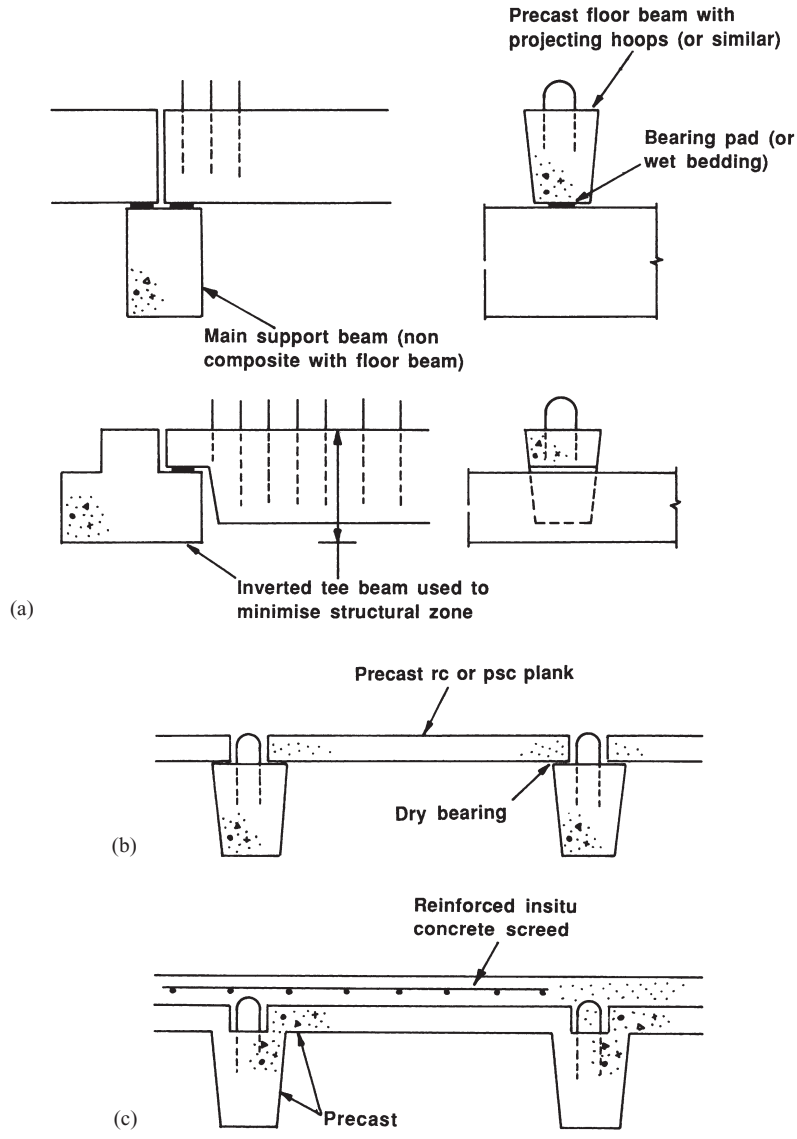

Figure 5.69 Prestressed beam and composite plank floor system. (a) Precast floor beam positioned; (b) precast plank fixed; (c) *in situ* topping added.

5.5 Precast Beam-and-Plank Flooring

5.5.1 General

The beam-and-plank floor is commonly known as the Precast Beam Composite (PBC) system, and is shown generally in Figures 5.1(e) and in detail in Figures 5.69(a)–(c). It is a three-part construction as follows:

(1) Prestressed beams are the major structural components that span between the primary beams in the structure. They are typically available in depths of up to 550 mm, and weigh up to 4.3 kN/m

run. The spacing between the beams varies between 900 and 2400 mm. The maximum span for roofs is then 20.9 m, and for office floors is 18.2 m.

(2) Precast planks, which are between 50 and 75 mm deep and of the specification given in Section 5.4, span transversely to the beams. The width of the plank may be up to 2.4 m, but smaller units, say 600 mm wide and weighing about 50 kg, may be manhandled into their final position, which is clearly beneficial from a construction point of view. The design of the plank is as given in Section 5.4.2.

(3) A 40- to 50 mm-thick grade C32/40 *in situ* concrete topping is added to the top of the planks, making the total construction span-to-depth ratio, inclusive of all three items, of about 25:1 for offices, and 30:1 for domestic buildings. Voids up to about 2.0 m wide may easily be formed between the prestressed beams. All the details given in Section 5.4 above may be incorporated into this system.

The PBC method is more versatile geometrically than the hollow-core or double-tee methods and may be adapted to suit a wide range of plan configurations. The floor system may be used in conjunction with *in situ* concrete, precast concrete, or steelwork frames.

5.5.2 Design of prestressed beams in the beam-and-plank flooring system

The beam's cross section is trapezoidal, with a 2.5° side splay. A single tapered mould may be used for any depth of unit, although the manufacturers prefer to work to a small number of depths, usually 400, 450, 500 and 550 mm. Similarly the width of the beam is restricted in size, usually to 320 mm at the bottom.

The beams are designed according to the basic prestressing principles. The depth of the ends of the beams may be reduced to form a half-joint in the same manner as for double-tee units. Cantilever balconies may be formed either by reinforcing the beam for the negative moment, or by utilising the top reinforcement in the structural topping. The hogging moment induced from the prestressing must be nullified (or reversed) in the cantilevered part.

5.6 Design Calculations

5.6.1 Hollow-core unit

This specimen calculation is used to determine:

(i) serviceability and ultimate moments of resistance
(ii) ultimate shear capacities in the flexurally uncracked and cracked regions
(iii) cracking moment of resistance and the decompression point
(iv) camber and short-term deflection at installation
(v) long-term deflection
(vi) deflection after the application of finishes
(vii) crack spacing and crack width
(viii) fire resistance
(ix) sound resistance
(x) thermal transmittance

for the nominally 1200 × 200 mm deep hollow-core unit shown in cross section in Figure 5.70. The unit contains 6 cores each 140 mm wide. The unit is the type produced in slip-forming machines manufactured by Echo Engineering in Belgium.

For the purpose of calculating deflections, the effective span is 8.5 m, bearing length = 100 mm, the floor finishes and services are 2.0 kN/m^2 and the live load is for offices at 5.0 kN/m^2. The required fire

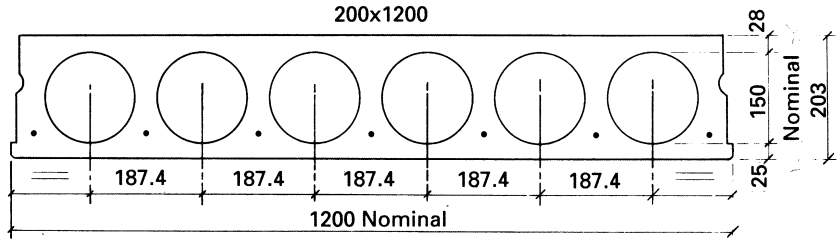

Figure 5.70 Cross-section of hollow-core slab used in design calculations.

resistance is R60 minutes {1 hour}. The unit is to be designed to BS EN 1992-1-1, f_{ctm} {BS 8110 Class 2} permissible tension. Exposure is XC1 taking 50 per cent relative humidity (RH) in service. Installation takes place at 28 days. The hcu is pretensioned using seven 12.5 mm plus five 9.3 mm diameter Class 2 helical strands f_{yk} $\{f_{pu}\} = 1770\,\text{N/mm}^2$ stressed to 70 per cent. Cover is 40 mm. Concrete is C45/55, with transfer after 18 hours, during which the mean curing temperature is 40°C and RH = 70 per cent. The cement is grade 52.5R and the aggregates are gravel. For the purpose of thermal properties the depth of finishes may be taken as 60 mm.

Unit properties per 1200 mm width

Depth = 200 mm
Width = 1197 mm (bottom), 1154 mm (top)
Concrete area $A_c = 152\,460\,\text{mm}^2$
Depth of concrete to core = 40 mm
$I = 696.67 \times 10^6\,\text{mm}^4$
$Z_b = 7.040 \times 10^6\,\text{mm}^3$
Eccentricity from centroid = 53.1 mm
Area of longitudinal joint = $7515\,\text{mm}^2$
Height to neutral axis $y_b = 99.0$ mm
Total breadth of webs $b_w = 303$ mm
$S = 4.768 \times 10^6\,\text{mm}^3$
$Z_t = 6.895 \times 10^6\,\text{mm}^3$
Area of strand $A_p = 7 \times 93 + 5 \times 52 = 911\,\text{mm}^2$

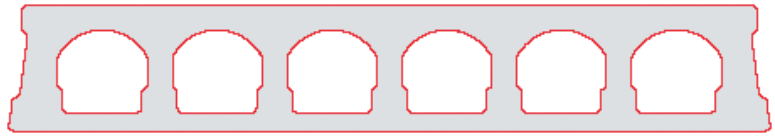

Material properties to BS EN 1992-1-1

Concrete:

$f_{ck} = 45\,\text{N/mm}^2$

Mean compressive and tensile strength (see Table 3.1.)

$f_{cm} = f_{ck} + 8 = 53\,\text{N/mm}^2$

$f_{ctm} = 0.3 \times 45^{2/3} = 3.80\,\text{N/mm}^2$ (see 3.1.6.(1)P)

Design strength in flexure or compression,

$\alpha_{cc} = 0.85$, otherwise $\alpha_{cc} = 1.0$,

$f_{cd} = 0.85 \times 45/\gamma_c = 25.5\,\text{N/mm}^2$ (see Eq. 3.15)

otherwise $f_{cd} = 30\,\text{N/mm}^2$

Design tensile strength $\alpha_{ct} = 1.0$ & $\gamma_c = 1.5$

5% fractile strength

$f_{ct,0.05} = 0.7 \times 3.80 = 2.66\,\text{N/mm}^2$ (see Table 3.1)

$f_{ctd} = 2.66/\gamma_c = 1.77\,\text{N/mm}^2$ (see Eq. 3.16)

Young's modulus

$E_{cm} = 22\ (53/10)^{0.3} = 36.3\,\text{kN/mm}^2$ (see Table 3.1.)

At transfer, values$_{(t)}$ with $t = 2$ days:

$f_{ck(t)} = 30\,\text{N/mm}^2$

$f_{cm(t)} = f_{ck(t)} + 8 = 38\,\text{N/mm}^2$

$f_{cd(t)} = 0.85 \times 30/\gamma_c = 17.0\,\text{N/mm}^2$

$f_{ctm(t)} = \beta_{cc(t)}^{\alpha} f_{ctm}$ where $\alpha = 1$ for 1 day

$\beta_{cc(t)} = f_{cm(t)}/f_{cm} = 38/53 = 0.72$ (see Eq. 3.4.)

$f_{ctm(t)} = 0.72 \times 3.80 = 2.72\,\text{N/mm}^2$

$f_{ctd(t)} = 0.7 \times 2.72/\gamma_c = 1.27\,\text{N/mm}^2$

$E_{cm(t)} = 22\ (38/10)^{0.3} = 32.8\,\text{kN/mm}^2$

Material properties to BS 8110

Concrete:

$f_{cu} = 55\,\text{N/mm}^2$

Design strength = $0.45 \times 55 = 24.75\,\text{N/mm}^2$

Tensile strength $f_{ct} = 0.45 \times \sqrt{55} = 3.34\ \text{N/mm}^2$

Design tensile strength $f_t = 0.24 \times \sqrt{55} = 1.78\ \text{N/mm}^2$

Young's modulus $E_c = 20 + 0.2 \times 55 = 31\,\text{kN/mm}^2$

At transfer:

$f_{ci} = 37\,\text{N/mm}^2$

Tensile strength $f_{ct} = 0.45 \times \sqrt{37} = 2.74\ \text{N/mm}^2$

Young's modulus $E_{ci} = 20 + 0.2 \times 37 = 27.4\,\text{kN/mm}^2$

Steel tendons

Characteristic strength $f_{pk} = 1770\,\text{N/mm}^2$

$f_{p,0.1k} = 0.9\ f_{pk} = 1593\,\text{N/mm}^2$

$\gamma_{p,fav} = 0.9$ at ultimate, and 1.0 at service (see 2.4.2.2.(1))

$r_{sup} = r_{inf} = 1.0$ for direct measurement (see 5.10.9)

$\gamma_s = 1.15$ (see 2.4.2.4)

Design stress at ultimate

$f_{pd} = 1593/1.15 = 1385\,\text{N/mm}^2$ (see 3.3.6. (7))

Young's modulus $E_p = 195\,000\,\text{N/mm}^2$ (see 3.3.6. (3))

Strain limit (3.3.6(7), Figure 3.10)

$\varepsilon_{uk} = \varepsilon_{ud}/0.9 = 0.02/0.9 = 0.0222$ (see 3.3.6. (7))

Relaxation class = 2 (see 3.3.2. (4))

Relaxation loss at 1000 hours $\rho_{1000} = 2.5\%$ (see 3.3.2. (6))

Detensioning rate = 'gradual' (see 8.10.2.2.(2))

Characteristic strength $f_{pu} = 1770\,\text{N/mm}^2$

Design stress at ultimate $f_{pb} = 1770/1.15 = 1539\,\text{N/mm}^2$

Young's modulus $E_s = 195\,000\,\text{N/mm}^2$

Relaxation loss at 1000 hours = 2.5%

Serviceability Limit State of Bending

Initial prestress = $0.7 \times 1770 = 1239\,\text{N/mm}^2$

Initial force = $1239 \times 911 = 1128.7\,\text{kN}$

Initial relaxation loss

$\mu = 0.7$ and $t = 18$ hours

$\Delta\sigma_{p,r} = 1239 \times 0.66 \times 2.5 \times e^{(9.1 \times 0.7)} \times (18/1000)^{0.75(1-0.7)} \times 10^{-5} =$ $\underline{4.84\,\text{N/mm}^2}$

$P_r = 1124.3\,\text{kN}$

Instantaneous deformation

$f_{cc} = 11.94\,\text{N/mm}^2$ (at tendon centroid)

$\Delta\sigma_{p,el} = 11.94 \times 195/32.8 =$ $\underline{70.88\,\text{N/mm}^2}$

Assume 8% loss at transfer due to half the relaxation loss and elastic shortening.

Initial relaxation = $0.5 \times 1.2 \times 2.5 = 1.5\%$

$f_{cci} = 11.02\,\text{N/mm}^2$ (at tendon centroid)

Elastic loss

$$= \frac{11.02 \times 195}{27.4 \times 1239} = 6.33\%$$

Total loss at transfer = 75.7 N/mm^2
Prestress at transfer σ_{pm0} = 1163.3 N/mm^2
f_{bc} = 14.95 N/mm^2 (bottom) < 17.0 N/mm^2
f_{tc} = −1.22 N/mm^2 (top) > −2.72
f_{cc} = 11.25 N/mm^2 (at tendon centroid)
BS EN 1992-1-1, equations 3.29, 5.44 and 5.46, together with Annexes B and D, give more scope for estimating losses in different circumstances. The prestress is required at installation only for reasons of calculating the deflection after installation of finishes. The temperature-adjusted concrete age is calculated using Eq. B.9 and B.10 and is used for the initial creep losses.

<u>Creep loss from transfer to installation</u>
t = 0.75 to 28 days
All surfaces exposed (excluding inside faces of cores)
h_o = 2 × 152 460/2751 = 111 mm
(Eq. B.9 and B.10) $t_{o,T} = e^{-(4000/313 - 13.65)} \times 0.75 = 1.79$ days
$t_o = 1.79 \times ((9/(2 + 1.79^{1.2}) + 1)^1 = 5.8$ days
(Eq. B.1 to B.8) Creep loss coefficient

$$= \left(1 + \frac{\left(1 - \frac{70}{100}\right)}{0.1 \times \sqrt[3]{111}} \times \left(\frac{35}{53}\right)^{0.7}\right) \times \left(\frac{35}{53}\right)^{0.2} \times \frac{16.8}{\sqrt{53}} \times \frac{1}{(0.1 + 5.8^{0.2})} \times \beta_{c(t,t0)} = 0.912$$

where

$$\beta_{c(t,t_0)} = \left(\frac{28 - 0.75}{1.5(1 + (0.012 \times 70)^{18} \times 111 + 250\left(\frac{35}{53}\right)^{0.5} + 28 - 0.75}\right)^{0.3} = 0.445$$

(Eq. 5.46) $\Delta\sigma_{p,c}$

$$= \frac{\frac{195}{36.3} \times 0.912 \times 11.25}{1 + \frac{195}{36.3}\frac{911}{152460}\left(1 + \frac{152460}{696670000}53^2\right)(1 + 0.8 \times 1.329)} = 50.6 \text{ N/mm}^2$$

Prestress at installation σ_{pmi} = 1112.7 N/mm^2
f_{cc} = 10.76 N/mm^2 (at tendon centroid)
<u>Creep loss from installation to life</u>

Total loss at transfer = 7.83%
Prestress at transfer = 1142.0 N/mm^2
Prestress at transfer
f_{bc} = 14.68 N/mm^2 (bottom) < 0.5 × 37
f_{tc} = −1.20 N/mm^2 (top) > −2.74
f_{cci} = 11.04 N/mm^2
BS 8110, Part 2, clause 7.3
Creep coefficient at installation = 0.4 × 1.8 = 0.72

$$\text{Creep loss} = \frac{0.72 \times 11.04 \times 195}{31.0 \times 1239} = 4.09\%$$

Prestress at installation = 1091.9 N/mm^2
f_{cci} = 10.56 N/mm^2
Creep coefficient installation to life = 1.80 − 0.72 = 1.08

$$\text{Creep loss} = \frac{1.08 \times 10.56 \times 195}{31.0 \times 1239} = 5.79\%$$

Shrinkage loss = 300 × 10^{-6} × 195 000 = 58.5 N/mm^2 = 4.72 %
Final relaxation = 1.5% = 1.50 %
Total Losses = 23.93%
Final prestress = 943 N/mm^2
Effective prestressing force = 911 × 943 = 859.2 kN

t = 28 to 20 833 days (500 000 hours)
Notional depth for soffit exposed
$h_o = 2 \times 152\,460/1200 = 255\,\text{mm}$
Creep loss coefficient

$$= \left(1 + \frac{\left(1 - \frac{50}{100}\right)}{0.1 \times \sqrt[3]{255}} \times \left(\frac{35}{53}\right)^{0.7}\right) \times \left(\frac{35}{53}\right)^{0.2}$$

$$\times \frac{16.8}{\sqrt{53}} \times \frac{1}{(0.1 + 28^{0.2})} \times \beta_{c(t,t_0)}$$

$= 1.636$

where

$$\beta_{c(t,t_0)} = \left(\frac{20833 - 28}{1.5(1 + (0.012 \times 50)^{18} \times 255 + 250\left(\frac{35}{53}\right)^{0.5} + 20833 - 28}\right)^{0.3}$$

$= 0.992$

Shrinkage losses

$\varepsilon_{ca} = 1 - e^{-0.2\sqrt{500000}} \times 2.5 \times (50 - 10) \times 10^{-6} = 0.000088$

$k_h = 0.80$ for $h_o = 255\,\text{mm}$

$$\varepsilon_{cd,0} = 0.83 \times 0.85(220 + 110 \times 6)e^{-0.11\frac{50}{10}} \times 1.55\left(1 - \left(\frac{50}{100}\right)^3\right) = 0.00045$$

Drying shrinkage strain (Eq. 3.9)

$$= \frac{(20833 - 1)}{(20833 - 1 + 0.04\sqrt{255^3})} \times 1 \times \varepsilon_{cd,0} = 0.000447$$

Total ε_{cd} = 0.000547

Post transfer relaxation loss

(Eq. 3.29) $\mu = 1163/1770 = 0.657$

$$= 1163 \times 0.66 \times 2.5e^{9.1 \times 0.657}\left(\frac{500000}{1000}\right)^{0.75(1-0.657)} 10^{-5} = 37.5\,\text{N/mm}^2$$

Total time-dependent losses (Eq.5.46)

$$= \frac{0.000547 \times 195000 + 0.8 \times 37.5 + \frac{195}{36.3} \times 1.636 \times 10.76}{1 + \frac{195}{36.3}\frac{911}{152460}\left(1 + \frac{152460}{696670000}53^2\right)(1 + 0.8 \times 1.636)} = 201.8\,\text{N/mm}^2$$

Final prestress = 1239 − 75.7 − 50.6 − 201.8 = 910.8 N/mm^2 (Losses 26.5%)

Effective prestressing force = 911 × 910.8 = 829.7 kN

Prestress after losses (bottom) $f_{bc} = 11.71\,\text{N/mm}^2$
(top) $f_{tc} = -0.96\,\text{N/mm}^2$

For XC1 exposure, allowable tension ($f_{ck} = 45\,\text{N/mm}^2$) = 3.8 N/mm^2

Service moment of resistance using compound section, based on $(m - 1)$, where later it is shown $\psi_{28} = 0.71$

$m = (1 + 0.71) \times 195/36.3 = 9.2$

Prestress after losses (bottom) $f_{bc} = 12.12\,\text{N/mm}^2$
(top) $f_{tc} = -0.99\,\text{N/mm}^2$

For class 2 elements, allowable tension ($f_{cu} = 55\,\text{N/mm}^2$) = 3.34 N/mm^2

Service moment of resistance using compound section where

$m = (1 + 0.72) \times 195/31 = 10.8$

where
$Z_{b,co} = 7.430 \times 10^3\,mm^3$
$Z_{t,co} = 6.924 \times 10^3\,mm^3$
M_{sr} based on bottom stress =
$(11.71 + 3.8) \times 7.43$ = 115.20 kNm
M_{sr} based on top stress
$= (0.96 + 0.45 \times 45) \times 6.924$ = 146.83 kNm
> 113.65

so not critical.

$Z_{b,co} = 7.505 \times 10^3\,mm^3$
$Z_{t,co} = 6.929 \times 10^3\,mm^3$
M_{sr} based on bottom stress
$= (12.12 + 3.34) \times 7.505$ = 116.03 kNm
M_{sr} based on top stress
$= (0.99 + 0.33 \times 55) \times 6.929$ = 132.62 kNm
> 116.03

so not critical.

Design service moment

Self-weight including infill = $25 \times (152460 + 7515)\ 10^{-6}/1.2 = 3.33\,kN/m^2$
$w_s = 1.2 \times (3.33 + 2.00 + 5.00) = 12.40\,kN/m$
$M_s = 12.40 \times 8.5^2/8 = 112.0\,kNm < 113.65\,kNm$. OK.

Self-weight including infill = $24 \times (152460 + 7515)\ 10^{-6}/1.2 = 3.20\,kN/m^2$
$w_s = 1.2 \times (3.20 + 2.00 + 5.00) = 12.24\,kN/m$
$M_s = 12.24 \times 8.5^2/8 = 110.5\,kNm < 116.03\,kNm$. OK.

Ultimate Limit State of Bending

$d = 200 - 45.8 = 154.2\,mm$
$b = 1154\,mm$
Final prestress = $910.8\,N/mm^2$
$\varepsilon_{po} = 910.8/195\,000 = 0.00467$
$\varepsilon_{LOP} = 0.9 \times 0.87 \times 1770/195\,000 = 0.0071$
By solving quadratic or iterative solutions, $X = 55.1\,mm > 40\,mm$ top flange. By considering concrete below top flange above the circular core
$X = 59.9\,mm$
$d_n = 22.1\,mm$
$\varepsilon_p = 0.010103 > \varepsilon_{LOP} < \varepsilon_{ud}$
$f_p = 1416\,N/mm^2$
$F_s = f_p\,A_p = 1416 \times 911 = 1290.0\,kN$
Ultimate moment of resistance
$M_{Rd} = 1290.0 \times (154.2 - 22.1)$ = 170.4 kNm

Final prestress = $943\,N/mm^2$
$\varepsilon_{po} = 943/195\,000 = 0.00484$
$\varepsilon_{LOP} = 0.696 \times 1770/195\,000 = 0.00632$
By solving quadratic or iterative solutions, $X = 52.5\,mm > 40\,mm$ top flange. By considering concrete below top flange above the circular core
$X = 63.6\,mm$
$d_n = 22.9\,mm$
$\varepsilon_p = 0.00982 > \varepsilon_{LOP} < 0.01290$
$f_p = 1396\,N/mm^2$
$F_s = f_p\,A_p = 1396 \times 911 = 1271.7\,kN$
Ultimate moment of resistance
$M_{Rd} = 1271.7 \times (154.2 - 22.9)$ = 167.0 kNm

Design ultimate moment

(Eq. 6.10(b))
$w_{Ed} = 1.2 \times (1.25 \times (3.33 + 2.00) + 1.5 \times 5.00) = 17.00\,kN/m >$
(Eq. 6.10(a)) 14.93 kNm
$M_{Ed} = 17.00 \times 8.5^2/8 = 153.5\,kNm < 170.4\,kNm$. OK.

$w_u = 1.2 \times (1.4 \times (3.20 + 2.00) + 1.6 \times 5.00) = 18.33\,kN/m$
$M_u = 18.33 \times 8.5^2/8 = 165.5\,kNm < 167.0\,kNm$. OK.

Ultimate Limit State of Shear

i) Uncracked

$f_{ctd(t)} = 0.7 \times 2.72/1.5 = 1.27\,N/mm^2$
$f_{pbt} = 3.2 \times 1.0 \times 1.27 = 4.06\,N/mm^2$
$\sigma_{pm0} = 1163.3\,N/mm^2$
$l_{pt2} = (1.2 \times 1.0 \times 0.19 \times 1163.3/4.06)\ \phi = 65.3\ \phi$
Mean dia = $(7 \times 12.5 + 5 \times 9.3)/12 = 11.17\,mm$

Mean dia = $(7 \times 12.5 + 5 \times 9.3)/12 = 11.17\,mm$

Mean $l_{pt2} = 65.3 \times 11.17$ = 729 mm

$l_x = 100 + 99 = 199$ mm
$\alpha_l = 199/729 = 0.273$
$\sigma_{cp} = 5.44$ N/mm^2
$f_{ctd} = 0.7 \times 3.80/1.5 = 1.77$ N/mm^2
Ultimate shear capacity

$$V_{Rd,c} = \frac{696670000 \times 303}{4768000} \times \sqrt{1.77^2 + 0.273 \times 0.9 \times 5.44 \times 1.77} = \underline{103.75\,\text{kN}}$$

Transmission length $= \dfrac{240 \times 11.17}{\sqrt{37}}$ = 441 mm

$f_{cp} = 5.64$ N/mm^2
f_{cpx} at 199 mm from end = 3.94 N/mm^2
$b_v = 303$ mm
$f_t = 0.24\sqrt{55} = 1.78$ N/mm^2
Ultimate shear capacity

$$V_{co} = 0.67 \times 303 \times 200\sqrt{1.78^2 + 0.8 \times 3.94 \times 1.78} = \underline{120.1\,\text{kN}}$$

ii) Cracked

$k = 2$

$$V_{Rd,cr} = \left(0.12k(100\rho_1 f_{ck})^{1/3} + 0.15\sigma_{cp}\right)b_v d$$

$$V_{Rd,cr} = \left(0.12 \times 2(100 \times 0.0195 \times 45)^{1/3} + 0.15 \times 0.9 \times 5.35\right)303 \times 154.2 = \underline{83.46\,\text{kN}}$$

$V_{Rd,cr,min} = 0.66 \times 303 \times 154.2 \times 10^{-3}$ = 64.66 kN

Cracked moment of resistance $V_{Ed} \le V_{Rd,cr}$
$M_{cr} = (11.71 + 1.77) \times 7.43 = 100.2$ kNm
For the given service loading and span, this occurs at $x = 2.72$ m from support. At this point $V_{Ed} = 26.0$ kN < 83.46 kN, not critical.

100 $A_s/b_v\, d = 1.95$
$\nu_c = 1.172$ N/mm^2
$f_{pe}/f_{pu} = 0.7\ (1 - 0.2388) = 0.533$
$M_o = 0.8 \times 12.12 \times 7.505 = 72.77$ kNm = 75.7 kN > 46.1 kN not critical
occurs at 1.75 m from support where $V_u = 46.1$ kN and $M_u = 109$ kNm.
At this point V_{cr} (Eq. 55) = (1 − 0.55 × 0.533) × 1.172 × 303 × 154 + 72.77 × 50.2/98.4 = 38.6 + 37.1
Deflections based on compound section

At transfer

$P_{pm0} = 1163.3 \times 911 = 1059.7$ kN
Camber

$$\delta_1 = \frac{1059700 \times 53 \times 8500^2}{8 \times 32800 \times 716.8 \times 10^6} = -21.6 \text{ mm}$$

Self weight at transfer (3.81 kN/m)

$$\delta_2 = \frac{5 \times 3.81 \times 8500^4}{384 \times 32800 \times 716.8 \times 10^6} = +11.0 \text{ mm}$$

Net deflection at transfer
$\delta_3 = -10.6$ mm < span/300

$P_t = 1142.0 \times 911 = 1040.3$ kN
Camber

$$\delta_1 = \frac{1040300 \times 53 \times 8500^2}{8 \times 27400 \times 720.6 \times 10^6} = -25.3 \text{ mm}$$

Self weight at transfer (3.66 kN/m)

$$\delta_2 = \frac{5 \times 3.66 \times 8500^4}{384 \times 27400 \times 720.6 \times 10^6} = +12.6 \text{ mm}$$

Net deflection at transfer
$\delta_3 = -12.7$ mm < span/300

At installation, effective change in Young's modulus gives creep coefficient

$$\varphi = \frac{32800}{0.5 \times (32800 + 36300)} \times 2.5 \times (0.4 - 0.1) = 0.71$$

Camber = 1.71 × −21.6 = −36.9 mm
Self weight = 1.71 × 11.0 = 18.8 mm
Net deflection at installation
$\delta_4 = -18.1$ mm
Long term creep coefficient
= 0.8 × 2.5 × (1 − 0.4) = 1.20

$$\varphi = \frac{27400}{0.5(27400 + 31000)} \times 0.4 \times 1.8 = 0.676$$

Camber = 1.676 × −25.3 = −42.4 mm
Self weight = 1.676 × 12.6 = 21.1 mm
Net deflection at installation
$\delta_4 = -21.3$ mm
Long term creep coefficient
= 1.8 − 0.676 = 1.124

Long term camber

$$\delta_5 = -36.9 - \frac{1.20 \times 829760 \times 53 \times 8500^2}{8 \times 36300 \times 716.8 \times 10^6}$$

$= -55.2$ mm

Long-term self-weight incl. infill = 4.00 kN/m

$$\delta_6 = 1.2 \times 18.85 + \frac{5 \times 4.00 \times 8500^4}{384 \times 36300 \times 716.8 \times 10^6}$$

$= +33.1$ mm

Long-term dead load = 1.2 × 2.00 = 2.40 kN/m subjected to $\varphi_{28} = 1.2$, plus quasi-permanent live = 0.3 × 1.2 × 5.00 = 1.80 kN/m subjected to $\varphi_\infty = 0.8 \times 2.5 = 2.0$

$$\delta_7 = \frac{5((1+1.2) \times 2.40) + ((1+2.0) \times 1.80) \times 8500^4}{384 \times 36300 \times 716.8 \times 10^6}$$

$= +27.9$ mm

Final deflection = −55.2 + 33.1 + 27.9 = +5.8 mm < span/250 = 34 mm

$$\delta_5 = -42.4 - \frac{1.124 \times 859200 \times 53 \times 8500^2}{8 \times 31000 \times 720.6 \times 10^6}$$

$= -63.1$ mm

Long-term self-weight incl. infill = 3.84 kN/m

$$\delta_6 = 1.124 \times 21.1 + \frac{5 \times 3.84 \times 8500^4}{384 \times 31000 \times 720.6 \times 10^6} = +35.4 \text{ mm}$$

Long-term dead load = 1.2 × 2.00 = 2.40 kN/m subjected to $\varphi_{28} = 1.124$, plus factor (0.25) × live = 0.25 × 1.2 × 5.00 = 1.50 kN/m subjected to $\varphi_\infty = 1.8$

$$\delta_7 = \frac{5 \times ((1+1.124) \times 2.40) + ((1+1.8) \times 1.50) \times 8500^4}{384 \times 31000 \times 720.6 \times 10^6}$$

$= +28.3$ mm

Final deflection = −63.1 + 35.4 + 28.3 = +0.6 mm < span/250 = 34 mm

Deflection after installation

Change in camber = −55.2 − (−36.9) = −18.3 mm

Dead load visco-elastic movement (subjected to φ_{28} after installation) = +20.0 mm

Live load static + visco-elastic movement (subjected to 1+ φ_{28} after installation) = +10.3 mm

Net movement = −18.3 + 20.0 + 10.3 = 12.0 mm < span/500 = 17.0 mm

Figure 5.71 shows the final deflections.

Crack spacing and width

w_s (frequent service load) = 1.2 (3.33 + 2.00 + 0.5 × 5.00) = 9.40 kN/m

$M'_s = 9.40 \times 8.5^2 / 8 = 84.9$ kNm

Frequent bottom stress = $f_{bc} - M'_s / Z_{b,co}$

$= 11.71 - 84.9 / 7.43 = +0.28$ N/mm^2 no decompression

$\Delta\sigma_p > 0$ and $c_w = 0$.

Change in camber = −63.1 − (−42.4) = −20.7 mm

Dead load visco-elastic movement (subjected to φ_{28} after installation) = +21.3 mm

Live load static + visco-elastic movement (subjected to 1+ φ_{28} after installation) = +9.7 mm

Net movement = −20.7 + 21.3 + 9.7 = 10.3 mm < 20 and span/350 = 24.2 mm

Fire resistance

Effective thickness = 200 mm.

Refer Table 3.3 gives R120.

Axis distance − 15 mm = 45.8 − 15 = 30.8 mm< 40 mm gives R90

Fire resistance = 90 minutes

Cover = 40 mm gives 2 hours

Depth = 200 × ((152460 + 9960) /1200 × 200) = 133 mm > 123 mm gives 2 hours

Fire rating = 2 hours

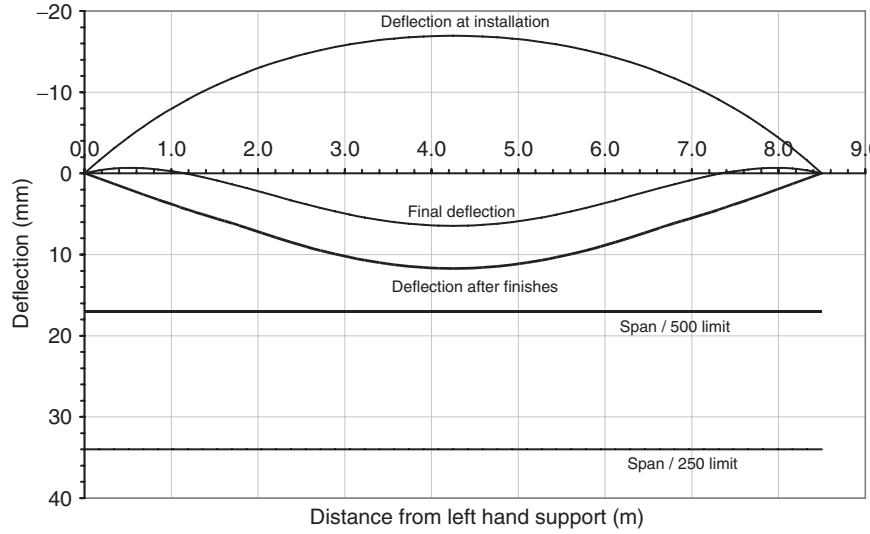

Figure 5.71 Final deflection profiles for the example in Section 5.6 to BS EN 1992-1-1.

Other data

Sound attenuation, including finishes

BS EN12354-1, Annex B2 [5.60] and similar data from National Physics Laboratory for voided elements:

$$D = 37.5\log_{10} m - 44 \text{ dB} = 37.5\log_{10}(102\times(3.33+2.00)) - 44 = 59 \text{ dB}.$$

Thermal resistance of uninsulated floor

BS EN 13369, clause 4.3.6 [5.7] refers to BS ISO 6946:2007 [5.61] and BS ISO 10456:2007 [5.62].

Estimate of thermal resistance, including finishes of basic unit. Refer to specialist information for effects of flanking at edges, air gaps and other obstructions:

Data λ for concrete = 1.7 W/m°K
R_{si} (internal) = 0.170 m²°K/W downwards and 0.100 m²°K/W upwards (BS EN ISO 6946, Table 1)
R_a = unventilated air space (hollow cores) = 100 mm dimension = 0.22 m²°K/W (Table 2)
$R = d/\lambda$ (Clause 5.1)

For internal to internal surfaces upwards:	m²°K/W
R solid section of concrete = (0.200 + 0.060)/1.7	= 0.153
Internal surfaces = 2 R_{si} = 2 × 0.100	= 0.200
Sum $R_{T,solid}$ at solid section of concrete	= 0.353

Equivalent thickness of flanges above and below the voids ≈ $(A_c - b_w\ h)/b$ = ((152460 + 7515) − (303 × 200))/1200 = 83 mm

R_T concrete flanges = (0.083 + 0.060)/1.7	= 0.084
Internal surfaces = 2 R_{si} = 2 × 0.100	= 0.200
Air space R_a	= 0.160
Sum $R_{T,void}$ at voided sections	= 0.444

(EN ISO 6946, 6.2.2)
Proportion of voided slab per unit width $f_{void} = (1200 - 303)/1200 = 0.748$

$1/R_T = f_{solid}/R_{T,solid} + f_{void}/R_{T,void}$ $= 2.399\,\text{W/m}^2\,^\circ\text{K}$
Final R_T $= 0.42\,\text{m}^2\,^\circ\text{K/W}$

CHAPTER 6

Composite Construction

The design and construction aspects of using precast concrete elements compositely with in situ *concrete are described.*

6.1 Introduction

Composite construction offers many advantages in precast concrete design, particularly in enhancing the flexural and shear strength of prestressed concrete beams, where greater axial stresses may be generated in the precast units than in ordinary non-composite designs. To most minds, composite construction means adding *in situ* concrete on top of precast components to form a single unit acting as though it were one. However, in the context of precast design there are many ways in which *in situ* concrete is used compositely in the structure. For example, composite action is used mainly to:

- increase flexural and shear strength of floor slabs
- tie floor slabs to beams, thereby ensuring a secure bearing, and increasing the flexural and shear strength of beams
- provide the compressive and/or shear transfer between adjacent precast units, e.g. between walls, shear walls and columns, and at column foundations
- provide interface shear between the *in situ* concrete infill and the outer leaf of a precast concrete twin-wall
- ensure floor diaphragm action, with or without a structural topping (see Section 8.2)
- anchor stability tie steel into precast components (see Section 9.2).

In all cases, *in situ* concrete surrounds the precast components to form a monolithic structure. Shear and compressive forces are carried through the *in situ* concrete by shear friction, wedging and/or bearing. Tension is effected by fully anchored rebar, or other mechanical means, so that the concrete is confined to prevent lateral splitting. Design values at the interface vary over a wide range depending on the surface characteristics of the joining faces, the loading, and the mode of failure, where non-ductile situations attract higher partial safety factors.

The strength of the two concretes may be different; usually the precast concrete is grade C30/37 to C50/60 and the *in situ* concrete is grade C20/25 or C25/30 (see Table 6.1), but this is taken into account in the analysis for both the service and ultimate limit states. Reference is also made to the design recommendations in BS EN 1992-1-1, clause 6.2.5 [6.1] {BS 8110, Part 1, clause 5.4 [6.2]}.

Non-structural finishing screeds may be applied directly onto precast concrete slabs, but allowances for precamber should be made in calculating overall floor depth. It is only in the presence

Multi-storey Precast Concrete Framed Structures, Second Edition. Kim S. Elliott and Colin K. Jolly.

Table 6.1 Strengths and short-term elastic moduli for typical concrete for composite construction

Type of concrete	f_{ck} (N/mm^2)	f_{ctd} (N/mm^2)	E_{cm}* (kN/mm^2)	f_{cu} (N/mm^2)	f_t (N/mm^2)	E_c (kN/mm^2)
In situ	20.0	–	30.0	25.0	–	25
In situ	25.0	–	31.5	30.0	–	26
Precast reinforced	30.0	–	32.8	37.0	–	28
Prestressed	40.0	1.64	35.2	50.0	3.2	30
Prestressed	50.0	1.90	37.3	60.0	3.5	32

* Gravel aggregates. Limestone × 0.9.

of very large line or point loads, or in cases where the dynamic or acoustic characteristics of the precast slab are judged to be inadequate, that a structural *in situ* reinforced concrete topping might be required. Note the terminology: 'topping' is a structural layer, 'screed' is a non-structural finishing layer. Structural toppings are nearly always necessary where double-tee units are used and are an obvious prerequisite for composite plank construction. For a topping to act compositely with the precast slab, in a structural sense, the concrete must be reinforced and unbroken by service chases, etc.

The two main areas where composite construction is carried out are in floor slabs and beams (Figures 6.1(a)–(e)). The structural function of some precast elements, e.g. precast planks (Figure 6.1(c)) such as 'Omnia' floor (Figure 5.1(d)), rely implicitly on composite action. However, composite action in other elements, e.g. hollow-core slabs and beams (Figures 6.1(a) and (e)), is optional and may be used at the discretion of the designer wishing to increase flexural and shear capacities, stiffness, fire resistance and vibration characteristics. Composite construction may also be used to create extended bearings at the ends of units, as shown in Figure 4.3.

The design is carried out in two stages, before and after the *in situ* concrete has reached its design strength. The main design criteria are:

- flexural and shear strength, serviceability and ultimate states
- confinement or reinforcing of *in situ* concrete to avoid separation, called 'delamination', from the precast concrete
- interface shear transfer
- constraint of *in situ* concrete shrinkage.

These items will be considered for the two cases of composite floors and composite beams, design of which are discussed in more detail later in this chapter.

Precast twin-wall construction, shown in Figure 6.2(a), relies on the interface shear between the *in situ* concrete infill and the outer leaf of the precast walls. Twin walls are most commonly used in wall frames as the direct support for floor slabs in multi-storey apartments, hotels, schools, etc., but may also be used in skeletal frames for shear walls, or in localised areas where beams and columns are not appropriate. The advantages over solid walls are mainly in the ease of continuity by placing additional reinforcement in the cavity. There is also reduced self-weight during transportation and erection. However, compared with solid walls, the complexity of manufacture and casting of the *in situ* infill reduces these bonuses. The twin walls are manufactured with light reinforcement in the outer leaves, typically H10 at 200 mm centres in a thickness of 75 to 100 mm, together with diagonal lattices, typically 5-, 6- or 7 mm-diameter bars inclined at between 45°and 65° to the wall, as shown in Figure 6.2(b). Total thickness varies between 250 and 400 mm. The surface roughness is classed as 'smooth, as cast, or slip formed/extruded'.

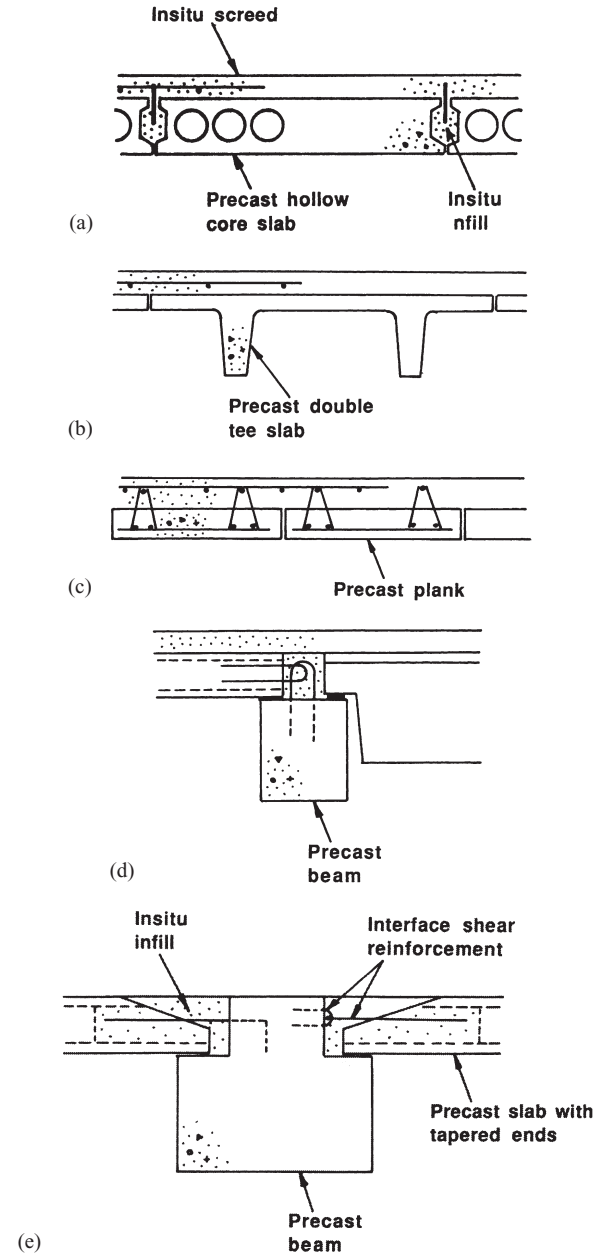

Figure 6.1 Composite slab and beam sections. (a) Composite hollow-core slab; (b) composite double-tee slab; (c) composite plank floor; (d) composite beam action with a structural topping; (e) requirements for composite beam action without a structural topping.

The design ultimate shear resistance at the interface is given according to BS EN 1992-1-1, clause 6.2.5, Eq. 6.25, and in BS 8110, Part 1, Table 5.5, as $v_u = 1.8\,\text{N/mm}^2$ for $f_{cu} = 30\,\text{N/mm}^2$ as:

$$v_{Rdi} = cf_{ctd} + \mu\sigma_n + \rho f_{yd}(\mu \sin\alpha + \cos\alpha) \leq 0.2(1 - f_{ck}/250)f_{ck} \tag{6.1}$$

i.e. the sum of cohesive bond $c = 0.2$, shear friction $\mu = 0.6$, and dowel action effects (according to BS EN 1992-1-1 amendment dated 30 June 2008). Inclination of the bars $\alpha =$ must be between 45°

(a) 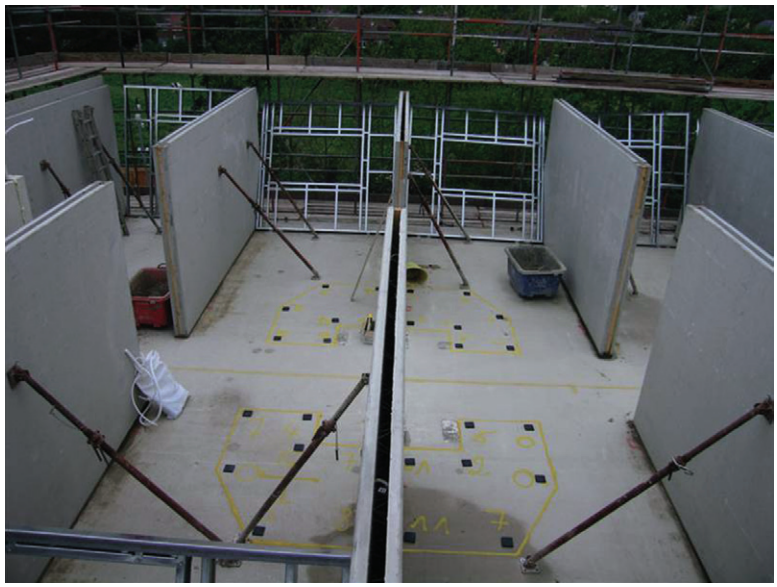 (b) 

Figure 6.2 (a) Precast twin-wall construction (courtesy of Precast Concrete Structures Ltd., UK); (b) diagonal lattices provide the interface resistance and tension across the cavity.

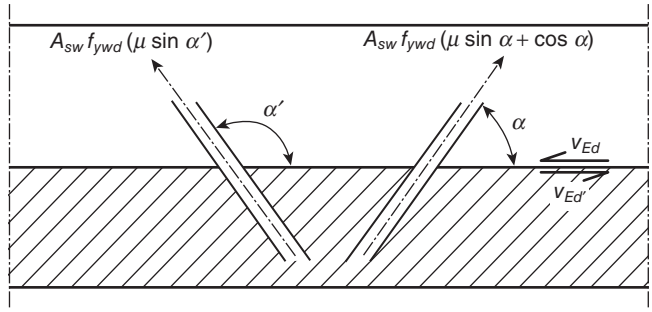

Figure 6.3 Definition of interface shear and normal resistances in lattice girders. Reproduced from BS EN 13747:2005 [6.3], Figure D2.

and 90°, i.e. acting against the shear flow, as shown in Figure 6.3, taken from BS EN 13747:2005 [6.3]. If $\alpha > 90°$, the cos α component will be negative and is deemed not to be active, such that:

$$V_{Rdi} = A_{sw} f_{yd} (\mu \sin \alpha + \cos \alpha + \mu \sin(180 - \alpha)) \tag{6.2}$$

There is no term for shear wedging, which, if the interface has a surface roughness of 1 to 2 mm, can be equal to or even greater than the other two terms. For this type of wall there is no externally applied normal stress, $\sigma_n = 0$. The steel area ratio $\rho = A_{sw}/ps$, where A_{sw} is the area of 2 diagonals inclined at α with the shear flow, and 2 diagonals inclined at $(180 - \alpha)$ opposing the shear flow; p = pitch of diagonals; and s = spacing of lattices. For example, if 7 mm diagonals at 60° are used in a lattice with a 150 mm pitch and 300 mm spacing, grade C25/30 *in situ* concrete, and $f_{yd} = 500\,\text{N/mm}^2$, then $\rho = 2 \times 38.5/150 \times 400 = 0.00128$ (note that $2\rho \sin \alpha = 2 \times 0.00128 \times 0.866 = 0.22\% >$ minimum 0.13%). Then $v_{Rdi} = 0.2 \times 1.20 + 0.00128 \times 0.87 \times 500 \times (0.6 \sin 60° + \cos 60° + 0.6 \sin 120°) = 0.24 + 0.86 = 1.10\,\text{N/mm}^2$. Also $v_{Rdi} \leq 0.2 \times 0.9 \times 25 = 4.5\,\text{N/mm}^2$, not critical. The critical resistance is much lower than in BS 8110, $v_u = 1.8\,\text{N/mm}^2$.

The technical report by FIP [6.4] on shear at the interface of precast concrete is also used to calculate the limiting shear strength. In this document, the surface characteristics are classed as Type viii, as per Figure 7 in the document. This is category 2 in the calculation for interface shear capacity

$$f_{vd} = \beta_1 \rho f_{yd} + \beta_2 f_{td} \tag{6.3}$$

where β_1 is a friction factor for mean inclination of a saw-tooth model of 42° = 0.9, β_2 is a cohesion factor = 0.4, $\rho = A_s$ sin α/ps, and $f_{td} = 0.25\sqrt{f_{cu}}$. Continuing the previous example, $f_{vd} = 0.9 \times 0.866 \times 2 \times 0.00128 \times 0.87 \times 500 + 0.4 \times 1.37 = 0.868 + 0.548 = 1.42\,\text{N/mm}^2$. The effect of the opposing inclination of the diagonals, giving rise to horizontal components in the direction of the shear force, may be disregarded when using the FIP approach.

The low value of v_{Rdi} in EC2 is not unexpected, but is surprising, particularly as the ratio with FIP values is 0.58, on which the Eurocode leans heavily. Of greater concern is the cohesive strength $c\,f_{ctd}$ for as-cast and slip-formed finishes. The effect of this may be the requirement to specify dowel action bars at interfaces where the interface stress is in the region of $0.25\,\text{N/mm}^2$, considerably lower than $0.55\,\text{N/mm}^2$ in BS 8110.

6.2 Texture of Precast Concrete Surfaces

6.2.1 Classification of surface textures

The types of surface which a precast unit may have, prior to receiving the *in situ* concrete to form a composite section, may be classified according to the following types given by the FIP Recommendations [6.4]. These options are presented in order of increasing roughness:

(1) smooth, as obtained by casting the unit against a steel or timber shutter
(2) trowelled or floated, to a degree where it is effectively as smooth as (1)
(3) tamped, so that the fines have been brought to the top, but where some small ridges, indentations or undulations have been left
(4) achieved by slip-forming and vibro-beam screeding
(5) produced by the extrusion technique
(6) textured, by brushing the concrete when wet, ideally to a specified depth of ridge
(7) brushing by a transverse screeder, by combing with a steel rake or tamping with a former faced with a suitable expanded metal
(8) the concrete has been thoroughly compacted but no attempt has been made to smooth, tamp or texture the surface in any way, leaving a rough surface with coarse aggregate protruding (but firmly fixed in the matrix)
(9) the concrete has been sprayed wet, to expose the coarse aggregate without disturbing it
(10) provided with mechanical shear keys.

Type (1) rarely occurs in the types of composite section illustrated in Figures 6.1(a)–(d). Type (2) is almost impossible to achieve and would rarely be attempted in practice. Type (3) is possibly the most common type of smooth surface considered in design, although in practice it will usually be rough to some extent. The remaining types all have some measure of roughness, whether naturally occurring or deliberately induced.

With some extrusion processes type (5), with high vibration, can cause bleeding and produce a very smooth surface, but generally this type of surface would have the same level of roughness as type (6). Types (6) and (7) are possibly the most common textured surfaces, type (7) probably being at least as effective as type (9) (which is specifically mentioned in many codes of practice).

Type (8) can produce a very rough surface, but there can be problems with it since the concrete near the top may be poorly compacted.

Some indication is given in the literature [6.4] of the degree of roughness covered by these descriptions, but there are no clearly defined boundaries between the different types, and what is actually achieved will depend very much on workmanship in individual cases. For example, the effectiveness of the smoother surfaces can be influenced by the concrete workability, and the presence and type of mould oil. All surfaces not roughened deliberately can be affected by casting procedures, concrete workability, and whether or not use is made of super-plasticisers. Whatever approach is adopted, it is essential that the surface is not weakened by destroying the aggregate bond.

Surfaces (5) to (9) inclusive could be generally considered as being at least adequate in providing a suitable surface for an effective construction joint using *in situ* construction, at least in terms of roughness. Surface types (1) and (2) clearly do not provide an equivalent surface. It is also impossible in practice to obtain this equivalence with type (3) and (4) surfaces.

6.2.2 Surface treatment and roughness

In designing the interface to ensure composite action, most previous codes have considered surface roughness to be the principal factor, giving limiting stresses for differently defined categories of roughness, which have not always related to the types of surface that can realistically be achieved in practice. Test data – for example, the work by Vesa [6.5] and Gustavsson [6.6] – indicate that the treatment of the precast surface is at least as important as the degree of roughness. Factors such as cleanliness, compaction, the presence of laitance, curing and wetting of the surface have a major influence on the shear strength of the interface. Indeed, with the optimum combination of these, and with good mix design and workmanship for the *in situ* concrete, it is possible to develop a strength with a smooth surface (types (3) and (4), and possibly (2), for example) that is equal to, or even greater than, that obtained with a rough surface (types (7) to (8)), where less attention has been paid to surface treatment prior to making the joint.

For these reasons, the FIP Recommendations [6.4] place great emphasis on surface treatment and on workmanship requirements for the *in situ* concrete topping. The major principle in following these recommendations is that any treatment of the surface – to clean it, or to produce the required level of roughness – should not impair the interface strength. This means avoiding any treatment causing cracks in the matrix or aggregate.

Roughness can influence the potential bond which may be achieved between the two concretes in the following ways:

- the increase in the interface surface area caused by roughness
- the fact that natural debonding factors, such as laitance skin, dust, water and so on, are concentrated at depressions in the surface, whereas projections tend to be less affected
- the rougher the surface, the less susceptible it is to the quality of the workmanship in cleaning and preparation. Angular aggregate is advantageous
- the shape and inclination of the ridges should ideally lead to a definite mechanical grip (interlocking) between the two concretes. The amplitude and pitch of the ridges or high spots (and their shear strength) should be such as to permit this interlocking to take place. It should also be noted that during curing, ridges will often be exposed to less favourable conditions than the rest of the concrete.

These characteristics of the adhesion between the two concretes are important in considering the deformations involved when failure occurs along an interface. Chemical bonds will be destroyed first, but the interlock effect can be destroyed only if all the ridges and high spots fail in shear. Even if this does happen, then if the two concretes are physically prevented from moving apart (by reinforcement, for example) it will be possible to mobilise shear resistance due to friction, where the rougher surface will give a greater frictional resistance. The opportunities to obtain a strength equivalent to a monolithic section (the maximum possible) are therefore considerable.

The qualities that affect bond and shear transfer at the interface are surface roughness, surface strength, and cleanliness. Where interfaces are to be bonded, the designer should prescribe the relevant category of roughness and, if bond is particularly important structurally, should consider whether or not to specify methods of achieving the required standard. As an aid to the specification, it is of considerable help if models, photographs or specimens are supplied to the factory.

Various kinds of micro-roughness may be achieved for surfaces that are cast against a mould and that, in general, are characterised as plane or smooth. The mould material itself has a considerable influence, as does the mould-release agent used. Thus wood, steel and resin moulds result in different kinds of surface, which may be differentiated further by the choice of demoulding agents used on their surfaces. An extreme example is the use of retarding release agents, providing exposed aggregate interfaces after surfaces have been demoulded, washed and wire-brushed.

Mechanical means to achieve suitable roughness vary from fibre and steel brushes to rake-like devices and groove-cutting saws, all dependent on the concrete consistency and roughness pattern intended. It is advisable to pretest the mechanical device chosen so as to ensure a surface pattern that conforms to the surface category required. The treatment should preferably be done in such a way that resulting ridges are directed normally to the main shearing forces to be transferred at the interface.

6.2.3 Effects of surface preparation

The main parameters for the surface preparation of precast floor units, in particular hollow-core or double-tee slabs, are roughness, moisture content and debris (including surface laitance after floor slabs are manufactured). Figures 6.4 and 6.5 show dried laitance, after sawing at the ends of hollow-core floor units, flaking off in the hand with a thickness of 0.7 to 1.0 mm. While most of this is removed prior to erection, there may remain sufficient dust to affect the integrity of the interface.

According to EC2 a 'smooth' surface is as cast, with no additional treatment apart from the usual removal of debris, as is typical of the extruded or slip-formed finish to hollow-core units. A 'roughened' surface has some post-casting treatment to create 3 mm roughness, and an 'indented' surface has 5 mm roughness. Surface moisture content is not specified, although the general rule is that surfaces should be dampened, yet without standing water or ponding in crevices. Ibrahim and Elliott [6.7–6.9] studied the combined effects of surface roughness and moisture on the interface shear capacity in some small-scale push-off tests and full-scale shear tests on composite hollow-core slabs. Mones and Breňa [6.10] studied surface preparation, such as sandblasting, raking and brushing of dry-cast (extruded) and wet-cast (slip-formed) hollow-core samples. Smooth surfaces were ex-production, with a surface roughness $R_a = 0.25$ to 0.32 mm [6.7] and macrotexture depth (determined using a fine sand volume method) of 0.25 to 0.35 mm [6.10], while roughened surfaces were raked transversely to a depth of 2 to 3 mm and had $R_a = 0.42$–0.48 mm [6.7] and 0.75–1.20 mm [6.10]. Typical hollow-core production is in the order of $R_a = 0.2$ mm for extruded and 0.3 mm for slip-formed. Three different surface moistures were prepared:

(a) 'dry' (indoor exposure at RH = 45% for a few weeks giving 12 to 13% moisture content at test)
(b) 'optimum wet' (as dry, plus 9.5 litres/m^2 of water, any excess allowed to evaporate with no standing water and giving 26 to 28% moisture content)
(c) 'ponded' (45 litres/m^2 of water to a standing depth of 1 to 2 mm, giving 53 to 55% moisture content).

Shear tests were carried out according to BS EN 1168, Annex J [6.11], and the interface shear capacity v_{Rdi} was calculated from first principles (see section 6.2.5) when the ultimate failure of the slab occurred. Mones's results are based on push-off tests. The results in Figure 6.6 are, as expected, greater than code values: by a ratio of 1.8 to 2.5 vs BS8110 and 2.7 to 4.8 vs EC2. The 'optimum wet and rough' condition gave the greatest capacity, with v_{Rdi} mean = 1.5 N/mm^2, and the 'ponded and rough' surface also achieved about 1.35 N/mm^2, although the mode of failure was less predictable in the ponded conditions. Mones's data, with a maximum strength of 2.23 N/mm^2, show further linear

Figure 6.4 Surface laitance on the top of hollow-core floor units.

Figure 6.5 Surface laitance measured as 0.85 mm thickness.

correlation of v_{Rdi} with roughness, with greater variation for the effect of surface wetting in the dry-cast hcu. The main conclusion is that good practice values are well in excess of code values, reasonably repeatable, and do not fail before the vertical ultimate shear capacity of the composite slab is attained.

The interface research also included a long-term bending test on a composite slab, as shown in Figure 6.7. The slab consisted of five 1.2 wide × 150 mm deep hcus with a 75 mm structural topping (f_{cu} = 43 N/mm^2), 6.0 m long, and was subjected to a uniformly distributed load equal to its service capacity of 10 kN/m^2 for two years. Creep strains, deflections and ambient top and bottom temperatures were monitored daily, giving the results in Figure 6.8. In spite of seasonal variations, the increase in creep deflections was as expected and some 2.45 times the initial static deflection. An ultimate load test on the composite slab gave values of v_{Rdi} of around 1.2 N/mm^2, and showed v_{Rdi} is not affected by exposure to external environmental effects.

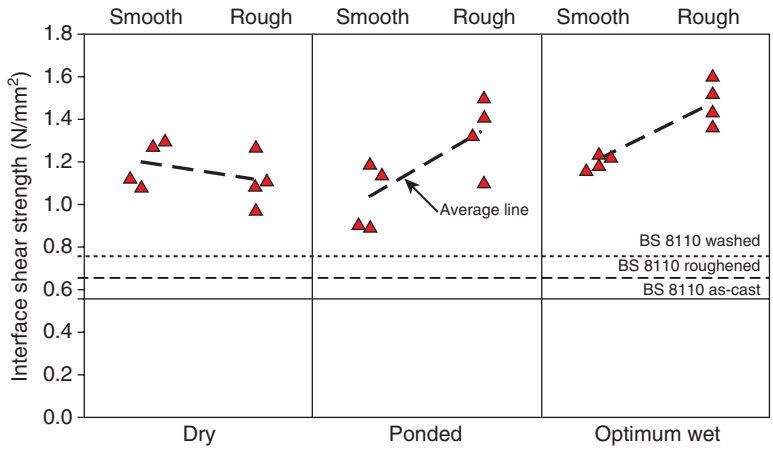

Figure 6.6 Results of interface shear tests on prestressed hollow-core slab with a structural topping [6.7, 6.10].

Figure 6.7 Prestressed hollow-core slab with a structural topping subjected to an outdoor bending test under full service load for 2 years.

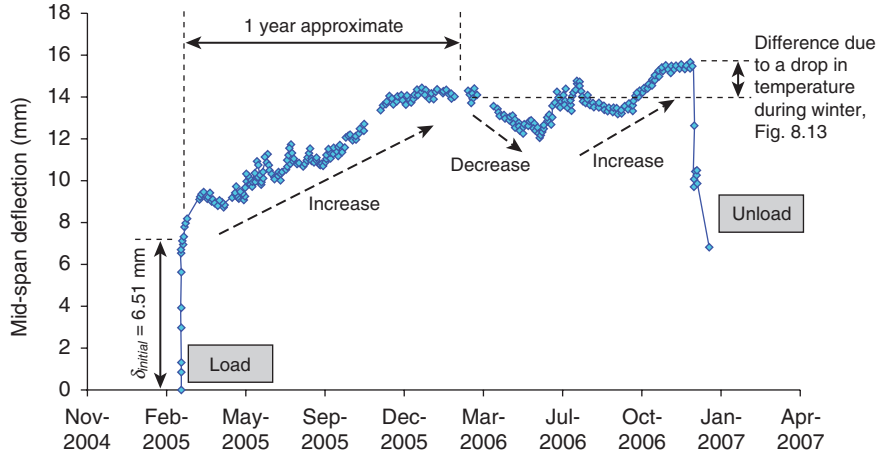

Figure 6.8 Mid-span deflection in the composite slab bending test shown in Figure 6.7 [6.7].

6.3 Calculation of Stresses at the Interface

Shear at the interface need only be checked for the ultimate limit state. The design method used, based on experimental evidence, will ensure that serviceability conditions are satisfied. The average ultimate shear stresses at the interface may be calculated using eq. 6.1. In EC2, the complementary vertical shear stress forms the basis for the calculation.

$$v_{Edi} = \beta \frac{V_{Ed}}{z b_i} \leq v_{Rdi} \tag{6.4}$$

where

v_{Rdi} = the design shear stress resistance at the section interface considered at the ultimate limit state;

v_{Edi} = the design transverse shear force in the concrete to one side of the interface;

β is the ratio of longitudinal force above the interface to the total longitudinal force;

z = the lever arm of the composite bending section;

b_i = the transverse width of the interface.

The design shear stress resistance is given by:

$V_{Rdi} = cf_{ctd} + \mu\sigma_n + \rho f_{yd}(\mu \sin\alpha + \cos\alpha)$

with an upper limit defined by

$V_{Rdi} \leq 0.5 \nu f_{cd}$

where

c and μ are surface roughness factors reproduced in Table 6.2.

$f_{ctd} = 0.14 f_{ck}^{2/3}$

$f_{cd} = 0.85/1.5\ f_{ck}$

σ_n is the normal force across the interface, compression positive. When σ_n is –ve, $c = 0$.

$\rho = A_s/A_i$, the ratio of rebar crossing the interface area

α is the angle between the rebar and the interface

ν is the reduction factor $0.6(1 - f_{ck}/250)$

The effect of reinforcement crossing the interface is included in the above formulation.

In many precast-to-*in situ* structural floor toppings, ρ is zero and σ_n is positive, but small and conservatively taken as zero.

If v_{Edi} is less than the capacity without reinforcement, then minimum orthogonal links should be provided (according to equation 9.4 in BS EN 1992-1-1), as follows:

$$A_{sw,min} = 0.08 \frac{\sqrt{f_{ck}}}{f_{yk}} b_w s \tag{6.5}$$

where

b_w is the mean width of the tension web below the interface

s is the longitudinal link spacing

$$v_{ave} = \frac{F_v}{b L_z} \tag{6.4}$$

where

v_{ave} = the average shear stress at the cross section of the interface considered at the ultimate limit state;

F_v = the design force in the concrete to one side of the interface;

b = the transverse width of the interface;

L_z = distance between the points of minimum and maximum bending moment.

The design values in Table 6.2 are based on the use of this formula, and allowance has been made for the small errors in defining the shear stresses that occur in the equation.

If the interface is in a compression zone, then F_v is equal to the compression force in the *in situ* concrete only, i.e. above the interface. If the interface is in a tension zone, then F_v is equal to the total compression or tension calculated from ultimate loads.

The force is distributed evenly over the contact interface breadth and over the length of the beam between points of maximum and zero moment, thus giving the average interface shear stress v_{ave}. The average stress is then distributed in accordance with the magnitude of the vertical shear at any section, to give the design shear stress v_h. Thus for uniformly distributed superimposed loading (self-weight does not create interface stress) the maximum stress $v_h = 2\ v_{ave}$. For a point load at mid-span $v_h = v_{ave}$ and so on.

Horizontal interface shear stresses v_h are checked for the uncracked section (BS 8110, Part 1, clause 5.4.7.2) against values in Table 6.2 (reproduced from BS 8110, Part 1, Table 5.5).

If v_h is greater than the ultimate stress in Table 6.2, then reinforcement (per metre run) is provided (according to equation 62 in BS 8110), as follows:

$$A_f = \frac{1000 b v_h}{0.87 f_y} \tag{6.5}$$

The reinforcement should be adequately anchored on both sides of the interface. If loops are used, as shown in Figure 6.9, the clear space beneath the bend should be at least 5 mm + size of aggregate. It is found that the bend radius need not comply with bursting requirements; only the minimum of 3ϕ is required.

Table 6.2 Design Ultimate Horizontal Shear at Interface

	EC2 coefficients			BS 8110 Stress (N/mm^2)			
					Grade of *in situ* concrete		
Precast unit	**Surface type**	***c***	***μ***	**Surface type**	**C20/25**	**C25/30**	**C30/37**
Without links	Cast against steel, plastic or surface-treated wood	0.025–0.1	0.5	As cast or as extruded	0.40	0.55	0.65
	Slipformed, extruded or only vibrated	0.2	0.6	Brushed, screeded or rough-tamped	0.60	0.65	0.75
	>3 mm roughness by raking, exposing aggregate, etc.	0.4	0.7	Washed to remove laitance, or treated with retarding agent and cleaned	0.70	0.75	0.80
With nominal links that project into *in situ* concrete	Indentations > 5 mm deep (shaped as specified)	0.5	0.9	As cast or as extruded	1.20	1.80	2.00
				Brushed, screeded or rough-tamped	1.80	2.00	2.20
				Washed to remove laitance, or treated with retarding agent and cleaned	2.10	2.20	2.50

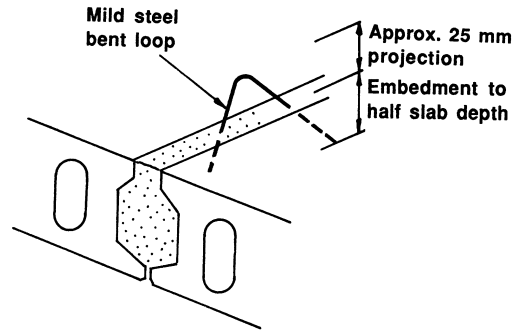

Figure 6.9 Projecting loops placed in the longitudinal joints between hollow-core units.

The bars are usually uniformly distributed along the length of the interface, although the spacing could in fact be reduced towards the point of zero shear. Nominal links should be at least equal to $0.08\sqrt{f_{ck}}/f_y$ {0.15} per cent of the contact area. The longitudinal spacing of links should not be too large, $0.75d$ or 600 mm, with their equivalent being concentrated in joints typically at 1.2 m maximum for hollow-core slabs. Where links are provided in ribs of tee-beams, the spacing should additionally not exceed four times the minimum thickness of the *in situ* concrete.

The minimum permissible interface shear stress for hollow-core units (hcu) and double-tee units is therefore 0.36 {0.4} N/mm^2 and 0.46 {0.6} N/mm^2, respectively, for normally produced units. For EC2 designs, this is constrained by the concrete topping strength. In short spans where the shear is large (compared with flexural requirements), interface links can be left projecting in the longitudinal joints between hollow-core units using loops (H10 at 1.2 m centres for example), as shown in Figure 6.9.

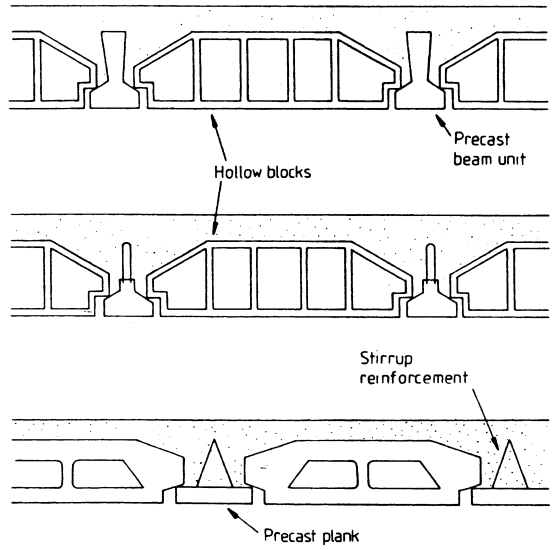

Figure 6.10 Definition of interface contact breadth [6.4]

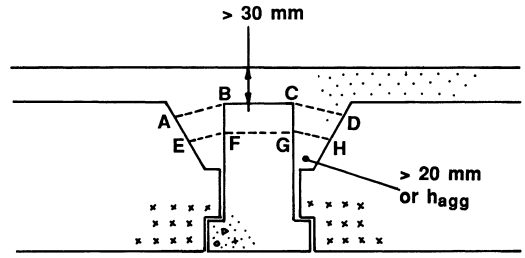

Figure 6.11 Examples of special cases for consideration in determining contact breadth.

The definition of b in Eqs. (6.4) and (6.5) is clear in most cases but, for example, in the situations given in Figure 6.10, b must be defined on its merits because it is not practical to define specific rules that cover all cases. It can, however, be recommended that those parts of the interface that are covered by *in situ* concrete of thickness less than 30 mm should normally not be considered as effective interface area, except in sections of the type shown at G–H in Figure 6.11. Because of the compacting pressure during casting, 20 mm or the maximum aggregate size can be considered to be the minimum thickness on the side of beams.

6.4 Losses and Differential Shrinkage Effects

6.4.1 Losses in prestressed composite sections

It is difficult to make an assessment of the losses of prestress that occur in a composite section, as they obviously depend on when the *in situ* concrete is added to the prestressed concrete, normally after between one and four months. Although it may be assumed that most of the losses occur before this addition, in many cases that will not be strictly correct and the effects of differential shrinkage and creep should at least be taken into account.

If little or no losses have taken place in the prestressed concrete before the topping is placed (i.e. in less than 7 days), then the shortening of the precast unit will be restrained to some extent by the added concrete, though the amount of the actual restraint will depend on the shape of the section and the quantity of the *in situ* concrete used.

Any bending moment that is induced in the composite section as a result of differential shrinkage affects only the elastic stress conditions, and does not affect the ultimate behaviour (in the same way that the level of prestress has a small influence on the ultimate strength). Because it is difficult (and probably unnecessary) to make a 100 per cent correct assessment of the differential deformations due to shrinkage and creep, it seems sensible to first compute the shrinkage and creep movement taking place in the precast beam, and then to add the effects of the relative movement in the topping concrete. To proceed in this manner will usually lead to slightly conservative results, as the relative shrinkage strain in the interface will be greater than if all the shrinkages are assumed to occur simultaneously.

6.4.2 Design method for differential shrinkage

The forces due to differential shrinkage may be calculated by the following method. In this analysis, the term 'differential shrinkage' is used to describe the difference in the free strains due to the shrinkage of the *in situ* concrete and the combined shrinkage and creep of the precast concrete. At the end of the span, the stress in the precast concrete due to self-weight and prestress is small and the differential strain should normally be taken as the difference in the free shrinkage values of the two concretes.

If the beam or slab reinforcement is placed non-symmetrically, a bending moment is induced by shrinkage owing to non-uniform restraint by the reinforcement and, as a result, shrinkage increases the curvature and consequently the flexural deflection of the components.

In the following equivalent tensile force method for estimating shrinkage-induced stresses, applied actions and shrinkage forces are resisted by an uncracked, cracked or partially cracked member. In the case of the cracked or partially cracked member, the assumption is made that the shrinkage occurring prior to cracking is insignificant. It is therefore possible to treat shrinkage-induced stress in a similar way to load-induced stress at the serviceability limit state.

Consider a unit length of the composite precast beam of precast depth h, and topping depth h_s, shown in Figure 6.12(a), in which, after any interval of time following the casting of the *in situ* concrete flange, the free shrinkage of the flange is ε_f and the combined free shrinkage and creep of the beam is ε_b at the centroid, with values of ε_{bt} and ε_{bb} at the top and bottom fibres respectively. Refer also to the design guidance given in BS 8110, Part 2, clause 7.4, and BS EN 1992-1-1, annex D. The analysis considers that the precast concrete member is free to shrink, and when this happens the compression and tension steels are compressed by fictitious forces $\varepsilon_b A'_s E_s$ and $\varepsilon_b A_s E_s$ respectively, where A'_s and A_s are the areas of the compression steel and tension steel, respectively, and E_s is the Young's modulus of the steel bars or tendons. When these loads are released, it is equivalent to eccentric tension loads $\varepsilon_b A'_s E_s$ and $\varepsilon_b A_s E_s$ applied at the steel level to the entire transformed area of the member, as shown in Figure 6.12(b). These forces produce a bending moment and consequently a curvature and flexural deflection of the concrete member. If $A_s > A'_s$, then the deflection is downwards. These forces also produce an interface shear stress as follows.

The bending moment M_b produced by the effects of beam shrinkage is given by:

$$M_b = \varepsilon_b E_s (A_s(d - X) - A'_s(X - d')) \tag{6.6}$$

where d and d' are the depths of the tension and compression reinforcement respectively, and X is the distance from the top of the topping to the neutral axis of the transformed composite section (see Section 6.5 for an explanation of transformed sections). In multi-layered reinforcement, use the sum of each layer for the term $A_s\,(d - X)$.

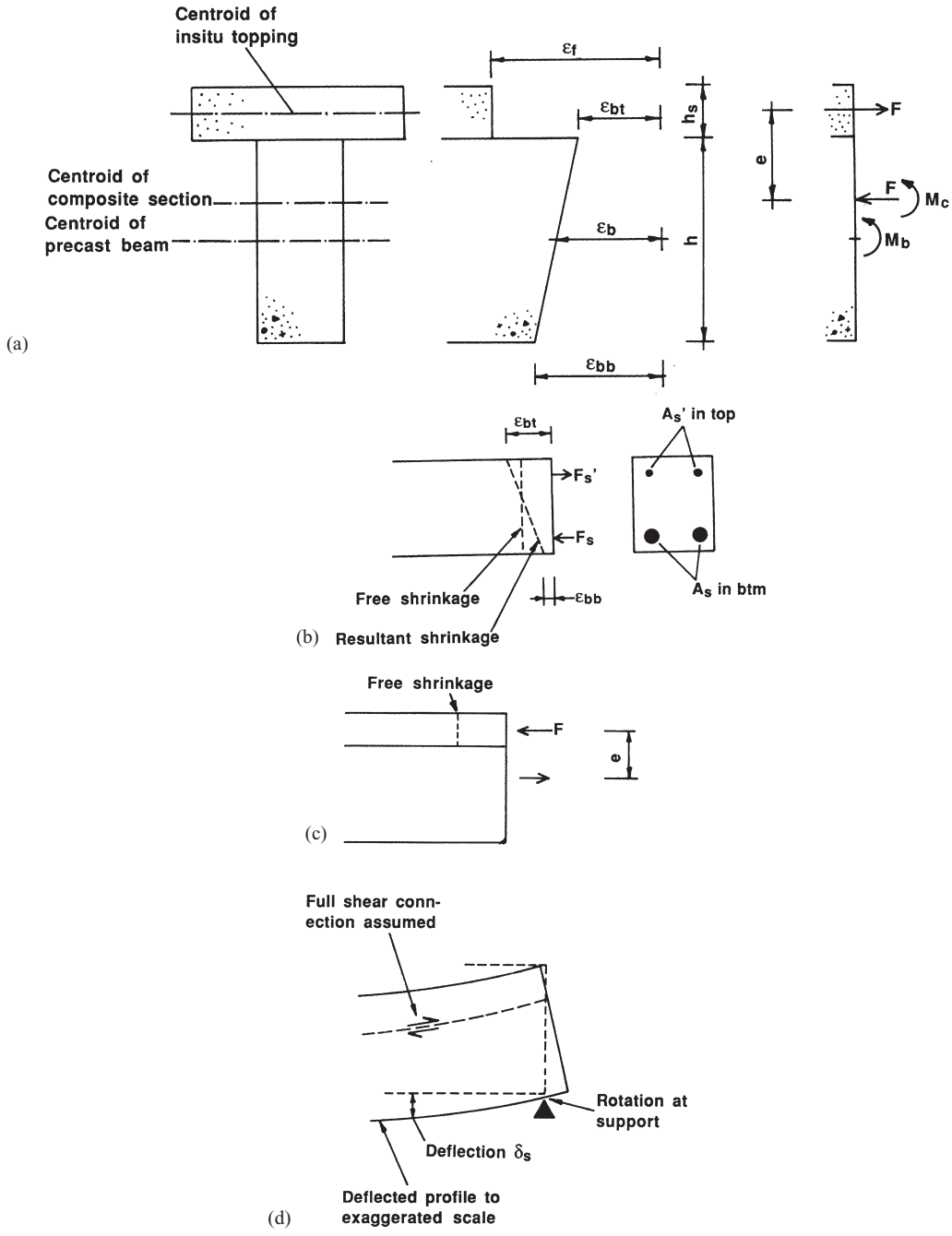

Figure 6.12 Theoretical approach to shrinkage-induced deflections in composite construction. (a) Definitions; (b) shrinkage effects in reinforced sections; (c) effective eccentric force due to differential shrinkage; (d) shrinkage-induced deflection.

For plane sections to remain plane, the strain gradient in both the composite and the precast beam is identical; hence the strains in the top and bottom surfaces of the beam are given by Eqs. (6.7) and (6.8) (assuming $\varepsilon_{bt} > \varepsilon_{bb}$):

$$\varepsilon_{bt} - \varepsilon_{bb} = \frac{M_b h}{E_c I_c} \tag{6.7}$$

where E_c is the modulus of elasticity of beam concrete, and I_c is the second moment of area of the transformed composite section. Also, the strain at the interface between the precast concrete and topping:

$$\varepsilon_{bt} = \frac{M_b(X - h_s)}{E_c I_c} + \varepsilon_b \tag{6.8}$$

The relative shrinkage strain between the flanged topping (ε_f) and the top surface of the precast concrete beam (ε_{bt}) is given by:

$$\varepsilon_s = \varepsilon_f + \varepsilon_b \tag{6.9}$$

The modification factor for the restraining effect of the mesh in the topping $(1 + K\rho)$ (where $\rho = 0.13$ to 0.24 per cent, and $K = 15$ to 25, typically) is not significant in toppings.

To restore a common strain at the interface, an equal and opposite force must be applied to both flange and beam. The tensile force F is applied at the centroid of the flange to overcome the strain differential between the flange and the beam (Figure 6.12(c)), and is given by:

$$F = \varepsilon_s E_c m A_f \tag{6.10}$$

where $m = E_c'/E_c$ is the modular ratio, and A_f is the area of flange section. In composite beams the effective width of the flange is the same as for any tee-section, so A_f can be determined.

The two concretes may now be joined together (theoretically) and the external actions released if a compressive force F and a balancing moment M_c are applied to the composite section, such that:

$$M_c = Fe + M_b \tag{6.11}$$

where e is the distance between the centroid of the flange and the centroid of the composite section. The contribution of M_b is usually not more than about 5 per cent of the total moment M_c. The resultant longitudinal force F_v (of these two actions) to one side of the interface (tension in the flange and compression in the beam) is given by:

$$F_v = F + M_c \frac{S_c}{I_c} \tag{6.12}$$

where S_c is the first moment of area to one side of the interface about the centroid of the transformed composite section, and I_c is the second moment of area of the transformed composite section. This is the value for F_v that must be used in Eq. (6.4).

The resulting induced bending moment M_c causes a maximum mid-span sagging curvature deflection δ_s (Figure 6.12(d)) over a simply supported span L of:

$$\delta_s = \frac{M_c L^2}{8 E_c I_c} \tag{6.13}$$

and so on, depending on the beam geometry and loading conditions. Note that in the unlikely event of $\varepsilon_f < \varepsilon_{bt}$, then F will be negative. In this case use $F = 0$, and so $M_c = M_b$ and $F_v = M_b\, S_c/I_c$.

Shear lag effects in the *in situ* concrete will reduce the relative shrinkage strains. This will be noticeable in depths of topping greater than about 100 mm. However, in most applications in precast work, where thicknesses of *in situ* concrete are usually less than 75 mm, the simplified version given above is adequate for design purposes.

A further complication in the analysis is the changing thickness of *in situ* toppings on precambered, prestressed beams and slabs. In a typical situation the depth of topping used on a hollow-core or double-tee floor slab is 50 mm at the crown (mid-span) of the floor slab and up to 80 mm at the supports. Thus the composite section properties calculated at the crown of the floor are not appropriate to the situation at the supports, where the effects of differential shrinkage are the greatest. For the same reason, neither are the section properties at the support correct. The usual practice is to calculate the interface stresses based on the composite section properties at the position of the mean depth of the topping.

Where non-rectangular beams, e.g. L- or inverted-tee beams, are designed compositely with floors and toppings the situation is more complicated, because the contact area between the precast and *in situ* concretes includes the sides of the upstand. This may be ignored if the width of the *in situ* infill is less than 30 mm. In Type II edge beams (Section 4.3.4.), where the *in situ* is much wider, the critical interface is at the ledge, rather than at the top of the beam.

Exercise 6.1 Shrinkage-induced forces in rc sections

The reinforced concrete inverted-tee beam shown in cross section in Figure 6.13 is simply supported over an effective span of 10 m. The beam supports 200 mm-deep hollow-core floor slabs clear spanning 6.6 m, and the mean depth of the topping over the line of the beam is 75 mm. Given that after the topping has been cast the predicted free shrinkages in the beam concrete and topping concrete are 80 με and 150 με, respectively, calculate the average interface shear stress between the top of the beam and the topping.

Use grade C30/37 concrete for the beam, grade C20/25 for the topping, with $E_s = 200\,\text{kN/mm}^2$, and 35 mm cover to the 10 mm-diameter links.

Solution

Step 1: Considering free shrinkage of beam acting over transformed composite section

Effective breadth of topping = 300 + 10 000/5 = 2300 mm

Depth to neutral axis of transformed section (ignore minor steel areas) = 208.2 mm

Eccentricity of topping, $e = 220 - 37.5 = 182.5$ mm

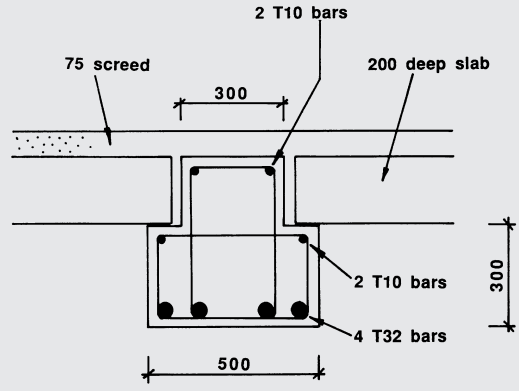

Figure 6.13 Details for Exercise 6.1.

Bottom reinforcement (four H32 bars) $A_s = 3216\,\text{mm}^2$
$d = 575 - 35 - 10 - 16 = 514\,\text{mm}$
Mid-reinforcement (two H10 bars) $A'_s = 157\,\text{mm}^2$
$d = 275 + 35 + 10 + 5 = 325\,\text{mm}$
Top reinforcement (two H10 bars) $A'_s = 157\,\text{mm}^2$
$d = 75 + 35 + 10 + 5 = 125\,\text{mm}$
$M_b = 80 \times 10^{-6} \times 200 \times 10^3 \times (3216(514 - 208.2) + 157(325 - 208.2) - 157(220 - 125)) = 16.03\,\text{kNm}$
From Table 6.1

$E_c = 33\,\text{kN/mm}^2$, $E'_c = 30\,\text{kN/mm}^2$	$E_c = 28\,\text{kN/mm}^2$, $E'_c = 25\,\text{kN/mm}^2$
Topping modular ratio = 30/33 = 0.909	Topping modular ratio = 25/28 = 0.893
$I_c = 1.461 \times 10^{10}\,\text{mm}^4$	$I_c = 1.455 \times 10^{10}\,\text{mm}^4$
$\varepsilon_{bt} = \frac{15.15 \times 10^{-6} \times (208.2 - 75)}{28 \times 10^3 \times 1.461 \times 10^{10}} + 80 \times 10^{-6} = 84.4 \times 10^{-6}$	$\varepsilon_{bt} = \frac{15.15 \times 10^{-6} \times (208.2 - 75)}{28 \times 10^3 \times 1.455 \times 10^{10}} + 80 \times 10^{-6} = 85.2 \times 10^{-6}$

Step 2: Considering free shrinkage of topping relative to top of beam

$\varepsilon_s = 150 \times 10^{-6} - 84.4 \times 10^{-6} = 65.6 \times 10^{-6}$	$\varepsilon_s = 150 \times 10^{-6} - 85.2 \times 10^{-6} = 64.8 \times 10^{-6}$
$F = 65.6 \times 10^{-6} \times (0.909 \times 2300) \times 75 \times 33000 \times 10^{-3} = 339.5\,\text{kN}$	$F = 64.8 \times 10^{-6} \times (0.893 \times 2300) \times 75 \times 28000 \times 10^{-3} = 279.3\,\text{kN}$
$M_c = 339.5 \times 0.1825 + 16.03 = 73.73\,\text{kNm}$	$M_c = 279.3 \times 0.1825 + 16.03 = 63.71\,\text{kNm}$
Now	Now
$S_c = (0.909 \times 2300) \times 75 \times 182.5 = 26.66 \times 10^6\,\text{mm}^3$	$S_c = (0.893 \times 2300) \times 75 \times 182.5 = 26.30 \times 10^6\,\text{mm}^3$
So	So
$F_v = 339.5 + \frac{16.03 \times 10^3 \times 26.66 \times 10^6}{1.461 \times 10^{10}} = 368.7\,\text{kN}$	$F_v = 279.3 + \frac{16.03 \times 10^3 \times 26.3 \times 10^6}{1.455 \times 10^{10}} = 308.2\,\text{kN}$

Average interface shear stress over half the length of the beam

$= \frac{368.7 \times 10^3}{300 \times 500} = 0.246\,\text{N/mm}^2$	$= \frac{308.2 \times 10^3}{300 \times 500} = 0.205\,\text{N/mm}^2$

6.4.3 Cracking in the precast and *in situ* concrete

The question often arises as to whether the *in situ* concrete at the interface cracks when the uniaxial cracking strain is exceeded, or whether the precast concrete unit restrains the *in situ* concrete. Some restraint is given to weaker concrete in these situations. If the bond at the interface is sufficient for the two concretes to act monolithically, then a linear strain distribution may be assumed throughout the entire section. Also flexural cracking at the interface propagates simultaneously in the precast and *in situ* concrete [6.12].

The precast unit, which covers the entire bottom surface of the *in situ* concrete, behaves in a similar manner to reinforcing bars, in that it eliminates any concentration of strain at any section where the concrete quality is below average for the specimen; thus the average strain before cracking occurs is greater than that for an unrestrained plain concrete having the same overall properties.

It has been seen that the assumption of linear strain distribution depends on the fact that the connection between the two concretes that make up the composite section is strong enough to ensure that the longitudinal shearing forces cause no relative movement at the interface. A rough-tamped top surface of the precast unit will be sufficient to ensure that a horizontal shear failure does not occur, although it may take place as a secondary effect after some other factor has caused the primary failure. As far as cracking is concerned, a rough surface by itself will also prove to be a better

Figure 6.14 Power floating a structural topping over hollow-core floors.

interlocking medium than the corresponding smooth surface that also has either castellations or projecting steel stirrups.

6.5 Composite Floors

6.5.1 General considerations

This section considers precast reinforced or prestressed concrete floor units with *in situ* concrete topping, or finishing screed (Figure 6.14). The screed may be floated (by power or hand) smooth to give a finished floor, but this prevents the placement of services in the screed. Firstly, horizontal diaphragm action resulting from horizontal wind or earthquake loads may be transmitted through the structural topping (not a finishing screed) acting as a deep beam or truss. The resulting diaphragm stresses are only in the order of 0.5 N/mm^2 and do not affect the flexural behaviour of the topping. Secondly, the reinforcement in the topping may be used to satisfy the requirements for stability ties, in which case the reinforcement should be continuously lapped across the whole floor.

The types of floor slab considered here are hollow-core floors, double-tee units and precast planks. In designing a composite floor, reference must be made to the basic section and material properties of the precast unit itself, i.e. h, d, b, $\{b_w\}$, A, I, Z, f_{ck}, $\{f_{cu}\}$, f_b, v_c, etc. The precast unit serves two functions, by providing permanent shuttering to the topping as well as contributing to the flexural and shear strength of the completed floor.

An enhancement in the ultimate moment of resistance is usually possible only in spans of up to about 10 m, because of the deleterious effects of additional self-weight. The optimum thickness of topping from a strength point of view is typically about 50 mm at mid-span. Figure 6.15 shows the enhanced load-versus-span characteristics of a range of 400- and 600 mm-deep double-tee units using 75 mm-thickness structural toppings. The increased performance of composite hollow-core slabs gives rise to increases in superimposed loading of between 20 and 40 per cent when using a 40 mm-thick topping, and between 60 and 110 per cent when using a 100 mm-thick topping. However, when these increased loadings are compared with the basic non-composite data, the efficiency of the flooring expressed in terms of the volume of concrete used is reduced by about 8 per cent. This is an

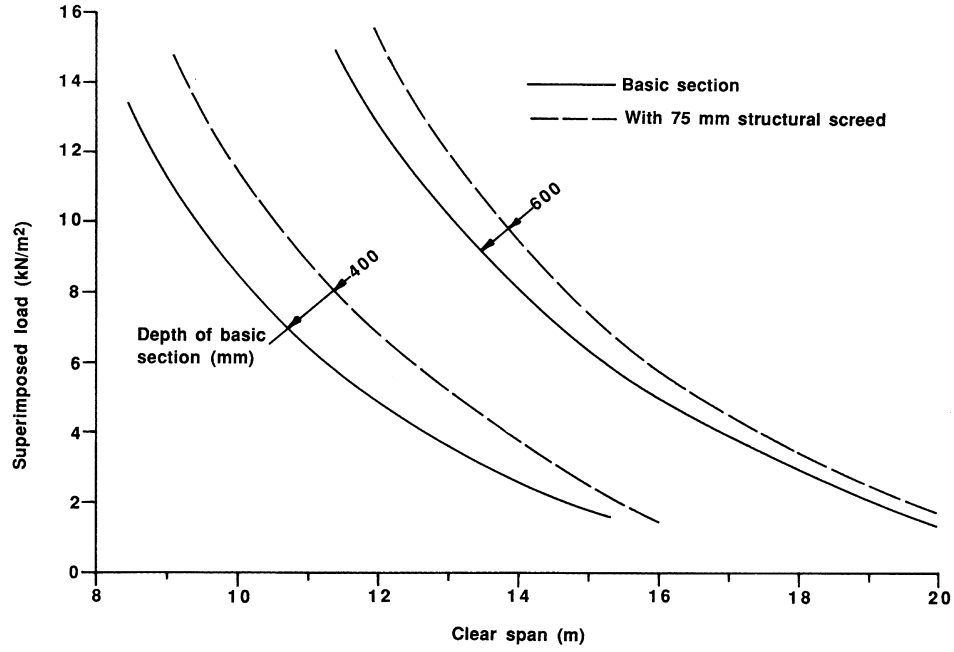

Figure 6.15 Load versus span characteristics of double-tee units using structural toppings.

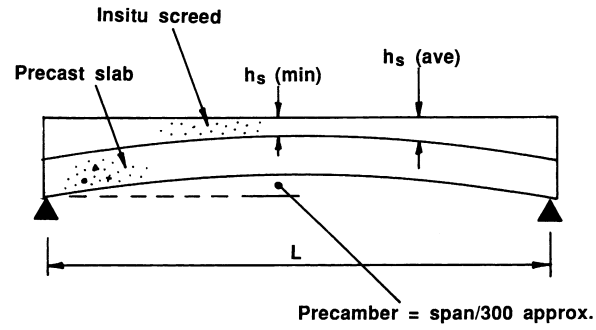

Figure 6.16 Effect of precamber on depth of topping.

obvious result, as a prestressed unit is structurally more efficient than an equivalent reinforced section. Further comparisons are made in Section 6.7.

Structural toppings can be made of ordinary Portland cement and a coarse aggregate with a size that should not exceed half of the minimum thickness. The thickness of the topping h_s should not be less than 40 mm, and the minimum grade of concrete is C20/25. It is important that the workability should be specified to suit the delivery (pumped or skipped) and compaction methods (mechanical vibrating bar or poker) used. A slump of 75 mm is usually suitable. When calculating the average depth of the topping, allowances for precamber should be made as shown in Figure 6.16. The normal levelling tolerances given in BS 5606 [6.13] are specified; this usually means a maximum deviation in thickness of 5 mm.

The topping is reinforced using a mesh of minimum area 0.13 per cent of A_c, or greater for the requirements of stability ties, usually using a square mesh with a bar spacing of 200 mm (typically A142 or A193), placed at mid-depth to resist shrinkage stresses. The mesh is lapped to peripheral

projecting reinforcement in the edge beams and is continuous over internal beams. Care has to be taken when lapping mesh and no more than three sheets of the mesh should meet at any point. A minimum lap length of 300 mm is required.

6.5.2 Flexural analysis for prestressed concrete elements

(a) At serviceability state

Permissible service stresses are checked for two loading conditions – Stages 1 and 2. These are checked before and after hardening of the *in situ* topping, respectively. Stresses and deflections are calculated by the superposition method, taking into account the following loads and section properties:

- Stage 1 for the action of self-weight of the precast slab, plus the self-weight of *in situ* concrete topping, plus an allowance for temporary construction traffic of up to 1.5 kN/m^2
- Stage 2 for superimposed loading.

Bending moments M_1 and M_2, and section properties Z_{b1} and Z_{t1}, and Z_{b2} and Z_{t2} are calculated for each stage. The support conditions are simple, or cantilevered. In the serviceability limit state, the stresses are distributed in proportion to the stiffnesses of the concrete components. Thus a modular ratio based on elastic response E_c (*in situ*)/E_c (precast) is used to calculate the effective section properties at Stage 2 for the service state, as shown in Figure 6.17. Stresses are compared with permissible values for compression and tension of $0.45f_{ck}$ and f_{ctm} respectively {$0.33f_{cu}$ from BS 8110, Part 1, clauses 4.3.4 and values in Table 5.4 of clause 5.4.6}. As with the non-composite unit, the various compound values for Z_{co} for the precast and composite section are used, using the appropriate modular ratios for the precast concrete and the composite topping. Referring to Figure 6.18(a):

$$\frac{M_1}{Z_{b1}}+\frac{M_2}{Z_{b2}} \le f_{bc}+f_{ctm} \quad \left\{\frac{M_1}{Z_{b1}}+\frac{M_2}{Z_{b2}} \le f_{bc}+f_{ct}\right\} \text{ in the soffit of the precast slab} \tag{6.14}$$

$$\frac{M_1}{Z_{t1}}+\frac{M_2}{Z_{t2}} \le 0.45f_{ck}+f_{ct} \quad \left\{\frac{M_1}{Z_{t1}}+\frac{M_2}{Z_{t2}} \le 0.33f_{cu}+f_{ct}\right\} \text{ in the top of the precast slab}$$

$$\frac{M_2}{Z'_{t2}} \le 0.45f_{ck} \quad \left\{\frac{M_2}{Z'_{t2}} \le 0.33f_{cu}\right\} \text{ in the top of the } \textit{in situ} \text{ topping,}$$

where Z'_{t2} is the section modulus at the top of the *in situ* concrete, f_{bc} and f_{tc} are the prestress values after losses in the bottom and top of the beam, respectively, and f_{ct} is the permissible flexural tensile stress allowed in Class 2 structures given in BS EN 1992-1-1, clause 3.1.6(2) {BS 8110, Part 1, Table 4.1}.

The critical situation occurs in the bottom of the slab, because the new position of the neutral axis is close to the top of the precast unit. Eq. (6.14) can be written as:

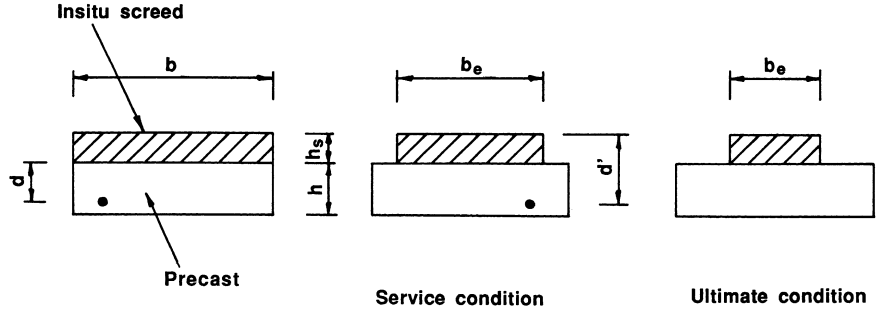

Figure 6.17 Transformed sections.

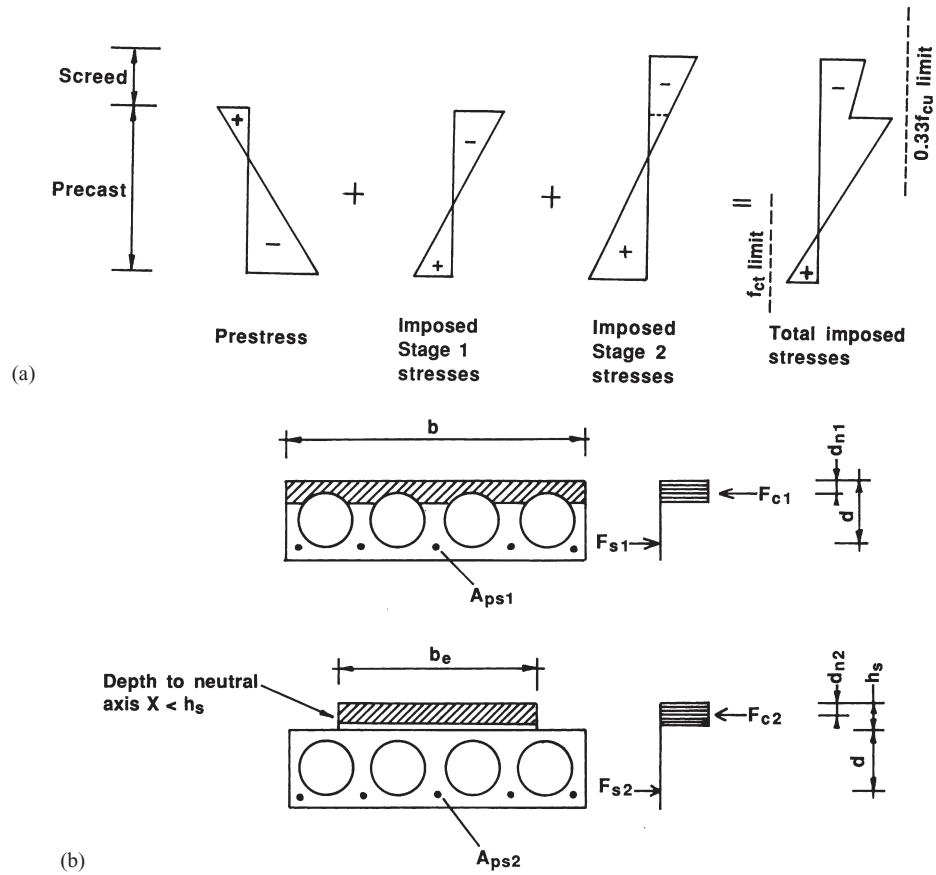

Figure 6.18 Composite section design. (a) State of stress in a prestressed composite section and (b) composite action at ultimate limit state.

$$M_2 = (f_{bc} + f_{ct})Z_{b1} - M_1\frac{Z_{b2}}{Z_{b1}} \tag{6.15}$$

For a specified geometry and prestress, values of f_{ct}, f_{bc}, Z_{b1} and Z_{b2} are known. Also, M_1 can be calculated for a given span L, and so the imposed load moment M_2 may be derived.

The construction traffic loading needs to be considered as contributing to M_1 only when checking Stage 1 service stresses. However, it does not have to be included in the final calculation of Eq. (6.15) because it is not a permanent load.

(b) At ultimate limit state

The design at ultimate conditions is also a two-stage process, with the flexural stresses resulting from the self-weight of the precast element plus any wet *in situ* concrete being carried by the precast unit alone. The lever arm in this calculation is obviously the same as in a non-composite design, i.e. *d*. The method entails calculation of the area of steel, A_{ps1}, required in Stage 1, and to add the area, A_{ps2}, required in Stage 2 using an increased lever arm. Some designers choose not to separate the stresses and moments as given in Eq. (6.16a), preferring to use Eq. (6.16b) for the total ultimate moment, and this is the approach in BS EN 1992-1-1, which assumes a completely fresh analysis of the now monolithic composite structure. The differences in using either method are small if the superimposed moment M_{u2} is more than twice the self-weight moment M_{u1}.

The effect of the structural topping is to increase the lever arm to the steel reinforcement by an amount equal to the thickness of the topping h_s, providing the depth to the neutral axis is less than h_s (Figure 6.18(b)). At ultimate limit state the stress is distributed in proportion to the strengths of the concrete components. Thus in Stage 2 the effective breadth of the *in situ* topping is taken as:

$b_e = b\dfrac{f_{ck}(in\ situ)}{f'_{ck}(\text{precast})}$, where b is the breadth of the compression flange of the precast unit. Then:

$$M_{Rd1}\{M_{u,1}\} = f_{pb}A_{ps1}(d - d_{n1}) \tag{6.16a}$$

$$M_{Rd2}\{M_{u,2}\} = f_{pb}A_{ps2}(d + h_s - d_{n2}) \tag{6.16b}$$

where each of the two values for f_{pb} and d_n are obtained from BS 8110, Part 1, Table 4.4 [6.2] for specific levels of prestress and strength ratios $f_{pu}A_{ps}/f_{cu}b_e(d + h_s)$. Thus before carrying out a composite design it is necessary to know the magnitude of the stresses in the precast unit.

The difficulty perceived in calculating a single moment of resistance is that the Stage 1 stresses must first be established. These are span-dependent and so the superimposed moment capacity M_{u2} is a function of span and Stage 1 loads, as given in Eq. (6.17). The alternative view is that the locked-in stresses from the earlier stage are negligible when the section yields as the ultimate limit state is approached.

$$M_{Rd2}\{M_{u,2}\} = f_{pb}\left(A_{ps} - \frac{M_{u1}}{f_{pb}(d - d_{n1})}\right)(d + h_s - d_{n2}) \tag{6.17}$$

6.5.3 Propping

During the normal course of construction it is very likely that the section will be unpropped, and that the slab will be positioned as it is meant to be used in the future – simply-supported with no intermediate props of any kind. However, additional benefits may accrue if the precast unit is propped while the *in situ* concrete is hardening, as shown in Figure 6.19. The benefit derives from the fact that the Stage 1 moments due to the weight of the wet concrete topping are determined over a continuous double span, each of $L/2$. When the props are removed, the prop reaction R creates a new moment (for a point load at mid-span or two point loads at 1/3 points, depending on the number of props used), which is carried by the composite section. Finally, the superimposed loads are added as before, as is also shown in Figure 6.19.

Under the action of a single prop, the hogging moment is $-0.03125\,wL^2$, where w is the self-weight of *in situ* topping and L is the effective floor span. The prop reaction is $R = 0.625\,wL$, so that when the prop is removed the sagging moment induced in the composite section is $+0.15625\,wL^2$. (See Exercise 6.3.) It is important to note that the critical position for the limiting service bending moment is not at mid-span, as shown in the bending moment distributions in Figure 6.20. This effect is exaggerated for greater depth of topping (relative to depth of precast unit) and greater imposed loads.

The benefits of the additional structural performance must be balanced against the cost and disruption in propping. Precast construction teams prefer not to prop slabs, since each unit (1.2 m wide) must be propped in an identical manner, which is not always easy to achieve in practice. Precise instructions must be relayed to site if propping has been assumed in design. Clear instructions should be visible on drawings.

Propping at two points, usually at 1/3 span positions, is sometimes used, even though the effort in raising two lines of props is clearly more than for a single prop. The main advantage in using two lines of props is in the assurance that if one line of the props does not perform correctly, the other line of props will do so. Under the action of two props at 1/3 span, the hogging moment at the props is $-0.0667wL^2$ and at mid-span it is (still positive) $+0.00278wL^2$, where w is the self-weight of *in situ* topping and L is the effective floor span. The prop reactions are both $R = 0.3667wL$, so that when the prop is removed the sagging moment induced in the composite section at 1/3 points and at mid-span is $+0.1222wL^2$. This shows that using two props is not quite as structurally efficient as using one prop.

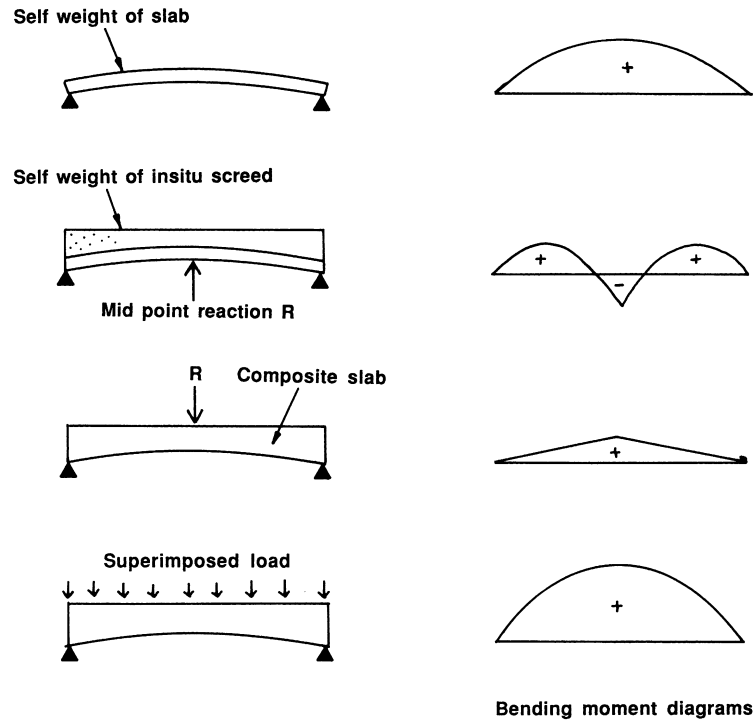

Figure 6.19 Bending moments in propped composite construction.

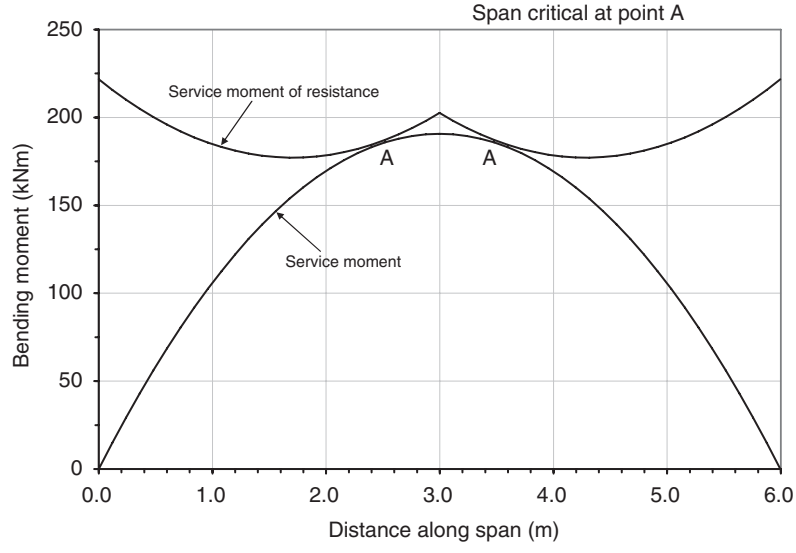

Figure 6.20 Bending moment diagrams for service moment and moment of resistance for a simply supported composite span propped at mid-span, showing that the critical design points A are not at mid-span.

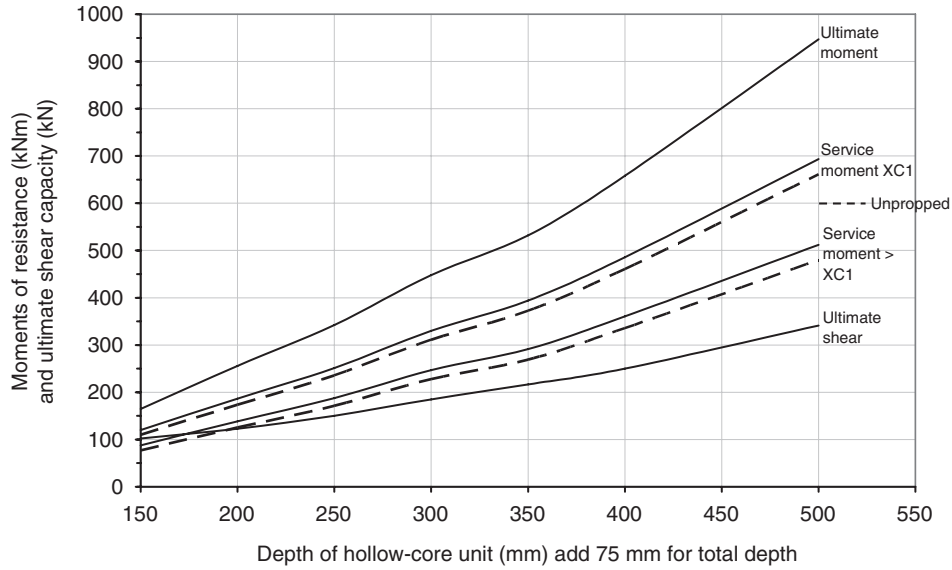

Figure. 6.21 Moments of resistance and ultimate shear capacity of composite hollow-core floor slabs with 75 mm structural topping.

For example, a 150 mm-deep hollow-core floor unit constructed compositely with a 100 mm-deep structural topping would have a service moment of resistance at mid-span of (i) 122 kNm without propping, (ii) 147 kNm with one prop, but only (iii) 142 kNm with two props.

Figure 6.21 shows the moments of resistance and ultimate shear capacities for a standard range of hollow-core composite slabs from 150 to 500 mm depth, with a 75 mm-deep structural topping (total depth 225 to 575 mm). The service moments of resistance are shown with two props at 1/3 points and without propping (dashed lines). The material properties are $f_{ck} = 45\,\text{N/mm}^2$, $f_{ck(t)} = 30\,\text{N/mm}^2$ at transfer, and $f_{cki} = 25\,\text{N/mm}^2$ for the *in situ* topping. Final prestress in the bottom fibre is set at about $f_{bc} = 12\,\text{N/mm}^2$. The permissible tension is f_{ctm} for exposure class XC1 and zero for > XC1. Because the service moment of resistance of the composite slab depends on the bending stress due to the self-weight of the precast unit plus the topping, which in turn is a function of span, the data are based on a span/depth ratio of 40. However, if span/depth = 30, M_{sr} increases by only 2 per cent.

6.5.4 Design calculations

Composite design for 200 mm-deep hcu using grade C20/25 *in situ* concrete topping, without propping

The section corresponds to the non-composite hcu design in Section 5.6. General equations are derived in which the depth T of the topping is variable. In the following, M_1 = maximum bending moment due to self-weight of precast unit plus *in situ* concrete topping, and M_2 = maximum bending moment due to superimposed loading (including partitions, finishes, ceilings, services and live loads). The effective span is again taken as 8.5 m.

Unit properties per 1200 mm width

Basic section as before.

$$Z_{b1,co} = \text{compound section modulus of precast unit} = 7.430 \times 10^3\ \{7.505 \times 10^3\}\ \text{mm}^3$$

Composite values obtained using modular ratio method.

$$Z_{b2,co} = \text{compound section modulus of composite section}$$

***In situ* concrete data**

$$f_{ck}\{f_{cu}\} \text{ at 28 days} = 20\ \{25\}\ \text{N/mm}^2$$
$$E_{cm}\{E_c\}\ (\textit{in situ}) = 30.0\ \{25.0\}\ \text{kN/mm}^2$$

Serviceability limit state of bending

Modular ratio at service $m_s = 30.0/36.3 = 0.826\ \{25/31 = 0.806\}$

Effective breadth of *in situ* concrete, $b_e = 1200 \times 0.826 = 991.7\ \{967.7\}$ mm

Then $y_{b2,co}$, $I_{2,co}$ and $Z_{b2,co}$ calculated using parallel-axis theorem

Considering bottom fibre stresses: $f_{bc} - (M_1/Z_{b1,co}) - (M_2/Z_{b2,co}) = -3.80\ \{-3.34\}\ \text{N/mm}^2$

Using $f_{bc} = 11.50\ \{12.12\}\ \text{N/mm}^2$ from Section 5.6 gives the service moment for stage 2 loads

$$M_{sr\,2} = (15.30\ \{15.46\} \times Z_{b\,2,co}) - (M_{s1} \times Z_{b2,co} / Z_{b1,co})$$

Service moment of resistance $M_{sr,c} = M_{sr\,2+} M_{s1}$

Ultimate limit state of bending

Strength ratio at ultimate $m_u = 20/45 = 0.444\ \{25/55 = 0.454\}$

$b_{eff} = 0.454 \times 1200 = 532.8\ \{545.4\}$ mm

Assume full stress $F_s = 1516 \times 911 = 1381.5\ \{0.87 \times 1770 \times 911 = 1402.8\}$ kN

$d = 200 - 45.8 + T = 154.2 + T$ mm

$F_c = 0.567 f_{ck} b_{eff}\ 0.8X\{0.45 f'_{cu} b_{eff}\ 0.9X\}$, hence $X = 127.0\ \{115.5\}$ mm.

If $T \leq 0.8 \times 127.0\ \{0.9 \times 115.5\} = 101.6\ \{103.9\}$ mm, neutral axis is in topping

$$\text{Lever arm } z = 154.2 + T - 0.4X\{154.2 + T - 0.45X\}$$

If $T > 101.6\ \{103.9\}$ mm, neutral axis is in top of precast unit and compression zone is in two rectangles as:

$$F_c = 0.567 f'_{ck}(b_{eff} T + b(0.9X - T)) \quad \{0.45 f'_{cu}(b_{eff} T + b(0.9X - T))\}$$

Solve for X with a centroid depth d_n

Check strain compatibility $\varepsilon_s = 0.0035\ (154.2 + T - X)/X + \varepsilon_{po}$ (prestrain) and hence calculate $f_p\ \{f_{pb}\}$ from stress-versus-strain curves. If $f_p < 1516\ \{f_{pb} < 0.87 \times 1770\}$, recalculate F_s and iterate to find X.

Lever arm $z = 154.2 + T - d_n$

Then $M_{Rd,c}\ \{M_{u,c}\} = F_s\ z$

Solutions to these equations for various topping thicknesses are given in Table 6.3.

The precast concrete units designed in this example will each have an upward camber of approximately span/300, or 20 mm. This must be taken into account when determining the minimum and maximum thickness of the topping.

Increasing the compressive strength of the *in situ* concrete topping has little effect on the performance of the composite floor. For example, using a 40 N/mm^2 strength and 75 mm depth of concrete increases the serviceability and ultimate moments of resistance by approximately 2 and 7 per cent, respectively. In the above example, increasing the depth of the topping from 40 mm to 100 mm increased the total self-weight of the floor by 32 per cent, yet the increased service moment capacity is only 20 per cent.

Propping the hcu during casting the topping will increase the service moment, the advantage increasing with increasing thickness. If two props are used, the ratio of $M_{sr,c}$ propped/unpropped for $T = 100$ mm, for a span $L = 8.5$ m is 186.2/160.2 = 1.16 {BS 8110 = 191.1/164.8 = 1.16}.

Table 6.3 Properties and Moment Capacities of Composite Section per 1200 mm width

	To EC2					To BS 8110				
Depth of *in situ* topping (mm)	**Height to neutral axis (mm)**	$I_{c,co}$ **(×10⁶ mm⁴)**	$Z_{b2,co}$ **(×10⁶ mm³)**	$M_{sr,c}$ **(kNm)**	$M_{Rd,c}$ **(kNm)**	**Height to neutral axis (mm)**	I_{co} **(×10⁶ mm⁴)**	$Z_{b2,co}$ **(×10⁶ mm³)**	$M_{sr,c}$ **(kNm)**	$M_{u,c}$ **(kNm)**
40	121.0	1207	9.973	$152.6–1.342M_1$	184.5	120.0	1206	10.048	$155.3–1.339\ M_1$	174.8
50	126.9	1352	10.656	$163.0–1.434M_1$	199.0	125.8	1350	10.735	$166.0–1.430\ M_1$	193.4
75	141.2	1761	12.469	$190.7–1.678M_1$	231.8	139.9	1757	12.558	$194.2–1.673\ M_1$	227.8
100	155.2	2242	14.442	$220.9–1.944M_1$	264.6	153.7	2236	14.544	$224.9–1.938\ M_1$	263.5

EC2 values are calculated from: w = self plus topping $1.2 \times (3.33 + 2.60) = 7.12$ kN/m. $M_1 = 7.12 \times 8.5^2/8 = 64.3$ kNm. M_{prop} for topping $= -11w_1L^2/90 = 11 \times 1.2 \times 2.60 \times 8.5^2/90 = -27.6$ kNm. Net $M_1 = 36.7$ kNm. $M_{sr,c,prop} = (220.9 - 1.944 \times 36.7) + 36.7 = \underline{186.2\,\text{kNm}}$. $M_{sr,c} = (220.9 - 1.944 \times 64.3) + 64.3 = \underline{160.2\,\text{kNm}}$. If $L = 12.0$ m, the ratio = 151.9/103.2 = 1.47.

6.5.5 Ultimate limit state of shear

Although ultimate shear capacities in the composite section are increased by as much as 15 per cent for a depth of topping of 100 mm, non-composite values are conservatively used mainly because the ultimate limit state of shear is not usually critical. However, individual values may be computed if an additional shear resistance is required.

The main exception is that where hollow-core units are designed compositely, BS EN 1168, Annex F [6.11] requires a two-stage design, with the shear stress generated under self-weight and topping loads to be subtracted from the ultimate shear capacity based on composite section properties. (There is nothing equivalent in BS 8110, but there is no reason why the same method could not be used.) Referring to clause F2.2:

$$V_{Rdc,c} = \frac{I_{cc} b_w}{S_{cc}} \left(\sqrt{f_{ctd}^2 + \alpha_1 \gamma_{p,fav} \sigma_{cp} f_{ctd}} - \frac{V_{u1} S_c}{b_w I_c} \right) + V_{Ed1} \qquad (6.18)$$

where

V_{Ed1} = ultimate dead load acting on the unit, including self-weight of wet topping
I_{cc} = 2nd moment of area based on the net composite section, excluding the transformed area of tendons
S_{cc} = 1st moment of area at the centroidal axis in the composite section.

In the above example (refer to Example 5.6.1) for $T = 100$ mm, the effective span for shear = 8500 – $2 \times (50 + 99) = 8.20$ m. $V_{Ed1} = 1.35 \times 7.12 \times 8.2/2 = 39.4$ kN. Then $v_{Ed1} = 39.4 \times 10^3 \times 4.768/303 \times 696.7 \times 10^6 = 0.89$ N/mm². Composite $I_c = 2149 \times 10^6$ mm⁴, $y_{b,c} = 185.5$ mm, area above the centroid $S_c = (991 \times 100 \times 91.5) + 1200 \times 41.5^2/2 = 10.1 \times 10^6$ mm³. (Note that b_w is at the narrowest part of the web, which may not necessarily be on the centroidal axis; however, this is where shear failure will begin, even if the centroid is above the webs.) Then $V_{Rdc,c} = (64470\sqrt{(1.77^2 + 0.273 \times 0.9 \times 5.35 \times 1.77)} - 0.89) \times 10^{-3} + 39.4 = 132.5$ kN. Had this been calculated in stage one $V_{Rdc,c} = 150.6$ kN, so the shear stress consumed in stage 1 reduces $V_{Rdc,c}$ by 14 per cent. The non-composite $V_{Rdc} = 103.3$ kN.

Exercise 6.2 Composite floor design

Repeat Exercise 5.2 using grade C25/30 × 50 mm minimum thickness *in situ* concrete structural topping. Check the design for serviceability and ultimate moments, ultimate shear both cracked and uncracked in flexure, and interface shear stresses between the precast and *in situ* concrete. Note that the finishes in Exercise 5.2 are now included as part of the structural topping. The precast unit is grade C40/50. $E_{cm} = 35.26$ $\{E_c = 30\}$ kN/mm^2.

Solution

Effective span = 6600 + 75/2 + 75/2 = 6675 mm. Span for shear (unit $y_b = 97.3$ mm) = 6.406 m.
Assume average topping thickness 60 mm.

Stage 1 loading (kN/m^2)		Service	EC2 Ultimate Eq. 6.10(b)**	BS 8110 Ultimate
Permanent actions:	Self-weight of slab and infill	3.00	3.75	4.20
	Structural topping*	1.50 {1.44}	1.88	2.02
Total		4.50 {4.44}	5.63	6.22
Stage 2 loading (kN/m^2)		Service	EC2 Ultimate	BS 8110 Ultimate
Permanent actions:	Partitions, services and ceiling	1.60	2.00	2.24
Superimposed actions:		5.00	7.50	8.00
Total		6.60	9.50	10.24

* average $h_s = 60$ mm due to 20 mm camber in precast floor unit
** found to be the greater of Eq. 6.10(a) and 6.10(b) from BS EN 1990.

Step 1: Serviceability limit state stresses
maximum bending moment per 1.2 m wide unit,

Stage 1, M_{s1}	= 30.07 kNm	Stage 1, M_{s1}	= 29.67 kNm
Stage 2, M_{s2}	= 44.11 kNm	Stage 2, M_{s2}	= 44.11 kNm
Total ultimate bending moment, M_{Ed}	= 101.12 kNm	Total ultimate bending moment, M_u	= 110.01 kNm
		Ultimate shear force,	
Stage 1 V_{Ed1}	= 21.64 kN	Stage 1 V_{u1}	= 23.91 kN
Stage 2 V_{Ed2}	= 36.51 kN	Stage 2 V_{u2}	= 39.36 kN

Section properties of composite slab at serviceability limit state (see also Chart 5.2).
Effective breadth of topping $b_e = E_c$ (*in situ*) × 1200 mm/E_c (precast) = 1074 mm {1040 mm} using Table 6.1
Compound sections for hollow-core unit based on $m = (1 + 0.72) \times 205/35.26 = 10.0$ {11.75}
Try unit reference R(0 + 19)

	EC2					BS 8110				
Component	A (mm^2)	y_t (mm)	Ay_t (mm^3)	I_{oo} (×10^6 mm^4)	Ay'^2 (×10^6 mm^4)	A (mm^2)	y_t (mm)	Ay_t (mm^3)	I_{oo} (×10^6 mm^4)	Ay'^2 (×10^6 mm^4)
In situ topping	53 700	25.0	1 342 500	11.19	477.02	52 000	25.0	1 300 000	10.83	472.47
Precast unit	145 670	154.0	22 433 180	638.30	175.91	146 321	154.2	22 562 698	640.30	167.95
Compound	199 370		23 775 680	1302.42		198 321		23 862 698	1291.55	

(*Continued*)

$Z_{b1,co} = 638.30/96.0$	$= 6.65 \times 10^6\,\text{mm}^3$
$Z_{t1,co} = 638.30/104.0$	$= 6.14 \times 10^6\,\text{mm}^3$
Composite	
$y_{t2,co} = 23\,775\,680/199\,370$	$= 119.25\,\text{mm}$
$y_{b2,co}$ (net) $= 200 + 50 - 119.25$	$= 130.75\,\text{mm}$
$Z_{b2,co}$	$= 9.96 \times 10^6\,\text{mm}^3$
$Z_{t2,co}$ (top of psc)	$=18.81 \times 10^6\,\text{mm}^3$
$Z_{t2,co}$ (top of *in situ*)	$=10.92 \times 10^6\,\text{mm}^3$

$Z_{b1,co} = 640.3/95.8$	$= 6.68 \times 10^6\,\text{mm}^3$
$Z_{t1,co} = 640.3/104.2$	$= 6.14 \times 10^6\,\text{mm}^3$
Composite	
$y_{t2,co} = 23\,862\,698/198\,321$	$= 120.32\,\text{mm}$
$y_{b2,co} = 200 + 50 - 120.32$	$= 129.67\,\text{mm}$
$Z_{b2,co}$	$= 9.96 \times 10^6\,\text{mm}^3$
$Z_{t2,co}$ (top of psc)	$=18.37 \times 10^6\,\text{mm}^3$
$Z_{t2,co}$ (top of *in situ*)	$=10.73 \times 10^6\,\text{mm}^3$

Step 2: Stresses at service

$$f_{bc} \geq \frac{M_{s1}}{Z_{b1}} + \frac{M_{s2}}{Z_{b2}} - 3.509$$

$$f_{bc} \geq \frac{30.07\times10^6}{6.65\times10^6} + \frac{44.11\times10^6}{9.96\times10^6} - 3.509 \quad = 5.44\,\text{N/mm}^2$$

$$f_{tc} \geq 0.45 f_{ck} - \frac{M_{s1}}{Z_{t1}} - \frac{M_{s2}}{Z_{t2}}$$

$f_{tc} \geq 18.0 - 4.90 - 2.34 \quad = 10.76\,\text{N/mm}^2$

$$f_c(\textit{in situ}) \geq \frac{M_{s2}}{Z'_{t2}} \quad = 4.04\,\text{N/mm}^2$$

$< 0.45 \times 25 \quad < 11.25\,\text{N/mm}^2$

Referring to Chapter 5, Chart 5.3, use unit ref. R (0 + 19) with 395.2 kN prestress force.

Final $\sigma_{po} = 432.8/372.4 = 1162\,\text{N/mm}^2$

$$f_{bc} \geq \frac{M_{s1}}{Z_{b1}} + \frac{M_{s2}}{Z_{b2}} - 3.182$$

$$f_{bc} \geq \frac{29.67\times10^6}{6.68\times10^6} + \frac{44.11\times10^6}{9.96\times10^6} - 3.182 \quad = 5.69\,\text{N/mm}^2$$

$$f_{tc} \geq 0.33 f_{cu} - \frac{M_{s1}}{Z_{t1}} - \frac{M_{s2}}{Z_{t2}}$$

$f_{tc} \geq 16.5 - 4.83 - 2.40 \quad = 9.27\,\text{N/mm}^2$

$$f_c(\textit{in situ}) \geq \frac{M_{s2}}{Z'_{t2}} \quad = 4.11\,\text{N/mm}^2$$

$< 0.33 \times 30 \quad < 9.9$

Referring to Chapter 5, Chart 5.3, use unit ref. R (0 + 19) with 358.2 kN prestress force.

Final $f_{pe} = 358.2/372.4 = 961.7\text{N/mm}^2$

Step 3: Ultimate limit state

$A_{ps} \times f_{pu} = 19$ No. at 30.82 kN per wire = 585.5 kN

New effective depth, d = total depth minus height to centroid of prestress wires (from Chart 5.3)

$d = 200 + 50 - 42.5 = 207.5$ mm

To determine the ultimate moment capacity, first find the depth of compression centroid, d_n

$b_e = (25/40) \times 1200 = 750\,\text{mm}$

$\sigma_{po} = 1061\,\text{N/mm}^2$

$\varepsilon_{po} = 1061/205000 = 0.00517$

$\varepsilon_{LOP} = 0.9 \times 0.87 \times 1570/205000 = 0.006 > 0.00517$

By solving quadratic or iterative solutions,

$X = 46.4\,\text{mm} < 50\,\text{mm}$ depth of topping

$d_n = 0.4 \times 46.4 = 18.6\,\text{mm}$

Check strain $\varepsilon_p = 0.00517 + 0.0035 \times (207.5\text{-}46.4)/46.4 = 0.0173 < \varepsilon_{LOP} < \varepsilon_{ud}$

$F_s = f_p A_p = 1366 \times 373 = 508.7\,\text{kN}$

$M_{Rd} = 508.7 \times (207.5 - 18.6) = 96.1\,\text{kNm} < 101.12\,\text{kNm}$ required.

Repeat above using unit R (0 + 21)

$d = 207.3\,\text{mm}$

Solve for $X = 50.8\,\text{mm}$

$d_n = 0.4 \times 50.8 = 18.6\,\text{mm}$

$\sigma_{po} = 1048\,\text{N/mm}^2$

$\varepsilon_{po} = 1150/205\,000 = 0.00511$

Check strain $\varepsilon_p = 0.00511 + 0.0035 \times (207.3\text{–}50.8)/50.8 = 0.01730 < \varepsilon_{LOP} < \varepsilon_{ud}$

$b_e = (30/50) \times 1200 = 720\,\text{mm}$

BS 8110, Part 1, Table 4.4

$$\frac{A_{ps} f_{pu}}{f_{cu} b_e d} = \frac{585500}{50\times720\times207.5} \quad = 0.0784$$

i.e. the section is under-reinforced.

$f_{pe}/f_{pu} = 961.7/1570 \quad = 0.613$

$f_{pb}/0.87\,f_{pu} = 1.0$

$X/d = 0.168$

hence $X = 34.9\,\text{mm} < 50\,\text{mm}$ depth of topping

$d_n = 0.45 \times 0.9 \times 34.9 \quad = 14.1\,\text{mm}$

$M_u = 0.87 \times 585.5 \times (207.5 - 14.1) \times 10^{-3} \quad = 98.2\,\text{kNm}$

$< 110.01\,\text{kNm}$ required.

Repeat above using R (0 + 23) with

$A_{ps} f_{pu} = 707.8\,\text{kN}$

$d = 207.1\,\text{mm}$

$$\frac{A_{ps} f_{pu}}{f_{cu} b_e d} = \frac{707800}{50\times720\times207.1} \quad = 0.09495$$

$f_{pe}/f_{pu} = 944/1570 = 0.601$

$X/d = 0.204$

$X = 42.2\,\text{mm} <$ depth of topping d_n

$F_s = f_p\, A_p = 1366 \times 412 = 562.2\,\text{kN}$
$M_{Rd} = 562.2 \times (207.3 - 20.3) = 105.1\,\text{kNm} > 101.12\,\text{kNm}$ required.

$M_u = 0.87 \times 707.8 \times (207.1 - 17.1) \times 10^{-3}$ = 17.1 mm
$> 110.01\,\text{kNm}$ required. = 116.9 kNm
It is unusual for the ultimate limit state to be critical in prestressed concrete design. However in the transformed composite section the breadth of the topping is reduced by a much larger factor in ultimate (where f_{cu} is used) than in service (where E_c is used). See Figure 6.16.

Step 4: Ultimate Shear

$V_{Rd,c}$ in Table 5.2 for uncracked values.
For unit R (0 + 21)
$V_{Rd,c} = 142.8\,\text{kN}$
$>>$ 58.15 kN required, not critical.

a) For shear where uncracked in flexure, use non-composite value V_{co} for unit ref. R (0 + 23) = 150.9 kN
$>>$ 63.27 kN required
b) For shear resistance of section cracked in flexure, use V_{cr} from BS 8110, equation 55;
$(1 - 0.55\, f_{pe}/f_{pu}) = 0.695$
$b_v = 544\,\text{mm}$

$$\frac{100A_{ps}}{b_v d} = \frac{100 \times 450.8}{544 \times 207.1} = 0.40$$

Table 3.8. $v_c = 0.58\,\text{N/mm}^2$
The moment M_o required to produce a stress in the bottom fibres of 0.8 f_{bc} for unit R (0 + 23) is given by:
$M_o = 0.8\, f_{bc}\, Z_{b2,co} = 0.8 \times 6.58 \times 9.96$ = 52.4 kNm
M_o occurs at 1.67 m from the support (using service loads).
The critical section is at 1.67 + 0.207/2 = 1.78 m from the support.
Thus, at the critical section
$V_u = 1.2 \times 16.46 \times ((6.675/2) - 1.78)$ = 30.8 kN
Also at the critical section
M_u = 85.9 kNm

$$V_{cr} = 0.669 \times 0.589 \times 544 \times 207.07 \times 10^{-3} + 52.4\frac{30.8}{85.9} = 62.8\,\text{kN}$$

$> 26.2\,\text{kN}$ required.

Step 5: Interface shear:
This is checked at the ultimate limit state on an effective interface width of 1200 mm (not 720 mm) × half span of slab.

$F_v = 0.567\, f_{ck}\, b_e\, 0.8\, X = 0.567 \times 25 \times 1200 \times 0.8 \times 50.8$ = 689.9 kN
$\beta = 1$
$z = 207.3 - 20.3 = 187\,\text{mm}$

$$v_{Edi} = \frac{1.0 \times 60.55 \times 10^3}{1200 \times 187} = 0.270\,\text{N/mm}^2$$

(See Eq. 6.25)
$V_{Rdi} = 0.2 \times (0.7 \times 0.3/1.5 \times 25^{2/3})$ = 0.419 N/mm²
which is $> 0.270\,\text{N/mm}^2$

$F_v = 0.45 f_{cu} b_e 0.9X$
$F_v = 0.45 \times 30 \times 1200 \times 0.9 \times 42.2$ = 707.8 kN/unit

$$v_{h(ave)} = \frac{707.8 \times 10^3}{1200 \times 6750/2} = 0.1767\,\text{N/mm}^2$$

$V_{h(ave)} = 2 \times v_{h(ave)}$ = 0.353 N/mm²
$< 0.55\,\text{N/mm}^2$ from BS 8110, Part 1, Table 5.5 [6.2] for extruded floor slabs

Exercise 6.3 Propped composite slab

Repeat Exercise 6.2 with the slab propped at mid-span. Check for flexure only.

Solution

The negative moment over a central prop is $-0.03125wL^2$, where w = self-weight of the topping, and L is the effective span of the slab.

Stage 1 loading for the precast slab self-weight minus the propped topping gives:

$M_{prop} = -0.03125 \times 1.50 \times 6.675^2$ $= -2.089$ kNm	$M_{prop} = -0.03125 \times 1.44 \times 6.675^2$ $= -2.005$ kNm
$M_{s1} = 1.2 \times (3.00 \times 6.675^2/8 - 2.089)$ $= 17.54$ kNm/unit	$M_{s1} = 1.2 \times (3.00 \times 6.675^2/8 - 2.005)$ $= 17.64$ kNm/unit
Prop reaction	Prop reaction
$= 0.625 \times 1.2 \times 1.50 \times 6.675$ $= 7.51$ kN/unit	$= 0.625 \times 1.2 \times 1.44 \times 6.675$ $= 7.21$ kN/unit

Stage 2 loading for superimposed load (as before) and prop reaction at mid-span gives service moments and stresses:

$M_{s2} = 44.11 + 7.51 \times 6.675 / 4$ $= 56.64$ kNm/unit	$M_{s2} = 44.11 + 7.21 \times 6.675 / 4$ $= 56.14$ kNm/unit
$f_{bc} \geq \frac{17.54 \times 10^6}{6.65 \times 10^6} + \frac{56.64 \times 10^6}{9.62 \times 10^6} - 3.509$ $= 5.03$ N/mm^2	$f_{bc} \geq \frac{17.64 \times 10^6}{6.68 \times 10^6} + \frac{56.14 \times 10^6}{9.96 \times 10^6} - 3.182$ $= 5.10$ N/mm^2

Referring to Chart 5.3, use R (0 + 16).

6.6 Economic Comparison of Composite and Non-composite Hollow-core Floors

A comparison was made between the *approximate* costs, applicable only in the UK, of providing a fully grouted unscreeded precast floor, and a composite *in situ* with precast floor. Cost data were collected from hollow-core producers for 150 mm, 200 mm and 250 mm (or 260 mm) deep × 1200 mm wide units. The data, which are presented in relative terms in Tables 6.2 and 6.3, were based on the following specification:

- floor clear span = 6.0 m
- loading: superimposed = 5.0 kN/m^2
  partitions = 1.0 kN/m^2
  services etc. = 0.5 kN/m^2
- fire resistance = 1 hour
- 28-day strength f_{cu} = 60 N/mm^2

The slabs are of the proprietary type, being either extruded ('Tembo', 'Dycore') or slip-formed ('Roth') and prestressed in the usual manner. Stability ties are provided in the unscreeded floor in the form of peripheral tie bars. The *in situ* concrete is grade C20/25.

In Table 6.4 the data are expressed in terms of the cost of an unscreeded floor of between 1000 m^2 and 5000 m^2 floor area. Although the actual costs supplied by the producers varied by as much as 20 per cent of the mean value, it was clear that the additional cost of a structural topping was about 45 per cent. The increased cost due to materials was 30 per cent, with labour and plant adding a further 15 per cent. For small projects of less than 500 m^2 the labour charges per square metre increase rapidly, such that the average increased cost of the topping is in the order of 55 per cent.

Table 6.4 Relative cost of delivered and screeded floor compared with unscreeded floor

	Depth of precast unit (mm)		
	150	**200**	**250**
Slab delivered to site	0.75–0.83	0.76–0.85	0.80–0.86
Slab fixed and grouted with tie steel*	1	1	1
Slab fixed and 50 mm screed laid with A142 mesh+	1.42–1.48	1.39–1.46	1.36–1.40

* for floor area < 500 m^2 add 8 to 10 percentage points.
\+ for floor area < 500 m^2 add 12 to 15 percentage points.

Table 6.5 Relative cost of 150 mm- and 250 mm-deep units compared with 200 mm-deep units

	Depth of precast slab (mm)		
	150	**200**	**250**
Slab delivered to site	0.92–0.95	1	1.15–1.20
Slab fixed and grouted with tie steel	0.93–0.95	1	1.10–1.18
Slab fixed and 50 mm screed laid with A142 mesh	0.95–1.00	1	1.05–1.08

Table 6.6 Comparison of self-weight of unscreeded and screeded floor (kN/m^2)

	Depth of precast slab (mm)		
	150	**200**	**250**
Precast slab only	2.35	2.93	3.66
Precast slab with 50 mm screed	3.79	4.37	5.10
Ratio	1.61	1.49	1.39

Table 6.5 shows that the cost of unscreeded floors increases rapidly for depths up to and including 250 mm, whereas the cost of a screeded floor does not vary by more than −5 to +8 per cent over the range considered.

The conclusion is that in a typical four-storey commercial building of about 2500 m^2 floor area, the structural topping will cost £35k (2010 prices). It will add a further 3000 kN to foundation loads, as indicated by Table 6.6, and also increase the height of the building by about 300 mm.

6.7 Composite Beams

6.7.1 Flexural design

There is more potential for enhancement in the flexural capacity of composite beams than with composite slabs, because the breadth of the compression flange can, if correctly specified, be increased to the maximum permitted value as in monolithic construction, i.e. $b_w + L_z/5$ (BS EN 1992-1-1, clause

Table 6.7 Loading conditions for composite beam analysis

Stage	Loading	Section properties based on
1	Self-weight of beam and slab, + *in situ* infill + construction allowance	Precast beam
2	As stage 1 + self-weight of topping + construction allowance	Precast beam + *in situ* infill near beam only
3	Total self-weight + superimposed	Final beam and topping

5.3.1(6) [6.1] or BS 8110, Part 1, clause 3.4.1.5 [6.2]). The minimum strength of *in situ* concrete is again taken as 20 {25} N/mm^2, and the appropriate modular ratios are used in serviceability and stiffness checks and strength ratios for the ultimate limit state. Early research work by Kajfasz *et al.* [6.14] showed the potential for economic design. There is also a greater potential for the use of propped composite beam design, and this will be given in Section 6.7.2.

As with composite floors, service and ultimate stresses are checked at two stages of loading (or three if a structural topping is added to the floor) and superimposed in the final analysis. If structural toppings are used, the loading conditions are as given in Table 6.7.

The essential features of the design procedure are given in Figure 6.22. Stage 1 stresses exist in the precast beam only, Figure 6.22(a). These are the result of prestress and relaxation (if the beam is prestressed), self-weight of the beam, slab, and wet concrete. Stage 2 stresses exist in the precast beam and *in situ* infill, Figure 6.22(b), and are due to the self-weight of the wet topping plus an allowance of about 1.5 kN/m^2 for construction traffic if the amount of *in situ* concrete to be placed is extensive, as is the case for a structural topping. Final Stage 3 stresses in the composite beam, Figure 6.22(c), which are in addition to the above, are the result of superimposed, services, and partition loading, differential shrinkage and the total creep relaxation after hardening of the *in situ* concrete. Ultimate moment and shear resistances are computed in the usual manner, noting that differential shrinkage and creep strains are ignored at the ultimate limit state due to the effects of yield.

An important point requiring clarification is the *effective breadth* of the compression flange, particularly if the cores in certain types of hollow-core floor slab are filled only intermittently, as is the common practice using slip-formed units (Figure 6.23). Here the minimum section is through the unfilled hollow core. This comprises only the top and bottom flanges of the slab – each usually 20 to 30 mm thick. Although interface shear transfer between beam and slab may be fully effective at the positions of the reinforced *in situ* filled cores (representing possibly only one-twelfth of the breadth of the slab), there is no analytical or experimental evidence to suggest that continuous horizontal shear stresses exist between these points. In such cases the effective breadth of the compressive flange is equal to the breadth of the supporting precast beam.

In instances where several or every core is opened, the vertical interface shear capacity must be justified so that the effective breadth of the flange (based on the full depth of the *in situ* concrete) may be taken as equal to the actual distance between the extremities of the opened core. Though the *in situ* concrete may penetrate up to 100 mm beyond these points, its compaction is uncertain. Openings in cores are usually about 600 mm in length, resulting in effective breadths typically 1350 mm or 700 mm wide in symmetrical or non-symmetrical arrangements, respectively.

Figure 6.24 shows a photograph of a test where composite action between the prestressed beam and *in situ* concrete placed in the broken-out cores of some hollow-core slabs was studied. The main objectives were to determine the effective widths of the *in situ*–precast top flange, and to reduce the overall construction depth to give a span: depth ratio in the region of 18 to 1. The tests have shown that full interaction between the precast components and the *in situ* concrete may be taken in design,

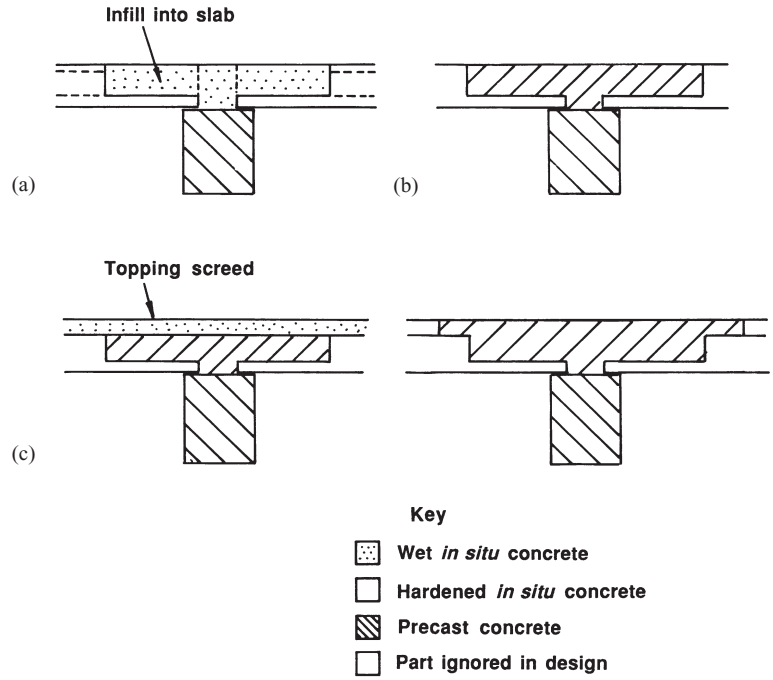

Figure 6.22 Composite beam design. (a) Stage 1, before hardening of *in situ* infill; (b) Stage 2, after hardening of *in situ* infill; (c) Stage 3, before (left) and after (right) hardening of structural topping.

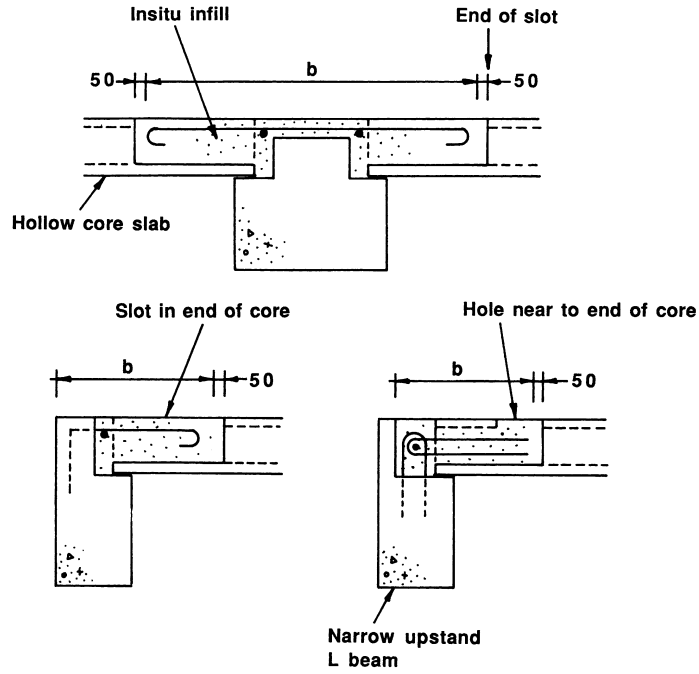

Figure 6.23 Effective breadth using hollow-core slabs.

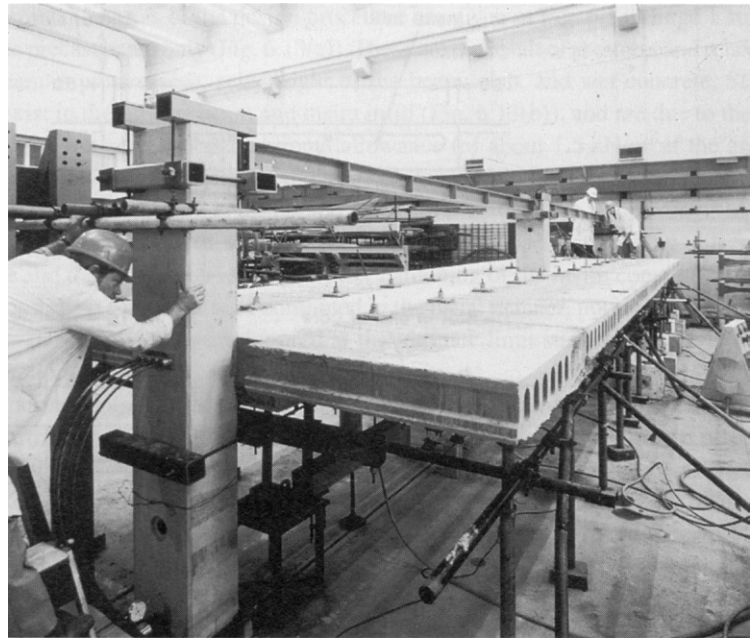

Figure 6.24 Composite beam – slab tests at London University (courtesy of Costain Building Products).

providing that minimum percentage interface shear reinforcement is present, and that the effective width of the *in situ* flange is equal to the actual width provided, i.e. 1.0 m in this case.

Effective breadths for the *in situ* concrete topping used with solid plank flooring are taken as for monolithic rc construction, i.e. span/10 either side of the supporting beam. Composite beam design is not usually carried out where double-tee flooring units and a relatively thin topping are used. The enhancement in strength is marginal and the topping's susceptibility to damage is increased in these cases.

Exercise 6.4 Composite reinforced edge beam in flexure

Determine the allowable imposed loading on the edge beam shown in Figure 6.25. The beam is supporting hollow-core floor slabs which weigh 3.0 kN/m^2 and span 8.0 m. The beam is simply supported over 6.0 m effective span. In this exercise, consider the stresses in the bars at both the construction and in-service cases.

Use concrete grade C32/40 (pc), grade C20/25 (*in situ*), f_{yk} $\{f_y\}$ = 500 N/mm^2, and 35 mm cover to 10 mm diameter links.

Solution

Stage 1 loading		Service
Permanent actions:	Self-weight of beam	3.50 {3.36}
	Slab 3.0 × 8.0/2	12.00
Total		15.50 {15.36}

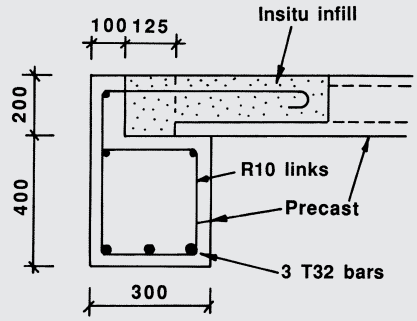

Figure 6.25 Details for Exercise 6.4.

Step 1: Stage 1 properties

$b = 100\,\text{mm}$

$d = 600 - 35 - 10 - 32/2 = 539\,\text{mm}$

$f_{ck} = 32\,\text{N/mm}^2$ | $f_{cu} = 40\,\text{N/mm}^2$

Step 2: Stage 1 design

Eq. 6.10(b) assumed, check at end

$$M_1 = 1.25 \times 15.50 \frac{6.0^2}{8} = 87.2\,\text{kNm}$$

$$k_1 = \frac{87.2 \times 10^6}{32 \times 100 \times 539^2} = 0.0938$$

$z_1 = 490\,\text{mm}$

$X_1 = 122.5\,\text{mm} < 200\,\text{mm}$ upstand

$$A_{s1} = \frac{87.2 \times 10^3}{0.87 \times 500 \times 490} = 409\,\text{mm}^2$$

$$M_1 = 1.4 \times 15.36 \frac{6.0^2}{8} = 96.8\,\text{kNm}$$

$$k_1 = \frac{96.8 \times 10^6}{40 \times 100 \times 539^2} = 0.090$$

$z_1 = 478.2\,\text{mm}$

$X_1 = 135\,\text{mm} < 200\,\text{mm}$ upstand

$$A_{s1} = \frac{96.8 \times 10^6}{0.87 \times 500 \times 478.2} = 465\,\text{mm}^2$$

As the total steel area is $2413\,\text{mm}^2$, the remainder may be used to carry imposed loads using the composite section stage 2 loading.

Step 3: Stage 2 properties

$b = 125 + 500$ slot in slab $= 625\,\text{mm}$

$d = 539\,\text{mm}$

$f'_{ck} = 20\,\text{N/mm}^2$

$A_{s2} = 2413 - 409 = 2004\,\text{mm}^2$

$f'_{cu} = 25\,\text{N/mm}^2$

$A_{s2} = 2413 - 465 = 1948\,\text{mm}^2$

Step 4: Stage 2 design

$F_{s2} = 0.87 \times 500 \times 2004 \times 10^{-3} = 871.7\,\text{kN}$

$F_{c2} = 0.567 \times 20 \times 625 \times 0.8\,X_2$

$$X_2 = \frac{871.7 \times 10^3}{0.567 \times 20 \times 625 \times 0.8} = 153.7\,\text{mm}$$

$F_{s2} = 0.87 \times 500 \times 1948 \times 10^{-3} = 847.3\,\text{kN}$

$F_{c2} = 0.45 \times 25 \times 625 \times 0.9X_2$

$$X_2 = \frac{847.3 \times 10^3}{0.45 \times 25 \times 625 \times 0.9} = 133.9\,\text{mm}$$

$X_2 \approx X_1$ so the strain compatibility is satisfactory, i.e. the neutral axis position for both stages is close.

$z_2 = 539 - 0.4 \times 153.7 = 477.5\,\text{mm}$

$M_{Rd2} = 871.7 \times 477.5 \times 10^{-3} = 416.3\,\text{kNm}$

Hence $w_{Ed2} = \dfrac{8 \times 416.3}{1.5 \times 6.0^2} = 61.67\,\text{kN/m}$ run of beam

From which it is clear that Eq. 6.10(b) is critical

$z_2 = 539 - 0.45 \times 133.9 = 478.7\,\text{mm}$

$M_2 = 847.3 \times 478.7 \times 10^{-3} = 405.6\,\text{kN}$

$= 56.3\,\text{kN/m}$ run of beam

6.7.2 Propping

The basic concept for propping composite sections before the *in situ* concrete is added was described in Section 6.5.3. The potential for structural enhancement is greater for prestressed beams than for slabs, because the Stage 2 stresses due to the self-weight of the floor slab, *in situ* infill and topping can be virtually eliminated by the use of two or three props.

The ratio of the Stage 1 moment in the mid-span propped and unpropped situation is given by the ratio β.

$$\beta = M_1 \text{ propped} / M_1 \text{ unpropped} = \frac{(w_0 - 0.25w_1)}{(w_0 + w_1)}$$

where

w_0 = self-weight of beam
w_1 = self-weight of precast slab and infill *in situ* concrete.

Typical values for β are between 0.1 and 0.3.
Then $M_1 = 0.125\ \beta\ (w_0 + w_1)\ L^2$
Prop force $R = 0.625\ w_1\ L$
and $M_2 = 0.125\ (w_2 + 1.25\ w_1)\ L^2$, where w_2 is the superimposed loading.

The resulting stresses are

$$f_{bc} \geq M_{s1} / Z_{b1} + M_{s2} / Z_{b2} - f_{ct} (\text{N/mm}^2), \text{ and so on as before.}$$

It is worthwhile propping beams of over 6 m to 10 m span with two or three props, respectively, particularly if a structural topping is being used and the ratio of the composite properties to the basic section properties exceeds 1.50. There are considerable advantages in keeping the possibility of propping in reserve in case of an unexpected request to drill a hole in the beam, or in case an error has occurred in the calculation. Propping reduces beam erection rates by about 15 to 25 per cent, and so the delicate balance between material saving and time lost on site has to be considered. Only the precast construction companies can give exact cost information on this.

6.7.3 Horizontal interface shear

The integrity of composite construction relies on the long-term continuity between the precast and *in situ* concrete. Although floor loading in buildings is predominantly static, there may be instances where it is variable and cyclic in nature, resulting in a fluctuation in shear stress levels. For this reason, primary composite beams are designed with interface shear links or other similar mechanical fasteners. Shear friction alone is not recommended for beams.

As with slabs, the ultimate interface shear stress v_{Edi} {v_h} is checked for the uncracked section (BS EN 1992-1-1, clause 6.2.5(1)), {BS 8110, Part 1, clause 5.4.7.2} against v_{Rdi} values in equation 6.25 in EC2 {or Table 5.5 of BS 8110}. Nominal interface shear links should always be provided. The minimum area of links is $0.08\sqrt{f_{ck}}/f_{yk}$ {0.15%} of the contact area. If v_{Edi} {v_h} is greater than the permitted value, shear steel to carry the *entire* shear force is provided according to BS EN 1992-1-1, equation 9.4 {BS 8110, Part 1, equation 62}. Note that the recently reduced value of c in BS EN 1992-1-1, clause 6.2.5(2) for 'very smooth' surfaces cast against a smooth mould (c = 0.025 to 0.1 for inverted-tee beams), and 'smooth' surfaces (c = 0.2 for rectangular beams), and with the normal stress σ_n being zero (inverted-tee beams) or small (rectangular beams), v_{Rdi} is effectively designed for the interface shear links alone.

6.7.4 Shear check

This is usually not a problem in beams of span greater than about 4.0 m. It is therefore often sufficient to check the applied ultimate shear against the basic shear capacity of the beam.

6.7.5 Deflections

Stage 1 (downward) deflections are subtracted from the (upward) precamber deflections produced during manufacture, such that the net upwards deflection prior to the superimposed loadings is (very) approximately span/1000. Stage 2 deflections, due to superimposed loads, creep, shrinkage, etc., which are usually controlled by ceiling deflections of not more than 20 mm, are based on the composite section properties.

Exercise 6.5 Composite beam calculation

The following exercise shows the calculation for an inverted-tee beam, comparing the design for both the basic section and the composite section. The construction details are shown in Figure 6.26. The precast beam is grade C50/60 and the *in situ* infill is C25/30. Aggregates are gravel.

Overall span of beam = 7000 mm
Effective span of beam = 7000 – (2 (150 + 50)) = 6600 mm
Overall floor span supported by beam = 7200 mm
Centre to centre distance between beams = 7500 mm

E_c (precast) = 37.28 {32.0} kN/mm^2. E_c (infill) = 31.48 {26.0} kN/mm^2.

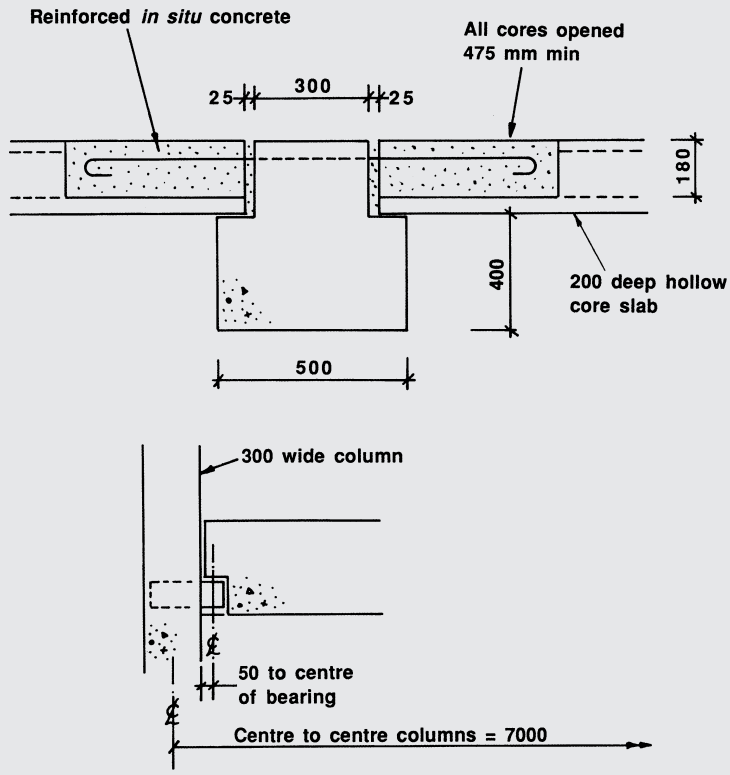

Figure 6.26 Details for Exercise 6.5.

(*Continued*)

Solution

Try a 500 mm wide × 400 mm deep inverted-tee beam (with 300 mm wide × 200 mm upstand).

Non-composite loading		EC2 Service	EC2 Ultimate Eq. 6.10(b)	BS 8110 Service	BS 8110 Ultimate
Permanent actions:	Self-weight of beam	6.50	8.125	6.24	8.74
	Psc slab	2.93 × 7.2	26.37	2.93 × 7.2	29.53
	Partitions	1.00 × 7.5	9.375	1.00 × 7.5	10.50
	Ceilings and services	0.60 × 7.5	5.625	0.60 × 7.5	6.30
Superimposed actions:		5.00 × 7.5	56.25	5.00 × 7.5	60.00
Total		77.10	105.75	76.84	115.07
Stage 1 composite loading					
Permanent actions:	Self-weight of beam	6.50	8.125	6.24	8.74
	Psc slab	2.93 × 7.2	26.37	2.93 × 7.2	29.53
	Construction	1.5 × 7.5	14.06	1.5 × 7.5	11.25
Total		38.85	48.55	38.59	54.02
Permanent total		27.60	34.50	27.34	38.27
Stage 2 composite loading					
Permanent actions:	Partitions	1.00 × 7.5	9.375	1.00 × 7.5	10.50
	Ceilings and services	0.60 × 7.5	5.625	0.60 × 7.5	6.30
Superimposed actions:		5.00 × 7.5	56.25	5.00 × 7.5	60.00
Total		49.50	71.25	49.50	76.80

Step 1: Non-composite design

$$M_s = \frac{77.10 \times 6.6^2}{8} = 419.8\,\text{kNm} \qquad M_s = \frac{76.84 \times 6.6^2}{8} = 418.4\,\text{kNm}$$

$$M_{Ed} = \frac{105.75 \times 6.6^2}{8} = 575.8\,\text{kNm} \qquad M_u = \frac{115.07 \times 6.6^2}{8} = 626.6\,\text{kNm}$$

$$V_{Ed} = \frac{105.75 \times 6.6}{2} = 349.0\,\text{kN} \qquad V_u = \frac{115.07 \times 6.6}{2} = 379.7\,\text{kN}$$

Referring to Chart 4.1 for capacities, use TB400/18 {TB400/21}, i.e. 18 {21} no. 12.5 mm-diameter strands, with a service moment capacity of M_{sr} = 457 {448} kNm, ultimate moment capacity M_{ur} = 727 {743} kNm, and ultimate shear capacity V_{co} = 509 {417} kN.

Section properties of basic beam and composite section

Try TB400/15 when composite.

$A_{ps} = 15 \times 94.2 = 1413\ \text{mm}^2$

$m = (1 + 0.72) \times 195 / 37.28 = 9.0 \quad \{(1 + 0.72) \times 195 / 32 = 10.48\}$

$(m - 1)A_{ps} = 8.0 \times 1413 = 11\,300 \quad \{9.48 \times 1413 = 13\,397\}\ \text{mm}^2$

Height to centroid of strands y_s = 269.2 − 99.2 = 170.0 mm; y_{st} = 430 mm from top

Actual breadth of infill concrete = 2 × (25 + 475) = 1000 mm

Depth of *in situ* infill = 200 − 20 bottom flange = 180 mm

Effective breadth of infill $b_e = E_c$ (*in situ*) × 1000 mm/E_c (precast)

$b_e = 1000 \times 31.48 / 37.28 = 844 \quad \{1000 \times 26 / 32 = 812.5\}\ \text{mm}$

	EC2					BS 8110				
Component	A (mm^2)	y_t (mm)	Ay_t (mm^2)	I_{oo} (×10^6 mm^4)	Ay'^2 (×10^6 mm^4)	A (mm^2)	y_t (mm)	Ay_t (mm^2)	I_{oo} (×10^6 mm^4)	Ay'^2 (×10^6 mm^4)
Beam upstand	60 000	100	6 000 000	200.0	3310.7	60 000	100	6 000 000	200.0	3330.4
Beam flange	200 000	400	80 000 000	2666.7	847.6	200 000	400	80 000 000	2666.7	829.5
Strands	11 300	430	4 859 000		459.3*	13 397	430	5 760 710		542.6*
Total	271 300		90 859 000	7484.3		273 397		91 760 710	7569.2	
In situ infill	151 920	90	13 672 800	410.2	3744.7	146 250	90	13 162 500	394.9	3744.0
Beam upstand	60 000	100	6 000 000	200.0	1296.5	60 000	100	6 000 000	200.0	1350.0
Beam flange	200 000	400	80 000 000	2666.7	4681.8	200 000	400	80 000 000	2666.7	4500.0
Strands	11 300	430	4 859 000		735.8*	13 397	430	5 760 710		857.3*
Total	423 220		104 531 800	13 735.7		419 647		104 923 210	13 712.9	

* Ay'^2 for the strands is calculated for each row, not for the centroid to all.

$y_t = \dfrac{99672800}{271300}$ = 334.9 mm

$y_b = 600 - 334.9$ = 265.0 mm

$Z_{t1} = \dfrac{7484.3 \times 10^6}{334.9}$ = 22.35 ×10^6 mm^3

$Z_{b1} = \dfrac{7484.3 \times 10^6}{265.0}$ = 28.24 ×10^6 mm^3

Composite

$y_{t2} = \dfrac{104531800}{423220}$ = 247.0 mm

$y_{b2} = 600 - 247.0$ = 353.0 mm

$Z_{t2} = \dfrac{13735.7 \times 10^6}{247.0}$ = 55.61 ×10^6 mm^3

$Z_{b2} = \dfrac{13735.7 \times 10^6}{353.0}$ = 38.91 ×10^6 mm^3

$y_t = \dfrac{91760710}{273397}$ = 335.6 mm

$y_b = 600 - 335.6$ = 264.4 mm

$Z_{t1} = \dfrac{7569.2 \times 10^6}{335.6}$ = 22.55 ×10^6 mm^3

$Z_{b1} = \dfrac{7569.2 \times 10^6}{264.4}$ = 28.63 ×10^6 mm^3

Composite

$y_{t2} = \dfrac{104923210}{419647}$ = 250.0 mm

$y_{b2} = 600 - 250.0$ = 350.0 mm

$Z_{t2} = \dfrac{13712.9 \times 10^6}{250}$ = 54.85 ×10^6 mm^3

$Z_{b2} = \dfrac{13712.9 \times 10^6}{350.0}$ = 39.18 ×10^6 mm^3

Step 2: Composite Stage 1 construction design

$M_{s1} = \dfrac{38.85 \times 6.6^2}{8}$ = 211.5 kNm

$M_{Ed1} = \dfrac{48.55 \times 6.6^2}{8}$ = 264.3 kNm

$V_{Ed1} = \dfrac{48.55 \times 6.6}{2}$ = 160.2 kN

$f_{t1} = \dfrac{211.5}{22.35}$ = 9.46 N/mm^2

< 0.45 × 50 = 22.5 N/mm^2

$f_{b1} = \dfrac{211.5}{28.24}$ = 7.49 N/mm^2

< 10.38 N/mm^2 for beam TB400/15 (Chart 4.2)

$M_{s1} = \dfrac{38.59 \times 6.6^2}{8}$ = 210.1 kNm

$M_{u1} = \dfrac{54.02 \times 6.6^2}{8}$ = 294.1 kNm

$V_u = \dfrac{54.02 \times 6.6}{2}$ = 178.3 kN

$f_{t1} = \dfrac{210.1}{22.55}$ = 9.32 N/mm^2

< 0.33 × 60 = 19.8 N/mm^2

$f_{b1} = \dfrac{210.1}{28.63}$ = 7.34 N/mm^2

< 10.4 N/mm^2 for beam TB400/15 (Chart 4.1)

(*Continued*)

Step 3: Composite Stage 1 permanent design

$M_{s1} = \frac{27.60 \times 6.6^2}{8}$	$= 150.3\,\text{kNm}$	$M_{s1} = \frac{27.34 \times 6.6^2}{8}$	$= 148.8\,\text{kNm}$
$f_{t1} = \frac{150.3}{22.35}$	$= +6.73\,\text{N/mm}^2$	$f_{t1} = \frac{148.8}{22.55}$	$= +6.60\,\text{N/mm}^2$
$f_{b1} = \frac{150.3}{28.24}$	$= -5.32\,\text{N/mm}^2$	$f_{b1} = \frac{148.8}{28.63}$	$= -5.20\,\text{N/mm}^2$

Step 4: Composite Stage 2 design

$M_{s2} = \frac{49.5 \times 6.6^2}{8}$	$= 269.5\,\text{kNm}$	$M_{s2} = \frac{49.5 \times 6.6^2}{8}$	$= 269.5\,\text{kNm}$
$M_{Ed2} = \frac{72.5 \times 6.6^2}{8}$	$= 394.5\,\text{kNm}$	$M_{u2} = \frac{76.8 \times 6.6^2}{8}$	$= 418.2\,\text{kNm}$
$V_{Ed2} = \frac{72.5 \times 6.6}{2}$	$= 239.1\,\text{kN}$	$V_u = \frac{76.8 \times 6.6}{2}$	$= 253.4\,\text{kN}$
$f_{t2} = \frac{269.5}{55.61}$	$= +4.85\,\text{N/mm}^2$	$f_{t2} = \frac{269.5}{54.85}$	$= +4.91\,\text{N/mm}^2$
$f_{b2} = \frac{269.5}{38.91}$	$= -6.93\,\text{N/mm}^2$	$f_{b2} = \frac{269.5}{39.18}$	$= -6.88\,\text{N/mm}^2$

Step 5: Composite Stage 3 design

Combining Stage 1 plus Stage 2 stresses gives values for comparison with the basic prestress limits for Class 2 members. The critical section is at the bottom of the beam.

$f_t = 6.73 + 4.95$	$= +11.68\,\text{N/mm}^2$	$f_t = 6.60 + 4.91$	$= +11.51\,\text{N/mm}^2$
$< 0.45 \times 50 = 22.5\,\text{N/mm}^2$		$< 0.33 \times 60 = 19.8\,\text{N/mm}^2$	
$f_b = -5.32 + -6.93$	$= -12.25\,\text{N/mm}^2$	$f_b = -5.20 + -6.88$	$= -12.08\,\text{N/mm}^2$
Permissible tensile stress	$= -4.07\,\text{N/mm}^2$	Permissible tensile stress	$= -3.49\,\text{N/mm}^2$
So $f_{bc} \geq -4.07 - (-12.25)$	$\geq 8.18\,\text{N/mm}^2$	So $f_{bc} \geq -3.49 - (-12.08)$	$\geq 8.59\,\text{N/mm}^2$
Refer to beam properties in Chart 4.2.		Refer to beam properties in Chart 4.1.	
Use TB400/15 with $f_{bc} = 10.38\,\text{N/mm}^2$		Use TB400/15 with $f_{bc} = 10.4\,\text{N/mm}^2$	
The saving compared with the non-composite beam is 3 strands.		The saving compared with the non-composite beam is 6 strands.	

The ultimate moment of resistance of the basic beam TB400/15 (698 > 575.8{638 > 626.6}) and the shear capacity of the basic beam (482 > 349.0 {380 > 379.7}) in Charts 4.1 and 4.2 are both greater than the design values, and so no further checks are necessary. The exercise may be repeated for the effects of propping the beam prior to fixing the floor slab. The likely outcome of this action would be a reduction in the size of the beam from 400 mm to 350 mm depth.

CHAPTER 7

Design of Connections and Joints

Connections form the most vital part of precast concrete structures. There are many varied types and methods of analysis. This chapter gives a full description of connections and joints, with numerous worked examples and test results.

7.1 Development of Connections

Connections form *the* vital part of precast concrete construction. *In situ* concrete joints were used extensively in the early development of precast structures, owing mainly to their simplicity of manufacture and the more relaxed attitudes to safe and rapid site progress. A temporary bearing, of about 40 mm to 50 mm contact width, was used to support the beam and carry only its self-weight, as shown in Figure 7.1, and an extended permanent bearing was formed using *in situ* concrete. The obvious disadvantages were shrinkage and flexural cracking in the top of the precast-to-*in situ* interface, which led to the use of non-shrink grouts and latex bonding admixtures. Projecting reinforcement from the lower column was lapped onto similarly offset projecting reinforcement in the upper column, but there were reported difficulties in stabilising the upper column due to the flexibility of the open reinforcement cage. The use of latticed column cages to stabilise upper-storey columns is still quite frequent.

Methods were sought of obtaining continuity at the connections. The Ministry of Public Works and Buildings, which existed during the early 1950s in the UK, copied an American solution called the H-frame, whereby pin-jointed site connections were made near the positions of frame contraflexure; i.e. mid-column height and 0.2 × beam span (see Figure 7.2). The solution removed one problem by shifting the connections to points of zero (or small) bending moment, but caused other difficulties elsewhere in manufacturing and transportation by creating large, two-dimensional units. Figure 7.3 is a better solution: a 'scarf joint', approximately $0.15L$ – say, 600 to 750 mm from the column – reduces the bending moment in the beam by around 40 per cent, resulting in a shallower beam. The scarf joint may be positioned at one end of the beam, or at both ends. This method of design has been used in multi-storey car parks in order to save headroom.

The most robust solution was found in a mechanical connection, brought about by relying on the precast concrete to firmly anchor rolled or fabricated steel sections in position so that a direct steel-to-steel joint was made. The number of different solutions was as great as the number of precast concrete frame manufacturers of the day – about twenty. Figures 7.4(a) and (b) show two examples of types of connector that have proved to be costly and difficult to position on site.

The reasons for the large number of variations stem partly from the fact that the greater the connectors' load-carrying capacity, the more complex they became in order to handle the resulting

Multi-storey Precast Concrete Framed Structures, Second Edition. Kim S. Elliott and Colin K. Jolly.

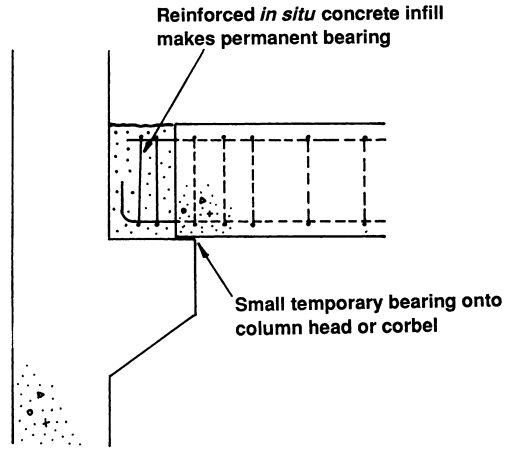

Figure 7.1 Early type of connection using cast *in situ* extended bearings.

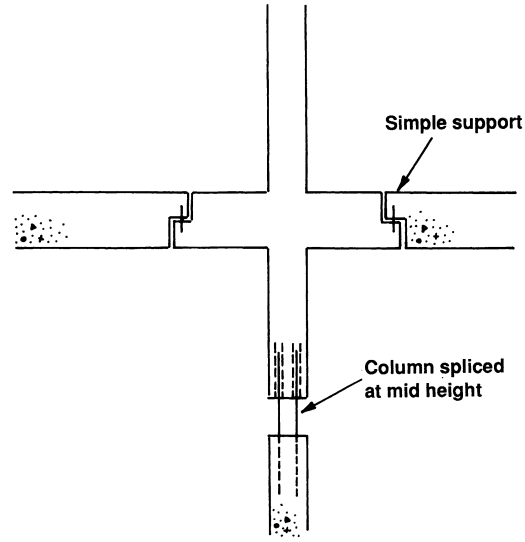

Figure 7.2 Connections to H-frames made at points of contraflexure.

stresses. The main cost elements are fabrication and material costs, and those rise steeply with increases in connector capacity. Precast designers prefer the complicated aspects of the connector to be under the control of the factory, reducing site operations to simple dowelling, bolting or welding.

The influence of patented connections in the 1960s and 1970s stifled the widespread use of the most efficient types of connection, and led designers towards ingenious designs that occasionally 'failed', not structurally but on practical grounds. Connector design is an iterative process in which no aspect of strength, compatibility, materials and tolerances can be considered in isolation. The example shown in Figure 7.5 illustrates how easy it is to lose sight of the functional principles.

Stanton *et al.* produced a special study for the PCI [7.1] on moment-resistant and simple connections, and stated: *The economic and functional success of a precast concrete structure depends to a great extent on the configuration and properties of its inter-element connections. Flexibility of the connections affects the distribution of creep, thermal and shrinkage strains and determines joint performance over time. The strength of the connections remaining after the demands of volume change, gravity loads and*

Figure 7.3 Reinforced concrete inverted-tee beams designed with a scarf joint at approximately 750 mm from the face of the column create a negative bending moment at the column that will reduce the depth of the beam.

dimensional or alignment corrections have been satisfied determines whether the structure will deform permanently under action of extreme wind or seismic forces. Ductility of the connections determines whether the permanent deformations will take place by a safe redistribution of load and dissipation of energy or by brittle connection failure.

This statement captures the essence of precast frame design in knowing *which* effects are to be considered in design, and not simply carrying out the mechanics of stress equilibrium and strain compatibility.

7.2 Design Brief

The structural requirement is the transfer of vertical shear, transverse horizontal shear, axial tension and compression, and occasionally bending moments and torsion, from one precast component to another in a safe and structurally sound manner.

All connections will resist compression, but it is necessary to check for the possible addition of stresses resulting from axial forces due to temperature effects, shrinkage and creep. These are becoming increasingly important as beam and floor spans are increased, and some precast components are tied into the structure at a lower age. Connector forces due to the effects of fire, impact and explosions, etc. have been virtually ignored in favour of alternative load path design methods or the use of peripheral and internal ties (see Section 9.4). Torsion has also been ignored and this has led to fears of rotational instability in the temporary construction stage.

While acknowledging that these forces do actually exist, the designer should not aim to design a connection that will resist every conceivable stress and strain, but should allow other parts of the structure to accommodate some of the effects.

One other functional requirement that is frequently ignored is the capacity to rotate and accept beam deflections. The problem is based around the concept of a pinned joint. The difficulty is that on the one hand, if a joint were designed to behave as a 'true' pin, the connection might be deemed unserviceable owing to cracking and deformation at the end of the beam. On the other hand, if the connection is capable of developing moment restraint, local stresses in the vicinity of the connection could give rise to other problems. An example of this is shown in Figure 7.6, where shear forces resulting from moment transfer across a beam-to-column connection caused a shear failure in the column.

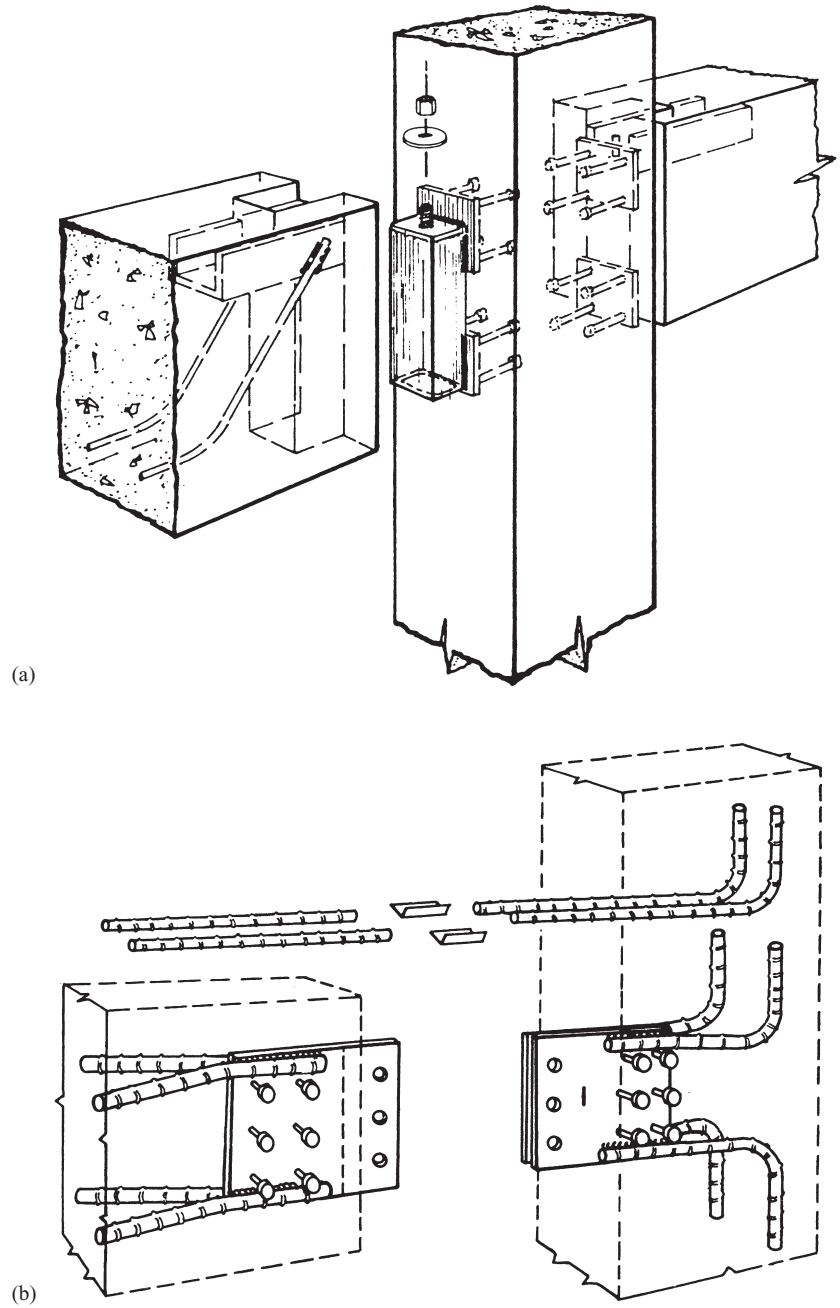

Figure 7.4 Unsuccessful types of beam-to-column connections.

The structural behaviour of connections is often complex and not conducive to normal reinforced concrete design methods. The simplest form of connection is a simple abutment-type bearing where, as shown in Figure 7.7, there is no restriction on the construction zone, and the transfer of forces from the beam to column is quite obvious from a single photograph. The need for shallower construction depths led to the concealed steel insert connection, where a combination of steel plates and rolled sections is used to carry extraordinarily high forces. Connections of the type shown in Figure 7.8 are

Figure 7.5 Beam-to-column connections designed with little regard for some of the practicalities associated with precasting.

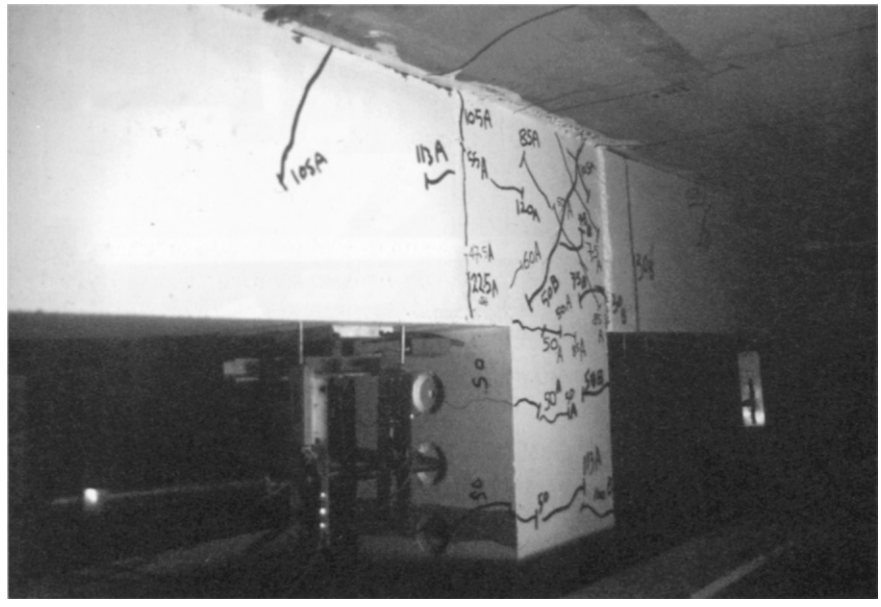

Figure 7.6 Shear cracking in inadequately reinforced column due to moment transfer from the beam.

capable of carrying a beam reaction in the order of 500 kN within a 500 mm depth of connection. This equates to a shear stress of about 3 N/mm^2. If the mode of failure is concrete crushing around the connector, then a lower safety factor may be used than if the concrete failure is due to tension or diagonal shear. This is because compressive failure may be controlled by the introduction of ductile reinforcement across the failure plane.

Local stress levels around the steel inserts become very important. They occur in small zones in areas where full concrete compaction may not be easy to achieve, and their distributions are

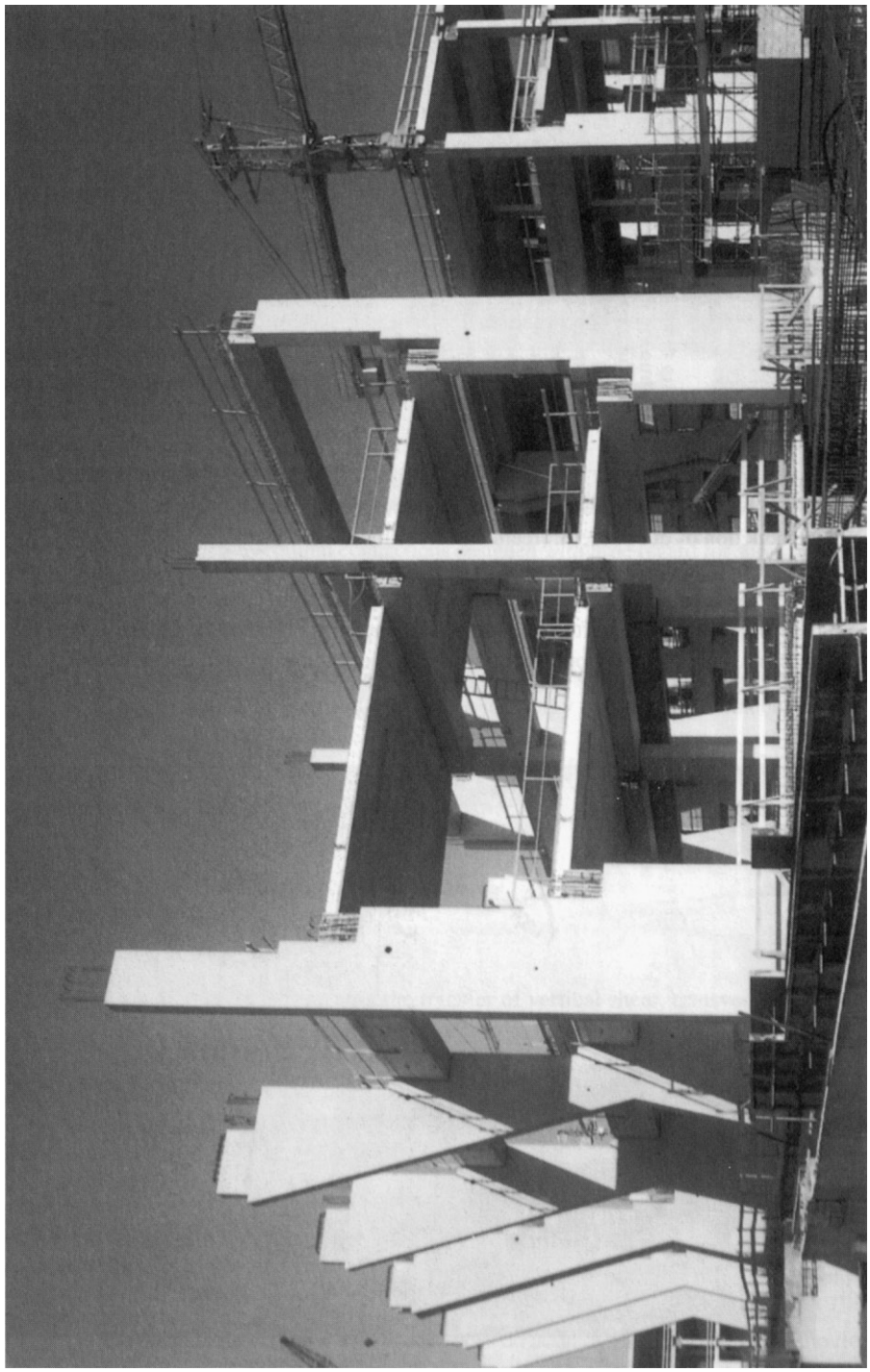

Figure 7.7 RAI Centre in Rome, 1990 (courtesy of BF+T. Wiesbaden).

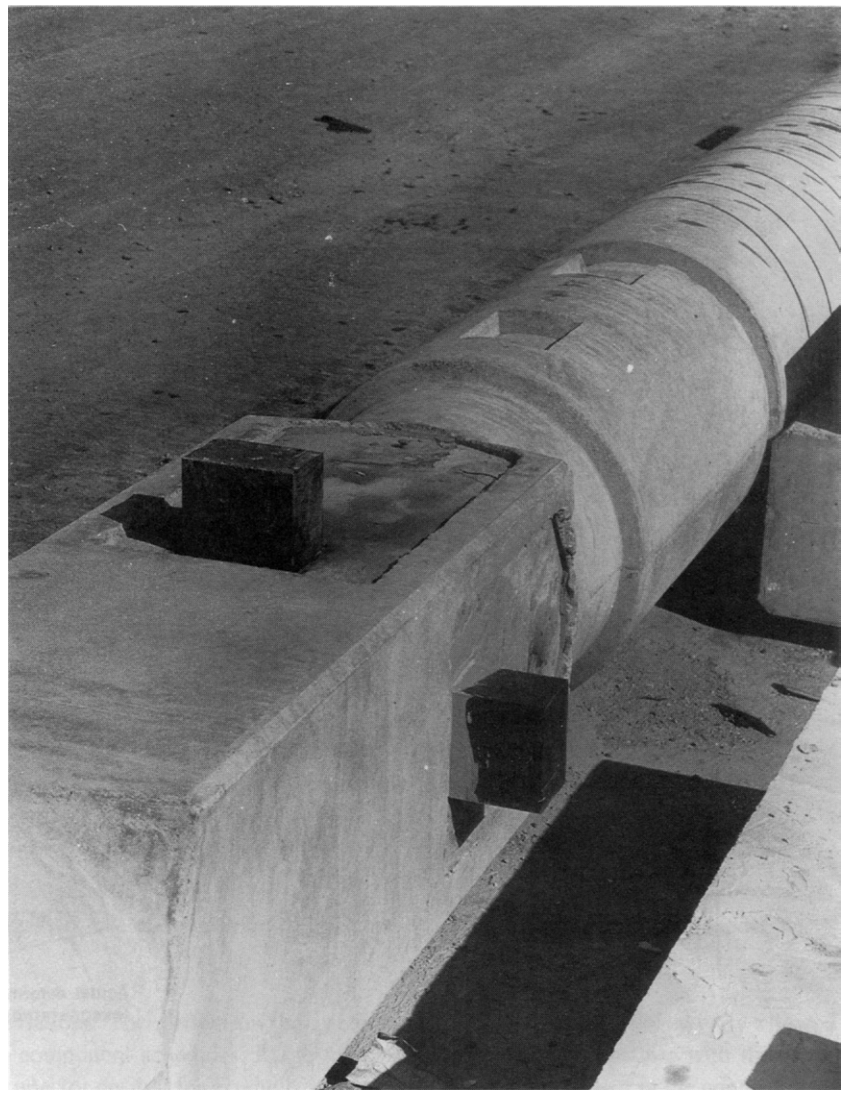

Figure 7.8 Solid mild steel billet cast into columns.

often unknown. The anchoring method is the greatest problem, and full-scale testing should not be overlooked in research and development. It is not uncommon for steel plates to be welded to reinforcement cages, as shown in Figure 7.9, in order to realise the full capacity of the connection.

The role of connector testing has been criticised in some circles, e.g. Colman [7.2], owing to the unavoidable restrictions of being unable to test the connections in a real frame environment – complete with sway and large deflections – and of being unable to study the effects of moment distribution after initial cracking. An example of this is the phenomenon of reverse end rotation resulting from high shear force in the traditional shear end tests, as shown in Figure 7.10. With this arrangement the deformation in the joint is greater than in the beam, resulting in a set of stresses in the test specimens that are not representative of real behaviour. Under circumstances such as these, there is a danger of an unsafe extrapolation of test results to other component and connector geometries and materials.

Figure 7.9 Steel plates being added to reinforcement cages at the factory.

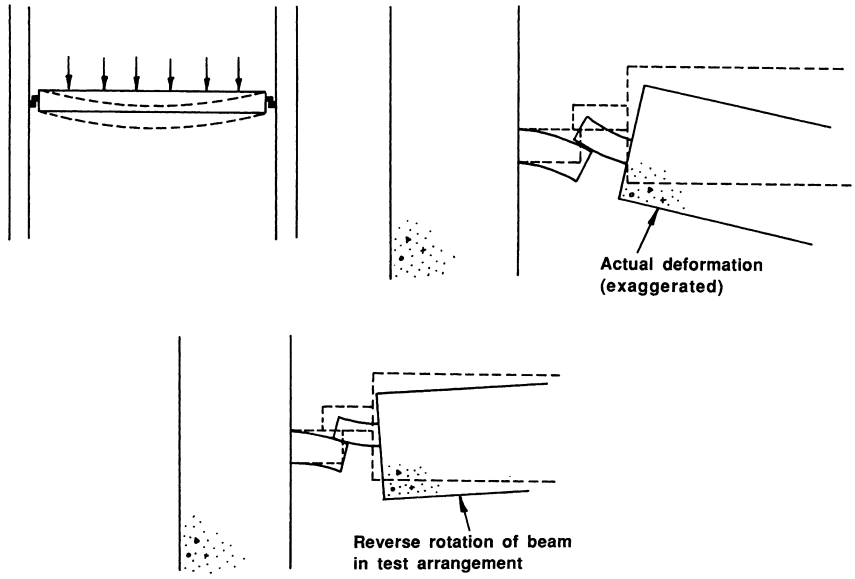

Figure 7.10 The phenomenon of reverse bending in column connector tests.

Designers should not be insensitive to the problems of tolerances. A lack of flatness, alignment and squareness will inevitably lead to the accumulation of physical dimensional deviations. Their effect on the strength and behaviour must be positively allowed for in component schedules. Large tolerances may not be compatible with the proposed connector design; for example, if vertical slots are not provided in the connector in Figure 7.11, then packing must be used and the connector set to a negative height tolerance.

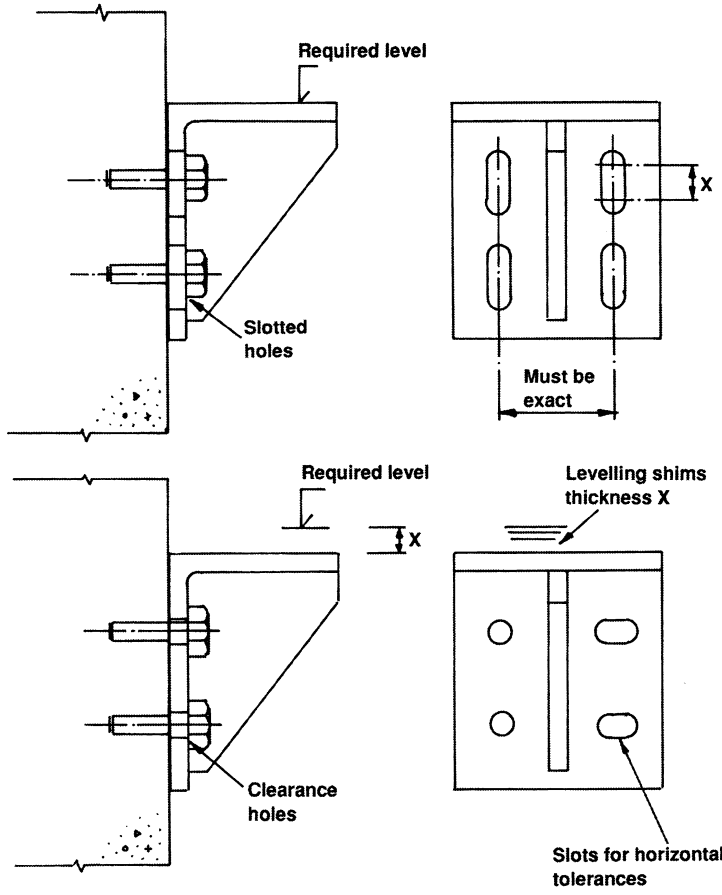

Figure 7.11 Use of negative fixing tolerances where alternative means are not possible.

7.3 Joints and Connections

Much confusion surrounds the difference between a 'connection' and a 'joint'. The correct definition is that a connection is the total construction, including the ends of the precast concrete components that meet at it, whereas a joint comprises the individual parts that form the connection. For example, in a beam-to-column situation a bearing joint is made between the precast beam and precast column; but when the assembly is completed by the use of *in situ* grout etc. the entire construction is called a connection. These terms are often transposed in casual conversation, but for the sake of clarity we shall use the correct definitions in this book.

It is not always necessary for loads to be transferred through a joint. For example, in the case of a sealing joint for waterproofing purposes, or an expansion joint for thermal movements, relative movement is allowed across the joint, but one would hardly call that a connection. However, a connection will always have a structural function.

Joints are made in several ways, for instance by:

- dowelling and securing with *in situ* concrete or grout
- welding and protecting with same

- bolting and protecting with same
- using resin anchors in combination with the above.

From a structural point of view there may be no preference for a particular approach. However, construction rates can be dramatically affected in some buildings (e.g. tall and with small plan area) if time is needed for the development of *in situ* concrete strength within a connection. The first step is to describe the general criteria for the design and construction of joints, and then to discuss the design of the functional types of connection in skeletal structures, i.e.:

- beam-to-slab connections
- beam-to-column connections
- wall-to-frame connections
- column splices, including to foundations.

7.4 Criteria for Joints and Connections

7.4.1 Design criteria

The four rules for satisfactory joint design are that:

- The components can resist ultimate design loads in a ductile manner.
- The precast members can be manufactured economically and be erected safely and speedily.
- The manufacturing and site erection tolerances do not adversely affect intended structural behaviour, or are catered for in a 'worst case' situation.
- The final appearance of the joint must satisfy visual, fire and environmental requirements.

Design engineers have satisfied these criteria by ensuring that the intended behaviour of the joint is guaranteed by careful attention to detail. In some instances, slight cracking is accepted as an indication that spurious load paths are not being created, and in others reinforcement is deliberately avoided or underdesigned in certain areas to prevent restraining moments from forming. The *FIB Manual* on structural connections [7.3] summarises the philosophy of connection design: *The main purpose of the structural connections is to transfer forces between the precast concrete elements in order to obtain a structural interaction when the system is loaded. By the ability to transfer forces, the connections should secure the intended structural behaviour of the superstructure and the precast subsystems that are integrated in it. . . . The design of the structural connections is not just a question of selecting appropriate dimensions of the connection devices, but the force path through the connection must be considered in a global view of the whole connection and the adjacent structural members*. The hidden message here is that the design of precast concrete structures is an iterative process, and one cannot separate the processes of design, manufacture and erection of the elements in isolation from the same processes for connections. A floor diaphragm comprising hollow-core units (see Chapter 8) is the perfect example, where the designer responsible for the whole structure must be aware of the particular features of hollow-core units used to create the floor diaphragm, e.g. shear transfer between the units, tie bars and coupling bars in the ends of units, and the orientation of the floor with respect to the positions of shear walls etc.

The *FIB Manual* [7.3] gives the main features of connection design as standardisation, simplicity, movement, ductility, durability, fire resistance and aesthetics. Vambersky [7.4] has similarly summarised the main criteria for the serviceability performance of joints in terms of strength, influence of volume changes, ductility, durability, fire protection, simplicity in fabrication and erection, temporary loading conditions, economy and appearance. It is important to note that heading the *fib* list are 'standardisation' and 'simplicity', i.e. use of a generic type – welded, bolted or grouted connection throughout a structure, and use of the least number of pieces, giving site operatives little choice in the sequence of construction. Requirements for some of these criteria are summarised below, with references to other sections where more detailed design information may be found.

7.4.1.1 Strength

A connection must have the strength to resist the forces to which it will be subjected during its lifetime. Some of these forces are apparent, caused by permanent and imposed gravity loads, wind, earthquake, and soil or water pressure. Others are not so obvious and are frequently overlooked. These are the forces caused by restraint of volume changes in the precast components, and by forces required to maintain stability.

Instability can develop from eccentric gravity loading and horizontal loads. Furthermore, additional capacity may need to be provided to resist unanticipated, accidental or abnormal loads, which may be caused by foundation settlement, explosion, collision, change of building usage, etc. These 'abnormal' loads may be accommodated in connections by a capacity for overload and ductility within the connection or, for example, by building redundancies into the total structure by using stability ties.

Joint strength can be categorised by the type of stress resisted, i.e. compressive, tensile, flexural, torsional or shear; see Sections 7.5.1. to 7.5.5. Connections may have a high degree of resistance to one type of stress, but little or no resistance to another. In many cases it may be unnecessary, or even undesirable, to provide a high capability to resist a combination of stresses. A better solution would be to utilise more than one joint type to achieve the same overall result. See Sections 7.7 to 7.13 for strength design methods.

7.4.1.2 Influence of volume changes, or movement

The combined shortening effects of creep, shrinkage and temperature reductions can cause tensile stresses in precast concrete components and their connections. If the connections restrain movement, the resulting stresses must be considered in the design, and they may be much harder to evaluate than from external forces. The solution to many problems associated with movement is to design the connections as pinned. See Section 8.5 for volume change design methods.

7.4.1.3 Ductility

This is the ability of a connection to undergo large deformations without failure, and is measured by the amount of deformation that occurs between first yield and ultimate failure. Ductility in building frames is usually associated with moment resistance. However, the connections in precast structures are designed using pinned joints between the components, and semi-rigid behaviour is considered as being adequate. See Section 9.2 for further details. The design should ensure that flexural yielding takes place at the chosen plastic hinge position, so that the post-elastic deformation capacity of the entire structure may be controlled. The design should avoid highly localised stress concentrations, use ductile reinforcement along load paths, and provide additional strength capacity to potentially brittle parts (e.g. welds, short bolts in tension, bolts subjected to shear, reinforcement anchorage zones).

7.4.1.4 Durability

Connections should be designed and constructed to give the same environmental protection as the elements connected. Connections exposed to an aggressive environment should be periodically inspected and maintained. Evidence of poor durability is usually exhibited by corrosion of exposed steel elements, or by cracking and spalling of concrete, as shown in Figure 7.12. Connections that will be exposed to weather should have steel elements adequately covered with concrete, otherwise they should be painted or galvanised. Alternatively, non-corroding materials should be used. The preferred method of protecting exposed steel connection elements is to cover with concrete or grout. Typical mix proportions are shown in Table 4.3. No chlorides should be permitted in the mix.

Most precast concrete components are of high quality, and flexural cracking is seldom a serious problem provided that tensile stresses are kept within code limits. However, local cracking or spalling can occur when improper details result in restraint of movement, or in stress concentrations. Tolerances should be increased to allow for misalignment on site.

Figure 7.12 Spalling of cover concrete around a steel plate connector due to corrosion. The cover distance was 12 mm minimum. The age of the building was about 15 years when the photograph was taken.

7.4.1.5 Fire resistance

Connections weakened by fire may jeopardise the structural stability and should be protected to give the same resistance as the structural frame, e.g. an exposed steel corbel supporting a beam, even though there is evidence that such steel is less susceptible to fire-related strength reduction because the larger concrete element absorbs more heat and reduces the temperature of the steel. The fire resistance of rc corbels attached to columns should be designed using the information provided for simply supported beams, even though they form a part of the column, as the stresses in the reinforcement are due to bending and shear in the manner of a deep beam.

7.4.1.6 Aesthetics

Connections that are not hidden can either be emphasised and become part of the architecture, as in the case of the corbel shown in Figure 7.13, or be finished in a manner that is functional but not expressive. There was no advantage in using a more complicated hidden connection in Figure 7.14.

7.5 Types of Joint

7.5.1 Compression joints

Compression is transmitted between precast concrete components either by direct bearing, or through an intermediate medium such as *in situ* mortar or concrete. The distinction is made depending on tolerances and the importance of the accuracy of the load transfer location. For example, vertical load transfer between two columns, one above the other, requires concentricity between member axes. This can be achieved only by using an intermediate medium of reasonable size.

On the other hand, direct contact between precast concrete components with no intermediate padding material may be used only where great accuracy in manufacture and installation is obtained and where bearing stresses are less than about $0.2f_{ck}$ (see clause 10.9.4.3(3)) $\{0.2f_{cu}\}$ of the weaker concrete. Only those parts of the components that are solid should be considered in any compression joint analysis, thus ruling out hollow-core slabs unless the ends are concreted solid. Special attention should be paid to convex surfaces, where contact widths may be small. Particular attention should also be given to detailing reinforcement in the precast components, especially if large cover distances, e.g. 50 mm, are required for severe fire or exposure categories, and large-diameter high-tensile bars (with large bend radii) are used. The minimum dimension for a direct contact area should be 50 mm

Figure 7.13 The architect has unwittingly demonstrated the design of the connection by contrasting the tiling in the beams and column.

(or 75 mm when using 20 mm-size aggregates in both components). The minimum contact area depends on the magnitude of the stress, but experience suggests that it should not be less than about 8000–12 000 mm^2.

In the transfer of forces through joint materials such as *in situ* mortar, neoprene bearing pads and other types of bedding, the aim is to ensure that irregular surfaces can transmit forces without damage to the contact surfaces. Unintentional eccentricities, and spurious shear forces and moments, etc. can lead to problems such as spalling and crushing, and splitting of the joined members. The thickness of the jointing material should be as small as possible, without impeding the normal tolerances. The recommended thickness is 10 mm to 15 mm. The elastic response of the bearing medium should be similar (i.e. Young's moduli differing by not more than about 20 per cent) to that of the precast concrete to avoid localised contraction and splitting forces, as shown in Figure 7.15(a). This is very important where the thickness of the joint is greater than 50 mm, because the effects of shear lag and lateral tensile stress will reduce concrete compressive stress capacity to less than 1.0 f_{ck} {0.8 f_{cu}}: Figure 7.15(b). The significance of this will be apparent later in the text, e.g. Table 7.1.

Bedded bearings are usually unreinforced. The mode of failure is by crushing of the mortar, or splitting of the precast components in contact with it. In spite of the fact that the mortar is highly confined and would, in a perfectly plain stress condition, achieve compressive strengths greater than the characteristic value, a low design strength is used because the edges of the mortar bed tend to spall off, leading to a non-uniform distribution of stress as shown in Figure 7.15(c). Poor workmanship may exacerbate the problem.

Vambersky [7.5] shows relationships between the bearing capacity of an unreinforced mortar joint in terms of the geometry of the joint, i.e. width-to-thickness ratio b/v, and compressive strengths of

Figure 7.14 The corbel is seen as a functional part of the structure, as there was no advantage in using a more complicated, hidden connection.

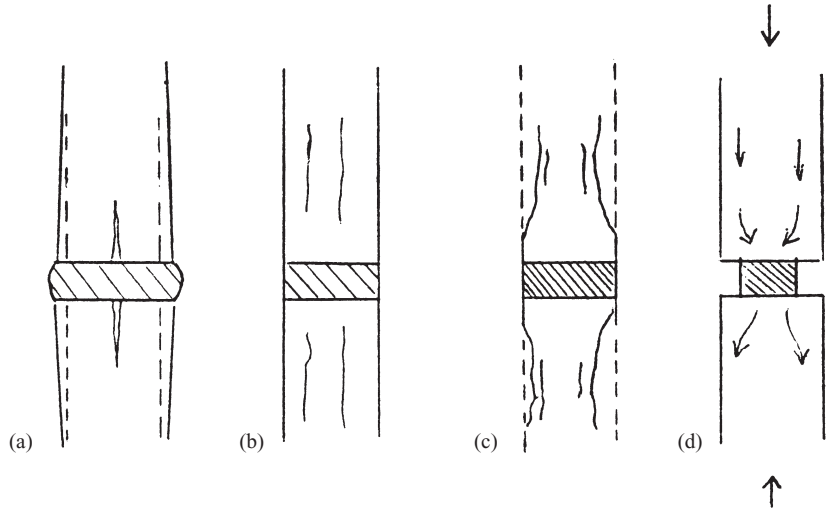

Figure 7.15 Force transfer through compression joints having an elastic modulus. (a) Less than the precast; (b) equal to precast; (c) greater than precast; (d) as (c) but with reduced breadth.

the precast concrete component f_{ck} $\{f_{cu}\}$ and *in situ* mortar $f'_{ck}\{f'_{cu}\}$. Two reduction factors are implemented – η_o reflecting the trapped air void content, and η_m to account for site-mixed mortar conditions being different from those under which the laboratory tests are conducted. For the case of precast components placed *on* to a mortar bed $\eta_o = 0.3$, and for fluid or dry-packed mortars placed after the component is in place $\eta_o = 0.9$ and 0.7, respectively. The value for $\eta_m = 0.75$ if site cubes are tested, or $\eta_m = 1.0$ if cores are cut and tested. The former is more likely.

From Vambersky's results, it is clear that a design stress of the mortar 0.4 f'_{cu} may be adopted as the bearing capacity for the joint, providing that the *b/v* ratio exceeds 8 to 10 and that the difference in strength between the mortar and precast materials does not differ by more than 25 per cent. In common practice both of these criteria are satisfied.

Barboza and El Debs [7.6] carried out ten compression tests on 175 mm square section precast stub columns, eight of which had mortar joint thickness varying from 15 to 30 mm. The ends of the columns were reinforced to prevent splitting or crushing failures before the mortars failed. Mortars were no-shrink (Fosgrout Plus®), fluid (Combextra P®), fluid with epoxy resin (Combextra EPR® for expected dynamic loads), and dry-pack/no-shrink. Compressive cylinder strengths for the mortars varied from $f'_{cm} = 25$ to $f'_{cm} = 80\ \text{N/mm}^2$, and for concrete $f_{cm} = 29$ to $68\ \text{N/mm}^2$ (mean not characteristic, $f_{cm} = f_{ck} + 8$).

The results are summarised in Figure 7.16, where the ratio $\alpha = f'_{cm}/f_{cm}$ is the basis for comparisons of experimental failure loads to the squash load of the precast column $\beta = P_{exp}/P_c$ and the mortar joint $\beta = P_{exp}/P_j$ according to Vambersky's equations [7.5]. The main concern is the high proportion of results where $\beta < 1$, particularly the experimental/design joint strength ratio, where more results should be just greater than 1. The 95 per cent confidence fit through both sets of data was surprisingly close, but was distorted by the data points for the high-strength specimens. Therefore, ignoring those points, the empirical relationship $\beta = 0.5 + 0.35\alpha$ is proposed. Thus the joint design strength $f_{cdj} = ((0.5 + 0.35 f'_{cm}/f_{cm}) - 8)/1.5$. For example, if precast $f_{cm} = 50\ \text{N/mm}^2$ and mortar $f'_{cm} = 40\ \text{N/mm}^2$, then the joint $f_{cdj} = (((0.5 + 0.35 \times 0.8) \times 50) - 8)/1.5 = 20.6\ \text{N/mm}^2$. BS EN 1992-1-1 (see clause 10.9.5.2(2)) states (with $\alpha_{cc} = 1$ for bearings) $f_{cdj} = 0.85\ f_{cd} - (\text{Min}(f_{cm}; f'_{cm}) - 8)$, which gives $f'_{cm} = 0.567(40 - 8) = 18.1\ \text{N/mm}^2$ in the same example, with good agreement.

Barboza notes that it was difficult to control the thickness of the 15 mm joint, preferring a 22 mm joint for successful filling and compacting. Where $\alpha \approx 0.75$, P_{exp} is 25 per cent greater than the squash load of the mortar. As α increases to 1.26 there is no significant increase in P_{exp}. However, when high-strength mortar is used, with $\alpha \approx 2.36$, splitting stresses in the column dominate and there is severe cracking of concrete cover. Additional links in the column close to the contact plane increase ductility, but not necessarily strength. The main conclusion is that triaxial mortar strength is approximately 1.25 times uniaxial strength, and high-strength mortars encourage cracking of cover concrete in the column – a potentially dangerous situation.

Figure 7.16 shows Vambersky's equations [7.5], based on $\eta_m = 0.75$, $\eta_o = 0.9$, and joint breadth/thickness (same value as Barboza) = 175/15 = 11.67. The results are in good agreement in the common range of $0.6 < \alpha < 1.2$.

Bljuger [7.7] presents the information in terms of an effective compressive strength $\eta_1 f_c$, where f_c is the uniaxial compressive strength of the precast members, and η_1 is a factor depending on the thickness of the joint v and the ratio of the joint strength f'_c to f_c. The data are given in Table 7.1.

A further strength-reduction factor is due to eccentricity, defined as e in Figure 7.17(a). The effect of e is to reduce the compressive strength of a joint by the factor η_1, where:

$$\eta_1 = 1 - 2e/b \tag{7.1}$$

Similarly the effect of lack of verticality, given by e' in Figure 7.17(b), reduces the strength by a factor η_3 as follows:

$$\eta_3 = 1/(1 + e'/b) \tag{7.2}$$

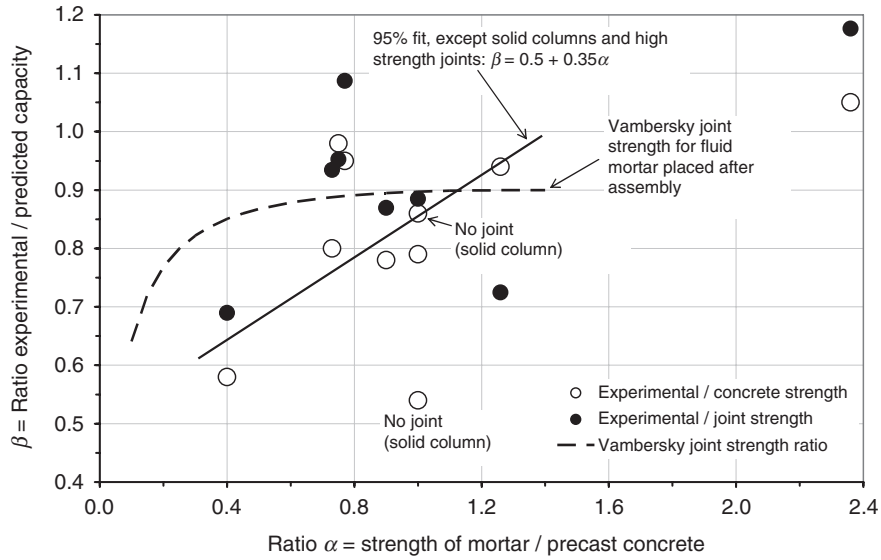

Figure 7.16 Normalised load capacity data versus mortar/precast column strength ratio [7.5, 7.6].

Table 7.1 Compressive joint strength ratios η_1 for mortar infill

	Ratio of mortar strength to concrete strength (f_c'/f_c)					
v (mm)	0.1	0.3	0.5	0.7	0.95	≥ 1.0
10	0.87	0.93	0.94	0.95	0.95	0.95
30	0.60	0.78	0.85	0.90	0.93	0.95
50	0.37	0.68	0.81	0.88	0.93	0.95

BS EN 1992-1-1 [7.8] permits the net contact area to be used with a generally lower stress, unless the requirements of Clause 6.7 for a partially loaded area are fulfilled.

In summarising the kind of information outlined above, BS 8110 suggests (in Part 1, clause 5.3.6) [7.9] that when calculating compressive strengths, the area of concrete in the joint should be the greater of:

- the area of the *in situ* concrete, ignoring the area of any intruding component, but not greater than 90 per cent of the contact area, or
- 75 per cent of the contact area.

The deformability of a compression joint also depends on the nature and number of contact surfaces between different media. In the joints shown in Figure 7.18, type (a) has two *in situ*–precast contact surfaces, while (b) has one precast–precast and one *in situ*–precast contact. The deformability of these joints differs owing to their different lateral distortion, splitting and frictional characteristics. The effect also differs between columns and walls, where splitting is unconfined in two directions in a column but only in one direction in a wall.

Generally, Table 7.2 gives the values for the basic deformability λ_o of different types of joint [7.10] expressed in linear elastic deformation per unit stress. These data may be used to determine the total

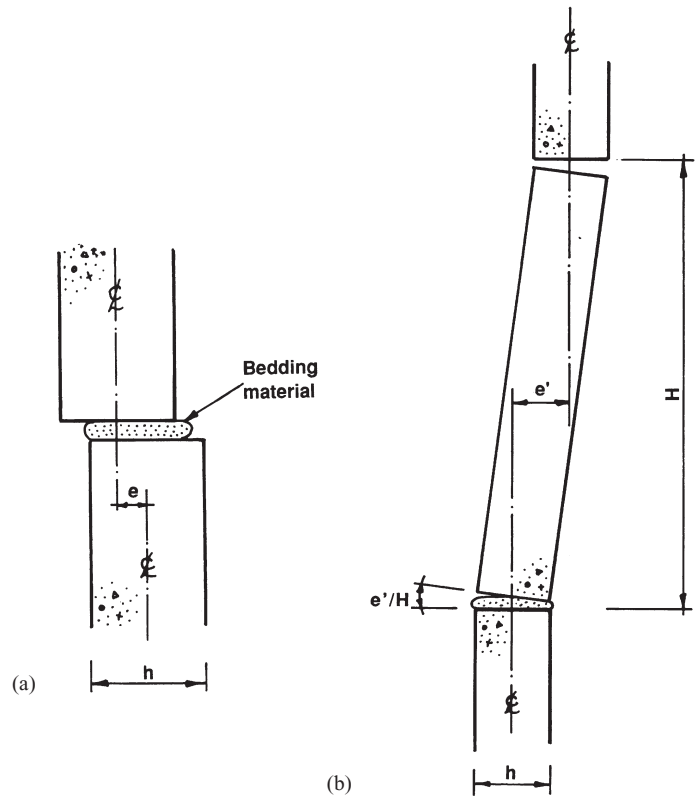

Figure 7.17 Load capacity reduction effects in compression joints. (a) Eccentricity in a compression joint and (b) lack of verticality in a compression joint.

deformability of joints and components by the method of addition of strains. For the purpose of structural analysis the members are considered homogeneous, of equivalent modulus E', and the strain in the equivalent material is that of the composite one. The deformability of a joint(s) reduces the stiffness of the connection, such that the net value for Young's modulus is given by:

$$E' = \frac{1}{1/E_c + \lambda_m/H} \tag{7.3}$$

where

E_c = Young's modulus for the infill concrete
H = storey height
λ_m = total joint deformability over the height of the storey obtained by summing the individual joint deformabilities λ_{mi} as follows.

Where an interface consists of different parts, e.g. Figure 7.18(a) and (b), the deformity of the entire interface is given by:

$$\lambda_{mi} = \frac{1}{\sum_j (n_j/\lambda_{oj})} \tag{7.4}$$

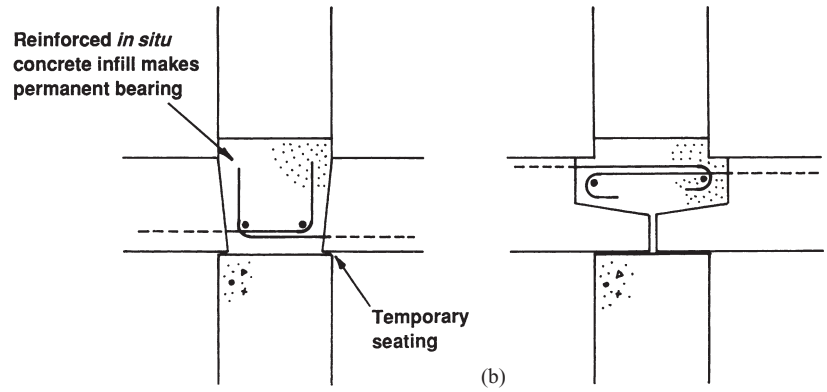

Figure 7.18 Compression joints with discontinuities. (a) Two *in situ*–precast contact surfaces and (b) one precast–precast and one *in situ*–precast surface.

Table 7.2 Deformability λ_o of different joints in compression (mm/N/mm^2)

		Grade of mortar		
Type of joint	**Diagram**	**<1 N/mm^2**	**5 N/mm^2**	**>10 N/mm^2**
Wall to wall	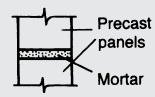	0.10	0.06	0.04
Wall to wall	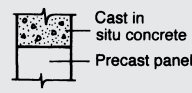	–	–	0.02
Column splice	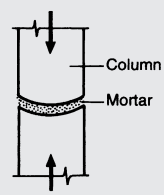	–	–	0.02

where n_j is the number of interfaces having a basic deformability λ_{oj}, as given in Table 7.2. Each value of λ_{oj} is proportional to the width of the bearing divided by the width of the interface b_j/h.

Elliott carried out tests on precast–*in situ* concrete compression joints using unreinforced 100 mm cube sections representing scaled-down versions of 300 mm-sized components. The specimens comprised a sandwich of grade C32/40 precast concrete with grade C15/20 infill of 100, 50, 25 and 0 mm thickness. The maximum size of aggregates used was 10 mm, and the sand was finely graded to allow for the scale factor. Figure 7.19 shows the failure of the 50 mm thick infill specimen, where the predominant cracking is seen in the lower strength infill. Figure 7.20(a) shows stress–strain data for the various tests, and Figure 7.20(b) the relationship between λ_m/H and b/v. The data show that the elastic compressive deformability of 25 mm to 50 mm-deep joints of grade C15/20 concrete between grade C32/40 precast components equates to a value between 0.03 and 0.06 mm per 1.0 N/mm^2 compressive stress for a storey height of 3.0 m. The results from this work are in good agreement with that of Bljuger.

Similar tests were also carried out by Elliott, in which the compression was induced over the precast–*in situ* interface by bending a prismatic section. These results are independent of the thickness of the infill, and give a single value of 0.02 mm per unit compressive stress for a storey height of 3.0 m, i.e. the flexural joint deformability is less than in the axial compression mode.

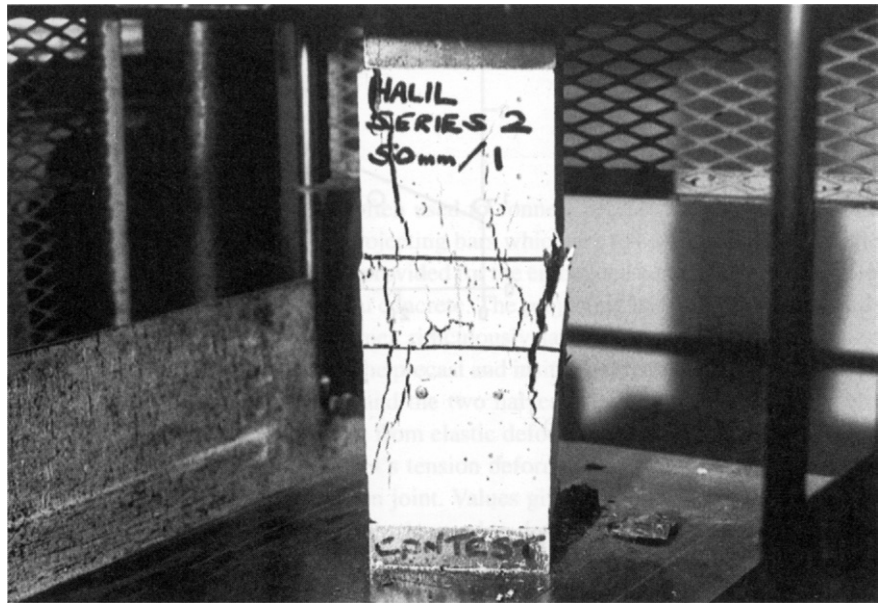

Figure 7.19 Compression test where precast is twice *in situ* strength.

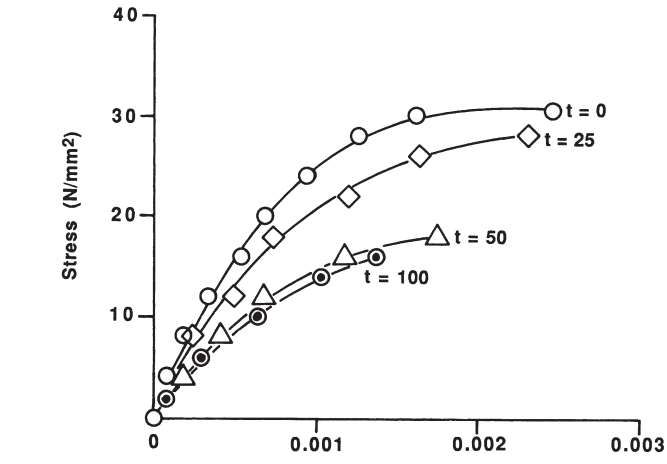

(a)

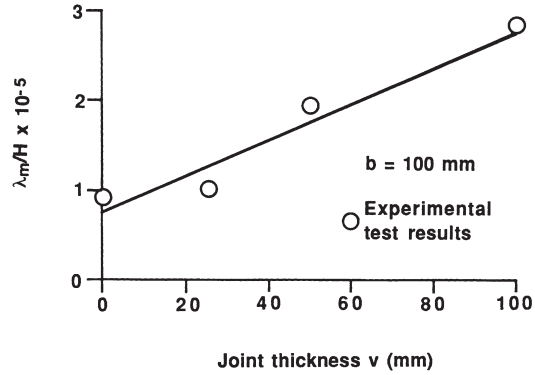

(b)

Figure 7.20 Deformation factors in compression joints. (a) Stress versus strain relationships at precast–*in situ* concrete interfaces and (b) values for λ_m versus b/v in compression tests.

Exercise 7.1

Determine the effective Young's modulus for the compression joint shown in Figure 7.21. The infill concrete and the mortar are grade C30/37 and C16/20, respectively. Coarse and fine aggregates are gravel and crushed gravel.

Solution

The deformability of the upper mortar bedding $\lambda_o = 0.04\,\text{mm/N/mm}^2$.
The deformability of the *in situ* infill $\lambda_o = 0.02\,\text{mm/N/mm}^2$.

For the slab bearing:

$n_1 = 2$ for the mortar bedding, with $b_1/h = 70/200 = 0.35$
$n_2 = 1$ for the *in situ* infill concrete, with $b_2/h = 60/200 = 0.30$

Then

$$\lambda_m = \frac{1}{(0.35\times 2/0.04)+(0.3\times 1/0.02)} = 0.031$$

The total deformation is the summation
$\lambda_m = 0.04 + 0.031 = 0.071$

E_c for the infill concrete = $29\,\text{kN/mm}^2$
Hence:

$$E' = \frac{1}{1/29000 + 0.071/3000}\times 10^{-3} = 17.2\,\text{kN/mm}^2$$

E_c for the infill concrete = $25\,\text{kN/mm}^2$
Hence:

$$E' = \frac{1}{1/25000 + 0.071/3000}\times 10^{-3} = 15.7\,\text{kN/mm}^2$$

i.e. a reduction of 32 {41} per cent compared with the modulus of the *in situ* infill.

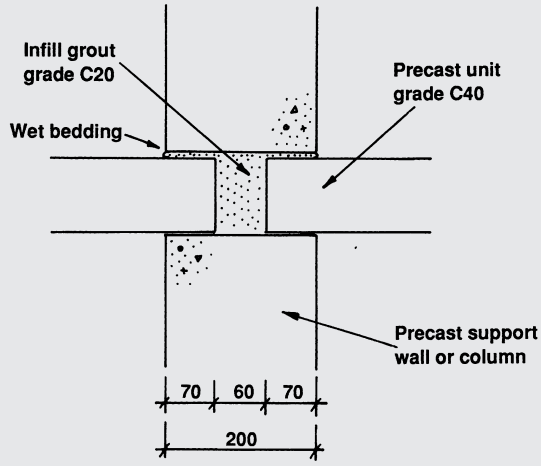

Figure 7.21 Details for Exercise 7.1.

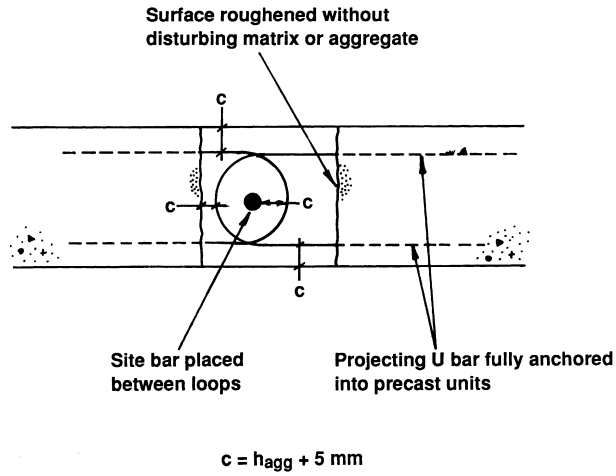

Figure 7.22 Tension joints by lapping reinforcement in cast *in situ* infill.

Table 7.3 Deformability λ_o of different joints in tension (mm/N) $\times 10^{-5}$

	Type and diameter of bar (mm)							
	Deformed bar				Plain bar			
Type of joint	**6**	**8**	**10**	**16**	**6**	**8**	**10**	**16**
Straight bar in tension	4.0	2.5	2.0	1.3	5.2	3.2	2.6	1.7
180° U-bar in tension	3.2	2.0	1.6	1.0	4.2	2.6	2.1	1.4
90° hooked bar in tension	6.4	4.0	3.2	2.1	8.4	5.2	4.2	2.8

Such differences in strain response between members connected in different locations and with different details lead to shear lag between adjacent components. These must be considered in the design.

7.5.2 Tensile joints

Lapping of reinforcement bars is often used to connect precast members, as shown in Figure 7.22. The precast units have projecting bars that interleaf vertically and are to be embedded *in situ* after erection. A full anchorage length is provided for the embedded bar, and this is calculated according to the same rules as for *in situ* concrete. The projecting bars are usually hooked a full 180°, otherwise the lap becomes ridiculously large. Despite the full anchorage provided for the bars embedded in the precast and *in situ* concrete, bond stresses quickly break down close to the interface and the two halves of the joint may be considered separately. A tensile crack resulting from elastic deformation in the bar and slippage is formed in the interface and the joint's tension deformability may be calculated in the same manner as for the compression joint. Values given in Table 7.3 are based on the work of Bljuger [7.11]. These data may be used to determine crack widths in flexurally loaded precast–*in situ* interfaces.

With vertical lapping, the main problem is to ensure that the *in situ* concrete forms a full and positive bond with the steel bars. Pressurised grout is inserted through a hole beneath the level of the lap, and the appearance of the grout at a vent hole above the top of the lap is used as an indication of complete filling, as illustrated in Figure 7.23. The annulus should be at least 6 mm clear on all sides of the bars [7.12].

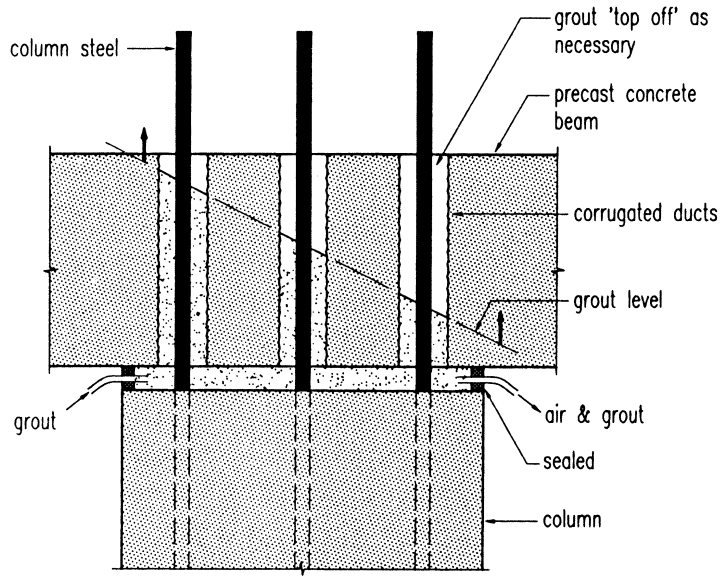

Figure 7.23 Grout injection at beam to column connections [7.8].

Use clean water to flush out any debris inside the hole before grouting. The water should wet the sides of the hole without ponding. The grout should be non-shrinking and be sufficiently flowable to allow pressure grouting through a 20 mm-diameter nozzle using a manually powered hand pump. A 2:1 sand–cement mix containing a proprietary expanding agent is used to give 24-hour strengths of 16 {20} N/mm^2 and 28-day strengths around 50 {60} N/mm^2. Note that the grading of the sand is crucial to the ultimate strength of this grout.

Grouting may be carried out by gravity pouring, but the annulus must be vented, or sufficiently large in diameter, e.g. 50 to 60 mm for a 25 mm bar, to prevent air pockets from forming.

Bolting is used extensively to transfer tensile and shear forces. Anchorages such as bolts, threaded sockets, rails or captive nuts attached to the rear of plates are anchored in the precast units. Tolerances are provided using oversized or slotted holes in the connecting member. The tensile capacity of bolted connections should be governed by the yield strength of the bolt, as this gives a ductile failure. In most types of bolted joint, tension is accompanied by shear. Shear capacities are governed by the local bearing strength of the concrete in contact with the shank of the threaded bolt. Shear bolt failures are brittle and should be avoided. The *PCI Manual* [7.13] gives design data for bolting.

Welding is used to connect components through projecting bars, fully anchored steel plates or rolled steel sections, etc. The joint is made either directly between the projecting bars, as shown in Figure 7.24(a), or indirectly using an intermediate bar or plate, as shown in Figure 7.24(b).

Post-tensioning is used to resist tension and shear forces by the application of clamping forces across the joint. Cable ducts are inserted into the precast concrete components, or in the spaces around the components and, after erection, the cables are placed in the ducts and post-tensioned. Tensile capacities are computed from the state of stress in the post-tensioned components, and shear resistance is calculated using the shear friction hypothesis.

7.5.3 Shear joints

It is most important that shear resulting from flexural actions, for example in composite precast–*in situ* beams in bending, must be considered separately from shear derived from shear forces. The former was discussed in Section 6.7, while the latter concerns the transfer of direct shear forces between precast components through bond, friction, welds, shear keys and shear reinforcement, as shown in Figure 7.25(c) with their associated failure modes. The graphs in Figure 7.25(b) are plots

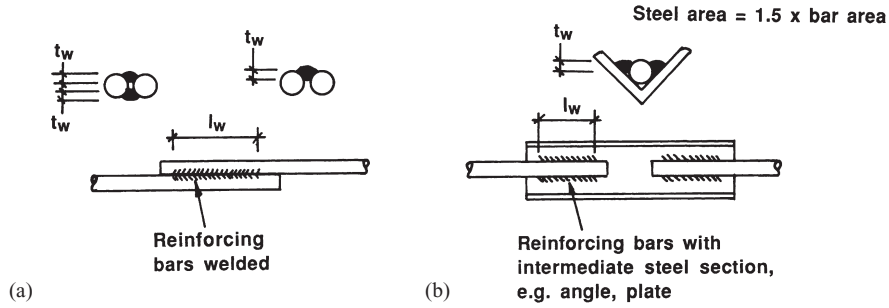

Figure 7.24 Tension joints by welding reinforcement. (a) Direct joint and (b) indirect joint.

of shear force versus shear slip. The gradient of these curves gives the shear stiffness, which forms the basis of shear deflections in precast construction, i.e. shear deformation is the sum of joint slip and element deformation.

When a joint face has surface roughness, shear forces can be transmitted by friction even if the joint is cracked, but normal compressive stresses must act across the joint, either actively by an external force, or passively by the clamping action of reinforcement, shown in Figure 7.26. In some joints, e.g. horizontal joints in precast infill walls (Section 8.7.1), the weight of the wall and the resultant of the diagonal reaction above the joint result in permanent compressive stresses in the joint.

Shear friction should be used where the available shear interface is large, e.g. between precast floor units and *in situ* structural topping, and the possibility of delamination, e.g. due to vibrations, is small. No attempt should be made to deliberately roughen the surface texture of precast units beyond the usual machine slip-formed, extruded or tamped finish. Large crevices harbour grease and debris, and provide possible sites for water to accumulate immediately before concreting commences (see Section 6.2.2). The shallow shear key provided by the normal trowelling procedures is not only structurally adequate in terms of interface stress, but has greater quality control. If no external normal force is present, then reinforcement should be provided across the shear plane to ensure that the shear friction is mobilised. The limiting ultimate shear stress is $v_{Rdi} = c\, f_{ctd}$, where c is given in Table 6.2 according to BS EN 1992-1-1, clauses 6.2.5(1) & (2) [7.8], e.g. if $c = 0.2$ and $f_{ck} = 25\,\text{N/mm}^2$, $v_{Rdi} = 0.24\,\text{N/mm}^2$, or $v_h = 0.23\,\text{N/mm}^2$, according to BS 8110, Part 1, clause 5.3.7(a) [7.9].

Deeper shear keys may be deliberately formed, as shown in Figure 7.25(c). The indented root depth should be at least 5 {10} mm. The design is satisfied by following a few simple rules regarding geometry and cover distances. The angle α depends on the dimensions of the keyed surface. The resulting force N has a magnitude $N = V \cot \alpha$ with $\alpha > 60°$ {$\alpha = 40°$ to $50°$}, which must be carried either by reinforcement of area A_s crossing the interface, a precompression P from external sources (post-tensioning for example), or a combination of both such that:

$$A_s = \frac{V \cot \alpha - P}{0.87 f_y} \tag{7.5}$$

Sufficient reinforcement should be provided to control cracking, and the water content of the *in situ* infill should be low, e.g. about $160\,\text{kg/m}^3$, with a superplasticiser being used to maintain medium workability.

Shear keys rely on mechanical interlock and the development of a confined diagonal compressive strut across the shear plane. A taper is usually provided to aid removal from formwork. Figure 7.27 shows the dimensional requirements of BS EN 1992-1-1, figure 6.9. This also assists in confining the concrete in the second direction. Failure is generally ductile owing to the warnings given by concrete cracking in this way. However, as with shear friction methods, the interfaces should be prevented from moving apart, either explicitly by external forces, or implicitly by placing reinforcement according to Eq. (7.5) across the shear plane.

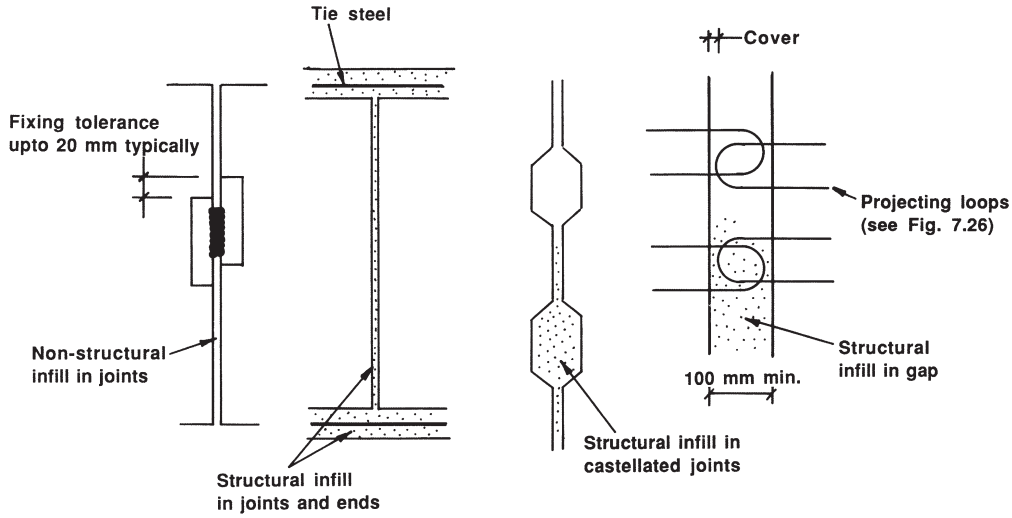

(a)

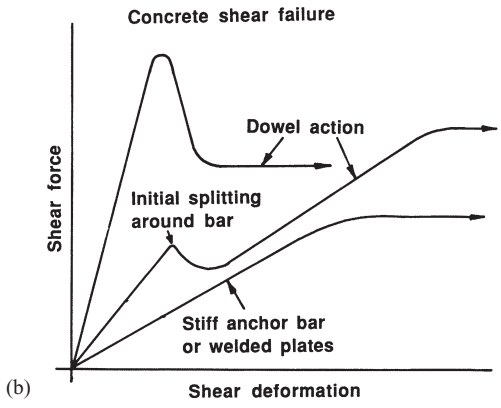

(b)

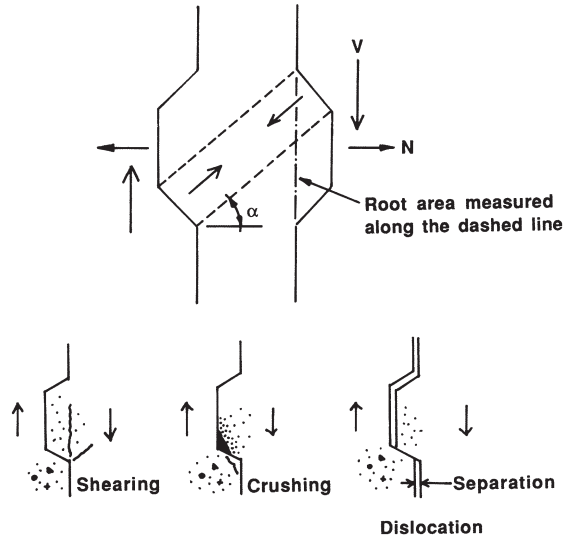

(c)

Figure 7.25 Design methods for shear joints. (a) Shear joints; (b) shear force versus slip behaviour; (c) deep keyed shear joint.

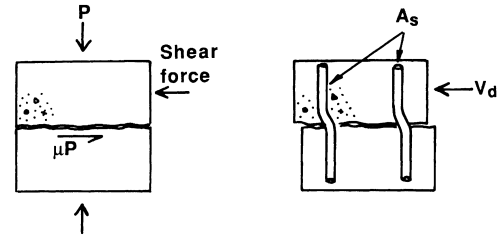

Figure 7.26 Shear friction hypothesis.

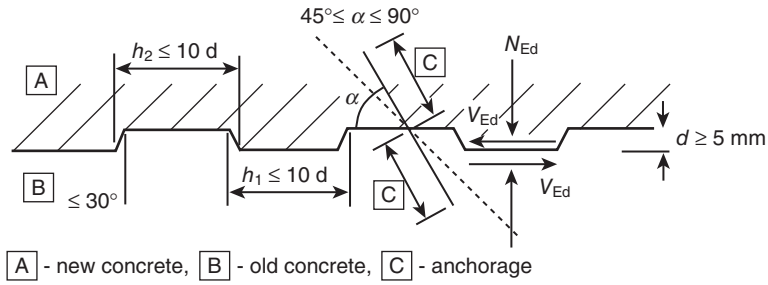

Figure 7.27 Indented shear key profile according to BS EN 1992-1-1, figure 6.9.

The approach to the ultimate shear resistance is different in BS EN 1992-1 and BS 8110. In BS EN 1992-1-1, for indented joints without dowel bars $v_{Rdi} = c\, f_{ctd}$, where $c = 0.5$ and $f_{ctd} = 0.14 f_{ck}^{2/3}$. If this is exceeded, $v_{Rdi} = c\, f_{ctd} + A_{sw}\, f_{yd}\, (\mu \sin\alpha + \cos\alpha)/A_j$ where $\mu = 0.9$, and reinforcement of area A_{sw}, inclined at $45° \le \alpha \le 90°$ to the shear plane, is acting over an area A_j. This clause is not applicable where $\alpha > 90°$, i.e. the $\cos\alpha$ component will be negative and is deemed not to be active, such that $v_{Rdi} = c\, f_{ctd} + A_{sw}\, f_{yd}\, (\mu \sin\alpha + \cos\alpha + \sin\,(180 - \alpha))$. Providing that the restraint is present, BS 8110, Part 1, clause 5.3.7(b) [7.9] states that no interface shear reinforcement is required if the ultimate shear stress $v_u \le 1.3\,\text{N/mm}^2$, when calculated on the minimum root area.

Where shear reinforcement is used the strength of the interface is based on the shear strength of the reinforcement alone, called 'dowel action' or 'dowel shear'. Dowel bars are usually H12 to H20, or may even use pretensioning helical strand of 9.3 to 15.2 mm diameter.

As shown in Figure 7.26, it is not possible to add concrete-to-concrete frictional forces to direct dowel forces, because when the latter is being mobilised the former is not, and vice versa. The shear capacity of a steel bar loaded in pure shear is estimated by adopting the yield criterion by von Mises, which is expressed as

$$V_{Rd} = f_y A_s/\sqrt{3} \approx 0.6 f_y A_s \text{ (note } \gamma_m = 1.15 \text{ not used here).} \tag{7.6}$$

Experimental results show this to be applicable. Test results [7.2] of headed dowel pins found $V_{Rd} = \alpha f_y A_s$ with α ranging from 0.55 to 1.0; therefore $\alpha = 0.6$ is a mostly conservative figure.

Referring to Figure 7.28, the dowel bar is loaded by shear V_d at the top of the beam, which is supported by a contact pressure along the part that is embedded in the column or beam, but not the sum of both. This results in flexural deformations (kinking) and flexural stresses (formation of one or more plastic hinges in the dowel). Local crushing occurs in the surrounding concrete at point A. The resistance V_{Rd} increases with increased dowel area A_s, f_{cu} and f_y. If a gap forms between the surfaces, or there is an initial eccentricity, V_{Rd} decreases considerably. An eccentricity of the same magnitude as the bar diameter results in a reduction of the shear capacity by about 0.4 to 0.6.

For concrete subjected to high bearing stresses in a local area, if splitting is prevented a near-triaxial state of stresses is obtained and hence a design bearing stress of $f_{Rdu} \le 3.0\, f_{cd}$, which may

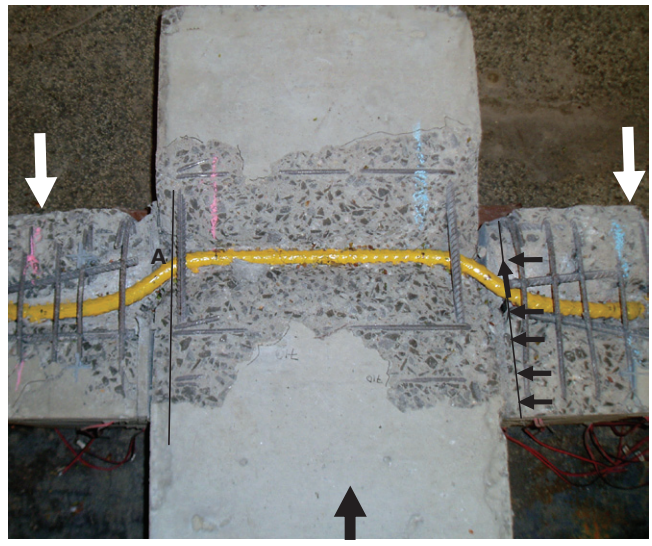

Figure 7.28 Mechanism of dowel action providing shear resistance by bending resistance and clamping pressures, as indicated.

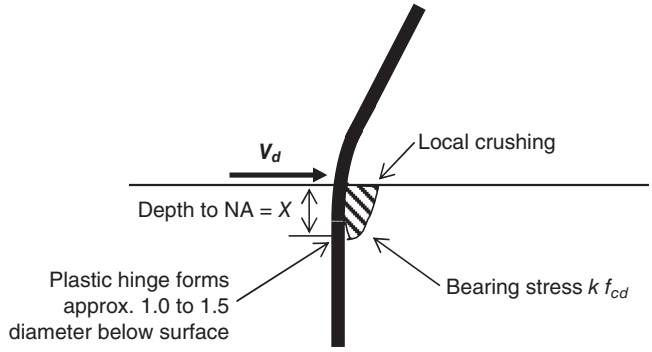

Figure 7.29 Plastic hinge model for dowel resistance.

be used in BS EN 1992-1-1, clause 6.5.4(6). In Figure 7.29 generally $f_{Rdu} = k\ f_{cd}$, where k varies depending on confinement. The *fib Manual* ([7.3], Section 8.2.1.4) reports on $k \approx 3$ to 4. At the formation of a plastic hinge, the depth to the neutral axis $X = V_{Rd}/k\ f_{cd}\ \phi$. The moment $M_{Ed} = V_{Rd}X - kf_{cd}\phi X^2/2 = V_{Rd}^2/2kf_{cd}\phi$. The plastic section modulus for a round bar $= \phi^3/6$; then $M_{Rd} = f_y\ \phi^3/6$. For example, for grade C40/50, $f_y = 500\,\text{N/mm}^2$ and $\phi = 20\,\text{mm}$, $k = 3$, $M_{Rd} =$ 666 667 Nmm, and $V_{Rd} = 46.1\,\text{kN}$. The pure shear capacity $= 0.6 \times 500 \times 314 = 94.2\,\text{kN}$. According to CEB/FIP model code MC90 [7.14], the shear displacement δ_s needed to mobilise the shear capacity is about 0.05ϕ, although the *fib Manual* shows it is closer to 0.2ϕ for $f_{cd} = 50\,\text{N/mm}^2$ and 0.3ϕ for $f_{cd} = 20\,\text{N/mm}^2$. Therefore a typical value is about $\delta_s = 0.25 \times 20 = 5\,\text{mm}$, which is quite large.

If a dowel bar is threaded into an insert, there will always be a projecting portion of exposed thread with a reduced cross section, typically about 75 per cent of the gross area; the plastic moment capacity is reduced compared to V_{Rd} above. According to the *fib Manual*, the reduction factor is $\sqrt{(1+(M_{p,thread}\,/\,M_p)}$, approximately 0.7 for $\phi = 20\,\text{mm}$.

Shear stresses in welded joints may arise from direct shear or torsion. The usual structural models and material properties for the design of welds are used. Due consideration should be given to manufacturing and construction tolerances when specifying weld lengths, because the adjoining elements are captured in the precast components. This means adding 10 mm to 15 mm to the length of a weld.

Figure 7.30 Shear jointing by site welding together steel plates in precast wall and column components.

Figure 7.30 shows an example of the use of welded shear joint in the construction of a shear wall panel-to-column connection.

Shear deformations are the result of localised damage at the shear interface. Walraven and Mercx [7.15], Bljuger [7.16], and others have produced expressions for shear deformations in cracked concrete interfaces. The theory assumes that sliding movement between two faces is the result of matrix damage, which is related to the stiffness of the cement paste and hence to E_c of the concrete. In addition, the state of stress at the interface influences the damage in the paste and therefore the normal stress σ_n, which is proportional to the area of reinforcement crossing the cracked plane, is also important.

Elastic shear deformabilities, expressed in units of mm displacement per kN applied shear force, are given in Table 7.4 [7.11].

where

ϕ = diameter of rebar (mm)
E_{c1}, E_{c2} = elastic moduli of precast and *in situ* concrete, respectively (kN/mm^2)
E_c = smaller of E_{c1} and E_{c2} (kN/mm^2)
A_k = contact area at root of castellation (mm^2).

Type I joints using grade C20/25 and C40/50 concrete were also studied by Elliott using pairs of equal-strength precast blocks containing one of three diameters of helical strand: 9.3, 12.5 and 15.2 mm, shown in Figure 7.31(a). The results given in Figure 7.31(b) are in good agreement with the

Table 7.4 Shear deformabilities (mm/kN)

Description of joint	Diagram	Shear deformability (mm/kN)
Type I	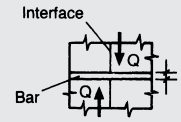	$\frac{6}{\phi}\left(\frac{1}{E_{c1}}+\frac{1}{E_{c2}}\right)$
Anchor bar cutting through shear plane	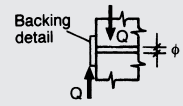	$\frac{6}{\phi E_{c1}}$
	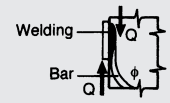	$\frac{1.5}{\phi E_{c1}}$
Type II	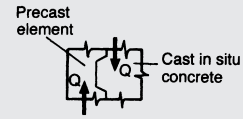	$\frac{0.5}{E_c A_k}$
Concrete element cutting through shear surface	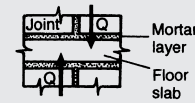	5×10^{-3}
Type III Reinforced concrete flexural member connecting walls	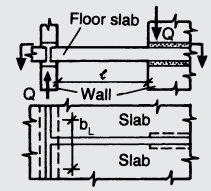	To be determined as given in text

values obtained from Table 7.4. For example, experimental joint deformations are in the range 10 to 24×10^{-3} mm/kN. Calculated values from Table 7.4 for the same geometry and material moduli are between 15 and 24×10^{-3} mm/kN for grade C20/25 concrete, and between 12 and 19×10^{-3} mm/kN for grade C40/50 concrete.

The results in Figure 7.31(b) also show that the increase in dowel capacity is proportional to the cube root of the concrete strength ratio, i.e. $\sqrt[3]{50/25} = 1.26$. Because the failure mode is governed by the shear-tension capacity of the concrete it is hardly surprising to find that the effect of increasing diameter is small, i.e. less than 25 per cent for increases in cross-sectional area of up to 2½ times. This observation does not agree with the data given in Table 7.4.

Shear deformations in Type III joints cause shear, bending and rotational deformations within the joint, idealised in Figure 7.32. The shear stiffness is given by k_s, where:

$$k_s = \frac{E_c bh}{3L} \tag{7.7}$$

where L, b and h are the length, breadth and depth of the element. Shear deformations are not influenced by end conditions.

The flexural stiffness is given by k_b, where:

$$k_b = \frac{12E_c I}{a_1 L^3} \tag{7.8}$$

(a)

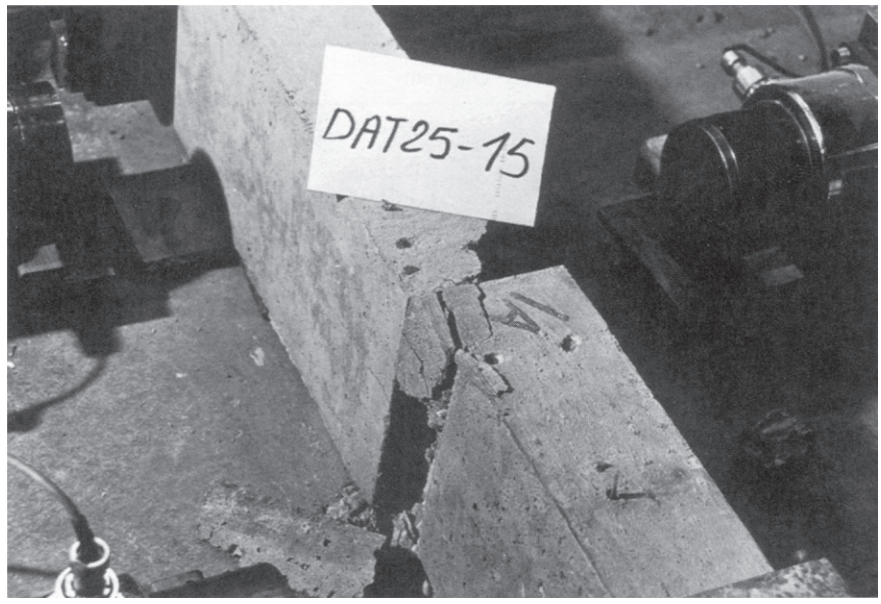

(b)

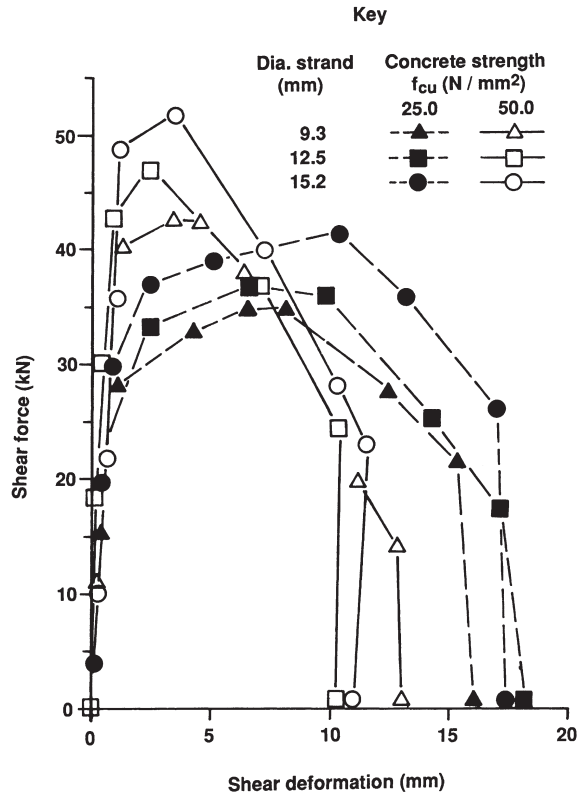

Figure 7.31 Shear joint tests by Bensalem at Nottingham University. (a) Experimental shear joint tests and (b) results from tests.

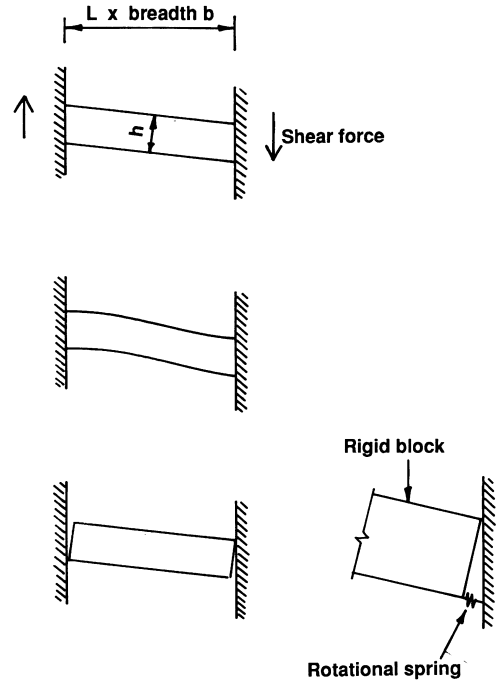

Figure 7.32 Components of shear deformations.

where I is the second moment of area of the element in the plane of bending, a_1 is a factor; $a_1 = 1$ if both ends of the element are clamped, and $a_1 = 4$ if one end is clamped and the other end pinned.

The stiffness due to joint rotation is given by k_j, where:

$$k_j = \frac{b}{a_2 K L^2} \tag{7.9}$$

where a_2 is a factor; $a_2 = 0.5$ if both ends of the element are clamped, and $a_2 = 1$ if one end is clamped and the other end pinned, and K = bending deformability within the joint itself according to Table 7.5 [7.16] and Figure 7.33.

7.5.4 Flexural and torsional joints

Flexural and torsional forces may be resolved into a couple generating direct tension, direct compression, and shear. The strain gradients across these joints are often large and so the materials making up the joint will behave differently under combined stresses of differing magnitude (rather in the same manner as the Brazilian and beam rupture tests give different tensile strengths). The main types of flexural joint are shown in Figure 7.34(a), where a couple is generated between concrete in compression and steel in tension and shear. A 'cold' joint should not be left between the precast and *in situ* concrete in the compression zone. This is the term used to describe the placement of wet concrete against an ex-mould precast surface with no preparation or applied bonding agents.

It is also important that the concrete is adequately confined, either by the use of binding links (see Section 10.2) or by the correct use of a bearing pad to prevent lateral bursting, as explained in Section 7.3.1. The main design criterion for the tension force is adequate anchorage, which is usually provided by casting a fully anchored steel plate or threaded socket, etc. into one or both adjoining members. Space is often at a premium in these joints and so use of a large number of smaller components in the joint is recommended, rather than a small number of large components. The former option has the added advantage of being able to yield and dissipate energy in case of overloading.

Table 7.5 Bending deformability of an element clamped over a distance L_s

L_s (mm)	50 min	100	150	> 200
K (mm/kNm/m)	0.00020	0.00015	0.00012	0.00010

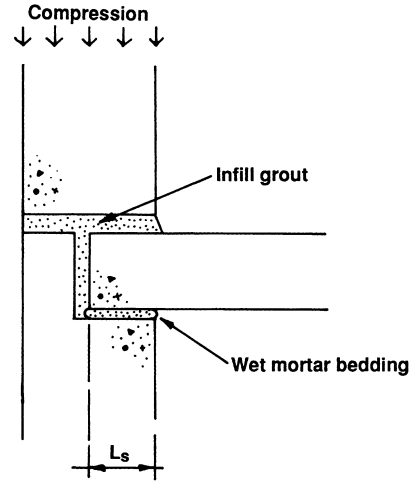

Figure 7.33 Definiton of clamping and restraint factors in flexure and shear connections.

Empirical rules for the detailing of projecting loops are given in Figure 7.34. The bearing stresses inside the loop are governed by BS EN 1992-1-1, clause 8.3(3), Eq. 8.1 [7.8] or BS 8110, clause 3.12.8.25 [7.9]. Semi-circular loops of internal radius approximately six times the bar diameter may be used to satisfy the bursting stresses; otherwise a straight portion must be added to the loops making the splice zone larger. Lateral reinforcement of at least equal cross-sectional area to the loops should be provided through the loops.

7.6 Bearings and Bearing Stresses

7.6.1 Average bearing stresses

It is inevitable that some of the joints in precast frames will rely on one member bearing directly onto the cast surface of another member. Bearings are designed for structural strength and integrity, and BS 8110 Part 1, clause 5.2.3 recognises the latter in stating that:

> *. . . the integrity of a bearing is dependent on two essential safeguards: (a) an overlap of reinforcement in reinforced bearings, (b) a restraint against loss of bearing through movement . . .*

and, it might be added, on avoiding partial loss of bearing due to accumulative manufacturing and site fixing tolerances. Similarly, BS EN 1992-1-1 [7.9] differentiates between connected (tied by normal reinforcement lap requirements), and isolated (not tied) bearings, requiring greater contact areas for the latter in clause 10.9.5.3.

The simple provision of an adequate bearing length should not be underestimated. It distinguishes precast from all other forms of construction in many ways. The physical and structural aspects of bearings should not be sacrificed on grounds of aesthetics, ease and speed of construction, saving on bearing mediums, reducing bearing thicknesses, etc. The problem is sometimes compromised because

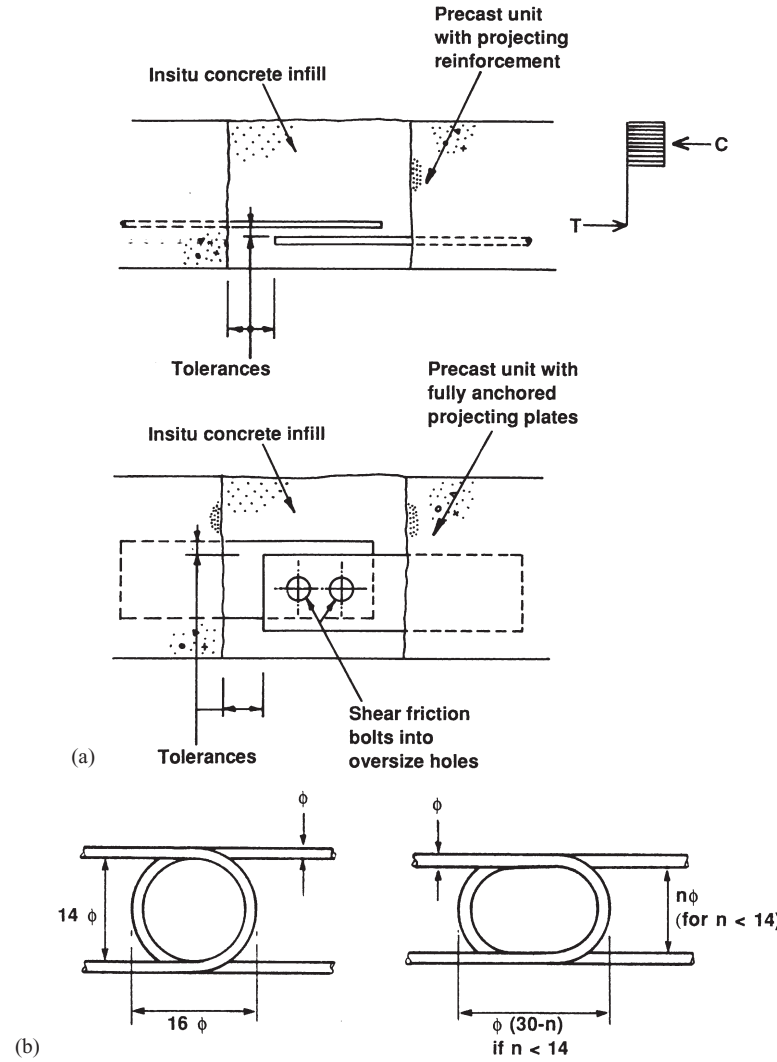

Figure 7.34 Flexural joint details. (a) Flexural jointing by welding or bolting projecting steel sections together to form a couple with the concrete in compression, and (b) dimensions of loops for correct load transfer.

it is known that actual bearing stress, when calculated using the recognised nominal dimensions, say 75 mm for a floor slab, is often less than 25 per cent of the ultimate strength; designers are therefore tempted to 'slim down'. Most of these indiscretions are shown in Figures 7.35 to 7.37.

The main types of bearing are:

- dry bearing of precast to precast or precast to *in situ* concrete
- extended bearings, where the temporary bearing is small and reinforced *in situ* concrete is used to complete the connection, seen in Figure 7.1
- dry-packed bearing, where components are located on thin (3 to 10 mm thick) shims and the resulting small gap is filled using semi-dry sand/cement grout; see Figure 7.38(a)
- bedded bearing, where components are positioned onto a prepared semi-wet sand/cement grout; see Figure 7.38(b)
- elastomeric or soft bearing using neoprene rubber or similar bearing pads; see Figure 7.38(c)
- steel bearing using steel plates or structural steel sections; see Figure 7.38(d).

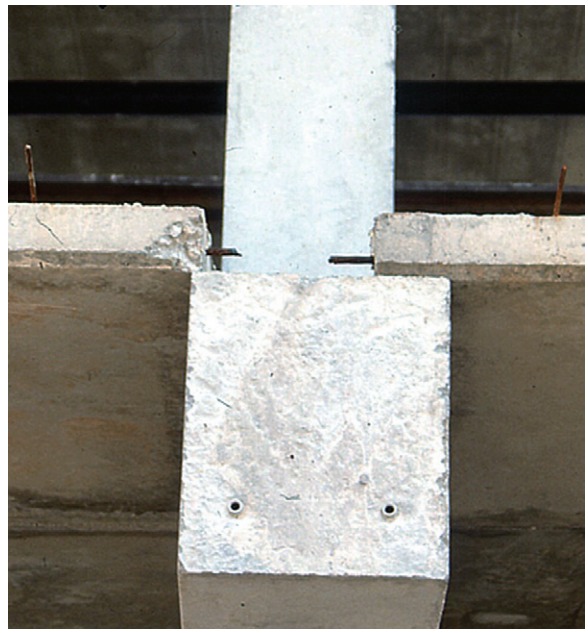

Figure 7.35 Inadequate bearing length, of around 15 mm, in the precast plank unit may not have structural implications after the topping is added, but the danger of it dislodging during construction is clearly more important.

Figure 7.36 Unequal bearing levels creating localised stress concentrations between precast floor units and beams, leading to spalling under certain conditions of movement and loading.

Figure 7.37 Omission of a bearing medium in a 200 mm-long joint enables clamping forces to cause failure in the end of the beam.

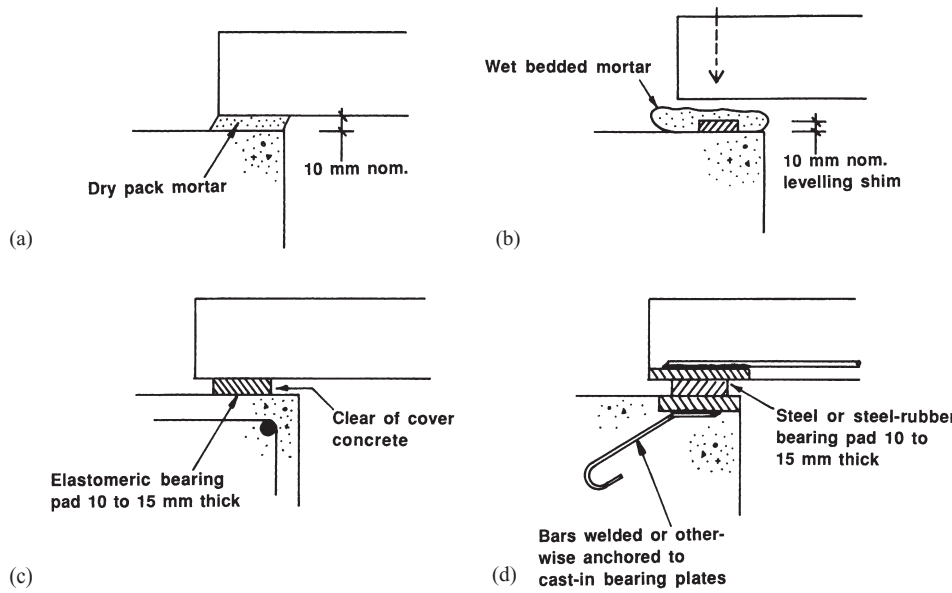

Figure 7.38 Bearing types. (a) Dry pack; (b) wet bedded; (c) elastomeric or soft; (d) anchored steel plates.

There is a broad division between precast components that are considered to be non-isolated and those that are isolated. Non-isolated components are connected to other components with a secondary means of load transfer, which would sustain loads in the event of failure in the primary support. For example, hollow-core flooring units that are grouted together would distribute shear forces to adjacent members in the event of a failure at the beam support, and would be classed as non-isolated. On the other hand, a stair-flight unit seated onto a dry corbel is an isolated component.

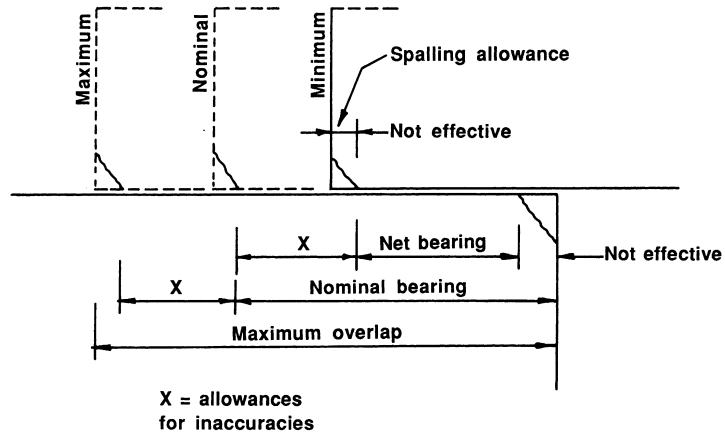

Figure 7.39 Definitions of bearing lengths and tolerances.

The design method considers the bearing stresses in both the abutting precast components and the sandwiched jointing material (if any) in between. Two values are determined in the plan dimension: bearing width, which is the greater dimension perpendicular to the direction of the span of the member, and bearing length. The effective bearing width is taken as the least of:

(1) the actual bearing width of the imposed member
(2) one-half of (1) plus 100 mm (or all of (1) if a compliant bearing pad is provided when the member is seated)
(3) 600 mm {600 mm}.

Conditions (2) and (3) are empirical values based on the acceptable degree of flatness possible in members exceeding about 1.0 m in the critical dimension.

The net bearing length, as defined in Figure 7.39 (see also Section 5.2.13), is equal to the actual bearing length minus twice the spalling tolerance, called an ineffective bearing length. Allowances for spalling are given in Tables 7.6 and 7.7. Note that the difference between the 'nominal' bearing length as cited in design details, and the actual bearing length, is equal to the sum of all inaccuracies. These equate to about 3 mm or 5 mm per m distance between faces of precast or *in situ* supports, respectively. The minimum net bearing length is usually 40 mm for non-isolated components or 60 mm for isolated components. BS EN 1992-1-1 requires increased values of 80 mm for ribbed floor or purlin bearings, and 140 mm for beam bearings, again increased by 20 mm if the supported member is isolated. The minimum nominal bearing width is about 70 mm. The ultimate bearing stress is given by:

$$f_b = \frac{\text{ultimate support reaction per member}}{\text{effective bearing length} \times \text{net bearing width}} \tag{7.10}$$

This should not exceed the design ultimate bearing stress, which is based on the cylinder {cube} crushing strength of the weakest of the two, or three, component materials (excluding masonry supports), as follows.

BS EN 1992-1-1, clause 10.9.5.2(2) ($\alpha_{cc} = 1$ for bearings) [7.8] and BS 8110, clause 5.2.3.4 [7.9]

(i) dry bearings on concrete: $0.4\, f_{cd} = 0.267\, f_{ck}$ {$0.4\, f_{cu}$}
(ii) bedded bearings on concrete or grout: $0.85\, f_{cd} = 0.567\, f_{ck}$ {$0.6\, f_{cu}$} (of the weakest medium)
(iii) elastomeric bearing (called flexible padding): between $0.4\, f_{cu}$ and $0.6\, f_{cu}$; use the lesser of $0.567\, f_{ck}$ {$0.5\, f_{cu}$} or f_c {f_c} of the bearing material.

Table 7.6 Spalling allowances at the *supporting* member

Method of support	To BS EN 1992-1-1, Table 10.3 [7.8]		To BS 8110 [7.9]
	Ineffective bearing at continuous (line) support (mm)	Ineffective bearing at concentrated support (mm)	Ineffective bearing (mm)
Steel	10	15	0
Concrete grade ≥ C30/37	15	25	15
Concrete grade < C30/37	25	35	25
Masonry	15 if stress ratio ≤ 0.4	25 if stress ratio ≤ 0.4	25
Reinforced concrete less than 300 mm deep at outer edge			Nominal cover to reinforcement at outer edge*
Reinforced concrete where loop reinforcement at outer edge exceeds 12 mm diameter			Nominal cover plus inner radius of bent bar*

* Chamfers occurring in the above zones may be discounted.

Table 7.7 Spalling allowances at the *supported* member

Reinforced at bearing	To BS EN 1992-1-1, Table 10.4 [7.8]		To BS 8110 [7.9]
	Ineffective bearing at continuous (line) support (mm)	Ineffective bearing at concentrated support (mm)	Ineffective bearing (mm)
Bars continuous over support	0	0	0
Tendons or straight bars exposed at end of member	5	15	0
Tendons, straight bars, or horizontal loops at end of member	5 but ≥ end cover	15 but ≥ end cover	10 but ≥ end cover*
Vertical loops ≤ 12 mm diameter	15	End cover + inner loop bend radius	10 but ≥ end cover*
Vertical loops > 12 mm diameter	15	End cover + inner loop bend radius	Nominal end cover plus inner radius of bent bar*

* Chamfers occurring in the above zones may be discounted.

Items (i) to (iii) are intended for wide bearings, such as slabs or nibs on walls, but not for concentrated bearings, e.g. column corbels, called 'nodes' under item (vii) and (viii) below.

(iv) concrete bearings in regions of flexural and compressive stress (e.g. where the stress distribution is more triangular than rectangular, with $\alpha_{cc} = 0.85$), $0.85 \times 0.85\, f_{cd} = 0.482\, f_{ck}$ $\{0.4\, f_{cu}\}$

(v) limiting concrete bearing stress at a node where there are *no* tension ties, and there is no bearing plate or other medium (clause 6.5.4(4), Eq.6.60):

$$\sigma_{Rd,1} = (1 - f_{ck}/250) f_{ck}/1.5 \quad \{0.6 f_{cu}\} \tag{7.11}$$

(vi) limiting concrete bearing stress at a node where there *are* tension ties in one direction (Eq. 6.61):

$$\sigma_{Rd,2} = 0.85(1 - f_{ck}/250) f_{ck}/1.5 \quad \{0.4 f_{cu}\} \tag{7.12}$$

(vii) steel bearing of width b_p cast into member or support and not exceeding 40 per cent of the concrete dimension b (in the same direction of bearing), assuming the length of bearing h is semi-infinite: $\alpha_{cc} f_{cd} \times$ confinement factor S_q; see Eq. (7.15) ($\alpha_{cc} = 0.85$ where there are transverse tension forces) $= 0.567\, f_{ck}\, S_q$ if the requirements for a partially loaded area are satisfied $\{0.8\, f_{cu}\}$. Higher bearing stresses may be used only if proved by adequate testing.

(viii) for wider bearing plates the allowable bearing stress f_b is given as follows [7.17]:

$$f_b = 0.567 f_{ck} S_q \quad \left\{ f_b = \min\left(\frac{1.5\, f_{cu}}{1 + (2b_p/b)}; 0.6 f_{cu} \right) \right\} \tag{7.13}$$

This reduced stress is to cater for diagonal tension that is directly beneath the insert and/or close to the outside face of the column. Thus for BS 8110 if $b_p/b > 0.44$, Eq. (7.13) will govern.

(ix) for a bearing plate $b_p \times h_p$ embedded in a section $b \times h$, the allowable bearing stress f_{Rdu} which may be known as $\sigma_{Rd,3}$ $\{f_b\}$ is given as follows [7.18] (BS EN 1992-1-1, clause 6.7(2), Eq. 6.63 [7.8]):

$$f_{Rdu} = \sqrt{\frac{A_{c1}}{A_{co}}} f_{cd} < 3 f_{cd} \quad \left\{ f_b = 0.6 f_{cu} \sqrt{\frac{bh}{b_p h_p}} < 2.0 f_{cu} \right\} \tag{7.14}$$

where

$$S_q = \sqrt{\frac{A_{c1}}{A_{co}}} < 3 \text{ (see Section 7.10.2)} \tag{7.15}$$

resistance area $A_{c1} = 3b_p \times 3h_p$
loaded area $A_{c0} = b_p\, h_p$.

This is based on a 2:1 sloping (63°) load spread over a depth that, in each respective direction, is the greater of $2b_p$ or $2h_p$. If the 63° line is interrupted by a free edge in one direction at $a < 2b_p$, $A_{c1} = (b_p + 2a)\ 3\ h_p$. If $a < 2h_p$, $A_{c1} = (h_p + 2a)\ 3\ b_p$. and so on. Figure 7.40, adopted with slightly different notation from the Norwegian precast manuals [7.19], shows the procedures. For example, using concrete C40/50, for 150 mm square bearing in a 500 × 300 mm section, then: from Figure 7.40, $b_2 = 3\ b_1$, but $c_a = (300 - 150)/2 = 75\,\text{mm} < 150\,\text{mm}$, and

$$f_{Rdu} = \sqrt{\frac{(3 \times 150) \times (150 + 2 \times 75)}{150 \times 150}} \times \frac{40}{1.5} = 65.3\ \text{N/mm}^2$$

$$\{f_b = 0.6 \times 50 \times 2.58 = 77.4\ \text{N/mm}^2\}$$

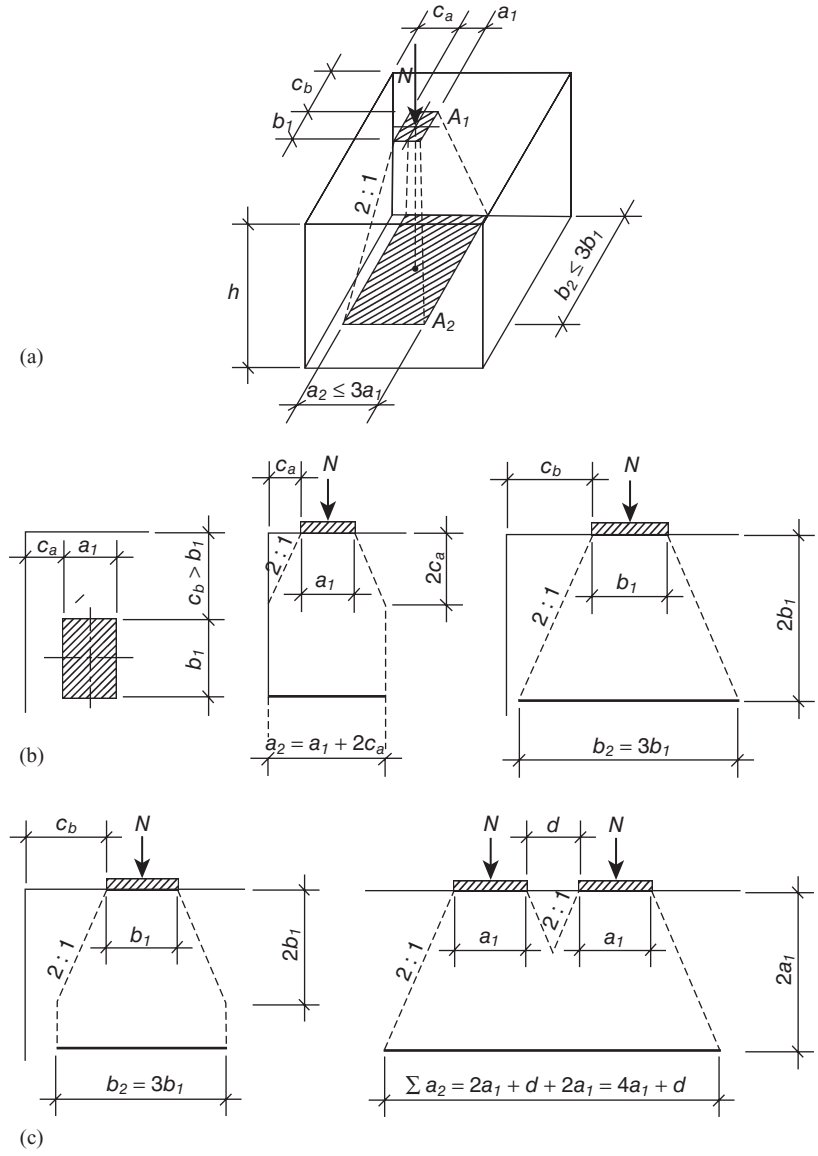

Figure 7.40 Compressive stress control, adapted from *Betongelementboken* (2005) [7.19]. (a) General load distribution; (b) edge distance; (c) overlapping loads. (Courtesy Betongelementforeningen (www.betongelement.no.)

7.6.2 Localised bearing stresses

In some cases localised bearing stresses will be much greater than the allowable ultimate values given above. Providing that the zones of localised high bearing stress are confined in the normal reinforced concrete manner, these stresses may be treated separately and considerable enhancements in allowable values are permitted. If steel inserts or bearing plates have cast-in reinforcement welded to their backs, local bearing stresses up to 0.85 f_{ck} {0.8 f_{cu}} may be used. Test results [7.20] show that in columns, ultimate values equal to 1.0 f_{cu} were achieved using H and I section inserts. The *IStructE Manual* [7.21] recommends:

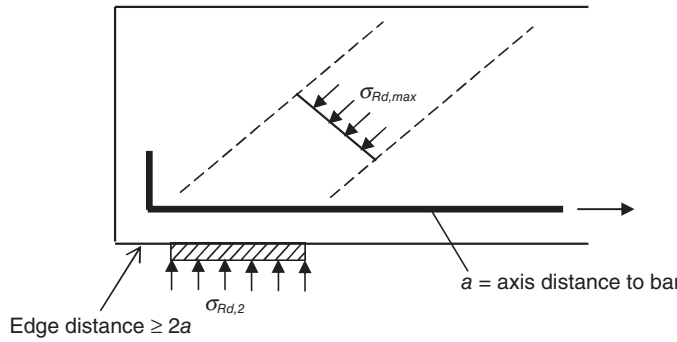

Figure 7.41 Concrete compressive stress in bearings with tension tie in one direction (after [7.8]) based on Eq. (7.12).

> *. . . where a local load represents a small part of the total loading, its influence can be neglected. It is difficult to provide clear guidance to cover all cases, but broadly, local effects can be ignored where the overall load does not exceed 80% of the allowable capacity, or where the local load does not represent more than 20% of the total load.*

BS EN 1992-1-1 [7.8] clearly defines in Clauses 6.5.4(5) & (6) the geometric and confinement conditions that permit such enhancement, but provide no exemption from design calculation.

Localised stresses may also result from the rotations of flexural members at simple bearings. Where rotations exceeding 0.01 radians are anticipated, suitable soft bearing membranes should be used to accommodate the rotation. A suitable material for 0.02 radians of rotation is 10 mm thick × 150 mm square neoprene pad. Otherwise, rotations will shift the line of action of loading onto a knife edge near to the end of the spalling zone.

Finally, the combination of vertical load V and a significant horizontal load H can reduce the vertical bearing capacity by causing splitting or shearing in the supporting member. Where $H > V \tan 20°$, allowances should be made by providing sliding bearings, lateral reinforcement in the top of the supporting member, or continuity reinforcement to prevent splitting in the supported member.

7.7 Connections

7.7.1 Pinned connections

Pinned connections transfer purely shear forces, both for (dominant) gravity and uplifting forces. The connections lend themselves to simple detailing and construction, and may be formed in the simplest manner by element-to-element bearing. To increase bearing capacities and reduce the localised spalling, steel inserts are frequently used by anchoring plates (or rolled structural sections) into the connecting elements. The connection is completed by surrounding the steel inserts with cementitious grout for fire and durability protection.

7.7.2 Moment-resisting connections

7.7.2.1 Full-strength and rigid moment connections

Fully moment-resisting connections, simulating monolithic ones in cast-*in situ* frames, are possible in many situations, in particular at foundations and between beams and columns. Cast-*in situ* connections are themselves not fully rigid, but have a flexural stiffness in the order of 70–90 kNm per mrad (10^{-3} radian). To place that in context, the flexurally cracked stiffness of a 6.0 m long × 600 × 300 mm beam (4H25 bottom bars) using $E = 30\,\text{kN/mm}^2$, $K = 3EI/L = 36\,\text{kNm/mrad}$, i.e. the

connection has twice the stiffness and same strength as the beam. The reason for this is that the column is also flexible, and unless the beam loading and span are exactly symmetrical, will introduce some flexibility there.

Moment-resisting foundation design is dealt with in Section 7.14, but the method of casting or bolting a steel plate onto the end of one component and then connecting the plate to another component through waiting bars may be exploited elsewhere if space permits, such as at upper-floor column splices.

If the connection is to be structurally useful, either in relieving sagging moments in beams or in increasing the global frame stiffness, moments of resistance of at least 50 kNm to 75 kNm are required for this purpose. If the moment is less than this, then it is probably better to design the connection as pinned. A lever arm of about 150 to 250 mm is required between the compressive and tensile forces that generate the moment; thus the couple will need to generate forces of about 300 kN. That is achieved by using an area of concrete of about 20 000 mm^2 (minimum grade C32/40 concrete assumed), and using two or three 16- to 20 mm-diameter high-tensile reinforcing bars (grade 500 assumed).

If welding is used to provide the continuity of forces, generous tolerances should be allowed in the positioning of the steel in the separate components to give the site operative the opportunity to place an intermediate bar if necessary between the bars and place a well-fashioned bead. Underhand welding should be avoided if possible, and the weld should be inspected afterwards.

Moment-resisting connections should be proportioned such that ductile failures will occur and that the limiting strength of the connection is not governed by shear friction, short lengths of weld, plates embedded in thin sections, or other similar details that may lead to brittleness. Many of the principles behind these requirements have evolved through years of seismic research and development, and the common practice in the US, Japan and New Zealand is to design and construct moment-resisting connections in the perimeter of the frame, where there is less size restriction on beams and columns [7.12]. Large deep beams with ample space for this purpose are specified as ring frames, while the interior frames' connections are all pinned-jointed shallow beams. Figure 7.42 shows details of a 457 mm square precast–*in situ* concrete beam end connection tested by Stanton *et al.* [7.1], which achieved a moment of resistance of 2100 kip-in (230 kNm). Versions similar to this have been studied by Park [7.22] and Pillai and Kirk [7.23].

Moment-resisting connections may be formed between columns and precast walls, or (sufficiently thick) cladding panels, because the latter are usually capable of accommodating the transfer moment. However, caution must be exercised in assuming that the places where splices are made will attain their ultimate design strength, i.e. the receiving element may not be able to carry the connecting moment.

Hasan [7.24] has designed and tested precast beam-to-column connections that are discontinuous in the construction stage, as shown in Figure 7.43 but, as shown in Figure 7.44, are made continuous by site-grouting additional rebars (e.g. 2H20 in this example) into a 100 mm-deep trough in the top of the beams. Continuity of the column is achieved by *in situ* grouting of protruding longitudinal bars (4H20 in this example) from the bottom column extending into galvanised steel ducts in the upper column and through the beam. The important reinforcement at the ends of the beams is shown in Figure 7.45 for two different designs. The cruciform joint is subjected to (i) balanced gravity load, producing a negative bending moment in the connection of about 150 kNm, and (ii) sway loads producing smaller negative and positive moments in the connection. The literature shows that little research has been carried out on this type of connection, the few exceptions being by Stanton [7.1], Vinha [7.25], deChefdebien [7.26], and Restrepo [7.27]. However, the connection shown in Figure 7.44 is much simpler in terms of site work, requires no special mechanical parts, no bolting or welding, and is structurally efficient by providing good continuity between the jointed elements.

Three reinforcement cages were designed (T1 to T3). Two are as shown in Figure 7.45, where additional horizontal links were provided, and 2H20 additional top bars were added in T3. Negative bending moments were applied to the beams to induce relative rotation θ at the face of the column, enabling a plot of M/θ to be made as shown in Figure 7.46. A summary of the results is shown in

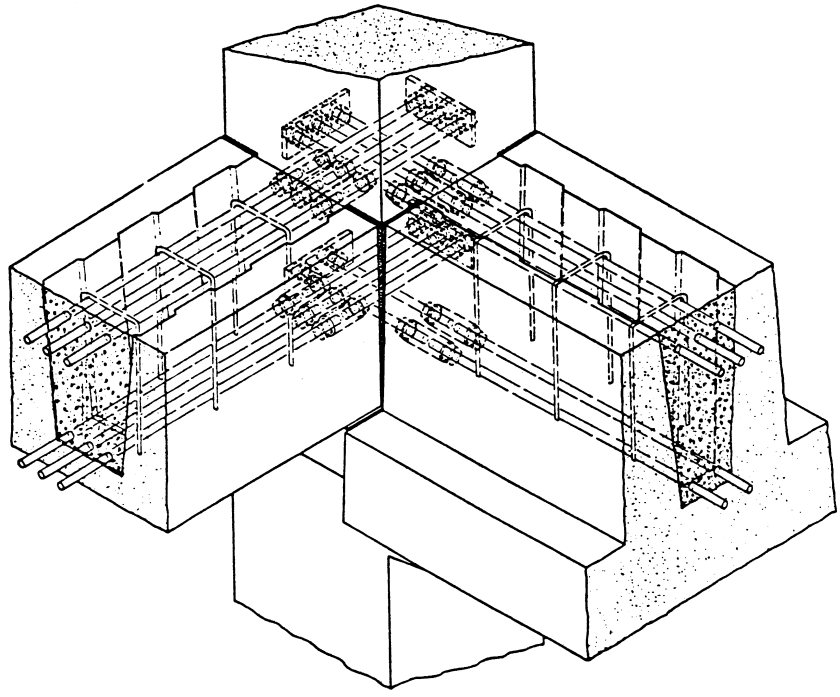

Figure 7.42 Moment resisting connections after Stanton [7.1].

(c)

(d)

Figure 7.43 (a) Discontinuous pinned jointed beam-to-column connection; (b) close-up view.

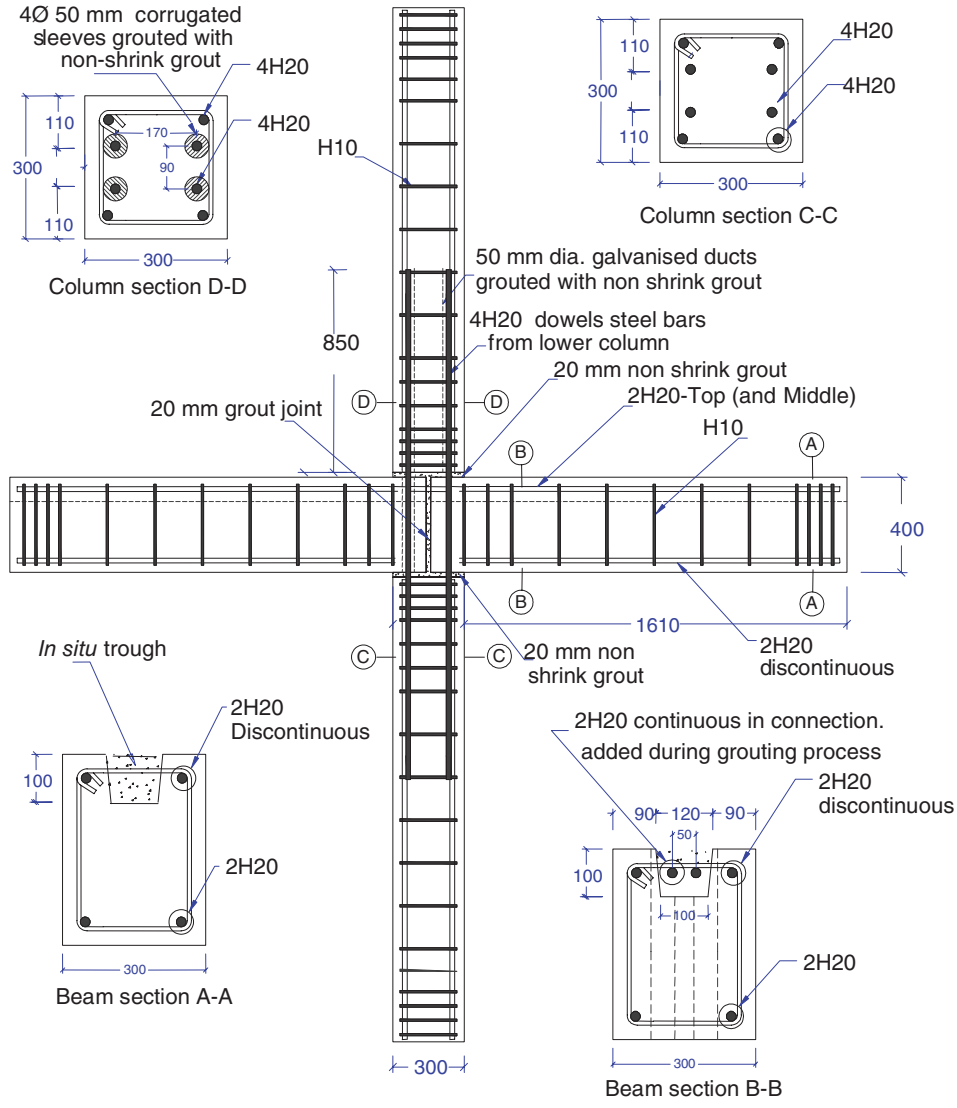

Figure 7.44 Design of precast concrete beam-to-column connection with discontinuous beam and column elements [7.28].

Table 7.8, where the ratio of the failure moment to the predicted ultimate moment is 1.01 to 1.37, although the sudden decrease in strength due to debonding of the top bars raises the question of whether this, or the final test moment of 159.4 kNm, should be quoted. The rotational stiffness of the connection S, given by the gradient in the M/θ graphs, is measured as the secant value at the intersection of the beam-line at point E (as defined later in Figure 7.50). The results in Table 7.8 show $S \approx 38$ kNm/mrad for tests T1 and T2, but $S = 83.3$ kNm/mrad in test T3, clearly a result of the additional continuity bars and extra U-links at the ends of the beam. These values may be compared with the flexurally cracked stiffness of beam T3 × (say) 6.0 m long, $K = 3EI/L = 8.52$ kNm/mrad ($E = 36.5$ kN/mm^2, $I = 473 \times 10^6$ mm^4, $L = 6000$ mm). The mode of failure of this connection is under-reinforced, and sufficiently ductile. Applying a factor of safety against the rebars of 1.15, and 1.5 for concrete, M_{Rd} for test T3 may be taken as approximately 130 kNm, i.e. $M_{Rd}/f_{cu}bd^2 < 0.45$ to BS

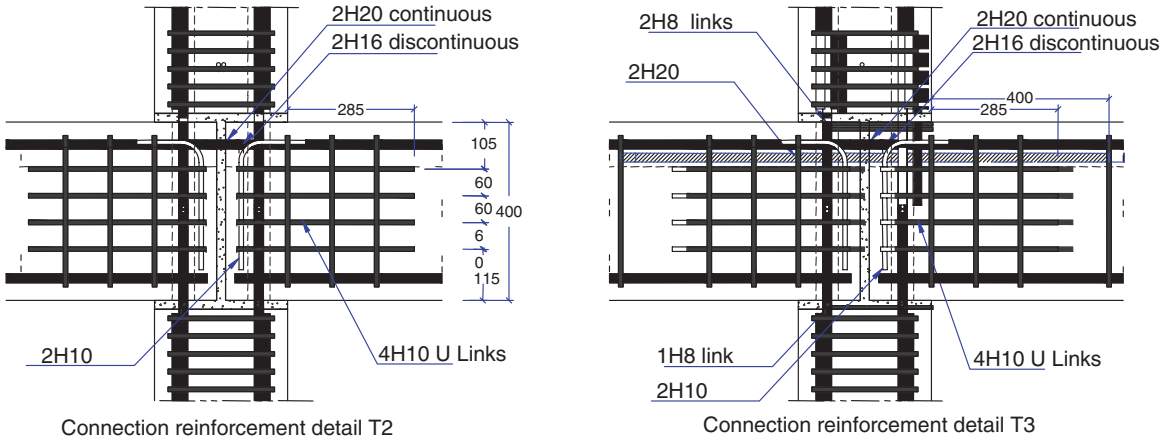

Figure 7.45 The important reinforcement details at the ends of beams required for successful beam-to-column behaviour [7.28].

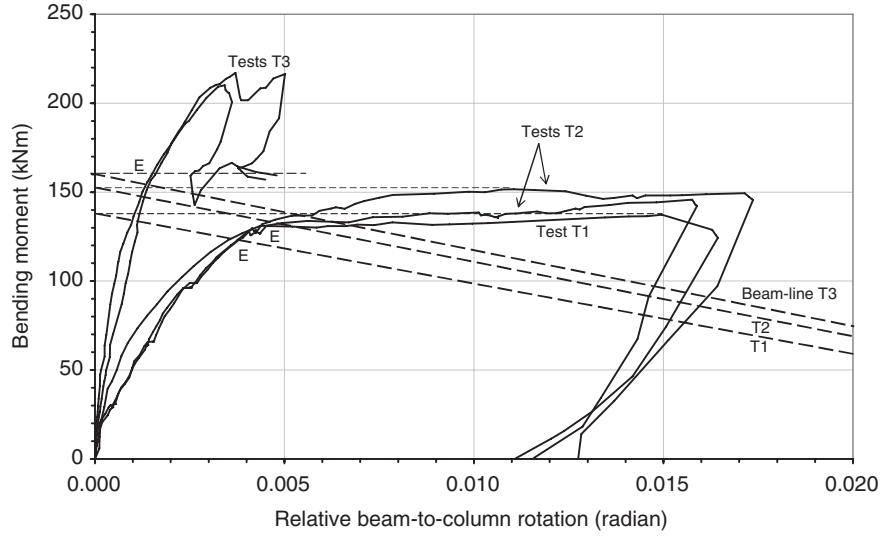

Figure 7.46 Moment versus rotation data for the cruciform precast beam-to-column connections [7.28].

Table 7.8 Results of the cruciform precast beam-to-column connections tests [7.28]

Test ref	Predicted ultimate moment kNm	Test failure moment kNm	Ratio test/ predicted	Secant rotational stiffness at E kNm/mrad	Precast concrete cube strength* N/mm^2	Infill mortar cube strength* N/mm^2
T1	121.3	137.3	1.13	32.4	63.0	65.7
T2	151.1	151.6	1.01	29.4	76.0	55.2
T3	157.8	159.4	1.01	113.6	82.8	59.7

* measured at date of test

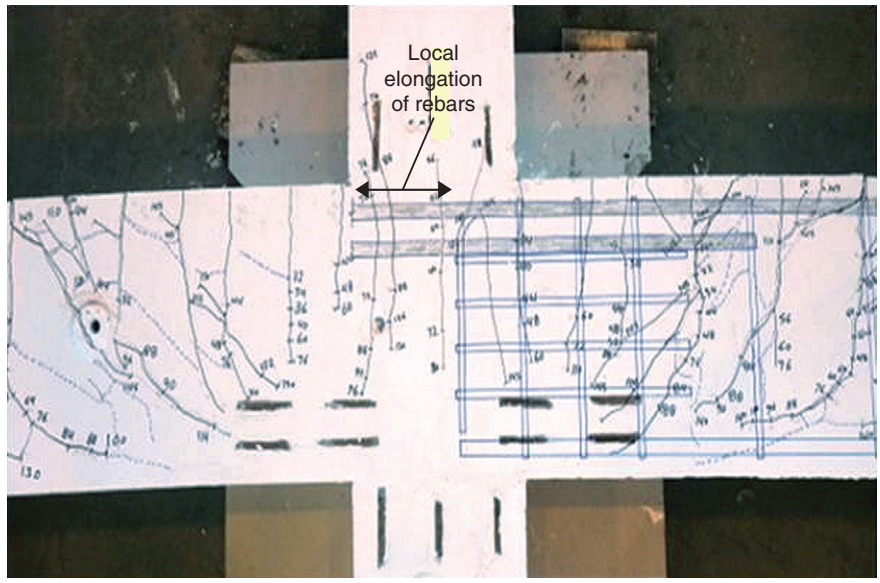

Figure 7.47 Flexural cracking in the cruciform precast beam-to-column connections [7.28].

EN 1992-1-1 for a rotational hinge {≈ 0.05, giving $x/d \approx 0.13 < 0.5$ to BS 8110}. Figure 7.47 shows extensive flexural cracking extending to the neutral axis at around 60 mm from the compression face. Clearly this is a practical type of connection to design and construct, with good mechanical properties.

To quantify the rotational stiffness S of the connection, which may be determined by testing or by calculation according to Section 7.7.2.2, a fixity factor γ according to Monforton [7.29] is adopted. This is a non-dimensional parameter that relates S to beam stiffness $3EI/L$ (the remote end of the beam is considered as pinned-jointed), varying from $\gamma = 0$ for pinned to 1 for fully rigid connections, respectively, and is given by:

$$\gamma = \left(1 + \frac{3EI}{SL}\right)^{-1} \tag{7.16}$$

Thus for the cruciform connection T3, $S = 29.4$ kNm/mrad and the beam stiffness $3EI/L = 5.9$ kNm/mrad. Then $\gamma = 0.83$. For T2, $S = 113.6$ kNm/mrad and $3EI/L = 8.5$ kNm/mrad, so $\gamma = 0.93$. It is now required to consider the effect of the fixity factors in assessing the behaviour of the connections in the beam-to-column structure, as follows.

7.7.2.2 Partial strength and semi-rigid moment connections

Not all precast skeletal structures are designed using pinned-jointed or fully rigid beam-to-column connections. The spectrum for the range of connection behaviour is the widest possible in precast concrete, more so than in other forms of construction. During the construction stage the beam is pinned-jointed to the column face, or seated on a corbel or on the column head. Afterwards, when floor units, together with reinforced cast-*in situ* infill and narrow strips around their ends (and sometimes a cast-*in situ* topping) are taken into account, the connection will possess appreciable flexural strength and rotational stiffness. Connections such as these, which in the past focused largely on the proprietary types of mechanical connector described in Section 7.10, were conveniently (and sometimes carelessly) designated 'notionally pinned' during construction, offering zero stability to columns and no negative moment in the beam. Once completed, the connection must then be classified according to its effect on the behaviour of the framed structure – not by its own resistance *per se* – as

Figure 7.48 Site-placed tie bars in both in-plane (parallel to beams) and out-of-plane directions generate semi-rigid behaviour with full-strength resistance in a 10-storey skeletal frame.

'semi-rigid' in terms of stiffness and 'partial or full strength', and reinforced appropriately so it is able to resist *imposed* dead and live gravity loads and, in the case of unbraced frames, reversals of sway loads. There should be no flexural cracking in the top of the beam in the connection zone, or debonding of rebars at the precast interfaces. In addition, negative (sagging) moment continuity must also be provided to counter the effects of relaxation of prestress, thermal movement, creep, and shrinkage, particularly in long-span and highly prestressed beams. The detailing of the reinforcement varies according to designers' and contractors' preferences, but the essential requirements are shown in Figure 7.48.

There has been considerable human resistance to the use of semi-rigid connections in skeletal structures in spite of the analytical, numerical, experimental and construction evidence. The PRESSS research program [7.30] led to the successful execution of a post-tensioned beam-to-column connector used in a 22-storey frame in the USA. Ozden [7.31] has modelled these connections by adding unstressed tendons though the centre of the beams, capable of resisting bending moments over 200 kNm at rotations up to 0.04 radians. Semi-rigid connections are commonly used in commercial and educational buildings of up to 5–10 storeys in South America, as shown in Figure 7.49. Reaction forces generated through welded steel plates at the corbel seating, and continuity rebars in the floor zone, are coupled to produce sufficient rotational stiffness to brace this structure in two mutually perpendicular directions.

This reluctance has not been helped in the past by the lack of information in codes of practice for structural concrete, which (unlike structural steelwork) do not cater for such connections. BS EN 1992-1-1, clause 5.8.3.2(3) allows the relative stiffness at the ends of the columns, expressed as $k = (E_{cm}I_{col}/l_{col})/(M_{col}/\theta_{joint})$, to be used in the effective length calculations. However, the effective relative stiffness of a precast beam to column in BS 8110, Part 2, clause 2.5.4, is 1/10. Unfortunately this information is not applicable to semi-rigidity where M/θ is required at beam ends, not in columns, and there is no mention of separating local joint rotations from the total rotation. In response to this, between 1990 and 2009 there were nearly one hundred full-scale (or reasonably sized model scale) tests carried out on precast beam-to-column connections, sub-frames, continuous beams, and so on. The leaders in this field have been Stanton *et al.* [7.1], Priestley *et al.* [7.30], Lindberg *et al.* [7.32, 7.33], Elliott *et al.* [7.34–7.36], Ferreira *et al.* [7.37–7.39], and at CERIB [7.40].

Figure 7.49 Semi-rigid and full-strength connectors in medium-rise precast frames (courtesy of T&A Prefabricados, Recife, Brazil).

Under the European action COST C1 (1991–1999) for the 'Control of the Semi-rigid Behaviour of Civil Engineering Structural Connections' in steelwork, precast concrete, timber and polymer sections, Mahdi [7.41] and Gorgun [7.42] and later Ferreira [7.43] tested 34 full-scale tests on a wide range of beam-to-column connections. Proprietary mechanical connectors, such as the steel T-cleat, welded plate or RHS billet (see Section 7.10) provided the initial notional pinned joint and, together with small quantities of reinforced *in situ* concrete in the joints, generated semi-rigid behaviour, as shown in Figure 7.49 and as defined by a *moment-rotation* M-θ diagram shown in Figure 7.50. The negative moment M is measured at the face of the column, and the relative (not absolute) beam-to-column rotation θ as close to this as possible, within $1.2h$ (h = beam or beam + slab depth). θ must not include rotations due to flexural curvature of the beam or column, otherwise these will be counted twice in frame analysis. It is important to recognise that test results cannot always separate these two effects.

The relevant properties of semi-rigid connections are defined in Figure 7.50 as (i) ultimate flexural strength M_R, (ii) rotational stiffness S, and (iii) ultimate rotational ductility capacity θ_u. M-θ behaviour in precast connections is typically linear up to about $0.3M_{Rd}$ and roughly parabolic afterwards. Elliott *et al.* [7.34] show this in a curve-fitting exercise. The rotational stiffness is required at the point where the end moment and rotation in the connection match those in the connecting beams – in other words, where the M-θ behaviour of connector *and beam-line* intersect, given by point E in Figure 7.50.

The beam-line represents the characteristic M-θ behaviour of a beam under certain conditions of loading. Consider a uniformly distributed imposed load w acting on a beam of span L; the moment of resistance of the beam (or composite beam + slab) M_{Rd} at point A is equated to the fixed end moment $wL^2/12$. The beam is theoretically fully rigid, such that $\theta = 0$. If the beam is pin-ended, then

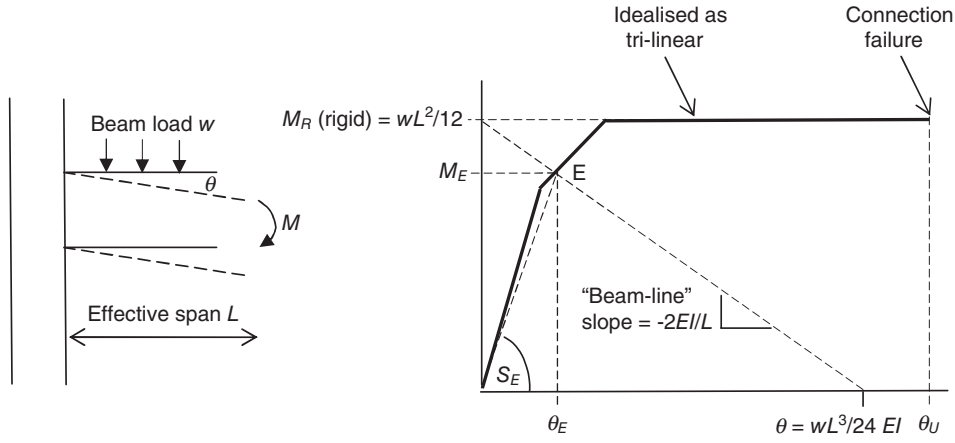

Figure 7.50 Definition of moment versus rotation parameters for connections.

at point B, $M = 0$ and $\theta = wL^3/24E_cI$, where E_c is the short-term value for Young's modulus, and I is the flexurally cracked second moment of area. The gradient of the beam line $= -2E_cI/L$. All points along the beam-line define the M-θ relationship of the beam. If M-θ for the connection is plotted on the same diagram, the intersection point 'E' (E represents beam *End*) simultaneously defines the end moment and rotation of *both* the beam and the connection. For a connection stiffness to be considered in frame design, point E must exist, as shown in Figure 7.50, and the rotational stiffness may be taken as S_E. If the connection fails prior to reaching the beam-line, it must be classed as pinned (even though there may be some small strength and stiffness present).

For very high values of stiffness the behaviour will resemble closely that of a rigid joint, and may be assumed to be rigid in frame analysis. Similarly, a connection of very low stiffness may be assumed to be pinned. Anything in between will be semi-rigid, but the boundaries between the three classifications are somewhat arbitrary. The *PCI Design Handbook* on connections [7.44] and BS EN 1993 [7.45] permit semi-rigid design for steel connections having a rotational stiffness in the range $0.5EI/L \le S \le 8EI/L$ for braced frames, and $0.5EI/L \le S \le 25EI/L$ for unbraced frames. Experimental tests on precast connections show that typically $4.5EI/L \le S \le 12.8EI/L$ and the ten tests shown here in Figures 7.46 and 7.51 gave $6.4EI/L \le S \le 40EI/L$, which by comparison must surely be suitable for semi-rigid design. Note that results given are ultimate test capacities, unfactored for design purposes.

The procedure is:

(i) First determine the experimental, numerical or analytical moment capacity of the connection, M_E and its stiffness, S_E.
(ii) Apply appropriate partial safety factors for materials to M_E, if not already applied.
(iii) Determine the fixity factor as

$$\gamma = (1 + 3EI/S_EL)^{-1} \tag{7.17}$$

(iv) Back-calculate maximum uniformly distributed imposed dead and live load w at the end of beam as:

$$M_E = \frac{wL^2}{12}\left(\frac{3\gamma}{2+\gamma}\right) \tag{7.18}$$

(v) Using w, calculate the mid-span beam moment M_{span} and deduct the bending moment due to self-weight and other dead loads before the connection is completed. If this cannot be achieved, reduce w to suit, and accept that the connection will not achieve its potential strength:

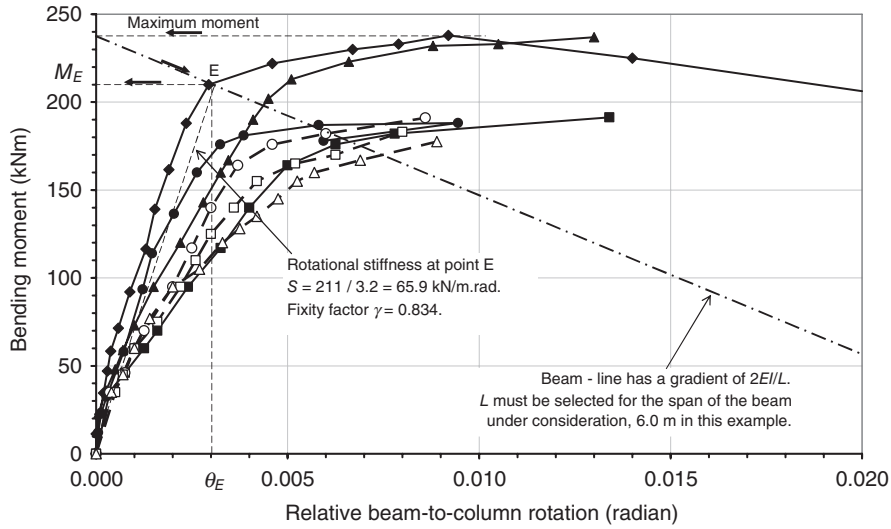

Figure 7.51 Moment versus rotation data for double-sided beam to continuous column connections using steel billet and welded plate (▲◆ symbols) connectors [7.41, 7.42].

$$M_{span} = \frac{wL^2}{12}\left(\frac{3-1.5\gamma}{2+\gamma}\right) \tag{7.19}$$

(vi) Calculate the beam end rotation using the smaller value of w from above, and use θ_E to calculate deflections due to connection rotation.

$$\theta_E = \frac{wL^3}{24EI}\left(1-\frac{3\gamma}{2+\gamma}\right) \tag{7.20}$$

Referring to Figure 7.50 at point E, where $M_E = 211\,\text{kNm}$ and $\gamma = 0.834$: Eq. (7.18), $w = 79.6\,\text{kN/m}$ for $L = 6.0\,\text{m}$. The mid-span moment $M_{span} = 147\,\text{kNm}$. The end rotation θ_E is based on $EI = 27\,600\,\text{kNm}^2$; then Eq. (7.20) $\theta_E = 0.117 \times 79.6 \times 6.0^2/(24 \times 27\,600) = 0.003$ radian.

Figure 7.52, which is reproduced after Ferreira [7.43], gives a design chart for the above parameters. The moments are normalised with respect to the fully rigid condition, and the rotation to the pinned condition. Studying this chart, Ferreira identified two important demarcation points:

$\gamma = 0.4$ distinguishes low strength from medium strength, because when $\gamma > 0.4$ the semi-rigid behaviour provides more than 50 per cent of full rigidity.
$\gamma = 0.67$ distinguishes medium strength and high strength, because $M_E > M_{span}$.

Therefore the proposed classification system after Ferreira [7.43] consists of five distinct zones, as indicated in Figure 7.52 as follows:

ZONE I (pinned connections): $\gamma \leq 0.14$. There is no semi-rigid behaviour, but connections must provide adequate rotation capacity in order to guarantee integrity when the beam end rotates.
ZONE II (semi-rigid with low strength): $0.14 < \gamma \leq 0.40$. Connections are not able to act as moment-resisting. However, numerical simulations under lateral loading show that for $\gamma > 0.14$ the lateral stiffness of the frame increases significantly, most significantly for taller frames.

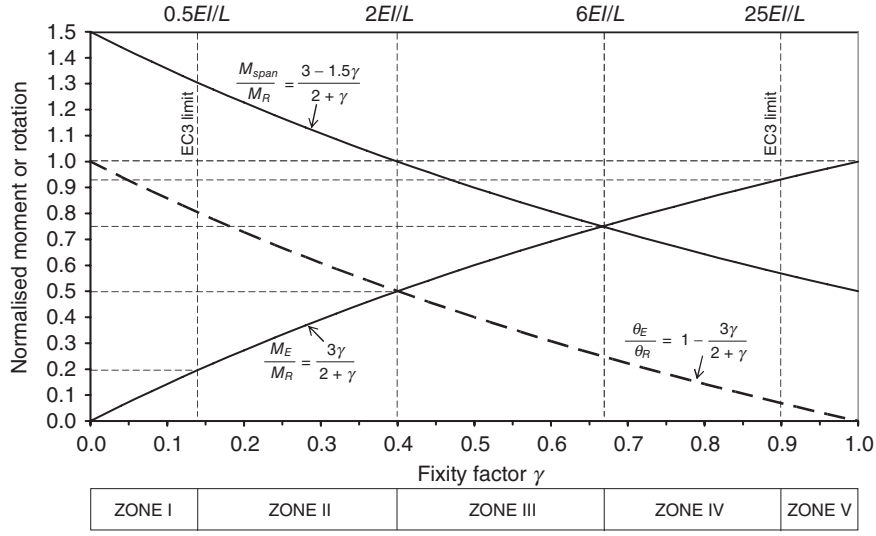

Figure 7.52 Classification system for pinned, semi-rigid and fully rigid beam-to-column connections. The text explains what must be checked in each category. After Ferreira [7.43] (courtesy fédération internationale du béton (fib), www.fib-international.org).

ZONE III (semi-rigid with medium strength): $0.40 < \gamma \leq 0.67$. Connections are suitable to act as moment-resisting connections, but still cannot provide semi-continuity to the adjoining beams. Since the connection resistance follows the beam capacity, rotations occurring in the connection zone will be mainly due to the beam end deformation, wherein the plastic hinge is developed, so that in this case there is no need to specify a rotation requirement.

ZONE IV (semi-rigid with high strength): $0.67 < \gamma \leq 0.90$. Connections are fully connected and provide semi-continuity to the adjoining beams. Confirming this indication, according to BS EN 1993, there is no need for semi-rigid analysis in braced frames when $\gamma > 0.75$.

ZONE V (rigid connections): $\gamma > 0.9$. There is no need to consider the semi-rigid behaviour. However, even rigid connections should be assessed in terms of ductility.

7.7.2.3 Theoretical derivations for the connection flexural strength and stiffness

Ultimate flexural strength may be calculated according to the same principles as for reinforced concrete sections. The small quantity of infill grout or mortar will generally have about the same compressive strength as the precast, say C40/50, as an early strength of about 30 N/mm^2 is required on site after 1–2 days. Thus, providing the continuity bars are fully anchored and wrapped by links or other rebars crossing the bending plane, the steel should attain yield strength. Thus $F_s = 0.87\, f_{yk}\, A_s$ $(0.87\, f_y\, A_s)$, $F_c = 0.567\, f_{ck}\, b\, 0.8X\{0.45\, f_{cu}\, b\, 0.9X\}$, and the lever arm becomes

$$z = 2.5d - 4.80 f_y A_s / f_{ck}\, b \quad \{2.22d - 4.77 f_y A_s / f_{cu} b\} \tag{7.21}$$

and

$$M_{Rd} = 0.87 f_{yk} A_s z \quad \{M_R = 0.87 f_y A_s z\} \tag{7.22}$$

Ferreira found that the top reinforcement lever arm, $z = 0.85d$ to $0.95d$.

Note that according to BS EN 1992-1-1, clause 5.6.3 limits $x/d \leq 0.45$ for continuous beams based on a connection's rotation capacity over a length of 0.6 × depth of section each side. This automatically allows 15 per cent moment redistribution at the connection, if required, providing the ductility of the connection is proven. There is no such restriction in BS 8110.

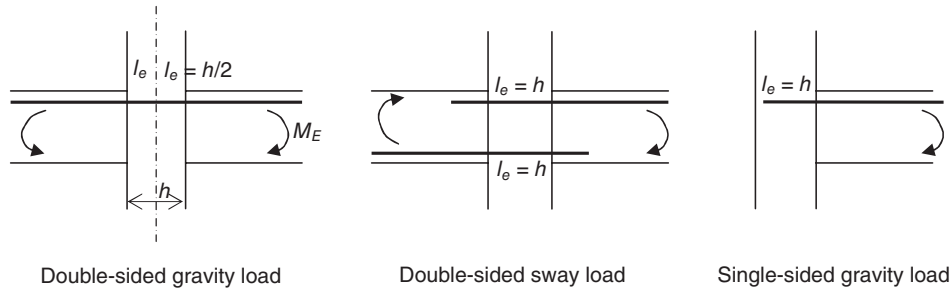

Figure 7.53 Embedment length of reinforcement across columns.

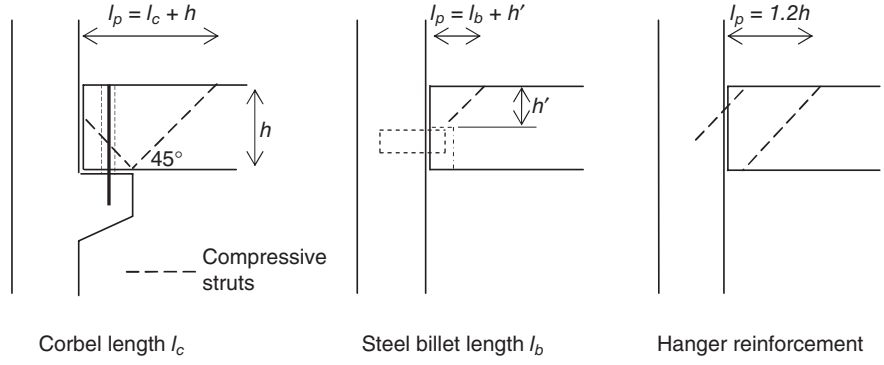

Figure 7.54 Plastic hinge lengths for types of precast connection.

The total end relative rotation θ_E arises from two primary deformations. These are:

(i) Beam-to-column rotation due to joint opening at the interface
(ii) beam end curvature along a plastic hinge length l_p.

Joint opening at the interface: This is due to the elongation of the top reinforcing bars, as shown in Figure 7.47. The local rotation $\phi_c = \delta/d$, where d = effective depth to top bars in the beam or composite beam + slab. The deformation is equal to the yield strain in the bars times embedment length, $\delta = l_e f_y/E_s$, where l_e is taken as the lesser of either a length over which the stress distribution along the bar is uniform or the length available, as defined in Figure 7.53. If the bar is stressed on both sides of the joint, the maximum embedment length is equal to half the depth of the column. Then:

$$\phi_c = \frac{f_y l_e}{E_s d} \tag{7.23}$$

Beam end rotational deformation: This is caused by curvature of the beam in the region where the curvature of the beam, and hence also the tensile stress in the top bars, are constant; see Figure 7.54. Cracking patterns obtained from experimental results [7.34] show that curvature is constant for approximately 0.5 times the anchorage bond length. There is a concentration of cracks causing the curvature that is constant within the plastic hinge length l_p. For rc beams $l_p = h_{beam}$. In precast connections l_p depends on the load path from the centre of rotation and the type of connector bearing, e.g. corbel, billet insert, or cleat, and whether the force is transferred to the beam by a cast-in steel plate or by suspension bars (Figure 7.53). Then:

$$\phi_c = \left(\frac{1}{r}\right)_{cr} l_p = \frac{M_R l_p}{E_c I_{cr}} \tag{7.24}$$

where $(1/r)_{cr}$ is the curvature of the beam (or beam plus slab) based on the flexurally cracked section.

The required moment capacity M_{ER} and the allowable design moment M_{Ed} for the connector at the ultimate limit state can be obtained from the intersection of $S = M_R/\phi_c$ with the beam-line (from $M_{ER}/M_R = S/S + 2EI/L$) as:

$$\frac{M_{ER}}{M_R} = \frac{M_{Ed}}{M_d} = \left(1 + \left(\frac{2E_c I_{cr}}{L}\right)\left(\frac{\phi_c}{M_R}\right)\right)^{-1} \tag{7.25}$$

Letting (7.22) $M_R = f_y\, A_s\, z$ and $\phi_c = (f_y\, l_e/E_s\, d) + (M_R\, l_p/E_c\, I_{cr})$, Eq. (7.25) is rewritten as:

$$\frac{M_{ER}}{M_R} = \frac{M_{Ed}}{M_d} = \left(\left(\frac{L + 2\ell_p}{L}\right) + \left(\frac{2E_c I_{cr}}{E_s d A_s z}\right)\left(\frac{\ell_e}{L}\right)\right)^{-1} \tag{7.26}$$

For example, using the 300 × 300 mm beam and composite 200 mm-deep hollow-core floor slab identified in Figure 7.50, use the above equations to compare with the test values $M_E = 210$ kNm and $\phi_E = 0.003$. In this test by Gorgun [7.42], column depth h_{col} =, section depth $h = 300 + 200 = 500$ mm, $d = 500 - 50$ cover = 450 mm, $A_s = 2$ no. H25 bars = 982 mm^2, f_y = (measured) 518 N/mm^2, $f_{cu(i)}$ = (measured) 45.0 N/mm^2, $E_c\, I_{cr} = 27.6 \times 10^{12}$ Nmm^2. The bond lengths, from Figures 7.52 and 7.53, are $l_e = h_{col}/2 = 150$ mm, $l_p = 150 + 60 + 200 = 410$ mm, where the bearing surface of the 60 mm projecting steel billet was at 150 mm from the top of the beam, the half bearing length = 80/2 = 40 mm, plus the 200 mm slab. The beam length is once more taken as 6.0 m.

Then, applying no material partial safety factors for a comparison with test data:

$F_s = 518 \times 982 = 508\ 676$ N
$X = 508\ 676/0.67 \times 45 \times 300 = 56$ mm $< 0.45d$
$z = 450 - 0.45 \times 56 = 425$ mm
$M_R = 508\ 676 \times 425 = 216.2$ kNm. Test result = 238 kNm, but ultimate strength of bars exceeded the design value.
$\phi_c = (518 \times 150/200\ 000 \times 450) + (216.2 \times 10^6 \times 410/27.6 \times 10^{12}) = 0.004$ rad. Test result = 0.003 rad.
$M_{ER}/M_R = (1 + (2 \times 27.6 \times 10^{12} \times 0.004/6000 \times 216.2 \times 10^6))^{-1} = (1 + 0.172)^{-1} = 0.854$.
$M_{ER} = 0.854 \times 216.2 = 185$ kNm. Test result = 210 kNm. The theoretical value is less than the experimental because the ultimate tensile strength, approximately 560 N/mm^2, was available in the test.

7.8 Design of Specific Connections in Skeletal Frames

7.8.1 Floor slab to beam connections

Floor connections can be divided into two main categories:

- connections at supporting joints
- connections at non-supporting longitudinal joints.

In the latter, beams or walls spanning parallel with the floor slab are essential to the integrity of the precast frame, and as such these joints are of equal importance to the main supporting joints.

Slab-to-beam connections using hollow-core and double-tee floors are designed as simple supports, despite the presence of reinforced *in situ* concrete strips cast in the ends of the units. Hollow-core floors are usually laid dry directly onto the shelf provided by the boot of the beam, but neoprene bearing pads or (less frequently) wet bedding onto grout can also be used in certain circumstances, e.g. double-tee floor slabs. Wet-bedded bearings are sometimes used on refurbished beams with uneven surfaces.

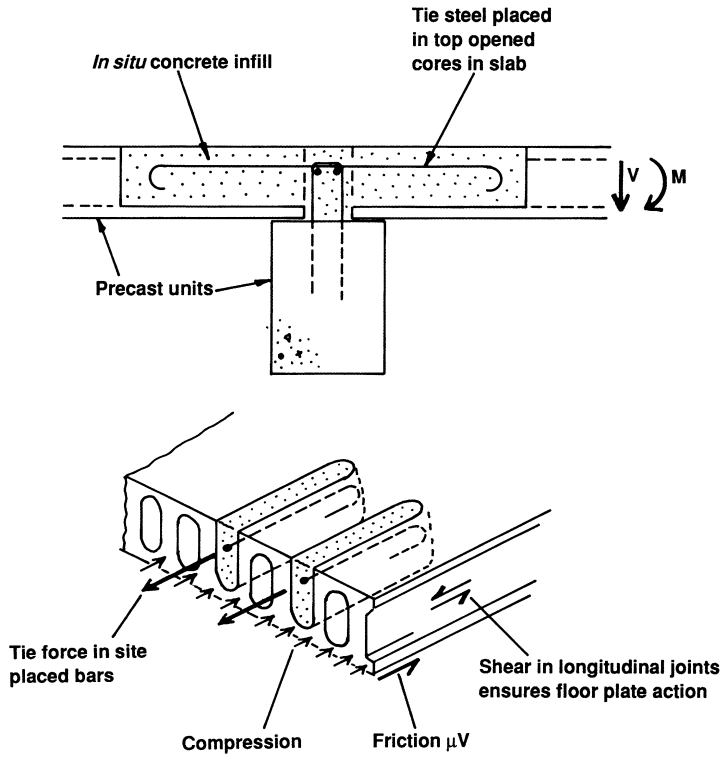

Figure 7.55 Spurious moment restraint at slab-to-beam connection.

7.8.2 Connections at supports

Although floor slab connections at supporting joints are normally designed as simply supported, a degree of end restraint may be present owing to the couple generated between the contact plane and tie back (rc or weld), as shown in Figure 7.55. Moments of resistance of up to 25 kNm per metre run have been measured by Mahdi [7.41] using only two H12 bars site-placed into the opened cores in the tops of the slabs. The magnitude of the restraint does not usually affect the flexural behaviour of the slab [7.46], because cracking in the top of the floor slab is often found only at the *in situ*-to-precast interface, and not in the slab itself. Longitudinal shrinkage of the floor slabs may also lead to cracking over the support, thus rendering the connection pinned in any case.

The objectives of design are to ensure transfer of vertical loading from the slab to the beam in both normal and abnormal (fire, accident, etc.) loading conditions. The connection has therefore to satisfy the requirements of load transfer, structural integrity, and ductility. Some of the means of achieving this are shown in Figure 7.56.

In hollow-core construction, Figure 7.56(a), openings are made in the top flanges of the units (during manufacture) to permit the placement of structural concrete (grade C20/25 minimum) on site. Continuity of reinforcement is achieved either by direct anchorage between the precast beam and *in situ* strips, or by dowel action between loops, or between loops and other bars. The bars may be placed in the longitudinal gaps between the slabs providing that the geometry of the gap corresponds to the details in Figure 5.11. Structural continuity, but not moment transfer, over internal beams is easily achieved, as shown in Figure 7.57(a)–(c). See *FIP Manual* [7.46] and the *BCA Guide* [7.47] for other possible details.

The length of embedment is taken as the greater of one anchorage bond length or the equivalent of the transfer length of the prestressing force in the precast unit. End hooks may be used to obtain

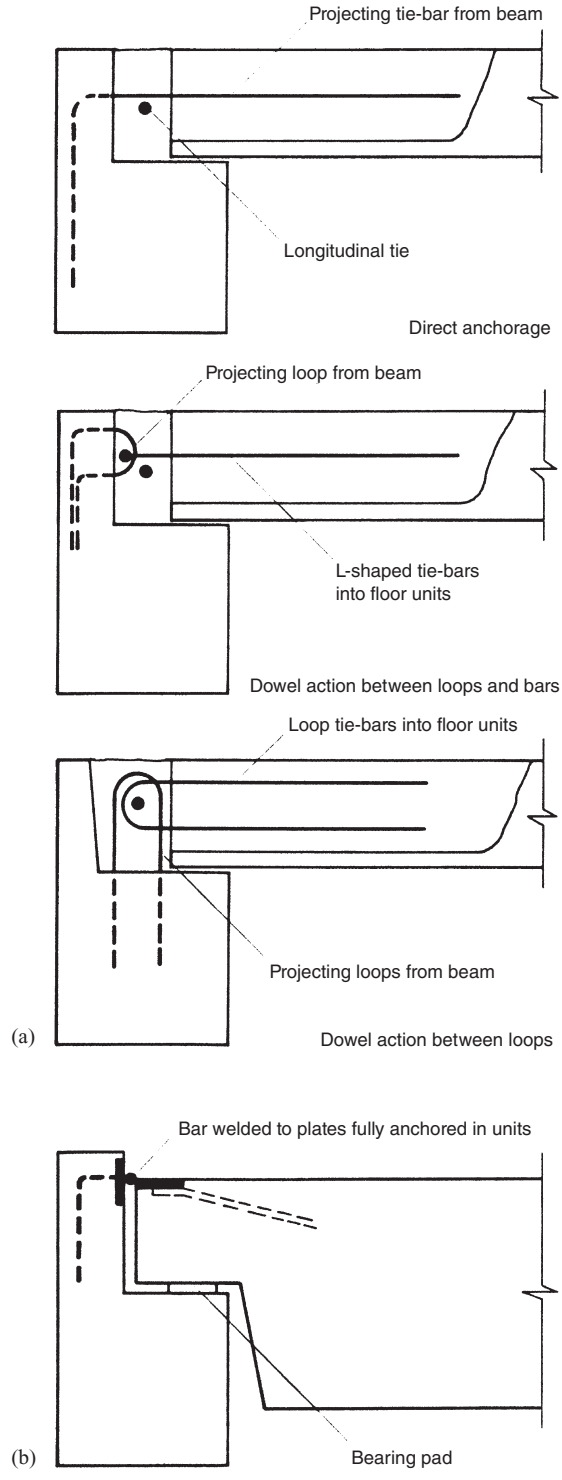

Figure 7.56 Floor slab to external beam connections [7.47]. (a) At hollow-core slabs connections and (b) at double-tee slab connections.

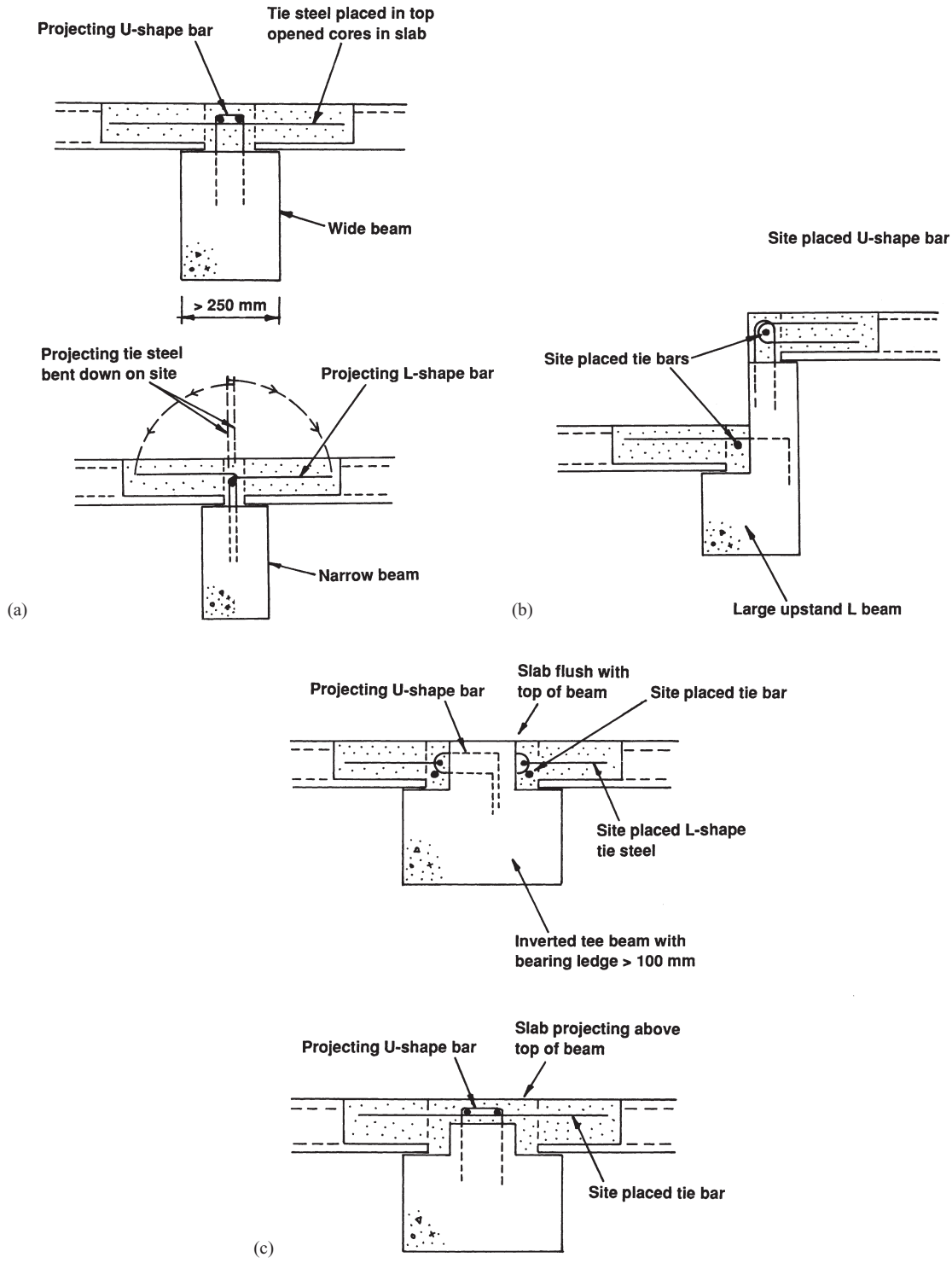

Figure 7.57 Floor slab to internal beam connections [7.22]. (a) Rectangular beams; (b) asymmetric beam; (c) inverted-tee beams.

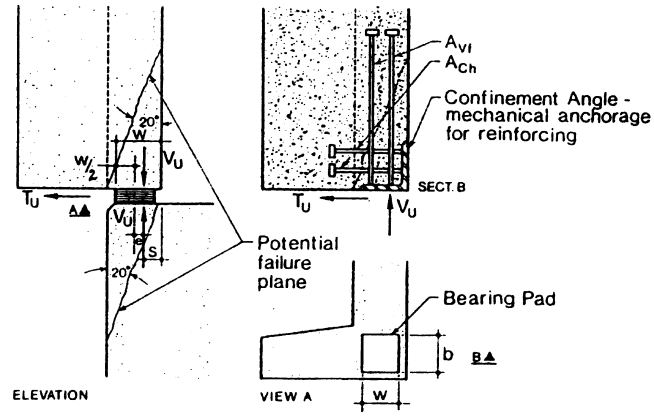

Figure 7.58 Shear friction hypothesis used to analyse edge bearings.

the required length. The openings are wide enough to ensure good compaction using a small-diameter poker vibrator. The infill usually penetrates the end of the opening to a distance greater than is structurally required.

Hollow-core units are laid directly onto dry precast beam seatings. The design ultimate bearing stress, $0.4\,f_{cd} = 0.267\,f_{ck}$ $\{0.4\,f_{cu}\}$ is rarely critical. A nominal bearing length of 75 mm, resulting in a net length of 60 mm after spalling allowances have been deducted, gives rise to a bearing capacity in the region of 800 kN/m run. Rigid neoprene strips or wet mortar bedding, which have been used in special circumstances, e.g. in refurbished buildings or on masonry bearings, ensure that a uniform bearing is made between them.

In double-tee floors a welded connection is made, Figure 7.56(b). Double-tee slab bearings require greater consideration, because it is vital that the loads should be equally shared between all four bearing points. A nominal bearing length of 150 mm minimum is recommended and the units should always be seated on rigid 100 × 100 mm neoprene (or similar) pads of about 8 mm to 10 mm thickness.

Design equations given in *PCI Manuals* [7.48] for ultimate bearing capacity take into consideration the dimensions s, w and the coefficient of friction $\mu = T_u/V_u$ defined in Figure 7.58. Using a static value for μ between dry elastomeric and concrete surfaces of 0.7, the analysis considers a potential shear failure crack inclined at 20° to 25° to the vertical free edge of the bearing. For typical double-tee geometry, the minimum bearing capacity (based on a design stress of 7 N/mm^2 for neoprene) is in the order of 170 kN/m. Again this is rarely critical. Bearing lengths of less than 100 mm are not recommended for double-tee units, because there is a chance that misalignment of the pads could easily reduce the actual bearing length to as little as 70 mm (Figure 7.59).

It is not advisable to attempt a flexural connection between double-tee units and support beams unless full anchorage of the force mechanisms providing the couple is guaranteed, both at the slab-to-beam and beam-to-column connections. The transfer moment is concentrated at the seating of the webs (usually at 1.2 m centres). Problems due to the combined effects of vertical and horizontal forces at the seating are difficult to avoid in such confined areas without the use of special anchorage devices.

Connections between flat plank flooring and supporting members present few problems, providing a soft sand/cement mortar is used to bed 2.4 m wide units onto precast (particularly prestressed, or with camber) beams. A 75 mm nominal bearing is used. Continuity of reinforcement is provided by the mesh lapping with projecting reinforcement in the beams or walls.

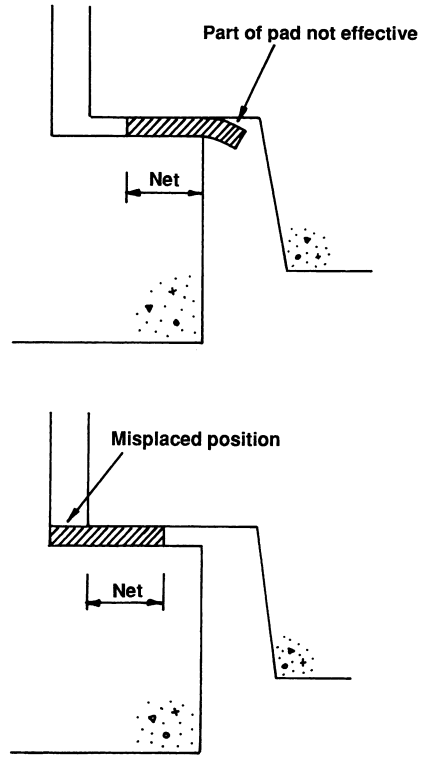

Figure 7.59 Misplacement of bearing pads to double-tee units.

7.8.3 Connections at longitudinal joints

Longitudinal joint connections are provided between the edges of precast floor units and beams (or walls) running parallel with the floor. Their main function is to transfer horizontal shears, generated in the floor plate by diaphragm action (see Section 8.3), between floor slab and beam while allowing for the differential movement between adjacent precast components. Details of this joint are shown in Figure 7.60(a)–(c).

In hollow-core construction, recesses may be formed by removing part of the top flange. An *in situ* rc joint is formed at intervals, usually at 2.4 m centres, along the edge of the slab. Full-depth *in situ* concrete strips may be preferred, to ensure a positive shear key. The slab is sufficiently flexible to accommodate differential vertical movements due mainly to temperature and loading effects.

Typical longitudinal joints between double-tee and edge units are also shown in Figure 7.60, where a welded connection (at 2.4 m intervals) is made between the units immediately after fixing. The strength of the weld is sufficient to maintain the position of the double-tee unit while the *in situ* concrete topping is hardening. The welded connection is designed to prevent separation of the reinforced topping (which is tied to the edge beam) from the flanges of the precast slab. The flanges of the slab are, in turn, reinforced (with mesh) to cater for flexural forces generated by the shear restraint provided by the weld to prevent differential movement. Longitudinal cracking in double-tee units is very rare indeed.

It is not always necessary to use parallel edge beams with solid precast plank floorings, because of the semi-monolithic form of the construction. However, if beams are used (to carry wall loads, for example), an *in situ* connection between the beam and structural topping is made by lapping site-placed mesh to projecting bars from the edge beam.

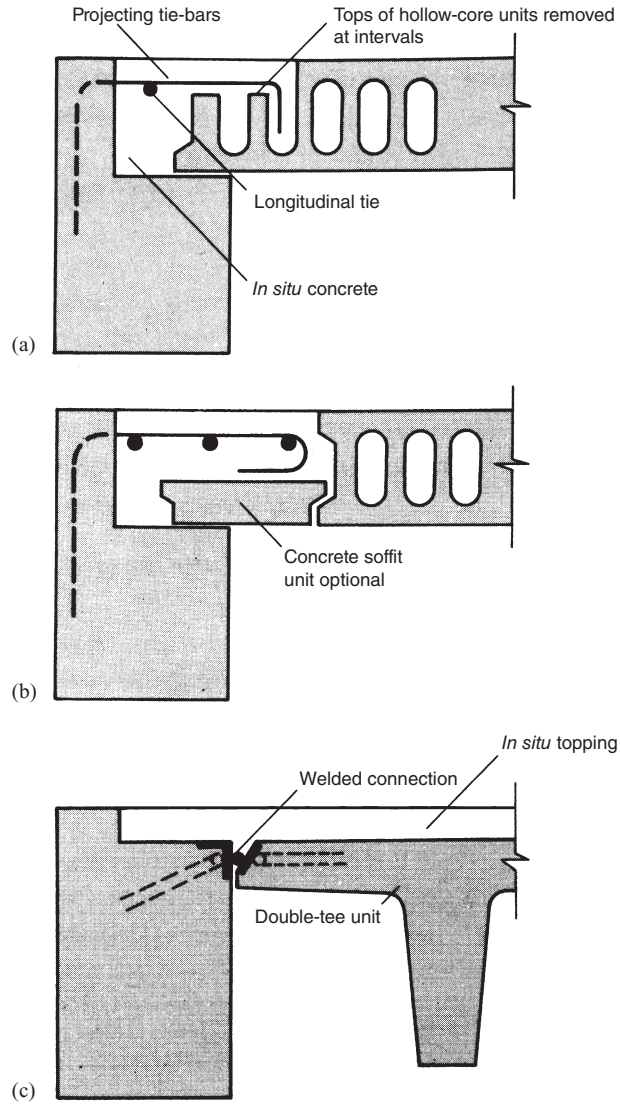

Figure 7.60 Floor slab to beam connections at longitudinal positions [7.47]. (a) Intermittent tie; (b) continuous *in situ* edge strip; (c) welded tie to double-tie.

7.8.4 Floor connections at load-bearing walls – load-bearing components

Horizontal joints in load-bearing walls occur at floor and foundation levels. Primary forces in the joint are due to vertical compression from upper-storey panels and horizontal shears from floor plate diaphragm effects. Secondary forces due to temperature, long-term shrinkage, and creep, or spurious bending moments induced by end restraints, are by comparison of minor importance. Connections at wall supports require careful detailing, particularly if the floor units are supported within the breadth of the walls, and large wall loads are imposed: see Figure 7.61. Some hollow-core units (e.g. 300 mm deep) may require strengthening to prevent web buckling by filling the voids to a depth coincident with the edges of the walls. Double-tee units may require rib end closure pieces to form a diaphragm.

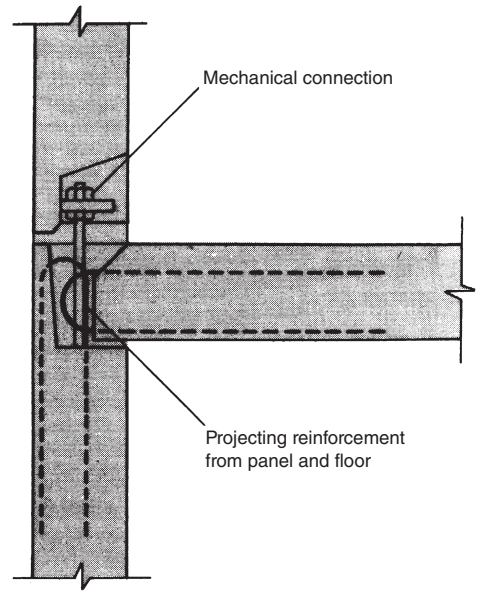

Figure 7.61 Floor slab to wall joints [7.47].

There is a wide range of solutions available for forming these joints, varying from an extensive use of *in situ* concrete and tie steel, Figure 7.62(a), to welded connections made between fully anchored plates, Figure 7.62(b). The former offers excellent structural integrity and ductility, whereas the latter offers immediate stability to the precast frame. For these reasons a combination of both is sometimes used, such that the bolt or weld design need only satisfy temporary stability conditions.

A general distinction is made between *continuous* joints (e.g. using hollow-core flooring) and *isolated* joints (e.g. using double-tee flooring where a connection is made at 1.2 m intervals). Typical details for continuous construction are shown in Figures 7.63 and 7.64(a) and (b) for internal and external use, respectively. It is important for the designer to allow easy access to make these joints, which is why the detail in Figure 7.64(a) using loose, U-shaped site bars is preferred to Figure 7.64(b), where the projecting L-shaped bars must be cast into the wall with an accuracy within about 50 mm.

Strength-controlling factors for the correct transfer of vertical load are:

- the extent and compressive strength of confined *in situ* concrete
- the 'effective' width of shims and the use of steel levelling shims in the upper-storey panel bearing
- the vertical splitting strength of the panel ends
- the strength of any mechanical connection.

A further subdivision of joints is where, for reasons of restricted access or bearing width, an extended bearing is formed, as shown in Figure 7.65. This is often referred to as an *open* joint, as opposed to the more frequently used *closed* joint. Differences in failure modes are due to the different stress-deformation characteristics of the *in situ* and precast concretes. Although crushing failure is theoretically possible, tensile splitting occurs first because transverse reinforcement is not present in most cores in hollow-core slabs. Furthermore, to restrict the penetration of *in situ* concrete to the width of the wall bearing reduces the risk of introducing hogging restraint moments to floor slabs that are not suitably reinforced.

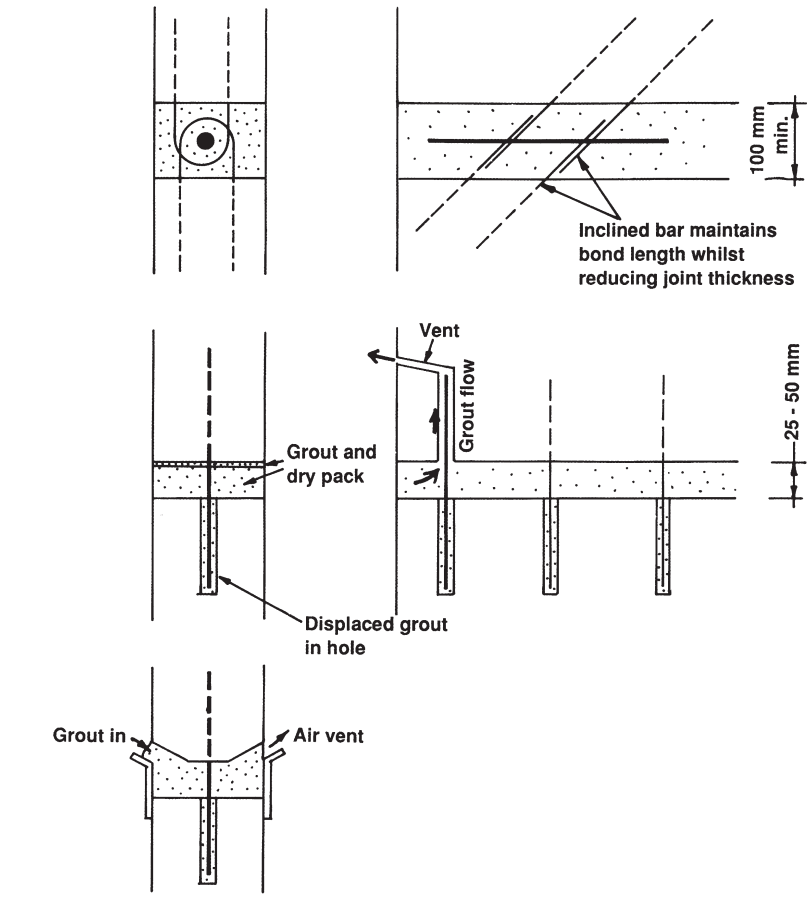

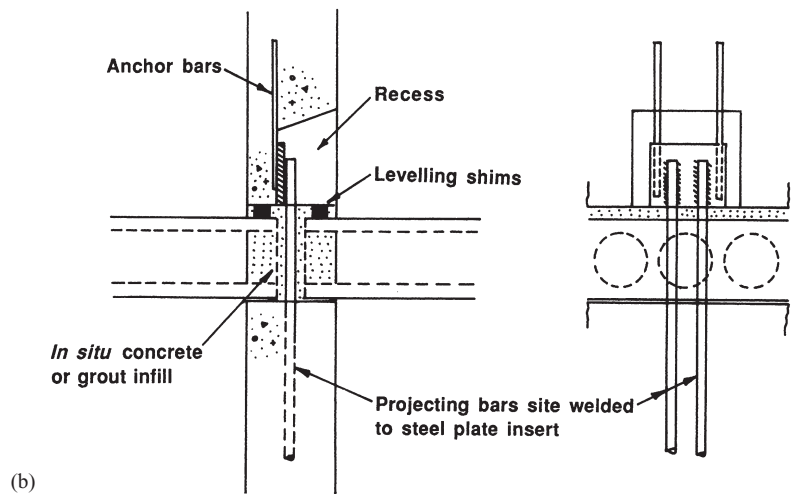

Figure 7.62 Load bearing wall-to-wall connections. (a) Using reinforced *in situ* joints, and (b) using welded joints.

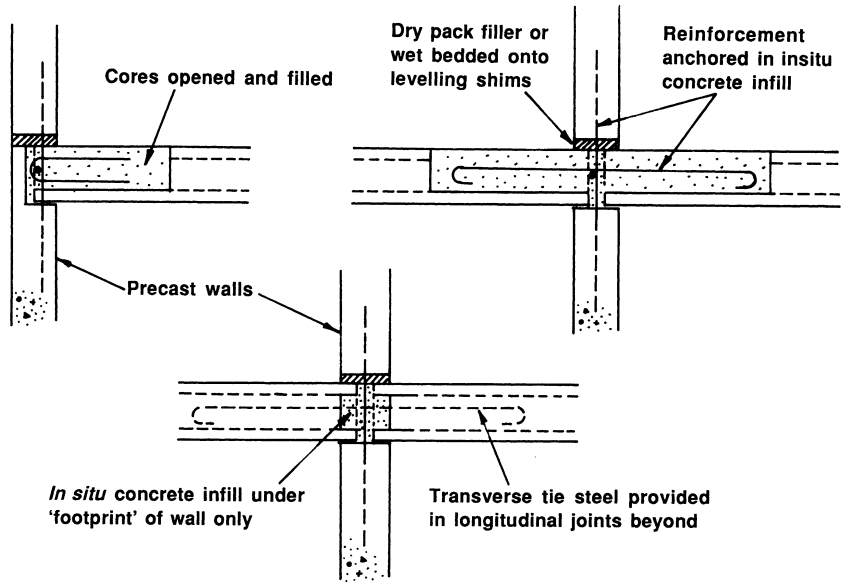

Figure 7.63 Continuous connections in floor slab to wall joints.

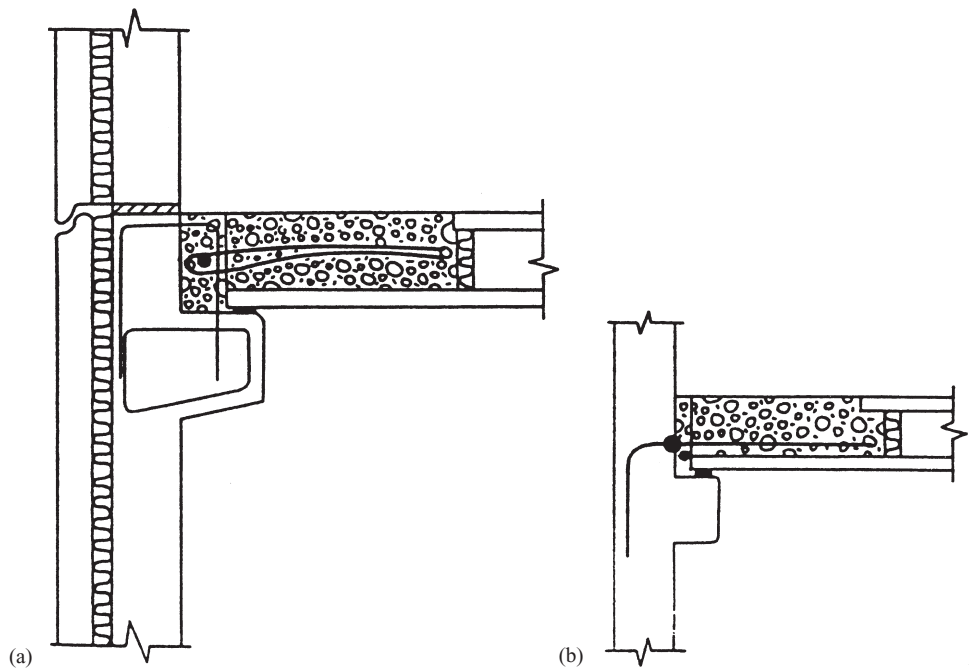

Figure 7.64 Continuous connections in floor slab to external wall joints: (a) using U-shape site bars and (b) using projecting L-shape bars.

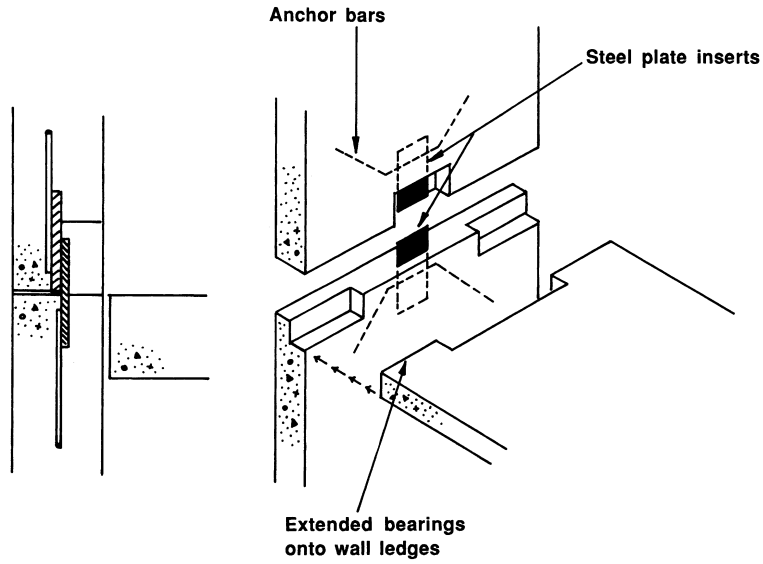

Figure 7.65 Intermittent connectons and extended bearings in an 'open' floor slab to wall joint.

7.9 Beam-to-Column and Beam-to-Wall Connections

7.9.1 Definitions for different assemblies

The most fundamental feature in the design of multi-storey precast frames is the connection between vertical and horizontal components. There is a broad subdivision in that either the vertical member is *continuous* (both in design and construction terms) and horizontal components are framed into it at various levels, or the vertical member is *discontinuous* (only in construction terms) and the horizontal components are either structurally continuous or separate across the junction. Although the former usually refers to skeletal column and beam construction and the latter to wall frames, there is an alternative approach, particularly in low-rise unbraced buildings, for single-storey columns to be erected floor by floor, and an important *in situ* concrete connection to be then made between precast components.

The *fib Manual* [7.3] on structural connections highlights some fundamental principles, which make a good starting point for this discussion:

> *Figure 7.66 shows a compression-loaded mortar joint for the columns and a half-joint for the beams. Solution A will give an excellent performance – the joints are easily accessible to workers and the large forces in the columns are readily transferred from one column to another. Solution B, with a beam passing over the column and one half-beam joint, say at one-fifth of the span, will give better moment distribution over the beams, but most probably a poorer performance at the column connection. The column connection, which now consists of two mortar joints, will have to overcome the following two handicaps:*
>
> - *As the beam passes over the column and has a certain negative moment, its top filaments will elongate. This elongation transferred through the mortar joint to the underside of the upper column will negatively influence the bearing capacity of this column, as it will tend to undergo the same deformation and split.*
> - *The joint at the underside of the beam is in turn difficult to reach. Placing of the mortar is difficult, resulting (most probably) in bad quality and subsequent poor force transfer.*

Fogarasi [7.49] gives a summary of many of the types of connection used in Europe, Asia and North America. Of the 20 or so types of connector cited, there is an even split between the use of concrete corbels with twin-rib or rectangular beams, and cast-in steel inserts forming what many people refer to as the 'invisible corbel'.

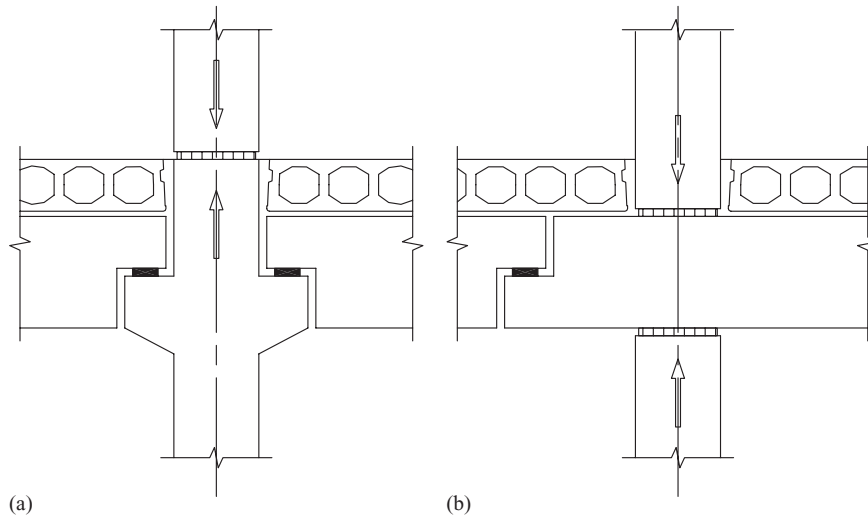

Figure 7.66 Alternative solutions for a beam-to-column connection, from [7.3] (Courtesy of fédération internationale du béton (*fib*), www.fib-international.org.)

7.9.2 Connections to continuous columns using hidden steel inserts

Steel insert joints are one of the commonest forms of beam-to-column connection. The structural mechanism, which is described in Figure 7.67, is based on static strength, stiffness, load transfer into the connecting components, temporary stability and structural integrity. A wide range of joints, some of which are shown in Figure 7.68(a)–(f), have evolved to satisfy these requirements. The basis of joint design is as follows (Figure 7.67):

(1) At A – to transfer the shear force carried by the reinforced (or uncracked prestressed) concrete at the ends of the beams into the connection. This usually takes the form of shear transfer from a combination of vertical shear links and/or bent-up bars into a prefabricated steel section, called a 'shear box'. The end of the beam is pocketed or recessed.

(2) At B – to ensure adequate shear capacity in the plane of the physical discontinuity between beam and column (or other supporting member), taking into consideration ultimate and working values of static strength, cracking, durability and fire resistance. This usually takes the form of either a projecting (solid or hollow) steel section, or a gusseted angle or T-cleat bolted into anchored sockets.

(3) At C – to transfer the compressive loads into the rc column. The effects of horizontal bursting forces, both above and below the connection in the case of eccentrically loaded columns, are controlled using closely spaced links. Column anchorages are generally either fully anchored cast-in-sockets, or steel box or H-section cast-in inserts.

7.9.3 Beam-to-column inserts

The options for beam-to-column inserts are as follows:

(1) Direct frictional bearing between beam and column inserts with no positive mechanical action between the essential precast components: a non-structural top fixing, comprising either a bolted or welded cleat or plate, or an arrangement of reinforcement to provide torsional stability to the connection (Figure 7.68(a)). Shear capacity is based on the net shear section of the projecting inserts.

(2) As (1), with the addition of a 'drop bolt' located between the top fixing and column insert and used to give immediate temporary stability to the connection and a positive mechanical tie between the precast components (Figure 7.68(b)).

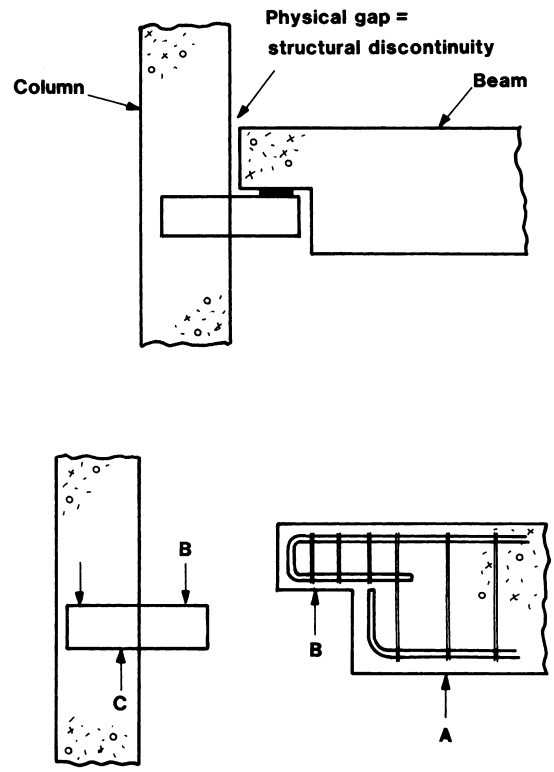

Figure 7.67 Basic principle for the design of beam-to-column connections using halving joints and cast-in steel inserts.

(3) A welded connection in which discrete weld preparations have been made to the adjoining beam and column inserts. Top fixings may be excluded because of the torsional stability provided by the weld (Figure 7.68(c)). The vertical shear capacity is as (1) and excludes the contribution of the weld.

(4) A sliding plate fitted into a rectangular slot in the beam. A notch at the end of the plate fits over a lip at the bottom of a steel box cast into the column (Figures 7.68(d) and 7.69).

(5) A separate intermediate cleat. Typically these are a rolled structural tee, rolled angle, fabricated plate angle, or fabricated box gusseted for strength and drilled to receive a bolted connection to both beam and column components. Top fixings may be excluded because of the stability provided by the bolt group (of at least two) (Figures 7.68(e) and 7.43). The shear capacity is based on the lesser of:

a) the single shear capacity of the bolt group (at least 2) to the column

b) the capacity of the gusseted cleat (or box) designed as a solid 'strut-and-tie'.

Side connections, shown in Figure 7.68(f), are also possible providing that the torsion moments are catered for in the beam.

The connection is designed for the least favourable position between contact surfaces, taking into account the accumulation of frame and component tolerances. The gap between the precast components is concreted using a sand/cement (or cement only) grout containing a proprietary expanding agent. In some instances, particularly where the cover to the surface of the nearest steel insert exceeds about 50 mm, small-diameter links are spot-welded or otherwise attached to the inserts to form a small cage. The grout, which has a minimum compressive design strength of 25 {30} N/mm^2 (but frequently exceeds 40 {50} N/mm^2 at 7 days), provides up to a 2-hour fire protection and total durability protection to the connection.

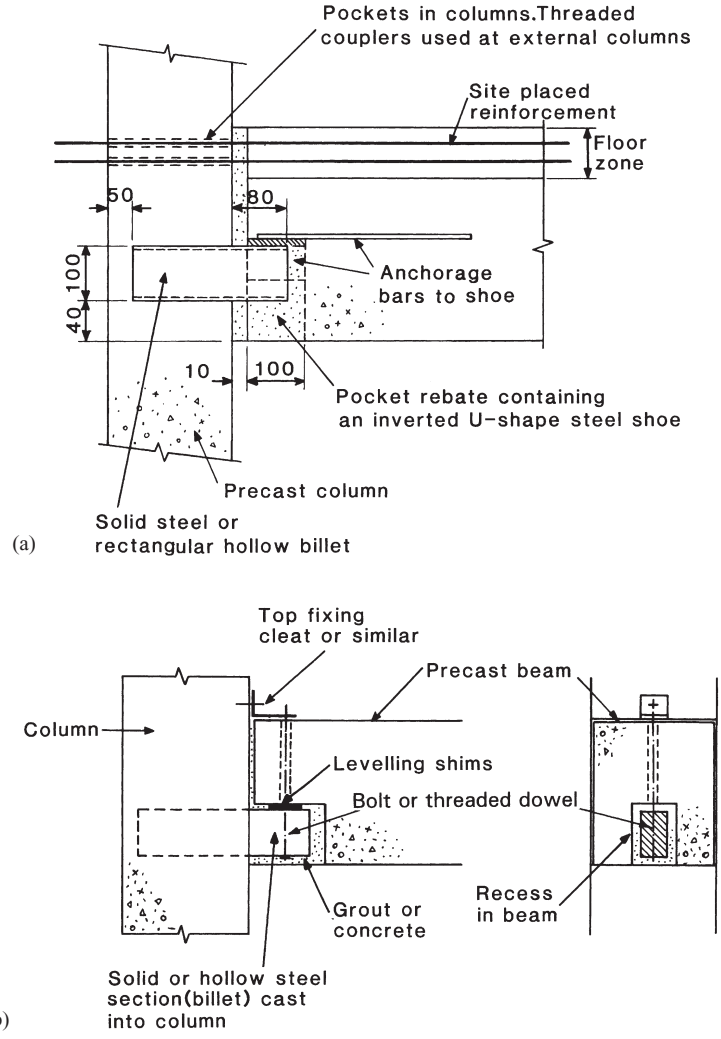

Figure 7.68 Types of cast-in steel inserts at beam-to-column connections.
(a) Using solid or hollow billet with top steel reinforcing bars
(b) Using solid or hollow sections with threaded dowel and top angle fixing
(c) Using solid billet with welded plate in beam
(d) Using open box and notched plate in beam
(e) Using rolled H-section and bolted on cleat
(f) Side billet connection (courtesy of Trent Concrete Ltd).

7.10 Column Insert Design

7.10.1 General considerations

A 'column insert' is the name used to describe a steel section that is embedded into precast columns in order to transfer shear and axial forces, and sometimes bending and torsion moments to the column. There are many types of insert, including:

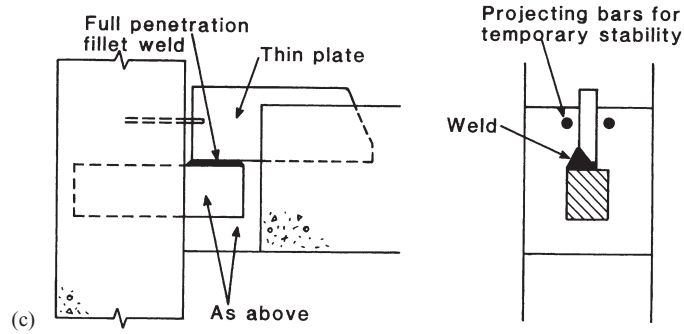

(c)

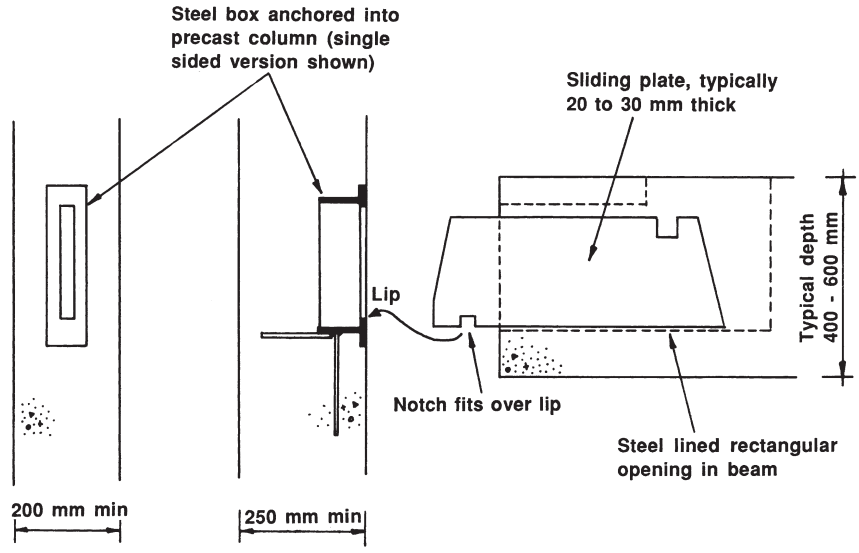

(d)

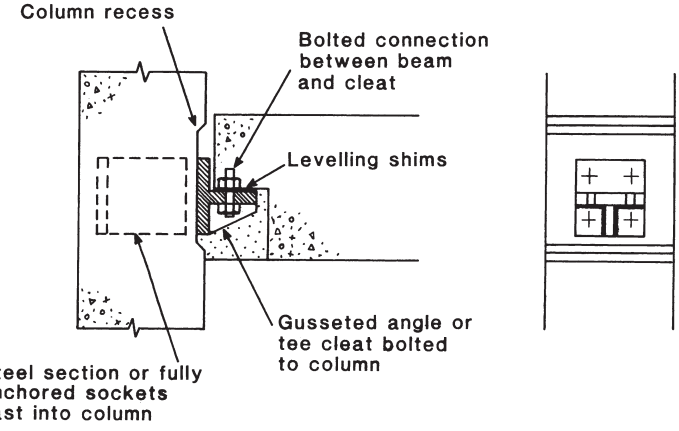

(e)

Figure 7.68 (*Continued*)

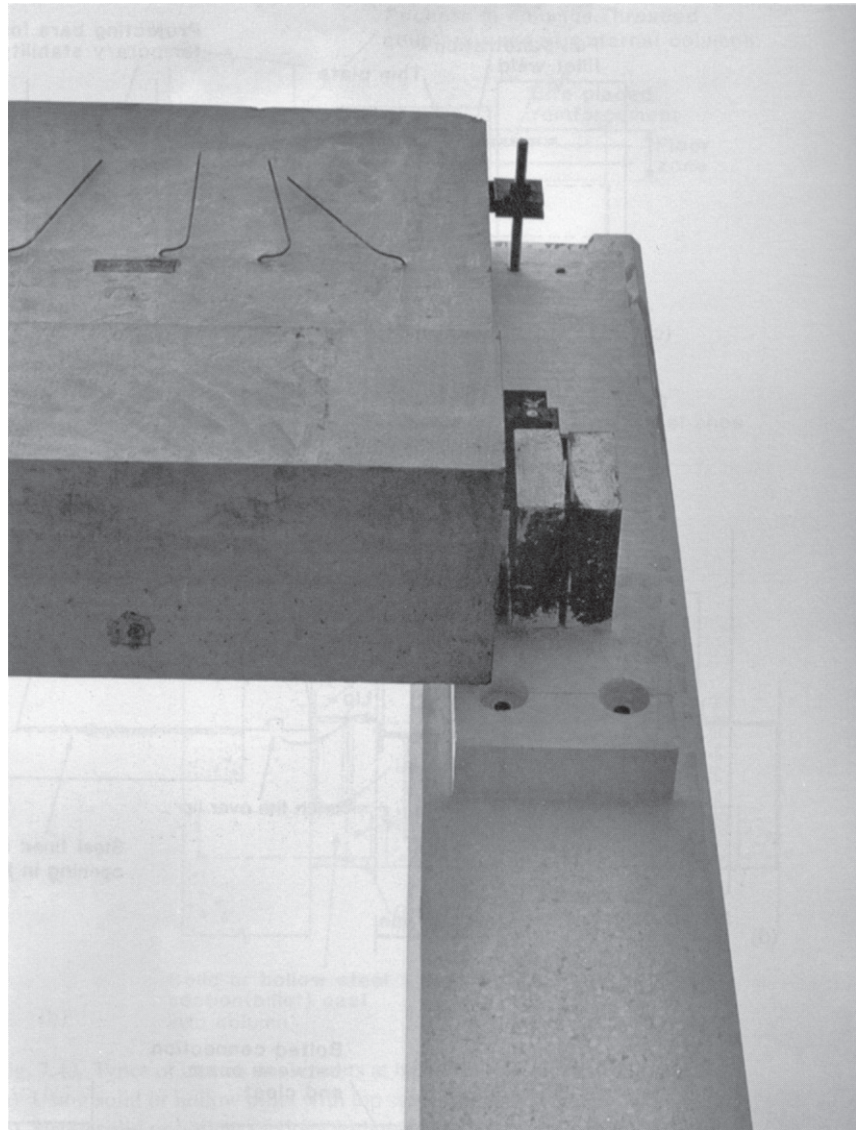

(f)

Figure 7.68 (*Continued*)

- Universal column or beam (UC, UB)
- rolled channel, angle, or bent plate
- rolled rectangular or square hollow section (RHS, SHS)
- narrow plate
- threaded dowels or bolts in steel or plastic tubes
- bolts in cast-in steel sockets.

Column insert design may be conveniently subdivided into the following:

- insert type
- breadth of insert to column width ratio, b_p/h
- beam topography, i.e. number and orientation of beams at each column.

(a) (b)

Figure 7.69 (a) Sliding plate connector steel plate is expressed from the beam after casting, and (b) is received into the steel box slots in the column.

Insert type may be either the solid or tubular (Figure 7.68(a)–(c)) or cast-in sections (Figure 7.68(d) and (e)). Inserts are classified as:

- 'wide sections', i.e. when the breadth of the bearing surface b_p is in the range 75 mm < b_p < 0.4h
- 'narrow plates', which includes thin-walled rolled sections with wall thickness less than 0.1h, or 50 mm. In general additional bearing surfaces are required in thin section connectors (see Section 7.10.5)
- 'broad sections', where the cover distance to the sides of the insert is small enough to cause concern over shear cracking, and as a consequence the permissible stresses in the joint are reduced.

This part of the beam-to-column connection has been the subject of considerable research and analysis (e.g. [7.17, 7.34–7.37, 7.50–7.54]) and is therefore designed with a greater degree of confidence than many other joints in the precast frame.

There are several aspects to embedded steel connections that require special attention, such as the need to minimise voids (and in particular lifting holes within 400 mm of the insert) under the embedded section; the need for fire protection; and the need to ensure that the concrete surrounding the embedded section is adequately confined by links. The most popular shape for the insert is the SHS or RHS, because they have the following beneficial characteristics:

- high shear to flexural capacity (greater than UBs)
- uniform shape (making it easy to weld additional plates and rebars to it)
- favourable torsional properties (in non-symmetrical situations)
- range of sizes and thicknesses available (100 × 50 mm to 250 × 150 mm being the usual range).

The shear span for any section is given by $a = M_u/V_u$, where $M_u = p_y\ S_{xx}$, and $V_u = 0.6\ p_y\ 2\ d\ t$. For SHSs and RHSs, a = 90 mm to 120 mm, which is a convenient shear span for the majority of

beam-to-column connectors (see Exercise 7.1, where the shear span is 114 mm). On the other hand, for UBs, $a = 150$ mm to 190 mm, making it uneconomical.

The most economical option in terms of minimising the size of the recesses in the beams is clearly the smaller, thicker sections. The minimum breadth of insert is taken as 75 mm. The minimum thickness for the steelwork is taken as 6 mm for rolled sections and 4 mm for box sections, providing that the insert is sealed to the passage of air and moisture when the joint is complete.

There are two ways of setting the insert in the column – either by casting directly into the column, or by forming a hole in the column and placing the insert into the hole using either grout or resin-mortar. In the former, the insert must penetrate the sides of the mould, which is made good by plating afterwards. Unless this operation is done well it may cause uneven surfaces in subsequent columns that are cast against the repaired mould. The latter option avoids damage to the mould. However, the main problem in this case is that cracking may propagate around the corners of the hole while the column is being lifted from the mould, particularly if the breadth of the hole is more than one-third of the breadth of the column. For heavily loaded connections, in which the *working* stress underneath the insert is greater than $0.567 f'_{ck}$ $\{0.4 f'_{cu}\}$ of the grout (calculated using a linear elastic analysis), an epoxy mortar should be considered. Apart from the obvious advantages in using a quick-setting material of considerable compressive and tensile strength, epoxy-based materials may be poured into a much smaller annulus than is possible with cementitious grout. This allows the hole in the column to be smaller, with its attendant benefits in detailing and crack resistance. A note of caution should be included here, and the specialist supplier of epoxies should be consulted about the long-term durability of certain epoxy mortars. The manufacturer's details should be strictly followed with regard to mix proportions, ambient conditions and cleanliness.

At ultimate, the confined localised stresses are often in excess of the cylinder {cube} strength of the concrete. Nonetheless, in the wide sections, design ultimate bearing stresses of only $0.567 f_{ck} \times$ confinement factor S_q $\{0.8 f_{cu}\}$ are used. For concentric loading, the ultimate bearing capacity is in the order of 800 kN (for a 300 mm-square column with a 100 mm-wide insert, allowing for 25 mm spalling in the cover concrete each side) and is rarely critical. The column connector is rated with respect to the design and ultimate load testing under eccentric loading. The *IStructE Manual* [7.21] proposes a method for determining the load and moment capacity of prismatic sections, which has found favour with many design engineers.

The design methods are adopted from the *PCI Manuals* using the design data given in BS EN 1992-1-1 [7.8] or BS 8110, Part 1, clause 5.3.5 [7.9] to replace those in the American standards. The method gives good agreement with the original PCI method and other, more rigorous analyses. The equilibrium of forces and moments at the ultimate limit state is achieved by reinforcing (or otherwise guarding) against bursting, spalling and splitting, etc. Figure 7.70 shows typical details of a multi-sided connection. The general practice is to guarantee the confinement of concrete directly above and below the column insert using closely spaced links and to ensure the main longitudinal reinforcement is not interrupted by the insert.

The centre line of the insert should not be less than $3b_p/2$ from the edge of the column. The insert must lie within the column reinforcement cage.

The beam's reactions due to patch loading give rise to non-symmetrically loaded connections. It is impossible for a column insert to be symmetrically loaded, and therefore the beam topography will always produce bending moments in the column. These may be as large as 150 kNm in extreme cases, but in general are in the order of 20 to 60 kNm. Corner columns are subjected to biaxial bending, although it is usual for one of the beams at a corner to be lightly loaded owing to the one-way spanning floor slabs. The most onerous design situation occurs in a single-sided insert.

7.10.2 Single-sided wide-section insert connections

The ultimate bearing capacity of the insert and the column into which it is cast is calculated as follows. Referring to Figure 7.71(a), the bearing stress is assumed to be uniform over limited areas of the insert.

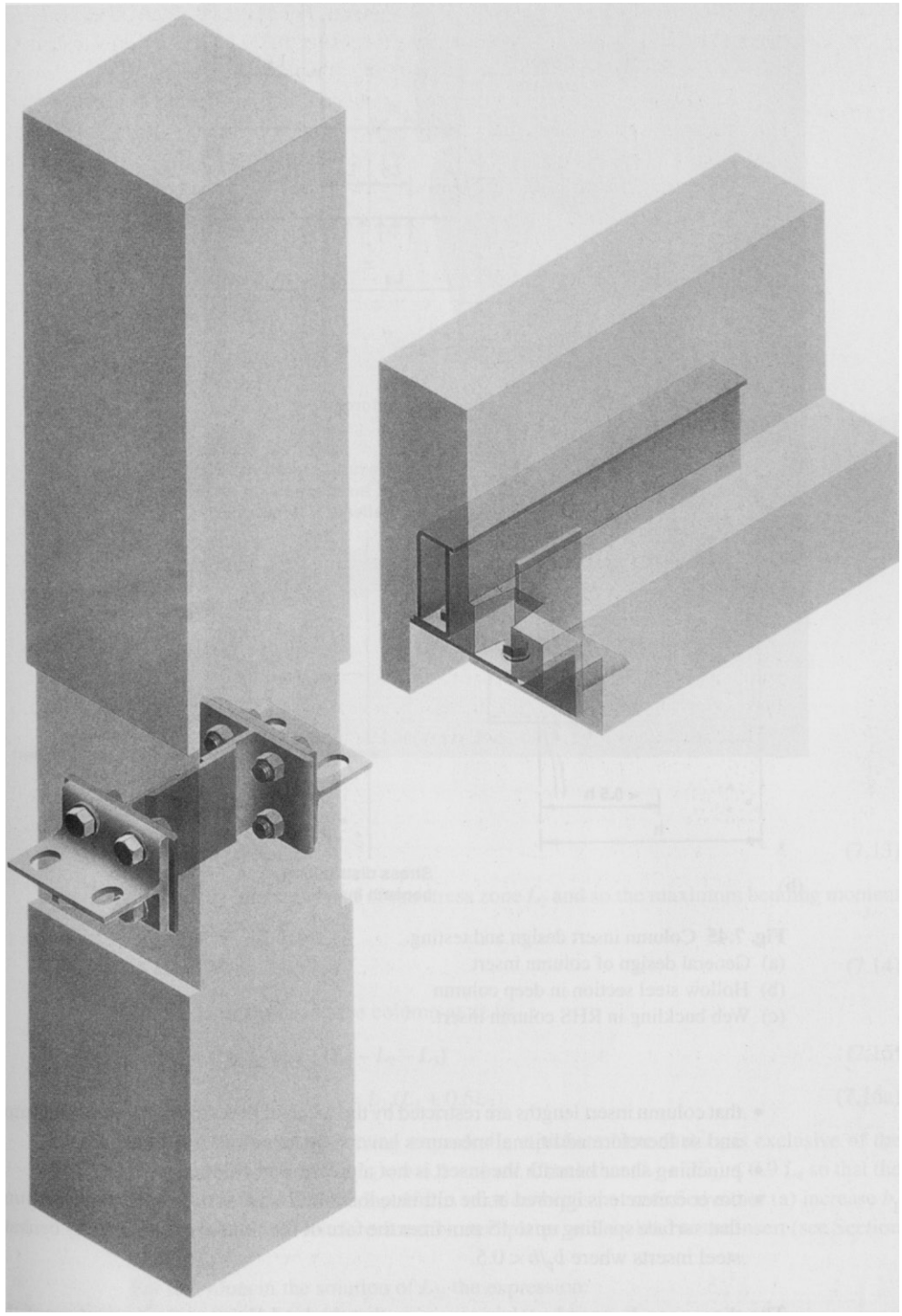

Figure 7.70 Multi-sided beam-to-column connection (courtesy of Trent Concrete Ltd).

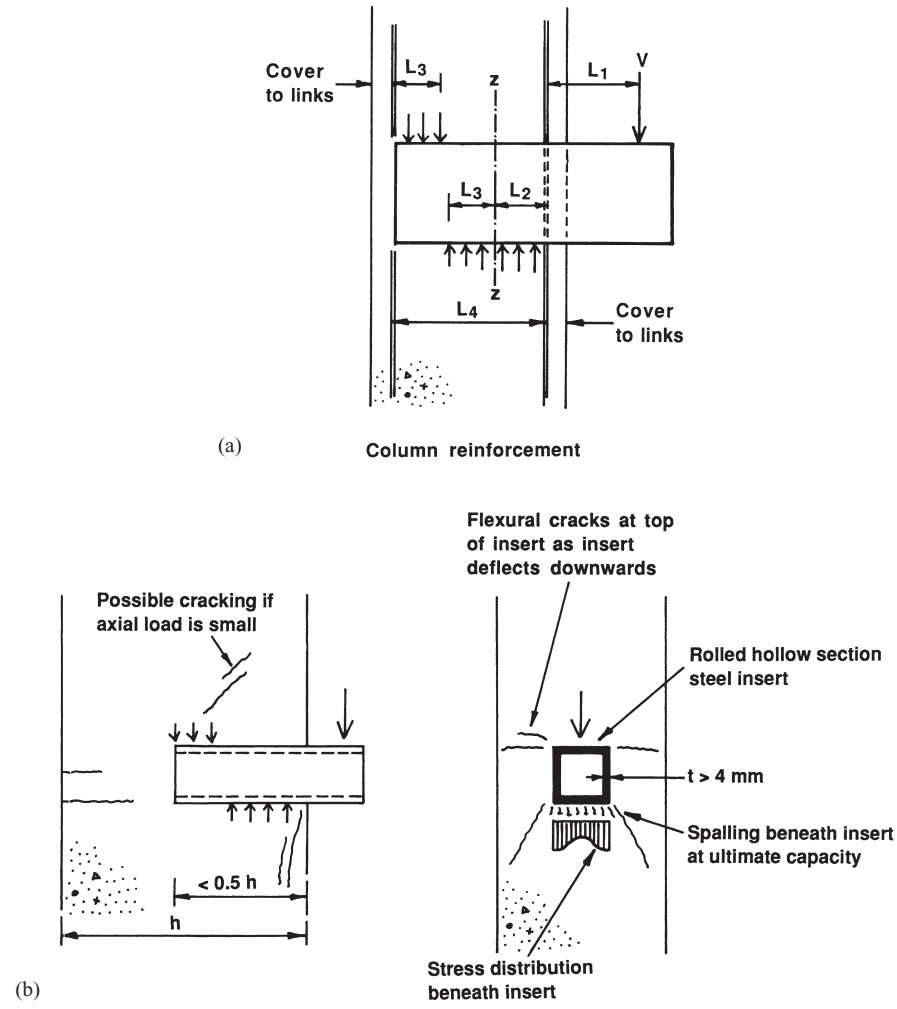

Figure 7.71 Column insert design and testing. (a) General design of column insert. (b) Hollow steel section in deep column.

To BS EN 1992-1-1 [7.8]. The ultimate bearing capacity of the insert is limited to $\alpha_{cc} f_{cd}$ ($\alpha_{cc} = 0.85$ where there are transverse tension forces) = $0.567 f_{ck}$. Clause 6.7(2) permits the zones beyond the areas of pressure to be treated as compressive struts underlying a partially loaded area, thereby taking advantage of enhanced pressures due to the confinement within the strut-and-tie system. The bearing stress used to calculate the strut force F_{Rdu} is enhanced by a factor $S_q \leq 3.0$: see Eq. (7.15).

To BS 8110 [7.9]. The ultimate bearing capacity of the insert is limited to $0.8 f_{cu}$ or f_b according to Eq. (7.13).

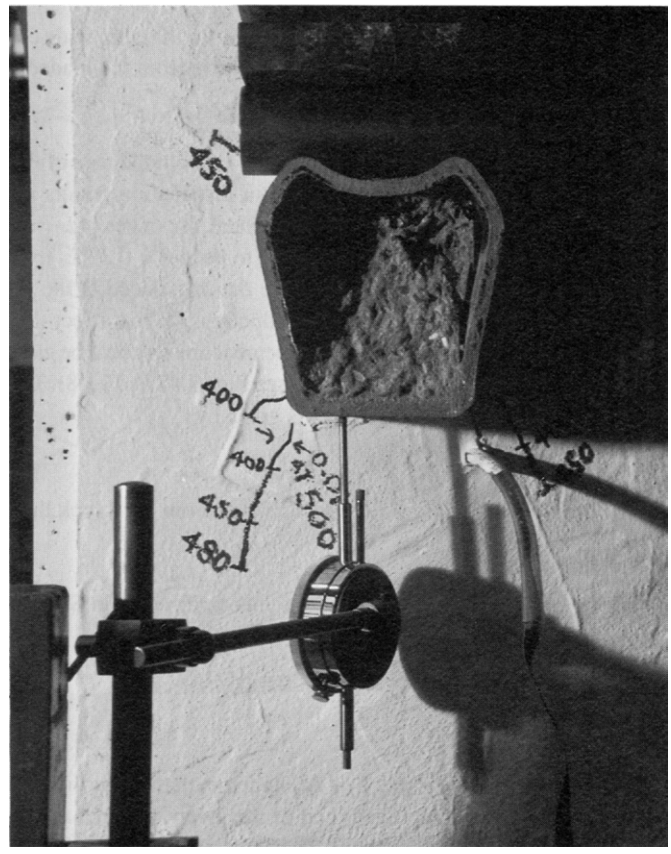

Figure 7.72 Web buckling in RHS column insert.

The line pressure consists of two components – one part to react the vertical load V, and a second part to produce a couple to react the bending moment. In reality the pressure distribution will be non-uniform [7.50], but because the columns are significantly less stiff than the beams, they will rotate to equalise the pressure. For the purpose of design it may be taken as shown in Figure 7.71(a).

The following design method is adapted from the *IStructE Manual* on joints [7.21] and is similar to the design of shear boxes in beams outlined in Section 4.3.11. The main differences here are that:

- column insert lengths are restricted by the width of the column, typically 300 mm, and so additional constraints arise
- punching shear beneath the insert is not a problem in columns
- cover concrete is ignored at the ultimate load other than to assist in pressure distribution. Full-scale testing by Elliott found that surface spalling up to 15 mm from the face of the column frequently occurs directly beneath steel inserts where $b_p/b < 0.5$.

The shear span L_1 must be obtained assuming that the load V acts at the centreline of the bearing area, plus an allowance for tolerances. Use the ultimate bearing pressure against the insert to find the contact length in compression, L_2 from the relationship:

$$L_2 = \frac{V}{0.567 f_{ck} S_{q23} b_p} \qquad (7.27)$$

in which S_{q23} is the confinement enhancing coefficient for the strut geometry defined by L_2 and L_3.

$$S_{q23} = \sqrt{\frac{A_{c1}}{A_{c0}}} \leq 3.0$$

in which A_{c0} is the area of bearing onto the strut, and A_{c1} is the maximum area of symmetrical strut that can exist along the orthogonal axis through the centroid of A_{c0}, with a limiting value for cover, c_{ov} of

$$S_{q23} = \sqrt{\frac{(b_p + 2c_{ov})(L_2 + L_3 + 2c_{ov})}{b_p(L_2 + L_3)}} \leq 3.0$$

$$L_2 = \frac{V}{0.8 f_{cu} b_p} \qquad (7.27)$$

Zero shear occurs at the end of the stress zone L_2 and so the maximum bending moment at plane z–z is given by:

$$M_{zz} = V(L_1 + 0.5L_2) \qquad (7.28)$$

Since the moment inside the column at z–z is:

$$M_{ZZ} = 0.8 f_{cu} b_p L_3 (L_4 - L_2 - L_3) \qquad (7.29)$$

$$M_{ZZ} = 0.567 f_{ck} S_{q23} b_p L_3 (L_4 - L_2 - L_3) \qquad (7.29)$$

Then

$$L_3(L_4 - L_2 - L_3) = L_2(L_1 + 0.5L_2) \qquad (7.30)$$

Note that L_4 is exclusive of the cover concrete to the links; $L_4 = h - 2 \times$ cover. L_3 can be found by solving a quadratic equation. For real roots in the solution of L_3, the expression $(L_1 + L_2)^2 - L_1^2 \leq 0.5(L_4 - L_2)^2$ must be satisfied. Check that the total depth of the rectangular stress blocks $(L_2 + 2L_3) \leq 0.9L_4$ so that the bearing surfaces do not overlap. If this relationship is not satisfied, either increase b_p or provide additional reinforcement or steel plates, etc. welded to the insert (see Section 7.10.3).

L_3 can be found by solving a quadratic or higher-order equation, depending on whether S_{q23} takes a limiting value or is itself a function of L_2 and L_3. Because derivation of L_2 and L_3 is interrelated by S_{q23}, it is most suited to a computer-based iterative solution.

In most practical cases the shear span L_1 for 300 mm-wide columns is between 60 and 120 mm. The position of the 'neutral axis' from the loaded face, X, is given by:

$$X = L_4 + c_{ov} - 0.5(L_4 - L_2) \qquad (7.31)$$

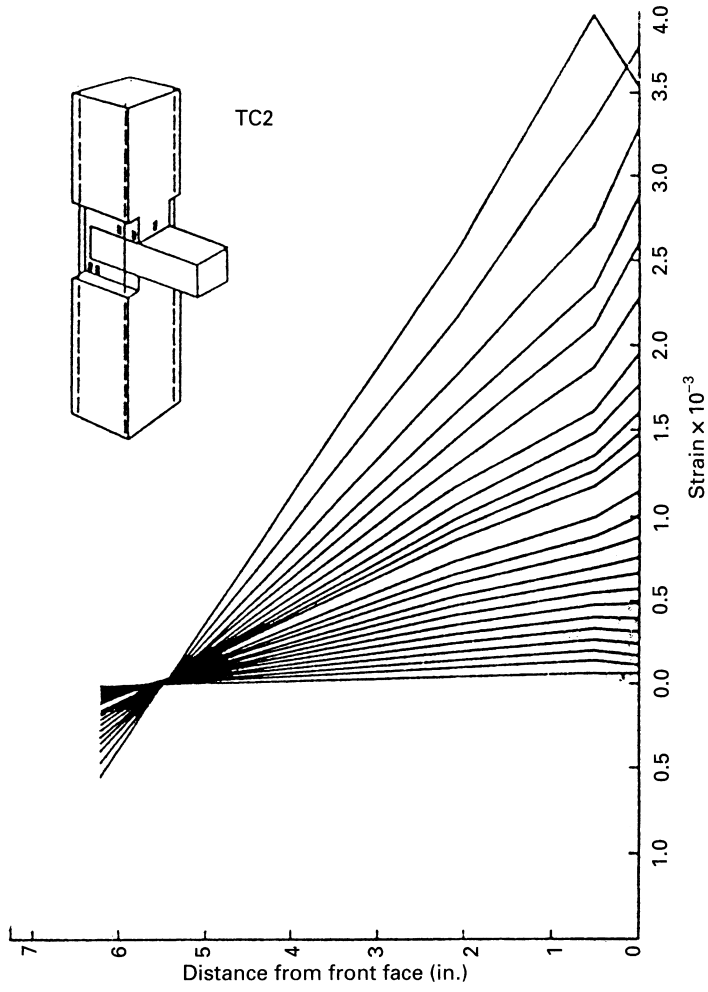

Figure 7.73 Strain distributions under steel billet in single-sided connector [7.52].

This works out at approximately $X = 0.7L_4$ from the face of the column. This is in good agreement with the experimental strain distribution results obtained by Marcakis and Mitchell [7.52] and shown in Figure 7.73 where, for values of $L_1 = 102\,\text{mm}$, $b = h = 203\,\text{mm}$, $L_4 = 184\,\text{mm}$, the neutral axis is found to be at $X = 0.77L_4$ from the face of the column.

Column reinforcement must not be cut or reduced at the position of the steel insert unless tests have shown that such reductions do not affect the capacity of the column. Displaced column links, called confinement links, should be grouped and placed at close centres (typically 50 mm) immediately above and below the insert (see Figures 7.74 and 7.75). The maximum compressive force occurs below the insert and is given by:

$$F = 0.567 f_{ck} S_{q23} b_p (L_3 + L_2) \qquad (7.32) \quad | \quad F = 0.8 f_{cu} b_p (L_3 + L_2) \qquad (7.32)$$

The horizontal bursting force is calculated from end block theory to give:

$$F_{bst} = \varsigma F \qquad (7.33)$$

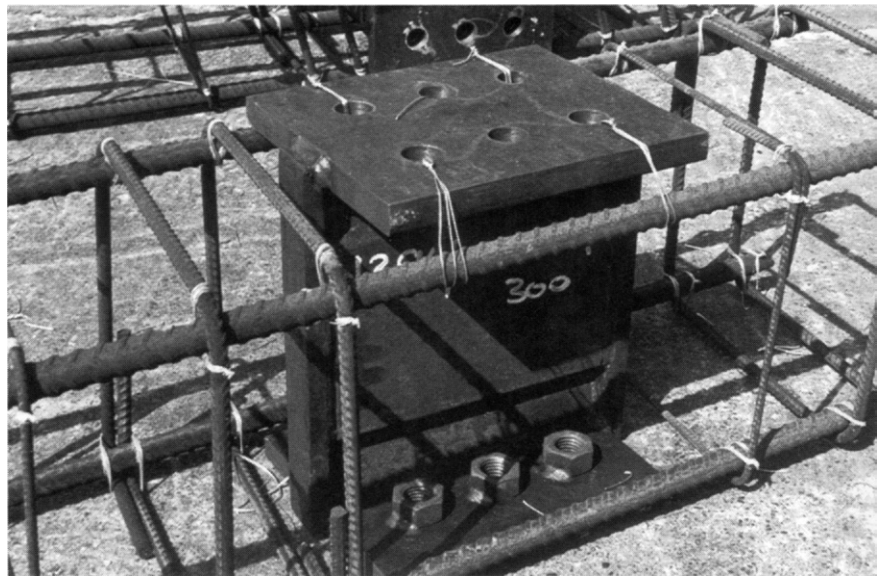

Figure 7.74 Confinement links near to cast-in rolled H-section.

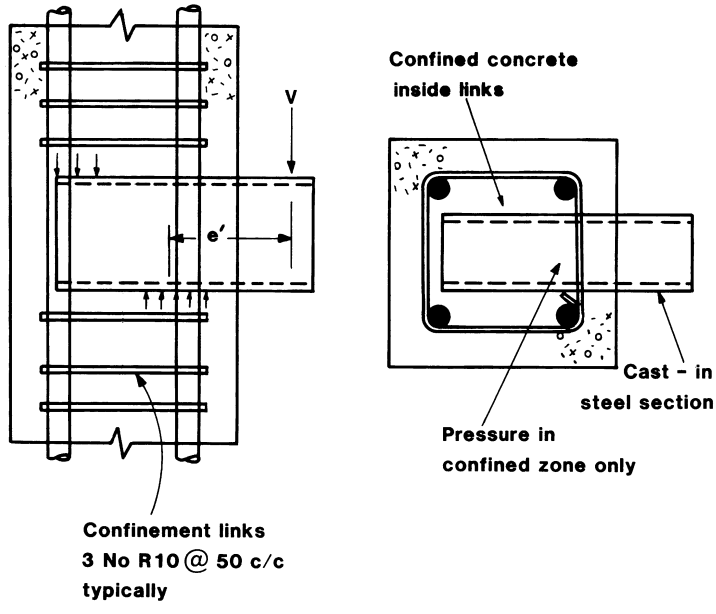

Figure 7.75 Design of confinement links around column connector.

where ς is the bursting force coefficient referred to in Section 4.3.10. Thus the area of confinement steel A_{bst} is given by:

$$A_{bst} = \frac{F_{bst}}{0.87 f_{yv}} \tag{7.34}$$

If the zone of pressure underneath the insert (i.e. $L_2 + L_3$) is small and located near the front end of the insert (i.e. nearest the load), the area A_{bst} should be only one leg of each of the confinement links. The links should be of the 'closed' variety, with proper anchorage. This is because the bursting forces will be present only in the front face of the column. Bursting forces will not affect the rear of the column until the pressure zone extends sufficiently far along the insert. Although there is a gradual increase in bursting forces in the column faces, the following is recommended from tests carried out by Elliott on asymmetrically loaded bearing plates:

If $L_2 + L_3 + c_{ov} < h/3$, all A_{bst} to be provided by one leg of the links.
If $h/3 < L_2 + L_3 + c_{ov} < h/2$, ⅔ of A_{bst} to be provided by one leg of the links.
If $L_2 + L_3 + c_{ov} > h/2$, ½ of A_{bst} to be provided by one leg of the links.

Short length billets (Figure 7.71(b)) may fail by diagonal cracking above the billet and so confinement steel is placed above the insert, based on the compression zone defined by L_3 as:

$$F_{bst} = \varsigma 0.567 f_{ck} S_{q23} b_p L_3 \qquad (7.35) \quad | \quad F_{bst} = \varsigma 0.8 f_{cu} b_p L_3 \tag{7.35}$$

using Eq. (7.34) to design the steel.

The maximum bending moment in the steel insert occurs at zero shear, when

$$L_2 = V/(0.567\, f_{ck}\, S_{q23}\, b_p) \qquad | \quad L_2 = V/(0.8\, f_{cu}\, b_p)$$

from the end of the stress block. The eccentricity e' is given by:

$$e' = (L_2/2) + \text{cover} + \text{distance from face of column to reaction point.} \tag{7.36}$$

Thus

$$M_{zz} = Ve' = V(L_1 + 0.5L_2) \tag{7.37}$$

Then the plastic modulus $S_{xx} > M_{zz}/p_y$, and the web area $> V/0.6\, p_y$.

In the case of rectangular hollow sections, web buckling and bearing are avoided by filling the hollow section with concrete or grout, either in the factory or during the grouting operation on site. Expanding agents may be used for the infill. In tests by Elliott, web buckling occurred at around 525 kN (see Figure 7.72) in joints designed for 400 kN ultimate load according to Figure 7.71(b). Any projecting parts must be checked to ensure that they will not distort excessively or buckle under the applied joint loads and rotations. Local spalling may result at the face of the columns under uneven loading created by distorted sections.

The foregoing analysis is highly simplified for the purpose of design, and conservative with respect to the real behaviour of the connection after construction. It is known that there are several inconsistencies in the assumptions used in the design manuals, some of which are explained in various papers on the strength of column inserts (e.g. [7.50, 7.53, 7.54]). For example, in Figure 7.71 the position of the neutral axis depth is assumed constant, when in reality it varies with the eccentricity and magnitude of loading, and is also dependent on the relative confinement of concrete above and below the steel insert. It is also supposed that in the fully grouted assembly the beam has a restraining effect on bending of the insert, and that the insert is actually behaving not as a short cantilever but

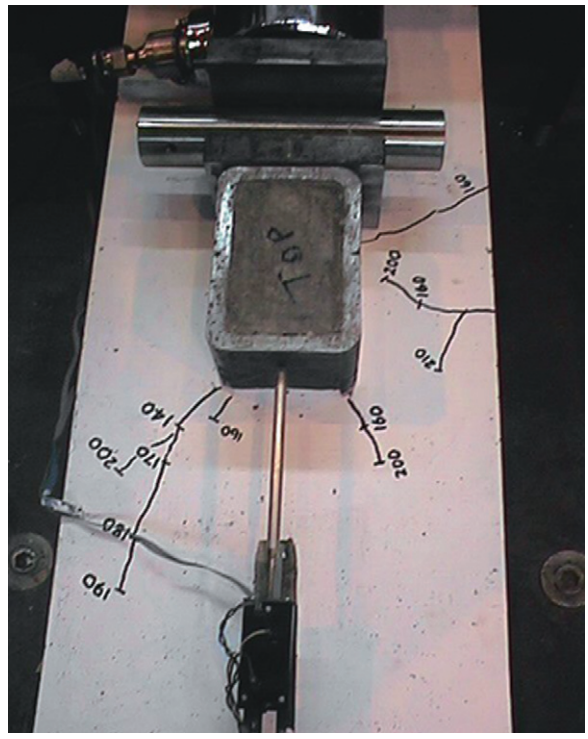

(a)

Figure 7.76(a) Steel billet column connector test incorporating concrete-filled steel RHS shows where the principal tension needs to be reinforced. The black box beneath the insert is a displacement gauge with a sensitivity of 0.001 mm.

as a stiff web. Holmes and Posner [7.50] also suggest that the calculation of bursting forces beneath inserts is more complicated than using a simple geometric relationship, and that the real effects of concrete shrinkage and compaction beneath the insert, and the presence of main longitudinal bars, should all be considered.

A full-scale demonstration test was carried out by Elliott on 150 kN ultimate capacity steel billets cast into 300×300 mm columns of compressive cube strength $f_c = 61\,\text{N/mm}^2$ and indirect axial tension $f_t = 5.4\,\text{N/mm}^2$ (both the mean of 3 specimens). Figure 7.76 shows the importance of providing reinforcement close to the corners of the steel billet, where strain and stress contours pack together. This example shows that the principal tension is parallel to the side of the billet and is across the corner of the billet, both places requiring reinforcement. While a close-fitting diagonal rebar would satisfy the latter, high-tensile links are provided in combination with the main rebars in the column. The predicted cracking load was 110 kN, based on a local shear stress at the bottom corner of the billet resulting in 45° principal tension of $5\,\text{N/mm}^2$, whereas the 55° crack was first observed at 140 kN. The ultimate capacity was about 220 kN, as a complete failure was unsafe (roller dislodging), giving a factor over design of 1.47. The stiffness up to the point of the design capacity was approximately 1130 kN/mm.

The effects of axial precompression, load eccentricity, shape and width of the insert and of additional reinforcement welded to the sides of the insert have also been studied [7.52]. The most important results showed that for $b_p < b/2$ the effective width of the insert extended to the width of the confined column region as bounded by the links. Closely spaced links, i.e. at less than 75 mm spacing, were necessary to ensure the connection failed in a ductile manner. Very high axial loads, e.g. 0.75 of the squash load, resulted in a decrease in ductility at failure. The insert is therefore underdesigned with respect to the biaxial failure strength of concrete. Design practice in the Eurocode has responded to many of these findings.

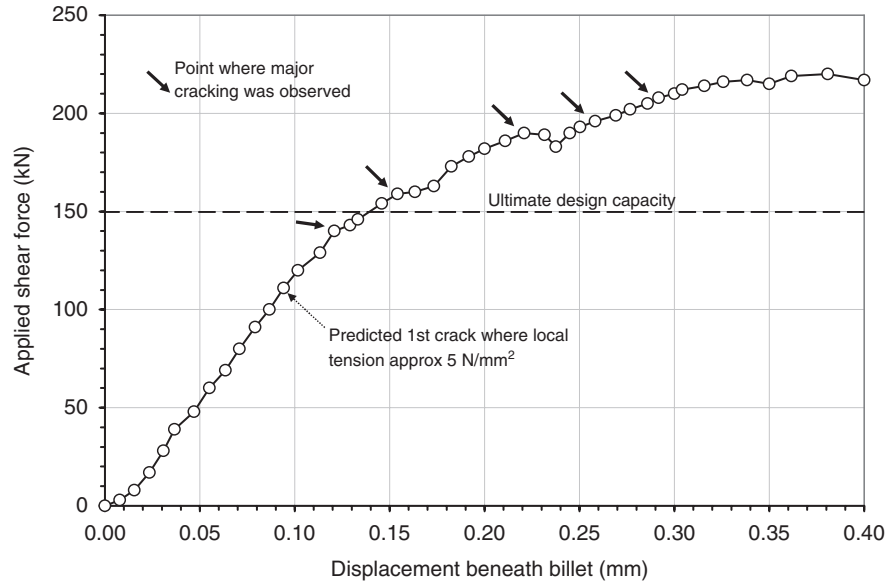

Figure 7.76(b) Steel billet column connector test: applied shear force versus displacement beneath the billet.

Exercise 7.2 Billet type single-sided column connector

Figure 7.77 shows the detail of a square, hollow, box-type billet column connector used to support a rectangular precast beam. The maximum distance from the face of the column to the centre of the beam bearing is 60 mm. Given that the ultimate beam reaction is 142.5 kN {equivalent to 150 kN to allow for increased partial load factors in BS 8110}, calculate the confinement reinforcement required below and above the billet.

Use concrete grade C40/50, $f_{yv} = 500\,\text{N/mm}^2$, cover to reinforcement = 35 mm, and grade S275 {43} steel.

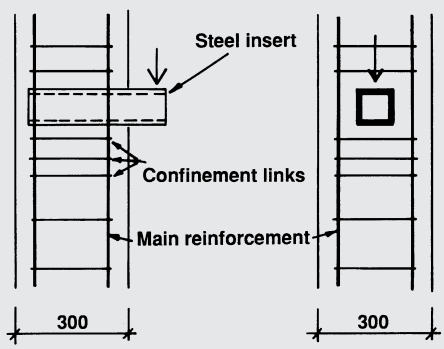

Figure 7.77 Details for Exercise 7.2.

(*Continued*)

Solution

Step 1: Column reinforcement

Assume $b_p = 100\,\text{mm}$

Calculate maximum pressure under billet as the lesser of:

S_{q23} is an iterative function of the line pressure lengths $L_2 + L_3$ and is shown later = 2.021	
$f_b = 0.567 \times 40 \times 2.021$	$= 45.81\,\text{N/mm}^2$
Line pressure under billet = 45.81×100	$= 4581\,\text{N/mm}$
$L_2 = \dfrac{142.5\times10^3}{4581}$	$= 31.1\,\text{mm}$
$M_{zz} = 142.5 \times (95 + 31.1/2)$	$= 15753\,\text{kNmm}$
Maximum length of billet = $300 - 35$	$= 265\,\text{mm}$
Distance between end of billet and start of pressure at L_2	
$= 265 - 35 - L_2 = 198.9\,\text{mm}$	
$M_{zz} = 4581L_3 \times (198.9 - L_3)$	
Solving gives L_3	$= 19.1\,\text{mm}$
$L_2 + 2L_3 = 69.4 < 0.9L_4 = 207\,\text{mm}$	
Check $S_{q23} = \sqrt{\dfrac{170\times(50.2+70)}{100\times50.2}} = 2.021$	
Total vertical force below connector	
$= 4581\ (19.1 + 31.1) \times 10^{-3}$	$= 230.1\,\text{kN}$
Total force above connector	$= 87.6\,\text{kN}$
(with $S_{q5} = 3.0$ and $L_5 = 12.65\,\text{mm}$)	
Bursting force coefficient $\varsigma = 0.25\left(1 - \dfrac{100}{300}\right) = 0.1667$	
$F_{bst} = 0.1667 \times 230.1$ below insert	$= 38.4\,\text{kN}$
$F_{bst} = 0.1667 \times 87.6$ above insert	$= 14.6\,\text{kN}$
$L_2 + L_3$ + cover	$= 85.2\,\text{mm}$
so all A_{bst} to be in one leg of confinement link	
$A_{bst} = \dfrac{38.4\times10^3}{0.87\times500}$ below the insert	$= 89\,\text{mm}^2$
$A_{bst} = \dfrac{14.6\times10^3}{0.87\times500}$ above the insert	$= 34\,\text{mm}^2$

$f_b = \dfrac{1.5f_{cu}}{1+(2b_p/h)} = \dfrac{1.5\times50}{1+(2\times100/300)}$	$= 45\,\text{N/mm}^2$
or $f_b = 0.8f_{cu}$	$= 40\,\text{N/mm}^2$
Line pressure under billet = 40×100	$= 4000\,\text{N/mm}$
$L_2 = \dfrac{150\times10^3}{4000}$	$= 37.5\,\text{mm}$
$M_{zz} = 150 \times (95 + 37.5/2)$	$= 17062\,\text{kNmm}$
Maximum length of billet = $300 - 35$	$= 265\,\text{mm}$
Distance between end of billet and start of pressure at L_2	
$= 265 - 35 - L_2 = 192.5\,\text{mm}$	
$M_{zz} = 4000L_3 \times (192.5 - L_3)$	
Solving gives L_3	$= 25.6\,\text{mm}$
$L_2 + 2L_3 = 88.7 < 0.9L_4 = 207\,\text{mm}$	
Total vertical force below connector	
$= 4000\ (25.6 + 37.5) \times 10^{-3}$	$= 252.4\,\text{kN}$
Total force above connector	$= 102.4\,\text{kN}$
(Table 4.11a) Bursting force coefficient for $b_p/b = 0.33$, $\varsigma = 0.21$	
$F_{bst} = 0.21 \times 2524$ below insert	$= 52.5\,\text{kN}$
$F_{bst} = 0.21 \times 1024$ above insert	$= 21.3\,\text{kN}$
$L_2 + L_3$ + cover	$= 98.1\,\text{mm}$
so all A_{bst} to be in one leg of confinement link	
$A_{bst} = \dfrac{52.5\times10^3}{0.87\times500}$ below the insert	$= 121\,\text{mm}^2$
$A_{bst} = \dfrac{21.3\times10^3}{0.87\times500}$ above the insert	$= 49\,\text{mm}^2$

Use two H10 ($157\,\text{mm}^2$) closed links below connector.
Use one H10 ($78\,\text{mm}^2$) closed link below connector.

Step 2: Insert design

The maximum moment in the steel insert occurs at zero shear, which is at

$L_2 = 31.1\,\text{mm}$	
from end of stress block	
$S_{xx} > 15\,753/275$	$= 57.29\,\text{cm}^3$
$2dt > 142\,500/165$	$= 863.6\,\text{mm}^2$

$L_2 = 150\,000/4000 = 37.5\,\text{mm}$	
from end of stress block	
$S_{xx} > 17\,062/275$	$= 62.05\,\text{cm}^3$
$2dt > 150\,000/165$	$= 909.1\,\text{mm}^2$

Use $100 \times 100 \times 5$ SHS ($S_{xx} = 66.4\,\text{cm}^3$ and $2dt = 1000\,\text{mm}^2$).

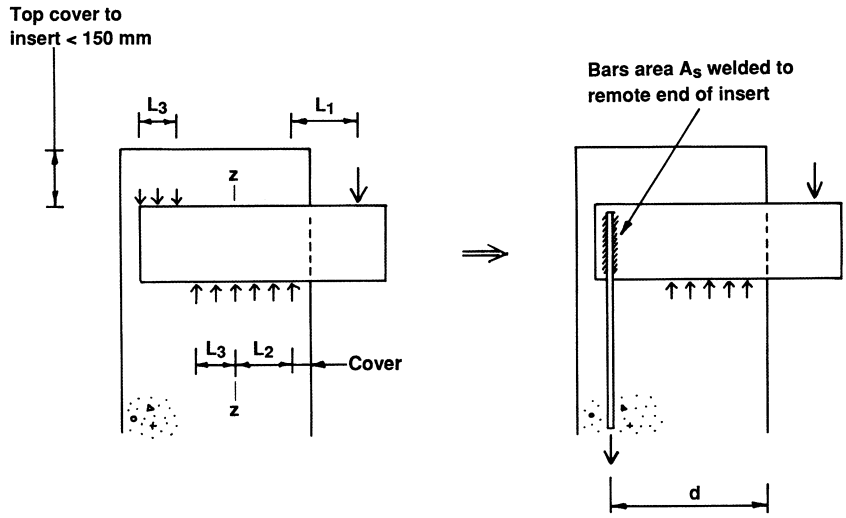

Figure 7.78 Additional tie-back reinforcement welded to insert.

7.10.3 Addition of welded reinforcement to wide-section inserts

Where the insert lies close to the top of the column such that the restraining force cannot develop above its end, reinforcement should be welded to the sides of the remote end of the insert and anchored by full bond development, as shown in Figure 7.78. The decision as to whether the top cover is adequate is made on practical grounds as well as assessing punching shear at the critical section. Generally, if the cover to the top of the insert is less than 150 mm, then it is certain that a designer will not allow the insert to rely on holding down pressure $0.567\ f_{ck}\ S_{q23}\ b_p$ $\{0.8\ f_{cu}\ b_p\}$. These stresses must ultimately be transferred back below the insert by the column's main reinforcement after development of bond stresses some distance from the stressed area.

Alternatively, the stress may be transferred directly down the column by bars welded to the insert. Referring to Figure 7.78:

$$M_{ZZ} = 0.567 f_{ck} S_{q23} b_p L_2 (L_1 + 0.5L_2) \quad (7.38)$$
$$M_{ZZ} = 0.567 f_{ck} S_{q23} b_p L_3 (d - c_{ov} - L_2 - 0.5L_3) \quad (7.39)$$

$$M_{ZZ} = 0.8 f_{cu} b_p L_2 (L_1 + 0.5L_2) \quad (7.38)$$
$$M_{ZZ} = 0.8 f_{cu} b_p L_3 (d - c_{ov} - L_2 - 0.5L_3) \quad (7.39)$$

hence L_3 may be determined.

Check $L_2 + L_3 < L_4$ so that a couple may be generated.

Check $L_2 + L_3 < 0.7\ L_4$ so that a couple may be generated.

The steel required to replace the upthrust is:

$$A_s = \frac{0.567 f_{ck} S_{q23} b_p L_3}{0.87 f_{yk}} \quad (7.40)$$

$$A_s = \frac{0.8 f_{cu} b_p L_3}{0.87 f_y} \quad (7.40)$$

Where the top cover to the insert is greater than 200 mm, at least three closed links may be provided and the concrete well compacted, thus allowing the bearing pressures to develop.

If the strength capacity of an insert is less than required owing to overlapping pressure around the insert, one remedy is to add extra bars to both the front and rear of the insert. In calculating the strength it is then assumed that the bars can act in tension or compression both above and below

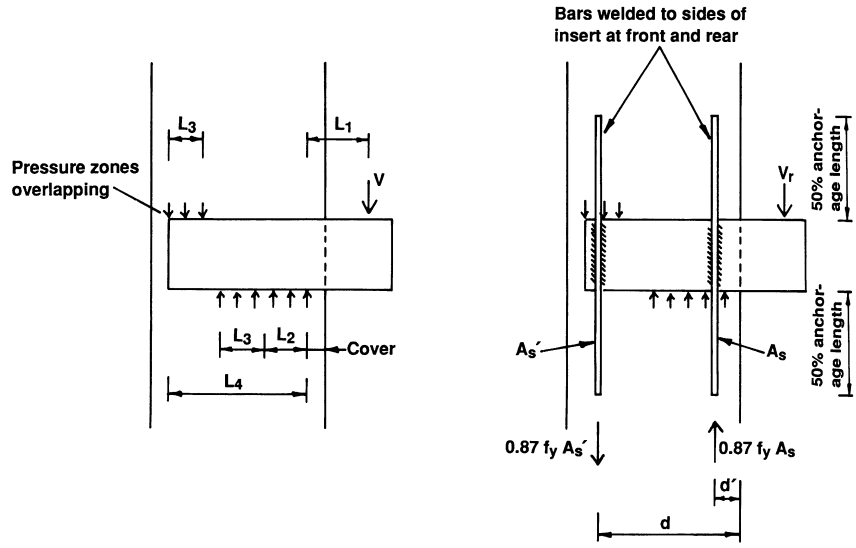

Figure 7.79 Additional reinforcement welded to insert.

the insert, and can develop their ultimate yield strength by the action of bond alone. The bars are placed projecting an equal distance either side of the insert, as shown in Figure 7.79. Although deformed bar is used in order to keep the anchorage bond lengths to a minimum, the bar is welded, so ultimate stress in the bar is taken as the value for mild steel reinforcement, i.e. 250 N/mm^2. In order to develop a full bond strength the bars should be positioned with a centroidal cover distance of at least 50 mm, and be enclosed within confining links of area not less than $0.5 \times A_s$, i.e. the bursting coefficient for rebars close to the edge of concrete is taken as 0.5. The weld can be deposited on both sides of the bar, i.e. effective thickness = 2 × throat thickness = 1.4 × weld leg. The weld design should be according to BS EN 1993-1-1 [7.55] {BS 5950, Part 1: 1985 [7.56] clause 6.6}.

The moment of resistance using this reinforcement increases from M, in the unreinforced case, to M_r. The corresponding vertical shear increases from V to V_r. The equilibrium conditions are obtained by reference to Figure 7.78, resolving vertically before the introduction of the bars and then taking moments:

$$V = 0.567 f_{ck} S_{q23} b L_2$$
$$V(L_1 + 0.5L_2) = 0.87 f_{yk} A'_s (d - d') \quad (7.41)$$

$$V = 0.8 f_{cu} b L_2$$
$$V(L_1 + 0.5L_2) = 0.87 f_y A'_s (d - d') \quad (7.41)$$

$A_s = A'_s$, because the vertical force V is resisted by the concrete alone. When V is increased to V_r, then:

$$V_r = 0.567 f_{ck} S_{q23} b L_2 + 0.87 f_{yk} (A_s - A'_s) \quad (7.42)$$

and

$$V_r - V\,(d + L_1 - c_{ov}) = 0.87\, f_{yk}\, A_s\, (d - d') \quad (7.43)$$

$$V_r = 0.8 f_{cu} b L_2 + 0.87 f_y (A_s - A'_s) \quad (7.42)$$

and

$$V_r - V\,(d + L_1 - c_{ov}) = 0.87\, f_y\, A_s\, (d - d') \quad (7.43)$$

where $A_s > A'_s$ and L_2 is assumed to remain unchanged from the previous case. This may not be strictly true because of the influence of the welded reinforcement on the strain distribution in the cast-in section, but the assumption is sufficiently accurate not to warrant further detailed analysis. To ensure that the lever arm between the pressure zone beneath the insert and the bars welded to the rear end is sufficient, it is necessary to restrict $L_2 < 0.7\ L_4$. See the experimental results in Figure 7.73 [7.52].

Exercise 7.3 Inserts close to the top of the column

A 300 × 300 mm column carries a single-sided asymmetrical ultimate load of 209 kN {220 kN owing to higher partial factors} at a maximum distance from the face of the column of 60 mm. The top of the insert is located at only 100 mm from the top of the column. Design a suitable rectangular hollow section to be cast into the column and suitable steel bars to be welded to the rear end of the insert.

Use concrete grade C40/50, f_{ywk} {f_{yv}} = 500 N/mm^2, f_{ykw} {f_{yw}} = 250 N/mm^2 if bar is welded, cover to reinforcement = 35 mm, and grade S275 {43} steel.

Solution

Step 1: Insert design

Assume $b_p = 100$ mm

S_{q23} is shown later = 1.656

Line pressure = 0.567 × 40 × 100 × 1.656
= 3754 N/mm

$L_2 = \dfrac{209\times10^3}{3754}$ = 55.7 mm

$M_{zz} = 209\left(95+\dfrac{55.7}{2}\right)$ = 25674 kNmm

$S_{xx} = \dfrac{25674}{275}$ = 93.4 cm^3

$2dt = \dfrac{209\times10^3}{165}$ = 1267 mm^2

Line pressure = 0.8 × 50 × 100
= 4000 N/mm

$L_2 = \dfrac{220\times10^3}{4000}$ = 55.0 mm

$M_{zz} = 220\left(95+\dfrac{55}{2}\right)$ = 26950 kNmm

$S_{xx} = \dfrac{26.95\times10^3}{275}$ = 98 cm^3

$2dt = \dfrac{220\times10^3}{165}$ = 1333 mm^2

Use 150 × 100 × 5 RHS (S_{xx} = 119 cm^3 and $2dt$ = 1500 mm^2).

Step 2: Tie-bar design

Maximum length of billet = 300 − 35 = 265 mm

Assume 12 mm dia. links and 32 mm dia. tie-down bars.

Edge distance to tie-down bars = 35 + 12 +16 = 63 mm

d = 237 mm

$M_{ZZ} = 0.567 f_{cu} S_{q23} b_p L_3 (d - c_{ov} - L_2 + 0.5L_3)$

$M_{ZZ} = 3754 L_3 (147 - L_3)$

Solving gives L_3 = 58.4 mm

$S_{q23} = \sqrt{\dfrac{170\times(114.7+70)}{100\times114.7}} = 1.656$

Total force in steel = 3754 × 100 × 58.4 = 219.2 kN

$A_s = \dfrac{219.2\times10^3}{0.87\times250}$ = 1007 mm^2

$M_{ZZ} = 0.8 f_{cu} b_p L_3 (d - c_{ov} - L_2 + 0.5L_3)$

$M_{ZZ} = 4000 L_3 (147 - L_3)$

Solution of this quadratic gives L_3 = 56.8 mm

Total force in steel = 4000 × 100 × 56.8 = 227.2 kN

$A_s = \dfrac{227.2\times10^3}{0.87\times250}$ = 1045 mm^2

Use two H32 bars (1608 mm^2) at 47 mm cover welded to side of insert.

(*Continued*)

Step 3: Weld design
Weld length required, assuming 8 mm continuous fillet weld to both sides of the bar (CFW)

(See Table 7.12) $f_{wd} = 275/1.25$
$= 220\,\text{N/mm}^2$

$$L_w = \frac{219.2\times10^3}{2\times1.4\times8\times220} = 44.5\,\text{mm}$$

Plus 16 mm run-outs, makes $L_w = 60.5\,\text{mm}$

$f_w = 215\,\text{N/mm}^2$

$$L_w = \frac{227.2\times10^3}{2\times1.4\times8\times215} = 47.2\,\text{mm}$$

Plus 16 mm run-outs, makes $L_w = 63.2\,\text{mm}$

Provide 8 mm CFW 150 mm long to both sides of bar.

Step 4: Link design

Total force below connector = 428.2 kN

Bursting force coefficient

$$\varsigma = 0.25\left(1-\frac{100}{300}\right) = 0.1667$$

$F_{bst} = 0.1667 \times 4282$ below insert = 71.4 kN

$L_2 + L_3$ + cover = 149.1 mm

so ⅔ A_{bst} to be in one leg of link

$$A_{bst} = \frac{71.4\times10^3}{0.87\times500}\times\frac{2}{3} = 110\,\text{mm}^2$$

below the insert

Total force below connector = 447.2 kN

(Table 4.10a) Bursting force coefficient for $b_p/b = 0.33$, $\varsigma = 0.22$

$F_{bst} = 0.22 \times 447.2$ below insert = 98.4 kN

$L_2 + L_3$ + cover = 146.8 mm

so ⅔ A_{bst} to be in one leg of link

$$A_{bst} = \frac{98.4\times10^3}{0.87\times500}\times\frac{2}{3} = 151\,\text{mm}^2$$

below the insert

Use two H10 closed links below connector (157 mm²).

Exercise 7.4 Billet with additional reinforcement

Repeat Exercise 7.3 for a beam end reaction of 285 kN {300 kN due to higher partial factors}. Check the adequacy of the insert and provide additional reinforcement to the insert if necessary.

Solution

Step 1: Insert design
Assume $b_p = 100$ mm

S_{q2} is shown later = 1.860

Line pressure = 0.567 × 40 × 100 × 1.860
= 4216 N/mm

$$L_2 = \frac{285\times10^3}{4216} = 67.6\,\text{mm}$$

$$S_{q23} = \sqrt{\frac{170\times(67.6+70)}{100\times67.6}} = 1.860$$

$$M_{zz} = 285\left(95+\frac{67.6}{2}\right) = 36\,707\,\text{kNmm}$$

$$S_{xx} = \frac{36707}{275} = 133.5\,\text{cm}^3$$

$$2dt = \frac{285\times10^3}{165} = 1727.3\,\text{mm}^2$$

Line pressure remains 4000 N/mm

$$L_2 = \frac{300\times10^3}{4000} = 75\,\text{mm}$$

$$M_{zz} = 300\left(95+\frac{75}{2}\right) = 39\,750\,\text{kNmm}$$

$$S_{xx} = \frac{39750}{275} = 144.6\,\text{cm}^3$$

$$2dt = \frac{300\times10^3}{165} = 1818.2\,\text{mm}^2$$

Use 150 × 100 × 5 RHS ($S_{xx} = 147\,\text{cm}^3$ and $2dt = 1890\,\text{mm}^2$).

Step 2: Tie-bar design
Retain length L_2.
Maximum length of insert = 300 − 35 = 265 mm
Assume 10 mm dia. links and 32 mm dia. tie-down bars.
Edge distance to tie-down bars = 35 + 10 + 16 = 61 mm
$d - d' = 178$ mm

$M_{ZZ} = 0.87 f_{yk} A_s (d - d')$, gives

$$A_s = \frac{36707 \times 10^3}{(0.87 \times 250) \times 178} = 949 \text{ mm}^2$$

$M_{ZZ} = 0.87 f_y A_s (d - d')$, gives

$$A_s = \frac{39750 \times 10^3}{(0.87 \times 250) \times 178} = 1027 \text{ mm}^2$$

Use two H32 bars (1608 mm^2) at 45 mm cover welded to side of insert.

Step 3: Weld design
Weld length required, assuming 8 mm continuous fillet weld to both sides of the bar (CFW)

Force in each bar $\frac{36707}{2 \times 178}$ = 103.1 kN

$$L_w = \frac{103.1 \times 10^3}{1.4 \times 8 \times 220} = 41.8 \text{ mm}$$

Plus 16 mm run-outs, makes L_w = 57.8 mm

Force in each bar $\frac{39750}{2 \times 178}$ = 111.7 kN

$$L_w = \frac{111.7 \times 10^3}{1.4 \times 8 \times 215} = 46.4 \text{ mm}$$

Plus 16 mm run-outs, makes L_w = 62.4 mm

Provide 8 mm CFW 150 mm long to both sides of bar.

Step 4: Link design

Total force below connector = 285.0 kN
Bursting force coefficient

$$\varsigma = 0.25\left(1 - \frac{100}{300}\right) = 0.1667$$

F_{bst} = 0.1667 × 2850 below insert = 47.5 kN
L_2 + cover = 102.6 mm
so ⅔ A_{bst} to be in one leg of link

$$A_{bst} = \frac{47.5 \times 10^3}{0.87 \times 500} \times \frac{2}{3} = 73 \text{ mm}^2$$

below the insert

Total force below connector = 300.0 kN
Bursting force coefficient for $b_p/b = 0.33$, $\varsigma = 0.21$
F_{bst} = 0.21 × 3000 below insert = 63.0 kN
L_2 + cover = 110 mm
so ⅔ A_{bst} to be in one leg of link

$$A_{bst} = \frac{63.0 \times 10^3}{0.87 \times 500} \times \frac{2}{3} = 97 \text{ mm}^2$$

below the insert

Use two H10 closed links below connector (157 mm^2).

7.10.4 Double-sided wide-section inserts

Internal column connectors supporting a symmetrical arrangement of beams may be designed along similar lines to the single-sided connector in Section 7.10.1, by finding the equivalent point load. Patch loading is used where the maximum and minimum beam reactions are:

V_{max} = 1.35 × permanent + 1.5 × imposed
V_{min} = 1.0 × permanent

V_{max} = 1.4 × permanent + 1.6 × imposed
V_{min} = 1.0 × permanent

The net overturning moment is obtained from the worst possible scenario when the construction tolerance Δ is added to the eccentricity of the greater load and deducted from the eccentricity of the smaller. Thus if the distance from the centroid of the column to the centre of the beam reaction is e, the net moment on the connector is:

$$M_{net} = M_{max} - M_{min} = V_{max}(e + \Delta) - V_{min}(e - \Delta) \tag{7.44}$$

The net eccentricity is given by:

$$e_{net} = M_{net}/V_{max} + V_{min} \tag{7.45}$$

The analysis may now proceed in the same manner as for the single-sided connection above. Note that L_1 may be negative if $e < h/2 -$ cover, and that the equation for overturning $M_{zz} = V\,(L_1 + L_2/2)$ is as follows:

$$M_{zz} = V(-(e - h/2 + c_{ov}) + L_2/2) \tag{7.46}$$

Only where the eccentricity e is greater than a certain value do we need to consider the effects of bending. Referring to Figure 7.80, we can adapt a kind of 'middle-third' rule used in combined stress analysis in prismatic sections to find a limiting value for the eccentricity. Bending stresses occur where e is given by:

$$e_{net} = \frac{L_4 - L_2}{2} \tag{7.47}$$

or

$$M > M_{\max} - M_{\min} = (V_{\max} + V_{\min})\left(\frac{h}{2} - \frac{V_{\max} + V_{\min}}{2 \times 0.567 f_{ck} S_{q2} b_p} - c_{ov}\right) \tag{7.48}$$

$$M > M_{\max} - M_{\min} = (V_{\max} + V_{\min})\left(\frac{h}{2} - \frac{V_{\max} + V_{\min}}{1.6 f_{cu} b_p} - c_{ov}\right) \tag{7.48}$$

where the maximum and minimum moments on either side of the connection are given by Eq. (7.44).

In these situations the pressure above the insert is very small (if not zero) and therefore no bursting steel is required. However, many precasters will always include at least one closed link, or even provide

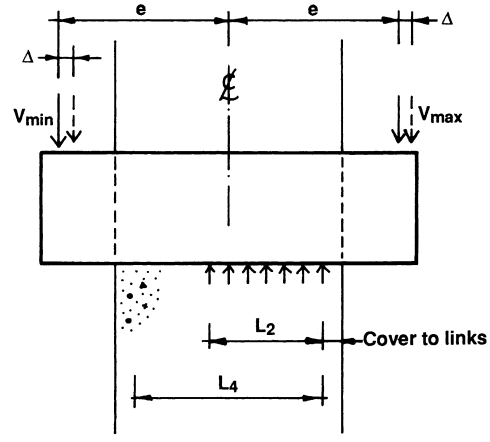

Figure 7.80 Double-sided billet design.

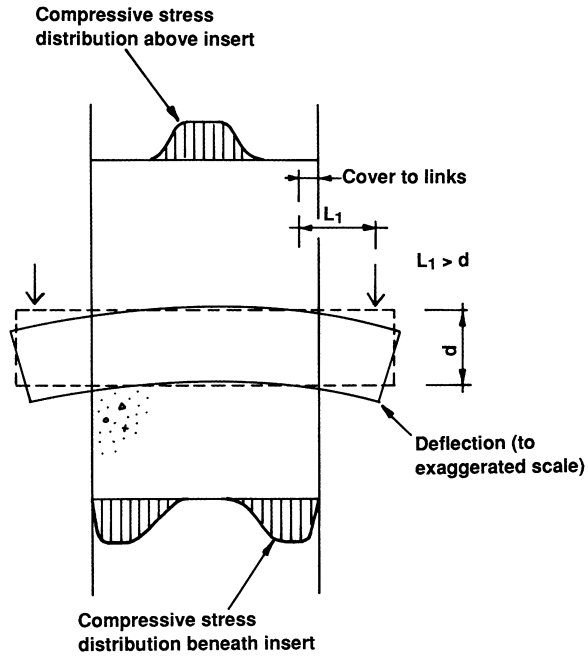

Figure 7.81 Pressure distributions under cast-in steel inserts.

the *same* links above and below the insert to avoid the risk of the steel being misplaced or transposed. Sometimes when casting a very long column it is easy to lose sight of which is the top of the column and which is the bottom!

A more realistic approach is to consider the steel billet supported by a deformable foundation, i.e. the concrete in the column. The distribution of the bearing pressure between the billet and the concrete depends on the relative stiffness of the two components and the position (or eccentricity) at which the load is applied to the billet. The analysis is akin to beams on elastic foundations subjected to end shear and end bending moment. For different permutations of M, V and the relative stiffness between billet and concrete it is, in theory, possible for the billet to rise clear of the concrete below its middle (see Figure 7.81). Thus in service (at which most of these connectors perform because of the large factors of safety used in the industry) the bearing pressure distribution is as shown in Figure 7.81.

Exercise 7.5 Double-sided steel billet design

A 300 × 300 mm column carries a double-sided symmetrical connector subjected to characteristic permanent and imposed loads of 99 and 81 kN {equivalent to 100 and 85 kN to allow for increased partial load factors in BS 8110}, respectively, at a distance from the face of the column of 55 mm. Using the appropriate loading combinations, design a suitable rectangular hollow section to be cast into the column. Design the confinement reinforcement in the form of high-tensile links in the vicinity of the connector.

Use grade S275 {43} steel for the insert and grade C40/50 concrete. Cover to all reinforcement is 25 mm. The construction allowance for the position of the beams is 6 mm.

(*Continued*)

Solution

Step 1, Load Case 1: Patch load design

	BS EN 1992-1-1		BS 8110	
Maximum beam reaction	$= (1.35 \times 99) + (1.5 \times 81)$	$= 255.2$ kN	$= (1.4 \times 100) + (1.6 \times 85)$	$= 276$ kN
Maximum eccentricity	$= (55 + 6)$	$= 61$ mm	$= (55 + 6)$	$= 61$ mm
Minimum beam reaction	$= (1.0 \times 99)$	$= 99$ kN	$= (1.0 \times 100)$	$= 100$ kN
Minimum eccentricity	$= (55 - 6)$	$= 49$ mm	$= (55 - 6)$	$= 49$ mm
Net maximum overturning moment	$= 255.2(150 + 61) - 99(150 + 49)$	$= 34135$ kNmm	$= 276(150 + 61) - 100(150 + 49)$	$= 38336$ kNmm
Net eccentricity	$= 34135/(255.2 + 99)$	$= 96.4$ mm	$= 38336/(276 + 100)$	$= 102.0$ mm
Net eccentricity from the start of the pressure zone		$= 28.6$ mm		$= 23$ mm

The effective reaction line is therefore within the column.
Assume breadth of insert $b_p = 100$ mm.
Maximum length of insert = 300 − 2 × 25 cover = 250 mm

S_{q23} is shown later = 1.440
Line pressure = 0.567 × 40 × 100 × 1.440 = 3266 N/mm

$$L_2 = \frac{(255.2+99)\times 10^3}{3266} = 108.5 \text{ mm}$$

$$M_{zz} = 354.2\left(\frac{108.5}{2} - 28.6\right) = 9081 \text{ kNmm}$$

Distance from far end of billet and pressure at L_2 = 250 − 108.5 = 141.5 mm
$M_{zz} = 3266L_3(141.5 - L_3)$
Solving gives L_3 = 23.6 mm

$$S_{q23} = \sqrt{\frac{150\times(132.1+50)}{100\times 132.1}} = 1.440$$

$L_2 + 2L_3 = 155.7 < 0.9L_4 = 225$ mm
Total force below connector = 3266 (108.5 + 23.6) × 10^{-3} = 431.2 kN
Total force above connector = 77.0 kN
$L_2 + L_3$ + cover = 157.1 mm > 150 mm
so ½ A_{bst} to be in one leg of link

Bearing pressure under insert = $0.8f_{cu}b_p = 0.8 \times 50 \times 100$ = 4000 N/mm

$$L_2 = \frac{(276+100)\times 10^3}{4000} = 94 \text{ mm}$$

$$M_{zz} = 376\left(\frac{94}{2} - 23\right) = 9024 \text{ kNmm}$$

Distance from far end of billet and pressure at L_2 = 250 − 94 = 156 mm
$M_{zz} = 4000L_3(156 - L_3)$
Solving this quadratic equation, L_3 = 16.1 mm

$L_2 + 2L_3 = 126.2 < 0.9L_4 = 225$ mm
Total force below connector = 4000 (94 + 16.1) × 10^{-3} = 440.4 kN
Total force above connector = 64.4 kN
$L_2 + L_3$ + cover = 135.1 mm
so ⅔ A_{bst} to be in one leg of link

Step 2, Load Case 2: Maximum axial load design

S_{q23} is shown later = 1.354
Maximum beam reaction = 2 × 255.2 = 510.4 kN

$$L_2 = \frac{510.4\times 10^3}{3069} = 166.3 \text{ mm}$$

$$S_{q23} = \sqrt{\frac{150\times(166.3+50)}{100\times 166.3}} = 1.354$$

Total force below connector = 510.4 kN
Total force above connector = 0 kN
$L_2 + L_3$ + cover = 216 mm
so ½ A_{bst} to be in one leg of link

Maximum beam reaction = 2 × 276 = 552 kN

$$L_2 = \frac{552\times 10^3}{4000} = 138 \text{ mm}$$

Total force below connector = 552 kN
Total force above connector = 0 kN
L_2 + cover = 163 mm
so ½ A_{bst} to be in one leg of link

Step 3, Load Case 3: Maximum axial load design with inaccuracies

$e = 6\,\text{mm}$
This is less than e_{net} from Eq. (7.47)
$e_{net} = (L_4 - L_2)/2$
$= (300 - 2 \times 25 - 160.5)/2 \quad = 44.8\,\text{mm}$

$e = 6\,\text{mm}$
This is less than e_{net} from Eq. (7.47)
$e_{net} = (L_4 - L_2)/2$
$= (300 - 2 \times 25 - 138)/2 \quad = 56\,\text{mm}$

Hence no positive design bending stresses need be checked. Total vertical force above and below insert will not exceed those already calculated for Case 2.

Step 4: Reinforcement design

Bursting force coefficient

$$\varsigma = 0.25\left(1 - \frac{100}{300}\right) = 0.1667$$

$F_{bst} = 0.1667 \times 510.4$ max. below insert $= 85.1\,\text{kN}$
$F_{bst} = 0.1667 \times 72.8$ max. above insert $= 12.8\,\text{kN}$

$$A_{bst} = \frac{85.1 \times 10^3}{0.87 \times 500} \times \frac{1}{2} \text{ below insert} = 98\,\text{mm}^2$$

$$A_{bst} = \frac{12.8 \times 10^3}{0.87 \times 500} \text{ above insert} = 30\,\text{mm}^2$$

Bursting force coefficient for $b_p/b = 0.33$,
$\varsigma = 0.21$

$F_{bst} = 0.21 \times 552$ max. below insert $= 115.0\,\text{kN}$
$F_{bst} = 0.21 \times 64.4$ max. above insert $= 13.4\,\text{kN}$

$$A_{bst} = \frac{115.0 \times 10^3}{0.87 \times 500} \times \frac{1}{2} \text{ below insert} = 133\,\text{mm}^2$$

$$A_{bst} = \frac{13.4 \times 10^3}{0.87 \times 500} \text{ above insert} = 31\,\text{mm}^2$$

Use two H12 ($226\,\text{mm}^2$) closed links below the insert and one H12 ($113\,\text{mm}^2$) closed link above the insert.

Step 5: Insert design

The maximum moment in the steel insert occurs 166.3/2 = 83.2 mm from end of stress block
$e' = 83.2/2 + 25$ cover $+ 61 \quad = 127.6\,\text{mm}$
$M_{zz} = Ve' = 255.2 \times 127.6 \quad = 32\,549\,\text{kNmm}$

$$S_{xx} = \frac{32549}{275} \quad = 118\,\text{cm}^3$$

$$2dt = \frac{255.2 \times 10^3}{165} \quad = 1546\,\text{mm}^2$$

The maximum moment in the steel insert occurs 138/2 = 69 mm from end of stress block
$e' = 69/2 + 25$ cover $+ 61 \quad = 120.5\,\text{mm}$
$M_{zz} = Ve' = 276 \times 120.5 \quad = 33\,258\,\text{kNmm}$

$$S_{xx} = \frac{33258}{275} \quad = 121\,\text{cm}^3$$

$$2dt = \frac{276 \times 10^3}{165} \quad = 1673\,\text{mm}^2$$

Use $150 \times 100 \times 6$ RHS ($S_{xx} = 141\,\text{cm}^3$ and $2dt = 1800\,\text{mm}^2$).

The final arrangement of reinforcement is shown in Figure 7.82.

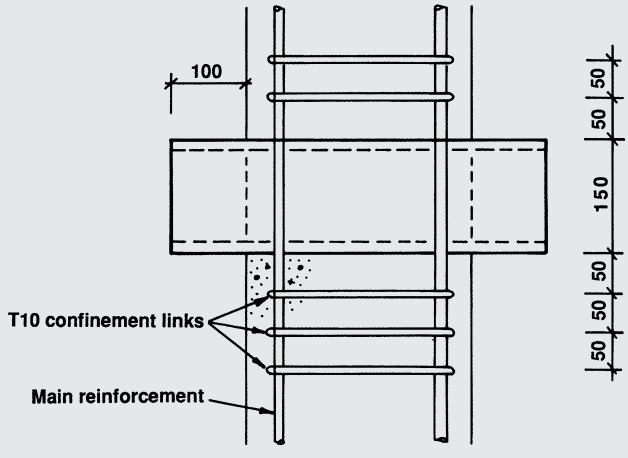

Figure 7.82 Details for Exercise 7.5.

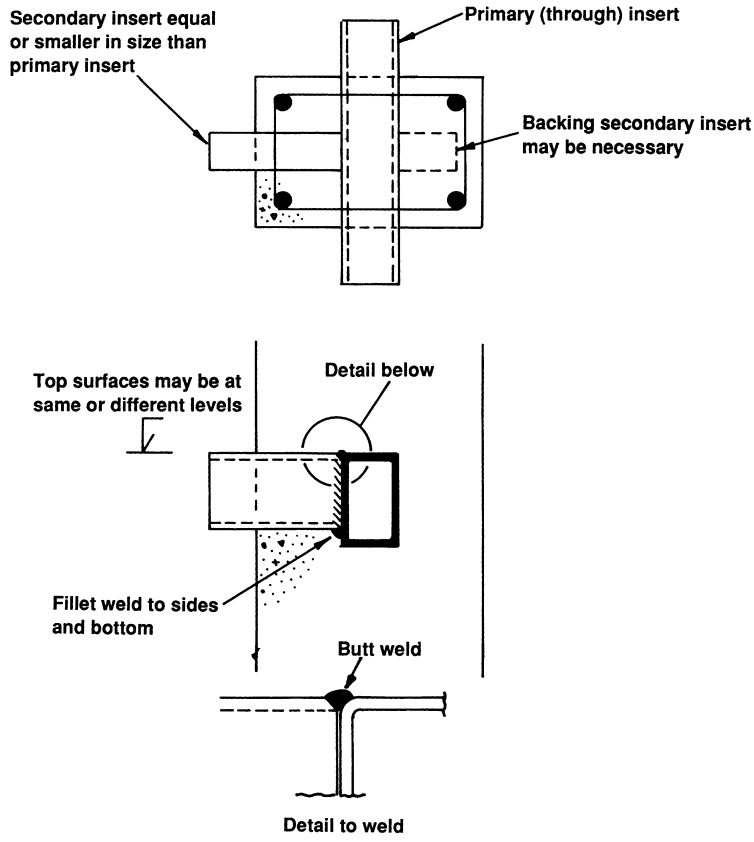

Figure 7.83 Main and secondary billets in a three- or four-way beam-to-column connector.

7.10.5 Three- and four-way wide-section connections

Three-way and four-way connections refer to the number of sides on which a column is loaded. Four-way connections are uncommon in precast structures (unlike steel structures where tertiary systems are used), but even where they are used, two of the reactions on opposite sides of the column are usually small and the connection may be conservatively designed as double-sided with a small eccentricity. In a multi-directional connection each leg may be designed as above, the welding between legs being carefully designed to transfer the loads. The problem is compounded if the inserts are not at right angles to one another.

The design of the welded joint between the two parts of the insert should be based on bending and shear, and torsion if the inserts are not at right angles. It is recommended that the major load(s) be carried on the primary continuous insert, and the secondary load(s) on inserts welded to the primary insert (see Figure 7.83). If the designer has a choice in the matter, it is better that the primary insert is slightly deeper than the secondary insert so that a fillet weld may be deposited around the full perimeter. If the inserts are equal depth, a butt weld must be used across the top and bottom and the end of the secondary insert must first be bevelled.

Three-way connections are more difficult to analyse because of the torsional behaviour caused by biaxial loading. Little analytical or experimental work has been carried out on this type of connection. It is quite common for all three reactions to be large and therefore a conservative design approach would be to consider the single-sided part of the insert first and to transfer the uplift reaction into the double-sided insert. The design of the steel insert itself would be based on bending and shear, as in the cases considered above.

Exercise 7.6 Three-way billet connector design

A 300 × 400 mm column carries a three-sided connector, as shown in Figure 7.84(a). The inserts are at right angles to each other. The distance from the face of the column to the centre line of the bearing is 60 mm in all cases, exclusive of a construction tolerance of 6 mm. Assume that the level of the top of the column connector is the same on all three sides.

Choose the most appropriate loading patterns and design suitable rectangular or square rolled hollow sections to be cast in to the column. The size of the single arm insert may be smaller than the through insert.

Design the confinement reinforcement in the column in the form of high-tensile steel links in the vicinity of the connector.

Use concrete grade C40/50, f_{ywk} {f_{yv}} = 500 N/mm^2, cover to reinforcement = 35 mm, and grade S275 {43} steel and weld.

The comparable characteristic beam end reactions to the three sides of the column are as follows:

	BS EN 1992-1-1			BS 8110		
Characteristic loading	Position A	Position B	Position C	Position A	Position B	Position C
Permanent actions:	70	40	85	70	40	85
Superimposed actions:	42	14	42	45	15	45

Solution

Step 1, Load Case 1: Maximum axial at Point B

Refer to Figure 7.84(b).

Assume b_p = 100 mm throughout.

Consider first the load at point B.

Breadth of column = 300 mm

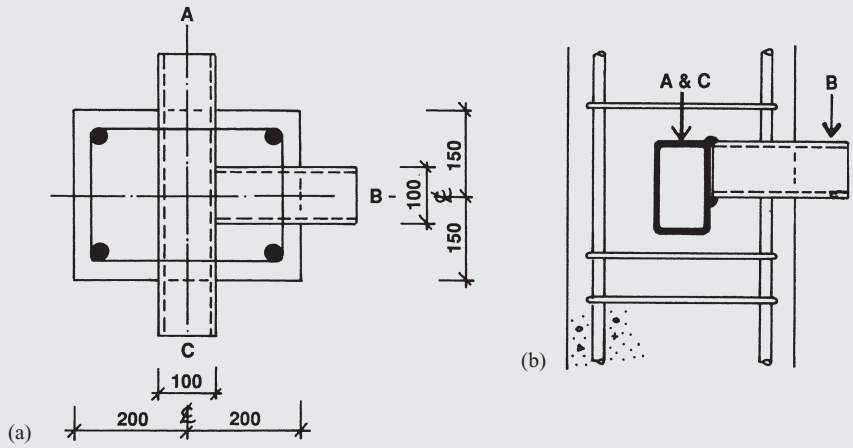

Figure 7.84 Details for Exercise 7.6. (a) Plan view of three-way connector, and (b) section through primary insert.

(*Continued*)

S_{q23} is shown later = 2.876
Line pressure = 0.567 × 40 × 100 × 2.876 = 6519 N/mm

Maximum beam reaction
$V_B = (1.35 \times 40) + (1.5 \times 15)$ = 76.5 kN
$L_2 = \dfrac{76.5 \times 10^3}{6519}$ = 11.7 mm
$M_{zz} = 76.5(35 + 66 + 11.7/2)$ = 8175 kNmm
$S_{xx} = \dfrac{8175}{275}$ = 29.7 cm^3
$2dt = \dfrac{76.5 \times 10^3}{165}$ = 464 mm^2

Calculate maximum pressure under billet as the lesser of:
$f_b = \dfrac{1.5 f_{cu}}{1 + (2b_p/h)} = \dfrac{1.5 \times 50}{1 + (2 \times 100/300)}$ = 45 N/mm^2
or $f_b = 0.8 f_{cu}$ = 40 N/mm^2
Line pressure = 40 × 100 = 4000 N/mm

Maximum beam reaction
$V_B = (1.4 \times 40) + (1.6 \times 15)$ = 80 kN
$L_2 = \dfrac{80 \times 10^3}{4000}$ = 20 mm
$M_{zz} = 80(35 + 66 + 20/2)$ = 8880 kNmm
$S_{xx} = \dfrac{8880}{275}$ = 32.3 cm^3
$2dt = \dfrac{80 \times 10^3}{165}$ = 485 mm^2

Use 100 × 100 × 4 SHS (S_{xx} = 54.9 cm^3 and $2dt$ = 800 mm^2).

Maximum length of billet = 300 − 35 = 265 mm

Distance from end of insert to pressure zone = 250 − 35 − 11.7 = 203.3 mm
$M_{xx} = 6519 L_3(203.3 - L_3)$
Solving gives L_3 = 6.4 mm
$S_{q23} = \sqrt{\dfrac{170 \times (18.1 + 70)}{100 \times 18.1}} = 2.876$
Total vertical force below connector = 6519 (11.7 + 6.4) × 10^{-3} = 118.0 kN
Total force above connector = 41.5 kN

Distance from end of insert to pressure zone = 250 − 35 − 20 = 195 mm
$M_{xx} = 4000 L_3(195 - L_3)$
Solving this quadratic gives L_3 = 12.1 mm
Total vertical force below connector = 4000 (20 + 12.1) × 10^{-3} = 128.6 kN
Total force above connector = 48.6 kN

Step 2, Load Case 1: Maximum axial at Points A and C combined with Step 1

Maximum beam reactions
$V_A = (1.35 \times 70) + (1.5 \times 45)$ = 162 kN
V_B = −41.5 kN from Step 1
$V_C = (135 \times 85) + (1.5 \times 45)$ = 182.3 kN
Force beneath insert = 162 + 182.3 − 41.5 = 302.8 kN
$L_2 = \dfrac{302.8 \times 10^3}{2267 \times 1.823}$ = 73.3 mm
$S_{q23} = \sqrt{\dfrac{170 \times (73.3 + 70)}{100 \times 73.3}} = 1.823$
Eccentricities
e_A = 150 + 60 − 6 = 204 mm
e_B = 0 mm
e_C = 150 + 60 + 6 = 216 mm
$M_{net} = (1823 \times 216) - (162 \times 204)$ = 6318 kNmm
$e_{net} = \dfrac{6318}{302.8}$ = 20.9 mm
$e_{net} < \dfrac{(230 - 73.3)}{2} = 78.4$
so ignore eccentricity effects.
Total force below insert = 302.8 + 118.0 = 420.8 kN
Total force above insert = 0 kN

Maximum beam reactions
$V_A = (1.4 \times 70) + (1.6 \times 45)$ = 170 kN
V_B = −48.6 kN from Step 1
$V_C = (1.4 \times 85) + (1.6 \times 45)$ = 191 kN
Force beneath insert = 170 + 191 − 48.6 = 312.4 kN
$L_2 = \dfrac{312.4 \times 10^3}{4000}$ = 78.1 mm

Eccentricities
e_A = 150 + 60 − 6 = 204 mm
e_B = 0 mm
e_C = 150 + 60 + 6 = 216 mm
$M_{net} = (191 \times 216) - (170 \times 204)$ = 6576 kNmm
$e_{net} = \dfrac{6576}{312.4}$ = 21.0 mm
$e_{net} < \dfrac{(230 - 78.1)}{2} = 76.0$
so ignore eccentricity effects.
Total force below insert = 312.4 + 128.6 = 441 kN
Total force above insert = 0 kN

Step 3, Load Case 2: Minimum axial at point B
Consider first the minimum reaction at point B.

$V_B = (1.0 \times 40)$	$= 40\,\text{kN}$
S_{q23} is shown later = 3.0	
$L_2 = \dfrac{40\times10^3}{6800}$	$= 5.9\,\text{mm}$
$M_{zz} = 40(35 + 60 - 6 + 5.9/2)$	$= 3678\,\text{kNmm}$
Distance from end of insert to pressure zone = 250 − 35 − 5.9	$= 209.1\,\text{mm}$
$M_{xx} = 6800L_3(209.1 - L_3)$	
Solving gives L_3	
$S_{q23} = \sqrt{\dfrac{170\times(8.5+70)}{100\times8.5}} = 3.962$	$= 2.6\,\text{mm}$
S_{q23} = max 3.0	
Total vertical force below connector $= 6800 \times (5.8 + 2.6) \times 10^{-3}$	$= 57.8\,\text{kN}$
Total force above connector	$= 17.8\,\text{kN}$

$V_B = (1.0 \times 40)$	$= 40\,\text{kN}$
$L_2 = \dfrac{40\times10^3}{4000}$	$= 10\,\text{mm}$
$M_{zz} = 40(35 + 54 + 10/2)$	$= 3760\,\text{kNmm}$
Distance from end of insert to pressure zone = 250 − 35 − 10	$= 205\,\text{mm}$
$M_{xx} = 4000L_3(205 - L_3)$	
Solving this quadratic gives L_3	$= 4.7\,\text{mm}$
Total vertical force below connector $= 4000\ (10 + 4.7) \times 10^{-3}$	$= 58.8\,\text{kN}$
Total force above connector	$= 18.8\,\text{kN}$

Step 4, Load Case 2: Minimum axial at point A and maximum axial at Point C combined with Step 3

$V_A = (1.0 \times 70)$	$= 70\,\text{kN}$
$V_B = -17.8\,\text{kN}$ from Step 1	
$V_C = (1.35 \times 85) + (1.5 \times 45)$	$= 182.3\,\text{kN}$
Force beneath insert = 70 + 182.3 − 17.8	$= 234.4\,\text{kN}$
S_{q23} is shown later = 1.858	
$L_2 = \dfrac{234.4\times10^3}{4211}$	$= 55.7\,\text{mm}$
Eccentricities, as before	
$e_A = 150 + 60 - 6 = 204\,\text{mm}$	
$e_B = 0\,\text{mm}$	
$e_C = 150 + 60 + 6 = 216\,\text{mm}$	
$M_{net} = (1823 \times 216) - (70 \times 204)$	$= 25086\,\text{kNmm}$
$e_{net} = \dfrac{25086}{234.4}$	$= 107.0\,\text{mm}$
$e_{net} > \dfrac{(230-55.6)}{2} = 87.2\,\text{mm}$	
so include eccentricity effects.	
$M_{zz} = 234.4(-(107 - 150 + 35) + 55.7/2)$	$= 8400\,\text{kNmm}$
Distance from end of insert to pressure zone = 230 − 55.7	$= 174.3\,\text{mm}$
$M_{zz} = 2267S_{q23}L_3(174.3 - L_3)$	
Solving gives L_3	$= 12.3\,\text{mm}$
$S_{q23} = \sqrt{\dfrac{170\times(67.9+70)}{100\times67.9}} = 1.858$	
Vertical force below insert $= 4211 \times (55.7 + 12.3) \times 10^{-3}$	$= 286.3\,\text{kN}$
Total vertical force below insert = 286.3 + 57.8 from Step 3	$= 344.1\,\text{kN}$
Total force above insert	$= 51.8\,\text{kN}$

$V_A = (1.0 \times 70)$	$= 70\,\text{kN}$
$V_B = -18.8\,\text{kN}$ from Step 1	
$V_C = (1.4 \times 85) + (1.6 \times 45)$	$= 191\,\text{kN}$
Force beneath insert = 70 + 191 − 18.8	$= 242.2\,\text{kN}$
$L_2 = \dfrac{242.2\times10^3}{4000}$	$= 60.6\,\text{mm}$
Eccentricities, as before	
$e_A = 150 + 60 - 6 = 204\,\text{mm}$	
$e_B = 0\,\text{mm}$	
$e_C = 150 + 60 + 6 = 216\,\text{mm}$	
$M_{net} = (191 \times 216) - (70 \times 204)$	$= 26976\,\text{kNmm}$
$e_{net} = \dfrac{26976}{242.2}$	$= 111.4\,\text{mm}$
$e_{net} > \dfrac{(230-60.6)}{2} = 76.0\,\text{mm}$	
so include eccentricity effects.	
$M_{zz} = 242.2(-(111.4 - 150 + 35) + 60.6/2)$	$= 8214.7\,\text{kNmm}$
Distance from end of insert to pressure zone = 230 − 60.6	$= 169.4\,\text{mm}$
$M_{zz} = 4000L_3(169.4 - L_3)$	
Solving this quadratic gives L_3	$= 13.1\,\text{mm}$
Vertical force below insert $= 4000\ (60.6 + 13.1) \times 10^{-3}$	$= 294.8\,\text{kN}$
Total vertical force below insert = 294.8 + 58.8 from Step 3	$= 353.6\,\text{kN}$
Total force above insert	$= 52.6\,\text{kN}$

(*Continued*)

Step 5: Reinforcement design

Maximum from Case 1		Maximum from Case 1	
Bursting force coefficient		Bursting force coefficient for $b_p/b = 0.33$,	
$\varsigma = 0.25\left(1-\frac{100}{400}\right) = 0.1875$		$\varsigma = 0.23$	
$F_{bst} = 0.1875 \times 420.8$ below insert	$= 78.9\,\text{kN}$	$F_{bst} = 0.23 \times 441$ below insert	$= 103.4\,\text{kN}$
Maximum from Case 2		Maximum from Case 2	
$F_{bst} = 0.1875 \times 51.8$ above insert	$= 9.7\,\text{kN}$	$F_{bst} = 0.23 \times 52.6$ above insert	$= 12.3\,\text{kN}$
$A_{bst} = \frac{78.9\times10^3}{0.87\times500}\times\frac{1}{2}$ below the insert	$= 91\,\text{mm}^2$	$A_{bst} = \frac{103.4\times10^3}{0.87\times500}\times\frac{1}{2}$ below the insert	$= 119\,\text{mm}^2$
$A_{bst} = \frac{9.7\times10^3}{0.87\times500}$ above the insert	$= 23\,\text{mm}^2$	$A_{bst} = \frac{12.3\times10^3}{0.87\times500}$ above the insert	$= 29\,\text{mm}^2$

Use two H10 ($157\,\text{mm}^2$) closed links below connector.
Use one H10 ($78\,\text{mm}^2$) closed link above connector.

Step 6: Through insert section design
The maximum moment in the steel insert occurs at zero shear:

$= \frac{182.3\times10^3}{2267\times1.823}$ mm from the end	$= 44.1\,\text{mm}$	$= \frac{191\times10^3}{4000}$ mm from the end	$= 47.8\,\text{mm}$
$e' = 44.1/2 + 35 + 60 + 6$	$= 123.1\,\text{mm}$	$e' = 47.8/2 + 35 + 60 + 6$	$= 124.9\,\text{mm}$
$M_{zz} = 1823 \times 123.1$	$= 22\,426\,\text{kNmm}$	$M_{zz} = 191 \times 124.9$	$= 23\,851\,\text{kNmm}$
$S_{xx} = \frac{22426}{275}$	$= 81.6\,\text{cm}^3$	$S_{xx} = \frac{23851}{275}$	$= 86.7\,\text{cm}^3$
$2dt = \frac{182.3\times10^3}{165}$	$= 1105\,\text{mm}^2$	$2dt = \frac{191\times10^3}{165}$	$= 1158\,\text{mm}^2$

Use $150 \times 100 \times 5$ RHS ($S_{xx} = 119\,\text{cm}^3$ and $2dt = 1500\,\text{mm}^2$).

Step 7: Weld design between inserts
Let the top surface of the secondary insert be 10 mm lower than the primary insert to allow a fillet weld to be deposited.

From load case 1, the moment at the face of the primary insert,

$= 76.5(200 + 66)$		$= 80(200 + 66)$	
$- 118.0(200 - 35 - 18.1/2)$	$= 4023\,\text{kNmm}$	$- 128.6(200 - 35 - 32.1/2)$	$= 4562\,\text{kNmm}$
The shear force $= 118.0 - 76.5$	$= 41.5\text{kN}$	The shear force $= 128.6 - 80$	$= 48.6\,\text{kN}$
Try 6 mm CFW		Try 6 mm CFW	
S_{xx} (parallel axis theorem)		S_{xx} (parallel axis theorem)	
$= (2 \times 100 \times 4.2 \times 50) + (2 \times 4.2 \times 50^2)$	$= 63\,000\,\text{mm}^3$	$= (2 \times 100 \times 4.2 \times 50) + (2 \times 4.2 \times 50^2)$	$= 63000\,\text{mm}^3$
$M_r = 220 \times 63000 \times 10^{-3}$	$= 13\,860\,\text{kNmm}$	$M_r = 215 \times 63000 \times 10^{-3}$	$= 13545\,\text{kNmm}$
$> 4022.8\,\text{kNmm}$ required		$> 4561.4\,\text{kNmm}$ required	
$V_r = 220 \times 2 \times 4.2 \times 100 \times 10^{-3}$	$= 184.8\,\text{kN}$	$V_r = 215 \times 2 \times 4.2 \times 100 \times 10^{-3}$	$= 180.116\,\text{kN}$
$> 41.5\text{kN}$ required		$> 48.6\,\text{kN}$ required	

Use 8 mm CFW between primary and secondary inserts.

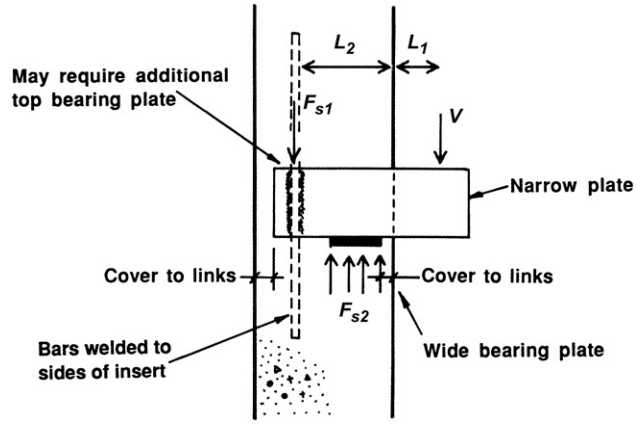

Figure 7.85 Narrow steel plate insert with additional reinforcement.

7.10.6 Narrow-plate column inserts

Narrow-plate inserts are steel plates not thicker than one-tenth of the column width, or 50 mm, whichever is less, set vertically in the column to support a beam reaction, as shown in Figure 7.85. When loaded such plates tend to produce a splitting effect in the columns under the bearing surface, unless they are supported by transverse bearing plates or welded reinforcement.

The inserts are nearly always supplemented either by a wider bearing plate near the loaded face of the column, or tensile anchorage reinforcement near the loaded face and remote face of the column. In the latter case, compressive bearing stresses are ignored in the thin plate and the total reaction, allowing for eccentricity of the imposed load, is carried in bond by reinforcement (which is additional to the overall compressive requirement of the column). The reinforcement is welded to the sides of the plate and, by placing small-diameter links (typically H8 at 50 mm centres) around the bars, the concrete immediately beneath the thin plate is highly confined. The compressive bond resistance of the bars is used if there is an insufficient tension anchorage bond length available above the connection, e.g. at roof level. Stirrups are used in the usual manner to prevent lateral buckling of these compression bars.

Narrow-plate inserts without either welded reinforcement or transverse plates were tested by Holmes *et al.* [7.50, 7.57], and the capacities obtained were very low. Only empirical relationships relating capacity to column size and cube strength were obtained. The capacities were affected by many variables, such as shape of bearing surface, proximity of column reinforcement, and shrinkage stresses in the concrete, and it is therefore not recommended that such unreinforced narrow plates be used without careful testing.

To calculate the maximum shear and moments on the plate with welded reinforcement both back and front, assume that load V acts as described in Section 7.10.1. Calculate the force in the steel, F_{s2} from the relationship:

$$F_{s2} = V \times L_1/L_2 \tag{7.49}$$

and calculate F_{s1} from the relationship:

$$F_{s1} = F_{s2} + V \tag{7.50}$$

Provide reinforcement A_{s1} and A_{s2} to carry ultimate loads F_{s1} and F_{s2} through adequate bond and anchorage. Place additional column confinement links above and below the plate, using bursting

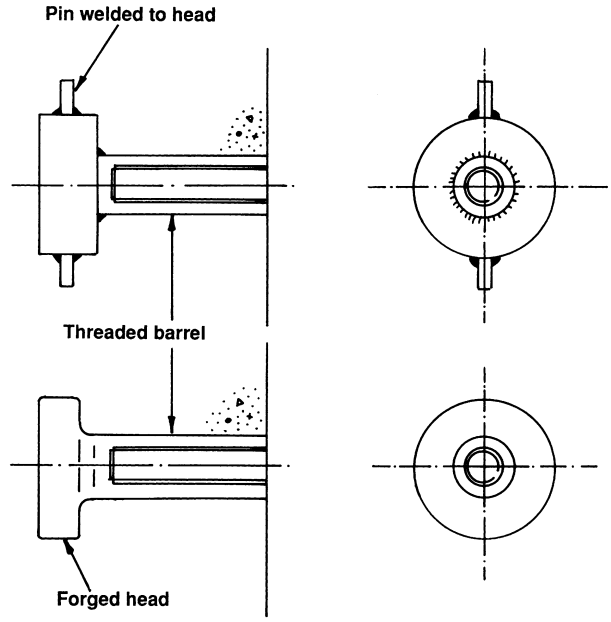

Figure 7.86 Cast-in threaded sockets.

coefficient of 0.5 for point loads in steel bars. Note that where a plate occurs close to the top of a column, force F_{s1} may be provided by reinforcement in compression, provided that sufficient links are arranged to restrain such reinforcement against buckling.

7.10.7 Cast-in sockets

The use of cast-in sockets as a means of transmitting vertical and horizontal forces to the column is not widely used. The design of inserts (and other fixings) in concrete is covered extensively in the CEB Report [7.58]. The pin anchor bar or welded pin head, attached to the rear end of the socket shown in Figure 7.86, provides a full tensile anchorage to the socket. Vertical shear is provided by direct bearing under the barrel of the socket itself – typically 24 mm diameter by 100 mm long. The *PCI Manual* on cladding [7.13] gives extensive design guidance.

The spacing between cast-in sockets should not be less than two diameters of the outer barrel, or the size of the aggregate + 5 mm, whichever is the larger. Confinement links are calculated on the assumption that the compression beneath the sockets produces a knife-edge effect (even though the barrel is circular) radiating at 45° away from the sockets. If there are two sockets in the same horizontal plane (the usual case), the stresses overlap and create a uniform pressure zone, as shown in Figure 7.87, such that = ς V_{Ed} {ς V} where $\varsigma = 0.175$ {0.23} and V_{Ed} {V} is the ultimate shear force in the sockets. The edge distance to a socket should be clear of any reinforcement, and be not less than the smaller of the cover to the main bars plus 10 mm, or 75 mm.

7.10.8 Bolts in sleeves

In this method of support, steel or hard plastic sleeves are cast in the column, surrounded by the usual confinement links and main steel. Steel bolts or threaded rods are placed through the sleeves to receive seating cleats or similar attachments to the face of the column, as shown in Figure 7.88. The structural mechanism is similar to cast-in sockets, but with the added complication that the bolt

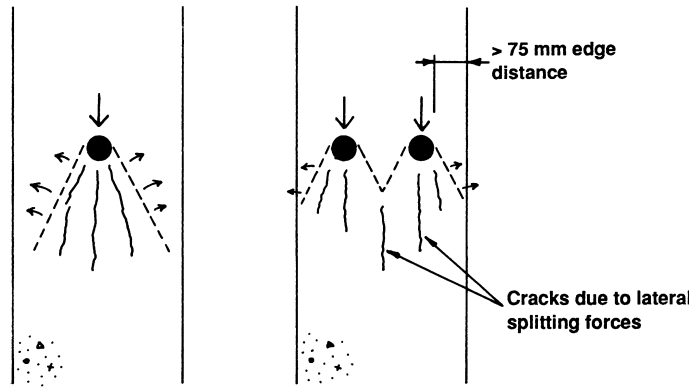

Figure 7.87 Stress distributions in columns beneath cast-in sockets subjected to shear forces.

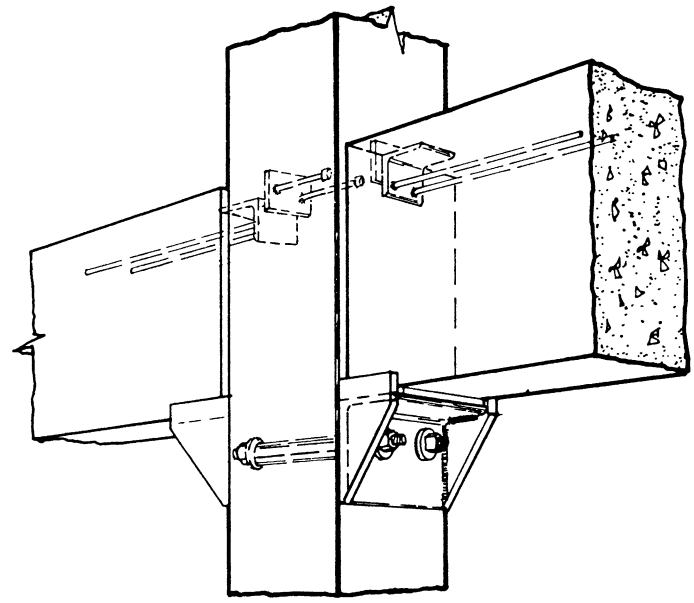

Figure 7.88 Bolts in cast-in sleeves in columns.

is not a tight fit in the sleeve. The resulting pressure distribution inside the sleeve is transferred directly to the concrete.

Full scale testing by Jolly and Mohamed [7.59, 7.60] used M24-grade 8.8 threaded bolts supporting angle cleats to the faces of 300 × 300 mm precast columns to study the effects of the concentration of bolts on connector capacity. The number of bolts making the connection varied from 1 to 4 (i.e. 2 rows × 2). Concrete strengths were varied from 61.9 N/mm^2 to 30.5 N/mm^2, and confinement reinforcement beneath the bolts was in the form of R8 links at 50 mm centres. The ratio of the failure load for the multi-bolt connection to that of a single bolt was as given in Table 7.9.

The failure mode for the high-strength concrete specimens was by flexure (due to the small connector eccentricity) and shear yielding of the bolts. Conversely the failure in the lower-strength concrete was by large ovalisation of the sleeves and concrete splitting beneath the connector (see Figures 7.89 and 7.90).

Table 7.9 Ratio of multi-bolt connection ultimate capacities to a single bolt capacity

Number of bolts in connection cleat	Load capacity/ single bolt cleat capacity
2	1.7
3	2.6
4	2.8

Figure 7.89 'Ovalisation' of bolt sleeves in shear connector tests [7.59].

7.11 Connections to Columns on Concrete Ledges

7.11.1 Corbels

A corbel is a short cantilever projection from the face of a column (or wall) that supports a load-bearing component on its upper horizontal ledge. Column corbels are not widely used in the UK compared with Continental Europe and North America. As in any type of frame, it is necessary to minimise the structural zone by containing the connection within the overall depth of the beam. For reasons of appearance this calls for 'shallow' corbels, which are defined in Figure 7.91 and designed as a short cantilever. Care is needed to ensure correct lapping and anchorage of reinforcement adjacent to contact surfaces, with full regard for fixing tolerances.

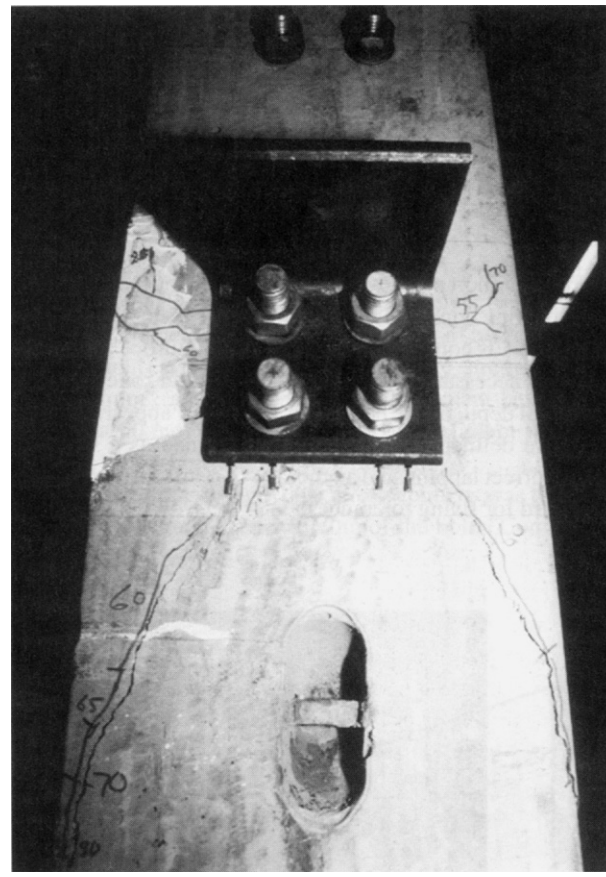

Figure 7.90 Column splitting beneath four-bolt angle connectors [7.60].

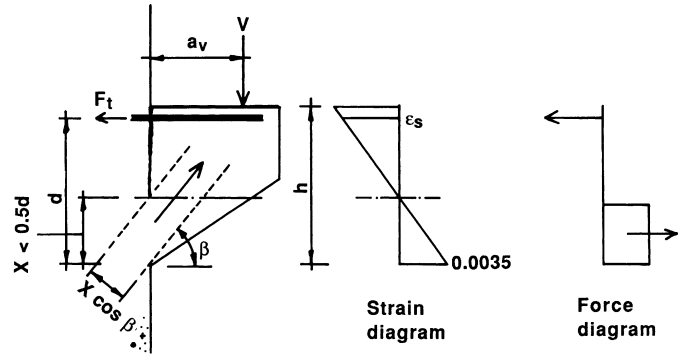

Figure 7.91 Shallow corbel definitions and design.

The usual beam connection is a single vertical dowel, which is either a waiting bar cast into the corbel, or is site-fixed into a hole. Care should be taken to ensure that the hole does not fill with water and freeze. The dowel diameter is between 16 and 25 mm typically, and the respective dowel hole is 35 to 50 mm in diameter. Non-shrink grout, grade C20/25 (or C30/37 if it is being used on the site elsewhere), is poured into the hole from the top.

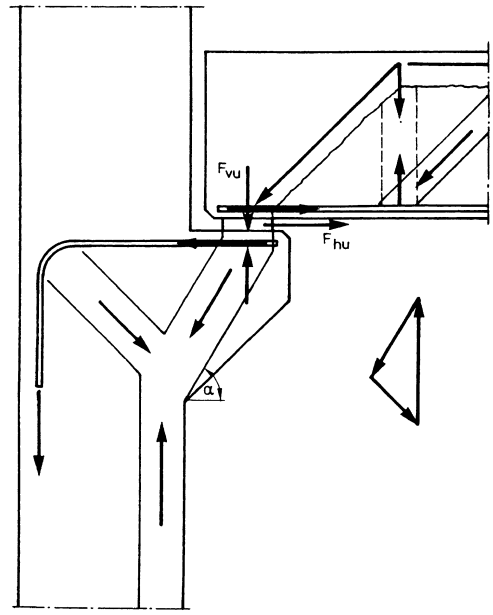

Figure 7.92 Shear force transfer between beam end and column corbel [7.18].

In precast frames, corbel design is carried out on an *ad hoc* basis to suit the specific requirements of the project. It is unusual to find a standard column corbel detail in production manuals. However, if used, the design and detailing is carried out with the usual attention to the prevention of spalling, cracking, etc. If a dowelled connection is made between the beam and corbel, horizontal hair-pin bars (typically 8 mm diameter at 50 mm centres) are used to prevent bursting of the thin covering to the dowel hole and projecting dowel bar.

There are many complications in reinforcing multi-planar corbels, particularly if the level of the shoulder is at the same level in two directions. Congestion of the horizontal tie-back steel may be relieved either by varying the height of the seating by at least 50 mm, or by casting in a special steel insert to transmit the tie forces as necessary.

A graphic illustration of the load transfer through a corbel is given by Bruggeling [7.18], reproduced in Figure 7.92. The notation in this diagram refers to individual joint designs within the connection, and may be found in Bruggeling's book [7.61]. Extensive testing of corbels (over 200 tests) was carried out by Kris and Raths [7.62] and showed the dependence on the shear span ratio a_v/d, and the percentage of horizontal reinforcement for the ultimate load. The loads were applied through bearing pads of well-defined size and position, with no attempt to simulate concrete-to-concrete contact. Somerville [7.63] also gives design recommendations.

Finite element programs, e.g. 'FIELDS' [7.64], have been used to verify the behaviour of highly loaded rc shallow corbels assumed in design, as shown in Figure 7.93. In all analyses, the problem of bearing stresses in the bends of the reinforcement leads to small-diameter bars being preferred, e.g. <25 mm diameter. The disturbed region of the column, known as the 'D-region', may extend for a distance equal to about $1.5h$ above the table of the corbel and $1.5h \cos \beta$ below the root of the corbel. Additional links should be provided in the column throughout these regions. All these features are evident in the photograph in Figure 7.94.

The design procedure is given in BS EN 1992-1-1, clauses 6.2.2(6) and (7) and Annex J.3 and Figure J.6(a) [7.8] and PD 6687, Annex B.3 gives the same information in Figure B.5(a) [7.65] {BS 8110, Part 1, clause 5.2.7 [7.9]}. To qualify as a corbel in design, the distance a_c $\{a_v\}$ from the centre of the load to the face of the support should not be greater than z_o, the lever arm between the compression in

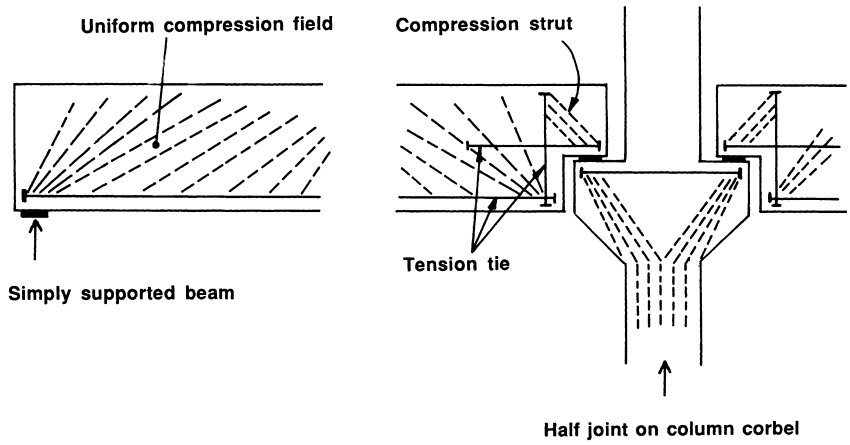

Figure 7.93 Stress trajectories in a corbel from the program FIELDS [7.64].

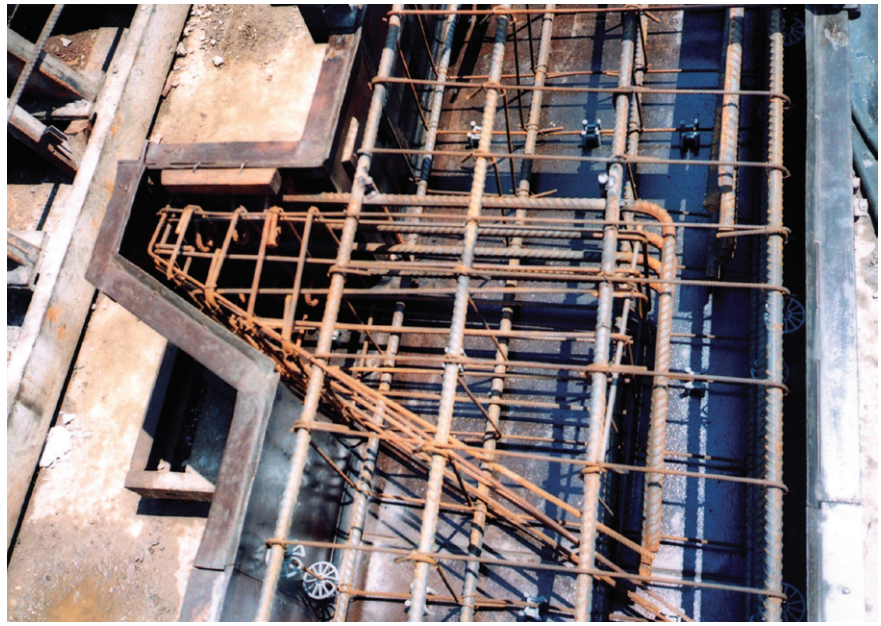

Figure 7.94 Reinforcement detailing in a shallow corbel.

the bottom of the corbel and the tension steel in the top (see Figure 7.95(d) {*d*, the effective depth of the 'root' of the corbel}. BS EN 1992-1-1, clause 6.2.3(8) defines a_v as the distance to the *edge* of the load, and a_c to the *line* of the reaction {BS 8110, clause 5.2.7.1 defines a_v as the distance to the *line* of the reaction}. The depth of the face of the corbel should not be less than half the total depth. The width of a corbel $b_1 \leq 600$ mm is recommended for continuous bearings, see BS EN 1992-1-1 clause 10.9.5.2(3) {must be less than about 500 mm, otherwise it qualifies as a continuous nib, where BS 8110, clause 5.2.8 is used}.

7.11.1.1 Shallow corbels

It is generally accepted that to qualify as a shallow corbel requires the distance to the centre of the load $a_c \leq 0.5h_c$ = approx. $0.45d$, where h_c is the total depth {$a_v \leq 0.6d$}, plus other criteria, shown in

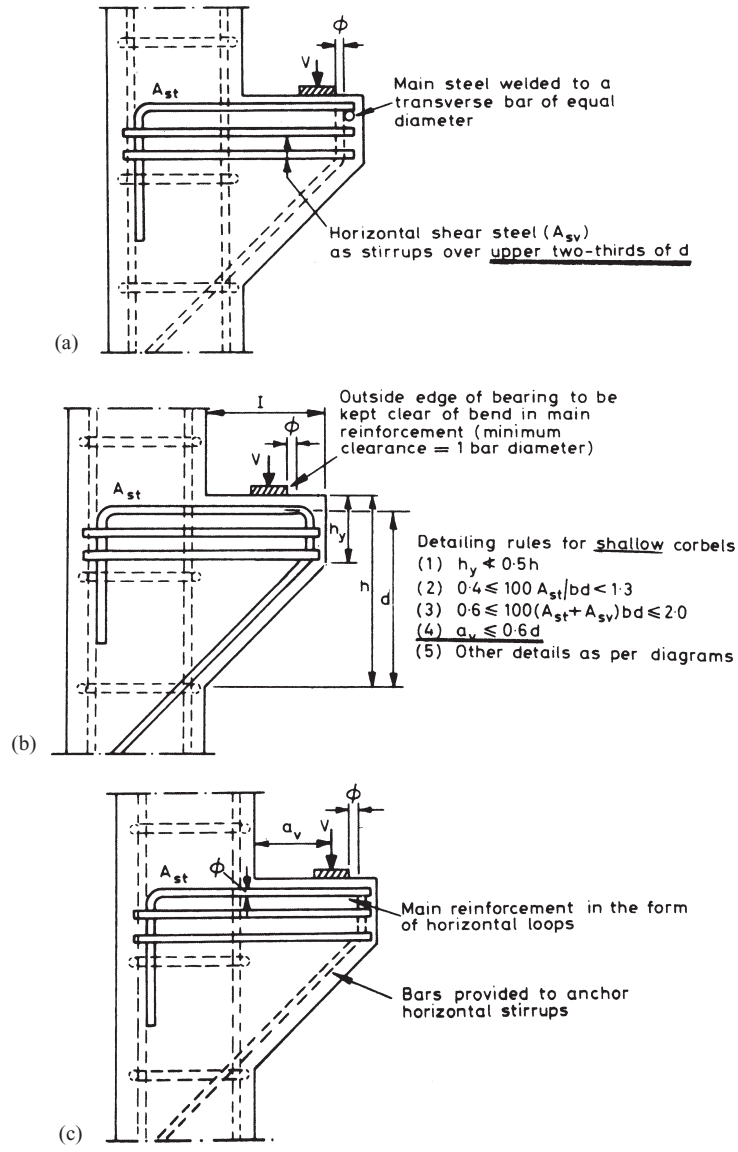

Figure 7.95 Reinforcement details for shallow corbels
(a) Main steel welded to an edge bar [7.21]
(b) Main steel as a continuous bar [7.21]
(c) Main steel in the form of a horizontal U bar [7.21]
(d) Corbel reinforced according to Figure 7.66(b).

Figure 7.95, must apply – otherwise it should be considered as a short cantilever beam. Figure 7.95 shows three different options for anchoring the main steel in the top corner of the corbel:

- welding the main steel to a bar of equal size across the front face of the corbel (Figure 7.95(a))
- contouring the bar to the profile of the corbel (Figure 7.95(b) and (d))
- using a horizontal U-shaped bar in the top of the corbel (Figure 7.95(c)).

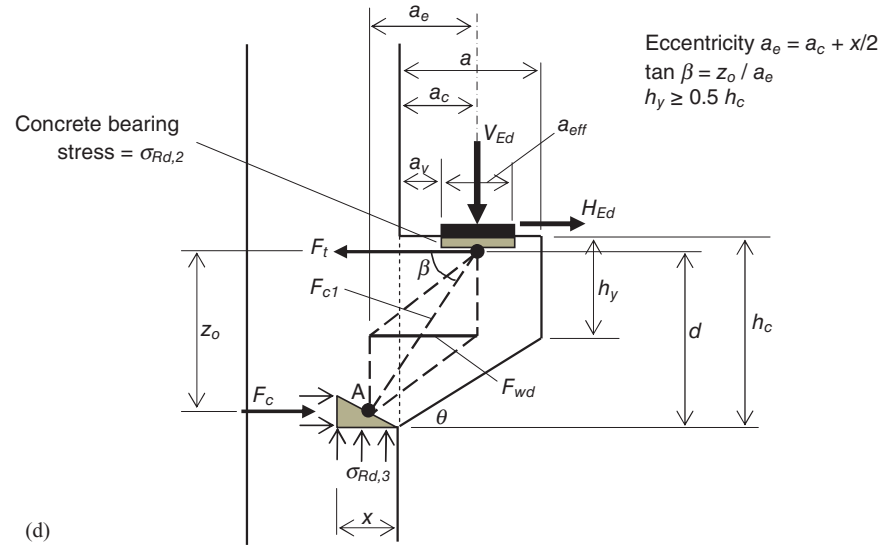

Figure 7.95 (*Continued*)

Of the three options, (a) represents the most economical solution, giving the shortest corbel length, but only if the bar diameter is less than about 16 mm.

The strut-and-tie design model is again used, which leads to a more favourable and accurate representation than by considering the corbel as a short cantilever in bending and shear. The use of the strut-and-tie method for short corbel design is well documented in The Concrete Centre's publication [7.66]. However it is first necessary to check that a shear failure will not occur, by proportioning the depth of the corbel according to the following.

First, the ultimate shear stress $v_{Ed} = V_{Ed}/bd$ {$v = V/bd$} at the face of the column should not exceed $0.5\ \nu\ f_{ck}/1.5$, where $\nu = 0.6(1 - f_{ck}/250)$ from Eq. 6.5 and 6.6N {$0.8\sqrt{f_{cu}}$}. V_{Ed} should not exceed $V_{Rd,c}$ {shear reinforcement is required if the applied shear stress v is greater than the enhanced concrete stress shear stress $v > v_c\ (2d/a_v)$}. Otherwise, A_{sw} {A_{sv}} is obtained from:

$$A_{sw} = \frac{a_v}{2d}\frac{V_{Ed}s}{z0.87f_{ywk}} > \frac{0.08b\sqrt{f_{ck}}s}{f_{ywk}} \qquad (7.51)$$

where a_v is the distance to the edge of the load according to clause 6.2.3(8), and z/s is the number of links, minimum 2, crossing a 45° shear plane originating from the centre of the load.

$$A_{sv} = \frac{a_v b(v - v_c(2d/a_v))}{0.87f_{yv}} > \frac{0.4a_v b}{0.87f_{yv}} > 0.2\%bh \qquad (7.51)$$

where a_v is the distance to the centre of the load according to clause 5.2.7.1.

The enhancement factor $2d/a_v$ can often be as large as 3 or 4 in certain cases, and therefore the amount of shear reinforcement is surprisingly small.

For the Eurocode method, PD 6687, Annex B.4 [7.65] presents a strut-and-tie model as adapted in Figure 7.95(d). The resultant of the compressive forces is a potential splitting tie force F_{wd} that, according to clause B4.2, requires closed horizontal or inclined links (two legs per link) A_{sw} (called $A_{s,link}$) $\geq 0.5\ A_s$ (called $A_{s,main}$), assuming f_{ywk} is the same as f_{yk}, although high-tensile bars tend to be used for both. $A_{s,link}$ is independent of A_{sw}, and is not additive, therefore $A_{sw,max} = \max(A_{sw}; A_{s,link})$.

An empirical equation for F_{wd} is given in the Model Code MC90, clause 6.8.2.2.1 [7.67], based on linear elastic finite element modelling as follows:

$$F_{wd} = \frac{\frac{2z_o}{a_e} - 1}{3 + tan\beta} F_c \tag{7.52}$$

where the eccentricity between nodes $a_e = a_c + x/2$, where for the vertical resolution of forces $x = V_{Ed}/b\ \sigma_{Rd,1}$. Typically, if $z_o/a_e = 1.5$ and $\tan\beta = 1.5$, then $F_{wd} = 0.44\ F_c = 0.44\ F_t$, and as such $A_{s,link}$ is close to 0.5 $A_{s,main}$.

BS 8110 specifies a minimum area of shear links of $A_{sv} = 0.5A_s$ (where A_s is from Eq. (7.41, 7.42a and 7.42b); min 0.4% × concrete section at the face of the support = 0.4%bh) should be provided to ensure the confinement of the concrete in the compressive strut. Thus the total area of steel must satisfy $A_s + A_{sv} \geq 0.6\%bh$.

Horizontal links are placed in the upper two-thirds of the corbel. (PD 6687, Annex B.4 requires the links to be closed, and to enclose the main steel to the front and rear of the corbel. The spacing is shown as uniform, but good practice would suggest placing them in the upper region.) The link diameter should not be more than 12 mm. The distance to the first link should not be more than 75 mm from the bearing surface. Zeller [7.68] measured failure shear stresses of 1.15 to $1.21\sqrt{f_{ck}}$ $\{1.06\sqrt{f_{cu}}$ to $1.12\sqrt{f_{cu}}\}$ in rc corbels, where $a_v/d = 0.5$ and the ratio of horizontal steel $\rho = 0.86\%$ was slightly greater than the minimum value of 0.6% specified.

The strut-and-tie forces are calculated from the triangle of forces; it being assumed that a node is formed at the intersection of the main tension steel and a point directly beneath the centre line of the bearing, as shown in Figure 7.95(d). This may not be strictly true, as the effective bearing point may move further from the column owing to construction tolerances and when beam end rotations (of up to 0.0001) take place, which are a function of span[3]. In BS EN 1992-1-1 this is allowed for in clause 10.9.5.2, in the construction deviation Δa_2 (e.g. columns are too far apart) plus the manufacturing deviation Δa_3 (e.g. beam is too short). Lindberg and Keronen [7.32] have shown that the bearing point in a beam-to-column portal frame connection will move sideways when rotations take place in pinned connections. Thus before proceeding with the analysis to BS 8110, it is wise to add up to 20 mm to a_v to allow for this effect.

The details in Figure 7.95(d) represent a 'node'. Owing to the presence of the tension tie H_{Ed} the bearing stress beneath the load $\sigma_{Rd,2} = 0.85(1 - f_{ck}/250)\ f_{ck}/1.5$ $\{f_b = 0.4\ f_{cu}\}$. Further from the node, a strut-and-tie model is used (according to clause 6.5.2). Here the compressive strut stress, which is subjected to lateral bursting tension in the midst of the corbel, $\sigma_{Rd,3} = 0.6(1 - f_{ck}/250)\ f_{ck}/1.5$ from clause 6.5.2(2), Eq. 6.56 $\{f_c = 0.4\ f_{cu}\}$. The effective bearing area is confined to within the rc zones, i.e. any net dimensions are exclusive of the cover concrete, c. If the width of the corbel is given by b, the bearing length is given by:

$$a_{eff} = \frac{V_{Ed}}{\sigma_{Rd,2}(b - 2c)} \tag{7.53}$$

$$a_{eff} = \frac{V}{f_b(b - 2c)} \tag{7.53}$$

where V_{Ed} $\{V\}$ is the ultimate applied force.

The length of the seating ledge, a in Figure 7.95(d), is determined from the sum of the distance to the centre of the load a_c $\{a_v\}$ plus half the bearing length a_{eff} plus an edge distance allowance, which includes the diameter of the links that surround the main bars.

The outside edge of the bearing is to be kept clear of the bend of the main bars; a distance equal to the diameter ϕ of the bar is recommended. This clearance requirement is replaced in BS EN 1992-1-1 by the construction deviation Δa_2. Therefore, according to Table 8.1N, the allowance for bars $\phi \leq 16$ mm is $r_i + c = 2\phi + c$; otherwise it is $3½\phi + c$. It may be made $2\phi + c$ by using end anchorages to the main bars (see Figure 7.95(f) later). The BS 8110 allowance is $5\phi + c$ (face cover to bar) for high-tensile bar with an inner bend radius $r_i = 3\phi$ and an outer bend $r_o = 4\phi$, and for mild steel bars it is $4\phi +$ cover.

The overall depth h of the corbel should be at least $1.2a$, and up to $1.5a$ if the volume of reinforcement becomes congested. The depth of the outer edge of the corbel should be $h_y \geq 0.5h$, Together this means that the slope of the soffit to the horizontal θ is about 30° to 40°, although of course corbels with horizontal soffits are possible (as shown in Figure 7.14). Finally the face depth $h_y \geq$ top cover + r_o + straight part of bar to attach the links, say 75 mm + distance at the bend at the bottom of the face = $(r_o + c) \tan(90 - \theta)/2$. Then $h = h_y + a \tan\theta \leq h_y/0.5$.

The effective depth d is given by:

$$d = 1.2(a_c + 0.5a_{eff} + 3.5\phi + c) \quad \text{(7.54-a)}$$

or if $\phi \leq 16\,\text{mm}$

$$d = 1.2(a_c + 0.5a_{eff} + 2\phi + c) \quad \text{(7.54-b)}$$

$$d = 1.2(a_v + 0.5a_{eff} + 5\phi + c) \quad (7.54)$$

The angle of the compressive strut to the horizontal is given by:

$$\beta = \tan^{-1}\frac{d - 0.5X}{a_c} \quad (7.55)$$

$$\beta = \tan^{-1}\frac{d - 0.5X}{a_v} \quad (7.55)$$

$$F_t = \frac{V}{\tan\beta} \quad (7.56)$$

$$F_c = \frac{V}{\sin\beta} \quad (7.57)$$

The tensile tie capacity F_{tR} is given by:

$$F_{tR} = A_{s1}0.87f_{yk} \quad \text{(7.58-a)}$$

$$F_{tR} = A_{s1}0.87f_y \quad \text{(7.58-a)}$$

There is often a need to add horizontal U-shaped steel bars directly beneath the bearing to cater for the horizontal friction force $H_{Ed} = \mu V_{Ed}$ $\{H = \mu V\}$, particularly in the case of long, prestressed beams in which the force is induced by creep shortening within the first six months or so. These bars are *additional* to the bars already required.

Thus, the tensile tie capacity H_{tR} is given by:

$$H_{tR} = A_{s2}0.87f_{yk} \quad \text{(7.58-b)}$$

$$H_{tR} = A_{s2}0.87f_y \quad \text{(7.58-b)}$$

The total area of main tension reinforcement $A_s = A_{s1} + A_{s2} \geq 0.4$ per cent of the section at the face of the column, $A_{s,min} = 0.2\%bh_c$ (BS EN 1992-1-1 does not specify; therefore use the same as for the column) $\{A_{s,min} = 0.4\%bh\}$. Figures 7.95 (a)–(c) show three different ways of reinforcing a shallow corbel. The diameter of the top bars is usually in the range $12 \leq \phi \leq 25\,\text{mm}$.

The main tension bars should be anchored at both sides of the bearing. Anchorage at tip of corbel may either be by a bend extending at the front face of the corbel, checking the inner bar radius (mandrel diameter $\phi_{m,min}/2$), or by a transverse bar welded to the main bar of diameter at least ϕ. The anchorage length is measured from the inner face of the bearing area or loading plate (PD 6687, clause B4.2), but the anchorage stress is calculated from the actual stress in the bar at the start of the bend, so there is a reduction in the tie force F_{bt} between these two points: see clause 8.3(3) {3.12.8.25.2}. A linear decrease in the force in the bar is taken over this straight part of the bar. Let this distance = $l_{straight}$. Then F_{bt} calculated per bar = $0.87\,f_{yk}\,A_s\,(A_{s,required}/A_{s,provided})\,(l_{bd} - l_{straight})/l_{bd}$, using 'good' or 'poor' bond conditions according to Figure 8.2b or c for corbels cast on their side $\{F_{bt} = 0.87\,f_y\,A_s\,(A_{s,required}/A_{s,provided})\,(l - l_{straight})/l\}$. The inner bend radius is then calculated according to Eq. 4.32.

The anchorage length into the column should be measured from the vertical bars in the near face of the column, and the inner bend radius should be checked as above. For double-sided corbels the anchorage lengths overlap, and are therefore automatically provided by the anchorages at the tip of the corbel.

The compressive capacity of the diagonal strut F_{cR} is given by:

$$F_{cR} = \sigma_{Rd,3} bX \cos\beta \qquad (7.59) \quad | \quad F_{cR} = 0.4 f_{cu} bX \cos\beta \qquad (7.59)$$

To prevent the concrete strain from exceeding 0.002175 at ultimate, then $X < 0.5d$. Thus Eq. (7.55) may be written:

$$\tan\beta = \frac{0.75d}{a_c} \qquad (7.60) \quad \Big| \quad \tan\beta = \frac{0.75d}{a_v} \qquad (7.60)$$

The required angle for β is $1.0 \leq \tan\beta \leq 2.5$ (about 45° to 65° to the horizontal).

The top cover to the steel should be 25 to 30 mm (the exposed side cover may be greater). This frictional force can be eliminated if continuity steel is carried across the beam-to-corbel interface (e.g. by stability ties), but this is not always possible at corners, nor is it required in single-storey portal frames where corbels are most often used. It is sometimes possible to provide a slip bearing such as a shear-deformable bearing pad, e.g. neoprene, which will prevent the frictional force being transferred to the corbel. However in order to make a positive site fixing, beams are nearly always dowelled to the corbel.

Bearing lengths are critical in corbel design, particularly if the main reinforcement in both the supported member and corbel comprise vertically bent bars in high-tensile steel, and where ineffective bearing lengths {widths} accumulate. Note that the terms in BS EN 1992-1-1 and BS 8110 are different; in BS EN 1992-1-1, Figures 10.5 and 10.6, bearing 'length' is parallel to the span and 'width' is perpendicular to span. The terms are opposite in BS 8110, Figure 5.4. This book adopts the terms used in BS EN 1992-1-1.

If concrete-to-concrete bearing surfaces are used, the net bearing width b_1 is taken as the lesser of the supported member or width of corbel minus the ineffective width of 2 × edge cover to the links in the top of the corbel.

Referring to Figure 7.95(e) (left), for BS EN 1992-1-1 the net bearing length a_1 after subtraction of ineffective lengths (a_2 and a_3) and deviations (Δa_2 and Δa_3) is according to clause 10.9.5.2, Figure 10.6 and Tables 10.2 to 10.5. Iteration is required because $a_1 = V_{Ed}/b\ \sigma_{Rd,2}$ is required to first determine the relative ultimate bearing stress ratio σ_{Ed}/f_{cd}, which in turn provides the distance a_1. For typical corbel design, σ_{Ed}/f_{cd} is usually 0.3–0.5, such that for a 'concentrated support' a_1 may be taken as 140 mm in the first instance. The allowance for ineffective bearing at the front edge of the corbel is a_2 according to BS EN 1992-1-1, Table 10.3, which may be taken as 25 mm (for precast concrete > C30/37). The ineffective bearing length of the supported member is a_3 according to Table 10.4. This may not be known at the time of designing the corbel, but is likely to be 15 mm, although not less than the end cover of say, 30 mm, or (for vertically bent rebars) end cover plus the inner bend radius of rebars of 2ϕ to $3½\phi$, i.e. some 60 to 100 mm. The construction deviation between supports (fixing tolerance) Δa_2 according to BS EN 1992-1-1, Table 10.5 is likely to be 10 mm (unless span > 12 m), and the manufacturing deviation for the length of the supported member Δa_3 is length/2500 = say 5 mm. Thus the total ineffective bearings plus deviations is at least 70 mm, and up to 140 mm if the supported member has vertical rebars, as shown in Figure 7.95(e). Together with the net bearing length of $a_1 = \max(V_{Ed}/b_1\ \sigma_{Rd,2}$; 140 mm), plus a nominal fixing gap of say 15 mm. This gives the minimum ledge length of the corbel $a \approx 225$ to 295 mm. Further requirements depend on whether the main bars are vertically bent at the face of the corbel, or there is a chamfer at the face, the cover and diameter of the links, or if the ends of the main bars are anchored to a transverse bar.

For BS 8110, the net bearing length a_{eff} after subtraction from the nominal bearing length of ineffective distances due to spalling is according to clause 5.2.3.2 and Tables 5.1 and 5.2. The ineffective bearing length in deep corbels with $h_c \geq 300$ mm is 15 mm. Otherwise, and most commonly, it is face cover if the main bars are anchored, or face cover plus the inside bend radius for vertically bent bars

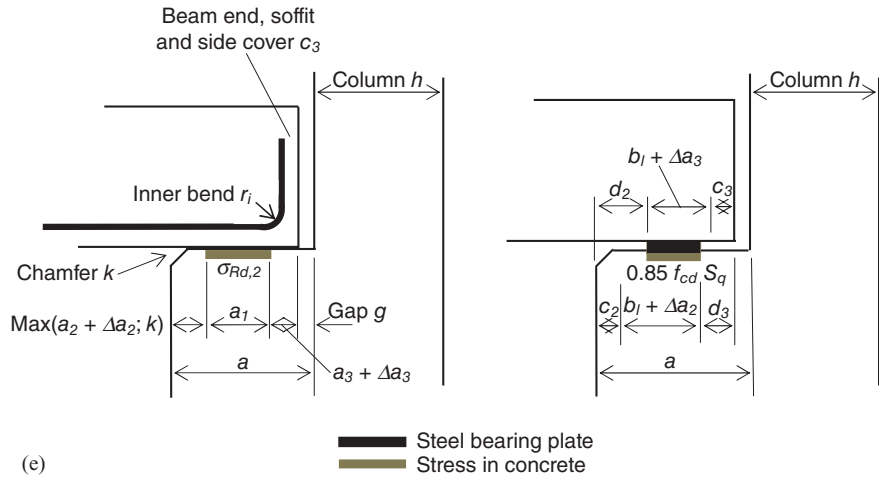

Figure 7.95(e) Bearing lengths and stresses for concrete bearing (left) and with steel plate (right), adapted from BS EN 1992-1-1, figure 10.5 [7.8].

$\phi > 12$ mm, typically 30 + 50 = 80 mm. In the supported member it is (i) zero for flush or exposed straight bars or tendons, or (ii) the greater of end cover or 10 mm, except end cover plus bend radius for vertically bent bars $\phi > 12$ mm, typically 80 mm. Manufacturing deviations, according to clause 6.2.8.3.(e), are taken as $\Delta a = 12$ mm for beams <12 m long. Construction deviations, according to BS 5606 [6.13], Table 1, clause T1.1, are taken as $\Delta a = 13$ mm for columns up to 7 m apart. As mentioned earlier, these may be replaced by an allowance for beam end movement of 20 mm. Together with the structural net bearing length of V/b_1 $0.4f_{cu}$ = say $400 \times 10^3/240 \times 20 \approx 85$ mm (minimum 40 mm), plus a nominal fixing gap of say 15 mm, this gives the minimum ledge length of the corbel $a \approx 150$ to 260 mm.

If steel plates are used, b_1 is the actual width of the plate b_p, typically specified by the designer as 0.4 b, but can, if required, be equal to the full bearing width minus 2 × cover. This is for fire and corrosion protection and will therefore require at least one cover distance, or more practically 50–75 mm, at the edges of the corbel. The ultimate bearing stress beneath a steel plate of width $b_p > 0.4$ b is according to Section 7.6.1 (vii), but when $b_p \leq 0.4b$, and confinement links are provided, $\sigma_{Rd,3} = 0.567\, f_{ck}\, S_q$ {$f_b = 0.8\, f_{cu}$}. In practice the concrete stress limits of $\sigma_{Rd,2}$ {$0.6\, f_{cu}$} are tried first, particularly since S_q requires iteration (the dimensions of the plate must be known to determine S_q); if the concrete stress is successful in terms of plate size the enhanced stresses are not needed. Elastomeric pads may remain exposed, but should have edge distances of about 50 mm. Although the characteristic compressive strength of the material is quite low, typically 7 N/mm^2 and therefore limiting, the design is based on concrete strength $\sigma_{Rd,2}$ {$0.6\, f_{cu}$}.

Minimum values for the net bearing length of steel plates b_l are not given in codes, but in practice would be the greater of $V_{Ed}/\sigma_{Rd,2}\, b_p$, 75–100 mm (depending on the forces and size of corbel); or $0.4a$ {$V_u/0.6\, f_{cu}\, b_p$, 75–100 mm ditto; or $0.4a$}. Note that steel plates do not need to comply with the requirements for a_1 in Table 10.2, as these are for dry or bedded concrete bearings. The ineffective bearing lengths are according to the dimensions d_2 and d_3 in Figure 7.95(e), adapted from BS EN 1992-1-1, clause 10.9.4.7(1) and figure 10.5 as follows:

(i) vertically bent bars (shown dashed) $d_i = c_i + \Delta a_i + r_i$, where r_i = inner bend radius
(ii) horizontal loops or end anchored rebars (e.g. transverse bar(s) shown in Figure 7.95(f)) $d_i = c_i + \Delta a_i$
(iii) pretensioned tendons or rebars exposed at the ends of units (i.e. end cover is effectively zero) $d_i = \Delta a_i$.

The main difference compared with a direct concrete bearing is that the ineffective concrete lengths a_2 and a_3 are consumed within d_i as the sum of the cover, deviations and, if present, vertical rebar bend radii.

Referring to Figure 7.95(e), the procedure is to determine d_2, d_3 and b_l as above, determine Δa_2 and Δa_3 from clause 10.9.5.2, and then, knowing the corbel bars cover c_2 and the beam end cover c_3, check the aggregate dimensions, where the symbol $|\,|$ means this term is zero if not present:

$$a \geq d_2 + d_3 + b_l + g \tag{7.61}$$

where

at the corbel face $d_2 = c_2 + \Delta a_2 \,|+ r_{i,\,corbel}|$ (if bent bars)
at the end of the beam $d_3 = |+ c_3| + \Delta a_3 \,|+ r_{i,\,beam}|$ (if bent bars)

Then

$$b_l \leq a - (c_2 \,|+ c_3| + \Delta a_2 + \Delta a_3 \,|+ r_{i,corbel}||+ r_{i,beam}| + g) \tag{7.62}$$

The two conditions *also* shown in Figure 7.95(e) are:

$$a \geq d_2 + b_l + \Delta a_3 + c_3 + g$$

Then

$$b_l \leq\ a - (c_2 \,|+ c_3| + \Delta a_2 + \Delta a_3 \,|+ r_{i,corbel}| + g) \tag{7.63}$$

and

$$a \geq c_2 + b_l + \Delta a_2 + d_3 + g$$

Then

$$b_l \leq a - (c_2 \,|+ c_3| + \Delta a_2 + \Delta a_3 \,|+ r_{i,beam}| + g) \tag{7.64}$$

cannot be critical, as all the terms are present in Eq. (7.62). For example, Eq. (7.62), let $a = 300$ mm, $g = 15$ mm, $c_2 = c_3 = 30$ mm, $\Delta a_2 = 25$, $\Delta a_3 = 5$, $r_{i,corbel} = 2 \times 16 = 32$ mm, $r_{i,beam} = 3½ \times 20 = 70$ mm, then $b_l \leq 300 - 207 = 93$ mm. Using Eq. (7.64), $b_l \leq 300 - 175 = 125$ mm.

In summary, steel plate length = seating length − gap − $\Sigma c - \Sigma \Delta a - \Sigma r_i$ of *both* corbel main bar (if bent) or beam main bar (if bent). If the rebars are anchored, as follows, then $|+ r_i| = 0$. If the main bars in the beam are cut flush or exposed at their ends, then $|c_3| = 0$.

One of the options is to anchor the end of main bars, as shown in Figure 7.95(f), rather than bending the bars. This has the advantage of reducing the corbel seating length by a distance equal to the internal bend radius of the bent bars. One or two bars, of diameter ϕ_t, may be welded to the underside of the main bar, with a spacing of $3\phi_t$. BS EN 1992-1-1, clause 8.6(2) and equation 8.8N [7.8] gives the end bearing capacity F_{btd} of a spot-welded transverse bar of length l_{td} (taken as the spacing between the bars being anchored) and diameter ϕ_t, in which the concrete is subjected to a compressive stress σ_{cm} = ultimate bearing stress, as follows:

$$F_{btd} = l_{td}\phi_t\sigma_{td} \leq F_{wd} \text{ the capacity of the spot weld} \tag{7.65}$$

where

$\sigma_{td} = (f_{ctd} + \sigma_{cm})/(0.015 + 0.14\ e^{-0.18x}) \leq 3\ f_{cd}$, where $x = 2\ (c/\phi_t) + 1$
$l_{td} = 1.16\ \phi_t\ (f_{yd}/\sigma_{td})^{0.5} \leq$ actual length

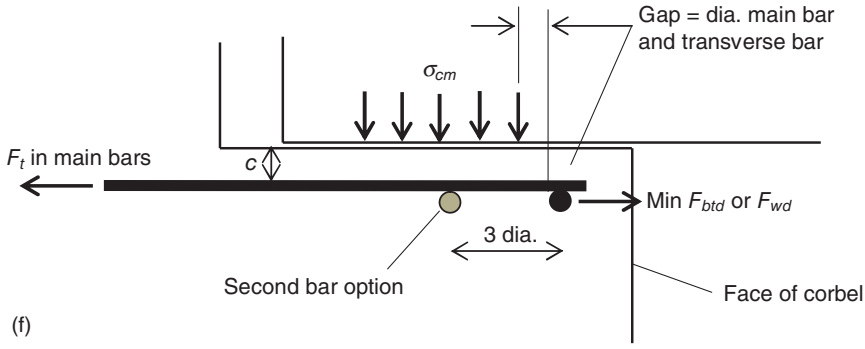

Figure 7.95(f) Welded transverse bar as main steel anchoring.

Iteration is required, taking the diameter of the main bar as a first value for ϕ_t. For example, $\phi_t = 20\,\text{mm}$, c = 25 mm, $f_{ck} = 40\,\text{N/mm}^2$, $f_{yk} = 500\,\text{N/mm}^2$ and letting $\sigma_{cm} = 10\,\text{N/mm}^2$, then $x = 3.5$, $\sigma_{td} = (1.64 + 10)/(0.015 + 0.14e^{-0.63}) = 130\,\text{N/mm}^2 > 3 \times 40/1.5 = 80\,\text{N/mm}^2$ and $l_{td} = 1.16 \times 20 \times (435/80)^{0.5} = 54\,\text{mm}$. Then $F_{btd} = 54 \times 20 \times 80 \times 10^{-3} = 86.4\,\text{kN}$ per bar $< F_{yd} = 0.87 \times 500 \times 314 \times 10^{-3} = 136.6\,\text{kN}$. Given the reduction in tensile capacity, two transverse bars may be used with a spacing of 60 mm; then $F_{btd} = 1.41 \times 86.4 = 121.8\,\text{kN}$. There is no design method in BS 8110.

The flared-V-groove welds made between the bars have a weld size of ½ bar diameter, and throat thickness $t_w = 0.7 \times 0.5\phi_t = 0.35\phi_t$. Using grade S355 electrodes, $p_w = 510\,\text{N/mm}^2$. Then $F_{wd} = p_w\, l_w\, t_w/\gamma_m$, where length of weld = transverse bar diameter plus the V-flare on either side, $l_w = \phi_t + 2\, t_w$ and $\gamma_m = 1.25$. Thus $F_{wd} = 510 \times 34 \times (0.35 \times 20) \times 10^{-3}/1.25 = 97.1\,\text{kN}$ > end bearing of bar.

One of the major drawbacks with corbels is that the mould must be specially shaped and built for each project (unlike with steel inserts, where the cross section of the mould is a continuous rectangle). To overcome this problem, corbels have been designed and cast in a two-part process. Initially, fully anchored threaded couplers are cast into the face of the column at the level of the tension reinforcement to receive the corbel steel after the column has been stripped from the mould. A retarding agent is applied locally to the surface concrete of the column mould in the region of the corbel to permit exposure of the aggregate without disturbing it when the column is demoulded. Subsequently, further concrete is added a few days later within a separate mould to form the projecting corbel.

7.11.1.2 Deep corbels

Deep corbels simulate inclined columns. To qualify as a deep corbel the distance a_v should not be greater than $0.2d$. The outer edge of the corbel does not always have to be vertical, but care should be taken at the top corner where a 25 mm chamfer should be detailed. Deep corbels are usually required, because the capacity of the shallow corbel is insufficient. However, the problem of local bursting stresses at the bearing surface is just as important as before, and so mild steel spreader plates are often cast into the bearing surface. The tension steel A_s is welded to the steel plate to form a positive anchorage.

The same design equations are used for deep and shallow corbels in BS EN 1992-1-1, {in BS 8110 Part 1, clause 5.3.7 [7.9] the shear stress in the compressive region should not exceed $1.3\,\text{N/mm}^2$}. The compressive strut must be restrained using horizontal bars, as shown in Figure 7.96. The *IStructE Manual* suggests that, apart from A_s, main strut reinforcement A_{sc} should be provided such that:

$$A_{sc} = \frac{0.5bX\cos\beta}{100} \tag{7.66}$$

and horizontal links of 0.4% of the concrete area be uniformly distributed over the full depth of the corbel. The size of the bars should be at least a quarter of the diameter, with the spacing not exceeding 12 times the diameter of the main strut reinforcement.

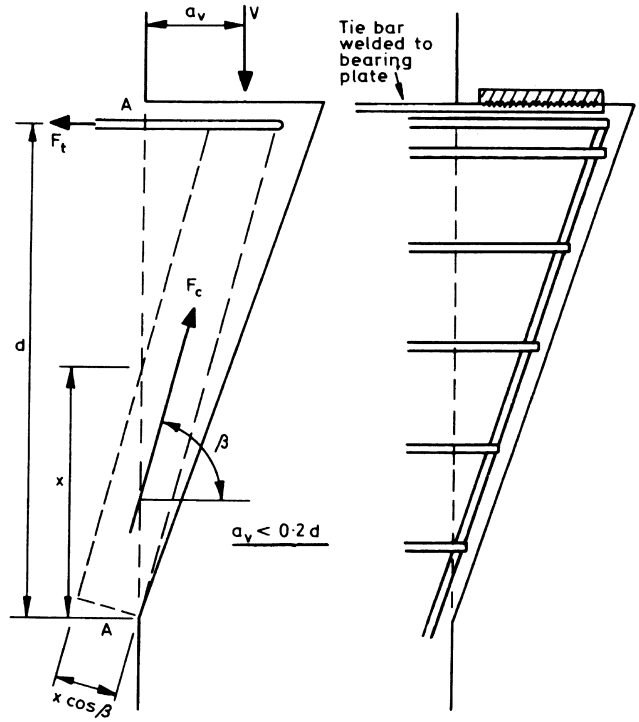

Figure 7.96 Deep corbel design [7.21].

Exercise 7.7 Shallow corbel design

A 300 × 300 mm precast column supports a 12.5 m span precast prestressed concrete beam on a single-sided corbel. The tendons in the beam are cut flush with the end of the beam. The nominal clear distance from the face of the column to the end of the beam is 15 mm. The beam is positioned onto a steel bearing plate on the centre line of the column. If the ultimate beam shear force is 190 kN {200 kN}, design a reinforced concrete shallow corbel. The allowance for the rotation of the beam may be taken as beam span/2500 {20 mm}.

Use concrete grade C40/50, $f_{yk} = f_{ywk}$ $\{f_y = f_{yv}\}$ = 500 N/mm^2 and 35 mm cover to main reinforcement, except 25 mm top cover to corbel.

Solution

Step 1: Bearing length and shear check

Assume main bar dia. = 16 mm and link dia. = 10 mm.

Initially try
$\sigma_{Rd,2} = 0.85 \times (1 - 40/250) \times 40/1.5$ = 19.04 N/mm^2
Bearing plate area = $190 \times 10^3/19.04$ = 9979 mm^2
$b_p \le 0.4 \times 300 = 120$ mm, use 100 mm
$b_l \ge 9979/100 = 100$ mm
Try 120 × 100 wide × 10 mm thick mild steel plate.

Initially try $f_b = 0.6 \times 50$ = 30 N/mm^2
Bearing plate area = $200 \times 10^3/30$ = = 6667 mm^2
$b_p \le 0.4 \times 300 = 120$ mm, use 100 mm
$b_l \ge 6667/100 = 67$ mm
Try 100 × 100 mm wide × 10 mm thick mild steel plate.
Distance to centre of bearing plate
a_v = gap + half plate + rotation allowance
= 15 + 50 + 20 = 85 mm

Distance to centre of bearing plate
a_c = gap + half plate + Δa_3 (only, as beam tendons are exposed)
= 15 + 60 + 12 500/2500 = 80 mm
Corbel length from face of column
$a = a_c$ + half plate + Δa_2 + bend allowance + face cover
= 80 + 60 + 10.4 + 2 × 16 + 35 = 217 mm
Due to anchorage, a is later found to be = 235 mm
To determine h:
assume $\theta = 30°$
$h_y \geq 25 + \text{bend} + 16 + 50 + (48 + 35)\tan(90° - 30°)/2$ = 185 mm
The bend is later found to be 48 mm
Try h between the limits:
$h \leq h_y/0.5$ < 340 mm
or $h \geq 185 + 235 \tan 30°$ > 320 mm
or $a_c/h \leq 0.5$, then $h \geq 80/0.5$ > 160 mm
or $h \geq 1.2a = 1.2 \times 235$ > 282 mm
Therefore use h = = 320 mm
$d = 320 - 25$ cover $- 8$ bar rad. = 287 mm
$z_o > a_c$, or $d > a_c/0.75 = 80/0.75$ = 107 mm
Soffit slope $\theta = \tan^{-1} 135/235$ = 29.9°
Shear check:

$$d > \frac{190 \times 10^3}{0.5 \times \frac{40}{1.5} \times 0.6\left(1 - \frac{40}{250}\right) \times 300} = 94\text{ mm}$$

< 287 mm provided
Then if $X = 0.5d$ in the limit

$$\beta = \tan^{-1}\left(\frac{0.75 \times 287}{80}\right) = 69.6°$$

The compressive strut force

$$F_c = \frac{190}{\sin 69.6°} = 202.7\text{ kN}$$

$\sigma_{Rd,3} = 0.6(1 - 40/250)\ 40/1.5$ = 13.44 N/mm^2
$F_{cR} = 13.44 \times 300 \times 0.5 \times 287 \times \cos 69.6° \times 10^{-3}$ = 201.7 kN
≈ 202.7 kN required, say OK.
Horizontal tie force

$$F_t = \frac{190}{\tan 69.6°} = 70.7\text{ kN}$$

$$A_{s1} = \frac{70.7 \times 10^3}{0.87 \times 500} = 162\text{ mm}^2$$

Frictional force = 0.4 × 190 = 76 kN

$$A_{s2} = \frac{76 \times 10^3}{0.87 \times 500} = 174\text{ mm}^2$$

Total $A_s = 162 + 174$ = 336 mm^2
$A_{s,min} = 0.2\% \times 300 \times 300$ = 180 mm^2
Use two H16 (402 mm^2).

Corbel length from face of column
$a = a_v$ + half plate + bend allowance + face cover (Δa included in rotation)
= 85 + 50 + 5 × 16 + 35 = 250 mm
To determine h:
assume $\theta = 30°$
$h_y \geq 25 + (4 \times 16) + 50 + (64 + 35)\tan(90° - 30°)/2$ = 196 mm
Try h between the limits:
$h \leq h_y/0.5$ < 392 mm
or $h \geq 196 + 250 \tan 30°$ > 340 mm
$h \geq 142 + 25$ cover $+ 8$ bar rad. > 175 mm
where $d \geq a_v/0.6 = 85/0.6$ = 142 mm
or $h \geq 1.2a = 1.2 \times 250$ > 300 mm
Therefore use h = = 340 mm
$d = 340 - 25$ cover $- 8$ bar rad. = 307 mm
Soffit slope angle = $\tan^{-1} 144/250$ = 29.9°
Shear check:

$$d > \frac{200 \times 10^3}{0.8 \times \sqrt{50} \times 300} = 118\text{ mm}$$

< 307 mm provided
Then if $X = 0.5d$ in the limit

$$\beta = \tan^{-1}\left(\frac{0.75 \times 307}{85}\right) = 69.7°$$

The compressive strut force

$$F_c = \frac{200}{\sin 69.7°} = 213.2\text{ kN}$$

$\sigma_c = 0.4 \times 50$ = 20.0 N/mm^2
$F_{cR} = 20.0 \times 300 \times 0.5 \times 307 \times \cos 69.7° \times 10^{-3}$ = 319.5 kN
> 213.2 kN required
Horizontal tie force

$$F_t = \frac{200}{\tan 69.7°} = 74.0\text{ kN}$$

$$A_{s1} = \frac{74.0 \times 10^3}{0.87 \times 500} = 170\text{ mm}^2$$

Frictional force = 0.4 × 200 = 80 kN

$$A_{s2} = \frac{80 \times 10^3}{0.87 \times 500} = 184\text{ mm}^2$$

Total $A_s = 170 + 184$ = 354 mm^2
$A_{smin} = 0.4\% \times 300 \times 340$ = 408 mm^2

(*Continued*)

$A_{s,link} \geq 0.5\,A_{s,main} = 0.5 \times 336 = 168\,\text{mm}^2$ to be forwarded to shear links calculation.

Anchorage length check

$f_{bd} = 2.25 \times 0.7 \times 1.0 \times 1.64 = 2.58\,\text{N/mm}^2$

$l_{bd,req} = 0.25 \times 16 \times 0.87 \times 500 \times (336/402)/2.58 = 563\,\text{mm}$

(See Table 8.2) $\alpha_1 = 0.7$ (edge cover $C_d = 51 > 3$ dia.)

α_2 = say 1.0

$l_{bd} = 0.7 \times 1.0 \times 563 = 394\,\text{mm}$

$l_{straight}$ = plate 120 mm

$F_{bt} = 0.87 \times 500 \times 201 \times (336/402) \times (274/394) \times 10^{-3} = 50.8\,\text{kN}$

(Eq. 4.32) a_b = 35 + link bend, say 16 + 16/2 = 59 mm

$$r = \frac{50.8 \times 10^3 (1/59 + 1/(2 \times 16))}{2 \times 40/1.5}$$

$= 45\,\text{mm} > 2 \times 16\,\text{mm}$, use 3 × dia radius, therefore add 48 − 32 = 16 mm to length of corbel, then $a \geq 217 + 16 = 233\,\text{mm}$, use $a = 235\,\text{mm}$

Main bar is positioned at the inner bend of links = 2 × dia., found later to be 8 mm.

Use two H16 with r = 3 × dia = 48 mm inner bend radius.

$A_{sv} \geq 0.5\,A_s = 0.5 \times 354 = 177\,\text{mm}^2$ to be forwarded to shear links calculation.

Anchorage length check

Anchorage $l = 35 \times 16 \times (354/402) = 493\,\text{mm}$

$l_{straight}$ = plate 100 + extra dia. 16 = 116 mm

$F_{bt} = 0.87 \times 500 \times 201 \times (354/402) \times (377/493) \times 10^{-3} = 58.9\,\text{kN}$

(Eq. 4.32) a_b = 35 + link bend, say 20 + 16 = 71 mm

$$r = \frac{58.9 \times 10^3 (1 + 2(16/71))}{2 \times 50 \times 16} = 53\,\text{mm}$$

just greater than 3 × 16 mm, but less than 5 dia. allowed, therefore no change required to length of corbel.

Main bar is positioned at the inner bend of links = 2 × dia., found later to be 10 mm.

Use two H16 with r = 3 × dia = 48 mm inner bend radius.

Step 2: Shear reinforcement

The ultimate shear capacity is

$$V_{Rd,c} = \frac{0.5 \times 300 \times 287}{10^3} \times 0.6\left(1 - \frac{40}{250}\right) \times \frac{40}{1.5} = 578\,\text{kN}$$

$> 190\,\text{kN}$

Reduced $a_v = 80 - 120/2 = 20\,\text{mm}$

$< 0.5d$, so use $0.5d$ in the reduction factor $= a_v/2d = 0.5 \times 287/2 \times 232 = 0.25$

(See Eq. 7.51)

$$A_{sw} = \frac{0.25 \times 190 \times 10^3}{0.87 \times 500} = 110\,\text{mm}^2$$

Minimum links calculated over a depth at the front face = 185 mm

$A_{sw,min} = 0.08 \times 300 \times \sqrt{40} \times 185/500 = 57\,\text{mm}^2$

But $A_{s,link} \geq 168\,\text{mm}^2$

Max A_{sw} = max(110; 57; 168) = 168 mm²

Use two H8 (200 mm²) at 50 mm centres.

$v = 200 \times 10^3/300 \times 307 = 2.17\,\text{N/mm}^2$

$100\,A_s/bd = 100 \times 402/300 \times 307 = 0.436 < 3$

$400/d = 400/307 = 1.303 > 1$

$v_c = 0.79 \times 0.436^{1/3} \times 1.303^{1/4} \times (40/25)^{1/3}/1.25 = 0.60\,\text{N/mm}^2$

Enhancement factor

$2d/a_v = \min(2 \times 307/85; 4) = 7.22$, use 4

$v_c = 4 \times 0.60 = 2.40\,\text{N/mm}^2$

$> 2.17\,\text{N/mm}^2$ required

$$A_{sv} = \frac{0.4 \times 85 \times 300}{0.87 \times 500} = 23\,\text{mm}^2$$

And $A_{s,min} + A_{sv,min} \geq 0.6\%\,bh$

Then $A_{sv,min} \geq 0.6\% \times 300 \times 340 - 402 = 210\,\text{mm}^2$

But $A_{sv} \geq 177\,\text{mm}^2$

Max A_{sv} = max(210; 23; 177) = 210 mm²

Use two H10 (314 mm²) at 50 mm centres.

Step 3: Lateral bursting

See Table 4.11b, where $b_p = a$.	See Table 4.11a.
$b_p = 100$, $b = 300$, then	$b_p/b = 100/300 = 0.33$, then
$\varsigma = ((300 - 100)/300)/4 = 0.167$	$\varsigma = 0.22$
$F_{bst} = 0.167 \times 202.7 = 33.8\,\text{kN}$	$F_{bst} = 0.22 \times 213.2 = 46.9\,\text{kN}$
$A_{bst} = \dfrac{33.8 \times 10^3}{0.87 \times 500} = \underline{78\,\text{mm}^2}$	$A_{bst} = \dfrac{46.9 \times 10^3}{0.87 \times 500} = \underline{108\,\text{mm}^2}$
$< 100\,\text{mm}^2$ provided above across front face.	$< 157\,\text{mm}^2$ provided above across front face.

The design method proposed in PD 6687, Annex B.4 is shown in Figure 7.95(c). It is informative to repeat the above calculations by way of comparison. Resolving vertically, $x = 190 \times 10^3/300 \times 13.44 = 48\,\text{mm}$. Then $a_e = 80 + 24 = 104\,\text{mm}$. To determine the lever arm ratio z_o/d, given that the height of the stress block at A $= 2(d - z_o)$, and $F_c = \sigma_{Rd,3}\ b\ 2(d - z_o)$, and taking moments about A, $F_c\ z_o = V_{Ed}\ a_e$, the following quadratic equation is solved:

$$(z_o / d)^2 - (z_o / d) + (V_{Ed} a_e / 2bd^2 \sigma_{Rd,3}) = 0 \tag{7.68}$$

In this example $V_{Ed}\ a_e/2\ d^2\ \sigma_{Rd,1} = 190 \times 10^3 \times 104/2 \times 300 \times 267^2 \times 13.44 = 0.0344$. Then $z_o/d = 0.964$, limited to 0.95, and $z_o = 0.95 \times 287 = 272\,\text{mm}$. Then $\beta = \tan^{-1} 272/104 = 69.0°$ (cp. 69.6°) and $F_t = 190/\tan 69° = 72.9\,\text{kN}$ (cp. 70.7 kN), giving reasonable agreement. Using Eq. (7.52) the tie force $F_{wd} = 72.9 \times (((2 \times 272/104) - 1)/(3 + \tan 69°)) = 55.0\,\text{kN}$, then $A_{s,link}$ per 2 links $= 55.0 \times 10^3/0.87 \times 500 = 126\,\text{mm}^2$ (cp. $168\,\text{mm}^2$), the design clearly giving a conservative result.

7.11.2 Haunched columns

Haunched column design involves only the provision of an adequate bearing surface at the level of the soffit of the beam (see Figure 7.97). This type of joint is not widespread in multi-storey frames because of the increased dimension of the column at each floor level. The detail may be used in low-rise unbraced structures, where the increased column geometry is beneficial in cantilever action, or in situations where the magnitude of the beam end reaction cannot practically or structurally be accommodated in a shallow corbel or steel insert, i.e. exceeding about 500 kN.

A bearing medium between the concrete surfaces of at least 10 mm thickness is highly recommended for many reasons:

- to ensure a uniform bearing pressure and ensure that the beam reaction is transferred to the column in the intended position
- to avoid eccentricity of load
- to prevent local spalling
- to accommodate tolerances, particularly in very long columns
- to allow beam rotations to take place.

The bearing pad may consist of neoprene, or be a composite construction of two thin (3 mm thick) steel plates with neoprene (10 mm) sandwiched between. In all cases the edge of the bearing plate should not extend beyond a point connecting a 45° line to the edge of the top steel in the column, i.e. 2 × cover. Some precasters provide a 25 × 25 mm chamfer to ensure that the bearing pad does not extend to the edge of the column. Also, the bearing pad should not project beyond the end of the

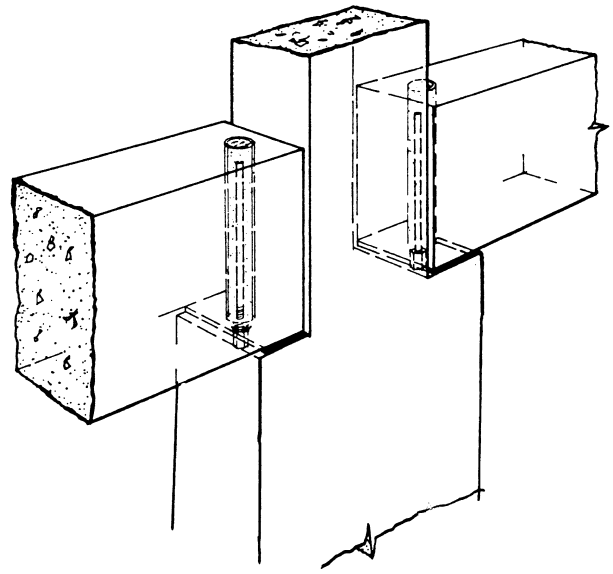

Figure 7.97 Column haunch general arrangement.

beam, where there is a clearance gap of 10 to 25 mm provided. Thus, referring to Figure 7.98(a), the length b_1 of the bearing plate is given by:

$$b_1 = \text{shoulder} - (2 \times \text{cover}) - \text{clearance gap} \tag{7.68}$$

In the presence of tension ties in one direction, if the bearing pressure is greater than $0.85\,(1 - f_{ck}/250)\,f_{ck}/1.5$ $\{0.4\,f_{cu}\}$ – see Eq. (7.12) – a steel plate must be cast into the column shoulder and, if necessary, additional bars welded to the underside of this plate. The designer has the choice of using a wide cast-in plate, say $b_p = b - (2 \times \text{cover})$, and accepting the lower bearing capacity given by Eq. 7.13, or a narrower plate ($b_p < 0.44b$) and using $0.567\,f_{ck}\,S_q$ $\{0.8\,f_{cu}\}$. Referring to Figure 7.98(b), if the line pressure beneath the cast-in plate is $f_b\,b_p$, then the pressure on the concrete f_c is given by:

$$f_c = \frac{V}{b_p b_l} < f_b \tag{7.69}$$

Adopting a strut-and-tie model with a $\theta = 20°$ load spread in the strut, the horizontal force $V \tan\theta$ is resisted by bars welded to the underside of the cast-in plate and anchored by bond in the column. As with the earlier column insert design, high-tensile ribbed bars are used, but the design stress for any welded bar is f_{ykw} $\{f_{yw}\} = 250\,\text{N/mm}^2$.

Horizontal frictional forces μV are treated in a similar manner to those for corbels and beam nibs. Unless the horizontal force can be restrained by continuity reinforcement or some other type of positive tensile fixing, tie bars inclined at α to the horizontal are required beneath the bearing surface, such that:

$$A_{sh} = \frac{V \tan\theta + \mu V}{\cos\alpha 0.87 f_y} \tag{7.70}$$

The thickness of the cast-in plate is determined from tie force considerations as normal, but typically should not be less than 8 mm. Anti-bursting confinement links are designed and positioned according to Section 7.10.2.

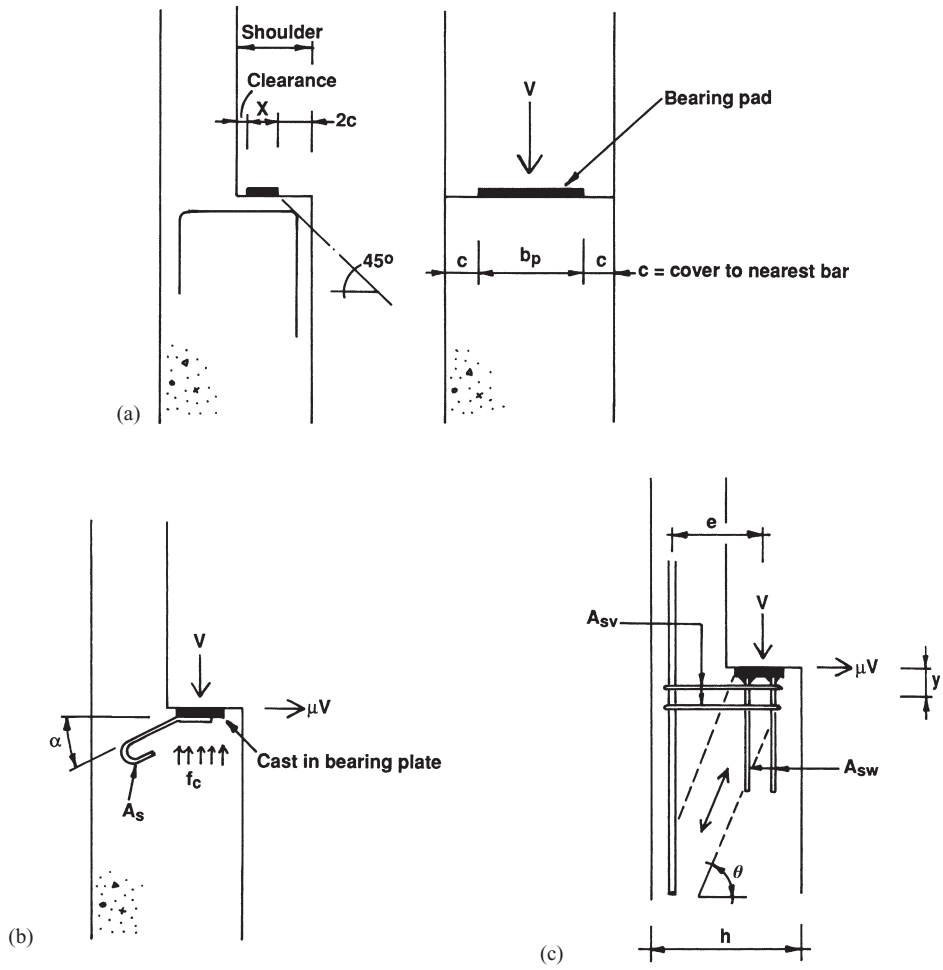

Figure 7.98 Design of column haunch. (a) Definitions used in column haunch design; (b) column haunch using welded anchor bar; (c) column haunch using tie bars.

Figure 7.98(c) shows an alternative method of transferring the horizontal forces into the column. A number of bars, usually four, are welded to the underside of the plate. Horizontal links of area A_{sv} are placed around these bars such that the centre of the group of bars is at distance y below the bearing surface (y should not be more than about 100 mm). Assuming a $\theta = 20°$ load spread from the vertical, the compression in the shoulder will act at a node at a distance $e/\tan\theta$, where e is defined in Figure 7.98(c). Then:

$$A_{sv} = \frac{V\tan\theta + \mu V\left(\dfrac{y + e/\tan\theta}{e/\tan\theta}\right)}{0.87 f_{yv}} \tag{7.71}$$

The size of the vertical bars A_{sw} welded to the plate and fully anchored into the column is given by:

$$A_{sw} = \frac{V\tan\theta + \mu V\left(\dfrac{y + e/\tan\theta}{e/\tan\theta}\right)}{0.6 \times 0.87 f_{yv}} \tag{7.72}$$

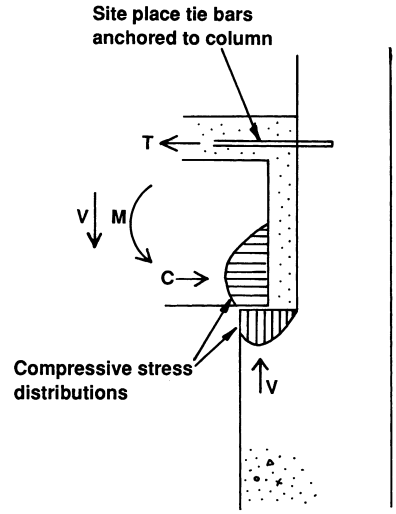

Figure 7.99 Principle of moment resisting connections at column haunches.

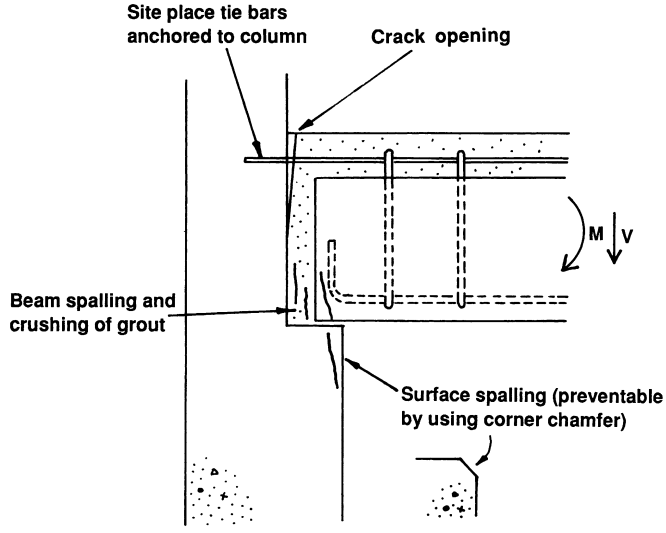

Figure 7.100 Spalling at support in moment-resisting connection.

A top fixing to the beam in the form of a bolted or a welded cleat or plate, or by using continuity reinforcement across the column, is specified in the same manner as for other beam-to-column connections.

The connection is essentially a pinned joint, but it has the potential of developing a hogging moment capacity of considerable magnitude by the use of extended bearings and reinforced *in situ* concrete in composite action with the precast beam. Figure 7.99 shows the basic principles involved. Careful detailing and specific instructions to site are required to ensure composite action at the ultimate design load.

The main requirement is for a rigid bottom connection that does not rely on horizontal shear transfer to the column. If the beams are connected rigidly at the top, but not at the bottom, rotations will occur instead of bending moments developing. Spalling of concrete due to such lack of strength and rigidity at the bottom of the beam is shown in Figure 7.100. See Chapter 8 in *Prefabrication With Concrete* [7.61] for further details.

Exercise 7.8 Haunched column design

The single-sided column haunch connection shown in Figure 7.101 is to be designed to carry an ultimate beam reaction of 380 kN {400 kN}. The beam is 12.5 m long and is reinforced at its end using horizontal loops. The nominal clear distance from the face of the column to the end of the beam is 15 mm. The allowance for the rotation of the beam may be taken as beam span/2500 {20 mm}. Design the reinforcement in the column, and specify any bearing and/or cast-in plates.

Use grade C30/37 concrete, f_{yk} $\{f_y\}$ = 500 N/mm^2 and f_{ykw} $\{f_{yw}\}$ = 250 N/mm^2, cover to reinforcement = 25 mm, and grade S275 {43} steel and welding electrodes.

Solution

Step 1: Bearing plate
Maximum bearing width b_p = 300 − 2 × 25 cover = 250 mm

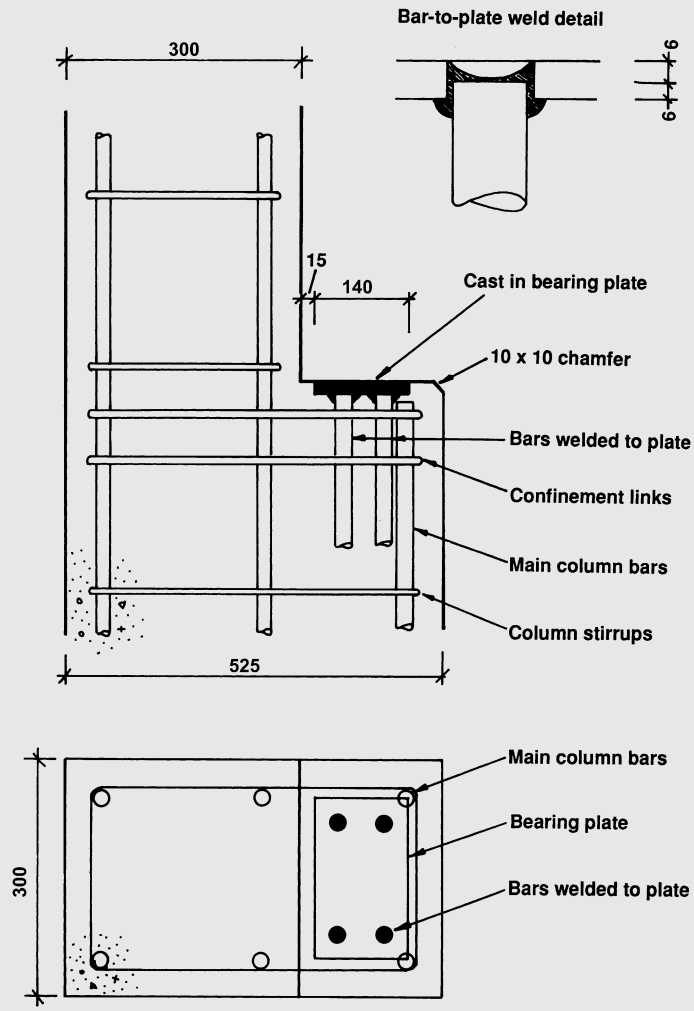

Figure 7.101 Details for Exercise 7.8.

(*Continued*)

Maximum bearing length		Maximum bearing length	
$b_l = 225 - \text{gap} - (\text{beam cover} + \Delta a_3) - (\Delta a_2 + \text{haunch cover})$		$b_l = 225 - 15$ gap $- 2 \times 25$ cover $- 20$ rotation allowance	= 140 mm
$= 225 - 15 - (25 + 12\,500/2500) - (10 + 25)$	= 145 mm	Try a 200 mm wide × 110 mm plate	
Try a 200 mm wide × 140 mm plate		Ultimate bearing pressure	
Ultimate bearing pressure		$= 400 \times 10^3/200 \times 110$	= 18.2 N/mm^2
$= 380 \times 10^3/200 \times 140$	= 13.57 N/mm^2	$< 1.5\, f_{cu}/(1+2b_l/\text{b}) = 23.8$ N/mm^2	
$< 0.567 \times 30 = 17.0$ N/mm^2 without the need for S_q		Plate thickness	
Plate thickness		$t = \dfrac{400\times10^3 \tan 20°}{200\times275}$	= 2.65 mm
$t = \dfrac{380\times10^3 \tan 20°}{200\times275}$	= 2.51 mm		

But this plate must be sufficiently thick to enable bars to be fillet welded through holes in the plate. Assume 6 mm weld (see detail in Figure 7.101).

Hence use 12 mm-thick mild steel plate.

Step 2: Vertical bars to plate

Using mild steel bars		Using mild steel bars	
$A_{sw} = \dfrac{380\times10^3 \tan 20°}{0.6\times0.87\times250}$	= 1060 mm^2	$A_{sw} = \dfrac{400\times10^3 \tan 20°}{0.6\times0.87\times250}$	= 1116 mm^2

Try four 20 mm-diameter bars into 12 mm-thick plate.

Step 3: Bearing inside hole in plate

$P_b = 12 \times 20 \times 190 \times 10^{-3} = 45.6$ kN × 4 (four bars) = 182.4 kN.

Axial force capacity of double-sided 6 mm fillet weld around 20 mm bar $= 2\times6/\sqrt{2}\times215\times20\pi\times10^{-3} = 114.6$ kN per bar or 458.5 kN total.

458.5 kN > 380 × tan20° required	= 138.3 kN	458.5 kN > 400 × tan20° required	= 145.6 kN
Length of 20 mm bar required		Length of 20 mm bar required	
$l_b = \dfrac{20}{4} \times \dfrac{0.87\times250}{2.25\times(0.21/1.5\times30^{(2/3)})} + 12$	= 370 mm	$= 30 \times 20 + 12$	= 612 mm

Use four H20 (1256 mm^2) bars × 620 mm long welded to plate, 6 mm fillet weld to plate.
Bars to penetrate hole in plate 6 mm.

Step 4: Horizontal links

$A_{sw} = \dfrac{380\times10^3 \tan 20°}{0.87\times500}$	= 318 mm^2	$A_{sw} = \dfrac{400\times10^3 \tan 20°}{0.87\times500}$	= 335 mm^2

Use two H12 (452 mm^2) links at 50 mm centres beneath plate.

Step 5: Confinement links (see Table 4.11)

Using $b_p = 200$, $b = 300$, then		Using $b_p/b = 200/300 = 0.67$, then	
$\varsigma = ((300 - 200)/300)/4 = 0.083$		$\varsigma = 0.104$	
$F_{bst} = 0.083 \times 380$	= 31.67 kN	$F_{bst} = 0.104 \times 400$	= 41.67 kN
$A_{bst} = \dfrac{31.67\times10^3}{0.87\times500}$	= 73 mm^2	$A_{bst} = \dfrac{41.67\times10^3}{0.87\times500}$	= 96 mm^2
on one face only < 226 mm^2 provided by links above.		on one face only < 226 mm^2 provided by links above.	

7.11.3 Connections to the tops of columns

There are many similarities in the principles involved in the design of this type of connection with those in wall-frame design, i.e. horizontal components are seated on the top of vertical members and an *in situ* concrete connection is made. The most common situation in beam-and-column construction occurs at the termination (usually at roof level) of a continuous column. The beam is seated and dowelled onto the column head, as shown in Figures 7.102(a) & (b), and 7.103, to form a simple support.

Bearing plates are provided between the components for the same reasons as given in Section 7.11.2. The size of the bearing pad should be at least 75×75 mm, or $h/3$ in larger columns. As before, the edge of the bearing plate should not extend into the cover concrete, and a 25×25 mm chamfer is provided so that the bearing pad does not extend to the edge of the column.

The connection can transfer the vertical forces by providing confinement links according to Section 4.3.10 and Table 4.10. The connection can also transfer applied horizontal forces, providing steel reinforcement is placed in the top of the column to prevent an inclined crack forming as shown in Figure 7.100. This steel is additional to the confinement links.

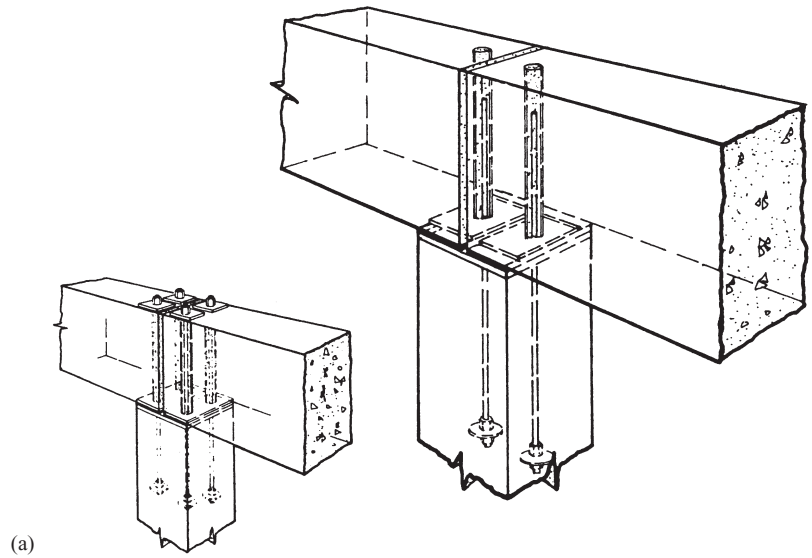

(a)

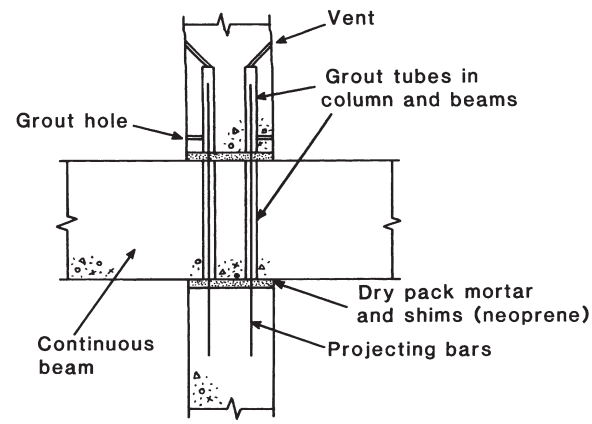

(b)

Figure 7.102 Beam-to-column head connections. (a) Simply supported column head details, and (b) continuous beam-to-column connection.

Figure 7.103 Welded connection at column head (courtesy of Blatcon Ltd).

Projecting column bars (or dowels), which are either cast into the column at the factory or grouted into holes in the top of the column on site, pass through circular corrugated ducts (of thin metal or plastic) cast within the beam. The inside diameter of the duct is two to three times the diameter of the bars passing through, but not less than 50 mm. U-shaped loops are placed around the dowel holes, typically R8 at 50 mm centres. The strength of these bars should be equal to the shear force in the dowels. The bars also provide the beam with lateral stability. The overturning moment, $M = \Sigma V\ e$ from floor slabs' reactions V placed on one side of the beam at an eccentricity e from the centre line of the beam, is resisted by a couple in the dowel. The dowel (area A_s and section modulus Z) is designed to carry the bending moment $M = 0.87\ f_y\ Z$ and the shear force $F = M/z = 0.6\ f_y\ A_s$, where z is taken as the lesser of the depth of the beam or length of projecting dowel.

Two methods are used when grouting the duct, depending on ease of access, the size of the annulus around the bar and the depth of the beam. If the beam depth is 300 mm or less and the annulus is more than about 15 mm, the grout may be dispensed from above, with a back-stop filler placed around the outside of the joint to prevent grout loss. Otherwise, for deeper beams, pressure grouting from beneath the beam is recommended. The reason for concern is not so much to do with bond around the vertical bars, although that is important, but because of entrapped air voids in the bearing area.

A further application of the use of single-storey discontinuous columns is at a balcony connection where cantilever beams are designed continuously over a column head. As before, projecting reinforcement in the lower lift of column passes through sleeves in the beam and is fully grouted to ensure vertical continuity in the column. A full compression lap length is provided to the projecting bars. The bearing area is usually sufficient to enable a dry-pack, e.g. plastic or steel shims, to be used with a solid structural expanding grout to form a joint of at least 20 mm thickness. At a node design, tension tie forces will be present, and so there is no requirement for steel-to-steel bearings providing that the design bearing stress does not exceed $0.85\ (1 - f_{ck}/250)\ f_{ck}/1.5\ \{0.4\ f_{cu}\}$, and that the strength of the grout or dry-pack infill is at least similar to that for the column.

The absence of a vertical joint at the face of the column ensures maximum efficiency in the use of precast concrete components subjected to shear and compression. The major disadvantage is that in jointing the column above and below each floor beam, two connections per floor level are made. The increased production and construction costs are in excess of the savings made in these simple connections.

7.12 Beam-to-Beam Connections

Where it is not possible to terminate a beam at a column, connections between secondary beams and primary beams may be made as shown in Figures 3.39, 7.104 and 7.105. This connection requires special attention, particularly in the primary beam, where the combined effects of bending, shear, torsion, and bearing stresses may cause problems within the shallow depth of the beam. Steel inserts are most widely used, particularly if the beam reaction is greater than about 150 kN. (Park [7.69] shows a number of details for beam-to-beam connections used in New Zealand.)

The *IStructE Manual* [7.21] makes a pertinent statement on this subject:

> *. . . These joints tend to be avoided . . . probably because their simplest forms are not normally appropriate to the client's requirements. In addition, pretensioned floors have excellent span potential so that the concept of main beams, secondary beams and slab can often be dispensed with and replaced by beam and slab.*

However there are occasions, particularly surrounding medium-sized voids in floor slabs, e.g. greater than about 2.5 m, where the floor slabs adjacent to the voids are too highly loaded to be supported without beams. The small beam span does not warrant adding extra columns to support the secondary beam, and so a beam-to-beam connection offers the most economical solution.

The design falls into three main categories, which depend mainly on:

- the magnitude of the shear force in the secondary beam
- the difference in the depths, in particular the soffit level, of the adjoining beams
- the distance to the secondary beam from the end of the primary beam.

Let the primary beam depth be h_1 and secondary beam depth be h_2, and the breadth of the beams be b_1 and b_2, respectively.

(a) Type 1 – a simple pocket bearing may be made as shown in Figure 7.104(a) where $h_1 - h_2 > 200$ mm, $b_1 > 250$ mm, and the end shear V is given by:

$$V < 0.5 \times 0.6(1 - f_{ck}/250) f_{ck}/1.5 \times b_1(h_1 - h_2) \quad (7.73) \quad \Big| \quad V < 0.8\sqrt{f_{cu}}\, b_1(h_1 - h_2) \quad (7.73)$$

If the primary beam is *not* torsionally restrained, the bearing may be recessed across a part of the primary beam a distance the greater of 100 mm or $b_1/2$, in order to ensure that torsional stresses are minimised. If the primary beam is torsionally restrained by the floor slab for example, the distance may be the greater of 75 mm or $b_1/3$.

(b) Type 2 – a direct bearing on the top of the primary beam is made, as shown in Figure 7.104(b), if $h_1 - h_2 < 200$ mm, or the depth of the primary beam $h_1 < 200$ mm itself. The same bearing length as above is used.

(c) Type 3 – a side shear connector is made to a steel insert, as shown in Figure 7.104(c), if $h_1 - h_2 < 200$ mm.

In the recessed Type 1 connections, the shear force from the secondary beam is carried into the main body of the primary beam in two ways. Firstly, a strut-and-tie model can be used acting

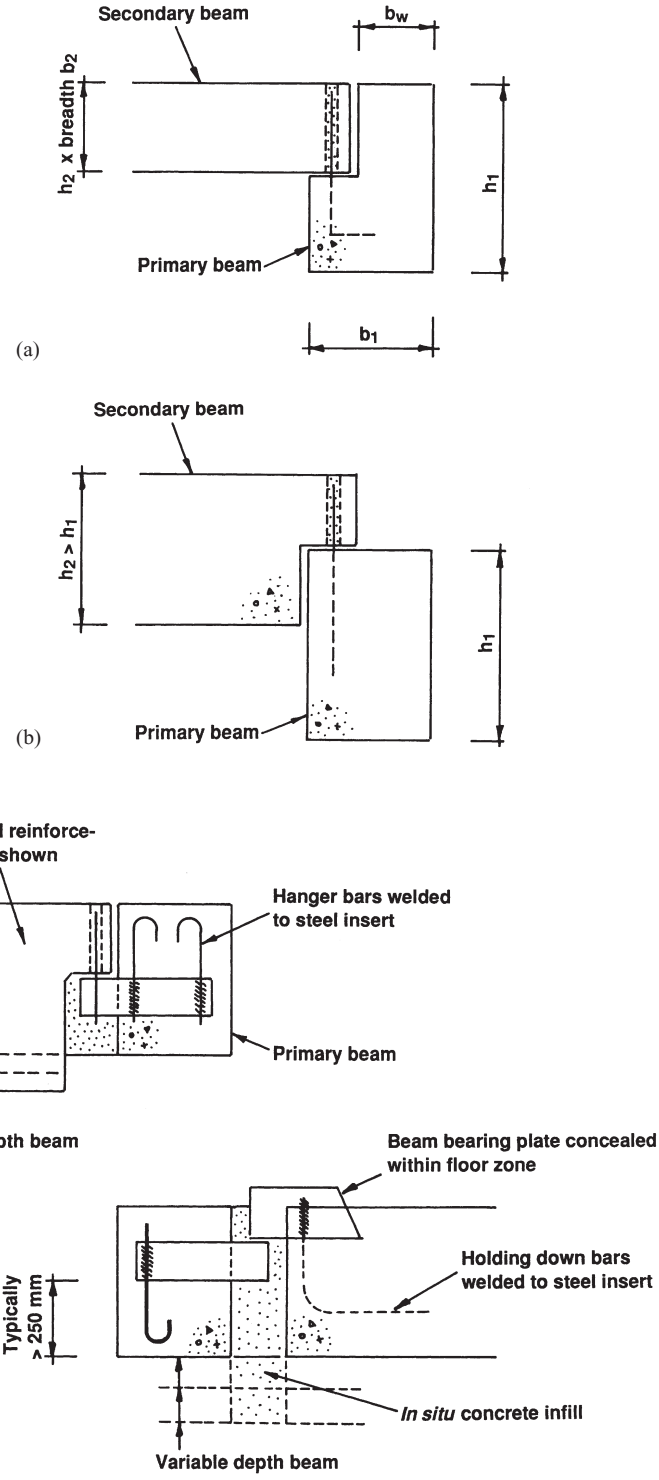

Figure 7.104 Beam-to-beam connections. (a) Pocket bearing type; (b) direct bearing type; (c) side shear box type; (d) making a beam-to-beam connection on site (courtesy of Trent Concrete Ltd).

(d)

Figure 7.104 (*Continued*)

underneath the bearing, in the same manner as for the L-shaped edge beam analysis in Section 4.3.5. The depth to the neutral axis X from the bottom of the beam should not exceed 0.5 d'', where d'' is the effective depth to the tie steel in the bearing nib. The horizontal frictional force μV is also included as before. Figure 7.104(d) shows the construction of such a connection; interestingly, the primary beam in this example is itself cantilevered at the column head, as shown in Figure 7.102(b).

Secondly, the forces may be resolved in the longitudinal direction. Referring to Figure 7.106(a), the beam geometry should be proportioned so that the line connecting the nodes in the diagonal compressive strut C is inclined at $\beta = 45°$ to 55° to the horizontal. Then the force C, and the diagonal-tension tie force T (also inclined at 45° to the horizontal) is given by:

$$C = T = \frac{0.5V}{\sin^2 \beta} \tag{7.74}$$

The bottom horizontal tie force H beneath the secondary beam bearing is given by:

$$H = 0.5V \cot \gamma \tag{7.75}$$

Figure 7.105 A double narrow-plate connector forming a beam-to-beam joint helps to maintain stability during erection and welding.

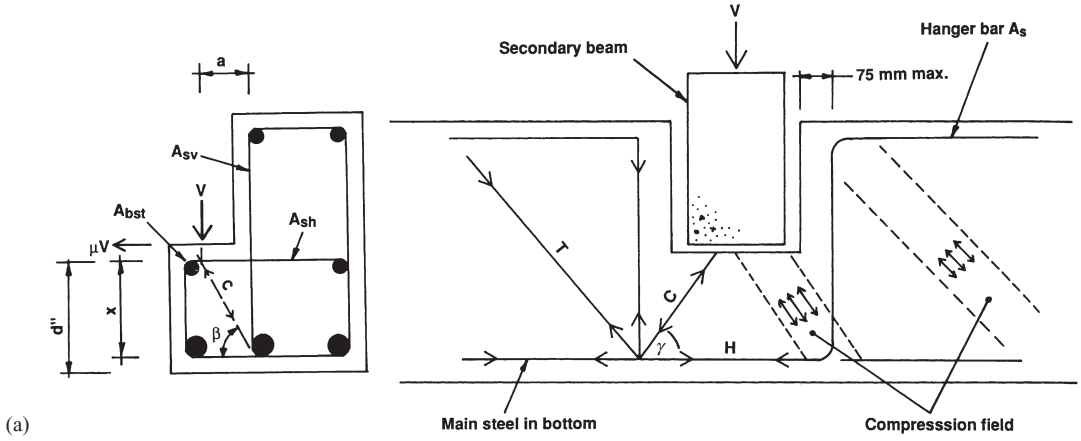

(a)

Figure 7.106 Practical beam-to-beam connections. (a) Reinforcement at primary beam.

A pair of hanger bars with area A_s may therefore be provided, as shown in Figure 7.106(b) such that:

$$A_s = \frac{H}{0.87 f_{yk}} \text{ or } \frac{0.5V}{0.87 f_{yk}} \qquad (7.76)$$

$$A_s = \frac{H}{0.87 f_y} \text{ or } \frac{0.5V}{0.87 f_y} \qquad (7.76)$$

whichever is greater. If the beam-to-beam connection is near the end of the primary beam, i.e. closer than $2d$ from the end, where d = effective depth of the primary beam, the compressive strut will be directed towards the end of the beam and will not induce the diagonal-tension force T.

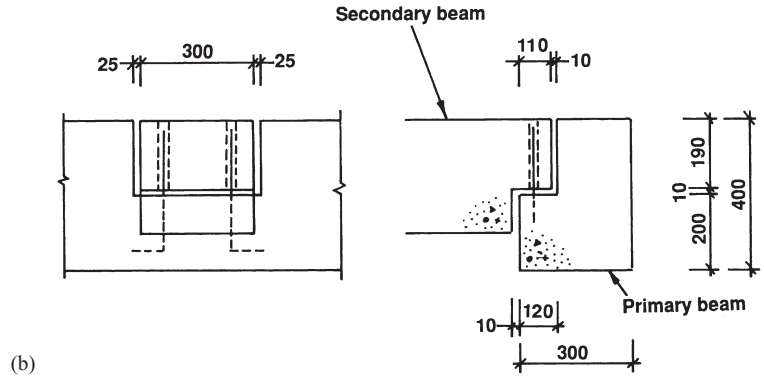

(b)

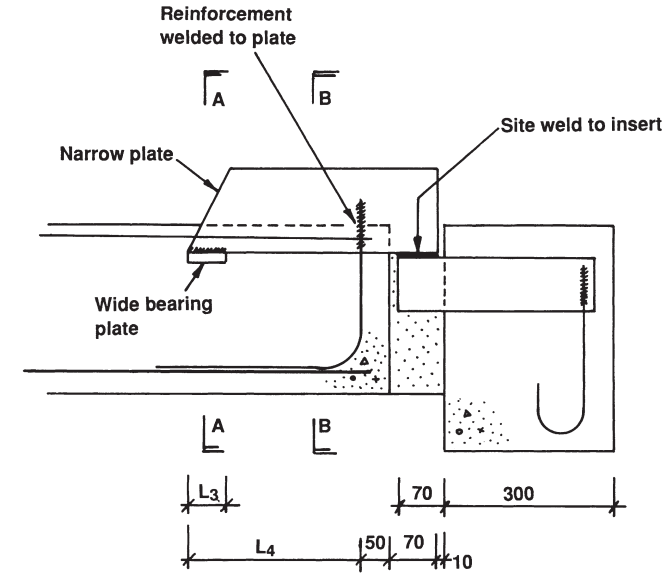

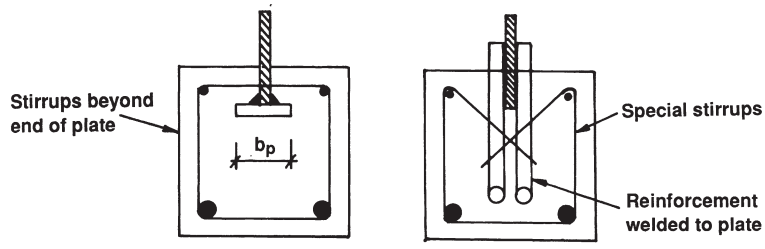

(c) Section A-A Section B-B

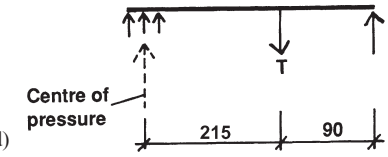

(d)

Figure 7.106 (*Continued*) Practical beam-to-beam connections. (b) Recessed half-joint option in Exercise 7.9. (c) Cast-in steel option for Exercise 7.9, and (d) force equilibrium for steel insert in Exercise 7.9.

Let the distances from the ends of the primary beam to the beam-to-beam connection be x_1 and x_2, where $x_2 > x_1$. Vertical shear links A_{sv} should be provided immediately to the sides of the recess in the primary beam, in order to generate the maximum shear force $x_2\ V/(x_2 + x_1)$ within the nodal distance equal to 0.75 d:

$$A_{sv} = \frac{x_2 V}{(x_1 + x_2)0.87 f_{yv}} \tag{7.77}$$

Finally, small lacer bars, H8 or H10, should be placed at the top corners of the tie steel in the boot.

The design methods used in the steel insert connections type 3 follow the same procedures as for beam end detailing in Section 4.3.12 and column insert detailing in Section 7.10. The major difference in the beam design is that the level of the bearing ledge is close to the top of the beam, and therefore a type of protruding Cazalay hanger is used. The protruding part is concealed within the floor slab zone. Narrow plates are the best option here, as large anchor tie forces are possible if the depth of concrete beneath the plate is substantial. Tie bars or plate straps can be fully anchored into the beam, producing a ductile failure mode (see Figure 9.2). A small bearing plate may be required at the remote end of the narrow plate.

The narrow plate is bevelled and fillet-welded to the column insert. Two temporary stability studs are needed at the end of the plate to prevent the beam from rotating on its knife edge bearing.

Exercise 7.9 Beam-to-beam connection design

A 300 × 400 mm-wide secondary beam is supported at the mid-span position of a 400 × 300 mm-wide primary beam. The ultimate shear force at the end of the primary beam is 95 kN {100 kN}. The tops of the beams are level, and the maximum allowable protrusion for any kind of connector above the beams is 75 mm. It may be assumed that the beams are torsionally restrained.

Design a suitable beam-to-beam connection using the two methods:

(1) recessed half joint
(2) cast-in steel inserts.

Use grade C30/37 concrete, f_{yk} {f_y} = 500 N/mm^2, f_{ywk} {f_{yw}} = 250 N/mm^2, cover to exposed faces = 35 mm, cover to protected faces = 25 mm, and grade S275 {43} steel and weld. Allow a 10 mm gap.

Solution

Step 1, Option 1: Recessed half joint – shown in Figure 7.106(b)
Let site fixing tolerance = 10 mm to all sides, except 25 mm to the sides of the pocket.
Half-joint depth to primary beam = 200 mm, and breadth = 300 mm.
Half-joint depth to beam = 190 mm.
Maximum bearing breadth = 300 − 2 × cover = 230 mm.

$\sigma_{Rd,2}$ = 0.85 (1 − 30/250) 30/1.5	= 15.0 N/mm^2
Bearing area without steel plates	
$= \frac{95 \times 10^3}{15.0}$	= 6333 mm^2
Bearing length = 6333/230	= 27.5 mm
Table 10.2. Try 110 mm. σ_{Ed}/f_{cd} = 3.56/20 = 0.178	
< minimum of a_1 = 110 mm	

f_b = 0.6 × 37	= 22.2 N/mm^2
Bearing area without steel plates	
$= \frac{100 \times 10^3}{22.2}$	= 4505 mm^2
Bearing length = 4505/230	= 19.6 mm
< minimum of 75 or b/3 = 100 mm	

Use plate 230 × 110 mm.

Step 2: Design of strut-and-tie steel beneath bearing

Assume 12 mm tie-bar diameter.

$d'' = 200 - 25 - 12/2 = 169$ mm

$x = 169 - 35 - 12/2 = 128$ mm

$a = 25 + 12/2 + 10\ \text{gap} + 110/2 = 96$ mm

$$\beta = \tan^{-1}\left(\frac{169 - 35 - 12/2}{96}\right) = 53.1° > 45°$$

Compressive strut force $= \dfrac{95 \times 10^3}{2 \times \sin^2 53.1°}$	$= 74.22$ kN	Compressive strut force $= \dfrac{100 \times 10^3}{2 \times \sin^2 53.1°}$	$= 78.13$ kN
Then $\sigma_{Rd,1} = (1 - 30/250)\ 30/1.5$	$= 17.6$ N/mm^2	Then $\sigma_c = 0.4 \times 37$	$= 14.8$ N/mm^2
$X = \dfrac{74.22 \times 10^3}{17.6 \times 300 \times \sin 53.1°}$	$= 17.6$ mm	$X = \dfrac{78.13 \times 10^3}{14.8 \times 300 \times \sin 53.1°}$	$= 22.0$ mm
$< 0.5\ d''$		$< 0.5\ d''$	
When the frictional force $\mu V = 0.7 \times 95 = 66.5$ kN acts, the tie force H is		When the frictional force $\mu V = 0.7 \times 100 = 70$ kN acts, the tie force H is	
$H = \dfrac{95}{\tan 53.1°} + \dfrac{66.5 \times (128 + 25 + 12/2)}{128}$	$= 153.9$ kN	$H = \dfrac{100}{\tan 53.1°} + \dfrac{70 \times (128 + 25 + 12/2)}{128}$	$= 162.0$ kN
$A_{sh} = \dfrac{153.9 \times 10^3}{0.87 \times 500}$	$= 354$ mm^2	$A_{sh} = \dfrac{162 \times 10^3}{0.87 \times 500}$	$= 373$ mm^2

Use four H12 (452 mm^2) links in boot at 100 mm centres.

Longitudinal hanger bars A_s inclined at 45° to horizontal

$A_s = \dfrac{47.5\sqrt{2} \times 10^3}{0.87 \times 500}$	$= 155$ mm^2	$A_s = \dfrac{50\sqrt{2} \times 10^3}{0.87 \times 500}$	$= 163$ mm^2

Use two H10 (314 mm^2) inclined hanger bars in front face of primary beam.

$A_s = \dfrac{47.5 \times 10^3}{0.87 \times 500}$	$= 110$ mm^2	$A_s = \dfrac{50 \times 10^3}{0.87 \times 500}$	$= 115$ mm^2

Use two H10 (157 mm^2) links either side of recess.

Splitting force directly beneath bearing point, using lowest value for the bursting coefficient ς

Table 4.11(b) $\varsigma = 0.075$		Table 4.11(a) $\varsigma = 0.11$	
$F_{bst} = 0.075 \times 95$	$= 7.1$ kN	$F_{bst} = 0.11 \times 100$	$= 11.0$ kN
$A_s = \dfrac{7.1 \times 10^3}{0.87 \times 500}$	$= 17$ mm^2	$A_s = \dfrac{11.0 \times 10^3}{0.87 \times 500}$	$= 25$ mm^2

Use one H8 (50 mm^2) bar in top corner of boot.

See Figure 7.106(a) for final reinforcement details.

(*Continued*)

Step 3, Option 2: Cast-in steel inserts. Secondary beam connector design – shown in Figure 7.106(c).
Choose narrow high-level beam plate, fillet-welded to RHS or SHS column insert.

The design requires an initial guess for the thickness of the narrow plate. Try 16 mm.

Steel-to-steel contact bearing length

$= \dfrac{95\times10^3}{16\times220}$	= 27.6 mm
$= \dfrac{100\times10^3}{16\times215}$	= 29.1 mm

plus weld run-outs, with 50 mm min. = 60 mm, say.

Eccentricity between centres of bearing and tie bar = 30 + 10 gap + 25 cover + 10 link + 16 bar radius = 91 mm.

Depth of narrow plate = 75 mm maximum protrusion plus embedded depth based on length of weld required to tie bars.

Assuming weld size = 8 mm, and referring to Figure 7.106(d), the tie force is approximately:

$T = 95 \times (215+91)/220$	= 132.1 kN
Weld length $= \dfrac{132.1\times10^3}{4\times0.707\times8\times220}$	
= 28 mm + weld run-outs	= 44 mm
$T = 100 \times (215+91)/215$	= 142.3 kN
Weld length $= \dfrac{142.3\times10^3}{4\times0.707\times8\times215}$	
= 30 mm + weld run-outs	= 46 mm

Use 50 mm.

Total depth of narrow plate = 75 + 50 = 125 mm

Narrow plate thickness

$t = \dfrac{95\times10^3}{125\times0.6\times275}$ based on shear or	= 4.61 mm
$t = \dfrac{95\times10^3\times91\times4}{125^2\times275}$ based on bending.	= 8.05 mm
Both are < 16 mm.	
$t = \dfrac{100\times10^3}{125\times0.6\times275}$ based on shear or	= 4.85 mm
$t = \dfrac{100\times10^3\times91\times4}{125^2\times275}$ based on bending.	= 8.47 mm
Both are < 16 mm.	

Use 125 × 16 mm narrow plate.

Assume b_p = 80 mm wide plate of length equal to the narrow plate. The concrete beneath the insert is not directly confined, therefore line pressure beneath plate:

= 0.567 f_{ck} t = 0.567 × 30 × 80	= 1360 N/mm
Maximum moment in plate	
M_{zz} = 95 × 91	= 8645 kNmm
Try narrow-plate length L_4 = 250 mm	
Also M_{zz} = 1360 L_3 (250 − 0.5 L_3)	
Hence L_3 = 26.9 mm, so use 30 mm wide narrow plate	
Then C = 1360 × 26.9 × 10^{-3}	= 36.6 kN
and T = 95 + 36.6	= 131.6 kN
Tie steel $A_s = \dfrac{131.6\times10^3}{0.87\times250}$	= 605 mm^2
Use two H20 (628 mm^2).	
= 0.6 f_{cu} t = 0.6 × 37 × 80	= 1776 N/mm
Maximum moment in plate	
M_{zz} = 100 × 91	= 9100 kNmm
Try narrow-plate length L_4 = 250 mm	
Also M_{zz} = 1776 L_3 (250 − 0.5 L_3)	
Hence L_3 = 21.4mm, so use 30 mm wide narrow plate	
Then C = 1776 × 21.4 × 10^{-3}	= 38.0 kN
and T = 100 + 38.0	= 138.0kN
Tie steel $A_s = \dfrac{138.0\times10^3}{0.87\times250}$	= 635 mm^2
Use two H25 (982 mm^2).	

Weld bars to narrow plate, with 8 mm CFW × 50 mm long.

Bend radius to H20 bars:	
to reduce stress inside bends,	
splay the bars to 150 mm centres	
along bottom of beam, then	
a_b = 150 mm	
Force per bar = 131.6/2 = 65.8 kN	
Bend radius to H25 bars:	
a_b = 16 + 25 = 41 mm	
Force per bar = 138.0/2 = 69.0 kN	
$r = \dfrac{69.0\times10^3\times\left(1+\dfrac{2\times25}{(16+25)}\right)}{2\times37\times25}$	= 82.8 mm

$$r = \frac{65.8\times10^3\times\left(\frac{2}{150+20}+\frac{1}{2\times20}\right)}{2\times30/1.5} = 61\,\text{mm}$$

< 3½ dia = 70 mm minimum
Let $r = 70$ mm
Horizontal shear in bar = μV = 66.5 kN

$$A_s = \frac{66.5\times10^3}{0.6\times0.87\times250} = 510\,\text{mm}^2$$

< 628 mm² provided.

> 3 dia = 75 mm minimum
Horizontal shear in bar = μV = 70 kN
is resisted by the shear in the tie bar, and friction-bond in the plate. Ignoring the latter, then:

$$A_s = \frac{70\times10^3}{0.6\times0.87\times250} = 537\,\text{mm}^2$$

< 982 mm² provided.

Step 4: Shear reinforcement design
Assume 25 mm main bars in beam. $b = 300$ mm, $d = 300 - 35 - 8 - 25/2 = 242.5$ mm

V required = 135.2 kN

$$V_{Rdc} = \frac{0.12\times\left(1+\sqrt{\frac{200}{242.5}}\right)\times(100\times0.00863\times30)^{(1/3)}\times300\times242.5}{10^3} = 49.3\,\text{kN}$$

The maximum design load

$$V_{Ed} = \frac{0.5\times300\times242.5}{10^3}\times0.6\left(1-\frac{30}{250}\right)\times\frac{30}{1.5} = 384.1\,\text{kN}$$

> 190 kN
$z = 0.9 \times 242.5$ = 218.2 mm

$$\frac{A_{sv}}{s_v} = \frac{135.2\times10^3}{218.2\times0.87\times500\times2.5} = 555\,\text{mm}^2/\text{2legs}$$

or

$$A_{sv,min} = 0.08\times\sqrt{30}/250\times300\times242.5 = 128\,\text{mm}^2$$

Use H8 links at 175 mm centres (571 mm²) for a distance to the end of the narrow plate plus d.

$$\frac{100A_s}{bd} = \frac{100\times982}{300\times242.5} = 1.375\,\text{N/mm}^2$$

Hence, $v_c = 0.902$ N/mm²

$$\frac{A_{sv}}{s_v} = \frac{300\times(1.375-0.902)}{0.87\times250} = 1.35\,\text{mm}^2/\text{mm} = 652\,\text{mm}^2/\text{m for 2 legs}$$

Use H8 links at 150 mm centres (666 mm²) for a distance to the end of the narrow plate plus d.

Step 5: Design of wide plate
Overhang beyond edge of narrow plate = (80 − 16)/2 = 32 mm
Average stress under wide plate

$$= \frac{36.6\times10^3}{80\times30} = 15.25\,\text{N/mm}^2$$

Shear, $V = 15.25 \times 30 \times 32$ = 14.64 kN
Bending, $M = 15.25 \times 30 \times 32^2/2$ = 234.3 kNmm

$$t = \frac{14.64\times10^3}{30\times0.6\times275}$$ based on shear, or = 3.0 mm

$$t = \sqrt{\frac{234.3\times10^3\times4}{30\times275}}$$ based on bending = 10.6 mm

$$= \frac{38.0\times10^3}{80\times30} = 15.85\,\text{N/mm}^2$$

Shear, $V = 15.85 \times 30 \times 32$ = 15.2 kN
Bending, $M = 15.85 \times 30 \times 32^2/2$ = 243.4 kNmm

$$t = \frac{15.2\times10^3}{30\times0.6\times275}$$ based on shear, or = 3.07 mm

$$t = \sqrt{\frac{243.4\times10^3\times4}{30\times275}}$$ based on bending = 10.86 mm

Use 100 × 30 × 16 wide plate.

(*Continued*)

Step 6: Design of primary beam steel insert and reinforcement

Distance to centre of secondary beam reaction from face of primary beam = 40 mm

Because the lever arm is smaller than in column inserts, use SHS rather than RHS. Try b_p = 80 mm.

Line pressure = 0.567 × 30 × 80	= 1360 N/mm	Line pressure = 0.8 × 37 × 80	= 2368 N/mm
$L_2 = 95 \times 10^3/1360$	= 69.9 mm	$L_2 = 100 \times 10^3/2368$	= 42.3 mm
$M_{zz} = 95 \times (40 + 35 + 69.9/2)$	= 10 443 kNmm	$M_{zz} = 100 \times (40 + 35 + 42.3/2)$	= 9612 kNmm
$S_{zz} > 10\,443/275$	= 37.97 cm^3	$S_{zz} > 9612/275$	= 34.95 cm^3
$2dt > 80 \times 10^3/165$	= 576 mm^2	$2dt > 80 \times 10^3/165$	= 606 mm^2

Use 80 × 80 × 5 mm SHS (S_{xx} = 41.7 cm^3, $2dt$ = 800 mm^2).

Maximum length of billet = 300 − 35 = 265 mm. Hence use additional bars to rear of insert, at edge distance to bars = 35 + 10 + 25/2 = 57.5 mm. Then d = 242.5 mm.

The lever arm	= 137.6 mm	The lever arm	= 165.3 mm
Using $M_{zz} = 1360\ L_3\ (137.6 - L_3)$, and solving the quadratic equation, L_3	= 77.7 mm	Using $M_{zz} = 2368\ L_3\ (165.3 - L_3)$, and solving the quadratic equation, L_3	= 26.7 mm
Total force in steel $= 1360 \times 77.7 \times 10^{-3}$	= 105.7 kN	Total force in steel $= 2368 \times 26.7 \times 10^{-3}$	= 63.3 kN
$A_s = \dfrac{105.7 \times 10^3}{0.87 \times 250}$	= 486 mm^2	$A_s = \dfrac{63.3 \times 10^3}{0.87 \times 250}$	= 291 mm^2
Use two H20 bars (628 mm^2).		Use two H16 bars (402 mm^2).	

Locate bars at 45 mm cover welded to side of insert.

Bar anchorage length $= \dfrac{20}{4} \dfrac{105.7 \times 10^3}{628 \times 2.25 \times 0.21/1.5 \times 30^{(2/3)}}$	= 277 mm	Bar anchorage length $= 32 \times (291/402) \times 16$	= 371 mm

> 225 mm to bottom of beam. Hence provide hook to give full anchorage.

Assume weld size = 8 mm.

Weld length $= \dfrac{105.7 \times 10^3}{4 \times 0.7 \times 8 \times 220}$		Weld length $= \dfrac{63.3 \times 10^3}{4 \times 0.7 \times 8 \times 215}$	
= 22.0 mm + run-outs < 80 mm available	= 38 mm	= 13.14 mm + run-outs < 80 mm available	= 29.1 mm

Use 8 mm CFW × 80 mm long to side of insert.

Confinement reinforcement beneath insert (see Table 4.11)

$F = 95 + 105.7$	= 200.7 kN	$F = 100 + 63.3$	= 163.3 kN
$b_p = 80$, $b = 300$, then $\varsigma = ((300 - 80)/300)/4 = 0.183$		$b_p/b = 80/300 = 0.229$, then $\varsigma = 0.23$	
$F_{bst} = 0.183 \times 200.7$	= 36.7 kN	$F_{bst} = 0.23 \times 163.3$	= 37.4 kN
$A_s = \dfrac{36.7 \times 10^3}{0.87 \times 500}$	= 85 mm^2	$A_s = \dfrac{37.4 \times 10^3}{0.87 \times 500}$	= 86 mm^2

Use two H10 bars (157 mm^2) at 50 mm and 100 mm below the front of the insert.

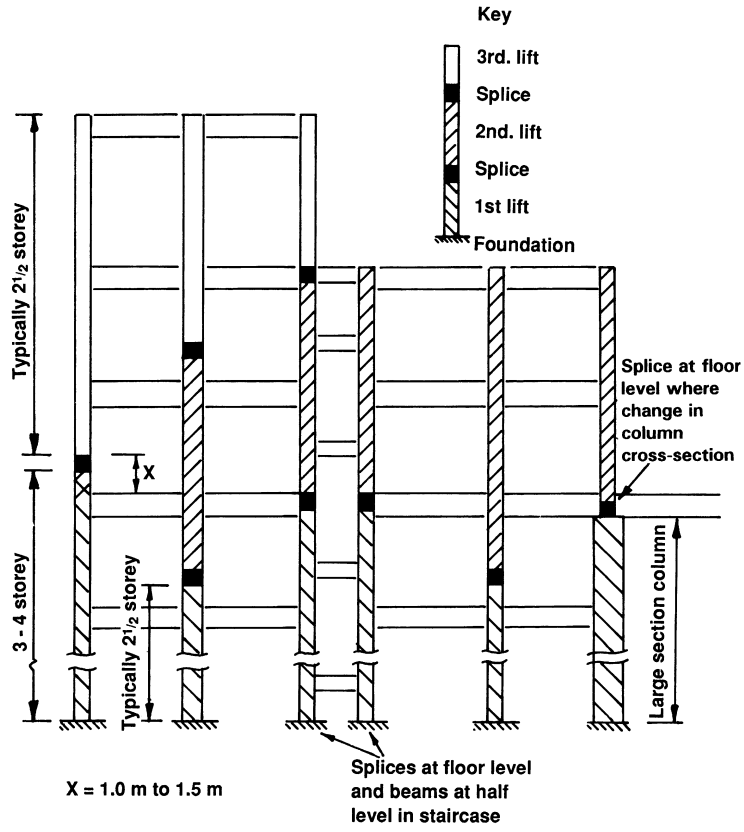

Figure 7.107 Preferred positions for column splices in a multi-storey multi-bay frame.

7.13 Column Splices

7.13.1 Types of splice

A column *splice* is the general term for a joint where a structural connection is made between a column and another precast component. The base member is usually a column, but it may also be a wall, structural cladding panel, beam, or in extreme circumstances a flooring unit. It does *not* include the connection to bases or other foundations.

Most precast concrete frame designers prefer to stagger the level of column splices, as shown in Figure 7.107, to avoid forming a 'plane of weakness'. The first level of splices is usually shared between the third and fourth floors, except in five-storey frames where the splices (if used at all) are made at the second and third floors. The second splice is at two or three storeys above the first splice. Splices are located either at a floor level (within the structural floor zone), where they may be concealed in the floor finishes, or at a convenient working height, e.g. 1.0 m above floor level, near the point of contraflexure in the frame where the bending moments are small (Figure 7.108). Column splices may be used only in a totally braced frame, or in the braced part of a partially braced frame, i.e. spliced columns may not be unbraced in any direction.

The choice of splice is often dictated more by site erection considerations than by structural strength. It is very important that the temporary stability of a structure is not placed at risk by using a connection that relies heavily on friction, wedging or other physical actions.

(a) (b)

Figure 7.108 A welded plate column splice: (a) alignment using templates and yokes, and (b) completed joint. (Courtesy of T&A Prefabricados, Recife, Brazil.)

7.13.2 Column-to-column splices

Column-to-column splices are made either by coupling, welding or bolting mechanical connectors anchored into the separate precast components, or by the continuity of reinforcement through a grouted joint. The compressive capacity of the splice is made equal to that of the parent columns by confining the *in situ* concrete placed into the joint. Although the 'design' strengths of the precast and *in situ* concrete are equal, it is almost certain that the 'actual' strengths will differ – the precast being greater. (In the authors' experience 28-day precast concrete cube strengths of 80 N/mm^2 are not unusual for columns where the 24-hour strength has been 40 N/mm^2.)

The effect of different concrete strengths on the compressive load capacity of columns and column splices was studied by Shu and Hawkins [7.70]. The test variables were height of splice v, breadth of the column b, and cylinder strength of the infill f_{cyl}. The effective (i.e. apparent) strength of the connection f_c' was measured. In all cases the ratio f_c'/f_{cyl} was greater than 1.0, but when the data for f_{cyl} are converted to cube strengths, the situation becomes non-conservative when $v/b > 1.5$. Thus, providing that the height of the splice is not more than 1.5 times the minimum breadth of the column, the connection will develop the design strength of the infill. The usual practice is to keep $v/b < 1$.

The essential features of design are to satisfy the requirements of ultimate strength and structural stability. This is achieved at every interface through the joint, either by coupling, welding or bolting mechanical connectors anchored into the separate precast components, or by the continuity of reinforcement through a grouted joint. The grout and concrete infill must also have adequate strength, in addition to providing durability protection for the steel components.

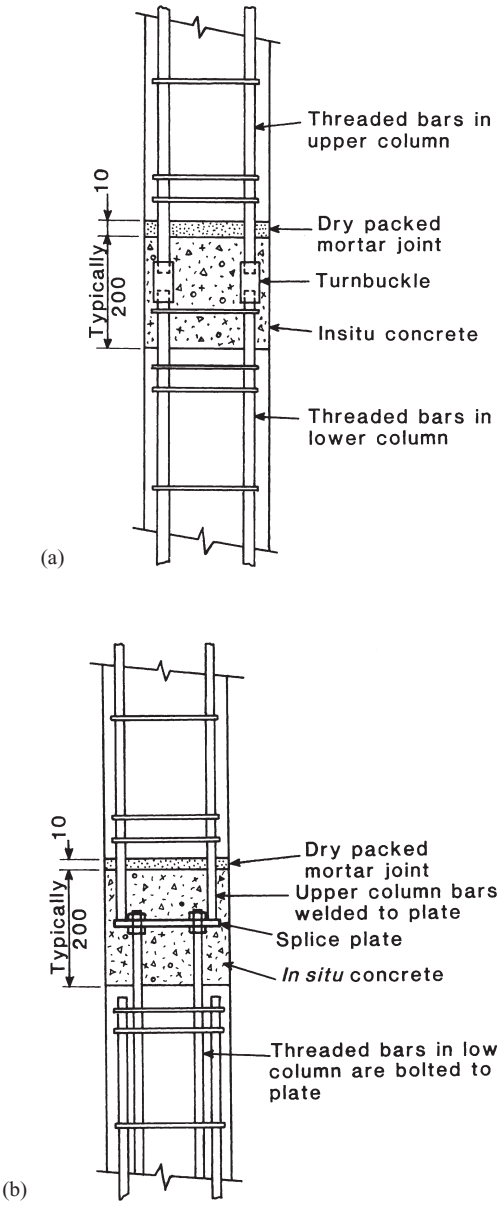

Figure 7.109 Types of splices. (a) Coupled joint; (b) welded plate; (c) grouted sleeve; (d) welded lap joint; (e) grouted splice sleeve.

7.13.3 Coupled joint splice

The coupled joint shown in Figure 7.109(a) provides a mechanical tie between the precast components that is capable of axial load and bending moment interaction. This connection requires absolute *precision* (to about ±3 mm) in placing projecting threaded bars, and should be used only if the designer is satisfied that such tolerances can be achieved both in the factory and on site. The other main drawback is the difficulty of adjusting all couplers simultaneously.

The strength of the splice may have to be down-rated owing to problems in the strain compatibility between the ordinarily reinforced precast components and the less ductile behaviour of the threaded

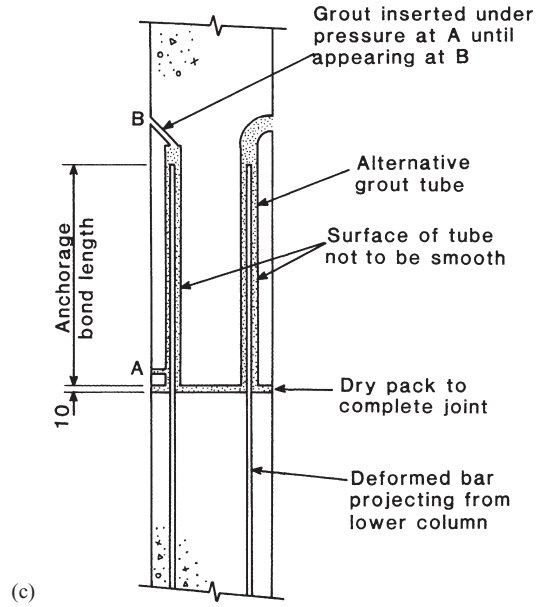

Figure 7.109 (*Continued*)

coupler. Designed links are provided in the infilled region to provide stability to the compression reinforcement and to increase the strength of the infill by confinement. The projecting reinforcement in the upper and lower columns is threaded to opposite hands, and the coupler is provided with opposite hand threads. A sufficient threaded length of bar within the coupler is assured by turning the coupler down to predetermined marks on the reinforcement.

The 28-day characteristic strength of the *in situ* infill is at least equal to the design strength of the column. A proprietary expanding agent is added to the cement/sand/6 mm aggregate mix to prevent shrinkage cracking between the different concretes. The height of the splice is generally less than 200 mm and is structurally adequate if the *in situ* connection is made in one pour. In dealing with larger volumes (greater than 0.05 m^3) or greater height (exceeding 300 mm), it is necessary to concrete in two stages by leaving a narrow 10 to 15 mm gap and dry-packing with a 2:1 sand/cement mortar at a later date.

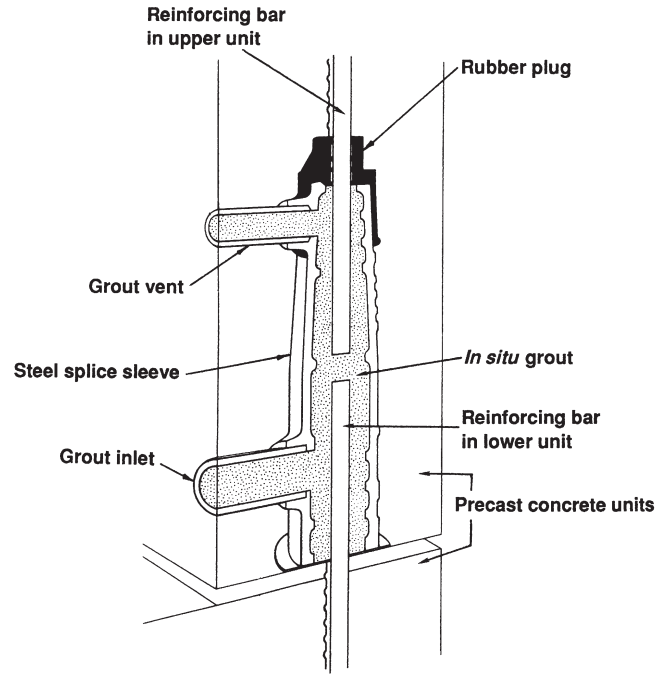

(e)

Figure 7.109 (*Continued*)

7.13.4 Welded plate splice

The splice, shown in Figure 7.109(b), is formed by allowing projecting reinforcement from the (usually) lower column to be clamped between pairs of nuts to a plate which is welded to bars projecting from the upper column. The compressive strength of this arrangement is based on the strength of the infill concrete plus either the load capacity of the threaded bar/nut system, or the load capacity of the welded mild steel reinforcement. The strength of the infill should be equal to that of the precast column, but not more than 40 N/mm^2 unless testing has shown that higher infill strengths may be used. The flexural and shear strength of the plate is enhanced by the confinement of the *in situ* concrete. However, flexibility of the plate can cause problems in the temporary condition, particularly if long columns (up to three storeys) are left free-standing.

The strength of the splice is governed either by the strength of the plate in bending, by shear across plane x–x in Figure 7.109(b), or by the strength of the bars. The upper column bars are considered mild steel because they are welded to the plate. The bars are placed into oversized holes such that there is an annulus of 4–5 mm around the bar to permit the placement of a full-penetration fillet weld. Fillet welds made directly onto the surface of the plate are not acceptable. Small-diameter (e.g. 3 mm) electrodes are used. The bar must penetrate the hole in the plate to a distance l_x, so that the strength of the weld is greater than the yield strength of the bar. A factor of safety of 2 is quite common to allow for variable workmanship, among other things. Thus, if the diameter of the bar is ϕ, then:

$$\pi\phi l_x f_{ykw}/1.25 > 2(0.87 f_{yk})A_s \qquad (7.78) \quad | \quad \pi\phi l_x p_{we/d} > 2(0.87 f_y)A_s \qquad (7.78)$$

If, for mild steel bar and grade S275 {43} steel weld, $f_{yk}/f_{ykw} = 250/220$ $\{f_y/p_{weld} = 250/215\}$, then

$$l_x > 0.5\phi \qquad (7.79)$$

Table 7.10 Metric threaded high-yield reinforcement data

Bar diameter	Area at root of thread (mm^2)	Tensile strength (kN)
16	157	66.9
20	245	104.4
25	353	150.4
32	561	239.0

Thus the rules are:

- the splice plate should be at least equal to the 'designed' bar diameter
- the bar should penetrate the plate to a distance equal to half its diameter.

Note that the actual bar used may be larger than the design value. In general the smallest size of bar used is 16 mm diameter, with 25 mm being the most common for supporting two-storey columns.

The lower bars are threaded high-tensile bars, with a reduced cross-sectional area measured at the root of the thread. For metric threads the effective diameter and strength of threaded reinforcing bars are given in Table 7.10.

If the splice is concealed in the floor zone, the size of the plate may be equal (or slightly greater if needed) to the size of the column. The cover to the threaded and welded bars may be equal to the main column reinforcement. However, if the splice is made above floor level then the plate must be protected by concrete cover, typically 35 to 40 mm. Thus the cover to the splice bars is about 70 mm. This has the effect of reducing the strength of the splice by reducing the lever arm between the bars.

The centroidal distance X between the bars is given by:

$$X = h/2 - \text{cover to bars} - \phi/2 \tag{7.80}$$

where ϕ = diameter of the threaded bar.

The lever arm from the centre of this bar to plane x–x is $X/\sqrt{2}$, and the effective breadth of the plate in plane x–x may be approximated as $\sqrt{2}X$. In the temporary construction phase before the splice is grouted, the thickness of the plate is given by the greater of:

$$t^2 = \frac{2F_s}{p_y} \tag{7.81}$$

and

$$t = \frac{F_s}{0.6p_y\sqrt{2}X} \tag{7.82}$$

where F_s is the force in the bar due to the self-weight of the column W and to the effects of overturning due to wind loads and lack of plumb. Wind pressures in the temporary stage cause moments M at splices in the order of 5 to 6 kNm in a two-storey column, and about 10 kNm in three storeys. For combined bending and axial force, the force in the bars (four per column) is given by:

$$F_s = 0.25\left(\frac{M}{X} + W\right) \tag{7.83}$$

This force is, of course, permanent and must form part of the overall calculation for the strength of the splice when completed. It is also vital that no signs of distress are seen in the splice during this stage. For these reasons the bars are often overdesigned, with a factor of safety of about two at ultimate.

After completion of the splice by grouting etc. the load path through the connection by-passes the plate, but not the bars. However, the role of the plate is essential to the satisfactory performance of a splice by helping to confine the infill concrete. No confinement links are used here.

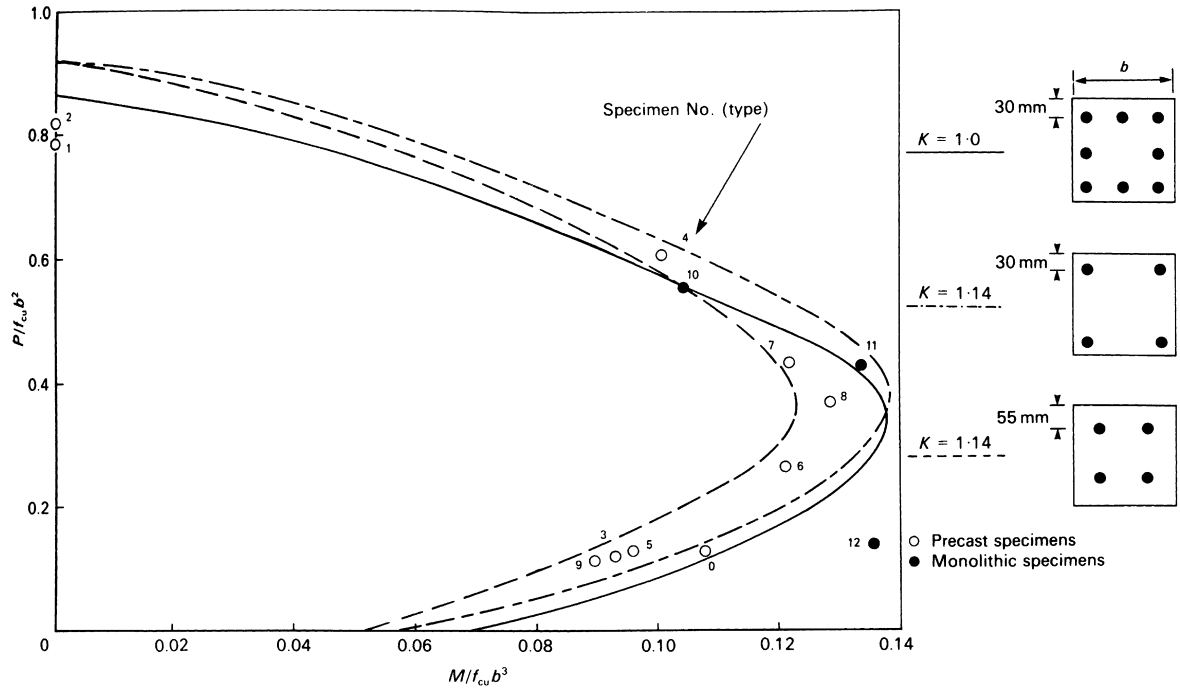

Figure 7.110 Moment versus axial load interaction failure data for grouted sleeve column splice tests by Kuttab & Dougill [7.71].

7.13.5 Grouted sleeve splice

One of the most popular (and most economical) column splice details is the grouted splice sleeve (see Figure 7.109(c)). Full-scale tests [7.71] have shown that the axial load-bending moment interaction characteristics of this joint are equal to those of the parent column. Figure 7.110 summarises the results. The joint possesses most of the advantages (confinement of concrete, thin dry-packed joint, continuity of high-tensile reinforcement, ease of manufacture and fixing) and few of the disadvantages (difficult to fully compact pressurised grout in the sleeves of the upper lift) associated with precast construction methods. Figure 7.111 shows that the lapped rebars in the sleeve may not always be perfectly central; however, that does not appear to inhibit full bond strengths developing at the bar–grout–sleeve interfaces.

Splices may be made in this way at virtually any level in the frame and are not restricted to column-to-column connections. The requirements for the size of the sleeve and the grouting method given in Section 7.5.2 and Figure 7.23 are also applicable here.

7.13.6 Welded lap splice

The welded lap joint solution, Figure 7.109(d), is not widely used because the height of unrestrained reinforcement, which is typically 500 to 700 mm in order to achieve the necessary weld length, cannot be justified. A single link can be placed in the gap, but this must then be made wider than is normally acceptable for dry-packed mortar. The main disadvantages are associated with accuracy in manufacture and site erection, and with the need for the upper column to be held rigidly while the welding is carried out. *In situ* concreting against such large 'dry' surface areas makes it difficult to avoid honeycombing and unsightly surface irregularities.

If these problems can be satisfactorily overcome, the splice may be considered structurally equal to a precast column reinforced with mild steel bars.

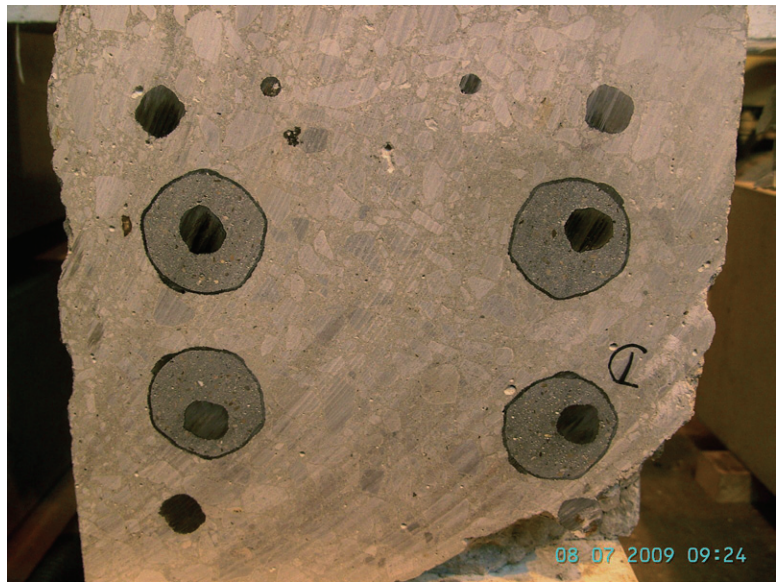

Figure 7.111 Cross section through grouted sleeve column splice [7.24].

7.13.7 Grouted sleeve coupler splice

Reinforcing bars to be connected are inserted end to end into a preformed steel sleeve and pressure-grouted in the same manner as the grouted sleeve given in Section 7.13.5. The original splice sleeve was invented by A. A. Yee in the US, and the proprietary system is patented. The splice detail shown in Figure 7.109(e) may be used for compression and tension, and is equally suited to horizontal as well as vertical (or inclined) splices.

The principle is simple in that the bond length of the bars may be reduced to about eight diameters, because the grout inserted into the annulus between the bars is highly confined by the tapered and ribbed inside face of the sleeve. The annulus is approximately 8 mm minimum thickness, but special large-opening sleeves may be used where site tolerances need to be greater than the standard practice. See Section 7.5.2 for the grouting specification. The sleeve contains a stop, formed at its centre, to ensure that each bar is embedded to the correct length. The bars may be of different diameter.

7.13.8 Steel shoe splices

Prefabricated steel shoes, Figure 7.112, are used where it may be necessary to generate bending moment and tensile forces in splices. The so-called 'column shoe' may also be used at foundation connections. It is an attractive alternative to the welded splice plate in large cross sections (greater than, say, 400 × 400 mm), where large plates may be wasteful. In all four shoes are used, one at each corner of a rectangular column. Modified versions of the standard shoe are possible for non-rectangular columns. The connectors are expensive in terms of materials and manufacture, but compensate for this by providing a very rapid and structurally safe fixing on site, accommodating large tolerances. Positioning errors of up to 10 mm are possible with the use of cleverly designed eccentric-hole plate washers.

For typical use in precast columns, each shoe consists of a thick (grade 50) steel plate, typically 12 to 40 mm thick and 100 to 150 mm square, joined to a thin plate-metal shroud forming an 80–100 mm

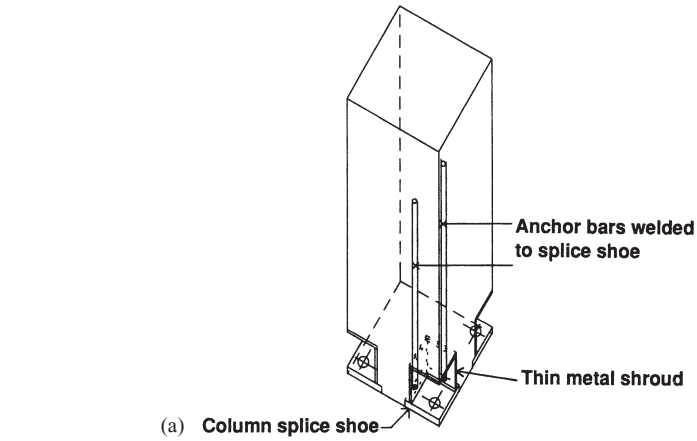

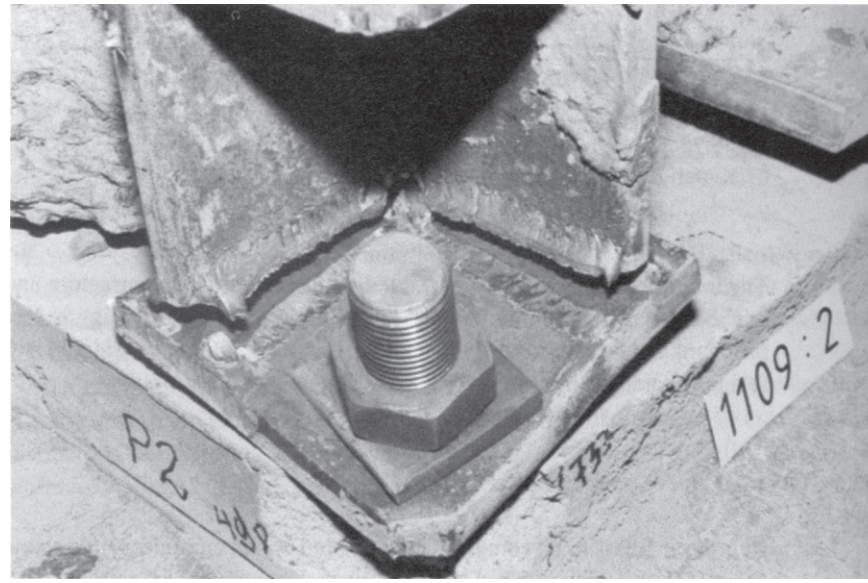

(b)

Figure 7.112 Column splice shoe details. (a) Column splice shoe tests by Bergström [7.72], and (b) ultimate failure condition at one corner of a column [7.72].

(approximately) open-box cube, with three weld-connected rebars in a triangular formation. The bars, which are typically 16 to 40 mm in diameter, provide the bond force to the concrete column. The base plate has a punched hole at its centre that receives the threaded coupler bars from the adjoining column (similar to the welded plate splice detail). The column shoe may be recessed in the column if the splice connection is exposed; otherwise the edge of the base plate is made flush with the column.

The tensile capacity of these connectors is always governed by the shroud welds or the strength of the threaded portion of the coupler bar, and never by the bond strength of the rebars. For typical sizes of grade C40/50 precast columns in precast frames, where the shoe size is about 100 mm square with M30 bolts, the static tensile strength is in the order of 300 kN per shoe.

Bergstrom [7.72] has carried out bending moment tests on columns with four shoe connections, as shown in Figure 7.112(a). The column size was 400 mm square. Applied moments of up to 230 kNm caused relative rotations between the foundation and the bottom of the column of up to 0.02 radians

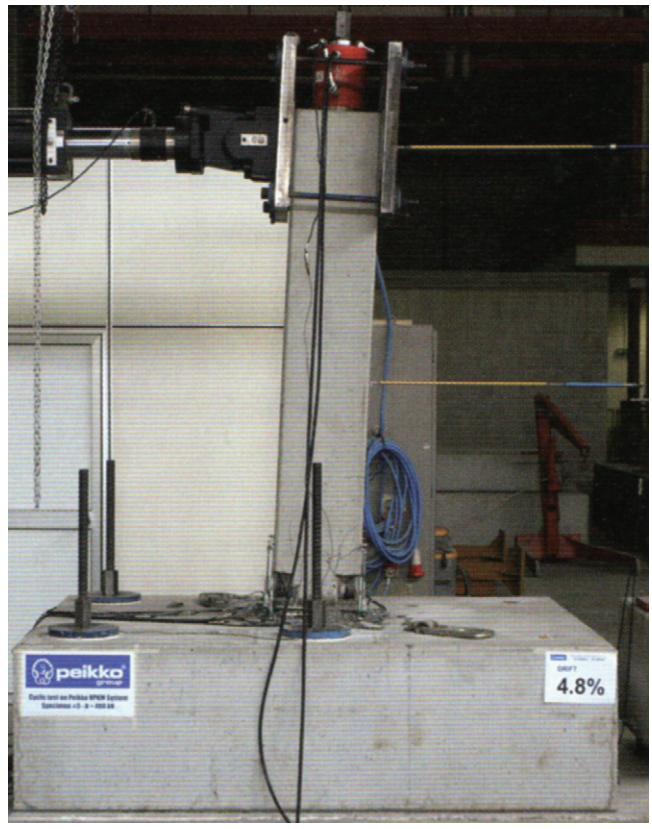

Figure 7.113 Column shoe test carried out by the manufacturer Peikko Group Corp., Finland [7.74] at 4.8% rotation giving a moment of resistance of 180 kNm (courtesy of Peikko Group Corp.).

at the limit of proportionality, and 0.1 rad at ultimate. The average rotational stiffness of these connections was 12 750 kNm/rad, which is equal to approximately 0.8 times the uncracked flexural stiffness of a 4.0 m long column of the same size as used in the test. This value compares reasonably closely with the value of 1.0 according to BS 8110 [7.9], although the test result is on the unsafe side. Figure 7.112(b) shows the ultimate failure condition at one corner of a column.

The flexural behaviour of bolted column-to-foundation connections was investigated by the Peikko Group Corporation in the European Centre of Earthquake Engineering in Italy. The experimental loading history consisted of a series of horizontal displacement cycles at the tops of the columns with increasing target drift, as shown in Figure 7.113. During the tests constant compression through internal tendons was applied, which represented the vertical loads of typical multi-storey buildings. Figure 7.114 shows the hysteretic behaviour of the connection up to a drift (inclination) equal to 4.8 per cent and the corresponding damaged pattern at the end of the tests. The results obtained highlighted the following facts [7.73]:

- The behaviour of the connection is governed by the failure of the bolts and is characterised by high values of ductility and dissipative capacity.
- The connection sustains its resistance for much larger drifts than the maximum drifts accepted for prefabricated columns, even under a design seismic event.
- No damage to the welding of the column shoes was observed. This is because of the high quality standards of the fabricator.

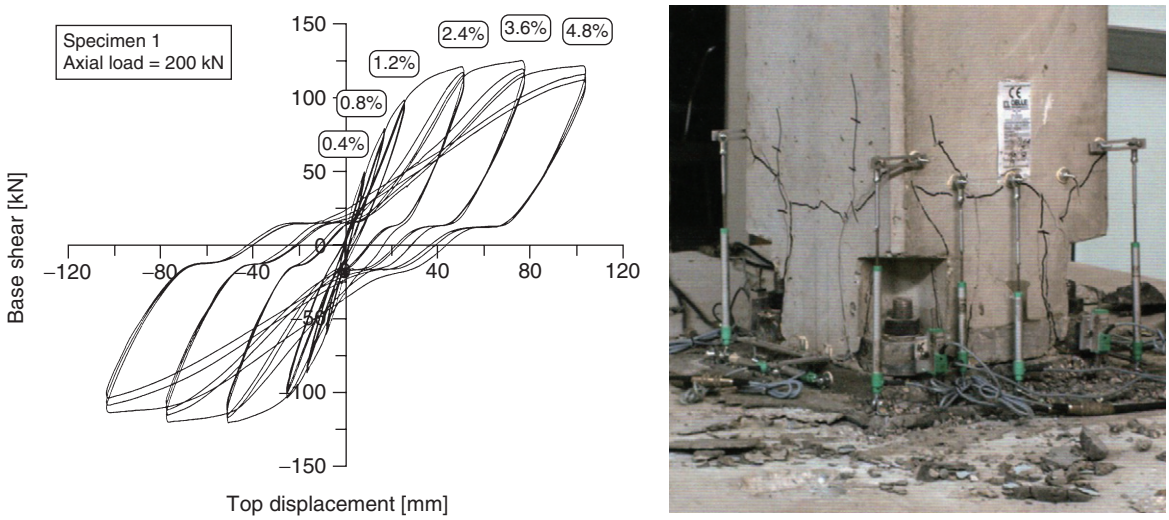

Figure 7.114 Test results for column shoe bending tests by the manufacturer Peikko Group Corp., Finland [7.74] (courtesy of Peikko Group Corp.).

Exercise 7.10 Welded plate splice design

Calculate axial load capacity of the welded plate splice shown in Figure 7.115, assuming that the bending moment is zero. Assume the edge distance to the holes in the plate = 20 mm.

Use grade C30/37 for *in situ* concrete, f_{yk} {f_y} = 250 N/mm^2 in the upper bars, f_{yk} {f_y} = 500 N/mm^2 in the lower threaded bars, 35 mm cover to the plate, grade S275 {43} steel plate and weld.

Solution

Step 1: During construction

Assume 25 mm threaded bar, then $X = 230/2 - 20 - 25/2 = 82.5$ mm

$b = \sqrt{2} \times 82.5 = 116.7$ mm

Plate bending capacity $M_R = 275 \times 116.7 \times 20^2 \times 10^{-3}/4 = 3209$ kNmm

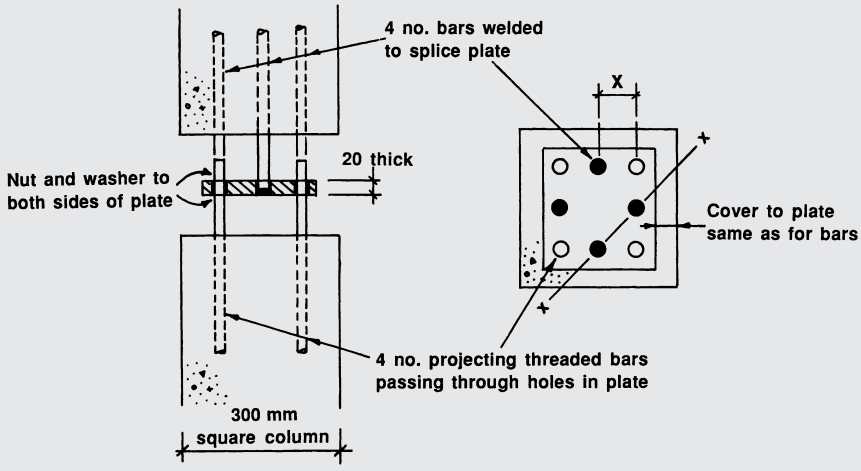

Figure 7.115 Details for Exercise 7.10.

(*Continued*)

$M_R = F_s X/\sqrt{2}$
Hence $F_s = 3209/58.35 = 55\,\text{kN}$
Plate shear capacity $V_R = 165 \times 116.7 \times 20 \times 10^{-3} = 385\,\text{kN}$
Hence $F_s = V_R = 385\,\text{kN} > 55\,\text{kN}$ bending capacity
Ultimate axial capacity of splice $= 4 \times 55 = 220\,\text{kN}$.

Threaded bar $A_s = \dfrac{55 \times 10^3}{0.87 \times 500} = 126.4\,\text{mm}^2$

Use H16 bars ($157\,\text{mm}^2$) threaded to M16.

Welded bar $A_s = \dfrac{55 \times 10^3}{0.87 \times 250} = 252.8\,\text{mm}^2$

Use R20 welded bars ($314\,\text{mm}^2$).

Weld capacity
Use penetration $x = 0.5 \times 20 = 10\,\text{mm}$
Contact area $= \pi \times 20 \times 10 = 628\,\text{mm}^2$
Weld strength $= 628 \times 220 \times 10^{-3} = 138.1\,\text{kN}$ {$628 \times 215 \times 10^{-3} = 135.1\,\text{kN}$} $> 55\,\text{kN}$ required.

Step 2: After concreting
Splice designed as an ordinary rc column

For the welded bars, $d/h = 0.857$
Use $d_2/h = 0.15$, $f'_{cu} = 30$ and $f_{yk} = 250\,\text{N/mm}^2$ (see Fig. 7.127). For maximum eccentricity for 3 m high column $e_i = 20\,\text{mm}$, and $A_s = 1257\,\text{mm}^2$
$N_{Rd}/f_{ck}\,b\,h = 0.57$
$N_{Rd} = 1540\,\text{kN}$
For the threaded bars, $d/h = 0.85$
Use $d_2/h = 0.15$ and $f_{yk} = 500\,\text{N/mm}^2$ and $A_s = 628\,\text{mm}^2$
$N_{Rd}/f_{ck}\,b\,h = 0.57$
$N_{Rd} = 1540\,\text{kN}$
Limiting ultimate axial capacity $= 1540\,\text{kN}$

BS 8110, Part 1, eq. 38 gives
$N = 0.4\,f_{cu}\,A_c + 0.75\,f_y\,A_{sc}$
For the welded bars
$N = (0.4 \times 37 \times 88743 + 0.75 \times 250 \times 1257) \times 10^{-3} = 1548\,\text{kN}$

For the threaded bars
$N = (0.4 \times 37 \times 89372 + 0.75 \times 500 \times 628) \times 10^{-3} = 1437\,\text{kN}$
Capacity of concrete in contact with plate, using $0.8\,f_{cu}$, and ignoring cover concrete
$N = (0.8 \times 37 \times 230^2) \times 10^{-3} = 1565\,\text{kN}$
Limiting ultimate axial capacity $= 1647\,\text{kN}$

Exercise 7.11 Grouted sleeve splice design

Calculate the ultimate moment of resistance of the column splice shown in Figure 7.116, if the maximum and minimum axial force is 1275 kN and 900 kN {1350 kN and 950 kN}, respectively. Determine the anchorage length of the projecting bars.

Use grade C30/37 for *in situ* concrete, f_{yk} {f_y} $= 500\,\text{N/mm}^2$.

Solution
Assume main bars in column are 25 mm dia. and links are 10 mm dia.
For minimum effective depth with splice bar touching inside face of sleeve
$d = 300 - 40\,\text{cover} - (50 - 12.5) = 222.5\,\text{mm}$

$$\frac{d}{h} = \frac{222.5}{300} = 0.742$$

Use $d_2/h = 0.26$ and $A_s = 1963\,\text{mm}^2$ (Fig 7.117)
$A_s\,f_{yk}/f_{ck}\,bh = 0.364$

Use BS 8110, Part 3, Column Chart 21 [7.75].

$$\frac{A_{sc}}{A_c} = \frac{1963 \times 100}{300 \times 300} = 2.02\%$$

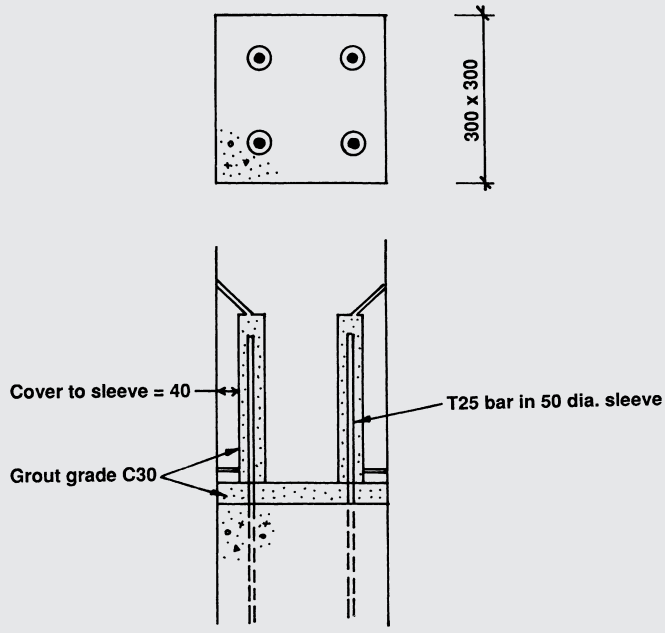

Figure 7.116 Details for Exercise 7.11.

For $\frac{N_{Ed}}{f_{ck}bh} = \frac{1275\times10^3}{30\times300\times300} = 0.472$

$\frac{M_{Rd}}{f_{ck}bh^2} = 0.109$

$M_{Rd} = 0.109 \times 30 \times 300 \times 300^2$ = 88.3 kNm

For $\frac{N}{f_{ck}bh} = \frac{900\times10^3}{30\times300\times300} = 0.333$

$\frac{M_{Rd}}{f_{ck}bh^2} = 0.122$, so not critical

$M_{Rd} = 0.122 \times 30 \times 300 \times 300^2$ = 98.8 kNm

Maximum safe moment capacity is = 88.3 kNm

To determine bond lengths, check stresses in bars.

Axial stress = 14.16 N/mm^2 or 10.00 N/mm^2

Bending stress $= \frac{6M}{bh^2}$ = 19.62 N/mm^2

Therefore not all bars are in compression. Supply all bars with tension bond length.

(See cl. 8.4, figure 8.2) Anchorage bond length for bars in tension. $h > 250$ mm. Casting conditions for top bars = poor

$f_{bd} = 2.25 \times 0.7 \times 1 \times 0.14 \times 30^{2/3}$ = 2.13 N/mm^2

(See cl. 8.4.4.) $l_{bd,req} = 0.25 \times 435 \times 25/2.13 = 1276$ mm

(See cl. 8.4.4., Table 8.2) $\alpha_1 = 1$

$\alpha_2 = 1 - 0.15 \times (65 - 25)/25 = 0.76$

$l_{bd} = 0.76 \times 1276 = 970$ mm

For $\frac{N}{bh} = \frac{1350\times10^3}{300\times300} = 15.0$

$\frac{M}{bh^2} = 3.127$

$M = 3.127\times300\times300^2$ = 84.4 kNm

For $\frac{N}{bh} = \frac{950\times10^3}{300\times300} = 10.56$

$\frac{M}{bh^2} = 3.815$, so not critical

$M = 3.815 \times 300 \times 300^2$ = 103.0 kNm

Maximum safe moment capacity is = 84.4 kNm

To determine bond lengths, check stresses in bars.

Axial stress = 15.00 N/mm^2 or 10.56 N/mm^2

Bending stress $= \frac{6M}{bh^2}$ = 18.76 N/mm^2

Therefore not all bars are in compression. Supply all bars with tension bond length.

Tension bond length for C30/37 concrete = 38 × 25 = 950 mm

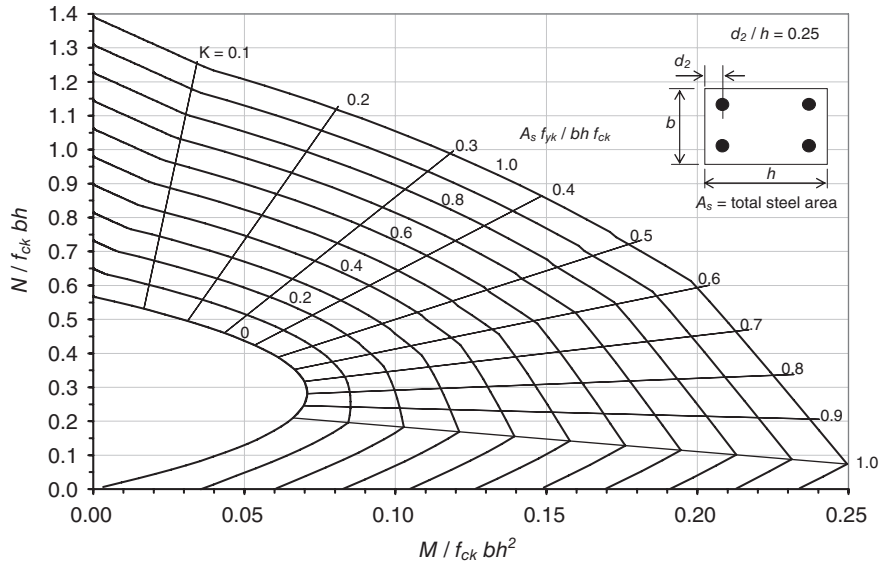

Figure 7.117 Column design chart to BS EN 1992-1-1, used in Exercise 7.11.

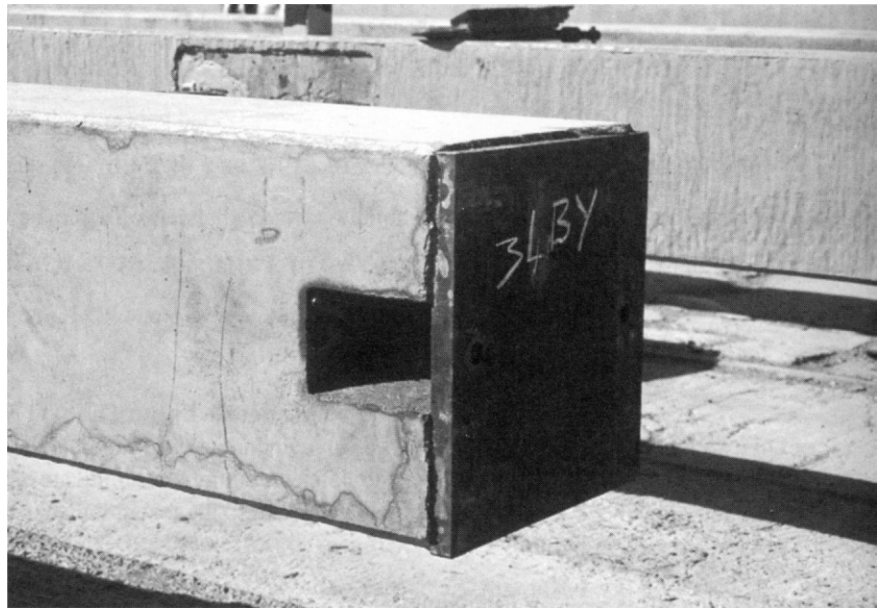

Figure 7.118 Pin-jointed base plate column-to-beam connection.

7.13.9 Columns spliced onto beams or other precast components

Pin-jointed splices are often formed between columns and precast beams, using any of the methods used in column-to-column splicing. The danger is that in unbraced sway frames large torsional moments will be induced in the beam unless the joint is specifically designed to eliminate moment transfer. A pin-jointed version of the grouted sleeve splice is shown in Figure 7.118, where two bolts are used in line to ensure that the connection actually behaves as a pin. Other similar welded or bolted details are easy to envisage.

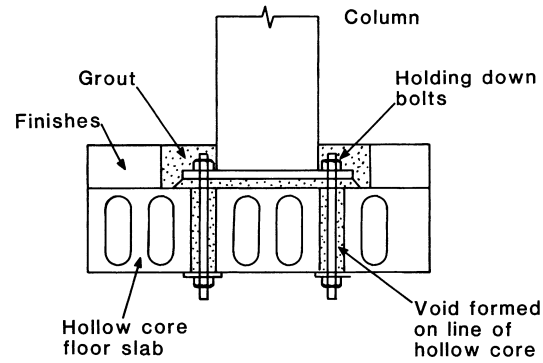

Figure 7.119 Column-to-hollow-core floor slab connection.

Moment-resisting splices may be formed between columns and precast walls and cladding, because the latter is usually capable of accommodating the transfer moment. However, caution must be exercised in assuming these splices will attain their theoretical ultimate design limit. Full-scale testing [7.72] under in-plane loading found that where the faces of the precast components were flush there was extensive cracking and a tendency for the cover to spall on the face of the supporting member, even though the connection was designed as pinned (see figures 33 and 34 in the *IStructE Manual* [7.21]).

Lightly loaded columns have successfully been spliced onto hollow-core flooring units, as shown in Figure 7.119. Although this practice is not entirely endorsed by all precast concrete engineers, there are occasions when, to satisfy an architectural feature almost exclusively at roof level (e.g. a mansard roof), there is no other feasible or practical solution. The column base is assumed pinned because of flexibility in the slab. Holes for holding-down bolts are pre-drilled during manufacture and the tops of the cores are opened to permit the placing of *in situ* concrete as appropriate. The dimensions of the position of the column and base plate are governed in part by the positions of the hollow cores in the finalised floor-slab layout. The maximum point load normally considered is about 50 kN.

Column splices have (very rarely) been formed on double-tee units. The position of the column is restricted to being central over the webs of the flooring units. The joint, which is made by welding or bolting to a base plate, is considered to be a *last resort* in the correct application of precast concrete frame design. However, lightweight steel columns have been spliced onto double-tee units to form a mansard roof or plant-room frame. The maximum point load normally considered is about 75 kN.

7.14 Column Base Connections

Column connections to pad footings and other *in situ* (or precast) concrete foundations (e.g. retaining wall or ground beam) are of three main types:

(1) grouted pocket
(2) base plate; (a) greater or (b) smaller in plan dimension than the dimensions of the column
(3) grouted sleeve.

Methods (1) and (2(a)) are most commonly used. The base plate has the advantage that the column may be stabilised and plumbed vertical by adjusting the level of the nuts on the holding-down bolts. This is particularly important when working in soft ground conditions, where temporary propping alone may not provide adequate stability.

Figure 7.120 Precast pocket foundations are an alternative to site-cast pockets, particularly if the foundations cannot be prepared in time for the installation of the column.

7.14.1 Columns in pockets

7.14.1.1 Basic requirements and principles

Pocket foundations are used for foundations on good soil. The pocket shall be large enough to enable good concrete filling below and around the column. When the inner surfaces of the pocket are smooth the vertical force is assumed to be transmitted directly to the base of the column, and so a depth of at least 300 mm is required beneath the column. If the inner surface is roughened to expose the coarse aggregate, or castellated with a shear key, as shown in Figure 7.120, the vertical force – and bending moments, if the foundation is suitable – are transferred successively by shear friction at the interface using a coefficient of friction which varies from $\mu = 0.3$ to 0.9, depending on the roughness of the surfaces.

Pocket foundations are located either in the centre of fairly large *in situ* concrete pad foundations, mostly isolated, but may be coupled with a ground beam, giving rise to a balanced foundation containing at least two pockets. The pocket may be offset or cantilevered if there are site restrictions. Alternatively, pockets may be partially or completely formed in precast pedestals, as shown in Figure 7.120, with so-called 'sockets'. The main difference between the two is that the wall thickness in the pedestal is narrow, around 175 to 250 mm, and requires careful detailing of reinforcement, whereas the side walls in the cast-*in situ* base are typically more than 500 mm. The gap between the pocket and column is filled using non-shrink concrete of minimum grade C30/37 or, more commonly, a non-shrinkable 2:1 mix of coarse sand (6mm aggregate) and cement grout that develops a strength of about 20 N/mm^2 in 2–3 days to allow the props and wedges to be removed as the precast frame progresses. The specification is often the same as for the grout used in splices. The *in situ* foundation is typically grade C25/30 or C30/37, depending on ground conditions or the contractor's preference.

The column pocket is the most economical solution from a precasting point of view, but its use is restricted to situations where fairly large *in situ* concrete pad footings can easily be constructed. The basic precast column requires only additional links to resist bursting pressures generated by end bearing forces, and a chemical retarding agent is used to enable the aggregate to be exposed in the region of the pocket. In cases where the column reinforcement is in tension, the bars extending into the pocket must be fully anchored by bond or by other means. In order to reduce the depth of the pocket to a manageable size, these bars may need to be hooked at their ends.

The *in situ* concrete foundation is cast using a tapered box shutter to form the pocket, with a taper of 3° to 5°. The taper eases the withdrawal of the formwork and the placement of grout in the annulus.

The gap between the pocket and the column should be at least 50 mm at the bottom and 75 mm at the top of the pocket. The foundation may also be cast integral with, or used to support, precast ground beams.

Vertical loads are transmitted to the foundation by skin friction and end bearing. The precast column requires only additional links at the bottom, say 2–3 H10 at 50 mm spacing, to resist bursting pressures generated by end bearing forces using $\varsigma = 0.075$ {0.11}.

Bending moments and shear forces are transferred to the foundation by forces on opposite faces of the pocket to provide a couple, together with skin friction. Figure 7.121(a) shows a structural model where the column and pocket surfaces are smooth or roughened. If the surfaces are cast from steel or timber formwork, a conservative value of the skin friction, $\mu = 0.3$ (see clause 10.9.6.3(2)), $\{\mu = 0.3\}$ is used, owing to possible cracking in all of the faces of the precast–*in situ* boundary. Exactly what constitutes a 'roughened' surface is never clearly defined in the literature, but we can assume that if the aggregate is exposed, but not damaged, then the surface may be classified as 'rough'. A retarding agent is applied to the moulded surfaces, enabling the laitance to be removed to expose fine and some coarse aggregates. If shear keys (indentations according to the dimensions given in Figure 7.25) are formed in the sides of both the column and pocket, axial load is transferred by the action of shear friction and shear wedging using $\mu = 0.90$; see Figure 7.124.

The failure mode may be by diagonal-tension shear across the corner of the pocket, as shown in Figure 7.121(b), so links must be provided around the top half of the pocket. The pocket taper, inclined at $\theta = 3°$ to 5° to the vertical, gives rise to a wedging force equal to $N \tan\theta$, where N is the ultimate axial load in the column, and a frictional resistance $\mu N \tan\theta$. This is in addition to the horizontal reaction F near the top of the pocket. The total force is in equilibrium with reinforcement in the upper part of the base. Several small links, say three to six H8 to H12, are preferred to larger bars in order to keep the corner bend radii small. Another mode of failure is by flexural and axial crushing of the *in situ* concrete in the annulus. This is guarded against by using an ultimate flexural/bearing stress of $0.85 \times 0.85 f'_{cd} = 0.482 f'_{ck}$ using $\alpha_{cc} = 0.85$ because it is flexural compression bearing $\{0.4 f'_{cu}\}$, working over a width equal only to the precast column, i.e. ignoring load spreading in the third dimension.

The recommended minimum embedment depth l is equal to 1.2 times the depth of column h, even though analysis may suggest values for $l < 1.2h$ for columns with small bending moments. The depth should not be less than h because of the need to develop a diagonal compressive strut in the column to resist shear forces. The most common value is $l = 1.5h$.

Bruggeling and Huyghe [7.61] propose that l is related to the ratio of the moment M and the axial force N as follows:

$$\text{If } M/N < 0.15h, \text{ then } l > 1.2h.$$

$$\text{If } M/N > 2.00h, \text{ then } l > 2.0h. \tag{7.84}$$

Their text [7.61] does not refer to intermediate values, but it is assumed that they may be linearly interpolated.

There is a lack of analytical or experimental data on the real behaviour of pocketed connections in large cast-*in situ* bases, but that is most probably due to an almost total absence of failures. The only research on this topic has been limited to considering the prevention of concrete splitting in the sides of the pocket, particularly where the cover thickness is less than about 200 mm [7.76], and in pockets with narrow side walls [7.77, 7.78].

7.14.1.2 Design methods for pocket foundations

No prescribed design method is given in BS 8110, and so the adopted model shown in Figure 7.122(a) is based on the principles of force and moment equilibrium and practical considerations, such as ignoring (i) poorly compacted, underfilled and unconfined concrete at the top of the pocket, and (ii) friction at the bottom of the pocket where filling voids may exist; there will be little frictional resistance, particularly if ceramic tiles are used to level the column. These are important points of practical

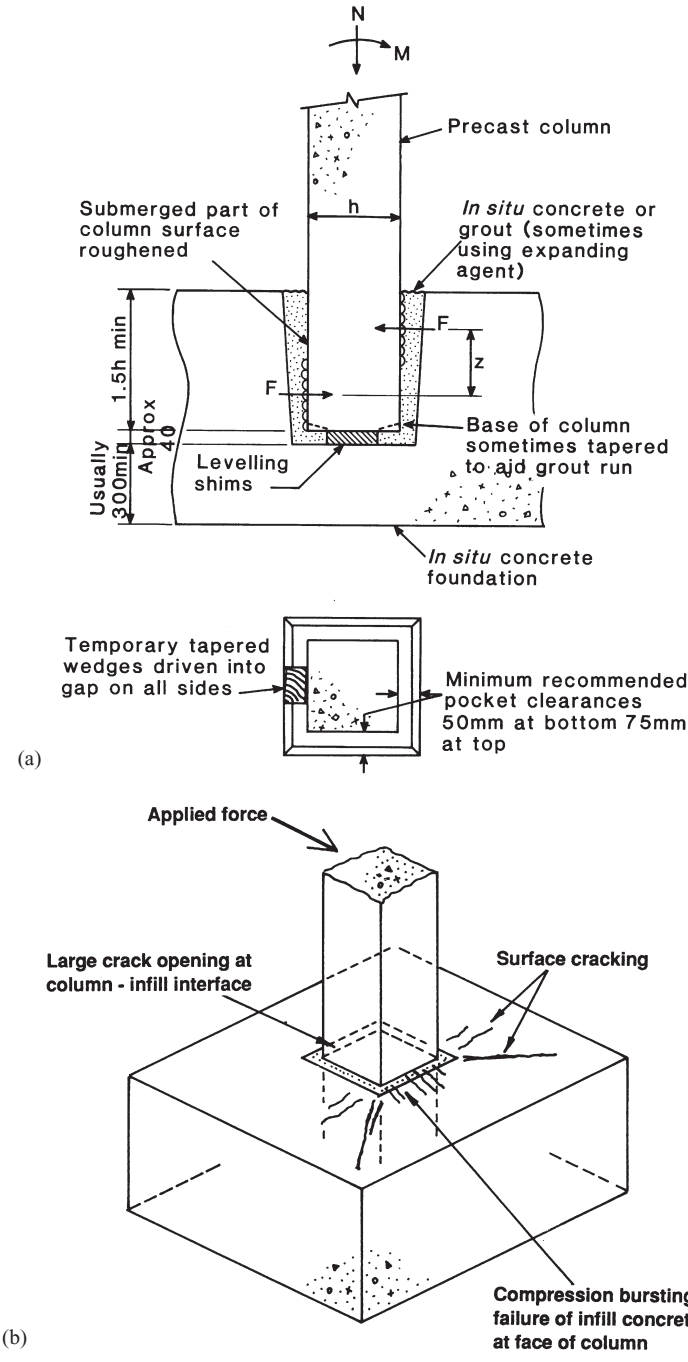

Figure 7.121 Pocket foundations. (a) Structural models in pocket foundations and (b) failure modes in pocket foundations.

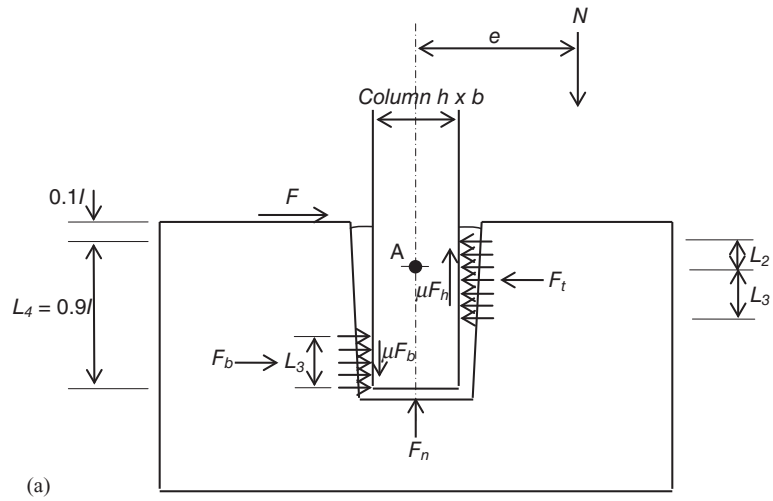

Figure 7.122(a) Pocket foundation model used for BS 8110 design.

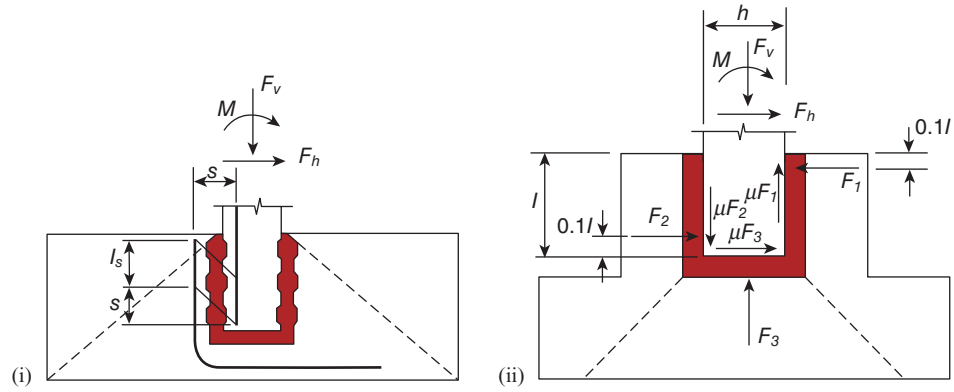

Figure 7.122(b) Pocket foundations as defined in BS EN 1992-1-1, figure 10.7, with (i) keyed joint surface, and (ii) smooth joint surface.

issue, which should not be disregarded in design. However, BS EN 1992-1-1, clause 10.9.6.3 presents the design model reproduced here in Figure 7.122(b), which excludes the aforementioned issues. Pockets with shear keys are designed to act monolithically with the column, thereby requiring full lap lengths between rebars in the column and foundation, with compression struts and ties.

The keyed joint model in Figure 7.122(b)(i) shows the requirement for the depth of embedment $l = l_s + s$, where $l_s = 1.5\ l_{bd}$ is a lap length according to BS EN 1992-1-1, clause 8.7, and the spacing, s = approx. 130 to 170 mm is greater than 50 mm or 4 × bar diameters (clause 8.7(3)). If the bars are fully stressed in tension $f_{yk} = 500\ \text{N/mm}^2$ and $f_{ck} = 30\ \text{N/mm}^2$, then $l \approx 45\phi + 150 \approx 1275$ mm for H25 bars, or 1590 mm for H32 bars – clearly impractical solutions for straight bars without hooks or bends. Transverse reinforcement for the lapped splice is provided by the links around the pocket.

For smooth/rough pockets, shown in Figure 7.122(b)(ii), the column bars should extend for one design anchorage bond length l_{bd} (typically 35 × bar diameter) and, for the same practical reasons as given above, starts 50 mm below the top of the pocket. If the area of rebar provided is greater than required, the actual tensile (or compressive) stress in the bars is calculated and a reduced bond length according to BS EN 1992-1-1, clause 8.4.2 [7.8] or BS 8110, clause 3.12.8.3 [7.9] is provided pro rata

to the full bond length. The designer also has the choice of either making the depth of the pocket relatively large with straight bars, or providing a bend or hook to the bars and making the pocket shallower. This may roughly halve the depth of the pocket. The minimum bond length, and hence pocket depth, must not be less than 12 bar diameters.

The ultimate moment M and axial force N may be resolved into a single force acting at a distance $e = M/N$ from the centre line of the column. The horizontal shear force F is effective a short distance below the top of the pocket, owing to the curvature of the column as it enters the pocket, but is assumed to act level with the top. The depth of the column is defined in the plane of bending = h and the breadth = b.

The analysis is for rectangular columns and uniaxial bending only. There is no method in BS EN 1992-1-1 {BS 8110} for dealing with biaxial bending, but the method for dealing with biaxial bending in columns may be adopted here, i.e. a separate design in each principal direction may be made to BS EN 1992-1-1, clause 5.8.9(2) provided that the relative eccentricities to clause 5.8.9(3) are satisfied, and an increased moment in the critical direction is considered as a uniaxial moment to BS 8110.

7.14.1.2(a) BS EN 1992-1-1 design

In this method the positions of the compressive reactions F_1 and F_2 between the column and foundation are assumed at $0.1l$ from the top and bottom of the pocket, respectively. The depth of the compressive stress areas is therefore $0.2l$ and, based on the limiting bearing stress of the infill grout $0.482 f'_{ck}$, the design fails when the line stress $0.482 f'_{ck} b$ is exceeded. The coefficient of friction $\mu = 0.3$.

Referring to Figure 7.123, resolving horizontally for the ultimate shear force F_{Ed}

$$F_{Ed} = F_1 - F_2 - \mu F_3 \tag{7.90-a}$$

Resolving vertically

$$F_3 = N_{Ed} - \mu F_1 + \mu F_2 \tag{7.90-b}$$

Combining equations (7.90-a) and (7.90-b)

$$F_3 = (N_{Ed} - \mu F_{Ed}) / 1 + \mu^2 \tag{7.90-c}$$

Check the grout strength that the resultant $\sqrt{(F_3^2 + mF_3^2)} \leq 0.482 f'_{ck} bh$.

Taking moments about the resultant F_2 at point A:

$$N_{Ed}(e + 0.5h) + 0.9F_{Ed}l - F_3(0.5h + \mu 0.1l) = F_1(0.8l + \mu h) \tag{7.90-d}$$

from which $F_1 > F_2$ may be calculated. The required compressive strength of the infill grout is:

$$f'_{ck} \geq F_1/0.482b, \text{ where } b = \text{column breadth} \tag{7.90-e}$$

The compression area at the interface of the infill grout and the *in situ* foundation is similarly checked using the breadth of the annulus at the top $b_p = b + 2 \times$ annulus, typically 75 to 100 mm. The required compressive strength of the foundation is unlikely to be critical, but is:

$$f_{ck(i)} \geq F_1/0.482b_p \tag{7.90-f}$$

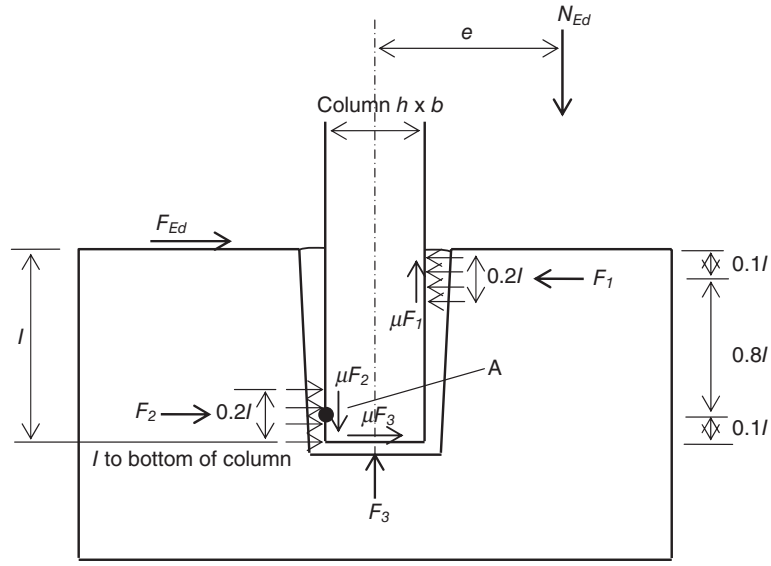

Figure 7.123 Pocket foundation model used for BS EN 1992-1-1 design.

7.14.1.2(b) BS 8110 design

In this method the positions and magnitude of the compressive reactions between the column and foundation are determined from the equilibrium or design forces and moments, based on the limiting bearing stress of the infill grout $0.4f'_{cu}$. The design fails if the calculated compression areas overlap or otherwise exceed the available depth of the pocket.

Let the embedment length = l'; then $L_4 = 0.9l$, as the top $0.1l$ of the pocket is ignored within the cover zone, typically 50 mm, to allow for underfilling, settlement, local shrinkage cracking and possible poor-quality infill. The moment is transferred to the foundation by a set of compressive struts as the resultant of:

(i) horizontal reaction forces in the top $F_t = p(L_2 + L_3)$ and at the bottom $F_b = pL_3$, where the line stress (N/mm units) $p = 0.4f'_{cu}b$

(ii) vertical frictional resistances μF_t and μF_b in opposing directions. The coefficient of friction $\mu = 0.35$

(iii) a vertical reaction force F_n at the base of the column.

The force F_t is distributed to the foundation using horizontal links, and particular attention should be paid to this if the edge cover is less than the smaller dimension of the column. A compressive strut develops at the sides of the column, at a gradient of about 45° vertically, connecting the reaction from links to the bottom corner of the pocket, which also spreads away from the pocket and dissipates stresses quickly. Only the local stresses acting before spreading need to be checked.

Referring to Figure 7.122, and considering the line stress $p = 0.4f'_{cu}b$, resolving horizontally

$$H = p(L_2 + L_3) - pL_3 \tag{7.85}$$

$$L_2 = H/p \tag{7.86}$$

where L_2 is measured from a point located 0.1 D from the top of the pocket.

Resolving vertically:

$$F_n = N - \mu p(L_2 + L_3) - \mu pL_3 = N - \mu pL_2 \tag{7.87}$$

Combining equations (7.86) and (7.87):

$$F_n = N - \mu H \tag{7.88}$$

Check that the grout strength $F_n \leq 0.4 f'_{cu} bh$.

Taking moments about the centre line of the column at the end of L_2 at point A:

$$Ne + H(0.1l + 0.5L_2) = pL_3(L_4 - L_2 - L_3) + \mu p(L_2 + 2L_3)0.5h$$

$$\therefore L_3^2 - (L_4 - L_2 + \mu h)L_3 + (Ne + H(0.1l + 0.5L_2) - 0.5\mu pL_2 h)/\mathrm{p} = 0 \tag{7.89}$$

from which L_3 may be calculated for real roots to the quadratic only. Note $0.1L$ is replaced by the cover to the top rebars if this is smaller. The stresses resisting the moment may not overlap on the interface (Section 7.10.2), such that $L_2 + 2L_3 \leq 0.9\ L_4$. Then:

$$F_t = p(L_2 + L_3), \text{ and } F_b = pL_3 \tag{7.90}$$

The analysis should be repeated for the line pressure acting beyond the column face at the interface of the annulus and the foundation, where breadth of the annulus $b_p = b + 2 \times$ annulus, typically 75 to 100 mm, e.g. $b_p = 300 + 2 \times 100 = 500$ mm. This is unlikely to be critical unless the strength of the foundation concrete is particularly low, as the foundation concrete (unlike the infill) contains confinement links around the top of the pocket.

The mode of action for smaller values of $M/N < 0.15h$ in shallow pockets will inevitably change from the above models where skin friction underneath the column will dominate more. In reality the skin friction will also act over the sides of the column parallel to the direction of the moment, and so Eq. (7.90) will be conservative in the presence of large axial forces and small moments.

7.14.1.2(c) Common aspects to pocket design

The area of the links at the top of the pocket is:

$$A_{sh} = F_l/0.87 f_{yk} \quad \{A_{sh} = F_t/0.87 f_y\} \tag{7.91}$$

The compressive strut through the side walls $F_c = \sqrt{2} F_l$ $\{F_c = \sqrt{2} F_t\}$. If the breadth of the *in situ* concrete side walls is t, the width of the compressive strut, idealised as prismatic is:

$$w = \sqrt{2} F_l/0.482 f_{ck(i)} t \quad \{w = \sqrt{2} F_t/0.4 f_{cu(i)} t\} \tag{7.92}$$

The horizontal projection of w down the side wall should not exceed half the depth of the pocket.

If the pocket is tapered at an angle θ to the vertical, lateral forces $N \tan\theta$ will act on the foundation (not the grouted annulus) on either side over the depth of the pocket. The true extent of this diminishing force down the pocket is not known, and so it is assumed to act over the top half. This will generate a frictional resistance $\mu N_{Ed} \tan\theta$ $\{\mu N \tan\theta\}$ acting on both sides of the foundation. Thus, the vertical equilibrium will become

$$F_3 = (N_{Ed} - 2\mu N_{Ed} \tan\theta - \mu F_{Ed})/1 + \mu^2 \quad \{F_n = N - 2\mu N \tan\theta - \mu H\} \tag{7.93}$$

Moment equilibrium is unaffected, because $\mu N \tan\theta$ is symmetrical. However, the area of the rebars across the top of the pocket will become:

$$A_{sh} = (F_l + \mu N_{Ed} \tan\theta)/0.87 f_{yk} \quad \{A_{sh} = (F_t + \mu N \tan\theta)/0.87 f_y\} \tag{7.94}$$

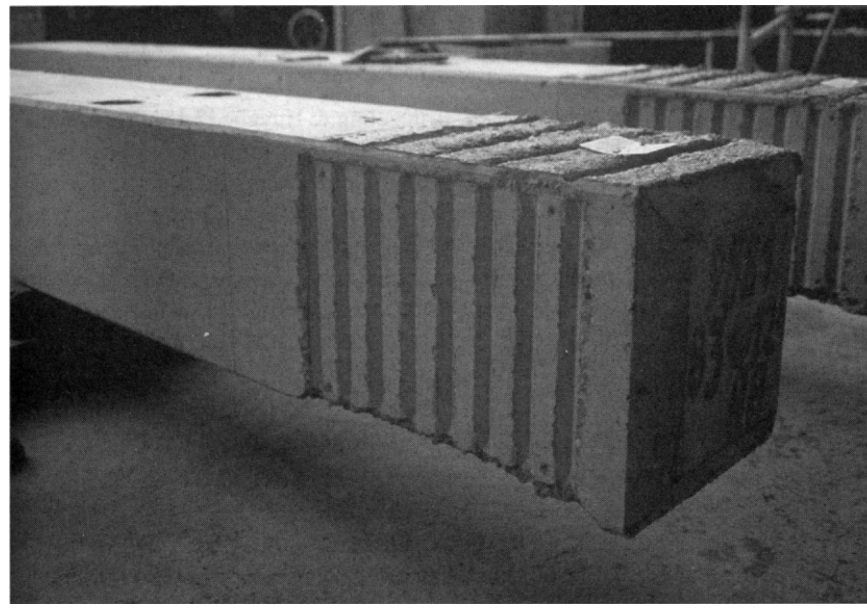

Figure 7.124 Castellations in column sides for pocket foundations.

The size of the pad foundation is governed by two main factors:

- bearing pressures at service conditions
- edge distance at top of pocket.

See Figure 7.121. The first is checked using any statical method, in order to avoid uplifting grouting pressures. The second is based on half the horizontal force in the top 0.5 F_1 {0.5 F_t} acting over the concrete on the same stress depth at the top of the pocket. If the effective depth from the pocket to the edge of the foundation is d_f, then the condition is satisfied if:

$$0.5F_1 \leq v_c 0.2ld_f \quad \{0.2f'_{cu}(L_2 + L_3) \leq v_c(L_2 + L_3)d_f\} \tag{7.95}$$

where v_c = shear stress of concrete.

7.14.1.3 Precast concrete pockets

Precast concrete pockets, e.g. Figure 7.125, have not been successful from a commercial viewpoint. This is because of the dual effort of preparing a level *in situ* concrete pad on which the precast foundation may sit, and afterwards bedding-in the pocket onto the pad. The precast pocket alone provides a pin-jointed foundation connection and may be used only in conditions of firm and level ground. This obviously rules out foundations onto pile caps, or on soft reclaimed land. One notable advantage of a precast pocket is that the reaction forces F_1 and F_3 {F_t and F_n} are resisted by high-strength precast concrete, say C40/50, whereas an *in situ* pocket may be limited by the strength of the *in situ* concrete, say C25/30.

For moment-resisting precast pockets, precast pedestals are designed with narrow walls and completed on site using *in situ* backfill and sometimes an integral ground beam, and are as analysed in Section 7.14.2.

Figure 7.125 Precast concrete pocket foundation.

Exercise 7.12 Column pocket design

Design a column-to-pocket foundation connection required to support a 300 × 300 mm column subjected to an ultimate axial force of $N = 950$ kN {$N = 1000$ kN} and a moment $M = 95$ kNm {$M = 100$ kNm}. The pocket has a 5° taper.

Use grade C40/50 concrete for the precast column, grade C30/37 for *in situ* infill, and grade C20/25 for the foundation, with f_{yk} {f_y} = 500 N/mm^2 for the reinforcement. Cover to column reinforcement = 35 mm, and cover to foundation reinforcement = 50 mm.

Solution

Step 1: Column main steel and concrete design

$e = 100 \times 10^3/1000 = 100$ mm $= h/3$, hence tension will develop in the column reinforcement.

Assume 16 mm dia. main bars and 10 mm dia. links. $D = 300 - 35 - 10 - 16/2 = 247$ mm

Column design: $d_2/h = 0.176$, use BS EN 1992-1-1 derived column design chart $d_2/h = 0.2$.
$N/bhf_{ck} = 0.264$ and $M/bh^2f_{ck} = 0.088$
$\therefore A_{sc} = 0.08\ bhf_{ck}/f_{yk} = 576$ mm^2
Use four H16 (804 mm^2) with H8 links at 175 mm centres.
Actual stress in bars
$= (576/804) \times 0.87 \times 500$
$= 312$ N/mm^2

Column design: $d/h = 247/300 = 0.823$
Use BS 8110 derived column design, equivalent to Part 3, Chart 47 [7.75].
$N/bh = 11.11$, and $M/bh^2 = 3.704$.
$\therefore A_{sc} = 0.728\%\ bh$ $= 655$ mm^2
Use four H16 (804 mm^2) with H8 links at 175 mm centres.
Actual stress in bars
$= (655/804) \times 0.87 \times 500$
$= 354$ N/mm^2

(cl.8.4, figure 8.2) Anchorage bond length for bars in tension. $h > 250$ mm.
Casting conditions for top bars = poor
$f_{bd} = 2.25 \times 0.7 \times 1 \times 0.14 \times 40^{2/3}$
$= 2.58\ \text{N/mm}^2$
(See cl. 8.4.4.) $l_{bd,req} = 0.25 \times 312 \times 16/2.58$
$= 484$ mm
(See cl. 8.4.4., Table 8.2) $\alpha_1 = 1$
$\alpha_2 = 1 - 0.15 \times (45 - 16)/16 = 0.728$
$l_{bd} = 0.728 \times 484 = 352$ mm
Hence $l = 50 + 352 + 35$ cover $= 437$, say 450 mm.
$\mu = 0.3$, $h = 0.3$ m, $e = 0.1$ m
(7.90 − c) $F_3 = 950/1.09 = 872.0$ kN
$\text{Resultant} = \sqrt{872.0^2 + 261.6^2} = 910.0$ kN
$f'_{ck} \geq 910.0 \times 10^3/(300^2 \times 0.482)$
$= 21.0 < 30\ \text{N/mm}^2$ provided.
(7.90-d) $F_1 = (950 \times 0.25 - 872 \times 0.1635)/0.45$
$= \underline{211.0\ \text{kN}}$
$f'_{ck} \geq 211 \times 10^3/(0.2 \times 450 \times 300 \times 0.482)$
$= 16.2 < 30\ \text{N/mm}^2$ provided.

Anchorage bond length for bars in tension $= 0.25 \times 354 \times 16/3.535$
$= 401$ mm
Hence $l = 50 + 401 + 35$ cover
$= 486$, say 500 mm
Then: $L_4 = \max(0.9 \times 500;$
$500 - 50) = 450$ mm
$p = 0.4 \times 37 \times 300 = 4400$ N/mm
$\mu = 0.35$, $h = 0.3$ m
(7.90-c) $L_3^2 - 0.555L_3 + 0.0227 = 0$
$L_3 = 45$ mm
$F_1 = 4400 \times 0.045 = \underline{198.0\ \text{kN}}$

Step 2: Column confinement steel

Using lowest value $F_{bst} = 0.075 \times 950$ $= 71.3$ kN
$A_{bst} = \dfrac{71.3 \times 10^3}{0.87 \times 500}$ per 2 legs $= 164\ \text{mm}^2$
Use two H8 ($200\ \text{mm}^2$) links at 50 mm centres.

Using lowest value $F_{bst} = 0.11 \times 1000$ $= 110$ kN
$A_{bst} = \dfrac{110 \times 10^3}{0.87 \times 500}$ $= 253\ \text{mm}^2$
Use three H8 ($300\ \text{mm}^2$) links at 50 mm centres.

Step 3: Reinforcement around foundation pocket

Bars to be placed in upper half of pocket, i.e. to a depth of 225 mm.
Horizontal force induced by taper
$= 950 \tan 5° = 83.1$ kN
Horizontal steel
$A_{sw} = \dfrac{(83.1 + 210.0) \times 10^3}{0.87 \times 500}$ $= 674\ \text{mm}^2$

Bars to be placed in upper half of pocket, i.e. to a depth of 250 mm.
Horizontal force induced by taper
$= 1000 \tan 5° = 87.5$ kN
Horizontal steel
$A_{sv} = \dfrac{(87.5 + 198.0) \times 10^3}{0.87 \times 500}$ $= 656\ \text{mm}^2$

Use three H12 ($678\ \text{mm}^2$) links at 75 mm centres around pocket.
Also provide nominal vertical hanger bars to support confinement links, three H10 bars.
See Figure 7.126 for final details.

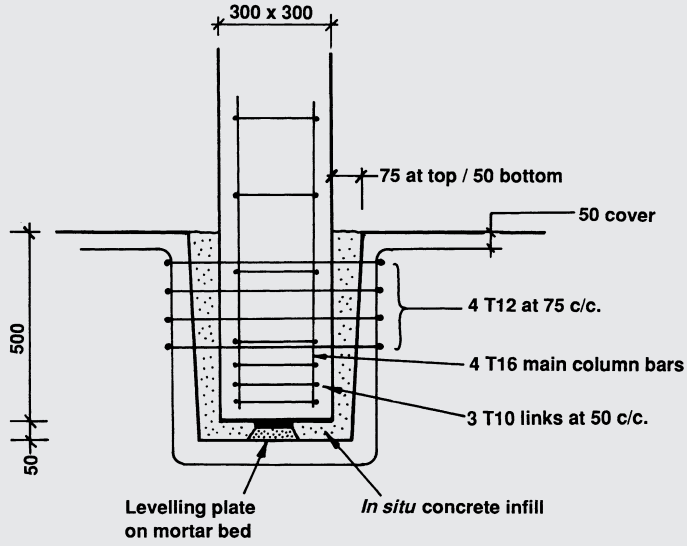

Figure 7.126 Details for Exercise 7.12.

Exercise 7.13 Moment-resisting column pocket design

A 400 × 300 mm column, with its major axis x–x aligned with the maximum moment, is subjected to the following ultimate loads and moments. Axial load $N = 475$ kN $\{N_{Ed} = 500$ kN$\}$, bending moments $M_{Ed,x\text{-}x} = 240$ kNm $\{M_{x\text{-}x} = 250$ kNm$\}$ and $M_{Ed,y\text{-}y}$ $\{M_{y\text{-}y}\} = 50$ kNm, and shear forces $H_{Ed,x\text{-}x}$ $\{H_{x\text{-}x}\} = 60$ kN. Calculate the minimum depth of pocket foundation, and the size of the pad foundation if the ground bearing pressure = 250 kN/m^2 and there is no uplift. Assume that the ultimate loads given above are based on $\gamma_f = 1.2$. Determine the reinforcement required in the column, around the pocket and in the bottom of the pad foundation. The pocket has a 5° taper.

Use grade C40/50 concrete for the precast column, grade C30/37 for *in situ* infill, and grade C20/25 for the foundation, with f_{yk} $\{f_y\} = 500$ N/mm^2 for the reinforcement. Cover to column reinforcement = 35 mm, and cover to foundation reinforcement = 50 mm.

Solution

Step 1: Column reinforcement design

Assume 25 mm dia. main foundation bars and 10 mm dia. links.

$h' = 400 - 35 - 10 - 25/2 = 342.5$ mm

$b' = 300 - 35 - 10 - 25.2 = 242.5$ mm

$M_{x-x}/h' > M_{y-y}/b'$

See cl. 5.8.9(3) $e_z/b_{eq}/e_y/h_{eq} = 0.156 < 0.2$, use separate moments.

Major axis $d/h = 342.4/400 = 0.856$

Use $d_2/h = 0.15$ (Fig. 7.127)

$$\frac{N}{f_{ck}bh} = \frac{475\times10^3}{40\times300\times400} = 0.1$$

$$\frac{M_{max}}{f_{ck}bh^2} = \frac{240\times10^6}{40\times300\times400^2} = 0.125$$

$A_{s,max} = 0.28 \times 300 \times 400 \times 40/500$
$= 2688$ mm^2

$N/f_{cu}\, b\, h = 0.083$, so

$\beta = 0.9$ (BS 8110, Part 1, Table 3.24)

Then $M'_{x-x} = 250 + \dfrac{0.9\times342.5\times50}{242.5} = 313.6$ kNm

$d = 342.5$ mm

$d/h = 0.856$. Use Chart 48.

Then $\dfrac{M_{x-x}}{bh^2} = 6.53$ and $\dfrac{N}{bh} = 4.17$

Then $A_{sc} = 3.12$ % $= 3744$ mm^2

Use eight H25 bars (3927 mm^2).

Minor axis $d/b = 242.5/300 = 0.808$
Use $d_2/b = 0.20$ (Fig. 4.53)

$$\frac{M_{min}}{f_{ck}hb^2} = \frac{50\times10^6}{40\times400\times300^2} = 0.035$$

$A_{s,min}$ = zero. Provide 0.2% = 240 mm^2
Total A_s required = 2928 mm^2
Use eight H25 bars (3927 mm^2)
Major axis provision pro rata = 3605 mm^2, keeping $N/f_{ck}bh = 0.1$, allows $M_{max}/f_{ck}bh^2 \approx 0.16$ giving M = 308 kNm
Minor axis provision A_s = 322 mm^2
allows $M_{min}/f_{ck}hb^2 \approx 0.055$ giving M = 79 kNm.
Check clause 5.8.9(4)

$$\left(\frac{240}{308}\right)^2 + \left(\frac{50}{79}\right)^2 = 1.01 \approx 1$$

Continue with fully stressed bars ($0.87 \times 500 = 435$ N/mm^2) and use the equivalent major axis moment = 308 kNm.
$f_{bd} = 2.25 \times 0.14 \times 40^{2/3} = 3.68$ N/mm^2
(See cl. 8.4.4.) $l_{bd,req} = 0.25 \times 435 \times 25/3.68 = 739$ mm
(See cl. 8.4.4., Table 8.2) $\alpha_1 = 1$
$\alpha_2 = 1 - 0.15 \times (45 - 25)/25 = 0.88$
$l_{bd} = 0.88 \times 739 = 650$ mm
Hence $l = 50 + 650 + 35$ cover = 735, say 750 mm.
Bruggeling's function for $e/h = 308 \times 10^3/475 \times 400 = 1.62$, by interpolation gives $l = 1.84h = 736$ mm < 750 mm.

Calculation of reaction F_1

$\mu = 0.3$, $h = 0.4$ m, $e = 0.65$ m
Then: (7.90-c) $F_3 = (475 - 0.3 \times 60)/1.09 = 457.0$ kN

$$\text{Resultant} = \sqrt{457.0^2 + 137.1^2} = 477.0 \text{ kN}$$

$$f'_{ck} \geq 477.0\times10^3/(300\times400\times0.482)$$

$= 8.3 < 30$ N/mm^2 provided.
(7.90-d) $F_1 = (475 \times 0.85 + 60 \times 0.675 - 457 \times 0.2225)/0.72 = \underline{475.8 \text{ kN}}$

$$f'_{ck} \geq 475.8\times10^3/(0.2\times750\times300\times0.482)$$

$= 21.9 < 30$ N/mm^2 provided.
Maximum shear stress at top of pocket

$$= 0.5\times0.6\left(1-\frac{20}{250}\right)\frac{20}{1.5} = 3.68 \text{ N/mm}^2$$

$$d_f = \frac{475.8\times10^3}{2\times150\times3.68} = 431 \text{ mm}$$

Total edge distance = 431 + 50 cover = 481 mm
Compressive strut $F_c = \sqrt{2}\times475.8$ = 672.8 kN
Strut width $w = 672.8 \times 10^3/(2 \times 481 \times 0.482 \times 20)$ = 73 mm, OK

Actual stress in bars = $(3744/3927) \times 0.87 \times 500$ = 415 N/mm^2
Anchorage bond length for bars in tension = $0.25 \times 415 \times 25/3.535$ = 734 mm.
Hence l = 50 + 734 + 35 cover = 819, say 850 mm.
Bruggeling's function for $e/h = 313.6 \times 10^3/500 \times 400 = 1.57$, by interpolation gives $l = 1.81h = 724$ mm < 850 mm.

Calculation of reaction F_t

$F_n = 500 - 0.3 \times 60 = 482.0$ kN
Line pressure in *in situ* infill
$= 0.4 \times 37 \times 300 = 4440$ N/mm
$L_2 = 60 \times 10^3/4440 = 13$ mm
$L_4 = \max(0.9 \times 850; 850 - 50) = 800$ mm
(7.90-b) $L_3^2 - 0.907L_3 + ((313.6 + 60\times0.0565 - 3.4)/4440) = 0$
Hence $L_3 = 86$ mm
$L_2 + 2\ L_3 = 185 < 0.9\ L_4 = 720$ mm
$F_t = 4440 \times (0.086 + 0.013) = \underline{439.6 \text{ kN}}$

Maximum shear stress at top of pocket

$$= 0.8\sqrt{f_{cu}} = 0.8\sqrt{25} = 4.00 \text{ N/mm}^2$$

Then $d_f = \dfrac{439.6\times10^3}{2\times99\times4.00} = 555$ mm
Total edge distance = 555 + 50 cover = 605 mm
Compressive strut $F_c = \sqrt{2}\times439.6$ = 621.6 kN
Strut width $w = 621.6 \times 10^3/(2 \times 605 \times 0.4 \times 25)$ = 52 mm, OK

(*Continued*)

Step 2: Perimeter bursting steel in foundation around pocket

Bars to be placed in upper half of pocket, i.e. to a depth of < 500 mm.

Horizontal force induced by taper
= 475 tan 5° = 41.6 kN
Force across pocket = 475.8 + 41.6 = 517.4 kN
Horizontal steel

$$A_{sv} = \frac{517.4 \times 10^3}{0.87 \times 500} \text{ per 2 legs} = 1190\,\text{mm}^2$$

Use six H10 (1356 mm^2) links at 70 mm centres around pocket.
Also provide vertical hanger bars to support confinement links, nominally three H10 bars.

Horizontal force induced by taper
= 500 tan 5° = 43.7 kN
Force across pocket = 439.6 + 43.7 = 483.3 kN
Horizontal steel

$$A_{sv} = \frac{483.3 \times 10^3}{0.87 \times 500} \text{ per 2 legs} = 1111\,\text{mm}^2$$

Use five H12 (1130 mm^2) links at 80 mm centres around pocket.
Also provide vertical hanger bars to support confinement links, nominally three H10 bars.

Step 3: Base size

Gap at top of pocket = 50 + 750 tan 5°
= 115.6 mm, say 115 mm
$B = 2 \times 481 + 2 \times 115 + 300 = 1492$ mm.
This is found to be too narrow and gives a base length of about 4 m. Thus use $B = 1800$ mm.
Depth of foundation
= 750 + 50 + 300 = 1100 mm
Base self-weight bearing
pressure = 25 × 1.100 = 27.5 kN/m^2
Net bearing pressure = 250 − 27.5
= 222.5 kN/m^2
Length of base H from the following at the front corner:

$$\frac{N}{BH} + \frac{6M_{x-x}}{BH^2} + \frac{6M_{y-y}}{HB^2} \le 222.5\,\text{kN/m}^2$$

where $N = 475/1.2 = 395.8$ kN
$M_{x\text{-}x} = (240 + 60 \times 1.1)/1.2 = 255.0$ kNm
$M_{y\text{-}y} = 50/1.2 = 41.7$ kNm
From which $H \ge 2.73$ m
And to prevent uplift at the rear corner:

$$\frac{N}{BH} - \frac{6M_{x-x}}{BH^2} - \frac{6M_{y-y}}{HB^2} \ge -27.5$$

From which $H \ge 3.541$ m
Use B × H = 1.80 × 3.55 m.
Maximum and minimum bearing stresses, including self-weight of base
= +178.6 kN/m^2 (<250) and +0.2 kN/m^2 (>0)

Gap at top of pocket = 50 + 850 tan5°
= 124.4 mm, say 125 mm
$B = 2 \times 605 + 2 \times 125 + 300 = 1760$, say 1800 mm

Depth of foundation
= 850 + 50 + 300 = 1200 mm
Base self-weight bearing
pressure = 24 × 1.200 = 28.8 kN/m^2
Net bearing pressure = 250 − 28.8
= 221.2 kN/m^2
Length of base H from the following at the front corner:

$$\frac{N}{BH} + \frac{6M_{x-x}}{BH^2} + \frac{6M_{y-y}}{HB^2} \le 221.2\,\text{kN/m}^2$$

where $N = 500/1.2 = 416.7$ kN
$M_{x\text{-}x} = (250 + 60 \times 1.2)/1.2 = 268.3$ kNm
$M_{y\text{-}y} = 50/1.2 = 41.7$ kNm
From which $H \ge 2.83$ m
And to prevent uplift at the rear corner:

$$\frac{N}{BH} - \frac{6M_{x-x}}{BH^2} - \frac{6M_{y-y}}{HB^2} \ge -28.8$$

From which $H \ge 3.50$ m
Use B × H = 1.80 × 3.50 m.
Maximum and minimum bearing stresses, including self-weight of base
= +190.0 kN/m^2 (<250) and 0 kN/m^2

Step 4: Reinforcement in bottom of base

Taking moments $M_{z\text{-}z}$ across face of column, lever arm $l_x = (H - 400)/2$

Considering bending about major x–x axis, where net pressure excludes self-weight of base:

$p_{max} = N/BH + 6M_{x-x}/BH^2 + 6M_{y-y}/HB^2$

$p_{min} = N/BH - 6M_{x-x}/BH^2 + 6M_{y-y}/HB^2$

$l_x = 1.575\,\text{m}$

$p_{max} = 151.1\,\text{kN/m}^2$

$p_{min} = 16.2\,\text{kN/m}^2$

$p_{z\text{-}z} = 91.3\,\text{kN/m}^2$

$$M_{z-z} = \frac{91.3\times1.8\times1.575^2}{2} + \frac{59.8}{2} \times \frac{2}{3}\times1.8\times1.575^2 = 292.9\,\text{kNm}$$

$M_{Ed,z\text{-}z} = 1.2 \times 292.9 = 351.5\,\text{kNm}$

$d = 1100 - 50\ \text{cover} - 16/2 = 1042\,\text{mm}$

$$k = \frac{351.5\times10^6}{20\times1800\times1042^2} = 0.009$$

$z = 0.95 \times 1042 = 990\,\text{mm}$

$$A_s = \frac{351.5\times10^6}{0.87\times500\times990} = 816\,\text{mm}^2$$

Use six H16 at 340 centres (1206 mm^2) in bottom of base.

See Figure 7.128 for final details.

$l_x = 1.55\,\text{m}$

$p_{max} = 161.2\,\text{kN/m}^2$

$p_{min} = 15.2\,\text{kN/m}^2$

$p_{z\text{-}z} = 96.55\,\text{kN/m}^2$

$$M_{z-z} = \frac{96.55\times1.8\times1.55^2}{2} + \frac{64.66}{2}\times\frac{2}{3}\times1.8\times1.55^2 = 302.0\,\text{kNm}$$

Then $M_{u,z\text{-}z} = 1.2 \times 302.0 = 362.4\,\text{kNm}$

$d = 1200 - 50\ \text{cover} - 16/2 = 1142\,\text{mm}$

$$k = \frac{362.4\times10^6}{25\times1800\times1142^2} = 0.00618$$

$z = 0.95 \times 1142 = 1085\,\text{mm}$

$$A_s = \frac{362.4\times10^6}{0.87\times500\times1085} = 768\,\text{mm}^2$$

Use six H16 at 340 centres (1206 mm^2) in bottom of base.

See Figure 7.128 for final details.

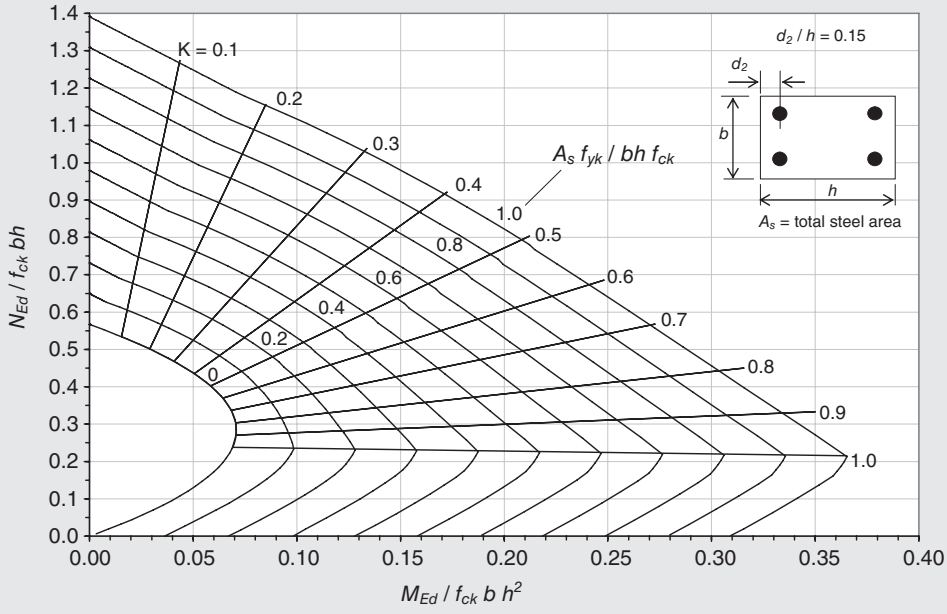

Figure 7.127 Column design chart to BS EN 1992-1-1, used in Exercises 7.13 and 7.10.

(*Continued*)

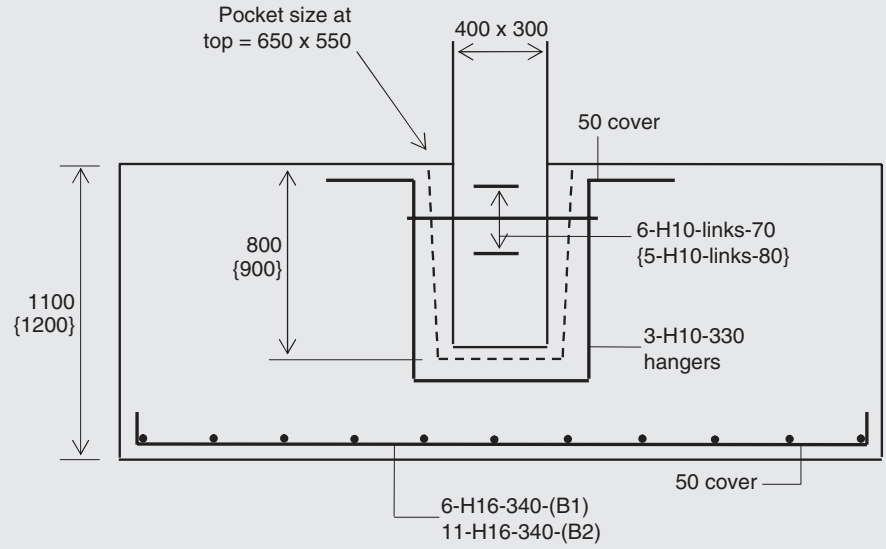

Figure 7.128 Reinforcement details for Exercise 7.13 {BS 8110 solution in brackets}.

7.14.1.4 Columns in pedestal sockets

Canha *et al.* [7.77] studied precast columns founded into pockets (or called 'sockets') in precast concrete pedestals, of the type shown in Figure 7.120, in order to determine the horizontal reactions, and hence design the reinforcement, in the pedestal walls as defined in Figure 7.129. The analysis is similar to that of pockets in mass foundations, up to the point where reinforcement is designed using a 45° strut, and vertical and horizontal ties in the pedestal walls. Using full-scale tests, subjecting 400×400 mm columns in keyed pockets of depth $1.6h$ to $2.0h$ (h = column depth) to combined axial force N_d, bending moment M_d and shear force V_d, failure loads were compared to the design methods given in the literature and in this textbook. The mean ratio of the failure load in the seven tests to the proposed analysis was 1.35 (minimum 1.25), which is acceptable.

Canha's analysis differs relative to the design method in Section 7.14.1, as follows:

(i) Reaction stresses are carried to the top of the *in situ* infill, where there is no allowance for underfilling, settlement, local shrinkage cracking and generally poor-quality infill in the top 20–30 mm.

(ii) The centroid of the bottom and top horizontal reactions H_B and H_T was based on a triangular concrete stress distribution, rather than rectangular ultimate stress blocks, thus making the lever arm between them greater. This introduces a paradox, because the reinforcement and diagonal strut are based on ultimate limit state.

(iii) A frictional reaction occurs across the bottom of the column, although when this is used some of the compression at the bottom of the pocket is obviously transferred to it. This force relies on good compaction beneath the column, even if the bottom of the column is flat.

(iv) The solution requires that the compressive strength of the infill in the annulus is the same as for the precast pedestal.

Referring to Figure 7.129, the pressure distribution beneath the column gives a reaction F_{nb} acting at an assumed distance $e_{nb} = h/4$ from the centre of the column (called a in Section 7.14.1). This may be greater than it should be, particularly for lower values of M_d/N_d, and makes quite a difference to the final result, as shown later. In this analysis μ = coefficient of friction at the precast–*in situ* interface,

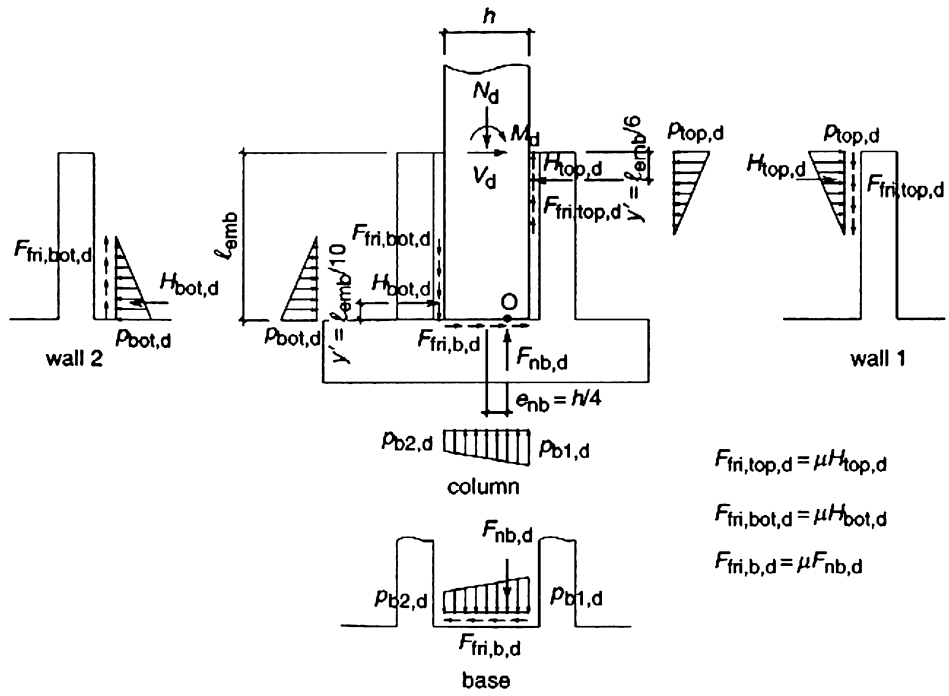

Figure 7.129 Force equilibrium to determine reaction forces and reinforcement in column pocket [7.77]. (Courtesy of fédération internationale du béton (*fib*), www.fib-international.org, and ICE Publishing.)

taken as $\mu = 0.3$ when both column and pocket are cast against steel formwork, $\mu = 0.6$ ditto for timber formwork, and $\mu = 1.0$ for the keyed profile.

The vertical resolution of forces is:

$$N_d = F_{nb} + F_{fri,top} - F_{fri,bot} = F_{nb} + \mu H_{top} - \mu H_{bot} \tag{7.96-a}$$

Horizontally

$$V_d = H_{top} - H_{bot} - \mu F_{nb}$$

Thus

$$H_{bot} = H_{top} - V_d - \mu F_{nb} \tag{7.96-b}$$

Solving these equations gives

$$F_{nb} = (N_d - \mu V_d)/(1 + \mu^2) \tag{7.96-c}$$

Taking moments about the resultant at H_{bot} on the side wall at point A:

$$M_d + V_d(l_{emb} - y') + N_d 0.5h - F_{nb}(0.5h + e_{nb} + \mu y') = H_{top}(l_{emb} - y - y' + \mu h) \tag{7.96-d}$$

from which $H_{top} > H_{bot}$ may be calculated. This procedure is similar to the BS EN 1992-1-1 equation (7.90-d).

Canha [7.77] proposed that the centroid to H_{top}, $y = l_{emb}/6$, based on the triangular stress block present halfway down the pocket, and the centroid to H_{bot} only $y' = l_{emb}/10$ due to the large rigidity

of the pocket on the compression side, following a CERIB report. The authors state that the design method is applicable to axial forces with large eccentricity, around $e = M_d/N_d = 2h$, but the assumptions that have been made in terms of pressure distributions means this is probably conservative and could be used for small eccentricities.

For example, try $h = 300\,\text{mm}$ column, $N_d = 1000\,\text{kN}$, $M_d = 600\,\text{kNm}$, $M_d/N_d\ h = 2$, $V_d = 50\,\text{kN}$; let $\mu = 0.7$, $e_{nb} = 75\,\text{mm}$, $l_{emb} = 2h = 600\,\text{mm}$, $y = 100\,\text{mm}$, $y' = 60\,\text{mm}$. Then:

$$F_{nb} = (1000 - 0.3 \times 50)/1.09 = 903.7\ \text{kN} \tag{7.96-c}$$

$$H_{top} = (600 + 50 \times 0.54 + 1000 \times 0.15 - 903.7 \times 0.243)/0.53 = 1051\,\text{kN} \tag{7.96-d}$$

Half this force will be transmitted through the two longitudinal walls (walls 3 and 4 in Figure 7.130) as tension, and $H_{top}/2$ will develop a 45° compressive strut resulting in a vertical tie force $F_{vm} = H_{top}/2$ in the longitudinal walls. If the pedestal wall is 200 mm thick and allowing 40 mm cover, the maximum diameter of bar that can form a tight enough bend to reach the corners of the walls is H16 (4 dia. mandrel). Using $f_{yk} = 500\,\text{N/mm}^2$, $A_{s,top} = 0.5 \times 1051 \times 10^3/0.87 \times 500 = 1208\,\text{mm}^2$. Use three pairs of H16 ($1206\,\text{mm}^2$) in the top half of the wall, i.e. at 50 cover to the top bar and then at 100 mm spacing.

The compressive strut force $= 0.5 \times 1051 \times \sqrt{2} = 743\,\text{kN}$. Using concrete $f_{ck} = 40\,\text{N/mm}^2$ for the precast pedestal, the width of the compressive strut to BS EN 1992-1-1 is $w = 743 \times 10^3/200 \times (0.482 \times 40) = 193\,\text{kN/m}$, which extends 136 mm down the wall $< l_{emb}/2 = 300\,\text{mm}$: OK. The vertical steel $A_{sv} = A_{s,top} = 1208\,\text{mm}^2$ and may be provided by using four H16 in the corners and two more in the side walls ($1206\,\text{mm}^2$). Figure 7.130 shows the final arrangement of rebars proposed by the authors.

The pressure distributions acting on the breadth of the column b for H_{top} and H_{bot} may be checked using a triangular distribution of stress according to Figure 7.129 or, more realistically as this is an

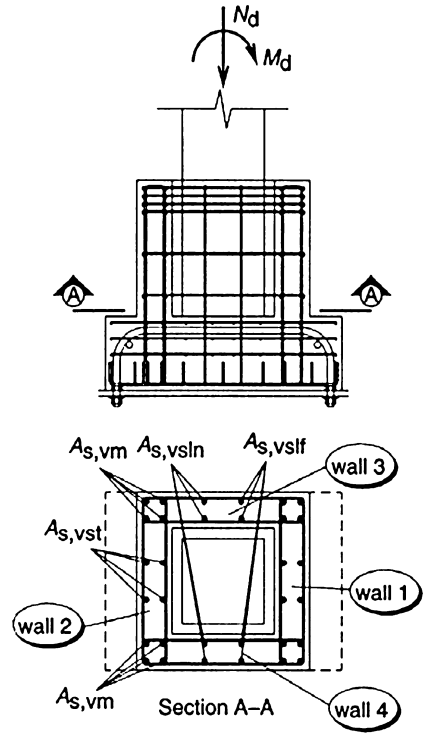

Figure 7.130 Arrangement of reinforcement in column pocket [7.77]. (Courtesy of fédération internationale du béton (*fib*), www.fib-international.org, and ICE Publishing.)

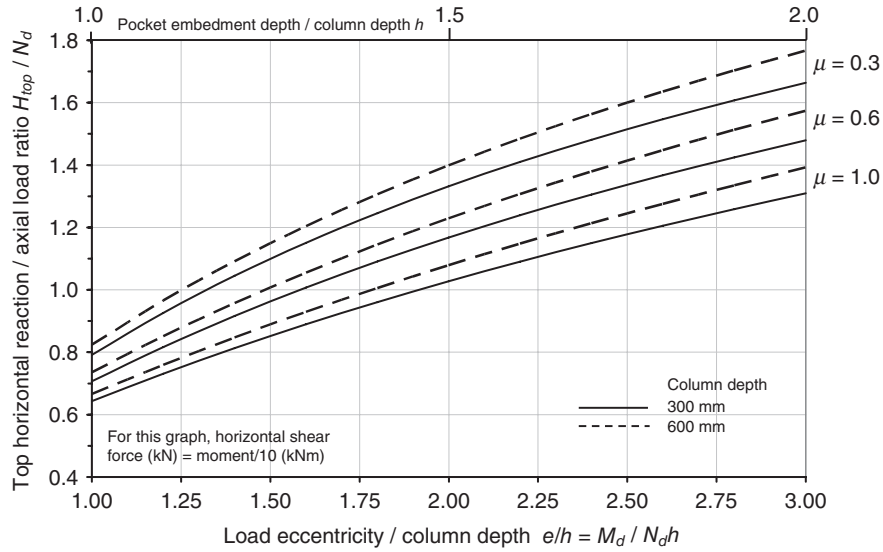

Figure 7.131 Design chart to determine horizontal reaction at top of pocket.

ultimate design, a parabolic-linear distribution. Taking flexural triangular stress distributions limited to $0.482 f'_{ck}$ for the infill concrete/mortar, and letting $b = 300$ mm, then if the depth to the centroid is y, the depth of the stress block is $3y$, such that:

$3y = H_{top}/b \text{ ½ } 0.45 f_{ck} = 1051 \times 10^3/(300 \times ½ \times 0.482 \times 40) = 363$ mm
$y = 363/3 = 121$ mm $\approx l_{emb}/6 = 100$ mm assumed at the start.

Similarly at the bottom, where (7.96-b)

$H_{bot} = 1051 - 50 - 0.3 \times 903.7 = 730$ kN, pro rata with H_{top}
$y' = 84$ mm $\approx l_{emb}/10 = 60$ mm assumed at the start.

Figure 7.131 may be used as a design chart to determine H_{top}/N_d in terms of the eccentricity $e/h = M_d/N_d h$, two column sizes, and three values for μ. Two assumptions have been made in order to present the data in a single chart: V_d (in kN) = $M_d/10$ (in kNm), and the depth of pocket $l_{emb} = 1.0h$ for $e/h = 1$ to $l_{emb} = 2.0h$ for $e/h = 3$. The former is based on a cantilever column 20 m in height subject to horizontal wind pressure, representing an upper limit. The reader can check other relationships. It should be noted that, because the magnitude of H_{top} is directly proportional to all the loads and moments, the ratio H_{top}/N_d is independent of the magnitude of N_d.

The effect of the resultant line of action for F_{nb} from the centre of the column, i.e. e_{nb}, is quite significant. Looking at the design chart in Figure 7.131, for $e/h = 1$, $\mu = 0.3$, and $h = 300$ mm. If $e_{nb} = h/4 = 75$ mm, then $H_{top}/N_d = 0.79$. If $e_{nb} = 25$ mm, then $H_{top}/N_d = 0.94$, 19 per cent greater. The increase diminishes as e/h becomes larger.

7.14.2 Columns on base plates

Base plates that are larger than the size of the columns are used where a moment connection is required. Figures 7.132(a) and (b) show the structural mechanism for this type of connection, and Figures 7.133 and 7.134 show photographs of the base plate before and after casting in the column. The disruption to manufacture of the precast column may be considerable, because the plate cannot be contained within the internal confines of the mould. However, base plates provide immediate

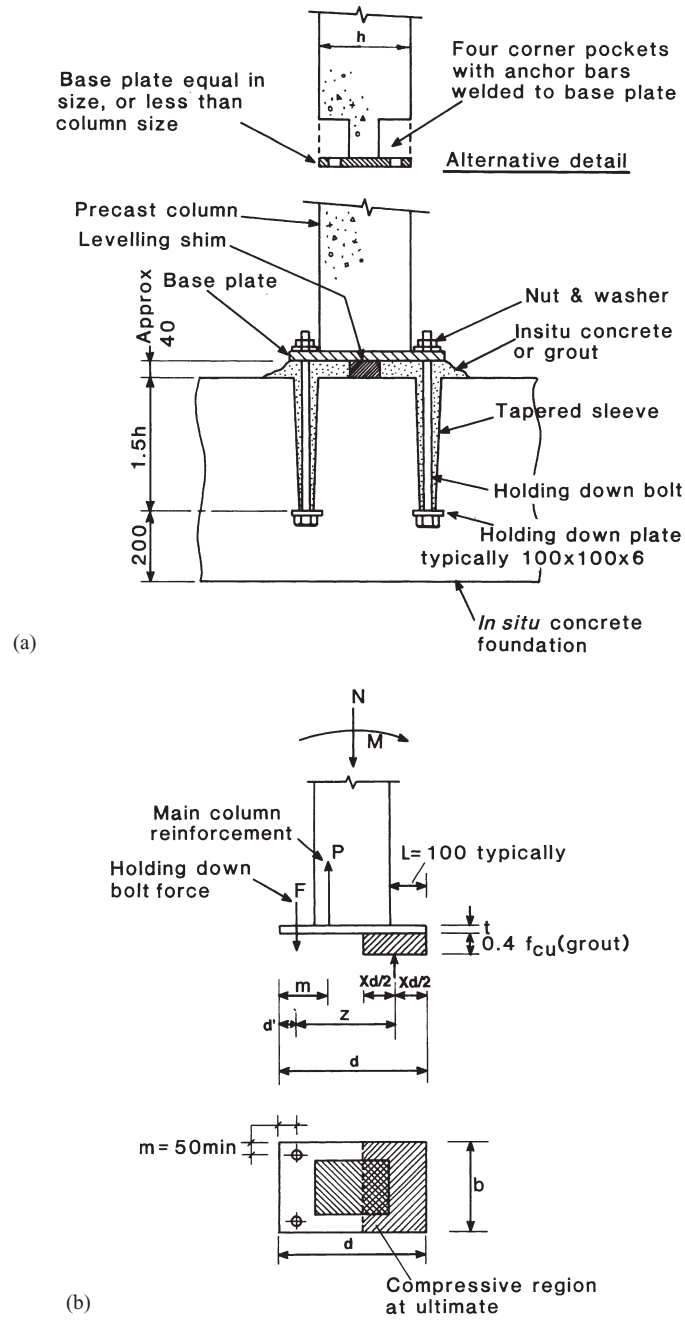

Figure 7.132 Base plate design principle. (a) General arrangement, and (b) notation.

stability when fixing the column on site, and the depth of the foundation is not excessive. The choice of using base plates rather than pockets tends to be made more on production rather than structural considerations.

An ultimate flexural/bearing stress of $0.85f_{cd} = 0.482f_{ck}\{0.4f_{cu}\}$ is used for the infill grout in the narrow gap beneath the plate and over the full width of the base plate. Because of confinement, this is a conservative stress limit and allows for the possible lack of filling at the very centre of the plate.

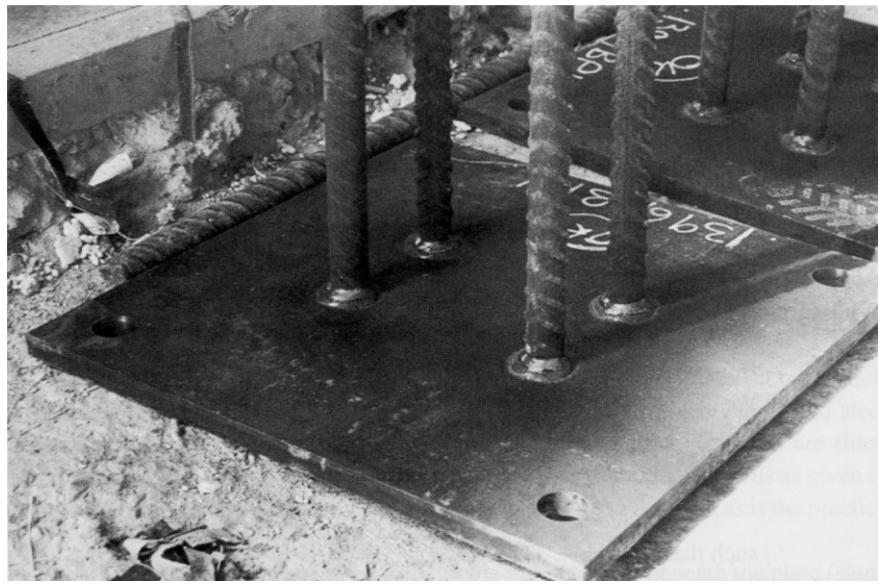

Figure 7.133 Column base plate with starter bars welded to plate.

Figure 7.134 Column-to-foundation connection with extended base plate.

The following design method may be used to calculate the base plate thickness in the completed structure. Referring to Figure 7.132(b) and resolving vertically, if $F > 0$:

$$F + N = 0.482 f_{ck} bXd \qquad (7.97) \quad | \quad F + N = 0.4 f_{cu} bXd \qquad (7.97)$$

where $X\,d$ = the compressive stress block depth.

Taking moments about the centre line of compressive stress block

$$M = F(d - d' - 0.5Xd) + N(0.5d - 0.5Xd) \qquad (7.98)$$

Also, $M = N\,e$, such that:

$$\frac{N(e + 0.5d - d')}{0.482 f_{ck} bd^2} = X\left(1 - \frac{d'}{d}\right) - 0.5X^2 \qquad (7.99) \quad \left| \quad \frac{N(e + 0.5d - d')}{0.4 f_{cu} bd^2} = X\left(1 - \frac{d'}{d}\right) - 0.5X^2 \right. \qquad (7.99)$$

from which X and F may be calculated.

We can simplify by letting a stress factor, K

$$K = \frac{M'}{f_{ck} bd^2} = \frac{N(e + 0.5d - d')}{f_{ck} bd^2} \qquad (7.100) \quad \left| \quad K = \frac{M'}{f_{cu} bd^2} = \frac{N(e + 0.5d - d')}{f_{cu} bd^2} \right. \qquad (7.100)$$

so that

so that

$$X^2 - 2X\left(1 - \frac{d'}{d}\right) + \frac{3K}{0.85^2} = 0 \qquad (7.101) \quad \left| \quad X^2 - 2X\left(1 - \frac{d'}{d}\right) + 5K = 0 \right. \qquad (7.101)$$

If $X > N/0.482 f'_{ck} bd$ $\{X > N/0.4 f'_{cu} bd\}$, then F is positive.

Assume N is number of bolts, each of root area A_b and yield strength f_{ykb} $\{f_{yb}\}$, providing the force F, then:

$$A_b = \frac{F}{N f_{yb}} \qquad (7.102)$$

The design strength f_{ykb}/γ_m {yield strength f_{yb}} and ultimate tensile strength for the holding-down bolts are given in Table 7.11.

Except in extreme cases of very high bending and low axial load, the worst bending on the base plate occurs on the compression side. Use a base plate of thickness t which is the greater of:

$$t = \sqrt{0.964 f_{ck} L^2 / p_y} \qquad (7.103) \quad \left| \quad t = \sqrt{0.8 f_{cu} L^2 / p_y} \right. \qquad (7.103)$$

(based on the compression side), or

(based on the tension side) $$t = \sqrt{4Fm / bp_y} \qquad (7.104)$$

where L = overhang of plate beyond column face, m = distance from centre of bolts to centre of bars in column, and p_y = yield strength of the plate. Steel grade S275 or S355 {43 or 50} is used; see Table 7.12.

If $X < N/0.482 f_{ck} bd$ $\{X < N/0.4 f_{cu} bd\}$, then F is negative and Eq. (7.100) is not valid. The analysis simplifies to the following:

$$X = 1 - \frac{2e}{d} \qquad (7.105)$$

Table 7.11 Yield and ultimate tensile strength of holding down bolts and base plates

	BS EN 1993-1-8, clause 3.1.1(3)		BS 5950
Bolt grade	**Bolt ultimate tensile strength f_{ub} (N/mm^2)**	**Bolt yield strength f_{ybk} (N/mm^2)**	**Bolt yield strength f_{yb} (N/mm^2)**
4.6	400	240	195
5.6	500	300	
6.8	600	480	
8.8	800	640	450
10.9	1000	900	
Plate grade		**Plate yield strength p_{yk} {p_y} (N/mm^2)**	**Plate ultimate tensile strength (N/mm^2)**
BS EN 1993-1-1	**BS 5950**		
S235		235	360
S275	43	275	430
S355	50	355	510
S420		420	520
S450		450	550

and

$$N = f_c bXd \tag{7.106}$$

because the grout is not fully stressed, Eq. (7.105) is modified to:

$$t = \sqrt{2 f_c L^2 / p_y} \tag{7.107}$$

The yield strength f_{ykb} {f_{yb}} and ultimate tensile strength for holding-down bolts are given in Table 7.12. The design value for bolts according to BS 5950 is equal to the yield strength, either f_{yb} = 195 or 450 N/mm^2 for grade 4.6 or (more commonly) grade 8.8. The design value to BS EN 1993-1-8:2005 [7.79] is f_{ykb}/γ_{M2} (γ_{M2} = 1.25). Thus f_{ydb} = 160 or 512 N/mm^2 for grade 4.6 or 8.8. These values should be adopted as characteristic values in design calculations.

The yield strength p_{yk} {p_y} and ultimate tensile strength for base plates are given in Table 7.11. The design value according to BS 5950 is equal to the yield strength. The design value to BS EN 1993-1-8: 2005 [7.79] is p_{yk}/γ_{M0} (γ_{M0} = 1.0).

The column is sometimes cast without the base plate, for convenience of fitting it into an existing mould. After casting, the base plate is welded onto the protruding column bars, and the final section of concrete between the precast column and the base plate is cast. To avoid difficulties due to shrinkage, this can be, say, 50 mm of dry-pack, or possibly a non-shrinking grout or concrete.

Reinforcement is fitted through holes in the base plate and fillet-welded at both sides (see Figure 7.133), using the same details as given in Section 7.13.4 on splices. The design strength of the column is therefore determined using mild steel reinforcement strength, which occasionally leads to cumbersome detailing. Additional links are provided close to the plate, as is the practice at splices.

Vertical loads are easily distributed through the grouted infill beneath the plate (with the specification for the grout as for use in splices). Overturning moments require a greater attention to detail, both in the precast column and *in situ* foundation. Tensile forces must be transmitted by bond in the precast column, bending and shear in the base plate, tension in the cast-in holding-down bolt, and bearing and shear in the foundation.

Holding-down bolts, most commonly of grade 4.6 or 8.8, are used as appropriate. The length of the anchor bolt is typically 375 to 450 mm for 20- to 32 mm-diameter bolts. The bearing area of the bolt head is increased by using a plate washer, nominally 100 × 100 × 8 mm. The bottom of the bolt is a minimum of 100 mm above the reinforcement in the bottom of the footing. Confinement reinforcement (in the form of links) around the bolts is usually required, particularly where narrow beams and/or walls are used and where the edge distance is less than about 200 mm. The steel is designed on the principle of shear friction, but should not be less than 4 R8 links at 75 mm centres placed near the top of the bolts. As a precaution against lateral bursting around the bolt, anchor loops are usually provided around the bolts in order to achieve the full strength of the bolt if the horizontal edge distance is less than about 200 mm.

Larger compressive forces beneath plates that project beyond the column face in two directions cause biaxial bending in the plate. The maximum projection of the plate is therefore usually restricted to 100 mm, irrespective of size (see Figure 7.134). 100 mm is also a minimum practical limit for detailing and site erection purposes. The resulting thickness of plate and size (and grade) of anchor bolts are given in Figure 7.135.

Pin-jointed footings can be designed by decreasing the in-plane lever arm. Base plates using two bolts on one centre line, or four bolts closely spaced, give the desired effect.

Base plates equal to or smaller than the column are used where a projection around the foot of the column is structurally or architecturally unacceptable – for example, where the connection is made at a floor level and cannot be hidden in the finishing screed. The holding-down bolt group is located in line with the main column reinforcement. The base plate is set flush with the bottom of the precast column and small pockets, typically 100 mm cube (for access purposes), leave the plate exposed at each corner (as shown in Figure 7.136 in the factory and Figure 7.137 on site), or at each mid-side of the column. Short starter bars are welded to the base plate (as previously described) in various configurations. The design of starter bars is a repeat of the design of the column at the foundation, except that the effective depth to the projecting bars is decreased to allow space for the starter bars to be welded to the plate. Diameter of holes around starter bars = bar diameter + 10 mm. Starter bars are to pass halfway through the base plate hole, and are welded above and beneath the plate. The weld throat thickness is usually 8, 10 or 12 mm. The fillet weld provided to the top of the plate is as follows:

Maximum diameter ϕ and area of starter bar = $A_{s,s}$

Ultimate force in starter bar

$$F_{Eds} = 0.87 f_{yk} A_{s,s} \quad \{F_{s,s} = 0.87 f_y A_{s,s}\} \tag{7.108}$$

Throat thickness of weld

$$t = F_{Eds}/0.7\pi\phi(f_{wk}/1.25) \quad \{t = F_{s,s}/0.7\pi\phi f_w\} \tag{7.109}$$

where f_{wk} $\{f_w\}$ = weld strength according to Table 7.12. (γ_m for welds = 1.25)

Table 7.12 Yield and ultimate tensile strength of welds

	BS EN 1993-1-8		BS 5950
Weld grade	**Weld yield strength f_{wk} (N/mm^2)**	**Weld ultimate tensile strength (N/mm^2)**	**Weld strength f_w (N/mm^2)**
S235	235	360	
S275	275	430	215
S355	355	510	

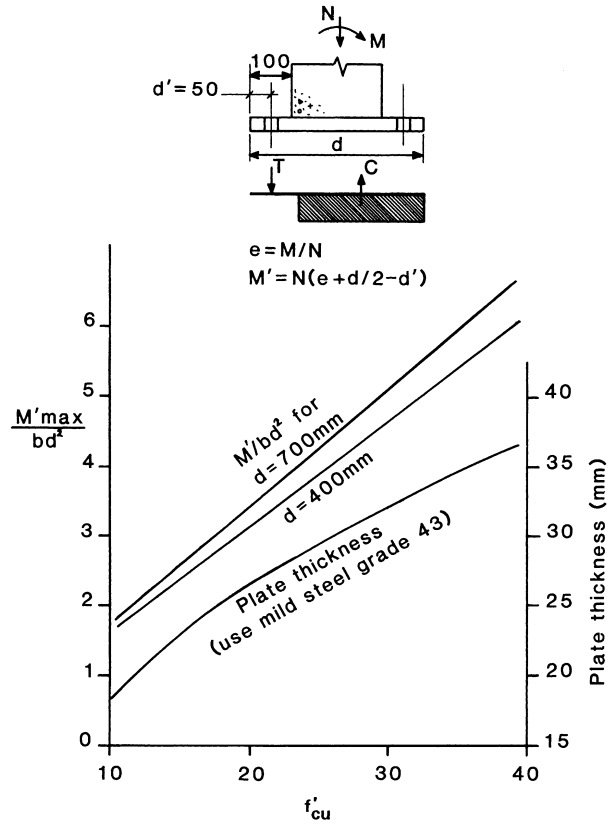

Figure 7.135 Column base plate design graph.

The plate is usually most critical in the temporary condition. In most cases, i.e. in columns less than 400 mm deep, these connections have a limited moment of resistance and are therefore considered pin-jointed. Again, two bolts may be used to form a truly pin-jointed connection, although site workers prefer four bolts to assist with vertical alignment and frame stability.

An alternative to casting the holding-down bolts into the foundation is to drill and fix resin-anchor or expanding bolts on site. The advantage in construction terms is obvious and it places less responsibility on the contractor to locate the bolts accurately. However the pull-out capacity of a drilled bolt is less than the capacity of a cast-in bolt of the same diameter. In some instances where the pull-out capacity is critical, the cost of drilled bolts may be greater. In other cases the smallest holding-down bolt used, typically 12 or 16 mm diameter, may still be overdesigned and the smaller drilled replacement may be more economical.

A fully welded option is shown in Figure 7.138. While the full axial and moment capacity of the connection is readily generated through the weld, the specialist welding equipment and technique make this a less popular choice for most contractors. The weld size is typically 12 mm throat thickness, using S355 electrodes to grade 450 plates. The control of a uniform input of power is a key issue, in order to prevent overheating of the concrete immediately above the plate cast into the column, and spalling is sometimes seen. The welded joint is protected using a dry-mix pack of at least grade C40/50.

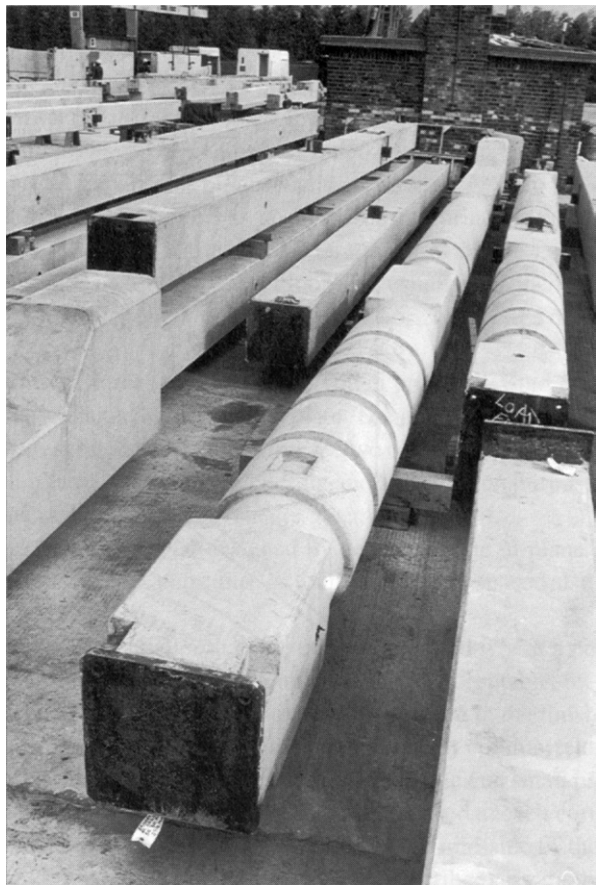

Figure 7.136 Column casting with flush base plate.

Figure 7.137 Column-to-foundation connection with flush base plate.

Figure 7.138 Steel base plate fully welded to cast-in plate in pile cap (courtesy of T&A Prefabricados, Recife, Brazil).

Exercise 7.14 Column base plate design

Design a column base plate connection required to support a 300 × 300 mm column subjected to an ultimate axial force of N_{Ed} = 950 kN {N = 1000 kN} and a moment M_{Ed} = 95 kNm {M = 100 kNm}.

Use grade C30/37 for the grout, grade S275 {43} steel for the base plate.

Solution

Try a 500 × 500 mm plate with L = 100 mm overhang and $d' = L/2$ = 50 mm

$e = 95 \times 10^3/950 = 100$ mm

Then $k = \dfrac{950\times10^3\times(100+500/2-50)}{500\times500^2\times30} = 0.076$

$X^2 - 2X\left(1-\dfrac{50}{500}\right)+\dfrac{3\times0.076}{0.85^2}=0$

Hence $X = 0.197$

Because $X < N/0.482 f_{ck}bd = 0.263$ then F is negative, so:

$X = 1-\dfrac{2e}{d} = 1-\dfrac{2\times100}{50} = 0.6$

and

$f_c = \dfrac{950\times10^3}{500\times0.6\times500} = 6.33\text{N/mm}^2$

Hence

$t = \sqrt{\dfrac{2\times6.33\times100^2}{275}} = 21.5\text{ mm}$

$e = 100 \times 10^3/1000 = 100$ mm

Then $k = \dfrac{1000\times10^3\times(100+500/2-50)}{500\times500^2\times37} = 0.065$

$X^2 - 2X\left(1-\dfrac{50}{500}\right)+5\times0.065=0$

Hence $X = 0.203$

Because $X < N/0.4\, f_{cu}bd = 0.27$ then F is negative, so:

$X = 1-\dfrac{2e}{d} = 1-\dfrac{2\times100}{50} = 0.6$

and

$f_c = \dfrac{1000\times10^3}{500\times0.6\times500} = 6.67\text{N/mm}^2$

Hence

$t = \sqrt{\dfrac{2\times6.67\times100^2}{275}} = 22.0\text{ mm}$

Use 500 × 500 × 25 mm mild steel base plate.

Exercise 7.15 Column base plate design

Repeat Exercise 7.14 using $N_{Ed} = 190\,\text{kN}$ {$N = 200\,\text{kN}$} and $M_{Ed} = 105\,\text{kNm}$ {$M = 120\,\text{kNm}$}.

Use grade C40/50 concrete for the precast column, C30/37 for the grout, with f_{yk} {f_y} = 250 N/mm^2 for the reinforcement welded to the plate, cover to column bars = 35 mm, grade S275 {43} base plate and grade 8.8 holding-down bolts.

Solution

Step 1: In the base plate

Try 500 × 500 mm plate with $L = 100\,\text{mm}$ overhang and $d' = L/2 = 50\,\text{mm}$

$e = 105 \times 10^3/190 = 552.6\,\text{mm}$

Then

$$k = \frac{190\times10^3\times(552.6+500/2-50)}{500\times500^2\times30} = 0.0381$$

$$X^2 - 2X\left(1-\frac{50}{500}\right)+\frac{3}{0.85^2}\times0.0381 = 0$$

Hence $X = 0.0927$

Because $X > N/0.482 f_{ck}\, b\, d = 0.053$ then F is positive, so:

$F = 0.482 f_{ck} bXd - N = 335.0 - 190 = 145.0\,\text{kN}$

Using $f_{ykb} = 640/1.25 = 512\,\text{N/mm}^2$

$$A_b = \frac{145\times10^3}{2\times512} = 142\,\text{mm}^2$$

$$t = \sqrt{\frac{0.964\times30\times100^2}{275}} = 32.4\,\text{mm}$$

$e = 120 \times 10^3/200 = 600\,\text{mm}$

Then

$$k = \frac{200\times10^3\times(600+500/2-50)}{500\times500^2\times37} = 0.0346$$

$$X^2 - 2X\left(1-\frac{50}{500}\right)+5\times0.0346 = 0$$

Hence $X = 0.102$

Because $X > N/0.4\, f_{cu}\, b\, d = 0.054$ then F is positive, so:

$F = 0.4 f_{cu} bXd - N = 376.9 - 200 = 176.9\,\text{kN}$

Using $f_{yb} = 450\,\text{N/mm}^2$

$$A_b = \frac{176.9\times10^3}{2\times450} = 197\,\text{mm}^2$$

$$t = \sqrt{\frac{0.8\times37\times100^2}{275}} = 32.8\,\text{mm}$$

Use two M24 grade 8.8 holding-down bolts in a 500 × 500 × 35 mm plate.

Step 2: In the column.

Before proceeding we need sizes of the starter bars in the column. These are designed as grade 250, owing to the weld to the plate, even though high-tensile bars will be provided. Assume the main bars are 32 mm and links 10 mm dia.

$$\frac{d}{h} = \frac{300-35-32/2}{300} = 0.83$$

$d_2/h = 0.17$,

use BS EN 1992-1-1 derived column design chart $d_2/h = 0.2$ (see Figure 4.53)

$$\frac{N}{f_{ck}bh} = \frac{190\times10^3}{40\times300\times300} = 0.053$$

$$\frac{M_{max}}{f_{ck}bh^2} = \frac{105\times10^6}{40\times300\times300^2} = 0.097$$

From column design chart:

$A_{sc} = 0.26\, bhf_{ck}/f_{yk} = 0.26 \times 300^2 \times 40/250 = 3744\,\text{mm}^2$

Use four H32 + two H20 (3845 mm^2) column bars.

Then $m = 50 + 35$ cover $+ 10$ links $+ 32/2 = 111\,\text{mm}$

$$t = \sqrt{\frac{4\times145\times10^3\times111}{500\times275}} = 21.6\,\text{mm}$$

$$\frac{d}{h} = \frac{300-35-32/2}{300} = 0.83$$

$$\frac{N}{bh} = \frac{200\times10^3}{300\times300} = 2.222$$

$$\frac{M_{max}}{bh^2} = \frac{120\times10^6}{300\times300^2} = 4.444$$

BS 8110 does not publish charts for $f_y = 250\,\text{N/mm}^2$; therefore column analysis is carried to show that for $d/h = 0.83$, and using $x = 65\,\text{mm}$, then $A_{sc} = 4230\,\text{mm}^2$ satisfies the above.

Use six H32 (4825 mm^2) column bars.

Then $m = 50 + 35$ cover $+ 10$ links $+ 32/2 = 111\,\text{mm}$

$$t = \sqrt{\frac{4\times176.9\times10^3\times111}{500\times275}} = 23.9\,\text{mm}$$

This is less than the 35 mm-thick provision above.

7.14.3 Columns on grouted sleeves

The design of these joints is identical to the grouted sleeve splice described in Section 7.13.5. Full compression or tension anchorage lengths are provided in both the precast column and *in situ* foundation. High-tensile deformed reinforcing bars are left protruding from the foundation, which is quite difficult to achieve with any accuracy (see Figure 7.139(a)). This is the main disadvantage in using this connection. The tendency is for the bars to touch the sides of the sleeves in the precast column, thus preventing full penetration of grout around the bar. Since the grout cannot be inspected afterwards, there is doubt that the bar is fully bonded. Allowance can be made for this by making the normal bond stress deductions as if the bar were one of a group.

Notwithstanding these difficulties, and because preventative measures can be taken, the joint may be considered in design as monolithic, providing that the bedding joint and grout sleeves are completely filled by pressure grouting to the satisfaction of the site engineer.

Work by Kuttab [7.71], Somerville [7.76], and Korolev and Korolev [7.80] has shown axial force–moment interaction characteristics of the joint are equal to those of the column itself. An added bonus is that high-tensile reinforcement is used throughout. The minimum internal diameter of the grout tube is 40 mm when using 25 mm-diameter deformed bar. Nominal cover to the tube and the minimum distance between tubes should be at least 75 mm. Confinement links are provided in the usual manner.

Protruding bars are often used with *in situ* slab foundation or foundation piles. The moment-resisting connection is realised with reinforcement bars, protruding from the foundation (more common) or from the column, as is the case in Figure 7.139(b). They are inserted in ducts to lap with the main reinforcement after grouting. The diameter of the ducts should be oversized to allow for placing tolerances.

(a)

(b)

Figure 7.139 Protruding bars from the column (a) and positioned into sleeves preformed in the foundation (b) to provide a full moment connection.

CHAPTER 8

Designing for Horizontal Load

This chapter deals with the transfer of horizontal load from the floor plate at every floor level to the foundations. The stability of the structure and the methods of achieving it are discussed.

8.1 Introduction

There is no doubt that precast multi-storey structures of up to about 50 m in height can be designed with economy, safety and excellent form. The main debate is in the manner in which horizontal forces are transmitted through the components and their connections, particularly in very large precast structures where the connections become highly stressed. The obvious relationship between stability and details is evident from the photograph of The Bourse in Leeds, UK, shown in Figure 8.1. The tallest precast (wall frame) structure in Europe is the 54-storey building for Nationale Nederlanden in Rotterdam, which consists of slip-formed *in situ* cores, precast load-bearing walls and precast double-tee floor units.

This increasing awareness towards the structural integrity of structural connections in prefabricated construction has been where most of the recent research effort has been directed. Most of the papers cited in this book are directed towards the structural integrity either of the structure or of the connections. The details used to achieve robustness in a structure have a significant effect on the structural mechanisms by which horizontal forces are distributed, and *vice versa*. Rarely has it been possible to test entire structures, the exception being the half-scale, three-storey precast structure tested at the University of California, San Diego, in 2008 [8.1]. A main feature of this 56 ft × 16 ft × 23 ft tall structure (17.1 × 4.9 × 7.0 m), shown in Figure 8.2, was to develop a diaphragm seismic design methodology for precast buildings, and these tests included 16 input ground motions, monitored by 640 sensors dynamically recording the various damage limit states. The floors comprised single-span 10 inch (255 mm) deep double-tee units and 4 inch (102 mm) deep hollow-core units, both with a 1½ inch (38 mm) thick topping. Subjected to peak ground accelerations of between 0.30g and 0.61g, the maximum roof drift ratio (sway/height) recorded at the centre of the floor diaphragms was 0.23 per cent and 1.88 per cent, respectively. The former sway of $h/434$ is close to the recognised ratio of $h/400$ in BS EN 1992-1-1 {$h/500$ used in BS 8110}. In the latter, where the sway = $h/53$, peak strains of 7700 με were recorded in the chord reinforcement at the centre of the floor, there were some floor–beam connections fractures, and there was some cracking up to 1.0 mm wide, but there was recovery of the floor diaphragm after loading.

Horizontal forces in precast structures derive mainly from wind loading and temperature gradients. In seismic zones earthquake loading is the predominant loading, but that is beyond the scope of this book. Secondary effects, such as linear changes in volume due to creep, tendon relaxation and

Multi-storey Precast Concrete Framed Structures, Second Edition. Kim S. Elliott and Colin K. Jolly.

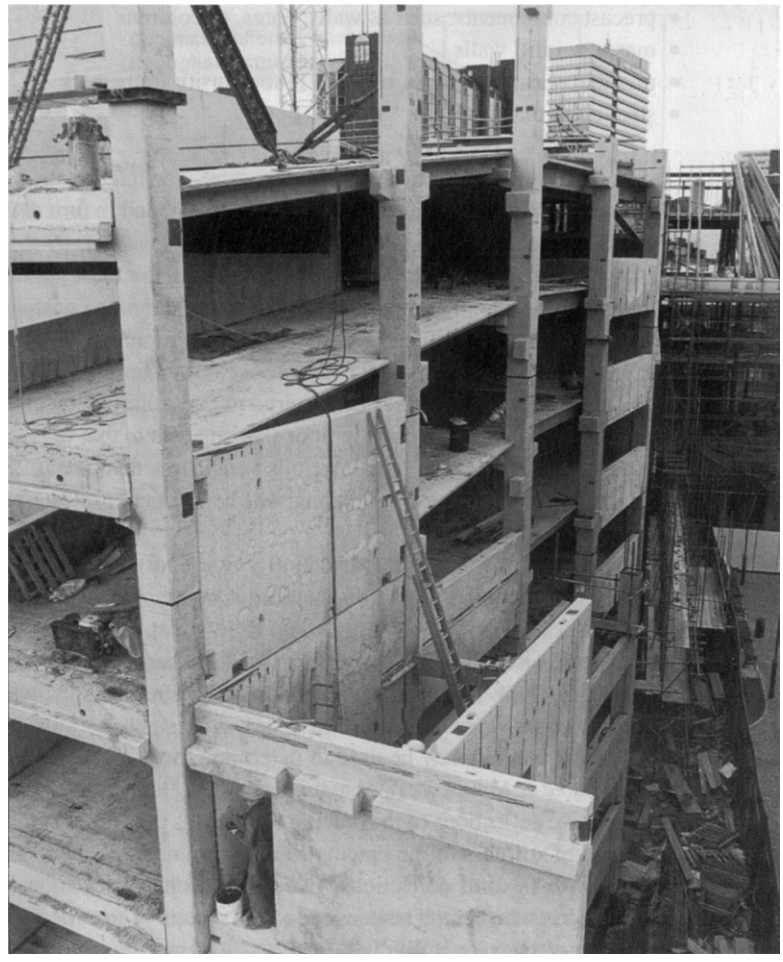

Figure 8.1 Construction of The Bourse, Leeds, UK (courtesy of Blatcon Ltd).

shrinkage, etc., are mostly (but not totally) eliminated by precasting, where factory controlled moisture loss is more effective than on site. The low water content and the low water/cement ratio used in the predominantly horizontal components ensure that shrinkage effects are minimised. The practice in design offices is to restrict these secondary effects to individual joints between the precast components under consideration and not to allow them to accumulate over large areas of the structure.

With the exception of structural toppings, the use of large quantities of *in situ* concrete is confined to situations where shrinkage cracking and minimal creep strains can be tolerated and allowed for in design. In situations where that is not acceptable, non-shrinkable concrete (or grout) is used.

Wind loading is in accordance with BS EN 1991-1-4 [8.2] {BS 6399-2:1997 [8.3]}, and force coefficients for rectangular-plan buildings are used for all building shapes. Although force and pressure coefficients are available [8.4] for non-rectangular plan forms (L, U, H shapes etc.) and unclad skeletal (lattices), the information is not widely used at present. An ultimate horizontal loading to BS EN 1992-1-1, clause 5.2(5) [8.5] of 0.5 per cent, based on an inclination of $\theta_o = 1/200$, of the total loading above each floor level 'together with other actions' as stated in clause 5.2(5) {BS 8110, Part 1 [8.6] of 1.5 per cent of the permanent loading G_k above each floor level replaces the ultimate wind force where appropriate}. This takes into account the effects of lack of verticality in construction.

Figure 8.2 Horizontal load testing of precast concrete diaphragm floors in a half-scale skeletal structure at University of California, San Diego's Englekirk Engineering Centre, in February 2008 [8.1] (courtesy of J. Restrepo, University of California at San Diego, USA).

Two key factors need to be satisfied in design: horizontal load transfer by diaphragm action in the precast concrete floor plate (Sections 8.3 and 8.4), and stability in the vertical bracing elements (Sections 8.6 to 8.7). Diaphragm action may also be divided into two distinct categories – behaviour with and without a structural topping. A general introduction to diaphragm action was given in Chapter 1, Section 1.4 and the reader should be familiar with this before proceeding.

8.2 Distribution of Horizontal Load

The distribution of horizontal loading between stabilising elements is determined from the position and stiffness of the bracing elements in the structure. The bracing elements may be either (in order of descending stiffness):

- precast components, such as walls, cores, or columns
- masonry infill walls
- moment-resisting frames, e.g. continuous *in situ* framework
- steel cross-bracing ties or diagonal tie/struts,

or some combination of each in the same structure. The relative stiffness of each bracing element determines the force carried by that element, and in turn defines the horizontal deflections in the floor plate.

Taking, for example, shear walls or cores as being the most popular type of bracing, and assuming that Young's modulus and shear modulus are constant for the materials used in the bracing, the stiffness of each unit is proportional to its second moment of area (I) in the uncracked condition (at the serviceability limit state). Thus the larger the I-value, the greater will be the force required to cause horizontal displacement, and the greater will be the shear force in the floor slab adjacent to that wall or core. If the unit is more squat, i.e. its height-to-length ratio is small (less than about 2), shear deflections will govern and the response to loading will be a function of the plan cross-sectional area, rather than I.

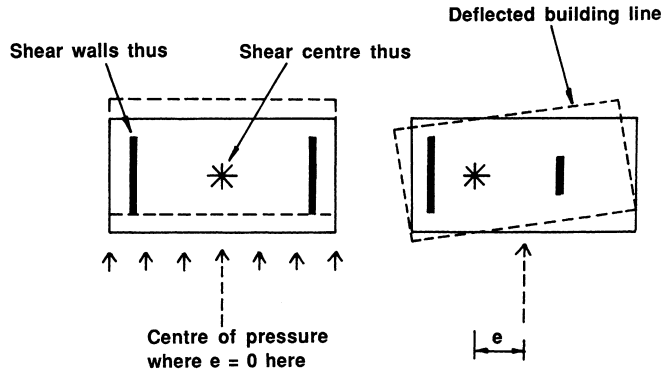

Figure 8.3 Definitions of floor plate and torsional stability in shear wall buildings.

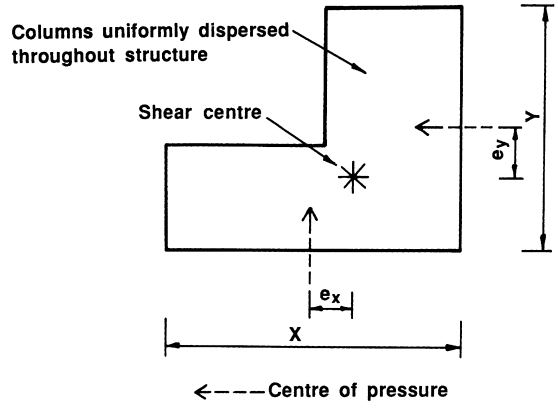

Figure 8.4 Eccentricity in shear wall systems.

Non-symmetrical walls (the vast majority) are considered for providing torsional stability, as shown in Figure 8.3, although the disposition of columns is usually such that the shear centre of the system coincides fairly closely with the centre of the external wind pressure. However, for L-shaped buildings, shown on plan in Figure 8.4, where the eccentricity ratios e_x/X and e_y/Y exceed 0.15, the torsional equilibrium may increase individual floor diaphragm reactions by up to 50 per cent.

Floor diaphragm forces also derive from a geometric imperfection caused by lack-of-plumb deformations, determined from the angular disposition of columns and right-angled walls, as shown in Figure 8.5. A design method is given by Bachmann and Steinle [8.7] based on DIN 1045-1 models, similar to the imperfection analysis in BS EN 1992-1-1, Figure 5.1c [8.5]. A uniform inclination of columns, particularly pin-ended single-storey columns – but less likely in continuous columns – reduces as the number of columns in the plane of sway increases. According to Figure 8.5, the inclination $\theta_i/2$ causing the diaphragm force H_i is given by

$$\theta_i = \sqrt{0.5(1+1/m)\alpha_h}\,/200 \tag{8.1}$$

where

$\alpha_h = 2/3 \le 2/\sqrt{h} \le 1$
h = storey height of column
m = number of columns contributing to the total force in the direction of imperfection

$$H_i = \theta_i(N_b + N_a)/2 \tag{8.2}$$

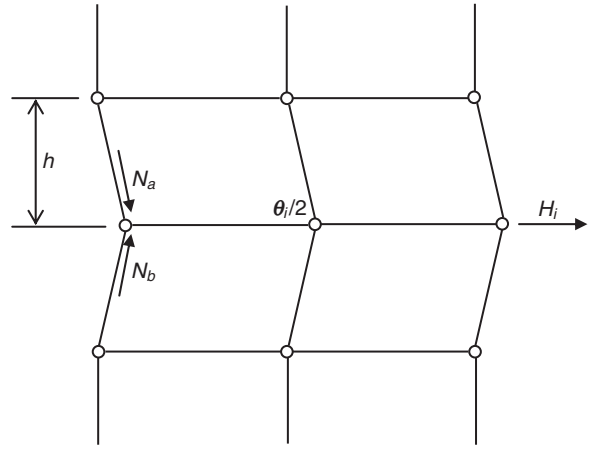

Figure 8.5 Horizontal diaphragm load caused by geometric imperfection.

and to a roof diaphragm

$$H_i = \theta_i N_a \tag{8.3}$$

For example, for a two-bay structure ($m = 3$ columns) of $h = 3.5$ m storey height, subjected to ultimate upper and lower column loads of 2000 and 2600 kN, $\alpha_h = 2/\sqrt{3.5} > 1$, $\theta_i = 0.816 \times 1/200 = 0.0041$ radians. $H_i = 0.0041 \times 4600/2 = 9.4$ kN per column $\times 3 = 28.2$ kN per floor bay. This compares with 0.5% $\Sigma N = 0.005 \times 6000 = 30$ kN, and wind pressure of (say) 1 kN/m$^2 \times 3.5$ m height $\times 8$ m bay width = 28 kN. Note that under large axial column loads, e.g. $N = 5000$ kN, H_i increases to around 60 kN per bay and that will govern.

Any statical method may be used to determine these reactions, but a design method given by Pearce and Matthews [8.8] assumes that the floor plate is a rigid diaphragm and that the relative deflections of the bracing elements are proportional to the distance *a* from the centroid of stiffness to the bracing. It also assumes that shear deflections are small compared with flexural deflections. Even though the distribution of forces will vary, depending upon whether the response in a wall system is governed by flexure, shear or a combination of both, or if one part of the wall system reaches its elastic limit before another, only one parameter is used in the calculation of stiffness.

In the following analysis the walls are assumed to be parallel with each other and to the direction of the load. Walls inclined to the direction of the load may have their resistance resolved into Cartesian components. Referring to Figure 8.6, the cantilevered walls may be considered as linear springs of stiffness $8EI/L^3$, and the floor as a rigid beam. The floor plate reaction in each bracing element H_1, $H_2 \ldots H_n$ is given by the general expression:

$$H_n = \left(\frac{I_n}{\sum I_i} + \frac{eI_n a_n}{\sum I_i a^2} \right) H \tag{8.4}$$

where

H_n = reaction in wall n
I_n and I_i = second moment of area in wall n and in all walls
e = distance from the centroid of stiffness to the centre of pressure of externally applied wind load
a = distance from the centroid of stiffness to each bracing element
H = total reaction = total applied load.

Note that where there are only two walls, the system is statically determinate.

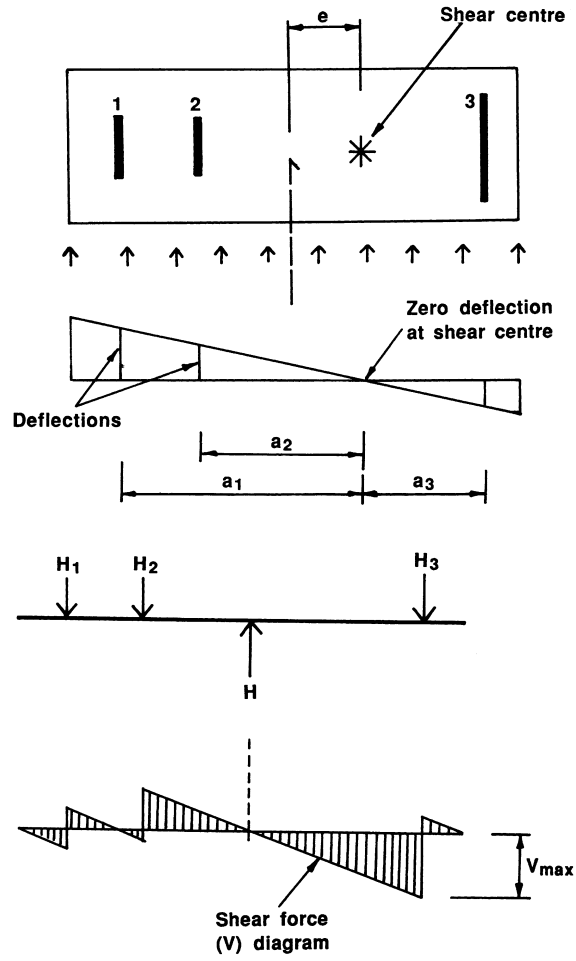

Figure 8.6 Distribution of horizontal load in statically indeterminate wall systems.

If a wall is composed of cross-walls, forming I-, T-, U- or L-configurations, as shown in Figure 8.7(a), the inertia of the composite elements is used in place of the above providing that the vertical joint at the intersections of the legs of the shape is capable of resisting the vertical interface shear force. If the walls are discrete components separated by columns (Fig. 8.7(b)), no interaction between the legs is considered.

In cases where 0.5 per cent of total loads {or 1.5 per cent G_k} is greater than the ultimate wind force, e is taken as the distance from the centroid of stiffness to the centroid of the permanent loads. This may be approximated from the summation of the centres of masses of the walls (external and internal) and floor slab at each level.

If the walls terminate at different floor levels, the structural response of the building will be different above and below each floor level. The theory suggests that each change in the wall position will cause an immediate change in the response of the structure. In fact, shear forces will develop in the floor plate and the changes will be gradual, with the continuous walls taking a slightly larger share of the total force than Eq. (8.4) gives.

A similar situation occurs in buildings containing blocks of different height, as shown in Figure 8.8(a). The reactions in the upper part of the taller block A must be transferred to the walls in the lower part of block A and to the walls in block B. In certain cases it is possible that the maximum wall reaction per floor will occur at an upper floor, possibly at the intersection of the two blocks,

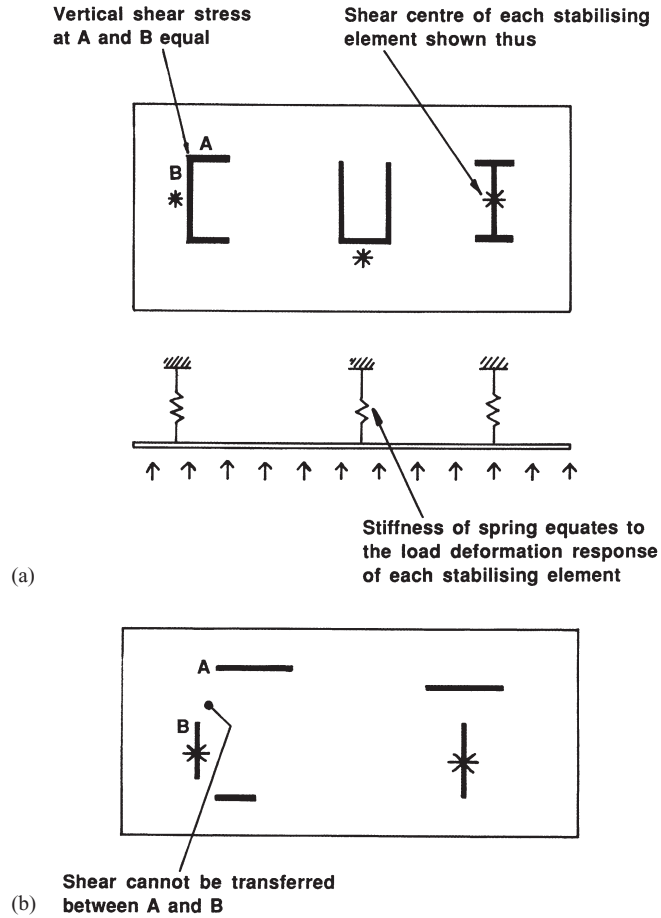

Figure 8.7 Distribution of horizontal load in two-dimensional wall systems. (a) Distribution in combined shear cores and (b) distribution in shear walls.

rather than at the foundation. However the maximum wall shear and maximum overturning moment will always occur at the foundation.

This kind of problem is solved by dividing the elevation of the building into component rectangles, and using superposition to obtain the centroid of horizontal pressure above each floor level. There are two ways of subdividing the elevation – block by block or floor by floor. The latter is more convenient in the calculation of horizontal reactions, because the eccentricity e has a single value throughout. However, when using the method of superposition the overturning moment cannot be extracted from the analysis because the reactions differ between the walls in the various blocks in the upper and lower parts of the building. It is therefore necessary to determine the reactions at every floor level so that they may be summed at the foundation.

A specific problem occurs where one part of the building is very tall in relation to the remainder, for example in Figure 8.8(b), where a one- or two-storey podium is connected to a multi-storey structure. At the level of the top of the podium the reactions in the walls in the tall building will suddenly be distributed through the floor plate as shear forces, moments and possibly torsion. It is better to isolate structurally the two parts of the building rather than risk possible floor plate cracking, as shown in Figure 8.8(c).

Torsional effects in non-symmetrical shear wall systems may be balanced by walls at right angles (or near-right angles) to the direction of the load, as shown in Figure 8.9. At least three walls are required, with at least two of the walls, called 'balancing walls', at right angles to the direction of the

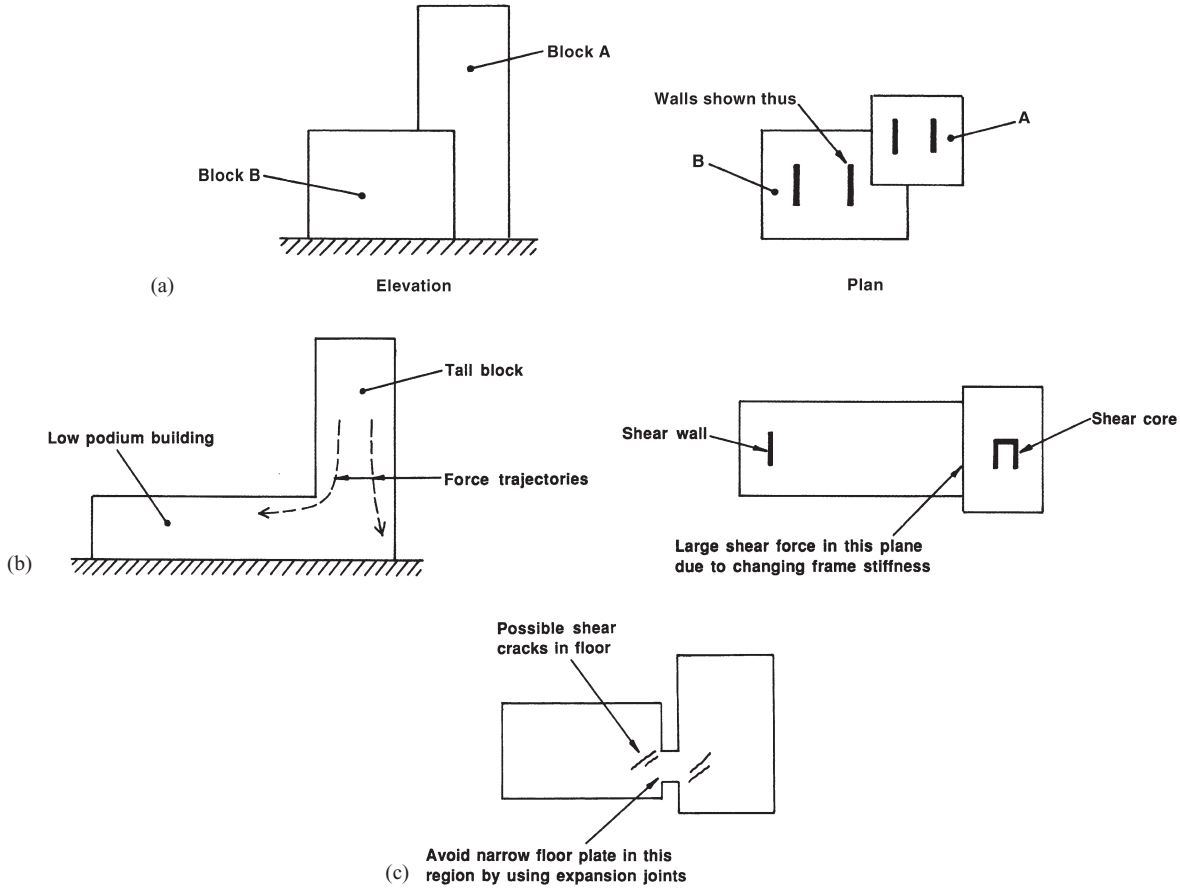

Figure 8.8 Effects of different building heights. (a) Distribution of horizontal load in buildings of different height. (b) Force trajectories between parts of building. (c) Floor plate behaviour at narrow sections.

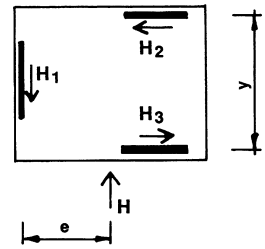

Figure 8.9 Shear system balanced by walls at right angles.

load. Provided there is shear continuity between the walls, any statical method may be used to determine the shear centre of the system and the reactions in the balancing walls. If the walls are not connected to one another, the shear centre is taken at the centroid of the main wall parallel to the load. If this is a distance e from the centre of pressure, then referring to Figure 8.9:

$$H_1 = H \quad \text{and} \quad H_2 = -H_3 = He / y \tag{8.5}$$

Normally y is at least 6 m. If there are more than two balancing walls, the statical method given by Eq. (8.4) may be used to determine the reactions in each of the balancing walls.

Exercise 8.1 Distribution of horizontal loading

Calculate the percentage reactions to a uniform lateral load against the large face of the building for each of the shear walls shown in Figure 8.10. The walls are all of equal thickness and manufactured using the same concrete strength and proportion of reinforcement.

Solution

Step 1: Calculations for determining wall stiffnesses
$I \propto L^3$, because t, f_{ck} and E {t, f_{cu} and E} are all constant.

Taking the origin for $x = 0$ at the left-hand side, then calculate the wall stiffnesses from:

Wall reference	Relative I	x	Ix	$a = x - \bar{x}$	Ia	Ia^2
A	27.0	12	324	–24.25	–655	15 872
B	8.0	39	312	2.75	22	61
C	42.9	51	2187	14.75	633	9333
Total	77.9		2823			25 266

$$\text{Shear centre distance} = \frac{2823}{77.9} = 36.25 \text{ m}$$

$$\text{Therefore } e = \frac{57.0}{2} - 36.25 = 7.75 \text{ m}$$

Step 2: Distribution of load between walls
The fraction of the total force in each of the walls is as follows:

$$\text{Wall A} \qquad H_A = \left(\frac{27}{77.9} + \frac{7.75 \times 655}{25266}\right) H = 0.547H = 54.7\%$$

$$\text{Wall B} \qquad H_B = \left(\frac{8}{77.9} + \frac{7.75 \times 22}{25266}\right) H = 0.096H = 9.6\%$$

$$\text{Wall C} \qquad H_C = \left(\frac{42.9}{77.9} - \frac{7.75 \times 633}{25266}\right) H = 0.357H = 35.7\%$$

Clearly the contribution of wall B is small, but it may be significant in reducing diaphragm bending moments and shears, as shown in Section 8.3.

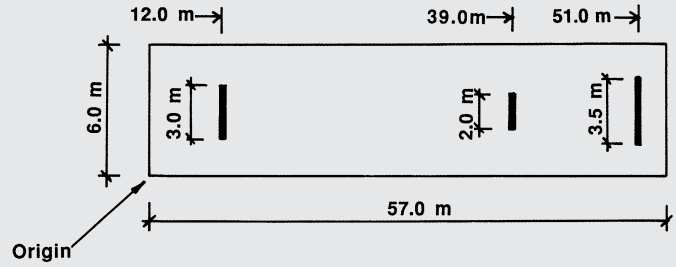

Figure 8.10 Details for Exercise 8.1.

Exercise 8.2

Repeat Exercise 8.1, but omitting Wall B.

Solution
Taking moments about wall A:

$(51 - 12)\ H_C = (57.0/2 - 12)\ H$
Then $H_C = 0.423\ H$, i.e. only an increase of six percentage points from Exercise 8.1.
Also $H_A = 0.577\ H$, a three percentage point increase compared with Exercise 8.1. Thus, unless there are other requirements for the introduction of Wall B, this could be omitted from the shear system. It is the reason that many shear wall structures have just one large panel wall at each end.

Exercise 8.3

Repeat Exercise 8.1, but omitting Wall C, and comment on the effectiveness of this new arrangement.

Solution
Taking moments about wall A:

$(39 - 12)\ H_B = (57.0/2 - 12)\ H$
Then $H_C = 0.611\ H$
This is a significant increase over the value 0.096 H in Exercise 8.1, particularly for such a small wall. Because the two-wall system is independent of the size of the wall, then the location of the wall should be consistent with its size, i.e. place larger walls near the centroid of the pressure.

Exercise 8.4 Distributions in buildings of different height

Calculate the horizontal forces in each of the shear walls in the y-direction for the braced structure shown in Figure 8.11. Block A is four storeys tall, while Block B is six storeys and contains a 3×3 m lift and a 3 m high lift-motor room. Each floor-to-floor level is 3.0 m.

Given that the design ultimate wind pressure is 0.8 kN/m^2, that the total characteristic uniformly distributed permanent and imposed actions are equivalent to 6 kN/m^2 and 5 kN/m^2 plan area respectively, determine the maximum horizontal shear force, and the maximum average shear stress in the walls.

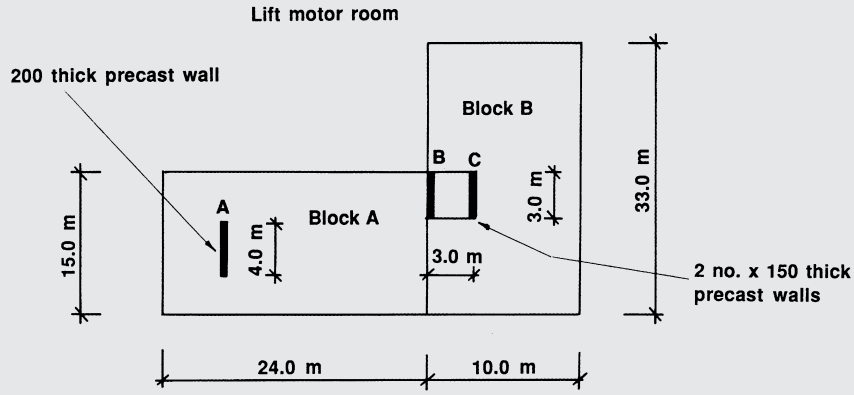

Figure 8.11 Details for Exercise 8.4.

Solution

Step 1: Calculations for determining wall stiffnesses

$I \propto L^3$, because t, f_{ck} and E {t, f_{cu} and E} are all constant.

Taking the origin for $x = 0$ at the left-hand side, calculate the wall stiffness. Using the block-by-block approach, and selecting the left-hand end of the building as zero datum, we have the following:

Wall reference	Relative I	x	Ix	$a = x - \bar{x}$	Ia	Ia^2
A	12.80	6.000	76.80	7.57	96.92	733.9
B	4.05	24.075	97.50	10.50	42.54	446.8
C	4.05	27.000	109.35	13.43	54.38	730.2
Total	20.90		283.65			1910.9

$$\text{Shear centre distance} = \bar{x} = \frac{283.65}{20.9} = 13.57 \text{ m}$$

Step 2: Considering ultimate wind pressure:

Total area of face of building in y-direction = $(24 \times 12) + (10 \times 18) + (3 \times 3) = 477\,\text{m}^2$

Design wind pressure, $H = 0.8 \times 477 = 381.6\,\text{kN}$

$$\text{Centroid of wind pressure} = \bar{x} = \frac{(288 \times 12) + (180 \times 29) + (9 \times 25.5)}{477} = 18.67 \text{ m from LHS}$$

$$e = 18.67 - 13.57 = 5.10 \text{ m}$$

Step 3: Considering eccentric load

Total floor area = $(4 \times 24 \times 15) + (6 \times 10 \times 33) + (1 \times 9) = 3429\,\text{m}^2$

$0.5\%\ (G_k + Q_k)$

$$= \frac{0.5 \times (1.35 \times 6 + 1.5 \times 5) \times 3429}{100} = 267.5\,\text{kN}$$

< wind load

$1.5\%\ G_k = 1.5 \times 6 \times 3429/100 = 308.6\,\text{kN}$

< wind load

The fraction of the total force, and the design shear force in each of the walls, are as follows:

Wall A $$H_A = \left(\frac{12.8}{20.9} + \frac{5.10 \times 96.92}{1910.9}\right) H = 0.353H = 135.0\,\text{kN}$$

Wall B $$H_B = \left(\frac{4.05}{20.9} + \frac{5.10 \times 42.54}{1910.9}\right) H = 0.307H = 117.3\,\text{kN}$$

Wall C $$H_C = \left(\frac{4.05}{20.9} - \frac{5.10 \times 54.38}{1910.9}\right) H = 0.339H = 129.3\,\text{kN}$$

The average maximum shear stress in each wall is given by H/Lt as follows:

Wall A $$\tau_A = \frac{135.0 \times 10^3}{200 \times 4000} = 0.169\,\text{N/mm}^2$$

Wall B $$\tau_B = \frac{117.3 \times 10^3}{200 \times 3000} = 0.261\,\text{N/mm}^2$$

Wall C $$\tau_C = \frac{129.3 \times 10^3}{200 \times 3000} = 0.287\,\text{N/mm}^2$$, which is the maximum.

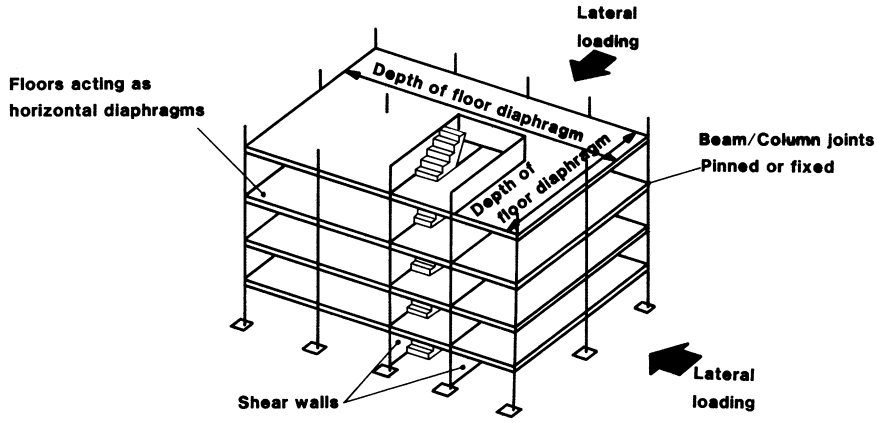

Figure 8.12 Horizontal load transfer in hollow-core floor slab.

8.3 Horizontal Diaphragm Action in Precast Concrete Floors without Structural Toppings

8.3.1 Background

The use of structural toppings in hollow-core flooring systems has long been a controversial issue, with the main emphasis of the debate centred not around the vertical strength and stiffness characteristics of the floor, which are well documented, but on the horizontal behaviour of the floor acting as a plate or diaphragm, as shown in Figures 8.12 and 8.13.

This debate has in part resulted from a lack of conclusive evidence of the real behaviour of the precast floor diaphragm, and a lack of understanding of the shear transfer mechanism between two precast units. The joint publication in Britain by the ICE and IStructE [8.9], specified:

> *In general it is advisable to use structural topping on precast floors, so that the risk of cracking in the screed and finishes is minimised and the diaphragm action of the floor is ensured. This topping should include light fabric reinforcement.*

There was conflicting opinion as to the need for an *in situ* reinforced concrete structural topping to provide the necessary diaphragm action in the floor plate. Floor screeds of more than about 30 m length require contraction joints to avoid cracking due to shrinkage. This will create occasional planes of weakness, where the shear must only be transferred through the precast slab. Research is looking at the use of steel-fibre reinforced concrete for use in thinner (30 mm maximum) and larger-area screeds. Staggered joints may be used in wider buildings, but these joints could be a crucial factor in certain situations. Structural toppings are known to be costly and time-consuming, and to counter the advantages inherent in a precast solution. However, their continued use has been based on the lack of understanding of an adequate shear transfer mechanism between adjacent hollow-core floor units, which are joined together on site by placing reinforced concrete infill at the ends of the precast units and *in situ* grout or small-aggregate concrete between them.

The precast industry was faced with having to justify the use of a wholly precast hollow-core floor diaphragm, but with no evidence of its actual behaviour. To add further confusion to the matter the Institutions' *Manual* was later revised to state that structural toppings were *not* necessary. In the

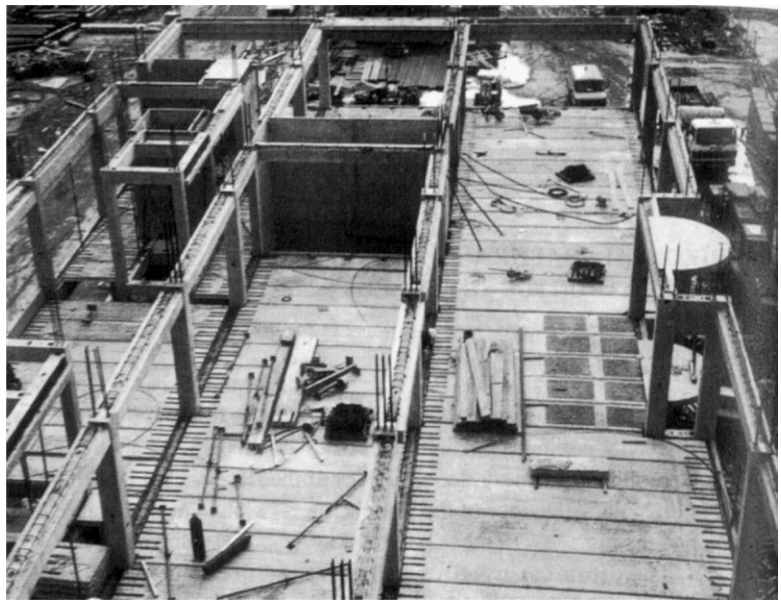

Figure 8.13 Multi-bay hollow-core floor prepared for *in situ* concrete ring beams to complete the diaphragm (courtesy of Reinforced Concrete Council).

meantime, however, considerable resistance to the use of an unscreeded precast floor was encountered by the precast industry. A library computer search carried out found fewer than six directly related publications (e.g. [8.10, 8.11]) and, prior to 1988, the only attempt to study the behaviour of a complete floor diaphragm using this type of proprietary unit was by Stroband and Kolpa (at 1/5 scale) [8.12], Sarja [8.13] and Svensson *et al.* [8.14]. Since then Stroband [8.15] has carried out some finite element work and Menengotto [8.16, 8.17] has done some experimental studies on undulating edge profiles, to try to clarify how the precast diaphragm actually works.

Diaphragm action is not considered without a structural topping in floors comprising precast double-tee slabs where the maximum depth of flange is 50 to 75 mm. Although double-tee slabs are intermittently welded together longitudinally and at their ends to beams (see Section 5.3.2), which would provide the necessary shear and tensile forces in the plate, diaphragm action is not considered in large floors because of the inability to generate the compression or maintain a uniform centroidal axis across contiguous floor panels. Secondly, it would not be wise to rely entirely on short welded connections for structural integrity.

Similarly, diaphragm action is not considered in unscreeded precast beam-and-block flooring for the obvious requirement of achieving shear transfer through the infill blocks. Diaphragm action is considered as being fully effective in the precast composite plank types of floor (Figure 5.1(d) and (e)), with no additional measures being taken other than to check the shear strength of the diaphragm at the critical positions, e.g. close to large voids, or narrow floor widths.

8.3.2 Details

The most important feature for ensuring horizontal diaphragm action in a hollow-core floor slab is the edge profile, shown in Figure 5.11. The edge is not made deliberately rough, but the drag of the casting machine on the semi-dry mix creates a surface roughness vital to diaphragm action. These units have edge profiles that permit the placement of *in situ* concrete in the longitudinal joints between adjacent units. Although different grades of *in situ* concrete are used in practice, the lowest strength is usually C20/25 (see Table 4.3). Despite a slight roughening of the edges during the manufacturing process, these joints may be considered plain (i.e. uncastellated) and unreinforced.

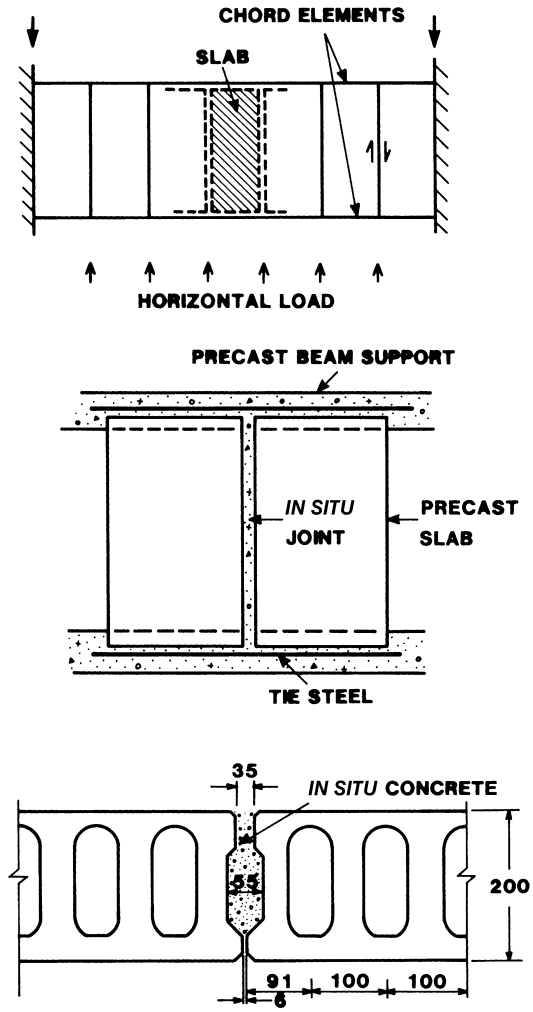

Figure 8.14 Shear transfer in longitudinal joints between hollow-core slabs.

It is also essential that the width of the gap between the units is large enough to permit the placement of properly compacted *in situ* concrete (or a sand/cement grout). Manufacturers have responded to this requirement in the last ten years by increasing the size of the former at the top edges of the units from about 10 to 20 mm (see Figure 5.11). This improved profile is also beneficial in the lateral distribution of vertical shear forces, moments and deflections. The integrity of the floor system in the vertical plane ensures the success of the floor acting as a horizontal diaphragm.

Thus the precast floor unit has large in-plane stiffness, and the flexural deformations between the discrete precast slabs are small. The design of a diaphragm is therefore essentially a joint design problem, as illustrated in Figure 8.14. The essential features in the construction of a typical hollow-core floor are:

- The precast units should be placed side by side such that there is no 'appreciable' gap between the units to allow shear-tension failure in the unreinforced *in situ* concrete. The size of this gap is not consistent, but its existence is thought to alter the shear failure mechanism by allowing diagonal tension to develop across gaps of more than 60 mm [8.18].

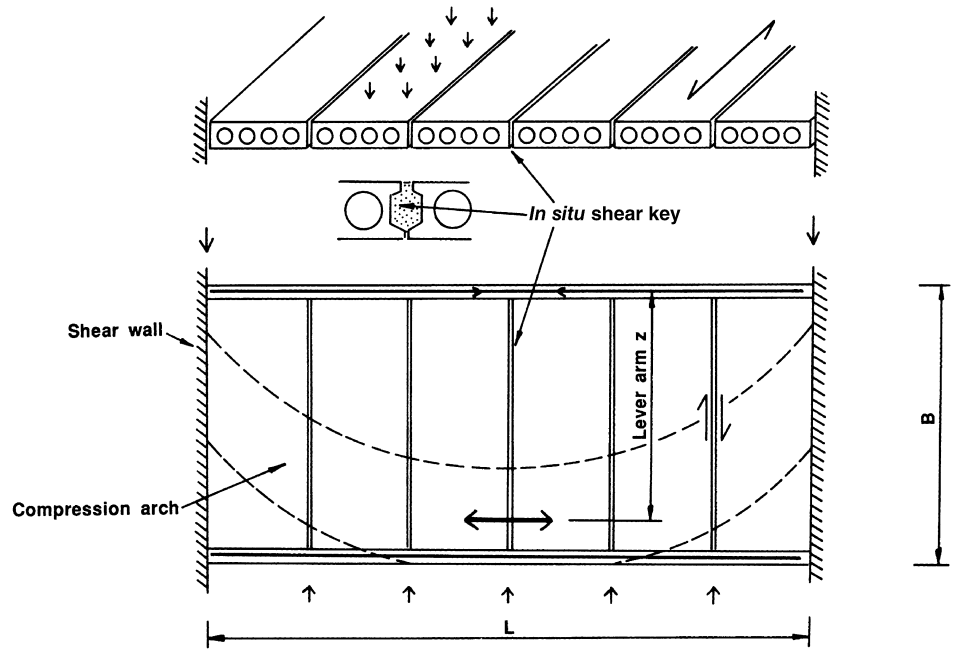

Figure 8.15 Peripheral tie steel is also used to ensure diaphragm action.

- Lateral tie steel, in the form of a continuous piece of 7-wire helical prestressing strand, or lapped high-tensile deformed bar, is placed into a narrow (typically 50–80 mm wide) *in situ* concrete strip between the ends of the flooring units and supporting beams. This reinforcement, shown in Figure 8.15, which is actually provided for stability purposes, provides the necessary tie forces required to prevent the precast slabs from moving apart sideways.
- L- or U-shaped shear friction bars are placed into *in situ* concreted slots formed in the broken-out cores (sometimes referred to as 'milled slots') of the hollow-core units, or placed into the longitudinal joints between the units. These bars also prevent longitudinal shrinkage movement, particularly if the precast slabs have been delivered to site at an early age, say three days. Shrinkage movements of 2–3 mm per 10 m-long slab has been seen where the slabs were seated, but not tied to the supporting member.

8.3.3 Structural models for diaphragm action

Horizontal loads due to wind (or earthquakes) are transmitted to shear walls or moment-resisting frames by considering the roof or floor, comprising individual precast concrete units, as a deep horizontal beam, truss or girder (see Figure 8.16). The structural walls or frames are supports for this analogous beam and the lateral loads are transmitted to these supports as reactions H_n in Eq. (8.4) and/or (8.5). The magnitude of the shear force at the wall may therefore be determined. The effective depth of the diaphragm is equal to the depth of the floor slab, and the parts of beams that are below the floor plate are ignored.

Various structural models have been proposed for the shear transfer mechanism, but the most critical situation is where the floors span parallel with the supporting shear walls. The web shear must also be transferred to the chord elements, i.e. the reinforced concrete edge or spine beams spanning perpendicular to the floor units. This is commonly known as horizontal 'Vierendeel girder action', in which the Vierendeel frame components are simulated by *in situ* concrete strips peripheral to the precast slab units. In longer floors, where the length-to-breadth ratio *L/B* is greater than about 5 or

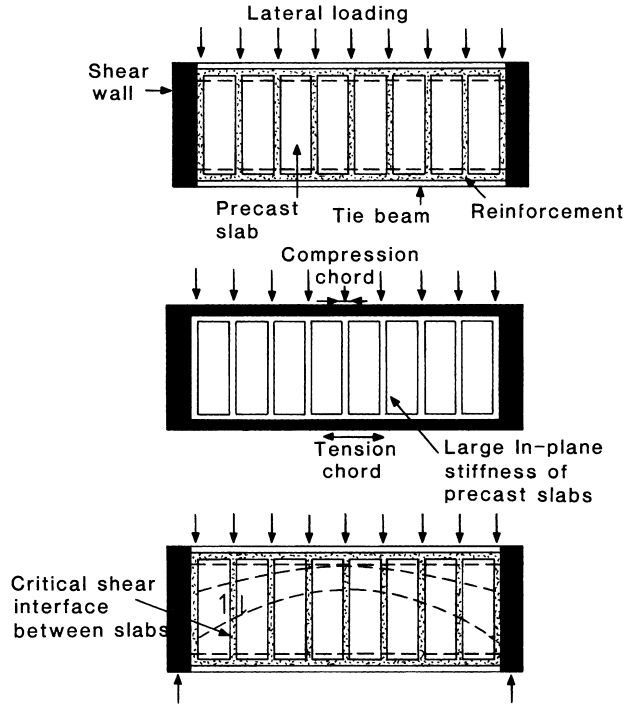

Figure 8.16 Structural models for floor diaphragm action.

6, the structural mechanism is probably closer to a deep beam than a Vierendeel girder. However, the problem is always one of shear transfer in the joints, irrespective of the assumed model.

Equilibrating shear parallel with the supporting beam is determined using any statical method. In multi-bay floors, where the slabs are spanning parallel to the direction of the applied load, as in Figure 8.17(a), the shear V_h at interior support between span L_1 and L_2 is given by:

$$V_h = \frac{VS}{I} = \frac{6V(B - L_1)L_1}{B^3} \tag{8.6}$$

for L_1 and L_3, where S and I are the first and second moments of the area above the interface.

Where the slabs are spanning perpendicular to the direction of the applied load, Figure 8.17(b), the maximum transverse shear between the slabs V_h occurs at the neutral axis and is given by:

$$V_h = \frac{VS}{I} = 1.5V \tag{8.7}$$

The shear force V_h is carried by dowel action using shear friction reinforcement, often called 'coupling bars', as indicated in Figure 8.18 [8.19]. The purpose of these bars is to transfer shear, caused by small, lateral, rigid-body translations in the slab, into the chord elements. A tie force is thus generated in the reinforcement in the beam and/or *in situ* perimeter strip. It is becoming increasingly popular to reinforce the *in situ* perimeter strip using 7-wire helical prestressing strand. The favourable mechanical properties of this type of strand and long lengths available on site make it an attractive alternative to high-tensile bar.

The ties prevent the slabs from moving apart and simultaneously generate the clamping forces that create the friction so essential to diaphragm action. In this manner, all the requirements specified

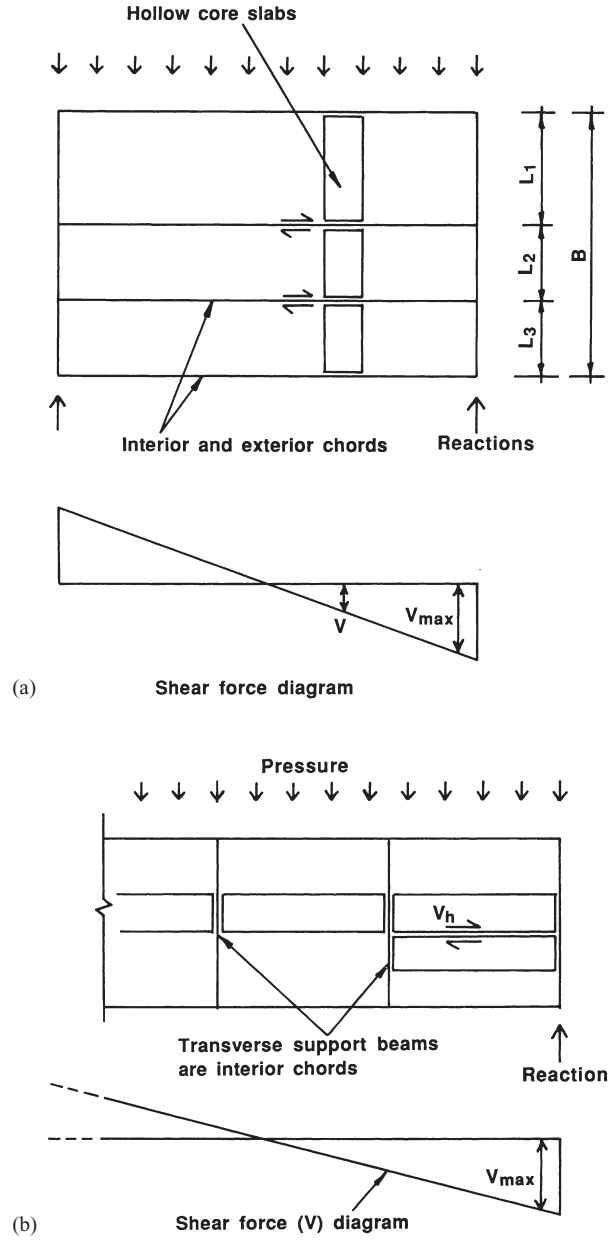

Figure 8.17 Shear forces along internal beams in floor diaphragm. (a) Slabs spanning parallel to wind loading and (b) slabs spanning perpendicular to wind loading.

in BS EN 1992-1-1, clauses 10.9.3(12) and 10.9.7 [8.5] and BS 8110, Part 1, clause 5.3.7(a) [8.6] are satisfied thus:

> *. . . the diaphragm should form part of a realistic structural model . . . transverse reinforcement for shear transfer across connections may be concentrated along supports, forming ties consistent with the structural model . . . for smooth and rough surfaces* (BS EN 1992-1-1), and *. . . these should be restrained to prevent their moving apart. No reinforcement need be provided in or across the joint, and the sides of the units forming the joint may have a normal finish . . .* (BS 8110).

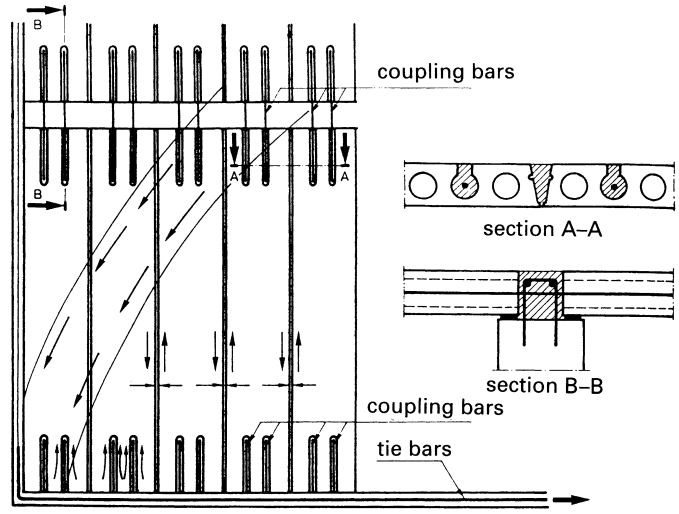

Figure 8.18 Tie bars cast into floor slots act as complementary shear friction reinforcement at the ends of the slabs [8.19].

An ultimate interface shear stress of 0.15 N/mm^2 {0.23 N/mm^2} is therefore used in design. The design clauses in the codes are based on work carried out by Mast [8.20]. In computing the magnitude of the interface shear stress $\tau = V/BD$, the depth of the unit can only be taken to the depth of the *in situ*–precast interface, i.e. $D - 30$ mm in most types of hollow-core slab. The reason for this derives from observations made of the compaction of the concrete in the joint. It is observed that grout loss occurs in the bottom of the joint and that the lower 10 to 15 mm is not grouted. Also, the lip at the bottom of the units prevents full penetration. The value also recognises that differential camber will be present, further reducing the net contact depth.

The interfaces between the hollow-core units and the *in situ* joint concrete are most likely to be the planes of cracking. Cracks occur owing to the shrinkage of the *in situ* concrete, or by the restraint in the precast floor system. In practice, cracks up to 1 mm wide have been found, shown in Figure 8.19, and it is assumed that in the majority of practical cases cracks exist in the joints between precast floor units. This is obviously detrimental to the shear transfer behaviour of the floor slab and as such the shear must be transferred in cracked concrete. In this case the shear resistance is a combination of [8.21–8.23]:

- aggregate interlock in cracked concrete, by wedging action and shear friction
- dowel action through bar kinking and shear capacity
- axial restraint stiffness provided by reinforcement perpendicular to the cracks, as shown in Figures 8.15 and 8.20.

If the shear force V and the shear slip δ in Figure 8.20 are plotted out, the relationship would be something like the graph in Figure 8.21(a). The gradient of the V-δ curve gives the stiffness K_s. Similarly, as the shear force is applied to the cracked interface, the two halves of the specimen would begin to move apart a distance given by c_w (as this is in fact a crack width). The relationship between δ and c_w is shown in Figure 8.21(b).

Shear strength and stiffness are provided by aggregate interlock, and the structural integrity by dowel action of the reinforcing bars crossing the cracked interface. Aggregate interlock may be separated into two distinct phases – namely 'shear wedging', where the inclined surfaces either side of the crack are in contact, and shear friction, where the contact surfaces are being held in contact by the

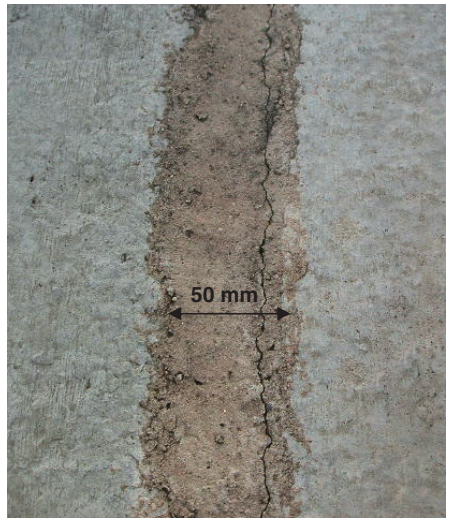

Figure 8.19 Shrinkage cracks in the *in situ* mortar-filled longitudinal joint between prestressed hollow-core floor units. Crack width varied from 0.35 to 1.15 mm wide, on average about 0.5 mm.

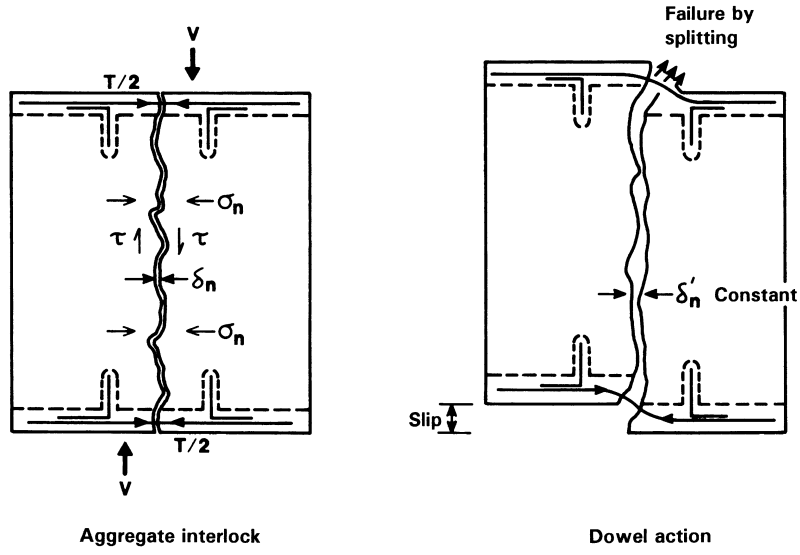

Figure 8.20 Shear transfer mechanisms of aggregate interlock and dowel action between discrete precast units.

normal stress. Shear wedging provides a very high resistance, but cannot be relied upon for very long if the interface cracks are wide.

As the crack width increases, tensile forces T are mobilised in the reinforcing bars, as shown in Figure 8.21(c). To understand this, a simple analogy is to slide one's knuckles of the hand over each other with an elastic band stretched around the fists. As the knuckles slide, the elastic band tightens and the resistance to movement increases. This is the shear mechanism that is active in a hollow-core floor diaphragm.

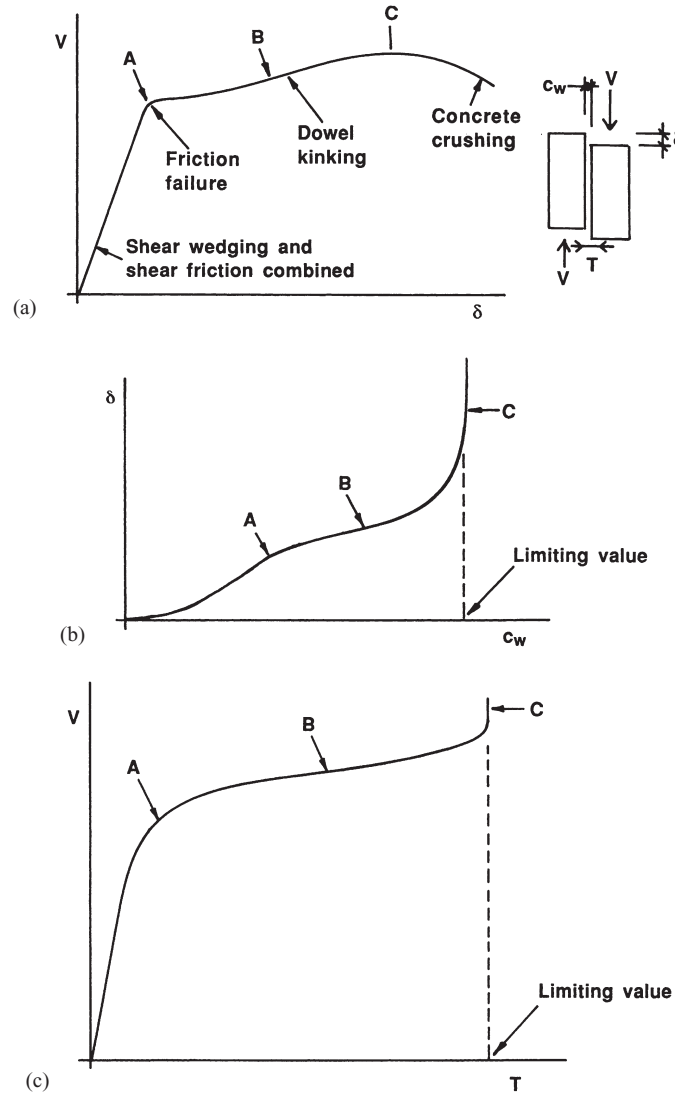

Figure 8.21 Idealised relationships in longitudinal slab joint. (a) Shear force versus shear slip, (b) shear force versus crack width; (c) shear force versus transverse tie force.

Cholewicki has developed a mathematical model to predict the strength and stiffness of the longitudinal joint between hollow-core units, based on shear friction and dowel action hypotheses [8.24]. Given this tool and a set of geometric and material properties, it is possible to predict shear behaviour by calculating the stiffness K_s and the strength V.

The floor plate is also subjected to horizontal bending where, as shown in Figure 8.15, internal equilibrium is maintained by tension and compression chords. The tie force $T = M_h/z$, where M_h is the applied diaphragm moment and z the lever arm. z depends on the aspect ratio for the floor, and on the magnitude of the bending moment. Maximum values for z/B at the points of maximum bending are as follows [8.25]: for $B/L < 0.5$, $z/B = 0.9$ and for $0.5 < B/L < 1.0$, $z/B = 0.8$.

Walraven [8.26] proposes a constant value for $z/B = 0.8$. BS EN 1992-1-1 does not restrict consideration of the floor plate as a normal rectangular bending section.

Where the aspect ratio $B/L > 1$, the behaviour will be closer to the strut-and-tied arch model than either the deep beam or truss models. The tie force is then given by:

$$T = \frac{0.5V}{B/LI} \tag{8.8}$$

as a diagonal compressive strut develops across the floor.

8.3.4 Diaphragm reinforcement

The maximum horizontal bending moment M_h is calculated from the equilibrium of external wind pressures and the reactions from the shear walls, obtained from Eq. (8.4). Referring to Figure 8.15 and given that the breadth of the diaphragm is B, the diaphragm reinforcement A_{hd1} to be positioned in the chord elements over the tops of the beams at the ends of the floor slab is determined with reference to Figure 8.15 from the following expression:

$$A_{hd1} = \frac{M_h}{z \times 0.87 f_{yk}} \tag{8.9}$$

where z is the lever arm of the slab as a normal rectangular bending section, with a minimum value of 0.76B.

$$A_{hd1} = \frac{M_h}{0.8B \times 0.87 f_y} \tag{8.9}$$

where the term $0.8B$ is the lever arm between the compressive zone and the diaphragm steel

A_{hd} should not exceed:

$$A_{hd1} = \frac{0.85/1.5 \times f'_{ck} \times 0.4dB}{0.87 f_y} \tag{8.10}$$

$$A_{hd1} = \frac{0.45 f'_{cu} \times 0.4dB}{0.87 f_y} \tag{8.10}$$

where d is the depth of the precast floor slab = $D - 30$ mm, and f'_{cu} is the strength of the *in situ* grout (or concrete) in the longitudinal gaps between the floor units. The 30 mm subtraction is applicable to hollow-core and other types of floor unit that have a lip at the bottom edge, which prevents the infill grout from penetrating the full depth of the floor slab. It also allows something for the differential camber often seen between adjacent prestressed units.

It is necessary to collect the floor diaphragm tie steel A_{hd1} in the chord elements. This may be achieved as follows:

- By utilising the reinforcement already provided in the chord elements, such as edge beams, and by providing a positive non-slip tie between the beams. This tie may be continuous through the column, as shown in Figure 7.68(a) for the billet connector, or may be provided as shown in Figure 7.68(b) by using steel dowels in shear.
- By placing tie steel additional to the steel provided in the chord members. (This steel may also be used as part of the stability tie steel determined in Section 9.4.) Some designers prefer to pass the reinforcement through small holes in the column. Alternatively if the beam is wider than the column, the bars are placed symmetrically on either side of the column.

Diaphragm reinforcement may be curtailed according to the usual rules governing lap lengths and anchorage. In many cases the point of maximum shear will coincide with minimum bending and therefore the full length of the slab B may be used in computing the average value for τ. However, where the maximum moment and shear coincide, the breadth of the diaphragm is reduced to z to allow for the decay in shear stress in the compression zone. Thus with Nmm units:

$$\tau = \frac{V}{x(D-30)} < 0.15\ \text{N/mm}^2 \qquad (8.11)$$

$$\tau = \frac{V}{x(D-30)} < 0.23\ \text{N/mm}^2 \qquad (8.11)$$

If τ exceeds this value, the shear force must be resisted by shear reinforcement placed across the ends of the slabs, as explained above. The steel area A_{hd2} is given in BS EN 1991-1-1, clause 6.2.3(3) [8.5] or BS 8110, Part 1, clause 5.3.7.(d) [8.6] as follows:

$$A_{hd2} = \frac{V}{z \times 0.87 f_{yk} \tan a_f} \qquad (8.12)$$

$$A_{hd2} = \frac{V}{0.6 \times 0.87 f_y \tan a_f} \qquad (8.12)$$

where $\tan(a_f)$ is the coefficient of friction, as given in BS EN 1992-1-1, clause 6.2.5(2) [8.5] {Table 5.3 of BS 8110 [8.6]}. Hollow-core slabs are considered as being untreated and smooth, and $\tan(a_f)$ = 0.6 {= 0.7}. Thus:

$$A_{hd2} = \frac{1.9167V}{zf_{yk}} \qquad (8.13)$$

$$A_{hd2} = \frac{2.737V}{f_y} \qquad (8.13)$$

Thus the total steel $A_{hd} = A_{hd1} + A_{hd2}$ may be determined. The minimum tie steel A_{hdmin} (mm^2) is provided as a perimeter tie and given as follows:

$$A_{hdmin} = \frac{(20 + 4n_o) \times 10^3}{f_{yk}} \qquad (8.14)$$

with f_{yk} in N/mm^2, and n_o the number of storeys.

$$A_{hdmin} = \frac{(20 + 4n_o) \times 10^3}{f_y} \qquad (8.14)$$

with f_y in N/mm^2, and n_o the number of storeys.

Exercise 8.5 Diaphragm reinforcement in floor slab

If the ultimate horizontal wind pressure acting on the floor slab used in Exercise 8.1 is 4 kN/m, calculate the maximum horizontal bending moment and shear force, and determine the floor diaphragm reinforcement. Check that the interface shear stress is no greater than the design value given in BS EN 1992-1-1 {BS 8110}. The overall depth of the precast floor slab is 150 mm. Choose a suitable position to curtail the chord reinforcement.

Use grade C20/25 concrete for the *in situ* infill, and f_{yk} {f_y} = 500 N/mm^2.

Assume five-storey height edge columns are 300 mm square and cover is 35 mm.

Solution

Step 1: At the point of maximum moment

Total wind force = 4 × 57 = 228 kN.

Wall reactions from Exercise 8.1 enable the horizontal shear force and bending moment diagrams to be drawn, as shown in Figure 8.22.

At point A in Figure 8.22, where the moment is maximum and the shear is zero:

$d = 6000 - 300 - 35 = 5665$ mm

$$k = \frac{449.4 \times 10^3}{150 \times 5665^2 \times 20} = 0.00467$$

Flexural lever arm

$$z = 5665(0.5 + \sqrt{0.025 - 0.88235 \times 0.00467}) = 5.641\ \text{m}$$

$$F_s = \frac{M_{max}}{z} = \frac{449.4}{5.641} = 79.7\ \text{kN}$$

$$A_{hd1} = \frac{79.7 \times 10^3}{0.87 \times 500} = 184\ \text{mm}^2$$

Flexural steel lever arm $z = 0.8 \times 6.0 = 4.8$ m

$$F_s = \frac{M_{max}}{z} = \frac{449.4}{4.8} = 93.62\ \text{kN}$$

$$A_{hd1} = \frac{93.62 \times 10^3}{0.87 \times 500} = 216\ \text{mm}^2$$

Use three H12 rebars continuous reinforcement.

Check compression in the *in situ* concrete, where the depth of the floor slab = D − 30 mm

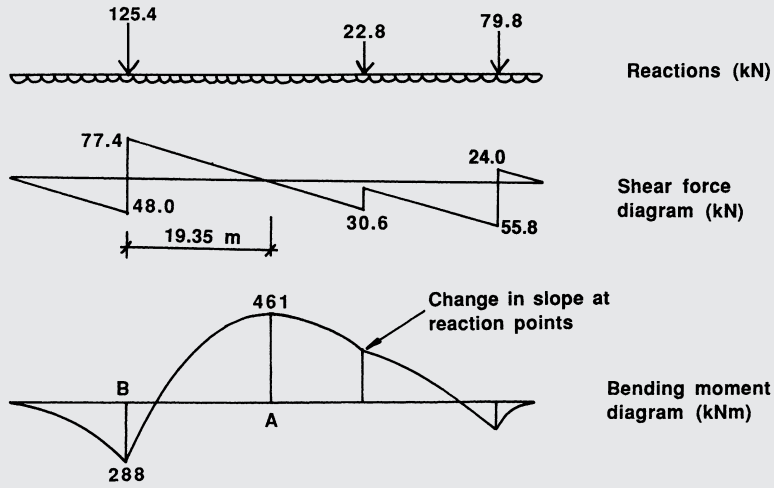

Figure 8.22 Details for Exercise 8.5.

$F_c = 0.85/1.5\, f_{ck}\, d\, 0.4B$
$= 0.85/1.5 \times 20 \times (150 - 30)$
$\times 0.4 \times 5665 \times 10^{-3}$ $= 3081\,\text{kN}$
$> 96.04\,\text{kN}$ required, OK.

$F_c = 0.45\, f_{cu}\, d\, 0.4B$
$= 0.45 \times 25 \times (150 - 30) \times 0.4 \times 6000 \times 10^{-3}$ $= 3240\,\text{kN}$
$> 96.04\,\text{kN}$ required, OK.

Step 2: With maximum shear combined with moment
At point B:

$$F_s = \frac{M_{max}}{z} = \frac{288}{5.641} = 51.1\,\text{kN} \qquad A_{hd1} = \frac{51.1 \times 10^3}{0.87 \times 500} = 118\,\text{mm}^2$$

$$F_s = \frac{M_{max}}{z} = \frac{288}{4.8} = 60.0\,\text{kN} \qquad A_{hd1} = \frac{60.0 \times 10^3}{0.87 \times 500} = 138\,\text{mm}^2$$

Check compression in the *in situ* concrete, where the effective depth of the floor slab

$t = D - 30\,\text{mm}$ and
$z = 5641\,\text{mm}$.
$F_c = 0.85/1.5\, f_{cu}\, d\, 0.4B$
$= 0.85/1.5 \times 20 \times (150 - 30)$
$\times 0.4 \times 5641 \times 10^{-3}$
$= 3069\,\text{kN} > 60.0\,\text{kN}$ required, OK.
Shear stress at B:

$$v_{ave} = \frac{76.8 \times 10^3}{120 \times 5641} = 0.113\ \text{N/mm}^2$$

$< 0.15\,\text{N/mm}^2$ permissible

$t = D - 30\,\text{mm}$ and
$z = 4800\,\text{mm}$.
$F_c = 0.45\, f_{cu}\, d\, 0.4B$
$= 0.45 \times 25 \times (150 - 30) \times 0.4 \times 4800 \times 10^{-3}$
$= 2592\,\text{kN} > 60.0\,\text{kN}$ required, OK.
Shear stress at B:

$$v_{ave} = \frac{76.8 \times 10^3}{120 \times 4800} = 0.134\ \text{N/mm}^2$$

$< 0.23\,\text{N/mm}^2$ permissible

Hence $A_{hd2} = 0$
Use two H12 bars.

Step 3: Chord reinforcement:

$$A_{hdmin} = \frac{40000}{500} = 80\,\text{mm}^2$$

Use one H12 bar ($113\,\text{mm}^2$) minimum.

Hence steel may be curtailed when $M = 0.87 \times 113 \times 500 \times 4800 \times 10^{-6} = 236\,\text{kNm}$. The position may be obtained from the bending moment diagram, at 10.86 and 43.85 m, say 10.4 and 44.3 m with anchorage bond lengths. (It is quite likely that the designer would choose to continue the three bars along the full length of the building, to avoid confusion and the possibility of misplacing the reinforcement.)

8.3.5 Design by testing

There has been extensive experimental work describing the shear transfer mechanism in cracked reinforced concrete, and the formulation of some basic relationships between the dominant material and geometrical effects that are based mainly on experiments using small specimens [8.27, 8.28]. However, there is a lack of experimental data on the monotonic and/or cyclic behaviour of large-scale units, and on the correlation between the small-scale testing and the full-sized diaphragm.

Tests carried out by Omar, Elliott and Davies [8.29–8.31] on full-scale, 200 mm-deep hollow-core units, shown in Figure 8.23, found that the attainable horizontal shear stress in the floor slab exceeded the permissible design stress for unreinforced, uncastellated joints. The laboratory tests were carried out in a 'realistic environment' regarding materials specification, geometry and on-site practice.

The results have shown interface shear stresses are in excess of the working load by a factor of at least 2.15, despite the presence of initial cracks in the interface of up to 0.55 mm wide. The working load is calculated by multiplying the working stress by the net contact area in the longitudinal joint. The working stress is defined as the ultimate shear stress of $0.15\,N/mm^2$ divided by γ_f of 1.5 {$0.23\,N/mm^2$ divided by γ_f of 1.4} for wind loading. Clamping forces normal to the precast units resulted in coefficients for the ratio between shear wedging and shear friction T/V of at least 5.

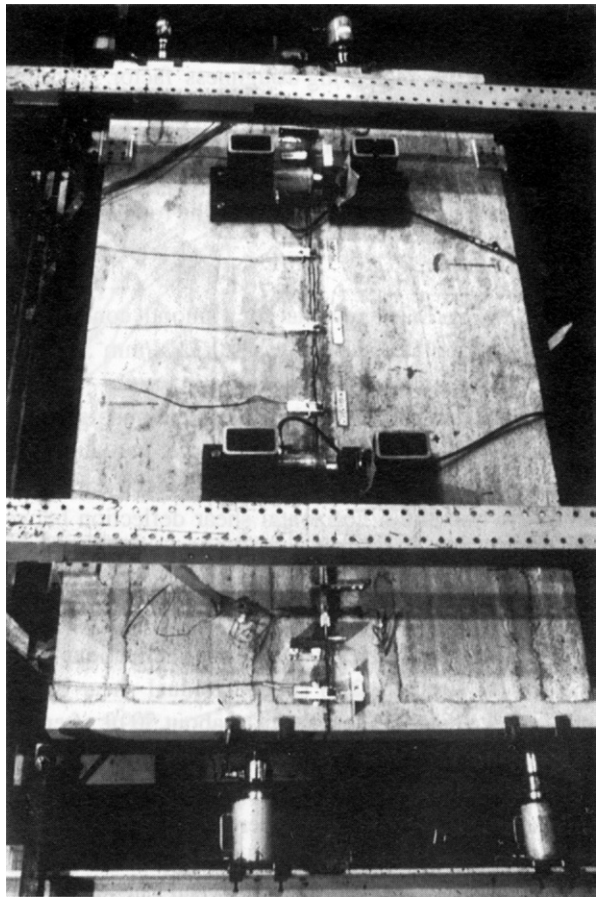

Figure 8.23 Experimental set up by Omar. (The precast floor slabs were manufactured by Bison Floors Ltd, UK.)

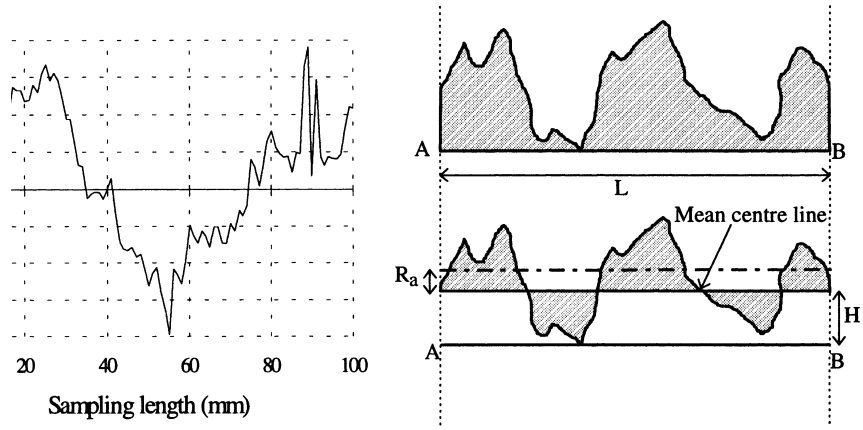

Figure 8.24 Tracing of surface roughness in the sides of proprietary hollow-core floor units.

It is also known that the behaviour of the interface depends on the roughness of the sides of the precast units. Physical measurements have been made on factory-produced units to quantify this parameter [8.32]. The surface roughness is measured using an instrument placed onto the sides of slipformed units to measure roughness along a sampling length of 100 mm, as shown by the plot in Figure 8.24. The roughness factor R_a is determined in accordance with BS 1134 [8.33] as the arithmetical mean deviation of the edge profile (in mm), which is the average value of departure of the profile above and below the mean centre line throughout the sampling length. Values for R_a in typical hollow-core production are between 0.2 mm and 0.3 mm.

Tests were carried out on slabs selected with different surface textures, in a manner similar to that shown in Figure 8.23. The specimens were grouted together in the longitudinal joint, using *in situ* concrete of 27 N/mm^2 cube strength with 10 mm aggregate. The behaviour was linear up to about ⅔ of the ultimate load. The crack width at the ultimate shear load increased with increasing roughness factor. This indicates that the interlocking mechanism is dependent on the texture of the adjacent surfaces. The peaks and valleys interlock the opposite surfaces until a critical crack width is reached, usually at about 2.5 mm, after which a shear friction failure occurs. The resulting shear stress τ_{ua} (N/mm^2) may be expressed in terms of the roughness factor R_a (mm) as follows:

$$\tau_{ua} = 0.22 + 0.207R_a \tag{8.15}$$

The results in Figure 8.25 show that for a smooth concrete surface with a roughness factor of zero, the extrapolated shear stress is 0.22 N/mm^2, i.e. just less than the BS EN 1992-1-1 [8.5] value of 0.15 N/mm^2 with an appropriate load factor of 1.5, and the BS 8110 [8.6] design value of 0.23 N/mm^2.

Designers also assume that the floor plate undergoes negligible shear deflection, i.e. the longitudinal shear stiffness is very large. In reality it is in the order of K_s = 500 kN/mm to 1000 kN/mm for 4 m long × 200 mm deep slabs [8.30]. Based on this experimental evidence, the maximum horizontal shear deflection between these slabs at a design working shear stress of up to 0.23/1.4 = 0.16 N/mm^2 would be approximately 0.02 mm. If this deflection was summed over a building length L (m), a total shear deflection at the midpoint would be 0.05L (mm).

A further deleterious factor is that shear deflections of this nature are not recoverable. Figure 8.26(a) (from [8.30]) shows residual shear deformations of between 0.1 and 0.2 mm, equivalent to a shear strain of about 50 με after several completed ultimate load cycles. However, when cycled at the working load the residual shear strain is less than 30 με (Figure 8.26(b)). Dislocations and abrasion across the tops of the asperities in cracked concrete are responsible for these permanent deformations. The resulting degradation in stiffness is about 50 per cent of the initial monotonic value.

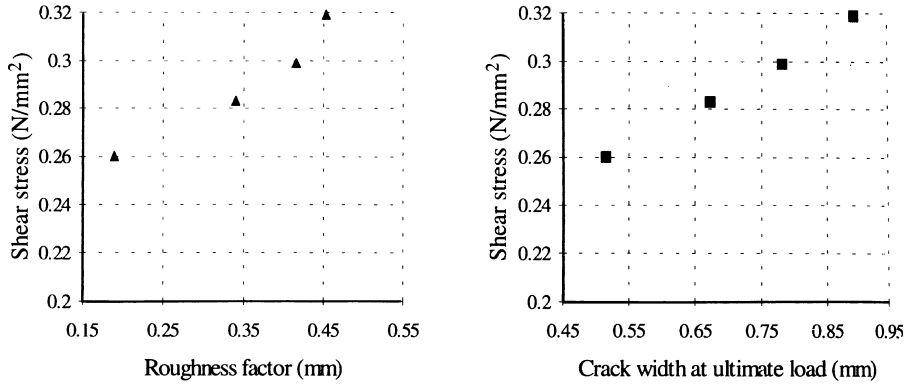

Figure 8.25 Effect of surface roughness and final crack width on interface shear stress capacity between hollow-core units.

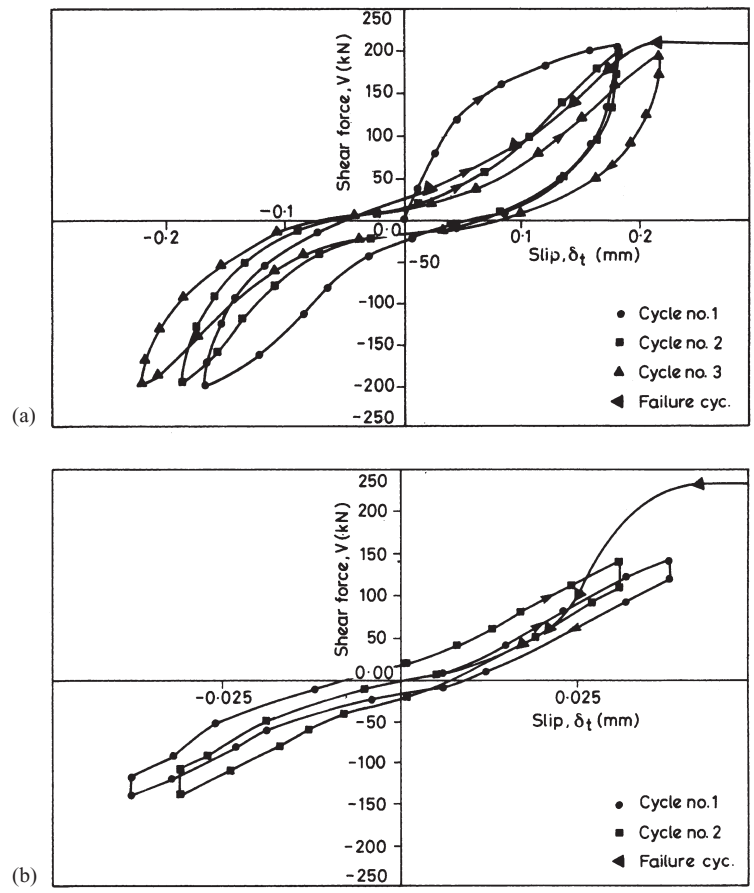

Figure 8.26 Results of cyclic load tests by Omar at Nottingham University. (a) Tested to ultimate load magnitude and (b) tested to working load magnitude. (Conversion factor: 200 kN force = 0.36 N/mm^2 stress.)

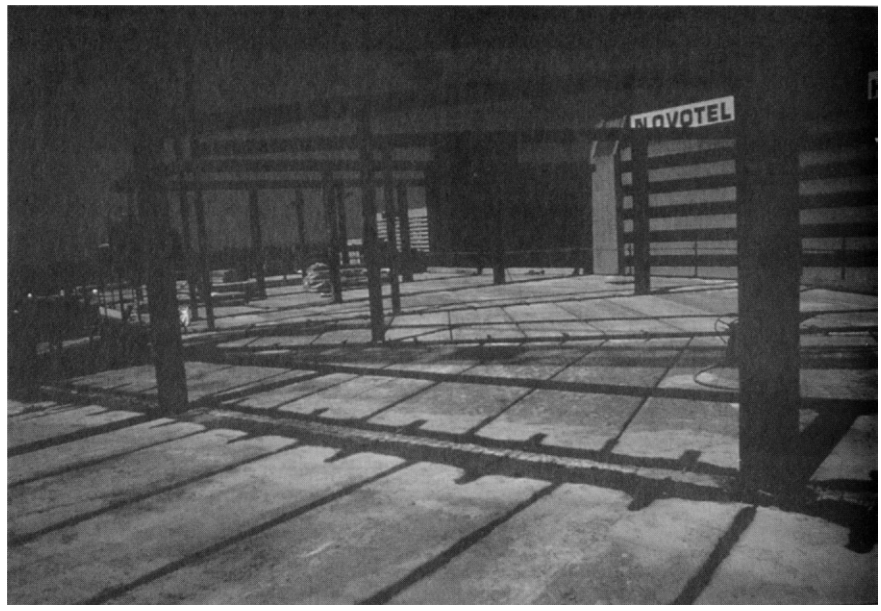

Figure 8.27 Hollow-core floor slabs used in The Ark, Hammersmith, London (courtesy of Bison Floors).

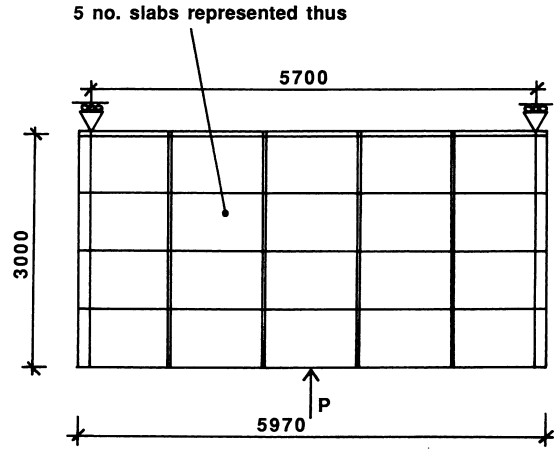

Figure 8.28 Test arrangement by Sarja [8.13].

Actual stresses at the interfaces between slabs and walls depend on the geometry of the building and the number of walls, but typical ultimate values (in the region of 0.05 N/mm^2 to 0.15 N/mm^2) are lower than the permissible design ultimate stresses. A rigorous analysis on the hollow-core floor diaphragm at the building known as 'The Ark' (at Hammersmith, London) determined maximum serviceability values of about 0.13 N/mm^2 in the longitudinal joints [8.34]. Figure 8.27 shows this form of construction.

Sarja [8.13] tested a large floor slab, shown in Figure 8.28, consisting of five 1.2 m wide × 265 mm deep hollow-core slabs. The slabs were tied together using an *in situ* ring beam containing either two 10 mm or two 16 mm-diameter rebars. The average strengths of the materials were $f_{cu} = 21$ to 24 N/mm^2 for the added concrete, and $f_y = 420$ and 475 N/mm^2 for the 10 mm and 16 mm bars, respectively. The stress distribution along the longitudinal joint in these tests is plotted in Figure 8.29.

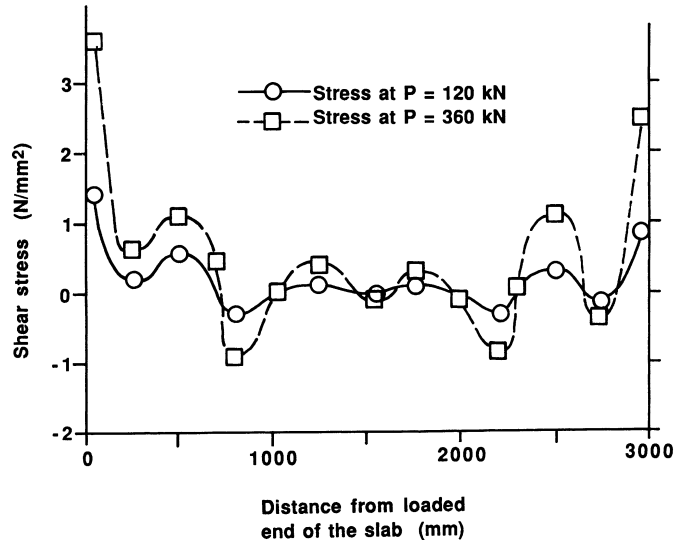

Figure 8.29 Stress distributions in longitudinal joint between hollow-core floor slabs [8.13].

Table 8.1 Test Results on Hollow-Core Floor Diaphragm in Bending and/or Shear [8.13]

Test reference	Loading regime	Tie steel bars (no. × mm)	Shear force (kN)	Average shear stress (N/mm^2)	Bending moment (kNm)
1	3 point bending	2 × 10	140	0.18	400
2			180	0.23	513
3			160	0.20	456
4			140	0.18	400
5	3 point bending	2 × 16	247	0.32	705
6			287	0.37	819
7	Pure shear	1 × 8	406	0.52	–
8			382	0.49	–

Shear tests were also carried out on pairs of slabs equal in size to the above. The tie steel in the ends of the slab was two 16 mm bars in one end and one 8 mm bar in the other end. No details are given in the report as to the effect of these differences.

The slabs were loaded in three-point bending over a span of 5.7 m (Tests 1 to 6) and pure shear (Tests 7 and 8). The resulting average shear stress and bending moment at failure are given in Table 8.1.

The results show that where the tie steel is two 10 mm-diameter bars, and the tensile strength of these bars is only 64.4 kN, the lowest recorded shear stress is 0.18 N/mm^2. Wahid Omar [8.30] found that the tensile tie capacity of the steel should be at least 115 kN in order to generate shear stresses of 0.25 N/mm^2 or greater. Sarja's results confirm this; when the tie steel force in tests 5 and 6 was at least 175 kN, the failure shear stress was 0.32 N/mm^2. The results for the pure shear tests are clearly greater than in the case of combined bending and shear.

8.3.6 Finite element analysis of the floor plate

Several attempts have been made by researchers to predict the behaviour of precast diaphragms composed of discrete elements. Early attempts to simulate behaviour were hampered by the large

number of variables to be studied, and the results resembled no more than the displacements between solid rectangular blocks connected by springs. The introduction of finite elements into structural analysis in the late 1970s enabled the modelling of both the precast concrete units and the interface between them.

The pioneering work by Sarja in 1978 [8.13] showed the early potential for these techniques, but unfortunately the input data relied heavily on known values, somewhat defeating the objective of the work. The numerical work modelled the experimental test slab shown in Figure 8.28. The most interesting result from this work was the variation of the interface shear stresses in one of the longitudinal joints. Figure 8.29 shows these distributions for three-point bending tests. The greatest values are close to the application point of the load. It is clear that these large stresses are due to compressive strut action and some arching stresses are being interpreted as shear. The reduction in shear to zero at ⅔ of the way across the slab suggests the presence of flexural cracking, although quite why the shear stress distribution increases again is unclear.

De Roo and Straman at Delft University of Technology [8.35] used the finite element package DIANA to simulate all the precast units, the longitudinal mortar joints and the transverse tie beams. Using non-linear interface slip surfaces to replicate the longitudinal shear-slip characteristics measured in tests, the relationship between the applied bending moment and the horizontal deflection of the diaphragm is shown in Figure 8.30. The deflection at the working load was about 1 mm, and the span-to-deflection ratio at failure was 1/4000. The results have shown that the floor diaphragm failed owing to yielding of the ties in the edge beam with a factor of safety of 3.13 with respect to the design strength. The compressive stresses were formed in a triangular distribution and concentrated across 2.5 m of the floor, giving a lever arm factor of $z/B = 0.97$. This suggests that the BS 8110 proposed design lever arm factor of 0.8 is very conservative and hence why it is not used in Eurocode designs.

The maximum compressive stress obtained in the modelling was 3.6 N/mm^2, and the maximum shear stress in the longitudinal joint was 0.4 N/mm^2. The final deformation pattern is shown in

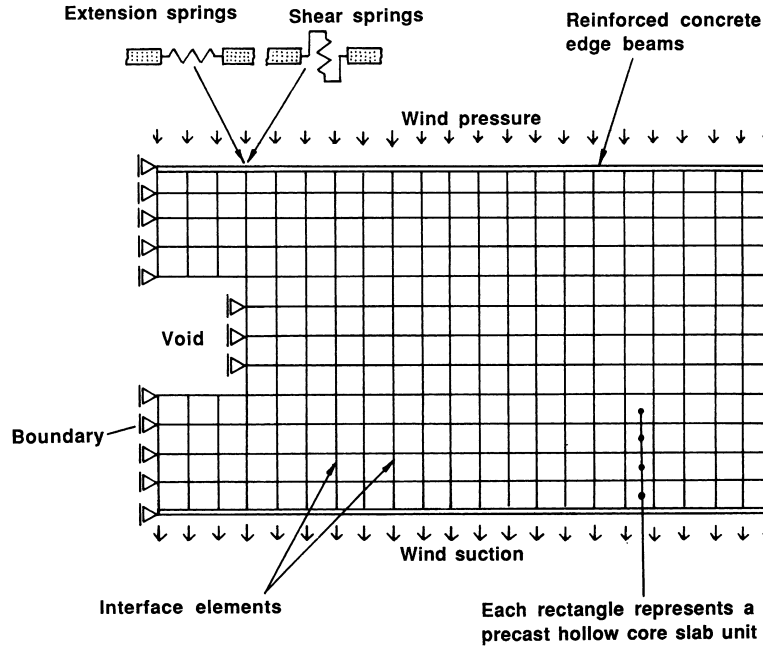

Figure 8.30 Finite element models used by de Roo & Straman [8.35].

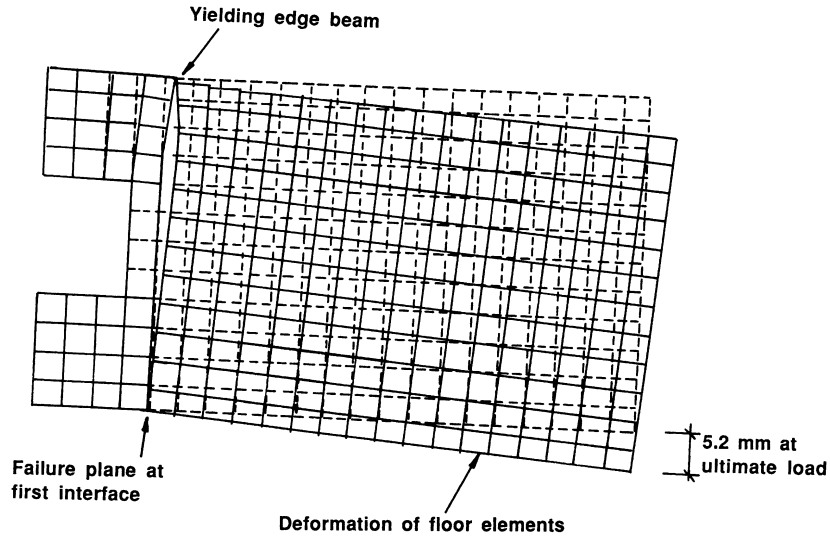

Figure 8.31 Floor diaphragm deformations [8.35].

Figure 8.31, where the critical longitudinal joint is not at the support but at the second interface between the slabs.

8.4 Diaphragm Action in Composite Floors with Structural Toppings

Composite floor systems are designed on the basis that the precast flooring units provide restraint against lateral (in this case vertical) buckling in the relatively thin topping. In other words, the precast floor is acting as permanent shuttering. The shear is carried entirely by the reinforced *in situ* concrete topping (the welded connections between double-tee units are ignored: see Figure 1.34). The minimum thickness of structural topping is 40 mm. The design ultimate shear stress is taken as at least 0.45 N/mm^2, for grade C25/30 concrete ($0.028 f_{ck}^{2/3}$ from clause 6.2.5(2) [8.5]) {BS 8110, Part 1, Table 3.9 [8.6]}, and the effective depth of the topping is measured at the crown (thinnest part) of the pre-stressed flooring unit.

Continuity of reinforcement in structural toppings is always extended to the shear walls or cores and it is safe to assume that the shear capacity of *in situ* diaphragms will not be the governing factor in the framing layout. Designers are careful not to allow large voids near external shear walls, and to ensure that if an external wall adjacent to a prominent staircase is used, then a sufficient length of floor plate is in physical contact with the wall.

Exercise 8.6

Calculate the horizontal shear force capacity in the *y*-direction in the screeded double-tee floor slab shown in Figure 8.32, if the maximum thickness of topping is 75 mm. The precamber in the precast unit may be taken as span/400. Use grade C20/25 concrete.

Solution

The maximum shear force occurs at a point of zero bending at the interface of the floor slab and shear wall. Maximum thickness of topping = 75 mm.

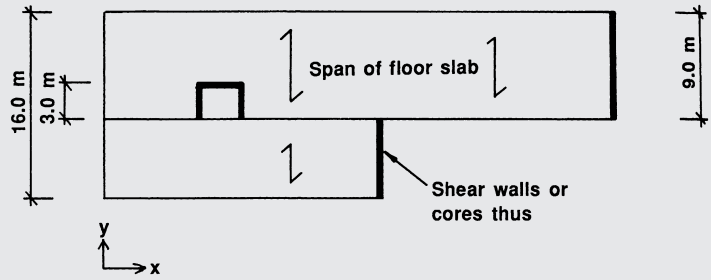

Figure 8.32 Details for Exercise 8.6.

A_s as % age of A_c from clause 9.2.1.1 is the maximum of 0.13 or

$$\frac{0.26}{100} \times \frac{0.3 \times 20^{2/3}}{500} = 0.13$$

Area of mesh = 0.13% × 75 × 1000 = 97.5 mm²/m

Area of mesh = 0.15% × 75 × 1000 = 112.5 mm²/m

Use A142 mesh.
Minimum depth of topping = 75 − (9000/400) = 52.5 mm
Minimum slab-to-slab contact length = 9 m
Effective area of topping = 9000 × 52.5 = 472 × 10³ mm²

Shear stress is maximum of
$0.12 \times 2 \times (0.13 \times 20)^{1/3}$ or
$0.035 \times 2^{3/2} \times 20^{1/2} = 0.443$
Shear resistance = 0.443 × 472 = 209 kN

Average shear stress for grade 25 concrete containing 0.15% reinforcement = 0.45 N/mm².
Shear force = 0.45 × 472 = 213 kN

8.5 Horizontal Forces due to Volumetric Changes in Precast Concrete

The effect of shrinkage and temperature changes during the period of cement hydration time is less significant in precast concrete than in cast-*in situ* work. Early-age deformations are unrestrained and therefore of little importance. In addition, precast connections are often designed such that volumetric changes do not generate large internal forces in the structure. This is achieved by assuming that once frictional forces are exceeded, the components are allowed only a very small free movement between one another before the *in situ* reinforced concrete strips accommodate the tensile forces. Skeletal structures are also sufficiently flexible to accommodate such movements.

In calculating volumetric changes in precast concrete, the two major obstacles in using standardised data intended for *in situ* concrete production are:

- the volume-to-surface area of many precast components is lower than normal, for example in double-tee units, where the exposed surface area is large
- water content in many precast components is low, e.g. in prestressed components such as hollow-core slabs.

Hence measured values tend to be used in place of general data. The following table gives specific information on shrinkage, temperature and elastic shortening obtained from the *PCI Manual* [8.36]. The axial strain induced from volumetric changes in a range of common precast concrete components is given in Table 8.2.

Table 8.2 Approximate axial volume changes for unrestrained precast concrete elements

Volume-to-surface ratio (mm)	Axial strain	Typical components
25	0.00062	300 deep double-tee slabs
37	0.00067	700 deep double-tee slabs
50	0.00069	150 deep hollow-core slabs
75	0.00086	250 deep hollow-core slabs
100	0.00086	Narrow beams or columns (300 wide)
125	0.00089	Wide beams or columns (600 wide)

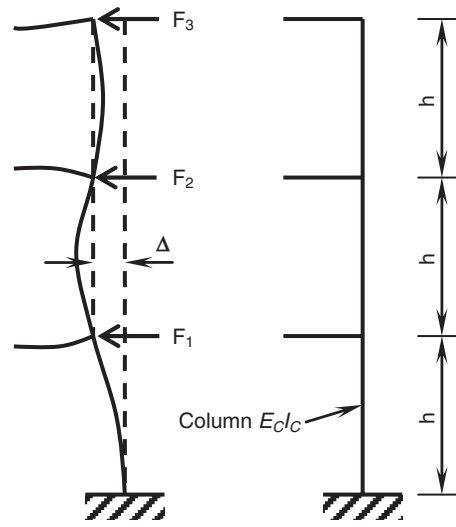

Figure 8.33 Horizontal forces and column bending moments due to drying shrinkage or temperature movement.

The data include elastic shortening strains in prestressed concrete, which equate to about 0.00035 (350 με). Data collected by Bensalem [8.37] on the lateral (i.e. side-to-side) shrinkage in extruded hollow-core slabs found that two-day-old units shrank 0.2 mm per 600 mm width after several months' exposure to moderate climatic conditions in the UK. The shrinkage strain is therefore $\varepsilon_{sh} = 0.00033$.

Horizontal forces and column bending moments due to drying shrinkage or temperature movement are shown in Figure 8.33. The deformation is given by:

$$\Delta = (\varepsilon_{sh} + \alpha t) L \tag{8.16}$$

where

$\alpha = 8 \times 10^{-6}$ per °C for concrete made with flint or quartzite aggregate,
$\alpha = 10 \times 10^{-6}$ per °C for concrete made with granite or basalt aggregate,

$\alpha = 12 \times 10^{-6}$ per °C for concrete made with limestone aggregate.
t = temperature range.

The shrinkage strain ε_{sh} may be taken either from BS EN 1992-1-1, clause 3.1.4(6) and Annex B [8.5], or from BS 8110, Part 2, Figure 7.2 [8.38], with appropriate modification factors for low water content mixes (because these data are for water contents of 190 l/m^3).

If the concrete maturity is t_m days when components are assembled, the autogenous shrinkage

$$\varepsilon_{ca} = \left(1 - e^{-0.2\sqrt{t_m}}\right) \times 2.5(f_{ck} - 10) \times 10^{-6}$$

and drying shrinkage using opc

$$\varepsilon_{cd(t)} = \frac{(t - t_0)}{(t - t_0 + 0.04\sqrt{h_0^2})} \times k_h \times \varepsilon_{cd0}$$

$$\varepsilon_{cd0} = 761\, e^{(-0.012(f_{ck}+8))} \times 10^{-6}$$

where, for an exposed perimeter u and drying depth $h_0 = 2\, A_c/u$
K_h is interpolated from

h_0	K_h
100	1.0
200	0.85
300	0.75
>500	0.7

$$\varepsilon'_{sh} = \varepsilon_{ca} + \varepsilon_{cd} \qquad (8.17)$$

Shrinkage strains ε_{sh} are modified according to the volume of reinforcement in the cross section $\rho = A_s/A_c$, and exposure parameter K as follows:

$$\varepsilon'_{sh} = \frac{\varepsilon_{sh}}{K\rho} \qquad (8.17)$$

where $K = 25$ for indoor and 15 for outdoor exposure.

In a multi-storey structure the force is greatest at the first-floor level, because the foundation does not move. The maximum axial force in the beams (elastic analysis) is given by:

$$F_1 = \frac{5.25 E_c I_c \Delta}{h^3} \qquad (8.18)$$

$$F_2 = -3.857 F_1 \text{ and } F_3 = 1.607 F_1 \qquad (8.19)$$

where E_c, I_c and h refer to the column.
The maximum bending moment is:

$$M = 2.357 F_1 h \qquad (8.20)$$

In the common situation when the ground floor is 1.2 times as high as the other floors, the coefficients for F_1, F_2, F_3, and M in Eq. (8.18 to 8.20) are 3.367, −2.832, 1.201, and 1.654, respectively. In multi-bay construction the forces accumulate in each successive bay. The connections must be designed to alleviate the forces to prevent tensile cracking in the connection and flexural cracking in the column.

Exercise 8.7 Shrinkage and temperature-induced moments

Determine the six-month drying shrinkage and temperature-induced horizontal deflections in the three-storey unbraced structure shown in Figure 8.34, and calculate the resulting axial forces in the rc beams and the bending moment at the foundation at column A. The floor slabs are simply supported on the beams and may be considered as being unconnected.

Use a temperature range of 20°C since the frame installation, and indoor exposure conditions. The age at loading is 28 days. Use grade C30/37 flint aggregate concrete with 190 l/m^3 water content.

Solution

Step 1: Beam properties

A = 180 000 mm^2. The exposed perimeter, u = 1500 mm. Drying depth of beam h_o = 180 000/1500 = 240 mm. Steel ratio = 4 × 491/180 000 = 1.091 %.

$\varepsilon_{ca} = \left(1 - e^{-0.2\sqrt{28}}\right) \times 2.5(30-10) \times 10^{-6}$	= 17.4 με
$K_h = 0.81$	
$\varepsilon_{cd0} = 761\ e^{(-0.012(30+8))} \times 10^{-6}$	= 482.2 με
$\varepsilon_{cd} = \dfrac{(182-28)}{(154+0.04\sqrt{240^3})} \times 0.81 \times 428.2$	= 199 με
$\varepsilon'_{sh} = \varepsilon_{ca} + \varepsilon_{cd}$	= 216.4 με
Free shrinkage per beam = $(\varepsilon'_{sh} + \alpha t)$	
$L_s = (216.4 + 8 \times 20) \times 10^{-6} \times 6000$	= 2.26 mm
The outer column displacement = $2L_s$	= 4.52 mm

Modification factor for the reinforcement = 1 + (25 × 0.01091)	= 1.273
Shrinkage strain (estimated from BS 8110, Part 2, Figure 7.2) = 140/1.273	= 110 με
Free shrinkage per beam = $(\varepsilon'_{sh} + \alpha t)$	
$L_s = (110 + 8 \times 20) \times 10^{-6} \times 6000$	= 1.62 mm
The outer column displacement = $2L_s$	= 3.24 mm

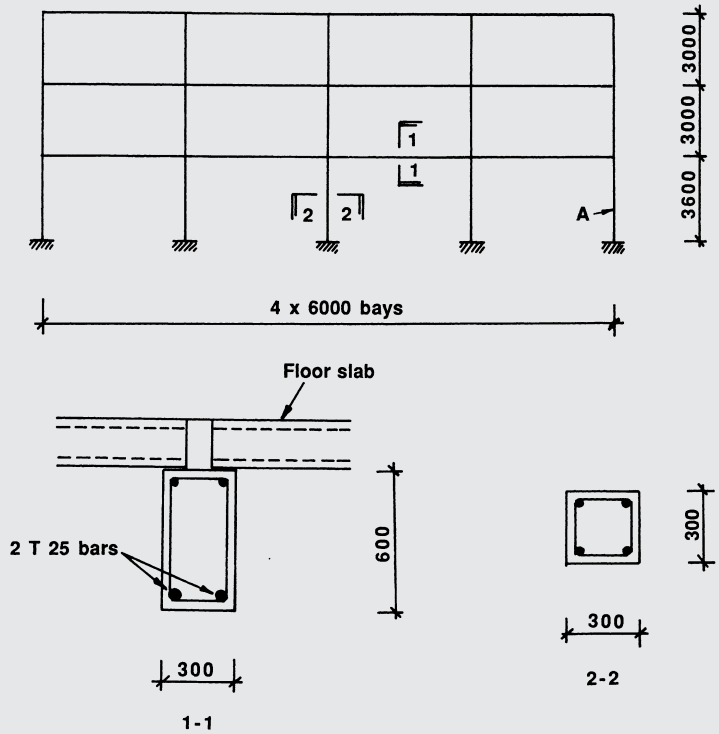

Figure 8.34 Details for Exercise 8.7.

Step 2: Column properties
Column properties: $I_c = 6.75 \times 10^8\,\text{mm}^4$.

Short term E_c (Table 6.1) $= 33\,\text{kN/mm}^2$

30-year creep factor (from BS EN 1991-1-1, Annex B)

$$\varphi_{RH} = \left(1 + \frac{\left(1 - \frac{50}{100}\right)}{0.1 \times 240^{(1/3)}} \times \left(\frac{35}{(30+8)} \right)^{0.7} \right)$$

$$\left(\frac{35}{(30+8)} \right)^{0.2} = 1.73$$

$$\beta_{(f_{cm})} = \frac{16.8}{\sqrt{30+8}} = 2.73$$

$$\beta_{(t_0)} = \frac{1}{(0.1 + 28^{0.2})} = 0.488$$

$$\beta_H = 1.5 \times 240(1 + 0.012 \times 50)^{18} + 250\sqrt{\frac{35}{30+8}} = 600$$

$$\beta_{c(t,t_0)} = \frac{(182-28)}{(600+182-28)} = 0.621$$

$$\varphi_{(t,t_0)} = 1.73 \times 2.73 \times 0.488 \times 0.984 = 1.432$$

Long term equivalent $E_c = 33/1.432 = 23.05\,\text{kN/mm}^2$

For $1.2h = 3600\,\text{mm}$, $h = 3000\,\text{mm}$

$$F_l = \frac{3.367 \times 23.05 \times 6.75 \times 10^8 \times 4.52}{3000^3 \times 10^3} = 8.76\,\text{kN}$$

$M = 1.654 \times 8.76 \times 3000 \times 10^{-3} = 43.48\,\text{kNm}$

Short term E_c (Table 6.1) $= 28\,\text{kN/mm}^2$

30-year creep factor (estimated from BS 8110, Part 2, Figure 7.1) = 2.58.

Proportion of long-term creep at 6 months = 60%.

Long-term equivalent E_c

$= 28/0.6 \times 2.58 = 18.09\,\text{kN/mm}^2$

For $1.2h = 3600\,\text{mm}$, $h = 3000\,\text{mm}$

$$F_l = \frac{3.367 \times 18.09 \times 6.75 \times 10^8 \times 3.24}{3000^3 \times 10^3} = 4.933\,\text{kN}$$

$M = 1.654 \times 6.68 \times 3000 \times 10^{-3} = 24.48\,\text{kNm}$

8.6 Vertical Load Transfer

8.6.1 Introduction

The reactions from the horizontal floor diaphragm calculated in Section 8.2 are transferred to the stabilising systems as point loads acting at the centroid of the area of the floor that is in contact with each bracing element, i.e. column, wall or core. The loads are reversible in nature and may not be coincident if floor levels differ in height.

In the split-level building example shown in Figure 8.35(a), the columns on Line A near the shear walls will be subjected to a horizontal shear force equal to the floor reaction in each shear wall. The columns on Line A are effectively loaded in the manner shown in Figure 8.35(b), with point reactions at a distance x from each floor level. In the worst situation, the shear is maximum when x is small, and (ignoring second-order deflections) bending is maximum when $x = h/2$, as shown in the figure. Flexural and shear checks should be made on these columns, particularly as the axial compression may be small in gable end columns, where many shear walls are located. If necessary a deeper column should be used. The usual outcome is that a shear wall is positioned in the split-level area to eliminate the reactions completely.

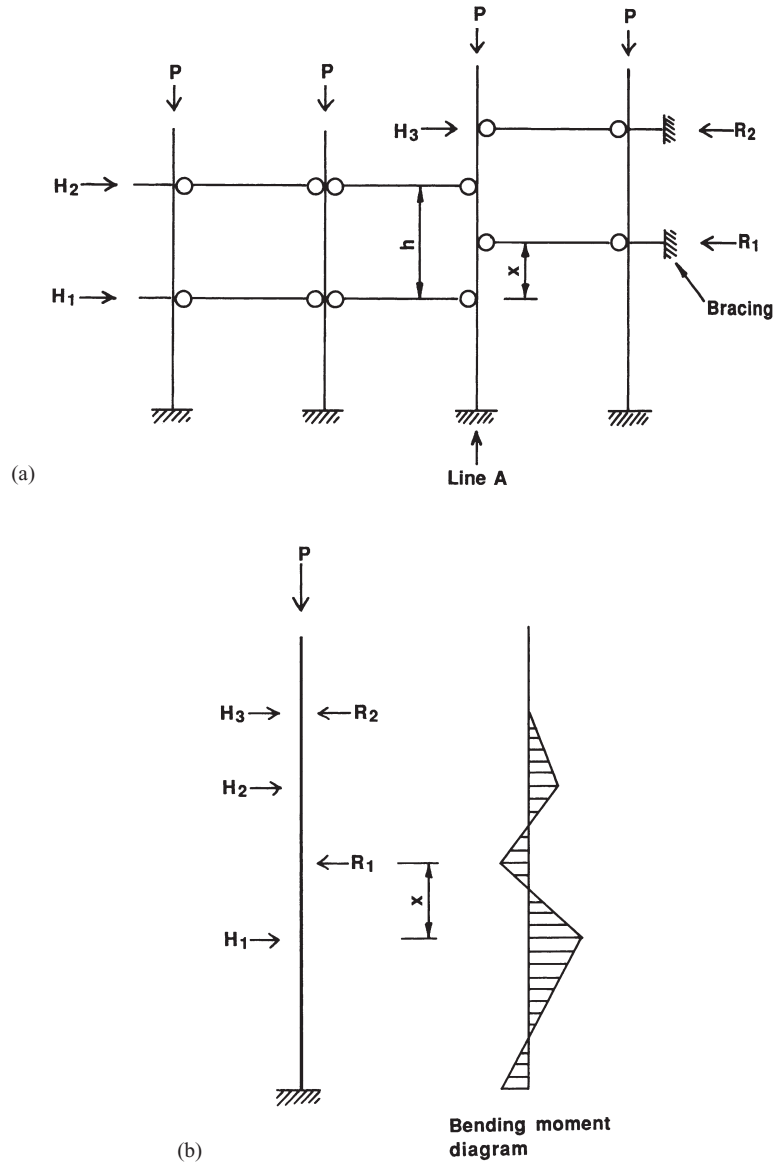

Figure 8.35 Design approach for split-level structures. (a) Horizontal load transfer in a split-level braced structure, and (b) column bending moments in a split-level braced structure.

This problem does not exist in unbraced structures, because the horizontal loads are shared equally between all columns.

In a skeletal structure the bracing elements will be either:

- walls or cores, in the case of a braced structure, or
- columns, in the case of an unbraced structure, or
- both, in the case of partially braced structures (refer to Sections 1.5 and 4.1).

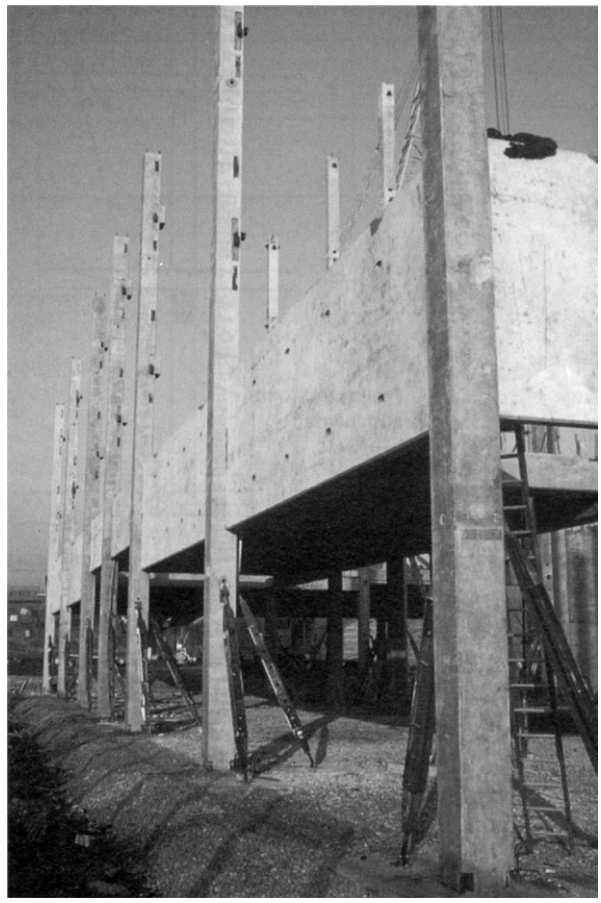

Figure 8.36 Spandrel beams in perimeter of frame.

As a point of information only, a method of strengthening pin-jointed precast structures, using roof diaphragms and external shear walls, is given in the *PCI Journal* by Kaplan *et al.* [8.39]. The external roof diaphragm operates as a ring beam, connected to a so-called shear wall, which is in reality a deep column located next to the pin-jointed columns of the original frame.

8.6.2 Unbraced structures

The stability of unbraced pin-jointed structures is provided entirely by columns designed as cantilevers for the full height of the structure (Figure 4.2(b)). Figure 8.36 shows a photograph of a typical unbraced structure, where any partial restraints provided by moment-rotation of torsionally stiff beam-to-column connections, deep external spandrel panels, or internal brick/block walls have ALL been ignored in the design.

The line of load application is at the centroid of the flooring system. The distribution of horizontal loading between columns is directly proportional to the second moment of area of the

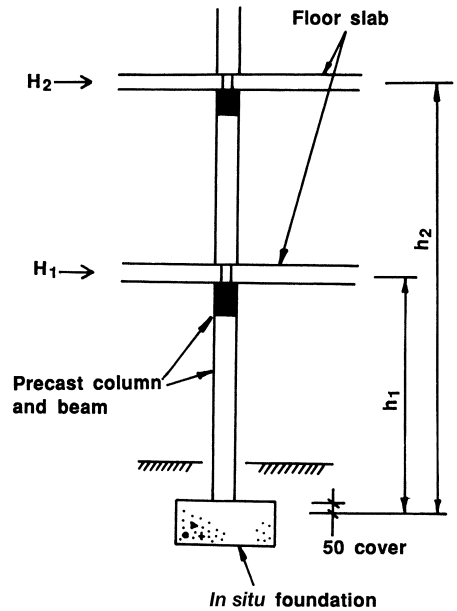

Figure 8.37 Definitions of lever arm for overturning moments in columns.

columns in the uncracked condition at the serviceability limit state, divided by the bending height cubed, h^3. Non-symmetrical buildings (the vast majority) are considered for torsional stability, but the disposition of columns is usually such that the shear centre of the system coincides fairly closely with the centre of pressure. In most instances the columns will be equally loaded horizontally.

The maximum overturning moment in each column is $\Sigma H_i\ h_i$, where H_i is the floor diaphragm reaction at each column, and h_i is the effective height from a point 50 mm below the top of the foundation to the centroid of the floor plate i (Figure 8.37). The overturning moment is additive to the frame moments derived under column design. There is no moment distribution into the beams if the connections are pinned, and therefore the columns are designed using an effective length factor of 1.0 between floors and 2.0 to the top.

The maximum height for an unbraced pin-jointed structure is about 10 m. Architectural restrictions on the sizes of columns and the magnitude of the moment-restraint required at the foundation are likely to be prohibitive for greater heights. The moment carried by the columns is dependent on the degree of fixity between the column and the footing, and on the resistance of the soil to footing rotation. The design codes give the total stiffness of the foundation (i.e. column-to-footing-to-soil) equal to that of the column, and this is assumed in design. *PCI Manuals* [8.36] are more explicit, but the result is approximately the same.

Columns are manufactured in a single length and therefore the design of splices is not applicable. There are occasions, however, where a column is founded onto floor beams or slabs; see Figures 7.119 and 7.120. This connection, which is designed as pin-jointed, does not contribute to overall stability (rather like a gable post in a warehouse).

Column reinforcement may be reduced at upper floor levels in accordance with the applied bending moment but, as in most precast components, increased fabrication costs (usually) outweigh savings in material.

Exercise 8.8 Overturning moments in columns in unbraced structures

Determine the maximum overturning moments in the columns shown in Figure 8.38. The bay centres are 6 m. The columns, which have identical cross sections, are founded in deep *in situ* concrete pockets with 50 mm cover to any reinforcement in the foundation. The storey heights are given to the centroid of the floor and roof slabs. Sway deflections are equal at roof level. The wind pressure may be taken as 0.7 kN/m^2.

Solution

The different floor spans have no effect on the overturning moments because the beam-to-column connections are pinned.

Add an extra 50 mm to bending heights of columns at foundation to allow for cover cracking.

Bending height of columns 1, 2, 3 = 10.0 + 0.050 = 10.05 m

Bending height of columns 4, 5 = 7.0 + 0.050 = 7.05 m

Relative stiffness of columns 1, 2, 3 = $EI/L_{1,2,3} = EI/10.05 = 0.0995\ EI$

Relative stiffness of columns 4, 5 = $EI/L_{4,5} = EI/7.05 = 0.1418\ EI$

Proportion of horizontal force in columns 1, 2, 3 $= \dfrac{3\times0.0995EI}{3\times0.0995EI + 2\times0.1418EI} = 0.513$, or 0.171 per column

Proportion of horizontal force in columns 4, 5 = 0.487, or 0.243 per column

Wind pressure acting on three-storey face gives maximum condition:

Wind at roof* = 0.7 × 6.0 × 1.5 = 6.30 kN acting @ 10.05 m above foundation

Wind at 2nd floor = 0.7 × 6.0 × 3.0 = 12.60 kN acting @ 7.05 m above foundation

Wind at 1st floor = 0.7 × 6.0 × 3.25 = 13.65 kN acting @ 4.05 m above foundation

* neglecting any beam parapet in this exercise.

Moment in columns 1, 2, 3:

$M = 0.171\times((6.3\times10.05)+(12.6\times7.05)+(13.65\times4.05)) = 35.47$ kNm

Moment in columns 4, 5:

$M = 0.243\times((6.3\times7.05)+(12.6\times4.05)) = 23.2$ kNm

Thus maximum moment = 35.47 kNm.

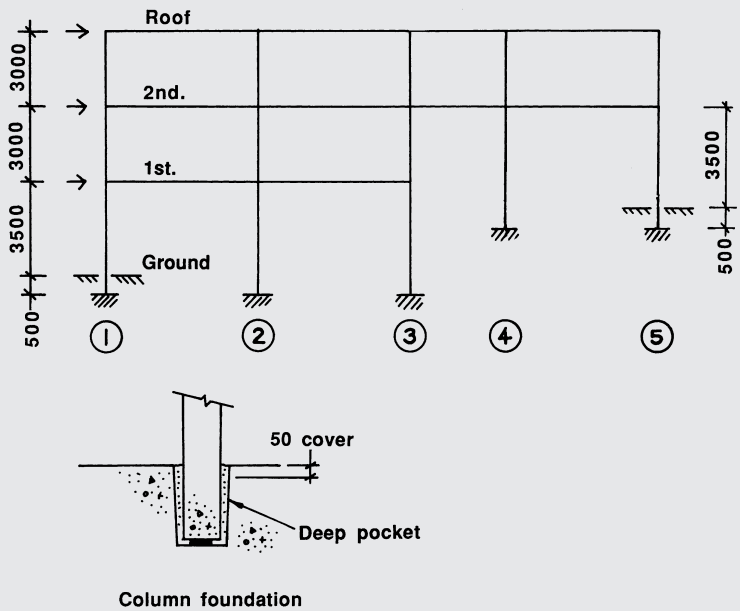

Figure 8.38 Details for Exercise 8.8.

8.6.3 Deep spandrel beams in unbraced structures

Deep beams, such as spandrel beams with a large upstand (say at least 750–1000 mm deep by about 150–200 mm wide), may be used to distribute sway moments into the frame by providing a vertical couple between the main connector, at the bottom of the beam, and a fixing at the top of the beam (see Figures 3.35 and 8.39). The principle is shown in Figure 8.40, where the stiffness and strength of the spandrel is considerably greater than in the column. For this to work, the horizontal forces in the fixings in the spandrel beam must generate a moment given by:

$$M = \frac{\sum H_i h}{n} \text{ at the 1st floor, and}$$
$$M = \frac{H_i h}{n} \text{ at upper floors} \qquad (8.21)$$

where H_i = horizontal floor load, h = storey height, and n = number of columns in the row. The compressive and tensile forces in the couple are given by $F = M/z$, where z = lever arm between the fixings. For this to be effective, z should be at least 600 mm.

The columns must be capable of resisting the same force by providing a tensile tie to the fixing and additional reinforcement surrounding it to carry the shear force, particularly in lightly loaded columns.

A fully effective vertical shear resistance, one that does not rely on shear friction, must be provided between the spandrel beam and the column. Two options include projecting reinforcement grouted in, or castellated or roughened shear keys. A vertical interface shear resistance between the end of the spandrel and the column must be equal to the shear fixing force F. The shear force will be upwards in direction at one end of the spandrel beam, and unless the beam is very lightly loaded (permanent action only) that will not cause a problem. At the other end of the spandrel beam the force will be additive to the total shear force, and must be allowed for in the design.

The most effective method of force transfer is to stitch the two components using projecting loops (typically H8 at 50–100 mm centres) and a vertical lacer bar concreted into a recess. Welded joints are often made at the top of the beam which, as shown in Figure 8.39, must be protected with grout. Bolted fixings usually require clearance holes, which do not give positive connectivity unless friction-grip bolts are used.

The columns are designed on the assumption that the spandrel is rigidly connected to it, both in terms of strength and stiffness. Thus the normal rules for column effective length factors β apply (see Section 4.4). A typical value for α_c = 0.2 to 0.3; hence β = approx. 1.1.

8.6.4 Braced structures

Braced structures offer the best solution to stability in multi-storey construction, irrespective of the number of storeys (Figure 4.2(a)). Connection details and foundation design and construction are greatly simplified. Precast concrete wall units are inexpensive, have high in-plane stiffness and strength, are easy to erect, and may be integrated with the structure using one of three methods:

- infill wall, either solid or hollow-core
- cantilever wall, either solid or hollow-core
- cantilever box.

Other methods of bracing are infill brick or block-work walls, and steel cross-bracing.

As shown in Figure 8.41, reproduced from the IStructE publication [8.40], floor diaphragm action occurs between vertical cores, composed of walls or a box. A centroidal line of load application from the floor plate to the core is once again assumed. The distribution of horizontal loading between shear walls or shear frames is dependent upon the following:

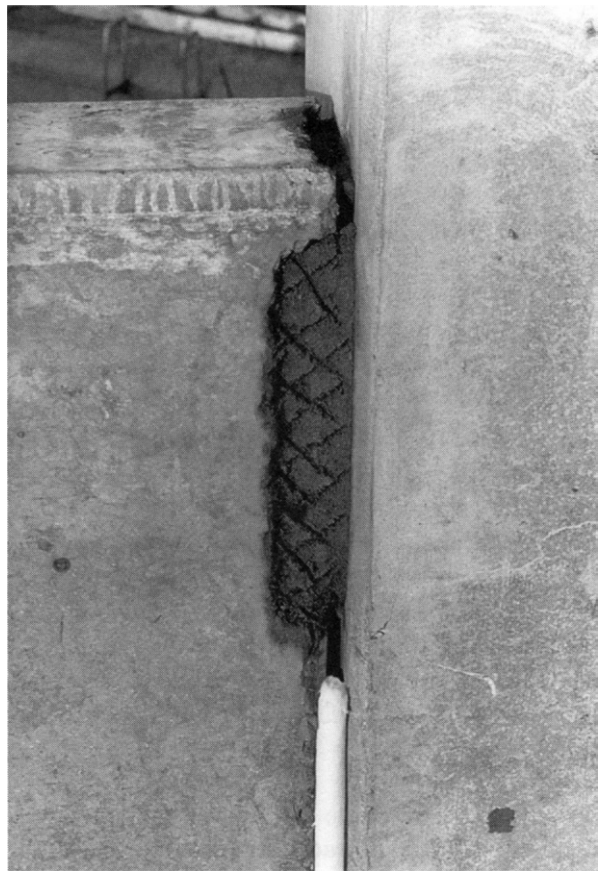

Figure 8.39 Welded joint at top of spandrel beam.

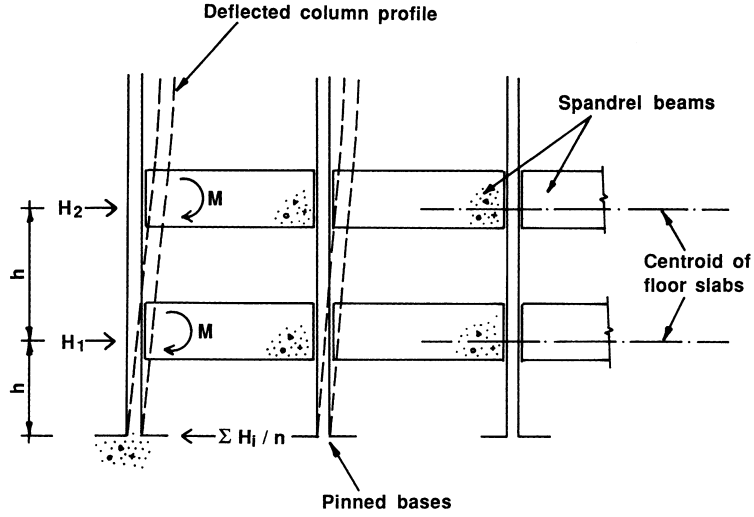

Figure 8.40 Spandrel beam restraint mechanism in unbraced structures.

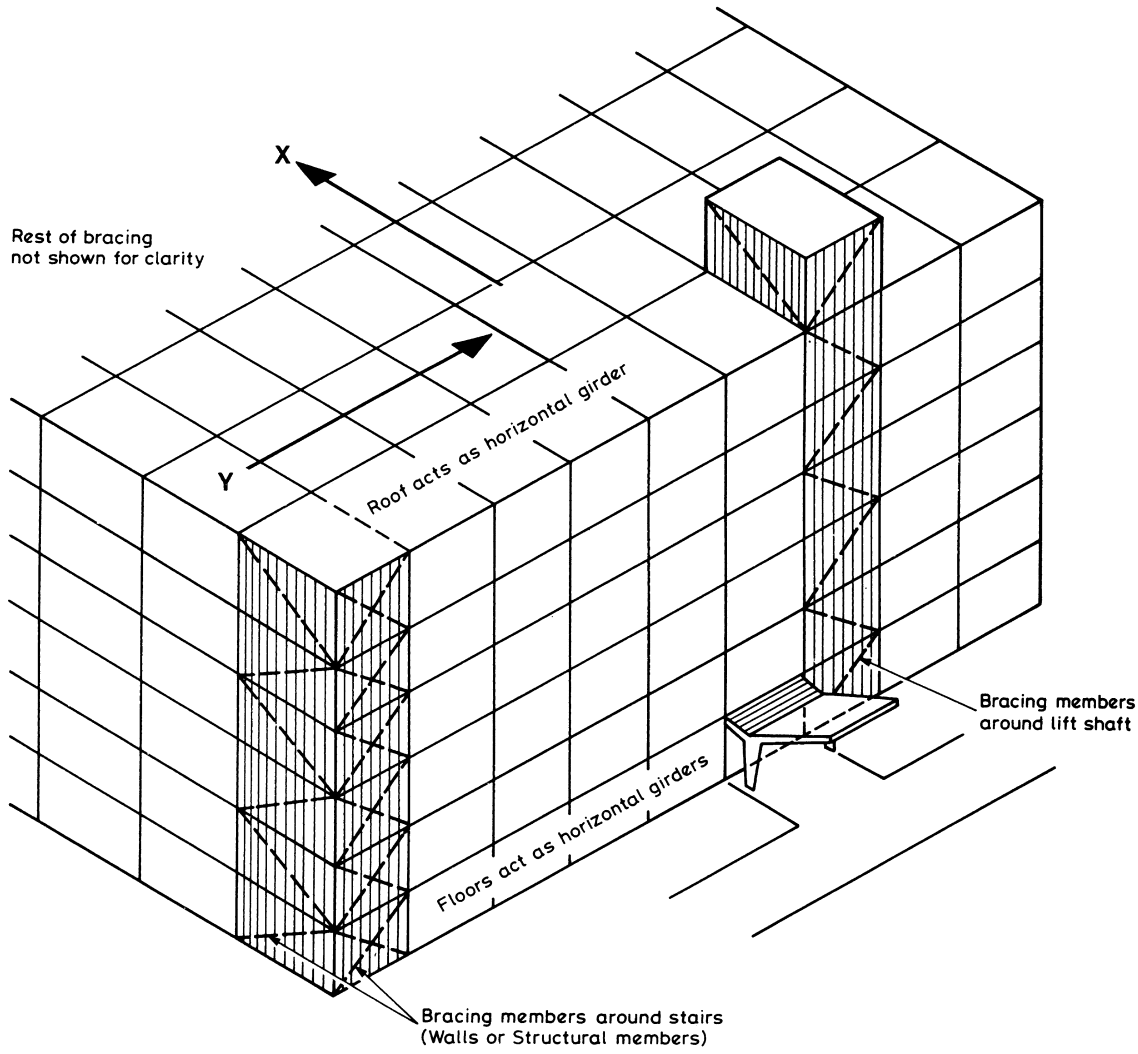

Figure 8.41 Stabilising system in braced structures [8.40].

(1) In-plane deflection response
This is predominantly a flexural deflection in cantilever walls (although shear deflection may govern in 'long' walls, i.e. length-to-height ratio > 2), a shear deflection in infill walls, and truss deflection in steel cross-bracing.

(2) Position
The structure must be balanced by disposing the walls according to their stiffness and in such a manner that the centre of pressure of horizontal loading lies between at least two of the 'larger' walls, as shown in Figure 8.3. Torsional effects, resulting from eccentricities, are statically determinate and modifications to the load distribution satisfy equilibrium in the direction of loading. If this cannot be achieved, lateral forces develop in the shear walls at right angles to the direction of loading, as explained in Section 8.2.

(3) Columns in the remainder of the structure
These may, if so desired, be designed to make a contribution to overall stability. This is rarely taken into account because:

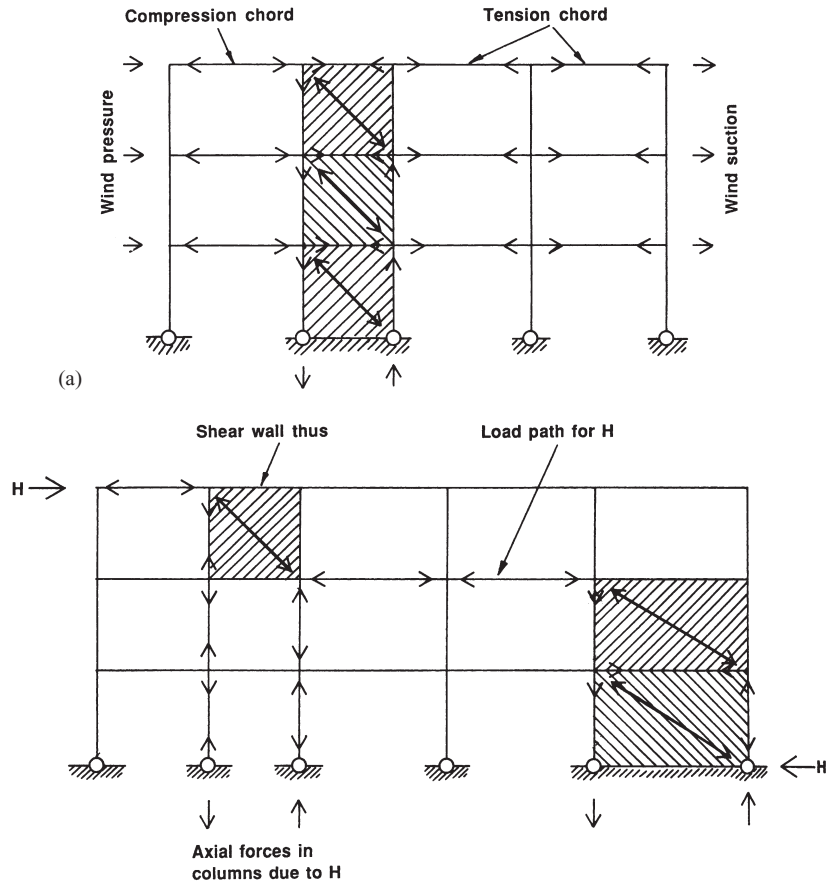

Figure 8.42 Horizontal load transfer in braced structures using coincident and non-coincident wall positions. (a) Walls in same vertical position and (b) walls in different vertical positions.

(a) the contribution is usually small
(b) similar problems associated with moment-resisting bases, etc. in sway structures are re-introduced
(c) shear walls are usually over-designed, because their size is often governed by lifting and pitching.

(4) Connections between walls, or between a wall and the foundation
Walls may be used in the structure for other purposes (e.g. supporting half-landings) than for stability. They may be designed so as not to be moment- or shear-resisting. This may be achieved by under-reinforcing the connections and allowing load redistribution to take place away from the wall, while maintaining structural integrity and load-bearing facility.

(5) Expansion joints in the floor diaphragm
In general, precast structures exceeding 60 to 80 m in plan dimension are usually isolated, depending on the plan configuration.

The horizontal forces are transmitted through the structure in the manner shown in Figure 8.42(a). It is not necessary for the walls to be located one above the other in the same vertical plane (Figure 8.42(b)), providing that the columns and beams surrounding the upper-storey walls are designed to carry the vertical wall reaction. This figure shows the load path for the horizontal force *H*.

The moments in the columns are small, but the axial forces have to be considered, particularly in the lightly gravity-loaded cases where walls are positioned between 'gable' columns and uplift may

occur, because gable columns support beams that do not carry floor slabs directly. However, large compressive forces may occur in the columns adjacent to infill walls, requiring a greater cross section (or reinforcement) than in the remainder.

Columns adjacent to cantilever shear walls are assumed not to carry additional axial forces due to overturning moments, despite the presence of a continuous vertical shear key between the column and wall. At ultimate, this shear key is assumed to break down and the shear wall is assumed to behave in isolation from the columns and beams.

8.6.5 Uni-directionally braced structures

Structures braced in one principal direction, and unbraced in the other, are considered separately as far as the design of walls is concerned. This means that the effects of sway in the unbraced direction are ignored when the walls in the braced direction are designed. On the other hand, the beneficial effect of lateral bracing is considered when the unbraced columns are designed, and this often leads to rectangular-section columns with the weaker axis in the plane of the bracing.

8.6.6 Partially braced structures

Partially braced structures are used in situations where stability walls are architecturally undesirable in the upper two (or maximum three) storeys (Figure 4.2(c)). The structure is designed as fully braced up to a specified level, and unbraced thereafter. This may not always be the same level throughout the entire building and may be different in the different directions of stability. The columns are cantilevered above this level as in an unbraced structure, but because they are not founded at a rigid foundation their behaviour is different from ordinary cantilever columns.

The advantages in using this system are many; for example:

- There are no bending moments at the foundation.
- Columns between ground and first floor, where greater headroom is usually required, are braced.
- Column sizes and reinforcements in most one- or two-storey cantilevered structures are no greater than if the structure were fully braced, i.e. stability is being provided 'for free'.
- Column splices may be made in the braced part of the structure.
- Clear floor areas for open-plan offices and staircases are punctuated only by columns.

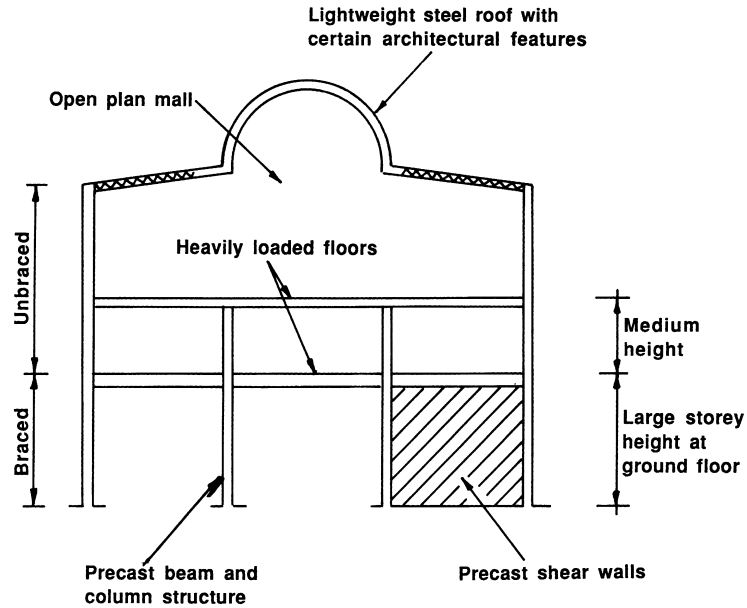

Figure 8.43 Mixed steel–precast concrete partially braced structure.

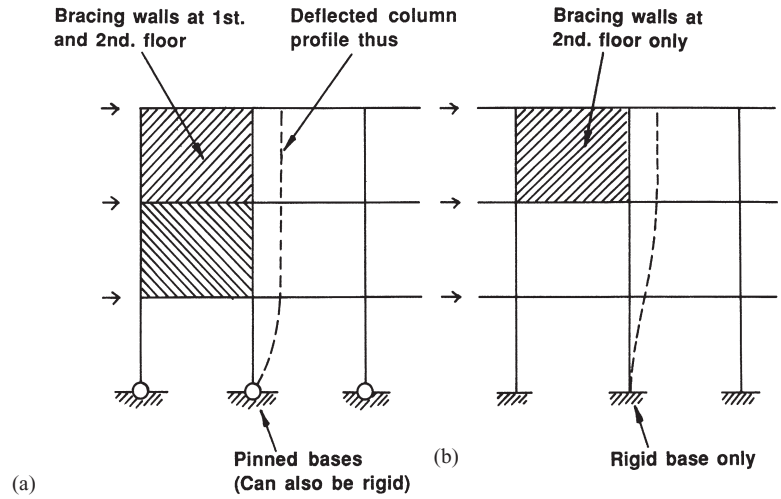

Figure 8.44 'Inverted' partially braced structure. (a) Bracing from first floor upwards and (b) bracing from second floor upwards.

An attractive application is the hybrid steel (or timber) roof/precast concrete structure, Figure 8.43, where the height of the structure is too great for a wholly unbraced structure, and the upper arcade prohibits the use of stabilising walls.

As explained in Section 4.4.4, columns in the unbraced part of the structure that are not in direct contact with the shear walls are designed as cantilevers, with a maximum effective length factor of 2.45 {2.3}. Columns supporting raking steelwork that is connected at its lower end to a rigid (no-sway) part of the structure are designed as propped cantilevers. The shear forces at the base of the unbraced columns are carried in the floor plate to the stiffening elements, in accordance with their stiffness and position. However, bending moments resulting from sway in the unbraced part are carried over into the unbraced part of the structure, diminishing to zero with distance to the level of the floor plate below. The effective length factor for the columns in this region is 1.0.

It is equally plausible to use a partially braced structure with the lower floor (or two floors) unbraced, as shown in Figures 8.44(a) and (b). The reason for doing this is to avoid shear walls at the ground floor. An open mall or car park may be required. However, there are few buildings today without service cores extending into the basement area, and so it is unlikely that this option would be used.

If the lower floors are unbraced, then the aforementioned rules for effective length factors are now reversed, except that it is possible to specify a moment-resistant foundation that would give an effective length factor in the ground-floor column (calculated using elastic stability functions) of 1.15.

Exercise 8.9 Columns in a partially braced structure

Repeat Exercise 4.8 where the structure is braced in both directions, using infill shear walls up to the second-floor level. The building is 36 m in length × 12 m wide. The 300 mm-square columns are at 6 m centres in both directions. The characteristic wind pressure is 1.0 kN/m^2.

Design the internal column. Assume that the horizontal out-of-plumb force 0.5%$(G_k + Q_k)$ {1.5% G_k} is not critical in this exercise.

Solution

Reference should also be made to Section 7.2.

In this exercise we are concerned only about the magnitude of the column bending moment at the second-floor level in both directions. Slenderness and second-order deflections can be obtained from:

(*Continued*)

For braced columns

$$l_0 = 0.5l\sqrt{\left(1+\frac{k_1}{0.45+k_1}\right)\times\left(1+\frac{k_2}{0.45+k_2}\right)} \quad = 0.5909\ l$$

with $k_1 = k_2 = 0.1$.

For unbraced cantilever columns, the

maximum of $l_0 = 2l\sqrt{\left(1+10\frac{k_1k_2}{k_1+k_2}\right)}$ or

$$l_0 = 2l\left(1+\frac{k_1}{1+k_1}\right)\times\left(1+\frac{k_2}{1+k_2}\right) \quad = 2.449\ l$$

with $k_1 = k_2 = 0.1$.

Then the slenderness ratio $\lambda = \frac{l_0}{r}$

and $\lambda_{lim} = \frac{20A\times B\times C}{\sqrt{n}}$ with initially

$A = 0.7$, $B = 1.1$, $C = 0.7$ and $n = 1$

Effective length factors β taken from BS 8110, Tables 3.21 and 3.22.

$\beta_a = \frac{1}{2000}\times\left(\frac{l_e}{b'}\right)^2$

$a_u = \beta_a kh$

where K is conservatively taken as 1.

Column	To BS EN 1992-1-1		To BS 8110			
	λ	λ_{lim}	Effective length factors	Slenderness ratios	β_a	a_u (mm)
Ground to first floor	24.9	10.78	$\beta = 0.9$ (braced)	10.8 < 15, so short		
First to second floor	20.5	10.78	$\beta = 1.0$ (braced)	10.0 < 15, so short		
Second to third floor	84.9	10.78	$\beta = 2.35$ (unbraced)	23.0 > 10, so slender	0.26	79.35 K
Third floor to roof	169.7	10.78	$\beta = 2.35$ (unbraced)	46.0 > 10, so slender	1.06	317.40 K

Step 1: Load case 1. For maximum gravity loading without wind. From Exercise 4.8:

From annex B of BS EN 1992-1-1
$\varphi_{ef} = 1.293$, so A increases to
$A = 1/(1 + 0.2\ \varphi_{ef}) = 0.795$, and assuming
2% reinforcement, B increases to
$B = \sqrt{1+2A_s f_{yd} / A_c f_{cd}} = 1.33$

N at 3rd floor = 306.1 kN
N at 2nd floor = 876.8 kN
The out-of-plumb moment from BS EN 1992-1-1, clause 5.2 with eccentricities at 3rd floor and roof:

$$e_{i3} = \frac{1}{200}\times 1\times 0.724\times 2.449\times\frac{3000}{2} = 13.3\ \text{mm}$$

$$e_{ir} = \frac{1}{200}\times 0.816\times 0.724\times 2.449\times\frac{6000}{2} = 21.7\ \text{mm}$$

$M_{ecc} = 306.1 \times 21.7 + 570.7 \times 13.3$ = 14.2 kNm
Second-order moments from clause 5.8.8.3
$m_{add} = 41.2 + 114.4$ = 155.6 kNm
Total moment = 169.8 kNm
$N/bh = 9.74$
$M/bh^2 = 6.29$
$A_{sc} = 2.75\%\ bh$

N at 3rd floor = 319.5 kN
N at 2nd floor = 918.9 kN
$M_{min} = 0.05 \times 0.3 \times 918.9$ = 13.8 kNm
(not critical, ignore further)
M_{ecc} due to column eccentricity = 0
$M_{add} = (319.5 \times 0.3174)\ K$
$+ (599.4 \times 0.07935)\ K$ = 149.0 K kNm
Then using
$N/bh = 10.21$ so $K = 1.0$
from BS 8110, Part 3, Chart 47, and
$M/bh^2 = 5.517$
$A_{sc} = 2.084\%\ bh$
$> 1\%\ bh$

Load case 2. For patch gravity loading

N at 3rd floor	= 237.6 kN	N at 3rd floor	= 244.3 kN
N at 2nd floor	= 635.5 kN	N at 2nd floor	= 656.6 kN
$M_{ecc} = 3.16 + 5.29$	= 8.45 kNm	$M_{add} = (244.3 \times 0.3174)\ K$	
$m_{add} = 53.5 + 32.0$	= 85.5	$+ (412.3 \times 0.07935)\ K$	= 110.26 K kNm
M_{patch} at 3rd floor $= 0.5 \times 41.18$	= 20.59 kNm	(but $K = 1.0$)	
Total moment	= 114.5 kNm	M_{patch} at 3rd floor $= 0.5 \times 43.34$	= 21.67 kNm
$N/bh = 7.06$		Total $M = 21.67 + 110.26 = 131.9$ kN	
$M/bh^2 = 4.24$		$N/bh = 7.296$	
$A_{sc} = 1.392\%\ bh$		$M/bh^2 = 4.886$	
< case 1		$A_{sc} = 1.89\%\ bh$	
		< case 1	

Load case 3. For combined gravity and wind loading in the *x*-direction

Horizontal wind force at roof $= 1.0 \times 1.5 \times 12 = 21.6\ \gamma_w$ kN per 21 no. columns

Horizontal wind force at 3rd floor $= 1.0 \times 3.0 \times 12 = 43.2\ \gamma_w$ kN per 21 no. columns

N at 3rd floor	= 306.1 kN	N at 3rd floor	= 264.6 kN
N at 2nd floor	= 876.8 kN	N at 2nd floor	= 747.6 kN
$M_{wind} = (21.6 \times 6.0 + 43.2 \times 3.0)\ 0.9/21$	= 9.26 kNm	$M_{wind} = (21.6 \times 6.0 + 43.2 \times 3.0)\ 1.2/21$	= 12.34 kNm
$M_{ecc} = 6.65 + 7.59$	= 14.14 kNm	$M_{add} = (264.6 \times 0.3174) + (483.0$	
$m_{add} = 41.2 + 114.4$	= 155.6 kNm	$\times 0.07935)$	= 122.3 kNm
		$M_{ecc} = 0$	
Total $M = 9.26 + 14.14 + 155.6$	= 179.0 kNm	Total $M = 12.34 + 0 + 122.3$	= 134.7 kNm
$N/bh = 9.742$		$N/bh = 8.307$	
$M/bh^2 = 6.632$		$M/bh^2 = 4.987$	
$A_{sc} = 3.011\%\ bh$		$A_{sc} = 1.83\%\ bh$	
> case 1		< case 1	

Load case 4. For combined gravity and wind loading in the *y*-direction

The larger windward face area causes a horizontal wind force in this direction three times the above.

$M_{wind} = 3 \times 9.26$	= 27.77 kNm	$M_{wind} = 3 \times 12.34$	= 37.03 kNm
Total $M = 27.77 + 14.14 + 155.6$	= 197.6 kNm	Total $M = 37.03 + 0 + 122.3$	= 134.7 kNm
$N/bh = 9.742$		$N/bh = 8.307$	
$M/bh^2 = 7.318$		$M/bh^2 = 5.901$	
$A_{sc} = 3.532\%\ bh$		$A_{sc} = 2.53\%\ bh$	
> case 3		> case 1	
Provide $A_{sc} = 3.532\% \times 300 \times 300$	= 3179 mm^2	Provide $A_{sc} = 2.53\% \times 300 \times 300$	= 2277 mm^2
Use four H25 + four H20 bars (3220 mm^2).		Use four H25 + two H20 bars (2591 mm^2).	

8.7 Methods of Bracing Structures

Attempting to use precast concrete as much as possible, the most common methods of bracing structures are (1) infill shear walls, and (2) cantilever panel or hollow-core walls. Figure 8.45 summarises the structural differences between the two types.

8.7.1 Infill shear walls

Unlike any other type of shear wall, infill shear walls rely on composite action with the 'individually unstable' pin-jointed column-to-beam structure for their strength and stiffness. Where an infilled wall

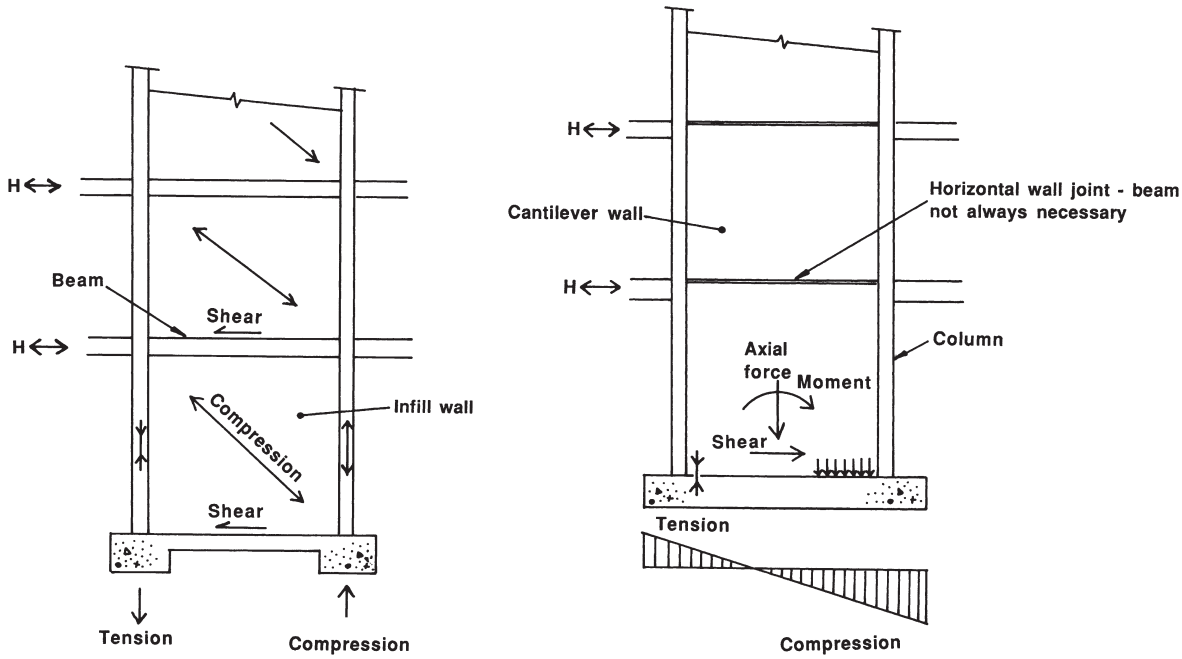

Figure 8.45 Behaviour of infill and cantilever shear walls in pin-jointed frames.

is built solidly, but not monolithically, into a flexible structure, its resistance to horizontal loading increases considerably owing to composite action with the structure. This is shown in the load-response sequence in Figure 8.46(a). Because the structure is (by design) flexible and the infill panel very stiff (having a large in-plane *EI*), there is a paradox in the fundamental use of infill structures. Theoretically the problem is similar to analysing stiff beams on elastic foundations [8.41], in that resistance to horizontal loading is affected by the amount of deformation and the interaction between the two media.

Optimum ultimate limit state design, i.e. collapse occurring in the structure and wall simultaneously, is very difficult to achieve because of the large number of variables used in the analysis. One of the most important of these is the quality of the vertical shear key connection, which for manufacturing purposes is usually unreinforced.

Most of the pioneering work on infilled frames – albeit using masonry infill – was carried out by Stafford-Smith and Carter [8.42], Mainstone [8.43] and Wood [8.44]. The design procedures suggested by these authors are widely used and respected in the UK. More recently Kwan and Liaum [8.45, 8.46] have proposed a plastic theory to deal with ultimate collapse mechanisms and suggested that an optimum design can be attained using reinforced joints with finite interface shear strength. Kwan's analyses further support the UK approach.

Commentaries on the behaviour of infilled shear walls are numerous, and therefore only the assumptions and methods used in current design will be raised here. Wright [8.47] produced a design method based on the principles developed by Stafford-Smith for masonry infill, which were combined with Mainstone's work using micro-concrete. The design assumptions are:

(1) Ultimate horizontal forces are resisted by a compressive diagonal strut across the concrete infill wall. The effective width of the strut depends primarily on the relative stiffness of wall panel and structure, and on the geometry h and θ as defined in Figure 8.46(b), but also reduces as the interface cracking load is exceeded.

(2) The tensile diagonal strength of the reinforced concrete wall is ignored, but the amount of reinforcement is sufficient to prevent excessive diagonal cracking and to maintain the intrinsic shape of the wall panel, particularly at the corners.

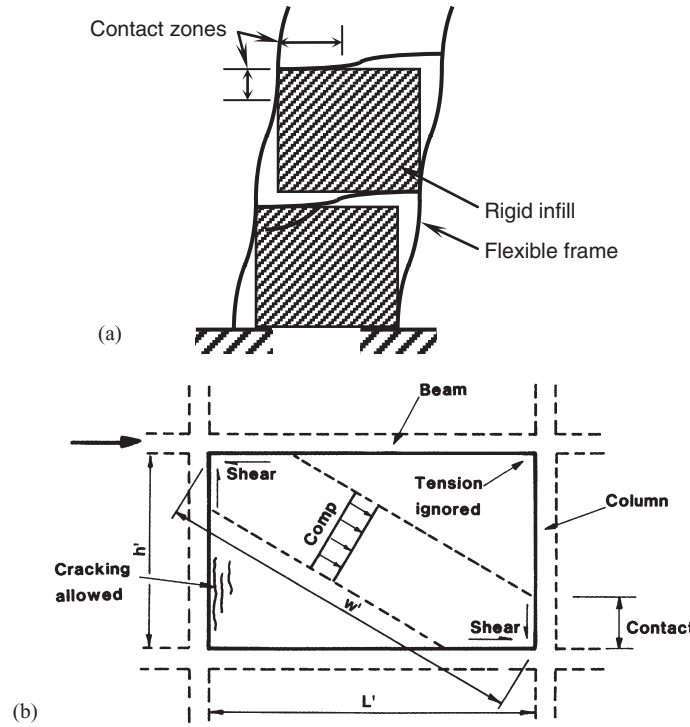

Figure 8.46 Infill shear wall design principles. (a) Precast infill frame strut analogy and (b) precast infill frame stresses.

(3) Slender wall panels are designed as slender braced *plain* concrete walls (reinforcement is usually less than 0.2 per cent {0.4 per cent}), taking into account manufacturing and site inaccuracies and deflection-induced bending moments.

(4) The shear resistance at the horizontal interface between beam and wall panel is also based on shear in plain concrete walls (normal aggregate, grade C20/25 minimum) using an ultimate average stress equal to $0.2 \times 0.14\ (f_{ck})^{2/3}$ plus 0.6 times the pre-compressive stress {$0.45\,N/mm^2$, or a value equal to 25 per cent of the vertical pre-compressive stress}.

(5) The wall is not subjected to vertical frame loading, i.e. floor beams are assumed structurally isolated from the wall units even though the gap between them is grouted solidly.

(6) The wall is not subject to simultaneous in-plane and out-of-plane wind loading. Eddy currents in enclosed courtyards of I-shaped buildings may in extreme circumstances present mutually perpendicular wind pressure to parts of the structure.

Some analyses have been so refined that the infill frame can often be misrepresented as a simple pin-jointed truss where the walls, columns and beams are singularly replaced by diagonal struts, chord elements and ties, respectively. This analogy is inadequate, because load transfer occurs over an extended region of the interface and the distribution of interaction over the contact length is semi-parabolic/triangular. The length of contact gives the effective width of the compressive strut and, together with the appropriate reductions for slenderness and spurious eccentricity, the ultimate diagonal compressive strength of the wall is computed. If the permissible horizontal shear stress is not exceeded, load versus infill panel size data may be presented as shown in Figure 8.47(a) {8.47(b)}. The derivation of these curves is given later. Note that the stiffness of the frame is based on 300×300 mm components throughout – a reasonable practical assumption.

The structural mechanism is as follows. On first application of a racking load there may be full composite action between the frame and wall if these are bonded together. At a comparatively early

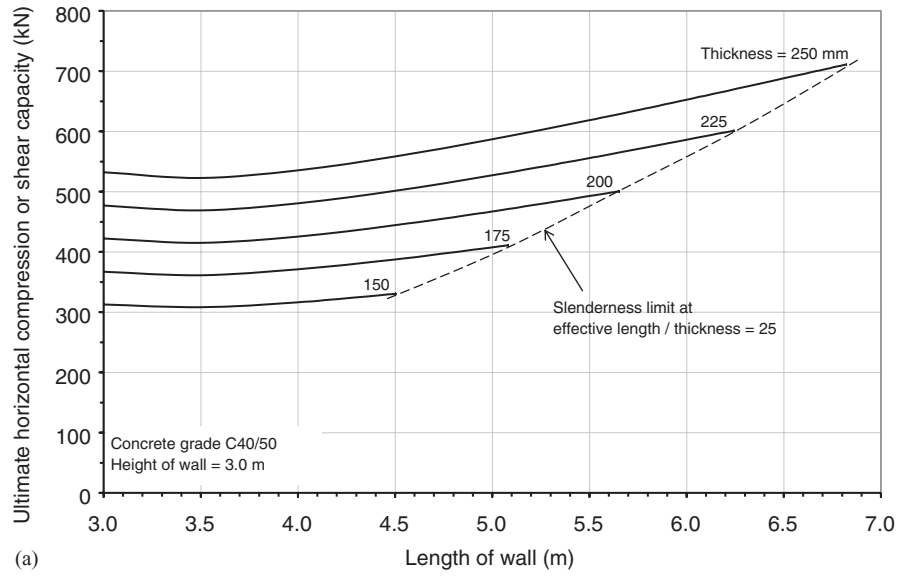

Figure 8.47(a) Horizontal shear capacity of infill precast concrete walls according to BS EN 1992-1-1.

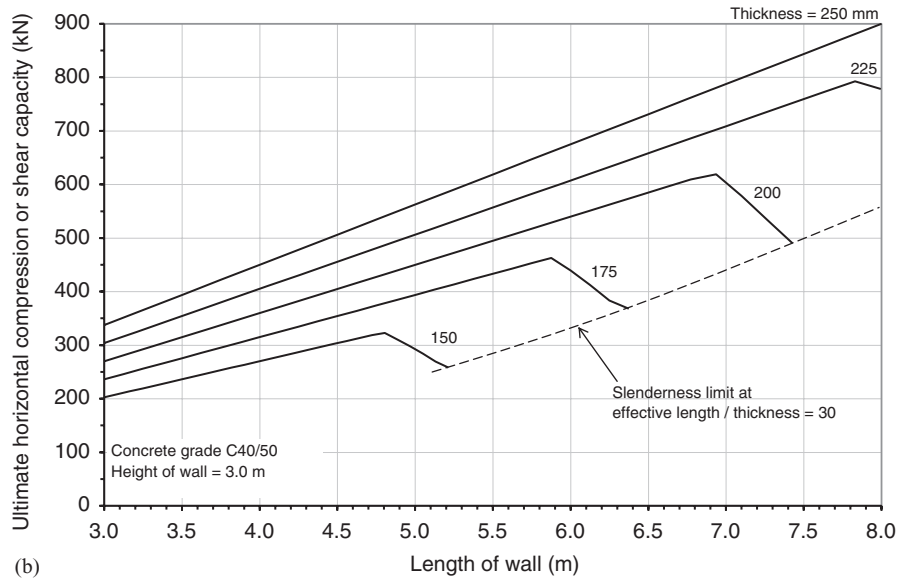

Figure 8.47(b) Horizontal shear capacity of infill precast concrete walls according to BS 8110.

stage, however, cracks will develop between the two components except in the vicinity of two of the corners, where the infill panel will lock into the frame and there will be transmission of compressive forces into the concrete wall. At this stage it is convenient to consider the concrete wall acting as a compression diagonal within the frame, the effective width of which depends on the relative stiffness of the two components and on the ratio of the height to the width of the panel. This action continues until the shear resistance is overcome and a crack, slightly inclined to the horizontal, is developed. Several more or less parallel cracks of this type may develop with further increase in load, and failure may finally result from the loss of rigidity of the infill as a result of these cracks, or from local

crushing or spalling in the region of the concentrated loads. In some cases the strength of the structure may be limited by the strength of the frame members or joints.

Essential problems in this approach are:

- determining the contact lengths between frame and wall;
- finding an effective width for the equivalent strut; and
- establishing the mode of failure and strength of the wall.

The contact length depends on the relative stiffness of the frame and infill, and on the geometry of the panel. Stafford-Smith first developed the analogy with a beam on an elastic foundation, by which the column of an unfilled frame under lateral load may be regarded as one half of a beam on an elastic foundation which under a central concentrated load, P, remains in contact with the foundation over a length known as the characteristic length, α, given by:

$$\frac{\alpha}{h} = \frac{P}{2\lambda h} \tag{8.22}$$

in which λh is a non-dimensional parameter expressing the relative stiffness of the frame and infill, where

$$\lambda = \sqrt[4]{\frac{E_i t \sin 2\theta}{4E_c I h'}} \tag{8.23}$$

where

E_i = infill modulus
E_c = concrete frame modulus
t = infill thickness
θ = slope of infill
I = minimum moment of inertia of beams or columns
h' = height of infill.

An 'equivalent' strut analogy is thus developed for the determination of α. This depends on aspect ratio h'/L'. Failure occurs either by local crushing at the corner, diagonal splitting due to excessive compression, or shear failure. Figures 8.48 and 8.49 (reproduced from [8.42]) are used to determine the failure loads appropriate to these conditions. Resulting ultimate design stresses are assessed against the following:

$\frac{0.6 f_{ck}}{\gamma_m}$ for concrete in compression
(with $\gamma_m = 1.5$)
$\frac{f_k}{\gamma_m} = \frac{0.5 f_b^{0.7} f_m^{0.3}}{\gamma_m}$ for group 1 clay brickwork laid with general-purpose prescribed mortar in compression
(with brick strength $f_b \leq 110\,\text{N/mm}^2$, mortar strength $f_m \leq 20\,\text{N/mm}^2$, $f_k \leq 75\,\text{N/mm}^2$, $\gamma_m \leq 3.0$) [8.49]
$\frac{f_{cvk}}{\gamma_{mv}}$ for brickwork in shear
(with $\gamma_{mv} = 2.5$) [8.49]. (8.24)

$\frac{0.67 f_{cu}}{\gamma_m}$ for concrete in compression
(with $\gamma_m = 2.2$)
$\frac{f_k}{\gamma_m}$ for brickwork in compression
(with $\gamma_m = 3.5$ [8.48])*
$\frac{f_v}{\gamma_{mv}}$ for brickwork in shear
(with $\gamma_{mv} = 2.5$ [8.48])*. (8.24)

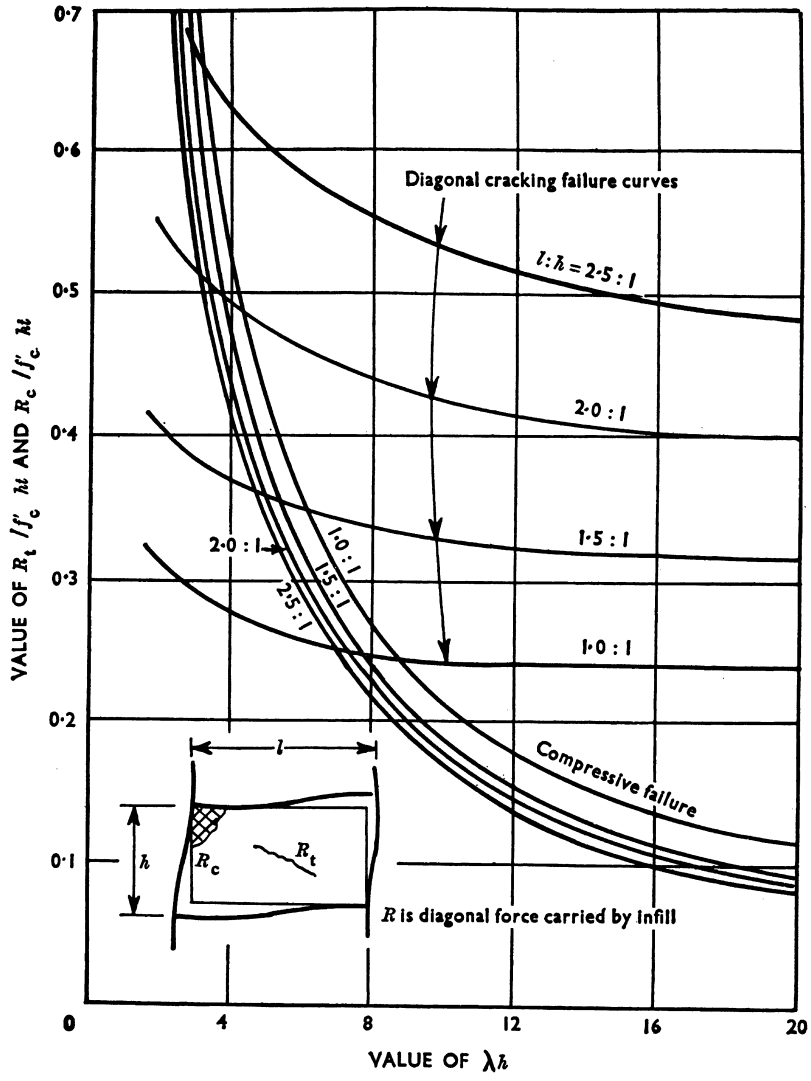

Figure 8.48 Infill wall design graph for limiting compressive strength [8.42].

Note that in reference [8.42] the compressive and shear strengths are given as f_c and f_{bs}, respectively.

Mainstone's method considered an upper-bound solution by restricting the width of an equivalent strut to 0.1 w', where w' = diagonal length of infill, but where the effects of slenderness must be considered. Vertical column reactions in compression or tension are carried to the column as appropriate.

Design methods are given in Sections 8.7.2 and 8.7.3 for concrete and brick infill walls, respectively.

8.7.2 Design methods for infill concrete walls

Concrete walls are considered to be plain walls, according to BS EN 1992-1-1, Section 12 [8.5] and BS 8110, Part 1, clause 3.12.5 [8.6] because the minimum area of reinforcement is provided only for

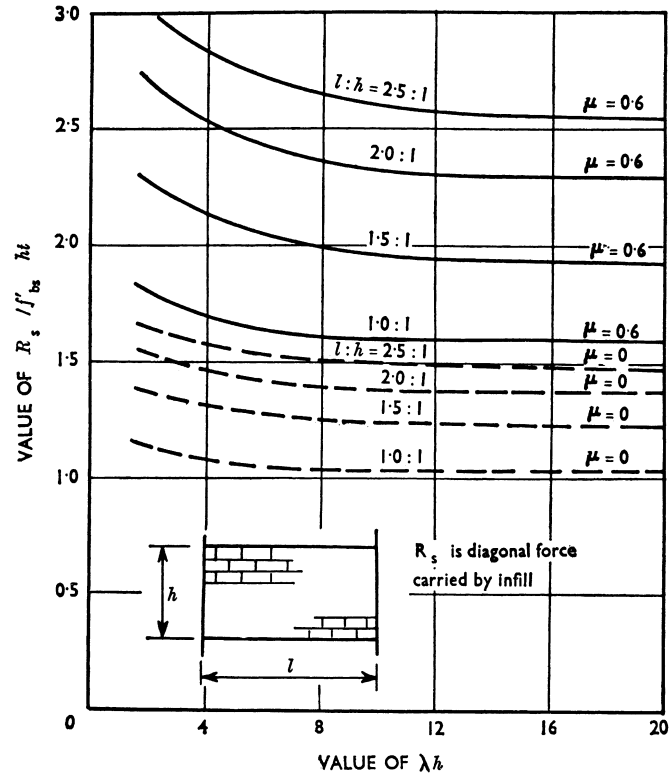

Figure 8.49 Infill wall design graph for limiting shear strength [8.42].

lifting purposes. In BS EN 1992-1-1, clause 12.3.1.1(1) the compressive design strength is multiplied by 0.8, giving $f_{cd,pl} = 0.8 \times 0.85\, f_{ck}/1.5 = 0.453\, f_{ck}$. The limiting strength of concrete to BS 8110, clause 3.9.4.15 is $0.3\, f_{cu}$. These reductions allow for the less ductile, and presumably the unconfined, nature of plain concrete in walls. The wall is built in on all sides and is therefore braced. Referring to Figure 8.46(a) the strength of the strut R_v is given by:

$$R_v = 0.453\, f_{ck} \times 0.1\, w'(t - 2\, e_i) \qquad (8.25)$$

where (clause 5.2(7)) the imperfection $e_i = h'/400$ as (Eq. 12.12) $e_o = 0$

$$R_v = 0.3\, f_{cu} \times 0.1\, w'\, t \qquad (8.25)$$

where f_{ck} $\{f_{cu}\}$ = compressive cylinder {cube} strength of the infill wall.

The horizontal component of R_v gives the resistance $H_v = R_v \cos\theta$ as:

$$H_v = 0.0453\, f_{ck}\, L'(t - 2\, e_i) \qquad (8.26)$$

$$H_v = 0.03\, f_{ck}\, L't \qquad (8.26)$$

To BS EN 1992-1-1, where the infill slenderness ratio $L_e/t >$ approximately 6.5 (see explanation later), the above equation is modified in accordance with clause 12.6.5.2, using a load factor Φ based on slenderness according to equation 12.11. Note that notation in BS EN 1992-1-1, Table 12.1 is: length of infill = b, height = l_w and thickness = h_w. The effective length $L_e = \beta w'$, where $\beta = b/2l_w$ if $b \le l_w$, or $\beta = (1 + (l_w/b)^2)^{-1}$ if $b > l_w$. If there is moment continuity along the top and bottom wall boundaries, β may be factored by 0.85 according to clause 12.6.5.1(4), but this is not usually the case in infill walls.

To BS 8110, where the infill slenderness ratio $w'/t > 12$, the above equation is modified in accordance with clause 3.9.4.16. As the wall is built in on two sides at the corner, the effective length of the wall $L_e = 0.75w'$.

The design is as follows:

There is a limit on the slenderness ratio, clause 12.6.5.1(5)

$$\lambda = \frac{L_e\sqrt{12}}{t} < 86 \text{ or } L_e/t \le 25 \quad (8.27)$$

$$R_v = 0.453\, f_{ck} \times 0.1\, w'\, t\, \Phi \quad (8.28)$$

(Eq. 12.11) where

$$\Phi = (1.14\,(1 - 2e_i/t) - 0.02\, L_e/t) \le (1 - 2e_i/t) \quad (8.29)$$

i.e. slenderness governs where $(1.14\,(1 - 2e_i/t) - 0.02\, L_e/t) \le (1 - 2e_i/t)$.

Then $L_e/t \ge 7\,(1 - 2e_i/t)$, e.g. if $h' = 3000$ mm and $t = 200$ mm, $e_i = 3000/400 = 7.5$ mm, and threshold $L_e/t \ge 7 \times 0.925 = 6.475$.

The horizontal resistance is:

$$H_v = 0.0453\, f_{ck}\, L'\, t\, \Phi \quad (8.30)$$

There is a limit on the slenderness ratio, clause 3.9.4.4.

$$\frac{L_e}{t} = \frac{0.75w'}{t} < 30 \quad (8.27)$$

$$R_v = 0.3\, f_{cu} \times 0.1\, w'\,(t - 1.2e_x - 2e_{add}) \quad (8.28)$$

where

$$e_x = 0.05t \text{ and } e_{add} = \frac{L_e^2}{2500t} \quad (8.29)$$

The horizontal resistance is:

$$H_v = 0.03\, f_{cu}\, L'\,(t - 1.2e_x - 2e_{add}) \quad (8.30)$$

Values of H_v in terms of L' and t are plotted graphically in Figure 8.47a {8.47b} for a specific wall height, together with respective slenderness limits.

At corners, Stafford-Smith shows that the length of contact with the column is $\alpha = \pi/2\lambda$, where λ = stiffness factor from Eq. (8.23). Although the contact length along the beam, as illustrated in Figure 8.46, is 0.5 L' in the case of precast concrete walls, where the interface cracking load is not exceeded, the horizontal contact is taken over the full length L'. BS EN 1992-1-1, clause 6.2.5(1) (equation 6.25) bases the interface shear resistance of a smooth surface (here called v_{Rv}) on cohesion $c = 0.2$ times the design tensile strength $f_{ctd} = 0.14 f_{ck}^{2/3}$, plus friction $\mu = 0.6$ times the normal compression σ_n. Owing to the diagonal strut theory, σ_n will always be acting on the beam from the vertical resolution of the diagonal force $= H \tan\theta$ acting near the corners of the wall over a length of $L'/2$; thus $\sigma_n = H \tan\theta/L't/2$. Normal compression does not act on the contact length of the column because the horizontal force H is resisted by the horizontal interface with the beam. In consideration of the vertical and horizontal shear forces, BS 8110, Part 1, clause 5.3.7 recommends an interface shear stress of 0.45 N/mm^2 without castellations or other shear key aids, because the joints are in compression as well as shear over the contact length.

Hence the vertical and horizontal contact contributions to R_v are respectively:

$$V_{Rv} = c0.14 f_{ck}^{2/3} \alpha t \le R_v \sin\theta \quad (8.31)$$

$$H_{Rv} = R_v \cos\theta \le (c0.14 f_{ck}^{2/3} + \mu\sigma_n) L't \quad (8.32)$$

$$V_{Rv} = 0.45\alpha t \le R_v \sin\theta \quad (8.31)$$

$$H_{Rv} = R_v \cos\theta \le 0.45 L't \quad (8.32)$$

Residual horizontal shear may be taken by added interface reinforcement passing through beams and grouted into holes in the wall, or otherwise fixed to wall panels. Excess vertical shear is carried by the beam-to-column connector.

Bearing under the corners of the wall, which extends a distance $L'/2$ from the corner, is checked for the weaker of the concretes used for the beam, wall or infill grout. The bedded bearing stress is given in Section 7.6.1. as $0.85\, f_{cd} = 0.567\, f_{ck}$ {$f_b = 0.6\, f_{cu}$}.

$$R_v \sin\theta = 0.567 f_{ck} L't/2 \quad (8.33)$$

$$R_v \sin\theta = 0.6 f_{cu} L't/2 \quad (8.33)$$

Exercise 8.10 Concrete infill wall design

The three-storey building shown in Figure 8.50 is 50 m long × 6 m wide and is braced at each end using infill concrete walls. Determine the minimum thickness of the wall at ground floor if the characteristic wind pressure w_k is 0.8 kN/m^2.

Use grade C30/37 concrete for the wall and grade C40/50 concrete for the frame.

Solution

Step 1: Estimate wall thickness

$L = 6000$ mm
$L' = 5700$ mm
$h = 4000$ mm
$h' = 4000 - 100 - 400 = 3500$ mm
$\theta = 31.55°$
$w' = \sqrt{5700^2 + 3500^2} = 6689$ mm
$I = 300 \times 300^3 / 12 = 6.75 \times 10^8$ mm^4
Characteristic wind load at first-floor level per end = 0.8 × 50/2 × (1.5 + 3.0 + 3.25) = 155 kN

$H_v = 1.5 \times 155$	= 232.5 kN
$R_v = 232.5/\cos 31.55°$	= 272.8 kN
$L' > h'$ (as per Table 12.1 with $b > l_w$)	
$L_e = 6689 \times (1 + (3500/5700)^2)^{-1}$	= 4858 mm
$L_e/t < 25$, hence	$t > 194$ mm
Eq. (8.28 and 8.29)	
$e_i = 3500/400$	= 8.75 mm
$R_v = 0.453 \times 30 \times 669\ t\ (1.14\ (1 - 17.5/t) - 97.16/t) \times 10^{-3}$	
i.e. $272.8 = 9.09\ (1.14t - 117.1)$	
Solving gives t	= 129 mm
< 194 mm, i.e. the design is governed more by slenderness than strength.	Let t = 200 mm

$H_v = 1.4 \times 155$	= 217 kN
$R_v = 217/\cos 31.55°$	= 254.7 kN
$L_e = 0.75 \times 6689$	= 5017 mm
$L_e/t = 5017/t < 30$, hence	$t > 167$ mm
Diagonal strength capacity R_v given Eq. (8.28 and 8.29)	
$R_v = 0.3 \times 37 \times 669 \times t \times \left(0.94 - \frac{5017^2}{1250t^2}\right) \times 10^{-3}$	
Solving this quadratic gives t	= 166 mm
< 167 mm, i.e. the design is well balanced for both slenderness and strength.	Let t = 170 mm

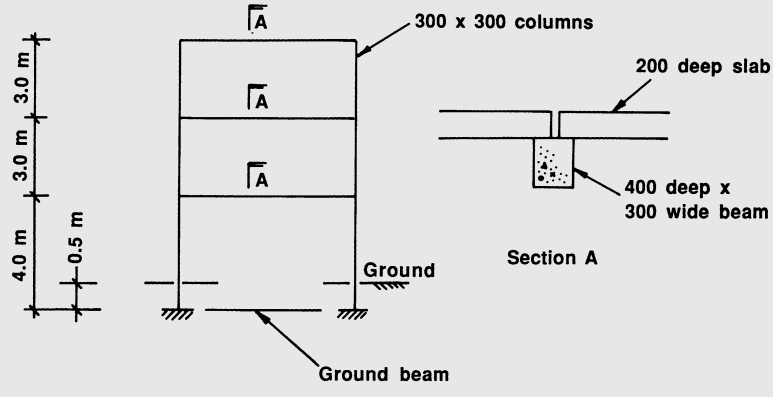

Figure 8.50 Details for Exercise 8.10.

(*Continued*)

Step 2: Check interface strength

Using relative stiffness parameter λ to give contact length against column α using Eq. (8.22)

$E_{wall} = 33\,\text{kN/mm}^2$		$E_{wall} = 28\,\text{kN/mm}^2$	
$E_{frame} = 35\,\text{kN/mm}^2$		$E_{frame} = 30\,\text{kN/mm}^2$	
$\lambda = \sqrt[4]{\frac{33\times200\times\sin(2\times31.55°)}{4\times35\times6.75\times10^8\times3500}}$	$= 2.054\times10^{-3}$	$\lambda = \sqrt[4]{\frac{28\times170\times\sin(2\times31.55°)}{4\times30\times6.75\times10^8\times3500}}$	$= 1.967\times10^{-3}$
$\frac{\alpha}{h} = \frac{\pi}{2\lambda h} = \frac{\pi}{2\times2.054\times10^{-3}\times4000}$	$= 0.191$	$\frac{\alpha}{h} = \frac{\pi}{2\lambda h} = \frac{\pi}{2\times1.967\times10^{-3}\times4000}$	$= 0.20$
Contact length with column		Contact length with column	
$= 0.191 \times 4000$	$= 765\,\text{mm}$	$= 0.2 \times 4000$	$= 800\,\text{mm}$
Eq. (8.31)		Eq. (8.31)	
$V_{Rv} = 0.2 \times 0.14 \times 30^{2/3} \times 765 \times 200 \times 10^{-3}$	$= 41.3\,\text{kN}$	$V_{Rv} = 0.45 \times 800 \times 170 \times 10^{-3}$	$= 61.2\,\text{kN}$
Vertical force $V_v = 272.8 \times \sin 31.55°$	$= 142.8\,\text{kN}$	$R_v = 254.7 \times \sin 31.55°$	$= 133.3\,\text{kN}$
$> 41.3\,\text{kN}$		$> 61.2\,\text{kN}$	
Residual force $= 142.8 - 41.3$	$= 101.4\,\text{kN}$	Residual force $= 133.3 - 61.2$	$= 72.1\,\text{kN}$
is carried to ground beam and does not transfer to column.		is carried to ground beam and does not transfer to column.	
Shear capacity along horizontal plane is given by Eq. (8.32)		Shear capacity along horizontal plane is given by Eq. (8.32)	
$\sigma_n = 232.5 \times 10^3 \tan 31.55°/0.5 \times 5700 \times 200$	$= 0.25\,\text{N/mm}^2$	$H_{Rv} = 0.45 \times 5700 \times 170 \times 10^{-3}$	$= 436.0\,\text{kN}$
$H_{Rv} = (0.2 \times 0.14 \times 30^{2/3} + 0.6 \times 0.25) \times 5700 \times 200 \times 10^{-3}$	$= 479.1\,\text{kN}$	$> 217\,\text{kN}$ design force.	
$> 232.5\,\text{kN}$ design force.		Use 170 mm-thick concrete wall.	
Use 200 mm-thick concrete wall.			

Exercise 8.11 Slender precast infill wall strength check

Calculate the ultimate horizontal shear capacity of the 200 mm-thick precast concrete shear wall shown in Figure 8.51, and determine the minimum strength of the precast concrete. The wall is built into a precast concrete frame on all sides.

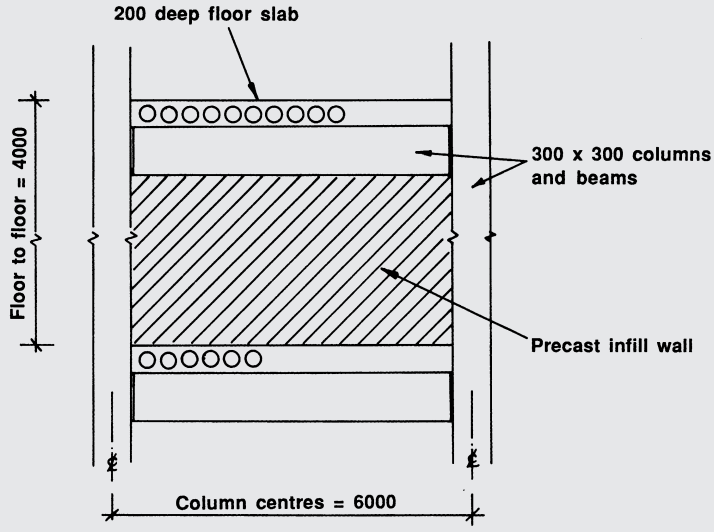

Figure 8.51 Details for Exercise 8.11.

Solution

Geometric and material data is as for Example 8.10.

$\theta = 31.55°$

$w' = \sqrt{5700^2 + 3500^2} = 6689$ mm

$t = 200$ mm

Ex. 8.10. $L_e = 0.726 \times 6689$	$= 4858$ mm
$L_e/t = 4858/200$	$= 24.2$
< 25	
Eq. (8.28 and 8.29)	
$e_i = 3500/400$	$= 8.75$ mm
$R_v = 0.453\, f_{ck} \times 669 \times 200\ (1.14\ (1 - 17.5/200) - 97.16/200) \times 10^{-3}$	$= 33.6\, f_{ck}$ kN
$H_v = R_v \cos 31.55°$	$= 28.64\, f_{ck}$ kN
Shear capacity on horizontal bedding is itself a function of H_v (in kN) and f_{ck}	
$\sigma_n = H_v \times 10^3 \tan 31.55°/0.5 \times 5700 \times 200 = 10.77 \times 10^{-4}\, H_v$ N/mm^2	
$H_{Rv} = (0.2 \times 0.14 f_{ck}^{2/3} + 0.6 \times 10.77 \times 10^{-4} H_v) \times 5700 \times 200 \times 10^{-3}$	
$H_{Rv} = 31.92 f_{ck}^{2/3} + 0.737 H_v$	
But in the limit $H_{Rv} = H_v = 28.64 f_{ck}$	
Then $28.64 f_{ck} = 31.92 f_{ck}^{2/3} + 21.11 f_{ck}$ for a limiting shear capacity $H_{Rv} = 2180$ kN.	$f_{ck} \geq 76.1$ N/mm^2

Ex. 8.10. $L_e = 0.75 \times 6689$	$= 5017$ mm
$L_e/t = 5017/200$	$= 25.08$
< 30, but because > 12, reduction factors apply	
Eq. (8.28 and 8.29)	
$R_v = 0.3 f_{cu} 669 \times 200 \times \left(0.94 - \frac{5017^2}{1250 \times 200^2}\right) \times 10^{-3}$	$= 17.52\, f_{cu}$ kN
$H_v = R_v \cos 31.55°$	$= 14.93\, f_{cu}$ kN
Shear capacity on horizontal bedding	
$H_{Rv} = 0.45 L' t = 0.45 \times 5700 \times 200 \times 10^{-3}$	$= 513.0$ kN
Then if 513.0 kN = 14.93 f_{cu} for a limiting shear capacity $H_{Rv} = 513$ kN.	$f_{cu} \geq 34.4$ N/mm^2

This exercise reinforces the conclusion from Exercise 8.10 that the design of infill shear walls to BS 8110 is better balanced than to BS EN 1992-1-1, where slenderness limit of 25 is restrictive on the strength.

8.7.3 Design method for brickwork infill panels

The ultimate horizontal forces are resisted by a diagonal compressive strut across the infill. The criteria are based on a stiffness factor λ, as before. The method is the same except that:

- A factor k replaces the constant 0.1 for the width of the diagonal strut.
- The crushing strength of the concrete is replaced with f_k, the strength of brickwork (masonry units in clay or calcium silicate) in compression. See BS EN 1996-1, clause 3.6.1.2, and Tables NA.2 and NA4 [8.48] {BS 5628, Part 1 [8.49]}.
- A further criterion is the local crushing resistance of the brickwork at the corners, obtained from Figure 8.48.
- Young's modulus for brick = 1000 f_k {450 f_k} (N/mm^2 units).
- The horizontal shear limit is obtained from Figure 8.49, with $f_s = f_v/\gamma_m$, where $f_s = 0.35$ N/mm^2 (BS 5628, Part 1, clauses 25 and 27.4)} and $\gamma_m = 2.5$. $v = 0.3 + 0.4\sigma_d \leq 0.065\, f_b$ (BS EN 1996-1, clause 3.6.2(3)) {$f_s = 0.35$ N/mm^2 (BS 5628, Part 1, clauses 25 and 27.4)} and $\gamma_m = 2.5$. $\mu = 0.6$ for solid (or unperforated) bricks, because vertical compressive stress acts at the same time as the shear.

$$\text{Hence } R_{vs} = f_s h' t \times \text{value from the design graph} \tag{8.34}$$

$$f_s = \frac{0.30 + 0.4\sigma_d}{2.5} \qquad (8.35)$$

Hence

$R_v \le f_s h' t \times$ value from graph in Figure 8.49.

$$f_s = \frac{0.35}{2.5} = 0.14 \text{ N/mm}^2 \qquad (8.35)$$

Hence

$R_v \le 0.14 h' t \times$ value from graph in Figure 8.49.

The compression limit is obtained from compressive failure curves in Figure 8.48:

$R_{vc} = (f_k/\gamma_m) h' t \times$ value from graph (8.36)

where, from BS EN 1996-1, clause 3.6.1.2, with group 1 bricks of strength $f_m \le 110 \text{ N/mm}^2$ and mortar strength $f_m \le 12 \text{ N/mm}^2$

$f_k = 0.5 f_b^{0.7} f_m^{0.3} \le 75 \text{ N/mm}^2$

$R_{vc} = (f_k/\gamma_m) h' t \times$ value from graph (8.36)

where f_k is from BS 5628, Part 1, clause 27.3, based on the strength of mortar from Table 1. The bricks should have a minimum crushing strength of 21 N/mm^2.

Exercise 8.12 Brickwork infill wall

The building in Exercise 8.10 is braced at each end between first and second floors using 215 mm-thick infill brick walls. Check the adequacy of these walls using 47 N/mm^2 strength brick in 1: ¼: 3 mortar.

Solution

$L' = 5700$ mm

$h = 3000$ mm

$h' = 3000 - 200 - 400 = 2400$ mm

$\theta = 22.83°$

$w' = \sqrt{5700^2 + 2400^2} = 6185$ mm

$I = 300 \times 300^3 / 12 = 6.75 \times 10^8$ mm^4

$t_{wall} = 215$ mm

$\gamma_m = 3.0$ for compression, and 2.5 for shear.

$f_b = 47 \text{ N/mm}^2$ for the bricks, and

$f_m = 12 \text{ N/mm}^2$ as 1:¼:3 is M12 mortar mix, so the masonry strength

$f_k = 0.5 f_b^{0.7} f_m^{0.3} = 15.6 \text{ N/mm}^2$

$E_{wall} = 1000 \times 15.6 = 15.6 \text{ kN/mm}^2$

$E_{frame} = 35 \text{ kN/mm}^2$

$$\lambda = \sqrt[4]{\frac{15.6 \times 215 \times \sin(2 \times 22.83°)}{4 \times 35 \times 6.75 \times 10^8 \times 2400}} = 1.804 \times 10^{-3}$$

$\lambda h = 5.411$

$$\frac{L'}{h'} = 2.375$$

From Figure 8.48

$$\frac{R_{vc}}{(f_k/\gamma_m) h' t} = 0.33$$ for compression failure, and 0.55 for diagonal splitting failure. The lower is critical, so

$$R_{vc} = 0.33 \times \frac{15.6}{3.0} \times 2400 \times 215 \times 10^{-3} = 885.6 \text{ kN}$$

From Figure 8.49, using $\mu = 0.6$

$$\frac{R_s}{(f_v/\gamma_m) h' t} = 2.65$$ for shear failure.

$\gamma_m = 3.5$ for compression, and 2.5 for shear.

From BS 5628 Table 2(a): $f_k = 14.28 \text{ N/mm}^2$

$E_{wall} = 450 \times 14.28/1000 = 6.43 \text{ kN/mm}^2$

$E_{frame} = 30 \text{ kN/mm}^2$

$$\lambda = \sqrt[4]{\frac{6.43 \times 215 \times \sin(2 \times 22.83°)}{4 \times 30 \times 6.75 \times 10^8 \times 2400}} = 1.502 \times 10^{-3}$$

$\lambda h = 4.505$

$$\frac{L'}{h'} = 2.375$$

From Figure 8.48

$$\frac{R_{vc}}{(f_k/\gamma_m) h' t} = 0.38$$ for compression failure, and 0.60 for diagonal splitting failure. The lower is critical, so

$$R_{vc} = 0.38 \times \frac{14.28}{3.5} \times 2400 \times 215 \times 10^{-3} = 800 \text{ kN}$$

From Figure 8.49, using $\mu = 0.6$

$$\frac{R_s}{(f_v/\gamma_m) h' t} = 2.73$$ for shear failure.

The shear capacity is a function of the normal compression σ_n; iteration is required. Try $H_v = 225\,\text{kN}$.

$$f_s = \left(0.3 + \frac{0.4 \times 225 \times 10^3}{0.5 \times 5700 \times 215}\right) \Big/ 2.5 \qquad = 0.179$$

$$R_s = 2.65 \times 0.179 \times 2400 \times 215 \times 10^{-3} \qquad = 244.4\,\text{kN}$$

$$H_{Rv} = 244.4 \cos 22.83° \qquad = 225.2\,\text{kN}$$

Design ultimate wind load at second floor level per end

$$H_v = 1.5 \times 0.80 \times 25 \times (1.5 + 3.0) \qquad = 135.0\,\text{kN}$$

$< 225.2\,\text{kN}$ capacity, and the design value of

$$R_v = 135.0/\cos 22.83° \qquad = 146.5\,\text{kN}$$

$$\frac{\alpha}{h} = \frac{\pi}{2\lambda h} = \frac{\pi}{2 \times 1.804 \times 10^{-3} \times 3000} \qquad = 0.29$$

Contact length with column $\alpha = 0.29 \times 3000 = 870\,\text{mm}$

Shear strength without σ_n is $0.3/2.5 = 0.12\,\text{N/mm}^2$

$$R_v = \frac{0.12 \times 870 \times 215 \times 10^{-3}}{\sin 22.83°} \qquad = 57.8\,\text{kN}$$

Residual force $= (146.5 - 57.8) \sin 22.83°$ $= 34.4\,\text{kN}$ is carried to first-floor beam and does not transfer to column

$$R_s = 2.73 \times \frac{0.35}{2.5} \times 2400 \times 215 \times 10^{-3} \qquad = 197.2\,\text{kN}$$

$$H_{Rv} = 197.2 \cos 22.83° \qquad = 181.8\,\text{kN}$$

Design ultimate wind load at second floor level per end

$$H_v = 1.4 \times 0.80 \times 25 \times (1.5 + 3.0) \qquad = 126.0\,\text{kN}$$

$< 181.8\,\text{kN}$ capacity, and the design value of

$$R_v = 126.0/\cos 22.83° \qquad = 136.7\,\text{kN}$$

$$\frac{\alpha}{h} = \frac{\pi}{2\lambda h} = \frac{\pi}{2 \times 1.502 \times 10^{-3} \times 3000} \qquad = 0.349$$

Contact length with column $\alpha = 0.349 \times 3000 = 1046\,\text{mm}$

$$R_v = \frac{0.14 \times 1046 \times 215 \times 10^{-3}}{\sin 22.83°} \qquad = 81.1\,\text{kN}$$

Residual force $= (136.7 - 81.1) \sin 22.83°$ $= 21.6\,\text{kN}$ is carried to first-floor beam and does not transfer to column

8.7.4 Infill walls without beam framing elements

The function of horizontal beams for the framing action in infill wall design may be replaced by using dowels between upper and lower walls, as shown in Figures 8.52 and 8.53. The units are economical to manufacture in shallow steel or timber moulds; see Figure 8.54. The dowels serve two functions – by providing horizontal shear forces as well as holding the walls together by developing tension across the interface. The diagonal strut analogy for infill walls is replaced by shear panel concepts, whereby both the horizontal and the complementary vertical shear forces are resisted by mechanical means. The vertical shear resistance between the wall and columns may be provided either by welding together cast-in plates on site, or by using projecting dowels grouted into a keyed joint along the full interface.

This method of construction, although more expensive than the infill method, has the advantage that fairly large voids may be formed in the walls, providing that there remains sufficient contact between the precast components to allow panel action to take place. The wall panels are also relatively inexpensive to manufacture, requiring simple rebar cages usually consisting of two sheets of A142 or A193 mesh. The units shown in Figure 8.54 also included projecting dowels, dowel holes and cast-in plates.

Figures 8.55 and 8.56 show a deep nib solution to providing a large, vertical shear capacity between connecting walls. This is an alternative to the use of interlocking loops or welding plates in the sides of the walls. Vertical tie bars pass through sleeves in the walls, which are grouted to form the continuity. The black ring in Figure 8.56 is a dam to enable a flowable, non-shrink grout to be used.

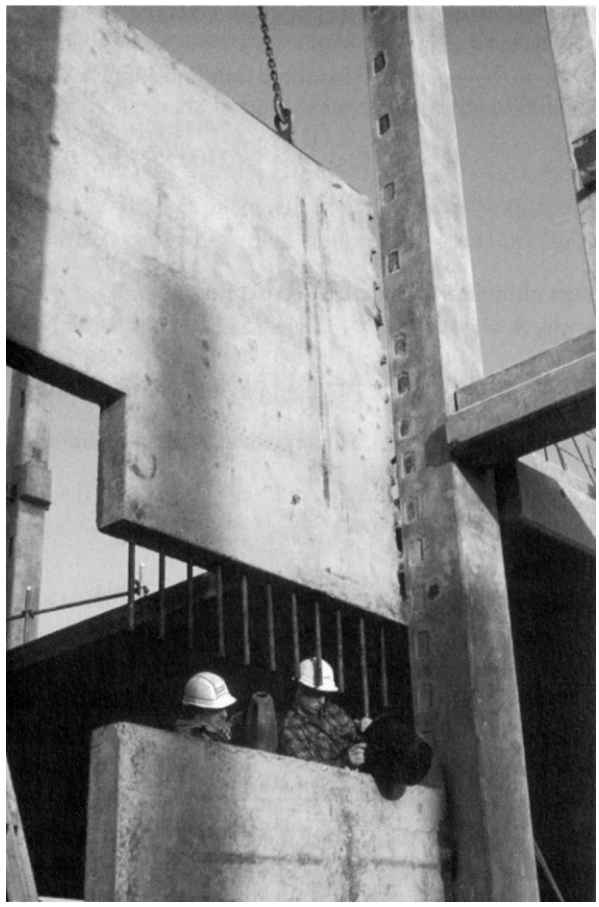

Figure 8.52 Construction of precast shear walls.

8.7.5 Use of slip-formed or extruded hollow-core walls as infill walls

Slip-formed or extruded hollow-core units, made in a similar manner to hollow-core slabs, may be used as infill walls, as shown in Figure 8.57 and Figures 8.58(a) and (b).The latter shows two alternative forms of construction. The method is not used extensively in some countries, and hardly at all in the UK, but it should not be dismissed as an alternative form of bracing, even though the thickness of the wall will inevitably be greater than for a solid wall of equal strength.

Slip-formed hollow-core walls are notoriously difficult to handle in the vertical position, owing to an absence of cast-in lifting points. Friction clamps provide the best method of lifting and pitching, but the safety of these devices must be guaranteed at all times.

The wall units must be symmetrical and lightly prestressed. In the first method (Figure 8.58(a)), the hollow cores lie in a horizontal plane and the ends of the cores are filled with *in situ* concrete (6 mm aggregate) for a distance of about 100 mm generally, and 500 mm to 600 mm in at least two cores per unit. Note the similarity with the hollow-core slab arrangement. The edges of the units are profiled to give a 'tongue-and-groove' joint, which helps to locate the walls one above another. Wall units are bedded onto wet mortar, with steel or plastic shims used to obtain the correct levels. Some form of temporary stability is required, usually in the form of sturdy clamps placed around the columns at the corners of each wall unit. This method of assembly relies on the columns for temporary stability.

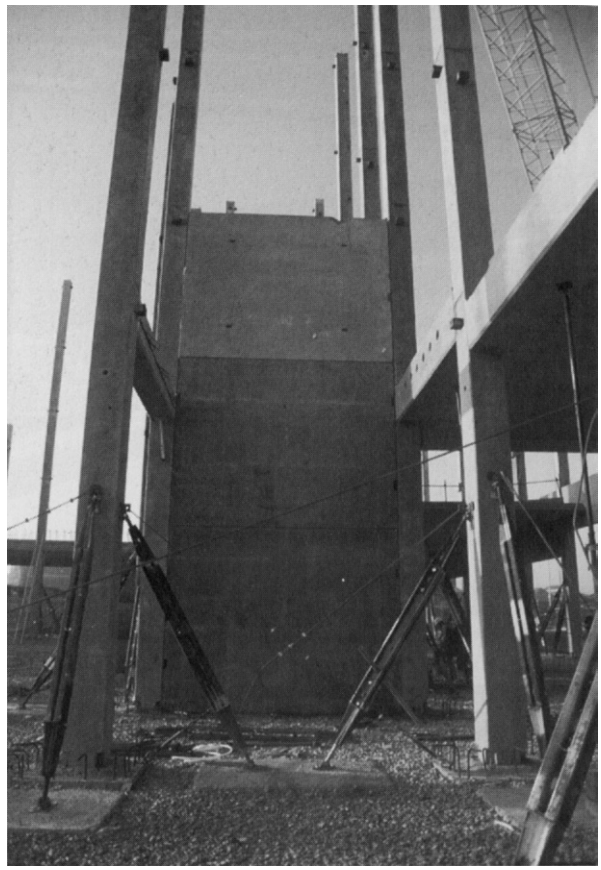

Figure 8.53 Partially complete construction of precast shear walls.

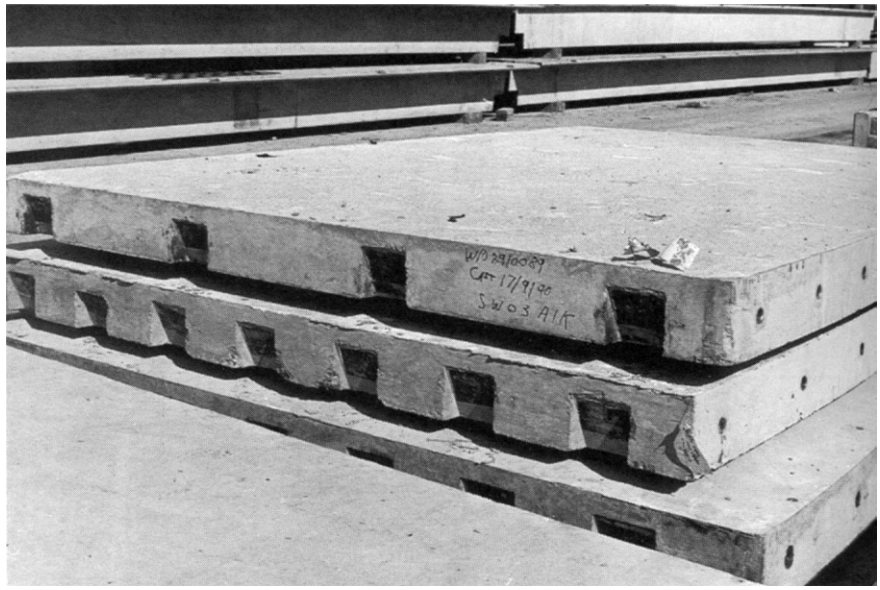

Figure 8.54 Wall panels in stock yard.

Figure 8.55 Precast concrete walls with deep nib vertical connection.

Figure 8.56 Vertical tie bars in deep nib connection between precast concrete walls.

Figure 8.57 Hollow-core shear wall under construction (in Far East).

The design method is an extension of the solid infill wall design, except that there are four additional considerations:

- the reduced cross-sectional area and inertia of the hollow-core wall unit compared with a solid wall of equal thickness
- the horizontal shear force in the longitudinal joint between the units
- the shear key to the column
- crushing of the webs in the corners of the wall panel.

The diagonal strut model is shown in Figure 8.58. Because the ends of the wall units are filled with grout, the contact width is equal to the full width of the wall. However, if Eq. (8.22) is to be used to determine the contact length α, the relative stiffness of the hollow-core wall must be modified to take into account the voids. The wall must also be checked for diagonal compressive capacity and for the effects of slenderness, as in the design of the solid wall in Section 8.7.1. Thus an effective thickness of wall t_{ef} is found by equating EI_{hcw} of a hollow-core unit to EI of a solid wall of equal thickness. Assuming that E is constant, and the breadth of the wall is b, then the conversion is made as follows:

$$t_{ef} = \sqrt[3]{\frac{12I_{hcw}}{b'}} \tag{8.37}$$

The effect of this reduction will have a compound effect on strength, especially if the wall becomes slender. The compressive strength of the wall is based on the total thickness of the two flanges – i.e. the webs between the hollow cores are ignored. As a result, the overall thickness of a hollow-core wall is likely to be greater than that of an equivalent solid wall. However, as the thickness of the greater proportion of solid walls is governed in practice not by ultimate design, but by lifting in the factory, the differences may not always be significant.

The second criterion concerns the development of sufficient vertical compression across the joint to enable the joint to be considered a compression joint, for which the ultimate shear stress is v_{Rdi}

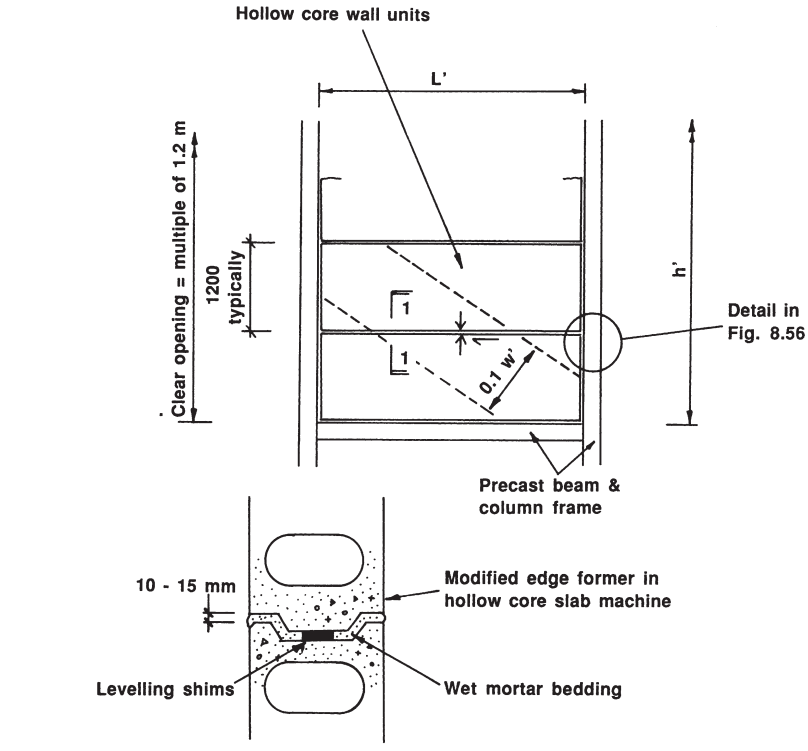

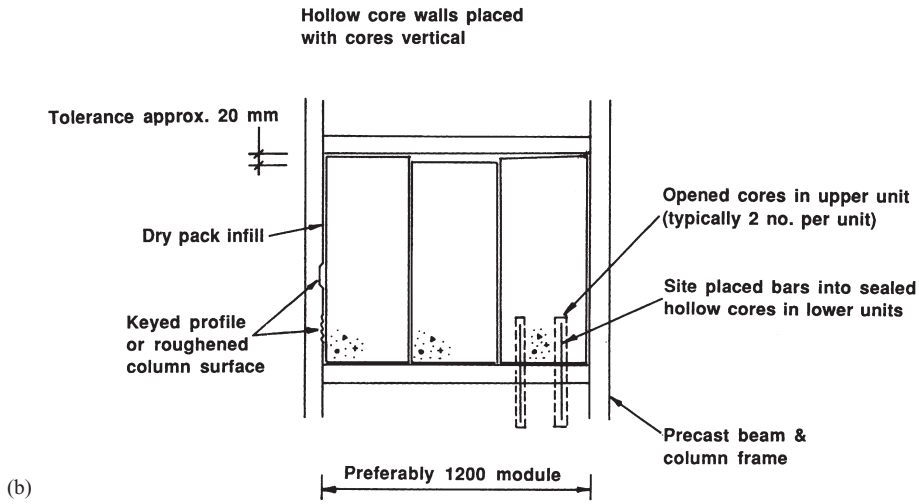

Figure 8.58 Hollow-core units used as infill shear walls. (a) Hollow cores and joints horizontal and (b) hollow cores and joints vertical.

which BS EN 1992-1-1, clause 6.2.5 [8.5], defines in terms of the normal stress σ_n {according to BS 8110, Part 1, clause 5.3.7(b) [8.6] this is 0.45 N/mm^2}. Neither code specifies the degree of compression that must exist across the joint, but it must be active in all design situations. The minimum compressive stress due to self-weight gives an ultimate compressive stress of about 0.04 N/mm^2, and is clearly insignificant. However, it is not possible for a horizontal shear force H_v to exist in the joint unless it is accompanied by a diagonal force R_v, where $R_v = H_v/\cos\theta$. The vertical component of $R_v = R_v \sin\theta$. The force R_v acts across a diagonal of width 0.1 × diagonal length of wall = $0.1w'$ and therefore compresses the joint over a distance $x = 0.1\ w'/\sin\theta$.

However, because the wall unit has large in-plane stiffness, EI_{xx}, it is known that diagonal forces acting across a hollow-core diaphragm exert uniform pressures and displacements over a considerable length of the interface. Wahid Omar [8.31] found differential crack openings of less than 0.05 mm in a 4 m long hollow-core slab when subjected to shear, and several investigators have measured greater shear capacities between hollow-core units when a diagonal force is acting across the joint.

Thus the compressive stress may be determined and, if necessary, added to the self-weight pressure of 0.04 N/mm^2. The ratio of the vertical to the horizontal stress will depend on θ, but for $\theta = 35°$ (a common value) it is between 0.70 and 0.75. This is equal to the required coefficient of friction in a plain surface (BS EN 1992-1-1, clause 6.2.5 [8.5]) {BS 8110, Part 1, Table 5.3 [8.6]}.

The wall units must in all cases be prevented from moving apart, and be shear-connected to the columns. The simplest method is to cast projecting U- or L-shaped tie bars into the columns and fill the mating opened hollow core with expansive concrete, as shown in Figure 8.59. The projection from the column should be a full anchorage length, typically 600 mm for a 16 mm bar. Mild steel bars are often cast against the inside of the mould and broken out as soon as the column is demoulded.

The area of steel required may be calculated as follows. The vertical shear force is complementary to the horizontal force and equal to $H \tan\theta$. If the vertical shear stress exceeds 0.15 N/mm^2

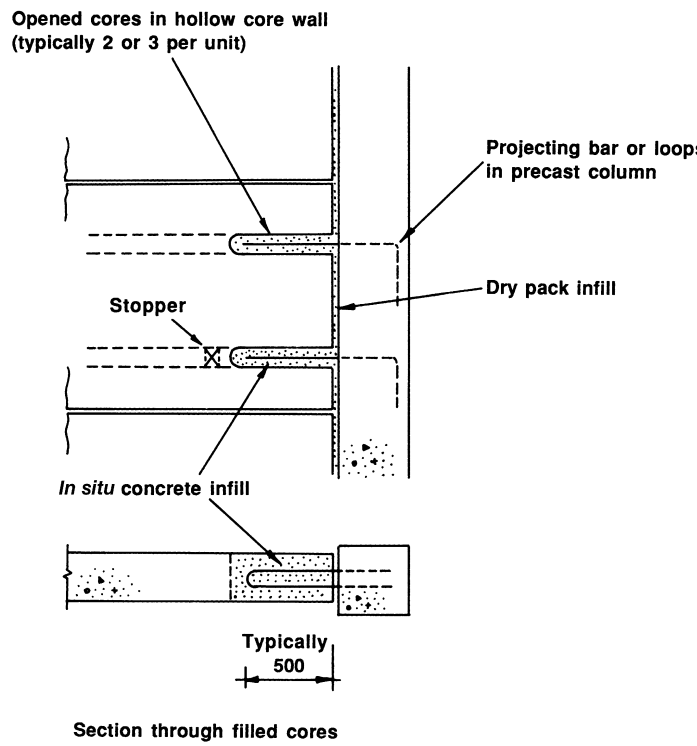

Figure 8.59 Shear connectors between infill hollow-core wall and columns.

{0.23 N/mm^2} (this is used because only a part of the vertical joint is under compression and because the column is flexible), reinforcement should be provided to resist the entire shear force. The area of shear steel projecting from the column is given by:

$$A_s = \frac{H_v \tan\theta}{0.6 \times 0.87 f_y} \tag{8.38}$$

This steel may be distributed uniformly over the storey height. At least two cores per wall unit should be opened. The opened core should be filled using a minimum concrete grade C30/37. Maximum bar size to permit on-site bending is 16 mm.

Local crushing of the webs in the corners of the wall panel may occur in flexible frames, where the contact zones, α are small. This may easily be prevented by filling the first one or two cores with concrete in the factory for a distance of about 600 mm.

In the second method, Figure 8.58(b), the wall-to-wall joints are *vertical*. The main differences with the former method are:

- the joint is rebated and filled (inside a shutter) in the same way as floor slabs
- the interface shear stresses are the result of complementary shear forces trying to rack the panel in a lozenging effect.

The largest force occurs in the vertical joint nearest the centre of the panel. The joints are all subjected to a normal compression $R_v \cos\theta$, which is equal to the shear force H_v. Thus a limiting value for the vertical interface shear stress of v_{Rdi} {0.45 N/mm^2} is used in the design. The surface of the column in contact with the wall is either roughened by removing laitance and revealing the coarse aggregate, or castellated to form a shear key (see Figure 6.9 [8.5]). The effects on slenderness and strength capacity of the hollow-core unit are the same as in the former method.

The horizontal joint between the top of the units and the floor beam is made by dowelling the hollow cores through holes (preferably slots) in the beam. The tolerance required in this joint to take care of variations in the height of the hollow-core units is at least 20 mm. The figure has exaggerated the effect. The dowels are grouted into two or three sealed hollow cores per unit prior to the upper-floor units being placed. The joint is completed by pouring *in situ* concrete through preformed openings in the upper wall units. Expansive cements are used throughout.

Hollow-core walls are reinforced longitudinally, using a symmetrical arrangement of prestressing wires, to produce a uniform prestress of around 2 N/mm^2. This is sufficient for lifting purposes. If the walls are exposed to lateral wind loading, they should be designed to span horizontally between columns or vertically between beams. It is unlikely that this will be a governing factor in the design of the units.

Exercise 8.13 Hollow-core shear wall design

Calculate the horizontal shear capacity of a 250 mm-thick hollow-core shear wall for the geometry and loading shown in Figure 8.60. Design the connecting reinforcement to the column for this capacity.

Use grade C40/50 concrete for the precast wall, grade C30/37 concrete for the *in situ* infill, and mild steel f_{yk} {f_y} = 250 N/mm^2 for the rebent loops in the joints.

Solution

Step 1: Ultimate shear resistance

Properties of hollow-core wall per 1200 mm-wide unit taken from manufacturer's literature are:

$t = 250$ mm

$I = 1250 \times 10^6$ mm^4

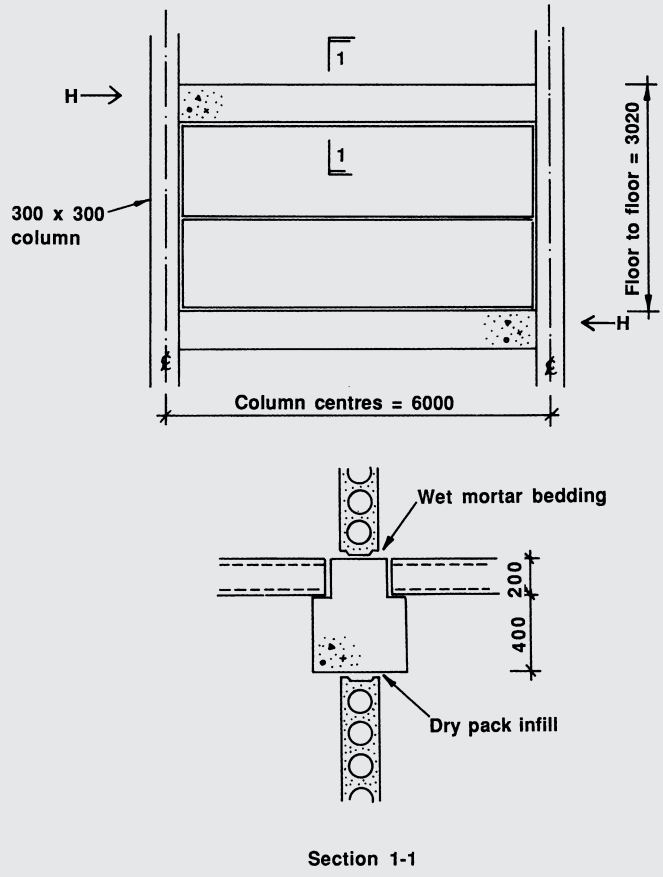

Figure 8.60 Details for Exercise 8.13.

Top and bottom flange thicknesses = 35 mm
$L' = 5700$ mm
$h = 3020$ mm
$h' = 3020 - 200 - 400 = 2420$ mm
$\theta = 23.0°$
$w' = \sqrt{5700^2 + 2420^2} = 6192$ mm
For the purpose of slenderness the effective thickness of the hollow-core unit is:

$$t_{ef} = \sqrt[3]{\frac{12 \times 1250 \times 10^6}{1200}} = 232 \text{ mm}$$

$L_e = (1 + (2420/5700)^2)^{-1} \times 6192$	$= 5246$ mm
$L_e/t_{ef} = 5246/232$	$= 22.6$
< 25	
For the purpose of strength the effective thickness is t_{ef}	$= 70$ mm
Eq. (8.28 and 8.29)	
$e_i = 2420/400$	$= 6.0$ mm
$R_v = 0.453 \times 40 \times 619 \times 70\ (1.14\ (1 - 6.0/232) - 0.02 \times 5246/232) \times 10^{-3}$	$= 517.0$ kN
$H_v = R_v \cos 23.0°$	$= 475.9$ kN

$L_e/t_{ef} = 0.75 \times 6192/232$	$= 20.0$
< 30, but because > 12, reduction factors apply.	
For the purpose of strength the effective thickness is $t_{ef} = 35 + 35$	$= 70$ mm
Eq. (8.28 and 8.29)	
$R_v = 0.3 \times 50 \times 619 \times 70\left(0.94 - \frac{20.0^2}{1250}\right) \times 10^{-3}$	$= 403.0$ kN
$H_v = R_v \cos 23.0°$	$= 370.9$ kN

Step 2: Check interface strength

Shear capacity on horizontal bedding joints using bedded width of 250 mm. For BS EN 1992-1-1 in the first instance, ignoring any friction contribution from vertical load on the beam (can be considered if necessary);

$H_{Rv} = 0.2 \times 0.14 \times 30^{2/3} \times 5700 \times 250 \times 10^{-3}$	$= 465.5\,\text{kN}$
≈ compression capacity	
Vertical shear force V	
$= 465.5 \times \tan 23.0°$	$= 197.6\,\text{kN}$
Mean vertical interface stress	
$= 197.6 \times 10^3/250 \times 2420 =$	$= 0.33\,\text{N/mm}^2$
$> 0.15\,\text{N/mm}^2$, then V to be resisted by projecting loops in shear.	
$A_s = \dfrac{197.6 \times 10^{-3}}{0.6 \times 0.87 \times 250}$	$= 1514\,\text{mm}^2$
Provide four H16 ($1608\,\text{mm}^2$) loops at equal spaces, two per unit.	

$H_v = 0.45 \times 5700 \times 250 \times 10^{-3}$	$= 641.2\,\text{kN}$
> compression capacity	
Vertical shear force V	
$= 370.9 \times \tan 23.0°$	$= 157.4\,\text{kN}$
Mean vertical interface stress	
$= 157.4 \times 10^3/250 \times 2420 =$	$= 0.26\,\text{N/mm}^2$
$> 0.23\,\text{N/mm}^2$, then V to be resisted by projecting loops in shear.	
$A_s = \dfrac{157.4 \times 10^{-3}}{0.6 \times 0.87 \times 250}$	$= 1206\,\text{mm}^2$
Provide four H16 ($1608\,\text{mm}^2$) loops at equal spaces, two per unit.	

8.7.6 Cantilever shear walls and shear boxes

Cantilever walls and boxes are generally very large physically because they are most often provided as stabilising elements around stairwells and lift shafts. The individual precast components are tied together vertically using site-placed continuity reinforcement or other mechanical connections, such as welded plates or bars.

Various failure modes are considered: shear slip failure occurs where L/h is greater than (approximately) 2.5 to 3, as shown in Figure 8.61(a); flexural tension failure occurs particularly if the wall is lightly loaded axially, Figure 8.61(b), and flexural compression failure occurs if the wall is heavily loaded, Figure 8.61(c). The wall panels themselves are designed as reinforced (not plain) concrete walls in the conventional rc manner.

The slenderness of the wall, out-of-plane eccentric loading and constructional tolerances are taken into consideration. Particular emphasis is given to the reinforcing of corners – particularly to avoid cracking at the early lifting age – and around windows and doors, etc. Figure 8.62 shows a typical detail for these regions. Large fenestrations, openings for doors or services, etc. are readily included by considering alternative load paths for the vertical and horizontal forces. The positions of the joints may have to be amended if particularly large voids fall on the proposed joint lines.

Complete storey-height units require only horizontal connections between them. Shear forces and overturning moments in the wall system generate regions of compression, shear and tension. Fully anchored reinforcing bars (or other mechanical devices, such as welded or bolted plates, or wall shoes, etc.) are used to transfer the tensile forces between units in addition to maintaining the pre-compression across the faces of the joint. The joint is assumed to be cracked only in flexure, and the shear friction theory is used to justify taking the full length of the wall into consideration in the determination of the average ultimate shear stress. The limiting value is f_{cvd} $\{0.45\,\text{N/mm}^2\}$. In reality the shear resistance of the concrete under high pre-compression is usually sufficient to resist the imposed shear.

Units assembled from individual flat panels are connected on site using vertical joints whose main function is to resist shear forces resulting from the cantilever action of the wall. The resistance to sliding depends on the size and shape of the joint, in addition to the amount of reinforcement projecting from the adjoining panels. Typically, the joint is at least 60 mm across the root (10–15 mm at the outside edges). Larger root gaps are occasionally necessary, although full-scale experimental work [8.18] has shown a reduction of 44 per cent in the ultimate shear strength when the root gap is increased to 120 mm. Vertical and castellated joints have been studied fairly extensively [8.50–8.53] and the ultimate design stress of $0.5\,f_{ctd} + 0.9\,\sigma_n$ according to BS EN 1992-1-1, clause 6.2.5(1) and (2) [8.5], typically $0.60 + 0.78 = 1.38\,\text{N/mm}^2$ for $A_s = 0.2\%\,A_c$ with $f_{ck} = 25\,\text{N/mm}^2$ and

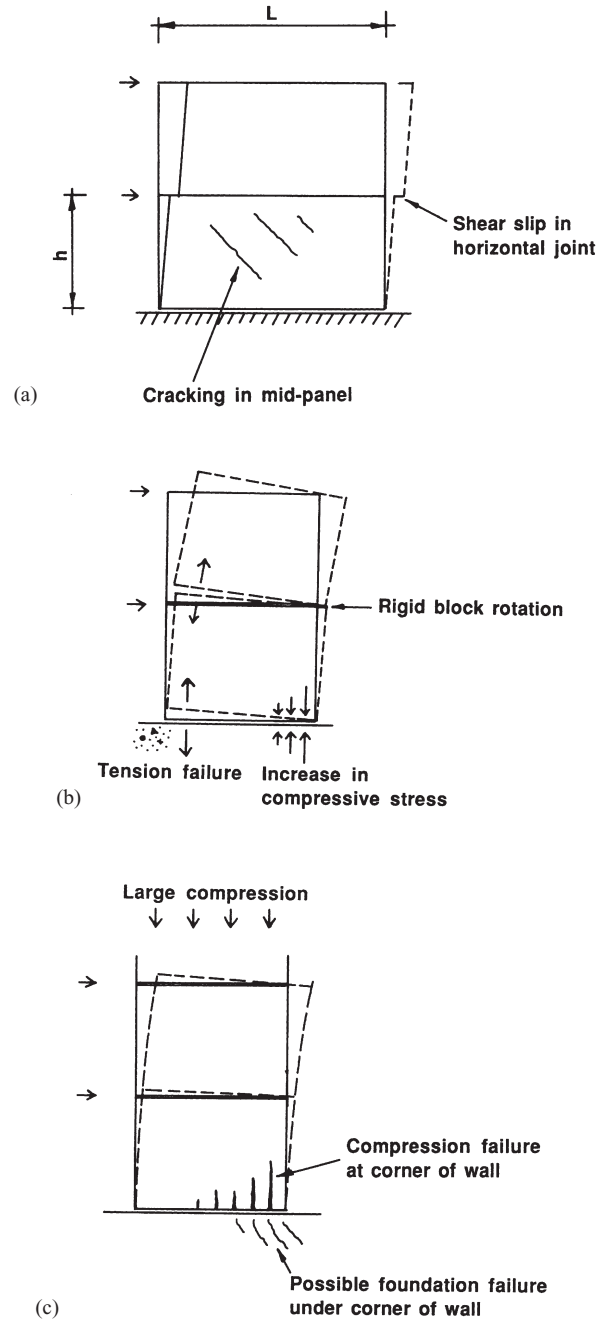

Figure 8.61 Deformations in wall panels. (a) Shear failure in long wall; (b) flexural tension due to large overturning moment; (c) compression failure due to combined axial forces and moments.

$f_{yk} = 500\,\text{N/mm}^2$ {$1.3\,\text{N/mm}^2$} has been shown to be conservative as long as sufficient reinforcement is provided to develop aggregate interlock by shear friction.

Mechanical connections are favoured by some engineers, because they provide immediate stability to the walls. Fully anchored plates are used to provide the site welder with easily accessible down-hand welding.

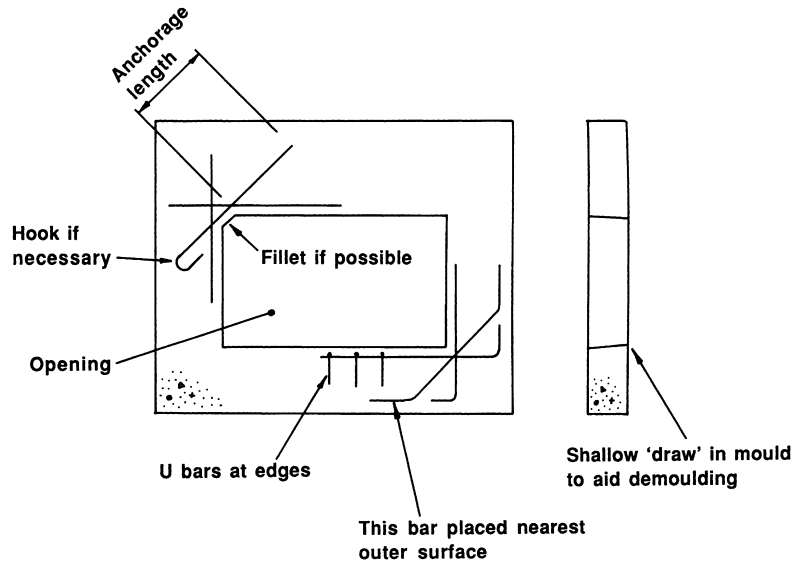

Figure 8.62 Reinforcement details at large openings in shear walls.

8.7.7 Hollow-core cantilever shear walls

The hollow-core walls described in this section are wet-cast, reinforced concrete panels with two or three preformed rectangular cores. The walls are used with the cores placed vertically and the design is different from that for the slip-formed infill walls discussed in Section 8.7.5.

The arrangement of these walls is shown in Figures 3.46 and 8.63. The walls must be placed between columns, even though they do not rely on composite action with the columns. The design section in BS 8110, Part 1, clause 3.9.3.6.3 is not very informative, and so design methods for columns are adopted with due consideration for transverse (out-of-plane) bending.

Hollow-core wall elements are manufactured using grade C30/37 to C40/50 concrete and contain typically 0.2 per cent reinforcement in each face. The hollow core is about 75 to 100 mm wide, depending on the overall thickness of the wall, and there are usually three or four cores in the length of the unit; see Figure 3.46. Typical sizes of wall are b = 200 to 250 mm, core size = 275 × 1200 mm, H = half or full storey height, and L = 3 to 5 m. The core is formed using a sacrificial polystyrene (or similar) former. The inside surface therefore provides a good shear key with the site-placed concrete. A rebate is provided in the sides of the unit to facilitate a keyed and grouted interface with the column.

Site-placed reinforcement includes starter bars cast into the foundation (the length of projecting bar is 1.0 × tension anchorage length), to which additional bars are lapped to provide the holding-down (tension) force F_s. *In situ* concrete (usually grade C30/37) is placed in the hollow cores to provide the compressive force F_c. The reinforcement is provided along the full length of the wall, with the larger bars, typically 16 mm-diameter high-tensile bars, nearest to the sides, or furthest from the neutral axis. The centre-most cores of the wall may be reinforced using 10- or 12 mm-diameter bars. The spacing of the bars is typically between 100 and 250 mm, depending on the strength requirements.

The design is carried out at the ultimate limit state as follows. Referring to Figure 8.64, the overturning moment M and axial compression N are calculated as before. Ignoring the compressive forces in the bars in the compression zone, the tensile force in the reinforcing bars F_s and the compressive force in the concrete F_c are given by:

$$F_s = 0.87nA_sf_{yk} \quad (8.39) \qquad F_s = 0.87nA_sf_y \quad (8.39)$$

$$F_c = 0.85/1.5f_{ck}b0.8X \quad (8.40) \qquad F_c = 0.45f_{cu}b0.9X \quad (8.40)$$

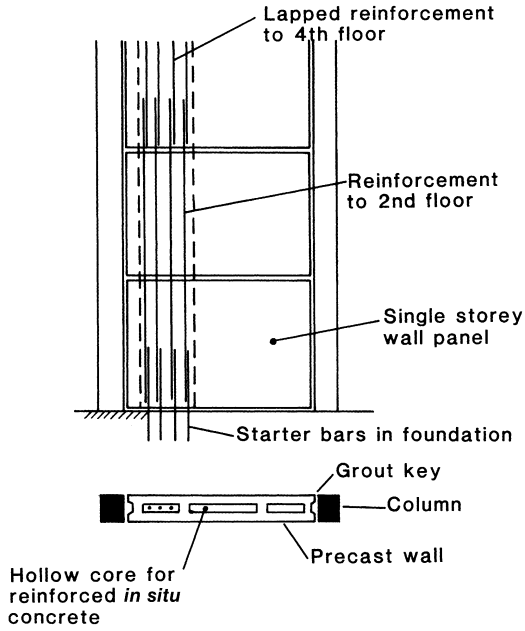

Figure 8.63 Cantilever hollow-core walls.

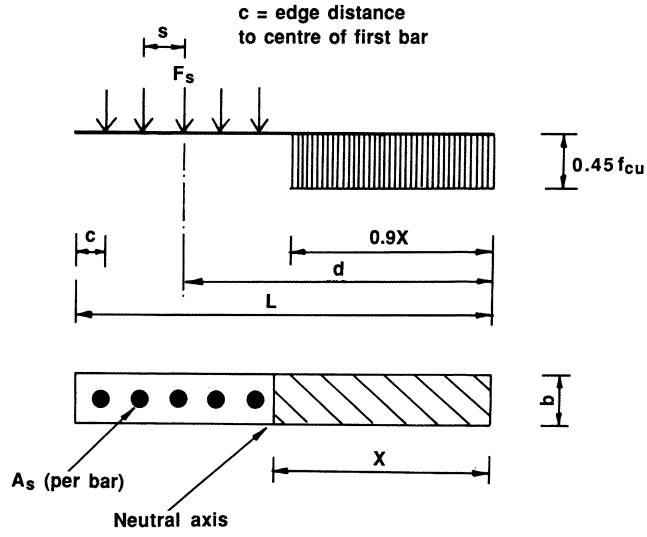

Figure 8.64 Design principles for cantilever shear walls.

where n = number of bars at a spacing s within the tension zone, i.e. in the zone $2(d - X)$, d is the distance to the centroid of the steel, and X is the depth to the neutral axis. The design value of 0.85/1.5 f_{ck} {0.45 f_{cu}} is used because the flexural stresses dominate compared with the smaller axial stress, and so the BS EN 1992-1-1 rectangular stress block, or the BS 8110 idealised rectangular stress block, devised for beam design, is appropriate here. The main difference between beam design and cantilever wall design is that the values of d and n will vary depending on the relative magnitudes of N and M. Then:

$N = F_c - F_s$	$N = F_c - F_s$
$N = 0.8 \times 0.567 f_{ck} bX - 1.74(d - X)A_s f_{yk}/s$ (8.41)	$N = 0.405 f_{cu} bX - 1.74(d - X)A_s f_y/s$ (8.41)
Taking moments about the centroid of the steel bars:	Taking moments about the centroid of the steel bars:
$M = 0.453 f_{ck} bX(d - 0.4X) - N(d - 0.5L)$ (8.42a)	$M = 0.405 f_{cu} bX(d - 0.45X) - N(d - 0.5L)$ (8.42a)
or about the centroid of the concrete in compression	or about the centroid of the concrete in compression
$M = 1.74(d - X)A_s f_{yk}(d - 0.4X)/s + N(0.5L - 0.4X)$ (8.42b)	$M = 1.74(d - X)A_s f_y(d - 0.45X)/s + N(0.5L - 0.45X)$ (8.42b)

depending on whether the steel or concrete is critical. From these equations X and d may be determined for a given geometry, materials and loads. The minimum length of wall is given by:

$$L = d + (d - X) + 2a, \text{ where } a = \text{axis distance to first bar (usually 50 to 60 mm)} \quad (8.43)$$

If this length is greater than the available length, either the value of b, f_{ck} $\{f_{cu}\}$ or A_s/s must be increased until it is less than the available length. The usual option is to decrease the bar spacing s so that the same size of bar may be used in all walls. However, if s becomes ridiculously small, say less than 75 mm, the size of bar should be increased. Some iteration, or trial and error, is required to find a unique solution to A_s/s, as shown in the following exercise. It is quite feasible to double up on the bars by placing them in pairs, providing that the bond lengths are increased accordingly.

Exercise 8.14 Hollow-core cantilever wall design

Redesign the long walls in Exercise 8.10 using hollow-core cantilever walls 2.7 m long × 200 mm thick, with the wall placed between 300 mm-square columns at 3.0 m centres. Assume that the flooring is supported by other beams and that the axial load on the wall is due only to self-weight.

Use concrete grade C30/37 for the precast concrete, and 12 mm-diameter high-tensile bars f_{yk} $\{f_y\} = 500\,\text{N/mm}^2$. Assume axis distance to centre of first bar = 50 mm.

Solution

Step 1: Determine reinforcement required

Height of wall = 4.0 + 3.0 + 3.0 = 10.0 m

Characteristic horizontal forces at:

roof = $0.8 \times 3.0/2 \times 50/2 = 30$ kN

2nd floor = $0.8 \times 3.0 \times 50/2 = 60$ kN

1st floor = $0.8 \times (3.0 + 3.5)/2 \times 50/2 = 65$ kN

Take moments at 0.05 m below top of foundation.

Try H12 bars at $s = 150$ mm centres, $A_s = 113\,\text{mm}^2$, $2a = 100$ mm.

Partial safety factors for loads: γ_f = gravity = 1.0 {1.0} and wind = 1.5 {1.4}

$N_{Ed} = 1.0 \times 0.2 \times 2.7 \times 10.0 \times 25$ = 135.0 kN	$N_u = 1.0 \times 0.2 \times 2.7 \times 10.0 \times 24$ = 129.6 kN
$M_{Ed} = 1.5 \times (30 \times 10.05 + 60 \times 7.05 + 65 \times 4.05)$ = 1481.6 kNm	$M_u = 1.4 \times (30 \times 10.05 + 60 \times 7.05 + 65 \times 4.05)$ = 1382.9 kNm
Then	Then
$N = 0.567 f_{ck} b0.8X - 1.74(d - X)A_s f_{yk}/\text{s}$	$N = 0.45 f_{cu} b0.9X - 1.74(d - X)A_s f_y/\text{s}$
$N = 0.453 \times 30 \times 200X - 1.74(d - X)113 \times 500/150$	$N = 0.405 \times 37 \times 200X - 1.74(d - X)113 \times 500/150$
$N = 2720X - 655.4(d - X)$	$N = 2997X - 655.4(d - X)$
$d = 5.150X - 206.0$	$d = 5.573\text{X} - 197.7$

Checking first the compression capacity, taking moments (8.42a):	
$M = 0.453\, f_{ck}\, bX\, (d - 0.44X) - N(d - 0.5L)$	
$M = 2718dX - 1087.2X^2 - 135.0 \times 10^3 (d - 1350)$	
$M = 2718\, (5.147X - 206.0)X - 1087.2X^2 - 129.6 \times 10^3\, (5.147X - 206.0 - 1350)$	
Solving this quadratic gives $X = 366$ mm and $d = 1679$ mm.	
The ratio X/d	$= 0.218$
< 0.5 preventing any danger of over-reinforcement.	
Eq. (8.43) $L = d + (d - X) + 2a$	$= 3092$ mm
> 2700 mm assumed. Therefore increase A_s/s. Iteration is required to find the solution thus:	
Try H16 at 194 centres. $A_s = 201\,\text{mm}^2$.	
Repeat above to give $X = 412$ mm and $d = 1506$ mm.	
Thus $L = d + (d - X) + 2a$	$= 2699$ mm
≈ 2700 mm required.	

Checking first the compression capacity, taking moments (8.42a): $M = 0.405\, f_{cu}\, bX\, (d - 0.45X) - N(d - 0.5L)$	
$M = 2997dX - 1348.7X^2 - 129.6 \times 10^3\, (d - 1350)$	
$M = 2997\, (5.573X - 197.7)X - 1348.7X^2 - 129.6 \times 10^3\, (5.573X - 197.7 - 1350)$	
Solving this quadratic gives $X = 324$ mm and $d = 1606$ mm.	
The ratio X/d	$= 0.202$
< 0.5 preventing any danger of over-reinforcement.	
Eq. (8.43) $L = d + (d - X) + 2a$	$= 2988$ mm
> 2700 mm assumed. Therefore increase A_s/s. Iteration is required to find the solution thus:	
Try H16 at 210 centres. $A_s = 201\,\text{mm}^2$.	
Repeat above to give $X = 355$ mm and $d = 1476$ mm.	
Thus $L = d + (d - X) + 2a$	$= 2697$ mm
≈ 2700 mm required.	

Step 2: Check ultimate moment of resistance based on rebars provided

Checking tensile capacity: taking moments about centre of concrete stress block (8.45b)

$M_{Rd} = 1.74(d - X)A_s f_{yk}(d - 0.4X)/s + N_{Ed}(0.5L - 0.4X)$	$= 1482$ kNm
$= M_{Ed}$, confirms the solution.	
Use H16 at 190 mm centres.	

$M = 1.74(d - X)A_s f_y(d - 0.45X)/s + N(0.5L - 0.45X)$	$= 1383$ kNm
$= M_u$, confirms the solution.	
Use H16 at 210 mm centres.	

Exercise 8.15 Hollow-core cantilever wall ultimate moment

A hollow-core cantilever wall 2.70 m long × 200 mm thick is to be reinforced using H12 bars at 150 mm centres. Determine the ultimate moment of resistance when the axial load is zero.

Use concrete grade C30/37, and f_{yk} $\{f_y\} = 500\,\text{N/mm}^2$. Assume cover to first bar is 50 mm.

Solution

$b = 200$ mm, $A_s = 113\,\text{mm}^2$ per bar, and $s = 150$ mm

$F_c = 0.453\, f_{ck}\, b\, X = 2718\, X$	
$F_s = 1.74\, f_{yk}\, (d - X)\, A_s/s$	
$F_s = 1.74 \times 500 \times \frac{113}{150}(d - X)$	
$= 655.4\, (d - X)$	
Then $2718\, X = 655.4(d - X)$	
$d = 5.147\, X$	
From the geometry:	
$d + (d - X) = 2700 - 100$	
$d = 1300 + 0.5\, X$	
$X = 1300/(5.147 - 0.5) = 280$ mm	
and $d = 1440$ mm.	
The ratio $X/d < 0.5$	$= 0.195$
Thus	
$M = 2718\, X\, (d - 0.4X)$	$= \underline{1010}$ kNm

$F_c = 0.405\, f_{cu}\, b\, X = 2997\, X$	
$F_s = 1.74\, f_y\, (d - X)\, A_s/s$	
$F_s = 1.74 \times 500 \times \frac{113}{150}(d - X)$	
$= 655.4\, (d - X)$	
Then $2997\, X = 655.4(d - X)$	
$d = 5.573\, X$	
From the geometry:	
$d + (d - X) = 2700 - 100$	
$d = 1300 + 0.5\, X$	
$X = 1300/(5.573 - 0.5) = 256$ mm	
and $d = 1428$ mm.	
The ratio $X/d < 0.5$	$= 0.179$
Thus	
$M = 2997\, X\, (d - 0.45\, X)$	$= \underline{1008}$ kNm

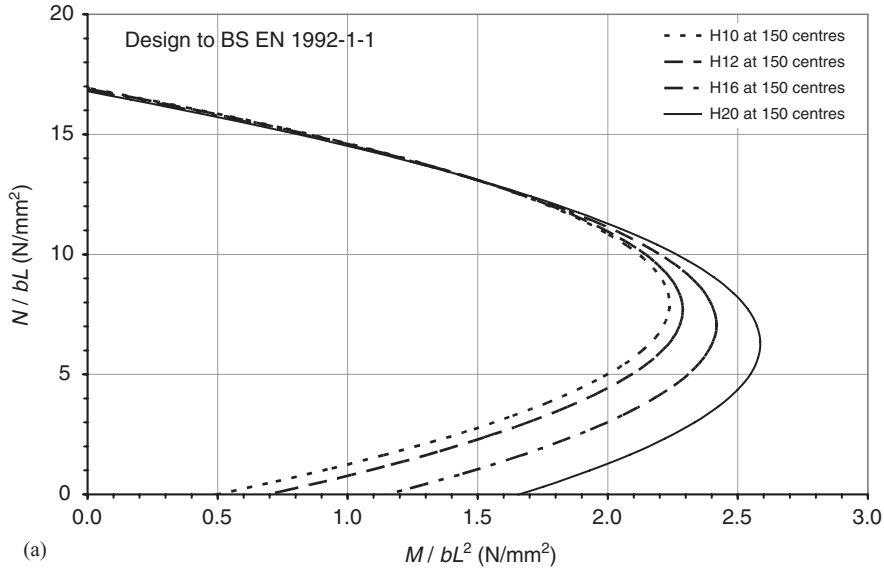

Figure 8.65(a) N/bL versus M/bL^2 interaction chart for reinforced hollow-core walls using concrete $f_{ck} = 30$ and $f_{yk} = 500\,\text{N/mm}^2$ to BS EN 1992-1-1.

Equations 8.42 to 8.45 may be used to develop the N versus M interaction charts shown in Figure 8.65, using the geometry and materials in Exercise 8.14. Note the diminishing contribution of the reinforcement when $N/bL > 12$ as the concrete pressure dominates.

8.7.8 Solid cantilever shear walls

Solid reinforced concrete shear walls rely entirely on the connections in the horizontal and vertical planes. The horizontal sway displacement of these types of wall is a function of the shear-stiffness k of both the wall panel and the joint. The latter is the more flexible (and weaker) part, possibly 1/100th of the former in terms of stiffness [8.54]. One of the reasons for this large difference is that the precast wall must be strong enough to resist lifting forces at the factory within 12 hours of casting. It must also have considerable stiffness and strength in service.

As with the hollow-core cantilever wall, the design is carried out at the ultimate limit state, with the moment M and axial compression N calculated as before. Referring to Figure 8.66, the idealised stress block given in BS EN 1992-1-1, clause 3.1.7 [8.5] {BS 8110 [8.6]} is used to give the following forces in the concrete F_c and reinforcing bars F_s:

$$F_{cs} = 0.567 f_{ck} b 0.8X \qquad (8.44) \quad | \quad F_{cs} = 0.45 f_{cu} b 0.9X \qquad (8.44)$$

where X = distance to neutral axis.

$$F_s = 0.87 A_s f_{yk} \qquad (8.45) \quad | \quad F_s = 0.87 A_s f_y \qquad (8.45)$$

Then:

$$N = F_c - F_s = 0.453 f_{ck} bX - 0.87 A_s f_{yk} \qquad (8.46)$$
$$M = 0.453 f_{ck} bX(d - 0.4X) - N(d - 0.5h)$$
or
$$M = 0.87 A_s f_{yk}(d - 0.4X) - N(0.5h - 0.4X) \qquad (8.47)$$

$$N = F_c - F_s = 0.405 f_{cu} bX - 0.87 A_s f_y \qquad (8.46)$$
$$M = 0.405 f_{cu} bX(d - 0.45X) - N(d - 0.5h)$$
or
$$M = 0.87 A_s f_y(d - 0.45X) - N(0.5h - 0.45X) \qquad (8.47)$$

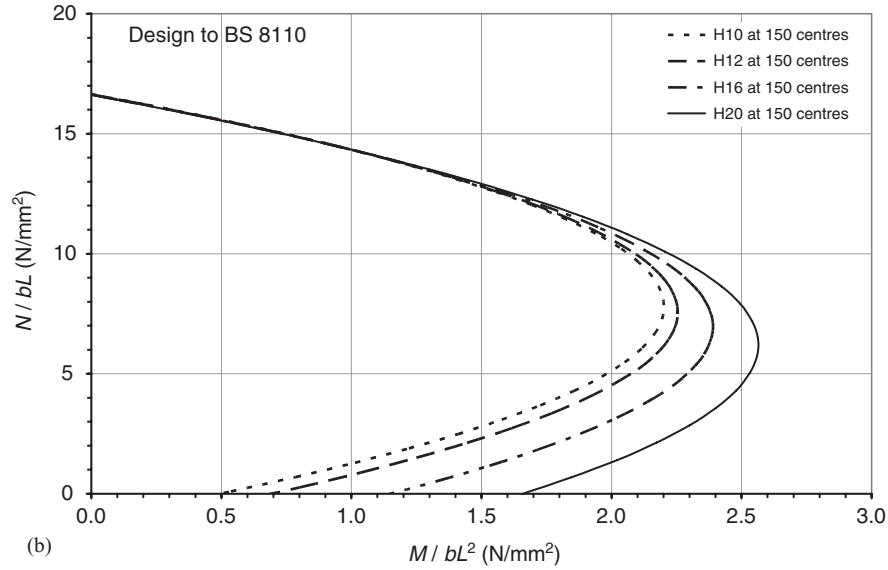

Figure 8.65(b) N/bL versus M/bL^2 interaction chart for reinforced hollow-core walls using concrete $f_{cu} = 37$ and $f_y = 500\,\text{N/mm}^2$ to BS 8110.

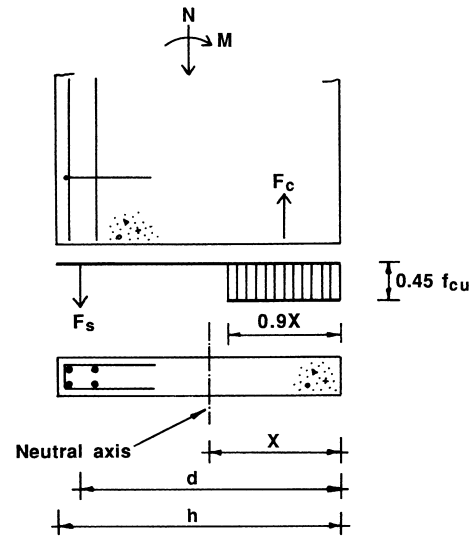

Figure 8.66 Design principles for solid cantilever shear walls.

depending on whether the steel or concrete is critical. Here h = length of wall, and d is the effective depth to the centroid of the steel bars in tension. This point should be coincident with the centroid of the group of holding-down bolts.

The side and end cover to these bars, and the clear horizontal distance between them, are very important and should not be less than 50 mm. This means that if two rows of bars are chosen, the minimum thickness of the wall should be 200 mm. If one row of bars is used, the wall thickness may be 150 mm – the minimum thickness for a precast wall.

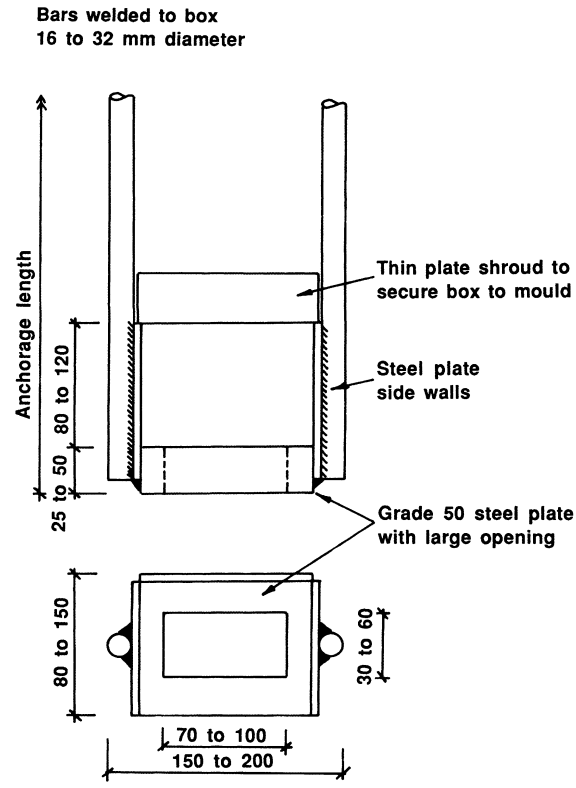

Figure 8.67 Details for wall shoe connector.

The steel bar(s) at the bottom of the wall are often welded to wall splices or shoes and are therefore considered as mild steel. The bar(s) at the top of the wall are often threaded, projecting through the splice plate. These bars are high-tensile. To ensure the complete transfer of force, the vertical bars must be surrounded by horizontal steel on either side of the vertical bars. This horizontal bar is usually U-shaped, with a minimum area of 0.2 per cent {0.4 per cent} × area of wall. Additional bars, typically two or three H10 at 50 mm centres, are added at the very top and bottom as an extra precaution against debonding.

Mechanical connectors between walls may be made using splice plates or the so-called 'wall shoe'; Figure 8.67. Designs vary according to load capacity and the breadth of wall available. In general, the cost of such connectors increases as the breadth reduces.

The principle of the wall shoe is similar to the column shoe (Figure 7.112) in that a punched hole plate is welded to a shroud box and to rebars for anchorage into the surrounding concrete. The hole in the plate receives a threaded bar from the adjoining wall (or foundation). Sizes and capacities vary from 140 × 80 × 80 mm boxes with 16 mm-diameter bars capable of resisting tensile forces of about 75 kN, to 250 × 150 × 150 mm with 32 mm bars having a capacity of at least 250 kN. As with the column shoe, the design strength is usually based on static strength of the threaded bar, and not the strength of the welded box, nor the bond strength of the rebars anchored into the wall.

Base plates may be used to connect the wall at the foundation, with the necessary modification to the design to allow for the fact that the compression plate and tension plate are separate. If the length of the wall = h, then the length of the base plate must be equal to the length of the compression stress block Xh. Note that in the design of base plates, the compressive stress is limited to $0.85 \times 0.85 f'_{cd} = f'_{ck}$ (using $\alpha_{cc} = 0.85$ because it is flexural compression bearing) $\{0.4 f'_{cu}\}$. The method given in Section 7.14.2 may be used with the following modification to Eq.(7.101):

$$\frac{N(e+0.5h-Xh/2)}{0.482 f'_{ck} bh^2} = X\left(1-\frac{Xh}{2h}\right)-0.5X^2 = X-X^2 \qquad (8.48)$$

$$\frac{N(e+0.5h-Xh/2)}{0.4 f'_{cu} bh^2} = X\left(1-\frac{Xh}{2h}\right)-0.5X^2 = X-X^2 \qquad (8.48)$$

because the distance to the centre of the bolts in tension is equal to $Xh/2$.

We can simplify by defining a new stress factor K

$$K = \frac{M'}{f_{ck} bh^2} = \frac{N(e+0.5h)}{f'_{ck} bh^2} \qquad (8.49)$$

$$K = \frac{M'}{f_{cu} bh^2} = \frac{N(e+0.5h)}{f'_{cu} bh^2} \qquad (8.49)$$

such that

$$X^2 - X\left(1+\frac{N}{0.9633 f_{ck} bh}\right)+2.076K = 0 \qquad (8.50)$$

$$X^2 - X\left(1+\frac{N}{0.8 f_{cu} bh}\right)+2.5K = 0 \qquad (8.50)$$

where b = breadth of wall and h = length of wall in plane of bending. (Note: K in Eq. (8.49) is not the same as K in Eq. (7.100).) The magnitude of the bracketed coefficient in Eq. (8.50) will be small (typically 0.005) in comparison with all other values, and so Eq. (8.50) may be approximated to:

$$X^2 - X + 2.08K = 0 \qquad (8.51)$$

$$X^2 - X + 2.5K = 0 \qquad (8.51)$$

without significant loss in accuracy.

The holding-down force in the bolts is given by Eq. (7.99), and the bolt size by Eq. (7.102). Usually there will be four bars per plate, two on either side of the wall.

The length of the base plate should be greater than Xd by at least 50 mm to allow for edge spalling beneath the plate. It is quite common for the size of the plate to be governed by the physical size of the bolts and the spacing between them – more for the contractor's benefit when casting them into the foundation than for the precaster's needs. The edge distance to the bolts should be at least 50 mm, and the centre distance between them at least 75 mm for bolts up to 25 mm diameter, and 100 mm for larger diameters.

As a final check on the arithmetic, the sum of the forces in the bars and underneath the base plate should be equal to M/z, where $z = (d - Xd)/2$.

For the base plates, splices and/or wall shoes to be structurally effective the reinforcement in the wall must be gathered near the connector to utilise the strength of the shoe. The recommended spacing between the bars is 200 mm vertically and horizontally. The walls may be symmetrically and partially prestressed (approx. < 4 N/mm^2), to assist in pitching the more slender walls. Prestressed walls would also be reinforced, as for ordinary rc walls. It is therefore necessary to design the connections first, before proceeding with the reinforcement design.

Exercise 8.16 Solid cantilever wall design

Design a solid reinforced concrete cantilever shear wall 2700 mm long × 200 mm thick with joints at each floor. Given the ultimate axial force in the wall is 142.5 kN {150 kN}, and the overturning moment is 1083 kNm {1140 kNm} at the foundation, design a steel base plate connection. If the ultimate axial force and moment at the first floor is 95 kN and 551 kNm {100 kN and 580 kNm}, also design a steel splice connection which is flush with the sides of the wall.

Use grade C30/37 for both precast and *in situ* concrete, f_{yk} {f_y} = 500 N/mm^2, f_{ykw} {f_{yw}} = 250 N/mm^2 for bars welded to plates, grade S275 {43} steel plate and welds. Cover to bars in wall = 35 mm.

(*Continued*)

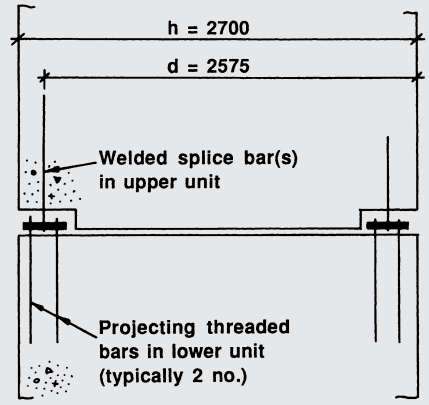

Figure 8.68 Details for Exercise 8.16.

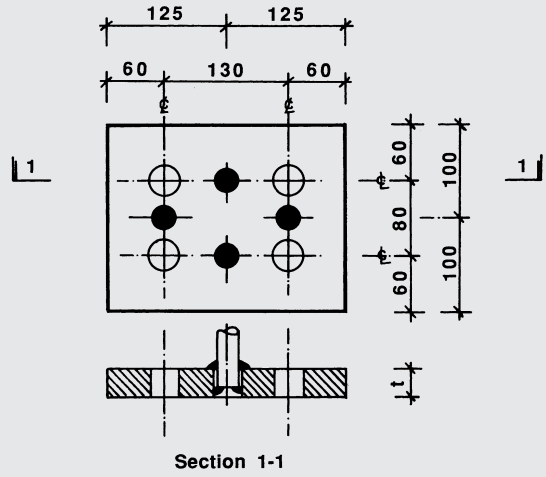

Figure 8.69 Details for Exercise 8.16.

Solution

Step 1: Design of base plate

Let $b_p = 200 + 2 \times 100 = 400\,\text{mm}$

$h = 2700$ mm

$e = 1083 \times 10^3/142.5$	$= 7600\,\text{mm}$	$e = 1140 \times 10^3/150$	$= 7600\,\text{mm}$
$K = \dfrac{142.5\times10^3\times(7600+2700/2)}{30\times400\times2700^2}$	$= 14.58 \times 10^{-3}$	$K = \dfrac{150\times10^3\times(7600+2700/2)}{37\times400\times2700^2}$	$= 12.44 \times 10^{-3}$
Hence $X = 0.03744$, and		Hence $X = 0.03182$, and	
$Xh = 101.1\,\text{mm}$.		$Xh = 85.92\,\text{mm}$.	
Then $F_c = 0.567 \times 30 \times 400 \times 0.8 \times 101.1 \times 10^{-3}$	$= 454.5\,\text{kN}$	Then $F_c = 0.45 \times 37 \times 400 \times 0.9 \times 85.92 \times 10^{-3}$	$= 515.0\,\text{kN}$
Bolt force $F = 454.5 - 142.5$	$= 312.0\,\text{kN}$	Bolt force $F = 515.0 - 150.0$	$= 365.0\,\text{kN}$

Use six M20 grade 8.8 holding-down bolts (626.4 kN), three each side of the wall at 75 mm centres.

Plate length > 50 + 75 + 75 + 50 = 250 mm to allow access for fixing bolts, or

101.1 + 50 = 151.1 mm < above.
Actual compressive stress beneath plate
$= \dfrac{491.3\times10^3}{400\times250} = 4.91\ \text{N/mm}^2$
Plate thickness given by Eq. (7.103) and/or (7.104) using $L = 100$ mm, $m \approx 110$ mm, $b = 250$ mm, and $F = 348.8/2 = 174.4$ kN

$t = \sqrt{\dfrac{2\times4.91\times100^2}{275}}$ = 18.9 mm
based on compression beneath plate, or

$t = \sqrt{\dfrac{4\times174.4\times10^3\times110}{250\times275}}$ = 33.4 mm
based on tension in bolts

85.9 + 50 = 135.9 mm < above.
Actual compressive stress beneath plate
$= \dfrac{515.0\times10^3}{400\times250} = 5.15\ \text{N/mm}^2$
Plate thickness given by Eq. (7.103) and/or (7.104) using $L = 100$ mm, $m \approx 110$ mm, $b = 250$ mm, and $F = 365/2 = 182.5$ kN

$t = \sqrt{\dfrac{2\times5.15\times100^2}{275}}$ = 19.35 mm
based on compression beneath plate, or

$t = \sqrt{\dfrac{4\times182.5\times10^3\times110}{250\times275}}$ = 34.2 mm
based on tension in bolts

Use two 250 × 400 × 40 mm mild steel plates.

Step 2: Reinforcement on the base plate
Place the welded reinforcing bars such that the effective depth $d = 2700 - 250/2 = 2575$ mm.
Using Eq. (8.46)

$N = 2720\ X - 217.5\ A_s$
So $X = 55.39 + 0.0780\ A_s$
Eq. (8.47) gives
$M = 1085 \times 10^6$
$= 217.5A_s\left(2575 - \dfrac{52.39}{2} - \dfrac{0.080A_s}{2}\right)$
$-142.5\times10^3\left(\dfrac{2700}{2} - \dfrac{52.39}{2} - \dfrac{0.080A_s}{2}\right)$
Hence A_s = 1660 mm^2
and $X = 185.1$ mm.

$N = 2997\ X - 217.5\ A_s$
So $X = 50.05 + 0.0726\ A_s$
Eq. (8.47) gives
$M = 1140 \times 10^6$
$= 217.5A_s\left(2575 - \dfrac{50.05}{2} - \dfrac{0.0726A_s}{2}\right)$
$-150\times10^3\left(\dfrac{2700}{2} - \dfrac{50.05}{2} - \dfrac{0.0726A_s}{2}\right)$
Hence A_s = 1750 mm^2
and $X = 177.1$ mm.

Use six H25 bars (2945 mm^2) at 75 mm centres, three for each face.
These bars should be aligned with the positions of the holding-down bolts.

Step 3: Reinforcement in the wall
High-tensile bars to be lapped with the above to carry tension up to first floor. Repeat the above using f_{yk} $\{f_y\} = 500$ N/mm^2

So $X = 52.39 + 0.1599\ A_s$
$M = 1083 \times 10^6$
$= 217.5A_s\left(2575 - \dfrac{52.39}{2} - \dfrac{0.1599A_s}{2}\right)$
$-142.5\times10^3\left(\dfrac{2700}{2} - \dfrac{52.39}{2} - \dfrac{0.1599A_s}{2}\right)$
Hence A_s = 819 mm^2

Then $X = 50.05 + 0.1451\ A_s$
$M = 1140 \times 10^6$
$= 217.5A_s\left(2575 - \dfrac{50.05}{2} - \dfrac{0.1451A_s}{2}\right)$
$-150\times10^3\left(\dfrac{2700}{2} - \dfrac{50.05}{2} - \dfrac{0.1451A_s}{2}\right)$
A_s = 865 mm^2

Use six H20 bars (1890 mm^2) lapped to welded H25 bars.

(*Continued*)

Vertical steel in remainder of wall
= 0.2% = 400 mm²/m per two faces
Horizontal steel in wall
= 0.2% = 400 mm²/m per both faces

Vertical steel in remainder of wall
= 0.4% = 800 mm²/m per two faces
Horizontal steel in wall
= 0.25% = 500 mm²/m per both faces

Use B503 fabric, plus H8 U-bars at 200 mm centres at ends of wall.

Step 4: Wall splice at first floor

Referring to Figure 8.68, maintain the effective depth to the bars in the splice at $d = 2575$ mm.

Design mild steel stress bars in upper wall welded to splice plate, again from Eq. (8.46):

$X = 95/142.5 \times 52.39 + 0.0800\,A_s$
Eq. (8.47) gives
$M = 551 \times 10^6$

$$= 217.5A_s\left(2575 - \frac{34.93}{2} - \frac{0.0800A_s}{2}\right) - 95\times10^3\left(\frac{2700}{2} - \frac{34.93}{2} - \frac{0.0800A_s}{2}\right)$$

Hence A_s = 773 mm²

$X = 100/150 \times 50.05 + 0.0726\,A_s$
Eq. (8.47) gives
$M = 580 \times 10^6$

$$= 217.5A_s\left(2575 - \frac{33.57}{2} - \frac{0.0726A_s}{2}\right) - 100\times10^3\left(\frac{2700}{2} - \frac{33.57}{2} - \frac{0.0726A_s}{2}\right)$$

Hence A_s = 816 mm²

Use four H20 bars (1257 mm²) in between the projecting threaded bars.
High-tensile threaded bars in lower wall. Repeat the above using f_{yk} {f_y} = 500 N/mm²

Then $X = 37.25 + 0.1451\,A_s$
$M = 551 \times 10^6$

$$= 435A_s\left(2575 - \frac{37.25}{2} - \frac{0.1451A_s}{2}\right) - 95\times10^3\left(\frac{2700}{2} - \frac{37.25}{2} - \frac{0.1451A_s}{2}\right)$$

A_s = 390 mm²

Then $X = 33.37 + 0.1451\,A_s$
$M = 580 \times 10^6$

$$= 435A_s\left(2575 - \frac{33.57}{2} - \frac{0.1451A_s}{2}\right) - 100\times10^3\left(\frac{2700}{2} - \frac{33.57}{2} - \frac{0.1451A_s}{2}\right)$$

A_s = 412 mm²

Use four H20 bars (628 mm²) threaded to M16.

Step 5: Splice-plate design

Referring to Figure 8.69, size of plate = 250 mm long × 200 mm wide

Upper bars welded to plate to be located in mid-sides of plate. Lower threaded bars to be located at corners of plate. Refer to Section 7.13.4 for design method.

Edge distance to bars = cover 35 + link 8 + bar radius 10 = 53 mm; use 60 mm.

Distance between bar centres = (250 − 120)/2 = 65 mm

Force in bars in splice plate
$= 0.87 \times 500 \times 390 \times 10^{-3}$ = 42.4 kN
Lever arm = 40 cos ($\tan^{-1}$(40/65)) = 34 mm
Effective breadth = $\sqrt{40^2 + 65^2}$ = 76.3 mm
Moment in plate = 44.2 × 34 = 1445 kNmm

$$t = \sqrt{\frac{4\times1445\times10^3}{250\times275}} = 16.6\text{ mm}$$

based on tension in bolts
Shear in plate = 42.4 kN

$$t = \frac{42.4\times10^3}{76.3\times0.6\times275} = 3.4\text{ mm}$$

Force in bars in splice plate
$= 0.87 \times 500 \times 412 \times 10^{-3}$ = 44.8 kN
Lever arm = 40 cos ($\tan^{-1}$(40/65)) = 34 mm
Effective breadth = $\sqrt{40^2 + 65^2}$ = 76.3 mm
Moment in plate = 44.8 × 34 = 1526 kNmm

$$t = \sqrt{\frac{4\times1526\times10^3}{250\times275}} = 17.1\text{ mm}$$

based on tension in bolts
Shear in plate = 44.8 kN

$$t = \frac{44.8\times10^3}{76.3\times0.6\times275} = 3.6\text{ mm}$$

Use 250 × 200 × 20 mm splice plate.

CHAPTER 9

Structural Integrity and the Design for Accidental Loading

This chapter describes how a precast structure is designed against possible progressive collapse, and looks at the way connections are designed so that alternative load paths are available in the event of an accident.

9.1 Precast Frame Integrity – The Vital Issue

Precast concrete frames are scrutinised by checking authorities more for structural stability, robustness and integrity than for the performance of the individual reinforced and prestressed concrete components and connections. This means that there is more concern for the way in which precast members interact with each other than for the structural performance of an individual beam, slab or column. The main question is whether the frame will react to forces as an entity or, as in the case of a Meccano set, will the removal of one bolt potentially cause the whole structure to collapse? Codes of practice refer to this topic as 'robustness'. BS EN 1992-1-1, clause 9.10 [9.2], quoting almost exactly BS 8110 [9.1], requires that:

> *. . . situations should be avoided where damage to small areas of a structure or failure of single elements may lead to collapse of major parts of the structure.*

The popular term for this is 'structural integrity' and the design aspects involve all the items dealt with in this book – namely component design, connections, diaphragm action and structural stability. These items cannot be dealt with in isolation, and precast frame design is an integrated process.

Frame stability is a crucial issue in multi-storey precast construction and adequate stiffness, strength, and the provisions to guard against the possibility of a collapse which is disproportionate to its cause must be provided. Tie forces between the precast components must be mobilised in the event of accidental damage or abnormal loading – nowadays termed 'accidental actions' – and alternative means of transferring loads to the foundations must be sought if a component is rendered unserviceable. In all cases the precast floor must act as a rigid, yet ductile, horizontal diaphragm.

Multi-storey Precast Concrete Framed Structures, Second Edition. Kim S. Elliott and Colin K. Jolly.

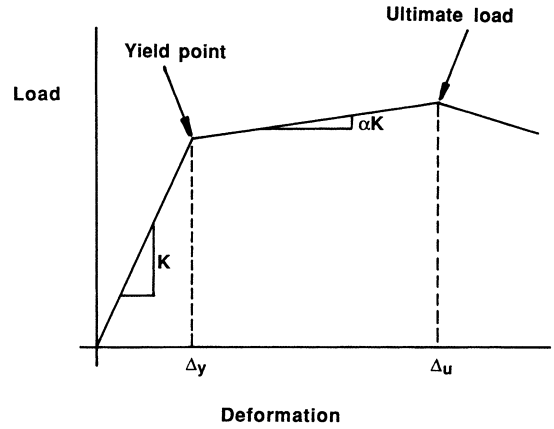

Figure 9.1 Idealised deformation behaviour in non-linear materials.

9.2 Ductile Frame Design

9.2.1 Structural continuity in precast skeletal frames

In precast work the design of ductile structures is entirely dependent on the stiffness and ductility of the connections. The stiffness is the rate of change of load versus deformation, i.e. the tangent gradient K in the idealised plot shown in Figure 9.1. Ductility is measured in terms of a ductility factor Φ, the ratio between the deformation at the ultimate load Δ_u and the deformation at the yield point Δ_y in Figure 9.1. These are simple definitions and the two characteristics are easy to understand in terms of a single element or joint. However, their effect on the behaviour of three-dimensional precast concrete structures is complex.

The flexural stiffness of many of the beam-to-column connections in use is between $0.1K_b$ and $1.3K_b$, where $K_b = 4EI/L$ is the flexural stiffness of a prismatic beam of length L to which the connector is attached [9.3]. The ductility factors Φ for these connections vary from about 1.5 to more than 6. Figures 9.2(a) and (b) show examples of moment versus connection rotation data obtained from the full-scale beam-to-column-to-hollow-core slab assembly shown in Figure 9.3. The relative beam-to-column rotations were measured at each side of the column, with the positive moment inducing hogging at the column face. Initial cracking occurred at the face of the column at approximately 5 mrad, but the connection responded to increased moment at four times this value.

Similarly, the stiffness of the half-joint connection tested (by Elliott) as shown in Figure 4.32 is only about twice the shear stiffness of the end of a beam subjected to an end shear force ($1.2\ VL/AG$). This information is hardly surprising, as the connections are designed as pinned joints with large shear capacities. The results of these and many other tests show that the designer is able to design the connections in order to control frame behaviour.

Precast frame design is not based on 'capacity' design procedures. The ductility of a component or connection is considered implicitly, and a value of Φ is aimed for in the way that strength and stiffness is. However, if a connection is found to be ductile, that is usually the result of features being introduced to the design for reasons other than making the particular connection respond in a ductile manner.

For example, consider the beam-to-column connection in Figure 9.4. The steel billet has been designed to fail in bending, rather than by shear, crushing or buckling. The column has also been designed such that the confinement links will yield and enable the concrete underneath the billet to fail gradually (more like the compressive failure of a cylinder than of a cube). The beam half-joint has been designed so that bursting and shear failures are controlled by strategically placed and fully

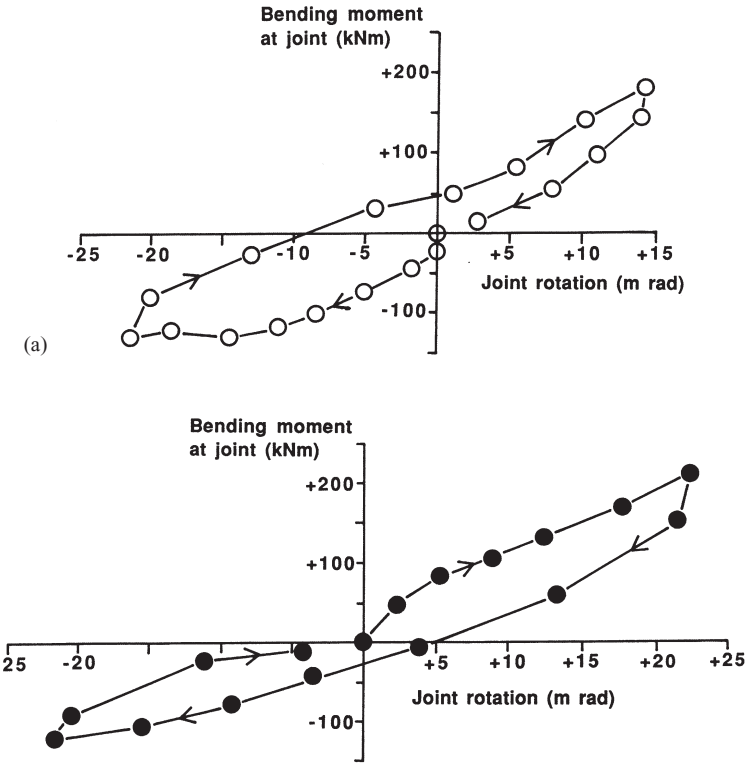

Figure 9.2 Moment versus rotation behaviour of beam-to-column connection tests [9.3].

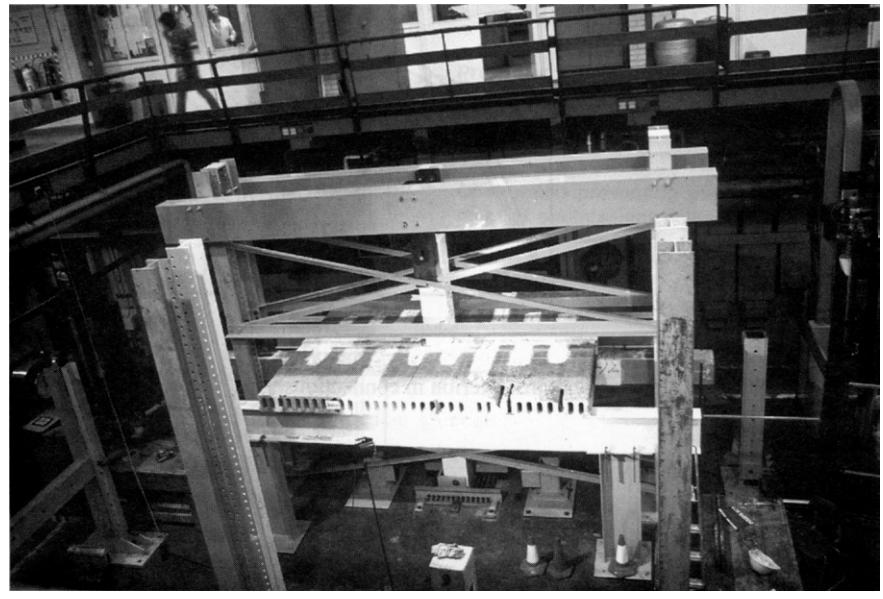

Figure 9.3 Test assembly used in flexural connection tests [9.3]. Column and beam size = 300 × 300 mm. Slab depth = 200 mm (Roth type). Tie steel across top of beam = 2 no. T 25 ribbed bars. Precast and *in situ* concrete strengths = 50 N/mm^2 and 25 N/mm^2, respectively.

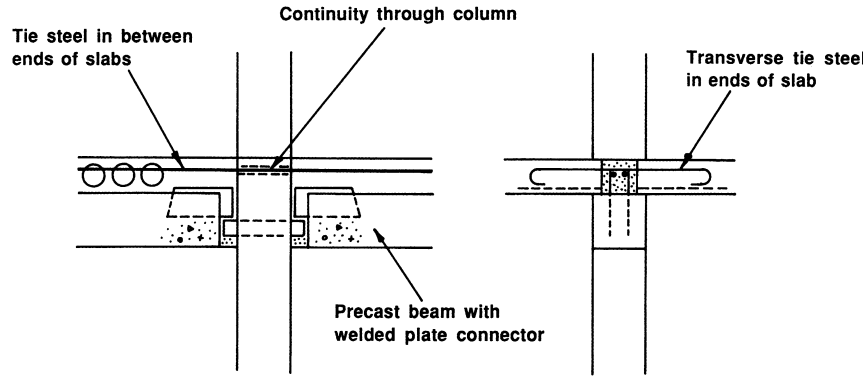

Figure 9.4 Principle of ductile beam-to-column connections because of continuous tie steel in the *in situ* infill strip over the beam.

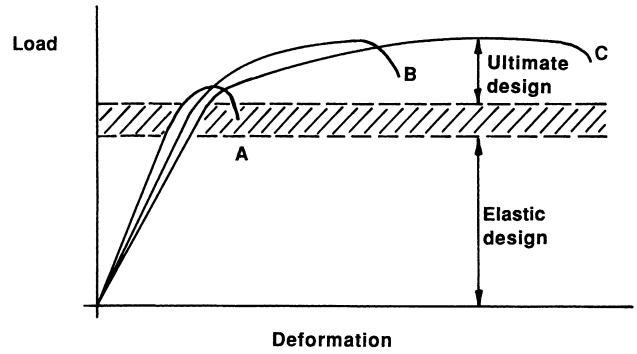

Figure 9.5 Different failure criteria in connections.

anchored reinforcement. If any one of these three elements were to fail prematurely and catastrophically, the connector load-versus-deformation behaviour might be as shown in curve A in Figure 9.5. If the connector was so designed that all three elements were to fail simultaneously, the deformation might be as curve B, with the changing stiffness in the 'grey' area reflecting the redistribution of forces from one zone to another. However, the presence of the continuity tie steel passing through the floor slab and column will increase the ductility of the entire connection by allowing more than one of the constituent parts of the connection to yield without total failure. The result is the ductile response shown by curve C.

The design of components and connections should be such that undesirable modes of failure are prevented. These include:

- shear-tension failures in incorrectly or unreinforced joints subjected to building movements etc.; see Figure 9.6 [9.4]
- buckling of compression reinforcement in site-made connections where confinement links have not been specified, or omitted because of fixing difficulties; see Figure 9.7
- anchorage failures in tie steel because of inadequate length of the projecting reinforcement and inadequate bearing lengths; see Figure 9.8 [9.5]
- large plastic rotations in connections that have been designed as pinned joints, but have been constructed so that bending moments and torque have been transferred into components that have not been designed to resist the resulting forces; see e.g. Figure 9.9 for torsion and Figure 7.6 for flexure.

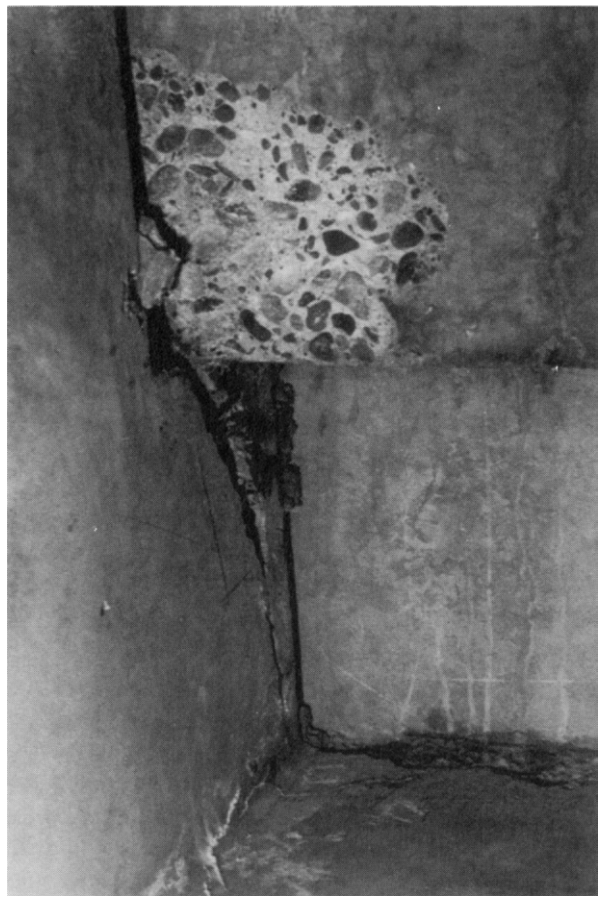

Figure 9.6 Shear failure by splitting of cover concrete [9.4].

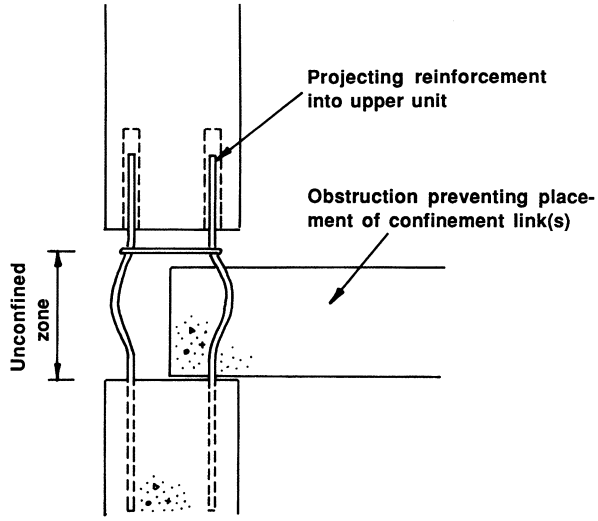

Figure 9.7 Buckling in unconfined compression bars.

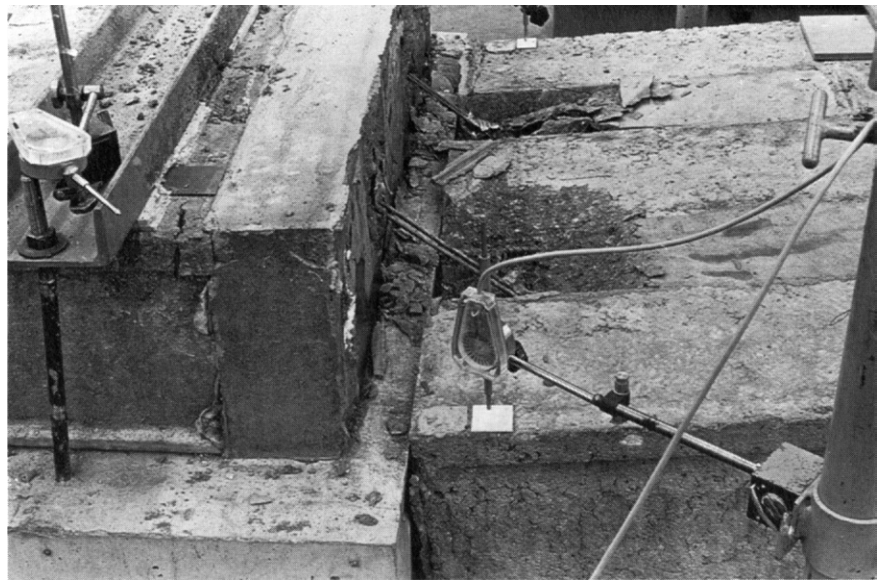

Figure 9.8 Ultimate failure of displaced hollow-core slab by Engström [9.5].

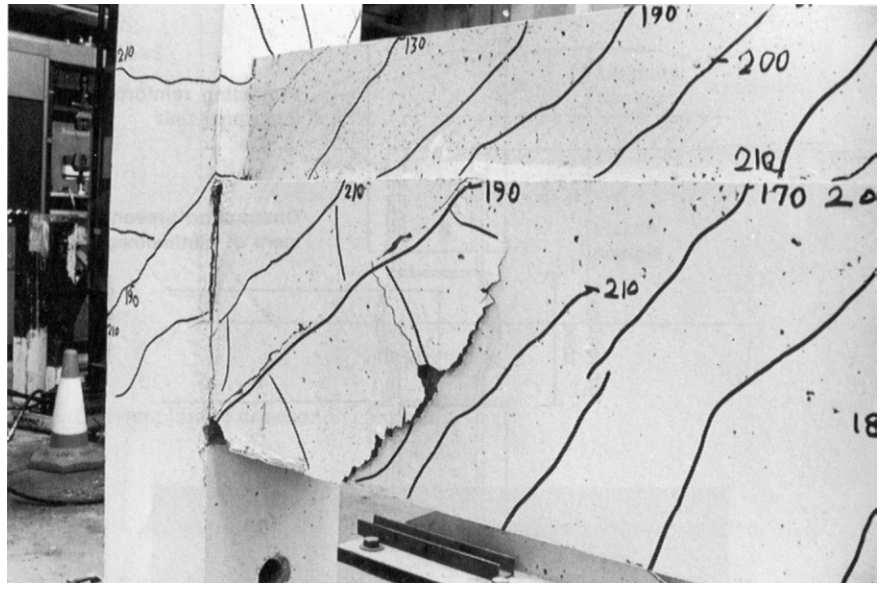

Figure 9.9 Torsional moments transferred into columns because continuity steel is provided in the floor slab.

The relationships between the stiffness and ductility of individual components/connections and the behaviour of the total structure form a complex, non-linear, three-dimensional problem with which, at the time of publication of the first edition of this book, research institutions were only just beginning to grapple [9.6]. However, from the past 15 years a considerable body of work now exists, as given in Chapter 7, Section 7.7.2.1, in which the partial strength and stiffness of slab-to-beam and beam-to-column connections were enhanced by the use of continuity ties placed within the beam/floor zone. Although this work did not extend to providing information directly applicable to the

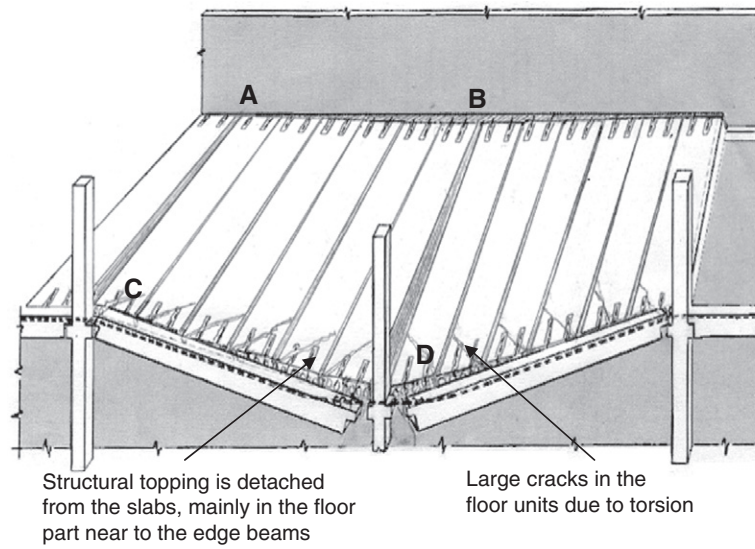

Figure 9.10 Possible scenario of the structural behaviour of a precast concrete frame structure after sudden column loss due to accidental actions (courtesy of fédération internationale du béton (*fib*), www.fib-international.org. Figure 26 in *fib* Bulletin 63 [9.7]).

design for robustness and continuity in 3-D frames, it nevertheless gave new methodologies and real experimental proof of ways of achieving continuity throughout a skeletal structure. These methods have formed the basis of the *fib* document *Design of Precast Concrete Structures against Accidental Actions* [9.7], and a substantial Unified Facilities Criteria document [9.8]. Some of the key points from the *fib* document are paraphrased as follows:

In a precast concrete structure, floor and beam interaction in the transfer of the accidental loading will depend on the structural layout and the positions of the connections. Two alternative models, based on the scenario in Figure 9.10, are given as follows:

In a 3-dimensional precast concrete slab field, tie forces may act in two mutually perpendicular directions, as 'beam ties' and along the slabs as 'floor ties'. The floor ties will only act in the vicinity of the beam where the bearing is lost, which could be estimated as 50% of the span from the ends.

Deformations will concentrate in the connections between the beams and floors, provided that the remaining columns can take the redistributed gravity load. The precast floor beams, supported previously by the removed column, will normally remain rigid and keep their original shape. Depending on the design assumptions and the actual details, either the connection of the beam above the remaining supports will act in full restraint, or the connection will behave as a hinge, plastic or not, depending on where the bars are located, and open up a gap between the beam and column as shown in Figure 9.10. In this situation the primary load transfer to the surrounding structure is assured by the floor beams alone, without major intervention of the transverse tie reinforcement in the floor slab (or structural topping if present). Because the floor–beam connections are in the upper part of the floors, during the downward movement of the beams the floor units are likely to slip from the beam ledge and remain suspended through the tie bars. The same is valid in the transverse direction. Consequently, the deformations during the transition to a catenary system will concentrate in the joints between the floor units mutually, and between the floor units and the supporting beams.

As the length of the deformed floor support (C–D Figure 9.10) is greater than A–B, the slabs will split apart, and will be subjected to torsion. Longitudinal joints here will show larger openings than the other joints. With hollow-core floors, the connecting reinforcement between floor units and beams should be positioned in top-opened cores (as shown in Figure 9.21) and ***not*** *in the longitudinal floor joints, since those will open during the deflection.*

The length of the deformed structure B–D is greater than at A–B, assuming that the column at D will not move inwards. The latter could happen when all the upper floors deform in the same way. During the collapse, any structural topping will most probably be detached from the floor units in the vicinity of C–D, unless the reinforcement in the topping is effectively anchored to the hollow-core units through projecting links in the opened cores, as those in the longitudinal joints between the floor units will be ineffective because of the splitting apart of the units. As a consequence, in the most unfavourable scenario, the full gravity load will be taken by the peripheral tie bars anchored to the floor beams, and the deformations in the transition to a catenary system will concentrate in the joints between these beams and the supporting columns.

9.3 Background to the Present Requirements

The term 'progressive collapse' was first used in Britain following the partial collapse of a precast concrete wall frame at Ronan Point, London, in May 1968 (see Figure 9.11). A gas explosion in a corner room on the eighteenth floor blew out one of the external walls, and because of inadequate structural continuity between the wall and floor elements, the removal of one wall element was sufficient to cause the total collapse of about 23 m^2 of floor area per storey over the height of the entire building. (It was originally rectangular on plan.)

Figure 9.11 Progressive collapse of part of Ronan Point (courtesy of the Brick Development Association).

Immediately following the accident several contracts were suspended for a time, until the results were known of structural investigations and testing at Imperial College, London, and the UK Building Research Station. The investigations found deficiencies in the manner in which the precast components were tied to one another, which together with poor detailing and unsatisfactory workmanship was blamed for the disproportionate amount of damage. However, the most crucial factor was that there was no suitable design information to guide the designer towards a suitably robust solution, although there were some existing building standards that contained some guidance and general warnings on the structural integrity, i.e. design beyond the normal static or dynamic equilibrium of large panel structures. The code of practice used for the design of Ronan Point was issued in 1952, and the building regulations contained a clause known as the 'functional requirement on structure', which contained no mention of progressive collapse, redundancy, etc [9.9, 9.10]. Changes to the UK Building Regulations swiftly followed in November 1968 after the publication of a government report [9.11], which now contained such concepts as 'the alternative load path when a structural element is removed', 'minimum tie forces for continuity' and 'an accidental static omni-pressure of 5 lb/in^2 (34 kN/m^2)'. The standards became part of mandatory building regulations in April 1970.

The situation is equally important during the construction stage, when the designer may not always command the levels of control prevailing in the finished structure. Each year there are a small number of localised failures of precast components, mostly limited to a single floor or stair unit – for example as shown in Figures 9.12 and 9.13 – but there have been also a number of highly publicised collapses, for example as shown in Figure 9.14, in which a single precast concrete slab at one floor level failed during construction owing to a combination of inadequate propping and overloading of wet *in situ* concrete.

The latest provisions for the assessment and design methodology for accidental actions are given in BS EN 1991-1-7:2006 [9.12]. This standard describes the principles and application rules for dealing with (a) impact forces from vehicles (road, rail, sea and air), (b) forces resulting from explosions, and (c) actions due to the local failure of elements from unspecified causes – for example, during erection of the building, damage during refurbishment or to changes to parts of the buildings. The standard is used for all building media and materials, and is compatible with other parts of BS

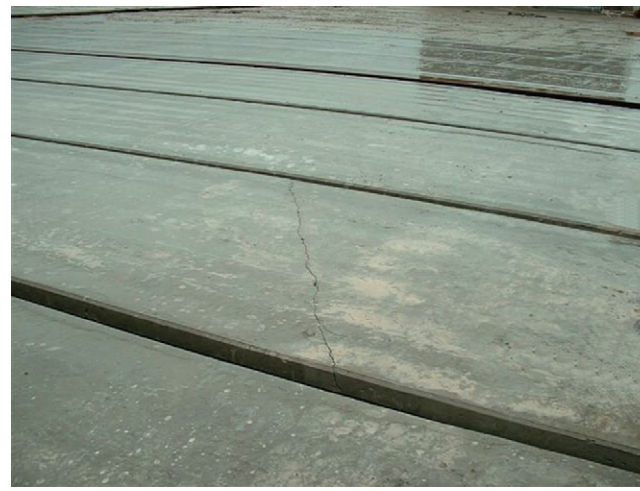

Figure 9.12 Torsion cracking in hollow-core floor unit, possibly caused by unequal bearing levels, i.e. three-point bearing, or by beam deflections at either end of the unit acting in opposite directions during installation.

Figure 9.13 Failure of a prestressed plank due to overloading during casting of topping.

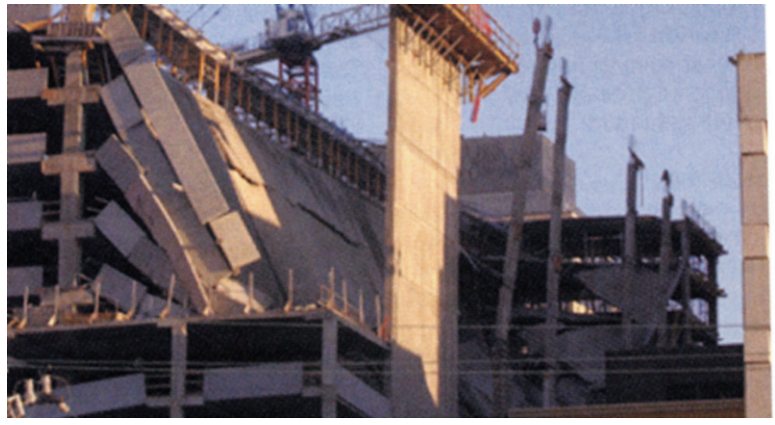

Figure 9.14 Progressive collapse of slabs and beams during erection at Atlantic City, USA (courtesy of *New Civil Engineer,* November 2003).

EN 1990 and the material codes BS EN 1992, 1993, etc. Its main objective is to present a strategy for identifying the accidental actions, thereby limiting the extent of localised failure. The strategy, given in BS EN 1991-1-7, clause 3.2, is to:

(i) take measures to prevent or reduce its severity
(ii) determine the probability of the action
(iii) determine the consequence of failure
(iv) address public perception
(v) determine the acceptable risk.

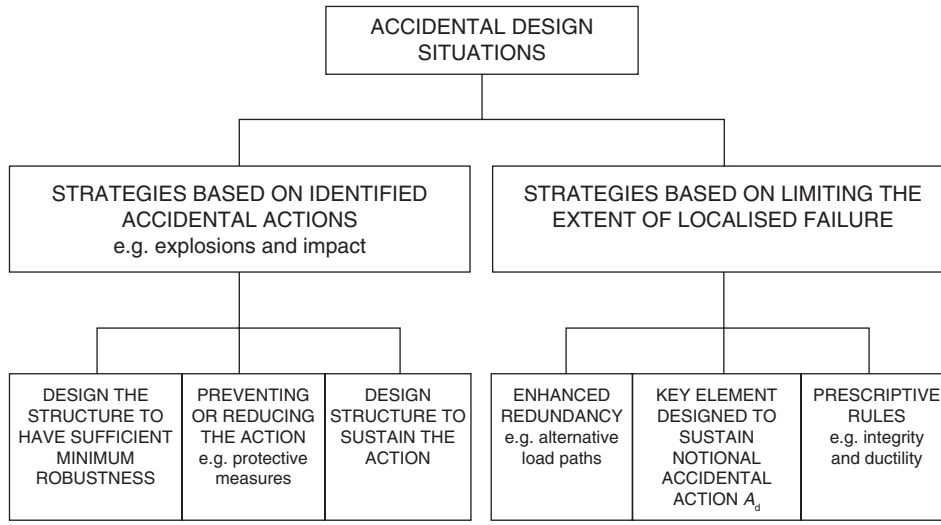

Figure 9.15 Strategies for accidental design situations according to BS EN 1991-1-7 [9.12].

Structures are designed for the relevant design situations given in BS EN 1990, clause 3.2(2), i.e. dead and imposed gravity loads, temporary loads, wind pressure, effects of fire and temperature, seismic effects and accidental actions. The strategies for the latter are summarised in Figure 9.15, reproduced from BS EN 1991-1-7, Fig. 3.2 [9.12].

According to the chart in Figure 9.15, three alternative methods are used to design for accidental actions. Referring to Figure 9.16 these are:

(a) 'key element' working as a protected member
(b) 'enhanced redundancy', known as alternative load paths
(c) 'prescriptive rules' by the use of ties.

The methods may be adopted separately or in combination in different parts of the same structure. It is not permitted to superimpose the mechanical effects of the three methods; for example, one cannot say that a member is partially protected and partially tied – it has to be either fully protected or fully tied.

Methods (a) and (b) are classified as 'direct' methods, because an appreciation of the severity and possible location of any accidental damage is known or assumed. The structure can be designed to withstand the occurrence of primary damage without an uncontrolled escalation of the damage. The key words here are 'uncontrolled escalation'. In method (c), in the event of accidental loading a notional tie force is capable of being activated at every location in the structure. Because the severity and possible location of the loads are not known, the method is classified as 'indirect'.

Following the Ronan Point collapse, tests were carried out [9.13] in which horizontal pressures, due to controlled gas explosions inside chambers, were monitored and measured. Pressures of 15.8, 16.9, 18.5 and 22.7 kPa caused structural damage without collapse. A pressure of 24.9 kPa caused considerable damage, with an outer wall showing a characteristic 'hipped roof shape' fracture-like crack pattern, but without collapse. From these (and other) test results, the 5th Amendment to the UK Building Regulations in 1978 [9.14] and today, the Building Regulations 2000, Part A [9.15], specified that any element on which the stability of the structure is to depend should, following an accident, be able to withstand a design ultimate pressure of 34 kPa, to which no partial safety factors should be applied. A simplified, less conservative robustness requirement had been adopted by most European design codes prior to the introduction of the Eurocodes. Such a protected member,

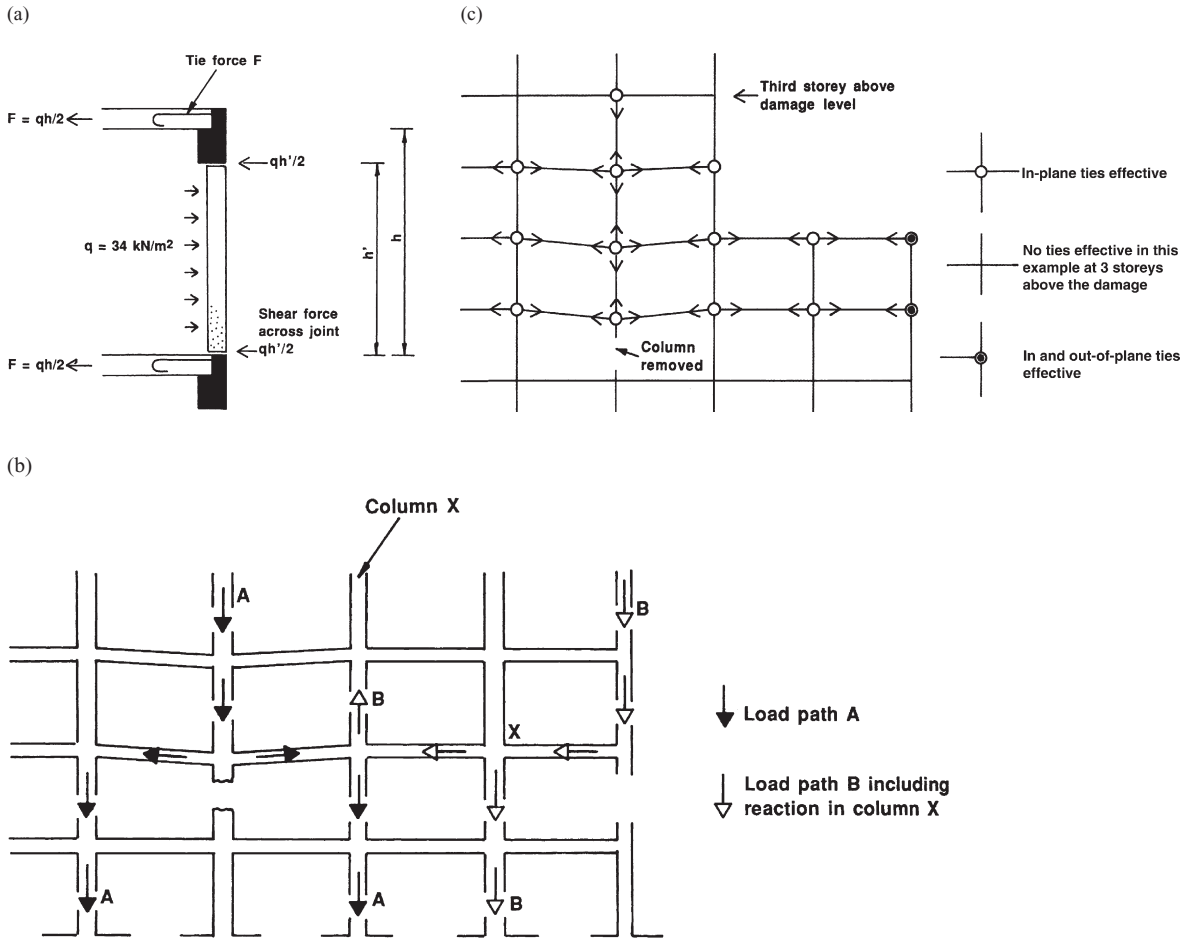

Figure 9.16 Alternative means of protection against progressive collapse. (a) Protected members; (b) alternative load paths; (c) use of ties.

including its connections to adjacent members, is called a 'key element' (BS EN 1992-1-1, clause 9.10 [9.1]) {BS 8110, Part 2, clause 2.6}.

Key elements should be designed, constructed and protected as necessary to prevent removal by accident. All other structural components that provide support vital to the stability of a key element must also be considered a key element. Few precast structures have incorporated protected members, although certain non-load-bearing precast cladding panels have been designed as such in high-risk buildings.

An alternative direct design method, called 'alternative path design', specifies walls, beams and columns, or parts thereof, that are deemed to have failed and the remaining structure is analysed based on these criteria. The components in the remaining structure are called 'bridging elements'. At each floor level in turn (including basement floors), every vertical load-bearing member, except for key elements, is sacrificed and the design should be such that collapse of a *significant* part of the structure does not result, as shown in Figure 9.17 [9.16]. Note that neither BS EN 1992-1-1 [9.1] nor BS 8110 [9.2] quantifies the permissible area of collapse, but the extent of damage is given in BS EN 1991-1-7 [9.12], Appendix A, Fig. A1.2, reproduced here in Figure 9.18. This method is not widely used in the UK because of the implicit legal necessity to satisfy the requirements of BS 8110, which permits the indirect and more fully defined method of using a tied solution.

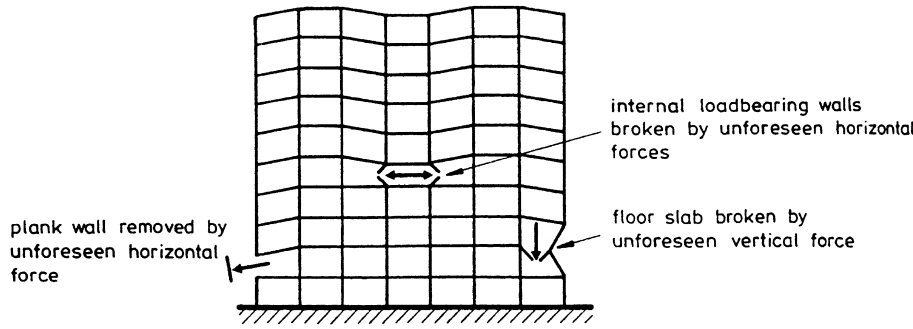

Figure 9.17 Containment of damage and debris loading in multi-storey structures [9.16].

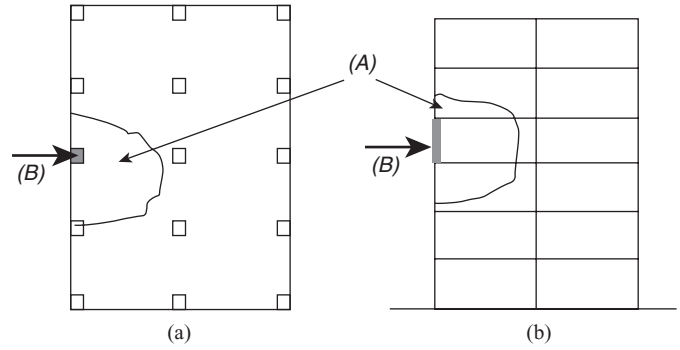

Key
(A) Local damage not exceeding 15% of floor area in each of two adjacent storeys
(B) Notional column to be removed
(a) Plan (b) Section

Figure 9.18 Recommended limit of admissible damage, adapted from BS EN 1991-1-7, Figure A.1 [9.12].

Izzuddin *et al.* [9.17] note some shortcomings: *Ties are unrelated to real structural performance, and ductility considerations are neglected. They are intended to provide resistance to gravity loading by means of catenary action upon removal of a vertical member, yet the associated ductility demands for specific structural forms can be unrealistically large, thus rendering the provisions unsafe. On the other hand, the alternative notional member removal provisions are more performance-based, but these are applied with conventional design checks, and hence they ignore the beneficial effects of such nonlinear phenomena as catenary and arching actions.*

The indirect approach to the control of accidental damage does *not* depend on the representation of the force vectors likely to be encountered, nor on the assessment of the effects of limited damage. The design is therefore based on empirical rules to provide minimum levels of strength, continuity and ductility. The first stage in securing stability is a satisfactory structural layout of slabs, beams, walls and columns, in which the smallest possible number of components rely upon others for safety. Figure 9.19 shows the kind of layout to avoid, where for various reasons columns are not permitted at certain locations. The load in the slab at Point X must pass through no fewer than six connections to reach the ground, i.e.:

(1) slab bearing
(2) beam-to-beam connection
(3) beam-to-stub column
(4) stub column-to-beam

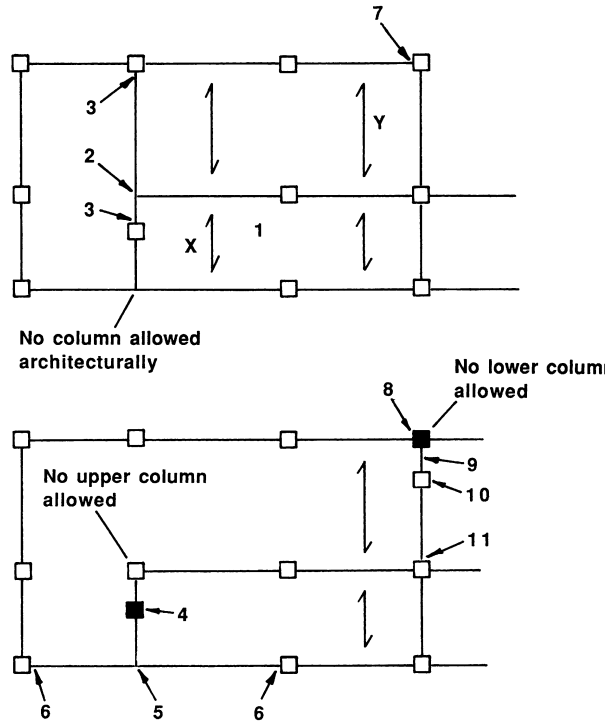

Figure 9.19 Floor layout details which may endanger the structural integrity of the building in the case of an accident.

(5) beam-to-beam
(6) beam-to-column.

Failure at one point (Point 6) would affect six structural components. Similarly at Point Y the load must be carried through several connections, including a cantilever beam end connection.

Continuity of tie steel placed in the slabs to span over beams or walls, and for beams either around the sides of or through sleeves in columns, as shown in Figure 9.20, affords the highest degree of protection. Continuity around corners is also important, Figure 9.21, where specially profiled hollow-core slabs are specified so as to enable the correct bend radius of 500 mm to be provided in the tie strands. If catenary action is assumed, as shown in Figure 9.22, allowance should be made for the horizontal reactions necessary for equilibrium.

To proceed with the design: BS 8110, Part 1, clauses 2.2.2.2. and 3.12.3 set out the requirements as to when and how the ties should be used, and this avoids *de facto* the requirement to design and construct key and bridging elements. Interaction between elements is obtained by the use of horizontal floor and vertical column and wall ties positioned as shown in Figure 9.23. These are as follows:

- horizontal internal and peripheral ties, which must also be anchored to vertical load-bearing elements
- vertical ties.

Horizontal ties are further divided into floor and beam ties (Figure 9.24) [9.16]:

- floor ties, to provide continuity between floor slabs, or between floor slabs and beams
- internal and peripheral beam ties, to provide continuity along lines of main support beams
- gable peripheral beam ties, to provide continuity between lines of main support beams.

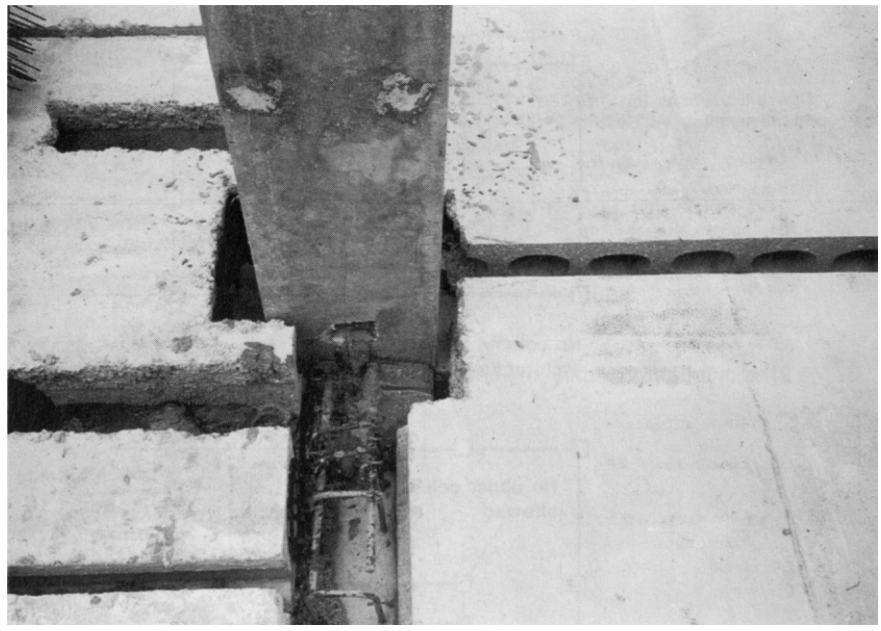

Figure 9.20 Sleeves in columns to receive continuity tie steel.

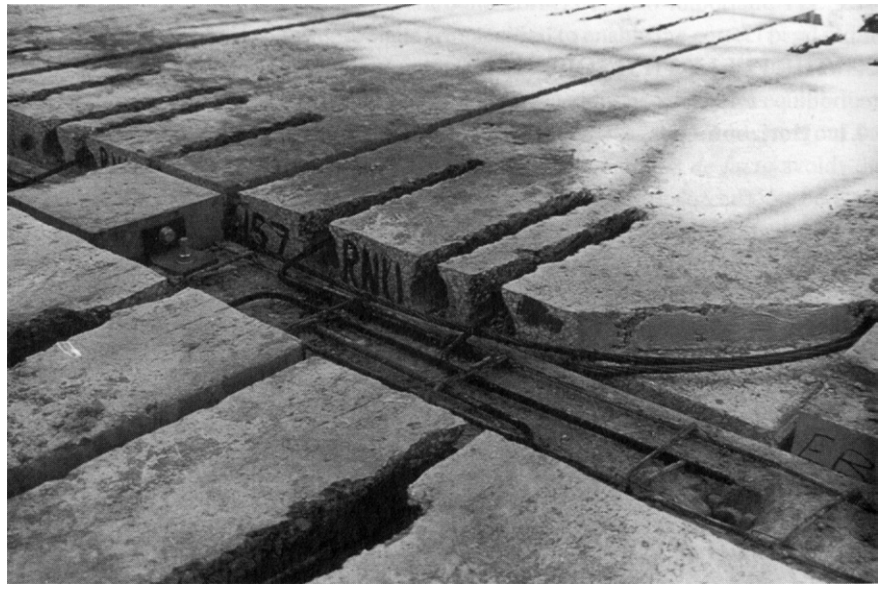

Figure 9.21 Use of helical strand as stability tie steel at external corners.

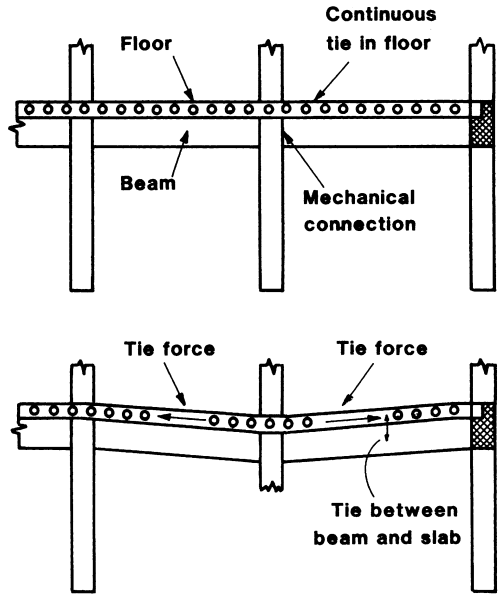

Figure 9.22 Catenary action between precast members.

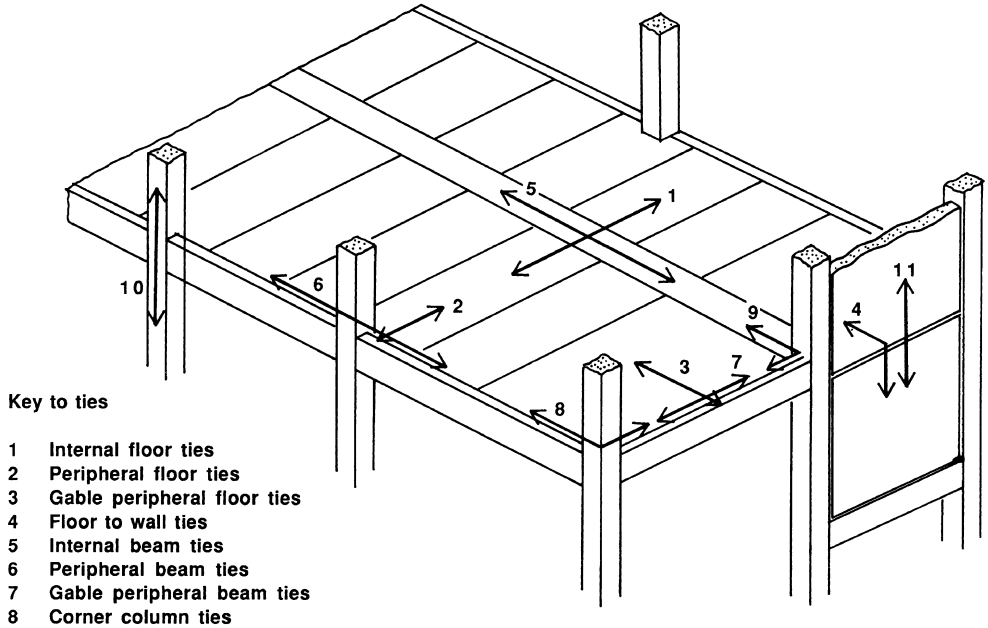

Figure 9.23 Types of ties in skeletal frames.

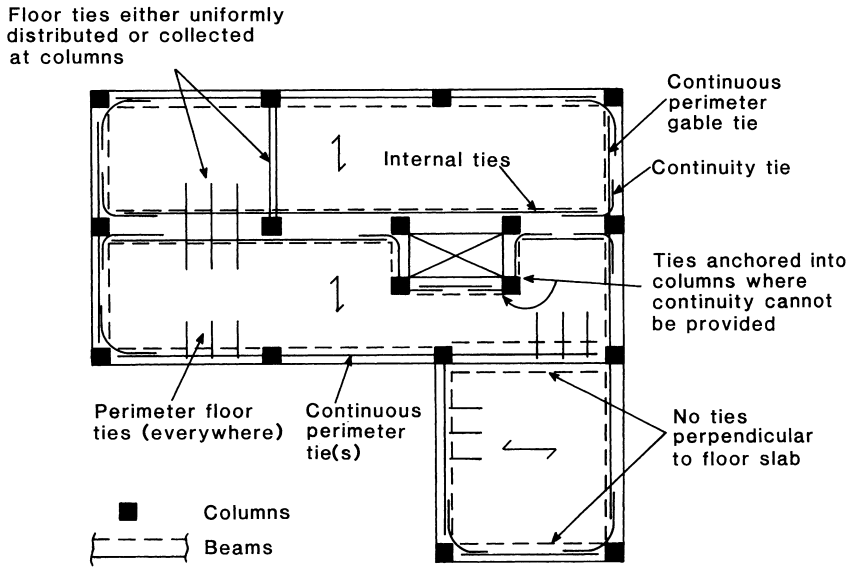

Figure 9.24 Definitions of floor ties [9.17].

9.4 Categorisation of Buildings

Building regulations classify a minimum level of protection against accidental actions in terms of possible consequences classes, depending on the height and the function of a building, as:

- Class 1: low (limited consequences)
- Class 2a: medium, lower
- Class 2b: medium, upper
- Class 3: high consequences.

Eurocode EN 1991-1-7, Annex A [9.12], recommends consequences classes for different types and occupancies of buildings. Table 9.1, reproduced from the *fib* publication [9.7], combines these recommendations with recommended design strategies. The type of approach and the recommended level of resistance to accidental actions are based on the potential consequences of the event. The most onerous class should be adopted for buildings with varying numbers of storeys, mixed-use buildings or those constructed with basements, which fall into more than one class. However, if the building is large in plan area and divided into separate structures to control movements, then the lower areas could be classed in a lower building class; e.g. two storeys of apartments over retail premises exceeding 2000 m^2 would require Class 2B for the retail floor, but 2A for the apartments. Basement storeys may be omitted from the total building storeys provided they meet Class 2B 'Upper risk group' robustness requirements.

9.5 The Fully Tied Solution

9.5.1 Horizontal ties

The specific requirements relating to ties in precast concrete structures are given in BS EN 1992-1-1, clause 9.10.2 [9.1] {BS 8110, Part 1, clause 5.1.8 [9.2]}. These are satisfied either by using individual continuous ties provided explicitly for this purpose in *in situ* concrete strips, or by using ties partly in the *in situ* concrete and partly in the precast components.

Table 9.1 Categorisation of consequences classes and design strategies [9.7, 9.11].

	Type of building and occupancy	Design strategies
Class 1 Low-risk Group	Single-occupancy houses not exceeding 4 storeys. Agricultural buildings. Buildings into which people rarely go, provided no part of the building is closer to another building or areas where people do go, than a distance of 1½ times the building height.	Provided a building has been designed in accordance with the rules given in national or international standards for satisfying stability in normal use, no further specific consideration is necessary with regard to accidental actions from unidentified causes.
Class 2a Lower Medium-risk Group	Five-storey single-occupancy houses. Hotels not exceeding 4 storeys. Flats, apartments and other residential buildings not exceeding 4 storeys. Offices not exceeding 4 storeys. Industrial buildings not exceeding 3 storeys. Retailing premises not exceeding 3 storeys of less than 1000 m^2 floor area in each storey. Single-storey educational buildings. All buildings not exceeding 2 storeys to which the public are admitted and which contain floor areas not exceeding 2000 m^2 at each storey.	Buildings should be designed in accordance with the requirements of *the indirect approach*. Effective peripheral and internal ties should be provided, respectively, for framed and load-bearing wall construction. Vertical ties are not strictly required, but always recommended.
Class 2b Upper Medium-risk Group	Hotels, flats, apartments and other residential buildings greater than 4 storeys but not exceeding 15 storeys. Educational buildings greater than single storey but not exceeding 15 storeys. Retailing premises greater than 3 storeys but not exceeding 15 storeys. Hospitals not exceeding 3 storeys. Offices greater than 4 storeys but not exceeding 15 storeys. All buildings to which the public are admitted and which contain floor areas exceeding 2000 m^2 but not exceeding 5000 m^2 at each storey. Car parking not exceeding 6 storeys.	Horizontal and vertical ties should be provided. As an alternative, the building should be designed in accordance with the requirements of the *alternative path approach*. The building should be checked to ensure that upon the notional removal of each supporting column and each beam supporting a column, or any nominal section of a load-bearing wall, the building remains stable and that any local damage does not exceed a certain limit. Where the notional removal of such columns and sections of walls would result in an extent of damage in excess of the agreed limit, then such elements should be designed in accordance with the *specific load resistance method*. In the case of wall frame buildings, the notional removal of sections of wall, one at a time, is likely to be the most practical strategy to adopt.

Table 9.1 (*Continued*)

	Type of building and occupancy	Design strategies
Class 3 High-risk Group	All buildings defined above as Class 2 Lower and Upper Consequences Class that exceed the limits on area and number of storeys.	Distinction is made between buildings with normal occupancy and buildings with a high occupancy or significant consequence of an accidental action.
	All buildings to which members of the public are admitted in significant numbers.	1) Buildings exceeding the limits of Class 2a and 2b. This category of building either:
	Stadia accommodating more than 5000 spectators.	a) should be designed in accordance with the requirements of the *alternative path approach* as specified in Section 9.3, or
	Buildings deemed to be high-risk targets.	b) should have a systematic qualitative risk assessment of the building performed and the required improvements based on this assessment implemented.
	Buildings containing hazardous substances and/or processes.	2) Buildings with high occupancy and stadia with a capacity of more than 5000 persons. For this category of building the consequences of accidental actions can be significant and a systematic risk assessment of the building should be undertaken and the required improvements based on this assessment implemented.
		3) Buildings deemed to be high-risk or buildings containing dangerous substances, or where dangerous processes are carried out.
		For this category of building a systematic risk assessment of the building should be undertaken and the required improvements based on this assessment implemented.
		4) The limit of admissible local failure may be different for each type of building. The recommended value is 15% of the floor, or 100 m^2, whichever is smaller, in each of two adjacent storeys, as shown in Figure 9.18.

Note 1: For buildings of more than one type of use, the 'consequences class' should be that relating to the most onerous type.
Note 2: In determining the number of storeys, basement storeys may be excluded, provided such basement storeys fulfil the requirements of 'Consequences Class 2b Upper Risk Group'.
Note 3: Consequences class for building types not specifically covered should be taken as the closest similar type.

The structural model is as follows. In the event of the complete loss of a supporting column or beam at floor level n, the floor plate at levels n and $(n + 1)$ must resist total collapse by acting in catenary, as shown in Figures 9.10 and 9.22. At the moment the accident occurs, an alternative load path for the floor beams that were previously supported by the damaged member may not be immediately available. If a column is removed, the tie forces over the beams must be mobilised. If a beam is lost, then it is the floor ties that do the work. With increasing deformation there will be a considerable amount of moment distribution away from the critical region. This will be followed by large

plastic hinge rotations at the column connections, which will lead to membrane action in the floor plate. A new equilibrium state will develop, as shown in Figure 9.22. The column that was directly above the damaged unit carries the beam end reactions of the beams at level *n* as a tie in vertical suspension. The column must therefore act as a tie according to Section 9.4.4, to prevent uncontrolled deflections leading to debris loading on the floor below.

This is a so-called 'collapse mechanism', which may be highly complex in buildings of irregular form. The problem is both three-dimensional and non-isotropic, depending upon the orientation of the floor slabs, walls and beams. A floor plate comprising structurally *in situ* topped double-tee units will be particularly difficult to analyse. A better term is a 'controlled collapse mechanism', for the aim is not necessarily to save the structure, but to save the lives of its occupants and of those in the vicinity. If localised repair can subsequently permit reuse of the structure, then that is a coincidental advantage.

With increasing deformation a new equilibrium state will develop, as shown in Figure 9.22, where the deflection reaches a critical value Δ_{crit}. If the deflection exceeds Δ_{crit}, the tie steel will either fracture or debond in the adjacent spans. This behaviour is applicable to uniformly distributed loads in the beam at the floor level under consideration, and to point loads from the column above this level.

If the sagging deflected shape of the beam is deduced from uniformly distributed loading (udl), and the tie steel is elastic–perfectly–plastic, it can be shown that for a characteristic udl w acting on a beam of length $2L$ (= two spans L affected by the loss of an internal column), the catenary force T is given as:

$$T = 2wL\left(\frac{0.208\,L}{\Delta_{crit}} + \frac{0.25\Delta_{crit}}{L}\right) \tag{9.1}$$

and for a point load P acting at mid-span of a beam of length $2L$:

$$T = 0.5P\sqrt{\left(\frac{L}{\Delta_{crit}}\right)^2 + 1} \tag{9.2}$$

In this equation, P is the characteristic axial force in the column from the storey above, i.e. $w(L/2 + L/2)$, because catenary action is taking place at all subsequent floors above the level under consideration. Δ_{crit} is related to the strain in the tie steel, which is a function of the type of reinforcement and detailing, and can be obtained only by testing. Test results [9.18] show that just prior to failure $\Delta_{crit} \approx 0.2L$.

The above equations may be used to determine catenary tie forces and assist in understanding the derivation of the stability tie forces that are given in BS EN 1992-1-1 and BS 8110.

Example 9.1

An internal column carries a symmetrical arrangement of two beams, which in turn carry a symmetrical arrangement of floor slabs. The column grid is 6.0 × 6.0 m. The characteristic dead plus live floor loading is 10.0 kN/m^2. If the central column were to be removed in an accident, calculate the magnitude of the beam and slab tie force required to establish a new equilibrium sagging position.

Solution

Beam load $w = 10 \times \left(\frac{6.0}{2} + \frac{6.0}{2}\right) = 60.0$ kN/m

$L = 6.0$ m

$\Delta_{crit} = 0.2 \times 6.0 = 1.2$ m

(Eq. 9.1) $T = 2 \times 60 \times 6 \times (1.04 + 0.05) = 785\,\text{kN}$

$$P = 60 \times \left(\frac{6.0}{2} + \frac{6.0}{2} \right) = 360\ \text{kN}$$

(Eq. 9.2) $T = 0.5 \times 360 \times 5.099 = 918\,\text{kN}$

Total tie force $T = \underline{1703\,\text{kN}}$.

Consider that the tie force may be distributed equally between the beam tie and the floor ties, owing to the rectangular grid dimensions.

Beam tie = 1703/2 = $\underline{851\,\text{kN}}$

Floor ties = 1703/2 = 851 kN distributed over 6 m wide floor = $\underline{142\,\text{kN/m run}}$.

The *fib* document [9.7] adopts an energy balance with regard to the linear extension of the tie bars from their original length L to $\sqrt{L^2 + \Delta_{crit}^2}$, in this example 6.11 m.

$$T = wL \left(\frac{L^2}{2\Delta_{crit}\sqrt{L^2 + \Delta_{crit}^2}} \right) \tag{9.3}$$

Then $T = 60.0 \times 6.0\ (6.0^2/2 \times 1.2 \times 6.11) = \underline{883\,\text{kN}}$, in reasonable agreement with 851 kN.

Tie bars are either high-tensile deformed bar, using a design strength of 500 N/mm^2 ($\gamma_m = 1.0$), or (increasingly popular) helical prestressing strand using its characteristic design strength, though some engineers make a 10 per cent strength reduction for strand to 1580 N/mm^2; see Figure 9.21. The strand is laid unstressed, but stretched tightly. The favourable mechanical properties of strand and the long lengths available on site make this an attractive alternative to high-tensile bar.

A tie is considered continuous if it is correctly lapped or spliced according to BS EN 1992-1-1, clause 8.7 [9.1] {BS 8110, clause 5.3.4 [9.2]}. However, strand should not be lapped in narrow site joints between precast units; mechanical fastenings are necessary here because bond stress transfer through small sections of concrete is uncertain. The details given for column splices in Section 7.12.2 may also be appropriate here. The lap length for deformed bar is usually taken as 40 diameters, in accordance with BS EN 1992-1-1, clause 8.7 [9.1], or from BS 8110, Part 1, Table 3.29 [9.2] for grade C25/30 concrete. The lapping length for the strand is based on the transmission lengths given in BS EN 1992-1-1, clause 8.7.3 [9.1] {BS 8110, Part 1, clause 4.10.3 [9.2]}. Using $f_{ck} = 20\,\text{N/mm}^2$ {$f_{cu} = 25\,\text{N/mm}^2$} in place of f_{ci}, and $K_t = 360$ for 7-wire drawn strand, a length of 72 × diameter is typical. Wahid Omar [9.19] undertook pull-out tests on a number of 12.5 mm-diameter helical strands embedded over a length of 1200 mm (94 diameters) into grade C20/25 concrete prisms 100 mm square. A maximum stress of 1790 N/mm^2 was measured in the strand prior to fracturing, with zero slip being recorded at the rear end of the strand. Thus a lap length of 1200 mm is usually specified.

The position of the lap is staggered to avoid a concentration of bars. The tie, of diameter φ, must be embedded in *in situ* concrete of at least $2(\varphi + h_{agg} + 5)$ mm width. In most instances this means that the *in situ* concrete must be at least 60 mm wide (as explained in beam design in Section 4.3.3). The partial safety factor for steel reinforcement may be taken as 1.0 (BS EN 1992-1-1, clause 2.4.2.4) {BS 8110, Part 1, clause 2.2.4.2}. The partial safety factor for concrete in flexure is 1.2 {1.3}, but moments of resistance are not normally determined in this situation.

Ties passing through precast columns or walls are fed through oversized sleeves (usually two to three times the diameter of the tie bar(s)) and later concreted in. Problems occur with this detail at external corners, where the tie bars change direction by up to 90°. These sleeves are impossible to form; also, the position of the sleeve must be known in advance and correctly positioned in the mould. This can often cause problems of two kinds. Firstly, many manufacturers prefer not to puncture the side of the mould unnecessarily; and secondly, too many slots and sleeves can weaken columns and lead to small diagonal cracking at the corners of the sleeve.

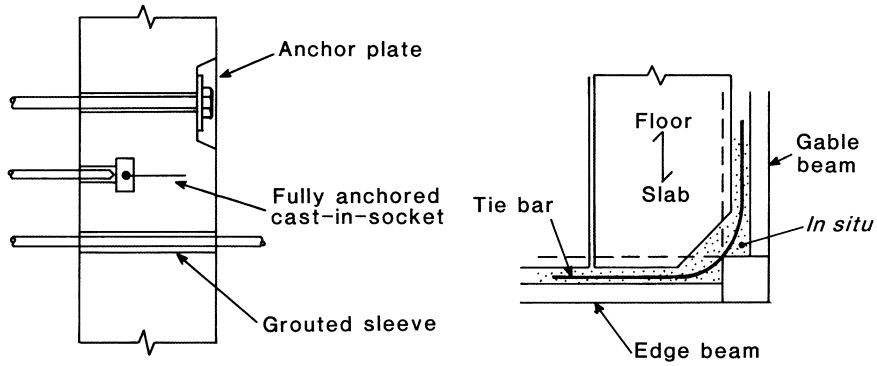

Figure 9.25 Ties anchored using cast-in sockets or bearing plates.

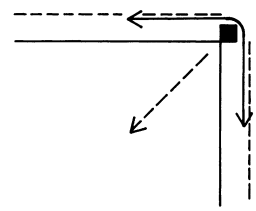

Figure 9.26 Stability ties at re-entrant corners.

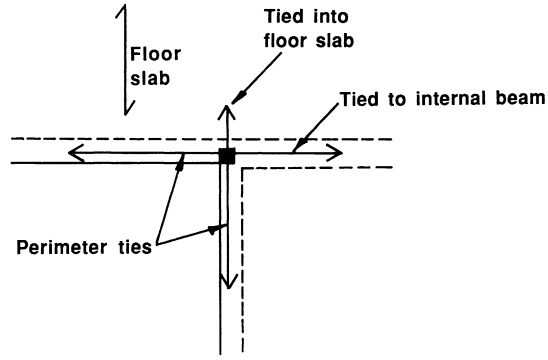

Figure 9.27 Continuity of ties at re-entrant corners.

To overcome these problems precast contractors prefer to run tie steel past the face of the column, rather than through it. This means that the width of the beam, over which the tie bars are placed, must be greater than the width of the column around which they will pass. Otherwise part of the floor slab has to be broken out to allow the ties to be bent and cranked around the corners of the column.

Continuity around corners is achieved either by concreting the tie into a 45° splayed corner, or by using threaded couplers or anchored plates, as shown in Figure 9.25. Continuity is not usually provided between the flights and landings in precast staircases, because these units are not essential to the stability of the frame. However, Figure 4.58(b) shows how this might be achieved, in the very rare event that continuity ties could be placed only in the floor landing.

The main problem with using gathered tie steel in this manner occurs at perimeter re-entrant corners where, as shown in Figure 9.26, the resultant force from the perimeter tie steel is pulling outwards into unconfined space. One cannot rely on the shear capacity of the column to restrain this force. Two alternatives, as shown in Figure 9.27, are possible:

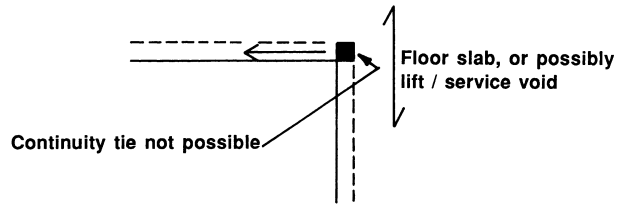

Figure 9.28 Difficulties in positioning ties at re-entrant corners.

(1) The tie steel continues through or past the side of the column as though it were an edge column. This is possible only if an internal beam is located in line with the edge beam, which is not always the case, as shown in Figure 9.28. In many buildings, particularly offices, a lift shaft or stairwell is located at re-entrant corners. This may cause additional tying problems because of the lack of space to place ties in walls, etc. Cast-in couplers (or similar) may be used to anchor the tie steel to the walls.

(2) A structural topping containing a steel fabric may be used in this localised area only, but that will probably cause embarrassment to the structural zone in the remainder of the floor. If the floor spans in that part of the building can be proportioned so that a shallower precast floor or precast beam is used in that area, a topping screed will not increase the overall floor depth. A 50 mm reduction is all that is required.

9.5.2 Calculation of tie forces

The requirements for all horizontal ties in BS 8110, Part 1, clause 3.12.3 [9.2] have been transferred exactly into the National Application Document for BS EN 1992-1-1 [9.1] in preference to adopting the Eurocode preferred methodology; the former is both simpler and less demanding. The requirements for column ties are a function of the load partial factors of 1.0 in BS EN 1992-1-1, and 1.05 in BS 8110, and therefore have changed.

The basic horizontal tie force F_t is the lesser of:

$$F_t = (20 + 4n) \text{ or } 60 \text{ kN/m width} \tag{9.4}$$

where n is the number of storeys, including basements.

F_t is considered as an ultimate value and is *not* subjected to the further partial safety factor of $\gamma_f = 1.05$ given in BS 8110, clause 2.4.3.2. These requirements have been retained in the UK National Application Document to [9.1]. In other European countries, equation 6.11(b) in BS EN 1990 [2.8] may be used, i.e. $G_k + \psi_2 Q_k$, where ψ_2 is the quasi-permanent factor, typically 0.3 for domestic, 0.6 for shopping, congregation and car parks, and 0.8 for storage.

If the total characteristic permanent (G_k) + imposed (Q_k) loading is greater than 7.5 kN/m^2 and/or the distances (l_r) between the columns or walls in the direction of the tie is greater than 5 m, the force is modified as the greater of:

$$F_t' = \left(\left(\frac{G_k + Q_k}{7.5} \right) \times \frac{l_r}{5} \right) F_t \tag{9.5}$$

or

$$F_t' = F_t \tag{9.6}$$

The catenary tie forces are calculated by simple statics, but the assumptions implicit in their formulations are rather arbitrary. The precast reinforced or prestressed members are designed so that

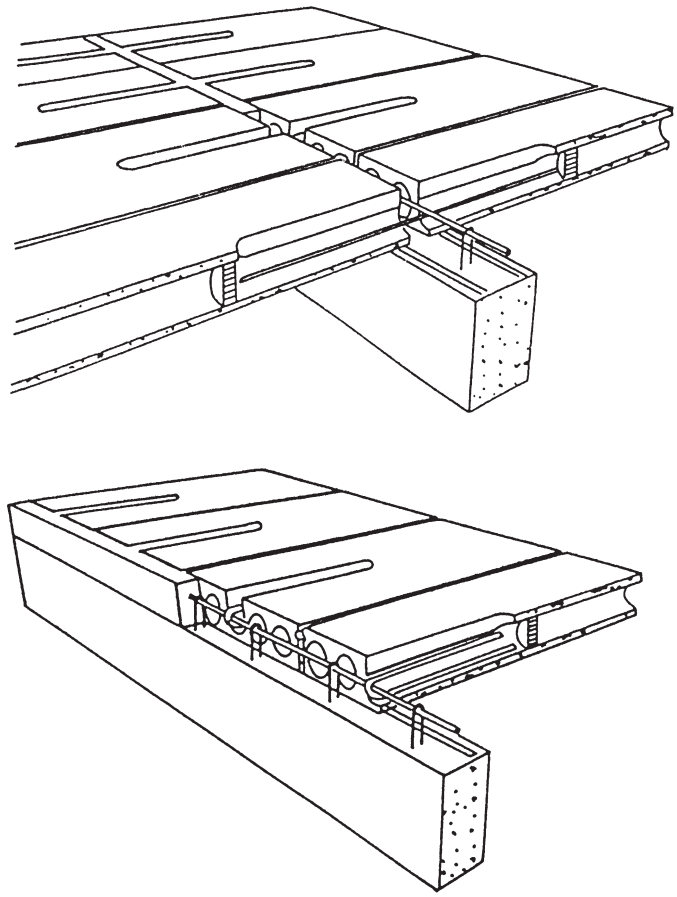

(a)

Figure 9.29(a) Continuity for floor ties in hollow-core slabs. Parallel with the floor slab.

they can generate the necessary tie forces, and so it is only continuity tie forces between the units that must be provided *in situ*.

Internal floor ties parallel with the span of the flooring are either distributed evenly, using short lengths of tie steel anchored by bond into the opened cores of the hollow-core floor units, or grouped in full-depth *in situ* strips at positions coincident with columns. The *FIP Manual* [9.20] on hollow-core floors shows a large range of alternative details, from which Figure 9.29(a) has been taken. However, this illustration shows ties positioned in the longitudinal joints between two adjacent units – this is not recommended, for the reasons mentioned in Section 9.2.1 and shown in Figure 9.10 in the event of catenary tie action splitting these joints. Figure 9.29(b) is an interesting example of using floor ties with end hooks positioned around the tie bars in beams, as these not only provide local confinement to the compression bars in the beam, but also ensure that the floor slab and beam would remain connected in the scenario shown in Figure 9.10. Floor ties should be positioned in the direction of the span of the floor unit and align across the beams, but on occasions it is necessary to incline the bars as shown in Figure 9.29(c). A small angle, as is the case here, is satisfactory, but anything greater will necessitate the tie bars kinking and straightening before the tie load is effective. However, because the straightened-out tie is designed to operate at ultimate load under large deformations, a larger anchorage length into the floor unit would enable the full resistance. Figures 9.29(d) and (e) show the welding of ties to obtain continuity through beams, using cast-in projecting bars in a precast beam, and welds to the sides of the web of a supporting steel girder, respectively.

In the first case, the mechanism relies on an adequate pull-out force generated by tie steel cast into *in situ* concreted hollow cores (see Section 9.5). A typical configuration is to use 12 mm-diameter

(b)

Figure 9.29(b) The solution of using floor ties looped around beam ties into the milled slots of hollow-core floor units.

(c)

Figure 9.29(c) Floor ties inclined or not in alignment will attempt to straighten and kink before taking the tie loads effectively.

high-tensile bar or 12.5 mm-diameter helical strand at 600 mm centres, i.e. two bars per 1200 mm-wide slab. For greater quantities it is better to decrease the bar spacing rather than increasing the size or number of bars. At no time should two bars be placed in one core. If high-tensile bars are cast into beams and arranged so that they are to be manually bent into the slots in the slab, the maximum size of bar that can easily be rebent on site is 12 mm diameter. Providing that the floor slabs are tied to edge beams or tied across internal beams, the tie force across the floor is provided in the precast floor

(d)

Figure 9.29(d) Floor ties passing into hollow-core slabs are welded to ties projecting from beams.

unit itself. Adequate reinforcement will be provided in all but the least reinforced units, using the minimum area of high-tensile steel of 0.13 per cent A_c.

Ties along gable edge beams are placed into the broken-out cores of slabs at intervals varying between 1.2 and 2.0 m. As shown in Figure 9.29(f), the success of the ties relies on adequate anchorage of small loops cast into *in situ* concrete, which itself is locked into the bottom of the hollow-core. Generous openings (say 300 mm long) should be made in the floor slabs to ensure that any projecting tie steel in the beam may be lapped without damage to the slab or tie bar. Figure 9.29(g) shows the minimum requirements, and is an example of where site cuts have been made in order to position the tie. Here the tie force is F_t.

The magnitude of the tie forces F_t' between precast hollow-core slabs is as given by Eq. (9.5) or (9.6). The area of steel is:

$$A_s = F_t' / f_y \tag{9.7}$$

since $\gamma_f = 1.0$ for the reinforcement (BS EN 1992-1-1, clause 2.4.4.2).

Continuity between beams is provided across the column line by calculating the magnitude of the internal and peripheral tie force F_t' according to Eq. (9.5) or (9.6). Here the tie force in the beam F_t' is the summation of all the internal tie forces across the span L of the floor, i.e.:

$$F_t'(\text{beam}) = F_t' L \tag{9.8}$$

If the spans of the floor slabs on either side of the beam are different, L_1 and L_2, the summation of half of each span, i.e. 0.5 $(L_1 + L_2)$, is used to replace L in Eq. (9.8). In an edge beam $L_2 = 0$. Where

(e)

Figure 9.29(e) Floor ties into hollow-core slabs are welded to the webs of steel beams.

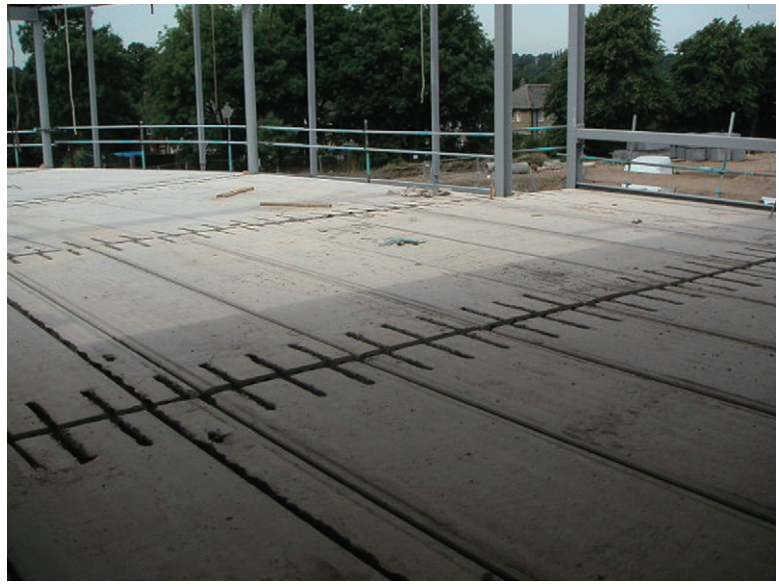

(f)

Figure 9.29(f) Floor ties are placed into the opened cores in the top of hollow-core floor slabs, which are then filled using *in situ* concrete.

(g)

Figure 9.29(g) Gable edge beam ties to the edges of hollow-core units executed by cut-outs into the first two hollow cores, which are blocked off prior to *in situ* concrete infill.

the floor slabs to one side of the beam are spanning parallel with the beam, and on the other side are spanning onto the beam with a span L_1, the beam tie force is taken as:

$$F_t'(\text{beam}) = 1.0F_t' + 0.5F_t'L \tag{9.9}$$

Where the floor slabs are spanning parallel with the span of an edge beam, only a nominal tie force 1.0 F_t' need be provided. The area of steel is calculated according to Eq. (9.7).

The internal tie bars should be distributed *equally* on either side of the centre line of the beam, be separated by a distance of at least 15 mm to ensure adequate bond (assuming the *in situ* fill has 10 mm-size aggregate), and be positioned underneath projecting loops from the beam. Peripheral tie bars should be similarly positioned and, according to BS EN 1992-1-1, clause 9.10.2.2 {BS 8110, clause 3.12.3.5}, should be located within 1.2 m of the edge of the building. This is not usually a problem, except in the case of cantilevers where there is no beam nearer than 1.2 m from the end of the cantilever. In this case the tie must be located in a special edge beam, which is cast for the sole purpose of providing the peripheral tie.

The success of the tie beams depends largely on detailing. Figure 9.30 illustrates the concept; two tie bars are fixed on site and pass underneath the projecting reinforcement loops. The hooked bars, which must pass underneath, are fully anchored into the hollow cores of the slab. Finally, the tie bars pass through small sleeves preformed in the columns, or pass by the side of the column. Figure 9.31 shows how continuity may be satisfied at external positions.

9.5.3 Horizontal ties to columns

Each external column is tied horizontally into the structure at each floor and roof level with ties capable of developing a force equal to the greater of (a) or (b), as follows (in the National Application Document to [9.1], a reiteration of BS 8110, Part 1, clause 3.12.3.6 [9.2]):

(1) the lesser of 2.0 F_t' or 0.4h F_t, where h is the storey height in metres
(2) 3 per cent of the vertical ultimate axial force carried by the column at that level using $\gamma_f = 1.0$ {1.05}.

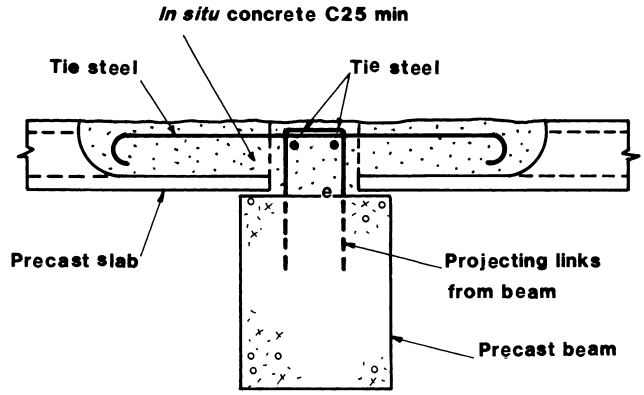

Figure 9.30 Stability ties at internal positions.

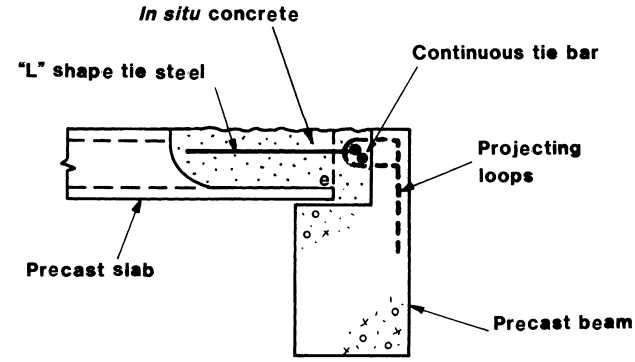

Figure 9.31 Stability ties at external positions.

Corner columns should be tied into the structure in two mutually perpendicular directions with the above force.

Ties may be provided at columns in one of two ways. If there is no positive tie force between the beam and column, e.g. the beam-to-column connector in Figure 7.68(a) where only a frictional bearing is provided, loose tie steel should be placed on site and be fully anchored, as shown in Figures 9.20 and 9.32. The net cross section of any threaded bar (to the root of the thread) is used in calculating the area of the tie bar. The column should be checked to ensure that the tie force can be resisted, and all anchor plates, cast-in sockets, etc. should be designed accordingly. Resin-anchored reinforcement may also be used, but this involves the use of proprietary materials and techniques. The manufacturer's specification with regard to the size of hole and insertion of the resin must be followed, with supervision and inspection implications.

The second method is to design the beam-connector so that the horizontal shear capacity may be used to provide the necessary tie force from the column to the beam. This imposes additional axial forces in the beam, which must be dealt with as explained in Section 4.3.7. There must be a positive, no-slip, horizontal connection between the beam and column. This is guaranteed by surrounding any mechanical connectors, such as bolts or dowels, with *in situ* concrete. The site workmanship should be especially well supervised in these situations, because evidence of poor compaction can easily be concealed.

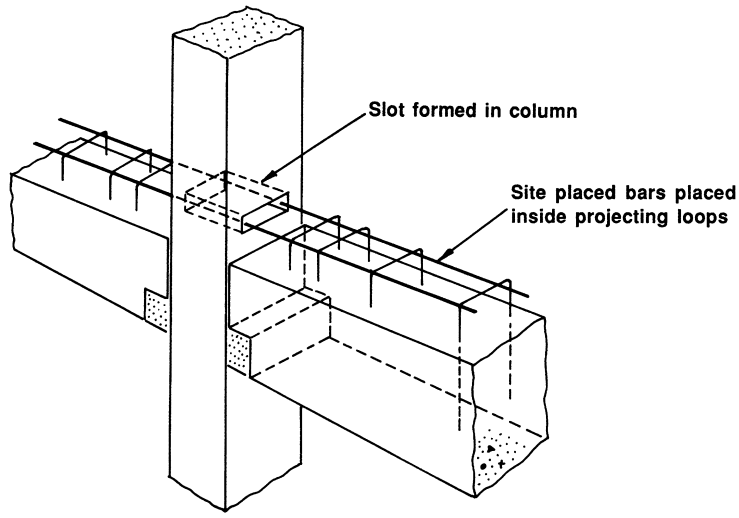

Figure 9.32 Continuity for beam ties through columns.

Exercise 9.1

Calculate the horizontal tie requirements in the floors of the four-storey building shown in Figure 9.33, where the floor-to-floor storey height = 3.2 m. All floors and roof slabs are 200 mm-deep hollow-core units. The characteristic permanent and variable floor loads are 1.6 kN/m^2 and 5.0 kN/m^2, respectively. The characteristic superimposed permanent and variable roof loads are 2.0 kN/m^2 and 1.5 kN/m^2, respectively. Assume that the building façade permanent load is 12 kN/m. Assume that the beam-to-column connector has no horizontal tie capacity.

Use grade C25/30 concrete for the *in situ* infill to limit anchorage length required, and $f_y = f_{yk} = 500\,\text{N/mm}^2$.

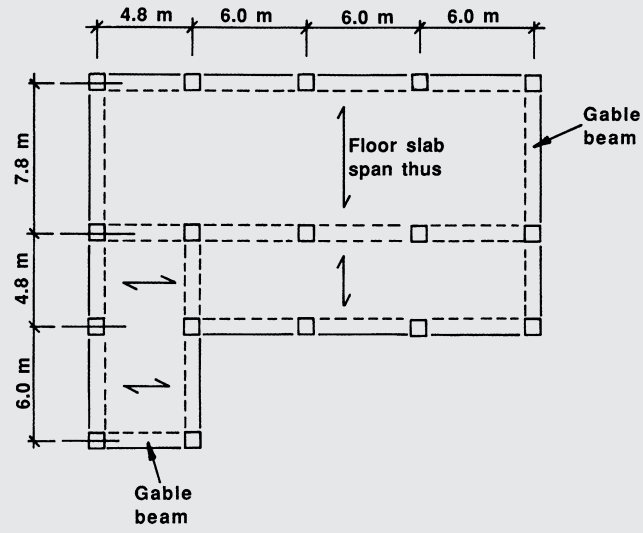

Figure 9.33 Details for Exercise 9.1.

Solution

Step 1: Loading

$$F = 20 + 4 \times 4 = 36 \text{ kN/m}$$

G_k = self-weight of slab (from Table 3.1) = 3.0 kN/m^2, plus superimposed permanent load = 1.6 kN/m^2
Total G_k = 4.6 kN/m^2

$$Q_k = 5.0 \text{ kN/m}^2$$

Then $(G_k + Q_k)/7.5 = 1.28$
Thus if $l_r < 5$ m then $F_t' = 36 \times 1.28 = 46.08$ kN/m, and if $l_r > 5$ m then $F_t' = 46.08 \times l_r/5$.

Step 2: Floor ties
(a) for span = 7.8 m
Ties are placed in slots at ends of hollow-core slabs. Preferable distance between ties = 600 mm, i.e. two per 1.2 m wide unit.

$$F_t' = 46.08 \times 7.8/5 = 71.9 \text{ kN/m run}$$

$$A_s = 71.9 \times 10^3 / 500 = 144 \text{ mm}^2/\text{m}$$

Use H12 ties at 600 mm centres (188 mm^2) at internal beams.
Anchorage length = $40 \times 12 = 480$ mm
Tie force in each bar = $0.6 \times 71.9 = 43.2$ kN must be resisted by shear in the projecting bars and loops in the edge beams. Then size of projecting bar is given by:

$$A_s = 43.2 \times 10^3 / 0.6 \times 500 = 144 \text{ mm}^2 \text{ per location.}$$

Use two H10 projecting bars in pairs, with H10 loops (157 mm^2) at edge beams.

(b) for span = 4.8 m < 5 m
$F_t' = 46.08 \times 1 = 46.08$ kN/m run, and A_s = 93 mm^2/m
Use H10 ties at 600 mm centres (131 mm^2) at internal beams.
Anchorage length = 400 mm
Tie force in each bar = $0.6 \times 46.08 = 27.7$ kN, and A_s = 93 mm^2
Use one H12 projecting bar with H8 loops (113 and 101 mm^2) at edge beams.

(c) at gable ends
$F_t' = 36 \times 1 = 36$ kN/m run, irrespective of span, and A_s = 72 mm^2/m
Use H10 ties at 1000 mm centres (78 mm^2).
Anchorage length = 400 mm
Tie force in each bar = 36 kN, and A_s = 120 mm^2
Use two H10 bars in pairs in H10 loops (157 mm^2).

(*Continued*)

Step 3: Peripheral ties to edge beams

(a) 6.0 m span beams supporting floors spanning 7.8 m

$F_t' = 46.08 \times 6/5 \times 7.8/2 = 215.6$ kN

$A_s = 215.6 \times 10^3 / 500 = 432$ mm^2

Use two H20 edge ties (628 mm^2).

(b) 6.0 m span beams supporting floors spanning 4.8 m

$F_t' = 46.08 \times 6/5 \times 4.8/2 = 132.7$ kN, and $A_s = 266$ mm^2

Use two H16 edge ties (402 mm^2).

(c) 7.8 m span gable beams

$F_t' = 46.08 \times 7.8/5 = 71.9$ kN, and $A_s = 144$ mm^2

Use one H16 gable edge tie (201 mm^2).

Step 4: Internal ties

(a) 6.0 m span beams supporting floors spanning 7.8 m and 4.8 m

$F_t' = 46.08 \times 6/5 \times (7.8 + 4.8)/2 = 348.4$ kN, and $A_s = 697$ mm^2

Use two H25 internal ties (982 mm^2).

(b) 4.8 m span beams supporting floors spanning 7.8 m only

$F_t' = 46.08 \times (7.8/2 + 1) = 225.8$ kN, and $A_s = 452$ mm^2

Use two H20 internal ties (628 mm^2).

Step 5: Horizontal column ties at first-floor level

(a) Edge columns at 6 m centres

Area of slab supported = 23.4 m^2

Axial load at roof = (3.0 + 2.0 + 1.5) × 23.4 = 152.1 kN

Axial load at floors = (3.0 + 1.6 + 5.0) × 23.4 + 12 × 6 = 296.6 kN

Tie force = greater of:

(a) lesser of 2 × 36 = 72 kN, or 0.4 × 3.2 × 36 = 46.08 kN

and **(b)** 0.03 × 1.05 × (152.1 + (3 × 296.6) + self-weight 28) = 24.2 kN

Use $F_t = 46.08$ kN

$A_s = 46.08 \times 10^3 / 500 = 93$ mm^2

Use one H12 edge column tie (113 mm^2).

(b) Internal columns at 6 m centres

Area of slab supported = 46.8m^2

Axial load at roof = 6.5 × 46.8 = 304.2 kN

Axial load at floors = 9.6 × 46.8 = 449.3 kN

Tie force = greater of:

(a) lesser of 2 × 36 = 72 kN, or 0.4 × 3.2 × 36 = 46.08 kN

and **(b)** 0.03 × 1.05 × (304 + (3 × 450) + self-weight 28) = 52.9 kN

Use $F_t = 52.9$ kN as above.

$A_s = 52.9 \times 10^3 / 500 = 106$ mm^2

Use one H12 internal column tie (113 mm^2).

If the beam ties are not tied to the columns in any way, the column ties must be used. However, if the beam ties pass through sleeves in the column and are enclosed within the main column reinforcement cage, then the H16 gable tie is already adequate to cater for the column tie force.

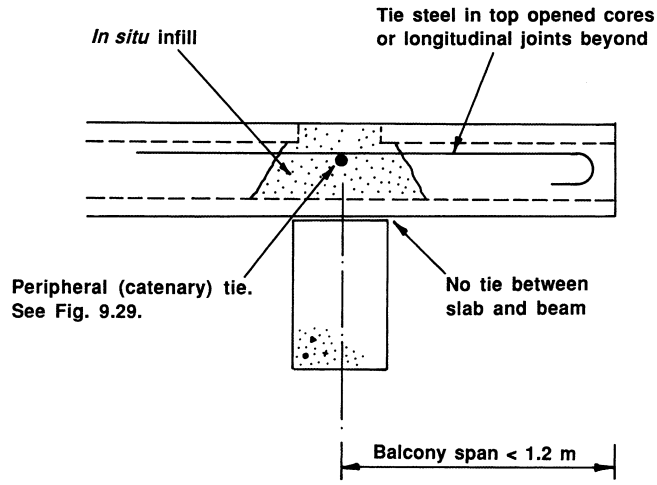

Figure 9.34 Perimeter floor ties across balcony slabs.

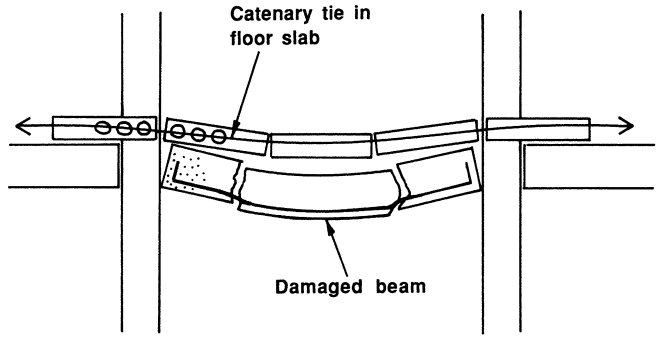

Figure 9.35 Catenary action in balcony slabs without beam-to-slab tie.

9.5.4 Ties at balconies

Where cantilevered floor or roof slabs are used to form balconies, there is a major problem in placing floor ties over the support beam. Figure 5.47 illustrates the problem. The simplest answer is to use a structural topping and provide the tie steel in the mesh, but where this is not desirable the designer is faced with having to provide a tie within the depth of the floor slab, as shown in Figure 9.34. Openings are formed in the sides of the floor slabs through which site bar(s) are placed. The site bars must pass beneath the top steel in the hollow cores of the floor slab (Figure 5.48) and *in situ* concrete is introduced into slots cut in the top of the slab. The method is not 100 per cent satisfactory, because of the problems in feeding the tie bars into the slabs. Also, in case of an accident to the supporting beam, the floor slabs would hang in catenary, as shown in Figure 9.35, but the beam would no longer be integral.

9.5.5 Vertical ties

The reason for vertical ties is to provide vertical suspension for the column in the situation shown in Figure 9.16(c). BS EN 1992-1-1 [9.1] {BS 8110, Part 1 [9.2]} calls for continuous vertical ties in all

buildings (the provision for ties in five or more storeys was deleted in 1993, and must be provided in all buildings because the Building Regulations [9.15] require it and legally override the design codes), capable of resisting the tensile force given in the NAD to the Eurocode {again a reiteration of BS 8110, clause 3.12.3.7}. The vertical tie force capacity is calculated from the *summation* of the ultimate beam reactions N only at the floor (or roof) immediately below where the tie is designed, not the total load from every floor below the tie. This means that the reinforcement provided in the column, and in any splice within that column, should be at least:

$$A_s = N / f_y \tag{9.10}$$

The loading on the floor may be taken as the permanent action plus 0.5 x variable action, but 0.7 x variable action if subject to public crowd loading (e.g. shops or meeting areas) or car access, or 0.9 x variable action for storage areas {characteristic permanent load plus one-third of the superimposed variable load (unless the building is being used for storage, when the full superimposed load is taken)}. The partial safety factor for all gravity loads γ_f may be taken as 1.0 {1.05}.

The tensile capacity of any column splice should also be able to resist the force N. In the case of grouted sleeve splices, the anchorage bond length for the reinforcement may be calculated using BS EN 1992-1-1, clauses 8.4.2 to 8.4.4 [9.1], {or BS 8110, Part 1, clause 3.12.8.3}, where the bond stress obtained from clause 8.4.2 {Table 3.28} is without the partial safety factor of 1.5 [9.1], {1.4 [9.2]}. The weld lengths in the welded splice are also determined without the partial safety factor.

In the welded plate splice the thickness of the plate is determined by considering the bare steel sections alone, i.e. the *in situ* concrete is ignored. The root thread area is used to determine the tensile capacity of the projecting bars, and the pull-out and anchorage bond capacity of the bars welded to the plate gives the tensile capacity of the upper bars. The strength of the plate is checked in bending and shear, as shown in Figure 9.36. The effects of two-dimensional plate bending and prying forces at the nut are ignored.

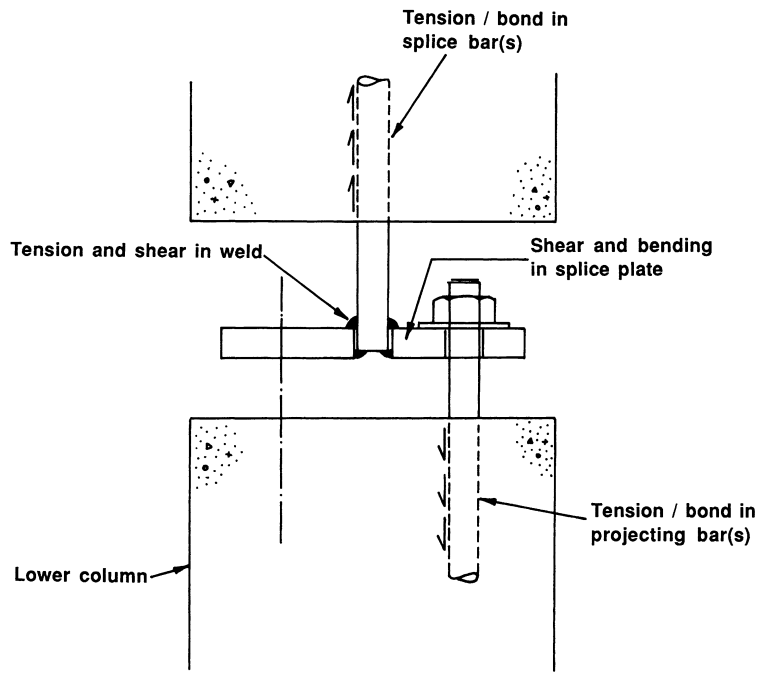

Figure 9.36 Stability vertical tie in welded plate column splice.

Exercise 9.2

Check the vertical tie requirements in the column and welded plate splice used in Exercise 7.10 and shown in Figure 7.115. The characteristic column permanent and variable loads at each floor level are 340 kN and 250 kN, respectively. The column concrete is grade C40/50.

Solution

Step 1: Column reinforcement

$N = (1.0 \times 340) + (1.0 \times 0.5 \times 250)$	$= 465\,\text{kN}$	$N = (1.05 \times 340) + (1.05 \times 250/3)$	$= 445\,\text{kN}$
$A_s = 465 \times 10^3/500$	$= 930\,\text{mm}^2$	$A_s = 445 \times 10^3/500$	$= 889\,\text{mm}^2$

Provide four H20 column bars ($1257\,\text{mm}^2$).

Column splice
Use mild steel stress, welded reinforcement to upper column and high-tensile threaded bar to lower column.

Upper column bars

$A_s = 465 \times 10^3/250$	$= 1860\,\text{mm}^2$	$A_s = 445 \times 10^3/250$	$= 1780\,\text{mm}^2$
Provide four H25 column bars ($1963\,\text{mm}^2$).		Provide four H25 column bars ($1963\,\text{mm}^2$).	

Bond length to column.

Force in each bar = 116.3 kN		Force in each bar = 111.1 kN	
Bond stress in grade C40/50 concrete for type 2 deformed bars in tension		Bond stress in grade C40/50 concrete for type 2 deformed bars in tension	
$= 2.25 \times 0.21 \times 40^{(2/3)} = 5.53\ \text{N/mm}^2$		$= 1.4 \times 0.5\sqrt{50} = 4.95\ \text{N/mm}^2$	
Tension lap length = Bond length		Tension lap length = Bond length	
$= \max(10 \times 25; 100;$		$= 111.1 \times 10^3/(4.95 \times 25\ \pi)$	$= 286\,\text{mm}$
$= 116.3 \times 10^3/(5.53 \times 25\ \pi)$	$= 375\,\text{mm}$		

Lower column bars

$A_s = 930\,\text{mm}^2$		$A_s = 889\,\text{mm}^2$	
Provide four H20 column bars with M20 thread ($980\,\text{mm}^2$ root area).		Provide four H20 column bars with M20 thread ($980\,\text{mm}^2$ root area).	
Tension lap length		Tension lap length	
$= \max(15 \times 20; 200;$		$= 111.1 \times 10^3/4.95 \times 20 \times \pi$	$= 358\,\text{mm}$
$= 116.3 \times 10^3/(5.53 \times 20\ \pi)$	$= 335\,\text{mm}$	Four H16 bars from before ($804 < 889\,\text{mm}^2$) must be increased to four H20.	
Four H16 bars from before ($804 < 930\,\text{mm}^2$) must be increased to four H20.		Compression lap length required with H20 bars	
Compression lap length required with H20 bars		$= 40 \times 20 \times$ (area required 889/area provided 1257)	$= 566\,\text{mm}$
same as tension lap	$= 335\,\text{mm}$	$> 286\,\text{mm}$ and $> 358\,\text{mm}$.	
$= 525\,\text{mm}$ and $> 375\,\text{mm}$.		Provide minimum lap length.	$= 575\,\text{mm}$
Provide minimum lap length.	$= 525\,\text{mm}$		

(*Continued*)

Plate design

Ignore the *in situ* concrete infill surrounding the plate and bars.

Plate size = 300 − 35 − 35 = 230 mm square

Eccentricity of upper to lower bars = 82 mm

Moment in plate $= 116.3 \times \frac{82}{\sqrt{2}}$	= 6741 kNmm	Moment in plate $= 111.1 \times \frac{82}{\sqrt{2}}$	= 6443 kNmm
Shear in plate	= 116.3 kN	Shear in plate	= 111.1 kN
Effective width of plate $b = 82\sqrt{2}$	= 116 mm	Effective width of plate $b = 82\sqrt{2}$	= 116 mm
Then modulus $S_{xx} = b\,t^2/4$		Then modulus $S_{xx} = b\,t^2/4$	
Using $p_y = 275\,\text{N/mm}^2$, then t	> 26.7 mm	Using $p_y = 275\,\text{N/mm}^2$, then t	> 26.1 mm
Shear area = $b\,t$		Shear area = $b\,t$	
Using $p_q = 165\,\text{N/mm}^2$ then t	> 6.1 mm	Using $p_q = 165\,\text{N/mm}^2$ then t	> 5.8 mm

Use 230 × 230 × 30 plate.

9.6 Catenary Systems in Precast Construction

There remains a popular belief that, under certain loading conditions, precast concrete frames cannot offer the ductility inherent in monolithic construction because of a lack of continuity in the joints. There is no evidence to support this argument, as a routine inspection of joint details, specifications and modern construction practice would show. To support the use of precast frame systems, the following is a summary of some of the experimental work carried out to test the integrity of precast connections and components

Various attempts to quantify the floor membrane forces present in precast catenary systems have been made by Regan [9.21], Burnett *et al.* [9.22, 9.23], Wilford at the UK Building Research Establishment (BRE) [9.24], Odgard [9.25] and Engström [9.5, 9.26]. In all cases the focus of attention has been on the development of a catenary system using hollow-core floor slabs without structural toppings. This is the worst possible scenario, since systems with toppings will perform better. The objectives were to show (or not, as the case might be) that short lengths of tie steel (either rebar or helical strand) embedded in the ends of the precast slabs would satisfy the new state of equilibrium shown in Figure 9.22, for example, without collapse.

The most appropriate work to the skeletal structure is by Burnett [9.22]. Full-scale experimental testing consisted of hollow-core slabs tied across their supports using short lengths of 7-wire helical strand in the longitudinal joints between adjacent units. Although it was not possible to achieve the new state of equilibrium, it was possible to achieve catenary action at loads of up to 80 per cent of the slab failure load, which suggested that by using continuous strand or increasing the anchorage length, and/or the amount of continuity reinforcement, full catenary action should be achieved. Failure at the centre joint was either by concrete splitting forces above the tie steel or by rupture in the ties, and at the outer joints by hogging bending cracks in the tops of the hollow-core slabs.

Tests carried out at the BRE [9.23] on precast floors and beams found that by the correct disposition of continuity reinforcement over a missing support, deformations up to 20 per cent of the adjacent single span could be achieved without collapse occurring. In some tests, failure occurred when reinforcement broke out through the soffit of the precast units, rather than in the *in situ* joints. It is debatable whether that is good or bad news.

Engström [9.5] has studied ductility of tie connections in precast floors, and rotation mechanisms in cantilevering wall frames. This is in fact an inverse catenary system, where the outside support is removed and hogging moments and tie forces develop in the top of the floor plate. The situation is particularly critical in the 'long floor' frame layout, where there are no transverse beams (Figure 1.36(a)) and the cantilevering floor system becomes the primary structural element.

The hollow-core specimens were tested as shown in Figures 9.37 and 9.38, which would effectively simulate the catenary action at point X in Figure 9.16(b). The tie steel consisted either of grade S400

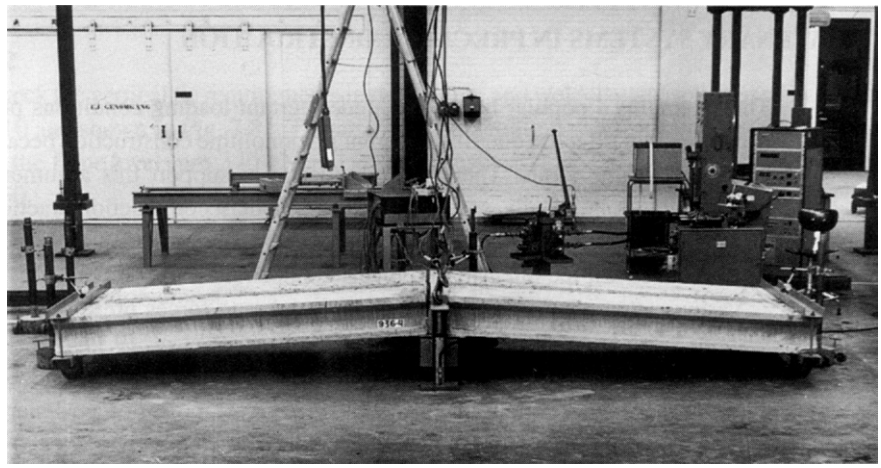

Figure 9.37 Arrangement of slab continuity tests by Engström [9.5].

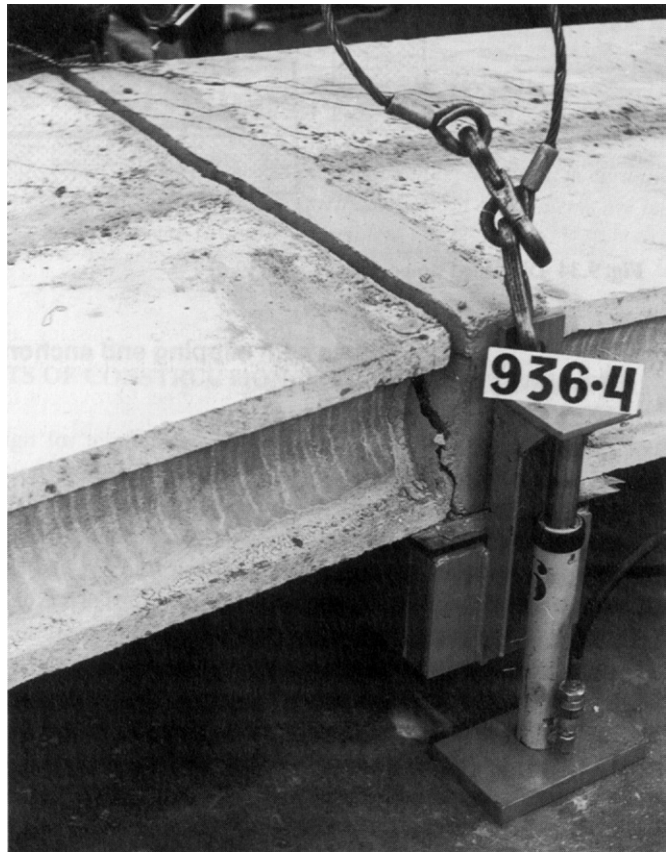

Figure 9.38 Initial cracking at precast hollow-core-to-*in situ* infill [9.5].

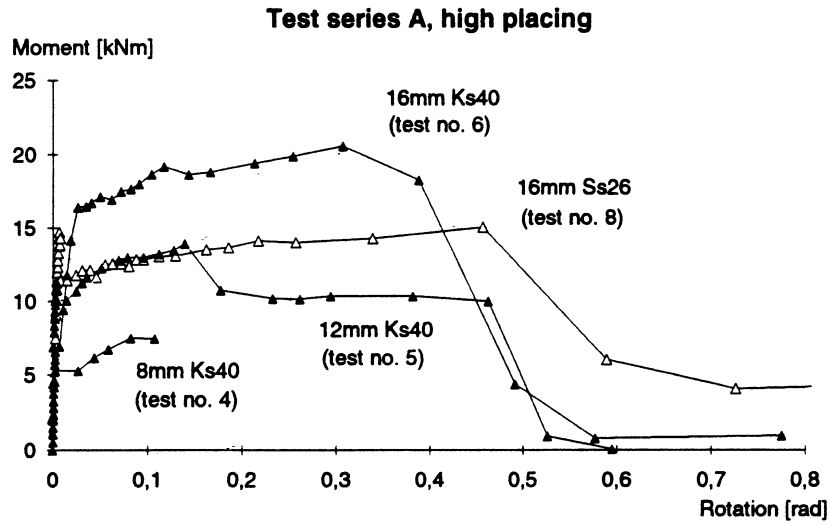

Figure 9.39 Moment versus rotation data from Engström's slab tests [9.5].

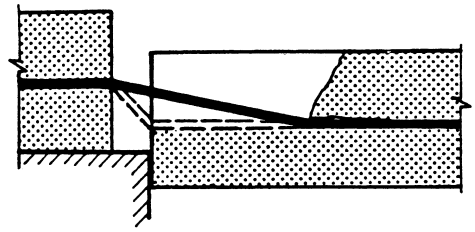

Figure 9.40 Displaced support mechanism [9.5].

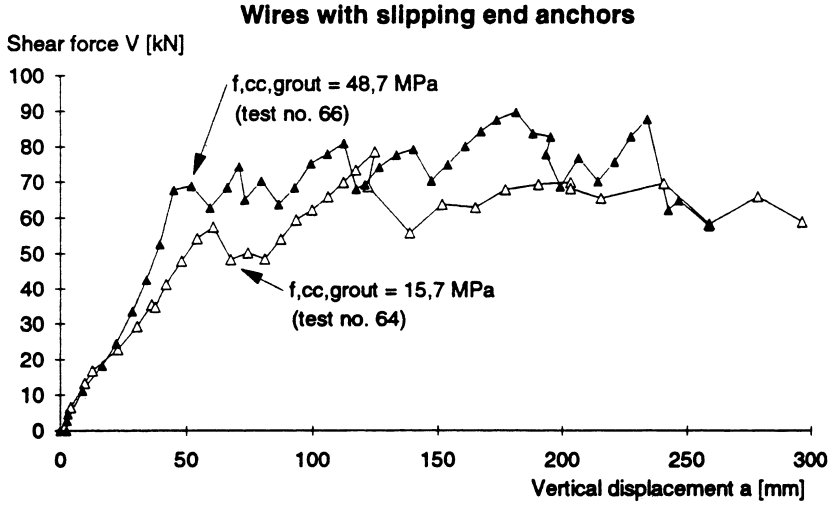

Figure 9.41 Shear force versus vertical deflection in Engström's tests [9.5].

high-tensile bar, grade S260 mild steel bar, or grade S1690 prestressing wire. The *in situ* concrete cube strengths varied from 24.6 to 33.3 N/mm^2. As expected, initial failures occurred abruptly owing to flexural tension failure in the interface between the precast slab and *in situ* infill, after which the slabs were connected by the tie steel alone. The important result, shown in Figure 9.39, is that the full tensile capacities of the bars were mobilised when the rotation of the slabs (given by Φ in Figure 9.39) was at least 0.1 to 0.2 radians. Generally, ultimate failure occurred at $\Phi > 0.3$ radians and the forces in the continuity bars were at least 60.5 kN per T12 bar (grade 460). This is equal to the upper limit of 60 kN for stability ties, Eq. (9.4).

Thus the tests show that adequate tensile forces can be mobilised in the tie steel without other modes of failure occurring first.

Engström also tested the behaviour of hollow-core floor slabs displaced off their bearings by the large sideways movement of roller supports; see Figure 9.40. High-tensile bar and prestressing wires were cast into the top opened cores of the slabs and, when the slabs were displaced from their bearings, the failure mode was by top-splitting of the concrete above the tie steel, as shown in Figure 9.8. The prestressing wires (two 6 mm-diameter per core) generated tie forces of 63 kN, i.e. two-thirds of the uniaxial yield strength, before splitting occurred. The vertical shear force versus displacement behaviour is shown in Figure 9.41, where maximum vertical displacements of 250 mm were possible. See also Figure 9.8. The minimum force for the high-tensile steel was 151 kN for one T16 bar (grade 460), i.e. 1.5 times the characteristic yield strength.

The conclusions from this work, which are relevant to the design of stability floor ties in accordance with BS 8110, is that providing that the tie steel is anchored 750 mm into the hollow cores and is correctly positioned with at least 30 mm top cover, the steel will generate tie forces greater than 60 kN before failure occurs by splitting of cover concrete.

CHAPTER 10

Site Practice and Temporary Stability

Temporary stability is an important part of design. This chapter explains that in certain situations the design of the frame is affected by the construction method. Certain components are more critical in the temporary condition than when the structure is complete.

10.1 The Effects of Construction Techniques on Design

The design for temporary stability, lifting of precast concrete components and site construction methods are an integral part of the overall design procedure. Careful instructions must be relayed from the design office to the site regarding the sequence of erection and, conversely, the design engineer should be aware of the contractor's chosen method of construction. In the majority of cases, precast design engineers are seconded to site to learn of the construction methods and see for themselves the practical methods of frame erection. This exchange of personnel and information, and the permanency of site-fixing gangs in the precast industry, are two of the major factors contributing towards the successful completion of structurally sound and undamaged frames.

The Construction (Design And Management) (CDM) health and safety regulations [10.1] mean that for each contract a single project coordinator will now be appointed, who is responsible for obtaining agreement from all parties on all safety issues, including the resolution of any conflicts between the construction contributors' working practices and methods. This is an important improvement in the operation of the construction industry in general, and particularly to more efficient construction sectors such as the precast frame sector, where there is increasing use of specialist designers, specialist construction teams, or specialist 'design and build' organisations. The project coordinator must approve staged or zoned handover between the main contractor, who will usually undertake groundworks and foundations, and the frame design and erection team, and subsequent handovers to the following trades. This formalises the best of safety practice. The regulations demand clear statements from those responsible for each part of the process and there will be:

(1) a designer's Method Statement, giving stability principles adopted, design standards used for components, and assumed construction sequence as it affects the design
(2) a producer's Statement of Compliance, with production legislation and with the designer's specification
(3) a contractor's Method Statement for the safe erection of the structural components, including such things as crane types, capacities and positions, sequence of construction, prerequisites for stability before erection progresses, etc.

Multi-storey Precast Concrete Framed Structures, Second Edition. Kim S. Elliott and Colin K. Jolly.

(4) a written statement of health and safety policy, with appropriate induction training for everyone entering the site.

It is because there is so much interaction between the first and third of these essentials, if the building is to be constructed efficiently and economically, that specialist design and construct organisations have developed. However, the legislation does not specify use of a single supplier or different suppliers for each responsibility; it merely enforces documented coordination of the process. Some clients will prefer a particular precaster's details and will use that precaster's in-house design team; others will prefer to adopt an independent designer (particularly if the building is part of a larger project or there is architectural input) who will obtain competitive tenders from precasters for the components. Some precasters prefer not to be directly involved with foundation work or site construction and will subcontract those parts of the process anyway.

All accredited precast frame producers will supply written statements of the principles of site erection, methods of making structural joints, and materials specifications. These are in general accordance with the requirements of BS EN 1992-1-1, clauses 9, 10 and 12 [10.2] {BS 8110, Part 1, clauses 5.3, 6.11.3 and 6.14 [10.3]} with regard to:

(a) critical jointing details, materials and methods
(b) critical dimensions, allowing for manufacturing and site tolerances
(c) temporary propping or fixings
(d) rules for advancing the construction ahead of completed and maturing sections of the building.

What is not always clear to the outside observer is where and how these criteria are met in the design, and the logic behind many of the decisions taken by precast designers is not always obvious. The two main aspects involved in the design for the temporary condition are:

- individual frame components and joints
- overall frame stability.

Checks are made to ensure that the young precast concrete components are handled correctly, both in the factory and on site, to prevent cracking, spalling and premature debonding, etc. This is particularly important in components such as plain stocky walls or lightly loaded columns, where the serviceability requirements for reinforcement are small, or near the sharp corners at openings where stress concentrations gather. In these situations additional reinforcement is provided to satisfy lifting and pitching criteria and, because the steel is not always designed according to the usual codes but is often according to previously tested configurations, these details may seem strange to the unaccustomed eye.

The components must be capable of supporting their own weight, often within 18 to 24 hours of production. Unlike cast-*in situ* concrete units, which only ever resist forces in the intended directions, precast components must also be designed to resist stresses of the types that are only possible during handling, pitching and the construction stage. These may occur within five days of casting. For example, the long, narrow spandrel beam of the type shown in Figure 3.35 will be lifted from the mould, and may even be delivered to site in a flat, horizontal manner with the weaker axis in the plane of bending, as shown in Figure 10.1. The handling reinforcement is provided in the front face of the beam, some of which will inevitably lie close to the neutral axis of the beam when it is in the upright position. Thus reinforcement is provided solely for the purpose of lifting.

Once positioned within the structure, the spandrel beam may require some temporary lateral or torsional bracing to prevent cracking while the flooring is being laid. Because the element may be subjected to horizontal wind loading before the flooring is fully tied to the beam, the element would have to be designed to resist the wind load by flexure about the weak axis. Horizontal shear forces

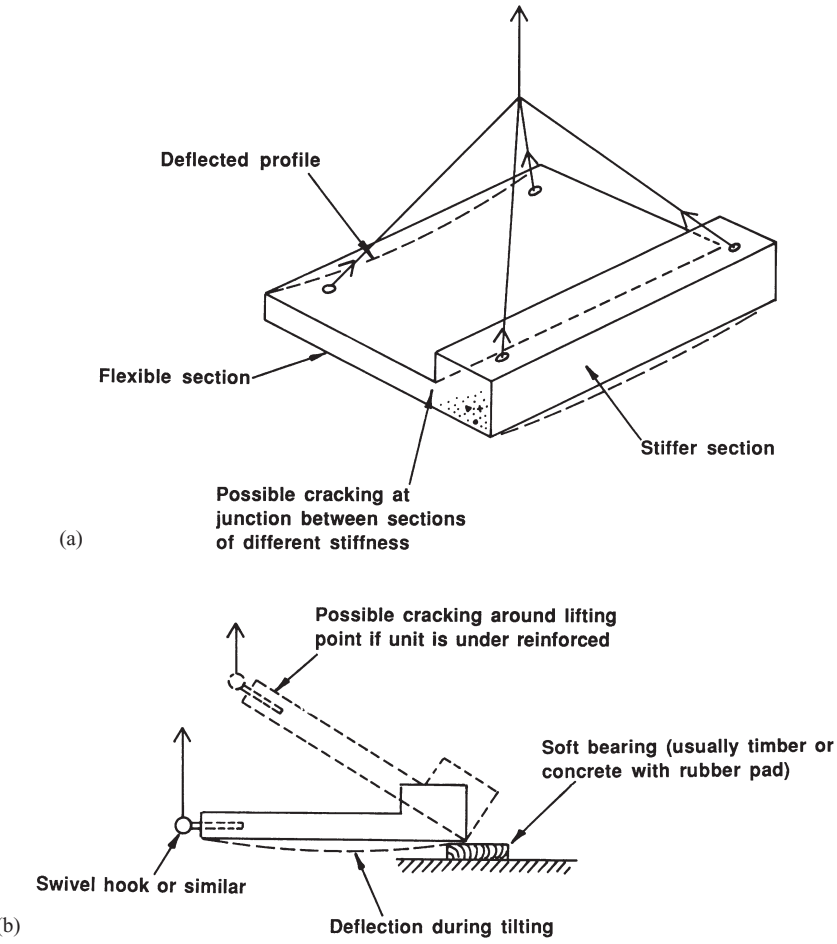

Figure 10.1 Flat handling of deep and narrow spandrel beams.

must be resisted by the end connectors, which means that certain types of beam-to-column connector are not suitable for this situation.

The second most important issue is that load paths through the partially completed structure may be different from those in the final form. An example is where floor slabs are placed on one side only of an internal beam, as shown in Figure 10.2. The connection is checked to resist the torsion and, if found to be inadequate, props are placed to prevent the beam rotations from damaging the connector. A more extensive discussion on this subject is given in the following sections.

Practical connection design is a very important aspect, and some examples of impractical connections were shown in Figure 7.4. Although there are a large number of connectors that may be used successfully in one situation but unsuccessfully in another, there are a number of basic 'rules' that lead to practical design and that in turn affect the design of the structure:

- Components should have a sufficiently wide bearing to assist the site operatives in positioning the component without excessive barring (levering into position). The seating area should be designed with tolerances and not, as shown in Figure 10.3, with a captive groove or restricted position.

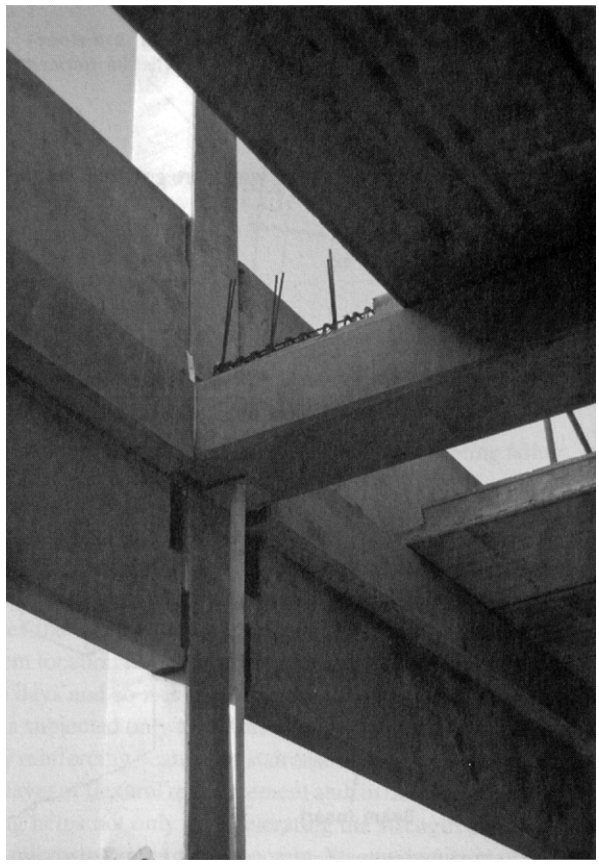

Figure 10.2 Non-symmetrical loading of slabs on beams.

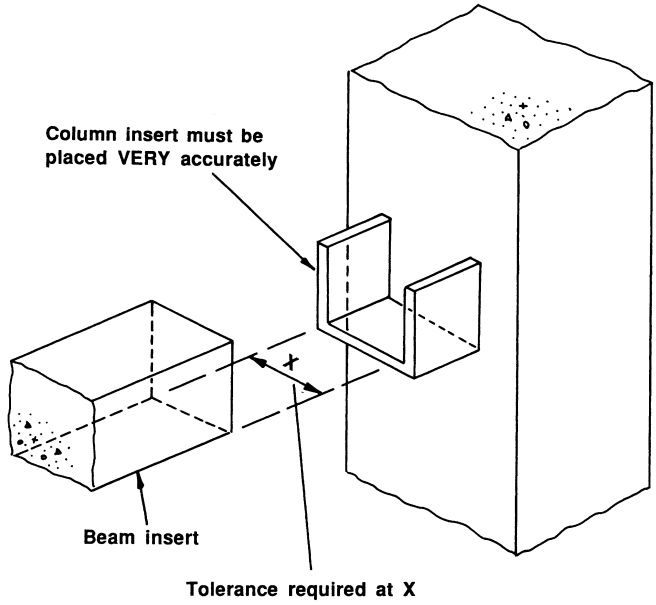

Figure 10.3 Restricted fixings.

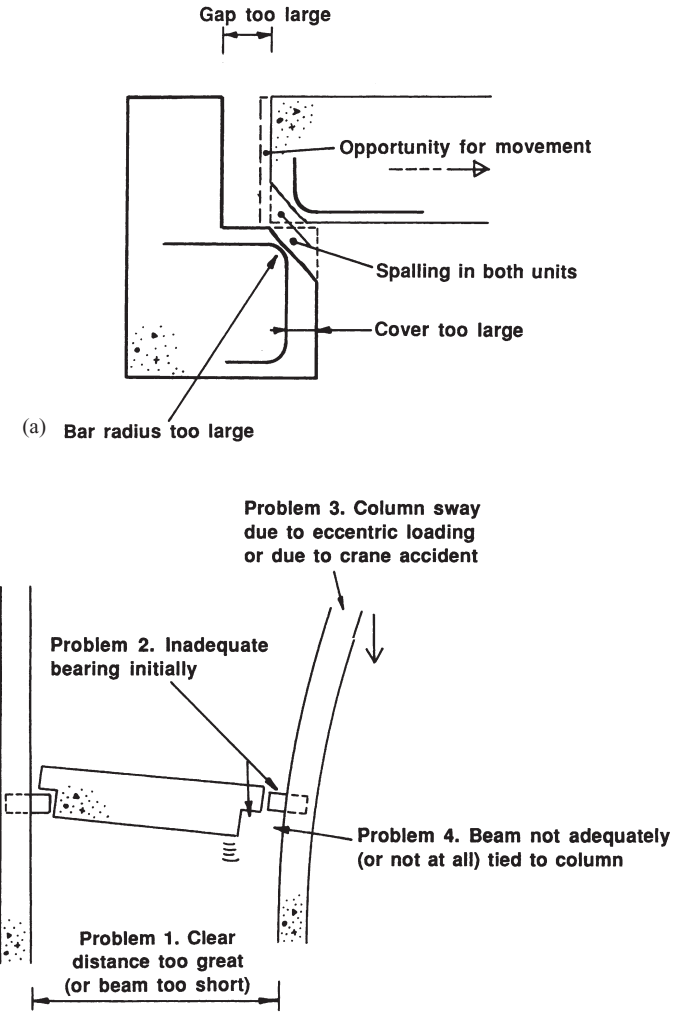

Figure 10.4 Problems due to inadequate precautions against bearing failure. (a) At slab-to-beam bearings and (b) at beam-to-coluumn connections.

- The seating should be designed so that the impact resistance associated with setting of precast units is at least twice the self-weight W of the unit. This figure should be increased to $3W$ in the case of large, two-dimensional units where the setting-down forces are not equally distributed between all fixing points.
- The seating capacity of temporary bearings, or extended bearings, should be similarly designed so that the cumulative effects of tolerances, shrinkage and movement resulting from accidental construction damage (e.g. crane impact causing a column to flex) do not cause failure of the seating as shown in Figures 10.4(a) and (b).
- Allow tolerance to at least one end of an element, and avoid captive dimensions that may cause a lack of fit in the connection.
- Avoid designing components or connections that rely on accumulative dimensions without tolerances in each individual element, e.g. shim allowance for vertical wall panels, or the layout of 1197 mm-wide hollow-core floor slabs for a 1200 mm modular dimension.

10.2 Designing for Pitching and Lifting

10.2.1 Early lifting strengths

Concrete strengths in a precasting works are governed by the 12- to 24-hour strength. This is usually between 20 and 25 N/mm^2 for reinforced components and about 40 N/mm^2 for prestressed concrete – values that enable the units to be lifted from the casting zone and moved to a more convenient stockyard for them to mature, ready for delivery to site. The maturity period can be as little as four or five days and so it is important that the internal microstructure of the young concrete unit is subjected only to strains *well* below the tensile cracking limit. This may involve doubly reinforcing beams and staircase units, which would otherwise have only a single bottom layer of flexural reinforcement, and, in the case of beams, providing nominal top steel.

Steam curing helps not only in accelerating the strength gain, but gives also an improved homogeneous microstructure to the concrete. Steam-cured units may be lifted after eight hours in the case of dry-cast concrete, and twelve hours for wet-casting. The use of surface retarders or colour pigments is not detrimental to the early strength of components.

10.2.2 Lifting points

Lifting points are selected so that the flexural and shear reinforcements provided in service are, as far as possible, fully utilised in lifting. The lifting points are also chosen to minimise deflections. Bending moments and shear forces are calculated in the usual manner. They are based on a loading that includes 25 per cent mould suction plus a 25 per cent impact allowance. It may be necessary to increase this allowance to 50 per cent in the case of units in contact with large mould surface areas, such as wall panels, spandrel beams or cladding units. The sides of the mould should be lifted clear of the unit so that it leaves the mould in a vertical ascent.

Lifting points are usually at $\frac{1}{4}$ to $\frac{1}{6}$ of span from either end of the units, although this varies depending on the type of unit. Prestressed units are lifted closer to the ends than reinforced units. The optimum situation for equal sagging and bending moment is where the lifting point is at $0.208L$ from the ends of a unit length L. Thus $0.2L$ is used if reinforcement is symmetrical; see Figure 10.5(a). One or two guide ropes are attached for the ground crew to control the suspended unit and manoeuvre it swiftly into position (Figure 10.5(b)).

Floor slab units, staircases, landings and flat wall units greater than about 750 mm wide require four-point lifting. Theoretically it should be possible to lift these units from two points, but any imbalance becomes more critical in wider units with higher centroidal positions. Very long columns and beams (approximately >13 m) of slender section (length/depth > 50 to 55) may also require four-point bending, because of unacceptable flexure stresses and deflections in a two-point lift. Spreader beams are used as shown in Figure 10.6(b) to keep the lateral force as small as possible. The line of the crane hook must coincide with the gravitational centroid of the unit. Temporary bracing across narrow legs or upstands in U- or L-shaped sections may be a more suitable alternative to excessive reinforcement or thicker sections, as shown in Figure 10.6(a).

Ductile reinforcement (for lifting hooks) is designed using service (not ultimate) stresses of roughly $0.6\,f_y$, together with an ultimate load factor of 1.35 {1.4} exclusive of the above suction and impact allowances. Round bar with ends deformed around component reinforcement is preferable to ribbed bars, to avoid potential overhead judder if the crane hook slips past a rib. For comparison, *The Chain Tester's Handbook* [10.4] suggests a factor of safety of 2.0 on steel design stresses, i.e. $0.87\,f_y/2 = 0.43\,f_y$, giving approximately the same result. Additional reinforcement may be required around the lifting points to prevent cracking due to radial bond stresses. This is particularly critical near corners where the cover distance to the lifting point is less than 50 mm. Small links (typically R6 or R8) are positioned to resist a lateral force equal to $0.2 \times$ lifting reaction.

Lifting loops and sockets are used to raise a unit through 90° to the vertical (or to turn a unit for finishing work). Not only is the socket fully anchored in the unit, but the concrete directly above the

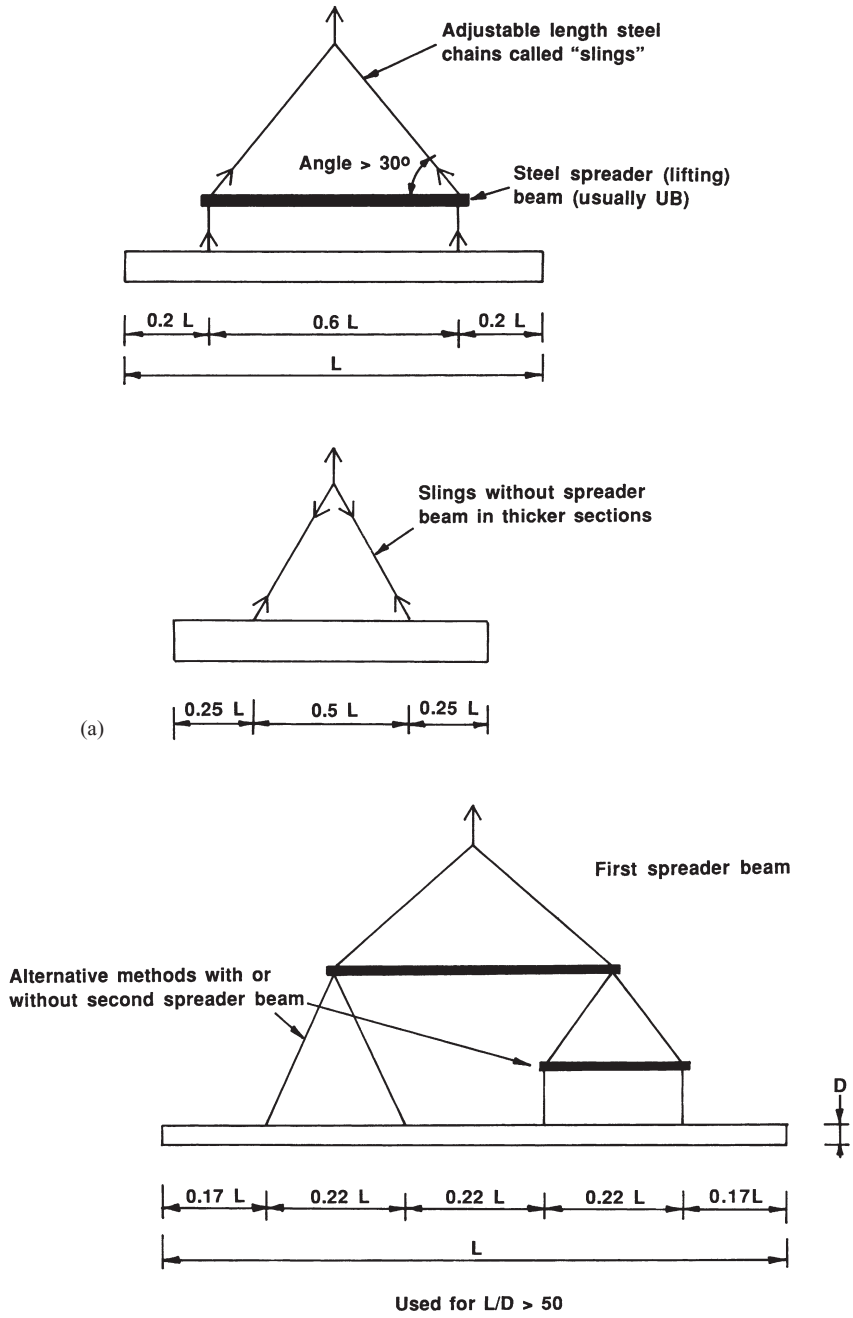

Figure 10.5 Flat handling of long components. (a) Two-point lifting positions and (b) four-point lifting positions.

socket in the flat lift position is reinforced to transfer the socket reaction into the body of the unit, as shown in Figure 10.7. A standard hook or bend may be used to reduce the anchorage length.

Most proprietary devices are designed to eliminate the need for additional steel (except when used for turning) by using a specially shaped shaft (e.g. conical, or bulbous), which produces wedging forces around the shaft. These help to confine the concrete radially, and reduce the need for additional

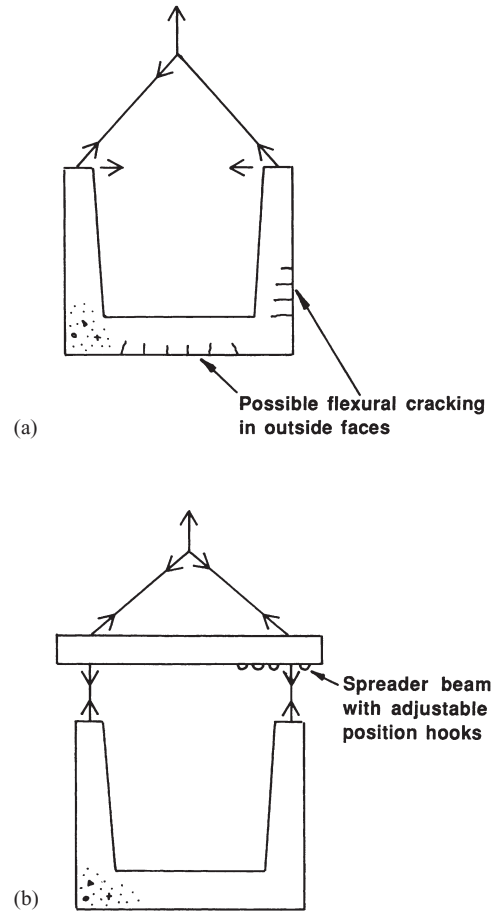

Figure 10.6 Handling methods in thin-walled components. (a) Incorrect procedure for lifting units and (b) correct procedure using a lifting beam.

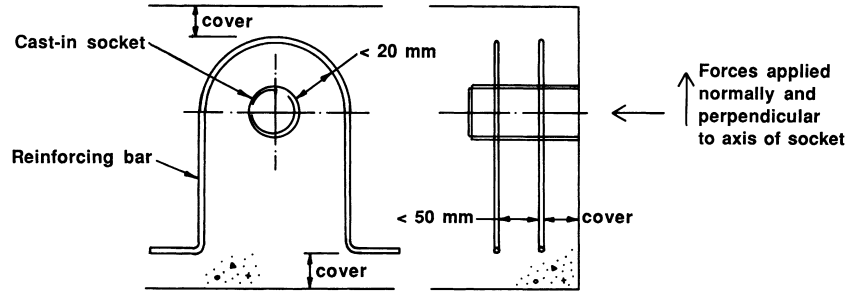

Figure 10.7 Hanger reinforcement around lifting holes or sockets.

confinement steel around the shaft. Figure 10.8 shows some of the more common types of swivel device.

Most precast components are delivered to site horizontally (although some large wall units greater than 2.5 m wide are dispatched close to vertical on A-frames). Columns are lifted to the vertical using a pitching point, usually at 0.3 times the height (L) of the column from the top (Figure 10.9). The

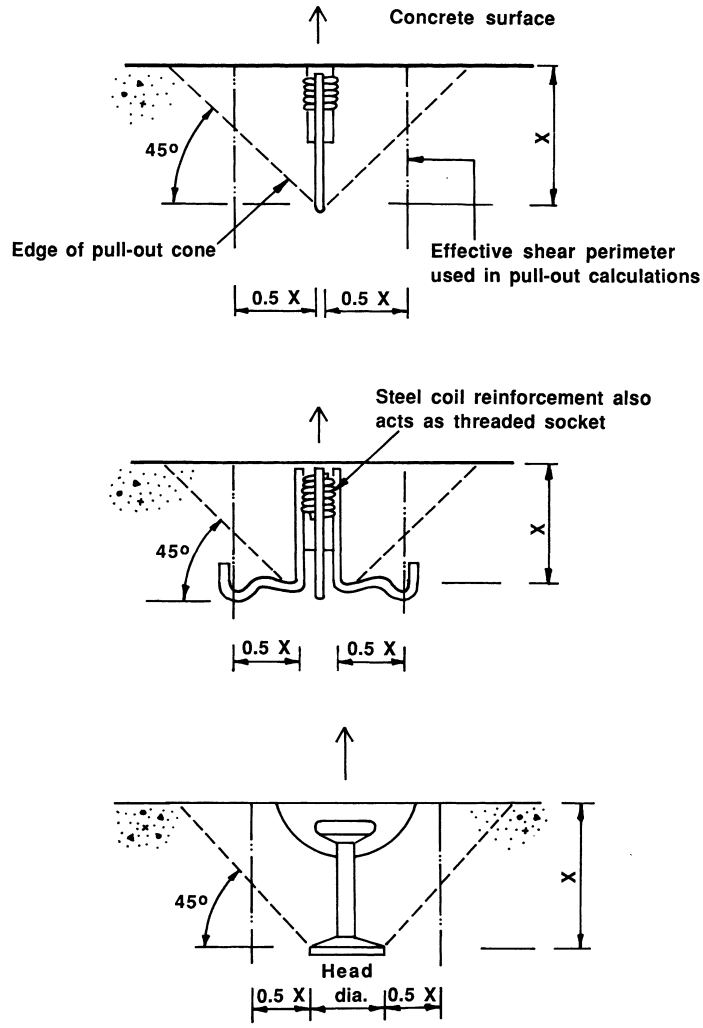

Figure 10.8 Types of lifting devices.

maximum reaction in the crane's chains is 0.72 wL, where w is the self-weight per unit length plus 25 per cent impact allowance. The maximum bending moment is 0.045 wL^2. Dual-pitching using sliding chains may be used for very long columns, say >15 m, as shown in Figure 10.10. The pitching points are placed at 0.16L and 0.60L from the top end of the column and the maximum bending moment is then 0.013 wL^2, i.e. a threefold reduction in moment compared to a single pitch point.

It is important that the pitching point is located at the centre of gravity of columns, to avoid tilting during the fixing operation. Although this has virtually no implication for the design of columns, verticality during placement ensures that all the reinforcement provided for the temporary condition is equally stressed, e.g. anti-bursting bars at the foot of the column.

The age at which most columns are pitched (7 to 14 days) has enabled the concrete to mature to its design strength, and in many cases more than that. This is particularly important if the unit has architectural finishes attached that are providing additional load. Using a single pitching point, the maximum vertical deflection in a 12 m long, 300 × 300 mm column is about 10 mm. Maximum tensile strains are less than the tensile cracking strain for grade C40/50 concrete. Columns 25 m long have been pitched using two points only, but these I-section columns were axially prestressed to permit that.

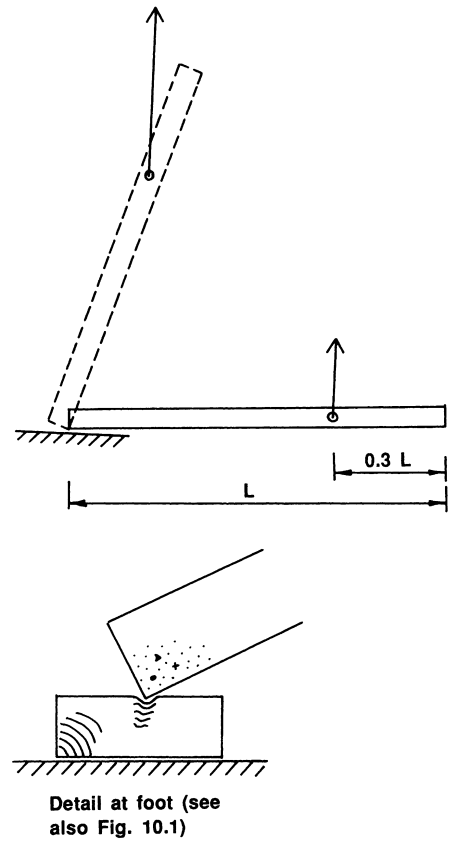

Figure 10.9 Single point pitching.

Walls and flat panels are pitched from the top. The maximum bending moment is 0.125 wL^2, where w is the self-weight per unit length plus 25 per cent impact allowance, and this may lead to the most onerous design situation. Lifting points are carefully located vertically over the centre of gravity of the unit, although that can prove impossible in some units. It is occasionally desirable to allow the unit to tilt slightly (no more than about 5°) inwards at the top or bottom to assist in the fixing. Special lifting devices have evolved to ensure that the concrete is not damaged during the pitching operation.

Hollow-core floor slabs are treated as a special case, because the manufacturing process by extrusion or slip-forming does not usually facilitate lifting hooks or pins, although some manufacturers have now automated this process immediately after casting. The alternative is to dig a short slot by hand, insert a hook or pin, and backfill using flowing concrete (self-compacting may be used), as shown in Figure 10.11. Compliance testing is according to BS 5808, with the distance from the edge of the hook/pin to the edge of the supports to the reaction frame equal to twice the embedment depth. Vertical static loads are used to fail the assembly either by (i) fracture of the hook or pin, (ii) shear cone failure (usually around the pin), or (iii) localised tension combined with shear around hooks or pins. The proof load for the assembly is based on a factor of safety (FoS) of 3.0 for the strength of the hook/pin, and 2.5 on the strength of concrete. A factor of 1.3 is applied to represent the snatch effect of the crane, and together with an allowance for the angle of the lifting chains approaching 45° (1/sin45° = 1.414), the safe working load for each hook/pin may be calculated, knowing the mass of the slabs. The proof load = 1.25 × SWL. Under test, the failure load cannot be greater than the uniaxial strength of the hook/pin, typically 510–530 N/mm^2. However, the embedment is so optimally designed that modes of failure may be concrete failure at a load greater than the uniaxial strength. Figures 10.12

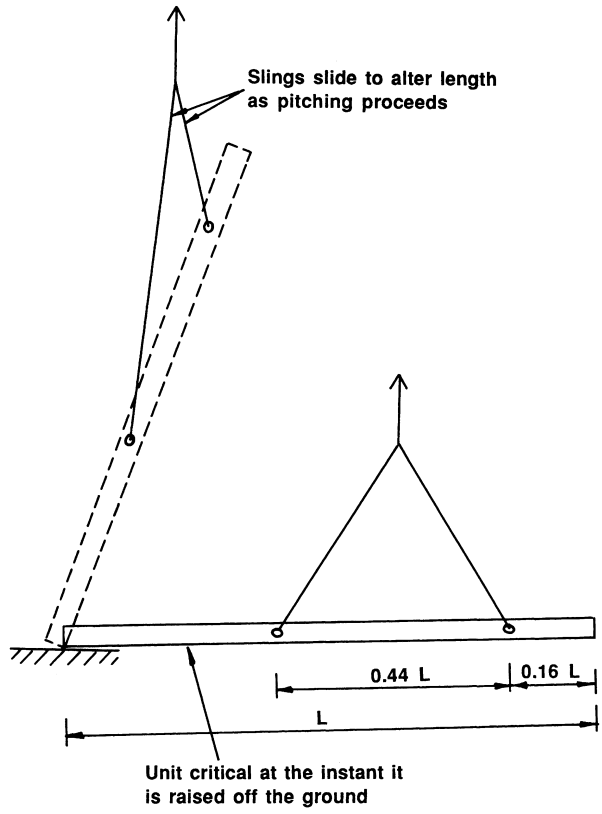

Figure 10.10 Double point pitching.

Figure 10.11 Lifting hooks cast locally into the cores of hollow-core units.

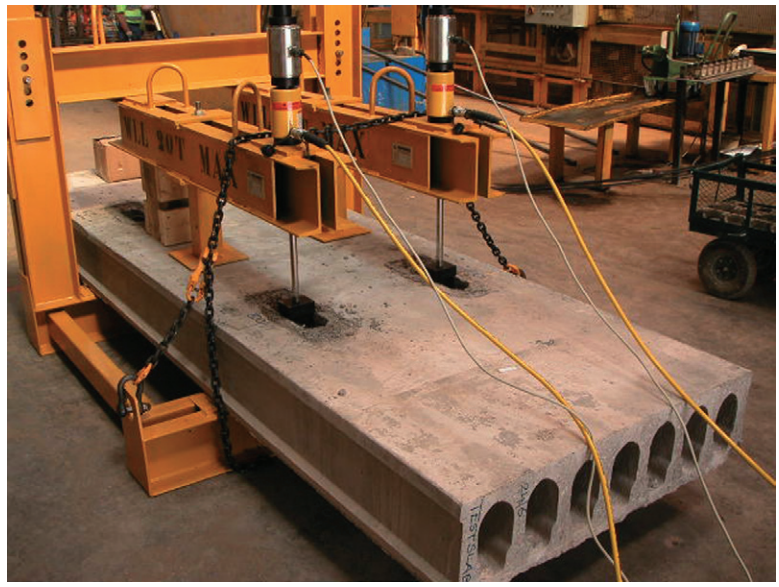

Figure 10.12 Testing arrangement for the simultaneous testing of a pair of lifting hooks (courtesy of Bison Manufacturing, UK).

Figure 10.13 Failure planes around a lifting hook in a 300 mm-deep hollow-core unit at a failure load of 143 kN per hook represent a factor of safety of 3.2 over the proof load, and a total factor of 9.6 assuming one leg of the slings is not fully engaged (courtesy of Bison Manufacturing, UK).

to 10.15 show examples of the results of load tests, and the different failure modes. In Figure 10.15, a 190 mm-diameter failure cone fails at a direct tensile stress of 69 per cent greater than f_{ctd} $\{3.25\ \text{N/mm}^2 = 0.42\sqrt{f_{cu}}$ (grade C60 cube strength concrete), 74 per cent greater than the design value in BS 8110$\}$. Overall, FoSs per hook/pin range from 3 to 7, depending on depth and mass of the slab. The practice in the UK is to use four lifters per unit, together with safety chains, but in some European countries only two are used.

(a) (b)

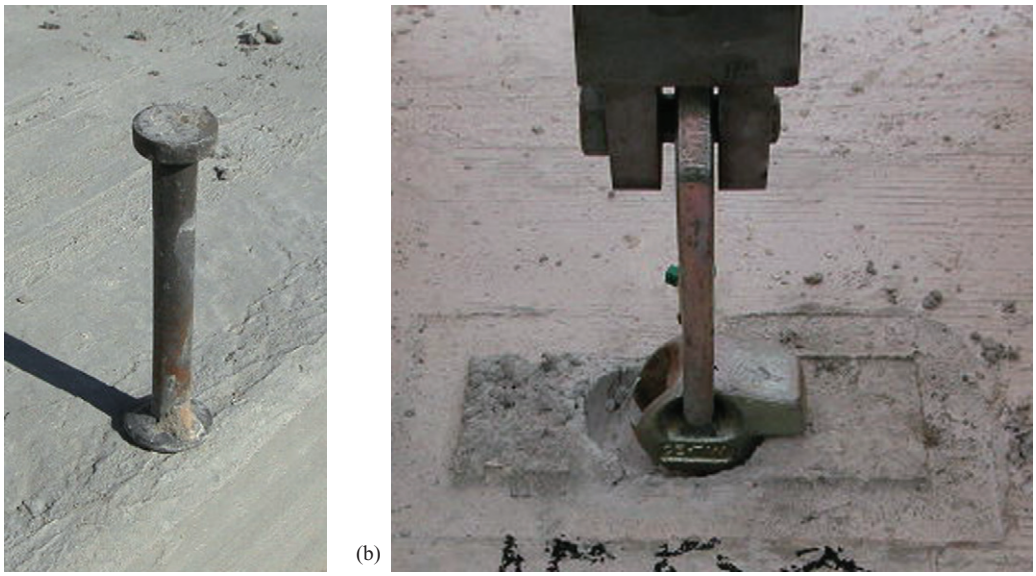

Figure 10.14 (a) Lifting pin, (b) clutch used to apply rapid vertical pull-out forces (courtesy of Bison Manufacturing, UK).

Figure 10.15 Cone failure at 92 kN load represents a factor of safety over the proof load of 4.6 (courtesy of Bison Manufacturing, UK).

Prestressing cambers (caused by negative moments) must be considered when the lifting points are not close to the ends, within about 400 mm from the ends of the unit. The design of these slabs is governed only by handling when the length is greater than the cut-off points shown in Figure 5.2.

Slabs are hoisted on site either by using slings or chains (Figure 10.16), lifting hooks/pins, or specially designed clamps (Figures 10.17(a) and (b)). The unit should be level during lifting so that an even contact is made with the supporting member. When slings or chains are used, the horizontal

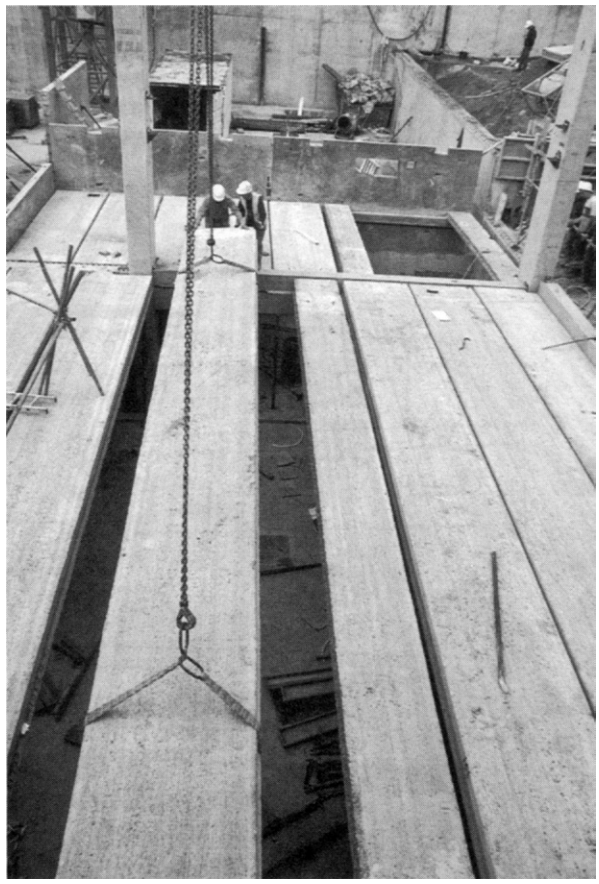

Figure 10.16 Hoisting 15 m long hollow-core floor units.

(a)

Figure 10.17(a) 'Scissors' clamps used for lifting hollow-core floor units both on site and in the factory some 16 hours after casting (courtesy of Spiroll Precast Services Ltd, UK).

(b)

Figure 10.17(b) Spiroll's 'Slablock' clamps used for hoisting hollow-core floor units (courtesy of Spiroll Precast Services Ltd, UK).

component of the reaction at the top of the unit creates a transverse bending moment in the unit. The tendency is for the force to try to collapse or to 'fold' the unit, as shown in Figure 10.18(a). Although the design of the unit is such that this does not happen, if large areas of the slab have been removed (Figure 10.18(b)) – e.g. to accept site-placed top steel at a cantilever – the problem may arise. Preventive measures include leaving small bridges of unbroken slab between the slots, usually 100 mm long at about 400 mm centres, or placing a temporary strut (acting as a spreader beam) across the chains to resist the horizontal forces.

Double-tee units are hoisted using four lifting points, in pairs over the line of the webs (Figure 10.19). Reinforcement details at these points may be obtained from the manufacturer, but typically comprise a large, inverted U- or V-shape of high-tensile reinforcement or helical strands embedded to the bottom of the web. Small bars are placed horizontally across the top of the lifting hook to prevent splitting cracks. Spreader beams are used on units of length greater than about 15 m, to prevent the horizontal component of the force in the low-inclination chains from causing splitting stresses in front of the lifting hook. Ideally the inclination of the chains should not be less than about $\theta = 35°$ to the horizontal. Low inclinations of θ also lead to greater forces in the chains themselves, given by $V/\cos\theta$, where V is the self-weight reaction at that point.

Precast planks are hoisted at four points, but the lifting criterion is not usually critical because the planks are used in relatively short lengths compared with other types of flooring.

Staircase units require two sets of chains for site fixing, one fixed and one adjustable, in order to maintain the correct inclination, as shown in Figure 10.20. The site lifting criterion is less onerous than at the factory because the same lifting points are used in both situations. This is because the unit must be seated level simultaneously at both ends to avoid the inclined edges from digging into the bearing ledge and causing horizontal frictional forces between the members. Three lifting points are used, two at the bottom of the flight and one at the top.

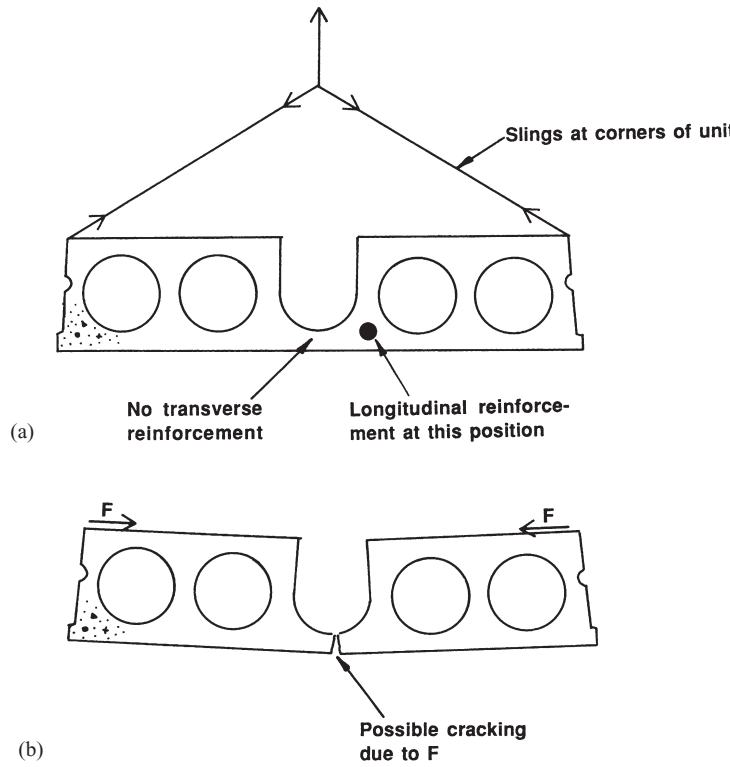

Figure 10.18 Problems encountered in lifting where top flanges are removed from hollow-core units.

Figure 10.19 Hoisting double-tee units (courtesy of Ergon, Belgium).

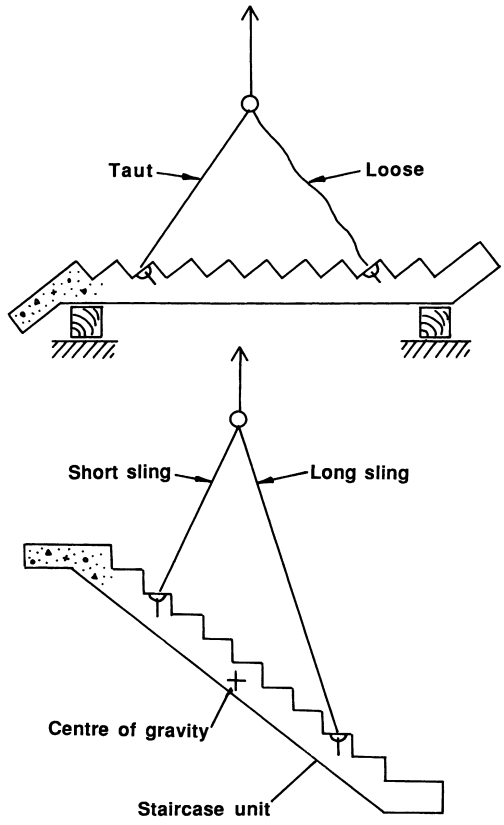

Figure 10.20 Adjustable lifting slings on inclined units such as stair flights.

Exercise 10.1

Check the lifting requirement for a 12 m long × 300 mm square column containing four H20 bars, which is lifted from the mould using only two points. When lifted the concrete strength is equivalent to grade C12/15, and the unit contains high-tensile reinforcement with 30 mm cover to 8 mm-diameter links.

Solution
Lifting points to be at 1/5 points = 2.40 m from ends.

Self-weight = $0.3 \times 0.3 \times 25$	= 2.25 kN/m	Self-weight = $0.3 \times 0.3 \times 24$	= 2.16 kN/m
Allow 1.5 for suction and impact	= 3.38 kN/m	Allow 1.5 for suction and impact	= 3.24 kN/m
Ultimate Moment		Ultimate Moment	
$M = 1.4 \times 2.7 \times 2.40^2 / 2$	= 13.12 kNm	$M = 1.4 \times 3.24 \times 2.40^2/2$	= 13.06 kNm
Shear $V = 1.4 \times 2.7 \times 2.4$	= 10.94 kN	Shear $V = 1.4 \times 2.7 \times 2.4$	= 10.89 kN
		$d = 300 - 30 - 8 -$ say $10 = 252$ mm	

(*Continued*)

$K = \dfrac{13.12\times10^6}{300\times300\times12}$ = 0.0622

$z = 252\times\left(0.5+\sqrt{0.25-0.882\times0.0622}\right)$ = 227.9mm

$A_s = \dfrac{13.12\times10^6}{227.9\times500}$ =115 mm^2

< 628 mm^2 provided; thus lifting is not critical. Shear stress

$V_{Rdc} = \left(0.12\times\left(1+\sqrt{\dfrac{200}{242}}\right)\times\left(\dfrac{100\times624}{300\times242}\right)^{1/3}\right)$

$\times\dfrac{300\times242}{1000}$ = 36.2 kN

> 10.94 kN

$K = \dfrac{13.06\times10^6}{300\times300\times15}$ = 0.0496

$z = 252\times$

$\min\left(\left(0.5+\sqrt{0.25-\dfrac{0.0496}{0.9}}\right);0.95\right)$ = 227.8mm

$A_s = \dfrac{13.06\times10^6}{227.8\times500}$ = 115 mm^2

< 628 mm^2 provided; thus lifting is not critical. Shear stress

$v = \dfrac{10.89\times10^3}{300\times227.8}$ = 0.15 N/mm^2

v_c = 0.72 N/mm^2 > 0.15 N/mm^2

Therefore the lifting condition is not critical.

Exercise 10.2

Design the lifting reinforcement for a 600 mm-deep double-tee slab weighing 12 tonnes, assuming that the angle of the four lifting chains is 60° to the horizontal. Allow 50% suction allowance at the mould and a factor of safety of 2 to the strength of the lifting hooks. Use high-tensile reinforcement $f_y = f_{yk}$ = 500 N/mm^2, and grade C25/30 equivalent concrete at the initial lifting. Assume cover to the bottom of the lifting hook = 50 mm.

Solution

Referring to Figure 10.21, use V-shaped lifting bar with the inclined bar at 45° to the horizontal.

Weight of unit = 12 tonnes = 117.7 kN

Maximum chain tension = 117.7 × 1.5/4 sin 60° = 50.95 kN

Axial forces in each leg of hook (by resolution of forces) in the inclined leg 0.5 × 50.95/sin60° = 29.4 kN and in the vertical leg = 0.5 × 50.95/sin 75° = 26.4 kN

Service stress in bar = 250/1.35	= 185.2 N/mm^2
Shear area A of lift bar based on f_q = 0.6 × 111.1 in double shear	= 100 N/mm^2
A = 50.95 × 10^3/2 × 111.1	= 230 mm^2
Maximum tensile area A_s = 29.4 × 10^3/185.2	= 159 mm^2
Largest bar area required = 230 × FoS of 2	= 460 mm^2

Service stress in bar = 250/1.4	= 178.6 N/mm^2
Shear area A of lift bar based on f_q = 0.6 × 178.6 in double shear	= 107.1 N/mm^2
A = 50.95 × 10^3/2 × 107.1	= 238 mm^2
Maximum tensile area A_s = 29.4 × 10^3/178.6	= 165 mm^2
Largest bar area required = 238 × FoS of 2	= 476 mm^2

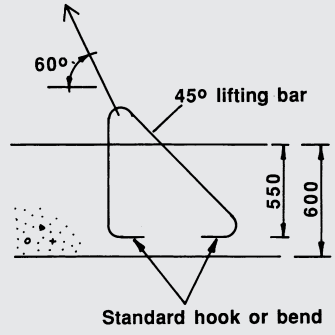

Figure 10.21 Details for Exercise 10.2.

Use one H32 bar (804 mm^2) to make anchorage easy.

Bond stress in grade C25/30 concrete
$f_{bs} = 2.25 \times 0.14 \times 25^{2/3}$ = 2.69 N/mm^2
Tensile anchorage bond length
$L_b = \max\left(\left(\frac{32}{4} \times \frac{250}{2.69} \times \frac{460}{804}\right); 10 \times 32; 100\right)$ = 424 mm
< (600 − 50) available depth = 550 mm
Bend bar if possible, so provide bob.

Tensile anchorage bond length in grade C25/30 concrete = 39 dia.
$L_b = 39 \times 32 \times 476/804$ = 739 mm
> (600 − 50) available depth = 550 mm
Bob provides an extra (12 − 4) × 32 = 256 mm
Hook provides an extra (24 − 4) × 32 = 640 mm
550 + 256 = 806 mm > 739 mm

Provide 550 mm anchorage plus standard bob.

10.2.3 Handling

Loading arrangements on delivery vehicles should be such that the components are not subjected to forces and stress that have not been catered for in the design. The components should be loaded evenly, so that the distribution of weight is uniform on each component. Components should have semi-soft (e.g. softwood) bearers placed along their length. Where components are stacked one above the other, the bearers should line over each other. The bearer should be large enough to keep the components vertically separated and strong enough to resist dynamic loads, so that the concrete components do not make contact with each other during transit.

When stacking units on the ground on site, the guidelines will be similar to the above. The ground should be firm, so that no differential settlement may take place and cause spurious forces and stress in the component (see Figure 10.22). Airbags may be used to avoid creating stress raisers during landing or turning of units. The height to which components may be stacked is about 1.5 m – the usual criterion is for an operative to be able to manually guide the crane-supported component while standing on firm ground. Figure 10.23 shows the possible result of not abiding by the rules!

The type of lifting equipment (crane, hoist, etc.) should be compatible with the geometry of the structure, weight and size of components, the nature of the ground, and site access. Consideration should be given to the maximum weight and radius of lift from the agreed area for lifting, so that the lifting equipment is able to lift and place the components smoothly, and without jerking, from suitably long chains.

Components that are to be inclined by pitching should be first placed on firm ground, and then pitched in a separate operation (Figure 10.9). A special shoe (steel, concrete or timber) may be required when pitching heavy and thin units, because it is not possible to reinforce the units for the very large point loads which develop on uneven surfaces. It is important that the point in contact with the ground does not slide or slew, which could disturb the stability of the lifting device and initiate a collapse.

Safety nets (Figure 10.24) or air bags (Figure 10.25) are installed for safety when erecting flooring units. A guard rail and toe board are immediately erected as fixing proceeds, as required by the UK Construction Health, Safety and Welfare Regulations 1996 and The Work at Height Regulation 2005.

10.2.4 Cracks

Small hairline cracks are sometimes seen near the lifting points of long, slender components, such as columns or beams. The decision as to whether these cracks are structurally detrimental in the final building must rest with the project designer, but the following may be taken as general guidance for cracks less than 0.3 mm wide:

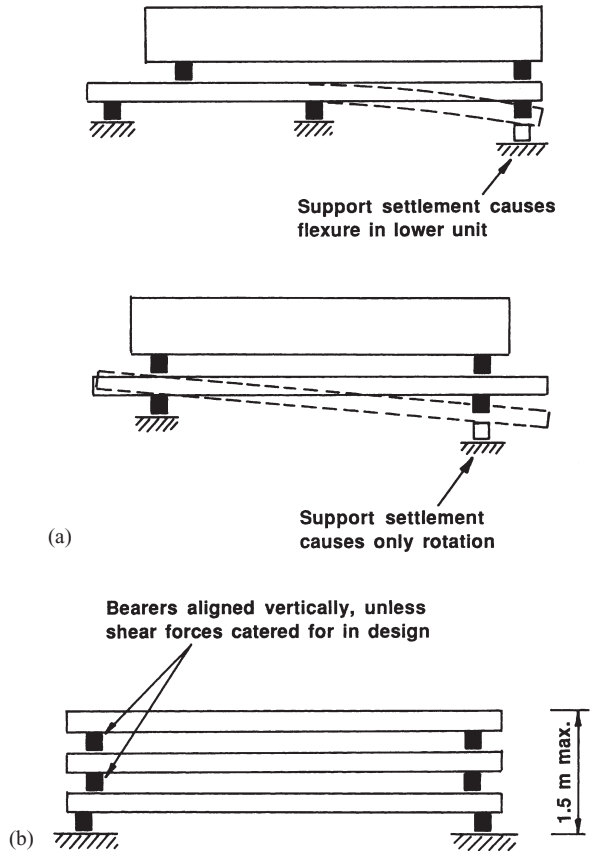

Figure 10.22 Difficulties in stacking units on soft ground.

Figure 10.23 Damaged prestressed slabs due to careless stacking.

Figure 10.24 Safety nets installed as one possible method of fall protection above heights of 2 m.

Figure 10.25 Safety air bag fall protection (courtesy of Beresford's Flooring Ltd).

(1) If the crack forms in a region that is permanently in compression: no action.
(2) If the crack closes completely to the naked eye when the unit is placed in its permanent location, which is not in an area of tension: no action.
(3) If the crack width is visible to the naked eye when the unit is placed in its permanent location, and is in an area of tension: measure the crack width using a graduated microscope before and after the construction of the components carried by the said unit. Then:
  (a) If the crack width does not increase: no action.
  (b) If the crack width increases but is no greater than 0.3 mm, check the serviceability limit state of deflection and crack widths based on the flexurally cracked section properties.
  (c) If the crack width increases to greater than 0.3 mm, refer to the designer to check both the serviceability calculations and the durability conditions. If necessary carry out structural repairs to the crack, but if that is not acceptable then consider replacing the unit or carrying out load testing to determine its flexural stiffness. Ultrasonic pulse velocity testing may be used to search for internal cracks in concrete, but the results must be treated with extreme caution if reinforcement is present between the measuring points.

Calculations to determine the onset of flexural cracking may be carried out by dividing the bending moment by the gross section modulus (ignoring the area of reinforcement if desired), and checking that this does not exceed about $1.3\times0.14f_{ck}'^{2/3}$ {$0.24\sqrt{f_{cu}'}$}. The lifting strength for precast units may normally be conservatively taken as grade C20/25. Hence the critical flexural cracking stress is about 1.35 N/mm^2 {1.2 N/mm^2}.

Crack widths may be determined from BS EN 1992-1-1, clause 7.3.4 [10.2] {BS 8110, Part 2, clause 3.8.3 [10.3]}, where, using the usual notation for serviceability calculations:

crack width, $w_k = s_{r,max}(\varepsilon_{sm} - \varepsilon_{cm})$ (10.1)
where, $s_{r,max} = 1.3(h - x)$ if the tension bar spacing $> 5\left(c + \dfrac{\phi}{2}\right)$, or

$s_{r,max} = 3.4c + 0.425k_1k_2\phi/\rho_{p,eff}$ (10.2)
with $k_1 = 0.8$ for deformed and 1.6 for plain bars and $k_2 = \dfrac{\varepsilon_1 + \varepsilon_2}{2\varepsilon_1}$ for the cracked section strains and $\varepsilon_1 > \varepsilon_2$

$$\varepsilon_{sm} - \varepsilon_{cm} = \frac{\sigma_s - 0.6\dfrac{f_{ct}}{\rho}(1 + m\rho)}{E_s} > \frac{0.6\sigma_s}{E_s}$$

$$\text{crack width} = \frac{3a_{cr}\varepsilon_m}{1 + 2\left(\dfrac{a_{cr} - c_{min}}{h - x}\right)} \quad (10.1)$$

$$\text{where } \varepsilon_m = \frac{M(a - x)}{E_cI_c} - \frac{b(h - x)(a' - x)}{3E_sA_s(d - x)} \quad (10.2)$$

It is unlikely that the tensile stress in the reinforcement will exceed 0.8 f_y during lifting. The term ε_m is calculated using the modular ratio method.

Shear cracks during handling are uncommon, but torsional cracks are possible in grade C15/20 concrete where the torsional shear stress is about 1 N/mm^2. According to Adlparvar [10.5] torsional cracking in asymmetrically loaded L-shaped beams commences when $v_t > 0.2\sqrt{f_{cu}}$ (for f_{cu} = 60 to 70 N/mm^2). In non-symmetrically loaded edge beams, e.g. those of the type shown in Figure 4.16, where the ends of the beam are restrained in the temporary condition against rotation, torsional shear stresses due to the self-weight of the beam plus impact allowances may result in helical cracking near the end supports (Figure 10.26(a)). The problem here is created by the temporary restraint, because the beam may have been designed on the basis that floor loads would equalise the torque *Fe*, even though the reactions F_1 and F_2 may be different, as shown in Figure 10.26(b). The solution is to prop the beam at two or three points before the crane is released. Care must be taken at upper-storey levels to ensure that all props line up vertically, otherwise the prop reaction may cause twisting of the component at the lower level.

Exercise 10.3

(a) Check the column in Exercise 10.1 for flexural cracks. Use the code of practice value for concrete tensile stress of $1.3 \times 0.14 f_{ck}^{2/3} \{0.24\sqrt{f_{cu}}\}$ as the limiting criterion for cracking.
(b) If the limiting tensile stress is exceeded, calculate the crack widths in the soffit of the section.

Use concrete grade C12/15.

Solution

Step 1: Uncracked serviceability limit state

(See Table 3.1) Young's modulus for grade C12 concrete E_{cm}	$= 27\,\text{kN/mm}^2$
Therefore modular ratio $m = 200/27$	$= 7.41$
Uncracked second moment of area for $A_s = 628\,\text{mm}^2$ and lever arm 102 mm	
$I_u = \frac{300 \times 300^3}{12} + (7.41 - 1) \times 2 \times 628 \times 102^2$	$= 759 \times 10^6\,\text{mm}^4$
Section modulus $Z_u = 759 \times 10^6/150$	$= 5.06 \times 10^6\,\text{mm}^3$
Service moment $M = 13.12/1.35$	$= 9.72\,\text{kNm}$
Then flexural stress $M/Z_u = 9.72 \times 10^6/5.06 \times 10^6$	$= 1.92\,\text{N/mm}^2$
> limiting flexural stress $= 1.3 \times 0.14 \times f_{ck}^{2/3}$	$= 0.95\,\text{N/mm}^2$

Young's modulus for grade C15 concrete $E_c = 20 + 0.2 \times 15$	$= 23\,\text{kN/mm}^2$
Therefore modular ratio $m = 200/23$	$= 8.7$
Uncracked second moment of area for $A_s = 628\,\text{mm}^2$ and lever arm 102 mm	
$I_u = \frac{300 \times 300^3}{12} + (8.7 - 1) \times 2 \times 628 \times 102^2$	$= 776 \times 10^6\,\text{mm}^4$
Section modulus $Z_u = 776 \times 10^6/150$	$= 5.17 \times 10^6\,\text{mm}^3$
Service moment $M = 13.06/1.4$	$= 9.33\,\text{kNm}$
Then flexural stress $M/Z_u = 9.33 \times 10^6/5.17 \times 10^6$	$= 1.80\,\text{N/mm}^2$
> limiting flexural stress $= 0.24\sqrt{15}$	$= 0.93\,\text{N/mm}^2$

Thus the section is cracked.

Step 2: Cracked serviceability limit state
Refer to Kong and Evans' design graphs [10.6] for cracked sections.

$d/h = 0.84$, $M/bh^2 = 0.36$, $A_s = 1257\,\text{mm}^2$, so from column design charts the steel stress σ_s	$= 66.79\,\text{N/mm}^2$
X	$= 141.1\,\text{mm}$
I_c	$= 214 \times 10^6\,\text{mm}^4$
and $Z_c = 214 \times 10^6/(300 - 141.1)$	$= 0.71 \times 10^6\,\text{mm}^3$
Tensile bar spacing $= 300 - 2(38 + 10)$	$= 204\,\text{mm}$
$> 5(30 + 20/2)$	$= 200\,\text{mm}$
Crack spacing $s_r = 1.3(300 - 141.1)$	$= 279.9\,\text{mm}$
and with $k_t = 0.6$	
$f_{ct,eff} = 0.3 \times 12^{2/3} = 1.57$	
$\rho_{p,eff} = 628/(2(30 + 8 + 20/2) \times 300) = 0.0218$	
The mean strain between cracks $= 66.79 - 0.6 \times \frac{1.57}{0.0218}\left(\frac{1 + 7.407 \times 0.0218}{200 \times 10^3}\right)$	$= 200.4\ \mu\varepsilon$
Crack width in soffit $w = 279.9 \times 200.4 \times 10^6$	$= 0.055\,\text{mm}$

< 0.3 mm, so durability not compromised.

If $mA_s/bd = 8.7 \times 628/300 \times 252$	$= 0.072$
then $I_c = 0.0479\ bd^3$ and X	$= 130.5\,\text{mm}$
$I_c = 0.0479 \times 300 \times 252^3$	$= 230 \times 10^6\,\text{mm}^4$
and $Z_c = 230 \times 10^6/(300 - 130.5)$	$= 1.36 \times 10^6\,\text{mm}^3$
Then flexural strain in the soffit $\frac{M}{E_c Z_c} = \frac{9.33 \times 10^6}{23 \times 10^3 \times 1.36 \times 10^6}$	$= 299\ \mu\varepsilon$
Then $\varepsilon_m = 299 - \frac{300 \times 169.5 \times 169.5}{3 \times 200 \times 10^3 \times 628 \times 121.5 \times 10^6}$	$= 111\ \mu\varepsilon$
To determine crack width in soffit over the longitudinal bar	
$a_{cr} = c_{min} = 30 + 8\,\text{mm}$ to main longitudinal bar, so crack width $= 3 \times 38 \times 111 \times 10^{-6}$	$= 0.013\,\text{mm}$

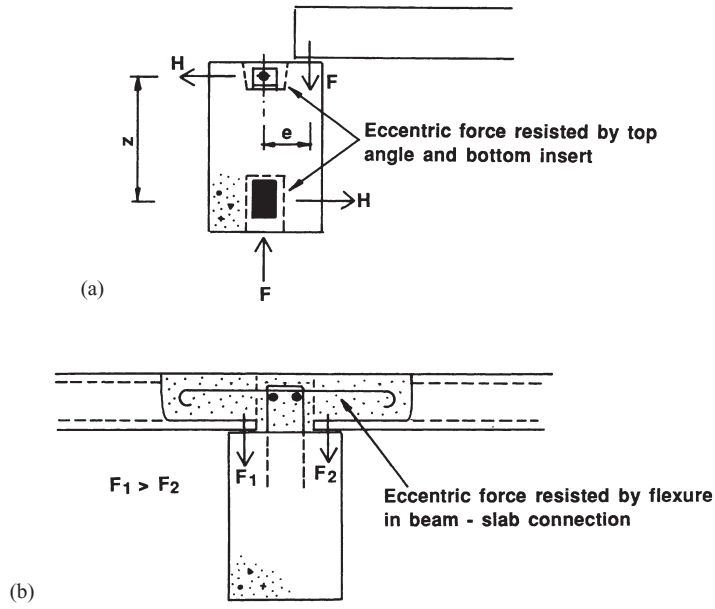

Figure 10.26 Non-symmetrical floor loading on beams. (a) Temporary restraint, and (b) permanent restraint.

10.3 Temporary Frame Stability

10.3.1 Propping

In some cases temporary propping will be required to stabilise a component prior to permanent stability being achieved. This will, or may, affect:

- columns and two-dimensional walls vertically
- beams, staircases and floor slabs horizontally.

Where propping is required, the ends of the props should rest against head-plates and sole-plates to spread point loads; see Figure 10.27 [10.7, 10.8]. The component should be reinforced to take the reaction(s) from the prop (both as an imposed load and a reaction), and special cast-in fixings should be provided if there is a chance that shear or tensile forces will develop.

The notion of propping refers not only to the use of adjustable length props, but includes any form of bracing in which a reactive force is developed. For example, timber wedges driven in between precast components at the foundation may create additional stresses for which the component should be designed. Great care should be taken when using hydraulically driven jacks to manoeuvre components into position, as large and unforeseen reactions, which may be present elsewhere, could lead to over-stressing. This is unlikely to happen with manually powered equipment.

Whenever jacks are used they should be correctly stabilised to prevent sideways forces developing. If jacking takes place from a lower-level floor, the precast contractor should be advised as to the maximum permitted load, and its position, to be carried by the floor below. The use of tow ropes, chain blocks, etc. to pull components into position should be correctly specified in all respects. The permitted positions at which ropes may be attached to components (in particular to any projecting fixings or reinforcing bars) should be clearly defined. If the ropes are tied to cast-in fixings, the fixing must have adequate anchorage and strength.

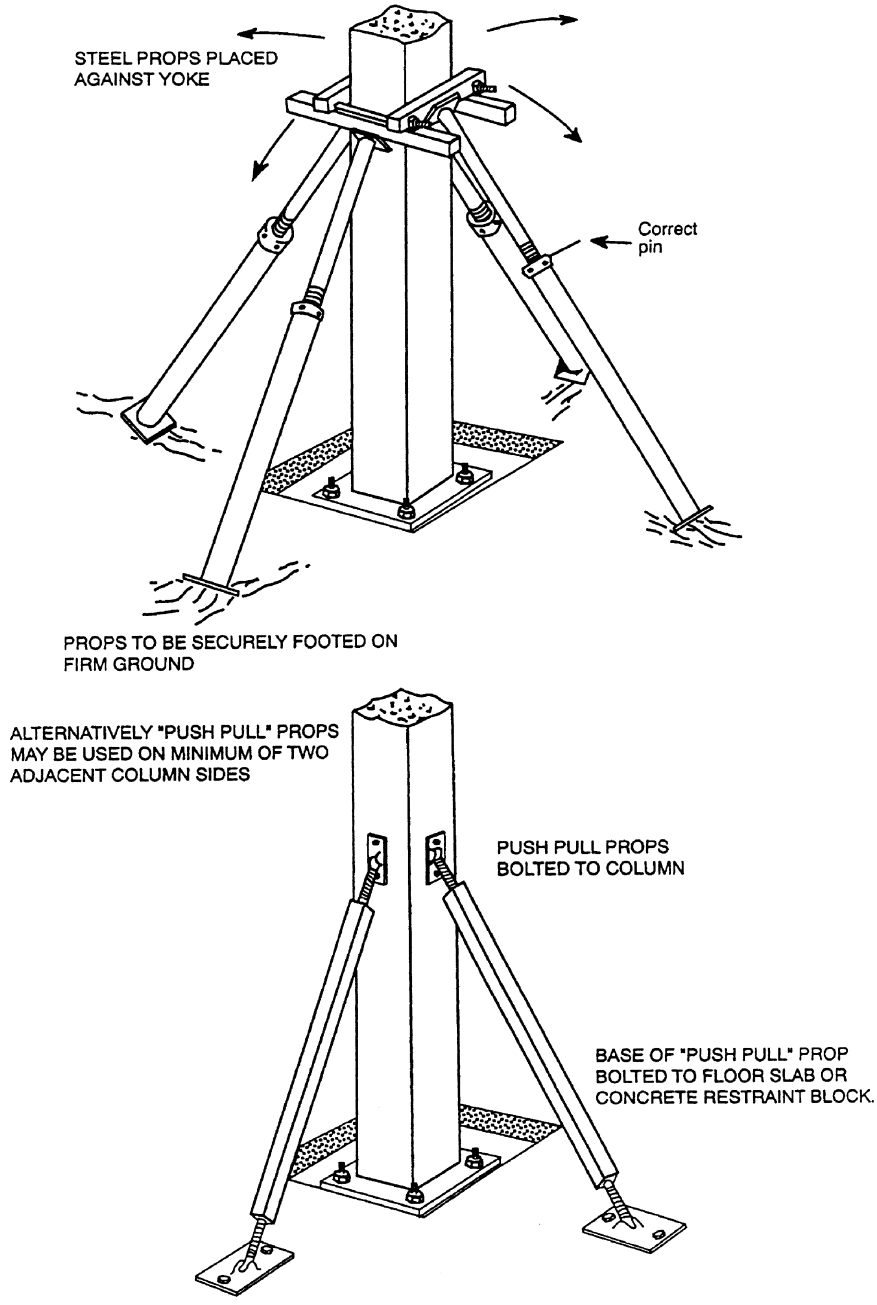

Figure 10.27 Head plates to props [10.8].

10.3.2 The effect of erection sequence

The sequence of erection is controlled by many factors, the more significant ones being crane accessibility, structural form (plan shape, unbraced/braced frame) and positions of stability walls. Lack of forethought, or delayed delivery of units, can result in novel site solutions.

Unbraced frames are inherently stable after completion of the moment connection at the foundation, but this does not mean that temporary stability may be ignored. A fully tied first-floor slab must

be assured before temporary props are removed from the columns, and the verticality of the columns is checked upon the completion of each floor level. Where more than one column is structurally tied into the frame, side-sway can occur only by simultaneous lateral movement of all columns. Because absolute rigidity cannot be achieved, the function of any bracing is to limit side-sway to within reasonable limits. The maximum permitted value is 0.05 times the width of the column, and this is well within the usual site fixing tolerances.

In braced frames, which rely on stabilising components, construction proceeds in an area that contains at least one stabilising element in the two orthogonal directions, and work proceeds outwards and upwards from that point. Temporary steel cross-bracing or diagonal propping is used if the geometry of the frame makes this sequence of fixing impossible. There is a degree of redundancy here, in that most 'pinned' bases have semi-rigid stiffness (the exceptions are columns founded on retaining walls or torsionally flexible *in situ* ground beams), and this may be called upon to assist in the temporary condition up to the level of the first column-to-column splice.

Two types of loading are considered at this stage: wind loading and eccentric loading due to lack of plumb or overhanging components. The effects of wind currents on rectangular blocks, plates, etc. have been reported by the Engineering Science Data Unit (ESDU) (e.g. [10.9, 10.10]) and by Cook on space frames [10.11]. Amplification factors on the basic wind pressure of up to 1.8 are possible on a partially clad building. However, these forces are not usually critical unless the frame is partially clad at the *same* level as the floor plate is incomplete. In this case, the line of columns on the windward and leeward external faces is checked against forces calculated using local wind pressure coefficients.

Eccentric loading due to non-symmetry is more easily calculated and allowed for. The main modes of possible failures are summarised in Figure 10.28. The divergent mode, Figure 10.28(a), is possible where particularly large concrete panels are fixed out of sequence, or too early with respect to the maturity of the structural frame. This may occur in cold weather, when *in situ* concreting is not permitted and the contractor is anxious to continue with the precast construction. These situations are always anticipated and temporary tie backs (e.g. using 'tirfors') are used. The alternative is the sway mode in Figure 10.28(b), where rotations between the beam and slab and between the column and beam, are both possible in the temporary condition. Props are used to prevent side-sway until the joints are grouted.

Lack of plumb is largely eliminated by very strict fixing tolerances, although frame movements due to temperature, shrinkage and self-weight loading will inevitably cause deviations in the order of ±10 mm for a 60 m long frame. Precast columns are surprisingly flexible to straightening and it cannot be emphasised too strongly that, unlike steel structures, precast frames are vertically aligned at every floor level before the *in situ* concrete tie beams are cast. 'Push–pull' props with tension as well as compression capacity are used extensively in this exercise, and fully anchored threaded sockets, brackets, etc. are supplied with the relevant precast units.

10.3.3 Special consideration for braced frames

The sequence of construction must ensure that floor diaphragm action be allowed to develop between the bracing frames or walls, particularly if the skeletal structure is to be clad, in part or in whole, around the perimeter or internally. Figure 10.29 shows the correct sequence. Point A lies on a critical plane and should be dealt with earlier rather than later in the fixing sequence. Floor slabs should not be omitted from the floor near bracing frames or shear walls.

Each floor slab level should be grouted such that the grout has time to mature before fixing of the floor (or roof) slab at the *second next* upper level commences. The usual maturity time is three to five days in temperate climates (10°–20°C), or one or two days in warm humid climates (25°–30°C). The tie connections between adjacent floor slabs, beams, columns and walls should be fixed according to the contract drawing. Cover distances and lap length should be checked, and the threaded penetration length into cast-in sockets marked before the threaded portion is mated.

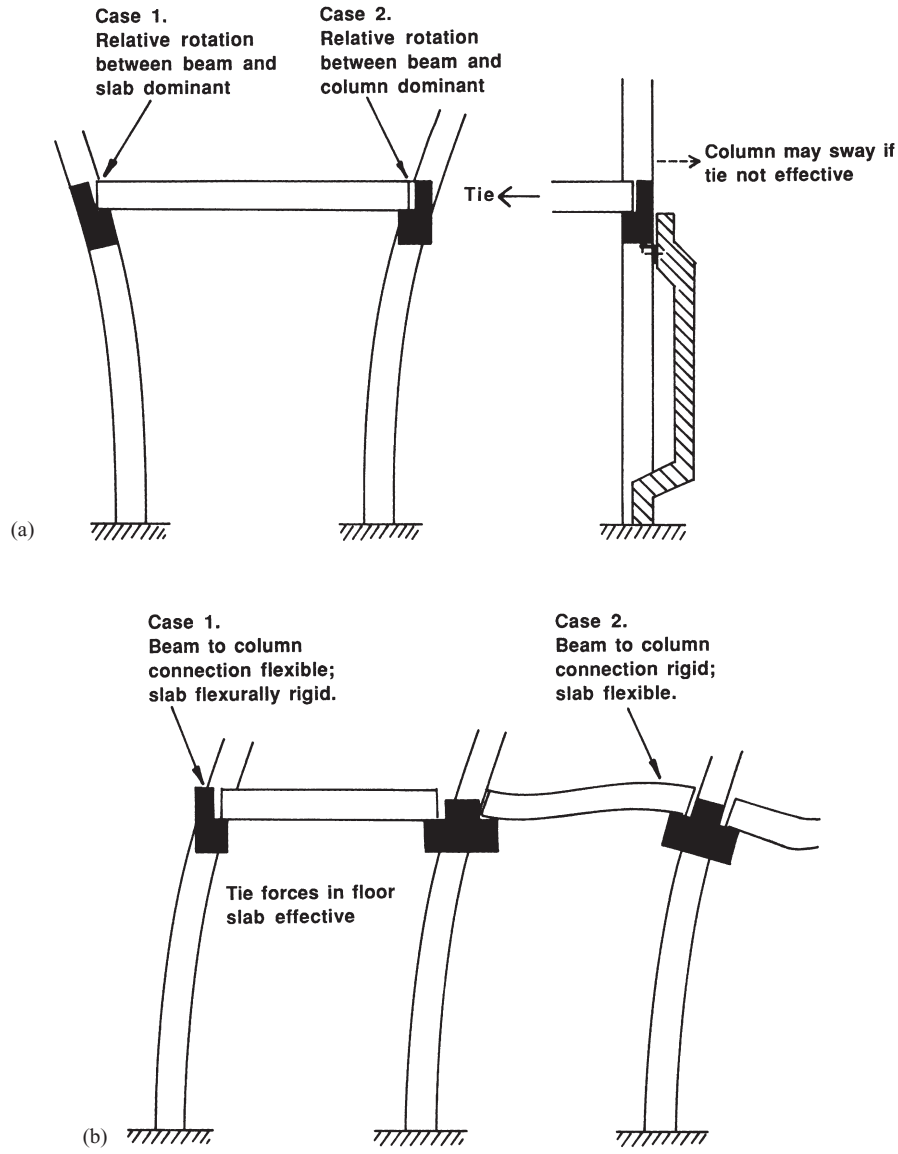

Figure 10.28 Sway modes of failure. (a) Divergent mode, and (b) sway mode.

The bracing frames, shear cores or shear walls, etc. should be constructed at least one storey ahead of beam, floor and staircase erection at any floor level. If the strength and stiffness of the wall rely wholly on composite action with the skeletal frame through an *in situ* grouted interface, the grout should be given time to mature before construction of the components at the floor level above the wall commences.

The wall should be temporarily propped or secured to the stabilised frame, perhaps using one of the methods shown in Figure 10.30(a) to (d). Temporary supports should remain in position until the *in situ* grout has matured and the wall is supported or tied into the frame (Figure 10.31). This may cause a delay in construction if the wall lies on the critical construction path. If the wall-to-frame connection is totally provided by bolting or welding, there need be no delay to subsequent construction.

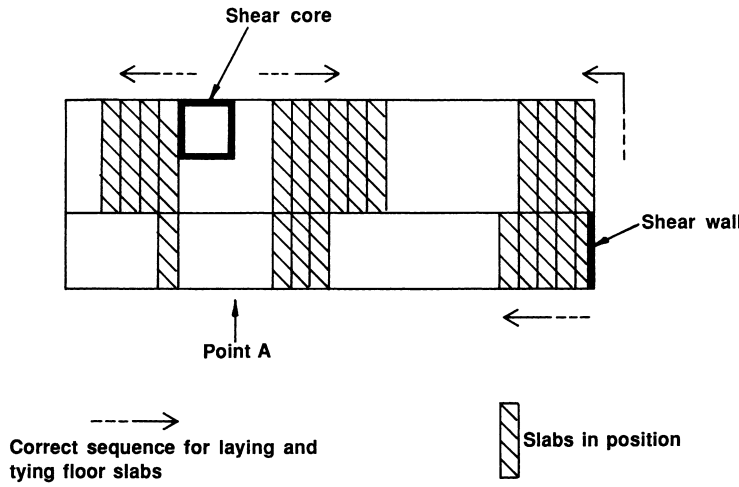

Figure 10.29 Unstable floor diaphragm.

The construction of column splices should be carried out exactly according to the specification, particularly with reference to the sequence of fixing upper columns and the mixing and placement of *in situ* concrete, grout, etc. The lower column should be fully tied into the skeletal frame to the floor level below the level of the splice. No splices should be made to columns that are not connected to a fully tied and braced part of the structure to within one storey level below the level of the connection.

The upper column should be propped for all types of column splice, even if the permanent connection between columns is made immediately, e.g. bolted, coupled or welded (Figure 7.109). The props should remain in position until the splice connection has developed its full strength and the upper column is tied to the skeletal frame at the next floor level above the splice. If the next floor level is staggered, the column should be tied into the lower floor level only, providing the column is connected in two mutually perpendicular directions.

Temporary stability is considerably enhanced if the level of the column-to-column splices is staggered in alternate rows of columns (Figure 7.107). This avoids a continuous plane of weakness in the permanent structure and enables construction to proceed with at least half the number of columns continuous above a critical horizontal plane. The axial force and bending moment capacity of some of the smallest column splices (for a 300×300 mm column) is sufficient to allow for about 15 mm of sway at the top of a two-storey column, a value which is unlikely to be exceeded in practice.

The floor slab is a convenient platform on which to work and therefore columns surrounding lift shafts, atria, etc. are particularly difficult to deal with. Special devices have been developed to stabilise these components, but it is the judgement of the erection foreman that guarantees temporary stability.

Frame erection continues no more than two storeys ahead of a fully tied framework. This may be restrictive in tall buildings of small plan area, e.g. 300 m^2, where the curing period for the *in situ* concrete infill is less than the fixing time for a complete floor. Bracing props may be left in position longer than normal to enable the precast frame erection to proceed.

10.3.4 Special considerations for unbraced frames

Unbraced frames are stabilised by cantilever action of the columns, or by frame action between the columns and floor plate, or the columns and beams. Therefore the sequence of construction is less critical, because each column is capable of carrying horizontal loads, both in the temporary and

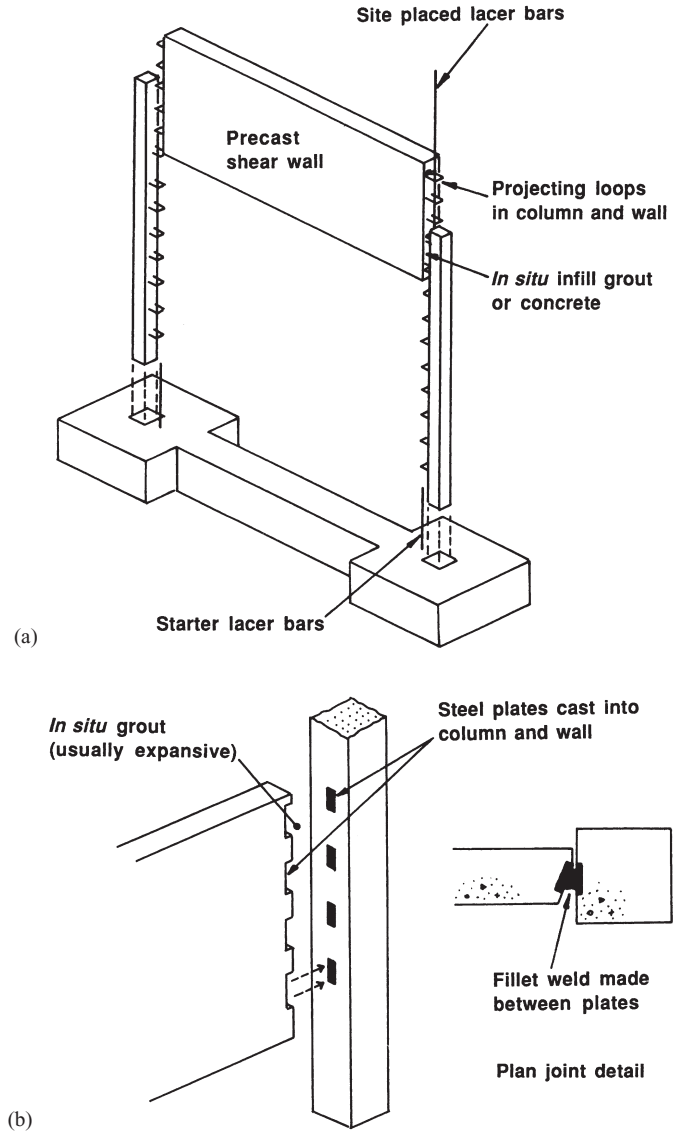

Figure 10.30 Wall-to-frame connections. (a) Lapped reinforcement; (b) welded plates; (c) temporary angle cleats; (d) temporary column clamps.

permanent situations. The columns should be adequately propped and column-to-frame connections completed and allowed to mature according to the same restrictions as given in Section 10.3.3.

The principle of concreting floor slabs no more than two floors behind the level of floor construction is also applicable in unbraced frames. The importance of this lies not so much in horizontal stability, because the columns can act as cantilevers by design, but in the safety and integrity of the floor slab in cases of accidental impact by slewing craned loads, or dropping of materials onto the floor slab. Experience has shown that ungrouted slabs can be dislodged from their seating by the impact loading from a slab unit dropped from the next upper floor level, whereas grouted slabs (more than three days' maturity of grout) are likely to survive the impact loading from two such slabs.

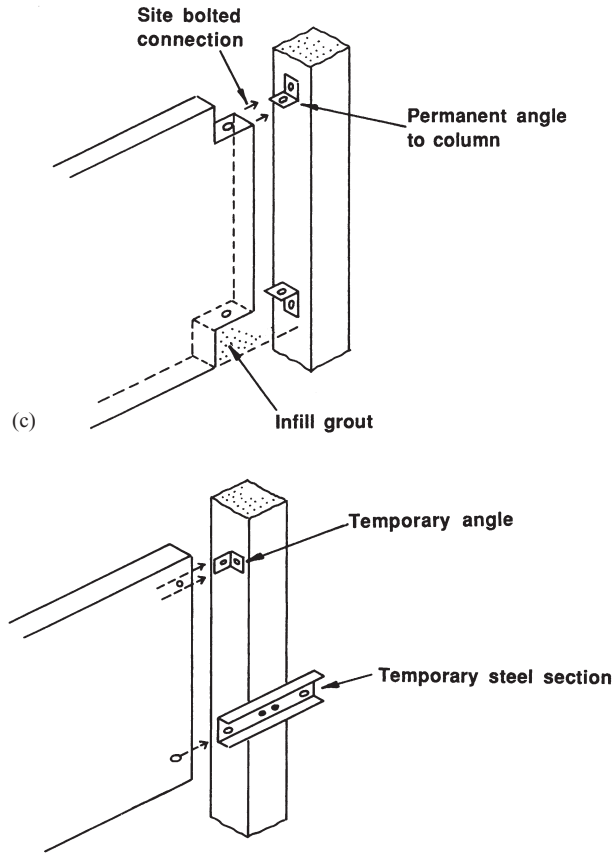

Figure 10.30 (*Continued*)

10.3.5 Temporary loads

Imposed loads due to the combined storage of materials, storage of precast components, and construction traffic and plant should be assessed and generous allowances given to the various parts of the framework. Strict guidance rules should be made available so that the precast contractor is aware of the limitations.

Where a precast component has been designed to act compositely with another medium, consideration must be given to the non-composite strength and stiffness of the component. Working drawings should carry this information in the form of allowable loads per unit area, or per individual component, irrespective of the location of the imposed load.

Wherever possible the stacking of precast components should be at ground level. Where this is not possible or practical, e.g. on confined sites, the weight and position of the component should be determined so as not to violate the above guidelines. The positions of stacked components should not impede the *in situ* site work necessary to achieve permanent stability.

In some instances damage will occur to the waiting components or to the components in the frame owing to impact. This may be the result of negligence on the part of the precast contractor, or of oversight on the part of the designer. Similar structural damage caused by following trades should likewise be reported and assessed. In some cases remedial structural work will be necessary, or the complete removal and replacement of the damaged part(s) may be required.

Figure 10.31 Wall and column props in position.

10.4 On-Site Connections

10.4.1 Effect of fixing types

The most important factors in practical connector design are:

- accessibility
- temporary stability
- tolerances.

Strength criteria may be satisfied simultaneously with the above, but new connector designs are most frequently unsuccessful owing to a lack of understanding of the erection sequences and the practical difficulties arising from cumulative manufacturing and site dimension deviations. The connection must allow for precast components to be lowered unhindered onto their supporting member, and for adequate access to the connection thereafter. There is an increasing range of safe-access equipment to assist in access for making connections during frame erection (e.g. cherry-pickers and scissor-lifts, shown in Figures 7.103 and 10.32, respectively. In difficult situations a slewed approach is sometimes permissible, but in general this is avoided.

(a)

(b)

Figure 10.32 Improved access equipment. (a) Cherry-picker, and (b) scissor-lift (both courtesy of Composite Ltd).

Structural joints between precast components require small quantities of materials. Small-aggregate concrete, cementitious mortars, epoxy mortars and adhesives must be carefully specified and accurately located and compacted. The *IStructE Manual* on joints [10.12] is widely used by designers for compliance with proposed jointing details.

There is a wide range of fixings and connections in a precast structure, many of which are used to perform a unique function. The precast contractor should be made aware of the importance, or not, of each fixing type, and of the permitted deviations. The designer should ensure that the fixings perform their intended function, either by strict compliance with the manufacturer's details, or by full-scale testing. In the former, the influence of the position of the fixing in the component, and the measures taken to ensure the full safe working capacity of the fixing, should be observed. Construction tolerances should be stated on the drawings.

Fixings should be clearly referenced and coded to avoid error. Where shims or packs are used to aid construction methods, the designer should ensure that they are capable of sustaining the necessary load, and can provide the degree of flexibility required. The load-bearing components should be designed for the effect of temporary point loads resulting from the use of small shims (particularly steel shims). The precast contractor should be informed of the permitted maximum load capacity through a shim.

The strength of bolted or welded connections should be assessed for both the temporary and permanent conditions, such that no element is overstressed at any time. The effect of torsion and shear stresses induced by non-symmetrical loading (e.g. slabs onto one side of a beam), which would not normally occur in service, should be catered for, e.g. see Figure 10.2.

The contribution to strength and stiffness from *in situ* concreted connections should be assessed with respect to the time taken for the concrete to mature. Although adequate strength may be achieved in compression, the bond resistance between rebar/dowel and the concrete may take longer to develop fully. The connections should be protected from rapid drying or rain penetration.

10.4.2 Strength and maturity of connections

Immediate strength is achieved by bolting or welding, although *in situ* concrete may be required for the joint to achieve full service strength. In this situation the strength of the partially complete joint is checked for temporary loading and, if necessary, the construction sequence is interrupted and work is carried out elsewhere until an adequate strength is achieved. Temporary propping is *not* always required during this operation. *In situ* concrete and grouts are specifically designed for early strengths and low shrinkage characteristics. Strengths around the $10\,N/mm^2$ mark are typical for temporary loading and are usually achieved within two days.

The most important joints are:

- column splices, where the joint must achieve adequate compressive strength before upper-storey beams and slabs are positioned
- floor slabs, where *in situ* concrete infill is used to complete the floor diaphragm to transfer horizontal loads to stabilising components
- shear walls etc., which must be integral with the frame at least one floor behind construction.

These different conditions are dealt with in Section 10.5.

10.5 Erection Procedure

10.5.1 Site preparation

The General Contractor (GC) should prepare well-consolidated and level ground around the full perimeter of the frame and within the interior of the frame. Any service pipes or similar must be

protected from crane and vehicle impositions. The extent of this working area depends on the type of crane being used by the precast frame erector, but should not be less than about 6 to 7 m wide, as measured from the edge of the frame. The working ground level should preferably not be more than 0.75 m above or below the finished ground-floor slab level.

A typical precast erection gang consists of four or five persons. The foreman is responsible for the works and will liaise, in the absence of a resident engineer, with the GC and the personnel at the precasting company. The foreman also orders the deliveries of precast components, and is often the most skilled person in the team for fixing and for directing the actions of the crane. Two other fixers assist the foreman, and two labourers carry out the duties after the precast components are fixed, e.g. shuttering, grouting, making good, etc.

In most instances the GC is responsible for the construction of the foundations and substructure in general (except where precast foundations are used). *In situ* concrete foundations should be cast at least 14 days before commencement of the frame erection. The strength of the *in situ* concrete to the foundations should be at least 10 to 15 N/mm^2 before frame erection commences, unless the precast designer specifies any special requirements. A levelling pad is prepared by the precast contractor at least three days before frame erection commences. If this is not possible, then 150 mm-square solid steel packs, or sandwich steel–clay tile packs, may be used. The clay tiles should not be more than 10 mm thick and the steel plates not less than 3 mm thick.

The precast contractor should prepare sound bases for the column props. Where props are used on either side of the column, the foundation for each prop need only be required to carry a compressive force. A timber or concrete spreader pad may be required if the ground conditions are poor. Where only one prop is permitted in any one direction, the foundation pad must be able to resist both compression and uplift. The precast designer should inform the GC of the size and position of the pad. The pad must be levelled horizontally and located centrally on the column line. Precasters will usually cast screw sockets into the precast members when push–pull props are to be used, but will usually omit them for compression-only props so as to maintain clean lines to visible faces.

10.5.2 Erection of precast superstructure

Figure 10.33 shows the fundamental erection sequence [10.13]. The important feature of this sequence is the time at which the temporary props are removed. The following sections discuss this sequence in detail.

10.5.2.1 Columns

Columns should be lifted off the delivery vehicle using at least two lifting points, and correctly stacked and pitched according to Section 10.2. The column may be inspected for any cracks when it is at an inclination of about 5° to the horizontal. Any cracks should be marked, measured and reported to the designer, whereupon any necessary corrective action will be taken.

At the ground-level connection, the column is lowered onto the foundation on the pre-levelled plate. If a pocket foundation is used, timber wedges (two per face) are forced down into the gap between the column and foundation, and the column is also propped at about 2.5 m to 3 m above foundation level. If the column is placed over projecting reinforcement to form a grouted sleeve connection, props are placed as above, together with horizontal wedges to prevent the bottom of the column from moving sideways. If holding-down bolts are used, the base plate is secured by fully tightening the nuts to *every* bolt, and no wedges are needed.

The props should be of adequate compressive strength and subtend an angle of approximately 45° to 60° to the horizontal; see Figure 10.34. The typical prop rating is 3 to 4 tonnes compression at 4 m extended length. The action of forces from the props should provide stability in two mutually perpendicular directions, and be coincident with the centroid of the column and the reaction from the wedges. This may be achieved using four compression props, or two tension–compression props, or a combination of both. The props should remain in position until all the columns supported by the said props are fully tied to the first-floor slab. It is not permitted to remove the props from one

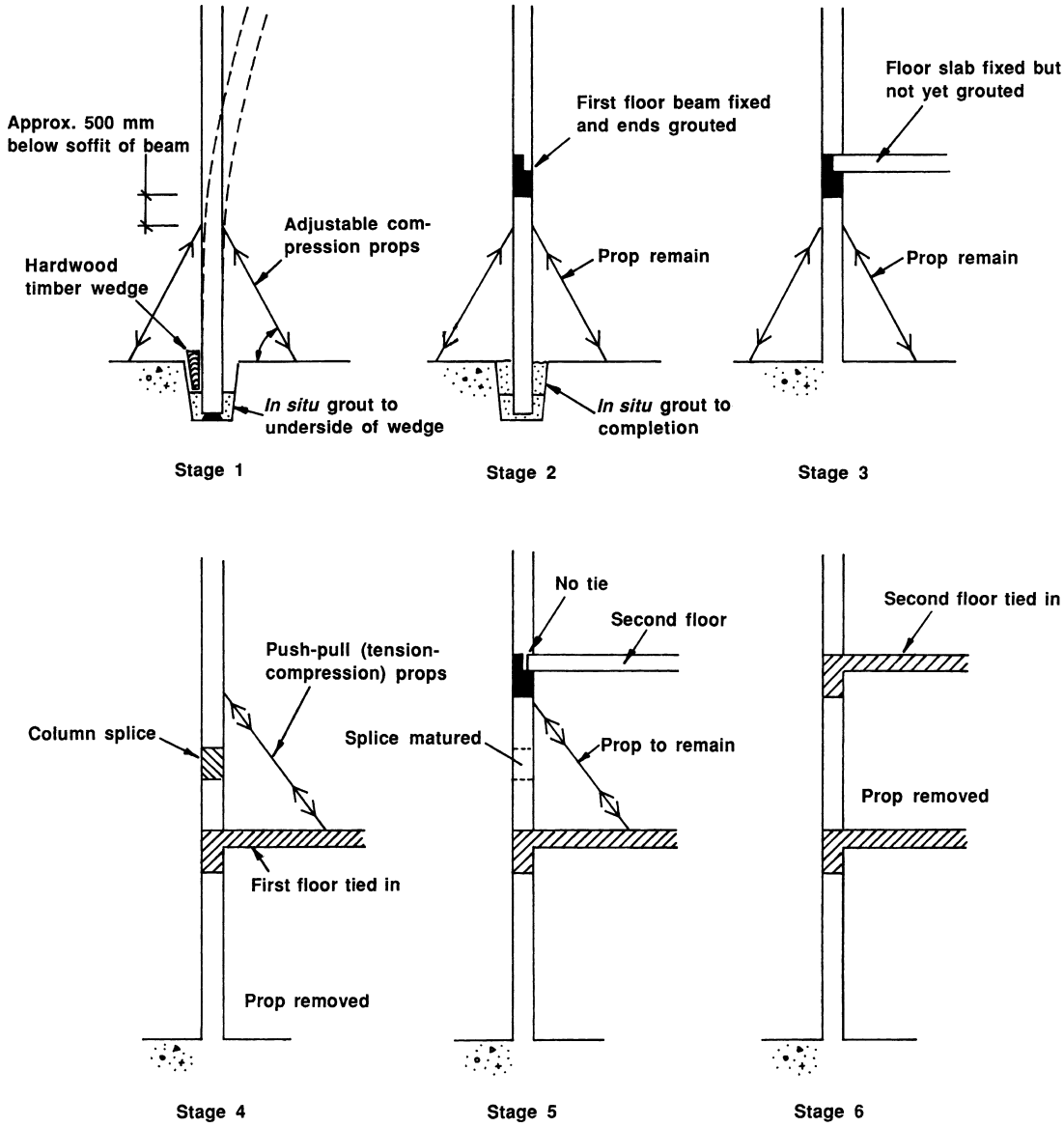

Figure 10.33 Precast frame erection sequence [10.13].

particular column on the premise that it is itself tied into the frame. Where the column is asymmetrically loaded, the props should remain in position until such time as the column is tied in at *two* floor levels. This is to provide the necessary horizontal prop reaction force (see Figure 10.35).

During bad weather, high winds or a disrupted fixing sequence, the precast contractor may wish to leave the props in position until the first and second floors are completed. Similarly, very tall columns, exceeding 15 m in height × 300 mm depth, may have to be propped at the first-floor level so that no more than 9 to 10 m height of column is unpropped while fixing commences at the second-floor level.

Columns founded in pockets are manoeuvred into position and aligned vertically using the tapered wedges and props, respectively. The wedges should be at least 250 mm long and tapered at

Figure 10.34 Fixing column props just below the level of the first-floor beam and into load-bearing footings capable of resisting compression and tension forces from the props.

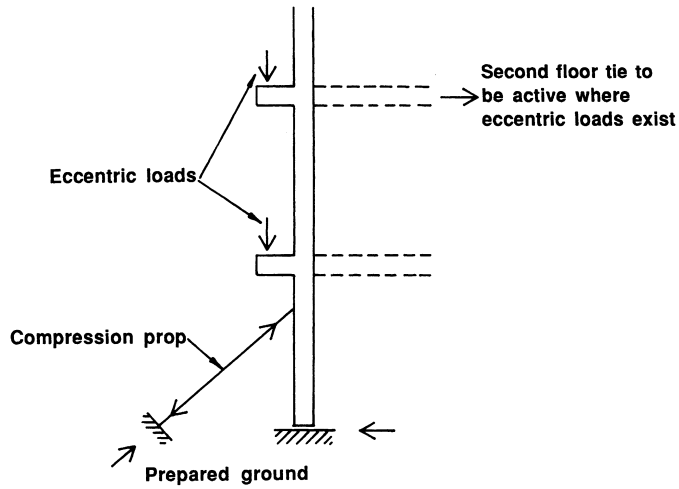

Figure 10.35 Stability of column subjected to eccentric load.

approximately 10°. It may be necessary to insert two wedges if the gap is particularly wide. Sturdy, seasoned hardwood should be used, because the wedges are driven downwards in order to drive the column into position. Crowbars (approx. 1 m long × 40 mm diameter) are also used to manoeuvre columns on base plates or projecting reinforcement. Optical instruments, such as two theodolites reading azimuth angles in two mutually perpendicular directions, are suitable (Figure 10.36). Plumb lines may be used for shorter (less than 10 m) columns, but are best suited to calm weather. When the column is correctly positioned, the annulus between the column and foundation should be filled

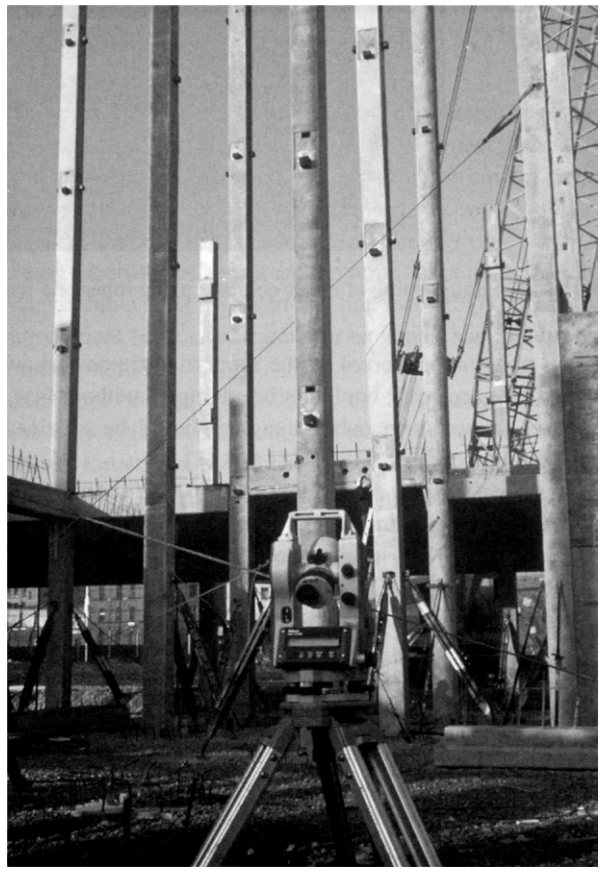

Figure 10.36 Vertical alignment of columns using optical methods.

to the level of the wedges or 250 mm depth, whichever is the greater, using a concrete grade C30/37 containing 6 or 10 mm size aggregate and an expanding agent. The slump should be 50 to 100 mm. A poker vibrator should be used to compact the concrete that is placed in pockets. The wedges may be removed a minimum of 24 hours later, or when the compressive cube strength of the *in situ* concrete reaches 10 N/mm^2. The foundation is then filled to the top using the same mix as before.

Columns founded on base plates assume a more immediate fixity, although a structural connection is not considered effective until *in situ* grout underneath the plate has achieved a reasonable strength.

Further vertical alignment of the column is possible after the base has been concreted. Columns are sufficiently flexible to allow horizontal movements of not more than 10 mm over a 3 m storey height for 300 × 300 mm sections. Realignment of columns from upper storeys may impose forces on the supporting framework that have not been allowed for in the design, and should not be attempted without first referring to the designer. In all cases compressive cube strengths should be obtained for the concrete used in the foundations, in accordance with BS EN 12390 [10.14].

It may be necessary during construction to adjust some of the columns vertically. This may be due to column curvature (asymmetrical curing, temperature variations, etc.), or to the forces imposed on the columns during frame erection to the upper floor levels. Figures 10.36 and 10.37 show wire ropes attached to these six-storey columns at the second-floor level. It is necessary to tension the rope by 'pulling' the column using a ratcheted wrench (e.g. Tirfor, or monkey wrench). Great care must be taken because tall concrete columns are surprisingly flexible. The column is secured by props at the floor level, as shown in Figure 10.38.

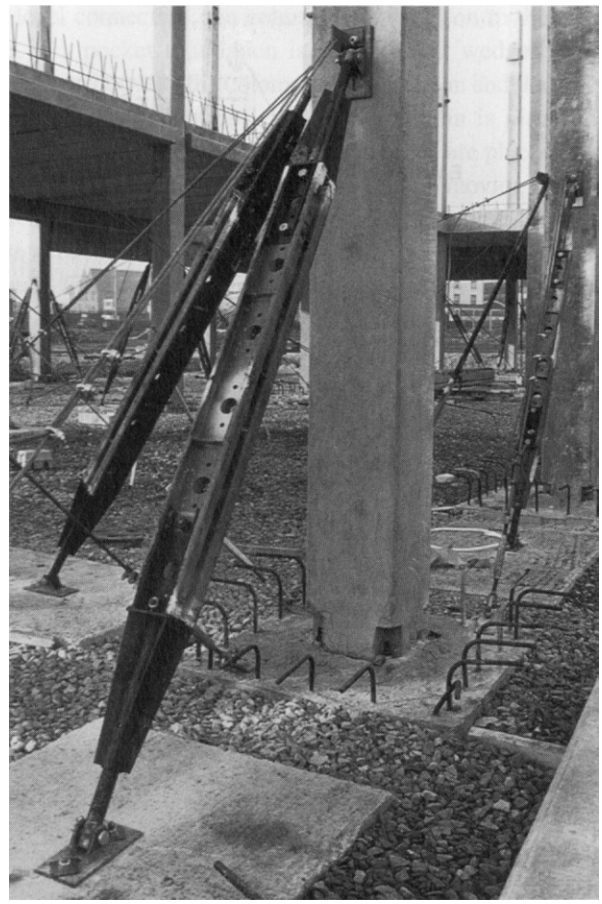

Figure 10.37 Straightening of upper columns using ropes and wrenches.

Where a threaded connection is made to the end of a projecting dowel, the threaded part of the dowel must be undamaged, and the protective covering placed over the thread at the factory must still be in place. Grout splashes should be removed from the thread. As before, the annulus around the dowel should be filled using a pourable grout before the holding-down plate (or washer) is placed over the end of the dowel hole. The entire length of the nut must be in *complete* contact with the threaded dowel.

No attempt should be made to manoeuvre precast components into position using the nut and dowel as leverage. If the element requires realignment, it should be lifted by the crane or raised off its bearing using jacks and moved in the correct manner.

10.5.2.2 Beams

The rules governing the lifting of beams are the same as for columns, except that beams may – and preferably should – be lifted directly onto the framework. The positions of the lifting points and lifting devices (spreader beams, for example) should not interfere with the connections or fixing methods.

Fixing procedures for beams depend largely on the type of connector used. A broad distinction can be made between those connectors that provide an immediate restraint to shear and torsional forces (e.g. bolted cleats, or billet with top fixing) and those that do not (dowelled corbel, or billet with *in situ* tie top fixing). In the latter case temporary propping may used, because the beam is unstable until the *in situ* grouted connection has matured. In all cases the shear capacity of the

Figure 10.38 'Push-pull' props for temporary column stability (courtesy of F.C. Precast Ltd).

connection is not affected by the sequence of erection and is not dependent on the strength of the *in situ* concrete infill.

The most onerous situation is the asymmetrically loaded spine beam shown in cross section in Figure 10.26(a). The eccentricity of the loading is about $e = 270$ mm and this results in a torsional moment of about 7 to 8 kNm in a typical frame. It must be resisted by the connector, or nullified by props and/or ties. With the exception of the welded plate-type connection, where propping is the preferred method, all connectors are capable of generating this restraint. Similar problems occur in some of the wider L-shaped edge beams and in special cantilevered sections, but in general they are easily overcome by the addition of an extra top-fixing cleat or by ad hoc site instructions to prop.

Beams of non-symmetrical shape, deep beams (exceeding 900 mm in depth), and spandrel beams are provided with a second fixing to improve temporary stability. The fixing may remain exposed, in which case stainless steel is used, or be covered in the general grouting operations. The operation is straightforward and has little effect on design.

Non-symmetrical perimeter components create torsional moments in their connections, and hence horizontal deflections in columns. This may lead to further deflections due to the P-Δ effect as subsequent floor loads are added. If column rotations occur, which will inevitably lead to beam or slab rotations, it is necessary to realign the perimeter components using push props or tethers. Dimensional checks should be made on column verticality, position and squareness during these operations.

If the orientation of the floor slab is such that a beam, or wall, is loaded non-symmetrically, or the fixing sequence is such that this effect cannot be avoided, the rotational stability of the support member should be ensured. That may be achieved in the form of props with crossheads, or brackets at the strategic positions such as beam-to-column, wall-to-column or wall-to-wall connections. The temporary supports should remain in position until such time as the forces causing the rotations are nullified by membrane action in the floor slab, as shown in Figure 10.26(b). Similarly the connection at the end of the beam or wall should be capable of resisting the torsional moments created under the temporary or permanent floor-loading arrangement.

Connector levels are positioned (by some but not all designers) up to 10 mm lower than the correct level, to enforce the use of levelling shims, which are to be used with due allowance for squashing.

It is important that the shims are accurately located to prevent large eccentricities occurring at the column face. The shim should be large enough to prevent local bearing problems, because it cannot be assumed that any *in situ* grout placed around the connector will penetrate to the bearing surfaces. The rules for using neoprene pads between concrete surfaces (e.g. column corbels) are similar, but for excessive thicknesses of packing a sandwich construction comprising a steel plate inserted between two neoprene pads is favoured. After the beam has been fixed to its supporting member, pourable grout or concrete using a 6 to 10 mm size aggregate, of minimum grade C20/25, fills the space around the connection. This applies to beams connected to continuous columns as well as to continuous beams fixed to column heads. An expanding agent may be added to the mix to enable a greater water content to be used. Leakage of grout (cement fines, etc.) should be prevented. Any gaps between the precast members should be filled using dry-pack mortar. The strength of the dry-pack should be equal to that of the (weaker) parent precast components.

If the torsional stability of the connection relies on the *in situ* infill, 24 hours' maturity should be provided prior to fixing floor slabs onto the beam. The strength of the grout should attain 10 N/mm^2 before the beam is loaded in a manner that will stress the connection. Alternatively the beam may be propped, in which case floor slabs may be fixed immediately afterwards. Connections offering immediate torsional stability allow the construction to proceed without delay. There is obviously some merit in this, particularly in buildings with a small number of beams per floor level.

10.5.2.3 Stability walls

Construction methods differ according to the type of wall. However, in all cases the walls should be braced against lateral movement, either:

- by using immediate permanent mechanical connections, such as angle cleats bolted or welded to the precast components
- by using immediate temporary connectors, such as clamps or temporary angle cleats, or
- by propping, using either a minimum of four compression props where the wall is internal and bound on both sides by floor slabs, or a minimum of two push–pull props where the wall is at an edge.

The props should subtend an angle of approximately 45° and be located at a position approximately one-fifth along the length of the wall (Figure 10.31). Where several wall panels are used to complete a storey-height wall, all individual panels should be braced to the main frame, and *not* to each other. The temporary bracing should remain in position until the *in situ* concrete ring beam to the floor slab above the level of the walls is completed and matured. Walls that are connected to the frame using permanent mechanical devices do not impose such restrictions on the fixing sequence.

Stability walls that rely on composite action with the framework via a cementitious interface should be fixed and concreted in position at least 24 hours before the floor slabs are positioned. This is because the floor slabs contribute a large part of the permanent weight at each storey level. The narrow annulus between the wall and framework should be equal around the perimeter of the wall, and should not be less than 10 mm if grout is being used, or less than 20 mm if small-aggregate concrete is used. The grout or concrete is usually a minimum of grade C20/25.

In the case where projecting reinforcement is used to tie walls and wall/columns together, it may be necessary to bend the projecting reinforcement against the face of the mould, later to be pulled out by hand. The reinforcement used for this purpose should be sufficiently ductile to be bent through a right angle. If radial cracks are seen around the embedded reinforcement, the surface concrete around the bar should be broken out in what will probably be a conical piece about 20 to 30 mm deep. The surface should be reinstated using an epoxy mortar or similar. Minor damage to the concrete, e.g. surface spalling, will be hidden beneath the infill grout and need not cause concern. There are proprietary systems marketed for this purpose, containing a nest of bars (partly surrounded by foam to avoid grout ingress) that can be readily fixed to the formwork and will provide the necessary anchorage.

10.5.2.4 Two-dimensional units, including floor slabs

Precast units of large plan area present few fixing problems, as long as adequate bearing is provided and the unit can be handled near the horizontal. A broad distinction in the fixing procedure is made between units on:

(a) *continuous* bearings (e.g. hollow-core flooring)
(b) *localised* bearings (e.g. double-tee units).

(a) Continuous bearings with uneven or cambered beams (or other supporting components) may cause 'rocking' in units that exceed about 2.0 m in width, which if restrained may lead to torsional cracking across one of the corners. The problem is overcome by wet bedding on mortar. Minimum bearing widths are achieved because flooring units are manufactured to positive tolerances. Flooring units are not propped unless a composite construction utilising propping forces is specified.

The sequence of fixing floor slabs should be continuous in one direction, progressing away from the frame's stabilising components. Hollow-core units are directly positioned by the use of lifting hooks or pins, or by using chains. Erectors claim that fixing times are about 30–40 per cent faster using the hooks or pins. Where chains are used (Figure 10.39), the units are levered into position using the edge of an adjacent unit as the fulcrum point for a (1 m long) crowbar. The hollow cores should be closed off at a distance of not more than 100 mm from the ends of the unit, or 100 mm beyond the end of broken-out cores, to prevent grout loss into the core. Plastic or polystyrene plugs are usually used for this, and can be factory-fitted by arrangement.

Bearing lengths at either end should be made equal except where, for reasons of restricted access at one end, the correct bearing length may be provided at one end and a greater length at the other end. The minimum permitted bearing length is equal to the nominal length minus the tolerance distance of 15 mm (see Section 7.6). If the bearing length is more than about 10 mm less than this value, the designer should be consulted as to whether the unit should be replaced

Figure 10.39 Fixing precast hollow-core floor units above safety nets.

Figure 10.40 Cracking and spalling has occurred due to only 45 mm physical bearing length for a 16 m long hollow-core unit.

or whether additional *in situ* concrete infill is necessary to make an extended bearing from the precast unit to the supporting member. Checks should be made for local cracking and spalling where there are inadequate bearing lengths, and the situation adjusted, such as is shown in Figure 10.40. In this case the net ultimate bearing stress, after deducting allowances for cover in the supporting beam leaving only 15 mm effective bearing, was approximately 18.0 N/mm^2, equating to $0.45f_{cu}$ and riding very close to the limit.

(b) Double-tee units are usually more massive in size and require careful attention during fixing. Four-point lifting enables the unit to be accurately located. The units should be positioned onto $150 \times 150 \times 10$ mm neoprene, or similar, bearing pads. The bearing length onto the supporting element, i.e. through the pad, should not be less than 130 mm, and the bearing width onto the pad not less than 140 mm (see also Figure 7.59). Contact with all four pads should be made, and if not the case, an additional thickness of pad should be provided at the non-contact point. Welded connections between adjacent floor units, and between floor units and their support, are made after the completion of a bay of flooring when deck load deflections of supporting beams are complete, and cumulative tolerances can be checked for the units to be adjusted where necessary.

Welded connections at the sides and at the ends of double-tee units are formed between pairs of plates cast into the slabs and beams. In order to cater for site fixing tolerances, a short, intermediate mild steel bar is placed in the gap between the plates. The diameter of the bar varies from 8 to 20 mm typically, and it is about 100 mm long. A range of dowels is kept on site and the selection is made to suit the circumstances. A fillet weld is made to both sides of the bar using electric arc techniques and electrodes are selected to match the grade of the parent metal, usually grade S275 {43}. Care should be taken not to generate large amounts of heat during the welding operation, particularly at low (<5°C) temperatures, as large thermal changes may cause cracking of the concrete at the ends of the plate. In extreme situations the crack will cause a large triangular piece of the flange to completely break off, thus exposing the plate from below. A small crack reliever – a slot cut into the concrete, or a compressible filler – will prevent such cracking.

The plates used for making welded connections between double-tee slabs and supporting beams are located over the tops of the webs of the slabs. This is the only place they can be located

in cases where the end flanges have been removed for service holes. Because of the need to allow for fairly large tolerances in the length of the slabs, the gap between the plates in the ends of the slabs and the beam may be as great as 30 mm. In this case a specially cut plate is used as the intermediate filler. The welded connection is made at one end of the slab to allow movement to take place between the ends of the slabs. The slabs are fully tied to the frame when the *in situ* structural topping is applied.

10.6 *In situ* Concrete

10.6.1 General specification

The requirements for the preparation, delivery, placement, compaction and curing of *in situ* concrete are given in Section 8 of BS EN 13670:2007 [10.15]. This refers to *in situ* concrete and grout, whether site-batched or delivered to site ready mixed. The following information should be given on the contract drawings and/or in the specification for the frame:

(1) mix specifications
- compressive cube strength at 3 and 28 days
- workability
- aggregate size
- additives

(2) procedures for placement of wet concrete and grout
(3) procedures for placement of dry-pack grout
(4) methods of compaction
(5) dimensional details and deviations
(6) reinforcement details and deviations
(7) formwork striking information
(8) defect assessment information and methods for making good.

In situ concrete can be supported in three ways:

- on permanent shutters (such as precast half-slab, soffit units)
- over beams
- on temporary formwork.

In the case of permanent shutters, these should be tight-fitting one to another and their size should be such that the total area of concrete is supported. Joints should be caulked, particularly if the units form the finished soffit. Permanent shutter units should be examined for cracking or other damage before any wet concrete is placed on them. They may need propping until the concrete is adequately cured. Where props are used they should be installed vertically (or as directed by the manufacturers), and where necessary they should be adequately braced.

The most common use of *in situ* concrete is as 'make-up' to floor units, and as such final dimensions may vary slightly from those shown on the contract drawing. Where major upward variances occur, e.g. in the order of +50 mm in width for 1200 mm-wide floor units, or proportionately less for narrower floor units, the precast contractor should consult the designer about the situation so that any design implications can be assessed.

When formwork is used, it must be of sufficient strength to support its own weight and that of the concrete, together with reinforcement and the weight of any operatives or plant engaged in the work. Temporary formwork should be designed and installed, including for any propping, according to BS EN 12812:2008 [10.16] {BS 5975:2008+A1:2011 [10.17] (2008 is withdrawn), in particular clauses 16.5.6 on precast concrete and 17.5.1 on wind loading}. Note that the National Foreword to BS EN

Figure 10.41 Storage of materials on individual floor units, e.g. 20 sheets of mesh weighing 700 kg, or 1000 kg palettes of cement, should be added to the general construction traffic loading.

12812 warns: *The design methodology within BS EN 12812:2008 is significantly different from that in BS 5975. Technical Committee B/514 advises that caution should be taken when applying BS EN 12812:2008*. It is beyond the scope of this book to discuss the details in these codes further.

The formwork load includes the total mass of concrete and reinforcement of density 2500 kg/m^3 plus the formwork self-weight, and the surcharge from storage and construction traffic, taken as (i) 1.5 kN/m^2 or (ii) the actual weight of the materials stored plus 0.75 kN/m^2 for operatives – see Figure 10.41.

Formwork should be tight-fitting so that grout loss is avoided. Narrow gaps may be filled using foam or other fillers. Gaps wider than 50 mm should be shuttered. Care must be taken when positioning props to support the formwork onto precast components below and with aligned props from there down to the ground. Small components, particularly narrow precast floor units, may not be strong enough to carry even the relatively small reactions from the props. Props should remain until the *in situ* concrete has achieved the necessary strength, as specified on the construction drawings or in the method statement. Props should be installed vertically, with back-propping to a foundation, and where necessary should be braced.

Surface preparation should be cleaned by brushing or air-jets to remove all debris, mortar, oil or other contaminants that could impair bond, in particular at joints.

Concrete should be compacted using a poker vibrator to liberate air until surface bubbles appear. The diameter of the poker should be appropriate to the dimensions of the infill, but is generally not more than 40 mm, or 25 mm if the minimum dimension is less than 200 mm. When using a mobile poker, care should be taken that the power unit is standing on a firm, level base and is operated in accordance with the manufacturer's instructions. Any damage to the precast units during compaction should be noted and an appropriate repair carried out. *In situ* concrete should be protected against rain and direct sunshine, using an appropriate membrane, for a minimum of 12 hours. Ponding using water is not recommended.

Fresh and hardened concrete should be tested according to BS EN 12350 [10.18] and BS EN 12390 [10.14]. Compressive cube strength results (N/mm^2 units), densities, and any unusual failure modes should be made known to both the precast contractor and designer within 24 hours and at the time of removal of the formwork. If the strength of the concrete is less than required, the precast contractor should postpone removal of formwork until further cube test results give strengths in excess of the required value.

10.6.2 Concrete screeds and joint infill in floors

A 'screed' is defined as a non-structural, unreinforced finishing layer, typically as a sand/cement mix or low-strength concrete with small-size coarse aggregate. If thermal or sound proofing is required on top of the precast slab, then the screed need not be in direct contact. A structural topping is a reinforced concrete layer, structurally bonded to the top of the precast slab, with or without interface shear links or dowels, to create an equivalent monolithic composite slab. In the construction sequence, if a structural topping is being used to provide horizontal floor diaphragm action it should be placed before the construction of the second next upper storey is completed, unless temporary horizontal bracing is provided, e.g. horizontal diagonal steel ties. Structural toppings should not be cast onto precast floor units that are themselves less than 14 days of age. Concrete can be delivered to the point of placement by concrete pump, crane and skip, or (for small areas) hoist and wheelbarrow.

Surface finishes produced by the slip-forming or extrusion technique will comply with BS EN 1992-1-1, clause 6.2.5(2) as 'smooth' {BS 8110, Table 5.5 as 'as-extruded' or 'as-cast'} unless tamping, raking or brushing with steel bristles is carried out perpendicular to the direction of casting immediately after casting, so as to comply as 'rough' {'brushed or rough-tamped'}. This is the maximum surface roughness advisable after machine production.

Surface preparation should be stated on the construction drawings. Prior to placing the topping, the surface shall be brushed clean to remove all loose debris, dirt, laitance or any other contaminants. Surface laitance due to cutting of hollow-core slabs, shown in Figure 6.4, should be removed at the factory. The surface of the floor element shall be wetted using approximately 1.5 litres/m^2 [10.19] of potable water, depending on the ambient conditions. The surface should not be allowed to dry out, and free water should be removed.

The reinforcement bars or sheets of mesh will be lapped (inverted nesting) and also lapped to ties projecting from edge beams and walls according to anchorage bond lengths, i.e. at least 40 diameters for welded fabric. Cover spacers should be used elsewhere to raise the reinforcement clear of the precast slab, typically 15 to 20 mm. The cover to the top of the screed must be maintained at all positions, including laps of at least 300 mm, which may mean that at certain places the reinforcement spacing from the precast slabs has to be compromised.

The concrete grade is usually grade C20/25 to C25/30 containing a 10 mm-size aggregate. The three-day cube strengths of the concrete should be at least 10 N/mm^2. The workability should give a slump of between 50 mm and 100 mm. A slump test should be carried out at the point of delivery. Self-compacting concrete may be used, using a flow table for compliance. The wet concrete should be uniformly distributed over the floor area, and should not be piled in excess of about 500 mm high at any point. It should be spread evenly over the floor area as quickly as possible, to within 50 to 75 mm of the specified final level.

The longitudinal joints between hollow-core units and precast half-slab planks, and the milled end slots in hollow-core floor units, should *first* be filled at least 24 hours before the topping is cast. This is to avoid longitudinal cracking of the topping due to differential deflections and camber of the individual units. Care should be taken not to allow laitance to dry on the surface of the units close to the infill. The construction bay widths should generally not be greater than 15.0 m along the span of the floor units and not greater than 6.0 m across the width of the units. The positions of the joints should not be where there are narrow, or small, isolated areas of topping. Mechanical vibrating beams are often used to compact the concrete. The screed may be de-watered and power-floated or

Figure 10.42 Power-floated structural topping onto precast hollow-core floor units. The mesh on the left has not yet been raised into position on cover spacers.

rough-tamped in the usual manner, depending on the nature of the subsequent floor finishes; see Figure 10.42.

Compressive cube strength results are required for all structural concrete. Day joints should be straight, preferably keyed, and have aggregate exposed prior to continuation.

Local shuttering and reinforcement for *in situ* concrete ring beams should be prepared as much as possible as the flooring is being laid, to minimise the time between the completion of the precast and the pouring of the *in situ* concrete. An area of about 1000 m^2 is the recommended maximum area of flooring that should be fixed without *in situ* tie beams being cast.

The longitudinal joints between precast units should be filled using concrete grade C20/25 to C25/30. The floor units should be dampened, without surface ponding, prior to placement of *in situ* concrete. The infill is best poured directly along the joint and swept into the gap using a stiff broom. Mechanical compaction is not often used.

10.6.3 Grouting

Grout is a sand–cement mix – or can be cement only, often with an admixture – and is used in situations where coarse aggregate concrete cannot penetrate. Wet grout may contain an expanding agent and/or a latex bonding agent, which may be added to the mix in accordance with the manufacturer's instructions. Bonding agents may alternatively be applied by painting to cold joint surfaces immediately prior to grouting.

Flowable grout can be cast either by (i) gravity into the annulus between precast elements or cast-in sleeves, e.g. grout tubes in beams and columns, or (ii) pressure from the bottom up. Gravity-fed grout should have a clear gap of at least 5 mm greater than the size of aggregate, or at least 20 mm. The grout should have a slump of at least 100 mm, or else use a self-compacting admixture. In the former, a small tamping rod (12 mm diameter maximum) or similar should be inserted to aid compaction. The operative should calculate the approximate volume of material required and report any variation in the grout consumed. Pressure grouting is best carried out using a grout pump of working pressure of about 1 bar, using a flexible hose connected to the input sleeves. An open vent should be provided

(a)

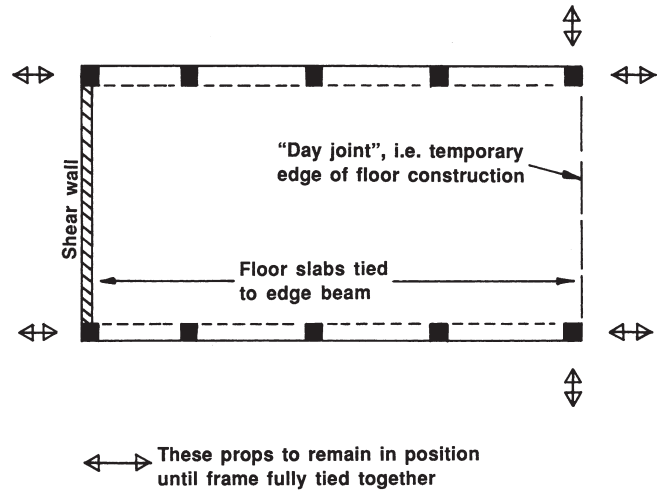

(b)

Figure 10.43 Location of props to maintain temporary stability: (a) positions requiring to be propped; (b) an example of propping retained until tie-restrained wall panel joints are complete (courtesy of Composite Ltd).

at an appropriate height, but not more than about 1 m, above the input hose. A formwork box or otherwise a dam should be formed around the infilling, using foam strips or dry pack to prevent grout loss.

Dry-pack grout should be used in circumstances where it is not possible to place the grout on the soffit or inclined surfaces of a precast component. Grout has a water/cement ratio of about 0.25 to 0.3 and is therefore mouldable in the hand. It should be placed by hand and trowel and hammered into position, which removes free air. It may be either 'structural' or 'non-structural' as above, but it is not possible to make control cubes.

The function of the grout is often identified on the contract drawing as either 'structural grout' or 'non-structural infill'. As well as meaning desirous of strength, the term 'structural' also refers to the protection of precast components or connections in which the integrity of the grout is necessary to ensure correct long-term structural behaviour. Thus strength tests are required for structural grout. The cube strength of the grout should be at least equal to the lesser design strength of the precast components in contact with the grout.

The preparation bed for the dry pack should be cleaned free of debris and mortar. Loose mortar around projected rebars should be chiselled free, and the surfaces made free from obstruction. A backing strip of formwork, or dry-pack mortar, should be made to prevent losses. Access to both internal and external faces of the joint should be possible. After filling the gap the mortar should be pointed off flush with the vertical faces. If dry-pack is used to complete a slab to beam or wall bearing, the dry-pack should be pointed off to give a recess or rake at the edge of the supporting member of at least 15 mm.

Cubes should be manufactured and tested for all dry-pack and grouting operations, according to BS EN 12390, Parts 2 and 3 [10.14]. Proprietary steel moulds should be used (not manufactured on site).

Non-structural infill is often used to complete a fascia, e.g. a vertical joint at a column face, but it is not serving any structural function and need not be subject to such close inspection, nor the strength tests referred to above.

10.7 Handover

As explained in Chapter 8, phased handovers of precast frames take many forms. There is a great temptation with prefabricated construction to allow following trades to move in immediately after the flooring has been fixed. The recommendation is that the precaster should not work directly above other labour, and that the trades who follow should desist until the precast at the next upper floor has been fixed and fully screeded/grouted.

Precast frames are readily released in self-contained and fully stable blocks. However, certain temporary props should be left in position even though the framework is stabilised at some point. Figure 10.43 shows the positions where props should be retained in partially completed frames. For this reason a phased handover should be carefully monitored, because the dominion of the frame is still with the precaster whenever the temporary bracing is present.

Final handover is achieved, of course, when all props and other temporary bracing are removed, and the *in situ* infill has achieved its design strength. The precaster will inspect the precast frame in the company of the engineer and/or architect to agree that the precast work is complete. The 'topping-out' ceremony follows shortly thereafter.

References

Chapter 1

1.1 White, R. B., Prefabrication: A History of its Development in Great Britain, National Building Studies Special Report 36, Ministry of Technology, Building Research Station, UK, 1965.
1.2 Morris, A. E. J., Precast Concrete in Architecture, George Goodwin Ltd, London, 1987.
1.3 Bachmann, H. and Steinle, A., Precast Concrete Structures, Ernst and Sohn GmbH KG, Berlin, Germany, 2011, 260 pp.
1.4 Glover, C. W., Structural Precast Concrete, C. R. Books Ltd, London, 1964.
1.5 National Building Frame Manufacturers' Association, The National Building Frame, UDC 693.9.691.327, undated.
1.6 Diamant, R. M. E., Industrialised Buildings, Iliffe Books Ltd, London, 1965.
1.7 Mokk, L., Prefabricated Concrete for Industrial and Public Buildings, Akademiai Kiado, Budapest, (in Hungarian) 1955, (in English) 1964.
1.8 Nilson, A. H., Design of Prestressed Concrete, 2nd edition, John Wiley, New York, NY, 1987.
1.9 Van Acker, A., Brussels North Skyline Now Dominated by Precast Tower Buildings, Concrete Plant International, Cologne, Germany, No. 5, 2006, pp. 174–182.
1.10 Goodchild, G. H. and Seilen, P., Project Profile, Merchant House and Woodchester House, Publication 97.324, British Cement Association, Crowthorne, 1992.
1.11 Egan, J., Egan Report, Rethinking Construction, Department of the Environment, Transport and the Regions, HMSO, London, 16 July 1998.
1.12 Fédération Internationale de la Précontrainte, FIP Recommendations, Design of Multi-Storey Precast Concrete Structures, Thomas Telford, London, 1986.
1.13 Lewicki, B., Building with Large Prefabricates, Elsevier, London, 1966.
1.14 Sarja, A., Industrialised Building Technology as a Tool for the Future International Building Market, Concrete Precasting Plant and Technology, B + FT, Vol. 58, No. 11, Nov. 1992, pp. 35–43.
1.15 Wilson, J. G., Exposed Concrete Finishes, vol. 1 & 2, CR Books, London, 1962 & 1964.
1.16 Monks, W., Appearance Matters, Nos 1 to 9, Cement and Concrete Association, Wexham Springs, Slough, Publication 47-101 to 47-109, 1985.
1.17 Taylor, H. P. J., Precast Concrete Cladding, Edward Arnold, London, 1992.
1.18 AMA Research Ltd., Precast Concrete Building Products Market UK 2007–2010, AMA Research Ltd., Gloucester, UK. GL50 1TY.
1.19 Precast Concrete Strategic Group, Precast Concrete Study Summary Report, Arup Economic Consultants, London, November 1989.
1.20 Van Acker, A., General Introduction, Prefabrication of Concrete Structures, International Seminar, Delft University of Technology, Delft University Press, Oct. 1990, pp. 7–12.
1.21 Scott, N., Precast Prestressed Concrete Beyond Year 2000 in the United States, Concrete Precasting Plant and Technology, B + FT, Vol. 60, No. 7, July 1994, pp. 46–58.
1.22 Elliott, K. S. and Filipowicz, S., High Specification Precast Concrete Structures, Proc. X11 Congress, PCI/FIP '94, Washington DC.
1.23 Elliott, K. S., The Design of Modern Precast Concrete Multi-storey Framed Structures in The United Kingdom, PCI Journal, Vol. 37, No. 3, May/June 1992, pp. 32–47.
1.24 Elliott, K. S., Precast Concrete Structures, Butterworth-Heinemann, Oxford, UK, 2002, 380 pp.
1.25 Goodchild, C., Webster, R. M. and Elliott, K. S., Economic Concrete Frame Elements to Eurocode 2, The Concrete Centre, Camberley, UK, 2009, 182 pp.
1.26 Elliott, K. S., Precast Concrete Structures – the Semi-Rigid Approach, Concrete, Vol. 39, No. 1, 2005, pp. 26–28.
1.27 Brigginshaw, G., A New Era for Structural Frames, Concrete, Vol. 21, No. 10, 1987, pp. 6–9.

Multi-storey Precast Concrete Framed Structures, Second Edition. Kim S. Elliott and Colin K. Jolly.

1.28 Precast Concrete Frames Association, Frames for Multi-Storey Buildings – An Economic Comparison, British Precast, Leicester, 1985.
1.29 Cholewicki, A. and Elliott, K. S., Diaphragm Action of Hollow-Cored Floors, Part 2 – Experimental Work, Betonwerk und Fertigteil-Technik, Vol. 65, No. 3, 1999, pp. 61–68.
1.30 Elliott, K. S. and Cholewicki, A., Diaphragm Action in Precast Concrete Hollow Cored Floor Slabs, Betonwerk und Fertigteil-Technik, Vol. 64, No. 11, 1998, pp. 76–90.
1.31 Bruggeling, A. S. G. and Huyghe, G. F., Prefabrication with Concrete, Balkema, Rotterdam, 1991, 380 pp.
1.32 Precast Concrete Industry Training Association, Code of Practice for the Safe Erection of Precast Concrete, British Precast, 60 Charles Street, Leicester, UK, March 2013.
1.33 Structural Products Association, Safe Erection of Precast Concrete Frameworks, 3rd edition, British Precast, Leicester, 2010.
1.34 Precast Flooring Federation, Code of Practice for Safe Installation of Precast Concrete Flooring and Associated Components, 3rd edition, British Precast, Leicester, 2010.
1.35 Tremi, S., The New RAI Technical Telecommunications Centre, Rome, Concrete Precasting Plant and Technology, B + FT, Vol. 60, No. 5, May 1994, pp. 67–82.

Chapter 2

2.1 *fib*. Website: http://fib.epfl.ch
2.2 Fédération Internationale du Béton (*fib*), Model Code 2010 – First complete draft, Vol. 1, April 2010, 318 pp.
2.3 Fédération Internationale du Béton (*fib*), Model Code 2010 – First complete draft, Vol. 2, May 2010, 312 pp.
2.4 Fédération Internationale du Béton (*fib*), Structural Concrete Textbook on Behaviour, Design and Performance, Volume 1: Design of Concrete Structures, Conceptual Design, Materials, 2nd edition, *fib*, Lausanne, Switzerland, November 2009, 306 pp.
2.5 FIP Recommendations, Planning and Design of Precast Concrete Structures, FIP Commission on Prefabrication, SEKO, Institution of Structural Engineers, London, May 1994.
2.6 Elliott, K. S. and Tovey, A., Precast Concrete Frame Buildings – A Design Guide, British Cement Association, Wexham Springs, Slough, May 1992, 88 pp.
2.7 British Standards Institution, BS 8110-1:1997, Structural Use of Concrete – Part 1: Code of Practice for Design and Construction, BSI, London, August 2007.
2.8 British Standards Institution, BS EN 1990:2002, Eurocode 0: Basis of Structural Design, BSI, London, March 2006.
2.9 British Standards Institution, BS EN 1991-1-1:2002, Eurocode 1: Actions on Structures – Part 1-1: General Actions – Densities, Self-Weight, Imposed Loads for Buildings, BSI, London, December 2004.
2.10 British Standards Institution, BS EN 1991-1-2:2002, Eurocode 1: Actions on Structures – Part 1-2: General Actions – Actions on Structures Exposed to Fire, BSI, London, December 2004.
2.11 British Standards Institution, BS EN 1991-1-3:2003, Eurocode 1: Actions on Structures – Part 1-3: General Actions – Snow Loads, BSI, London, June 2007.
2.12 British Standards Institution, BS EN 1991-1-4:2005 +A1:2010, Eurocode 1: Actions on Structures – Part 1-4: General Actions – Wind Actions, BSI, London, January 2010.
2.13 British Standards Institution, BS EN 1991-1-5:2003, Eurocode 1: Actions on Structures – Part 1-5: General Actions – Thermal Actions, BSI, London, December 2004.
2.14 British Standards Institution, BS EN 1991-1-6:2005, Eurocode 1: Actions on Structures – Part 1-6: General Actions – Actions during Execution, BSI, London, June 2005.
2.15 British Standards Institution, BS EN 1991-1-7:2006, Eurocode 1: Actions on Structures – Part 1-7: General Actions – Accidental Actions, BSI, London, July 2006.
2.16 British Standards Institution, BS EN 1991-2:2003, Eurocode 1: Actions on Structures – Part 2: Traffic Loads on Bridges, BSI, London, December 2004.
2.17 British Standards Institution, BS EN 1991-3:2006, Eurocode 1: Actions on Structures – Part 3: Actions induced by Cranes and Machinery, BSI, London, July 2006.
2.18 British Standards Institution, BS EN 1991-4:2006, Eurocode 1: Actions on Structures – Part 4: Silos and Tanks, BSI, London, June 2006.
2.19 British Standards Institution, BS EN 1992-1-1:2004, Eurocode 2: Design of Concrete Structures – Part 1-1: General Rules and Rules for Buildings, BSI, London, December 2004.
2.20 British Standards Institution, BS EN 1992-1-2:2004, Eurocode 2: Design of Concrete Structures – Part 1-2: General Rules – Structural Fire Design, BSI, London, December 2004.
2.21 British Standards Institution, BS EN 13369:2013, Common rules for precast concrete products, BSI, London, April 2013.
2.22 British Standards Institution, BS EN 1168+A3, 2011, Precast concrete products – Hollow-Core Slabs, BSI, London, 2005.

2.23 British Standards Institution, BS EN 13747:2005, Precast concrete products – Floor Plates for Floor Systems, BSI, London, 2010.
2.24 British Standards Institution, BS EN 15037-1, Precast concrete products – Beam-and-Block Flooring, BSI, London, 2008.
2.25 British Standards Institution, BS EN 13224:2004, Precast concrete products – Ribbed Floor Elements, BSI, London, 2004.
2.26 British Standards Institution, BS EN 13225:2004, Precast concrete products – Linear Structural Elements, BSI, London, 2004.
2.27 British Standards Institution, BS EN 14843, 2007, Precast Concrete Products – Staircases, BSI, London, 2007.
2.28 British Standards Institution, BS EN 14992:2007, Precast Concrete Products – Wall Elements, BSI, London, 2007.
2.29 British Standards Institution, BS EN 13670:2009, Execution of Concrete Structures, BSI, London, 2009.
2.30 British Standards Institution, PD 6687:2010, Background Paper to the UK National Annexes to BS EN 1992-1 and BS EN 1992-3, BSI, London, 2010.
2.31 CONSTRUCT Concrete Structures Group, National Structural Concrete Specification Edition 4:2010, NSCS-4, The Concrete Centre, Camberley, UK, April 2010, 123 pp.
2.32 Institution of Structural Engineers, Structural Joints in Precast Concrete: Manual, IStructE, London, August 1978, 56 pp.
2.33 Fédération Internationale du Béton (*fib*), Bulletin 43, Structural Connections for Precast Concrete Buildings, Guide to Good Practice, February 2008, 370 pp.
2.34 The Prestressed Concrete Institute, Design and Typical Details of Connections for Precast and Prestressed Concrete, 2nd edition, PCI, Chicago, 1988.
2.35 Prestressed Concrete Institute, Design Handbook, 7th edition, PCI, Chicago, IL, 2010.
2.36 FIP Recommendations, Precast Prestressed Hollow-Core Floors, FIP Commission on Prefabrication, Thomas Telford, London, 1988, 31 pp.
2.37 Fédération Internationale du Béton (*fib*), Bulletin 6, Special Design Considerations for Precast Prestressed Hollow-Core Floors, Guide to Good Practice, 2000, 180 pp.
2.38 Study Group of the New Zealand Concrete Society, Guidelines for the Use of Structural Precast Concrete in Buildings, Study Group of the New Zealand Concrete Society, and National Society of Earthquake Engineering, Christchurch, New Zealand, 1991, 174 pp.
2.39 The Concrete Centre, Precast Concrete in Buildings: A Guide to Design and Construction, The Concrete Centre, Camberley, UK, January 2008.
2.40 Goodchild, C. H., Hybrid Concrete Construction, Reinforced Concrete Council, (former British Cement Association), Camberley, UK, 1995, 64 pp.
2.41 Fédération Internationale du Béton (*fib*), Bulletin 43, Precast Concrete in Mixed Construction, State-of-art Report, 2002, 68 pp.
2.42 Narayanan, R. S., Precast Eurocode 2: Design Manual for the Design of Precast Concrete Building Structures to BS EN1992-1-1:2004 and the UK National Annex:2005, British Precast, Leicester, 2007, 93 pp.
2.43 Narayanan, R. S., Precast Eurocode 2: Worked Examples, British Precast, Leicester, 2008, 76 pp.
2.44 Bond, A. J. et al., How to Design Concrete Structures using Eurocode 2, The Concrete Centre, Camberley, UK, 2006, 98 pp.
2.45 Institution of Structural Engineers, Manual for Designing Concrete Building Structures to Eurocode 2, Institution of Structural Engineers, London, UK, 2006, 141 pp.
2.46 Goodchild, C., Webster, R. M. and Elliott, K. S., Economic Concrete Frame Elements to Eurocode 2, The Concrete Centre, Camberley, UK, 2009, 182 pp.
2.47 Sheppard, D. A. and Phillips, W. R., Plant-Cast Precast and Prestressed Concrete, 3rd edition, McGraw-Hill, New York, NY, 1989.
2.48 Haas, A. M., Precast Concrete Design and Application, Applied Science Publishers, London, 1983.
2.49 Bachmann, H. and Steinle, A., Precast Concrete Structures, Ernst and Sohn GmbH KG, Berlin, Germany, 2011, 260 pp.
2.50 Bljuger, F., Design of Precast Concrete Structures, Ellis Horwood, Chichester, 1988.
2.51 Levitt, M., Precast Concrete, Applied Science Publishers, London, 1982.
2.52 Levitt, M., Precast Concrete Materials, Manufacture, Properties and Usage, Routledge, London, September 2007.
2.53 Kromer, R., Tammer Elementti – A Nearly Automated Precast Works, Concrete Precasting Plant and Technology, B + FT, Vol. 58, No. 3, March 1992, pp. 166–180.
2.54 Richardson, J. G., Precast Concrete Construction, Cement and Concrete Association, London, 1973.
2.55 Richardson, J. G., Quality in Precast Concrete: Design – Production – Supervision, Longmans, Harlow, 1991.
2.56 National Precast Concrete Association of Australia and Concrete Institute of Australia, Precast Concrete Handbook, NPCAA, 8–10 Palmer Street, North Parramatta, NSW, 2002.
2.57 PCI Secretariat, 209 West Jackson Boulevard, Chicago, Illinois 60606-6938, USA.

2.58 FIP Secretariat, The Concrete Society, Riverside House, 4 Meadows Business Park, Station Approach, Blackwater, Camberley, GU17 9AB.
2.59 Department of Environment and CIRIA, The Stability of Precast Concrete Structures, Seminar, London, 1973.
2.60 Prefabrication of Concrete Structures, International Seminar, Delft University of Technology, Delft University Press, Delft, The Netherland, Oct. 1990.
2.61 Noteworthy Developments in Prestressed and Precast Concrete, Singapore, November 1989.
2.62 Institute of Engineers Malaysia, Trends, Innovation and Performance of Prestressed and Precast Concrete, Institute of Engineers Malaysia, Kuala Lumpur, May 1993.
2.63 Website: http://ukfib.concrete.org.uk/publications.asp.
2.64 Elliott, K. S. and Van Acker, A., Best Practice in Precast Concrete Structures and Materials for Industrialised Building Systems, Malaysian Construction Research Journal, Vol. 11, No. 2, November 2012, pp. 1–20.

Chapter 3

3.1 Building Research Establishment, Some Recent Work at the Building Research Establishment, Concrete Plant and Production, July/August 1993, p. 104.
3.2 Evans, B., Underfloor Heating and Cooling, Architect's Journal, Vol. 30, August 1993, pp. 40–41.
3.3 Strangbetong, A. B., TermoDeck, P O Box 5074, S 131 05, Nacka, Sweden, 1995.
3.4 Website: http://eco-structures.net/performance.html (sourced January 2011).
3.5 Website: http://www.precastfloors.info/news/press-precastfloors.html.
3.6 Bailey, C. G. and Lennon, T., Full-Scale Fire Tests on Hollow-Core Floors, The Structural Engineer, Vol. 86, 18 March 2008, pp. 33–39.
3.7 Ergon, P., Système de Construction Ergon, Marnixdreef, B-2500 Lier, Belgium, May 2012.
3.8 Fédération Internationale du Béton, (*fib*), Bulletin 43, Precast Concrete in Mixed Construction, State-of-art Report, 68, pp. 2002.
3.9 Vambersky, J. N. J. A., VNO/NCW Office Building, The Hague, Netherlands, FIP Notes, Vol. 2, 1996, pp. 15–18.
3.10 Lam, D., Elliott, K. S. and Nethercot, D. A., Push-off Tests on Shear Studs with Hollow-Cored Floor Slabs, The Structural Engineer, Vol. 76, No. 9, 1998, pp. 167–174.
3.11 Lam, D., Elliott, K. S. and Nethercot, D. A., Experiments on Composite Steel Beams with Precast Concrete Hollow-Core Floor Slabs, Proc. Inst. of Civil Engineers Structures and Building, Vol. 140, May 2000, 127–138.
3.12 Lam, D., Elliott, K. S. and Nethercot, D. A., Designing Composite Steel Beams with Precast Concrete Hollow-Core Floor Slabs, Proc. Inst. of Civil Engineers Structures and Building, Vol. 140, May 2000, 139–149.
3.13 Lam, D., Elliott, K. S. and Nethercot, D. A., Parametric Study on Composite Steel Beams with Precast Concrete Hollow-Cored Floors, Journal of Constructional Steel Research, Vol. 54, 2000, pp. 283–304.
3.14 Evans, B., Prefabricating the Superstructure, Architects' Journal, London, 16 June 1993, pp. 41–52.

Chapter 4

4.1 Elliott, K. S. and Tovey, A., Precast Concrete Frame Buildings – A Design Guide, British Cement Association, Wexham Springs, Slough, May 1992, 88 pp.
4.2 Prestressed Concrete Institute, PCI Architectural Precast Concrete Manual, 3rd edition, PCI, Chicago, IL, 2007.
4.3 Raths, C. H., Spandrel Beam Behaviour and Design, PCI Journal, Vol. 29, March–April 1984, pp. 62–131.
4.4 British Standards Institution, BS EN 1992-1-1, Eurocode 2: Design of Concrete Structures – Part 1-1: General Rules and Rules for Buildings Code of Practice for Dead and Imposed Loads, BSI, London, 2004.
4.5 British Standards Institution, BS 8110-1, Part 1: Code of Practice for Design and Construction, BSI, London, 1997.
4.6 Building Research Establishment, Design of Normal Concrete Mixes, 2nd edition, B. R. E., Watford, UK, 1997, 42 pp.
4.7 British Standards Institution, BS EN 206-1:2000, Concrete – Specification, Performance, Production and Conformity, BSI, London, 2001.
4.8 British Standards Institution, BS EN 934-1:2008, BS EN 934-2:2009+A1:2012 and BS EN 934-3:2009+A1:2012, Admixtures for Concrete, Mortar and Grout, BSI, London, 2009.
4.9 British Standards Institution, BS EN 206-9:2010, Concrete – Additional Rules for Self-Compacting Concrete, BSI, London, 2010.
4.10 British Standards Institution, BS EN 10080:2005, Steel for the Reinforcement of Concrete, BSI, London, 2005.
4.11 British Standards Institution, BS EN ISO 3766:2003, Construction Drawings – Simplified Representation of Concrete Reinforcement, BSI, London, 2004.
4.12 British Standards Institution, BS 6744:2001, Stainless Steel Bars for the Reinforcement of and Use in Concrete, BSI, London, 2001.

4.13 British Standards Institution, BS 4483:2005, Steel fabric for the reinforcement of concrete. Specification, BSI, London, 2005.
4.14 British Standards Institution, BS EN 10138-1. Prestressing Steels – General Requirements, in draft for technical review in 2012.
4.15 British Standards Institution, BS EN 1168+A3:2011, Precast Concrete Products – Hollow-Core Slabs, BSI, London, 2005.
4.16 Institution of Structural Engineers, Structural Joints in Precast Concrete: Manual, IStructE, London, August 1978.
4.17 British Standards Institution, BS 5400 Part 2: Steel, concrete and composite bridges: Part 2 – Specification for loads, British Standards Institution, London, 1978.
4.18 British Standards Institution, BS EN 1991-1-5. Eurocode 1: Actions on structures – Part 1-5: Actions on Structures – Thermal actions, British Standards Institution, London, 2003.
4.19 CERIB, Precast Concrete Safety Factors, European Research Final Report, Contract SMT4 CT98 2276, CERIB, Paris, July 2002.
4.20 British Standards Institution, BS EN 13369:2013, Common Rules for Precast Concrete Products, BSI, London, April 2013.
4.21 Mayfield, B., Davies, G. and Kong, F. K., Some Tests on the Transmission Length and Ultimate Strength of Pretensioned Concrete Beams Incorporating Dyform Strand, Magazine of Concrete Research, Vol. 22, No. 73, Dec. 1970, pp. 219–226.
4.22 Kong, P., Transfer of prestress by prestressed wire tendons, MEng thesis, Curtin University, Perth, Australia, 1993.
4.23 Institution of Structural Engineers, Manual for the Design of Reinforced Concrete Building Structures to Eurocode 2, Institution of Structural Engineers, London, 2006.
4.24 British Standards Institution, BS6399-1, Loadings for buildings: Part 1 – Code of Practice for Dead and Imposed Loads, BSI, London, 1996.
4.25 Adlparvar, M. R., Torsional Behaviour of Precast Concrete Beans and Connections, MPhil thesis, University of Nottingham, 1993.
4.26 Elliott, K. S., Davies, G. and Adlparvar, R. M., Torsional Behaviour of Joints and Members in Precast Concrete Structures, Magazine of Concrete Research, Vol. 164, Sept 1993, pp. 157–168.
4.27 Calavera, J., Calculo, construccion, patologia y rehabiliacion de forjados de edificacion, (Calculation, construction, pathology and rehabilitation of buildings), 5th edition, INTEMAC S.A., Instituto Technico de Materiales Y Construcciones, 28022 Madrid, Spain, 2003, 1008 pp.
4.28 Mitchell, D. and Marcakis, K., Precast Concrete Connections with Embedded Steel Inserts, PCI Journal, Vol. 25, 1980, pp. 88–116. Chicago, USA, July.
4.29 Holmes, M. and Posner, C. D., The Connection of Precast Concrete Structural Members, CIRIA Report 28, London, Feb. 1971.
4.30 Cook, W. D. and Mitchell, D., Studies of Disturbed Regions near Discontinuities in Reinforced Concrete Members, ACI Structural Journal, Vol. 85, March 1988, pp. 206–216.
4.31 Martin, L. D. and Korkosz, W. J., Connections for Precast Prestressed Concrete Buildings, including Earthquake Resistance, The Consulting Engineers Group, Inc., Illinois 60025, March 1982, 285 pp.
4.32 Prestressed Concrete Institute, Design and Typical Details of Connections for Precast and Prestressed Concrete, 2nd edition, PCI, Chicago, IL, 1990.
4.33 Beeby, A. W., Short-term Deformations of Reinforced Concrete Members, Technical Report 42.408, Cement and Concrete Association, Wexham Springs, Slough, 1968.
4.34 Clark, L. A. and Thorogood, P., Serviceability Behaviour of Reinforced Concrete Half-Joints, The Structural Engineer, Vol. 66, No. 18, September 1988, pp. 295–302.
4.35 Mattock, A. H. and Chan, T. C., Design and Behaviour of Dapped-end Beams, PCI Journal, Vol. 24, No. 6, 1979, pp. 28–45.
4.36 Windisch, A., Strut-Crack-and-Tie Model in Structural Concrete, Structural Concrete, IABSE Colloquium, Stuttgart, 1991, pp. 539–544.
4.37 Noor, R., Steel Fibre Reinforced Precast Concrete Half-Joints, PhD thesis, University of Nottingham, 2009.
4.38 Noor, R. and Elliott, K. S., Behaviour of Steel Fibre Self-Compacting Concrete under Biaxial Compression Loading, Proceedings of 5th International Symposium of Self-Compacting Concrete, Ghent, Belgium, 3–5 September 2007.
4.39 Mitchell, D. and Cook, W. D., Design of Disturbed Regions, Structural Concrete, IABSE Colloquium, Stuttgart, 1991, pp. 533–538.
4.40 Ife, J. S., Uzumeri, S. M. and Huggins, M. W., Behaviour of the 'Cazalay Hanger' Subjected to Vertical Loading, PCI Journal, Vol. 13, No. 6, 1968, pp. 48–66.
4.41 Elliott, K. S., Davies, G. and Mahdi, A. A., Semi-rigid Joint Behaviour on Columns in Precast Concrete Buildings, COST C1 Proceedings of the First State-of-the-Art Workshop, Semi-rigid Behaviour of Civil Engineering Structural Connections, ENSAIS, Strasbourg, Oct. 1992, pp. 282–295.

4.42 Mahdi, A. A., Moment Rotation Effects on the Stability of Columns in Precast Concrete Structures, PhD thesis, University of Nottingham, 1992.
4.43 Cranston, W., Analysis and Design of Reinforced Concrete Columns, Research Report 20, Cement and Concrete Association, Wexham Springs, Slough, Aug. 1972.

Chapter 5

5.1 British Standards Institution, BS EN 1992-1-1, Eurocode 2: Design of Concrete Structures – Part 1-1: General Rules and Rules for Buildings, BSI, London, December 2004.
5.2 British Standards Institution, BS 8110-1, Part 1: Code of Practice for Design and Construction, BSI, London, 1997.
5.3 Institution of Structural Engineers, Structural Joints in Precast Concrete: Manual, IStructE, London, August 1978.
5.4 Elliott, K. S. and Tovey, A., Precast Concrete Frame Buildings – A Design Guide, British Cement Association, Wexham Springs, Slough, May 1992, 88 pp.
5.5 FIP Recommendations, Precast Prestressed Hollow-Core Floors, FIP Commission on Prefabrication, Thomas Telford, London, p. 31, 1988.
5.6 Fédération Internationale du Béton (FIB), Bulletin 6, Special Design Considerations for Precast Prestressed Hollow-Core Floors, CEB-FIP Guide to Good Practice, Lausanne, Switzerland, 2000, 180 pp.
5.7 British Standards Institution, BS EN 13369:2013, Common Rules for Precast Concrete Products, BSI, London, April 2013.
5.8 British Standards Institution, BS EN 1168+A3,2011, Precast Concrete Products – Hollow-Core Slabs, BSI, London, 2005.
5.9 British Standards Institution, BS EN 13747:2005, Precast Concrete Products – Floor Plates for Floor Systems, BSI, London, 2010.
5.10 British Standards Institution, BS EN 15037-1, Precast Concrete Products – Beam-and-Block Flooring, BSI, London, 2008.
5.11 British Standards Institution, BS EN 13224:2004, Precast Concrete Products – Ribbed Floor Elements, BSI, London, 2004.
5.12 Narayanan, R. S., Precast Eurocode 2: Worked Examples, British Precast, Leicester, 2008, 76 pp.
5.13 Prestressed Concrete Institute, Manual for the Design of Hollow-Core Slabs, 2nd edition, PCI, Chicago, USA, 1998.
5.14 Walraven, J. C. and Mercx, W., The Bearing Capacity of Prestressed Hollow-Core Slabs, Heron, 28, No. 3, University of Delft, Netherlands, 1983, 46 pp.
5.15 Johnsson, E., Shear Capacity of Prestressed Extruded Hollow-Core Slabs, Nordic Concrete Research, Vol. 7, Oslo, 1988, pp. 27–31.
5.16 Pajari, M., Load-Carrying Capacity of Prestressed Hollow-Core Slabs, Nordic Concrete Research, Vol. 7, Oslo, 1988, pp. 232–249.
5.17 Pisanty, A., The Shear Strength of Extruded Hollow-Core Slabs, Materials and Structures, 25, 1992, pp. 224–230.
5.18 Juvas, K., The Workability of No-Slump Concrete for Use in Hollow-Core Slabs, Nordic Concrete Research, Vol. 6, The Nordic Concrete Federation, Oslo, 1987, pp. 121–130.
5.19 Den Uijl, J. A., Bond Properties of Strands in Connection with Transmission Zone Cracks, Concrete Precasting Plant and Technology, B + FT, Vol. 51, No 1, Jan. 1985.
5.20 Van Acker, A., Transversal distribution of linear loadings in prestressed hollow-core floors, Calgary Symposium, Fédération Internationale de la Précontrainte, 1984.
5.21 Lundgren, K., Broo, H. and Engström, B., Analysis of hollow-core floors subjected to shear and torsion, Structural Concrete, Vol. 5, No. 4, Thomas Telford, April 2004, pp. 161–172.
5.22 Venkateswarlu, B. *et al.*, Roof and floor slabs assembled with precast concrete hollow-cored units, ACI Journal, Vol. 79, No. 6, January 1982, pp. 50–55.
5.23 Stanton, J., Proposed Design Rules for Load Distribution in Precast Concrete Decks, ACI Structural Journal, Vol. 84, No. 5, Sept.–Oct. 1987, pp. 371–382.
5.24 Aswad, A. and Jacques, F. J., Behaviour of Hollow-Core Slabs Subject to Edge Loads, PCI Journal, Vol. 37, No. 2, March–April 1992, pp. 72 –84.
5.25 FIP, FIP Technical Report, Design Principles for Hollow-Cored Slabs Regarding Shear and Transverse Load Capacity, FIP Commission on Prefabrication, Wexham Springs, Slough, 1982.
5.26 Bernardi, P., Cerioni, R., Garutti, N., Michelini, E. and Non-Linear, A., Approach for the Analysis of Hollow-Core Floors with Large Openings – Part 1, Concrete Plant International, Cologne, Germany, No. 2, April 2012, pp. 166–171.
5.27 Bernardi, P., Cerioni, R., Garutti, N., Michelini, E. and Non-Linear, A., Approach for the Analysis of Hollow-Core Floors with Large Openings – Part 2, Concrete Plant International, Cologne, Germany, No. 2, April 2012, pp. 144–149.

5.28 Pajari, M., Shear-torsion Tests on 400 mm Hollow-Core Floor, VTT Research Notes 2274, Espoo, Finland, 2004.
5.29 Suikka, A. and Parkkinen, I., Load Distribution in 400 mm Deep Hollow-Core Floors, Proceedings of IECA Conference, Paris, 1991.
5.30 Mosley, W., Bungay, J. and Hulse, R., Reinforced concrete design to Eurocode 2, Palgrave Macmillan, 2007, 408 pp.
5.31 O'Brien, E., Dixon, A. and Sheils, E., Reinforced and prestressed concrete design to EC2 – The complete process, Spon, 2012, 524 pp.
5.32 Kong, F. K. and Evans, R. H., Reinforced and prestressed concrete, 3rd edition, Van Nostrand, 1987, 508 pp.
5.33 British Standards Institution, BS 5896, Specification for High-Tensile Steel Wire and Strand for the Prestressing of Concrete, 1980.
5.34 British Standards Institution, BS EN 10138-1, Prestressing Steels – General Requirements; EN 10138-2, Prestressing Steels – Wire; EN 10138-3, Prestressing Steels – Strand – Bars. 2006. All in draft.
5.35 Association of Manufacturers of Prestressed Hollow-Core Floors, Hollow-Core Floor Design and Applications, Manual 1st edition, ASSAP, Verona, 2002.
5.36 Girhammer, U. A., Design Principles for Simply Supported Prestressed Hollow-Core Slabs, Structural Engineering Review, Oxford, Vol. 4, No. 4, 1992, pp. 301–316.
5.37 ACI, Standard 318-89, Building Code Requirements for Reinforced Concrete, American Concrete Institute, Detroit, 1989.
5.38 Vecchio, F. J. and Collins, M. P., The Modified Compression Field Theory for Reinforced Concrete Elements Subjected to Shear, ACI Journal, Proceedings, Vol. 83, No. 2, 1986, pp. 219–231.
5.39 Araujo, C. A. M., Loriggio, D. D. and Da Camara, J. M. M. N., Anchorage Failure and Shear Design of Hollow-core Slabs, Structural Concrete, Journal of FIB, Vol. 12, No. 2, 2011, pp. 109–119.
5.40 Bertagnoli, G. and Mancini, G., Failure Analysis of Hollow-core Slabs Tested in Shear, Structural Concrete, Journal of FIB, Vol. 10, No. 3, 2009, pp. 139–152.
5.41 Collins, M. P., Mitchell, D., Adebar, P. and Vecchio, F. J., A General Shear Design Method, ACI Journal, Proceedings, Vol. 93, No. 1, 1996, pp. 36–45.
5.42 Lin, Y., Design of Prestressed Hollow-Core Slabs with Reference to Web Shear Failure, Journal of Structural Engineering, ASCE, Vol. 120, No. 9, September 1994, pp. 2675–2696.
5.43 Palmer, K. D. and Schultz, A. E., Experimental Investigation of the Web-shear Strength of Deep Hollow-Core Units, PCI Journal, Vol. 56, No. 4, Fall 2011, pp. 84–104.
5.44 Logan, D. R., Discussion to reference [5.12], PCI Journal, Vol. 57, No. 3, Summer 2012, pp. 132–134.
5.45 Russell, B. W. *et al.*, Measurement of Transfer Lengths on Pretensioned Concrete Elements, Journal of Structural Engineering, Vol. 123 (5), May 1997, pp. 541–549.
5.46 Oh, B. H. and Kim, E. S., Realistic Evaluation of Transfer Lengths in Pretensioned Prestressed Concrete Members, ACI Structural Journal, Vol. 97, No. 6, Nov.–Dec. 2000, pp. 821–830.
5.47 Akesson, M., Fracture Mechanics Analysis of the Transmission Zone in Prestressed Hollow-Core Slabs, Publication 93.5, Chalmers University of Technology, Göteborg, Sweden, 1993, 62 pp.
5.48 Tassi, G., Bond Properties of Prestressing Strands, Proceedings of FIP Symposium, Jerusalem, Israel, 1988, 8 pp.
5.49 Gylltoft, K., Bond Properties of Strand in Fatigue Loading, Research Report TULEA 1979:22, Lulea University of Technology, Lulea, Sweden, 1979, 73 pp.
5.50 Kong, P. Y. L., Transfer of Prestress by Pretensioned Wire Tendons, MSc thesis, School of Civil Engineering, Curtin University of Technology, Australia, 1993, website http://espace.library.curtin.edu.au.
5.51 FIP, Quality Assurance of Hollow-Core Slab Floors, Guide to Good Practice, 1992.
5.52 Evans, R. H. and Robinson, G. W., Bond Stress in Prestressed Concrete from X-ray Photographs, Proc. ICE, part 1, Vol. 4, No. 2, 1955, pp. 212–235.
5.53 Concrete Society, Technical Report 43: Post-Tensioned Concrete Floors – Design Handbook, 2nd edition, The Concrete Society, Camberley, UK, 2005.
5.54 Barney, G. B., Corley, W. G., Hanson, J. M. and Parmelee, R. A., Behaviour and Design of Prestressed Concrete Beams with Large Web Openings, PCI Journal, Vol. 22, No. 6, Nov.–Dec. 1977, pp. 32–60.
5.55 Adus, S. S. and Harrop, J., Prestressed Concrete beams with Circular Holes, ASCE Journal of the Structural Division, Vol. 105, No. 3, March 1979, pp. 635–652.
5.56 Savage, J., Tadros, M., Einea, A. and Fischer, L., Precast Prestressed Concrete Double Tees with Web Openings, Proc. X11 Congress, PCI/FIP '94, Washington DC, 1994, pp. C48–C54.
5.57 Land, H., Precast Concrete Floors, Special Points on Section Values Determination – Design and Construction, Part 1, Concrete Precasting Plant and Technology, BFT, Vol. 60, No. 5, May 1994, pp. 93–95.
5.58 Land, H., Precast Concrete Floors, Special Points on Section Values Determination – Design and Construction, Part 2, Concrete Precasting Plant and Technology, BFT, Vol. 60, No. 6, June 1994, pp. 108–118.
5.59 British Standards Institution, BS EN 1993-1-1, Eurocode 3: Design of Steel Structures – Part 1-1: General Rules and Rules for Buildings, BSI, London, September 2006.

5.60 EN, 12354-1:2000, Building Acoustics – Estimation of Acoustic Performance in Buildings from the Performance of Elements: Airborne Sound Insulation between Rooms. BSI, London, July 2000.
5.61 International Organization for Standardization, ISO 6946:2007, Building Components and Building Elements – Thermal Resistance and Thermal Transmittance: Calculation Method, BSI, London, 2007.
5.62 International Organization for Standardization, ISO 10456:2007, Building Materials and Products – Hygrothermal Properties: Tabulated Design Values and Procedures for Determining Declared and Design Thermal Values, BSI, London, 2007.

Chapter 6

6.1 British Standards Institution, BS EN 1992-1-1, Eurocode 2: Design of Concrete Structures, Part 1-1: General Rules and Rules for Buildings – Code of Practice for Dead and Imposed Loads, BSI, London, 2004.
6.2 British Standards Institution, BS 8110-1, Part 1: Code of Practice for Design and Construction, BSI, London, 1997.
6.3 British Standards Institution, BS EN 13747:2005, Precast Concrete Products – Floor Plates for Floor Systems, BSI, London, 2010.
6.4 FIP Recommendations, Shear at the Interface of Precast and *In Situ* Concrete, Fédération Internationale de la Précontrainte, Wexham Springs, Slough, Jan. 1982, 31 pp.
6.5 Vesa, M., Shear Strength at the Interface between Topping and Concrete Element, Helsinki Technical University, 1979, 96 pp.
6.6 Gustavsson, K., Shear at the Interface – Tests on T-slabs with Thin Top Layers, FIP Commission on Prefabrication, Lulea, Sweden, June 1980, 7 pp.
6.7 Ibrahim, I., Behaviour of Precast Concrete Hollow-Core Units with Structural Topping, PhD thesis, University of Nottingham, 2008.
6.8 Elliott, K. S. and Ibrahim, I., Composite Construction in Prestressed Precast Concrete Floors, CONCET 2006, 9th International Conference on Concrete Engineering, Kuala Lumpur, Malaysia, Institution of Engineers Malaysia, Sept. 2006, pp. 104–116.
6.9 Ibrahim, I. and Elliott, K. S., Long-term behaviour of precast, prestressed hollow-core slabs with concrete toppings, 7th Asia Pacific Structural Engineering and Construction Conference (APSEC) and 2nd Asian European Civil Engineering Forum (EACEF), 2009.
6.10 Mones, R. M. and Breňa, S. F., Hollow-core slabs with cast-in-place concrete topping: A study of interfacial shear strength, PCI Journal, Vol 58, No. 3, Summer 2013, pp. 124–141.
6.11 British Standards Institution, BS EN 1168+A3, 2011: Precast Concrete Products – Hollow-Core Slabs, BSI, London, 2005.
6.12 Evans, R. H. and Parker, A. S., Behaviour of prestressed concrete composite beams, ACI Journal, Vol. 51, No. 43, 1955, pp. 861–881.
6.13 British Standards Institution, BS5606, Guide to Accuracy in Building, BSI, Milton Keynes, 1990.
6.14 Kajfasz, S., Sommerville, G. and Rowe, R. E., An Investigation of the Behaviour of Composite Concrete Beams, Cement and Concrete Association Research Report No. 15, London, Nov. 1963.

Chapter 7

7.1 Stanton, J. F., Anderson, R. G., Dolan, C. W. and McCleary, D. E., Moment-Resistant Connections and Simple Connections, Final Report to PCI, Specially Funded R & D Projects Nos 1 & 4, 1986, and PCI Journal, Vol. 32, No. 2, March–April 1987, pp. 62–74.
7.2 Colman, D. G., A Study of Precast Concrete Beam-to-Column Joints using Steel Connections, Applied Science Publishers, London, 1982.
7.3 Fédération Internationale du Béton, (*fib*), Bulletin 43, Structural Connections for Precast Concrete Buildings, Guide to Good Practice, February 2008, 370 pp.
7.4 Vambersky, J. N. J. A., General Design Philosophy, Prefabrication of Concrete Structures, International Seminar, Delft University of Technology, Delft University Press, Delft, Oct. 1990, pp. 15–28.
7.5 Vambersky, J. N. J. A., Mortar Joints Loaded in Compression, Prefabrication of Concrete Structures, International Seminar, Delft University of Technology, Delft University Press, Delft, Oct. 1990, pp. 167–180.
7.6 Barboza, A. d. S. R. and El Debs, M. K., Load-bearing Capacity of Mortar Joints Between Precast Elements, Magazine of Concrete Research, Vol. 58, No. 9, November 2006, pp. 589–599.
7.7 Bljuger, F., On an Estimation Methodology for Wall Bearing Capacity in Precast Concrete Construction, Proceedings 10th International Congress of the Precast Concrete Industry, Jerusalem, Sept. 1981, pp. 259–271.
7.8 British Standards Institution, BS EN 1992-1-1, Eurocode 2: Design of concrete structures – Part 1-1: General rules and rules for buildings, Code of Practice for Dead and Imposed Loads, BSI, London, 2004.

7.9 British Standards Institution, BS 8110-1, Part 1: Code of practice for design and construction, BSI, London, 1997.
7.10 Bljuger, F., Non-linear Characteristics of Joints in Compression, RILEM-CEB-CIB, Athens, Greece, Vol. 1, Sept. 1978, pp. 159–169.
7.11 Bljuger, F., Determination of Deformability Characteristics of Vertical Shear Joints in Precast Buildings, Building and Environment, Vol. 11, 1976, pp. 277–282.
7.12 Study Group of the New Zealand Concrete Society, Guidelines for the Use of Structural Precast Concrete in Buildings, Study Group of the New Zealand Concrete Society and National Society of Earthquake Engineering, Christchurch, New Zealand, 1989, 174 pp.
7.13 Prestressed Concrete Institute, PCI Architectural Precast Concrete Manual, 3rd edition, PCI, Chicago, IL, 2007.
7.14 Fédération Internationale du Béton, CEB/FIP Model Code MC90, Lausanne, Switzerland, 1992.
7.15 Walraven, J. C. and Mercx, W., The Bearing Capacity of Prestressed Hollow-Core Slabs, Heron, 28, No. 3, University of Delft, Netherlands, 1983, p. 46.
7.16 Bljuger, F., Wall Clamping of Floor Slabs, Building and Environment, Vol. 17, No. 1, 1982, pp. 17–21.
7.17 Clarke, J. L. and Simmonds, R. M., Tests on Embedded Steel Billets for Precast Concrete Beam–Column Connections, Technical Report No. 42.523, Cement and Concrete Association, Wexham Springs, Slough, August 1978, 12 pp.
7.18 Bruggeling, A. S. G., Development Towards Structural Concrete, Concrete Precasting Plant and Technology, BFT, Vol. 58, No. 3, March 1992.
7.19 Betongelementboken, Bind B, Avstivning og kraftoverføring (Design manual for precast concrete, Shoring and transmission, Vol. B). Betongelementforeningen, SB Grafisk, Asker, Norway, 2005, 296 pp. (in Norwegian).
7.20 Fawzi, H. T., Concrete bearing with steel inserts in precast column-to-beam connections, MPhil thesis, University of Nottingham, 1976.
7.21 Institution of Structural Engineers, Structural Joints in Precast Concrete, IStructE, London, August 1976, 56 pp.
7.22 Park, R., Seismic Design Considerations for Precast Concrete Construction in Seismic Zones, Seminar on Precast Concrete Construction in Seismic Zones, Japan Society for the Promotion of Science & US National Science Foundation, Tokyo, Vol. 1, 1986, pp. 1–38.
7.23 Pillai, S. U. and Kirk, D. W., Ductile Beam–Column Connections in Precast Concrete, ACI Journal, Vol. 78, Nov.–Dec. 1981, pp. 480–487.
7.24 Hasan, S., Discontinuous Precast Concrete Beam–Column Connections, PhD thesis, University of Nottingham, UK, 2011.
7.25 Vinha, J. and Lindberg, R., Beam-to-column Connections in Storey-height Concrete Frame, Report 57, Department of Civil Engineering, Tampere University of Technology, Finland, 1992.
7.26 deChefdebien, A., Precast beam-to-column head connections, Control of the Semi-rigid Behaviour of Civil Engineering Structural Connections, COST C1 International Conference, Liege, 1998, pp. 35–44.
7.27 Restrepo, J. I., Park, R. and Buchanan, A. H., Tests on Connections of Earthquake-resisting Precast Reinforced Concrete Perimeter Frame of Buildings, PCI Journal, Vol. 40, No. 4, July–Aug 1995, pp. 44–61.
7.28 Hasan, S., Elliott, K. S. and Ferreira, M., An Experimental Investigation on the Moment Continuity of Precast Concrete Beam–Column Connections under Gravity Loads, Proceedings, fib Symposium, Prague, May 2011.
7.29 Monforton, G. R. and Wu, T. S., Matrix Analysis of Semi-Rigidly Connected Frames, Journal of Structural Division, ASCE, Vol. 89, No. 6, 1963, pp. 13–42.
7.30 Priestley, M. J. N., Sritharan, S., Conley, J. R. and Pampanin, S., A Summary of Test Results from the PRESSS Five-Storey Precast Concrete Building, SESOC Journal, Structural Engineering Society, New Zealand, Vol. 13, No. 1, April 2000, pp. 21–37.
7.31 Ozden, S. and Ertas, O., Modelling of Precast Concrete Hybrid Connections by Considering the Residual Deformations, International Journal of the Physical Sciences, Vol. 5, No. 6, June 2010, pp. 781–792.
7.32 Lindberg, R. and Keronen, A., Semi-rigid Behaviour of a RC portal frame, COST C1 Proceedings of the First State-of-the-Art Workshop, Semi-rigid behaviour of civil engineering structural connections, ENSAIS, Strasbourg, 1992, pp. 53–63.
7.33 Lindberg, R. *et al.*, Beam-to-Column Connections in Storey-Height Concrete Frame, Report 57, Tampere University of Technology, Finland, 1992, 104 pp.
7.34 Elliott, K. S., Davies, G., Ferreira, M., Mahdi, A. A. and Gorgun, H., Can Precast Concrete Structures be Designed as Semi-Rigid Frames? – Part 1: The Experimental Evidence, The Structural Engineer, Vol. 81, No. 16, 19 August 2003, pp. 14–27.
7.35 Elliott, K. S., Davies, G., Ferreira, M., Mahdi, A. A., Gorgun, H. and Precast, C., Concrete Structures be Designed as Semi-Rigid Frames? – Part 2: Theoretical Equations and Applications for Frame Design, The Structural Engineer, Vol. 81, No. 16, 19 August 2003, pp. 28–37.
7.36 Elliott, K. S., Davies, G. and Gorgun, H., Semi-Rigid Connections in Precast Concrete Frames, FIP Notes, Vol. 1997/4, September 1997, pp. 6–12.
7.37 Ferreira, M. A., Deformability of Beam–column Connections in Precast Concrete Structures, PhD thesis, School of Engineering of São Carlos, University of São Paulo, Brazil, 1999.

7.38 Ferreira, M. A., El Debs, M. K. and Elliott, K. S., Theoretical Model for Design of Semi-Rigid Connections in Precast Concrete Structures, Proceedings 44th Brazilian Concrete Congress, IBRACON Brazilian Concrete Institute, Belo Horizonte, Brazil, August 2002, pp. 100–116.
7.39 Ferreira, M. A., El Debs, M. K. and Elliott, K. S., Analysis of Multi-storey Precast Frames with Semi-Rigid Connections, Brazilian Conference on Concrete, IBRACON 2003, 45th Brazilian Concrete Congress, Brazilian Concrete Institute – IBRACON, Vitoria, Brazil, 16–21 August 2003.
7.40 deChefdebien, A. and Dardare, J., Experimental Investigations on Current Connections between Precast Concrete Components, COST C1 Proceedings of the Second State-of-the-Art Workshop, Semi-rigid Behaviour of Civil Engineering Structural Connections, 1994, Prague, pp. 21–30.
7.41 Mahdi, A. A., Moment-Rotation Effects on the Stability of Columns in Precast Concrete Structures, PhD thesis, University of Nottingham, 1992.
7.42 Gorgun, H., Semi-rigid Behaviour of Connections in Precast Concrete Structures, PhD thesis, University of Nottingham, 1997.
7.43 Elliott, K. S., Ferreira, M., de Aranjo, D. and El Debs, M. K., Analysis of Multi-storey Precast Frames considering Beam–column Connections with Semi-rigid Behaviour, Keep Concrete Attractive, FIB Symposium, Budapest, 23–25 May 2005, pp. 496–501.
7.44 Prestressed Concrete Institute, Design and Typical Details of Connections for Precast and Prestressed Concrete, 2nd edition, PCI, Chicago, IL, 1990.
7.45 British Standards Institution, BS EN 1993-1-1:2005, Design of steel structures – Design of steel structures: General rules and rules for buildings, BSI, London, 2008.
7.46 Fédération Internationale de la Préconstrainte, FIP Recommendations. Precast Hollow-Core Floors, FIP Commission on Prefabrication, Thomas Telford, London, 1988, 31 pp.
7.47 Elliott, K. S. and Tovey, A., Precast Concrete Frame Buildings – A Design Guide, British Cement Association, Wexham Springs, Slough, May 1992, 88 pp.
7.48 Prestressed Concrete Institute, Design Handbook, 7th edition, PCI, Chicago, IL, 2010.
7.49 Fogarasi, G., Precast Concrete In Buildings: Design, Manufacture and Construction, Precast Concrete In Buildings, Seminar, Precast Concrete Manufacturers' Association of NSW and Concrete Institute of Australia, April 1988, pp. 1–45.
7.50 Holmes, M. and Posner, C. D., Factors Affecting the Strength of Steel Plate Connections between Precast Concrete Elements, The Structural Engineer, Vol. 48, No. 10, 1970, pp. 399–406.
7.51 Regan, P. E., Billet Insert Joints for Precast Concrete Frames-Two Beam Joints under Symmetrical Loads, Report to Dowmac Concrete Ltd., Polytechnic of Central London, Oct 1981.
7.52 Marcakis, K. and Mitchell, D., Precast Concrete Connections with Embedded Steel Members, PCI Journal, Vol. 25, No. 4, July–Aug. 1980, pp. 88–115.
7.53 Mattock, A. H. and Gaafar, G. H., Strength of Embedded Steel Sections as Brackets, ACI Journal, Vol. 79, No. 2, March–April 1982, pp. 83–91.
7.54 Holmes, M. and Bond, D., Tests on a Beam-To-Column Connection for Precast Concrete, The Structural Engineer, Vol. 41, No. 9, Sept. 1963, pp. 293–297.
7.55 British Standards Institution, BS EN 1993-1-1:2005, Eurocode 3: Design of steel structures – General rules and rules for buildings, BSI, London, 2005.
7.56 British Standards Institution, BS 5950, Structural Use of Steelwork in Buildings, Part 1, Code of Practice for Design in Simple and Continuous Construction: Hot Rolled Sections, BSI, London, 1985.
7.57 Holmes, M. and Posner, C. D., The Connection of Precast Concrete Structural Members, CIRIA Report 28, Thomas Telford, London, February 1971.
7.58 Comité Euro-International Du Béton, Fastenings To Concrete and Masonry Structures, CEB State-of-the-Art Report, Thomas Telford, London, 1994, 249 pp.
7.59 Jolly, C. K. and Mohamed, S. A. M., Behaviour of Bolted Beam–column Joints in Precast Concrete Frames under the Application of Symmetrical Shear Loading, ASEC-94 Conference, Australian Society of Engineers, September 1994, pp. 1133–1138.
7.60 Jolly, C. K., Sleeve-Bolted Joint Constraints In Precast Concrete Beams: Structural Assessment – The Role of Large and Full Scale Testing, Paper 056, Proceedings of the Joint Institution of Structural Engineers/City University International Seminar, City University, London, July 1996, pp. 1–10.
7.61 Bruggeling, A. S. G. and Huyghe, G. F., Prefabrication with Concrete, Balkema, Rotterdam, 1991, 380 pp.
7.62 Kris, L. B. and Raths, C. H., Connections in Precast Concrete Structures: Strength of Corbel Brackets, PCI Journal, Vol. 10, No. 1, 1965, pp. 1–61.
7.63 Somerville, G., The Behaviour and Design of Reinforced Concrete Corbels, Publication No 12.069, Cement and Concrete Association, Wexham Springs, Slough, 1972, 60 pp.
7.64 Cook, W. D. and Mitchell, D., Studies of Disturbed Regions Near Discontinuities in Reinforced Concrete Members, ACI Structural Journal, Vol. 85, No. 2, March 1988, pp. 206–216.

7.65 British Standards Institution, PD 6687:2010, Background paper to the UK National Annexes to BS EN 1992-1 and BS EN 1992-3, BSI, London, 2010.
7.66 Goodchild, C. H., Morrison, J. and Vollum, R., How to Design Concrete Structures using Eurocode 2, Strut-and-Tie Models, The Concrete Centre, Camberley, UK, August 2012, 56 pp.
7.67 Comité Euro-International du Béton, CEB–FIP Model Code MC90, Thomas Telford, London, 1990, 437 pp.
7.68 Zeller, W., Conclusions from Tests on Corbels, Structural Concrete, IABSE Colloquium, Stuttgart, 1991, 577–582.
7.69 Park, R., Trends, Performance of Precast Concrete in Buildings, Seminar, Trends, Innovation and Innovation and Performance of Prestressed and Precast Concrete, Institute of Engineers Malaysia, Kuala Lumpur, May 1993.
7.70 Shu, C.-C. and Hawkins, N. M., Behaviour of Columns Continuous through Concrete Floors, ACI Structural Journal, Vol. 89, No. 4, July–Aug. 1992, pp. 405–416.
7.71 Kuttab, A. and Dougill, J. W., Grouted and Dowelled Jointed Precast Concrete Columns: Behaviour in Combined Bending and Compression, Magazine of Concrete Research, Vol. 40, No. 144, Sept. 1988.
7.72 Bergstrom, S., Inspanning Av Betongelementpelare Med Grundskruv Och Stalfot, Chalmers University of Technology, Göteborg, Report 94:1, May 1994.
7.73 Peikko Group Corp., Private communication, Finland, June 2012.
7.74 Bianco, L., Santagati, S., Bolognini, D. and Nascimbene, R., Seismic Response of Columns Connected to the Foundation through a Fastening Technique, Peikko News, Edition 1/2009, Peikko Group, 15101 Lahti, Finland, 2009, pp. 13–20.
7.75 British Standards Institution, BS 8110-3:1985, Structural use of concrete: Design charts for singly reinforced beams, doubly reinforced beams and rectangular columns. BSI, London, 1985.
7.76 Somerville, G., Tests on Column–Column Joints for the Ministry of Public Building and Works, Cement and Concrete Association, Wexham Springs, Slough, Note DW/30, July 1967.
7.77 Canha, R. M. F., El Debs, A. L. H. and El Debs, M. K., Design Model for Socket Base Connections Adjusted from Experimental Results, Structural Concrete, Journal of fib, Vol. 8, No. 1, Jan.–March 2007, pp. 3–10.
7.78 Osanai, Y., Watanabe, F. and Okamoto, S., Load Transfer Mechanism of Socket Base Connections with Precast Concrete Columns, ACI Structural Journal, Vol. 93, No. 3, March 1996, pp. 266–276.
7.79 British Standards Institution, BS EN 1993-1-8:2005, Design of steel structures – Part 1-8: Design of joints, BSI, London, September 2006.
7.80 Korolev, L. V. and Korolev, H. V., Joint Between Prefabricated Reinforced Column and Foundation, Promyshlennoe Sroitel'stvo, Vol. 16, No. 9, Sept. 1962.

Chapter 8

8.1 Schoettier, M. J., Belleri, A., Zhang, D., Restrepo, J. I. and Flieschman, R. B., Preliminary Results of the Shake-Table Testing for the Development of a Diaphragm Seismic Design Methodology, PCI Journal, Precast and Prestressed Concrete institute, Vol. 54, No. 1, Winter 2009, pp. 100–123.
8.2 British Standards Institution, BS EN 1991-1-4:2005 +A1:2010, Eurocode 1: Actions on structures – Part 1–4: General actions – Wind actions, BSI, London, January 2010.
8.3 British Standards Institution, BS 6399-2:1997, Loading for buildings. Code of practice for wind loads. BSI, London, July 1997 (withdrawn in 2010 and replaced by reference 8.2).
8.4 Cook, N., The Designer's Guide to Wind Loading of Building Structures, Butterworth, 1985.
8.5 British Standards Institution, BS EN 1992-1-1, Eurocode 2: Design of concrete structures – Part 1-1: General rules and rules for buildings, Code of Practice for Dead and Imposed Loads, BSI, London, 2004.
8.6 British Standards Institution, BS 8110-1, Part 1: Structural use of concrete – Code of practice for design and construction, BSI, London, 1997.
8.7 Bachmann, H. and Steinle, A., Precast Concrete Structures, Ernst and Sohn GmbH. KG, Berlin, Germany, 2011, 260 pp.
8.8 Pearce, D. J. and Matthews, D. D., An Appraisal of the Design of Shear Walls in Box Frame Structures, Property Services Agency, April 1973.
8.9 ICE/IStructE, Manual for the Design of Reinforced Concrete Building Structures, Institutions of Civil and Structural Engineers joint publication, London, 1985.
8.10 Moustafa, S. E., Effectiveness of Shear-friction Reinforcement in Shear Diaphragm Capacity of Hollow-core Slabs, Journal of the Prestressed Concrete Institute, Vol. 26, No. 1, January–February 1981, pp. 118–132.
8.11 Svensson, S., Diaphragm Action in Precast Hollow-core Floors: Description of a Pilot Test Series, The Nordic Concrete Federation, Nordic Concrete Research, Publication No. 4, 1985.
8.12 Stroband, J. and Kolpa, J. J., The Behaviour of a Demountable Floor, Proceedings of Symposium on Demountable Concrete Structures, Delft University Press, Delft, 1985, pp. 201–216.

8.13 Sarja, A., Analysis of the Statical In-plane Behaviour of Prefabricated Hollow-Core Slabs Field, Concrete Laboratory Report No 51, Espoo, Finland, June 1978, 36 pp.
8.14 Svensson, S., Engstrom, B. and Cederwall, K., Diaphragm Action of Precast Floors with Grouted Joints. Nordisk Betong, Feb. 1986, pp. 123–128.
8.15 Stroband, J., Diaphragm Action, Prefabrication of Concrete Structures, International Seminar, Delft University of Technology, Delft University Press, Delft, Oct. 1990, pp. 203–214.
8.16 Menengotto, M., Seismic Resistant Extruded Hollow-Core Slabs, International Symposium on Noteworthy Developments in Prestressed and Precast Concrete, Singapore, November 1989.
8.17 Menengotto, M., Hollow-Core Floors Tests for Seismic Action, FIP Symposium, Jerusalem, Sept. 1988, pp. 477–484.
8.18 Abdul-Wahab, H. and Sarsam, S., Strength of Vertical Plane Joints Between Large Precast Concrete Panels, The Structural Engineer, Vol. 66, No. 14, July 1988, pp. 211–215.
8.19 Bruggeling, A. S. G. and Huyghe, G. F., Prefabrication with Concrete, Balkema, Rotterdam, 1991, 380 pp.
8.20 Mast, R. F., Auxiliary Reinforcement in Concrete Connections, Proceedings of the American Society of Civil Engineers, Vol. 94, No. ST 6, 1968, pp. 1485–1504.
8.21 Jimenez, R., Gergely, P. and White, R. N., Shear Transfer across Cracks in Reinforced Concrete, New York, Cornell University, Dept. of Structural Engineering, Report No. 78-4, August 1978.
8.22 Tassios, P. T. and Vintzeleou, E. N., Concrete to-concrete friction, Journal of Structural Engineering, Proc. ASCE, Vol. 113, No. ST4, April 1987, pp. 832–849.
8.23 Divinkar, M. P., Fafitis, A. and Shah, S. P., Constitutive Model for Shear Transfer in Cracked Concrete, Journal of Structural Engineering, Vol. 113, No. 5, May 1987, pp. 1046–1062.
8.24 Cholewicki, A., Shear Transfer in Longitudinal Joints of Hollow-Core Slabs, Concrete Precasting Plant and Technology, B + FT, Vol. 57, No. 4, April 1991, pp. 58–67.
8.25 Norges Betongindustriforbund, Konstrucksjonshandbok Betongelementer, Norges Betongindustriforbund, Oslo, 1988.
8.26 Walraven, J. C., Diaphragm Action in Floors, Prefabrication of Concrete Structures, International Seminar, Delft University of Technology, Delft University Press, Oct. 1990, pp. 143–154.
8.27 Millard, S. G. and Johnson, R. P., Shear Transfer across Cracks in Reinforced Concrete due to Aggregate Interlock and to Dowel Action, Magazine of Concrete Research, Vol. 36, No. 126, March 1984, pp. 9–21.
8.28 Walraven, J. C. and Reinhardt, H. W., Concrete Mechanics: Part A – Theory and experiments on the mechanical behaviour of cracks in plain and reinforced concrete subjected to shear loading, Heron, Vol. 26, No. 1A, 1981, pp. 1–68.
8.29 Davies, G., Elliott, K. S. and Omar, W., Horizontal Diaphragm Action in Precast Hollow-Cored Floors, The Structural Engineer, Vol. 68, No. 2, Jan. 1990, pp. 25–33.
8.30 Elliott, K. S., Davies, G. and Omar, W., Experimental and Theoretical Investigation of Precast Hollow-Cored Slabs used as Horizontal Diaphragms, The Structural Engineer, Vol. 70, No. 10, May 1992, pp. 175–187.
8.31 Omar, W., Diaphragm Action in Precast Concrete Floor Construction, PhD Thesis, University of Nottingham, 1990.
8.32 Elliott, K. S., Davies, G. and Bensalem, K., Precast Floor Slab Diaphragms without Structural Screeds, Concrete 2000 – Economic and Durable Construction Through Excellence, Dundee, Sept. 1993, pp. 617–632.
8.33 British Standards Institution, BS1134, Methods for the Assessment of Surface Texture, Part 1, BSI, London, 1972.
8.34 Bison Manufacturing Ltd., Private communication, Dec. 1990.
8.35 de Roo, A. M. and Straman, J. P., Krachtsverdeling in en vormverandering van een in zynvlak belaste prefab vloerconstructie (Distribution and deformation of a loaded prefabricated floor construction), PhD thesis, Delft Precast Concrete Institute, Delft University of Technology, 1991.
8.36 Prestressed Concrete Institute, Design Handbook, 7th edition, PCI, Chicago, IL, 2010.
8.37 Bensalem, K., The Structural Integrity of Precast Concrete Floor Systems used as Horizontal Diaphgrams, PhD Thesis, University of Nottingham, 2001.
8.38 British Standards Institution, BS 8110-1, Part 2: Structural use of concrete – Code of practice for special circumstances, BSI, London, 1985.
8.39 Kaplan, H., Nohutcu, H., Çetinkaya, N., Yilmaz, S., Gönen, H. and Atimtay, E., Seismic Strengthening of Pin-connected Precast Concrete Structures with External Shear Walls and Diaphragms, PCI Journal, Precast and Prestressed Concrete institute, Vol. 54, No. 1, Winter 2009, pp. 88–99.
8.40 Institution of Structural Engineers, Stability of Buildings, IStructE, London, Dec. 1988.
8.41 Hekenyi, M., Beams on Elastic Foundations, University of Michigan Press, Ann Arbor, MI, 1946.
8.42 Stafford-Smith, B. and Carter, C., A Method of Analysis for Infill Frames, Paper 7218, Proc. Institution of Civil Engineers, Vol. 44, Sept. 1969.
8.43 Mainstone, R. J., On the Stiffnesses and Strengths of Infill Frames, Building Research Establishment Paper CP2/72, Feb. 1972.

8.44 Wood, R. H., Plasticity, Composite Action and Collapse Design of Unreinforced Shear Wall Panels in Frames, Paper 8110, Proc. Institution of Civil Engineers, Vol. 65, June 1978.
8.45 Kwan, K.-H. and Liaum, T.-C., Non-linear Analysis of Multi-Storey Infilled Frames, Paper 8577, Proc. Institute of Civil Engineers, Vol. 73, June 1982.
8.46 Kwan, K.-H. and Liaum, T.-C., Plastic Theory of Infilled Frames with Finite Interface Shear Strength, Paper 8718, Proc. Institute of Civil Engineers, Vol. 75, Dec. 1983.
8.47 Wright, R., Design of Wind Walls, Internal Paper, Trent Concrete Ltd, Nottingham, June 1981.
8.48 British Standards Institution, BS EN 1996-1-1, Eurocode 6: Design of masonry structures, Part 1-1 – General rules for reinforced and unreinforced masonry structures, BSI, London, 2005.
8.49 British Standards Institution, BS 5268-1, Code of practice for the use of masonry – Structural use of unreinforced masonry, BSI, London, 2005.
8.50 Chakrabarti, S. C., Nayak, G. C. and Paul, D. K., Shear Characteristics of Cast-in-place Vertical Joints in Storey-high Precast Wall Assembly, ACI Structural Journal, Vol. 85, No. 1, Jan.–Feb. 1988, pp. 30–45.
8.51 Chakrabarti, S. C., Bhise, N. N. and Sharma, K. N., Failure Criterion of Vertical Shear Key Joints in Prefabricated Wall Panels, Indian Concrete Journal, Vol. 55, No. 3, March 1981, pp. 63–67.
8.52 Foerster, H. R., Rizkalla, S. H. and Scott Heuvel, J., Behaviour and Design of Shear Connections for Load-bearing Wall Panels, PCI Journal, Vol. 34, No. 1, Jan.–Feb. 1989, pp. 102–118.
8.53 CIRIA, The Behaviour of Large Panel Structures, Construction Industry Research and Information Association, Report 45, London, March 1973.
8.54 Straman, J. P., Precast Concrete Cores and Shear Walls, Prefabrication of Concrete Structures, International Seminar, Delft University of Technology, Delft University Press, Oct. 1990, pp. 41–54.

Chapter 9

9.1 British Standards Institution, BS EN 1992-1-1, Eurocode 2: Design of concrete structures – Part 1-1: General rules and Rules for Structures, BSI, London, 2004.
9.2 British Standards Institution, BS 8110-1, Structural Use of Concrete – Part 1: Code of practice for design and construction, BSI, London, 1997.
9.3 Mahdi, A. A., Moment Rotation Effects on the Stability of Columns in Precast Concrete Structures, PhD thesis, University of Nottingham, 1992.
9.4 Study Group of the New Zealand Concrete Society and National Society of Earthquake Engineering, Guidelines for the Use of Structural Precast Concrete in Buildings. Christchurch, New Zealand, 1991, 174 pp.
9.5 Engström, B., Ductility of Tie Connections in Precast Structures, PhD thesis, Chalmers University of Technology, Göteborg, Sweden, 1992.
9.6 Numerous contributors, COST C1 Proceedings of the First State-of-the-Art Workshop, Semi-rigid Behaviour of Civil Engineering Structural Connections, ENSAIS, Strasbourg, Oct. 1992.
9.7 Fédération Internationale du Béton, (fib), Bulletin 63, Design of Precast Concrete Structures Against Accidental Actions – Guide to good practice, January 2012, 72 pp.
9.8 United Facilities Criteria UFC 4-023-03, Design of Buildings to Resist Progressive Collapse, January 2005.
9.9 Bignell, V., Peters, J. and Pym, C., Catastrophic Failures, Open University Press, Milton Keynes, 1977.
9.10 Griffiths, H., Pugsley, A. G. and Saunders, O., Report of the Inquiry into the Collapse of Flats at Ronan Point, Canning Town, Her Majesty's Stationery Office, London, 1968.
9.11 UK Ministry of Housing and Local Government, Standards to Avoid Progressive Collapse – Large Panel Construction, November 1968.
9.12 British Standards Institution, BS EN 1991, Part 1-7:2006, General actions – Accidental actions, BSI, London, 2006.
9.13 Astbury, N. F. *et al.*, Gas Explosions in Load-bearing Brick Structures, British Ceramic Research Association, Report No. 68, 1970.
9.14 The Building Regulations 1976, No. 1676, Her Majesty's Stationery Office, London, 1978.
9.15 Office of the Deputy Prime Minister, The Building Regulations Approved Document A – Structure (2004 edition), Schedule 1: A3, Disproportionate Collapse, London, 27 April 2006.
9.16 Bruggeling, A. S. G. and Huyghe, G. F., Prefabrication with Concrete, Balkema, Rotterdam, 1991, 380 pp.
9.17 Izzuddin, B. A., Vlassis, A. G., Elghazouli, A. Y. and Nethercot, D. A., Assessment of Progressive Collapse in Multi-storey Buildings, Proceedings of the Institution of Civil Engineers, Structures and Buildings, Vol. 160, August 2007.
9.18 Baker, A. L. L. and Yu, C. W., Research to Investigate the Strength of Floor-to-outside Wall Joints in Precast Concrete, The Stability of Precast Concrete Structures, Department of Environment and CIRIA Seminar, Ref. B387/73, March 1973.
9.19 Omar, W., Diaphragm Action in Precast Concrete Floor Construction, PhD thesis, University of Nottingham, 1990.

9.20 FIP Recommendations, Precast Prestressed Hollow-Cored Floors, FIP Commission on Prefabrication, Thomas Telford, London, 1988, 31 pp.
9.21 Regan, P. E., Catenary Tests on Composite Precast–In situ Concrete Composite Floors, Report to the Department of Environment, The Polytechnic of London, 1974.
9.22 Schultz, D., Burnett, E. and Fintel, M., A Design Approach to General Structural Integrity – Design and Construction of Large Panel Concrete Structures, Supplemental Report A, Portland Cement Association, Stokie, USA, 1978.
9.23 Hanson, N. and Burnett, E., Wall Cantilever and Slab Suspension Tests, Design and Construction of Large Panel Concrete Structures, Report 4, Portland Cement Association, Stokie, USA, 1977.
9.24 Wilford, M. J. C. and Yu, C. W., Catenary Action in Damaged Structures: Paper No. 6, Department of Environment and CIRIA, The Stability of Precast Concrete Structures, Seminar, London, March 1973, pp. 1–24.
9.25 Odgard, A., Connections between Precast Floor Slabs, CIB Symposium, Bearing Walls, Sept. 1975.
9.26 Engström, B., Connections Between Precast Components, Nordisk Betong, Journal of the Nordic Concrete Federation, Vol. 2, No. 3, 1990, pp. 53–56.

Chapter 10

10.1 Health and Safety Executive, CDM or ConDaM Regulations, Managing Health and Safety in Construction. Construction (Design and Management) Regulations 2007 Approved Code of Practice, Health and Safety Executive, 2010 edition, HMSO, London.
10.2 British Standards Institution, BS EN 1992-1-1, Eurocode 2: Design of Concrete Structures – Part 1-1: General Rules and Rules for Buildings, Code of Practice for Dead and Imposed Loads, BSI, London, 2004.
10.3 British Standards Institution, BS 8110-1, Part 1: Code of Practice for Design and Construction, BSI, London, 1997.
10.4 McCaully, C. H. A., Chain Tester's Handbook, 2nd edition, Chain Testers' Association of Great Britain, London, 1975.
10.5 Adlparvar, M. R., Torsional Behaviour of Precast Concrete Beans and Connections, MPhil thesis, University of Nottingham, 1993.
10.6 Kong, F. K. and Evans, R. H., Reinforced and Prestressed Concrete, 3rd edition, Van Nostrand, London, 1987, 508 pp.
10.7 Precast Flooring Federation, Code of Practice for Safe Erection of Precast Concrete Flooring, 2nd edition, British Precast, Leicester, UK, 2010.
10.8 Precast Concrete Industry Training Association, Code of Practice for the Safe Erection of Precast Concrete, British Precast, Leicester, UK, 2010.
10.9 Engineering Science Data Unit, Fluid Forces and Moments on Flat Plates, ESDU Item No. 70015, London, September 1970.
10.10 Engineering Science Data Unit, Fluid Forces, Pressures and Moments on Rectangular Blocks, ESDU Item No. 71016, London, September 1971.
10.11 Cook, N., The Designer's Guide to Wind Loading of Building Structures – Background, Damage Survey, Wind Data, and Structural Classification, Building Research Establishment, Dept. of the Environment, 1985, 371 pp.
10.12 Institution of Structural Engineers, Structural Joints in Precast Concrete. IStructE, London, August 1978, 56 pp.
10.13 Elliott, K. S. and Tovey, A., Precast Concrete Frame Buildings – A Design Guide, British Cement Association, Wexham Springs, Slough, 1992, 88 pp.
10.14 British Standards Institution, BS EN 12390, Parts 1–8, Testing of Hardened Concrete. BSI, London, various dates.
10.15 British Standards Institution, BS EN 13670:2009, Execution of Concrete Structures, BSI, London, 2009.
10.16 British Standards Institution, BS EN 12812:2008, Falsework – Performance Requirements and General Design, BSI, London, 2011.
10.17 British Standards Institution, BS 5975:2008+A1:2011, Code of Practice for Temporary Works Procedures and the Permissible Stress Design of Falsework, BSI, London, October 2011.
10.18 British Standards Institution, BS EN 12350, Parts 1–12, Testing Fresh Concrete, BSI, London, various dates.
10.19 Ibrahim, I., Behaviour of Precast Concrete Hollow-Core Units with Structural Topping, PhD thesis, University of Nottingham, 2008.

Index

Multi-storey Precast Concrete Framed Structures, Second Edition. Kim S. Elliott and Colin K. Jolly.